WINDPOWER '96

June 23-27, 1996

Denver Marriott City Center Hotel

Denver, Colorado

Annual Conference and Exhibition of
the American Wind Energy Association

Co-sponsored by:

U.S. *Department of Energy*

National Renewable Energy Laboratory

PacifiCorp

DISCLAIMER

WINDPOWER '96 *Proceedings was produced by*
the American Wind Energy Association.
For additional copies of this document,
please call or write to:

122 C Street, NW, Fourth Floor
Washington, DC 20001
phone (202)383-2500
fax (202)383-2505

WINDPOWER '96

June 23-27, 1996

SESSION 1: Opening
Monday, June 24
Chair: Randall Swisher, American Wind Energy Association

SESSION 2: Views on World Markets
Monday, June 24
Chair: Kevin Rackstraw, American Wind Energy Association

SESSION 3: Europe
Monday, June 24
Chair: Ruud de Bruijne, Netherlands Agency for the Environment

Copyright article removed

SESSION 10A: Utility Issues
Wednesday, June 26
Chair: Gail Miller, PacifiCorp

SESSION 12A: Resource Assessment - 1
Wednesday, June 26
Chair: Robert Baker, Impact Weather

SESSION 13A: Resource Assessment - 2
Wednesday, June 26
Chair: Ed McCarthy, Wind Economics & Technology, Inc.

SESSION 10B: Small Wind Turbine Aerodynamics & Applications
Wednesday, June 26
Chair: R. Nolan Clark, USDA-Agricultural Research Service

SESSION 11B: Wind-Diesel Simulation Models and Applications
Wednesday, June 26
Chair: Lawrence Flowers, National Renewable Energy Laboratory

SESSION 12B: Aerodynamics
Wednesday, June 26
Chair: Tim Olsen, Tim Olsen Consulting

SESSION 13B: Dynamic Models
Wednesday, June 26
Chair: Paul Veers, Sandia National Laboratories

POSTER PRESENTATIONS

WIND ENERGY IN 1996: LOOKING FORWARD, LOOKING BACK

Randall Swisher, Executive Director
American Wind Energy Association

What is the state of Windpower in 1996?

It was the best of times, it was the worst of times.

On the positive side, wind energy technology continues to progress very impressively in terms of reliable and cost-effective performance. The technology has achieved cost goals no one would have thought possible a decade ago. WINDPOWER '96 is in part a celebration of that technology progress and of the wind industry's partnership with US DOE and NREL in pursuing collaborative R&D. That partnership and wind technology's progress will be highlighted by our visit later this week to the National Wind Technology Center.

WINDPOWER '96 is also a celebration of the growing worldwide market for wind, a growth that has been made possible in large part because of wind's increased cost-effectiveness and reliability. Wind's growing worldwide market is reflected in the conference agenda, where we have tried to bring in experts from around the world to provide details on selected markets. I would also like to extend a special welcome to our many guests from around the world who are participating in the Wind Energy Applications and Training Symposium.

Finally, we are also here to celebrate continuing partnerships with utilities, including our conference cosponsor PacifiCorp, or other leading utilities such as Northern States Power, Central & South West, Green Mountain Power, Lower Colorado River Authority, Sacramento Municipal Utility District, CARES, the Waverly, Iowa municipal utility or Traverse City Light & Power.

What is the down side for today's wind industry?

The bankruptcy of Kenetech, the wind industry's largest player, is clearly the most striking event of the past year. And perceptions matter. Our industry will be hurt in the eyes of many utilities and financial institutions around the world. But most of you realize that the failure of Kenetech should in no way be taken as a failure of the wind industry as a whole. Although Kenetech made some significant mistakes, its bankruptcy is also a fitting monument to the failure of U. S. energy policy to successfully facilitate a sustainable market for wind and other renewable technologies.

A second major negative is that at least temporarily, the restructuring of the U. S. electric industry has slowed the market for wind and any other new capacity. The U.S. electric industry is in the midst of the most momentous changes in its history, moving from a series of heavily regulated monopolies to a competitive power market in which electricity is a commodity bought and sold on futures markets.

This trend toward greater reliance on market forces is not confined to the U.S.--it is a

worldwide trend--and greater reliance on market forces can bring broad public benefit if market rules reflect the long-term public interest.

Today, the U.S. utility industry is busily preparing itself for competition. Little new capacity of any kind is being added. Wind should not feel singled out. As part of the preparation for competition, we see utility mergers, downsizing, assaults on PURPA and PURPA contracts and anything else utilities perceive as higher cost increasing their risk of financial exposure. We see a host of new market entrants such as power brokers and marketers. And we see an unrelenting emphasis on price with little attention to value, the long-term or the broader public interest beyond low-cost power.

The new competitive market holds advantages and disadvantages for renewables. We believe customer choice can work for wind. The time is quickly coming--in some parts of the country by 1998--when you as generators of electricity (or through brokers) will have the opportunity to sell on a direct access basis to the retail customer. As every survey or poll has demonstrated, people want renewables. Any utility or marketer looking to differentiate its product in this emerging commodity market will not be able to ignore the green market.

On the other hand, renewables have certain disadvantages in this new market. We have higher capital costs and are disadvantaged in a market which emphasizes short-term costs and doesn't properly value our long-term cost and environmental advantages. And wind plants don't operate like fossil fuel plants. The new market rules for transmission pricing and operation of power pools could exclude or seriously disadvantage intermittent renewables like wind.

So wind could do well in competitive markets, but the system must be set up in ways that are compatible with wind and its characteristics. The new market rules which will be imposed by federal and state policymakers must engage the power and efficiency of competitive markets while including market-oriented protections for the environment and the long-term public interest.

That's really what AWEA's Renewables Portfolio Standard is all about--harnessing the power of the market to bring renewables into the main stream. You'll be hearing more about the RPS tomorrow from Nancy Rader, who developed the concept for AWEA as a way to advance renewables in restructured markets.

The RPS was endorsed by the California Public Utilities Commission last December as a way of maintaining and increasing California's resource diversity. It has been increasingly embraced by other renewable industries, and we are now working with the biomass, geothermal and solar thermal industries (as well as environmental allies such as the Union of Concerned Scientists) to pass such a bill.

The RPS has some key advantages:

First is its Administrative Simplicity--each retail supplier would simply have to certify that the required percentage of their power came from renewables. In California's case, the

Commission has set a requirement of ten percent renewables. There are no complex bureaucratic procedures and minimal regulatory burden. Just do it.

Secondly, the RPS would be competitively neutral and imposed on all competitors, not just regulated utilities. By engaging all competitors, it would transform the market for renewables, giving all market participants a stake in building alliances that will allow them to achieve the standard in the most efficient and cost-effective way.

Third, the RPS is a market-based regulatory program that would rely on a system of tradable renewable energy credits to achieve policy goals in the least-cost way.

There are three primary policy options currently under consideration as ways of advancing renewables in restructured electric markets. All of these options can co-exist compatibly. The first is the RPS, which AWEA believes is the policy that most effectively advances wind in competitive markets. For more information on the RPS, consult AWEA's World Wide Web site at <http://www.igc.apc.org/awea/>.

Second is the "Systems Benefits Charge," a surcharge on electric rates which is intended to pay for a host of social benefits that could be stranded by competition--demand side management, low-income programs, research and development, and advancement of pre-commercial renewable technologies. But we don't believe a surcharge is the most effective way to advance commercially ready bulk power renewables. It really doesn't really transform the market. Depending upon a surcharge to pay the above market costs of renewables ensures that renewables will be no more than a sidebar to the market.

Third is Green Pricing, leaving renewables deployment up to voluntary contributions of customers who are willing to pay prices beyond their normal utility bill. There are a few examples, such as Sacramento or Traverse City, where utilities have implemented green pricing well, with real long-term vision. Unfortunately, they are exceptions. In most cases, including the proposal announced recently here in Colorado, the projects proposed to be supported are so small as to invariably be higher cost, setting up a vicious cycle, in which renewables are condemned to a marginal status as a higher cost resource in a sort of Green Ghetto.

All three mechanisms--a Renewables Portfolio Standard, a Systems Benefits Charge or Green Pricing--have a place in advancing renewables in competitive markets, but let's be aware of the limitations of each as we focus on ways to move wind from the margins to a more central role in the utility portfolio. Although Green Pricing has a role to play, it does not take the place of good public policy. And while AWEA favors the RPS, it is not the perfect policy tool to advance the interests of all renewable technologies. We require a portfolio of policy options to advance the interests of all renewables.

Most of the legislative action in regard to utility restructuring thus far has been on the state level, but there is growing interest in Congress in addressing the issue. One of the leaders in that debate will be Rep. Dan Schaefer, Chairman of the House Energy and Power Subcommittee.

We are lucky that Dan Schaefer is in such a key position. Wind and other renewables have been fortunate to have very strong support from a number of legislators on both sides of the aisle. But none has been stronger, more consistent or more effective than Dan Schaefer.

Schaefer led the way in defending DOE's renewable energy budget last year, winning the Klug-Schaefer Amendment on the House floor, standing up to much of the Congressional leadership in the process.

When the wind-biomass production tax credit was threatened last year, again Schaefer led the way, providing House leadership with a letter signed on to by scores of his colleagues, underscoring our strong political support and successfully defending the production tax credit. Recognizing that many of his colleagues lacked knowledge in regard to renewables, Schaefer established the House Renewable Energy Caucus as a vehicle for educating and organizing a Congressional constituency for renewables.

Now Schaefer is working on legislation that would accelerate the transition to customer choice, and we are all eagerly awaiting the provisions in his bill which would address renewables. We have had an opportunity for a great deal of dialogue with his staff on these issues, and our suggestions in regard to establishing a national renewables portfolio standard featuring tradeable renewable energy credits as a means of advancing renewables in competitive markets have been well received by his staff.

It has been a pleasure working so closely with Chairman Schaefer and his staff on so many issues, and it is a great pleasure to introduce him to you here at WINDPOWER '96.

CUSTOMER CHOICE AND RENEWABLE ENERGY

Congressman Dan Schaefer
Chairman, House Energy and Power Subcommittee

It has been almost a year now since I publicly announced my intention to introduce and move legislation ending the government-protected monopoly over the generation of electric energy. What a difference a year makes. At this time last year, the idea that retail consumers of electricity should have the power to choose among competitive suppliers of electricity was a notion limited to the academic journals. Today, it is fast becoming one of the most closely watched debates on Capitol Hill.

A year ago, the electric utility monopolies' motto was "just say no." Today, few utility executives will deny, at least in public, that retail choice for their customers is coming. The battle against consumer choice in Washington has become simply a rear-guard action of delaying the inevitable for as long as possible. It has gone from "just say no" to "just go slow."

A year ago, the Administration was saying there is no reason to consider retail choice legislation this year, giving a long list of excuses why we should wait until after the election to start the debate. Today, rumor has it that the Administration is drafting retail choice legislation to answer the Republican plan.

A year ago, less than one half of the States were even considering retail competition. Today, 47 states are at least studying retail choice, and a few are actively trying to implement their own plans. And just recently, the American Legislative Exchange Council, made up of state legislators, voted unanimously in favor of a model resolution calling for a "pro-consumer, pro-competition, and pro-market" retail choice plan for consumers.

A year ago, the Senate had adopted the industry's "just say no" position. Today, the Senate has completed a number of hearings on the issue and, reportedly, plans to hold even more.

A year ago, the House Commerce Committee and the leadership were being pressed to repeal federal monopoly statutes like PUHCA and PURPA without considering consumer choice. Today, it is taken as a given that all of these issues must be addressed in a comprehensive manner, and even EEI admits that piecemeal deregulation is dead now.

A year ago, the general media had hardly even heard about retail choice for consumers. Today, not a week goes by that the Wall Street Journal, the Washington Post or other major media do not run a story on utility deregulation.

Why have we seen all this dramatic movement toward retail choice for consumers? It is not because I have been giving a lot of speeches and holding a bunch of hearings. It is because

consumers of electricity understand the benefits of competition to their wallet and to the economy as a whole. As a result, competition is inevitable. What consumers want, they get.

Consumers want the same power of choice over electricity services as they have over other essentials of life like food, clothing and shelter. In fact, the very fact that electricity is so important to our lives is all the more reason why the power over electricity rates and services should be taken away from the government and given to a much higher authority -- the consumer.

A recent study by Citizens for a Sound Economy shows that even the smallest residential or small business consumer stands to save big -- if only they are given the opportunity to choose who provides their electricity service. The report estimated that consumers could see short term savings of 25 percent off the average monthly electric bill, and save up to 43 percent over the long term.

Whether or not you agree with these specific findings, it is clear that consumers -- not the Congress -- are the driving force behind competition. In the face of such momentum, Congress has two choices. It can shield government-protected monopolies from competition, or it can help consumers get what they want. I, for one, want to stand beside consumers.

That is why I will soon introduce legislation to give all consumers the power to choose among competing providers of electricity. Since I am still putting the finishing touches on my legislation, I cannot talk today about the details of the bill. However, I think it is important to understand why Congress must act, and why we must do so sooner rather than later.

As states and the Congress have begun to study how best to implement consumer choice, it has become clear that states have run into a number of obstacles that only Congress can remove.

For example, there is significant confusion in current law about where federal jurisdiction stops and state jurisdiction starts in a competitive world. As states move to do the right thing and give their consumers choice, they potentially risk losing their traditional jurisdiction to the FERC. This uncertainty has understandably slowed down state efforts to implement competition. Without congressional action to help define jurisdictional responsibilities of the federal government and the states, the only reward states may get for their trouble is never-ending litigation and uncertainty.

If we are being honest about allowing the states to take the lead in implementing consumer choice -- and I strongly believe that is the right way to go -- we have to recognize that the federal government must, at a minimum, clarify state jurisdiction, remove federal barriers to competition and provide states the tools they need to bring the benefits of consumer choice to all.

The nine hearings I have held to date in my subcommittee clearly show that each state varies in terms of how to introduce competition, and that the details of implementing customer choice to the states. My bill will do that. You will see much leeway given the states to implement customer choice in a manner that best suits their situation.

However, the one thing that is not subject to variations between states or regions is the need for customer choice in electricity. It is up to Congress to clear the way for the states to implement

customer choice, let them choose their own path to get there, but ensure that they get there in a reasonable time frame. Accordingly, my bill will also set a time-certain for the states -- following any appropriate model they choose -- to give consumers the ability to choose among competing providers of electricity.

Not only does Congress need to act, it needs to do so sooner, rather than later. Nevertheless, I am constantly asked: Why now? Shouldn't we let nature run its course and let the states act at their own pace? Or at least wait until after the election? And so on and so on.

Those who are urging Congress to "just go slow" often say we should wait to see how the new FERC transmission order and wholesale competition develops before even considering retail competition. It is, first of all, unclear how much benefit small consumers will see from wholesale competition.

In fact, it is becoming increasingly clear that stopping at just wholesale competition actually puts small consumers at risk. Utilities are giving special breaks to their largest customers to keep them as customers -- and residential and small business users that have no option to leave are picking up the tab. If we stop at just wholesale competition -- if we do not give all customers choice -- it will be the smallest consumers will be the ones who are left behind and "stranded."

Those urging Congress to "just go slow" also usually point to the existence of stranded costs as the reason not to do anything. The fact is the every dollar of stranded costs that exists is just one more reason why the system of monopoly regulation has failed consumers and one more reason why we should give consumers choice sooner rather than later.

As I said earlier, the hearings held by the Energy and Power Subcommittee to date have demonstrated that a one-size-fits-all approach to implementing consumer choice is not appropriate and that the details need to be left to the states. However the states decide to resolve the stranded costs problem, the sooner we begin the transition to consumer choice for electricity, the sooner we can get the stranded costs behind us and start realizing substantial gains to the economy and to the average ratepayer's wallet. The very existence of stranded costs is the reason to act now, not a reason to delay.

Once consumers have been given a taste of the benefits available to them in a competitive electricity marketplace, the monopoly which currently holds dominion will cease to exist. Both consumers of electricity and policy makers are beginning to understand the opportunities competition has in store for them. It is my hope that introducing legislation will be the first step in bringing those benefits home to the consumer.

I am also hopeful that introducing my legislation will be the first step toward putting the future of renewable energy generation in this country on a solid competitive footing.

As everyone in this room knows, U.S. renewable energy industries are at a vulnerable stage in their development. During the past two decades, solar, wind, biofuels, geothermal and other renewable energy technologies experienced significant technological advancements, cost

declines and marketplace successes. We are so close, and yet so far, to achieving our goal of making renewable technologies viable and competitive alternatives to traditional fuel sources.

While renewables generation is growing at record rates, the government support that has fostered that growth is increasingly endangered. The Energy Policy Act of 1992 created a five-year plan that authorized funding to help demonstrate and commercialize new renewable technologies. Nevertheless, four years into that authorization, the program has never been adequately funded. Last year's budget nearly cut federal renewables funding in half. In fact, we considered it a great victory that we were able to restore enough funding to end up with only a 30 percent cut. This year, not only are we working hard to safeguard research funding, we are also striving to keep the wind and biomass tax credit, which is also threatened by budgetary pressures.

After last year's budget fight, I decided to form the House Renewable Energy Caucus, in preparation for the inevitable fight this year. From the original seven members, our caucus has already grown to nearly 90 members of both parties representing 38 states. Many observers of Congress note that this caucus has already had a positive impact on what promises to be a difficult appropriations process again this year.

But the fact is that government resources for renewable technologies are scarce, and getting scarcer. Further, relying on the political process to support renewable development is an incredibly inefficient way to allocate those resources that do exist. Who does or does not get government support often depends as much on political connections and lobbying skills as on the merits that really matter most in a marketplace -- which technologies are the most promising, which are the closest to being competitive, and which companies are the best managed.

Renewable energy is too important to the future of this country to leave, year after year, to the uncertainties of the appropriations process and tax politics. Electricity is the cornerstone of our economy. Ensuring the security and diversity of generation resources is a critical but neglected aspect of our overall national security preparedness, not to mention the defense of our environment. But the never-ending uncertainty of government support retards the development of renewable technologies, slows innovations and consumes immense amounts of time and resources in the political process that could be better spent elsewhere.

The free market is the only place where the merits that matter most for the future of renewables development are recognized and rewarded. If our goals are to speed the commercialization of renewable technologies and allow them to compete on an even footing with traditional generation as soon as possible, the future of renewables is with the free market, not the government.

In writing legislation to open the retail generation market to competition, I am committed to ensuring that renewable energy sources have a place in that market. Again, because I am still putting the finishing touches on my bill, I am not prepared to discuss any details today. However, let me say that the objectives of my legislation will be to finally free renewable energy generation from the inefficient, costly and uncertain reliance on government hand outs. I believe that subjecting renewable technologies to the disciplines of the market will reward the most

promising technologies, bring innovations to market faster, and make renewables competitive with traditional fuels years sooner than if they simply continue to rely on government support.

The renewables community should not fear retail customer choice and competition in generation. It presents a unique opportunity for renewables to end their dependence on the government and to flourish in the marketplace. I look forward to working with you as my committee works to bring competition and consumer choice to all electricity customers as soon as possible.

WINDPOWER '96 OPENING SESSION REMARKS

Christine A. Ervin
Assistant Secretary
Energy Efficiency and Renewable Energy

Thank you, Randy.

I'm delighted to join you all this morning for this celebration here in Colorado -- home of great wind resources and home to the great National Renewable Energy Laboratory and National Wind Technology Center. And a special welcome to our many international visitors.

The wind industry is one of our finest success stories. The image of turbines turning against the sky has become a powerful symbol for clean energy around the world. At the same time, we are at a crossroads for determining how quickly we can exploit the promise of our labors together. Over the next couple of days you will be sharing your successes and ideas for moving ahead. But this morning I will focus on our challenges with a special emphasis on the budget debate in the U.S.

I'm also privileged to follow Congressman Schaefer this morning. May I say, sir, that your leadership in the House Renewable Energy Caucus helps restore my confidence that clean energy can once again be bipartisan. Your efforts not only serve Coloradans but the country and beyond. I say that also so you'll know this story I'm about to tell does not refer to you! But it illustrates, I believe, current Congressional thinking about clean energy, energy efficiency and renewable energy.

Picture a time of great turmoil, a time like the French revolution. A guillotine stands in the town square. The executioner drags a doctor up to the guillotine and straps him down. The executioner pulls the lever, but the blade gets stuck and doesn't fall.

- "This is providence," the doctor shouts. "I'm meant to live so that I can continue to heal my patients. You must release me!" The executioner releases him.

- Next comes a lawyer. The executioner straps him to the guillotine and pulls the lever, but it gets stuck again.

- "This is a matter of precedent," the lawyer yells. "You let the doctor go, and you must let me go!" The executioner releases him.

- Next, the executioner drags up a Member of Congress and straps him down. But the blade sticks again. The Congressman turns to the executioner and says, "You know, I could fix that."

Think of the guillotine blade as America's growing addiction to foreign oil, much of it coming from a troubled Persian Gulf. Think of it as the risk of losing many American jobs as we back away from an international market for renewable energy that is heating up fast. Think of it as the enormous environmental damage that can occur as nations undertake unprecedented economic development campaigns, and decide on whether they will use clean technologies or dirty technologies.

Clean energy technologies are the key to keeping that blade from falling. And in many cases, Federal clean energy programs are the catalyst that brings these new technologies into existence, and into the marketplace. But our partnership with this industry and others is seriously being compromised.

I'd like to offer three "no-holds-barred" observations about Congress' attempts to "fix the guillotine."

Observation No. 1: The assault now underway in Congress on Federal clean-energy programs is nothing less than a sneak attack on the environment. (The cuts being imposed on these programs will be just as devastating to the quality of the environment in our nation as attempts last year to roll back major environmental regulations.)

Observation No. 2: Those who argue that the Federal Government has no place in the marketplace -- that the "free market" will take care of the nation's need to develop promising new energy technologies -- are naive. They are operating in an economic fantasy world. And if allowed to shape national policy, their naiveté will make America a second-rate economic power in the next century.

And observation No. 3: Those who say America cannot afford Federal spending on clean energy -- those who argue that these programs must be sacrificed to reduce the Federal budget -- are saying in effect that we cannot afford clean air. We cannot afford good health. We cannot afford new jobs. We cannot afford the kind of America we want to leave for our children.

We all know the historic roller coaster we've taken in the U.S. in support of clean energy. Huge budgets in the early 1980s as we learned the right and wrong ways to forge new technologies. Business plans and investments ventured then swept away with the advent of the Reagan Administration. Difficult rebuilding during the late 1980s with slow, steady progress. And then bipartisan support emerged with the Bush Administration and was reinforced by President Clinton. The future was bright and we were poised for the expanding markets.

And then the new Congress came to town (about the same time as utility restructuring), along with their plans to fix the guillotine aimed at many environmental programs. The public rebelled. Many Republicans objected. The President vetoed. Largely as a result, Speaker Gingrich created a new Environmental Task Force to help moderate environmental reform. To develop a kinder, gentler, stance on the environment. But the Task Force missed what sneaked through in the Interior Bill for efficiency technology -- another 10 percent cut after a 30 percent cut last year. The Appropriations Committee's press release was entitled "take care of the environment." I'll say. But I don't think that's what the public had in mind.

The Energy and Water Appropriations Committee hasn't marked up renewables yet. But we know the House Budget Resolution called for eliminating wind and reducing other renewables once again. We all have hopes for what the Caucus can and will accomplish, but protecting renewables from the deepest of cuts is still a far cry from enthusiastic bipartisan support.

Let me lift the fog from this issue. An attack on clean energy programs is an attack on the environment. Clean energy and a clean environment are inextricably linked.

Here's a little-known fact: The production and use of energy cause more environmental damage than any other economic activity in the world today. And as I mentioned earlier, the problem is growing worse. Many countries are building new energy systems on an unprecedented scale. Unless clean energy technologies are available to them, their economic progress will mean major new pollution on a global scale.

We don't have an energy crisis today like we did in the 1970s. There are no gasoline lines, no cardigan sweaters in the White House. Today's problems are far more subtle, and are far more serious than gas lines. Our energy use is changing the environment in destructive and long-lasting ways -- global climate change, the disappearance of rain forests and the species that occupy them, the dumping of pollutants into our air, water and soil. Our job must be to find and deploy clean new sources of that energy so that our nation and other nations can continue meeting our economic needs without ignoring our environmental needs.

Here's another little-known fact: Most of the Federal Government's research in voluntary pollution prevention technologies is done by the Department of Energy -- most of it right here in the Office of Energy Efficiency and Renewable Energy.

Let's be clear about the consequences of this disinvestment in the environment. When we talk about pollution prevention, we aren't simply talking about making life safe for flora and fauna, although that's critical. It's about our health. Renewable energy can reduce the emissions that contaminate the air we breathe. And overseas, a wind machine, a PV module, or hybrid systems can replace the wood smoke and kerosene fumes that are breathed by young and old alike. Preventing pollution is preventing illness and disease.

About my second observation that concerns the role of the Federal Government in the marketplace, we continue to hear the argument on the Hill and among conservative think tanks that the Federal Government has no business being involved in the so-called "free energy market."

One of the most vocal advocates of this dogma is the Cato Institute. Cato asks: "Why is it that the Department of Energy is so much smarter than every energy company, any energy executive and any long-term, investor?"

The 1997 House Budget Resolution mirrors this unrealistic view of the marketplace. It says, "The Budget Resolution reflects the conviction that the nation's energy problems will be solved by the people and industries of this country . . . not by government spending."

I'd like to respond with a couple of reality statements.

First, let's talk about the idea of the "free market." I believe in the power and the magic of the marketplace as much as anyone. But any student of economics knows that in the real world, the marketplace is filled with subsidies, distortions, uncounted costs and benefits, information gaps and barriers. In the real world, cheapest is not always best. Market forces of the moment don't always look after the nation's long-term security interests. For example, cheap oil may be great for the economy in the short term, but insofar as it encourages us to use more imported oil, it's not necessarily good for national economic security in the long term, or for the balance of trade, or for the quality of our air.

If the marketplace were as infallible and intelligent a source of national leadership as some believe, then we wouldn't need Congress or a White House or a Supreme Court. We wouldn't need governors or mayors or city councils. We wouldn't need conservative think tanks.

The marketplace would make all of our decisions for us. But in reality, it cannot. It is a marvelous force, but it is no substitute for intelligent leadership that protects and helps guide our long-term interests. And that's why I tell economist jokes every chance I get. My very first one goes back many years to Economic 201 class.

- It's about three people stranded on a desert island with nothing but a can of food.

  The physicist said they must find ways to concentrate the solar rays into a beam that would burn through the tin.

  The engineer said they must look for tools that could be used to pry open the can.

  But the economist simply turned to his companions and said: "all things being equal, let us assume we have a can opener."

Well you can assume anything you fancy but it won't change reality.

The market purists make other mistakes too. They forget the Federal Government is the largest consumer in the country. So the purchasing decisions we make can greatly affect markets. Second, they assume that Federal researchers are trying to impose their own judgments on the private sector. And that our efforts are failures.

As you well know, the research we carry out is a partnership with industry. Industry plays a lead role in shaping our business plans, which is why modest Federal dollars leverage so many private dollars. Once again the U.S. is fretting about whether or not the Federal Government should work with industry to create technologies that serve a public good -- something many countries represented here take for granted as good common sense.

As for successes -- the wind industry epitomizes the conundrum clean energy faces. On one hand, critics claim your technologies are failures, not ready for prime time and never will be

anything more than a tiny niche market. On the other, they say wind power is now so successful it can compete on its own without any support.

The reality is that clean energy technologies are winning a disproportionate amount of R&D awards, that our partnerships are relentlessly improving the technology and steadily bringing costs down.

And the wind investments being made around the world testify to how far we've come in just a few years. It's that kind of progress that leads Dutch Royal Shell's strategic planning unit to project that renewable energy will provide 50 percent of the world's energy in 2040 -- a scenario based on a hard, cold analysis of world demand, supply options, environmental drivers and capital markets. But there are many market hurdles yet as wind competes with fossil fuels that dominate markets and boardrooms.

So, the market polarization that the House Budget Resolution speaks of is a myth. The Government certainly can act contrary to the positive influence of market forces, but it need not. It is not the natural enemy of American industry, or American consumers. The Government is an inevitable part of the marketplace, as a consumer, an information provider, and a technology partner with industry.

My third and final observation has to do with the Federal budget deficit. Deficit reduction is a critical national goal. We all realize that. But we must be selective and intelligent in deciding how to reduce Federal spending. It should not be an excuse for cutting into our nation's best investments for the future.

Its difficult to understand just what some Republicans stand for in this budget -- if not more pollution, higher regulatory costs, fewer jobs, and the folly of handing over technologies we helped develop to other countries. But what if they stood for something like this instead. Let me read several principles adopted by a group whose identity you'll have to guess:

- We regard sustainable development, defined as development that meets the needs of the present without compromising the ability of future generations to meet their own needs, as a fundamental aspect of sound business management.

- We believe that sustainable development is best achieved by allowing markets to work within an appropriate framework of cost effective regulations and economic instruments. Government has a leadership role in establishing and enforcing long-term priorities and values.

- We recognize the precautionary principle in that research is needed to reduce uncertainty but cannot eliminate it entirely.

What if <u>that</u> were the platform of the Speaker's new Environmental Task Force? But whose is it? -- some environmental association? university group? liberal think tank? No -- its a statement of environment commitment by nearly 100 insurance companies from 20 different countries.

An industry that is wakening to the fact that unbridled development of traditional energy sources and resulting changes in climate could bankrupt their industry.

And who said: "Sometime, our children will have to pay a carbon pollution cost. That could be a great big number -- it could be bigger than the budget deficit. We think there is a big market out there and we're going for it?" Bob Kelly, Executive Vice President of Enron -- one of the larger natural gas companies in the world -- explaining why they're investing in solar technologies.

These are the ingredients to success for clean energy today:

- Government leadership in looking beyond next year's ledger to the future of our children.
- Private sector vision and leadership in creating the future.
- Innovative ways of channeling the world's financial capital into the bridge for a sustainable future.

For when all is said and done -- we are all responsible. The future doesn't just happen to us. It's a place we create. The wind industry is at the cutting edge of creating a clean, prosperous, future. Now we need to broaden and deepen the strategic alliances that will make it a reality.

WIND ENERGY:
A REVIEW OF TECHNICAL AND MARKET ISSUES

A D Garrad
Garrad Hassan & Partners Ltd, Bristol, UK

Introduction
This paper is divided into three sections: the market, the technology and some more general conclusions.

1. Market

Figure 1 will come as no surprise to most readers. This figure shows the capacity in the European Union and the US. For the time being at least, considerable growth is being maintained within the EU. The figure shows that although the installed capacity in the EU exceeded that in the US in 1994, it took a much longer time to achieve that result. The EU growth has also been much more cautious. The reason for both features is that the EU figures are a geographical average of 12, and now 15, political regimes whereas the US figures are the result of one federal system plus, of course, some local state influence.

Figure 1

Growth of Wind Energy in EU and USA

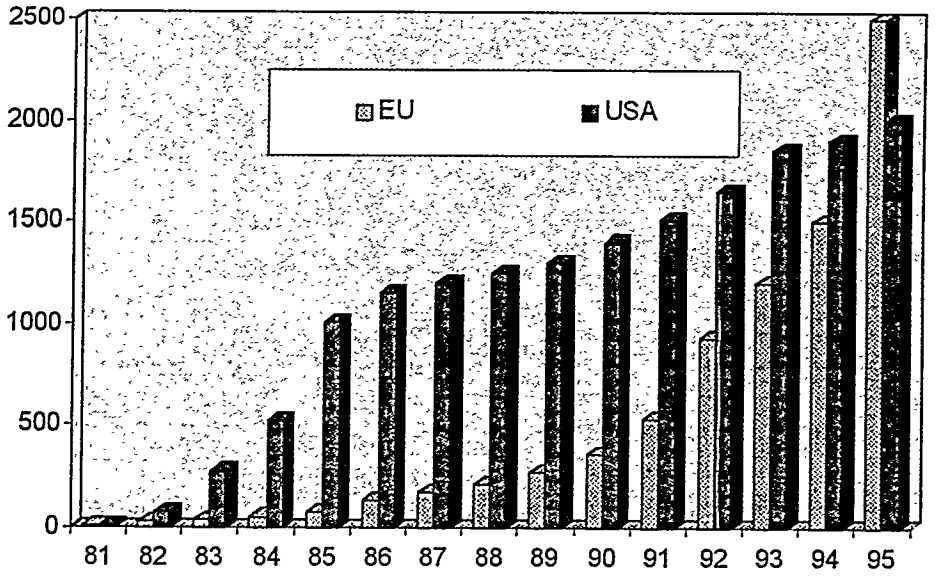

Figure 2 shows the European growth in the context of the goals published by the European Wind Energy Association in their policy document "Time for Action". The major goal was 10% of Europe's electricity from the wind by the year 2030 but some intermediate goals were also introduced, namely 4,000 MW by the year 2000 and about 11,000 MW by the year 2005. Progress towards the first goal has been very good. If present trends continue then the turn of the century goal should be exceeded. The most active market is in the developed world - the "conscience" market. This market is stimulated by a desire to produce clean electricity rather than to produce more electricity to satisfy an increased demand.

There is another rapidly expanding market - the "necessity" market in which wind energy is being used to satisfy a demand for more generating capacity, for example, in India where there is a shortfall of 25% in electrical capacity, in China and Brazil where there are major expansion plans for electricity production from both conventional and traditional forms.

Figure 2

Time for Action Goals
10 % of EU electricity by 2030

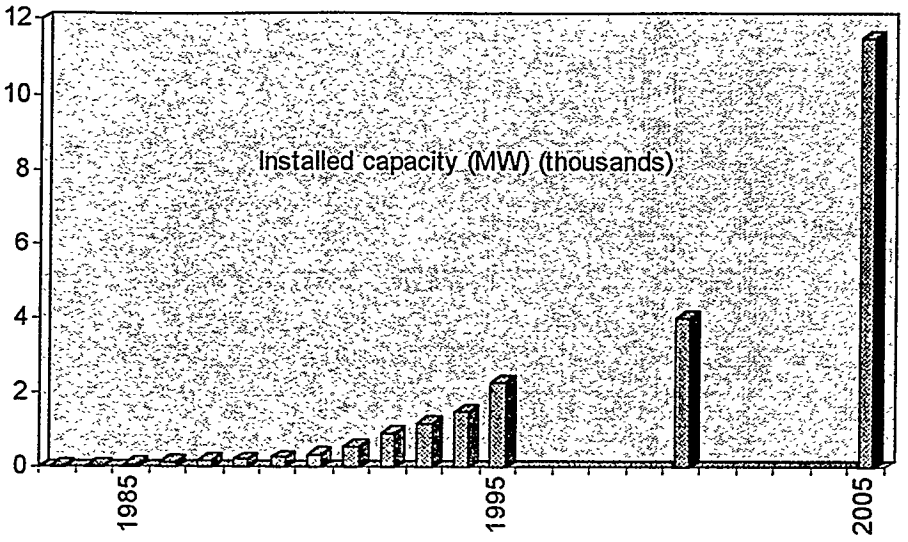

Consider first the conscience market. The apparently healthy growth towards the EWEA goals hides some important barriers in individual countries. These barriers may be considered under three headings. First there is the physical barrier: Is there enough space in which to place the wind turbines and, equally important, is there an electrical grid to make a connection? The second barrier is social. The social barriers have occurred in countries where there has been a rapid growth in wind energy. At the moment, although these barriers are a nuisance, they are probably not of long term significance. However, as the installed capacity grows, public acceptance will eventually prove to be a barrier to further expansion of wind energy in populated areas.

The biggest barrier of all, at least in the early days, is politics. Looking at each country in which there has been significant wind energy activity, that activity can be clearly traced to specific political decisions. Underlying these three barriers is the "economics". Economics, or cost has become increasingly important as some of the other barriers are overcome. Indeed, cost is the central issue as the industry moves out of Europe into other parts of the world. The long term future for wind energy depends crucially on its cost relative to conventional energy.

In the present markets the barriers have been overcome by market incentives. This statement appears surprisingly simple , almost trite, but experience suggests that it really is pretty simple. It is clear that where market incentives have been put in place there has been substantial and almost immediate growth, and where they have not existed there has been none. The details of a market incentive are crucial. Although the general intention may be well defined there have been a number of examples where the voracity of the incentive itself has been undermined by the details of the legislation. For example, access to the grid has been highly contentious in Germany, Denmark and in the UK. The wisdom of capital incentives rather than premium energy prices needs careful examination. The experience in the early days of California was that capital incentives could cause the market to overheat and tended to place inadequate emphasis on the good operation and efficient maintenance of the machines.

The role of the utility is also crucial. There is a growing move towards privatisation of many utilities, most advanced in the UK but also elsewhere in Europe. As these new look utilities emerge, it may well be that they play a different role in the promotion of renewable energy, and in wind energy in particular. Instead of being merely political tools, if devices are put in place which allow them to make money out of renewable energy then they may well play a more positive and supportive role than they do at present. There are, of course, some examples of public utilities which have been supportive, but by and large these are not responsible for some of the

windiest areas of Europe. Spotting the friendly utility is, therefore, an important part of expanding the market for wind energy. Even more important is making hostile utilities friendly. This is a demanding task!

In Figure 3, which is rather contentious, the characteristics of the different European Union countries are assessed under several different headings, some of which have already been itemised above. The physical assessment is self-explanatory. Under the political heading, there is either a "✓" or a "x" except in the case of Germany which has been particularly positive politically. Under the "Utility" heading is an attempt to sum up the perception of the utility attitudes in the different countries. Again, this is highly contentious but, to the author's knowledge, reasonably accurate. Finally, an attempt has been made to assess the level of activity in each country. The most active country at present is most definitely Germany. This is something of an irony since it is the only European Union country which is unable, in ideal terms, to produce all of its electricity from the wind. Nevertheless, because of the firm political support which is presently available, it is by far the most active country. This demonstrates the important point that, at this stage at least, political support is by far the most important characteristic for the development of wind energy.

Figure 3

	The Important Ingredients				
	Physical	*Social*	*Political*	*Utility*	*Activity*
DK	✓✓	x	✓	✓	✓
NL	✓x	✓	✓	✓	x
S	✓✓	✓	✓	x	✓
UK	✓✓✓	x	✓	✓	✓
H	✓✓	✓	x	x	x
ES	✓✓	✓	✓	✓	✓
EI	✓✓✓	✓	✓	x	✓
D	x	✓	✓✓	x	✓✓✓
F	✓✓	✓	x	x	x
B	x	?	x	x	x
L	x	?	x	x	x
I	✓	?	x	✓	x
P	✓✓	?	x	✓	x
US	✓✓✓	✓	x	-	x
INDIA	✓✓	✓✓	✓✓	✓	✓✓✓

To this discussion of the European scene, the US and India have been added. Little activity is shown in the US since the political climate is positively discouraging whereas in India there is a strong political will to support wind energy.

The same theme is illustrated in a slightly different way in the next figure, Figure 4. The installed capacity in each of the European Union countries and also the amount of the capacity that has been added this year are shown. In the case of Germany and India the capacity added in the first quarter is also shown. In both cases, although figures are not yet available, the capacity in the second quarter of 1996 will be substantially smaller. This clearly shows that major growth has taken place in Germany and India - the two most politically positive countries.

Figure 4

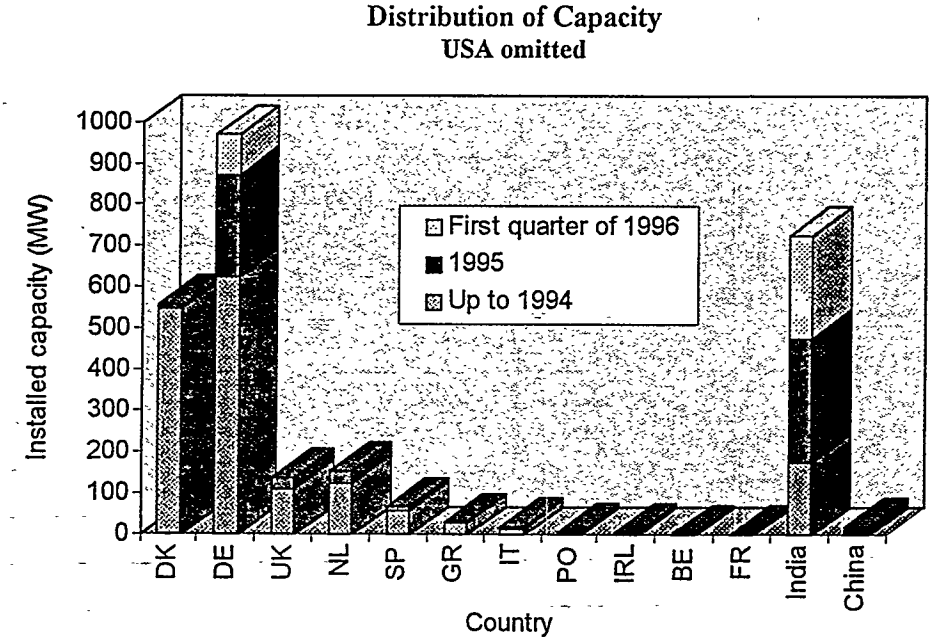

So, where is the growth now? Although Europe is still very much involved, there is major activity in India, and shortly to take place in Central and South America; there is also activity in Egypt, China and New Zealand. This trend away from European developments, although the technology may well stay in Europe, is going to be a feature of the next ten years or so. The present obsession with utility restructuring in the US makes it is difficult to envisage any major activity there, nevertheless it seems impossible that a more active market will not emerge over the next few years.

To go one stage further an attempt has been made to indicate how the market may develop over the next five years in three different sectors, in Europe, on the American continent and elsewhere in the world - see Figure 5. The annual installations in Europe will grow a little bit over the next five years or so, and then flatten off and perhaps later on even decline a little. We may expect to see the market on the American Continent to start to grow gently over the next few years and then continue to grow steadily. The growth is also expected to continue elsewhere in the world and by the turn of the century, we may expect the annual market outside Europe and the United States to exceed either of those two individual markets. This chart is the integral result of a much more detailed nation by nation study.

Figure 5

Market forecast - Capacity required per annum

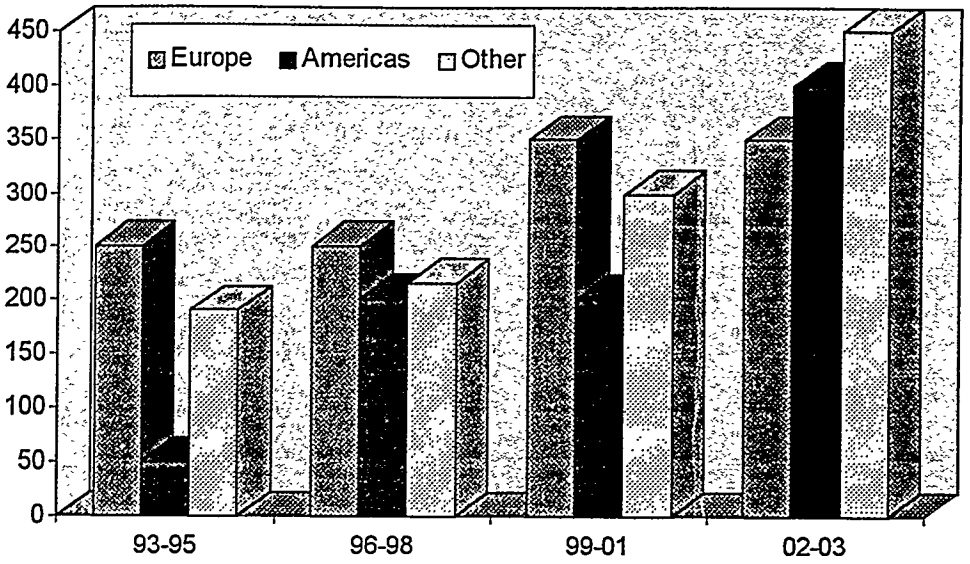

2. Technology

It would be wrong to write such an overview without any mention of technology. There is still a terrific lack of consensus about the basic parameters of the optimum machine. There is, perhaps, one exception to that rule which is variable speed, which seems to have been chosen by the vast majority of people developing large machines. Figure 6 presents the proportion of commercial machines which fall into different "concept categories". This demonstrates that the "3-bladed DK stall" regulated approach still dominates. The labels on this graph are rather coy. The "3-bladed US var speed" is, of course, Kenetech and hence this market share will reduce for 1996. "3-Bladed gearless" is Enercon and fixed speed, "3-bladed DK pitch" is Vestas. Gearboxes, aerofoils and other components are still receiving much attention, but by far the most popular area for development at present are variable speed and direct drive systems. Perhaps the most important underlying trend is the effort on mass reduction, which goes hand in hand with mass production.

Figure 6

Wind turbine concepts

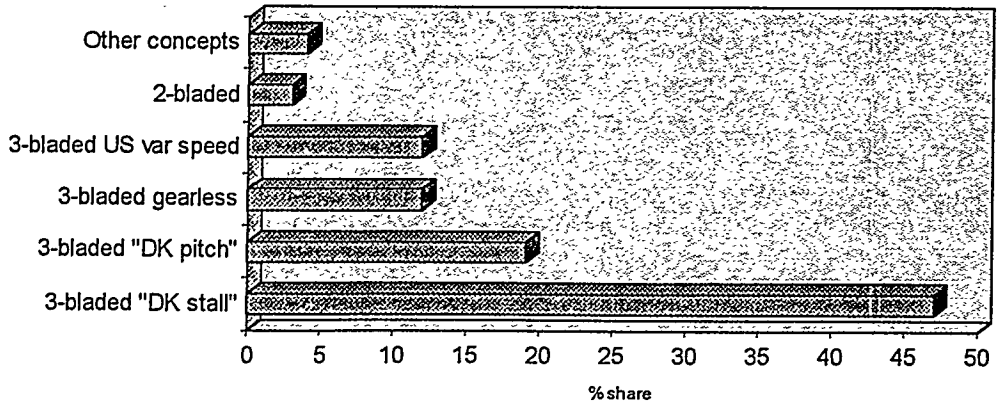

Figure 7 attempts to show the effect of mass reduction. The range of specific masses for the old big machines, the WEGA1 machines, back in the eighties, is shown together with those for the WEGA2 machines. There is a clear downward trend. The specific mass of a typical commercial Danish machine - a 300 kW variety rather than the 500 kW - which are now standard used in increasing numbers, and also the specific mass of the Carter 300kW machine, which is roughly half that of its Danish counterpart, are also shown. The trend for the bigger machines is certainly downwards towards the existing commercial or Danish style, but there may well still be quite a substantial quantum leap to be made between the typical European machines and the more lightweight American style.

Figure 7

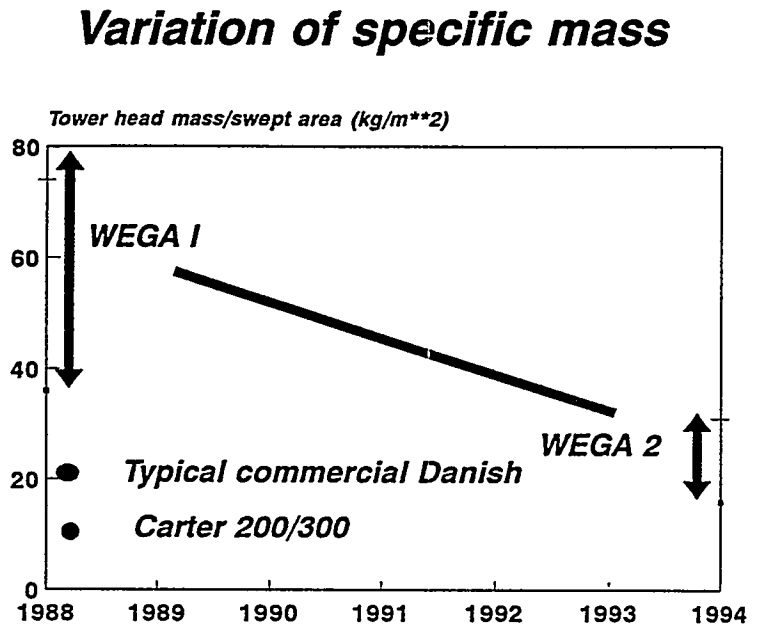

Garrad Hassan has recently undertaken a very detailed study, both computational and experimental, of the Carter machine, and some example results are shown in Figure 8. This figure shows very clearly how the flexibility of this machine has a marked effect on the loads. Only the steady loads are shown in this figure. The dynamic loads may be deduced from the slope of the curves. The flexibility of this machine reduces the loads by almost an order of magnitude.

Figure 8

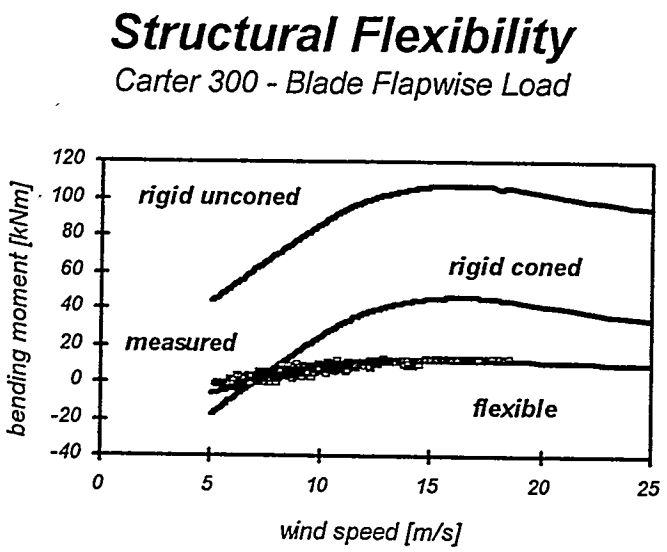

It is interesting to look at the machine trends in the commercial field. In Figure 9 some data for Vestas machines are presented. The figure shows their commercial range of machines from the 80's until the present day: from the small 60 kW machines up to the 1.5 MW machine which was launched this year.

Figure 9

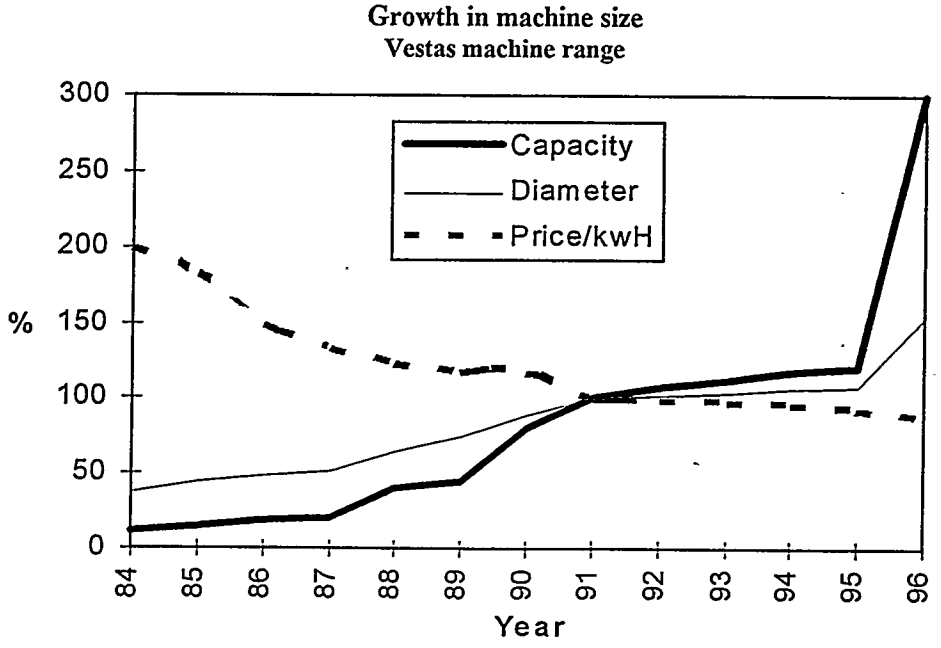

The price curve shown in this graph suggests that there is a levelling off of the price achievable from this type of technology and further major reductions in the price can only be achieved by very high volume or through a major change in design philosophy. It should be noted that these numbers have simply been reproduced from data published by Vestas.

Indigenous manufacture is already an important consideration for the industry, and as developing world markets grow its importance will increase. Wind energy is particularly well suited to such an approach. Figure 10 shows the financial value of components used on typical Danish machines. It is clear from this chart that much of the effort is the assembly of imported parts many of which could be supplied by local companies.

Figure 10

Country of origin of turbine components for a typical Danish machine by value

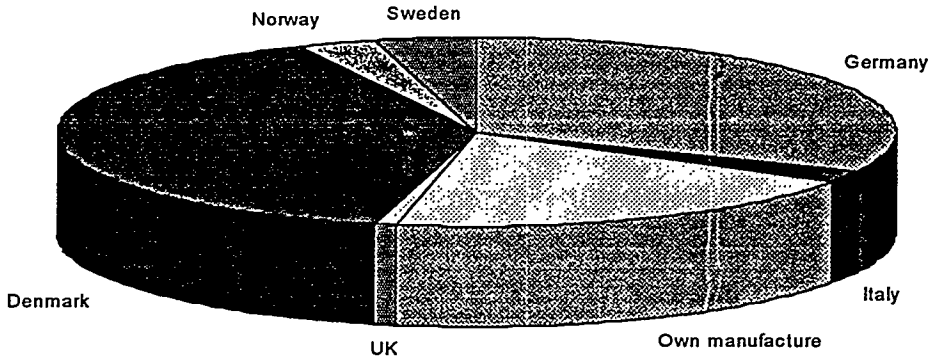

3. Overview

In the final figure, Figure 11, an attempt has been made to bring together all the issues which have been discussed in this paper. The result is a very complicated chart but one which shows a lot of the characteristics of wind energy over the last decade throughout the world. The left hand ordinate is installed capacity with no particular units, the x-axis is time. Consider first the two market routes: the straight line towards the bottom labelled "utility route" and the line with various plateaux on it. In plotting this line, an analysis has been made of past events and also some conjectures made about what may happen in the future.

Figure 11

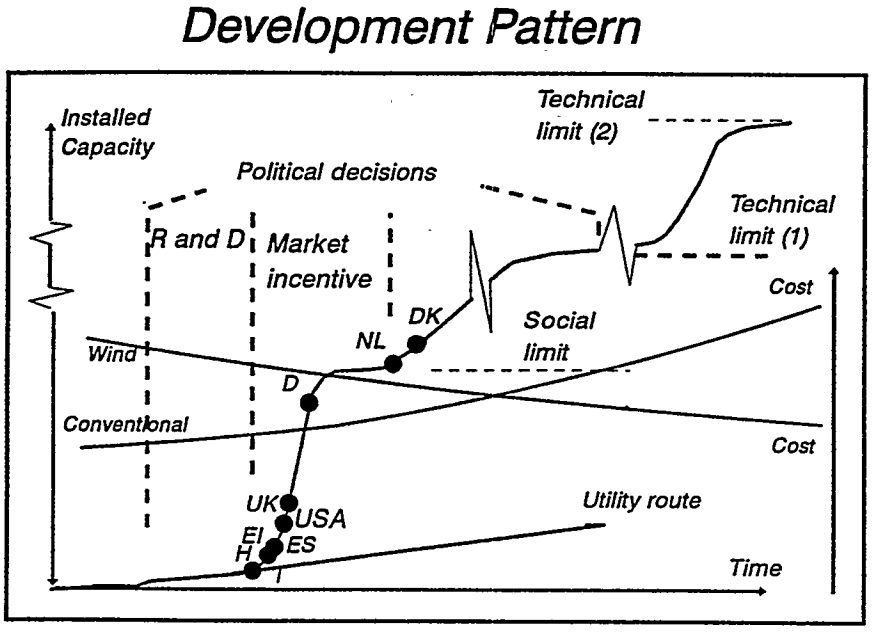

At the extreme left there is no activity. Then a decision is taken, labelled a "political decision" on this chart to initiate some research and development on wind energy. A little growth then takes place but nothing significant. A further political decision is taken to introduce a market incentive and then there is dramatic growth, which is followed by some public reaction labelled here "social limit". This social limit is the general public saying that they are not happy with the rate of growth of wind energy and they wish to slow it down for further consideration. Further growth then takes place only if a further political decision is taken to the effect that, despite the fact that there may be some public opposition to this type of electricity generation, there is sufficient benefit from it to promote its use. The growth under these circumstances is rather more gentle and eventually limited by access to the grid in windy parts of that country. This limit has been labelled "the first technical limit". To develop wind energy beyond this point will require major investment in the infrastructure, and in particular major grid reinforcement. That is only likely to take place as a result of another political decision or as a result of the cost of wind energy becoming cheaper than the cost of electricity generated by more conventional forms. In the context of this last comment, it is necessary to look at the two graphs labelled "conventional" and "wind" which are intended to show costs plotted to an arbitrary scale. This simply shows that, as wind energy starts to develop, its cost decreases but remains above that of conventional sources until at some point the two curves cross. It has been assumed that conventional sources of electricity will tend to become more expensive whereas wind energy will become cheaper.

Eventually the growth will reach a second technical limit which is a very high installed capacity indeed - 10-20% of the European Union electrical capacity. At this point it may prove difficult for the high tension grid to organise and absorb an increase in wind energy capacity.

The other market route, labelled "utility route", describes growth without a market incentive. Some countries have followed this and have tended to produce extremely slow growth. Having examined, in general terms, the significance of the curves, each active country has been placed on the curve at an appropriate point. There are many clustered around the bottom, there are some moving up the market incentive growth line, in particular the UK, Spain and Germany which is placed quite high up approaching the social limit. Both Denmark and the Netherlands have been placed beyond the social limit. In these two countries there have been periods of very little growth, largely been due to the public reaction to the introduction of wind turbines. Nevertheless, as a result of exactly the type of political decisions which were discussed earlier, growth is now taking place again. It is clearly difficult to place these individual countries accurately on this graph but it does nevertheless appear that there is a pattern which is being followed in most countries.

In this talk a "snapshot" of the present situation, a look into the future, and finally an attempt to summarise the different trends, characteristics and future for wind energy within the European Union and, to some degree, the rest of the world have been presented.

INTERNATIONAL WIND FARM MARKETS: AN OVERVIEW

Kevin Rackstraw
American Wind Energy Association
122 C St., NW
Washington, DC 20001
USA

ABSTRACT

More wind energy capacity was installed in 1995 than in any previous year. Two markets, Germany and India, accounted for nearly two-thirds of those installations, while the largest single market in the world historically, the US, ground nearly to a halt. Market supports in Germany and India, however, are vulnerable to political forces largely beyond the control of the wind industry. This paper examines the growth of international wind farm markets worldwide and notes that future markets will be more broadly based, leaving the industry less vulnerable to political changes. The paper also concludes that an additional 18,500 MW could be installed by the year 2005 even without assuming a dire ecological scenario that would create environmental drivers to accelerate wind market growth.

INTRODUCTION

The great irony of 1995, the year that the wind industry enjoyed over 35% growth world-wide, is that firms in the wind industry continue to struggle. The news for 1995 was decidedly uneven, with some markets slowing drastically while others flourished (see Figures 1 and 2). The US market was particularly hard hit by dramatic changes in the power sector. While many projections[1] for 1996 and beyond, including this one, are optimistic about the prospects for growth of the wind industry, the market dynamics upon which the 1995 installations were built are quite narrow (more than two-thirds of the 1995 installations were in two countries, Germany and India) and therefore unstable, as shown by the decline of the US market in 1994 and 1995. An interesting, and very positive, development contained in most projections through 2005 is the fact that growth is expected to be spread among many more markets, making the industry less vulnerable to changes in major markets (see Figure 3).

[1] Two independent but similar projections were conducted in mid-1995 for Nordtank Energy Group by Garrad Hassan & Partners and BTM Consult, two leading European wind energy consulting firms.

AWEA, as well as other organizations such as the World Energy Council (see Figure 4), anticipates over 18,500 new MW of wind energy to be installed by the year 2005, representing a market of over $18 billion. Even with allowances for much slower growth in Germany, Western Europe should continue to lead the world in new installations, barring significant political changes that would threaten the generous wind market support structure that is now in place. The Americas as a whole should not be far behind as the US market recovers in 1997 and then expands rapidly after the year 2000. The Asian market should continue to expand rapidly but is highly dependent on India, which is driven by tax incentives and uncertain politics, and the People's Republic of China, whose wind market may be constrained by its difficulty in providing a stable, acceptable investment and trade environment. One of the key questions regarding China is how much of that market over time will be open to foreign vendors, since the Chinese are keenly interested in developing their own industry.

Salient results of AWEA's projections are the following:

- projections for new wind installations from 1996 through the year 2000: over 7,500 MW
  2005: over 18,500 MW
- regional projections for new wind installations by 2005:
  - . Western Europe: 7,250 MW
  - . Asia: 4,685 MW
  - . US and Canada: 3,315 MW
  - . Latin America/Caribbean: 2,161 MW
  - . Other: 1,470 MW
- by the year 2005, as many as 29 countries would have at least 50 MW installed by the year 2005, representing at least 22 new countries compared to today.

REGIONAL INSTALLATIONS BY 2005

Western Europe

Western Europe will continue to dominate new installations for the next several years. In countries such as Denmark and the Netherlands, growth is likely to be somewhat slower in 1996 than in 1995. This is due largely to uncertainties of government and utility support. For example, changes in Danish law regarding cooperative or individual ownership of turbines will make it more difficult in 1996 to find sites and get hardware in the ground. Because of high population density and scarcity of land, some public opposition on the issue of siting wind turbines is springing up in many parts of Europe. Fortunately, this is unlikely to cause a major drop in expected installations.

Spain and Greece are the two new markets that could see strong growth in 1996 and even stronger growth in 1997 and beyond. France has recently announced its intentions to join the wind race, although it will take several years to get significant projects in place. Italy seems poised to get into the action as well, given strong new incentives recently put into place, and a significant amount of wind installations should occur within the next few years.

The next several years in the UK should be very strong years as the recent Non-Fossil Fuel Obligation (NFFO) projects are implemented, but after that there is quite a bit of uncertainty about the future of incentives (or at least a fair playing field) for wind projects under deregulation.

Germany was the leading market for wind energy in 1995 with close to 500 MW of newly installed capacity. The entire industry will once again look to Germany's favorable pricing structure and continue to install new wind capacity in '96 at a rate comparable to 1995 levels. However, momentum in the German wind market has probably crested as growing resistance from utilities to the current pricing structure builds and some public opposition to siting of wind farms emerges.

The Americas

The US market will continue to stagnate in 1996 as restructuring sweeps across the country. Several of the projects that were left standing after the cancellation of hundreds of MW of wind projects under the Biennial Resource Plan Update (BRPU) have been delayed by politics or legal entanglements. Entry of new projects in the pipeline will slow to a trickle until more clarity is brought to the restructuring process. Adoption of AWEA's portfolio standard proposal (requiring all generators to include a percentage of renewables in their portfolio and making that percentage a tradable commodity such as with emissions credits) would put the wind industry back on track, but it is much too early in the process to predict outcomes and relief would not likely come until at least 1998.

The near-term outlook northward in Canada doesn't fare too well either. While Canada has made the positive steps of passing a tax measure that could accelerate wind development, and created some momentum toward a federal "green power" purchase mandate, virtually nothing is likely to be built in Canada in 1996 and possibly in 1997 as well other than the occasional wind turbines purchased by individuals or remote communities. A strong market for very small wind farm projects to supplement remote diesel power systems should finally develop in Canada within the next several years.

One area where AWEA is more optimistic than other recent projections is in the Americas outside of the US, despite the fact that no countries in the region are moving toward a heavily subsidized and/or heavily tax favored support system for wind such as in Germany or India. Already, one of the three 20 MW Costa Rican wind projects began operation in May of this year, while the other two are expected to move ahead later this year and in 1997.

Several more projects in Mexico and Central and South America are likely to follow in rapid succession as countries move to diversify their sources of energy away from reliance on hydro. Honduras and Guatemala are very interested in developing small to moderate sized projects in the near future, while Nicaragua and Panama might follow suit within several years. Brazil, Mexico, Argentina, Chile and Peru are potential candidates for larger developments. It appears that Mexico may not significantly delay its plans for an additional 27 MW in the next year, despite its shaky economy.

Argentina is a big question mark. While there is a phenomenal wind resource in certain areas of the country, the price of electricity on the spot market is around 3 cents. This is not very attractive for doing wind projects even given 10-12 m/s winds that can be found in a number of locations in Argentina. Privatization in Argentina, which has moved far and fast in the last 2-3 years, has meant existing generation assets were sold off at significant discounts. Little greenfield activity has occurred until recently because new projects are competing against fully depreciated, cheap generation assets, and no long-term market has been allowed to develop. The energy market is completely driven by the spot market. Those projects that are going to be built in 1996 and 1997 are essentially merchant plants selling on the spot market.

Brazilian utilities are especially keen on wind energy as they push the limits of exploiting their hydro capacity. Brazilian plans are far more ambitious than AWEA has projected, and if inflation is kept under control there, Brazil could be a significant market for wind companies within several years.

Asia

India will continue to be one of the top two markets in 1996 and could overtake Germany in terms of installations in 1996 or, more likely, in 1997. Investment tax incentives have been primarily responsible for the growth of India's wind energy market. India will likely begin moving away from an investment tax credit toward a production type tax credit by 1997, and issues regarding grid integration and financial stability of the Indian electric sector are likely to slow things as well by about 1998.

Future developers should note however, that despite the booming Indian market, politics in India, specifically the volatile brand of nationalism that has bedeviled other foreign projects in India, could rear its head and throw wind development into a tailspin. A backlash against wind (in the form of a withdrawal or major reduction of tax benefits) could develop if significant numbers of projects go bad or poor business practices are publicized.

China is an emerging potential market being eyed with tremendous interest by wind firms, but significant development there will be difficult to achieve anytime soon. First, China will rely heavily on tied aid to build initial projects, with more commercial projects staying in the slow lane for some time to come. US firms will struggle to match the tied aid that European competitors are likely to bring to bear on China. Second, doing business in China is complex and risky. Primary issues include foreign exchange availability for direct investments, contract sanctity, proprietary technology protection, bureaucracy and corruption. Third is the plethora of inevitable trade and political disputes between China and the rest of the world as it lumbers onto the world economic stage and reabsorbs Hong Kong. These issues will only make it more difficult for companies in the wind industry, which typically have limited resources, to pursue a market which requires patience and stamina.

Despite the formidable road ahead for China, the government is taking steps to encourage renewable energy development. China has a very ambitious goal of 1000 MW of wind energy by 2000. While that goal seems to be overly optimistic, it is reasonable that 500 to 600 MW can be developed by that time.

Another Asian market of interest could be the Philippines. The Philippines government has made significant efforts to attract foreign wind projects but very little has yet happened. The government was solidly behind an effort to develop geothermal resources and that led to an extremely attractive package of incentives and support (primarily building transmission lines and absorption of risks that industry did not want to take) by the government that led to the development of a major market for geothermal companies. While the Philippines government wants to absorb fewer risks in the case of wind, the environment is still relatively attractive, and some moderate-sized projects are likely to move forward within the next five years.

Indonesia and Vietnam are relative unknowns at this point. These two markets are unlikely to develop anytime soon into major wind farms markets, but significant markets for small wind farms or village systems to displace diesel use could develop within the next five years.

SUMMARY

The overall picture for wind technology utilization worldwide is quite encouraging. By the year 2005, AWEA projects that installed wind capacity will be more evenly dispersed throughout the world. This trend toward broadening of the number of markets where wind farms will be built over the next 10 years will generally be positive for market stability. Industry members will need to adjust their marketing and financing efforts to meet the needs of a variety of different markets. Western Europe should continue to be the largest market for wind on a regional basis, although the trend toward protection of home markets for the benefit of European firms may make it more difficult for US firms to compete in some of those markets.

Given the prevalence of government support for the development of national wind industries, both in terms of direct subsidization of firms through research and development budgets and in terms of subsidized export credits (often disguised as development aid), there will be continued pressure on the profitability of wind firms from the US, where subsidized support is dwindling and competitive export credits are difficult to find. This difficult financial environment for US firms is ironic at a time when wind markets worldwide are growing at a record pace.

Figure 1

1995 Additions (MW)

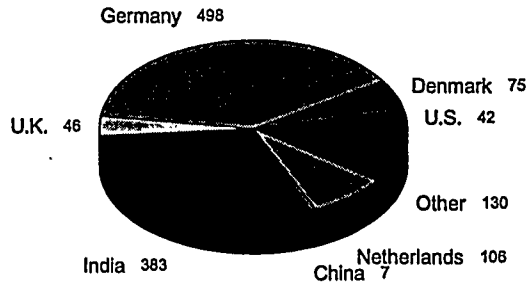

Figure 2

'95 Total Installed Capacity (MW)

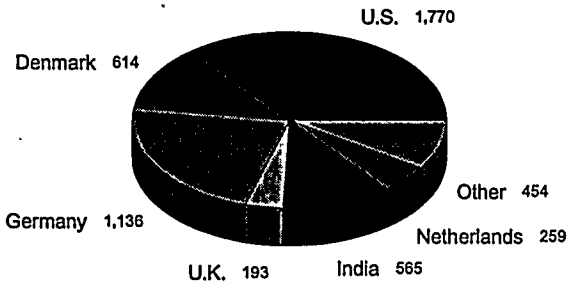

Figure 3

Countries Predicted To Have More Than 50 MW of Wind Energy By 2005

1. United States
2. Canada
3. Denmark
4. Netherlands
5. Germany
6. United Kingdom
7. Italy
8. Greece
9. Spain
10. Portugal
11. Ireland
12. Sweden
13. France
14. Mexico
15. Brazil
16. Argentina
17. Chile
18. Costa Rica
19. Honduras
20. Guatamala
21. Peru
22. China
23. India
24. Philippines
25. Japan
26. New Zealand
27. Australia
28. Morocco
29. Egypt

Figure 4

AWEA's Projections Compared With WEC's Projections: 1996 - 2005 (MW)

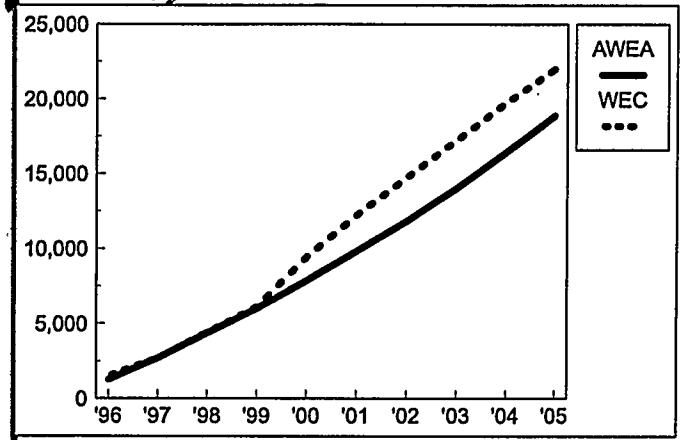

View on world Market

By: Johannes Poulsen
Vestas Wind Systems A/S
DK 6940 Lem, Denmark

I wish to thank AWEA for this opportunity to present my view on the world market for wind power.

Need of energy:
There is general agreement that on a world wide basis we will face a growing need of energy in the future. The International Energy Agency estimate an increase in world wide energy comsumption of 50% over the next 15 years. This together with replacement of worn out power plants during the same period means -as I see it- a need of all available energy sources to meet the demand.

Increased pollution:
As the majority of this addition to generating capacity is anticipated to be based on fossil fuel the consequence will be a dramatic increase in pollution and CO_2 emision and potential damage to the environment. It is therefor reasonable to believe that clean and renewable energy sources will be given increased attention during the period and possibly even a priority.

Wind power is clean and cheap:
Wind power is one of the cleanest energy sources available and one of the cheapest. Already to-day wind generated energy can compete with energy from new coal fired power plants, not to mention nuclear power plants which cost as much to dismantle as wind power plants cost to establish. As I understand it only existing hydro power plants and maybe -in the short term- also gas fired power plants established close to the source of gas produce cheaper energy than wind power plants. The only weakness or limitation by using wind power is the lack of guaranteed capacity. Obvious combinations in the short term would therefor be wind/hydro and wind/gas installations. In a longer term vision I believe wind/hydrogen installations will become economically feasible, especially if one takes the increasing need of clean water into consideration; but some R&D and full scale testing is still needed.

Enormous potential for wind power:
As a logical consequence of the above mentioned I see a huge world wide potential for wind power plants. The fuel is for free and unlimited, wind power plants are competitive with most other sources of energy, they do not harm the environment, they can be built using local labour, they can be built quicker than most other power plants and they can usually be placed close to the point of consumption.

Rapid growth in the wind industry:
Actual growth in installed wind power plant capacity in 1995 was approx. 80% compared to the previous year and total installed new capacity reached 1400 MW in 1995. These are record figures in the wind industry but still only a tiny drop in the sea of potential.

Obstacles for more rapid expansion:
Why is it then that the activity in the wind industry is not even higher that what we have seen last year?

First of all I must admit that I have obviously not yet succeeded and the wind industry has not yet succeeded in getting through with the message; but having said this I believe the responsibility lies mainly with politicians especially those active in countries with sufficient short term generating capacity, as politicians are the ones to make decisions regarding long term environmental issues. This cannot be left to utilities or individuals to do, as they -as per their nature- are short term profit oriented.

Fortunately we see more and more countries making programmes to support the use of environmentally friendly energy sources such as wind energy. In most EU countries such programmes exist and the growth in the wind industry is therefor to be found in the EU in spite of the fact that many utilities use more ressources to oppose such programmes than to support them.

We hear more about a handful of birds being killed by wind turbines than about accidents killing or injuring human beings by coal mining. We always hear about ratepayers money being used (unreasonably) and at the same time we know that ratepayers generally accept to pay more for and are in favour of environmentally friendly energy.

We need somehow to have this negative utility approach turned into a positive approach. This can probably only be done by putting a price tag on pollution. As long as pollution is for free one cannot expect utility- and financial people to do much to avoid it as the only argument they seem to understand is short term profit.

Therefor politicians are left alone to make the necessary long term decisions and they only seem to have two options (i) either to tax pollution or to force utilities by quotas for clean energy. I guess a lot can be learned from the EU in this respect. Most countries in the EU have to-day established programmes for wind power plants.

If it is just left to individuals to decide -for instance in the form of green pricing- it will be a slow process. You cannot expect individuals to take responsibility for the future of the society. That is what we have elected politician to do on our behalf. But it takes that politicians understand the issue and are prepared to take the responsibility and to make the necessary decisions.

Where will the development happen?
In spite of the obstacles mentioned I believe the future is generally bright for the wind industry.

In markets with an immediate demand for additional capacity wind power plants should be an obvious choice as they (i) can be built quicker than most other power plants, (ii) in small scale can be added on to existing relatively weak distribution grids and actually improve stability and therefor save investment in distribution grids, (iii) are competitive with most other power plants, (iv) can be built locally and therefor have a positive effect on unemployment and trade balance and (v) are not hurting environment.

I therefor expect to see a continued rapid development in countries in need of new capacity such as for instance India and China including the development of strong local manufacturing entities.

In countries with sufficient generating capacity a similar development may be seen; but only if strongly supported by political decisions to protect the environment. Examples are plenty but mainly inside the EU.

In countries with sufficient generating capacity and no political decisions to protect future environment the development will be slower and will in the worst case not happen until the effects of pollution and CO_2 emission becomes more visibel. Examples are plenty, but one obvious one is USA.

Summary:
I see a huge potential market for wind power as I am convinced that wind power is already to-day long term competitive.
Actual markets will be found in countries with demand for new capacity and countries with firm political decisions to protect environment. Short term profit oriented countries will need more time.
More and more countries make firm political decisions to protect environment and consequently I expect the world market for wind power plants to grow some 20-40% per year for the next several years.

Finally I wish to thank you for your patience and to underline that if someone should feel offended by what I have said it has certainly not been the intention.

WIND POWER SOARS

Christopher Flavin
Worldwatch Institute
1776 Massachusetts Avenue, N.W.
Washington, D.C. 20036

Wind power is now the world's fastest growing energy source. Global wind power generating capacity rose to 4,900 megawatts at the end of 1995, up from 3,680 megawatts a year earlier.[1] (See Figure 1.) Since 1990, total installed wind power capacity has risen by 150 percent, representing an annual growth rate of 20 percent.[2] By contrast, nuclear power is growing at a rate of less than 1 percent per year, while world coal combustion has not grown at all in the nineties.

If the world's roughly 25,000 wind turbines were spinning simultaneously, they could light 122 million 40-watt light bulbs or power over a million suburban homes. In the windy north German state of Schleswig-Holstein, wind power already provides 8 percent of the state's electricity.

Although it still generates less than 1 percent of the world's electricity, the rapid growth and steady technological advance of wind power suggest that it could become an important energy source for many nations within the next decade. The computer industry has demonstrated the potentially powerful impact of double digit growth rates. The fact that personal computers provided less than 1 percent of world computing power in 1980 did not prevent them--a decade later--from dominating the industry, and changing the very nature of work.

Wind power is being propelled largely by its environmental advantages. Unlike coal-fired power plants, the leading source of electricity today, wind power produces no health-damaging air pollution or acid rain. Nor does it produce carbon dioxide--the leading greenhouse gas now destabilizing the world's atmosphere.

In many regions, wind power is now competitive with new fossil fuel-fired power plants. At an average wind speed of 6 meters per second (13 miles per hour) wind power now costs 5-7 cents per kilowatt-hour, similar or slightly lower than the range for new coal plants. As wind turbines are further improved, with more aerodynamic and lighter blades as well as better control systems, and as they are produced in greater quantity costs could fall even further, making wind power one of the world's most economical electricity sources.

The modern wind power industry has its roots in Denmark and California in the early eighties. Spurred by government research funds, generous tax incentives, and guaranteed access to the electricity grids, a sizable wind industry was created. However, wind power development slowed dramatically at the end of the decade as government tax incentives were withdrawn and utilities became more resistant to higher-cost electricity.

Even as political support for wind power waned in the late eighties, the technology continued to mature. Many of the small wind turbines installed in the early days were expensive and unreliable, but the lessons learned from those first generation turbines were soon translated into new and improved models. The turbines that entered the market in the early nineties incorporated advanced synthetic materials, sophisticated electronic controls, and the latest in aerodynamic designs.

In the effort to make wind power more economical, most companies have built larger and larger turbines. In Germany, the average turbine installed in 1995 had a capacity of 480 kilowatts, up from 370 kilowatts in 1994 and 180 kilowatts in 1992.[12] Several manufacturers will soon introduce machines that can generate between 1,000 and 1,500 kilowatts--with blade spans as great as 65 meters.[13]

The 1,290 megawatts of wind generating capacity added in 1995 was almost double the capacity added a year earlier, and up sixfold from the 1990 figure.[6] (See Figure 3.) In 1995, the country with the most new wind capacity was again Germany, which added 505 megawatts, the most any country has ever installed in a single year.[7] India added 375 megawatts to easily take the number two position.[8] Next in line was Denmark with 98 new megawatts, followed by the Netherlands with 95 and Spain with 58.[9]

The European wind industry is now growing at an explosive pace: Altogether, Europe had 2,500 megawatts of wind power capacity at the end of 1995, up nearly threefold from 860 megawatts in 1992.[4] (See Figure 2.) In national terms, the United States still leads the world with 1,650 megawatts of wind power capacity in place at the end of 1995, but Germany is closing in fast with 1,130 megawatts. Denmark was third with 610 megawatts, and India fourth at 580 megawatts.[3]

Europe is now home to most of the world's leading wind power companies, which are introducing larger and more cost-effective models. Unlike the United States, where most wind power development has consisted of large groups of 20–100 turbines, called "wind farms," Denmark and Germany have pursued a decentralized approach to wind power development. Most of their wind machines are installed one or two at a time, across the rural landscape. This has made them popular with local communities, which benefit from the revenues and jobs that result.[14]

Europe's leadership also stems from the financial incentives and high purchase prices established for renewable energy in response to concern about the atmospheric pollution caused by fossil-fuel-fired power plants. In Germany, this approach has allowed determined investors and environmental advocates to beat back efforts by the electric utilities to reverse the 1991 "electricity in-feed law," which provides a generous price of about 11¢ per kilowatt-hour to electricity generators relying on solar, wind, and biomass energy. In a landmark vote in 1995, the Bundestag decided to uphold the law, though it remains under review by the courts.[15]

Wind energy is also advancing rapidly in the Netherlands, Spain, and the United Kingdom. The U.K. has Europe's largest wind power potential, and hundreds of megawatts of projects

are now being planned. European wind industry leaders are also hopeful that sizable wind power markets could soon emerge in Finland, Greece, Ireland, and Sweden, each of which has a large wind resource. Even France, the last bastion of the European nuclear industry embarked on a sizable wind power development plan in 1995, aimed at adding 250–450 megawatts of wind power over the next decade.[11] [10]

Just as wind energy development takes off in Europe, it has stalled in the United States, where the industry is buffeted by uncertainty about the future structure of the electricity industry. In fact, the country's total wind capacity has hardly increased sine 1991.[5] The country that led the world into wind power in the eighties actually saw a net decline of 8 megawatts in its installed capacity in 1995.[18] Some 50 megawatts were added—mainly in Texas—but 58 megawatts of old turbines were torn down in California.[19] Kenetech, the leading U.S. wind power company, file for bankruptcy in May 1996 after the combined effects of a slow market and mechanical problems with its new turbine led to large financial losses.

Prospects for developing nations are far brighter. Although most wind turbines are currently installed in industrial countries, much of the world's wind power potential is in the developing world. The leader so far is India, which is the first developing country with a real commercial market for wind power. India's roughly 1,500 wind turbines have virtually all been installed since the government opened the electricity grid to independent power producers and enacted tax incentives for renewable energy investments in the early nineties. According to the government, 730 megawatts had been installed by April 1, 1996, which would make India the world's most active wind market in 1996. However, there are also indications that uncertainty surrounding the Indian elections in May have since slowed the pace of development.

Some of India's wind turbines are being imported, but others are manufactured in India, either by domestic companies or in join ventures with foreign companies. Already, the Indian industry has more than 20 indigenous manufacturers and suppliers. In the windy southern state of Tamil Nadu, hundreds of jobs have been created as a result.[16]

Many other developing countries, including Argentina, Brazil, China, Egypt, Mexico, and the Philippines are surveying their wind resources and installing small numbers of turbines on an experimental basis. Although none of these countries have yet encouraged or even permitted the development of a sustained, market-driven wind industry, some may be on the verge. China, for example, already has 36 megawatts installed and has plans to reach 1,000 megawatts by the year 2000.

In most developing countries, wind power development will be driven not by environmental concerns as it is in industrial countries, but by a desperate need for electricity which is in short supply throughout the Third World. In areas such as western China and northeast Brazil, wind power is the only indigenous source of electricity ready to be developed on a large scale.

The global wind energy potential is roughly five times current global electricity use--even

excluding environmentally sensitive areas. In the United States, where detailed surveys have been conducted, it appears that wind turbines installed on 0.6 percent of the land area of the 48 contiguous states--mainly in the Great Plains--could meet one-fifth of current U.S. power needs--double the current contribution of hydropower. By comparison, the total cropland used to grow corn in the United States is nearly 3 percent of the country's land area. And unlike corn, wind power does not preclude the land from being used simultaneously for other purposes, including agriculture and grazing.

Other countries that have enough wind potential to supply most or all their electricity include Argentina, Canada, Chile, Russia, and the United Kingdom. China's wind energy potential is estimated by the government at 253,000 megawatts, which exceeds the country's current generating capacity from all sources by 40 percent. Much of that potential is located in Inner Mongolia, near some of the country's leading industrial centers.

India's potential is estimated at 80,000 megawatts, which equals the country's total current generating capacity. Europe could obtain between 7 and 26 percent of its power from the wind, depending on how much land is excluded for environmental reasons. Offshore potential in Europe's North and Baltic Seas is even greater.

Wind power cannot fully replace fossil fuels, but it has the potential to meet or exceed the 20 percent of world electricity provided by hydropower. Moreover, though wind power is more abundant in some areas than others, it is in fact one of the world's most widely distributed energy resources. More countries have wind power potential than have large resources of hydropower or coal.

Combined with other renewable energy sources such as solar and geothermal power, and by a new generations of gas-fired micro-power plants located in office and apartment buildings, wind power could help transform the world electricity system. These technologies could quickly replace coal and nuclear power--which together supply two-thirds of the world's electricity--and allow a sharp reduction in world carbon emissions.

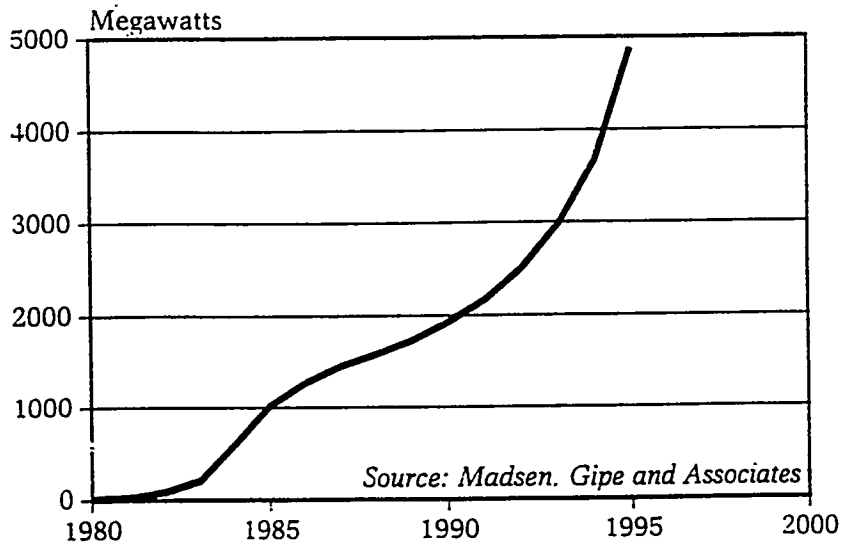

Figure 1: World Wind Energy Generating Capacity, 1980–95

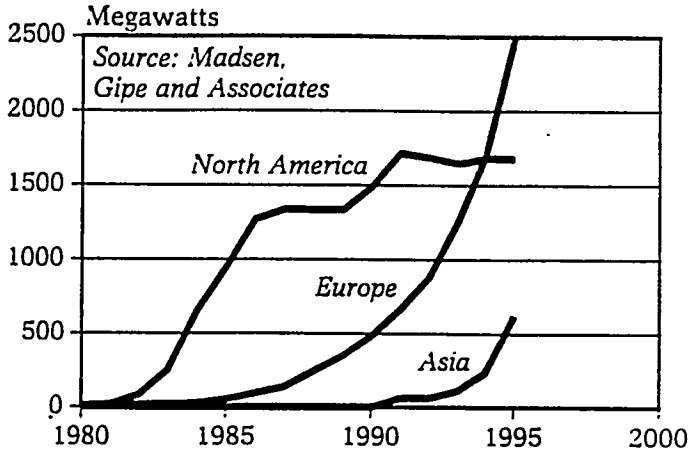

Figure 2: Wind Generating Capacity by Region, 1980–95

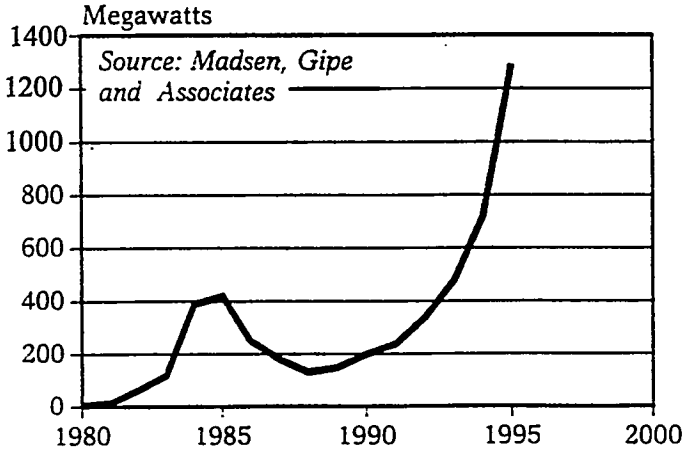

Figure 3: Net Annual Additions to World Wind Energy Generating Capacity, 1980–95

STATUS OF WIND ENERGY IN GERMANY

G.Gerdes, J. P. Molly, K. Rehfeldt
Deutsches Windenergie-Institut, DEWI
Eberststr. 96
26382 Wilhelmshaven
Germany

Abstract

By the end of 1995 in total 3655 wind turbines (WT's) were installed in Germany with a total capacity of 1,136 MW. In the year 1995 alone the WT installations grew by 1,070 units with 505 MW. About 40 % of the 1995 installations were sold to inland states of Germany with their lower wind speed potential. This fast development occurred in parallel to continuously reduced local state and federal subsidies. The further development is based mainly on the guaranteed reimbursement due to the Electricity Feed Law. But since some time the electricity utilities fight back on all legal and political levels to get cancelled the unloved Electricity Feed Law and since two years the building construction law with the foreseen privilege for WT's is discussed without any result. All these difficulties affect investors and credit giving banks in such a negative way, that the further annual increase in wind power installation for 1996 could be 10 to 20% less than in 1995. Many of the new commercial Megawatt WT's have pitch control and variable rotor speed which cause better electrical power quality and lower life time loads. From statistical evaluations on technical data of WT's a good overview of the further development is derived.

1 Status of Wind Energy Utilisation

In Germany at the status of December 31st., 1995[1] there are 3,655 wind turbines (WT's) in operation with an installed power of 1,136.517 MW (Fig. 1). The average installed power per WT therefore amounts to 310.9 kW/unit [1]. Only in 1995 a total of 505.291 MW and 1,070 units were installed resulting in an average power installation per unit of 472.2 kW. From this a potential annual energy yield of calculated 2,619 GWh or 3.29 % of the current consumption of the German coastal states (demand 1992: 79,600 GWh [2]) can be calculated. In relation to the demand of the Federal Republic of Germany (1992: 467,200 GWh [2]) the share of the wind energy is 0.56 %. The shares of wind energy to electricity supply in the states of Lower Saxony and Schleswig-Holstein are depicted in figure 1a and 1b.

It is interesting to note that the portion of WT's below 400 kW steadily declines. From the 1995 installations 455.4 MW (90.1 %) installed in 822 units (76.8 %) belong to the class over 400 kW. This class produces about 75% of all wind generated energy today.

The installation rate of 505 MW in the year 1995 is 69.5 % higher than the rate for 1994 (Fig. 1), whereas the respective number of installed WT's only grew by 32.4 % (Fig. 2). The goal to reach a total of 2,000 MW installed power in the year 2000 in Germany now needs in the course of the next five years an

[1] The data are exclusively based on manufacturer informations. The inquiry was made in December 1995/January 1996. On the average the data are applicable. They are based on the fact that the manufacturers specify the units actually installed during the last weeks before the critical date.

installation rate of only about 170 MW/year, a rate which will be certainly matched even if the legal and public opinion hindrances are growing.

Inhabitants	7.2Mio.
Annual electrical energy consumption	46TWh/a
Status1995	
Installed capacity	320MW
Share of wind energy	2%
Planned capacity 2015	
Installed capacity	1300MW
Share of wind energy	8%

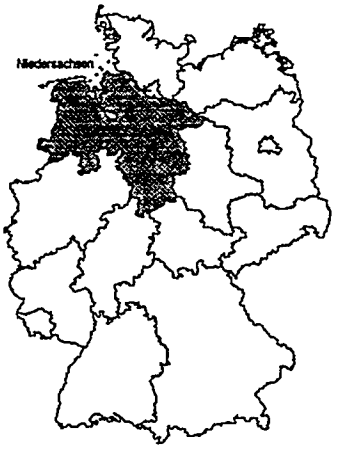

Figure 1a: Share of wind energy production on consumption in Lower Saxony

Inhabitatants	2.6 Mio.
Annual electrical energy consumption	12TWh/a
Status1995	
Installed capacity	449MW
Share of wind energy	8%
Planned capacity 2010	
Installed capacity	1200MW
Share of wind energy	~25%

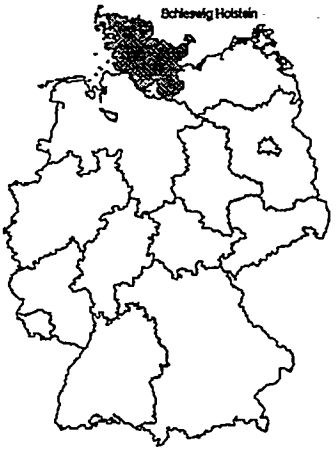

Figure 1b: Share of wind energy production on consumption in Schleswig-Holstein

The number of units and the annually installed power in Germany show that an average rated power of 472.2 kW was installed for each WT in 1995. In the Federal State of Schleswig-Holstein, this value amounted even to 544.1 kW per WT. In earlier years the average power installation per WT diminishes rapidly the larger the distances of the WT sites are from the windy coast. Now this trend is broken. The typical inland WT user is no longer a farmer who supplies his farm with electricity but is an investor who sells electricity on a commercial base to the utility.

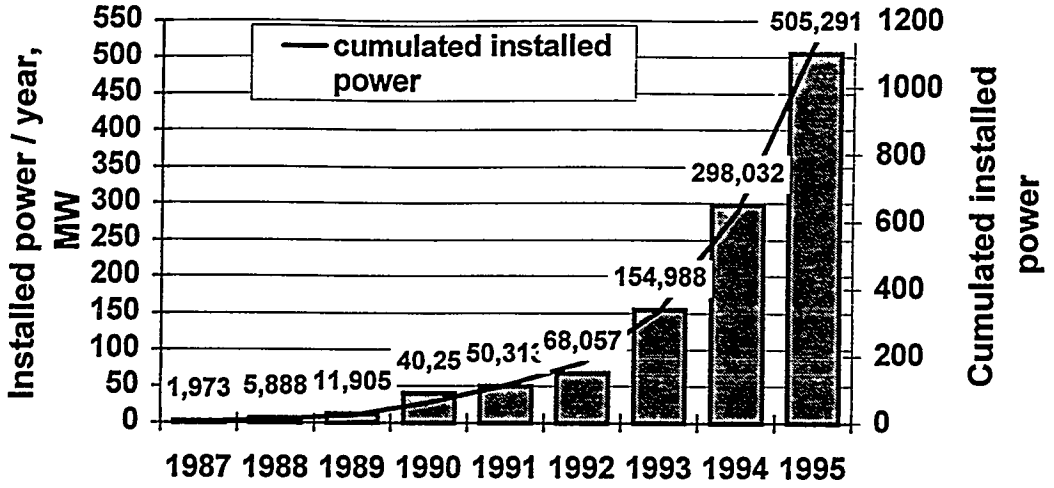

Figure 1:Installed WT power in Germany since 1987

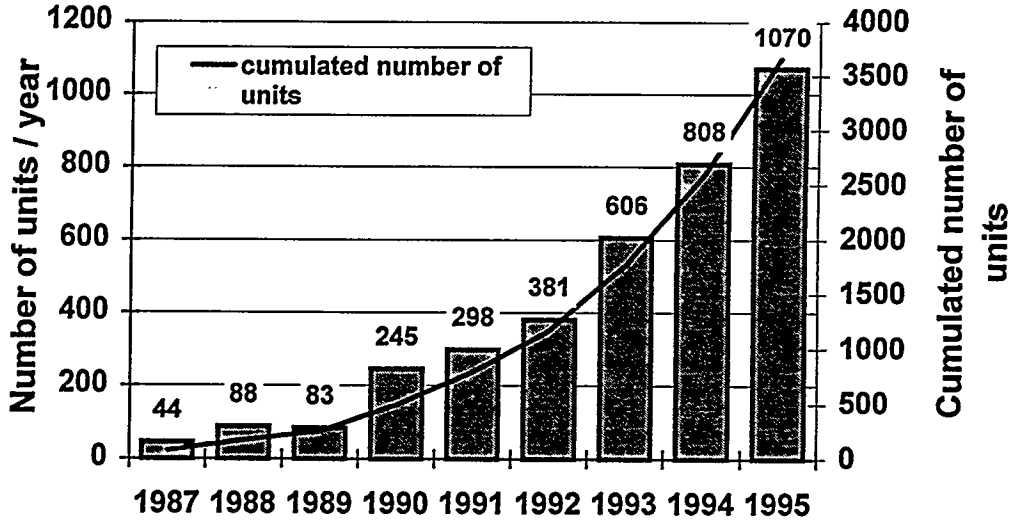

Figure 2:Installed number of WT's in Germany

The market shares of the firms offering WT's to the German market are shown in Fig. 3. Only the ten leading manufacturers are listed in order to present a clear layout. The hit list of the most successful manufacturers since 1982 concerning the power installed is led by the firm of Enercon whose share in the total market has again slightly increased from 28.4 % to 28.6 % when compared with 1994. Tacke Windtechnik, now on the second place increased its market share from 13.3 % to 16.4 %. Vestas which lost 1.5 % and its second place, has now 14.0 % whereas Micon took over fourth position from AN-Maschinenbau with an increase of 2.2 % to 10.3 % now.

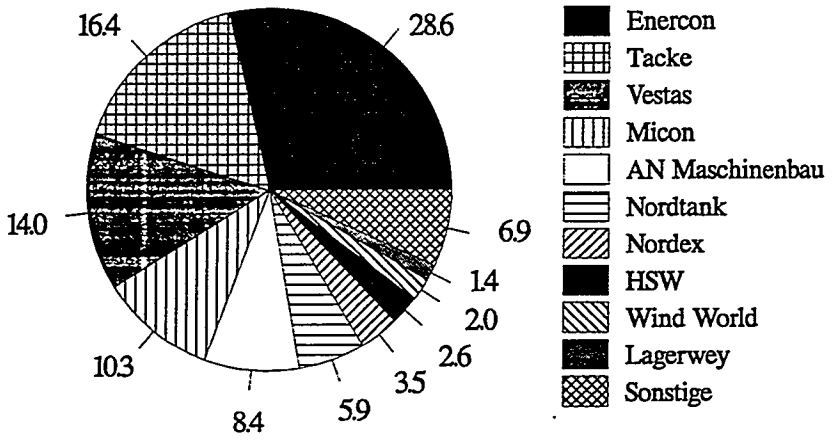

Status 31.12.1995

Figure 3: Shares of the suppliers on the German Market in per cent of the installed rated power since 1982.

To get a realistic view of the actual situation it is also of interest to break down the market shares for 1995 exclusively. Again only the 10 leading offering firms will be specified, differentiated by their installed rated power (Fig. 4).

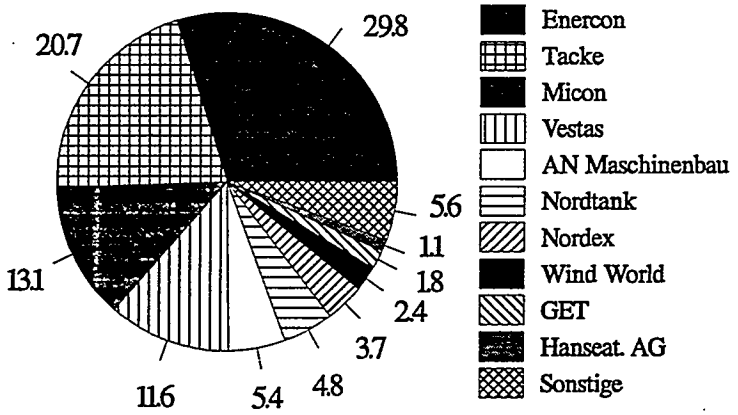

Status 31.12.1995

Figure 4: Shares of the suppliers on the German Market in per cent of the installed rated power in 1995.

The German Market in 1995 is dominated by the two Lower Saxonian firms Enercon and Tacke Windtechnik who together supplied 50.5 % of the installed rated power and 46.3 % of all units. The share of the six leading firms related to installed power was in 1995 85.4 % or 3.4 % smaller than in 1994. After several years of a steadily growing market share of the first six firms the rest of the competitors where able to increase a little bit their importance.

The companies' selling in 1995 with 541 MW (including export) matched exactly the expectations of 540 MW announced in January 1995. Now the companies are less optimistic with their predictions for 1996 due to the actual difficulties caused by the utilities and the unsolved situation concerning the Building Construction Law. The attempt of the utilities to get an examination and a final decision of the Electricity Feed Law by the Federal Constitutional Court failed in beginning 1996. The court refused to handle the

case because of not sufficiently described reasons. Beginning of May 1996 a Superior Administrative Tribunal decided that the Electricity Feed Law is in conformity with the federal constitution. Main concern of the utilities responsible in the windy areas is the unequal distribution among themselves concerning the additional cost they have due to the legally settled reimbursement of wind energy which is with 0.17 DM/kWh about 0.08 to 0.10 DM/kWh more expensive than the energy generated by conventional plants. In addition the change of §35 of the Building Construction Law in August 1994 has effect from 1996 on. Before that date, single WT's were privileged in areas outside of the building planning areas of a community and therefore could be erected there. In December 1995 and March 1996 the desired modification of the law failed with the result that for a further undefined time single WT's cannot be approved outside the building planning areas. Manufacturers don't complain that they don't have contracts. But the prosecution depends on the building licence of the local community authorities. These two legally unsolved problems cause severe irritations of the credit giving banks. A withdrawal of the §35 privilege and the Electricity Feed Law would have fatal consequences on the German wind energy market.

2 Economical Situation

Since 1991 the costs of wind generated energy has decreased considerably in Germany. The average WT prices have been higher during the last years in Germany than for example in Denmark, basically because of the relatively high subsidies available in Germany. But this high WT prices had a decisive effect on the market and technical development which made wind energy in Germany a self maintaining business and pushed German manufacturers to the top of the technological development, well in contrary to other forms of renewable energies. A simplified evaluation of the energy production cost of WT's of 32 to 45 m rotor diameter, based on the WT price ex-works, indicates a remarkable reduction of the kWh-production cost of about 45% (Fig. 5) since 1991. This reduction was caused by two factors. First by a cut-down on the governmental subsidies, second by the inflation influence of nearly 14 % which gave in 1996 a net reimbursement by the utilities of only about 0.1463 DM/kWh compared to 0.1661 DM/kWh in 1991. In extreme cases an operator achieved up to 0.28 DM/kWh in 1991. In 1996 for most of the investors it is not more than 0.1721 DM/kWh, the guaranteed reimbursement by the Electricity Feed Law. The advantage of the cost-price development is diminished by an increase of the grid connection cost during the same period [3]. The concentration on the near coast sites, which is necessary for all projects which cannot count on subsidies, urge the grid connection costs to increase due to the grid reinforcements necessary in many places.

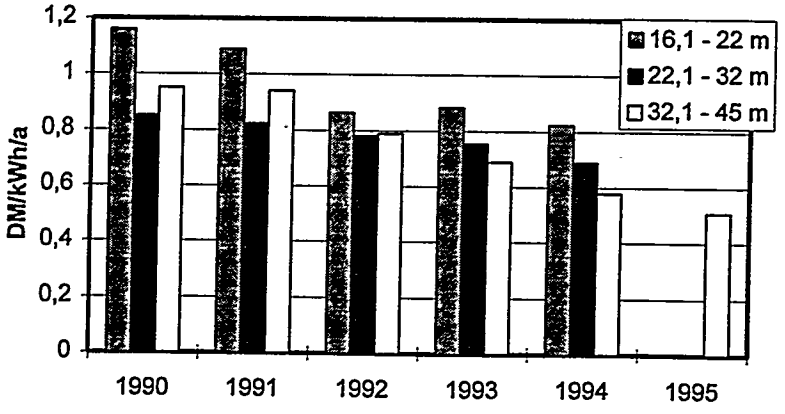

Figure 5 Development of the WT prices in DM value of 1991 with respect to the annual energy yield.

Reason for the positive cost development was the 500/600-kW-class of wind turbines, which replaced the smaller 250 to 400 kW machines since 1993. As Fig. 6 shows the smaller WT's have a considerably worse economic efficiency than the actual 500/600 kW class. Most of the European manufacturers are engaged in the development of WT's in the size of up to 1.5 MW, forced by the market, which requires for the largest WT available, due to their expected energy generation cost advantage. WT's of 800 and 1000 kW are already available on the market and took over about 5 % of the total wind power installation in Germany in 1995. But this step seems to be an intermediate step done by only some manufacturers. The leading ones in the ranking of the German market, like Enercon, Tacke Windtechnik, Vestas, Nordtank, etc. are going for 1.5 MW. The first prototypes of them were erected end of last and beginning of this year and are in test operation now.

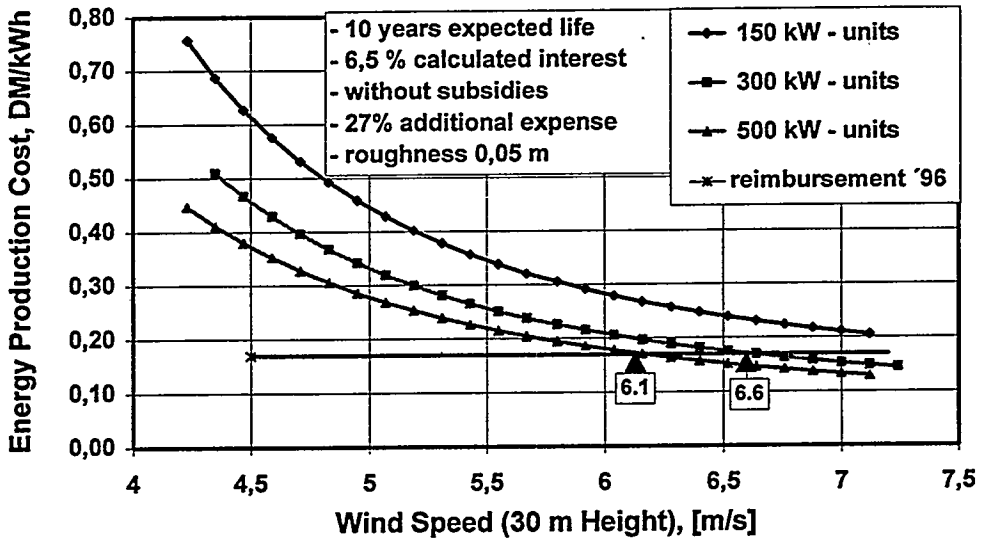

Figure 6: Wind energy production cost for different WT sizes with respect to same financial conditions [6]

3 Technical Development

Seven years ago an evaluation based on physical dependences [4], showed a possible electricity generation cost reduction with rotor diameters up to about 60 m. The evaluation took into consideration that economic advantages can be achieved by certain design drivers. Tower head mass (nacelle plus rotor) is one of the most important for optimised WT's because machined material has it's price. For a number of commercially available WT's the price for one kg tower head mass dependent on the rotor diameter is shown in Fig. 7. The line indicates more or less the average value for each rotor diameter group. If the curve is extrapolated to rotor sizes of about 60 m a kg-price of 28 DM/kg is reached.

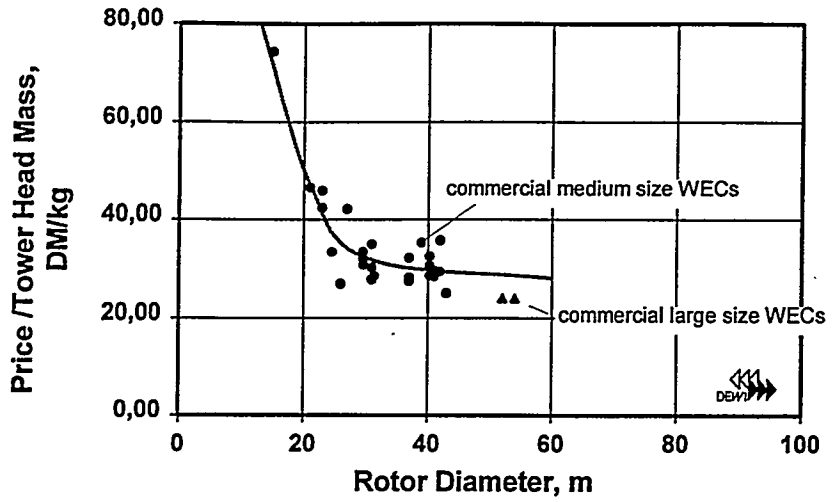

Figure 7: Price of 1 kg tower head mass of some WT's

Two already available 1-MW-WT's shown in the graph support the assumption that the coming 1.5-MW-WT's could reach about 28 DM/kg. Normally light weight WT's have a somewhat higher kg-price than the heavy ones which gives a possible kg-price variation between 23 to 33 DM/kg for the future 1.5-MW-class. Several possibilities exist to reduce the mass of the tower head. Increase of rotor speed to decrease the torque to be transmitted between rotor and generator is one of the possibilities. But Fig. 8 indicates that industry is very carefully with higher rotor tip speeds of large WT's. Reason for this is the increasing aerodynamic noise which grows with nearly the sixth power of the tip speed change, a fact which is commercially unacceptable under the local conditions of Germany.

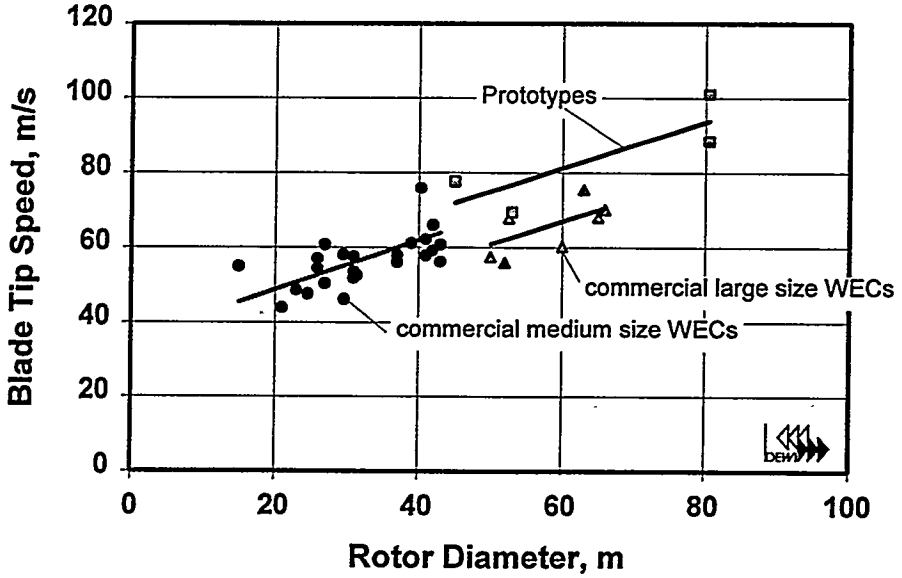

Figure 8: Blade tip speed of medium and large size WT's

An other way to get more cost effective is to increase the torque per kg of tower head mass. This can be done by better knowledge of material properties, load cases and a decrease of loads due to changes in rotor speed and power control. Again a statistic evaluation of the respective values of commercial WT's

indicates the technical development of today. Fig. 9 shows the changes in torque per kg tower head mass of medium size WT's and the same values for the new MW-class. Different to the nearly constant tip speed the torque per kg has a clear tendency to steadily increase with rotor size.

With the measured power curve, or in case of the new commercial MW-WT's a calculated power curve, annual energy yields for each particular WT at a specific site can be calculated. The site characteristic chosen for comparison reasons has an average wind speed of 6 m/s at 10 m height and a 1/7 power law change of wind speed with height.

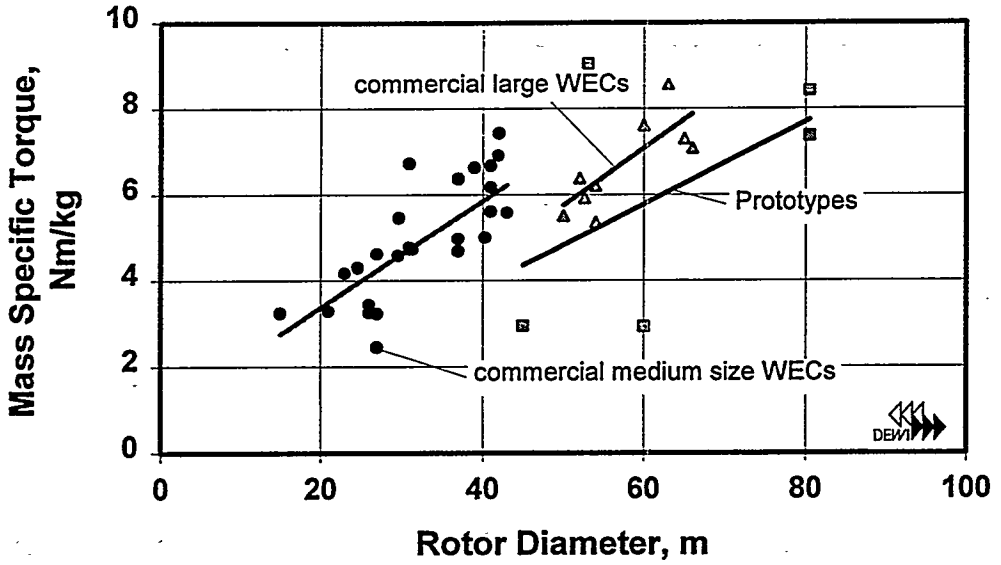

Figure 9: Torque per kg tower head mass of some WT's

With the informations above mentioned it is now possible to compare the seven years old energy cost prediction tendency (lines in Fig. 10) [4] with the achieved energy production costs of today. The two lines assume a conservative and an optimistic technology development with WT rotor size. To get the specific energy production cost for each real WT, the investment costs of the WT's were devided by their energy yield of only one year! Prices for WT's are known only for medium size WT's from catalogues. Selling prices for large WT's can be calculated, assuming the 28 DM/kg mentioned above and their known tower head mass. Both, theoretical large WT's and real medium size WT's energy generation costs fit quite well with the predicted size dependent energy cost tendency. Further more one can expect from the new MW-WT's to be at least competitive with the economics of the smaller commercial 500/600 kW size of today. As Fig. 10 demonstrates, the predicted minimum of the theoretical cost development curve, is quite flat so that even WT's of 80 to 90 m rotor diameter could be expected to become economic. In contrary most of the manufacturers of larger WT's express today their doubts that larger WT's than those developed today could become economic one day.

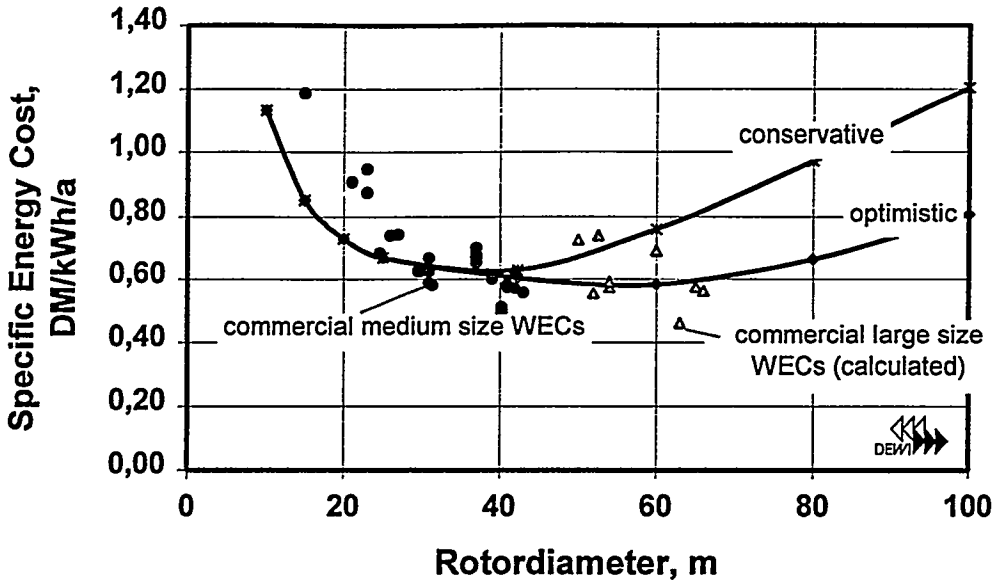

Figure 10: Energy generation costs related to annual energy yield at a 6 m/s (10m height) site with the assumption of a conservative and an optimistic technological development in comparison with today's values of commercial WT's.

The development in noise reduction during the last years, forced by the German subsidy formula, was very successful. The best WT's of more than 40 m rotor diameter are down at 98 to 99 dB(A) [5], or with other words 4 to 6 dB(A) lower than the expected tendency taken from older and smaller WT's. To give an idea, the minimum distance for a 500 kW WT to the nearest neighbouring house is only about 250 m, if a noise immission of 45 dB(A) shall not be surpassed. In most of the German windfarms this value of 45 dB(A) during night is applied because the windfarms are built outside the normal building planning areas of the communities where normally a mixed area of industry and residential houses is assumed.

The subsidy system applied in some German states also takes into account the electrical power quality of WT's. Power quality measurements are successfully done since more than one year by DEWI and others. Utilities more or less oblige the WT manufacturers to provide a data sheet with the respective power quality measurement results. An actual overview an power quality measurement results is given in [8].

4 Literature

[1] Rehfeldt, Knud 1996, Windenergienutzung in der Bundesrepublik Deutschland, Stand 31.12. 1995. DEWI-Magazin Nr. 8

[2] Die Elektrizitätswirtschaft in der Bundesrepublik Deutschland im Jahre 1992: Statistischer Jahresbericht des Referats Elektrizitätswirtschaft im Bundesministerium für Wirtschaft. Frankfurt a.M.: VWEW-Verl. 1994. ISBN 3-8022-0400-X

[3] Everding, H.; Keuper, A., Veltrup, M., 1993, Der steinige Weg zur eigenen Windkraftanlage. DEWI-Magazin Nr. 3

[4] Molly, J.P., 1990, "Windenergie, Theorie Anwendung, Messung", Kap. 6.3. Verlag C.F. Müller, Karlsruhe

[5] N.N., 1996, Datenblätter für die Landesförderung. Deutsches Windenergie-Institut, Wilhelmshaven

[6] Rehfeldt, K.; Schwenk, B 1996, Entwicklung der Energieerzeugungskosten von WEA. DEWI-Magazin Nr.8

[7] Rehfeldt, K. 1996, Entwicklungstendenzen der Anlagentechnik in unterschiedlichen Einsatzbereichen. Energie'96, 24.-26.4.1996

[8] Gerhard J. Gerdes, Fritz Santjer
Results from power quality measurements in germany - an overview
American Wind Energy Association Windpower'96 Conference, Denver June 1996

NEW DEVELOPMENTS IN THE DANISH WIND ENERGY POLICY

Jørgen Lemming
Ministry of Environment and Energy
Danish Energy Agency
44 Amaliegade
DK-1256 Copenhagen K
Denmark

INTRODUCTION

Wind energy resources in Denmark are among the best in Europe. In recent years there has been a rapid growth in number of wind turbines connected to the grid in Denmark. By the end of 1995 more than 3800 wind turbines were installed on-shore with a capacity of over 600 MW. The total production of electricity from these turbines in 1995 was more than 1200 GWh, corresponding to approximately 3.6 % of the Danish electricity consumption.

For several years Denmark has pursued an energy policy with an increasing weight on environmental aspects and new and renewable energy sources like wind energy. Therefore wind energy already plays an important part as supplement to the traditional sources of fuel in the electricity production, and the share of wind energy and other renewables is expected to increase significantly in the years to come.

ENERGY POLICY IN GENERAL

Denmark has a long tradition of conducting a vigorous energy policy, and implementing it with broad political support and the keen commitment of a wide range of actors: energy companies, industry, grass roots, municipalities, research circles and consumers.

The aim of the first energy strategy, *Danish Energy Policy 1976,* was to secure Denmark against crises in supply such as the energy crisis of 1973-74. The following plan, *Energy 81,* could build further, given the drastic price rises of energy after the crisis in 1979-80; it also emphasised socio-economic and environmental considerations. After a period of building up large projects for facilities and markets for natural gas and heat and power generation, the action plan, *Energy 2000,* followed in 1990, introducing the goal of sustainable development of the energy sector.

Each of these plans has been followed up continuously, partly through political agreements and legislation. *Energy 2000 - follow-up,* from 1993, comprises such action, and in 1995 the Government carried legislation through Parliament on "the green packet for trade and industry". In 1995, too, decisions were made on increased future utilisation of renewable energy. These initiatives are to be part of securing the fulfilment of the target of reducing CO_2 emissions during the period up to 2005.

The need for a new energy plan has come not least from international challenges. The development within the European Union of opening energy markets has brought a need for a new foundation for energy policy to ensure that overall environmental objectives can be maintained under new market conditions, while taking advantage of increased integration.

Denmark's Energy Futures, a discussion paper published in December 1995, contains a technical analysis of future scenarios for energy consumption and supply in Denmark. It has been followed and extended by *Energy 21,* the fourth of the energy strategies, which lays down the energy-policy agenda for the coming period.

ACTIONS CONCERNING CLIMATE CHANGE

Denmark is a highly industrialised country that emits large quantities of substances that burden the environment. For the energy sector, this is primarily the greenhouse gas, CO_2, where Danish *per capita* emissions are constantly among the highest in the world. The country has thus a particular duty to reduce these emissions (figure 1&2).

The increasing greenhouse effect is a global problem, in every sense of the word, that demands international actions to resolve it. It is the Government's wish that Denmark shall continue to have an active role in implementing these international efforts, and that the EU and other international cooperation should be used to maximum effect to support this effort.

Denmark has set a national target for reducing the greenhouse gas, CO_2. As by far the greatest part of these CO_2 emissions derive from the use of energy, the target shall continue to be pursued mainly through comprehensive actions in the energy sector.

Ratified by Denmark and 154 other countries, the UN Climate Convention requires all its signatories to act concerning emissions of greenhouse gases. Its target is to stop the growth in the atmosphere of greenhouse gases at levels of concentration that do not cause dangerous climate changes.

As a first step on the way, the industrial countries have undertaken to ensure that their emissions in 2000 do not exceed those in 1990. Denmark is living up to this obligation.

The Government is maintaining this obligation so as to stabilise, by 2000, total Danish CO_2 emissions into the atmosphere at a level below that in 1990 and, by 2005, to have reduced them by 20% from their 1988 levels.

This target includes the transport-sector target of stabilising its CO_2 emissions at their 1988 levels by 2005. This means that to achieve the overall national target of a 20% reduction, the other energy areas must achieve much larger proportional reductions than those of the transport sector. This is to be secured by a substantial effort especially as to the consumption and supply of heat and power, including an increased use of renewable energy.

DANISH CO_2 ACTIONS AFTER 2005

With *Energy 21* the Government wishes to demonstrate its abiding will to fulfil its obligations. The long-term perspective is that a further reduction of environmental impact shall be achieved after 2005.

As already stated, Denmark is willing to accept in international climate negotiations the reduction targets that follow from the conclusions of the International Panel on Climate Change. Should this be decided, Denmark and other highly-developed industrial countries with high CO_2 emissions would strive to reduce them, by 2030, to half their 1990 levels (figure 2).

In contrast to the shorter-term target, that is a 20% reduction before 2005, the establishment of a longer-term reduction is not to be understood as a new national target, but as the interim proposal for international

negotiations on the climate and as a starting point for formulating both short-term and longer-term energy policies.

A condition for the Government's decision to aim at halving CO_2 emissions before 2030 is that international efforts in both technological development and design of market conditions and mechanisms support this Danish effort.

THE ROLE OF RENEWABLE ENERGY IN ENERGY 21

The long-term perspective over a period of 30 years is the development of an energy system in which an increasing proportion of the energy consumption is covered by renewable energy. The assumption is that there will be a gradual phasing in of renewable energy as technological and economic conditions make the various renewable energy solutions commercially viable.

On the basis of the initiatives that have been launched, it is estimated that domestic renewable sources of energy will contribute some 12-14% of the total gross energy consumption by 2005. The Government intends to continue the development of renewable energy at an average annual rate of 1%. This entails renewable energy increasing its share of the energy supply to about 35%, a development which will also be necessary if it is decided to halve CO_2 emissions by 2030 relative to 1988 (figure 3&4).

In the short term, the development of renewable energy is expected to take place primarily by means of increasing the use of bioenergy and wind power, which are also expected to provide the largest contribution in the longer term. As a consequence of technological developments within individual fields, other renewable energy technologies such as solar cells, heat pumps, and wave energy will become of increasing importance (figure 5).

As early as in the autumn of 1995, the Government decided to intensify its activities in the field of renewable energy by launching a number of concrete initiatives designed to increase the use of renewable energy. It is estimated that these initiatives will result in a reduction of CO_2 by at least 1.5 million tonnes in 2005, while at the same time supporting the Government's wish to see cleaner sources of energy gaining increasingly larger importance in the energy supply of the future.

There will still be unexploited renewable energy resources available for increased use of renewable energy in Denmark's energy supply, but further extension still calls for the application of a number of instruments. It is necessary to support research and development in new and existing renewable energy technologies. Other instruments include support for demonstration projects, investment grants, and a suitable structure of taxation. In connection with the coming liberalisation of the electricity market, it must be ensured that the instruments for continued expansion of the use of renewable energy in power production will be available.

At the same time it is planned to increase the use of goal-oriented information campaigns.

WIND POWER IN ENERGY 21

In Denmark there are at present more than 3,800 wind turbines with a total capacity of about 600 MW and annual power production of more than 1,200 GWh (figure 6). The most recent large wind turbines are so competitive today that the use of electricity from wind turbines is one of the cheapest ways of reducing CO_2 emission from power production. It is also expected that wind power from large new turbines already in year 200 will competitive with coventional power production including a 20% capacity-backup factor for the turbines. (figure 7).

The total capacity in 2005 is presumed to be 1,500 MW and, as appears from the Government's Renewable Energy Initiative Package from November 1995, a large number of the wind turbines are to be built by the utilities. A considerable number will, however, still be privately owned. To meet the target for 2005, it will be necessary to maintain a development rate of at least 100 MW/year.

The most economical way is still to erect wind turbines on land. But area resources on land are limited when housing as well as nature and landscape considerations are to be taken into account. Furthermore, wind conditions at sea are considerably better than at sites on land, and wind turbines erected offshore are expected to become competitive in step with the development of technology.

The Government expects that a significant part of the expansion until 2005 will take place on land. As wind turbines become larger and hence more difficult to place in landscapes, the number of new sites will become limited. The increase of wind turbine capacity on land after 2005 will have to be effected, among other things, by renovation of wind turbine areas as well as by removal or replacement of existing wind turbines in accordance with regional and municipal planning. In the longer term it is to be expected that the main part of new development will take place offshore.

The Government intends to continue its promotion of the employment and export opportunities by continued research and development. This will support the Danish wind turbine industry, which is the largest in the world, with a turnover in 1995 of more than DKK 4 billion, and exports of wind turbines and wind turbine components of some DKK 3.5 billion corresponding to approx. 475 turbines. The total share of the world market is shown in figure 8. The number of jobs in the sector has increased to over 9,000.

In order to provide individual households outside areas with district heating and natural gas supplies with better opportunities to contribute to the use of cleaner energy, the Government will support development of small wind turbines (household turbines) producing electricity for heat and power. The small wind turbines are seen as a supplement to the general development of wind power.

The Government intends to:

* reach a decision on development of offshore wind turbines on the background of the action plan for offshore wind turbines which will be completed before July 1, 1997

* make wind turbine planning a regular feature of regional and municipal planning

* present proposals on revision of the scheme for replacement of older wind turbines.

* on the basis of the outcome of the ongoing demonstration programme on household turbines, evaluate the opportunities for promoting a development.

EFFECTS OF THE PLAN OF ACTION

Impacts of the Energy Plan are evaluated in relation to a reference scenario. It describes the development that is expected should the existing energy policy with associated initiatives be continued without further change (figure 4).

In the reference scenario, the taxes and subsidies and the like used hitherto are kept in force, and, as energy demands increase and scrapping occurs, the present supply system is developed, maintained and made more efficient.

The main assumptions for the reference scenario are that the efficiency of electrical appliances, processes and so forth improves only as a consequence of 'natural' technological development, and that such improvements are implemented only as old equipment wears out or is replaced. Extensions of industrial and combined heat and power plants continue as expected up to now, and the existing central power stations and heat and power plants are replaced with the newest and most efficient coal-fired plants.

The biomass action plan is realised and the use of renewable energy is increased in accordance with the Government's publication, *Renewable energy - new initiatives* (November 1995). Initiatives regarding wind energy being implemented are:

* The electric utilities must build 200 MW wind power capacity over the next 4 years

* The electric utilities must prepare an action plan off-shore wind farms, which will be ready in 1997

* New regulations with improved access for private persons and companyies to invest in wind turbines

* an information strategy for wind energy will be launghed

THE SENARIO OF THE ENERGY PLAN

Assumptions about economic developments and demands for energy are the same in the energy plan and reference scenarios.

Up to 2005 calculations assume that besides the initiatives decided in the reference scenario, a number of new initiatives are also realised within the main areas established in the action plan. Within the area of renewables a further development of combined heat and power utilising natural gas and developing 200 MW offshore wind turbines, about 1 PJ landfill gas, and about 1 PJ geothermal heat.

ASSUMPTIONS AFTER 2005

After 2005, efforts increase to promote measures that include conservation of heat and electricity; production and use of energy-efficient appliances, processes and cars; and use of renewable energy plants. It is expected that the measures regarding renewable energy in 2030 will entail in the following:

- developing wind turbines to a total output of 5,500 MW (of which 4,000 MW are from offshore sites) - or alternatively solar cells and wave energy, provided these are competitive with wind energy

- annually utilising about 100 PJ biomass and biogas, as well as about a further 45 PJ biomass, including energy crops

- establishing geothermal facilities and large heat pump plants corresponding to basic heating of about 25 PJ annually in district-heating areas; conversion of individual natural-gas supplies to CHP; further extending heat supplies outside district-heating areas to renewable-energy based facilities.

In the main, the aim is that, after 2005, the individual elements in the energy plan are given priority over economic costs and CO_2-shadow prices. This does not exclude, however, the incorporation of new but socially attractive technologies as and when they are developed.

Roughly speaking, the electricity-saving initiatives of the energy plan correspond to all the electricity conservation (with a 6-year simple pay-back time at current electricity prices for households and the public sector) being implemented in step with the ongoing replacement of appliances etc.

A prioritised development has taken place on the basis of cost evaluations of renewable energy supply plants. Top priority is now given to developing wind turbines on land and in coastal waters, immediately followed by utilisation of hitherto unexploited resources of waste, wood, straw and biogas.

Further electricity and heat demand is met by biomass, including energy crops as well as geothermal energy and heat pumps. Utilisation of the accessible biomass resources and priority given to their use in larger rather than smaller plants ensures that far the most important part of these extensions are achieved at relatively low CO_2-shadow price. In figure 9 is shown the actual CO_2-shadow prices for different renewable energies.

RESULTS OF THE PLAN SCENARIO

According to the plan scenario, the eventual energy consumption in 1994-2030 falls by about 14%, while the gross consumption of energy falls by about 17%; developments in distribution of various fuels are shown in figure 4.

In sum, the costs of fuel, operations and maintenance, as well as investments and reinvestment in supply facilities and consumers' installations, comprise on average 28 billion DKK annually in 1995-2005, increasing to 41 billion DKK annually in 2020-30. These figures exclude investments in the transport sector and the costs of the various measures.

References: Energy 21. Ministry of Environment & Energy. April 1996 (English version is available in July 1996).

CO2-emission pr. indbygger

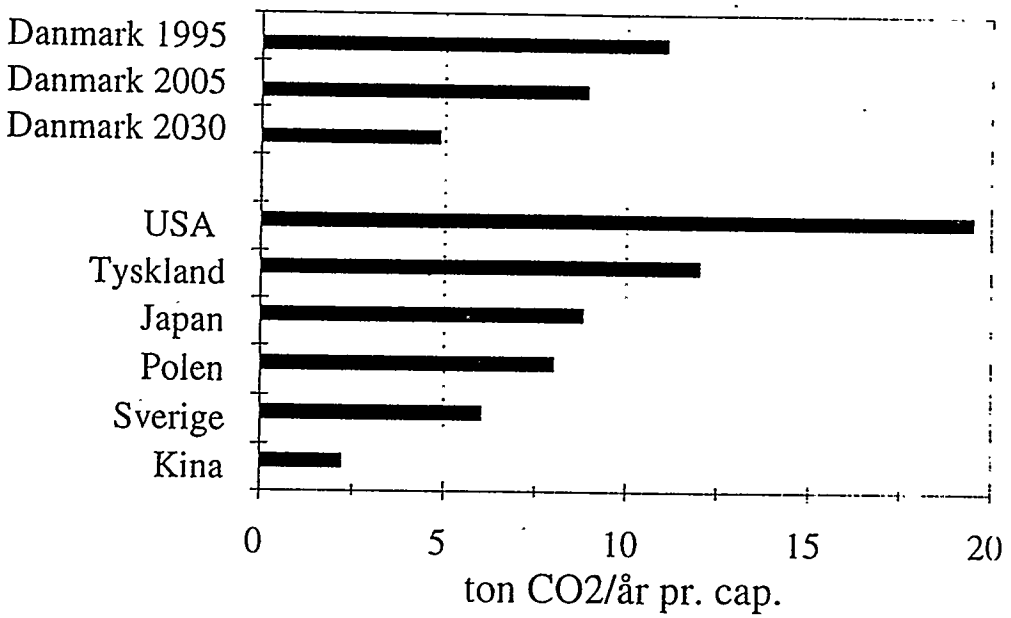

Figure 1.

Planforløbet 1991-værdier

Energistyrelsen
Miljø- og Energiministeriet
07.06.96

ENERGY 21

CO_2 - emission

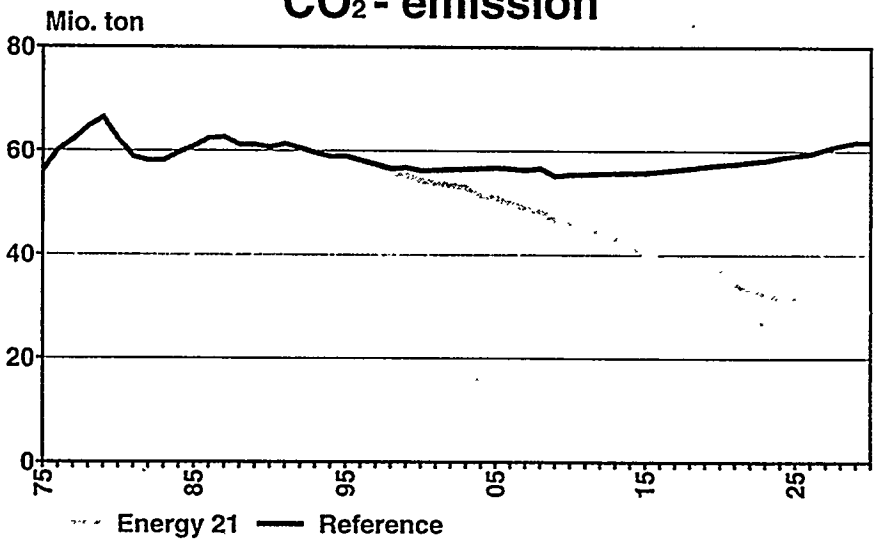

Figure 2.

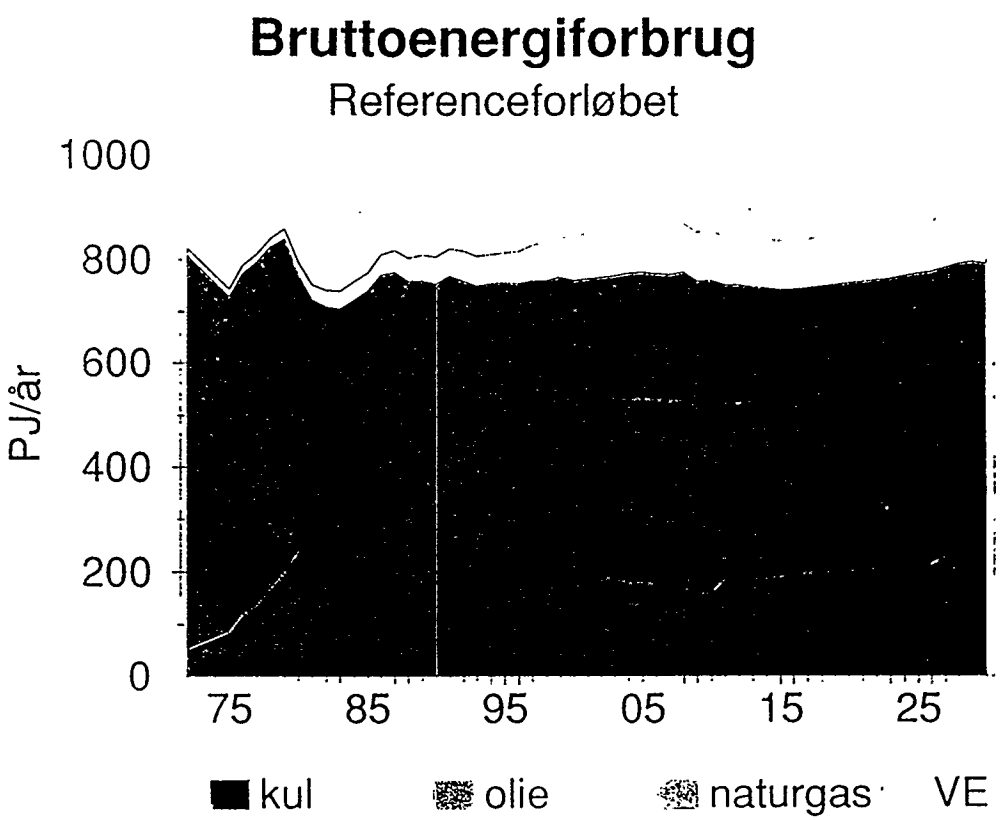

Figure 3.

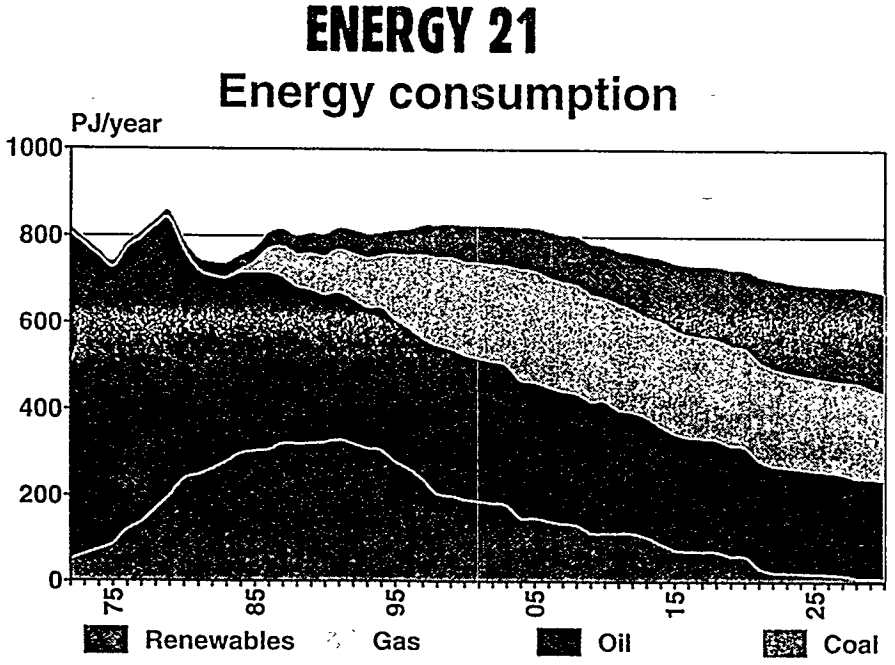

Figure 4.

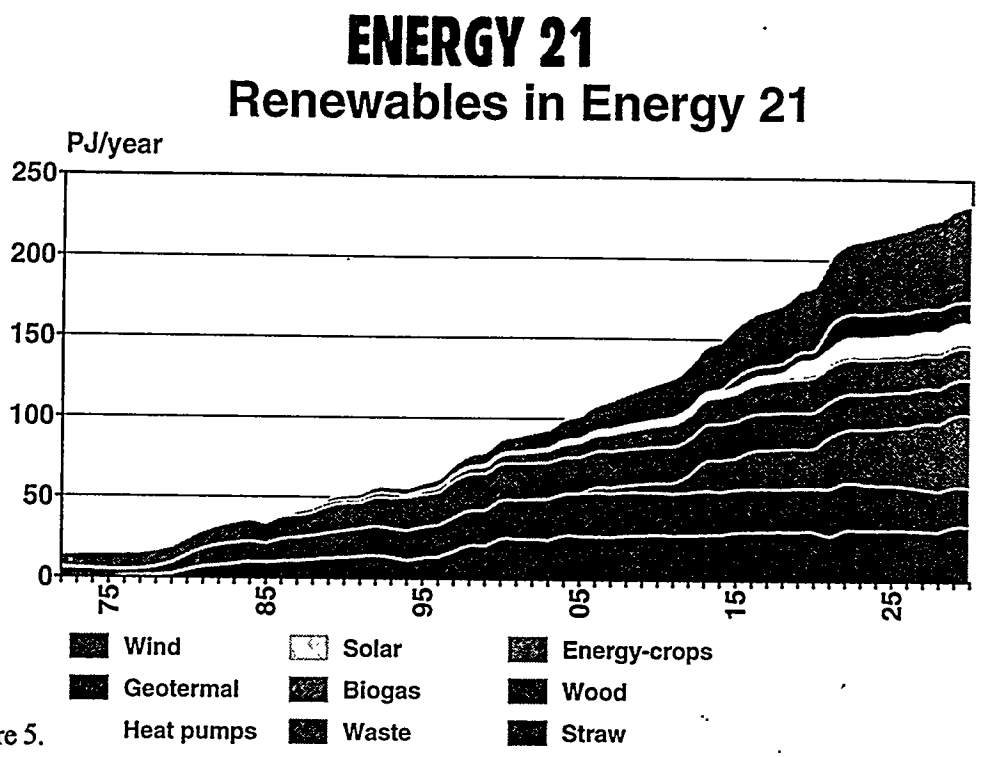

Figure 5.

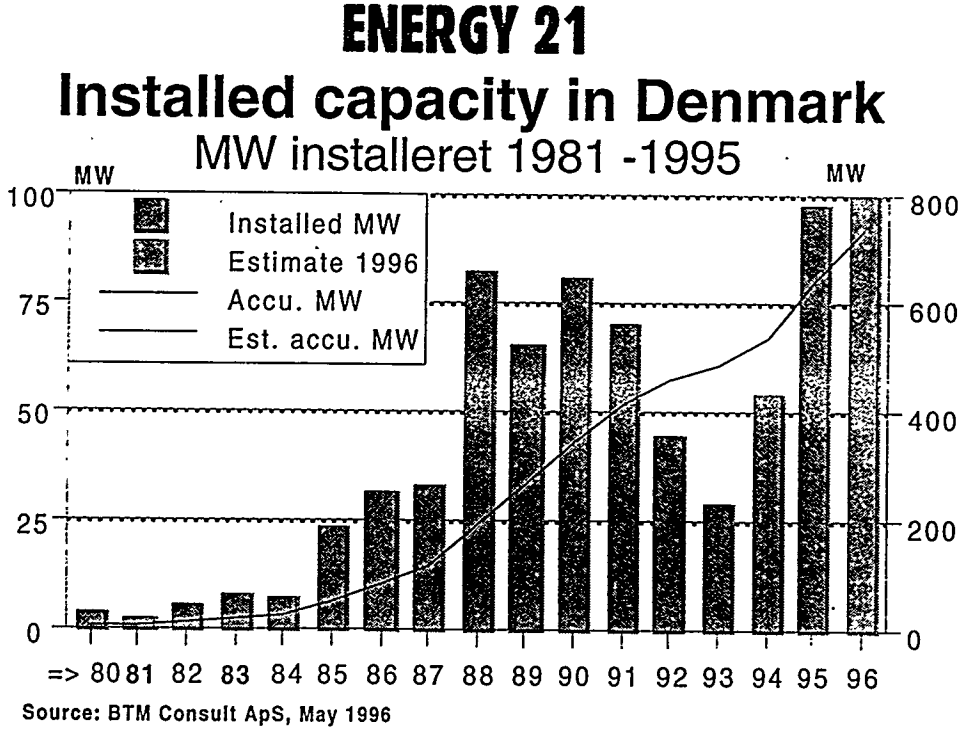

Figure 6.

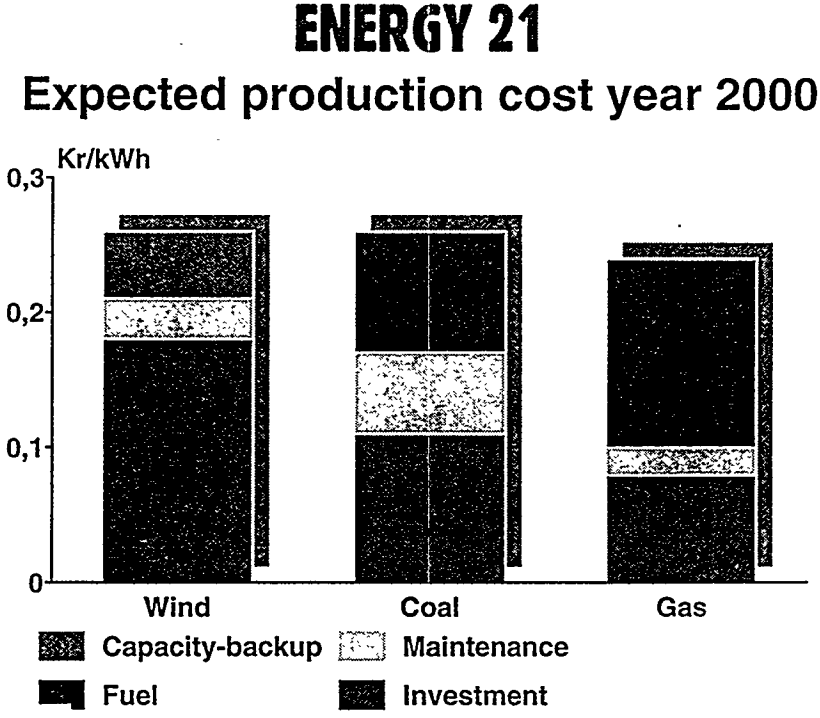

Figure 7.

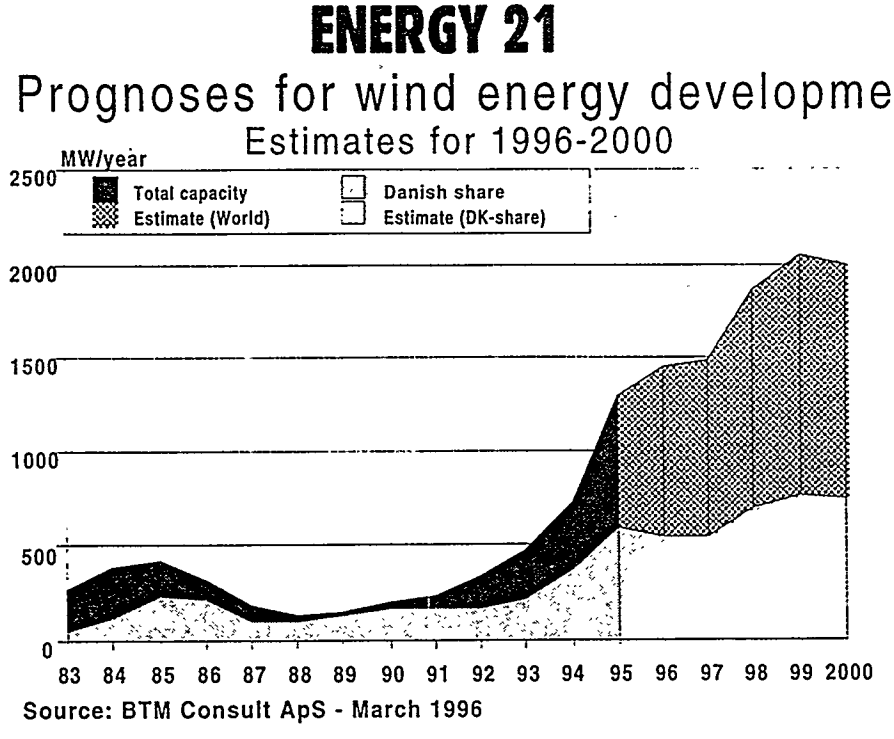

Figure 8.

ENERGY 21

Socio - economic costs in dkr per saved ton CO_2

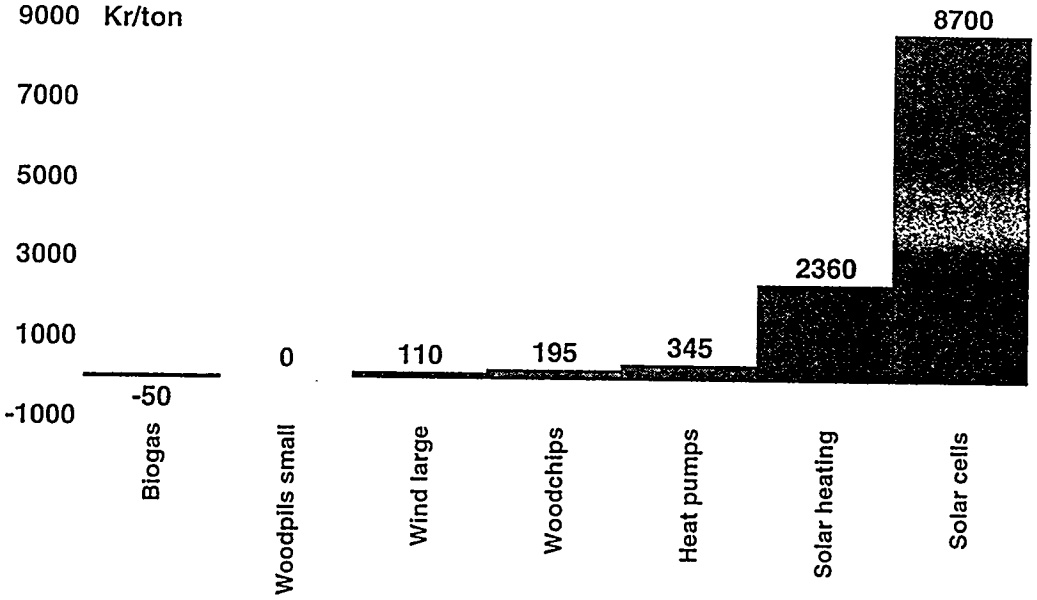

Figure 9.

THE WIND ENERGY MARKET IN THE U.K. AND IRELAND

David Lindley
Lindley and Associates
Woodfield House, Farm Lane, Jordans, Buckinghamshire HP9 2UP
United Kingdom

ABSTRACT

The market for renewable energy projects has been created in England and Wales by measures established by the Electricity Act 1989 which created the Non-Fossil Fuel Obligation (NFFO). Identical market enablement mechanisms now exist for Scotland and Northern Ireland whilst yet another version of the NFFO mechanism has been established in Ireland. As a result, the UK now has 31 operational windfarms with a total rating of 195MW whilst the completion of the first windfarm in Ireland is expected in early 1997. This paper gives details of these mechanisms and the impact they have had on the creation of a renewables market. Current expectations are that additional wind energy capacity of about 900MW will be added in the UK and Ireland by the end of the millennium. This implies a market worth between US$525 million and US$600 million in turbine sales and a total turnkey investment cost of between US$1.2 billion and US$1.5 billion.

THE UK RENEWABLES MARKET

The UK market for Renewable Energy power projects was created as a by product of the financial provision established by the Electricity Act 1989 to support the nuclear industry via the so called Non Fossil Fuel Obligation (NFFO). Since the Act, three NFFO 'orders' for renewables projects have been awarded, thus enabling the sponsors of these projects to proceed to finance and construct over 1200 MW Declared Net Capacity (DNC) of new renewable energy electricity generating schemes. The announcement of a new fourth tranche (NFFO 4) was made on 2 November 1995 and a fifth tranche is expected in 1998. At the same time that the third NFFO order was announced, both a Scottish Renewables Obligation (SRO) and a Northern Ireland Order (NIO) were announced. The intention was that the Scottish orders were made at the same time as the third, fourth and fifth NFFO orders.

The announcement made on 2 November 1995 by Mr Richard Page, the Parliamentary Under-Secretary of State at the Department of Trade and Industry reaffirmed that Government policy was to work towards 1500 MW DNC of new-renewables-based generation capacity in the UK by 2000. He said that the DTI expected that a total of 900 MW of capacity will be built as a result of the first three NFFO orders in England and Wales, from current Scottish and Northern Ireland (SRO and NI-NFFO) orders, from prospective future SRO and NI-NFFO orders, and from capacity built outside the NFFO/SRO arrangements. The DTI have assumed that only two-thirds of projects (and capacity) contracted under future NFFO arrangements will proceed to commissioning and they have concluded that new NFFO orders for England and Wales would have to contract for 900 MW of new capacity in order to deliver 600 MW of operational capacity. He said that he expected the fourth and fifth orders would each contract for between 400 to 500 MW of new capacity. On the same day of the DTI's press release for NFFO 4, George Kynoch, Minister for Industry at The Scottish Office, announced the second order under the Scottish Renewables Obligation (SRO) and said he would oblige Scottish Power and Hydro-Electric to secure between 70 to 80 MW (DNC) from renewable sources.

The Office of Electricity Regulation (OFFER) has provided a detailed analysis of the results of the 1990 NFFO (NFFO 1) and the 1991 NFFO (NFFO 2) and these are shown in Tables 1 and 2 (from Ref. 1). OFFER has also provided details of bids made in the NFFO 3 and SRO 1 competition (References 1 and 2). Tables 3 and 4 show the breakdown of the contracts awarded to different technologies in NFFO 3 and SRO 1 respectively.

The first Northern Ireland order awarded contracts for a total of 15.6 MW (DNC) of renewables.

The net result of these orders is that by the year 2000 about 2500 MW (DNC) of contracts will have been awarded under the three different Renewable Obligations in the UK in an attempt to obtain 1500 MW (DNC) of operational capacity. Financing this capacity will require a total investment of well in excess of US$2.25 billion.

THE TERMS OF THE NFFO CONTRACTS

Under the terms of contracts let in the first two NFFO's (NFFO 1 and NFFO 2), projects were paid a premium price for any electricity generated prior to the end of 1998. Once contracts were awarded, developers had to get their projects constructed as soon as possible so that they could earn the premium price as quickly as possible in order to maximise project revenues.

The 1998 contract termination date had a serious impact on the perception of renewables in two major ways. The 1998 end date meant that any loans raised from banks would usually need to be repaid by 1998 (because the bank would look only at the NFFO contract period as being the only significant and secure source of revenue). This in turn resulted in the prices paid in NFFO 2 being in the range 5.9 p/kWh (for sewage gas) to 11 p/kWh for wind energy. Very few commentators seemed to understand at the time that these high prices resulted from the short term of the contract.

TABLE 1: STATUS OF 1990 NFFO PROJECTS [1]

Technology	Projects Contracted		Projects Generating		Projects Terminated		Projects to be Commissioned		Completion Rates(%)	
	No	MW	No	MW	No	MW	No	MW	No	MW
Wind	9	12.21	8	11.7	1	0.51	-	-	89	96
Hydro	26	11.85	20	8.87	5	1.85	1	0.66	77	75
Landfill gas	25	35.5	20	30.31	5	3.82	-	-	80	88
Waste Combustion	4	40.63	4	39.63	-	-	-	-	100	98
Other Combustion	4	45.48	4	45.48	-	-	-	-	100	100
Sewage Gas	7	6.45	7	6.45	-	-	-	-	100	100
TOTALS	75	152.11	63	142.44	11	6.18	1	0.66	84	94

NOTE: TABLE 1 EXCLUDES A COLUMN FOR EXISTING PROJECTS. OF THE 75 PROJECTS AWARDED CONTRACTS, 35 WERE ALREADY EXISTING AND GENERATING ELECTRICITY. THUS, OF THE 150 MW DNC GRANTED PROJECTS, AROUND 100 MW DNC WAS NEW OR REFURBISHED AND ABOUT 50 MW DNC WAS ALREADY GENERATING.

TABLE 2: STATUS OF 1991 NFFO PROJECTS [1]

Technology	Projects Contracted		Projects Generating		Projects Terminated		Projects to be Commissioned		Completion Rates (%)	
	No	MW	No	MW	No.	MW	No	MW	No	MW
Wind	49	84.43	23	47.15	21	25.32	5	10.83	47	56
Hydro	12	10.86	7	10.05	-	-	5	0.81	580	93
Landfill gas	28	48.45	26	44.73	2	2.06	-	-	93	92
Waste Combustion	10	271.48	2	31.5	6	214.38	2	25.6	20	12
Other Combustion	4	30.15	1	12.5	1	8.45	2	9.2	25	41
Sewage gas	19	26.86	19	26.86	-	-	-	-	100	100
TOTALS	122	472.23	78	172.79	30	250.20	14	46.34	64	37

NOTE: TABLE 2 ALSO EXCLUDES A COLUMN FOR EXISTING PROJECTS. OF THE 122 PROJECTS, 25 WERE EXISTING WITH AROUND 37 MW DNC ALREADY GENERATING. MORE OR LESS ALL OF THE HYDO CONTRACTS WERE FOR EXISTING PROJECTS.

TABLE 3: 1994 NFFO CONTRACTS

Technology Band	Contracted Capacity MW DNC	Number of Projects	Lowest Contracted Price p/kWh	Weighted Average Price p/kWh	Highest Contracted Price p/kWh
WIND exceeding 1.6 MW DNC	145.92	31	3.98	4.32	4.8
WIND below 1.6MW DNC	19.71	24	4.49	5.29	5.99
HYDRO	14.48	15	4.25	4.46	4.85
LANDFILL GAS	82.07	42	3.29	3.76	4.00
MUNICIPAL and INDUSTRIAL WASTE	241.87	20	3.48	3.84	4.00
ENERGY CROPS & AGRICUL-TURAL & FORESTRY WASTE Gasification	19.06	3	8.49	8.65	8.75
Residual (Other)	103.81	6	4.9	5.07	5.23
TOTAL	626.92	141	-	4.35	-

SOURCE: DTI PRESS RELEASE, 1994, WARDLE MAKES THIRD RENEWABLE ENERGY ORDER, 20 DECEMBER.

TABLE 4: 1994 SRO 1 CONTRACTS

Technology Band	Contracted Capacity MW DNC	Number of Projects	Lowest Contracted Price p/kWh	Weighted Average Price p/kWh	Highest Contracted Price p/kWh
WIND	45.6	12	3.79	3.99	4.17
HYDRO	17.3	15	3.24	3.84	4.15
WASTE	3.8	2		(5 to 6)	
BIOMASS	9.8	1		(about 5)	
TOTAL	76.5	30			

Prior to the third NFFO (NFFO 3) the Government established the Renewable Energy Advisory Group (REAG) which reviewed the potential for Renewable Energy in the UK [3]. REAG recommended that longer term contracts would result in more competitive prices and suggested that the contract length should be closer to the maximum loan period that banks were prepared to contemplate. As a result, NFFO 3 contracts are of 15 years duration and may be taken up within five years of the contract being awarded. This 5 year 'period of grace' in which to obtain planning consent and construct a particular project also dealt with the second of the problems caused by the short contract term of NFFO 1 and NFFO 2. The 1998 end date had had a particularly serious impact on waste to energy projects where the time taken to obtain planning consent and negotiate construction and waste supply contracts meant all too often that there was too short a time left of the NFFO contract period to generate revenue sufficient to secure the investment required.

The new 15 year contract period now more closely matches the loan period (of typically 12 years) that banks are willing to offer for a limited recourse or non-recourse loan. Thus the repayments of principal and interest are a smaller percentage of the revenue and as a result prices bid in NFFO 3 and SRO 1 fell substantially and went a long way to dispel the image that electricity from renewables was expensive.

Table 5 (from reference 4) shows how this change in contract period coupled with reducing hardware costs lowered the winning bid prices.

The table shows that many of these technologies are now generating electricity at a price that is comparable to the 'embedded generation' value of electricity from conventional sources which has been estimated by some to be about 3.5p/kWh.

TABLE 5: NFFO PRICE FALLS

Technology	Technology Band Price 1991 NFFO p/kWh	Technology Band Price 1994 NFFO p/kWh (average)
Wind	11	4.32 (1.6 MW DNC +) 5.29 (under 1.6 MW dnc)
Hydro	6.00	4.46
Landfill gas	5.7	3.76
Waste Combustion	6.55	3.84
Other Combustion	5.9	5.07
Sewage Gas	5.9	-
AVERAGE	6.84	4.45

NOTE: [THE REDUCTION IN PRICE OF DIFFERENT TECHNOLOGIES (THE 'BAND PRICE') SHOWN IN TABLE 5 IS DUE TO THREE MAIN REASONS. FIRST, NFF03 CONTRACTS ARE FOR 15 YEARS RATHER THAN FOR 6-8 YEARS AS WITH NFFO1 AND NFFO2 CONTRACTS. THIS MEANS THAT CAPITAL REPAYMENTS ARE LESS PER kWh FOR NFFO3 CONTRACTS. SECOND, THERE HAS BEEN A MARKED FALL IN THE ECONOMIC COSTS OF RENEWABLE ENERGY TECHNOLOGY HARDWARE. THIRD, IT IS LIKELY THAT THE COST OF APPOINTING PLANNERS, LAWYERS AND OTHER INDIVIDUALS NECESSARY TO DEVELOP A PROJECT HAVE ALSO FALLEN AS THEY HAVE GAINED MORE EXPERIENCE.

THE 1996 COMPETITION FOR NFFO, SRO AND NI-NFFO

In March 1996, the Department of Trade and Industry (DTI) announced that the bids for nearly 900 projects had been received from potential generators of electricity from renewables for the fourth competition (NFFO 4) for England and Wales. Bids had been invited for seven renewable energy technologies and the results are shown in Table 6.

TABLE 6: EXPRESSIONS OF INTEREST BY RENEWABLE ENERGY TECHNOLOGY IN NFFO 4

Technology	Number	Capacity MW (DNC)
Landfill Gas	177	358
Waste Fired Combined Heat and Power	89	1982
Waste by Fluidised Bed Combustion	195	3801
Wind Power	227	1461
Hydro Power	79	40
Agricultural Waste by Anaerobic Digestion	34	48
Energy Crops by Gasification / Pyrolysis	89	707
Total	**890**	**8397**

The table shows that a staggering 227 wind energy projects were bid, representing 1461 MW (DNC), equivalent to about 3400 MW (nameplate) of turbines. By January 15, 1997, generators will be required to go firm on their bids and it is expected that the lowest bids will be awarded contracts sometime in the first quarter of 1997. The NFFO 4 order is expected to require the Regional Electricity Companies (REC's) to contract for 400 to 500 MW (DNC) of new capacity and the Government expects the prices to fall below those for NFFO 3. If this occurs, the price for wind will perhaps fall from its current NFFO 3 average (see Table 3) of 4.32 pence/kWh to less than 4 pence/kWh (about 6 cents/kWh). In a similar time scale, bids were received for the second Scottish Renewables Order (SRO 2) and the number of bids received for each technology is shown in Table 7.

TABLE 7: EXPRESSIONS OF INTEREST BY RENWEWABLE ENERGY TECHNOLOGIES IN SRO 2

Technology	Number	Capacity MW (DNC)
Wind	177	198.3
Hydro	46	43.8
Waste to Energy	19	105.2
Biomass	7	51.2
Total	249	398.5

Again, a huge number of 'expressions of interest' have been shown for wind energy with 177 projects amounting to 198.3 MW(DNC), equivalent to about 930 MW nameplate. It is expected that contracts will be issued (as in England and Wales for NFFO 4) in the first quarter of 1997 and that the total order will amount to about 50 MW (DNC) (i.e. about 116 MW nameplate).

The scope for the development of wind energy in Northern Ireland is likely to be limited. In the first Northern Ireland NFFO (NI - NFFO 1), six, 5 MW (nameplate) projects were awarded contracts. It is widely expected that a large waste to energy project will dominate the second set of contract awards and it is therefore unlikely that there will be more than six new windfarm contracts (amounting to no more than 30 MW nameplate) awarded.

Putting the English and Welsh (NFFO 4), Scottish (SRO 2) and Northern Ireland (NI - NFFO 2) orders together, it seems likely that an additional 600 MW (nameplate) of contracts for wind will be let. If a similar size of order is given in 1998/99, the total new market potential for the UK amount to about 1200MW by the year 2000. If two thirds of these fail (as the DTI assumes) because of planning and other difficulties, the actual market will amount to about 800 MW, equivalent to about 1300 - 600 kW rated turbines with a sales value of about US$525 to US$600 million and a total turnkey construction cost of between US$1.2 billion and US$ 1.5 billion.

THE MARKET IN IRELAND

The Irish Government in Dublin has itself created a market enablement mechanism for Renewable Energy and this has been called the Alternative Energy Requirement (A.E.R). In the first award under this scheme in March 1995, ten contracts for wind energy projects with a total nameplate rating of 73.5 MW were made with winning bid prices of about 6 to 6.5 cents/kWh. Not one of these projects has yet commenced construction, though two projects are said to be close to proceeding. One of these, a 15 MW project being developed by Scottish Power was awarded final planning approval by Donegal County Council in March but is currently awaiting the outcome of a last minute planning appeal. Another small 1.2 MW project at Arigna received planning approval in the second week of June 1996. Other projects are still in various stages of the planning process.

On 27 April 1996, the Irish Government announced a completely new long term strategy for renewables. The announcement said that the Government expected to secure electricity supply from an additional 100 MW of installed capacity from renewable energy sources by the end of 1999 and that it would allow third party access to the electricity network for Renewable Generators who wish to sell 'green' electricity directly to consumers. For wind energy, it has set a target of 30 MW (nameplate) of installed capacity each year for 1997, 1998 and 1999 to be procured through an annual competition. It is to offer capital grant aid of up to £65,000/MW installed. Contracts will be awarded through competitive bidding and the maximum price that will be paid is 4 pence/kWh (about 6 cents/kWh). The next competition will be in August 1996. A further target has been set to have 30 MW of wind capacity installed each year between 2000 and 2010 with an overall target of 470 MW of installed wind energy capacity by 2010. This is reportedly seen as a minimum target.

Another key element of strategy was the announcement that the Government is to examine the strategic impact of taxation on environmental policy and will bring forward specific tax measures for the 1997 Budget. It says that in this context it proposes in addition to the current Business Expansion Scheme eligibility, to pursue other fiscal measures to make investment in the renewables and energy efficiency sectors more attractive.

UK WINDFARMS UPDATE

A list of existing windfarms in the United Kingdom is given in Table 8.

TABLE 8: UK WIND FARM STATUS (AS AT 15 JUNE 1996)

Wind Project	Developer or Operator	Order No:	Start date	Turbine make	No.	Size (kW)	Wind farm capacity (MW)	Rough homes equivalent
Operating:								
Delabole, Cornwall	Wind Electric	1	Nov-91	Vestas	10	400	4	3,185
Haverigg, Cumbria	Windcluster	2	Aug-92	Vestas	5	225	1.125	896
Carland Cross, Cornwall	Renewable Energy Systems	2	Aug-92	Vestas	15	400	6	4,778
Cemmaes, Powys	National Wind Power	1	Nov-92	WEG	24	300	7.2	5,734
Blood Hill, Norfolk	Euros Power	2	Dec-92	Vestas	10	225	2.25	1,792
Chelker Reservoir, Yorkshire	Yorkshire Water Services	1	Dec-92	WEG	4	300	1.2	956
Rhyd-y-groes, Anglesey	EcoGen	2	Dec-92	Bonus	24	300	7.2	5,734
Blyth Harbour, Northumberland	Border Wind	2	Jan-93	WindMaster	9	300	2.7	2,150
Great Orton, Cumbria	Carter Wind Technology	2	Jan-93	Carters	10	300	3	2,389
Llandinam	EcoGen	2	Jan-93	Mitsubishi	103	300	30.9	24,608
Coal Clough, Lancashire	Renewable Energy Systems	2	Feb-93	Vestas	24	400	9.6	7,645
Cold Northcott, Cornwall	National Wind Power	2	Apr-93	WEG	21	300	6.3	5,017
Goonhilly Downs, Cornwall	Cornwall Light and Power	2	Apr-93	Vestas	14	400	5.6	4,460
Llangwyryfon, Dyfed	National Wind Power	2	Jun-93	WEG	20	300	6	4,778
Ovenden Moor, Yorkshire	Yorkshire Windpower	1	Jun-93	Vestas	23	400	9.2	7,327
Taff-Ely, Mid Glamorgan	East Midlands Electricity	2	Aug-93	Nordtank	20	450	9	7,167
Kirkby Moor, Cumbria	National Wind Power	1	Sep-93	Vestas	12	400	4.8	3,823
Royd Moor, South Yorkshire	Yorkshire Water Services	2	Dec-93	Bonus	13	450	5.85	4,659
Bryn Titli, Powys	National Wind Power	2	Jul-94	Bonus	22	450	9.9	7,884
St Breock, Cornwall	EcoGen	2	Jul-94	Bonus	11	450	4.95	3,942
Caton Moor, Lancashire	New World Power	2	Dec-94	WindMaster	10	300	3	2,389
Dyffryn Brodyn, Dyfed	New World Power	2	Dec-94	Nordtank	11	500	5.5	4,380
Corkey, Antrim	B9 Energy Services	NI 1	Mar-95	Nordtank	10	500	5	3,982
Four Burrows, Cornwall	New World Power	2	Mar-95	Bonus	15	300	4.5	3,584
Rigged Hill, Limavady	B9 Energy Services	NI 1	Mar-95	Nordtank	10	500	5	3,982
Elliot's Hill, Antrim	B9 Energy Services	NI 1	Apr-95	Vestas	10	500	5	3,982
Bessie Bell, Tyrone	Colham Energy	NI 1	Oct-95	Vestas	10	500	5	3,982
Hagshaw Hill(S10),Lanarkshire	Trigen	SRO1	Nov-95	Bonus	10	600	5.9	4,699
Hagshaw Hill(S15),Lanarkshire	Trigen	SRO1	Nov-95	Bonus	15	600	9.4	7,486
Slieve Rushen, Fermanagh	Sean Quinn Group	NI 1	Dec-95	Vestas	10	500	5	3,982
Trysglwyn, Anglesey	National Wind Power	3	Apr-96	Bonus	14	400	5.6	4,460
Total Commissioned					505		195.68	155.83
Under construction								
Werfa, Mid Glamorgan	Windstar Turbines	2	-	Wind Harvest	20	25	0.5	398
CarnoA, Powys	National Wind Power	3		Bonus	28	600	16.8	13,379
CarnoB, Powys	National Wind Power	3		Bonus	28	600	16.8	13,379
Siddick, Cumbria	Windcluster	3			7	600	4.17	3,321
PolwhatRig, Kirkcudbrightshire	National Wind Power	SRO1		Nordtank	18	600	10.8	7,796
Gallow Rig, Kirkudbrightshire	National Wind Power	SRO1		Nordtank	18	600	10.8	7,796
Awaiting construction								
Bendealt, Ross-shire	National Wind Power	SRO1					8.81	7,016
MeallanTuric, Ross-shire	National Wind Power	SRO1					7.84	6,243
Rheidol, Dyfed	PowerGen	3					2.33	1,856
Laggan, Islay	Windcluster	SRO1					2.98	2,373
Largie, Kintyre	Trigen	SRO1					14.86	11,834
Kirkstanton Airfield,Cumbria	Windcluster	3			4	600	2.98	2,373
Oldside, Cumbria	Windcluster	3			9	600	5.36	4,269
Harlock Hill,Cumbria	The Wind Company Ltd	3					3.46	2,755
Llanbabo	MANWEB/Kenetech	3					25	

About 20 other windfarms with NFFO 3 and SRO 1 contracts are in various stages of the planning process whilst about 30 others with NFFO 3 contracts are recorded as having 'planning applications not yet submitted or status unknown'.

CRITICISMS OF THE NFFO MECHANISM

It is generally accepted that the NFFO/SRO mechanism has been extremely successful in driving down the prices of wind generated electricity to the lowest anywhere in Europe. Unfortunately, the intense competition results in the exploitation of the highest wind speed sites, and these often coincide with areas valued for their scenic beauty. This has resulted in about 15 Public Inquiries for specific projects and what is perceived as increasing opposition from some quarters. The low winning bid prices means that lower wind speed sites (often at least as good as those that are being developed elsewhere in Europe) are not favoured.

The 'tranche' system, which requires a competitive bidding process at a given time results in flurries of activity, interspersed with long periods of inactivity. This causes problems for local authorities as well as developers, manufacturers and others in the industry. For the wind industry, the stop-start nature of the process has meant it has been difficult to support project development teams through long periods of inactivity. The extraodinarily competitive nature (i.e. over 400 projects with nameplate rating of over 3800 MW registered for NFFO 4 and SRO 2) means there is less than a 1 in 6 chance of being awarded a contract.

Combining this low probability of success with a 1 in 3 (or greater) chance of failing to obtain planning consent and/or finance results in the developer having about a 1 in 10 chance of being awarded a contract for a project that eventually gets built. This implies a fairly substantial high risk investment in the development process and this has already resulted in many organisations withdrawing from the business. The mechanism has also been criticised by some because of its failure to encourage a British Wind Turbine Manufacturing Industry. The competitive nature of the process is such as to give advantage to established wind turbine suppliers. As a result, UK windfarms have been supplied by 7 different manufacturers, only two of which are UK based. The others are Danish (3), Japanese (1) and Belgian (1). Less than 14% of the UK's operational turbines have been made in the UK and only the Wind Energy Group and Carter remain as UK manufacturers.

There is also some concern that the price has been driven to such a low level that margins are too small to support refurbishment and major maintenance of the plant in the second half of its expected life. The price levels of the bids themselves are mostly driven by the rate of return requirements of the investors and this to a large extent explains why most investors in UK windfarms are major 'blue-chip' lowly geared companies, many of which are already in the electricity generation and distribution business.

For this and other reasons, the UK has so far got no 'community' owned windfarms such as exist in Germany and Denmark where windmill guilds, cooperatives and individuals own the majority of the 1750 MW of wind turbines that exist in those two countries (5, 6).

CONCLUSIONS

The creation of the Non Fossil Fuel obligation and similar schemes in Scotland and Northern Ireland as market enablement mechanisms for Renewable Energy in the UK has proved successful in driving down prices of electricity from wind energy. The highly competitive nature of the bidding process combined with its cyclical nature has so far however inhibited the development of wind energy at anything other than high altitude high wind speed sites and has already driven many developers and investors out of the business.

Some modification to the market enablement structure is now needed to encourage development at lower wind speed sites and to encourage a wider spread of ownership. The total potential market for the UK and Ireland to the year 2000 is likely to approach 1300 MW of which it is estimated that about 800 to 900 MW will be constructed unless the planning environment deteriorates.

REFERENCES

1. THIRD RENEWABLES ORDER FOR ENGLAND AND WALES, published by Office of Electricity Regulation, November 1994.

2. FIRST RENEWABLES ORDER FOR SCOTLAND, published by Office of Electricity Regulation, November 1994.

3. Renewable Energy Advisory Group (REAG): Report to the President of the Board of Trade, November 1992, Energy Paper Number 60, HMSO, ISBN 0-11-414287-4.

4. Mitchell, C., "Renewable Energy in the U.K." - Financing Options for the Future, a paper for the Council for the Protection of Rural England, August 1995, ISBN 0 946 044 15 5.

5. Lindley, D., (1996) 'Financing the U.K.'s Renewable Energy Boom', Int. Journal of Global Energy Issues, vol. 8, Nos. 5/6.

6. Lindley, D., (1996) 'A study of the Integration of Wind Energy into the National Energy Systems of Denmark, Wales and Germany as illustrations of success stories for Renewable Energy'. Proc. of 1996 European Union Wind Energy Conference, 20 - 24 May, Goteborg, Sweden. To be published by H.S. Stephens, U.K.

Large Wind Turbine Development in Europe

Prof. Arthouros Zervos
Center for Renewable Energy Sources
19 klm Marathonos Avenue
19009 Pikermi, Attikis
Greece

ABSTRACT

During the last few years we have witnessed in Europe the development of a new generation of wind turbines ranging from 1000-1500 kW size. They are presently being tested and they are scheduled to reach the market in late 1996 early 1997. The European Commission has played a key role by funding the research leading to the development of these turbines. The most visible initiative at present is the WEGA program - the development, together with Europe's leading wind industry players of a new generation of turbines in the MW range. By the year 1997 different European manufacturers will have introduced almost a dozen new MW machine types to the international market, half of them rated at 1.5 MW.

STRATEGIES AND TRENDS OF EUROPEAN TECHNOLOGY

Wind Energy has created an important new market. The total installed European capacity 5 years ago was limited to a few hundred MW while in spring 1996 had exceeded 2500 MW. At the same time quality was dramatically improved and prices have come down and are currently slipping below $1.100/kW for turn key installations.
On the other hand the size of commercially available grid connected horizontal axis wind turbines has evolved from 50 kW in the early 80's to 500 to 800 kW today.

Wind energy technology has developed tremendously over the last decade. At the same time the European industry has reached a certain level of technological matureness and competitiveness. European Union and National R, D and D programs played an important role in this direction.

Some highlights of European trends are shown in Table 1. This global picture of the European situation shows an impressive technical improvement : on average European machines produced 1700 kWh per kW installed in 1994 while in 1986 only 580 kWh per kW were produced. This trend is confirmed for the 20 top machines: in 1986 the best machines had a specific energy production between 800 and 1200 kWh per m2 and year, in 1994 1800 kWh per m2 were reached by the very best ones.

R&D, which was by and large industrially based, contributed to this improvement in quality and a reduction in the cost of wind turbines: efficiency, reliability, availability and noise have been greatly improved and machines have become simpler and lighter.

Table 1

Trends in Turbine Sizes		
1977/78		± 10kW unit size
1984/85		± 100kW unit size
1996/97		± 1500kW unit size
Trends in Quality (kWh m^{-2} a^{-1})		
	20 Top machines	Europ. average of all machines
1986	800-1200	± 200 (580 kWh a^{-1} per kW)
1994	1400-1800	± 680 (1700 kWh a^{-1} per kW)

Many different design concepts are in use, the most used being three bladed, stall or pitch regulated, operating at near fixed rotational speed. However, there was also at least one technological breakthrough, i.e. the gearless turbine introduced by Enercon in Germany at the beginning of the 1990's. These new direct drive generators have become an important target for research and technological innovation in Europe with the aim of exploring all possible modifications to the basic concept.

Much emphasis in European R&D is also devoted to the improvement of blades, better profiles and new materials.

A central issue in development is the increase in size. Large-size machines are desirable mainly because they permit a better exploitation of wind in a given land area: doubling the turbine diameter from 25 to 50 m will approximately double the energy yield of the location. Larger machines also offer economic savings in production and grid connection and are easier to operate and maintain. These savings largely offset the greater complexity of transport and erection of large machines.

The range of sizes is a critical issue. During the 1980's when commercial turbines had a diameter of not more than 20m, leading R&D programs in the US and Germany were focusing on much larger machines up to 100m in diameter. Today we know that the MOD and GROWIAN projects failed as they were premature and their diameters were excessive. Instead, the trends observed over the last few years were a diameter increase from 20m (100 kW+/-) to 40m (500 kW - today's leading machines in the commercial market). This trend will continue over the next 2 or 3 years up to 66m diameter (+/- 1,5 MW).

Only in the longer term we will know if there can be 80 or 90m diameter multi MW machines. That will rather remain as an interesting question for technological strategy beyond the year 2000.

THE EUROPEAN COMMISSION'S WEGA PROGRAMS

WEGA I was initiated by the Directorate General XII for Science Research and Development (DG XII) of the European Commission in the mid 1980's. Three machines were developed, two of 60m diameter, one of 55m. They were erected in 1988/89, one in Tjaereborg (DK) on the North Sea coast, one at Cabo Villano (Spain) on the Atlantic coast and one at Richborough in England, also on the North Sea coast. With specific towerhead masses of 111 kg/kW, 153 kg/kW and 83 kg/kW respectively they were too heavy and consequently not economical. Nevertheless the WEGA I program can be considered a success. It's goal was not the development of commercial machines but an experimental exploration. [1]

The program lead actually to the following results:

- a good knowledge of the problems involved in MW size machines. A detailed investigation carried out on behalf of DG XII reviewed the critical design elements and concluded that weight and cost of all 3 turbines could have been reduced by between 30 and 45%.
- a subsequent study by a European team, relating to the principles of MW machines, established a clear analysis of the scope for the next development step, the WEGA II program [2].
- the sites in Denmark and Spain have become centres for broader wind development, e.g. wind farms were installed later in Cabo Villano, while Tjaereborg hosted new innovative prototypes.

At the beginning of the 90's a certain number of large wind turbines ranging from 750 kW to 3 MW were installed in several European countries (Table 2). They tried to avoid the mistakes of the past, to introduce innovative elements and to reduce the weight.

Table 2 : Large Wind Turbines in Europe
installed in 1992-1993

Manufacturers	Rated Power (kW)	Diam (m)	Number of blades	Power Control	Generator	Head Weight (tons)	Total Weight (tons)
Kvaerner Turbin AB	3000	80	2	pitch	induction	162	1661
MBB-(AEOLUS II)	3000	80	2	pitch	synchronous	162	1562
WEST-(Gamma 60)	1500	60	2	yaw	synchronous	110	231
HMZ/Windmaster	1200	45	2	stall + pitch	induction	98	200
Husumer Schiffswerft	750	46	3	pitch	induction	-	-

At the same period the WEGA II program was initiated by DG XII of the European Commission. The overall cost of the program is approximately 25 Mio ECUs. Most machines are already installed.[3] The sizes of machines are about the same as those in WEGA I. However, there are many improvements which can be seen on Table 3.

Table 3 :New Generation of Large Wind Turbines in Europe
(installed after 1994)

Manufacturers	Rated Power (kW)	Diam (m)	Number of blades	Power Control	Generator	Head Weight (tons)	Total Weight (tons)
Enercon*	1500	66	3	pitch	synchronous; direct drive	100	220
Nordtank**	1500	60	3	stall	induction	98	193
Tacke	1500	65	3	pitch	induction	97	237
Vestas***	1500	63 (or 57)	3	pitch	induction variable slip10%	76	156
Husumer Schiffswerft**	1000	54	3	pitch	induction	73	161
NedWind***	1000	52.6	2	stall + pitch	induction	65	110
Nordex (NW53)	1000	52.6	3	stall	induction	74	164
Nordic Wind Power*	1000	53	2	stall	induction	42	93
Bonus*	750	50	3	stall	induction	59	107

*supported by Joule **supported by THERMIE ***supported by JOULE and THERMIE

They can be summarized as follows:

- the work is carried by Europe's leading industry which is more motivated and experienced in innovation and developement than were most of the organizations involved in WEGA I.
- there is reasonable involvement of electric utilities to address the problem of grid integration.
- there is a larger number of machines and a much wider range of different technologies and concepts than in WEGA I. All together, there is a unique richness and a variety of new approaches which only a broad European dimension and the corresponding EU program could deliver.
- this time the outcome is very positive in terms of weight, technological quality and cost prospects. Virtually all machines have lower "towerhead" masses than the best of the WEGA I turbines, one as low as 42 kg/kW. The prototypes of WEGA II will be used to solve teething problems. Some of them will lead directlly to commercialization as early as the end of 1996.
- eventually the WEGA II machines can play the same role as WEGA I did for future developments: a broad and extensive measuring and monitoring program is being carried out on all machines in the frame of a Commission contract. WEGA II will not

only strengthen European wide understanding and agreements towards norms and standards, but also lay the ground for still further developments in what could become WEGA III.

Eventually WEGA II became the European pilot program and trend setter for MW turbines in as much as most leading European manufacturers followed in this direction. As Table 3 shows the European Commission is currently funding three 1.5 MW turbines and three 1 MW turbines. As part of the Joule program they are either official parts of WEGA II or at least involved in the WEGA II monitoring project.

As mentioned already, others have followed : Tacke has completed a 1.5 MW turbine and Nordex and HSW are each completing a 1.0 MW turbine. All in all we currently see the completion of 9 different turbines in the MW range from Europe's leading industry, four 1.5 MW turbines and four 1 MW ones.

From all the above we can conclude that wind energy in Europe has not only been a tremendous recent commercial success but has also seen an impressive development of technology innovation especially in the large wind turbine sizes.

REFERENCES

1. E. Hau, J. Langenbrinck, W. Palz: 'WEGA Large Wind Turbines', Springer Verlag, 1993.
2. 'Design and Costs of Large Wind Turbines - Study on the next generation of large wind turbines', Commission of the European Communities, JOUR-0011-D (AM), to be published in 1996.
3. 'WEGA II Large Wind Turbine Scientific Evaluation Project', Commission of the European Communities, Directorate-General XII for Science, Research and Development, EUR 16902 EN, April 1996.

STATUS REPORT OF WIND ENERGY PROGRAM IN THE PHILIPPINES

Pio J. Benavidez
National Power Corporation
Agham Road corner Quezon Avenue, Quezon City, 1100
Philippines

Abstract

This paper discusses the wind resource assessment activities being undertaken by the National Power Corporation at the extreme northern part of Luzon island. Preliminary results from the 10-month wind data are presented. This will give prospective wind developers an idea on the vast resources of wind energy available in the northern part of the country. This paper will also discuss briefly the stand-alone 10 kW wind turbine system that was commissioned early this year and the guidelines being drafted for the entry of new and renewable energy sources in the country's energy generation mix.

1.0 Overview

The Philippines has joined international efforts in harnessing wind for power generation along with other clean sources of energy. The government has made one of its priorities the development and utilization of renewable energy sources, as enunciated in the country's Energy Plan.

In 1995, the National Power Corporation (NPC) in cooperation with the Department of Science and Technology has launched an extensive wind resource assessment for large scale wind park in northern Luzon island particularly Ilocos Norte. As of July 1995, seven (7) multi-level wind monitoring stations were set-up to measure and record wind speeds and direction.

NPC has successfully commissioned a 10 kW Bergey Excel-R wind turbine situated in a remote fishing village in Ilocos Norte. This project will undergo 2 years performance monitoring to demonstrate the technical and economic viability of harnessing wind energy for power generation. NPC personnel are expected to gain experience in the installation, operation and maintenance of the wind turbine machine.

The guidelines which will pave the way for participation of the private sector in power generation using new and renewable energy sources (NRES) is being drafted by NPC. The ultimate goal is to have installed 300 MW of generating capacity from NRES by year 2003.

2.0 Wind Resource Assessment Activities in Northern Luzon

Documentation of the Philippine wind resources has indicated that the extreme northern Luzon is potentially a very attractive site for wind power generation. In July 1995, NPC launched an extensive wind resource assessment project for large scale wind park in Ilocos Norte, about 500 kilometers north of Manila. A total of seven (7) 30-meter multiple level wind monitoring stations were set up encompassing the municipalities of Burgos, Bangui and Pagudpud. The sites, stretching about sixty-five (65) kilometers of coastline at the northwestern corner of Luzon, are characterized by ridgelines, mountains, gently rolling plains and some plains at the lowlands. A load-end substation rated at 50 MVA, 115/69 KV is situated in Laoag City, approximately 35 km south of Burgos and 75 km south of Pagudpud. The nearest utility grid to the sites is the 13.2 kv distribution line owned by the local electric cooperative. NPC is currently constructing a new transmission line going to Laoag Substation with a rated capacity of 150 MVA. Location map is presented in Figure 1.

At present, there are 10 months of wind data collected from wind monitoring stations in Ilocos Norte. The mean wind speeds during northeast monsoon (October - April) are far stronger and consistent compared to the mean wind speeds during southwest monsoon (May - September). Table 1 shows the monthly mean wind speeds.

Considering the wind data collected at Subec, Pagudpud, the highest monthly mean wind speed was recorded on December 1995 at 32 mph. Figure 2 shows the distribution of wind speeds at Subec site from June 1995 to March 1996. It is anticipated that a typical 225 kW wind turbine installed at the site would be able to operate 1462 hours at rated capacity. The total wind kinetic energy is computed by multiplying the power of the wind per square meter of cross section for each bin with the number of hours of wind in that bin. Using that formula, Subec site had 6,184 kwh of wind energy per square meter. Figure 3 shows the wind energy at Subec site.

3.0 10 kW Bergey Excel-R Wind Turbine

The 10 kW wind turbine generator is a stand-alone system that supplies electricity to a remote community, small fishing village of 23 rural houses, in Pagudpud, Ilocos Norte, approximately 80 km northeast of Laoag City. The project consists of the following: 10 kW Bergey Excel-R wind turbine generator mounted on top of a 24 m lattice tower, voltage system controller, DC control panel, 700 AH deep cycle lead acid batteries, 10 kVA static inverter and the associated transmission lines. The WTG is located about 800 meters from the fishing village, its load center. The load is composed of compact fluorescent lamps and small appliances. Figure 4 shows the schematic diagram of the stand-alone WTG.

The mini power plant was commissioned on March 1996. It will undergo (2) years testing and performance monitoring to demonstrate the technical and economic viability of harnessing wind

energy for electricity production. The plant is being operated by four (4) technical personnel shifting every 8 hour daily. Recording of the wind speeds and direction, system voltage, frequency, energy consumption and specific gravity of the battery cells are done on hourly basis to monitor the performance of the plant. It is also equipped with automatic data acquisition system which monitors the wind speeds and direction, system voltage and power output of the wind turbine generator.

4.0 New and Renewable Energy Sources (NRES)

NPC is opening a window for the entry of 50 MW per year of NRES starting the year 1998. Its objectives are to support the establishment of renewable energy power project that could be economically added into the grid, to sign a long-term power purchase agreement (PPA) with a broad spectrum of renewable energy technologies, and to supplement petroleum-based generation in small islands with indigenous NRES technologies. A total of 300 MW of generating capacity from NRES is expected to have been installed from 1998 - 2003. Solicitation of proposal will start from 01 July and end on 01 December 1996.

Table 1

Mean Wind Speed in Ilocos Norte

(in Miles per Hour)

Monitoring Period	Burgos				Bangui	Pagudpud	
	Bayog*	Pagali*	Saoit*	Agaga*	Bangui**	Caparispisan*	Subec*
Jan-95							
Feb-95							
Mar-95							
Apr-95							
May-95							
Jun-95	10.3		9.7	13		11.7	8.9
Jul-95	8.8	8.7	8.2	10.7	8.8	9.6	7.9
Aug-95	7.3	7.7	6.4	8.2	7	10	8.3
Sep-95	11.4	13.4	9.9	11.2	10	14.5	13
Oct-95	16.7	20.4	14.3	16.1	14.9	18.9	18.9
Nov-95	22.7	25.3	18.2	20.4	19.4	22.8	25.7
Dec-95	27.7	28.8	22.4	25.9	25.1	26.6	32.1
Jan-96	18.5	20.5	14.8	14.8	14.8	22.4	23.6
Feb-96	21.2	22	17.2	18.3	18.2	22.7	24.8
Mar-96	13.4	14.1	10.8	10.3	10.9	17.5	16.2
Apr-96							
May-96							
Jun-96							
Jul-96							
Aug-96							
Sep-96							
Oct-96							
Nov-96							
Dec-96							

Note: * - data taken @ 30 m height tower
** - data taken @ 20 m height tower

Figure 1 - LOCATION MAP

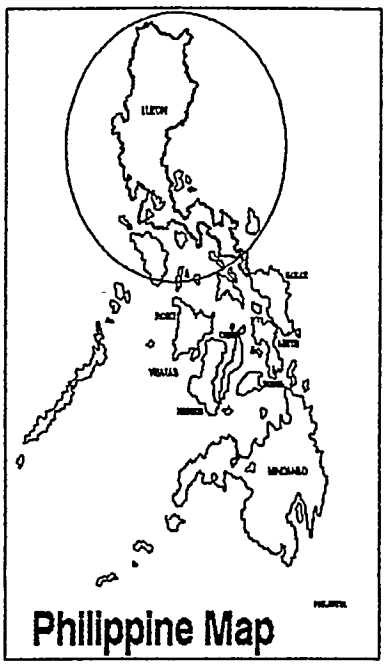

Ilocos Norte

Luzon Island

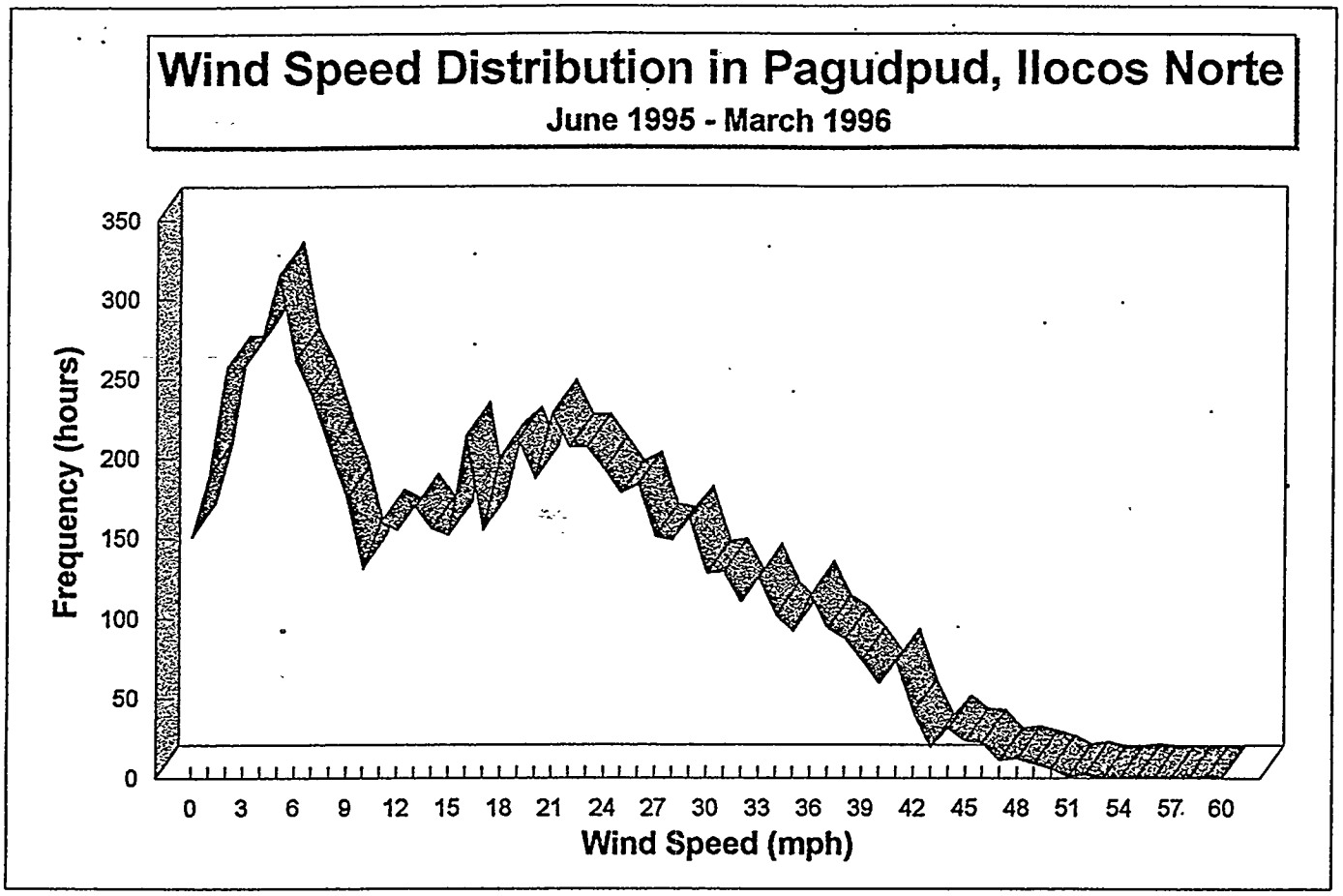
Wind Speed Distribution in Pagudpud, Ilocos Norte
June 1995 - March 1996
Frequency (hours)
350
300
250
200
150
100
50
0
0 3 6 9 12 15 18 21 24 27 30 33 36 39 42 45 48 51 54 57 60
Wind Speed (mph)

Figure 2

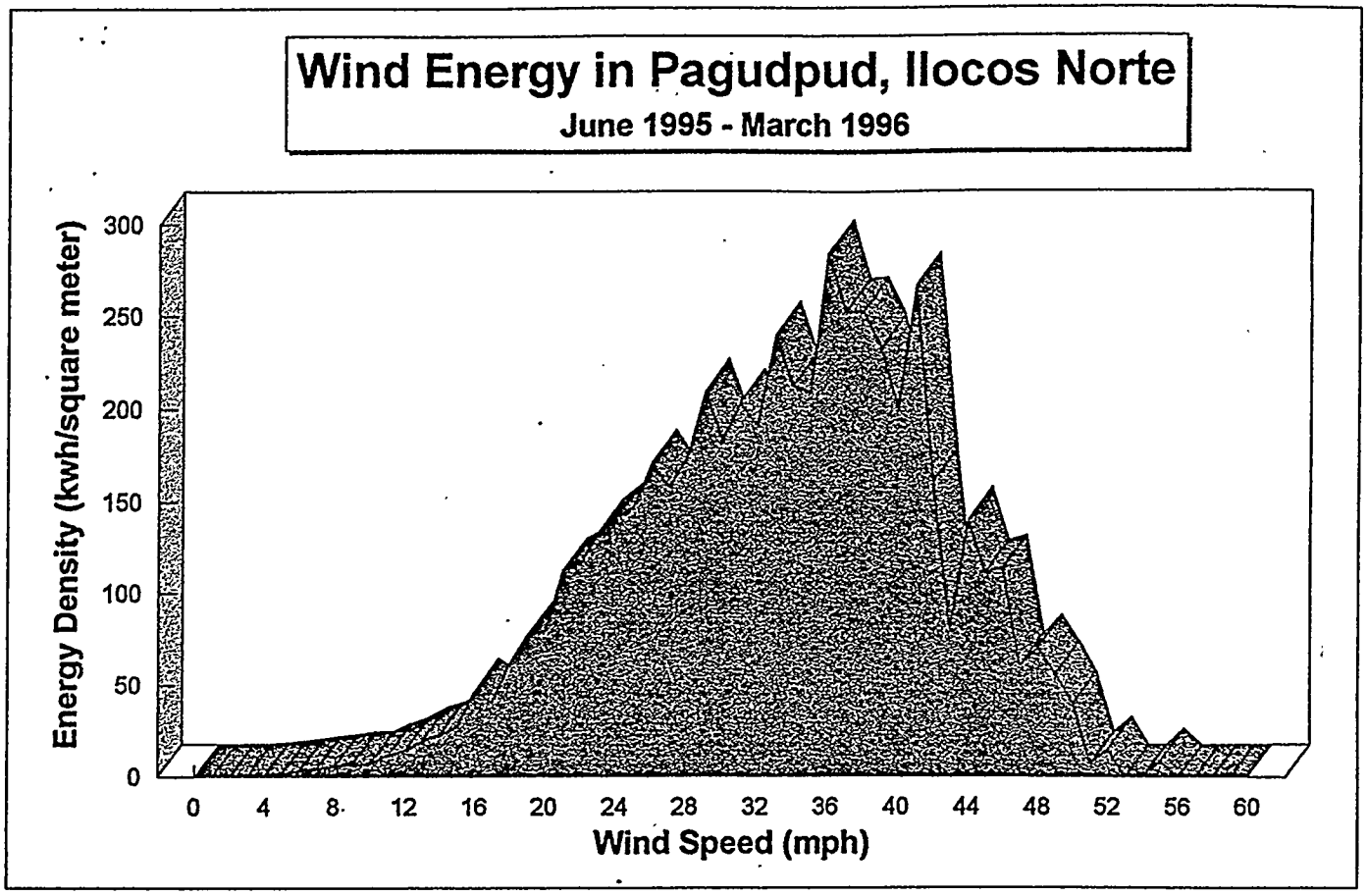
Wind Energy in Pagudpud, Ilocos Norte
June 1995 - March 1996
Energy Density (kwh/square meter)
300
250
200
150
100
50
0
0
4
8
12
16
20
24
28
32
36
40
44
48
52
56
60
Wind Speed (mph)

Figure 3

10 kW Remote Power System

Pagudpud, Ilocos Norte, Philippines

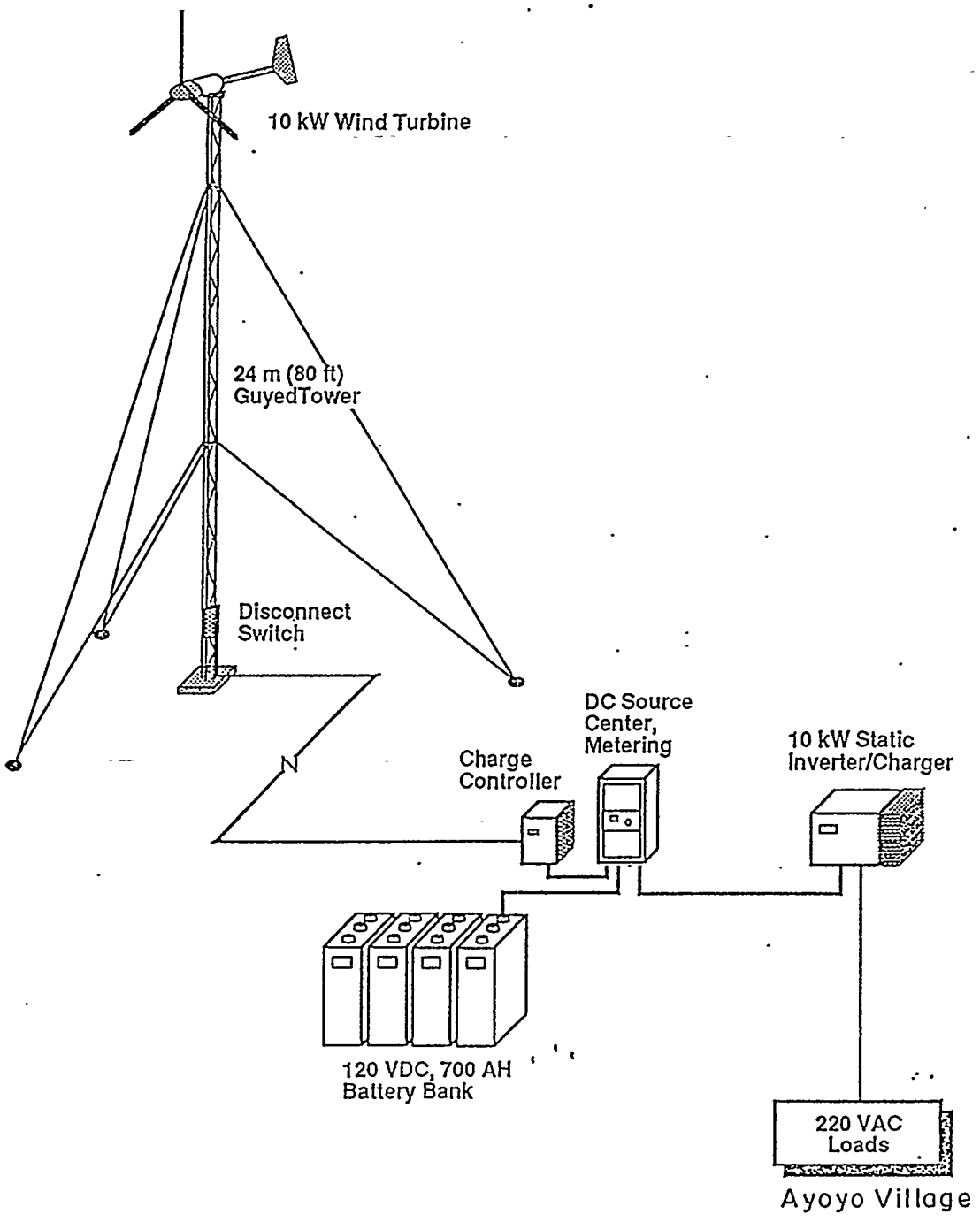

Figure 4

POTENTIAL MARKET OF WIND FARM IN CHINA

Pengfei Shi
New Energy Division
Hydropower Planning General Institute
3 Yiqu Zhongjie, Liupukang, Beijing 100011
CHINA

ABSTRACT

Wind energy resources are abundant in China, in southeast coast area along with the rapid economic growth, electricity demand has been sharply increased, due to complex terrain detailed assessments are in urgent need. Advanced methodology and computer model should be developed. In this paper the existing wind farms, installed capacity, manufacturers share and projects in the near future are presented. For further development of wind farm in large scale, different ways of local manufacturing wind turbine generators (WTG) are going on. Current policy and barriers are analyzed.

WIND ENERGY RESOURCE

Estimated by the Chinese Academy of Meteorological Science, wind energy potential near surface ground in China is 253 GW. This data reflects the total amount of wind energy technically available to be utilized, without consider the social and economical conditions. Provinces and Autonomous Regions favorable to wind farm construction are located in southeast coast areas and north of inland China, see Fig.1.

Along the coastal areas of southeast China, for lack of coal mine and oil resources, the fuel for thermal power plants have to be transport from far away. Hydro-power resources in Zhejiang and Fujian province have been fully exploited, due to autumn and winter are dry seasons, hydro-power generation reduced. However, wind is very strong in these seasons, so losses of hydro-power could be compensated by wind power. Many windy sites with annual average wind speed over 7 m/s are found in coastal areas and nearby islands.

In addition, Guangdong, Fujian and Zhejiang are more open to the outside world. During last decade the highest economic growth rate has been achieved in this region and the demand of electric power has sharply increased. High price of electricity could be afford by many enterprises. Hundreds MW of diesel generators were installed to ease the tension of power supply, which makes wind power more attractive in competition.

TABLE 1 WIND ENERGY POTENTIAL FAVOURIBLE FOR WIND FARM IN SOME PROVINCES

Province	Wind Potential (MW)	Province	Wind Potential (MW)
Inner Mongolia	61 780	Shandong	3 940
Xinjiang	34 330	Jiangxi	2 930
Heilongjiang	17 230	Jiangsu	2 380
Gansu	11 430	Guangdong	1 950
Jilin	6 380	Zhejiang	1 640
Hebei	6 120	Fujian	1 370
Liaoning	6 060	Hainan	640

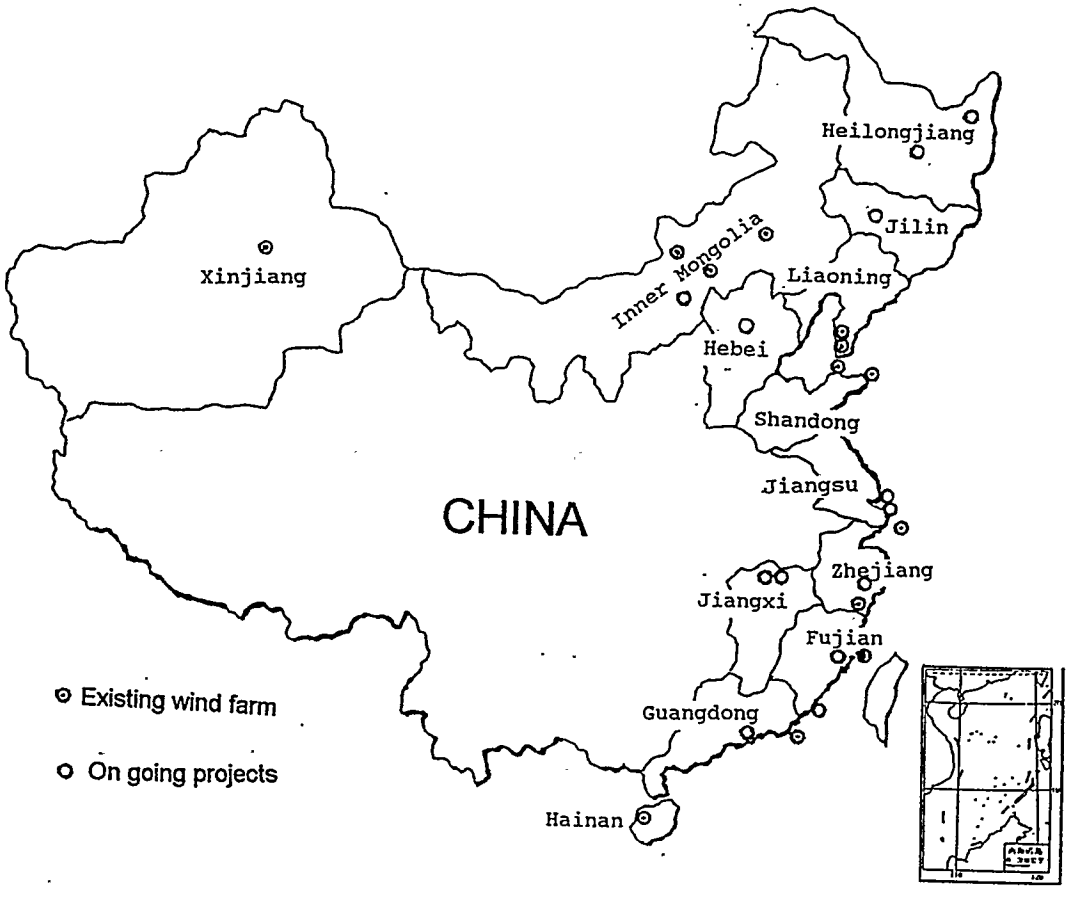

FIG. 1 PROVINCES IN CHINA FAVORABLE TO WIND FARM

In northwest of China there are many sites located in vast and flat terrain with annual mean wind speed over 6 m/s. These sites are suitable for large wind turbine generators, such as Dabancheng windy site in Xinjiang Autonomous region, where 1000 sq. km of areas are available for wind farms; Huitengxile site in Inner Mongolia Autonomous Region with 300 sq. km land ready for wind farm construction. More good sites could be found along with the further macro siting.

The study on wind potential that could be economically exploited is a vital issue in the implementation of wind energy programs. The government intends to raise more allocated funds for the detailed survey of wind energy resource.

New macro siting methods are being developed by the National Renewable Energy Laboratory (NREL) of U.S.A.. A computer based map of the favorable wind resource areas superimposed on the hill-shaded relief map, has been produced by the wind resource assessment team at the NREL, for the Nan'ao Island Wind Farm Case Study supported by the World Bank. The map provide a comprehensive guide to siting viable wind farms on the island. The comparison between real site survey and computer-based map has been made and the results are satisfactory.

EXISTING WIND FARMS

By the end of 1995 the installed capacity of grid connected wind turbine generators (WTG) had

TABLE 2 EXISTING WIND FARM SITES IN CHINA
AND INSTALLED CAPACITY BY END 1995

No.	Site	Province	Installed kW	No. of units
(1)	Dabancheng	Xinjiang	12 750	47
(2)	Nan'ao	Guangdong	8 680	43
(3)	Zhurihe	Inner Mongolia	4 200	28
(4)	Shangdu	Inner Mongolia	3 875	17
(5)	Donggang	Liaoning	1 555	6
(6)	Cangnan	Zhejiang	1 255	4
(7)	Pingtan	Fujian	1 055	6
(8)	Hengshan	Liaoning	1 000	4
(9)	Xilin	Inner Mongolia	1 000	4
(10)	Shengsi	Zhejiang	426	15
(11)	Rongcheng	Shandong	165	3
(12)	Changdao	Shandong	110	2
(13)	Dongfang	Hainan	55	1
	Total		36 126	180

been up to 36 MW. The details on the existing wind farms and manufacturers market share are shown in Table 2, Table 3, the development of installed capacity during past 10 years see Fig. 2.

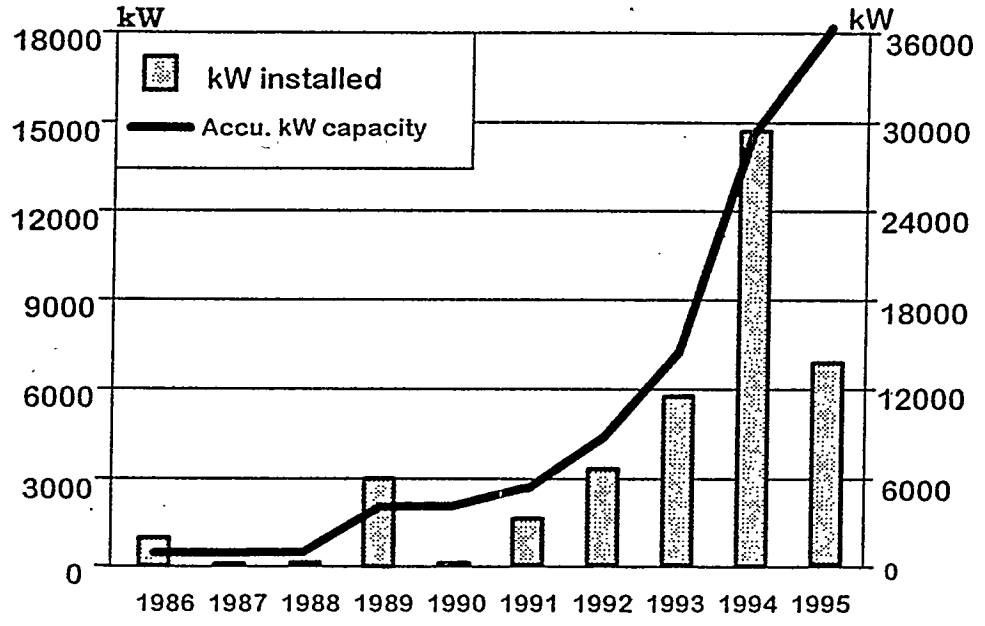

FIG. 2 INSTALLED CAPACITY IN CHINA DURING 1986-1995

The current largest wind farm was constructed at Dabancheng of Xinjiang Autonomous Region. It is the first one with the capacity over 10 MW, and also with the biggest machine 500 kW WTG installed. This wind farm was initiated with the aid from Danish Government, and later continue the development by using foreign soft loan. The Regional authority agreed to purchase electricity generated by wind at the rate of 0.87 Yuan/kWh, in order to pay back bank loan within the period of 8-10 years.

Better economic benefits have been achieved in Nan'ao wind farm, Guangdong Province. Nan'ao is an island county, very rich in wind energy potential, more than 8 m/s of annual average wind speed has been recorded on site. The government of Nan'ao County paid more attention on wind power generation, the planning of wind farm construction was initiated in 1985, as the first phase two 150 kW and one 90 kW wind turbine generators were erected and connected to power grid in June 1989. Based on this demonstration project, 40 machines were installed in following years, totaled 8680 kW by the end of 1995.

TABLE 3 MANUFACTURERS MARKET SHARE IN 1995

Company	Nordtank	Bonus	Nordex	Husumer
Country	Denmark	Denmark	Denmark	Germany
Installed kW	18 790	6 350	4 000	3 000
Share	52.0 %	17.6 %	11.1 %	8.3 %

Company	US Windpower	Chinese	Windmaster	Newind
Country	USA	China	Belgium	Sweden
Installed kW	1 100	1 076	800	390
Share	3.0 %	3.0 %	2.2 %	1.1 %

Company	Aeroman	Vestas	Micon
Country	Germany	Denmark	Denmark
Installed kW	300	220	100
Share	0.8 %	0.6 %	0.3 %

Good performance has been shown during operation, the average capacity factor of Nan'ao wind farm is 30.8%. In 1995 total wind power generation up to 12.3 million kWh, equivalent to 44% of total power consumption of the whole county, this figure shows the important role of wind farm in island economy
development and daily life of islanders. Electricity sold to power company at the rate of 0.70 Yuan (USD 0.084) per kWh, it is the same as the nearby oil thermal power plant on mainland, a reasonable profit has been obtained for further development.

Inner Mongolia is rich in wind energy potential, there are three wind farms with 9MW in total are in operation, another new site, Huitengxile, the most promising one with vast area of flat terrain, available to install 400 MW of WTGs and the local grid which has already been connected to the very strong North China Power Network, as an energy base, it might be available to export wind power to Beijing in the future.

CURRENT POLICY AND BARRIERS

In order to facilitate the progress of making huge potential market into real market, following measures for administration and market incentive have been taken by the Ministry of Electric Power (MEP).

- The electric power administrative bureaus at different levels should positively assist to conduct the pre-construction work of local wind farm, including planning, feasibility study and wind energy resources measurement. Meanwhile they are also responsible for the review of

wind farm's design and coordination in wind farm's connection with power networks.

- The network management department should allow connecting wind farm with power network at the nearest distance and purchase all electricity generated by wind and transmitted to power network.

- The pricing of electricity selling to power networks from a wind farm shall be made on the basis of the generation cost, plus pay-back of principle and interest from investment, plus reasonable profit. In case this price is higher than the average price of the network, the difference should be shared by the whole network. The electric power companies will be responsible for the purchase.

The development of wind farm to be hindered by the following barriers: High cost of imported WTGs; high rate of import duty for WTG (12%) and rate of VAT (17%) and other taxation; also high interest (15%) loan from domestic bank. Under such conditions during the period of pay back bank loan, price of electricity generated by wind farm should be as high as 1 Yuan/kWh (USD 0.12), it is difficult to be accepted by local authorities. In China the final dicision maker for electricity price is the government at provincial level.

ON GOING PROJECTS AND POTENTIAL MARKETS

In 1996 a big progress could be made on the construction of wind farm, since many contracts were finally signd, and the domestic investment up to 800 million Yuan is available from the State Economy and Trade Commision (SETC), enough for 70-80 MW installed capacity. Foreign investment up to 40 million USD are also available for 40-50 MW. The distribution reference to Table 4.

In January 1995, 12 provincial (regional) power companies submitted their preliminary wind power development plans (1995 - 2000) to the Ministry of Electric Power (MEP). The Hydropower Planning General Institute, as the administration institution of the pre-construction period of wind power development designated by the MEP, summarized all local plans as shown in Table 4.

Local plans are ambitious to result in the total installed capacity nationwide by the year 2000 reaching 1300 MW. However, considering that wind power development in large scale is just at the beginning, many difficulties have to be overcome, the target of 1000 MW nationwide is announced by the MEP. Based on the available domestic funds, the goal of 400

MW was set by the State Planning Commission (SPC) in May 1996, this plan has also been listed in Table 4, shown as upper figures marked with "*".

TABLE 4 ESTIMATED INSTALLED CAPACITY OF WIND POWER IN CHINA (MW)

Location (reference to Fig. 1)	End of 1995	Increased in 1996	Increased in 1997-2000		End of 2000	
			SPC*	MEP	SPC*	MEP
Nationwide	36.13	141.5	222*	1124	400*	1302
North China			35*		80*	
Hebei	0	0.6		52		53
Inner Mongolia	9.08	35.0		337		381
Northeast			48*		60*	
Liaoning	2.56	9.0		101		113
Jilin	0	0		56		56
Heilongjiang	0	0		55		55
East China			44*		80*	
Shandong	0.27	0		54		55
Zhejiang	1.68	28.2		70		100
Fujian	1.06	4.8		96		102
Jiangxi	0	0		50		50
South China			32*		60*	
Guangdong	8.68	8.1		194		211
Hainan	0.06	11.4		14		25
Northwest			23*		80*	
Xinjiang	12.75	44.4		45		102
Others			40*		40*	

(Based on the development plan submitted by local electric power bureaus in January 1995 and the plan from State Planning Commission in May 1996)

The development of wind power in China as an industry has been initiated. From now on to the year 2000, the achievements must be obtained via international cooperation, both in technology and finance, the main fields are specified as follows:

- Grants from international organizations, to support demonstration projects, resource assessment, technology transfer and indigenous manufacture, measurement instrumentation and personal training;

- Soft loans provided by international financial facilities and the government of industrialized countries;

- Encouragement to all potential foreign investors, public or private, to set joint venture, or cooperation production or by means of BOT, etc.

- Manufacture of medium and large size WTGs, importing matured technology and establishing production lines. At the beginning most of the components may come from foreign firms and are assembled in China, then the local made qualified parts could be increased gradually;

- Research, Development and test of WTGs.

CONCLUDING REMARKS

Detailed assessment of wind energy resources should be continued, computer-based new methodologies are being developed, and a common standard classification should be adopted by developers, that would be beneficial to the growing wind power market.

To utilize wind energy in large scale for power generation will improve the structure of power industry in China, reducing the pollution caused by coal fired power plants. Incentives should be formulated by the government at state level.

In the next two to three years, large WTGs have to be imported, international cooperation is crucial for technology transfer, to establish domestic wind industry in the near future.

REFERENCE

[1] Xue, H., et al. "ASSESSMENT AND ANALYSIS OF WIND ENERGY POTENTIAL IN CHINA"(in Chinese), Project report, China Academy of Meteorological Sciences, Beijing, 1995.

[2] Zhu, R.Z., et al. "WIND ENERGY RESOURCES AND ITS DIVISION IN CHINA"(in Chinese), SOLAR ENERGY, 1992.

[3] He, D.X., et al. "WIND ENERGY DEVELOPMENT IN CHINA", Proceedings of SOLAR ENERGY SEMINAR, Beijing, 1995.

[4] Xiao, G.R., "1000 MW WIND POWER IN CHINA - THE GOAL FOR YEAR 2000"(in Chinese), WIND POWER MAGAZINE, No.4, 1995.

NEW ZEALAND AND AUSTRALIA WIND ENERGY IN A NON SUBSIDISED MARKET ENVIRONMENT

by Paul van Lieshout
National Engineering Manager
Developing Technologies and Wind Power Group

New Zealand
DesignPower New Zealand Ltd.
PO Box 668, Wellington New Zealand
e-mail lieshout@designpower.co.nz

Australia
DesignPower New Zealand Ltd
Level 3, Waterfront Pl, 1 Eagle St
Brisbane, Queensland, Australia

Abstract

A great amount of preliminary work has been undertaken by many New Zealand and Australian Power/Generation Companies regarding Wind Power. Turbines are installed in Australia and New Zealand to test the wind and the technical applicability in the Australian wind diesel and the New Zealand high wind speed environment. Projects in Esperance, Thursday Island and King Island illustrate Australia's willingness to embrace wind power in hybrid wind diesel applications. A single Wind Turbine Generator (WTG) has been successfully operational in New Zealand's Capital for the last 3 years. A new 3.5 MW wind farm is operational and Resource Consent has been granted for a 65 MW wind farm in New Zealand. DesignPower is very proud to be involved in many of the New Zealand and Australian projects. It is obvious that wind power is just starting here, however the start has been promising and it is expected that wind power is here to stay.

This paper will address some of the issues associated with wind power in New Zealand and Australia, particularly those that are different from Europe and America. It shows the opportunities and challenges regarding the operation of WTGs in these countries. It addresses the non subsidised electrical pricing structure and the influence of the economically necessary high wind speeds or diesel systems on the choice of technology, particularly the control algorithm of WTGs and the subsystems. It reviews several of the issues associated with predicting the amount of energy that a WTG can generate, again taking into account the high wind speed control algorithms. It further addresses the issue of embedded generation and the influence that a wind farm might have on the electrical network. It continues to address issues associated with wind diesel systems. The paper concludes that wind power will be viable in the near future both in New Zealand and Australia, but also that care should be taken with data analysis and hardware choices during the next phase of implementation of wind power in New Zealand and Australia.

Introduction

It is well recognised within the wind industry that New Zealand is a windy country with wind speeds at many locations exceeding an annual average wind speed of 10 m/s. It has been mentioned that New Zealand is one of two new international markets that holds promise to generate a large amount of electricity with wind turbine generators.

Australia does not have a resource as large as New Zealand. Australia however has many communities isolated from a large coal fired electricity networks. Many of these communities are situated in moderately windy locations. Australia will have its own unique opportunities for wind generated electricity.

In New Zealand, the Electricity Corporation of New Zealand (ECNZ) has been investigating the potential for wind generation for some years now, having undertaken resource, siting and economic studies with DesignPower as lead consultant. One WTG has been operated by ECNZ in Wellington for the last 3 years with record breaking outputs, during which time DesignPower has been researching its operation on ECNZ's behalf.

A number of Power Companies in New Zealand have also been active with wind power investigations, and the first fully commercial 3.5 MW wind farm is now producing power in the southern Wairarapa. Resource Consents (planning approval) have been granted for another wind farm with a total installed capacity of 65 MW. Several power companies have secured land for future wind farm developments.

In Australia wind power is being generated in Western Australia, the Northern territories and Tasmania. The Western Power 2.3 MW wind farm at Esperance in Western Australia has been successful in replacing a large percentage of fuel usage in an existing diesel mini grid. Several power companies are investigating the possibility of utilising the wind by undertaking studies to find prime wind sites in their area followed by undertaking anemometer and feasibility studies. It is expected that future wind farms in Australia will be similar to the Esperance wind diesel system. This is evident in potential projects on Thursday Island, King Island (4 MW diesel grid) and the halted 10 MW Toora wind farm development.

This paper will address some of the issues associated with wind power in New Zealand and Australia. In particular it looks at the opportunities for wind power generated electricity in these countries and what kind of technological advancements and solutions will help the integration of more wind power in the existing energy generation mix in both countries.

At present there are not many turbines installed in both countries. However the opportunities are there if the bottom line economic hurdle can be taken.

This hurdle is in New Zealand in regards to the cost of existing and new generation projects. The system is largely fuelled by existing cheap hydro power, and newly built gas fired cogeneration projects are not expensive either. However there is a growth of electricity usage of between 2-4% on an annual basis. This will require additional installed capacity and it is expected that wind power can then be economically utilised particularly as embedded energy projects in areas with an average annual wind speed exceeding 10 m/s.

The economic hurdle in Australia can be overcome particularly in areas not connected to the low cost coal fired electricity networks. Such systems are characterised by small, normally diesel fuelled, mini grids. Many dozens of these mini grids have been identified throughout the coastal area in the west, south and east of Australia and its islands where moderate wind speeds occur which might be economic if compared with non subsidised diesel fuel prices.

Wind Power Economics

Much has been written about wind power economics. It is an important issue because every wind farm project has to be economic in itself and thus competitive with other available existing or new energy options in New Zealand and Australia[1]. It is different from European or American analysis where governmental subsidies are available for this form of renewable energy.

The economics of a wind power project are evaluated by researching the cost of installing a wind farm (including the cost of financing the installation which in itself includes a project risk factor), the cost of Operating and Maintaining the wind farm and the cost of replacing components during its lifetime (see Figure 1).

[1] South Australia seems to be willing to give some subsidy to wind power. In a report entitled "Towards the renewable Energy Target for South Australia" the ministry sets a 300 MW wind power target with a A$45 million subsidy.

The amount of energy that the wind farm will produce is estimated and the monetary worth of this energy determined from present electricity (energy and transmission) prices and/or from fuel prices.

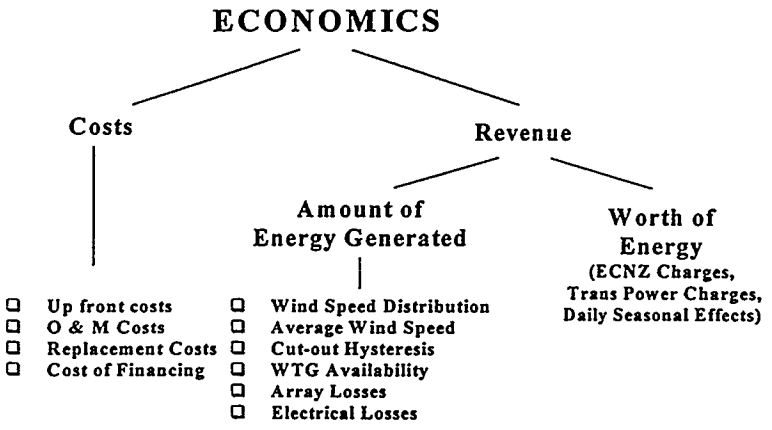

Figure 1- ECONOMICS OF WINDFARMING

The cost of wind energy depends on many variables including transportation cost of the WTG to the wind farm site. This factor might be particularly important in the more remote locations in Australia. The cost of energy in New Zealand is estimated to be around NZ$0.07-0.09 (US$0.05-0.06) per kWh for the 10 m/s wind sites. In the windy areas in Australia this cost is estimated to be around A$0.10 (US$0.08) per kWh.

This energy price tag would suggest that wind power is only economic at a very few, high wind speed sites in New Zealand and expensive diesel mini grids in Australia. It is believed however that present electricity prices will increase over the next few years due to an increase of energy usage in New Zealand and a removal of diesel fuel subsidies in Australia. Obviously wind power also has other advantages which are in line with governmental policies, such as the reduction of greenhouse gas emissions. These advantages are at present not translated to a monetary benefit for wind power.

Most industrial power generation projects are economically evaluated by combining a Life Cycle Cost analysis with the project's revenue to derive an Internal Rate of Return for the evaluated project. The revenue is based on the worth of electricity and the amount of electricity that is generated by the wind farm project.

Value of Wind Power Energy

The prices of electricity in New Zealand and Australia for utility connected areas are based on energy and transmission charges. Roughly the combined average cost is at present around NZ$0.07 (US$0.05) per kWh.

A more detailed study reveals that the energy charge in both countries is built up from several different components depending on time of day and the season. Hence it is not possible to simply equate average energy charges to the average wind generation value, since the wind value depend on the diurnal and seasonal wind patterns which are normally synchronised with energy demand. This makes the value of wind power generated electricity more valuable than just the average energy charge (see Figure 2).

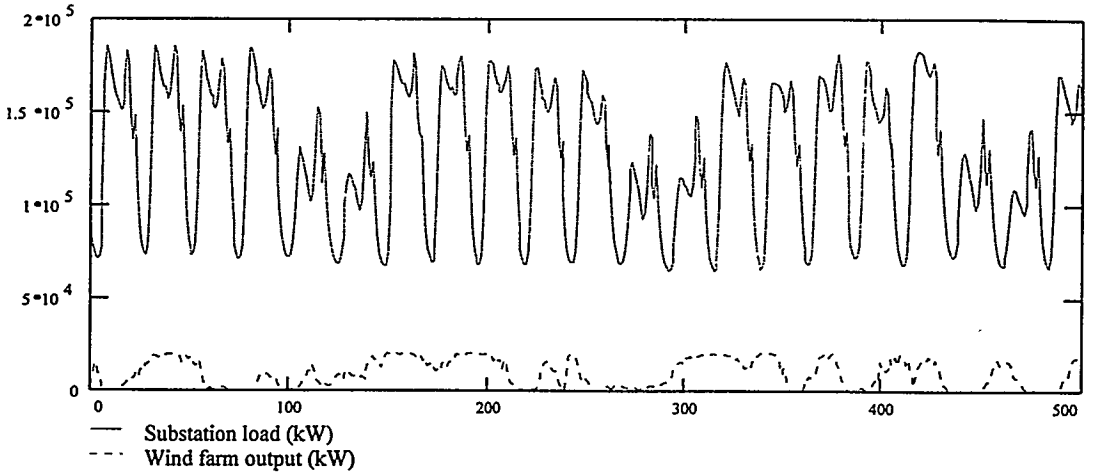

Figure 2 - TIME TRACES OF LOAD AND WIND FARM OUTPUT

For simplicity it can be said that the energy part of the total electricity charge in New Zealand is about 70% or $NZ0.04.5-0.05 (US$0.03-0.035) per kWh.

The transmission charge (Trans Power charges in New Zealand) at present are all based on the assets value of the transmission network and again in simple terms equate to about 30% of the total energy charge or about NZ$0.02-0.022 (US$0.015) per kWh in New Zealand. These prices and price variations are somewhat similar in Australia. The difficulty in both countries is that these transmission and distribution charges are normally based on the value of the asset. Embedded generation projects (and for that matter energy efficiency matters as well) will thus not have a 100% benefit for their portion of energy that is bypassing the transmission network. It is estimated that only a part of the transmission charges can be avoided which depends on the local situation.

Annual Energy Production

Accurate annual energy generation forecasting methodologies are expected to be different from those methodologies employed in other countries which have a lower annual average wind speed than those speeds encountered in New Zealand. Annual energy productions are normally calculated in lower wind speed countries based on average hourly or 10 minute wind speed observations from a specific site, which is cross correlated with a long term historical data set to obtain long term representative values. A distribution curve, based on this data, in combination with a WTG power curve yields the possible amount of energy that a WTG could generate at that particular site if its availability is 100 %.

Wake effects, historical or expected availability of the chosen WTG, as well as topographical characteristics and electrical losses will result in an expected net energy production. These calculations are crucial to the evaluation of the economic viability of a wind farm project.

This approach however is not accurate enough for the New Zealand situation because the wind speeds encountered in New Zealand are higher than the wind speeds of European and Australian wind farms. Particularly, because the New Zealand wind climate is driven by weather fronts with high peak wind speeds and a return period of about 5 days. The Fourier Transformation shown below illustrates both the diurnal wind speed effects, the 5 day weather-front recurrence and the high wind speeds (see Figure 3).

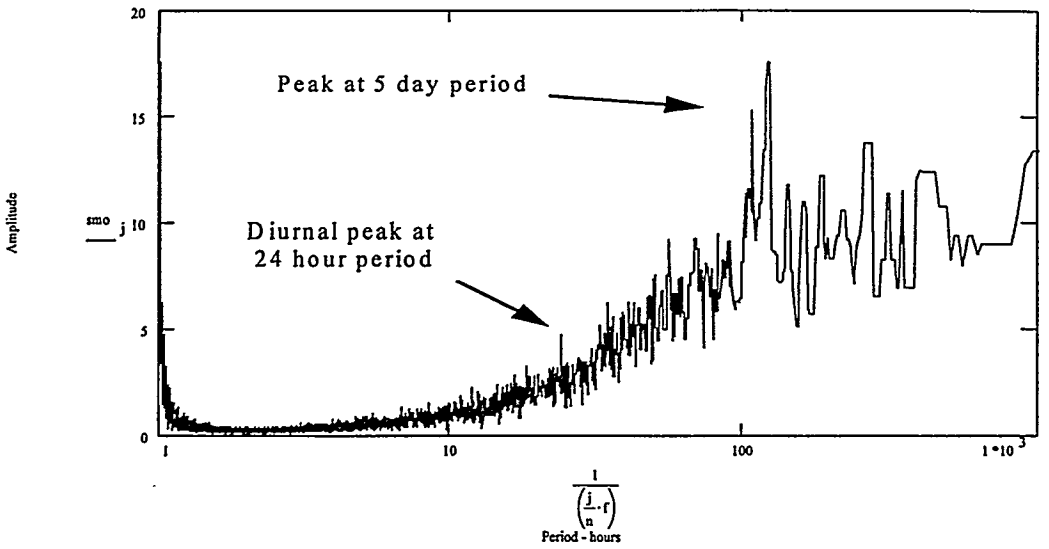

Figure 3 - FOURIER TRANSFORM - DIURNAL AND WEATHER FRONT EFFECTS

It is possible that large amounts of energy can be lost due to hysteresis effects of the power curve around the cut-out wind speed due to these high wind speeds (see Figure 4).

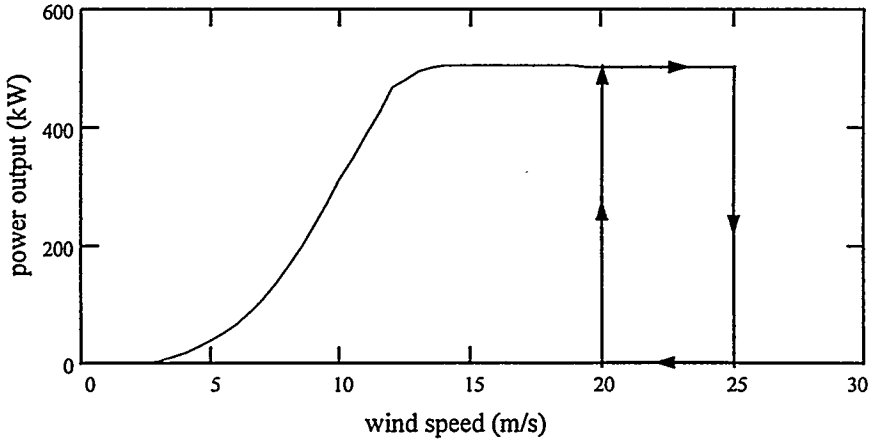

Figure 4- POWER CURVE HYSTERESIS EFFECT

This phenomena is not taken into account in the 'normal European' energy calculations. Using these normal European calculation methodologies which combines distribution curves and WTG powercurves might overestimate the annual energy production. The New Zealand high wind speed regime might greatly reduce the amount of energy that is thought to be generated using the European methodology. Deficits of more than 10% can occur when using the European methodology without considerations to the control methodology of the WTG and the wind speed versus time relationships. DesignPower has recently been awarded a research project related to these hysteresis effect. It is hoped that results and recommendations regarding improved WTG control methodologies which will reduce these hysteresis losses, will be published in 18 months time.

Another issue relates to the fatigue life of WTGs which is among others a function of the average wind speed. The higher the average wind speed is, the more time that a WTG operates to control the power output. It is this particular operating window when the wind speed is between rated wind speed and cut-out wind speed that fatigue accumulates the fastest.

Based on a Rayleigh wind speed distribution curves it can be calculated that WTGs installed in the high wind speed sites in New Zealand could spend 7 times longer in this fatigue sensitive operating window.

Both factors might have a detrimental effect on the cost of wind power, especially if they are not well defined in which case financiers might require a higher rate of return to cover for the uncertainties (risk) of the project. It is thus most important to address these issues accurately.

Extreme Wind Speeds

Extreme wind speed events have always been important in designing WTGs and in choosing the right WTG for a specific development. This again is more important to the New Zealand environment than most of the Australian environment[2]. Numerous overseas failures are attributed to extreme events even though many of them have actually occurred below the specified maximum design wind speeds. It is important to have a clear understanding of the maximum wind speeds that can be expected at the New Zealand sites particularly because of the correlation between average wind speed and maximum wind speed.

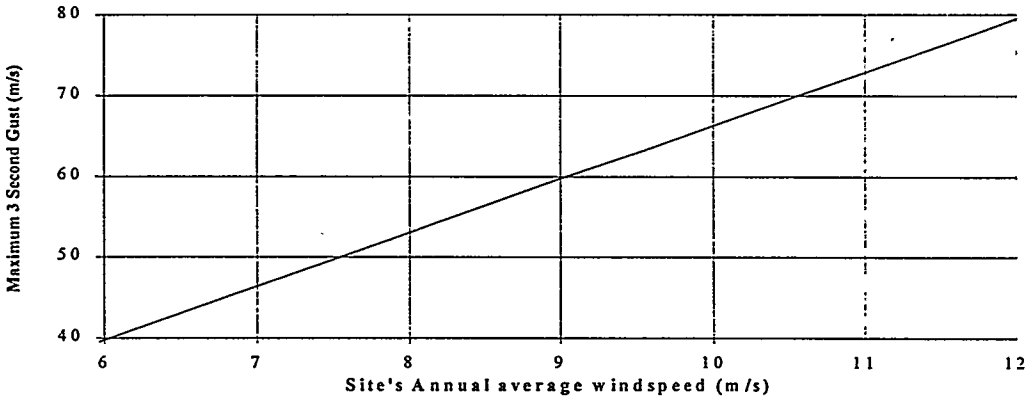

Figure 5- GENERIC EXTREME WIND SPEEDS GRAPH (20% accuracy)

The higher the average wind speed (which is advantageous for the economics of wind generation) the higher the maximum expected gust wind speed can be (which is disadvantageous for the economics of wind farming).

The New Zealand Building Code gives an indication as to the maximum expected wind speed for a specific site. However it is believed that more accurate maximum gust wind speed predictions are necessary to minimise investment risks. DesignPower is involved in research carried out by Victoria University regarding these extreme high wind speeds.

Figure 5 gives a generic relationship between maximum gust wind speed and average annual wind speed. It should be noted however that at many potential New Zealand wind farm sites, the maximum expected 3 sec gust wind speed with a return period of 50 years can be between 70 and 80 m/s.

Hysteresis Effects

It was mentioned earlier in this paper that energy predictions should take into account power curve hysteresis effects. Such calculations should use WTG specific control algorithms. Energy calculations

[2] Generally speaking the wind speeds are higher in New Zealand than Australia. Although wind speeds have been measured in excess of 9 m/s annual average wind speed in Tasmania (at 30 mAGL).

are then based on high sample rate wind speed observations or simulations based on the interpolation of hourly or 10 minute wind speed information. This in combination with the control algorithm gives the aerodynamic behaviour of the investigated WTG. Specific control parameters like maximum generator slip, rpm, power values, wind speed values and standard deviation values among others can then be investigated and taken into account in calculating the annual energy production of a single WTG within a wind farm. Either a hysteresis factor for a whole wind farm can be calculated or several calculations should be performed on representative WTG locations throughout the wind farm.

It should be mentioned that these calculations do not necessarily mean that the energy production is lower than those calculated using the 'normal European' methodology. This advanced methodology will highlight those turbines types and models that will be most advantageous to be installed on the investigated high wind speed sites. It will thus give developers and investors a better understanding of the energy production of proposed wind farm developments. This will reduce the risk involved in developing a site which will have a positive effect on the acceptable Internal Rate of Return.

Network Issues

Hysteresis effects and maximum wind speed issues are not of such a great concern in the Australian market. More important in Australia is the integration of wind power into an existing diesel mini grid. In New Zealand, which has an extensive transmission and distribution system, diesel networks are not that important (although there are some on small islands). Network issues related to New Zealand have to deal with weak electricity distribution lines will be used in embedded energy projects.

Network Issues; wind diesel hybrid systems (Australia)

In order to adequately integrate a WTG into an existing diesel generation system, there must be a concerted effort to optimise the total system for the specific community. This requires investigating load management opportunities in order to lessen the seasonal and diurnal variation in electricity demand. This might also includes very short term load management in order to cope with wind variations of the order of 1 minute. This again very much depends on the local system and the penetration rate of the WTGs.

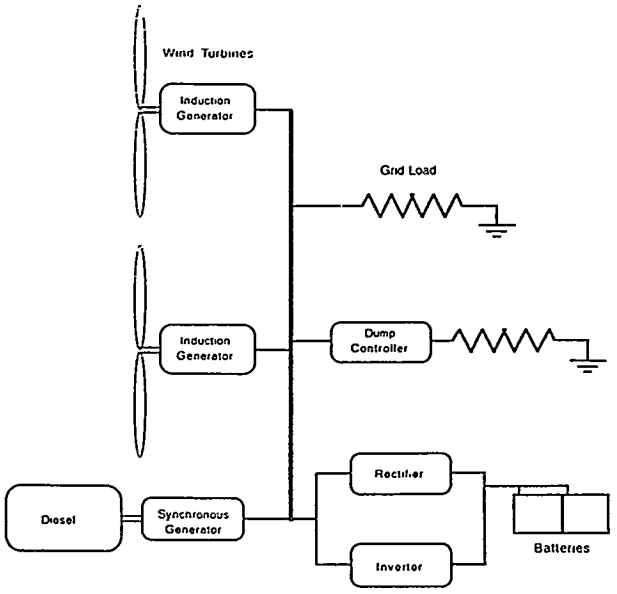

Figure 6 - GENERAL WIND DIESEL SYSTEM SCHEMATIC

It is important to determine whether existing diesel sets are capable of performing to the required level or if one or more replacement diesel sets would be more suitable. The older diesel sets may well be near the end of their useful life, and thus require replacement soon anyway. It will always be easier to develop an optimum wind diesel system if the diesel engine can be specifically chosen to suit the duty as dictated by the overall control system.

In order to cope with the variable nature of wind generated electricity either a high degree of load management is necessary, or short term energy storage or one has to settle for a non optimum energy system. Energy storage can be in the form of batteries, flywheel or hydraulic accumulator. Approximately 30 seconds of energy storage provides a major reduction in both fuel consumption and diesel start/stop cycles, with very little benefit beyond 5 minutes energy storage (unless storage greater than 4 days is applied). In reality an non optimum system from a technological point of view might be chosen to make a system cost effective. Most systems will not have a storage system.

Recent developments are investigating running diesel engines at negative loads to absorb surplus energy from the WTG, and to significantly reduce fuel consumption. This appears to be potentially viable, though practical matters of low lubricant temperatures and glazing of the cylinder bores needs to be researched.

Examples of good wind diesel systems is the Esperance system in Western Australia which has an annual fuel reduction of more than 30% over the previous diesel only mini grid. It is estimated that many other communities like Esperance will be looking at wind diesel option in the near future.

Network Issues; embedded generation projects (New Zealand)

New Zealand is expected to have many wind farm projects embedded in the local power companies distribution area. Many future wind farms will be similar in size to the 3.5 MW Haunui wind farm in the Wairarapa although there will be exception like the 65 MW Tararua Wind Farm development.

DesignPower is involved in carrying out Electrical Load Flow studies on the effect of embedding a wind farm into a local distribution network. Such an analysis determines whether the existing distribution network or transmission system can cope with the extra power generated by a wind farm (bi-directional power flow). Studies such as these are important due to the varying and directional nature of the new load flow. The studies involve both static and dynamic analysis and are recommended for all embedded generation projects.

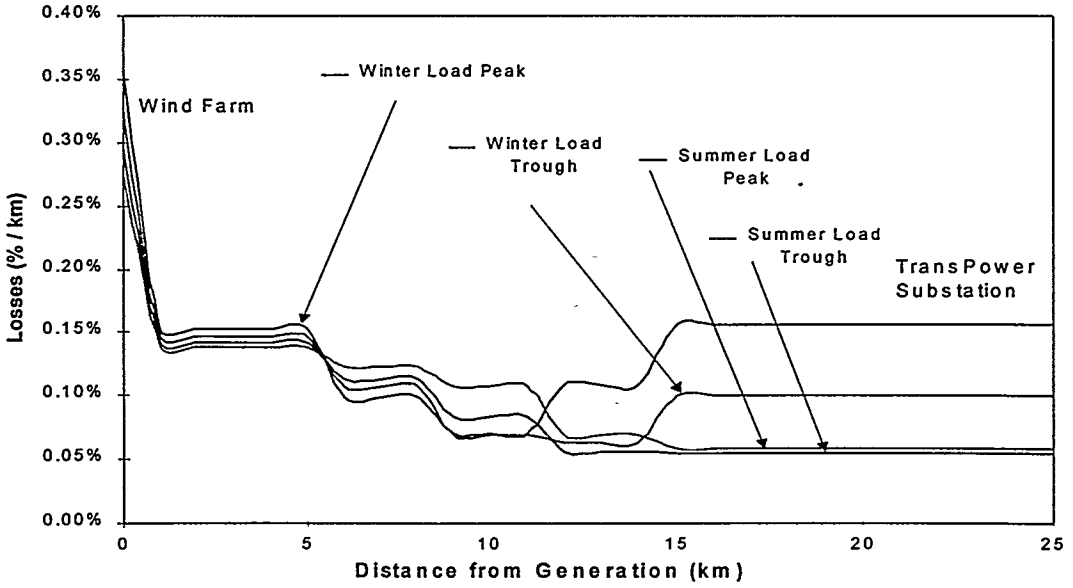

Figure 7- ELECTRICAL LINE LOSSES

The voltage of an existing distribution network affects the ability of the network to cope with new generation. If the network voltage is low, it may mean that excessive distribution losses will occur if the new energy injection has to be carried any distance to the load which is often the case in those remote embedded wind farm projects. It may in fact be advisable to upgrade the distribution network to a higher voltage than that required for load capacity in order to reduce inherent losses to an economic level.

Voltage fluctuations with long time constants may arise because wind turbine generators employing induction generators do not have the capability to control the reactive power. Such voltage fluctuations can be eliminated by introducing voltage regulators into the system. Whether voltage fluctuations will occur depends on the specific characteristics of the system being studied. Both synchronous generators and AC-DC-AC converter systems can compensate the reactive power component if actively controlled.

As well as the static load flow modelling (under different load conditions) that results from an electrical Load Flow analysis, it is important to incorporate the dynamic behaviour of a wind farm to ensure that flicker curves are adhered to. This is also important in wind diesel systems.

Summary and Conclusion

This paper has discussed the opportunities that New Zealand and Australian Power Companies see regarding generating utility grade electricity with Wind Turbine Generators. Several companies are now accumulating site specific data to evaluate the suitability of economically converting the wind into electricity. Several factors, but not all, that should be taken into account in the economic evaluation of wind farm developments have been discussed in this paper, particularly the importance of understanding the control algorithms of WTGs and their effects on energy production. It can be concluded that wind power will be technically and economically viable in the near future but also that care should be taken during the next phase of the implementation of wind power in New Zealand.

Acknowledgment

The author of this paper wishes to thank the organisers of the American Wind Energy Association for inviting him to prepare and present this paper. He also would like to thank the Electricity Corporation of New Zealand and the individual members of DesignPower's Developing Technologies and Wind Power Group for contributing to and assisting him in preparing this paper. Last but not least, the author wishes to thank the management of DesignPower New Zealand Ltd for allowing him to present this paper at this conference.

VIEWS ON WORLD MARKETS - CANADA

Jeff Passmore
President
Canadian Wind Energy Association
c/o 600 - 99 Bank Street
Ottawa, Ontario K1P 6B9
Canada

ABSTRACT

If "market" is defined by hardware in the ground (as it should be), then the Canadian wind power market has been virtually non-existent (only 23 MW to date). The potential on the other hand is enormous (6400 MW likely to be developed). This potential has not been pursued because of unregulated electric utility monopolies, lack of political knowledge and interest, and punitive tax treatment for renewables. Recent initiatives including utility restructuring, federal plans for green power procurement, and proposed tax measures suggest that situation has potential for change. Interested parties should start familiarizing themselves with the Canadian players / market now, in order to be ready to move when the time comes (likely in the next three years).

INTRODUCTION

With worldwide installed wind capacity projected to grow from the current 5000 MW to 18,500 MW by 2005, and with that growth representing a market opportunity of more than $18 billion, why would anyone want to invest time and money in Canada - especially when you consider there are only 23 MW currently installed, and a single 600 kW Tacke machine was the only significant installation in 1995?

THE BAD NEWS - WHAT CANADA DOES NOT HAVE

Canada's electric utilities are, with a couple of exceptions, self-regulated (an oxymoron) generation monopolies. In other words, they do what they want. Yes, Canada is a developing country. To date, Canada's electric utilities have not wanted non-utility generation competition, and they have not wanted wind power.

There is no federal, national electricity policy and nothing akin to U.S. PURPA legislation. Electricity policy is provincial jurisdiction and most provinces elect not to regulate their own utility. Provincial governments have certainly never attempted to suggest what kind of power utilities should buy at what price.

There is no equivalent to the British non-fossil fuel Obligation

Most of Canada's electric utilities are, or claim to be, in capacity surplus. This becomes a problem even in a restructured market like Alberta where one has to wait for the existing capacity to reach retirement age.

Electricity in Canada is cheap. Or at least we pretend it is. Actually it isn't cheap, but rather than have the price reflect cost, our electric utilities have elected to accumulate huge debts to keep rates artificially low. Ontario Hydro's debt, for example, is $Cdn32 billion. Hydro Quebec is in a similar position.

There is very little knowledge in Canada about the benefits of wind power, and as such, there is very little political interest or will.

There is certainly nothing approaching a renewable energy set-aside or equivalent of "Renewables Portfolio Standards" (Note possible exceptions in Ontario where we are awaiting the results of a 60 MW renewables request for proposals, and Quebec where a set-aside was recently recommended but is not as yet in place).

While Canada's electric utilities are under pressure from customers and independent producers to restructure and permit competition, it is only in two or three provinces where anything is happening and, with the exception of Alberta, Canada is far behind what has been happening in the U.S. or U.K., for example.

The recent problems at Kenetech have erected a roadblock in the Quebec market. Hydro Quebec does not want to commit to any further projects beyond their 100 MW contract with Energie Eolienne Kenetech because the original plan was to complete this one project and then, based on a performance evaluation, decide how to proceed from there. But it is not clear how, if at all, this project will proceed. This contract will be in default by mid-March, 1997 after which time, if it has not proceeded, new opportunities may open up in Quebec.

THE GOOD NEWS - WHAT CANADA DOES HAVE

Canada has no technology to speak of and almost no manufacturing. This may not be good news for Canadians, but it is for those of you who want to set up joint ventures with Canadian firms for the use and potential manufacture of your technology in Canada.

The public is interested in wind. CanWEA receives 50 calls a week from Canadians seeking information on wind power. While most of these inquiries don't have to do with utility scale projects, this level of interest speaks well for the under 100 kW stand alone machines or small clusters of machines.

There is an enormous wind resource in Canada. Assuming a very conservative assumption of seven percent penetration of each provincial utility's currently installed capacity, and taking into account utility concerns about wind penetration levels and power quality, the likely potential for wind in Canada is 6400 MW. Based on wind resource assessments the actual potential is far greater than this, but it appears to us to be a realistic starting point.

In January 1996, the federal government announced its intentions to pursue the concept of green power procurement. The green industry has been encouraging Ottawa to think of itself as a customer and wind proponents have already had discussions with government officials about how they can deliver the green kWhrs to them.

In March, 1996 after much effort by the Independent Power Stakeholder Task Force, the federal government announced a new tax class - the Canadian Renewable and Conservation Expenses (CRCE) intended to assist renewable energy exploration and development. It's a small step in the right direction and we hope for more policy in subsequent budgets

Canada's electric utilities face considerable pressure to restructure. In some provinces like Alberta, the electric system has been restructured (as of January 1, 1996) and there is a growing opportunity to deal directly with customers. (About 10% of generation is now "playing" in the power pool. The remainder is existing capacity and discussions are ongoing as to how long this "entitlement / obligation" or transition phase will last. It is likely that over the next three years, about 200 MW of new capacity will be required). In others like Ontario, there is a lot of talk about restructuring and a lot of resistance from the utility against moving too quickly. In places like Quebec, Saskatchewan or Manitoba there is no talk of change. Nova Scotia Power, a public monopoly, was replaced by a private monopoly which achieved nothing in terms of competition.

In Quebec, the recent (March, 1996) report on the public debate on energy called for renewable energy set-asides to aid in the development of wind technology and take advantage of the considerable resource. This report is now in the hands of the Quebec government which is to issue a new provincial energy policy this autumn. It remains to be seen whether the government will mandate Hydro Quebec to be more proactive with respect to wind procurement.

Canada is in the process of negotiating greenhouse gas emission reductions on the international stage. Like a lot of other nations involved in the post-Rio initiative, national governments have to devise strategies to deliver on the CO_2 reduction targets as agreed to in international protocols. Wind generated kWhrs offers one of the solutions to the question, how do we get there from here.

All this takes place in the context of utilities and governments that are broke which should translate into industry involvement on a performance basis only.

LEARNING MORE ABOUT THE CANADIAN MARKET

As the overheads suggest, there are many markets in the world more attractive than Canada - at least at first blush. But patience may be a virtue and if you have patience and perhaps pockets of medium depth, you should start positioning yourself to take advantage of the 6400 MW Canadian potential.

In fact, of course, some companies are already in the process of doing just that. Some decide to establish a small branch office, or to joint venture with an existing Canadian company, or retain a local representative to keep them posted on developments as they occur prior to deciding when to get involved in a more serious way. In the past, these approaches have been and are being used by Tacke, Vestas, Kenetech and Atlantic Orient Corporation.

The message here is that there are Canadian companies who know the regulatory environment, know the environmental assessment process, know the wind resource, know the technology (even though it comes from offshore), and know how to do systems packaging. They are looking for partners in financing, partners in hardware, partners in project development. Canadian companies

don't expect to do it all on their own and the same partnering approach should apply to any offshore firm hoping to be successful in Canada.

Certainly to me, though I am a happy warrior Canadian, the most important goal is to get that wind hardware in the ground. In other words, it matters not that the technology is Danish, Dutch, German or American. What matters is that we get, as quickly as possible, the environmental and economic wealth generation benefits to be derived from an aggressive policy of wind power procurement.

If you are going to succeed in the Canadian market, it is no different than succeeding in any other market - you need to understand the marketplace, you need to understand how Canada works, you need to find yourself a Canadian collaborator. To find out more about what could potentially be the most exciting market in the world in the period 1998 to 2010, come to the 12th annual conference of the Canadian Wind Energy Association to be held in Alberta, October 6 - 9, 1996.

NEW WIND CAPACITY INSTALLED IN 1995
(SELECTED COUNTRIES)

GERMANY	498 MW
INDIA	383 MW
HOLLAND	106 MW
DENMARK	75 MW
SPAIN	73 MW
U.K.	46 MW
U.S.	41 MW
CANADA	.6 MW

SELECTED GROWTH MARKETS FOR WIND ENERGY TO 2005
(Taken from AWEA Projections)

U.S.	2730 MW
INDIA	2500 MW
CHINA	1300 MW
GERMANY	1300 MW
SPAIN	1275 MW
CANADA	585 MW

ACHIEVABLE POTENTIAL, TARGETS, AND PROJECTIONS OF WIND POWER DEVELOPMENT IN CANADA (in MW)

Year	AWEA (Projections)	CanWEA (Targets)	Passmore (Potential)
2000	183	500	1000
2005	585	1500*	3000
2010	1100*	5000	6400

* Extrapolations

ELECTRIC RESTRUCTURING: OBSERVATIONS ABOUT WHAT IS IN THE PUBLIC INTEREST

Commissioner James J. Hoecker
Federal Energy Regulatory Commission

[Commissioner Hoecker was unable to attend;
these are his prepared remarks]

I.

The electric utility industry has changed and it is likely to change even more. That much is axiomatic. We know that, as a matter of good public policy (not to mention good politics), electric service must continue to be universally available, reliable, and reasonably priced. But, beyond that, I will bet that each of us views the road ahead and the possible destination somewhat differently. What level of service quality, what discipline on price, and what innovations will be attained after we prescribe a dose of competition for traditional electric utilities? Will the economic response of the industry be relatively uniform, in terms of the number of cents it takes to produce a kilowatt-hour? Will utilities choose to divest themselves of certain functions? Or, will they be forced to do so? And, what will become of the relationship between the local utility and its customers? These are questions worthy of discussion and, indeed, electricity regulators across the country are trying hard to ascertain the right answers for their jurisdictions. The process is turning out to be anything but simple.

In the final analysis, we are reshaping what we collectively deem to be "in the public interest." More and more, the public interest is becoming identified with "competition" -- known variously as customer choice, open access, or light-handed regulation by its many advocates. Electric generation is now widely perceived to be competitive and the public interest increasingly requires access to more than one source of supply. The best illustration of how the public interest is being redefined involves the FERC's standards for approving mergers among major investor-owned utilities. At one time the courts told the Commission not to break a sweat reviewing mergers under section 203 of the Federal Power Act. The public interest required only that the Commission ensure circumstances (mainly, rates) were not made worse by a specific merger. Today, given the effort being expended to infuse the world of regulated monopoly with the forces of competition, the FERC must examine more closely whether the consolidation of vast generation resources under one corporate roof might subvert the very competition we seek to create through open access. "Consistent with the public interest" has new and added meaning.

I submit to you that, at this moment, we may more confidently conduct a post mortem on the bad old system and announce why it is being discarded than we can foretell the net gains which the consuming public will obtain from restructuring. There is no indication that the public will cease to demand electric service that is both efficient and reliable, or that it is prepared to take risks in exchange for cheaper power. So, we had better take care to ensure

that competition is both "in the public interest" as we have come to understand it and as the new competitive realities dictate.

What does all this mean? Will the price of power be the only determinant of the success or failure of restructuring? Sometimes it seems so. When the FERC recently adopted Order No. 888, it projected annual savings of $3.8 to $5.4 billion from transmission open access. In fact, that was the big story. That indeed will constitute a major shot in the economic arm of the country. And, the Commission's efforts to open the bulk power market are a necessary, if not sufficient, predicate for retail competition, a broadly-competitive industry, and even greater savings. But, Order No. 888 and the scores of state restructuring proceedings necessarily raise important issues in addition to reducing the price of power.

These non-price aspects of restructuring have not proved very newsworthy, as far as I can tell. In two or three pretty good speeches this spring, which were (lamentably) widely ignored, I talked about the "other" restructuring -- that is, how competition will affect not just the efficiency of established utilities, their organizational structures, the nature of the regulatory compact, and the evolution of regional markets, but how competition will affect the industry's work force, the environment, energy conservation efforts, renewable energy, utility-supported social programs, and even regulators themselves and the nature of their work. These are key subtexts to the debate about how to restructure. But, I find that these are topics not calculated to bring the Fourth Estate to its feet. I am nevertheless pleased to see many groups, among them the American Wind Energy Association (AWEA) paying attention to stranded benefits and to long-term "public goods" -- including energy diversity, environmental protection, and jobs -- which ought to be a part of any calculation of the risks and benefits of restructuring.

Today, I want to continue my quixotic pursuit of this theme -- even though it is less within our purview in Washington than it is within that of the states. First, however, a word from my sponsor -- I mean by that, of course, the Commission's recent Order Nos. 888 and 889.

II.

On April 24 of this year, the Commission adopted a Final Rule requiring open access transmission service (or Order No. 888) and a Final Rule requiring Open Access Same-time Information Systems or "OASIS" (Order No. 889). It also issued a Notice of Proposed Rulemaking which could lead to uniform capacity reservation tariffs for transmission services. Our intent was simple: open the U.S. electric transmission system to competitive generation on a non-discriminatory basis and good things will happen. Order No. 888 challenges the monopoly power of investor-owned utilities by integrating and even commoditizing network transmission services, while also ensuring continued state control of end-user markets.

Let me be slightly more specific. First, Order No. 888 requires that transmission-owning utilities must offer transmission services to all eligible customers on a non-discriminatory basis. To ensure this result, the Order requires utilities to file, within 60 days, open access transmission tariffs that contain minimum terms and conditions of service. A

model pro forma tariff for utilities to follow is included in the rule. The utilities may propose their own rates for service.

Second, utilities must "unbundle" their services. In other words, they must take transmission service under the same tariffs with which they serve others, separately pricing each service, including ancillary services. Entities that are not jurisdictional public utilities (e.g., municipal utilities or cooperatives), but which obtain open access transmission from investor-owned utilities pursuant to our rules, must reciprocate by providing comparable transmission service if they own transmission facilities.

Third, the Commission will allow utilities to seek recovery of all legitimate, prudent, and verifiable costs that may be stranded because their customers use open access transmission service to obtain power elsewhere.

Finally, recognizing that competitive markets do not consist of wires and turbines alone, we require utilities to create or participate in an information system, the "OASIS." The OASIS will provide transmission customers with electronic information about available transmission capacity, prices, and other information necessary to obtain services; it must do so according to the technical standards and protocols of Order No. 889.

Open access in the bulk power market will exert strong pressure for retail markets to "open up." While the restructuring of the electric utility industry will be substantially more complex than the same realignment among natural gas pipelines, I expect that competition within retail markets will occur much more quickly. Where gas markets tend to be discrete and the city-gate has permitted LDCs to be more insular, retail electricity markets are part of a more integrated whole and price disparities between service areas or among jurisdictions are more difficult to justify according to purely local economics. The pressure from captive customers to access cheaper supplies off-system will prove irresistible. In sum, the shake-up in this industry will be from stem to stern.

I believe that FERC's actions are healthy preconditions for wholesale competition. Order No. 888 does not prescribe any industry structure. Nor does it predetermine how regulated utilities will respond to the possibilities it creates. We know that, as of July 9, 1996, utilities will have formulated and filed open access tariffs that ensure a minimum quality of transmission service. We know that the California utilities, pursuant to a CPUC-inspired search for a more rational market model, are moving farther and faster in redesigning their large and highly influential markets. We know that power pools will have to change their lifestyles by year's end. And, many state PUCs are working hard examining what will be best for their jurisdictional ratepayers in the brave new world. Like the FERC, they will have to deal with stranded costs, the role of municipal utilities and cooperatives, and the status of current requirements contracts. Unlike the FERC, however, the states will have the virtually exclusive task of deciding the future of so-called stranded benefits.

III.

Because I am sure you have read FERC's ponderous work product in its entirety, I need not expound upon it further. Let me therefore turn to three important questions. First,

can renewables successfully participate in an increasingly competitive marketplace? Second, is there a continuing role for federal and state governments with respect to renewables? And, if so, can such actions be taken without distorting the marketplace?

The role of renewable resources as well as energy efficiency and conservation efforts will be tough to figure out in a restructured industry. There exist well-founded apprehensions about the future of private and public efforts to promote the economically-, environmentally-, and socially-responsible uses of energy resources because the focus of all the talk the industry's transformation is seemingly on lower electricity prices. And, as you know, government funding to support research and development of renewable technologies is anything but abundant. The House of Representatives, for example, recently proposed to cut $285 million from the Energy Department's renewable and energy efficiency programs for FY 1997. On the other hand, the House Renewable Energy Caucus, a bipartisan caucus with 78 members from 36 states, supports continued funding for renewable resources. The Caucus argues persuasively that continued investment in renewables is necessary for, among other things, diversification of the domestic energy market, reduction of our dependence on foreign suppliers, and retention of America's competitive edge through exports of more than $1 billion in solar, photovoltaics, and other renewables applications.

So what can safely be said about the future of renewables?

A. Can renewables and conservation compete?

I believe that the two main competitors to fossil fuel generation -- conservation and renewables -- can effectively compete in the restructured environment. Investments by utilities in their customers' energy efficiency have both deferred capacity additions and helped mitigate utility risk. It is also encouraging that non-utility generation from renewable electric sources grew 8.6 percent between 1990 and 1994. The wind industry, in particular, has made important strides over the last 10 years; it has increased the reliability and efficiency of wind turbines to as much as 98 percent availability, while decreasing costs by more than 80 percent to prices as low as 3.9 cents per kWh. All this was in a less competitive, cost-driven environment, but such statistics suggest that wind energy, in its second decade of existence, can be a strong competitor in domestic and international energy markets. Other technologies may not fare so well, however.

For well-positioned technologies, a more competitive marketplace characterized by transmission access offers positive opportunities for renewable resources. Yet, it is important to acknowledge that new technologies are particularly vulnerable to market barriers erected in situations involving market dominance.

- New technologies generally are not favored by incumbents, and firms that own existing generating facilities can use their position in the market to block entry;

- Manufacturers and developers of innovative technologies are usually small entrepreneurs and new market entrants with less in the way of economic leverage;

- Innovative technologies may not be easily accommodated by traditional accounting and operational practices;

- Financing for innovative technologies may be difficult; for example, renewable projects have high up-front capital costs and typically require long-term financing; and

- New technologies cannot compete where there is excess generation capacity (as is the case in much of the country today), unless the new technology is incredibly cheap, the existing technology is very expensive, or some regulation or legislation causes the economics to change.

Many of these obstacles to development of renewable resources may be eased as the electric generation marketplace becomes increasingly competitive. FERC's open access policies may benefit renewables by encouraging greater regionalization of the electric market through transmission pricing innovations, regional transmission groups, independent system operators, and so forth. This trend toward regionally-based transmission services will help to facilitate the participation of renewable generating facilities in the marketplace. High quality renewable resources are often remote from load centers and, therefore, are more affected by the terms and conditions of transmission service than conventional generating facilities. If transmission must be secured across the territories of several utilities under current circumstances, pancaked rates could make remote generation less economic and could lead to inefficient choices of generation resources. The regional planning and operation of transmission will allow resource areas to be matched to demand areas and will lead to more competitively priced power.

Energy efficiency will have advantages as well. The market will place a premium on technologies that improve efficiency and performance. As the popularity of traditional cost-of-service ratemaking declines, the drive to add to rate base will be replaced with a strong cost-consciousness. Furthermore, an open market environment will encourage generation suppliers to minimize their risks. Investments in renewable resources and conserving energy offer relatively stable costs as compared to the risk of fluctuating fossil fuel prices. For these reasons, renewable resources and efficiency measures should prove to be attractive components of a utility's overall generation portfolio.

Finally, it must be remembered that, as restructuring makes electricity a more customer-driven business, utilities will no longer be the sole decisionmakers about generation resources. Customers also will play a significant role in determining the market for renewables. Numerous studies and polls have shown that consumers would even tolerate higher prices for electricity in order to take advantage of environmentally benign generation sources. Several utilities have already begun offering their customers "green pricing." The marketing techniques being employed in New Hampshire's retail wheeling pilot program, including Green Mountain Power's "eco-credit" concept, suggest that more of these programs are likely to follow as the electricity market opens to competition.

B. Does government have a role?

There is the very pressing question about the continuing role for regulators or other government entities in helping "manage" the production, transmission, and sale of electric energy or in financially assisting renewable technologies. I confess that, for the most part, the need to address such questions is not in my job description. I have some limited observations to make, however.

First, some commenters have expressed concern that Order No. 888 and full competition will reduce the ability of the states to provide renewable energy programs. This is incorrect. Influence over energy conservation, efficiency, and resource procurement strategies fall largely to state regulators. Nothing in FERC's open access initiative should inhibit the exercise of traditional state authority over these issues. Order No. 888 leaves state jurisdiction over the retail market essentially untouched. Even in an unbundled retail environment, where some transmission facilities used to serve retail customers may become FERC jurisdictional, states retain exclusive jurisdiction over local distribution and related social and efficiency programs.

I wish to emphasize that states will retain authority over utility resource procurement decisions. This will not simply involve the authority to site facilities and manage utility construction and procurement decisions through IRP. I believe the FERC can and will make clear that state regulators can prescribe portfolio standards, such as that proposed for renewables by AWEA. Those standards will determine the acceptability of any and all power sold to customers within those jurisdictions, even if delivered from outside, according to the source of that power. There's a tough Commerce Clause question here, naturally. But I have few doubts about state authority to order retail utilities to develop portfolio standards.

The only federal interest in all this is that such state requirements must be applied on a non-discriminatory basis (e.g., that the program treats in-state and out-of-state suppliers similarly) and in a way that avoids an undue burden on interstate commerce. At bottom, the future of renewable, conservation, and efficiency programs, and other utility-supported social programs is tied heavily to the ability of state and federal regulators to reach workable jurisdictional accommodations.

C. Will government involvement with renewables distort the market?

One could argue more than plausibly that government involvement in promoting renewables is increasingly inappropriate. Some regulatory attempts to promote conservation and renewable resources in the past have unquestionably frustrated economic efficiency or placed uneven burdens on energy providers. This may make these programs targets for elimination. Renewable technologies and efficiency strategies are very competitive with many kinds of installed capacity. However, renewables that are not competitive at the margins (i.e., against gas turbine generation) will tend to raise the average system cost of power. In a market dominated by short-term objectives, this is a significant disadvantage.

However, I would argue that some governmental support for renewables and conservation is both helpful and, for the time being, necessary. It is part of government's job to think long-term; industry must assist that process. AWEA's proposed portfolio standard

provides an interesting example of how to develop a program that both supports renewable resources and conforms to the realities of a competitive marketplace. Under AWEA's proposal, retail suppliers would be free to meet minimum renewable resource requirements by the least-cost means available -- either by owning renewables, purchasing renewable energy, or purchasing renewable "credits" if such a credit trading scheme were developed. This proposal closely resembles the SO2 allowance trading scheme endorsed by the Congress in the Clean Air Act as a way to achieve environmental protection through effective use of market mechanisms.

I clearly am not alone in my assessment that renewable programs can be successfully incorporated into fully competitive markets through the good offices of regulatory agencies. Both California and New York have included renewable provisions in their restructuring plans. The CPUC's final rule governing restructuring includes a minimum renewables purchase requirement and makes credits for meeting this requirement tradeable. A recent New York ruling on retail competition requires a system benefits charge that will be used to fund energy efficiency and renewables. According to the New York Public Service Commission, the environmental surcharge will be non-bypassable because it will be assessed on distribution charges.

IV.

The coming competitive environment that FERC envisions is one characterized by access, choice, and equity. The opportunities presented in this market can be significant. So can the risks, admittedly. To what extent are the industry and public policymakers prepared to support renewable resources and conservation efforts in a climate heavily influenced by the push for low-priced electricity? This is a key policy question for all of us in the future. I believe that, for a time at least, free market competition must be tempered by protection for certain fundamental principles, including reliability, conservation, environmental protection, equitable and universal access, and promotion of economic development. The task for regulators is to identify areas where the market may fail to provide adequately those benefits that most Americans will continue to regard as "in the public interest" and then to compensate for those failures.

In the future, regulators and the proponents of alternative generation and conservation will be challenged to find competitively-neutral, market-based ways to provide the same social and economic benefits formerly derived only pursuant to state mandate. I believe we are up to this challenge and that a vital and viable renewable energy industry will yield end-results for our society and our environment that will be well worth the effort.

Thank you.

SOME PERSPECTIVES ON THE ELECTRIC INDUSTRY

Jonathan H. Winer
Vice President & Chief Operating Officer
Mountain Energy, Inc.
35 Green Mountain Drive
South Burlington, VT 05403 USA

INTRODUCTION AND BACKGROUND

To assess and predict future directions in the electric industry, consideration of the past may be helpful. The 1960's were characterized by declining unit energy costs, resulting from economies of scale in large generating facilities. The 1965 Northeast blackout raised concerns about reliability; the North American Reliability Council was formed, and transmission system reinforcements were the order of the day.

The 70's saw the dramatic rise of oil prices, with some shortages. Nuclear power reliance increased substantially, but Three-Mile Island's troubles in 1979 caused a dramatic change in direction. PURPA was passed in 1978 as was the Fuel Use Act, which essentially banned the use of natural gas for electric generation.

In the early 80's, as utility power plant costs escalated, we implemented PURPA, relying on continuation of the previous decade's oil price escalation. Reacting to concerns about over-reliance on foreign energy sources, substantial state government initiatives fostered the growth of all domestic alternatives, including wind. Later in the decade, long-term integrated resource planning including demand-side management became the way to address the spectre of expensive central station power plants and the expected resumption of oil and gas price escalation. This approach continued even though

oil prices declined 50% during the decade! Utilities in many regions could not actively market electricity (their product) because the mandate was conservation. We began to see that power generation could be a competitive activity, utilities conducted large scale resource bidding programs often receiving offers totalling 30 to 50 times more power than they were seeking. It also became increasingly difficult to site transmission facilities, at least in the northeast.

In the early 90's, most of the generation was being built by independents. But just as this trend has taken hold, further shifts are occurring. Trade journals have few articles about new power supply needs in the United States, but instead cover buyouts of long-term contracts for power that is not priced competitively in the long-term or the short-term. There is far more text on international opportunities, including such distant locations as Sri Lanka, than on domestic needs. And the international needs are, indeed, huge.

Fuel prices continue to be relatively low and generally are below the pre-1974 embargo prices on a real basis. The building of large central station generating and transmission facilities is rare and risky financially. First, utilities and consumers have become more efficient in the use of generating capacity. Second, these facilities are hard to permit and cause a big impact on rates in their early years. Sales growth does not normally occur in such large blocks. Accordingly, many utilities look to smaller scale generation with shorter lead times that can often be located closer to the customers, reducing transmission needs and providing electrical system support. Long-term resource planning has become very difficult as we no longer know who will be whose customer in a few years, or even now as various pilot programs unfold. Certainly, taking the long view on resource decisions during these uncertain times may be inconsistent with short-term financial survival.

To sum up this is where we have been:

1960's	Reliability, Transmission
1970's	Large plants (many nuclear), Escalating Oil Prices
1980's	PURPA, Conservation
1990's	Transmission Access, Unbundling, Deregulation

So, where are we going from here?

INDUSTRY SHIFTS

Current Rules	New World
Revenue requirement	Profit/cash flow analysis
Allowed Rate of Return and Cost Recovery	Market prices and efficiency determine any profit margin
Regulator is proxy for customer choice	Direct access of customers to suppliers
Bundled service that affects all customers similarly	Unbundled service with greater variability of risk allocation and greater direct account-ability to customers
Obligation to serve	Some obligation, but with an emphasis on identifying and pursuing other markets

COMPONENTS OF THE NEW ELECTRIC WORLD

1. ELECTRICITY IS BECOMING A COMMODITY - many utilities are not oriented to commodity transactions.

2. PRICE IS VERY IMPORTANT, with certain customers providing low profit margins - in Argentina recently, wholesale electricity was being given away as part of competition.

3. HOW LOYAL WILL CUSTOMERS BE? Phone service and UK results show not very.

4. People will treat CALLS FROM CUSTOMERS AS OPPORTUNITIES not interruptions.

5. CUSTOMIZED SERVICE will be more prevalent as we move further away from the "one size fits all" requirements. This will utilize and drive major technology advances.

ISSUES FOR CONSIDERATION

1. How will capital assets be financed? Will the merchant plant model work?

2. Will consolidation result in too few sellers? Great capital capability may be needed.

3. Will all customers have access to the new market?

4. Will R&D funding continue to be available to support the development of new technologies?

5. How will customers be informed? Will they really pay more for certain types of power? In New Hampshire, Green Mountain Power has staked out a green position with favorable reaction from customers. It is still too early to assess, of course.

HOW WILL RENEWABLES FARE IN THE INCREASINGLY COMPETITIVE WORLD?

1. The ability to add smaller increments of generation efficiently is an advantage. Wind plant "clusters" such as our Searsburg site are consistent with this advantage.

2. Some (many) customers favor renewables and they will be able to chose.

3. If price is king, and the direct cost of renewables is higher than new "traditional" generation, will renewables survive? Certainly, many utilities recognize the need to have renewables well-represented in their generation portfolio.

4. GMP's studies and observations are that the public will support some higher price for renewables. Low external costs and dispersed generation are important factors.

WHAT CAN BE DONE?

1. We need continued R&D funding at the national level to promote technology improvement for new and existing technologies that are disadvantaged in the price focused market.

2. The full cost of producing power, including external costs, needs to be considered. Emission taxes at the national level would allow this to happen through the market.

3. Put some "societal" costs of renewables on the T&D charges to level the playing field.

4. Greater consumer information. Lack of information causes consumers to be skeptical about renewables. Education may increase consumers' willingness to pay for the benefits of renewables. We must also guard against overselling the benefits. In obtaining approval for our Vermont project, GMP was careful to address the costs and the benefits of windpower. If we promote both sides, potential opponents feel we are being evenhanded and are less concerned.

5. Remind people not to be 100% committed to one energy strategy. Such an approach requires major changes every five to ten years. Some reliance on the domestic wind resource should reduce the risk of energy portfolios.

CONCLUSION

The era of "regulators knowing best" is changing. Now, the "rules" are or are about to be set directly by customers. And the new "rules" will differ based on the variety of customer needs. We must talk directly to customers and find out what they are willing to support financially. This will require careful listening to people who have usually been told what they had to do regarding electricity. At Green Mountain Power, we think many customers want renewables including windpower. And this has been a basis for our company's approach in Vermont, in New Hampshire and through other parts of the country.

BUILDING A SUSTAINABLE MARKET FOR RENEWABLES

Nancy Rader
AWEA West Coast Representative

My comments today are going to be a little bit California-centric, since I've been representing AWEA in California for the last 2 years. But we've done a lot of thinking in California about how to assure that the benefits of renewables are not lost in competitive electric markets, and we've thought a lot about how different policies might work. I think that much of what we've learned applies to other areas of the country as well, and perhaps internationally.

The reason we've chosen to aggressively pursue the Renewables Portfolio Standard in California is because it will create a stable economic environment for the wind industry and other renewable energy industries during this very unstable transition to a more competitive electric industry.

But it also fits with competitive, deregulated markets because the whole reason the electric industry is being deregulated is because we think that markets are more efficient in delivering the electric services we want than are regulators and public agencies. In the same way, this market-based renewables policy will deliver the renewable energy that we know consumers want at the lowest possible cost.

So, first, let me briefly describe the Renewables Portfolio Standard concept. Since the California Public Utilities Commission adopted this policy approach in its December 1995 restructuring order, we've put a lot of thought into the details of how it would work.

Essentially, in California, what this policy says is that it makes sense to ensure that a meaningful fraction of our electric supply come from non-polluting, renewable energy that also acts as a hedge against over-reliance on fossil-fuel, and which directly supports about 5,000 jobs and rural economies across state. And, further, that these goals are too important to gamble on and risk losing as we move to retail competition.

Therefore, we're going to create a simple market rule that says, if retail suppliers want to do business in California, they must maintain a resource portfolio that includes at least 10% renewable energy--about the amount of energy in California that is currently supplied by wind, solar, biomass and geothermal resources. And this level would rise to 11% over five years. It's a tradable obligation, because it is based on a system of tradable "renewable energy credits," -- RECs for short -- which makes it flexible and which allows for maximum efficiency in meeting the standard.

So, for example, when a wind generator sells its power, it also generates RECs -- one REC for each kWh it generates. Those RECs are an entirely separate product from the power itself. So, the generator might sell its power into the power market, and RECs into the REC market or bundle power together with RECs. And retail sellers, who must purchase these credits, have the same options.

The only thing the government does is certify that renewable energy generation has occurred and issue the RECs, and then verify that each retail seller has enough RECs at the end of the year. A penalty exceeding the cost of compliance would be imposed on those not in compliance, which will result in virtually full compliance.

I'm often asked how much the RECs are worth. But no one sets the value of these credits--the market sets the value. Based on the laws of economics, the price of credits should reflect the difference between the marginal cost of generic power, and the marginal cost of renewable power. So, it sets up a market competition among renewables--but renewables do not have to compete against non-renewables, that is, fossil fuel, nuclear power plants (whose cost recovery will be guaranteed in California), and even hydropower, which is not included in this policy as a renewable for a variety of reasons.

The system of renewable energy credits works just like the tradable allowance system under the federal Clean Air Act that is working so well, and which has dramatically reduced the cost of sulfur dioxide reduction, compared to what was expected.

What the Portfolio Standard does, then, is put in place a simple market rule and let the market decide how to meet the rule at the least cost.

Think of it -- every retail seller now has an interest in driving down the cost of renewables, because they are in competition with every other retail seller who must also meet its renewables obligation. Now it's not you on your own trying to raise low-cost capital, and trying to get the market rules to work right for wind. Now it's you and the largest players in this industry trying to figure out how to drive your costs down.

That's what makes the difference in this approach. That's what makes it efficient, and that's what will drive the cost of renewables down.

Now, compare this to the other most frequently mentioned approach to supporting renewables in competitive markets--at least in California. And that is the "systems benefits charge" -- a surcharge on the bills of all customers which would create a pool of funds to support renewables.

Like Randy Swisher said yesterday, the systems benefits charge approach is necessary and appropriate for supporting low income and RD&D programs, but it is not the best approach for supporting market-ready renewables in competitive markets.

In California, the Environmental Defense Fund, EDF, has proposed an "Auctioned Renewables Credit" as the most efficient way to spend the funds that are collected through the systems benefits charge. Even though the PUC specifically rejected this approach, a number of parties continue to advocate it (and I must say that these parties are not exactly renewable energy's best friends).

Under EDF's approach, developers would bid for a per-kWh production subsidy which would be paid out for 10 years. The lowest bid wins. Then, the winning project must meet milestones to

make sure the project is advancing -- if milestones are missed, the funds are turned back into the pot, and we start all over again.

So, first of all, you have that inefficiency: if you miss getting a permit by one week, for example, you lose your funds. That kind of arbitrary rule--which is necessary when you're tying up the public's funds--creates inefficiencies that would not exist under a market-oriented approach.

Second, funds are only awarded to new projects, even if it is cheaper to support an existing project that would otherwise cease to operate. This is clearly inefficient, but, under this approach, only new projects would be allowed to bid.

Third, this approach creates an opportunity for speculative bidding, because--in a price-only competition--no weight is given for holding a contract, having the necessary permits, having a good company track-record, or any of the other barometers of success that are commonly used in business transactions. So there is nothing to prevent a bidder from imposing his wishful thinking on the program, and stalling the public benefits that are supposed to flow from the program.

Of course, all of these details are almost beside-the-point since the system benefits charge as proposed in California would do nothing to support existing projects or the 10% level of diversity currently provided by renewables in California.

In fact, the current surcharge proposal would support the operation of only about 200-600 MW of capacity at most -- in its fifth effective year -- which could be 2003 or later just due to the nature of the program. This compares to the 3,600 MW of renewables that are currently operating and would be immediately supported under the Portfolio Standard.

So, clearly, if the goal is sustainability, the surcharge approach being put forward in California is certainly not aimed at getting us there, nor would it be the most efficient way to get us there. The Portfolio Standard is much more suitable for achieving the goal of sustainability because it simply puts electric markets on a more sustainable path, as opposed to the circuitous route of the surcharge.

And, by the way, any economist who is true to economic theory knows that markets can be very efficiently unsustainable, and that achieving sustainability doesn't mean we have to compromise efficiency. (See the July 1996 edition of *The Electricity Journal* for an article by myself and economist Richard Norgaard on this point.)

Similarly, if the goal is to correct the market barriers that we can expect to hinder renewables in competitive markets, then the Portfolio Standard most directly overcomes those barriers. Once you create a market for renewables by requiring retail sellers to get engaged with renewables, you automatically overcome the difficulty of obtaining long-term financing in short-term markets, and the transactions costs and institutional barriers associated with marketing a unique resource, especially on a retail level.

By contrast, under the surcharge approach, these barriers are not removed, they will just result in increasing the amount of the subsidy that is required in order to get the project over these hurdles and into the market -- so that our limited public dollars will go less far.

Now I'd briefly like to address the argument that is often made that retail choice -- that is, "green pricing" and "green marketing" programs -- are all that renewables need in restructured markets.

There's nothing wrong with the concept of consumers having the ability to choose more environmentally-sound sources of electric power. Done right, it's a fine idea. By "done right", I mean that consumers need to know what they're getting and not pay more than they need to for renewable power.

But I worry about it being done wrong. I worry that utilities may invest in the highest-cost renewables instead of the lowest-cost ones. I worry that retail suppliers may overcharge for the renewable power they are supplying--kind of like putting a higher price tag on a cheap bottle of wine and watching sales increase. And I worry about putting a "green seal-of-approval" on gas and large hydro, which is already happening in New England.

For meaningful customer choice, I think we will need some meaningful consumer disclosure requirements--not some generic green stamp, but exactly how many kilowatt-hours of renewable energy the consumer is paying for, so that consumers can really do some comparison shopping and so that suppliers truly diversify their supply, and don't just put a lot of pretty pictures of windfarms in their TV commercials. This will require a system of tradable credits just like what would occur under the Portfolio Standard--which is one reason why the Portfolio Standard fits very well with green marketing.

But, more fundamentally, our environmental problems, the value of resource diversity, and the value of local economic development are too important to leave to volunteerism. As Christine Ervin said, we know from Econ 101 that markets contain many barriers to goods that create public benefits--that is, benefits that accrue to society at large, not to the purchasing consumer.

For the same reason that no one advocates repealing the Clean Air Act once we get retail competition -- even though consumers will have the ability to choose something besides coal -- we cannot assume that consumer choice alone will be sufficient to sustain the renewable energy industries in this country or to achieve a more sustainable electric system, even though public opinion polls clearly show that there is strong public support for these goals.

In fact, creating a stable economic environment for the renewable energy industries -- putting in place the market floor and infrastructure that would be established by the Renewables Portfolio Standard -- is essential if consumers are going to have much choice at all, because the industries need a healthy base from which to compete for additional "green" sales.

The notion that consumer choice, by itself, is enough actually disempowers consumers -- in their dual role as citizens -- from their right to affect, through our democracy, the rules that govern the marketplace.

In closing, I want to take this opportunity to emphasize how critically important it is that anyone with a stake in the California wind industry get involved in AWEA's effort to pass the RPS this summer. Our bill, AB 1202, is now in a Senate-Assembly conference committee, and what happens in the next 8 weeks will be critical to getting it to the Governor's desk in September. We need for all of you to get involved, and I urge anyone connected with the California industry to stop by our Portfolio Standard booth out in the hall to find out how you can get involved in this campaign which is so critical to the future of the wind industry.

Thank you very much.

Comments in Response to Questions:

Comments on Green Pricing -- The flipside of green pricing, another way of viewing it, is that it lets commercial and industrial consumers off the hook for paying for their fair share of clean energy and a diverse resource base. It's important to remind ourselves that this would really be the consequence of relying solely on residential consumers to promote renewables in a more competitive electric industry.

Also, I think it's very important to remind ourselves that electricity is "invisible" -- most consumers don't even know where electricity comes from. It's not like cans and bottles sitting on your kitchen floor making you feel guilty. It's much less tangible. Unlike organic produce, you can't see it and enjoy it, and it doesn't contribute directly to your own personal health.

People often make the comparison between green pricing and the fact that people recycle cans and bottles and buy recycled paper. But remember that these markets, and the infrastructure to support these markets, was developed through laws, like municipal recycling laws and state and federal minimum content requirements for recycled paper. These laws allowed consumers to have a choice at all. In the same way, renewable energy needs a policy floor to strengthen our industry -- a base from which we can market to consumers.

How will the different renewables be supported by a policy that doesn't distinguish between renewables? In California, the wind, geothermal and solar thermal electric industries have agreed that we're willing to compete amongst each other -- that we're in close enough competitive range not to need separate policies to support each of our technologies. We're promising competition in the RPS, and I think that's what helps sell the policy. The biomass industry, because of the extra costs associated with its fuel collection and processing, does need some extra policy support, and it can justify that support because of the extra benefits that that industry brings. So, within our 10% standard, there is a 1.8% biomass standard. This is less than what is currently provided by biomass, which will force them to compete.

For technologies that are not yet ready to compete and do not currently have significant market share, like photovoltaics, we are advocating that the system benefits charge include funds to help leverage these technologies into the market created by the Portfolio Standard.

STRATEGIES FOR PROMOTING RENEWABLES IN A NEW ELECTRIC INDUSTRY

BRUCE C. DRIVER
ATTORNEY & CONSULTANT

2260 BASELINE ROAD
SUITE 101
BOULDER, CO 80302

I. INTRODUCTION & SUMMARY

This paper describes strategies for promoting renewable resources in an era characterized by competitive pressures in the electric industry. It begins with a background section to describe the perspective from which I am writing and the nature of the pressures confronting renewables in 1996. Then, the paper turns to a discussion of the regulatory and other options to promote renewables in this environment.

The major conclusion of the paper is that there is no "magic bullet" to guide the development of renewables through the developing competitive era within the electric industry. Indeed, it appears that the job can get done only through a combination of different measures at all levels of government. The author believes that among the most effective measures are likely to be:

--a national renewable resources generation standard;
--conditions attached to restructuring events;
--regional interstate compacts;
--regional risk-sharing consortia supported by federal and state tax and fiscal policy; and
--state "systems benefits charges;"

II. BACKGROUND

A. Perspective I write this paper from the perspective of an environmental organization that has developed a 20-year "blueprint" for the electric industry in the six-state region in which it is active. The organization is the Land and Water Fund of the Rockies (LAW Fund), whose Energy Project advocates for clean power in a six-state region--Arizona, Colorado, Nevada, New Mexico, Utah and Wyoming. I am Special Counsel to the Energy Project as well as an author of its blueprint, "How the West Can Win: A Blueprint for a Clean and Affordable Energy Future," published in April, 1996.

The LAW Fund's goal is to reduce the environmental impacts of meeting the demand for electric energy services. In our region, where we face the need for over 15,000 megawatts (MW) of new

electric resource capacity (demand- and supply-side) in the next 20 years, we cannot achieve our goal without renewable resources. Indeed, the LAW Fund believes that the region should right now start figuring out how we can add roughly 5,000 MW of solar electric generation capacity, nearly 3500 MW (1500 effective on peak) of wind power capacity and almost 2000 MW of geothermal capacity to the region's electric resource capacity by 2015 without unacceptable economic costs.

B. The Problem A higher share of the life-cycle costs of most renewable technologies than of fossil fuel technologies is capital rather than fuel or operating and maintenance expenses. Moreover, some renewable technologies are presently more expensive than fossil fuel technologies, even on a life cycle basis.

These characteristics place renewable resources at a disadvantage as competition advances in the electric industry. In particular, vertically-integrated monopoly utilities, fearing the loss of captive retail customers, are increasingly reluctant to incur new capital costs the recovery of which from ratepayers is in doubt. These utilities also do not want to incur costs that could raise their rates and, thus, make their electricity less competitive.

As a result, utilities are attempting to abandon their commitments to acquire renewable resources, at least where they rely on regulated electricity customers to recover costs. The effect of this development on renewable resources could be devastating. In the LAW Fund's region the effect could be to choke off the supply of capital to emerging technologies at the very time that we must be learning how to rely on them to meet a significant fraction of new electric loads.

III. ELEMENTS OF A STRATEGY TO PROMOTE RENEWABLES

A. State Level Policies

1. Utilities Regulation-General

In theory, there are three ways to respond to the situation described immediately above. The first is to use existing regulatory power over still-vertically-integrated utilities to encourage them to invest in renewables. Integrated Resource Planning (IRP) that is sensitive to competitive pressures is the principal tool. There are still some states, including some in the LAW Fund's region, where this approach has remaining validity, at least in the short to mid-term, while states decide if or when they will move towards retail competition.

A second model is to expedite the transition to competitive markets. The three main steps here are disaggregation of today's vertically-integrated utilities, retail customer choice and implementation of measures to overcome market failures which may

place renewables at a disadvantage in a fully competitive market. This model is also a model in which renewables can survive, indeed, prosper.

A third model, what some utilities in the LAW Fund's region seem to want, is "unregulated monopoly" status, or the lifting of IRP and the abandonment of clean power programs even while the utility stays vertically integrated and struggles to prevent retail customer choice. This model will not work for renewables.

2. **Utilities Regulation--the Specifics**

(a) IRP/Rate-basing Renewables

Most utilities are backing away from this means of promoting renewables. They fear that "mandating" investments in renewables through IRP will place them at a competitive disadvantage.

The author makes reference to this strategy, however, because, in most states, it will likely be many years before retail electric competition is fully implemented. As a result, many utilities will continue to serve mainly captive customers. Arguably, these utilities owe these customers a modicum of investment in renewable resources, even though the investment may be expensive relative to the market price of power in the short run. The duty stems from the fact that, as long as most of us have no choice of utility supplier, we have to depend on the local utility to acquire resources that are not only the best for the utility's short-term financial position, but also meet other public objectives, such as environmental protection, risk diversity and sustainability.

(b) Green Marketing

At least some utilities believe that their sole obligation to the public interest in promoting renewable resources is to implement a green marketing or green pricing program.

Green marketing refers to providing consumers with the option of buying products that are made with less environmental impact than traditional products. There is no reason why this concept cannot be applied to the sale of electricity and, indeed, several utilities have established green pricing programs by which customers are usually given a choice to pay (more) for electricity generated cleanly.

Nonetheless, there are two kinds of problems with green pricing. One is that it depends solely on the market for promotion of renewables. Arguably, there are "market failures" (among them, high discount rates that excuse present-day purchasers of energy from ignoring the long-run) that undervalue investments in renewables. Too, green pricing focuses on the expense of renewables while ignoring the risks and costs associated with less

clean resources. To level the playing field, why not have "brown pricing" for power from dirty resources, or at least the identification on utility bills of the amount of power purchased by a customer from such resources?

As a result of these problems with green-pricing, some rate basing of renewables through IRP is appropriate public policy, pending the establishment of a portfolio standard, systems benefit charge or, ultimately, competition that is fair to renewables.

(c) Portfolio Standard

One theoretically forceful way of promoting renewables is to require that, by a certain date, a fixed percentage of the electricity supplied in a state be generated by renewable technologies. The requirement should fall on all power suppliers (so as to overcome anti-competitive effect), namely utilities, independent power producers and self-generators. Obligations to supply renewable energy could be freely tradeable, leaving the market to select the least-cost means of meeting the standard.

Legislation would be necessary to implement a standard in most states because many PUCs regulate neither municipal or cooperative utilities nor independent power producers or self-generators.

One question raised by a portfolio standard that includes tradeable obligations is whether it will bias the market towards relatively inexpensive renewables technologies. If so, how will more expensive technologies with great long-term potential find reliable funding? Another issue is whether the establishment of a portfolio standard for renewables might divert capital into renewables and away from other clean power investments, especially energy efficiency. Both concerns can be addressed through the creation of Systems Benefits Charges in addition to a portfolio standard.

If the effect of the implementation of a portfolio standard were predictably to raise electric rates in a state, one wonders whether many individual states will, on their own, implement a standard. This concern suggests that a national standard may need to be established by Congress.

(d) Systems Benefits Charges

Systems Benefits Charges, applied to "non-bypassable" distribution assets, have been proposed to fund Demand-Side Management and low income energy assistance. These charges could also be used to fund research, development and demonstration of more expensive renewables technologies.

One question raised by using a systems benefits charge for this purpose is whether there will exist the political will in most states to provide assistance to renewables both through a portfolio

standard and a systems benefits charge.

(e) Net Metering and Other Ways of Promoting Distributed Generation

Certain renewables, especially photovoltaics and wind, may in the short run at least expand market penetration primarily in distributed generation configurations.

One way of encouraging distributed generation is through net metering, in which a distributed energy producer's meter runs backwards at time in which its energy production exceeds its on-site needs. Of course, the economic impact on the utility of this proposal depends on whether its avoidable costs exceed or fall below the rates it charges to this customer.

(f) Breaking up vertically-integrated utilities

Arguably, vertically-integrated utilities will be able to exercise market power to find markets for their often above-market and sometimes dirty power, even though transmission assets are now subject to FERC's open-access order. Thus, many have concluded that fair and open competition in retail electric markets is unobtainable without disaggregation of vertically-integrated utilities.

Vertical disaggregation also creates the possibility to "re-charter" the distribution or transmission/distribution utility that is left after generation assets are spun off. The new T&D entity might be a non-profit company directed to acquire renewable resources as part of its portfolio of resources. For an intriguing proposal of this nature, see the LAW Fund proposal to disaggregate Nevada Power Company, described in "Breaking up is not so hard to do: A Disaggregation proposal," Eric Blank, Rick Gilliam and Jon Wellinghoff, The Electricity Journal, May, 1996.

(g) Attaching Conditions to Restructuring Transactions

Some utilities need regulatory approval of mergers and other restructuring transactions. Why not urge that PUCs condition such approval on the allocation of some fraction of transaction benefits to renewable resources? This is the LAW Fund's strategy in the pending Public Service Company of Colorado/Southwestern Public Service Company merger.

Other restructuring decisions offer greater possibilities. For example, why not provide that, if a utility is to be permitted to recover uneconomic generation costs when retail competition is implemented, a portion of the revenues accumulated go to funding renewable resources? And states might be urged to condition the implementation of retail competition on establishment of a renewables portfolio standard or systems benefits charge.

3. Tax policy

Several studies suggest that state and local governments could give a boost to renewables simply by establishing tax parity between renewable resources and their fossil fuel competitor. In this regard, state and local taxes based on the assessed value of an asset are biased against renewables because of their capital intensity relative to fossil fuel resources.

B. Federal Level Policies

The federal government has been involved in the promotion of renewable resources for nearly 25 years. During that time Congress has appropriated billions of dollars to encourage the development of renewable resources for their resource diversity, environmental and other attributes. The emergence of electric industry restructuring is justification to maintain federal support for renewables, if only to assure that the focus on short-term price in electric markets does not result in loss of the benefits of the federal investment in renewables. Of special importance is the role of the federal government in helping to overcome the tendency among the states to avoid the support of renewables out of the fear that to promote them will have an anti-competitive effect if other states do not follow suit.

1. Utility and Environmental Regulation

There is a long list of federal regulatory measures, some of which require legislation, which could be taken to encourage renewables at the national level. Among them are a national minimum renewables generation standard, which could be implemented by the states and which could be met by any means, such as through a portfolio standard applying to power generators, a systems benefits charge or even green pricing.

A second idea is to clarify federal electricity regulation so that states may continue to promote renewables, energy efficiency and other similar investments without preemption under the Federal Power Act. Such preemption was threatened under opinions rendered by the Federal Energy regulatory Commission in 1995.

In this regard, however, the electric industry is increasingly a regional industry, characterized by large-scale regional power flows, regional transmission groups and other indicia of regionalization. In this environment it may prove difficult for any one state to muster the strength to encourage utilities, independent power producers and others to invest in resources for other than their short-term economic value, regardless of clarification that, to do so, is not preempted by federal law. It may be essential for states to pool their electric regulatory and siting authorities in interstate bodies so that the states can have some effect on power investments. Thus, a third idea for federal

involvement is for Congress to pass legislation to encourage states to form interstate compacts for the purpose of promoting renewables and/or clean power technologies generally. Any such compact might also be useful in establishing a regional market for the trading of renewable credits under a national or state renewable supply requirements.

Another idea is for the federal government to encourage disaggregation of vertically integrated utilities such as through reduction of the federal tax consequences of disaggregation. Disaggregation should alleviate the pressure of utility market power on competitive markets.

Federal involvement in encouraging renewables could also extend to the establishment of environmental regulatory comparability between old and new power plants in the name of fostering fair competition. Applying New Source Performance Standards to old power plants--those that the drafters of the original Clean Air Act thought would be retired by now--may cause some of these plants finally to be retired, opening up a place for new renewable resources to meet loads.

Congress could also attach conditions to any mandate to the states to implement retail wheeling. Similarly, if Congress should order that states allow utilities to recover stranded costs, it might also order that a share of those costs be allocated to the financing of renewable resources.

Finally, federal power marketing administrations, especially the Western Area Power Administration (WAPA), could encourage renewables through power purchase set-asides. Indeed, WAPA has proposed a renewables purchase of 30 MW. Congress is also considering legislation that would transfer the ownership of PMA facilities to non-federal ownership. Authorization of these transactions is another opportunity to promote renewables, in this case through conditions to any such transfer. For example, a new, non-federal owner of a federally constructed dam might be required to use a portion of the output of the dam to firm up intermittent renewable resources.

2. Tax and Fiscal Policy

Federal support of the National Renewable Energy Laboratory has been critical to the development of new renewables technologies as has the wind tax credit been important to wind power development. There may be other ways in which the federal government can help through tax and fiscal measures. For example, federal financial support is at the core of the Solar Enterprise Zone in southern Nevada. Renewables developers and advocates need to be creative in thinking up ways to garner federal support, support that is sensitive to federal budget realities.

C. Other strategies

A number of mechanisms exist by which to spread the financial risk of renewables development that do not directly depend on government. For example, renewable developers, especially those seeking to gain experience with less-developed and/or more expensive technologies, may gain a toehold in the electric market by sharing the fuel input of generating facilities with natural gas in so-called hybrid facilities. Another way of spreading development risk is to form consortia with other interests, such as exemplified by the Arlington, Wyoming windfarm.

IV. CONCLUSION

The road ahead for renewables may look rocky, especially when compared with the favorable regulatory environments of California in the early 1980s or Maine later on. However, these halcyon days have been gone for some time and there is no returning to them. In any event, there are many techniques for promoting renewables in the new electric industry. The problem will be in deciding where the community should put its energy to provide the best basis for encouraging private capital to flow to renewables.

STRATEGIC PLANNING IN ELECTRIC UTILITIES: USING WIND TECHNOLOGIES AS RISK MANAGEMENT TOOLS

Thomas E. Hoff
Pacific Energy Group
108 C. Escondido Village
Stanford, California 94305

Brian Parsons
National Renewable Energy Laboratory
1617 Cole Blvd.
Golden, Colorado 80401

ABSTRACT

This paper highlights research investigating the ownership of renewable energy technologies to mitigate risks faced by the electric utility industry. Renewable energy technology attributes of fuel costs, environmental costs, lead time, modularity, and investment reversibility are discussed. Incorporating some of these attributes into an economic evaluation is illustrated using a municipal utility's decision to invest in either wind generation or natural gas based generation. The research concludes that wind and other modular renewable energy technologies, such as photovoltaics, have the potential to provide decision makers with physical risk-management investments.

INTRODUCTION

Regulatory and technical forces are causing electric utilities to move from a natural monopoly to a more competitive environment. Associated with this movement is an increasing concern about how to manage the risks associated with the electric supply business. There are several approaches to managing these risks. One approach is to purchase financial instruments such as options and futures contracts (Ref. 1). Another approach is to own physical assets that have low risk attributes or characteristics (Refs. 2, 3).

This research investigates the potential of mitigating risk by owning renewable energy technologies. Explicit consideration is given to the attributes of fuel costs, environmental costs, lead time, modularity, and investment reversibility. Ownership perspectives include investor-owned utilities (IOUs), municipal utilities, independent power producers (IPPs), and power consumers. Analytical approaches include risk-adjusted discount rates within a dynamic discounted cash flow framework, option valuation, decision analysis, and future/forward contract comparisons. See Ref. 4 for complete study results.

The research concludes that renewable energy technologies, particularly the modular technologies such as wind and photovoltaics, have the potential to provide decision makers with physical risk-management investments.

RENEWABLE ENERGY ATTRIBUTES

Fuel Costs

One of the most often stated positive attributes of renewable technologies is that they have no fuel costs. As a result, there is no uncertainty associated with the future fuel costs to operate a renewable power plant. All ownership perspectives mentioned earlier can benefit from this attribute. Different ownership

perspectives, however, will benefit to a different degree with those experiencing the most uncertainty realizing the greatest benefit. Currently, this includes IPPs and power consumers because fluctuations in fuel costs (or electricity prices) directly affect the profit of IPPs, the profit of commercial and industrial users of electricity, and the well-being of residential consumers who use power for their residential needs. IOUs and municipal utilities that generate power realize less benefit from a reduction in fuel cost variability because they currently pass this uncertainty on to customers through fuel adjustment clauses. In a more competitive environment, however, it is unlikely that this practice will continue.

When comparing renewable plants to fossil-based plants, the absence of fuel cost uncertainty must be added as a benefit of the renewable plant or counted as a cost of the fossil-based plant. Cost analysis for fossil-based plants typically projects a stream of expected fuel costs, discounts the results, and considers the present value cost as part of the cost of the plant. This analytical approach, however, improperly converts the uncertain stream of future fuel costs into a stream of certain costs without accounting for the reduced uncertainty.

One way to account for this uncertainty is to determine the premium charged for a fixed-price long-term fuel contract (e.g., a natural gas contract) over a series of spot-market based purchases (Ref. 5). Such a contract is analogous to a financial swap (i.e., a series of forward contracts). A second approach is based on utility theory and involves assessing the decision maker's utility function to determine his or her willingness to pay for "certainty" fuel instead of "risky" spot-market based fuel.

Environmental Costs

Another attraction of renewables is that they produce low or no environmental emissions. Quantifying the value of this benefit, however, is controversial. A good part of the debate stems from the fact that the various participants in the process may have vastly different valuations.

The perspective taken in this paper is that of the plant owner, including investors in IPPs, utilities, or power customers. Plant owners can incur two types of costs associated with emissions. First, there is the additional cost of building the plant to comply with current environmental standards. This cost, which is minimal when environmental standards are low, is usually included in evaluating all types of plants, both fossil-based and renewable.

Second, there is the cost associated with future environmental standards that have not yet been established. As Swezey and Wan point out, "prospective environmental cleanup costs of fossil-fuel-based plants are never considered up-front when generation investment decisions are made (Ref. 6)." These future costs have the potential to be quite high. Pacific Gas and Electric Company, for example, estimates that compliance with NO_x emissions rules for its existing power plants could require capital expenditures of up to $355 million over the next ten years (Ref. 7). It is likely that these costs were not anticipated by Pacific Gas and Electric Company when the plants were initially constructed. Power plants that are considered to be very clean by today's standards (e.g., natural gas based generation) may fare very poorly in five years.

A conceptual framework that can be used to view this future cost is that the decision to build any pollution generating source includes the plant owner's decision to give a valuable option to the government. The option gives the government the right (but not the obligation) to change emissions standards or impose externality costs (i.e., environmental taxes) associated with environmental damages at any time and require that all generators meet the standards. The result of this is that there is a positive probability that the plant owner will incur costs in the future. The cost of this option must be accounted for when comparing fossil-based to renewable plants. Either fossil-based plant owners require

compensation for the option that is given to the government or renewable plant owners need to be given a credit. The benefit of low or zero future environmental costs depends on who owns the plant, because some owners are more likely to incur environmental costs. For example, utilities and IPPs are likely to experience more stringent regulation than power consumers who own plants.

Lead Time

Projects with short lead times tend to have greater certainty associated with their installed cost because of fewer cost overruns and less lost revenue caused by plant delays. This is of interest to any party that is responsible for plant construction, although it is most significant for IPPs because utilities and power consumers frequently install generation facilities through a contracting procedure, thus shifting the construction risk away from themselves to the contractor.

IOUs and municipal utilities are still considered to be regulated natural monopolies, which requires them to serve all customers regardless of whether or not it is profitable to do so. The interaction between demand uncertainty, plant lead time, and capacity additions is of concern to these utilities. The smaller the utility, the greater the concern. For this reason, municipal utilities might be particularly concerned about demand uncertainty at the generation system level.

A typical approach to assessing the interaction between demand uncertainty, plant lead time, and capacity additions is to develop scenarios of high, medium, and low demand (Ref. 8) and to calculate the expected present value cost of meeting demand using plants with different lead times.

This approach, however, does not capture the dynamic nature of demand growth. Demand growth can change over time so that demand can grow or not grow at each point in time. For example, rather than always having high, medium, or low demand growth, actual demand may be high the first year, low the second year, and medium the third year. This leads to the situation where the number of scenarios equals the possible growth rate at each time period raised to the power of the number of time periods. For example, if demand growth rate can take on three levels at any time and there are ten time periods, there is a total of 3^{10} or almost 60,000 possible scenarios.

Taking the dynamic nature of demand growth into account rather than simply examining three scenarios results in a valuation that more accurately captures the effect of demand uncertainty. This will often result in an increase in the value of plants with short lead times over the value of plants with longer lead times.

Modularity

Plant modularity affects plant availability in several ways. First, from a revenue perspective, modular plants begin producing power (and thus revenue for utilities and IPPs or cost-savings for power consumers) earlier than non-modular plants. Modular plants begin producing power earlier than non-modular plants because each segment of a modular plant can come on line as it is completed.

Second, from an operational perspective, modular plants have less variance in their equipment availability than non-modular plants when equipment failures in the modular plant are independently distributed. A non-modular plant can be considered to be either operating or not operating. Modular plants, by contrast, can have partial availability. For example, a modular plant with two identical segments has three possible levels of availability: the plant is 100% available if both segments are functional; it is 50% available if either the first or the second segment is functional; and it is unavailable if both segments are non-functional.

The greater the number of segments in the modular plant (i.e., the more modular the plant is) the lower the variance. This means that there is a greater reliability associated with the availability of modular plants than with non-modular plants. Wind and photovoltaic plants are modular and are composed of a large number of identical parts.

In addition, a modular plant ties up fewer capital resources during the construction of the total plant. The project developer needs only enough working capital to finance one segment at a time. Once the first segment is completed, it can be fully financed, and the proceeds used to finance the next segment. This benefit is of particular interest to companies with limited financial resources, such as IPPs.

This benefit is similar to the benefit realized by a developer that chooses to build single-family dwellings rather than an apartment building. The full financial resources are tied up in the apartment building before it is sold while the single family dwellings can be sold as they are completed, thus requiring less working capital.

Moreover, continued construction of a modular plant is often contingent on the success of the previous phase so that there is the opportunity to stop the project without incurring a total loss after each segment is completed. This is because the completed increments of the project are used to produce revenue whether or not the project is fully completed. The same is not true for non-modular projects. While there is always the opportunity to halt construction, doing this on a non-modular project results in a loss of all capital invested to date, less the partially completed project's salvage value. While modularity thus provides value to utilities who want to control demand uncertainty, it is also of value to investors who are funding an IPP and are unsatisfied with the project's progress.

For these reasons, utilities are investing in small plants, such as gas turbines. Even smaller investments may further increase the risk-mitigation value.

Investment Reversibility

Investment reversibility is the degree to which an investment is reversible once it is completed. This is of interest to plant owners because they need to know if a plant can be salvaged and what its value is in an alternative application. Modular plants are likely to have a higher salvage value than non-modular plants because it is more feasible to move modular plants to areas of higher value or even for use in other applications. The degree of reversibility is a function of the difficulty and cost in moving the technology to another location and the feasibility of using it in different applications.

This value is not merely a hypothetical one. Consider, for example, the case of the 6 MW Carrisa Plains PV plant facility (California). Its original owner (Arco Solar) sold the plant for strategic reasons to another company. This company dismantled the plant and resold the modules at a retail price of $4,000 to $5,000 per kilowatt at a time when new modules were selling for $6,500 to $7,000 per kW.

ILLUSTRATION OF PRINCIPLES

Municipal Utility Purchases Wind Generation

Municipal utilities represent an important market for wind technologies for several reasons. First, they are likely to continue investing in power plants as opposed to only purchasing power from other power producers. Second, they appear to be able to represent the preferences of their customers for renewable energy technologies in their purchase decisions. Third, they have a lower cost of capital, thus reducing some of the bias against generation technologies that have high initial capital costs and low operation and

maintenance costs. Fourth, their tax-exempt status eliminates the tax benefit of expenses (e.g., fuel costs) over long-term capital costs.

This illustration compares the cost of a municipal utility's investment in wind generation with its cost of an investment in natural gas-based generation. The risk-mitigation benefits associated with the wind generation that are presented include the elimination of natural gas fuel price uncertainty, the elimination of potential future environmental costs associated with carbon emissions, and the value of more effectively matching generation system capacity with demand. The following discussion is meant for purposes of illustration and is not meant to imply that these are the only attributes of importance in this scenario.

Capacity and Demand

The municipal utility's historical and projected peak demand and its existing generation system capacity are presented in Figure 1. The current year is 1995 and the peak demand for this year is 480 MW. The lower solid line describes what historical peak demand has been from 1991 to 1995. The dashed lines describe projected peak demand with the light lines corresponding to the possible peak demands and the heavy line corresponding to the average peak demand. The utility has been experiencing an annual load growth of either 10 MW/year or 0 MW/year, each with an equal probability of 0.5. The utility believes that this same trend will continue in the future. The figure suggests that there will be no excess system capacity if peak demand increases for two consecutive years.

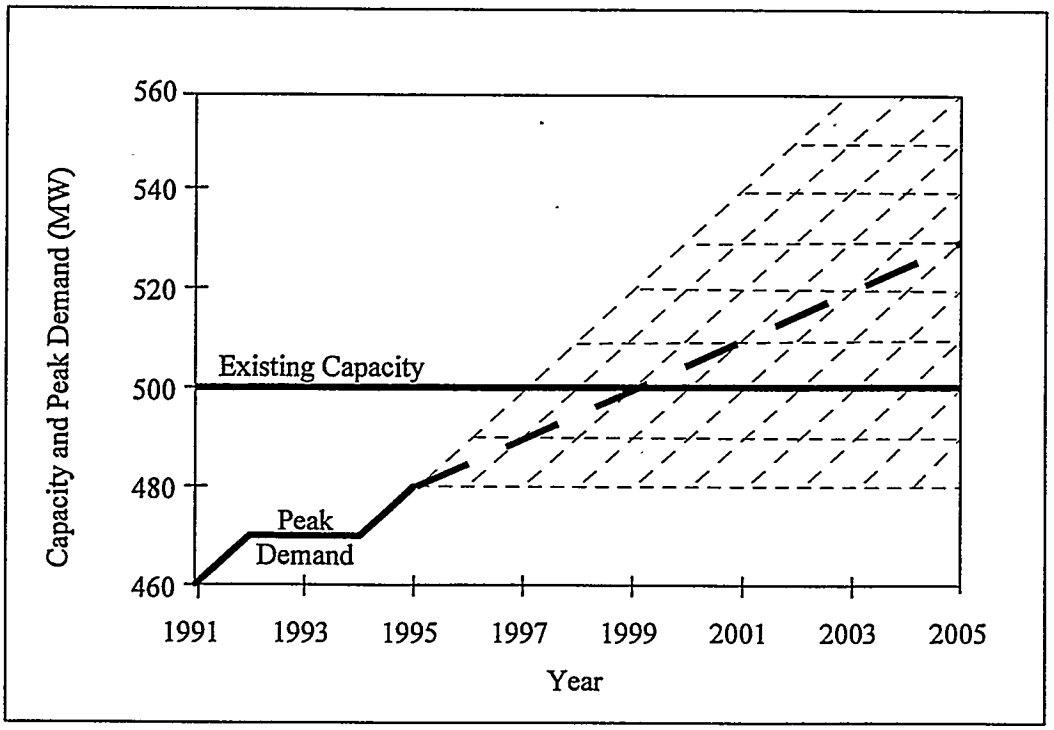

Figure 1. System capacity and peak demand.

Generation Alternatives

The utility has decided that it will either purchase a 50-MW natural gas-based plant or an equivalent amount of wind generation. It has completed a detailed, multi-year wind resource assessment program and has evaluated the match between the wind plant output and its peak load. Results indicate that a wind plant would have a 40% annual capacity factor (combined wind resource and equipment availability) and would provide generation system capacity equal to 40% of its nameplate capacity.

The natural gas-based plant can be operated at an 80% annual capacity factor for 20 years and has a 20% forced outage rate. Thus, a 100-MW wind plant is needed to provide the same generation capacity and the same amount of energy as the natural gas-based generation (i.e., a 50-MW natural gas-based plant with a 20% forced outage rate and 80% capacity factor increases system capacity by 40 MW and produces 350 GWh/year; a 100-MW wind plant increases system capacity by 40 MW and produces 350 GWh/year). Both alternatives will be fully financed by tax-free municipal bonds at 5%.

The plants differ in two major ways. First, the natural gas plant must be constructed all at one time, while the wind plant can be constructed in 25-MW segments so that each segment increases system capacity by 10 MW. Second, the natural gas plant has a 2-year lead time while each segment of the wind plant has a 1-year lead time.

Construction on the natural gas plant must begin immediately in 1995 so that the plant will be available if demand increases by 10 MW/year for two consecutive years. The top dashed line in Figure 2 presents system capacity with the natural gas-based generation.

In terms of the wind plant, the time at which each of the 25-MW wind plant segments must be built is uncertain. For example, construction on the first segment will begin when peak demand reaches 490 MW for the first time. This can happen in 1996 (0.5 probability), 1997 (0.25 probability), 1998 (0.125 probability), etc. The mathematical formulation of how to calculate the probability of demand reaching a certain point for the first time is fully developed in Reference 4. When this calculation is repeated for each of the four segments and the results summed, the expected increase in system capacity is as presented by the lower dashed capacity line in Figure 2.

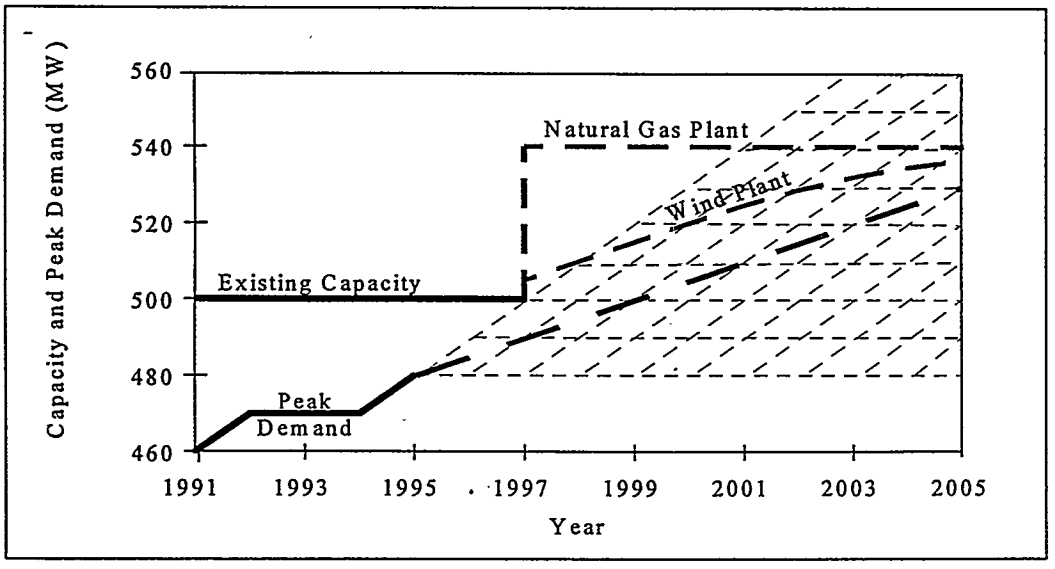

Figure 2. Capacity increases associated with gas and wind plants.

Wind Plant Costs

Two costs associated with the wind generation are its initial capital cost and its O&M cost; it is assumed that there are no firming costs and no added transmission costs. The wind plant capital cost is $800/kW and the O&M cost is $0.005/kWh. The annual O&M cost is $18/kW-year based on a 40% capacity factor. Using a discount rate of 5% (equal to the municipals cost of capital) for the 20 year life, the total present value cost equals $\$800+\sum_{i=1}^{20}\frac{\$18}{1.05^i}=\$1{,}025/\text{kW}$. Thus, the total cost of a 25-MW segment equals $26 million.

The total present value cost of the wind plant equals the expected discounted cost of when each segment is installed. As discussed in Reference 4, the expected cost of an investment equals $C_0\left(\frac{1}{1+r/p}\right)^L$, where C_0 is the investment cost, r is the real discount rate, and p is the probability of the load growing in a given year (0.5). In this analysis, L equals 1, 2, 3, and 4 for the first, second, third, and fourth wind plant segments. Since $\left(\frac{1}{1+r/p}\right)$ equals $\left(\frac{1}{1.1}\right)$, the total expected wind plant cost is $26\left[\left(\frac{1}{1.1}\right)^1+\left(\frac{1}{1.1}\right)^2+\left(\frac{1}{1.1}\right)^3+\left(\frac{1}{1.1}\right)^4\right]$, or $82 million.

Natural Gas-Based Plant Costs

Three costs associated with the natural gas-based plant are its capital cost, fuel cost, and potential future environmental costs. In terms of the capital cost, a 50-MW natural gas plant has a $25 million capital cost if its per unit cost is $500/kW.

In terms of the fuel cost, the natural gas plant is operated so that it produces the same amount of energy per year as the wind plant. For example, if only one segment of the wind plant is on-line, then the gas plant has a 20% annual capacity factor. The risk associated with natural gas price fluctuations is mitigated by committing to purchase four sets of 20-year natural gas contracts, one for when each of the four wind plant segments would have been needed. Each contract will supply 87.5 GWh/year worth of fuel (i.e., the same amount of electricity as produced by the 25-MW segment of the wind plant).

This requires a natural gas contract of 525,000 MBtu, assuming a constant heat rate of 6,000 Btu/kWh for simplicity. If the contracted natural gas price is $2.50/MBtu, then the annual contract cost is $1.3 million (this translates to an annual energy cost of $0.015/kWh). If this is the contracted price for 20 years, then this cost, discounted at the rate of debt over a 20-year period, equals $\sum_{i=1}^{20}\frac{1.3}{1.05^i}=\$16$ million.

The expected present value cost of these four fuel contracts must be calculated because the contracts are not entered into until each segment of the wind plant would have begun operation. The calculation is similar to that performed for the wind plant cost. The only difference is that the contract costs occur one year later (and thus must be discounted by an additional year) than the wind plant costs because there is

no lead time associated with the fuel contracts. The present value cost of the four fuel contracts equals $\left(\frac{16}{1.05}\right)\left[\left(\frac{1}{1.1}\right)^1+\left(\frac{1}{1.1}\right)^2+\left(\frac{1}{1.1}\right)^3+\left(\frac{1}{1.1}\right)^4\right]$, or \$48 million.

The third cost is the potential cost associated with future environmental regulations. While there are many potential regulations that could affect the cost of the natural gas-based plant, only the potential cost of carbon emissions because of the government developing regulations because of problems with global warming is considered.

There are 0.0145 tons of carbon/MBtu of natural gas (Ref. 9). Thus, the annual carbon emissions for each fuel contract equals 7,600 tons of carbon (0.0145 tons of carbon/MBtu times 525,000 MBtu). There is a total annual emissions of 30,450 tons of carbon when all four contracts have been purchased.

Bernow, et. al. (Ref. 10) have developed a set of scenarios of the potential future costs associated with carbon emissions. They have cases of no taxes, medium taxes (\$37/ton), and high taxes (\$110/ton).

By year 10, Figure 2 indicates that the full output of the wind plant is needed and thus the natural gas-based generation will be producing at its full power (i.e., demand will have grown sufficiently to require all of the generation). Assume that the carbon taxes are instituted in 2005 and that they last for 10 years of the plant's life. The total present value cost equals $\sum_{i=11}^{20}\frac{(tax)30,450}{1.05^i}=(tax)(144,350)$ so that the present value cost is \$5 million at a tax rate of \$37/ton and \$16 million at a tax rate of \$110/ton. If it is assumed that each of the three possible tax rates are equally likely, then the expected cost associated with carbon emissions equals \$7 million.

The total cost of the natural gas-based generation equals the sum of its capital, fuel, and potential environmental costs. This total equals \$25 million + \$48 million + \$7 million, or \$80 million. This cost is almost identical to the wind plants cost of \$82 million.

CONCLUSIONS AND FUTURE DIRECTIONS

Regulatory and technical forces are causing electric utilities to move from a natural monopoly to a more competitive environment. This change is causing an increasing concern about how to manage the risks associated with the electric supply business. This paper discussed the risk-mitigation potential of renewable energy technologies from several ownership perspectives. Specific attention was given to the attributes of fuel costs, environmental costs, modularity, lead time, availability, initial capital costs, and investment reversibility.

The conclusion of this research is that renewable energy technologies, particularly the modular technologies such as wind and photovoltaics, have attributes that may be attractive to a variety of decision makers depending on the uncertainties that are the greatest concern to them.

An illustrative example of a municipal utility considering either wind or natural gas-based generation shows that the consideration of risk attributes could significantly affect the decision process.

A full report that develops the equations for the discussed risk factors as well as presenting illustrative examples for wind and photovoltaic technologies with different project owner perspectives is forthcoming. We plan to carry the work further by applying a comprehensive set of risk factors to actual utility situations and future potential decisions through collaboration with decision makers and plant owners.

ACKNOWLEDGMENTS

Special thanks to Shimon Awerbuch (Independent Economist) and Howard Wenger (Pacific Energy Group) for their helpful comments and to Christy Herig (National Renewable Energy Laboratory) and Jack Cadogan (U.S. Department of Energy) for their support of this work and for their comments.

BIBLIOGRAPHY

1. Jones, S. T., and Felder, F. A., "Using Derivatives in Real Decisionmaking," Public Utilities Fortnightly, 132, 18-21, and 25, Oct. 15, 1994.
2. Cadogan, J. B., et al., "The Risks of Conventional Utility Supply Sources and the Rewards of Renewable Energy," Windpower 1992.
3. Logan, D. M., et al., "Integrated Resource Planning with Renewable Resources," The Electricity Journal, 8, 56-66, Mar. 1995.
4. Hoff, T. E., Integrating Renewable Energy Technologies in the Electric Utility Industry: A Risk Management Approach, forthcoming National Renewable Energy Laboratory Report, 1996.
5. Awerbuch, S., "Market-Based IRP: It's Easy!!!" The Electricity Journal, 8, 50-67, Apr. 1995.
6. Swezey, B. G., and Wan, Y., "The True Cost of Renewables," Solar Today, 9, 30-32 Nov./Dec. 1995.
7. Pacific Gas and Electric Company, Annual Report, p. 20, 1994.
8. Price, S., Clauhs, B., and Bustard, J., "Profitability and Risk Assessment of T&D Capital Expansion Plans," Distributed Resources 1995: EPRI's First Annual Distributed Resources Conference, Kansas City, Missouri, Aug., 1995.
9. Masters, G. M., Introduction to Environmental Engineering and Science, New Jersey: Prentice Hall, 1991, p. 398.
10. Bernow, S., et. al., Resource and Compliance Planning: A Utility Case Study of Combined SO2/CO2 Reduction, Final Report, U.S. Environmental Protection Agency, Acid Rain Division, 1994.

EVALUATING THE RISK-REDUCTION BENEFITS OF WIND ENERGY

Michael C. Brower
Brower & Company
154 Main Street
Andover, MA 01810

Kevin Bell
Convergence Research
6001 Phinney Avenue North
Seattle, WA 98103

Stephen Bernow and Max Duckworth
Tellus Institute
11 Arlington St.
Boston, MA 02116

Peter Spinney
Charles River Associates
John Hancock Tower
200 Clarendon Street T-33
Boston, MA 02116

ABSTRACT

This paper presents preliminary results of a study to evaluate the risk-reduction benefits of wind power for a case study utility system using decision analysis techniques. The costs and risks of two alternative decisions—whether to build a 400 MW gas-fired combined cycle plant or a 1600 MW wind plant in 2003—were compared through computer simulations as fuel prices, environmental regulatory costs, wind and conventional power plant availability, and load growth were allowed to vary. Three different market scenarios were examined: traditional regulation, a short-term power pool, and fixed-price contracts of varying duration. The study concludes that, from the perspective of ratepayers, wind energy provides a net levelized risk-reduction benefit of $3.4 to $7.8/MWh under traditional regulation, and less in the other scenarios. From the perspective of the utility plant owners, wind provides a significant risk benefit in the unregulated market scenarios but none in a regulated market. The methodology and findings should help inform utility resource planning and industry restructuring efforts.

INTRODUCTION

The question of uncertainty and risk in electric utility resource planning has received considerable attention in recent years. During the 1980s, many utilities suffered losses because of unexpectedly high plant construction costs and low growth in electricity demand. Since then, the introduction of competition to the electric industry has created additional risks for power companies. No longer will utilities be able to count on regulatory protections and a base of captive consumers to provide a stable market and adequate return on their investments. New risk management strategies will have to be considered.

One approach to managing risk is for a utility company to invest in diverse power sources such as wind power plants. Since wind plants consume no fuel, can be built in relatively small increments with short construction lead times, and generate no pollutants, it is often said that they offer significant protection from risks associated with conventional fossil-fuel power plants. There have been few efforts to quantify these benefits, however.[1]

This study compares the costs and risks of two competing resource options, a gas-fired combined cycle plant and a wind plant, both utility-owned, through decision analysis. The case study utility is Texas Utilities Electric, a very large investor-owned company serving an area with substantial, high-quality wind resources. We chose a specific moment in the future—the year 2003—when the utility currently plans to build a large fossil-fueled power plant, and examined the implications for the utility's expected revenues, costs, and profits if a wind plant were to be built instead. The uncertain inputs include fuel prices, environmental regulations (specifically, CO_2 controls), wind and conventional power plant availability, and load growth. The study did not address any benefits of modularity or short construction lead time, although the model could be adapted to do so.

OVERVIEW OF THE MODEL

The model we developed and used, the Strategic Resources Planning (SRP) model, generates resource expansion plans and estimates capital and operating expenses for the utility over a 20-year period. The resource plans and their estimated costs differ with each Monte Carlo draw of the uncertain inputs. For example, if gas prices increase sharply relative to coal prices in a particular draw, the model may select coal or wind instead of gas in its build decisions. The results of all the simulations are collected and presented as both an expected value and standard deviation of any indicator of interest (such as present-value revenue requirements or annual net income). Simulations are run until the relative standard error of mean revenues is less than one percent. This usually takes about 300 runs. The wind and gas scenarios are run simultaneously, using the same uncertain inputs, resulting in a very precise determination of the differences between them.

The capital costs and operating characteristics of new and existing fossil plants are based on TU Electric FERC Form 1 data as well as filings before the Texas Public Utilities Commission. The wind capital cost is assumed to decrease from $908/kW in 1996 to $845/kW in 2003. The wind capacity factor, 36 percent, is derived from DOE Candidate Wind Site data collected near Amarillo, Texas, assuming a 40 meter tower height and a power curve for the Enercon E-40 wind turbine. The initial 1600 MW of wind capacity is assumed to have a capacity value of 25 percent, which is in accordance with several studies of capacity value on other utility systems. Additions beyond 1600 MW are assumed to have decreasing capacity value.

Fuel Price Trends and Variations

The purchase of fossil fuels for use in power plants is one of TU Electric's largest expense items, constituting about $1.2 billion out of total operating revenues of $5.6 billion in 1994. It is also

---

[1] Two exceptions are Shimon Awerbuch, "Measuring the Costs of Photovoltaics in an Electric Utility Planning Framework," *Progress in Photovoltaics*, vol. 1, 153-164 (1993); and Jonathan M. Jacobs and Thomas E. Huntley, Pacific Gas and Electric Company, "Valuation of Fuel Diversity," Submitted for Hearings before the California Energy Commission (February/March 1992). Both consider only risks resulting from uncertain fuel prices.

one of the most variable and unpredictable and hence important to simulate in this study. From 1976 to 1985, gas prices paid by TU Electric rose at an average real (inflation-adjusted) rate of 15.7 percent, while coal prices rose at an average rate of 10.2 percent; from 1986 to 1993, however, gas prices fell at a 5.8 percent rate, while the rate of decline of coal prices averaged 1.5 percent. These large variations are reflected in the standard deviation of annual real price changes, which from 1976 to 1993 was 16.6 percent for gas and 10.2 percent for coal.

TU Electric's recent fuel price projections indicate that the company expects fuel prices to be much more stable in the future, however. Filings for the 1995 Integrated Resource Plan show an expected real growth rate in gas prices of 1.9 percent per year from 1994 to 2014, with a possible high rate of 2.8 percent and low rate of 0.5 percent. Little or no change is expected in the price of coal or lignite.

In the SRP model, it is assumed that fuel price variations follow a random-walk process, with an adjustment for price "shocks" caused by weather, temporary supply shortages or surpluses, and other factors. This approach is easy to model and can readily reproduce historical price behavior. In a random walk, each annual change in price establishes a new starting point from which the next year's price is calculated. Price shocks are assumed to disappear after one year.

The initial gas price is $2.10 per million Btu, and the initial coal price is $1.55 per million Btu (both 1996 dollars). The random changes in price are drawn from a normal (Gaussian) distribution. The mean of this distribution is taken from TU Electric's median price forecasts, i.e., 1.9 percent for gas and zero for coal. For the standard deviations, we consider two cases. In the high-risk case, we assume that prices will be about as unpredictable and volatile in the future as they have been in the past 25 years. This implies, for gas, a standard deviation of 12 percent in the random walk and 10 percent in the price shocks, resulting in a combined standard deviation of 16 percent. The random walk process results in a long-term range of variation in price that is about three times as large as TU's forecast range. The low risk case is defined by TU's forecast range, which leads to a standard deviation of 4 percent in the random walk and of 6 percent in the price shocks. The volatility of coal prices is assumed to be about two-thirds that of gas prices in both cases.

Load Growth

Unexpected changes in loads can affect the utility company's revenues and profits as well as prices paid by its customers. The past record shows that loads have been variable, although not as variable as gas and even coal prices have been. From 1977 to 1993, the standard deviation in annual changes in TU's loads has been 5 percent. TU Electric's 1995 load forecast suggests a continuation of historical load behavior in the future. The company predicts an average rate of growth in peak loads of 2.5 percent (compared to the historical 3.4 percent) from 1994 to 2004, with a 40 percent chance that the rate may be as high as 3.9 percent and a 40 percent chance that it may be as low as 0.9 percent.

Loads are modeled in the same way as fuel prices, with a combination of a random walk and one-year load shocks due to weather, short-term economic activity, and other factors. As before, the random variables are generated from a normal distribution. Based on TU Electric's projections (and taking into account planned demand-side management efforts), we assume a mean rate of increase of 1.93 percent, with a standard deviation of 3.8 percent to match the range of TU Electric's ten-year forecast. The one-year load shocks are assumed to have a standard deviation of 3.25 percent, yielding a combined standard deviation in load changes of 5 percent. Annual

energy demand is assumed to vary in an identical fashion, following the same random walk but with an independently generated energy shock.

Environmental Costs

Environmental regulatory risks are more difficult to simulate because of the paucity of meaningful historical data on which to base predictions. Nevertheless, the potential liability for electric utilities and their customers appears large. According to EIA data, investor-owned utilities have invested about $60 billion in environmental compliance costs over the past several decades; TU electric's cumulative investment is $2.4 billion. The greatest future cost may be that of greenhouse-gas regulation, although additional NO_x and SO_x controls as well as new limits on toxic metals such as mercury and cadmium may also prove expensive. For simplicity, we have chosen to represent all potential environmental regulatory costs as a CO_2 tax or fee, which may be implemented through an emissions allowance trading regime.

The characterization of the CO_2 regulatory risk in the SRP model has two components. The first is the probability that CO_2 controls will be imposed. We assume that in the high-risk case, that probability is 70 percent over the 20 years after the first year of operation of the wind or gas plant. In the low risk case, the probability that some kind of controls will be imposed over the same period is assumed to be just 30 percent.

The second component is the probability distribution of CO_2 taxes or emissions allowance costs. In an emissions allowance trading regime, the price of an allowance should be equal to the average marginal cost of reducing CO_2 emissions to the level mandated by law. Different studies have produced estimates of the marginal control cost ranging from $10 to $150 per ton for reductions of 20 to 50 percent. Costs near the upper end of this range are not likely to be politically supportable, however, unless the impacts of greenhouse warming prove very severe indeed. We believe a fair range of estimates for the probable cost of control under an emissions trading regime would be $5 to $35 per ton, with a mean value of $25 per ton. The assumed probability distribution is Gaussian with a zero mean from which only positive values are drawn. In order to yield the desired mean control cost, the standard deviation of this distribution is $31.3 per ton.

Plant Availability

Uncertainty in plant availability has frequently been ignored in utility resource planning, even though it can have a powerful impact on reliability and cost of service when a utility system is dominated by a few very large plants. It is especially important to consider in this study because the availability of wind plants is likely to vary much more than that of fossil-fuel plants.

The variability in the annual output of wind power plants is well understood and easily modeled. To estimate its magnitude we simulated the performance of a wind plant using the Enercon E-40 wind turbine and four years of wind data collected in the DOE Candidate Wind Site program near Amarillo, Texas. The resulting annual average capacity factor of the wind plant is approximately 36 percent (assuming a 5 percent wind speed reduction due to wake losses and a 2 percent average power reduction caused by individual turbine outages), with a standard deviation of 6.5 percent.

The uncertainty in wind plant output is incorporated into the model by randomly selecting a capacity factor in each year from a normal distribution with the given mean and standard deviation. When the capacity factor is lower than expected, the model draws more generation

than usual from fossil resources. When the capacity factor is higher than expected, the opposite occurs.

Estimates of fluctuations in the availability of fossil-fuel and nuclear plants are more difficult to come by directly, but can be derived from five-year historical data for large numbers of plants published in the National Electric Reliability Council *Generating Availability Report*. Over the five-year period of record, approximately 5 percent of all fossil-steam units had an FOR of more than 20 percent, whereas 40 percent had an FOR of less than 5 percent. From the NERC data one can derive an implied standard deviation in FOR for individual units by multiplying the observed standard deviation for different unit classes by the square root of the number of units in each class. Since the figures no doubt include some plants that are especially prone to failure, we scaled down the resulting estimates for this study. For existing plants as well as new coal plants, we assume a standard deviation in FOR of 10 percent. For gas-fired combustion turbines and combined cycle units, the standard deviation was assumed to be 5 percent. Since the variations in output of individual fossil units are uncorrelated, the standard deviation in the average FOR of all units in the TU system is only about 1 percent.

RESULTS

First, we review the base (fossil) and alternate (wind) plans under expected conditions, that is, allowing no deviations in fuel prices, load growth, environmental costs, or plant availability. The cost streams are discounted at two different discount rates, the utility's weighted average cost of capital (WACC), 9.64 percent, and the presumed risk-free discount rate, 7.5 percent. In either case, the forced addition of the wind plant in 2003 increases revenues and net income and decreases costs. (Note that net income equals revenue minus cost.) The higher net income is necessary to compensate company shareholders for their larger investment in the wind plant, as is evident from the fact that the return on equity (ROE) in both cases is the same.

Table 1. Comparison of Base and Alternate Plans (million 1996 dollars)*

Parameter	Discounted at WACC			Discounted at Risk-Free Rate		
	Base Plan	Alternate Plan	Change	Base Plan	Alternate Plan	Change
PV of Revenues	$69,737	$70,059	$322	$83,598	$83,906	$308
PV of Costs	$63,817	$63,685	-$132	$76,674	$76,469	-$205
PV of Net Income	$5,920	$6,374	$454	$6,924	$7,437	$513
Average ROE (%)	10.76%	10.76%	0.00%	10.76%	10.76%	0.00%

*Regulated market scenario, expected conditions.

If risks and environmental externalities were ignored, the gas-fired combined cycle unit would appear to be the preferred choice, since it is approximately $300 million less expensive for ratepayers. The following sections describe the effects of taking risk into account on the expected means and variances of the key parameters. Three market scenarios are examined: a regulated market, a power pool market, and a market dominated by fixed-price contracts.

Regulated Market Scenario

In this scenario, electricity prices are not market-determined but set by the regulatory system to achieve a target rate of return on equity (ROE) for TU Electric's stockholders. Changes in fuel prices and environmental costs are passed on to customers through a fuel-cost adjustment to the base electricity rate. Consequently, it can be expected that shareholders will have the least to gain from investing in wind as a risk-management strategy, whereas ratepayers will have the most to gain.

Table 2. Summary of Results (High Risk Assumptions)

Scenario		Revenues		Costs		Net Income		ROE	
		Mean	Std. Dev.	Mean	Std. Dev.	Mean	Std. Dev.	Mean	Std. Dev.
Regulated Market	Gas	$91,159	$17,503	$83,629	$16,337	$7,530	$1,843	10.70%	1.14%
	Wind	$91,180	$17,039	$83,154	$15,846	$8,026	$1,857	10.71%	1.11%
	Change	$21	-$464	-$474	-$492	$496	$14	0.00%	-0.03%
Unregulated Market	Gas	$100,270	$23,705	$88,111	$17,973	$12,159	$7,379	21.80%	11.32%
Power Pool	Wind	$100,053	$23,759	$87,595	$17,667	$12,459	$7,523	21.50%	11.01%
	Change	-$216	$55	-$516	-$306	$300	$144	-0.31%	-0.31%
Unregulated Market	Gas	$91,902	$16,143	$84,079	$15,954	$7,823	$2,098	11.01%	2.68%
Fixed-Price Contracts	Wind	$91,984	$15,755	$83,609	$15,474	$8,375	$2,085	11.14%	2.47%
	Change	$82	-$388	-$470	-$480	$552	-$13	0.13%	-0.21%

*All figures are present values over 20 years (2003-2022) discounted at 7.5 percent, converted to 1996 dollars. Revenu and net income are in millions of dollars. Standard deviations reflect variations between iterations, not between years.

This is confirmed by the first row of Table 2, which shows the expected present value and standard deviation of revenues, costs, net income, and average return on equity for both the gas and wind cases and the differences between them. (High-risk environmental and fuel cost distributions are assumed.) The mean present value of revenues in the regulated scenario is $21 million greater with wind than without wind, indicating that this case is still likely to be slightly more expensive for ratepayers, despite the possibly of CO_2 regulation. However, the standard deviation in revenues is $464 million less, indicating that the wind investment is significantly less risky. By contrast, the mean return on equity is virtually the same in both cases.

Different views of the data provide additional insights into the effects of replacing the gas-fired plant with the wind plant. Figure 1 shows a scatter plot of present-value revenues for the wind and gas cases in the regulated market scenario. The points in the closely spaced, upward sloping group show the intersection of values for the wind and gas cases. The points in the larger, downward sloping group show the difference in revenues between the wind and gas cases as a function of the gas case revenues. The important thing to observe is that when the present value of revenues is high, the wind case tends to be less expensive than the gas case, whereas when the present value is low, the converse is true. This graphically illustrates the point that wind plants can act as an insurance policy or hedging strategy against fossil-fuel risks.

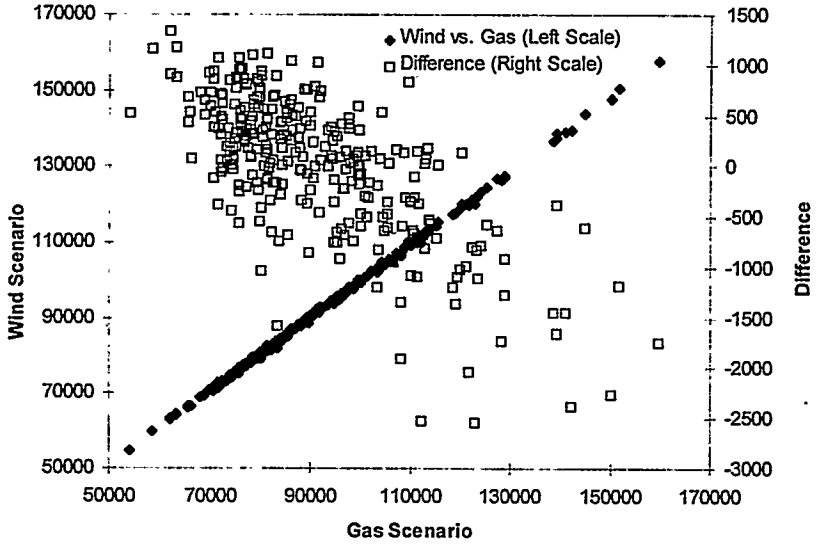

Figure 1. Present value of revenues, regulated market

Yet another view of the data is provided in Figure 2, which shows the differences between the mean revenues and standard deviations of the gas and wind cases for each year of the study period. As

might be expected, the wind case starts out more expensive than the gas case on average, but then becomes less expensive. In every year but the first, the standard deviation for the wind case is lower than that of the gas case by amounts ranging up to $150 million.

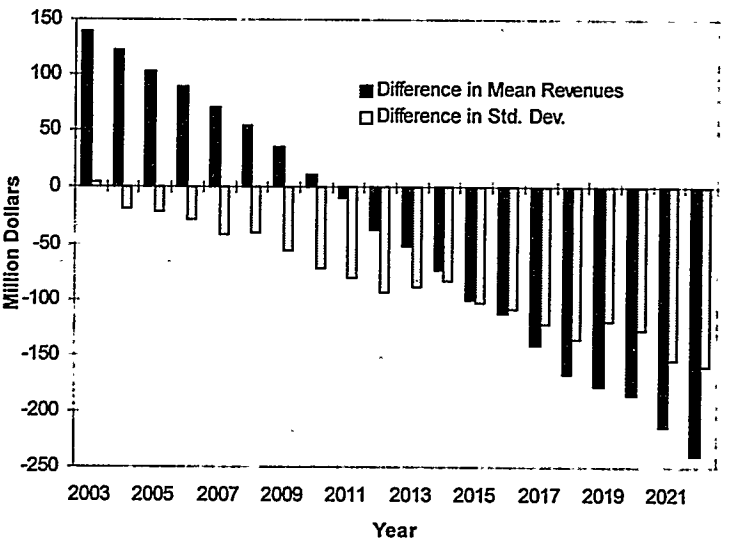

Figure 2 Difference between wind and gas scenario revenues (regulated market)

Unregulated Market Scenarios

The unregulated market is more complicated to model than the regulated market. The risks seen by the utility and its customers depend on many factors, such as the nature and degree of competition, corporate structures, the role of regulation, the design and functioning of the power pool, and the contractual relationships between the utility company and its customers and fuel suppliers. We cannot incorporate all such factors into the model. Instead, we consider two scenarios that illustrate a plausible range of sensitivity to risk: a power pool scenario, and a fixed-price contract scenario.

The critical difference between the two scenarios is that, in the power pool, TU Electric's plants compete against comparable fossil, nuclear, and renewable plants on the basis of short-term variable operating costs. Capacity payments are proportional to loss-of-load probability, as is done in the UK Pool. In the fixed-price contract scenario, the price of power is fixed for periods ranging from one to five years. In both cases, the capacity build decisions are assumed to be the same as in the regulated market scenario.

The results are summarized in the bottom two rows of Table 2. It is important to note, first, that the power pool scenario poses much greater risks for both customers and company shareholders than the fixed-price contract scenario, whether wind is present or not. The reason is that the capacity payments in the power pool are highly volatile, as they depend on reserve margin, which varies with fluctuations in load.

Moreover, the effect of substituting wind for gas varies strikingly between the two unregulated market scenarios. In the power pool scenario, the addition of wind appears to *increase* the standard deviation of revenues, but it decreases the standard deviation of the return on equity. The expected revenues, net income, and return on equity are all somewhat lower with wind, to the benefit of electricity consumers but to the detriment of company shareholders. The main reason is that the wind plant slightly reduces the amount of high-cost fossil generation needed to supply loads at the margin and therefore reduces the variable portion of the electricity price. The results of the contract scenario, on the other hand, closely resemble those of the regulated market scenario. The main difference is the reduction in the standard deviation of return on equity resulting from the wind addition, which is accompanied by a slight increase in the mean ROE.

VALUING RISK REDUCTION

A critical issue in interpreting the results of this study is estimating the value of changes in risk either for ratepayers or utility company shareholders. There is, first, the possibility of a change in the expected, or mean, outcome, which occurs if the probability distributions of the input parameters are skewed in some fashion. In our study, the only such skewed distribution is that of environmental regulatory costs, which we believe are far more likely to increase than to decrease. The effect of this bias is easy to account for, and indeed we already see its effect in the difference in mean revenues between the gas and wind cases in the regulated market scenario, which in Table 1 (with no variations in the input parameters) is $308 million, but in Table 2 is $21 million. Thus, one can say that accounting for high environmental regulatory risks reduces the mean revenues of the wind case relative to the gas case by $287 million.

More challenging is the problem of assigning a value to changes in the variability of a cash flow. This is accomplished in decision analysis by calculating a risk premium, which is proportional to the variance (or standard deviation squared) of the parameter of interest, an approach derived from expected utility theory. The *certainty equivalent* of the cash flow, which is the amount it is worth to a decision maker absent any risks, combines the mean with the risk premium in the equation,

$$CE = \langle CF \rangle - \frac{\alpha}{2}\sigma_{CF}{}^{2},$$

where α is known as the risk aversion coefficient. In the case of future cash flows, the certainty equivalent can be converted to a present value by discounting at a suitable risk-free discount rate.

The risk aversion coefficient can be measured directly by surveying the opinions or observing the investment behavior of the key decision makers or stakeholders. Absent such information, decision analysts generally assume that it is approximately equal to the reciprocal of one to two times expected income. In this study, we assume that, from the perspective of ratepayers, the risk aversion coefficient equals the reciprocal of 1.25 times revenues, whereas from the perspective of shareholders, it equals the reciprocal of 1.25 times expected return on equity.[2]

When the above equation is applied to the annual means and standard deviations calculated by the model, and the wind and gas cases are compared, the result is an estimate of the total risk-reduction benefit of wind energy, shown in Table 3.

The total benefit has two components, a change in mean revenues (due entirely to environmental regulatory risks), and a change in the risk premium. Together, they indicate the consequences of taking risks into account in the comparison of the two resource options. For example, the total wind risk benefit from the ratepayer perspective in the high-risk, regulated market scenario is $385 million, which includes the $287 million shift in mean revenues noted previously, and a $98 million shift due to a reduction in the risk premium. This implies that when risks are considered, the certainty equivalent of the wind case revenues will be $77 million less ($308 million minus $385 million) than the certainty equivalent of the gas case revenues, making the wind plant the more attractive option for ratepayers. If low risks are assumed, the total ratepayer benefit is $171 million, which is not enough to tip the scales in favor of the wind plant.

---

[2] Support for these assumptions is provided in Jonathan M. Jacobs and Thomas E. Huntley, Pacific Gas and Electric Company, "Valuation of Fuel Diversity," Submitted for Hearings before the California Energy Commission (February/March 1992).

Table 3. Summary of Wind Risk Benefits*

Scenario	Risk	Ratepayer Perspective			Shareholder Perspective		
		Change in Mean Revenue	Change in Risk Premium	Total Wind Risk Benefit	Change in Mean ROE	Change in Risk Premium	Total Wind Risk Benefit
Regulated Market	High	($287)	($98)	$385	0.00%	-0.02%	0.02%
	Low	($144)	($27)	$171	0.00%	-0.02%	0.02%
Power Pool	High	$29	$36	($65)	0.52%	-0.97%	1.48%
	Low	($100)	$35	$65	0.13%	-0.89%	1.03%
Contract	High	($260)	($78)	$338	0.12%	-0.38%	0.50%
	Low	($123)	($21)	$145	0.05%	-0.12%	0.17%

*Figures for the ratepayer perspective are in millions of 1996 dollars.

Regardless of its ultimate effect on the build decision, the risk benefit of the wind plant for ratepayers in the regulated market and contract market scenarios appears substantial. In the regulated market scenario, for example, the benefit is equivalent in real levelized terms to $3.4 to $7.8/MWh of wind generation. In contrast, the wind risk benefit for the ratepayer in the power pool scenario appears to be much smaller, and under high risk assumptions, is actually negative. The explanation for this effect is unclear, but is likely connected to the way wind energy affects the dispatch of high-cost fossil-fuel plants operating at the margin.

The risk benefits from the shareholder perspective are the mirror image of those from the ratepayer perspective. In the power pool scenario, shareholders receive a major risk benefit from the wind plant that is equivalent to an extra return on equity of 1 to 1.5 percentage points. In the contract scenario, the benefit to shareholders appears smaller but still substantial—0.17 to 0.5 percentage points. As already noted, there is little or no risk benefit for shareholders in the regulated market scenario.

CONCLUSIONS

The initial findings of this study suggest that risk should be an important consideration in evaluating competing wind and gas-fired combined cycle plants. For the most part, accounting for risk appears to act to the benefit of wind energy. The benefits of reduced exposure to fuel-price and environmental regulatory risks are not offset by the greater uncertainty in the annual average availability of wind plants compared to conventional plants.

Risks are distributed much differently in a regulated market than in an unregulated market, however. In a regulated market, utility company shareholders see few of the risks of fossil fuels and hence have little incentive to invest in risk-mitigation options such as wind power. This may help explain why many utilities have not eagerly embraced wind technology. An unregulated market may provide greater incentive for utility investment in wind energy based on risk considerations. Although this incentive is theoretically largest in a power pool, the extreme volatility of prices in such a market may serve to mask the incentive to a considerable degree. A market dominated by fixed-price contracts may be most favorable to wind, as the risk benefits will then be distributed more or less evenly between customers and utility company shareholders, giving both a modest incentive to go with wind. (This analysis did not consider the possibility that fossil-fuel risks may be passed on to or shared with fuel suppliers, however, which may reduce the risk benefits of wind but could also result in higher fuel prices.)

Most importantly, this study has demonstrated that decision analysis can be a useful tool for estimating the risk-reduction benefits of wind energy under a range of market conditions. Analytical tools like the SRP model should be used to help inform traditional methods of utility

resource planning as well as regulatory and legislative efforts to create a level playing field for wind and other renewable technologies in a deregulated electricity market.

The results presented in this paper are preliminary and undergoing review. The authors wish to thank the U.S. Department of Energy and National Renewable Energy Laboratory for their support of this work.

CHARACTERIZATION OF WIND TECHNOLOGY PROGRESS

John B. Cadogan
U.S. Department of Energy
1000 Independence Ave, S.W.
Washington, D.C., 20585, U.S.A

Brian Parsons
National Renewable Energy Laboratory
1617 Cole Boulevard
Golden, CO, 80401, U.S.A.

Joseph M. Cohen and Bertrand L. Johnson
Princeton Economic Research, Inc.
1700 Rockville Pike
Rockville, MD, 20852, U.S.A.

INTRODUCTION

The U.S. Department of Energy (DOE) Wind Energy Program, the National Renewable Energy Laboratory (NREL) and Sandia National Laboratories periodically re-evaluate their characterization of the state of wind technology and revisit wind research and development cost and performance goals. These characterizations, goals and supporting analyses are part of a larger effort in the DOE Office of Energy Efficiency and Renewable Energy to establish a consistent data base of technology progress information for its major programs. The data developed are used to communicate the competitive status of wind to various stakeholders, and to support various analytical exercises such as market impact studies and analysis of alternative research paths.

1995 marked the conclusion of a number of DOE-supported advanced turbine design efforts. Results from the next major round of DOE-supported research contracts are expected near the latter part of the century. This timing presents an opportunity for incorporating recent progress and results from the federal program, and from industry progress, into technology goals and projections for the end of the century and beyond. This paper discusses future trends for domestic wind farm applications (bulk power), incorporating recent turbine research efforts under significantly different market assumptions than assumed in previous DOE estimates. Updated cost/performance projections are presented, along with underlying assumptions and discussions of potential alternative wind turbine design paths. Additionally, issues regarding the market valuation of wind technology in a restructured electricity market are discussed.

TECHNOLOGY CHARACTERIZATION BACKGROUND

The U.S. Department of Energy (DOE) Wind Energy Program's current work in expressing wind technology trends for the U.S. bulk power market, termed "Technology Characterizations," (TCs) is the third in a series of efforts dating from 1989, at which time input was prepared for the National Energy Strategy. That initial work included an industry survey and the use of Electric Power Research Institute (EPRI) and other outside data, as well as national laboratory input.[1,2] The second effort in 1993 had a more detailed analytical basis, with information taken from the DOE/NREL Advanced Wind Turbine Near Term Conceptual Design Studies and other development programs of the period.[3,4] Current work

utilizes data from ongoing DOE/NREL Next Generation Turbine Research, and other industry turbine development and DOE research efforts. The latter DOE information includes results from the recently-completed Near-Term Product Improvement projects and Next Generation Phase I Concept Definition Studies. Currently three contracts are under negotiation for design and prototyping of next generation turbines. DOE plans to complete an updated (1996) version of its "Technology Characterization for Advanced Horizontal Axis Wind Turbines in Windfarms" in July, 1996.

DOE technology characterizations are used for responding to numerous requests for an overall description of technology cost and performance trends. The data is commonly used to answer questions from a variety of private and government sources, to provide input for market studies, for internal DOE quantification of potential benefits from program research efforts, and as one of the inputs to the Energy Information Agency's (EIA) annual market projections.

ANALYTICAL BASIS FOR CHARACTERIZATIONS

Approach to Trend Description

The Technology Characterization is presented as time trends of sets of cost and performance figures ("figures of merit") for wind farms that are considered to be broadly representative of each time period. Characterizations for current and near-term technology are based on a composite description of existing and proposed machines. The decision to represent a composite is based on the recognition that there is more than one design currently on the market and that there is more than one pathway to improved cost and performance characteristics. For later years, a representative technology path is built up from broader expectations of advances in certain subsystems or in certain technology areas (such as materials).[5,6] In formulating overall cost and performance figures of merit, estimations of expected cost and performance improvements for particular turbine subsystems were compared against known overall bounds (such as the Betz limit, raw material cost, etc.) as a reasonability check on projections, particularly in study end years.

Composite descriptions of windfarm cost and performance are not projections of the future for specific turbine designs. Rather, they are constructed to represent projected overall trends. For instance, actual capital and O&M costs, as seen in the market, may not follow a smooth downward curve as shown in the TC. As new turbines are introduced, costs may be higher until production increases and sufficient experience with O&M is developed in the field. Thus, although one might expect to see a downward trend over time, the path may be "saw-toothed" along the way as new technology is developed. This will be especially true with a technology in the earlier phases of commercial maturity (such as wind turbines) when large improvements are realized with each new generation of technology.

Figure 1 shows composite trends expected in wind turbine development. One of the concepts that the figure illustrates is that while there may be incremental advances in the technology, (technology "jumps" from one horizontal arrow to another), at the same time, there is an ongoing process of optimization. (This is shown as the bottom arrow "feeding" the incremental improvements above). It is recognized that designs are not driven solely by economic and technical factors. Manufacturer inertia and the nature of the market will also dictate the length of time that design features remain in the market. Additionally, designs will be driven in part by the need to conform to certain design standards in order to receive certifications that enable sales in some areas overseas.

Uncertainty In Assumptions

There is a higher level of certainty regarding near-term characterizations. However, some uncertainty

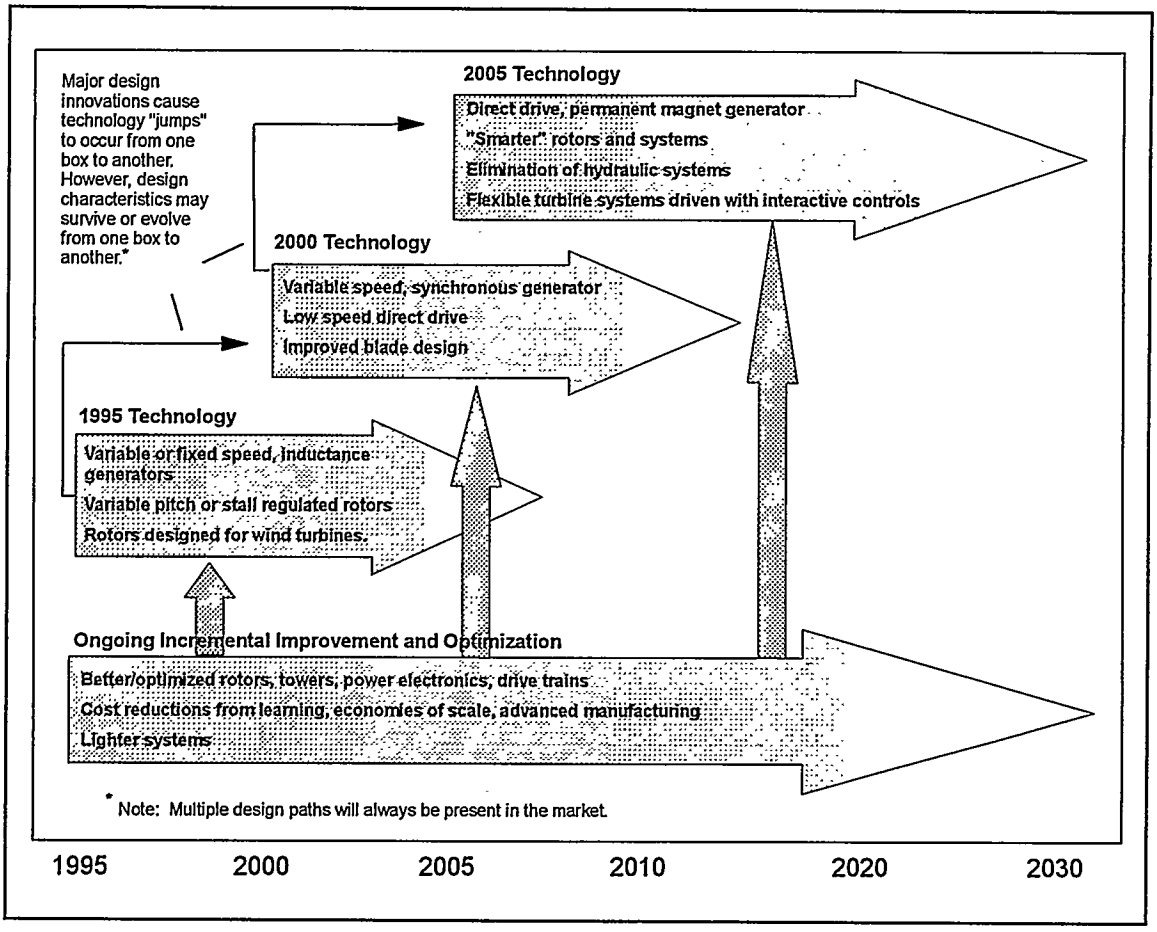

FIGURE 1. WIND ENERGY TECHNOLOGY EVOLUTION

exists even in these projections. The description of 1995 technology, for instance, is not considered validated until a sufficient number of turbines have proven their performance and operating cost characteristics over a number of years. A major source of uncertainty in turbine capital cost estimates comes from trying to infer turbine and windfarm costs from quoted prices. That is, pricing strategies can make it difficult to determine true costs. There are also key uncertainties in several assumptions made in the TC for combining cost and performance into an overall cost of energy (COE) figure of merit. These include values for balance of station (BOS) costs (all initial project costs other than the wind turbine capital cost), losses, and values of O&M. Although values for these assumptions have been formed from information collected from various industry and research sources, DOE welcomes additional industry and other stakeholder comment and input to improve the level of certainty regarding these values.

Description of 1995 Technology

1995 technology is a composite of fixed and variable speed options, but generally involves the use of one or more low cost induction generators. It is distinguished from earlier technology (1993 in the previous Technology Characterization) by the substantial use of power electronics (for power conversion and/or dynamic braking) and the use of NREL advanced airfoil designs. Projects using these types of technology currently exist. Turbine availability is high, and not expected to appreciably increase in following years. Windfarms for all years are assumed to be comprised of 100 turbines. A key assumption for 1995

technology is that costs are based on a cumulative production volume of approximately 500 units. This level of production serves as the baseline for future cost reductions due to volume effects.

2000 Technology Trends

Projections for the year 2000 include as their basis, information from the NREL Next Generation Turbine Research program. The direction of the 2000 technology, as reflected in the TC, is generally toward larger generators and rotors, variable speed or multiple speed, increased used of power electronics, more sophisticated control electronics, taller towers, and in some cases advanced generators. Figure 1 lists two alternative technology paths for 2000: 1) a variable speed synchronous generator with fully rated converter (electronics that allow elimination of the gear box), and 2) a doubly fed generator, that is seen as an interim, low cost variable speed generation option, with a geared transmission.

These two alternatives hardly begin to cover the possible configurations that could encompass, for example, vertical axis wind turbines, but they provide examples of potentially popular viable technologies for the time period. It is expected that all configurations for 2000 will incorporate advanced airfoils. It will be possible to design turbines for greater reliability based on a better knowledge of wind inflow characteristics and how they impact structural design, and appropriately improved modeling tools. It is expected that there will be improvements in turbine blades, particularly with respect to better integration of blade structural and aerodynamic design with appropriate manufacturing processes.

Progress is also expected in areas outside of cost and performance of the individual turbine. For example, more accurate micrositing models are expected to be developed, which will contribute to a reduction in wind farm array losses. Better local weather forecasting, along with appropriate utility operator training, is expected to raise the value of wind generation to the utility. A discussion of the importance of such value issues in today's market is found later in the paper.

2005 Technology Trends

Advances in 2005 are expected to be driven in part by an additional cycle of NREL-sponsored turbine development projects. As indicated in Figure 1, it is expected that a move will begin toward direct drive systems, with lower cost power electronics and increasing sophistication in control electronics, and rotor aileron or pitch activation. Permanent magnet generators may become cost-effective for wind farm-size turbines. The trend is expected to continue toward larger machines and higher towers in this time frame.

2010 and Future Technology

Performance gains are expected to level off in later years, with cost gains impacted primarily by volume effects (learning effects for customized components and volume discounts for off-the shelf components) and new manufacturing processes made viable by higher levels of turbine production. Specific technical advances are expected in the areas of materials (especially blade materials), advanced techniques and components to enhance turbine "load shedding" ability, and resultant ability to use larger rotor diameters (and so increase energy capture without increasing rotor efficiency). Continuing advances in electronics and electronics cost reduction are expected. Turbine generator rating is not expected to increase significantly during the period, as inverse economies of scale may hinder turbine development much beyond one megawatt.

QUANTIFICATION OF PERFORMANCE AND COST PROJECTIONS

For the trend information above to be fully useful in DOE program activities, expected progress must

be quantified. Multiple metrics, or "figures of merit" are used in the characterizing progress. This is necessary in order to portray the three basic categories of performance advances, cost advances, and overall cost/performance ratio. Additionally, different figures of merit for each of these categories allows description of advances from a number of different perspectives. Presenting turbine efficiency, for example, lends perspective on single turbine engineering performance, while net capacity factor clearly shows total turbine (or wind farm) productivity after all losses and availability have been accounted for.

System-Level Characteristics

Turbine Characteristics: Figure 2 shows representative turbine and windfarm characteristics between 1995 and 2030. Turbine size is shown increasing from 300 kW in 1995 to 1 MW in 2005, remaining at this size through the latter years. Tower hub height is shown rising throughout the years, to 100 meters in 2030. This is indicative of a general trend toward taller towers. However, tower height is a site-specific choice and actual heights for turbines will probably be found on either side of those presented in the characterizations for any given year.

System Performance Characteristics: Performance gains are shown in Figure 2 in terms of capacity factor and net annual energy output per unit of rotor swept area. Net capacity factor increases substantially in the years 2000 and 2005, with less dramatic gains in the later years, from 26.2% in 1995 to 36.9% in 2030 (in a Class 4 wind regime). Changes in assumed losses reflect improvements in control losses and blade soiling losses in the early years, and array losses in 2005. Note that there is an attempt in the TC to differentiate between ridge and plain sites, since turbine siting and corresponding array losses will vary significantly. As an analytic convention, "plain" sites are assumed to be wind class 4 regimes, while, "ridge" sites are assumed to be class 5 and above. Although this does not precisely represent reality, the use of these two assumed sites allows a range of sites to be represented in analysis. Availability, having increased substantially over the last decade, is

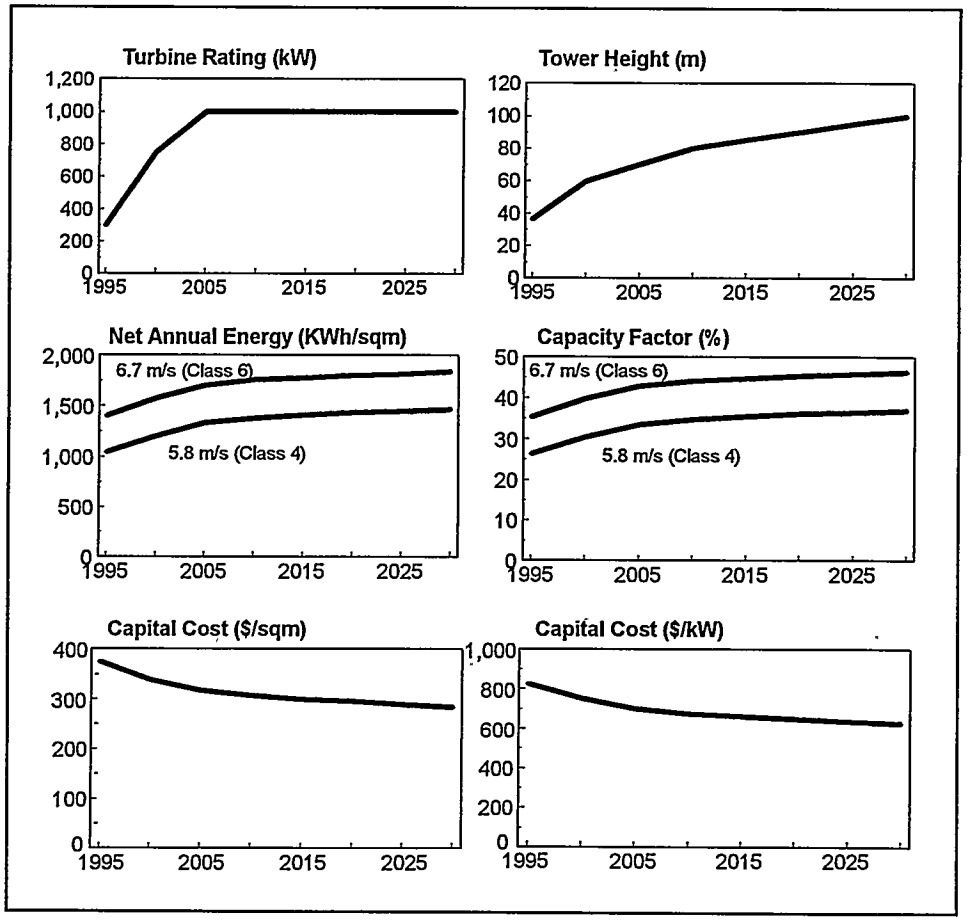

FIGURE 2. WINDFARM PROJECTED CHARACTERISTICS

characterized as level at 98%.

System Cost Characteristics: Installed farm cost numbers include turbine cost, shipping, installation and balance of station (grading, substation, engineering fees, etc). Costs are shown in Figure 2 moving from a current $825/kW to $625/kW in 2030. These reductions are influenced primarily by reductions in materials and eliminations in subsystems (geared transmission) in the near-term. In the long-term, the majority of weight (and therefore cost) reduction is assumed to have been extracted through improved design. The remaining gains therefore come from increased volume of production and improved manufacturing processes associated in part with the production volume increases. Although lower costs are not an inevitable result of higher sales volume, there are several specific volume effects that reasonably can be expected to lower turbine and windfarm costs in the future. First, increasing sales may allow a move to a new manufacturing technologies that lower production costs. Second, there is an established learning effect in similar products that indicates (logarithmically) decreasing product costs as cumulative sales increase. Third, as production volume increases, there is an opportunity for larger volume discounts on off-the-shelf components for turbines.[7]

Subsystem Performance Improvements

Estimates of performance for all years are formed using turbine energy output simulation software that takes into account overall system characteristics starting from rotor performance curves. This enables rapid evaluation of the effect on economics of changes in various subsystems. The C_p (coefficient of performance) curve for 1995, for instance, is modeled as a fixed speed, fixed pitch machine, while the 2000 turbine has a power curve typical of a variable speed machine (maintaining rated power above the rated wind speed). Generally, progression in rotor performance is characterized less by increases in peak C_p and more by maintenance of a relatively high C_p over a larger wind speed range. Additionally, a lower turbine cut-in speed is modeled as an advance in 2000 and beyond. Generator, transmission and power electronics performance (efficiency) are not explicitly modeled. Currently, these efficiencies are incorporated into the C_p curves used.

Tower heights increase throughout the projection period. This is not an indication that in the real world towers will gradually increase in height, but rather an indicator that the optimized system will trend toward higher towers, with specifics defined by the project site. Improvements in design software and general reductions in turbine weight per unit output will permit this shift in the optimum design point for turbine towers.

Other performance gains are reflected in changes in losses for turbines and farms. Blade soiling losses, specifically, are expected to be reduced early on. Array losses will be slightly reduced as micrositing software improves. Greater understanding of wind inflow characteristics and more sophisticated control algorithms should allow reductions in control losses.

Subsystem Cost Improvements

Table 1 summarizes the key qualitative assumptions driving subsystem cost improvements. The rotor subsystem is a significant cost driver. Cost increases (per kilowatt of generator rating) in the rotor subsystem are assumed for the years 2000 and 2005. The 2005 increase is due to the combined effects of a move to variable pitch blades and a significant increase in rotor diameter. (A percentage of blade cost tends to increase approximately with the cube of rotor diameter.) However, cost increases in 2005 are offset somewhat from improved manufacturing techniques resulting from the DOE/industry cost-shared Blade Manufacturing Project.

TABLE 1. ASSUMPTIONS FOR MAJOR SUBSYSTEM COST DRIVERS

	1995-2000	2000-2005	2005-2010	2010-2030
Rotor	Increase from larger size	Increase from size. Reduction from advanced manufacturing	Increase from size	Incremental reductions from lighter & smarter rotors
Tower	Largest increase from largest height increase	Decrease from smarter lighter, flexible top of tower system	Incremental increases with height (less than linear due to lighter components at top of tower)	
Generator	Induction - cheapest, off-the-shelf	Synchronous - a little higher cost	1st generation permanent magnet - highest cost	Incremental improvements in permanent magnet cost
Electrical	1st generation variable speed is expensive	Major cost drop as technology matures	Incremental improvements	
Drive Train	Direct drive - No transmission			
BOS	Incremental reductions from learning, maybe warranties			

Tower costs increase significantly in 2000, with incremental variations in the per kilowatt costs in out years. In the later years, cost per kilowatt increases at a rate lower than the tower height increases due to assumed advances in the ability to shed aerodynamic loads and design lighter turbine structures. Generator cost increases (per kW) up to 2005, as a result of moves to higher performance technologies. Sample technologies might be synchronous or doubly fed generators in 2000, and permanent magnet generators in 2005. Advances in manufacturing and design, and volume effects account for the cost decreases in the latter years.

Power and control electronics and other electrical costs show a significant increase in year 2000, as variable speed power electronics are used to enable direct drive to be implemented. Cost decreases through 2010 result from power electronics technology advances and, to some extent, increases in sales. Cost reductions in the latter years result primarily from volume effects. A major cost decrease in the transmission system is realized in 2000 as gearing is eliminated. This more than offsets the higher electronics, tower and rotor costs experienced during the same period.

MARKET CHANGES AND DOE COST GOALS

The domestic market for wind energy has changed dramatically and continues to change, presenting a serious challenge for the wind energy industry. Five years ago, after a decade of substantial wind progress and with natural gas prices seen as heading toward $4.00 per MMBtu by 2000, wind energy looked like a likely candidate for utility/Independent Power Producer (IPP) use as a fuel saving technology. Now, although the technology continues to progress steadily and recent international turbine deployment has been substantial, installation of large scale windfarms has stalled domestically, due to the confluence of low fossil fuel prices, utility restructuring and continuing improvements in natural gas-fired turbine efficiencies. With an increasing emphasis on spot market purchases (at less than 2 cents/kWh in many cases) and a trend toward natural gas combined cycle installations on those occasions where new facilities are needed, current wind installations tend to be fewer, smaller, and based on benefits other than cost. "Value," not "cost," will continue to be a key determinant of market success.

Cost of Energy Projections

The highest level and most commonly used figure of merit is levelized cost of energy (COE), expressed in cents per kilowatt-hour. This is a useful metric as it combines both elements of cost and performance and is recognized outside of the wind industry. COE figures used by DOE, however, have often differed from the (wide-ranging) numbers quoted for wind industry installations and project bids. It is important to point out that these apparent discrepancies have stemmed not from fundamentally differing opinions concerning the state of technology, but rather primarily from different financing and wind resource assumptions. For instance, current market projects and bids usually include federal renewable energy production incentives (REPI) or tax credits, depending on whether the project is for supply to investor-owned or municipally-owned utilities, respectively. DOE's COE figures do not include these incentives. Also, financial aspects may vary widely for different projects.

Another common difference between market and DOE Technology Characterization numbers is that DOE quotes COE in constant dollars because of the ease of use for technology tracking and in economic modeling (such as the national energy modeling performed by the Energy Information Administration). In contrast, bids and contracts are in current dollars, which appear higher than constant dollar figures.

DOE has historically quoted COE for Class 4 winds, in line with DOE goals to help make wind energy economically competitive in these regimes. Industry installations have tended to be at higher wind sites, with consequent confusion over "real" costs of wind energy. Although near-term wind installations will continue to target good wind resource sites, in order for wind to contribute large amounts of electricity to the nation's supply, opportunities in regions of the U.S. that have lower wind resources must also become economic by improving the technology. Figure 3 indicates the relative quantities of wind resource in various regimes, emphasizing the tremendous depth of the Class 4 resource.[8] Note, however, that current turbine deployments still use only a fraction of the available Class 5 and 6 lands.

The current Technology Characterizations partially address these issues and the changing nature of the marketplace by presenting a matrix of COE's, corresponding to various combinations of wind regimes and ownership/financing structures and using the cost and performance numbers from the TC. Figure 4 shows COEs from this matrix for year 2000 and 2030. It is important to note that these COE values are draft numbers and are subject to small changes as work is completed later this summer. The range of COEs is representative of different potential markets that are emerging as market restructuring continues.

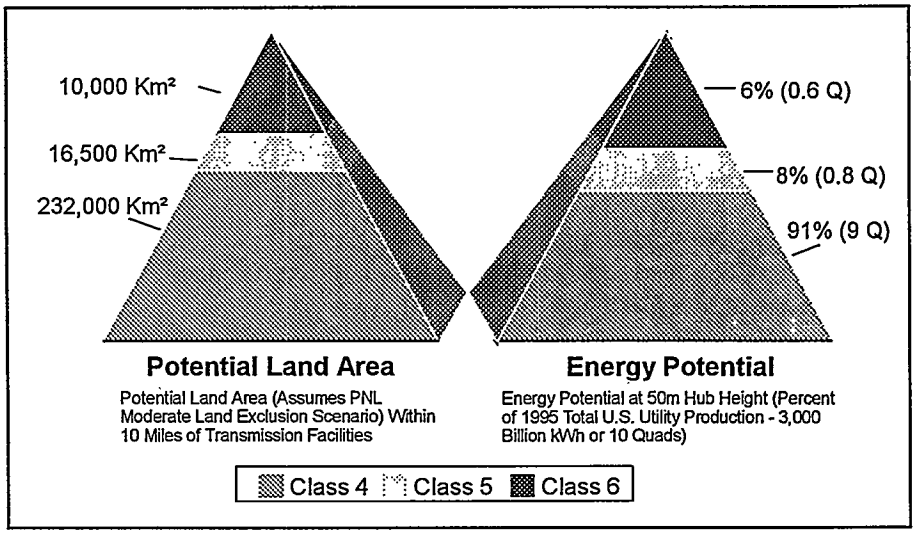

FIGURE 3. AVAILABLE WIND RESOURCE

COE figures were obtained using cash flow modeling with realistic financing and tax assumptions for the different scenarios. Investor Owned Utility (IOU) and Municipally- or publicly-owned

ownership cases (MUNI) use the cost-based revenue requirements method to figure COE, while Independent Power Producer (IPP) Ownership uses a market-based Discounted Cash Flow-Return On Investment (DCF-ROI) method. The MUNI projects are most advantageous to wind because financing is 100 percent tax-free debt (no expensive equity) over the plant lifetime, assumed to be 30 years. MUNIs also pay no income or property taxes. IOU is next costly, financed with 50 percent debt and 50 percent equity over the plant life (again, 30 years). IPPs use project financing which retires debt over the shortest period (for example, 15 years), and uses more debt financing than IOUs, but with a much higher equity rate. Together, these characteristics make IPP the highest cost form of financing. A more detailed discussion of financial assumptions can be found in the 1996 Technology Characterization.

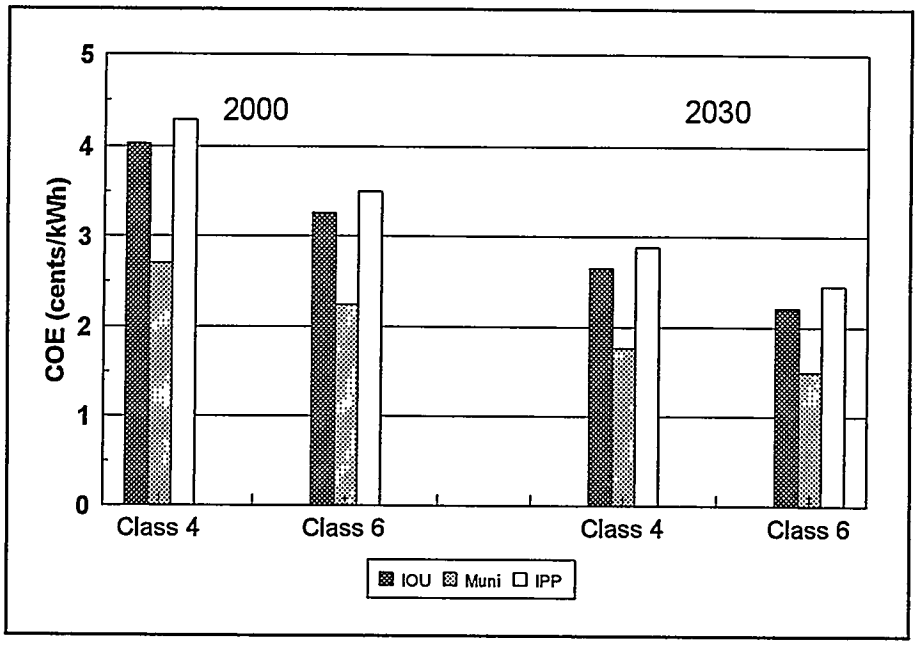

FIGURE 4. FINANCING AND RESOURCE IMPACTS ON COE

The figure shows that COEs for the same technology could conceivably range from a low of about $0.023/kWh (Muni, class 6) to a high of about $0.043/kWh (IPP, class 4) in year 2000. Obviously, the resource and ownership/financing structure have a large effect on the COE. How well these COEs will enable a specific wind project to compete will depend on the payment the windfarm developer/owner can collect plus any additional value of the windfarm, as perceived by the utility and its customers. In fact, a windfarm with a higher COE may be competitive in some locations while one with a lower COE is not competitive in others.

MARKET WILL EMPHASIZE VALUE

The Technology Characterizations put a heavy emphasis on cost of energy to evaluate progress and viability of individual renewable electric generating technologies, and to compare technologies against each other. However, as a key determinant of market success, value issues ("what is it worth" versus "what it costs") are particularly important to examine and, if possible, quantify in this difficult market environment. Table 2 lists some of these cost and value factors. Other papers presented in this conference session detail recent DOE efforts to analyze certain factors listed in the table.[9,10]

In arenas where values beyond short-term price are recognized, wind power is currently being adopted. For example, in Minnesota, a regulatory mandate reflecting public preferences and non-monetary values, combined with a good wind resource area and utilization of the federal production credit has resulted in an independent power project with levelized purchase prices of around 3 cents/kWh. For the near-term market, wind energy will need to continue to exploit niches where additional value is reflected. In addition to treatment of value, other characteristics make for suitable wind customers. Low cost of

TABLE 2. MARKET SUCCESS DETERMINANTS

Cost Factors	Value Factors
Technology performance, capital and operating costs	Capacity and energy avoided costs
Wind resource quality	Price certainty (i.e., no fuel escalation risk)
Financing	Generation mix diversity
Taxes	Environmental impacts
Policy incentives	Modularity, short lead times
Project ownership	Economic development
Permitting processes	Regulatory directives
Land cost/lease/royalty terms	Public preferences
Transmission (construction/upgrades and access/wheeling)	Distributed utility value

financing is a particularly desirable characteristic for capital-intensive technologies such as wind. Publicly owned utilities, with their access to favorable financing, their responsiveness to customers, and a less cumbersome regulatory environment, are likely candidates for wind development. Other examples of potential markets are cooperatives, power marketers, renewable power aggregators and direct access customers. The Federal Wind Program will continue to work to increase the understanding and recognition of various aspects of value to utilities and their customers. Specifically, DOE is looking forward to working closely with National Wind Coordinating Council (NWCC) members and others to identify near-term market openings and to help package wind for these opportunities.

REFERENCES

1. J.M. Cohen, S.M. Hock, J.B. Cadogan, "A Methodology for Computing Turbine Cost of Electricity Using Utility Economic Assumptions," Proceedings, Windpower '89, San Francisco, CA, September 24-27, 1989.
2. S.M. Hock, R.W. Thresher, J.M. Cohen, "Performance and Cost Projections for Advanced Wind Turbines," SERI/TP-257-3795, August, 1990.
3. "Technology Characterization for Advanced Horizontal Axis Wind Turbines in Windfarms," U.S. Department of Energy, Wind Energy Program, December, 1993.
4. "Technology Evolution for Wind Energy Technology," U.S. Department of Energy, Wind Energy Program, December, 1993.
5. J.L. Tangler, D.M. Somers, "NREL Airfoil Families for HAWTs," Proceedings, Windpower '95, Washington, DC, March 26-30, 1995.
6. C.H. Weigand, D.A. Marckx, Variable Speed Wind Generation: Electrical Options and Power Systems Issues," Proceedings, Windpower '94, Minneapolis, MN, May 10-13, 1994.
7. "The Effects of Increased Production on Wind Turbine Costs," Princeton Economic Research, Inc. for National Renewable Energy Laboratory, (publication pending), 1996.
8. B. Parsons, Y. Wan, D. Elliott, "Estimates of Wind Resource Land Area and Power Potential in Close Proximity to Existing Transmission Lines," Proceedings, Windpower '95, Washington, DC, March 26-30, 1995.
9. T. Hoff, "Strategic Planning in Electric Utilities: Using Wind Technologies as Risk Management Tools," Windpower '96, Denver, CO, June 23-27, 1996.
10. M. Brower, "Quantifying the Risk Benefits of Wind Power," Windpower '96, Denver, CO, June 23-27, 1996.

MODELING THE RELIABILITY AND MAINTENANCE COSTS OF WIND TURBINES USING WEIBULL ANALYSIS

William A. Vachon
W. A. Vachon & Associates, Inc.
9 Sea Street
Manchester, MA 01944 USA
(508) 526-4315

ABSTRACT

A general description is provided of the basic mathematics and use of Weibull statistical models for modeling component failures and maintenance costs as a function of time. The applicability of the model to wind turbine components and subsystems is discussed with illustrative examples of typical component reliabilities drawn from actual field experiences. Example results indicate the dominant role of key susbsystems based on a combination of their failure frequency and repair/replacement costs. The value of the model is discussed as a means of defining (1) maintenance practices, (2) areas in which to focus product improvements, (3) spare parts inventory, and (4) long-term trends in maintenance costs as an important element in project cash flow projections used by developers, investors, and lenders.

1. INTRODUCTION

During the past one to two years, perhaps half of the current wind energy projects in California reached the 11-th year in the Interim Standard Offer Number 4 (ISO4) Power Purchase Contracts at which time the utility buyback rate dropped from 13 to 14 to less than 5 cents per kWh. Over the next one to two years a majority of the remaining projects will reach that same price "cliff". A major concern to any project operator, that is working under such conditions, is to be able to understand and reduce the operation and maintenance (O&M) costs for the project. It is especially important to be able to project O&M costs if the owner seeks to refinance or sell the project.

For older projects with mature equipment, a major portion of O&M costs is driven by the unscheduled maintenance costs associated with equipment replacements due to wear out or failures. A recognized method of predicting component wear out or failures is to apply a Weibull analysis method [1]. The analytical procedure is based on a knowledge of historical failure-rates for similar equipment that is operated in a similar environment. The approach has been applied by the military and is used widely in several industries that manufacture mechanical and electronic components [2, 3] - where suppliers must understand and control equipment reliability and know their costs well. Much has been written about the use and value of Weibull analyses [eg., refs. 4 and 5] since Waloddi Weibull published his seminal paper on the subject in 1951 [6].

2. WEIBULL THEORY

Definitions: If turbine components and subsystems are not subject to design or manufacturing defects that can lead to "infant mortality" (i.e., early failures based on poor quality control or

defects), a given population will wear out or fail, as a function of time, in a manner that is described by a "bell-shaped" curve. The Weibull function is a two-parameter distribution that describes the failure rates, and provides sufficient mathematical flexibility to adjust the description to match most cases observed by components in service. Equation (1) is the generalized Weibull distribution :

$$f(t) = [b/\theta(t/\theta)^{b-1}] \exp[-(t/\theta)^{-b}] \qquad (1)$$

where: t is time (typically hours of service),
b is the Weibull Shape (also called slope) Parameter,
θ is the Characteristic Life (also called scale parameter) at which time 63.2 percent of the initial population of components is expected to fail or wear out.

Application: To determine the percentage of expected component failures after the passage of time T, equation (1) is integrated from time zero to time = T and results as follows:

$$F(T) = \int_0^T f(t)dt = 1 - \exp[-(T/\theta)^b] \qquad (2)$$

Figure 1 is a typical symmetric, or normal Weibull distribution of failure rate, and indicates that the cumulative failures at time T as the area under the curve from time zero to time T. For the case shown, the figure also indicates the mean life as the peak of the failure rate and the Characteristic Life as the time at which 63.2 percent of the area under the curve has been consumed.

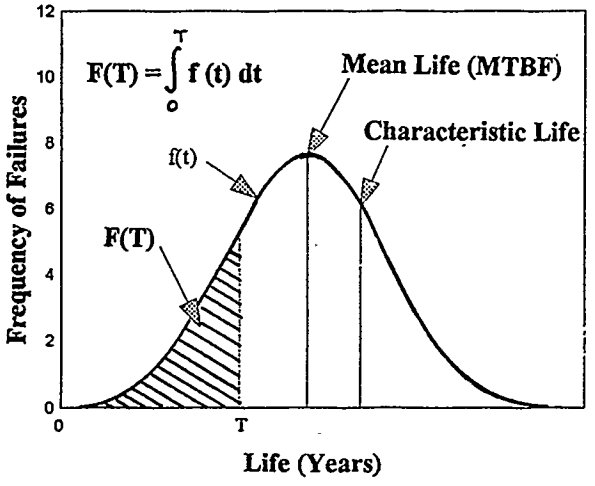

Figure 1. Weibull Distribution and Definitions

The value of b, the Shape Parameter, dictates whether the "bell-shaped" curve is symmetric about the mean life (when b=3.5), skewed left (for b<3.5), or skewed right (b>3.5) - as shown in Figure 2. Shape Parameters of less than 3.5 typically indicate "infant mortality" due to design or quality issues. Shape parameters greater than 3.5 indicate good component longevity and nor-

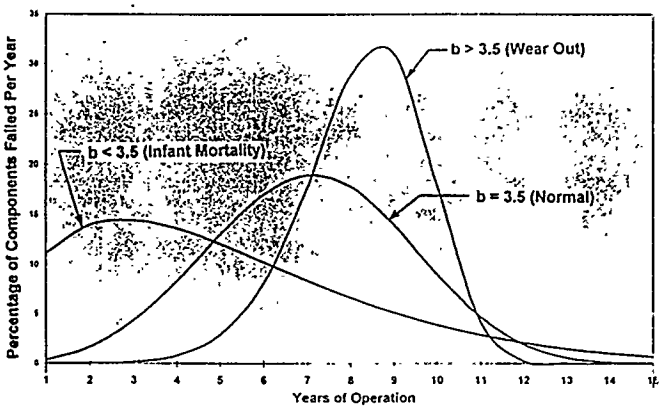

Figure 2. Effect of Weibull Shape Parameter (b) on Distribution

mal wear out. For most wind turbine components, and the data that we discuss in this paper, it has been assumed that b=3.5 (i.e., a symmetric bell curve) until more is known from field experiences.

The expected failure rate in a given year (eg., between year T and year T+1) is determined as the difference between the cumulative failures after successive years (i.e., years T and T+1) by applying equation (2) for each year - to determine F(T+1) - F(T). In addition, the Characteristic Life, is determined most simply by solving for θ in Equation (2) - that results in:

$$\text{Characteristic Life} = \theta = \frac{T}{[\ln[1/(1-F(T))]]^{(1/b)}} \qquad (3)$$

...where ln is the natural logarithm.

The mean life (i.e. MTBF or mean time between failures), in which 50 percent of the components are expected to fail, is a frequently reported parameter in reliability data. It is related to θ through Equation (4), which is derived by solving Equation (2) for t, while setting F(T) equal to 0.5, the probability of failure at the mean life.

$$\text{Mean Life} = \theta * (\ln 2)^{(1/b)} \qquad (4)$$

Failure Rates With Replacements: The annual failure rates described by equations (1) through (4) apply to a fixed population of components that are not replaced. Thus, the Weibull failure-rate curve (Figure 1) rolls off after the peak failure rate, because the population of remaining components is so reduced that the failure rate falls. In real life, however, as components fail, they are replaced - usually with new or completely rebuilt units that usually display the same reliability characteristics of the original population. Then, the subset of new components that are added each year creates their own bell-shaped curve of projected failures, but the first year in each new curve is displaced from the time of initial equipment startup by the number of years of service of the original components. When replacements are taken into account in this manner, the "normal" failure-rate curve does not drop off as shown in Figure 3. Rather it asymptotically approaches a failure rate that is equal to the inverse of the Mean Time Between Failures (MTBF) multiplied by the population of components in the project. During the years immediately after the MTBF period for the initial population, the failure rate for an ideal system oscillates with a period equal to the MTBF, but with lower amplitudes over time. Figure 3 compares the failure-rate curves for the case of no replacements (a symmetric bell-shaped curve) and full replacements of all components when failures occur.

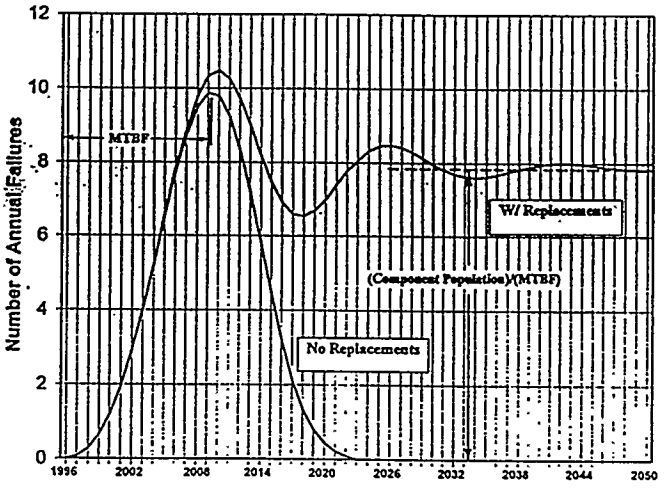

Figure 3. Comparison of Failure-Rate Curves Both With and Without Replacements

Wind Turbine Reliability/Availability Relationships: Average wind turbine availability is perhaps the best, simple yardstick by which the reliability of a wind turbine is judged. Under ideal operating conditions, the availability of a fleet of wind turbines is driven by historical component reliability data that define MTBF and Mean Time To Repair (MTTR) as indicated in equation (5):

$$\text{Availability, } A = 1 - \left[\frac{\text{Outage Time/yr}}{\text{Total Time/yr}}\right] = 1 - \left[\frac{\text{(Op Hrs/yr)}}{8760}\right] \sum_i \left[\frac{\text{MTTR}_i}{\text{MTBF}_i}\right] \qquad (5)$$

...where Op Hrs/yr is the total number of hours per year that the turbines operate and the summation of fractions involving MTBF and MTTR applies across all turbine components. In reality, in the wind turbine industry it is not generally reasonable to expect to know the MTTR and MTBF of the thousands of turbine components (including electronic components). However, in military programs such is typically expected. Equation (5) points out several important factors to consider in designing for high reliability, projecting reliability, or assessing reliability projections:

(1) The equal, but inverse importance of MTTR and MTBF in achieving availability goals shows that it is as important to cut repair time in half as it is to double MTBF. This factor supports the need for quick response to problems and the availability of a proper spare parts inventory.
(2) Due to the summation of the reliability fractions over all components, the importance of following a general design philosophy aimed at increasing reliability: "...keep it simple stupid", or KISS, is demonstrated mathematically. This is true because the fewer the number of components that can result in an outage, the higher is the expected availability.
(3) The more turbine operating hours per year at a site, the lower the availability (due to wear out) unless careful preventive maintenance is practiced.

3. KEY WIND TURBINE COMPONENTS OF CONCERN

Table 1 lists the major categories of components that are a concern for horizontal-axis wind turbines (HAWTs) and, where there is enough experience to develop data, the ranges of typical values for Mean Time Between Failure (MTBF) when 50 percent of the components are expected to fail. As a crude guide, Table 1 also indicates the typical types of failure modes. The components shown are of key importance, because if they are unreliable, they can incur significant costs, and most importantly, cause significant losses of operating time and revenue. The MTBF values are generally applicable to well designed turbines (i.e., electrical and mechanical loads within allowable levels, minimal degradation due to environment, etc.) that are maintained in accordance with manufacturers requirements. Some of the components listed are not always found on HAWTs - such as pitch hydraulic systems, bearings, and linkages that are omitted from fixed-pitch rotors.

3.1. Expected Component Life

The ranges of expected component life indicated in Table 1 are based on real experiences in the wind industry and vary with the factors that are discussed below. Because well-designed, wind turbines have only operated for up to 14 years in the U. S., some of the MTBF expectations listed in Table 1 that exceed 14 years are projections based on observations of current condition and wear factors as well as Weibull projections based on current failure history.

Table 1. Key Wind Turbine Components with Reliability Concerns and Ranges of Typical Lives

Component or Subsystem	Typical Expected Mean Time Between Failures (MTBF) *#	Typical Failure Modes #
Blades	> 10 years	Uncertain (variable)
Gearbox	12 - 20	Rubber oil seals (if present)
	12 - 20	Bearings and gears
Main Bearings	> 10	Brinelling, spalling
Yaw pinion	5 - 12	Gear wear or breakage
Yaw slew ring gear	8 - 16	Gear wear or breakage
Yaw Bearings	> 10	Brinelling, spalling
Pitch Bearings	> 8	Brinelling, spalling
Pitch Linkages	4 - 8	Bearings
Hydraulics, Pitch	5 - 10	Seals
Brakes	3 - 8	Pads, Calipers, Valves
Generators	8 - 12	Bearings, seals & windings
Electronic Boards	5 - 8	Uncertain (variable)
Sensors (eg., tachs)	3 - 6	Uncertain (variable)

*** MTBF is when 50 percent of population is expected to fail.**
 # Failure Modes and Lives Vary Substantially with Stresses, Lubrication, Cleanliness, Temperature and Other Environmental Factors

3.2. Failure Modes and Major Factors Influencing Component Longevity

A major failure mode of current large, maturely designed, utility-interconnected wind turbines is through the loss of control (a "runaway") under adverse or emergency conditions (lightning, loss of utility load, loss of brakes, etc.). If such does not occur, and turbines are maintained properly, they will generally operate with reasonable reliability for several years. Most of the failure modes listed in Table 1 are self explanatory. For specific components such as bearings, the typical failure mechanisms are listed. The discussion below outlines design practices and factors that contribute to lengthening or shortening the life of wind turbine mechanical and electrical components.

3.2.1. Mechanical Components

Preventive Maintenance: Similar to automobiles, every commercial wind turbine has a specified set of scheduled maintenance steps that should be carried out periodically to assure that a reasonable life is achieved. If such practices are carried out regularly, the mechanical components on mature, well-designed machines will often operate reliably for prolonged periods. If scheduled maintenance is not properly executed at reasonable intervals, it can lead to high wear and safety concerns in the following areas:

- High bearing wear from dirty or old oil (dirty oil and/or filters, burned oil, etc.);
- Ineffective solenoid valves from clogged hydraulic lines (lack of filters or dirty filters);
- High gear wear from lack of proper adjustment of bearing shims and gear clearances; and
- Overall turbine safety concerns under emergency conditions if brake pads or hydraulic actuators are worn or acting sluggishly.

Load Environment: The loading spectrum applied to wind turbine components must be properly specified and, at least analytically, the components must accommodate the loads for a prolonged

period of operation (several years) without significant wear. Excessive mechanical loads are often indicated through structural cracking or high wear.

Modal Dynamics: A key factor that often does not show up in loads analyses is the modal dynamic response of various subsystems to forced excitation. The forcing on a wind turbine is largely provided by the turbine rotor. If the forced oscillation occurs at frequencies that coincide with a natural resonance of a structural member, large oscillations and loads can result. On most structures, high modal excitation is not permitted unless the response is highly damped.

Design Margins: The design margins of mechanical components (i.e., allowable stress limits of material versus applied stress) in fatigue and in limit loads (i.e., maximum or survival load) are the best indicators of whether a component will exhibit long-term reliability. These factors are derived through a knowledge of the loads and stresses applied, and are computed from either (1) detailed analyses of stresses in the member or (2) direct stress measurements made during service.

Surface Wear and Fatigue: A high-incidence failure mode of mechanical components is associated with various surface wear mechanisms or fatigue cracks in structures due to repetitive stress cycles. Rapid surface wear can result from (1) brinelling (denting), (2) spalling (surface breakdown/loss due to rolling contact), or (3) fretting (material loss due to abrasion/adhesion during oscillation of contacting surfaces). Such wear factors depend on the design margins, proper clamping of bolts and preloads, stress concentrations, and lubrication. Wear and fatigue failures lend to Weibull failure modeling and are amenable to prediction, but only through field experience or accelerated life tests can one gain high confidence in the durability of product wear surfaces.

Contamination of Rolling and Sliding Surfaces: Bearings, gears, sliding sleeves and seals can wear rapidly if subjected to high loads, high duty cycle, contaminants, and/or lack of lubrication. Lubricants become largely ineffective in the presence of contaminants, so cleanliness and maintenance of filters is a first line of defense in avoiding mechanical wear.

High Duty Cycles: Wear of components, such as hydraulic actuators, brake pads, pitch bearings, and rotating and sliding seals can increase dramatically over the levels planned if the duty cycle (i.e., number of rotations or actions per year) substantially exceeds the design level. For example, reliability analysis indicates that a failure mode must be clearly understood in order to define the Weibull factors that govern the failure rates. In some cases, such as normal household light bulbs, failure rates of components may be more a function of the number of start/stop cycles than of total operating time. It is recognized in the design of wind turbines that it is important to reduce the number of start/stop cycles - especially for those machines in which there is sudden shock load to the drivetrain and/or high generator in-rush current each time that the turbine synchronizes with the network. These factors become a part of the overall design for maximum reliability, availability, and project profit.

Environmental Factors: Environmental factors; such as heat, dust, dirt, humidity, salt, acid, lightning, and ice; have been implicated in reducing component reliability and must be taken into account (minimized or accommodated) in the design and in developing realistic life projections.

Quality Assurance: Well-designed parts can fail because they may not have been manufactured properly. Quality assurance during manufacturing strives to assure that the material properties, component dimensions, heat treatment, or assembly procedures are as designed and specified.

3.2.2. Electrical Components

Environmental Factors: The majority of the above-listed environmental factors also influence the life projections of encased electrical components. A predominant factor in most applications is the thermal environment, because most components are housed in sealed or air-filtered boxes and subjected to particularly harsh vibration environments. Depending on the selection process applied to electronic components, some components in military applications can operate with acceptable reliability up to temperatures approaching 100 °C. For wind turbines, very high temperature environments are generally not encountered, so less selective components can often be used. Lightning can also create significant problems at sites with a high incidence of lightning and/or with turbines that have a poor grounding system. A significant reliability (and outage) concern for wind turbines as they age is that sensors and non-solid-state circuit elements, such as tachometers, relays, current transformers, etc., although relatively inexpensive, can fail at a relatively high rate. Older, reliable turbines often find that the predominant source of unscheduled outage is related to electronic and electrical components.

Loading Versus Rated Capability: Overloaded components with excess voltage or current will always lead to shorter lives. Very often the relationship of age to load is very non-linear - similar to relationships between mechanical loading and age.

4. RESULTS FROM WIND TURBINE FIELD EXPERIENCES

Historical Reliability Data. To derive statistical failure-rate data for wind turbines, specific reliability data were acquired from several wind projects that have operated for periods of up to 12 years. High quality reliability data are difficult to obtain from most current operational wind plants, because budget constraints have often led to inadequate record keeping. However, the small quantity of data that we acquired were screened to remove information that was based on faulty designs that were later redesigned and retrofitted. Estimates were made of future component failures, permitting the computation of θ (Characteristic life) and the mean life (i.e., MTBF) using Equations (3) and (4). A Shape Factor value of b=3.5 was also assumed. The results of these calculations for a 12-year old project are shown in Table 2.

The underlying failure-rate data that led to the values listed in Table 2 were not available for the first five years of wind park operation, but good data were available for the second five years of operation. However, through the application of Weibull analysis it was possible to reasonably project that the expected failure rates that occurred during the first five years of operation were 25 percent of the cumulative

Table 2. Component Failure Experiences from Field Operation

Turbine Subsystem	% Failed	No. of Yrs	b	63.2% Charact. Life (yrs)	50.0% Mean Life (yrs)
Gearbox Seals	2.7	10	3.5	28.0	25.2
Yaw Twist Sensor	25.9	10	3.5	14.1	12.7
Yaw Gearbox	13.8	10	3.5	17.2	15.5
Yaw Slew Ring	12.9	10	3.5	17.6	15.9
Yaw Pinion	93.4	9	3.5	6.8	6.1
Yaw Motors	30.5	10	3.5	13.3	12.0
Brake System	9.1	10	3.5	19.6	17.6
Hydraul. Pump Motor	4.6	10	3.5	23.9	21.6
Brake Valves/Switches	37.5	10	3.5	12.4	11.2
Generators	21.3	10	3.5	15.0	13.5
Generator Contactor	80.1	10	3.5	8.7	7.9

failures in the second five years. A sensitivity study was carried out to determine the effect of the estimated failure percentages for the first 5 years on the calculation of θ and MTFB for each component. The results showed that key failure parameters were relatively insensitive to the data from the first five years of operation - due to the relative strength of the data from the second five years of operation. By extending the analysis, it is possible to project the future failures for each subsystem.

Figures 4 through 6 are plots of measured and projected reliability data for brakes, generators, and yaw gearboxes, respectively, from one wind project that has operated for more than 10 years. The data show that the subsystems had actual, cumulative failures of 32, 80, and 303, respectively, during the 5-year period of 1990 through 1994. The Weibull analysis allowed us to fill in the assumed failures in the first five-year period.. The Figures clearly show that there was a "campaign" to replace badly worn or failed generators (in 1991) and yaw gearboxes (in 1994). It is often less costly to carry out several similar maintenance actions at once, if actions can be temporarily delayed until quantity purchases can be negotiated or the proper crane and/or personnel are available. The same types of plots can readily be developed for all components in the turbine for which detailed replacement data are available.

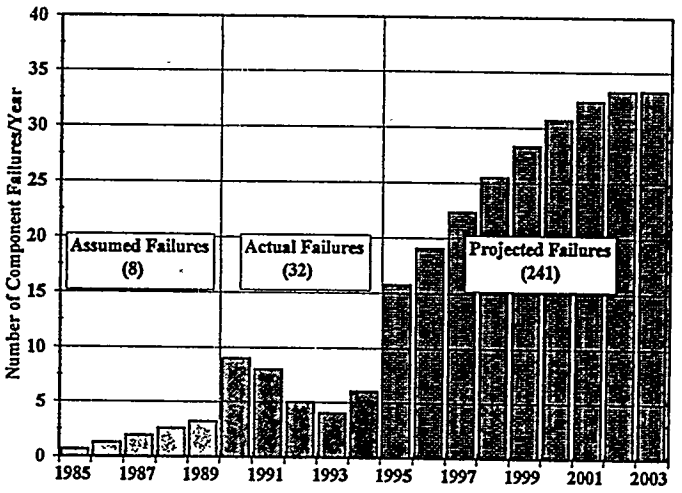

Figure 4. Weibull Reliability Projections for Brake Systems

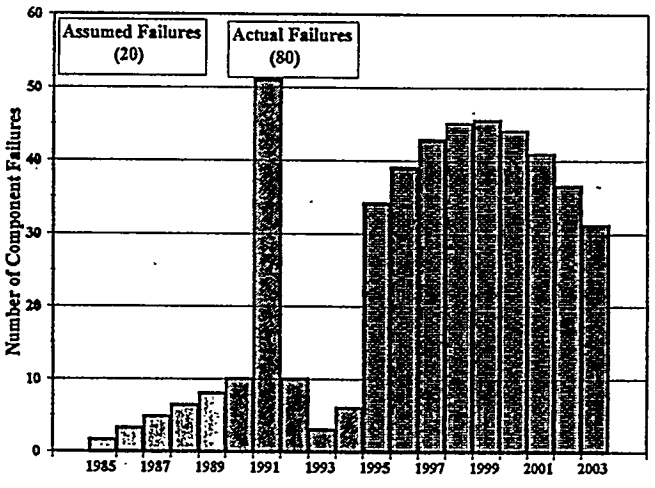

Figure 5. Weibull Reliability Projections for Generators

As shown in the figures, the Weibull analysis (without replacements), made it possible to project the annual failure frequency of the remaining components installed in the original turbines. If replacements were properly taken into account, as indicated in Figure 3, the annual failure rates would eventually settle out at a value approximately equal to 70 or 80 percent of the peak value - depending on the MTBF value and the total population in the wind park. Thus, knowing the failure frequency and cost for various key parts, as well as the personnel and crane time required for replacements, it is possible to credibly project unscheduled maintenance costs over the life of a

project. Most importantly, it is possible to project the life and costs during the period of a bank loan or when a major investment seeks to receive a good rate of return. If product improvement efforts lead to improved reliability, the historical database on which projections have been made will have to be altered to reflect the changes. Generally, such data must await a few years of field service to be reasonably accurate.

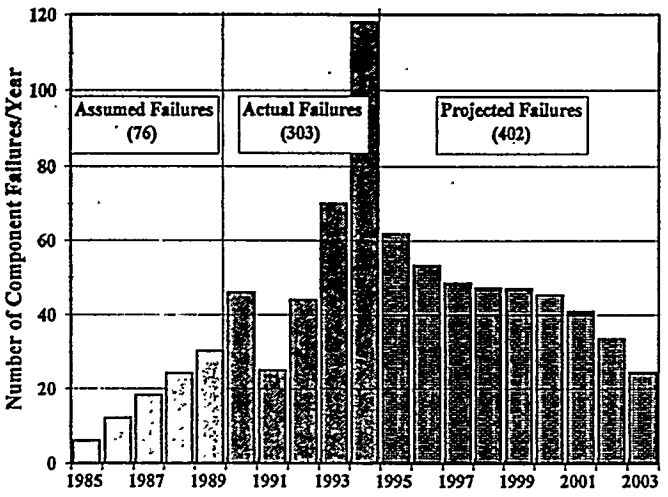

Figure 6. Weibull Reliability Projections for Yaw Gearboxes

Reliability Modeling. Based on a knowledge of how well-designed wind turbine components perform in service, prior to project inception it is possible to reasonably estimate operation costs as well as scheduled and unscheduled maintenance costs. Generally, both operations and scheduled maintenance costs can be predicted accurately. As known from prior projects, unscheduled maintenance costs are largely governed by reliability and replacement experiences on large components such as those listed in Table 3. The values listed in Table 3 are estimates based on (1) a knowledge of the component design margins, (2) results from prior field tests of prototypes, and (3) accelerated life tests conducted in the laboratory - using simulated but representative loads. The information listed in Table 3 make it possible to predict replacement frequency and unscheduled maintenance costs.

Table 3. Weibull Parameters For Estimating Maintenance Costs

Turbine Subsystem	Percent Failed	No. of Years	b	63.2% Char. Life (yrs)	50.0% Mean Life (yrs)
Gearbox	5	8	3.5	18.7	16.8
Blades	5	10	3.5	23.4	21.0
Hydraulics	10	6	3.5	11.4	10.3
Pitch System	10	6	3.5	11.4	10.3
Yaw System Gearbox	10	8	3.5	15.2	13.7
Yaw Slew Ring	10	10	3.5	19.0	17.1
Yaw Pinion	25	7	3.5	10.0	9.0

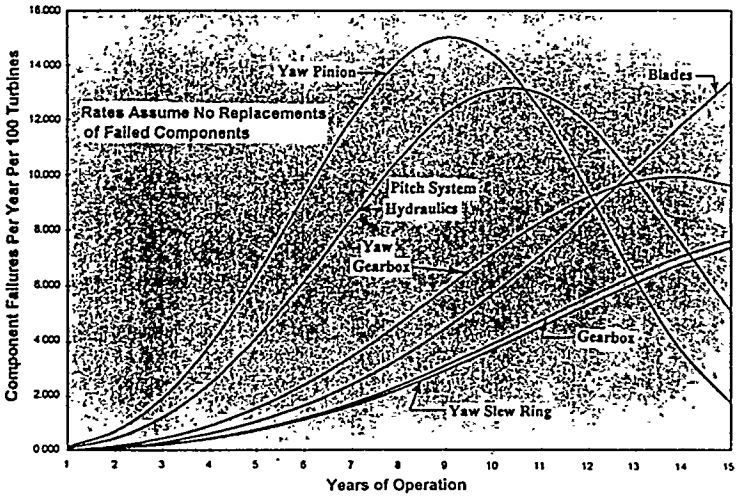

Figure 7. Projected Rate of Major Component Failures

Figure 7 is a plot of the projected failures per

year for the major components listed in Table 3 - when failures of replacements are not taken into account. It is clear that the yaw pinion, pitch system, and hydraulic system are dominant factors based only on repair frequency.

When actual replacement costs and typical hourly rates for personnel and cranes are included in a cost model, the costs projections shown in Figure 8 result. The estimates show that the major items such as blades and main gearboxes, which generally exhibit high reliability, can be the most significant unscheduled cost items. If such items are even slightly more unreliable than expected, very high maintenance costs can result. The estimates shown in Figure 8 also indicate that unscheduled maintenance costs for up to a five-year warranty period can be expected to be minimal compared to those following the expiration of the warranty.

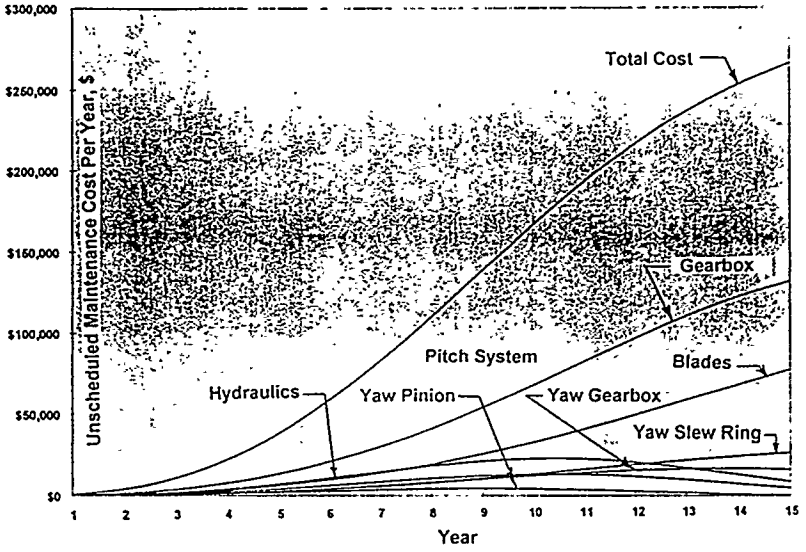

Figure 8. Estimated Unsched. Maint. Costs, Major Subsystems

5. SUMMARY

Annual wind turbine unscheduled maintenance costs can be expected to increase non-linearly in the early years (first 15 to 20 years) of wind project operation. Such costs can be modelled by a Weibull frequency distribution for annual component failures, that describes a "bell-shaped" curve. Sufficient historical component and subsystem reliability data are becoming available so that they can be analyzed through such procedures to project future reliability rates and costs for unscheduled maintenance. Such projections can be very useful in avoiding surprises, planning future costs, turbine upgrade programs aimed at reducing significant maintenance costs, and credibly estimating project financial performance over a multi-year period.

6. REFERENCES

1. Abernethy, Robert B., **The New Weibull Handbook**, Published by the author, 536 Oyster Road, North palm Beach, FL, 33408-4328.
2. Department of Defense, **Military Handbook, Reliability Prediction of Electronic Equipment**, MIL-HDBK-217F, Dec. 2, 1991.
3. Savage, M., and D. G. Lewicki, "Transmission Overhaul and Component Replacement Predictions Using Weibull and Renewal Theory," **J. Propulsion**, V. 7, No. 6, Nov-Dec. 1991.
4. Kececioglu, Dimitri, **Reliability Engineering Handbook**, Vols 1 and 2, Prentice Hall, 1991.
5. O'Connor, Patrick D. T., **Practical Reliability Engineering**, John Wiley, 1991.
6. Weibull, W., " A Statistical Distribution Function of Wide Applicability," **J. of Applied Mechanics**, 1951.

CHOOSING THE APPROPRIATE SIZE WIND TURBINE

Robert Lynette
FloWind Corporation
900 A Street, Suite 300
San Rafael, California, USA

Within the past several years, wind turbines rated at 400 kW and higher have been introduced into the market, and some manufacturers are developing machines rated at 750 - 1,000+ kW. This raises the question: What is the appropriate size for utility-grade wind turbines today? The answer depends upon the site where the machines will be used and the local conditions. The issues are:

- **Site-Related**
  - Visual, noise, erosion, television interference, interference with aviation
  - Siting efficiency
- **Logistics**
  - Adequacy of roads and bridges to accept large vehicles
  - Availability and cost of cranes for erection and maintenance
  - Capability of local repair/overhauls
- **Cost Effectiveness**
  - Capital costs
    - Wind Turbine
    - Infrastructure costs
  - Maintenance costs
- **Technical/Financial Risk**

The interests of the involved parties are shown in Figure 1.

Party	Social*	Resource Use**	Reliability	Cost of Energy	Profit	Risk
Governments	●	●	●	●		●
Community	●	●	●			●
Customers			●	●		●
Land Owners	●	●	●		●	●
Investors			●		●	●
Bankers			●		●	●

*** Visual, noise, flora, fauna, erosion, TVI, aircraft interference**
****Land and wind resource**

Figure 1, Interests of the Involved Parties

Site-Related Issues

Visual issues are a matter of local preferences and will not be addressed here, except to note that:

- Fewer, larger machines, with ratings up to 600 kW have proven more acceptable than larger numbers of lower-rated machines in Western Europe where space is limited; and

- Television and aircraft interference may become a problem with multi-megawatt wind turbines.

Siting efficiency refers to a measure of the wind energy capacity that can be installed on a given piece of land. On flat, or semi-flat land, the same capacity can be installed per unit of land regardless of the size of the machines, as long as the ratio of the ratings of the machines to the swept area is constant. (This is not intuitive, but those readers that are new to the technology can prove it to themselves by making the calculations.) However, where land is predominately of a ridgeline character, higher installed capacities can be achieved with bigger machines. This is a desirable characteristic of larger machines in such areas, especially where space is severely limited (e.g., Western Europe).

Logistics Issues

In many parts of the world, the transportation infrastructure is a barrier to moving large rotor blades, and in some areas, the roads and bridges are not sound enough to accommodate the heavy trucks required to bring very large machines to the wind sites. Such issues are easily settled by analyses of the local conditions.

The availability and cost of cranes, booms, and other materials handling machinery is most important when choosing a wind turbine. Large cranes are readily available in developed countries, but can be difficult to obtain in many developing countries, and their maintenance is a specialized business that must be considered. Further, in many rapidly developing countries, cranes that are available today may become more expensive, or not be available for extended periods, due to competing demands for their use. Purchase of a crane for maintenance is only cost effective for large wind power stations, and again crane maintenance must be considered. Gin poles can be used in place of large cranes, but the setup costs are very high. Fairly large cranes (75 tons or higher) are also required to remove and replace large wind turbines' major components. Purchasers of wind turbines for wind power station applications are advised to examine all of these issues carefully before deciding on the size of the wind turbines they will use.

Cost Effectiveness and Risk Issues

The wind energy industry has debated the issue of wind turbine size vs. cost for at least 20 years. No clear answer has emerged because:

1. Technology changes impact the relative cost of different sized wind turbines, so the answers are constantly changing. This includes materials technology, production processes, as well as the machine technology.

2. The industry has never reach production levels that allow significant economies in the production of wind turbine-unique components. Off-the-shelf components are rare in our industry, particularly on the larger machines.

3. There is insufficient experience with the larger machines to accurately determine their operation and maintenance costs.

For the present, machines rated at 200 - 500 kW appear to have approximately the same costs per kWh, although some manufacturers are claiming that the larger machines are more cost effective. There is general agreement within the industry however, that there is not a major capital cost differential among machines rated at 500 - 800 kW. The answer to the size vs. machine cost is still open, and will remain so for some time.

However, one area of agreement within the industry is that the wind power stations' infrastructure costs decrease with wind turbine size. Most of the savings are realized with machines rated at 250 kW, but further savings are being realized with higher-rated machines. The potential savings with machines rated higher than 250 kW appear to be about $10 - $30 per kW, or 1 - 3% of the turnkey cost of a project. An exception to this generalization may be in developing countries, where materials handling equipment and the transportation infrastructure are frequently not adequate to handle the larger components.

Another important logistics consideration is the ability to repair and overhaul major components in-country. If a gearbox or generator is very large, and can only be worked on in the supplier's country, it will cost far more than indigenous repairs. Unless the wind turbine seller is willing to provide a 10-year warranty, such issues must be carefully examined by buyers, and realistic maintenance costs that reflect these logistics issues should be factored into the financial projections. Most manufacturers of large wind turbines are claiming lower maintenance costs per kWh. Such assumptions may or may not prove true in the long run. Since most wind turbine fatigue problems do not appear until 2 - 4 years of operation, the lack of experience with the larger machines means that we do not yet know their long-run costs.

Finally, and most importantly, buyers must realistically asses the technical and financial risks associated with different sized machines. The 1980s provide us with some good experience with newly-introduced wind turbines. During the 1980s, machine sizes grew from 40 kW to approximately 250 kW. Many new-generation machines experienced structural/fatigue problems during the first five years of operation. The problems were serious enough to put more than 70% of all the wind turbine companies into bankruptcy. Today we know much more about the aerodynamics and structural dynamics of wind turbines, and our experience base in much larger than in the 1980s, so we should expect to see fewer problems. But the problems become more expensive to correct as the size of the machines increase. Perhaps this is why most manufacturers are offering only one or two-year warranties on the larger machines.

In the 1980s, many manufacturers offered five-year warranties that were backed by third-party insurance. The wind turbine owners were loss payees on the insurance policies, so that if a manufacturer got into financial trouble and was unable to correct the machines' problems, the insurance company paid for the corrective actions. Unfortunately, the insurance industry lost several hundred millions of dollars in the wind energy industry, and, with a few exceptions, they stopped providing comprehensive five-year coverage for large arrays of wind turbines. The industry must earn a reputation for reliability before the insurance industry will come back into this industry in earnest. Recent blade problems with at least three different machines rated at 400 kW and higher do not help the situation.

Perspective buyers must devise ways to protect their investment. If third-party insurance is not available, owners could insist that wind turbine manufacturers provide a five-year warranty covering the machines' performance (power curve), availability, and design, manufacturing, and materials defects. But, this protects the buyer only as long as the manufacturer is financially viable, and many wind turbine manufacturers do not have the financial reserves to cover major problems. Imagine a manufacturer who

has produced 1,000 wind turbines rated at 600 kW, and in the third year of operation the gearboxes begin to fail. Since most gearbox suppliers will only provide one or two year warranties, the financial burden falls on the wind turbine manufacturer. A retrofit of the gearboxes could easily cost $10,000 - $20,000 each, or $10 - $20 million dollars for the fleet of 1,000 machines. This is well beyond the financial capabilities of most of the industry's manufacturers, and they would be forced into bankruptcy, leaving the machine owners with the financial burden.

The technological risks associated with the newer, larger machines (or for that matter, new smaller machines) has not yet been internalized in the price of the machines. Table 1 shows the potential risks to the investors and lenders. The best method of protection is to obtain warranty insurance. However, insurance companies also recognize the risks associated with the newer, larger machines, and are reluctant to provide such coverage. One way to provide a reasonable level of protection is to require the seller to place a portion of the sales price into an account that must be maintained for five years, and can only be used to correct machine problems. Of course, to safeguard the buyers, they must have a security interest in the account, so that should the manufacturer go into bankruptcy, the funds would become available to the buyers, and not the general creditors. Based on experience and the example in Table 1, a reserve account representing 15 -20% of the project cost appears prudent.

Table 1, Potential Exposure to Costly Retrofits

Worst Case Outcome	Exposure*
Replace wind turbine	65 - 70%
Lost revenues (1 - 2 years)	30 - 40%
Total	95 - 110%

Very Possible Outcome	
Retrofits (2 - 3 major)	5 - 15%
Lost revenues (6 months)	5 - 10%
Total	10 - 25%

*Percent of project turnkey cost.

Today, investors have a wide range of choices of turbine configurations and sizes. Like most business decisions, they must make a choice based on the perceived risk-reward ratio. If investors and lending institutions insist that manufacturers reduce the technology risk by providing extended warranties, backed up by third-party insurance or a protected reserve account, those companies who will not stand behind their products will be quickly weeded out and the industry will begin to rebuild its reputation.

FROM MEDIUM-SIZED TO MEGAWATT TURBINES ....

Willem van Dongen
NedWind bv
P.O. Box 118
3910 AC Rhenen
The Netherlands

ABSTRACT

First and Further Generations

One of the world's first 500 kW turbines was installed in 1989 in the Netherlands. This forerunner of the current NedWind 500 kW range also represents the earliest predesign of the NedWind megawatt turbine.
After the first 500 kW turbines with steel rotor blades and rotor diameter of 34 m, several design modifications followed, e.g. the rotor diameter was increased to 35 m and a tip brake was added. Later polyester blades were introduced and the rotor diameter was increased with 5 m. The drive train was also redesigned. Improvements on the 500 kW turbine concept has resulted in decreased cost, whereas annual energy output has increased to approx. 1.3 million kWh.
Wind energy can substantially contribute to electricity supply. Maximum output in kiloWatthours is the target. Further improvement of the existing technology and implementation of flexible components may well prove to be a way to increase energy output, not only in medium or large sized wind turbines.

INTRODUCTION

To keep abreast in the wind energy industry, a turbine manufacturer must continually dare to invest in development of new products. NedWind, a Dutch pioneer in wind energy and a long established producer of wind turbines, has proven its capabilities in producing innovations more than once. The current product range includes the series NedWind 30 (250 kW), NedWind 40 (500 kW) and NedWind 50 (1,000 kW).

Developments since the first generation of the 500 kW Series has resulted not only in the worldwide installation of many wind farms including the first off shore wind farm in the Netherlands using 500 kW turbines, but also in the production of several 1,000 kW turbines.
NedWind further improved on earlier versions of 250 kW turbines and reduced the amount of components in the nacelle with 50% resulting in a turbine with either two or three blades to fit a range of wind conditions.

NedWind turbines are fitted with two independent braking systems, i.e., an aerodynamic brake effected by negative pitching of the blades and a mechanical brake of extaordinary high reliability. Both systems are of the 'fail safe' type.

Industrial computer systems control and protect the entire turbine. The latest system also stores important parameters for later retrieval, enables downloading of turbine status and performance information as well as allowing operation of turbines by remote control. The monitoring system can be connected to turbines located anywhere in the world. Via a modem and computer, over 200 turbine control functions can be monitored. Such parameters as wind speed, performance, availability and turbine status etc. can be tracked.

SUMMARY OF METHODOLOGY

NedWind constantly looks for ways to better the price performance ratio of its turbines.

Active Stall Control (ASC)

Maintenance of tip brakes in earlier turbine generations which had steel blades required cranes or other equipment. Furthermore, steel blades attracted lightning. Therefore NedWind began using polyester blades with full span pitch control. This was followed by the introduction of NedWind's Active Stall Control system (ASC) for the purpose of promoting design flexibility and power curve optimization.

All NedWind turbines feature ASC. The active negative pitching system combines the advantage of stall controlled behaviour in high winds with the means of accurately adjusting rotor power to the desired nominal value. Actively forced stall is very effective in regulating maximum power by eliminating damaging power spikes. Blade pitching also is used to optimize the power curve. Finally, negative pitching of the blades is applied as an aerodynamic brake.
In addition, ASC allows adjustments of the turbine characteristics. If noise emission is to be attenuated, for example at night or in certain wind directions, blade pitch can be automatically adjusted for minimum noise production. Alternately, the blades can be pitched for maximum performance. Blade pitch can also be used to allow turbine operation on heavily loaded grids.

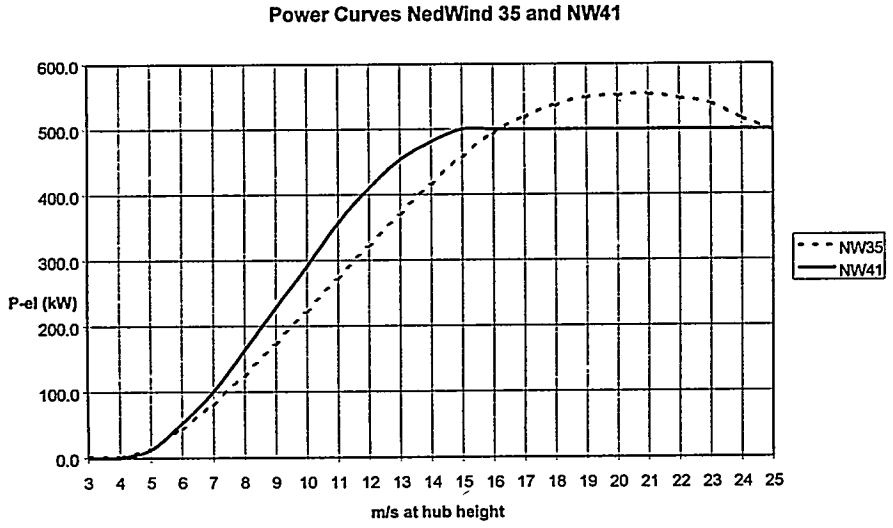

FIGURE 1 - COMPARISON OF POWER CURVES

Dual speed

Dual speed offers benefits for wind turbine operation in areas with low average wind speeds.
In combination with Active Stall Control, dual speed turbines have several advantages over a single speed version.

- At a site with low average wind speeds, the power curve is optimized by switching to lower rotor speed near 8 m/s.
- Decreasing noise level, which is relevant especially in densely populated areas or

at night time, is possible by operating at low rpm in low wind speeds. Whereas formerly a turbine had to be shut down in order to meet strict noise emission levels, noise can now be regulated by adjusting the blades for minimum noise production while maintaining maximum performance in the given conditions.

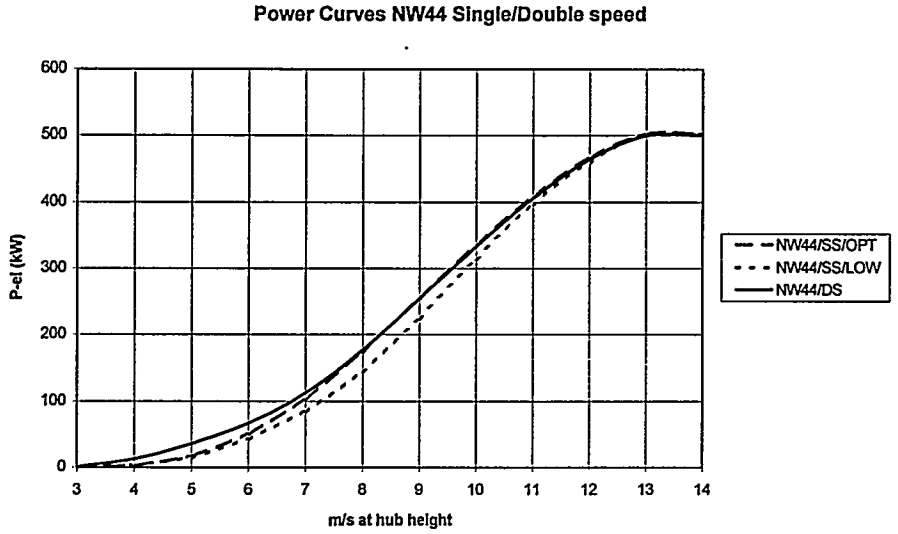

FIGURE 2 - COMPARISON OF POWER CURVE (SINGLE SPEED VERSUS DUAL SPEED)

Flexibility in Design

In order to allow wind energy utilization in coastal areas as well as in regions with lower wind speeds, the design of rotor and tower can be varied to meet the requirements of a specific site.
Since the first generation of 500 kW turbines, the rotor diameter for NedWind's 500 kW turbines have increased from 35 to 41 to up to 44 meters. This has resulted in optimum performance of the turbines.

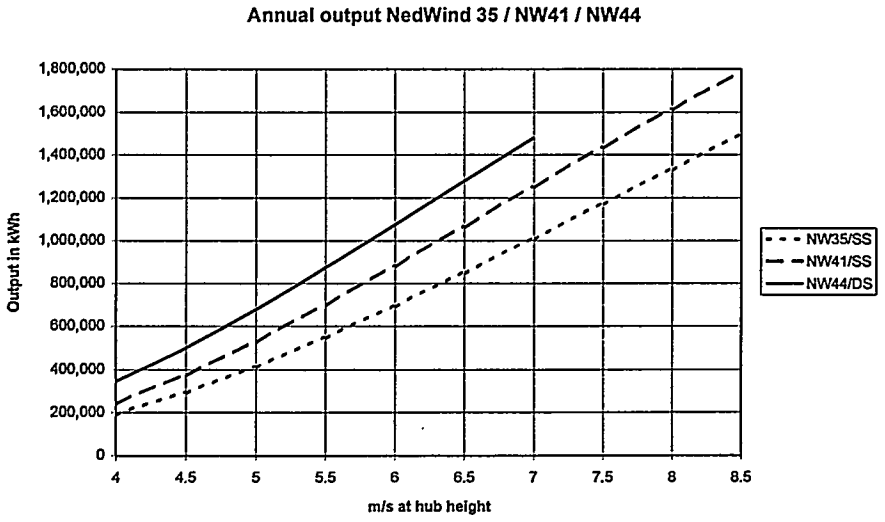

FIGURE 3 - COMPARISON OF ANNUAL OUTPUT

Extension and design improvement of turbine towers is another means to maximize output at a low average wind speed site. In the 500 kW turbine range, hub heights have increased from 39 to 50 to up to 65 meters.

Towers are dimensioned according to specific wind environments and wind speed classifications. The difference in tower shape is influenced by the following requirements:

1. The design must withstand (heavy) buckling loading standards.
2. The tower must have a natural vibrational frequency which lies within the desired range.
3. The weight of the tower should be minimal.
4. The maximum allowable tower section length is 23 meters.

Requirements 1. and 3. are influenced by changing the shape of the tower. If the tower wall thickness is changed (to meet the buckling standard) the frequency of the tower will change. Tower stiffness is then adjusted to arrive at the proper natural vibrational frequency by choosing the shape.

A tower can be made more stiff when the "bottle shape" is chosen, and less stiff by choosing the "tapered/cylindrical" shape.
The design of a tower for specific wind regime is a continuing process in which several designs are considered after which a design which best fits the requirements, is chosen.

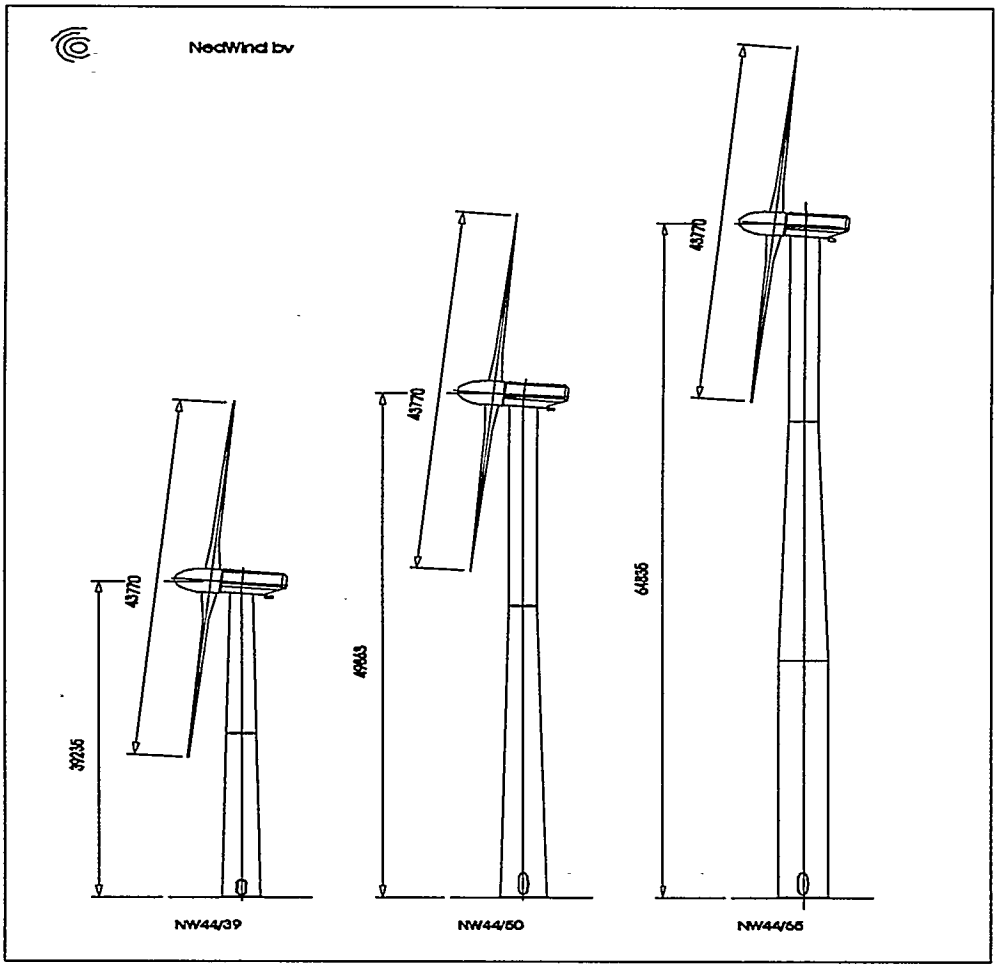

FIGURE 4 - TOWER SHAPES

Yawing device

A unique device for yawing the turbines has been used in all of the NedWind 500 kW Series turbines. This device uses a high tensile steel cable and double action hydraulic cylinders.

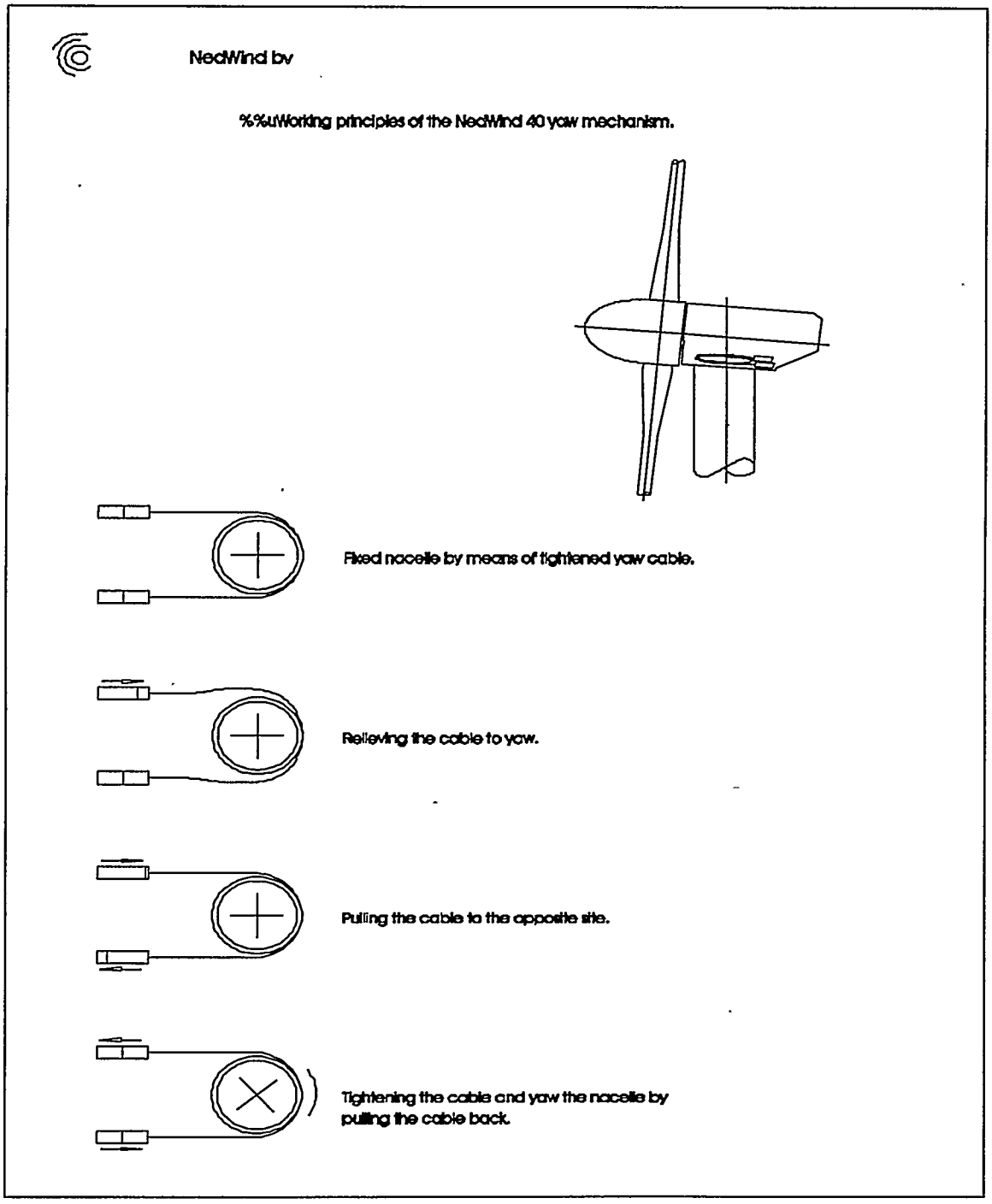

FIGURE 5 - WORKING PRINCIPLES OF YAW MECHANISM

The megawatt turbines do not feature the above described yawing device. Due to the larger dimensions of the turbines, yawing is accomplished by the conventional means of a yaw motor driven pinnion engaged with a bull gear which is attached to the tower.

Modular Drive Train/Power Conversion System

NedWind applies one (or more) standard 250 kW generator(s) in its turbines, for the purpose of improving efficiency and power factor. At full power, all generators are grid connected. Depending on the power produced at a given time, one or more generators are connected to the grid. In this way generator efficiency is optimized.

RESULTS

Price Performance Ratio

NedWind has made continuous improvement in turbine design and performance, which has resulted in turbines which are low in both capital and maintenance costs.

It will not be long before the wind turbines surpasses fossil fuels both in terms of cost effectiveness and price.

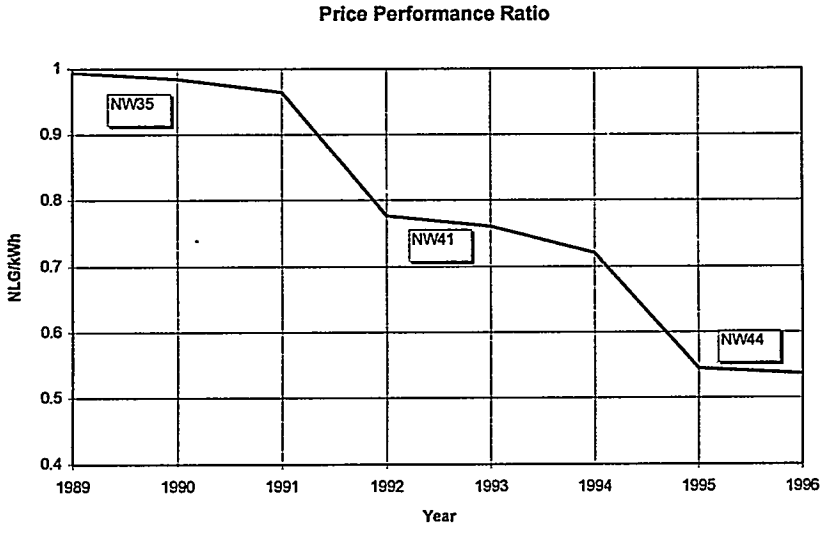

FIGURE 6 - PRICE PERFORMANCE RATIO

Flexibility

NedWind turbines are remarkable items of modern Dutch state-of-the-art innovative technology. NedWind's turbines are designed to make use of scarce sites for implementation of wind energy, on shore as well as off shore.
Dimensioning of rotor diameters, towers and other components will further evolve with the focus on designing turbines to fit a specific wind regime.

Off-shore application

Some five years back wind turbines were relatively rigid generators, designed for application in a coastal wind climate and constructed in accordance to respective wind conditions and load spectra.
On inland sites performance of such wind turbines decreased, however application off-shore in the IJsselmeer proved feasible, with certain modifications to turbine construction and installation.

The project has established proof that off-shore wind energy is a promising option for the Dutch energy supply and has given insight in the effect of this wind turbine project on its surrounding (water landscape, birds, fish).

Four NedWind turbines with a capacity of 500 kW were installed in a line configuration parallel to the dyke around the Wieringermeer.

The distance to the coast is 800 meters; the water depth is some 5 meters. The NedWind turbines were at that time the largest commercially available and were therefore chosen in order to achieve minimal operational costs

The turbines are placed on steel monopiles. This type of foundation is more flexible than the conventional concrete foundation usually used on land.

FIGURE 7 - WIND FARM LELY - OFF-SHORE

Parameters for the design calculations include ground data, ice loads, permissible material load and wind turbine data on frequencies and loads at the foot of the tower. Foundation design is such that natural frequencies of foundation/turbine do not coincide with those of the rotor or their harmonic frequencies.

Other reasons to apply steel monopiles for the foundation are that this type of foundation can be delivered pre-fabricated, can be placed quickly, can easily be adapted to the turbine placed on top of it. Natural frequency of the construction required the diameter of the monopiles to be 3.7 meters. The monopiles stand on clay in the sand layer in the bottom; the length of the piles was determined by the depth of this sand layer and varies from 26 to 28 meters.

The diameter of the turbine tower is 3.2 meters; a concrete floor on the monopile amchors the tower to the foundation. At 2.5 meters above water surface a base with mooring facility with special rubber shock absorbers is constructed around the tower to prevent serious damage to ship and foundation in case of a collission.

For connection to the grid each turbine has a 10 kV station in the tower, containing a transformer from 400 to 10,000 Volt and a switching system which could be used to turn off the particular turbine.

The wall of the transformer station is insulated to prevent condensation on the inside and mechanical ventilation prevents high temperatures in the transformer area. Moulding resin transformers were applied in order to prevent oil leakage. Since the water in the IJsselmeer is used for the drink water supply, the turbines were additionally fitted with double oil sealing rings and oil throughs.

In order to keep maintenance costs low, extra hoisting facilities were fitted in the nacelle for the inspection and maintenance of the rotor blades. A new control system for remote monitoring limits the number of inspection tours to the wind farm.

In view of extensive nautical activities in the vicinity of the wind farm and to limit hazard to shipping, security measurements were taken. Red colour accents are used on the towers and nose cones; horizontal positioning of the blades when the turbines are not operational is implemented; at night the wind turbines are marked with orange flashing lights; instruction signs for shipping on the bases are illuminated.

An innovative aspect is the implementation of a detection system for fog and thunder storms, which stops the turbines and ensures horizontal parking of the blades at certain weather conditions, thereby reducing the chance of lightning strokes by 50%.

The installation of the wind farm was realised within a few months. Foundation work started mid April 1994. Within four weeks monopiles and concrete floors on top of the piles were realized. Cables were laid and turbines bases were placed. Early June preparations for mounting the turbines were started. Towers were pre-assembled and rotors were mounted on the nacelles in the nearby working harbour. Due to calm weather and tight planning mounting the four turbines off-shore was done in two days. After that the transformer stations were installed and remaining assembly work was completed. The turbines were put into operation before the end of June 1994.

Building wind turbines on water is more expensive than a comparable project on land, primarily due to costs for foundations, grid connection, hoisting and security measurements for shipping.
This first off-shore project in the Netherlands proved to be some 30% higher in cost as compared to an identical windfarm constructed on land.

Since output and performance of modern wind turbines are steadily increasing, expectations are that an off-shore project consisting of several larger turbines can operate even more cost efficiently. However, due attention should be given to the choice of foundation, mooring and hoisting facilities, provisions for connection to the grid. These aspects will vary and are directly related to the projected site for a wind farm on water.

Important factors in favour of implementing wind energy off-shore are:
- growing scarcity of suitable sites for wind energy on land;
- limited terrain roughness and unimpeded wind supply;
- less opposition with respect to visual impact of the turbines;
- length of licencing procedures.

The Megawatt Series

Important factors in favour of implementing megawatt scale turbines on land are:
- growing scarcity of suitables sites for wind energy;
- optimal utilization of a site with higher installed capacity;
- advantages relating to costs for infrastructure and grid connection.

In 1991 NedWind started the development of a megawatt turbine. Subsidies were granted by the European Committe and the NOVEM. Design and construction of the prototype in Spijk and the second turbine in Medemblik were covered by Thermie projects; the measurement program and verification of the Spijk turbine was covered by a Joule project.

The two-bladed megawatt NedWind 50 Series design, available in single or two speed version, meanwhile consists of turbine types NW53 and NW55. Dimensioning of rotor diameter and hub height is adjusted to match the requirements of a specific wind environment.

Certification according to NEN6096/2: type NW53 - November 1994; type NW55 - March 1996.

Objectives of the measurement program for the prototype:
- Obtain detailed dynamic load and response data from a large stall regulated turbine.
- Evaluate the current design methods against measured data and hence to improve the predictive tools.
- Verify the NedWind 50 Series design.

Main conclusions of this measurement program are:
- An extensive measurement program has shown to be of major importance for verifying design models when upgrading turbine designs.
- Both noise and performance improvements could be achieved by optimized control strategy. Measured noise levels: 102.9 dB(A) at high rpm and 90.4 dB(A) at low rpm.
- Optimizing of yawing procedure resulted in a higher performance.
- Measured blade loads are generally in reasonable agreement with the calculations. At higher wind speeds the dynamic loads are somewhat higher than predicted. Ongoing analysis of measurements will reveal more details.

The prototype of the NedWind megawatt turbine was installed in Spijk in February 1994. The Spijk turbine has a rotordiameter of 52.6 meters and a hub height of 40.7 meters. These dimensions negatively influenced the aesthetic value and in the installation of later turbines this fact was taken into consideration.
The prototype was tested as a dual speed turbine, consisting of 6 generators of which 2 were operated in lower wind speeds respectively at lower rpm. In current megawatt turbine types of the dual speed version 4 double wound generators are implemented.

Results of the measurement program on the Spijk turbine convinced NedWind of the feasibility of the megawatt turbine and the NW53 turbine type became commercially available. Design of the turbine is basically similar to that of the 500 kW-series. The modular drive train, Active Stall Control and dual speed are comparable. However, in view of the weight of the nacelle, yawing by means of steel cables as is done by medium-sized turbines proved to be cumbersome and this system was substituted for a yawing device with a gear ring and two yaw engines.

The world's first megawatt turbine to be commercially operated, situated at Medemblik, was installed in May 1995 at the same spot as the NEWECS-45 experimental 1,000 kW turbine was erected at the end of 1985.
In April 1995 the old turbine was taken down and the 60 meter tower was shortened to 53 meters. The new megawatt turbine was then mounted on the exisiting tower on May 23. Annual output is estimated to be approx. 2.3 million kWh. Output in the first year (including the test period) totalled 1.8 million kWh.

The now proven megawatt technology resulted in the development of turbine type NW55, which dimensioning is fit for implementation on inland sites.

The first windfarm featuring megawatt turbines in the Netherlands is situated in Moerdijk on an industrial location along the Hollands Diep waterway.
The annual output of this wind farm consisting of 4 NedWind turbines type NW55 is prognosed to be some 6.8 million kWh. Rotordiameter is 55 meters, hub height is 60 meters. The Moerdijk wind farm became operational in May 1996.

CONCLUSIONS

Wind energy is a renewable source and can substantially contribute to the supply of electricity. Installation of wind farms require a short time period compared to the installation of traditional power plants.
Generating electrical power by means of wind energy has no harmful effect on the environment because the emission of toxic substances, which contribute to global warming and acid rain, are avoided. It is thus critical that use of wind energy is further expanded and in order to do so a low price performance ratio is important for wind energy to be able to succesfully compete with fossil fuels.

Maximum output in kilowatt hours is also important. This can be accomplished by optimizing turbine performance to a specific wind zone.

During the past five years, the wind energy industry trend has been to improve on the output of a turbine by increasing turbine size. NedWind is also engaged in increasing turbine size.
Further improvement of the existing technology and using flexible components may well prove to be a way to increase energy output and cost effectiveness in both medium and large size wind turbines.

THE 1.5 MW WIND TURBINE OF TOMORROW

BY

THEO J. DE WOLFF
HENRIK SONDERGAARD

NORDTANK ENERGY GROUP
North American Office
3311 Church Road, Suite 210
Richmond, VA 23233
U.S.A.

AT

WINDPOWER 1996
DENVER, COLORADO

ABSTRACT:

The Danish company Nordtank is one of the pioneers within the wind turbine industry. Since 1981 Nordtank has installed worldwide more than 2300 wind turbine generators with a total name plate capacity that is exceeding 350 MW.

This paper will describe two major wind turbine technology developments that Nordtank has accomplished during the last year:

* Site Optimization of Nordtank wind turbines: Nordtank has developed a flexible design concept for its WTGs in the 500/600 kW range, in order to offer the optimal WTG solution for any given site and wind regime.

* Nordtank's 1.5 MW wind turbine: In September 1995, Nordtank was the first company to install a commercial 1.5 MW WTG. This paper will document the development process, the design as well as operations of the Nordtank 1.5 MW WTG.

I. INTRODUCTION

The Danish company Nordtank is one of the pioneers within the wind turbine industry. Since 1981 Nordtank has installed worldwide more than 2300 wind turbine generators with a total name plate capacity that is exceeding 350 MW.

This paper will discuss:

* Site Optimization of Nordtank Wind Turbines
  Nordtank has developed a flexible design concept for its WTGs in the 500/600 kW range, in order to offer the optimal WTG solution for any given site and wind regime.

* Nordtank's 1.5 MW wind turbine:
  In September 1995, Nordtank was the first company to install a commercial 1.5 MW WTG. This paper will discuss the development process, the design as well as operations of the Nordtank 1.5 MW WTG.

II. SITE OPTIMIZATION OF NORDTANK WIND TURBINES

The opening up of new and widely divergent markets has demanded an extremely flexible approach towards wind turbine construction. The Nordtank product range has expanded considerable in recent years, with the main objective to develop wind energy conversion machines that can run profitable in any given case.

In the following you will find the site specific parameters that affect the wind turbine choice:

* Wind Regime:
  - Mean Wind Speed;
  - Turbulence;
  - Shear Factor;
  - Exposure to extreme wind speeds;
  - Air Density.

* Climate:
  - Monthly Mean Temperatures;
  - Extreme Temperatures;
  - Exposure to Lightning and other extreme weather conditions.

* Site Conditions:
  - Site Accessibility;
  - Terrain Conditions.

* Power Quality
  Specific grid requirements;
  Isolated or Independent Grid.

* General:
  Availability of sites;
  Permitting;
  Available Infrastructure;
  Visual impact;
  Noise.

It is impossible to develop an all-round wind turbine, that will perform optimally in all wide ranges of above mentioned parameters. For example: the windy mountain ridges in Southern California require a different wind turbine than the off-shore wind projects in the Netherlands.

In order to meet the demands of the various sites (and countries), Nordtank has developed for its wind turbines in the 500-600 kW range, a site-customizing concept that will result in the optimal solution for any given situation. The following components of the Nordtank turbines in the 500 - 600 kW range can be adapted to the specific project requirements:

* Rotor Diameter:
  Nordtank's WTGs in the 500-600 kW range can be equipped with either a 37m, 41m and/or a 43m rotor.

* Tower Height:
  Nordtank's 500-600 kW WTGs can utilize various tower designs, which will result in hub heights from 35m up to 60m.

* Fixed Pitch Setting of the blades:
  Based upon the actual air density at the site, Nordtank will pitch the blades upon installation, in order to compensate for air density. In this way Nordtank will minimize potential losses due to reduced air density.
  The turbulence intensity at the site has also influence on the pitch setting of the blades. For example, off shore wind regime have typically a low turbulence, which will allow a more positive pitch setting of the blades.

* Type of Generator:
  In addition to generators with various name plate ratings, Nordtank's WTGs in the 500-600 kW range can be equipped as an option with dual wound generators, which give the turbine a lower name plate rating at lower wind speeds and therefore the efficiency at lower wind speeds will improve. This option is feasible in lower wind regimes.

* Drive Train:

* Type of Tower:
  As a standard Nordtank uses tubular towers. As an option Nordtank has lattice tower designs available for its wind turbines in low to moderate wind regimes.

* Power Conditioning Equipment:
  Nordtank's wind turbines are equipped with full power factor correction equipment, in order to meet the IEEE 519 standards. In addition, Nordtank can add other power conditioning equipment to meet the requirements of the specific grid condition.

* Cold Weather Package:
  If the wind turbine has regularly exposure to ambient temperatures lower than -20 degrees Celsius, Nordtank recommends to utilize different steel grades for some components; to add heating elements to some components; different cabling insulation, etc.

Nordtank is currently offering the following configurations of turbines in the 500-600 kW range (identification WTG: nameplate capacity / rotor diameter):

* NTK 500/37H
* NTK 500/37
* NTK 500/41
* NTK 550/41
* NTK 600/37
* NTK 600/41
* NTK 600/43
* NTK 600/180/43

In the following you will find two case histories that will illustrate Nordtank optimal solution concept for its wind turbines in the 500-600 kW range:

* Corkey Wind Power Plant, Ireland:
  + Host Utility: Irish Utility.
  + Current owner and operator: Scottish Power, U.K.
  + Years of Operation: 1.5 year (start up December, 1994).
  + Capacity: 5 MW.
  + Current Availability: > 98%.
  + Nordtank's responsibility: supply and installation of WTG.
  + Wind Regime: Mean wind speed > 10 m/s
  + Remarks: During first year of operation: nett capacity factor 46.3%
    During the winter months nett capacity factor > 60%
  + Wind Turbine Optimization:
    10 NTK 500/37H WTGs
    Rotor: 37 m
    Tubular tower, hub height 35 m.
    Reinforced drive train in order to withstand the extreme high winds

* NUON Off-shore Wind Power Plant, the Netherlands:
  + Host Utility: Nuon (Dutch utility).
  + Current owner and operator: Nuon.
  + Years of Operation: under construction, start up October '96.
  + Capacity: 11.4 MW.
  + Nordtank's responsibility: turnkey installation of off-shore wind power plant.
  + Wind regime: Mean wind speed approx. 7.5 m/s
  + Wind Turbine Optimization:
    19 NTK 600/43 WTGs
    Rotor: 43 m
    Tubular tower, hub height 50 m.

III. NORDTANK'S 1.5 MW WIND TURBINE

A. THE DEVELOPMENT PROCESS OF THE NTK 1.5 MW WTG.

The development process of the Nordtank 1.5 MW Wind Turbine started in 1992. At that time Nordtank got awarded a grant to develop a 1.1 MW wind turbine under the THERMIE (Demonstration program) and JOULE (Research program) programs of the European Union.

The development program of Nordtank 1.5 MW WTG can be divided in the following phases:

* Phase 1: Design & Engineering; from January 1993 to January 1995.
* Phase 2: Implementation; from January 1995 to September 1995.
* Phase 3: Commissioning; from September 1995 to October 1995.
* Phase 4: Operation, data collection; from October 1995 to January 1997.

The objective of the development program was to design a one-MW-plus wind turbine, which would be competitive with medium sized wind turbines (500 kW class) on price per kWh basis.

Nordtank has designed the wind turbine in collaboration with the reputable design company, Jacob Jensen Design from Denmark (well-known worldwide as designer of Bang & Olufsen audio equipment). Several design alternatives have been evaluated, taking aesthetic, economical and technical criteria into consideration.

During the summer of 1994 five scale (1:40) models were made for the final evaluation and selection of the "solution". The solution expresses Nordtank's design philosophy:

* To create turbines with a smooth, aerodynamic look, which reduces the visual impact on the landscape.

* "Things should be made as simple as possible"

Some basic design parameters of the Nordtank 1.5 MW WTG:

* Three blades, upwind, rotor diameter: 60 m

* Double conical tubular tower, resulting hub height 60m

* nameplate rating: 1500 kW at 16 m/s

* total weight of the turbine (incl. tower and transformer): approx. 193 tons

B. THE DESIGN OF THE NTK 1.5 MW WTG

The design of the Nordtank 1.5 MW WTG has quite some similarities with the Nordtank wind turbines in the 500-600 kW range. The main design characteristics, such as stall-controlled power output regulation, constant speed rotor, active yaw system, induction generator and blade tip brakes, have remained the same. However, the design of Nordtank 1.5 MW WTG differs from Nordtank previous wind turbines in various design aspects, such as:

* Design of the machine foundation:
  The nacelle of Nordtank 1.5 MW WTG has been designed as a hollow box profile in comparison with a single curved steel shell (known as the submarine) for Nordtank's smaller WTGs.

* Design of drive train:
  The design of the drive drain of Nordtank 1.5 MW WTG has the following characteristics:

  + Three point suspension of main shaft and gear box, which minimizes alignment problems and simplifies the suspension compared to four point suspension of the smaller turbines.

  + Two generators.

  + Two output shafts in the gear box, which make it possible to apply two separate brake discs which renders a higher safety level for the mechanical braking system.

* Design of tower:
The design of the tower is constrained by a maximum diameter of 4.2 m, due to transportation considerations. Furthermore, the double conical tower is a result of the Jacob Jensen Design studies: the double conic tower results in a smoother change from the tower to the nacelle, which is improving the aesthetics. The transformer is placed in the top of the tower, in order to reduce energy losses in the cables.

* O. & M. aspects:

+ The turbine can, to a large extent, be serviced without an external crane; By mounting an internal crane it is possible to replace the generators if any damage should occur. Separate hoisting equipment is available for possible replacement of the blades.

+ As an option, it is possible to access the nacelle through a internal elevator. This option has been utilized at the first NTK 1.5 MW WTG.

* Improved noise reduction:
The following steps have been taken to reduce the noise emission from the 1.5 MW turbine:

+ Most importantly, the rotor is designed to rotate with a tip speed of only 60 m/s, which is relatively low compared to other turbines.

+ Supports for the gear box and generators are mounted on a stiff structure reducing the noise emission.

+ The air intake and outlet in the nacelle are mounted with noise reducing material.

+ Furthermore, the whole nacelle cover is constructed as a sandwich of glass fibre reinforced polyester (GRP), which also reduces the noise emission.

* Lightning protection:
Lightning protection is important due to the extreme height (90 m) of the WTG. Therefore, the following lightning protection features have been included in the design of the Nordtank 1.5 MW WTG:

+ Down-conductors positioned in the blades leading to the rotor.

+ Two aerials placed on top of the nacelle near the rotor.

+ One aerial placed on top of the wind vane.

+ Spark gaps at main shaft and yawing system.

C. OPERATING EXPERIENCE WITH THE 1.5 MW TURBINE

The first Nordtank 1.5 MW Wind Turbine was fabricated during the first half of 1995. The installation of the first Nordtank 1.5 MW WTG took place in early September, 1996, at the Tjaereborg site on the Western Coast of Denmark.

The turbine was connected to the grid for the first time on September 7, 1995, at 8:30 pm, at a mean speed of 14-15 m/s. Within 10 minutes, the turbine reached 1.5 MW, its name plate rating!

At the end of September, the turbine was operating in a storm with gusts up to 32 m/s and operated at the nominal power for nearly 6 hours, resulting in a lot of operating experience.

On the 18th of October, RISO, the independent Danish test institution allowed the turbine to operate in automatic mode after the blade test was performed: measuring flapwise and edgewise deflection, applying a shear force at the measuring blade (pulling from the tower).

Despite the fact that the overall performance of Nordtank's 1.5 MW WTG has met its expectations, various minor adjustments have been made since the inauguration of the WTG, such as:

* In October 1995 and February 1996, the blades were pitched to adjust the stall-power, and the stall point is now 1.5 MW, its design name plate capacity. Actually, the turbine was overproducing up to 1700 kW.

* In January 1996, the inner bearing on the high speed shaft No. 2 burned and had to be changed. The fault arose apparently because of incorrect mounting of the bearing. No problems have been experienced after the modification.

Up till June 1, 1996, the turbine has been operating for 2838 hours and has produced approximately 1800 MWh (average effective capacity 605 kW). The maximum technical availability was reached in December: 97.5%.

A preliminary noise measurement has been performed and showed results well below the 104 dB(A), which is the criteria on the Tjaereborg site. The measurement indicated a level of approximately 101.3 dB(A) pressure level, which is relatively low compared to the noise level of 500 kW turbines (characteristic noise level 97-98 dB).

D. FUTURE UTILIZATION OF THE NORTANK 1.5 MW WTG

Nordtank Energy Group is very pleased with the development of its 1.5 MW WTG. The development process has resulted in the following achievements:

* It is possible to manufacture a commercial 1.5 MW stall-regulated turbine with a cost price per kWh nearly the same as for the medium sized wind turbines.

* The Nordtank 1.5 MW WTG is a MW+ turbine with a reduced visual impact, making the turbine a nice element in the nature and more acceptable to opponents of wind energy.

* The stall regulation of the 1.5 MW Wind Turbine functions well.

* The 1.5 MW wind turbine supplies power with an acceptable power quality: The two generator concept in combination with the thyristor soft connection application reduces the possibility of power peaks during grid-connection remarkably.

* The turbine operates at a very low noise level. By utilizing Nordtank's 1.5 MW wind turbines, the total installed capacity per square meter would increase significantly, if the noise level on the ground area would be the critical design parameter: A 6 MW wind power plant utilizing 4 NTK 1.5 MW WTG would require 40% less site area than a 6 MW wind park, consisting out of 12 NTK 500 kW WTGs.

The major disadvantage of Nordtank 1.5 MW WTG is that the turbine can only be utilized, if sufficient infrastructure is available at the site, such as access roads, crane availability, etc. These factors have a huge influence on the economics of the 1.5 MW wind turbine.

Currently, Nordtank's 1.5 MW WTG is competitive for the European markets, that have site constraints: By using Nordtank's 1.5 MW WTG, the available site will be utilized most efficiently. Various installations of the Nordtank 1.5 MW wind turbine are planned for the near future.

Nordtank R. & D. department is continuously working on the further improvement of the Nordtank 1.5 MW Wind Turbine, in order to make the turbine more competitive for a wider range of markets. Nordtank is working on the development of additional configurations of its 1.5 MW WTG: larger rotor diameters and higher towers, in order to make the 1.5 MW wind turbine more efficient for low wind regimes.

RESULTS FROM POWER QUALITY MEASUREMENTS IN GERMANY - AN OVERVIEW

Gerhard J. Gerdes, Fritz Santjer
German Wind Energy Institute, DEWI
Ebertstr. 96
D-26382 Wilhelmshaven
Germany

Abstract

Grid interferences caused by wind turbines (WT) are getting a severe problem in Germany with the fast increasing number of installed turbines. The wind energy capacity was doubled annually in the past three years. The actual situation and the plannings for the next years will lead to a situation, where high wind energy penetration will exercise a big influence on the power and voltage quality of local utility networks. Measurements performed in Germany according to a national guideline show a big variety in power quality performance of WT's, which does affect the requirements for grid connection and thus the economical situation of wind energy projects to a large extent. The results from more than 25 power quality measurements will be discussed in this paper.

1 Introduction

Power Quality of wind turbines (WT's) is getting an important issue in Germany now. The reason lies on one hand in the high power and voltage quality ensured by the utility to the customers on the other hand in the relatively high installation densities of WT's of the 500 kW class in relatively low populated areas.

Germany during the past five years had the largest wind energy installation growth in the world. 300 MW installation in 1994 and 500 MW in 1995 contributed to the world wide annual installation to nearly 50 %. By the end of 1995 in Germany 1136 MW wind energy were installed, until the year 2010 more than 2500 MW are planned. Alone in the State of Schleswig-Holstein 1200 MW will be installed in 2010, if plannings become true. This means an average contribution of wind energy to the electricity supply in Schleswig-Holstein of more than 25 % (no growth in electricity consumption is assumed), in an agricultural structured area with comparatively low density and low infrastructure of the electrical network. A share of 25 % in average could mean in situations, where high wind speeds occur at the same time as local consumption is low, a penetration of more than 100 %. In this situation, where Schleswig-Holstein is rather exporting wind energy, the network power quality is strongly influenced by the electrical performance of the installed WT's. In order to use the existing grid capacities most efficiently and to keep network reinforcement to a minimum, the power quality performance of the connected WT's has to be as high as possible to keep grid interferences to a minimum.

In Germany power quality certifications are required for connecting a WT to the grid. The data given in the certification sheets are used by the utilities to calculate grid connection costs according to the electrical performance of the WT, to determine the grid capacity required and to examine the influence of the WT on the network power quality. The costs for grid connection strongly depends on the grid capacity used and thus on the power quality of the WT.

2 What is power quality?

The term power quality of a WT describes the electrical performance of the turbine's electricity generating system. It reflects the generation of grid interferences and thus the influence of a WT on the power and voltage quality of the grid. Grid interferences caused by WT's are mainly voltage distortions, which can be described in different time domains:

- harmonics above 50 Hz
- flicker 0.01 - 35 Hz
- voltage rise < 0.01 Hz
- transients random

In addition to the voltage distortions reactive power consumption and power factor have to be considered.

The grid interferences are induced by different distortion causes, which are mostly turbine specific. The influencing parameters are listed in table 1. Causes like average power production, turbulence intensity and wind shear are determined by meteorological and terrain conditions. The remaining causes are all due to the technical performance of the WT's, which are not only given by the characteristics of the electrical components like generators, transformers etc. but include also the aerodynamical and mechanical characteristics of rotor and drive train.

TABLE 1: Grid interferences caused by wind turbines.

Parameter	**Cause**
Voltage rise	average power production
Voltage fluctuations and flicker	switching operations, tower shadow effect, blade pitching error, yaw error, wind shear, fluctuations of wind speed, turbulence intensity
Harmonics	frequency inverter, thyristor controller, capacitors
Reactive power consumption	inductive components or generating systems

An example showing the extent of WT power fluctuations is depicted in figure 1. The 40 s-time-print shows active power output of a stall controlled 500 kW WT with induction generator and the line voltage. The WT is operating at an average power of approx. 10 - 15 % related to rated power. The peak-to-peak power fluctuation amounts to 20 % of rated power and to more than 100 % of average power. The frequency of the fluctuation of 1.5 Hz is corresponding to the blade passing frequency of the rotor and shows, that the fluctuation is due to the tower shadow effect.

The influence on the line voltage is low, below 1 % of the nominal value, which is due to the relatively high stiffness of the grid and low mean power production. In a situation of low grid short circuit power the voltage change will be distinctly higher. The example shows not the typical behaviour of a WT, most turbines have a better performance but single turbines will show an even worse performance.

This example shows how big power fluctuations are, compared to other, conventional power generation methods, which are not depending on stochastical input sources. The influence of a single WT on grid power quality will be smoothed by installation of large numbers of turbines connected to a utility grid. In

relation to the total installed power the short term power fluctuations will decrease with increasing number of turbines. But still the grid capacity has to be dimensioned according to the total occurring interferences. Investigations /1/ show, that a general rule of $1/\sqrt{n}$ can be assumed for flicker and harmonics, if the single interferences are statistical random. In case of mutual interferences, see /2/ and /3/, or resonance problems grid interferences may result, which are not smoothed by the number of WT's but may lead to severe distortions.

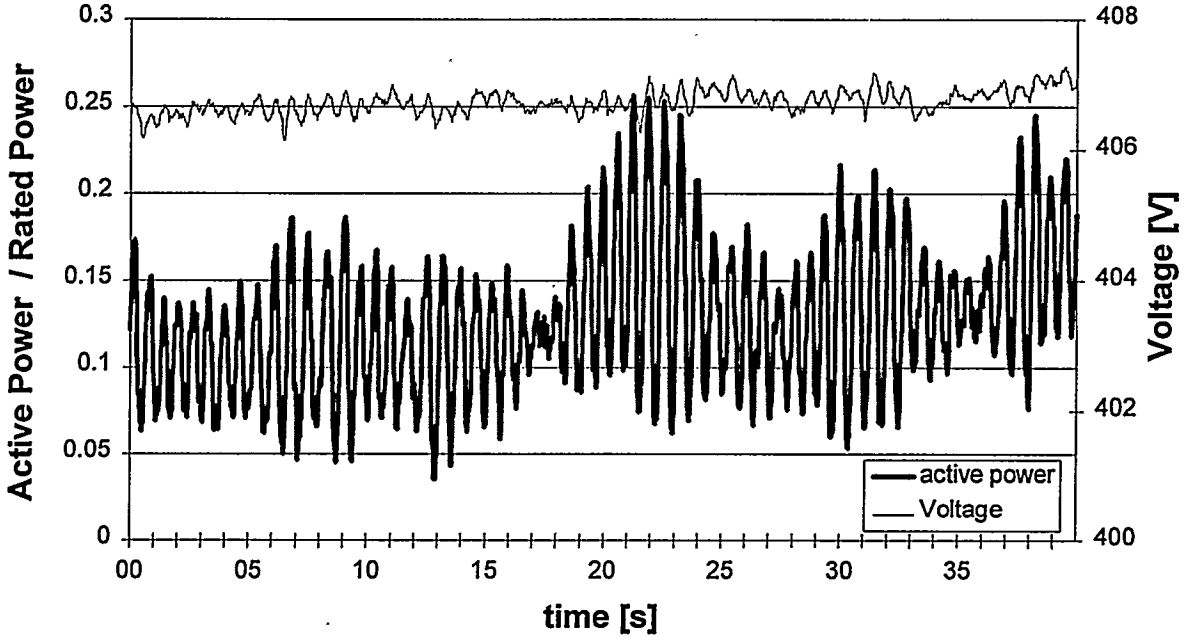

FIGURE 1: Power output fluctuations of a stall controlled 500 kW turbine with induction generator. Frequency of the fluctuation is 1.5 Hz, corresponding to the blade passing frequency.

3 Results from power quality measurements

As mentioned above, in Germany power quality measurements are required in case of connection of a WT to the utility grid. Due to missing European and international standards a guideline for power quality measurements on WT's was developed by a group of governmental authorities, utilities, manufacturers, research and measuring institutes, /4/. The initial guideline was established in 1993 and a number of changes and improvements resulting from the continuous application in daily measurement work went into the guideline. This guideline is acknowledged by the association of German electricity suppliers (VDEW) and is referred to in their recommendation for connection of local generation units to the medium voltage line /5/.

According to the guideline the power quality measurements are performed for harmonics, flicker and transients during normal and switching operations separately as well as for power factor, reactive power consumption and power peaks. An overview of measurements on more than 25 WT's performed by the measuring institutes Windtest Kaiser-Wilhelm-Koog, WindConsult and by the German Wind Energy-Institute will be given in the following.

All grid interferences produced by a WT are strongly influenced by the short circuit power and grid impedance angle of the connected network. To suppress the network influence on the evaluation results, all measurements are carried out current and/or power based. Especially flicker, which is defined as a voltage distortion, has to be determined by current and voltage measurements and the results have to be recalculated to standard grid impedance angles and short circuit powers, which are given in the German guideline.

The flicker coefficient c for different WT classes is depicted in fig. 2. The WT's are divided in three rated power classes and in two power control types, pitch and stall. A solid horizontal line is indicating the average flicker value for an entire class, while the bar shows the difference between the worst, maximum achieved value and the best, minimum achieved value in the class. Flicker is a measure for voltage fluctuations leading to a visual recognition of light flickering by the human eye. The flicker level should be below the recognition level of the human eye in 99 % of the time of a year. If it exceeds this level, the flicker has to be reduced either by grid reinforcement or constructural changes at the WT.

The flicker coefficient c determines the ratio between short circuit power and generator rated apparent power to acchieve a long term flicker level of $P_{LT} = 1$. With known short circuit power, generator rated power, grid impedance angle and generator phase angle the flicker level can be calculated from c for a given point of common coupling (see /5/). The flicker coefficient c gives a normalised, dimensionless measure of the flicker, independent from network situation and thus suitable to compare WT's of different size and type.

A large difference can be seen between maximum and minimum values of different classes as well as for values within one class. In the > 600 kW-class a difference of factor 9 can be recognised between the best and the worst WT. The average values are also showing a big variance ranging from a flicker coefficient c = 11 to c = 64. Generally a value below 20 is of no relevance for power quality considerations. A value up to 40 will be acceptable in many cases, where other power quality parameters are exceeding their minimum levels.

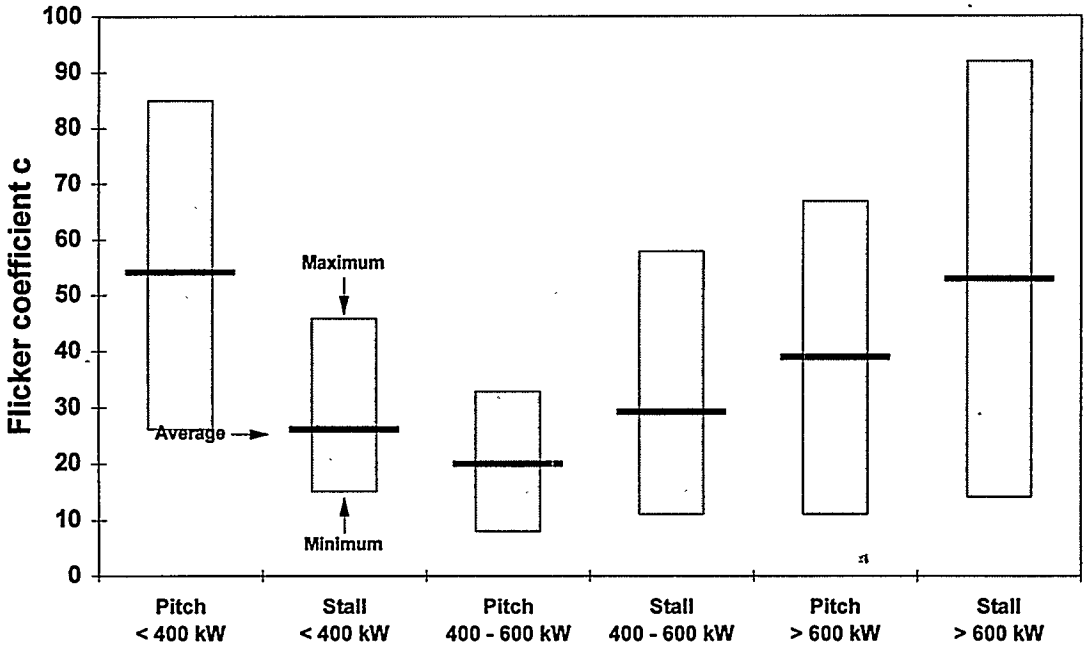

FIGURE 2: Flicker coefficient c for 6 WT classes

Figures 3 and 4 show in the same way the differences in power output fluctuation for instantaneous values (fig.3) and 10-minute average values (fig.4). The instantaneous power peaks give the relation between the maximum occurred power peak during the measurements, recorded with an averaging time of 8 to 16 line periods, related to the rated WT power output. The measured values are varying between a minimum of 1.04 for a 400 - 600 kW-class pitch controlled turbine to 2.2 for a stall controlled WT in the same power class. This means the latter WT produces a short term power of more than twice the rated power, while the first WT limits the maximum short term power output to nearly the rated value.

The average values, reflecting all WT's instead of just single turbines, show a smaller difference between the lowest value of 1.21 and the highest value of 1.59. The pitch machines in the classes 600 kW show in average a better performance than the stall machines, which is due to that fact, that the most investigated pitch WT's are full or partially speed variable.

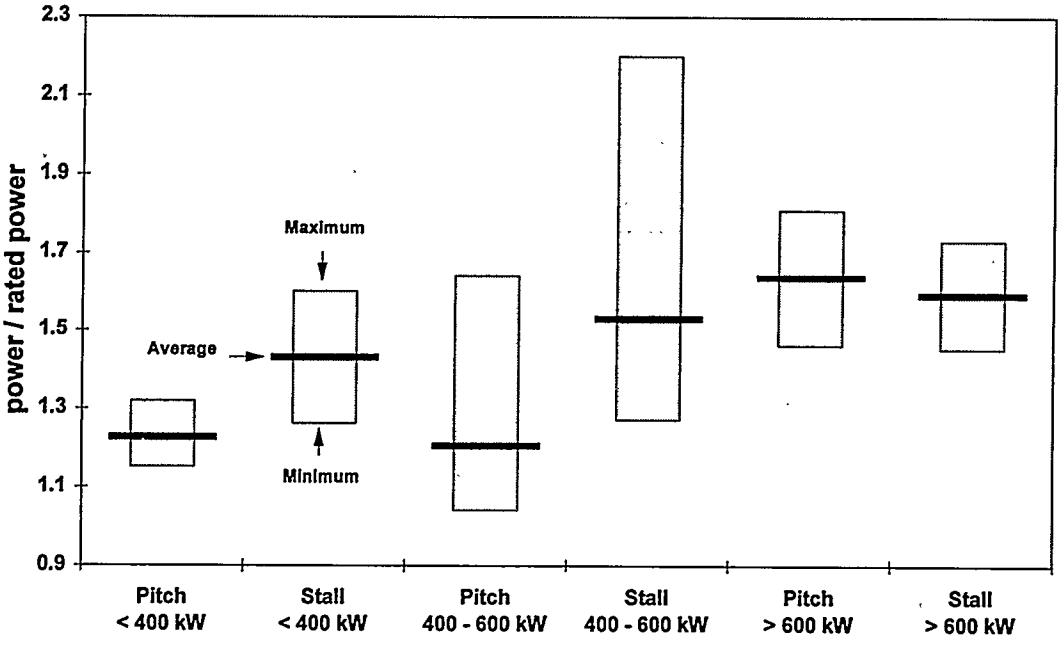

FIGURE 3: Instantaneous power peaks

The comparison of 10-minute average power output related to the rated power of the WT's in fig. 4 reflects a much smoother behaviour of the turbines. The 10-minute value is important for the grid capacity layout considering the thermal load of the transmission lines. The extreme values are varying between 1,0 for the best and 1.25 for the worst machine. This means, the thermal grid capacity has to be dimensioned 25 % larger in the worst case. If no other power quality parameters are of importance, the difference in grid connection costs would also be 25 % in this case.

The average values of the WT-classes are ranging from 1.01. to 1.15. The pitch controlled WT's in the range above 400 kW have very low 10-minute power peak values, which is typical for pitch machines, if the control is adjusted properly. The average values of the stall WT's are generally higher due to the typical exceeding of rated power by the stall control, which can be seen in the most stationary power performance characteristics of stall turbines. In the 400 - 600 kW-class the 10-minute peak of the average stall WT lies 13 % above that one of the average pitch WT.

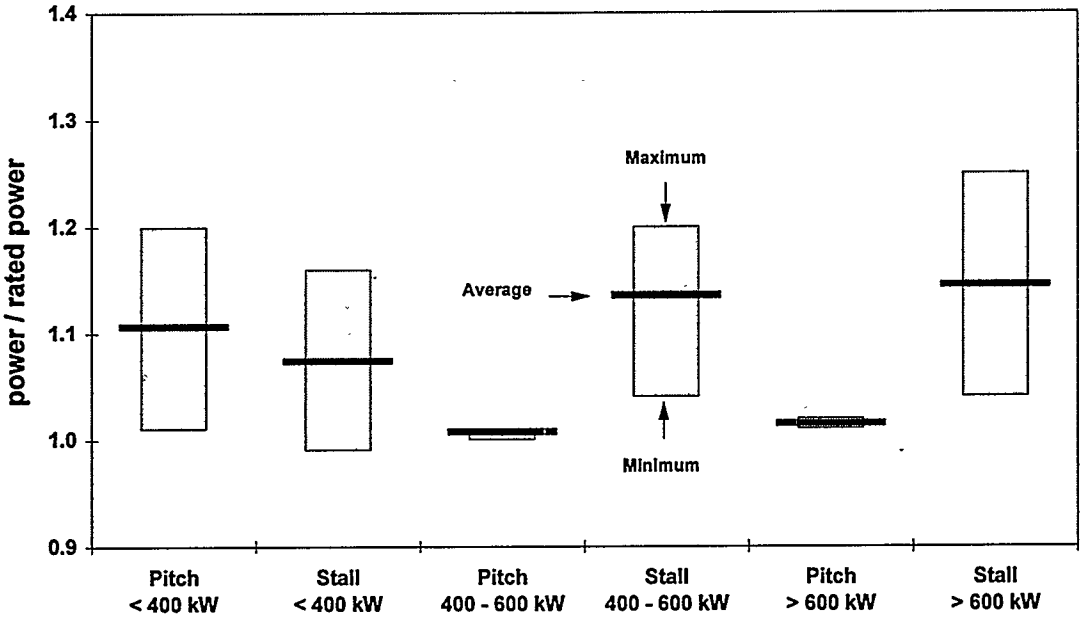

FIGURE 4: 10-minute-average power peaks

The relation between the maximum occurring current to the rated current is defined as the k-factor. The highest k-factors typically occur during switching operations and are caused by inrush currents. The maximum current is an important parameter in dimensioning the electrical equipment like transformers, switches, fuses etc..

Figure 5 shows the variations of the k-factor for different WT classes. The absolute minimum is 1.04 while the maximum of 4.6 is more than four times higher. The class mean values vary between 1.1 and 2.4. In general pitch controlled WT's show lower inrush currents than the stall turbines, which is due to the better active control characteristics of the pitch machines. The gradient of rotational speed at the moment when the WT reaches the synchronising speed can be rather steep for stall turbines. Pitch turbines can be controlled towards a very slow increase of rotational speed.

It can be stated in general, that the k-factor of WT's should not exceed a value of 2. The mean values of the stall turbines are distorted by only a few WT's with rather high k-factors. The most turbines already have a k-factor below 2. The limitation of the inrush current is a matter of the design of the soft start controller.

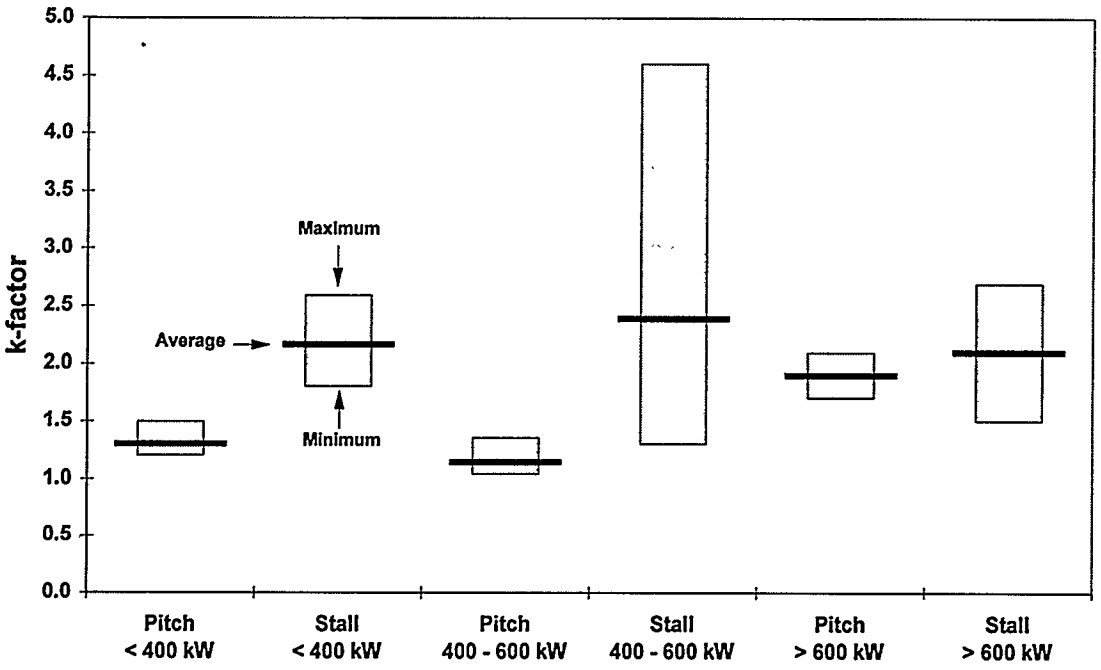

FIGURE 5: k-factor, relation between maximum occurring current and rated current, for 6 WT classes.

4 Summary

The measurement overview shows that power quality mainly not depends on the converter type or size. Good or poor power quality can not be assigned to specific WT classes and in several classes a wide span of performance can be recognised.

To a large extent high power quality is a matter of construction and control design. Aerodynamical and mechanical characteristics of rotor and drive train have a big influence on the electrical power output performance. Stall or pitch controlled turbines both can show either good or bad power quality. It can be seen from the single measurements, that only the pitch controlled WT's with partial or full variable speed not differ much from each other, these turbines are all lying in the range of good power quality measures.

The broad band of power quality measurement results show a span of factor 2 in performance for a large number of WT's and a factor of 3 or 4 for only a few turbines. In case of grid connection a performance difference of factor 2 means also that the grid capacity required varies by a factor 2 and thus the costs for grid connection may also be doubled, if the poorer machine is chosen.

In Germany the grid connection costs depend very much on the local network situation and on the already installed wind energy capacity. In areas with high wind energy penetration in the local networks the grid connection costs are ranging up to 20 % of the total turbine installation costs. Due to this big influence of electrical performance on the economic situation of wind energy projects, the WT's of high power quality will have better chances in future wind energy installations in Germany. And looking towards growing interests in wind energy installations in other countries, where the grid infrastructure may be comparatively weak, power quality will also become an important factor in other parts of the world.

5 References

[1] G.J. Gerdes, F. Santjer, J. Berding, R. Klosse
Reduction of grid interferences in wind farms
European Union Wind Energy Conference, Göteborg, Sweden, May 1996

[2] G. Gerdes, F. Santjer
Power quality of wind turbines and their interaction with the grid
European Wind Energy Association Conference EWEC '94, Thessaloniki, Griechenland, October 1994

[3] G. Gerdes, F. Santjer
Grid Interference and Mutual Interaction af Wind Turbine Generators and Wind Farms
American Wind Energy Association Windpower'95 Conference, Washington, March 1995

[4] Richtlinie zur Bewertung der elektrischen Eigenschaften einer WKA hinsichtlich der Netzanbindung. May 1996;
Hrsg.: Deutsches Windenergieinstitut GmbH, Wilhelmshaven; WINDTEST Kaiser-Wilhelm-Koog GmbH, Kaiser-Wilhelm-Koog; WINDconsult GmbH, Sievershagen

[5] Technische Richtlinie: Parallelbetrieb von Eigenerzeugungsanlage mit dem Mittelspannungsnetz des Elektrizitätsversorgungsunternehmens (EVU).
1. Ausgabe 1994, Hrsg.: VDEW e.V.; VWEW-Verlag, Frankfurt

Dual-Speed Wind Turbine Generation

E. Muljadi
C.P. Butterfield
National Wind Technology Center
National Renewable Energy Laboratory
1617 Cole Blvd.
Golden, Colorado 80401

D. Handman
Flowind Corp.
990 A Street, Suite 300
San Rafael, CA 94901

Abstract

Induction generator has been used since the early development of utility-scale wind turbine generation. An induction generator is the generator of choice because of its ruggedness and low cost. With an induction generator, the operating speed of the wind turbine is limited to a narrow range (almost constant speed). Dual-speed operation can be accomplished by using an induction generator with two different sets of winding configurations or by using a dual output drive train to drive two induction generators with two different rated speeds.

With single-speed operation, the wind turbine operates at different power coefficients (Cp) as the wind speed varies. Operation at maximum Cp can occur only at a single wind speed. However, if the wind speed varies across a wider range, the operating Cp will vary significantly. Dual-speed operation has the advantage of enabling the wind turbine to operate at near maximum Cp over a wider range of wind speeds. Thus, annual energy production can be increased. The dual-speed mode may generate less energy than a variable-speed mode; nevertheless, it offers an alternative which captures more energy than single-speed operation.

In this paper, dual-speed operation of a wind turbine is investigated. Annual energy production is compared between single-speed and dual-speed operation. One type of control algorithm for dual-speed operation is proposed. Some results from a dynamic simulation will be presented to show how the control algorithm works as the wind turbine is exposed to varying wind speeds.

I. Introduction

Utility-size wind turbines have been developed for many years [1]. The reliability of wind turbine generators has improved dramatically. More attention is directed to improve energy capture, load alleviation, and other characteristics that will bring down the cost of energy. Many avenues have been explored and considered such as the development of variable-speed wind turbines [2-5] and some variable-speed systems use direct drives to eliminate the operation and maintenance and the losses of the gearbox even in small scale applications [6-8].

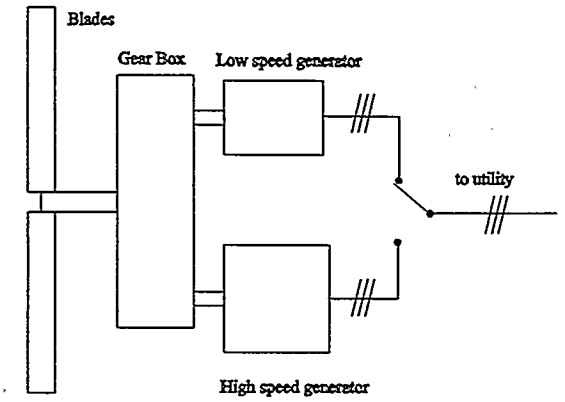

Figure 1. The physical diagram of a dual-speed wind turbine generation

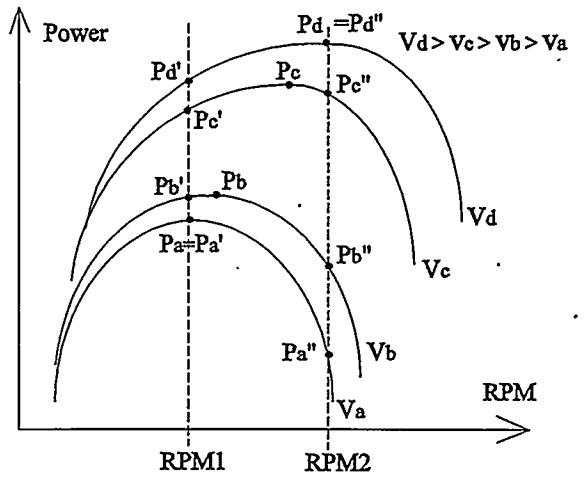

Figure 2. Power versus RPM for dual-speed operation

The system under consideration is shown in Figure 1. The wind turbine is connected to two induction generators via a gearbox. The smaller generator (generator 1) has a slower synchronous speed and the larger generator (generator 2) has a higher synchronous speed. Dual-speed operation can also be implemented by using an induction generator with two sets of windings; each winding has a different number of poles [9]. Using two speed systems instead of single-speed generation has several advantages. In the starting mode, for direct on-line start, the smaller induction motor (higher leakage inductances and resistances) is used to start the wind turbine, thus the inrush current will be lower. The efficiency of an induction generator is normally designed to have an optimum efficiency near its rated power. Thus in the lower power region (lower rpm), the wind turbine can be operated with a smaller generator and it is operated until it reaches its rated power. At low power output, the efficiency can be improved by using the smaller generator.

This paper is divided into 5 sections. In section II, the background of dual-speed operation will be discussed. In section III, the control algorithm will be presented and in section IV the energy calculation will be explored (detailed information regarding energy calculation can be found in reference [10]). Finally, the conclusion will be discussed in section V.

II. Dual-Speed Operation

In a fixed-frequency operation, a wind turbine starts generating power when the rpm reaches a certain rotor speed. An induction generator starts to generate power when the rpm is higher than synchronous speed. The synchronous speed can be computed as:

$$\text{Synchronous rpm} = 120 * \text{frequency} / \text{poles}. \quad (1)$$

Thus for a constant frequency operation, the more poles the generator has, the lower the synchronous rpm. It can be expected that the higher the synchronous rpm, the higher the wind speed will be before the generator starts generating. Figure 3 shows the power generated by the wind turbine for different rotor speeds (high-speed shaft rpm). For an induction generator, the rotor rpm varies with the slip. The slip is normally very small (<5%). Thus practically, the rotor speed in this paper is considered to be constant.

In Figure 2, the output power of a wind turbine for different wind speeds are shown as a function of rpm. The peak power operating points for different wind speeds are given as Pa, Pb, Pc, and Pd. Suppose that the wind turbine is operated only at RPM2, in the higher wind speed region (Vc and Vd), the wind turbine may operate close to its peak Cp (Pc" and Pd"); thus the difference from maximum power generated is small. However, in the lower wind speed region (Va and Vb), operation at RPM2 of the wind turbine will generate a much lower power than maximum power at maximum Cp. Similarly, if the wind turbine is operated only at RPM1, it will be optimized for lower wind speed regions and the operation in the higher wind speed region will be inefficient.

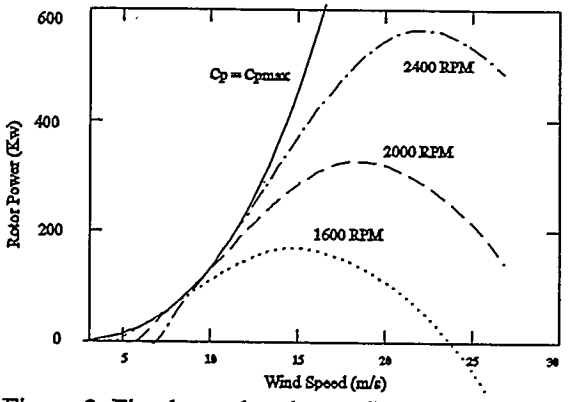

Figure 3. Fixed speed and max Cp operation of a wind turbine

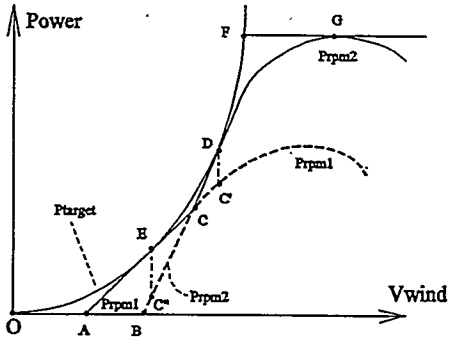

Figure 4. Power versus wind speed for dual-speed operation

From the Cp characteristic, the power versus wind speed can be drawn for different rpm. It can be expected that at higher rpm settings, peak power will occur at a higher wind speed. The maximum power that can be generated by the wind turbine operating at fixed speed does not correspond to the Cpmax. At the rotor speed settings, the system starts generating at higher wind speed (i.e., at 1600 rpm, the system starts generating below 5 m/sec while at 2400 rpm it starts generating at about 7 m/sec). A fixed speed turbine operates at maximum Cp only at one particular wind speed. Operation at other wind speeds is not at maximum Cp.

Dual-speed generation can be accomplished by using a single generator with a two winding arrangement (generator with dual pole configuration 4/6 or 6/8 poles). It can also be implemented by using two different generators (i.e., one generator has four poles and the other one has six poles). The dual-speed operation of a wind turbine generator has the advantage of capturing more energy compared to single-speed operation.

III. Control Algorithm of the System

The operation of a wind turbine at two different speeds is described by Figure 4. The system can be started by operating the induction machine at lower rpm to start the wind turbine. As the rotor speed reaches the (lower) synchronous speed, the wind turbine starts generating and continues to generate until another set point is reached. For example, we may specify a preset power (Pchosen) as the set point. Once the Pchosen is reached, and the wind continues to increase for ΔT seconds, the wind turbine should be transferred to the higher rpm mode, rpm2. During the transition, the rotor is accelerated by the wind. In the acceleration mode (from rpm1 to rpm2), there is no electrical connection to the utility, thus the energy from the wind is converted entirely to kinetic energy to increase the rotor speed.

At low wind speeds, the generator is started by motoring the lower speed motor. Unless any kind of soft start is in place, the start-up is a direct on-line start which will draw current from the utility. Fortunately, with a

smaller induction motor to start, the current drawn from the utility will not be as large as the larger induction motor. When the rotor speed reaches the rpm1, the wind turbine starts generating at rotor speed rpm1 (with a variation of a few percent of slip). The generated power increases until it reaches a chosen power (Pchosen) setting. The operation can be determined from the following simple logic:

```
if (power < Pchosen) then
  use rpm1
else if (power > Pchosen) then
  use rpm2
end if
```

where

power	= measured power	
rpm1	= lower rotor speed (smaller generator)	(along A E C .....)
rpm2	= higher rotor speed (larger generator)	(along C D G .....)
ptarget1	= $0.5\ \rho\ C_{ptarget}$ Area $(Radius/TSRtarget)^3\ \omega_{m1}^3$	(point E)
ptarget2	= $0.5\ \rho\ C_{ptarget}$ Area $(Radius/TSRtarget)^3\ \omega_{m2}^3$	(point D)

ptarget1<pchosen < ptarget2

The Pchosen is the set point at which the transfer from rpm1 to rpm2 should be initiated. This power should be chosen between point C' to C" as shown in Figure 4. As shown in Figure 4, the best possible power choice would be point C. At this point the power that can be generated has the maximum gain with respect to power generated by single-speed operation. The difference in power generation between variable-speed (VS) and single-speed rpm2 is area OBDFG. The difference in power generation between dual-speed (DS) generation and single-speed-rpm2 is area ABC and will be called ΔP.

With this option, the generator must be wound to operate at two different speed settings (for example, the generator might be wound to operate at switchable poles such as six and eight). Another option is to operate the wind turbine with two generators of different pole number, such that the lower-speed generator is sized to Pchosen, and the higher-speed generator is sized to take the whole power. For a four pole and a six pole generator, the size of the smaller generator (six poles) can be estimated with a cube relationship, about 8/27 (about 30%) of the size of the larger generator.

The transfer can also be implemented by sensing the rotor slip. When the generated power reaches Pchosen and the wind speed keeps increasing after some ΔT, the wind turbine operation must be transferred to another setting, i.e., operation in high speed rpm (rpm2). Unlike variable-speed operation, the dual-speed operation will have a transient operation during the transition from rpm1 to rpm2. During the transfer of operation of the wind turbine from rpm1 to rpm2, the low-speed generation must be deactivated, and thus the generated power will go to zero. As the wind speed increases, the energy from the wind accelerates the rotor speed and the energy from the wind is fully converted into kinetic energy and stored in the inertia of the rotor. When the rotor speed reaches rpm2, the generator is reconnected again with new synchronous speed at rpm2. Thus the transfer at point C is not instantaneous. We could expect that there are transient phenomena in the wind turbine during this transition.

To illustrate the implementation of dual-speed wind turbine generation, Figure 5 and Figure 6 are given to represent a simulation of the system. In Figure 5, the wind speed input is shown. The wind speed used is ten-minute data that has an average of 6 m/s with a rough wind condition. In Figure 6, the rotor speed is shown to follow the wind speed variation, in the low wind speed region the system operates with rpm1 and in the higher

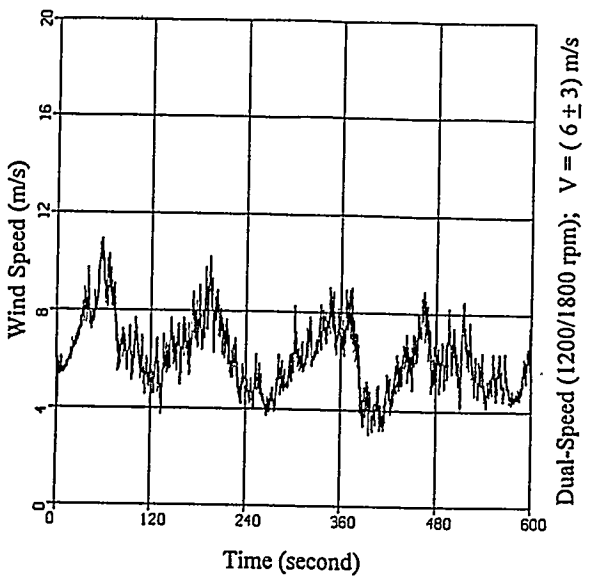

Figure 5. Typical wind speed for rough condition 6 m/s average

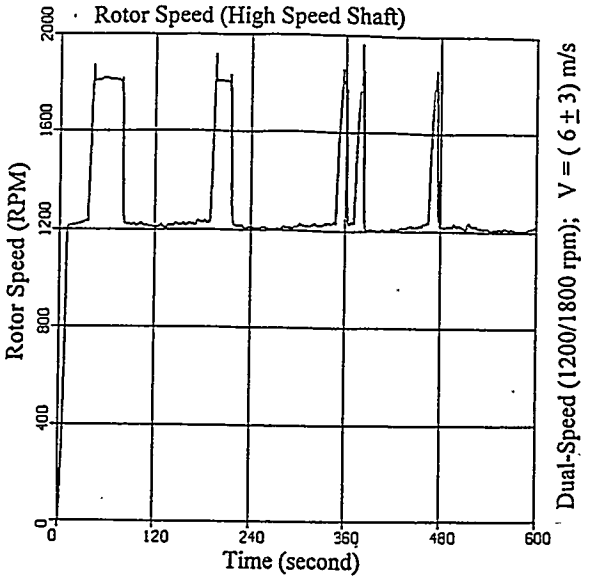

Figure 6. Rotor speed variation as the wind speed changes

wind speed region the system operates with rpm2. When the wind speed increases, the power generated increases until it reaches the power limit which can be detected by power sensor or slip sensor. The transfer from generator 1 to generator 2 can happen if there is enough wind to accelerate the wind turbine from rpm1 to rpm2. During the transfer, both generators are off-line. The system is in an idle condition for a preset idle-time. If during that time the wind speed decreases, the rotor speed will not increase to rpm2, the system will reconnect the wind turbine to generator 1. On the other hand, if there is enough energy in the wind to bring the rotor speed to rpm2 within the preset idle-time, the system will be connected to generator 2.

When generator 2 is operated, and the wind speed decreases, the system will be transferred back to generator 1. The transfer from generator 2 to generator 1 happens by switching from generator 2 to generator 1, thus there

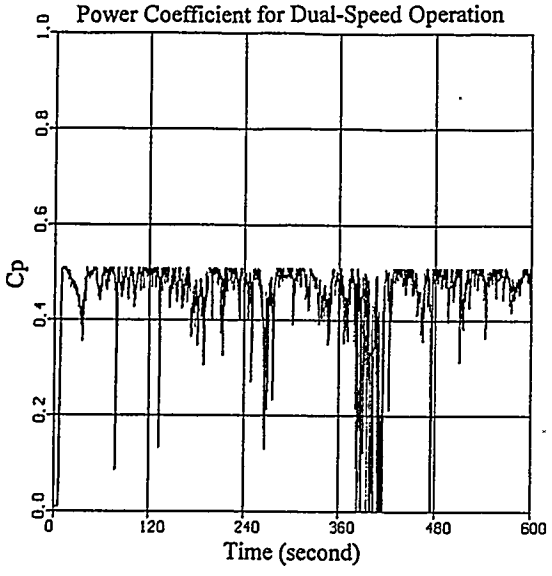

Figure 7. Power coefficient, Cp, for dual-speed operation.

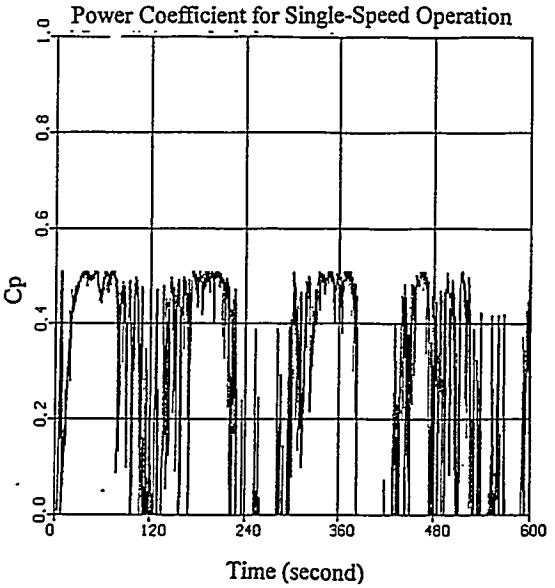

Figure 8. Power coefficient for single-speed operation.

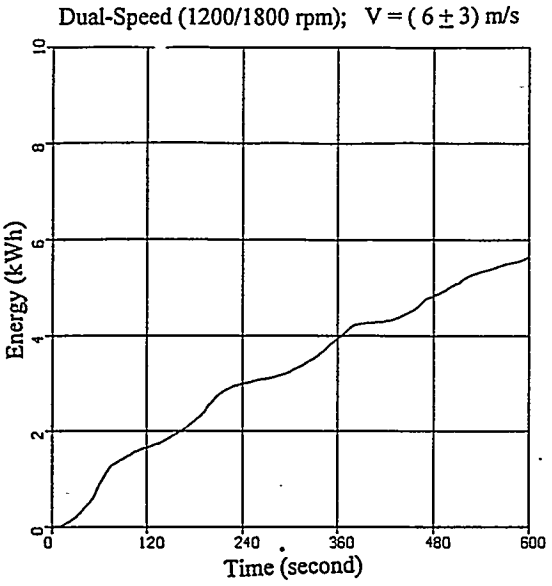

Figure 9. Energy generated for dual-speed operation

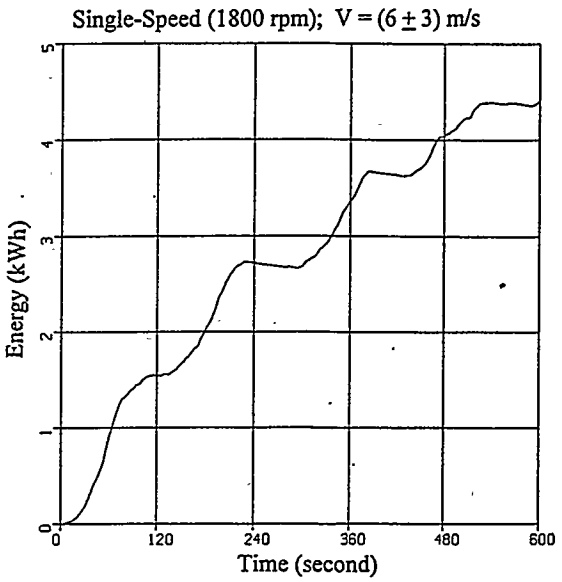

Figure 10. Energy generated for single-speed operation

is no idle time during the transfer from generator 2 to generator 1. Thus generator 1 is operated in the braking mode to change the rotor speed from rpm2 to rpm1. To limit the number of speed transitions, a more sophisticated algorithm must be used. The algorithm must be designed to maximize energy while minimizing the number of times the wind turbine changes its speed.

IV. Energy Production

The energy production can be illustrated by showing the characteristics of the wind turbine in dual-speed mode using the wind speed input presented in Figure 5. In Figure 7, the power coefficient Cp of dual-speed operation is shown. The power coefficient varies as the wind speed varies and the rotor rpm follows the trends of the wind speed in two discrete values. As a comparison, a wind turbine with generator 2 only is shown in Figure 8 to illustrate single-speed (rpm2) wind turbine operation. As can be expected, the operating Cp for a single-speed system in general is lower than the Cp for a dual-speed system.

The energy collected by the two different systems is shown in Figure 9 and Figure 10. In Figure 9, the dual-speed energy captured during the 10-minute simulation is shown. Note that this is the total energy generated by both generators. The energy generated by a single-speed wind turbine system (generator 2) is shown in Figure 10. It can be seen that there is a significant difference between dual-speed operation and single-speed operation.

The annual energy production (AEP) can be computed by employing a Rayleigh Distribution at a specific site, for example at a 5.8 m/s site. The AEP is computed for different wind turbine systems. In Figure 11 and Figure 12, annual energy is computed from steady-state analysis. Energy can be computed by multiplying the power generated at each wind speed by the density function at a particular wind site and then integrating the result and multiplying by the number of hours per year to get annual energy.

The annual energy distribution generated for different wind speeds is given in Figure 11. From Figure 11, it can easily be seen that dual-speed operation has a significant gain in the lower wind speed region for the site of 5.8 m/sec annual wind speed average. Annual energy generated for different wind speed averages can be illustrated in Figure 12. It can be seen that the AEP for dual-speed operation is higher than the AEP of a single-

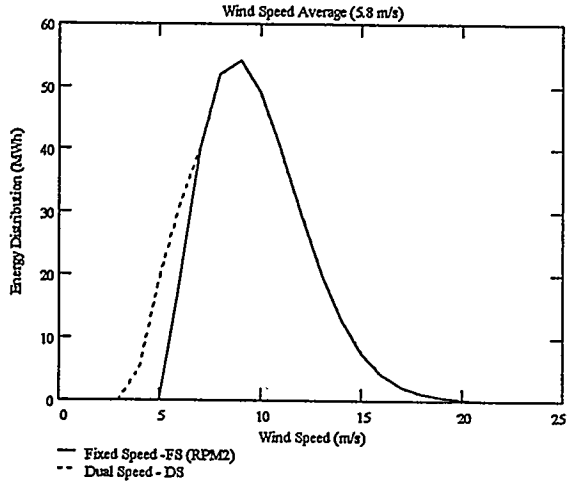

Figure 11. Annual energy distribution at different wind speeds for annual wind speed average of 5.8 m/sec

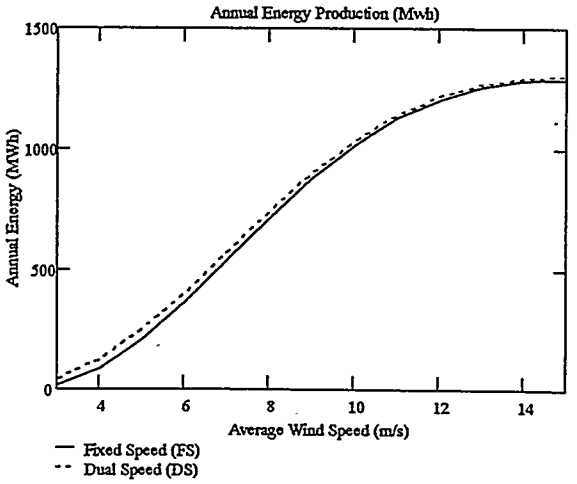

Figure 12. Annual energy production for different annual wind speed averages

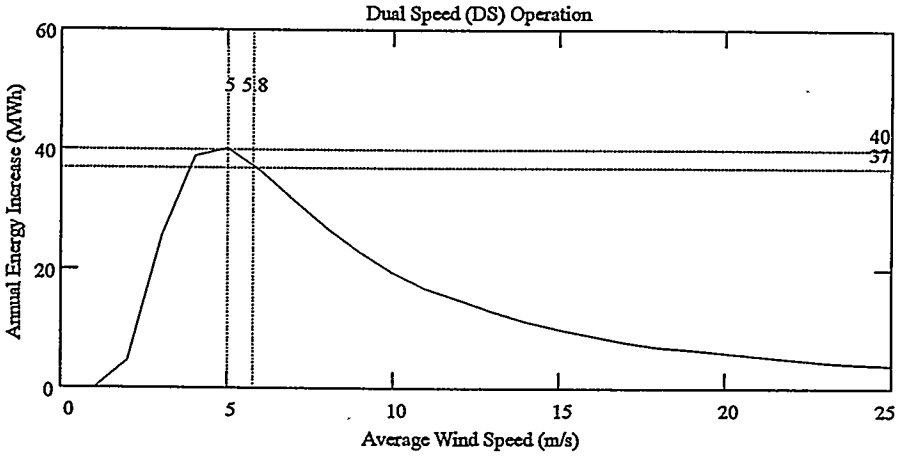

Figure 13. Annual energy increase for dual-speed system

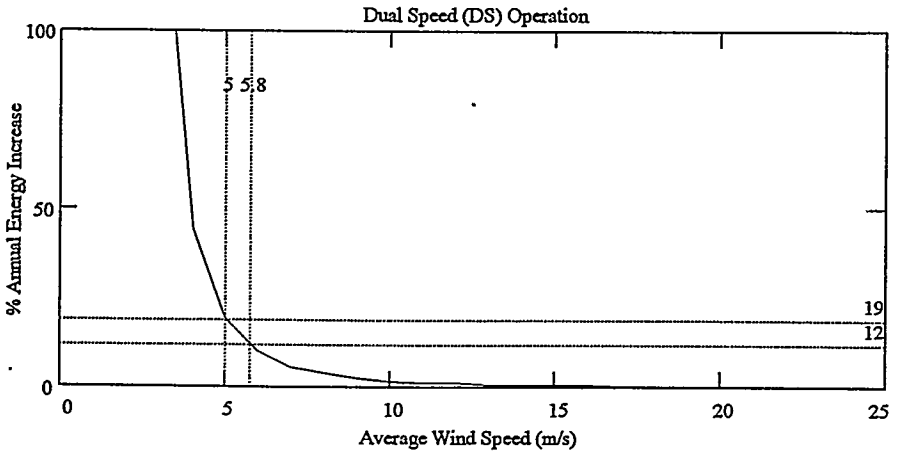

Figure 14. Percent annual energy increase for dual-speed system

speed/fixed-speed system especially in the lower annual-wind-speed average, the contribution of generator 1 (lower rpm) is very significant. The annual energy increase can be computed and the percent change can be plotted. In Figure 13 and Figure 14, the annual energy increases (actual and percentage) are shown. The baseline for annual energy is single-speed operation at rpm2. The annual energy increase is computed as shown in Equation 2 and Equation 3:

$$AEI = (\text{Annual Energy New System} - \text{Annual Energy RPM2}) \quad (2)$$

$$\%AEI = (AEI / \text{Annual Energy RPM2}) \times 100\% \quad (3)$$

Two points are marked on each curve; one corresponds to 5.8 m/s sites and the other corresponds to maximum points.

V. Conclusion

Dual-speed operation has advantages over single-speed operation in terms of the energy capture, higher efficiency in the low power output, and lower starting transients. The initial investment is slightly higher than for single-speed operation; however, it is lower than for variable-speed operation. Induction generation is a mature technology and is very rugged. Thus operation and maintenance is easier and cheaper. The control strategy used in this simulation can be improved and modified for different wind sites.

Acknowledgements

The authors wish to thank Neil Kelley of the National Wind Technology Center (NWTC), for providing the wind data for this simulation. Thanks also to V. Gevorgian of the NWTC and D. Zinger of the Northern Illinois University, DeKalb, for valuable technical discussions. They also wish to thank Kristin Tromly for her timely editing.

References

[1] D.F. Warne, "Generation of Electricity from the Wind," Proc. IEE, Vol. 124 no. 11R, November 1977, IEE Reviews.

[2] E. Muljadi, C.P. Butterfield, P.Migliore, "Variable Speed Operation of Generators with Rotor-Speed Feedback in Wind Power Applications," ASME Conference, Houston, Texas, Jan.28-Feb.2, 1996.

[3] L. Xu, Y.F. Tang, "A Novel Wind Power Generating System Using Field Orientation Controlled Doubly Excited Brushless Reluctance Machine", IEEE Industry Application Society Annual Meeting, Houston, TX, October 1992.

[4] D.S. Zinger, A. Miller, E. Muljadi, C.P.Butterfield, M.C. Robinson, "Laboratory Implementation of Variable Speed Wind Turbine Generation," Windpower 96, American Wind Energy Association Conference, Denver, CO, June 23-26, 1996.

[5] B.T. Meritt, *An Asynchronous AC/DC/AC Link for Wind Power Application*, Ph. D. Thesis at the University of Wisconsin, Madison 1977.

[6] E. Muljadi, S. Drouilhet, R. Holz, and V. Gevorgian, "Analysis of Wind Power for Battery Charging," ASME Conference, Houston, Texas, Jan. 28-Feb. 2, 1996.

[7] A.A. Fardoun, E.F. Fuchs and P.W. Carlin, "A Variable Speed, Direct Drive Transmission Wind Power

Plant," American Wind Energy Association Conference, San Fransisco, CA 1993
[8] David A. Torrey and M. Hassanin, "The Design of Low Speed Variable Reluctance Generators," Conference Record of the 1995 IEEE Industry Applications Society, Orlando, Florida, Oct. 8-12, 1995.
[9] Z.M. Salameh and L.F. Kazda, "A Design Method for Matching of a Double Output Induction Generator (DOIG) with the Performance of Characteristics of Wind Turbines," IEEE Power Engineering Society, Midwest Power Symposium at the University of Wisconsin, Madison, Nov. 22-23, 1982.
[10] Gary L. Johnson, *Wind Energy Systems*, Gary L. Johnson, Manhattan, KS, 1994, 2nd Edition.

Appendix: General data of the wind turbine generation systems.

The wind turbine parameter:

Blade diameter = 26 m

Rated power = 285 kW

Highest rpm = 57 rpm (low speed shaft)

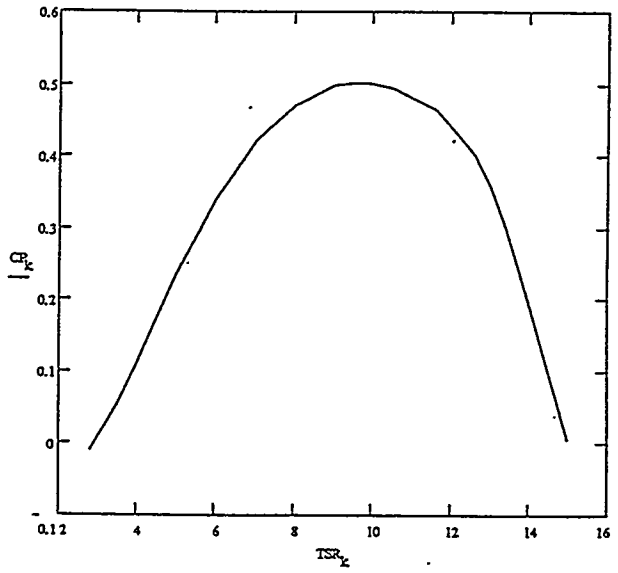

Cp_TSR of the wind turbine

TECHNICAL AND COMMERCIAL ASPECTS OF THE CONNECTION OF WIND TURBINES TO ELECTRICITY SUPPLY NETWORKS IN EUROPE

Paul Gardner
Garrad Hassan & Partners Ltd
Unit 2.04, Kelvin Campus,
West of Scotland Science Park,
Glasgow G20 0SP,
UK

email: gardner@glasgow.garradhassan.co.uk

ABSTRACT

This paper reviews some technical and commercial issues now topical for wind energy developments in Europe. The technical issues are important because of the weak nature of the existing electricity systems in rural or upland areas. Several commercial issues are considered which may improve the economics of wind energy as market incentives are gradually withdrawn.

1. TECHNICAL ISSUES

In Europe, wind turbine installations vary from single machines around 50 to 500 kW rating, to large wind farms. The former may be connected to the public low-voltage (< 1000 V) or medium-voltage (< 35 kV) networks. The latter are connected to networks in the range 10 to 220 kV.

Particularly in the less densely populated parts of Europe, the existing electrical networks in the areas of good wind resource are sparse and 'weak' (in the sense of low short-circuit powers). Whenever permitted by the utility, it is advantageous to connect the proposed wind farm to the closest feasible point on the existing network, because:

- capital cost is reduced;
- construction time is reduced;
- problems with obtaining permission for the new overhead line may be reduced.

Clearly the ultimate limit on the generation that can be connected to a particular point on an existing network is the thermal rating of plant such as transformers and lines (though it should be noted that wind farm developers may well be prepared to accept curtailment of output on a few occasions per year when the network is operating near its limits, for example due to planned outages or high ambient temperatures). However, on weak networks, other factors can often limit the installed generation capacity, and these are discussed below.

1.1 Steady-state voltage

The real and reactive power due to the wind farm will affect voltages on the network as it flows through the network impedances. For weaker networks (low short-circuit power or 'fault level', i.e. high system impedances), the effects are greater. Fault levels can be less than 70 MVA at 33 kV. The effect will (except in unusual circumstances) be greatest at the 'point of common coupling' (pcc), the point on the network where other consumers are (or could be) connected. Usually the pcc is also the boundary between the utility and the wind farm.

The ratio of the inductive component of the equivalent system impedance to the resistive component (X/R ratio) is also important. This ratio is often found to be around 2, which fortunately tends to minimise the effects on network voltage.

A simple analysis requires only the equivalent network impedance as seen from the pcc. The voltage variation (from zero to full wind farm output) can be compared with any limit specified by the utility. The disadvantages of this simple approach are:

- the utility is likely only to specify the acceptable voltage range due to all loads and generation, not just the wind farm;
- the simple analysis takes no account of the effect of customer loads on the network;
- the effects of automatic network voltage control (by transformer tap-changers or switched capacitor banks) are ignored.

Therefore if the simple analysis or the network configuration give cause for concern, a more detailed study using power-system analysis software is required.

Typical accepted ranges are:

- Spain: $\pm$ 7%
- UK: < 132 kV $\pm$ 6%, ≥ 132 kV $\pm$ 10%
- EN 50160 : $\pm$ 10%

EN 50160 [2] is a recent European Standard produced as part of the move towards a 'single market' in electricity trading within Europe. Its purpose is to define common limits for the 'quality' of power (more correctly, the quality of voltage) experienced by a consumer. Currently the standard has no legal force: if and when the single market for electricity is established, it is likely that existing national or utility requirements will have to be superseded by this standard or its successors.

If steady-state voltage is a problem for a particular development, the solutions are:

- connection to a stronger part of the network, in particular a transformer station fed from a higher-voltage network;
- choosing variable-speed turbines which permit optimum control of power factor;
- for fixed-speed machines, choosing the level of power-factor correction capacitors to minimise the effect on voltage, rather than to minimise reactive power charges. This may require additional switched capacitor banks.

1.2 Voltage step changes

This issue is closely related to steady-state voltage, and the same calculation methods are used. Utilities specify limits on the maximum instantaneous step change in voltage that a customer (load or generation) can cause. Typical values are:

- Spain: 5% for embedded generation with induction generators, or 2% for wind turbines
- UK: 3%
- Germany: 2%
- EN 50160: 5% frequently, 10% infrequently

There is plenty of scope for discussion on the cases to be considered. An argument that has been accepted by utilities in the UK is as follows:

- turbine start-up is not an issue, because starts are unlikely to be coincident (some manufacturers can ensure this through their wind farm supervisory control system), and because soft-start units are fitted to reduce inrush currents;
- simultaneous shut down of all turbines in a wind farm will only occur in fault conditions (due to faults on the network, or if network voltage or frequency go outside the acceptable range), and therefore does not need to be considered.

Therefore the case to be considered is where one or (for a large wind farm) possibly two wind turbines shut down simultaneously from full power, due to high winds.

Usually, a wind farm which meets the limits on steady-state voltage range is likely also to meet the voltage step change limits, unless it consists of only a small number of turbines.

Note however that when calculating the steady-state voltage range, the effect of automatic network voltage control (transformer tap-changing, or switching of capacitor banks) can be taken into consideration, as the 'steady-state' implies these have had time to operate. For step voltage changes, this cannot be assumed. Therefore for situations where the impedance of a transformer with automatic tap-changer control forms a significant part of the total equivalent system impedance, step voltage changes may assume greater importance.

1.3 Flicker

Wind turbines result in fluctuations in real and reactive power, and hence voltage, in the utility network. Voltage fluctuations can cause customer annoyance through the phenomenon of 'flicker' [3,4]. For any given sequence of voltage fluctuations, it is possible to determine the flicker severity, a measure of the likelihood of customer annoyance. Both short term (10 minute measurement period, P_{ST}) and long term (120 minute measurement period, P_{LT}) measures of flicker severity are recognised.

Typical accepted limits for the flicker produced by an installation are:

- UK: $P_{ST} \leq 0.5$ [5]
- Germany: $P_{ST} \leq 0.46$ [6]

In Spain, the same objective is aimed for by a requirement that the total generator rating is no more than 5% of the short-circuit power of the network at the point of connection. This requirement can be much more restrictive than limits on flicker.

Concerns about flicker are forcing manufacturers towards variable-speed or similar solutions: see, for example, the Vestas Optislip system [7].

Work is currently underway within IEC to develop a standard which allows the flicker caused on a particular network by a group of wind turbines to be predicted. Measurements of flicker on a single turbine of the same type are required. Turbulence intensity needs to be taken into account, but the principal effect is the 'smoothing' of power fluctuations from multiple turbines. Theory and experience both indicate that flicker increases with the square root of the number of wind turbines. Because of this, flicker is usually only an issue for small numbers of wind turbines, and in that respect is similar to the issue of voltage step changes.

1.4 Harmonics

Harmonics are generated by soft-start units, but this is generally ignored because of the short duration and the low probability of coincident starts.

For variable-speed turbines, where harmonic currents are generated continuously, filters are often necessary. Filter design can be site-specific, and filters are bulky and add cost, and so there is a move towards wind turbines with pulse-width modulated (PWM) control of the network-side converter, using power transistors, despite the increased cost.

National and utility regulations all set limits on harmonic distortion, but use different methods of calculation. Some set absolute current limits, others set limits proportional to the short-circuit level. This makes comparison difficult.

On weak rural networks, there can be significant existing levels of harmonics, from domestic consumers.

1.5 Voltage unbalance

On weak networks in rural areas, the majority of customer loads are single-phase. If these are not correctly shared out between the phases, voltage unbalance will result. Induction machines connected to such networks will act to reduce the unbalance [8], but in the process will be subject to overheating. It is known that in some cases voltage unbalance has been above the specified levels, and significant wind turbine downtime has occurred. If this problem is anticipated in advance for a particular site, it can be avoided by suitable specification of the electrical equipment.

2. COMMERCIAL ISSUES

In European countries, wind turbines exist because of 'market stimulation' or similar measures. This support is expected to reduce to zero as the technology improves. It is therefore necessary to examine all avenues to improve wind energy economics. There are three main options, which are discussed below. The issue of the value of pollution avoided is not covered here. The emphasis in this section is on the situation in the UK, as in some respects liberalisation of the electricity market is far advanced.

It should be noted that a 'premium price' for wind-generated electricity, or capital subsidies, are not necessarily the only benefits enjoyed by wind energy developers under current support arrangements. The existence of a guaranteed purchaser, contracting in advance to buy all the wind farm output, no matter how variable, at an agreed price for a period of many years, is a major benefit not available to other generators.

2.1 Benefits to the network

Embedded generation (generation of any kind which is connected to a distribution network with significant local load) can confer benefits on that network, for which payment may be possible. Some of these potential benefits are discussed here.

2.1.1 Losses

Overall losses in a large electricity system can be in the range 5 to 10%, with the higher values appropriate to networks where power has to be transported long distances. Most of the losses occur at the lower voltage (distribution) levels. Embedded generation can clearly reduce these losses if its output is similar to the demand in the area. But equally, for example in upland areas with low load density, a large development can increase overall losses. Accurate calculation of the benefit is site-specific. In the UK, loss adjustment factors can be calculated, and applied to the output of the wind farm.

2.1.2 Capacity credit

The value of intermittent generation in replacing the need for conventional generation capacity has been extensively studied, but usually for large systems with dispersed generation. A similar analysis for embedded generation [3] has to take into account the lower reliability of the distribution system. The particular problem for intermittent generation is that the correlation of output and demand is crucial in determining the capacity credit value, but clearly (for wind) this can vary significantly from year to year. In the UK, a mechanism exists which seems to deal with this issue satisfactorily. The electricity distribution companies are charged on their demand during the three half-hours of highest total system demand in any year (the 'triad periods'). Embedded generation running during triad periods clearly reduces the distribution company's demand, and creates a 'triad benefit', a percentage of which will be paid to the generator. For two National Windpower wind farms [9], the benefit is of the order of 5% of annual energy output. The procedure is clear and unambiguous, and satisfactorily credits wind for the good correlation (in northern Europe) between wind speed and demand, on an annual timescale. The disadvantage is that the generator takes the risk of the coincidence of peak demand with high wind farm output: although this can be treated statistically, there may be significant interannual variations.

2.1.3 Use of system charges

These are charges levied in the UK to cover the costs for provision of the distribution system plant. Recent judgements by the regulatory authority are establishing a principle that, if the effect of the wind farm will always be to reduce the currents flowing through the network (i.e. to reduce the required distribution plant capacity), some of these charges should not be applied.

2.1.4 Other issues

There are some other areas where embedded wind turbines could in theory provide benefits to the network. These are:

- Deferral of system reinforcement
- Network voltage control
- Harmonic filtering (specifically for variable-speed wind turbines)

However, it is difficult to argue that there is any real benefit from an intermittent generation source. The potential worth, in financial terms, is not likely to be significant, and there is currently no mechanism by which a developer could be paid for these benefits.

2.2 On-site generation

If an industrial consumer generates on-site, the value of the electricity generated is the value of the electricity purchases displaced. This is significantly more than the price that would be obtained by direct sale to an electricity distribution company. With seasonal-time-of-day (STOD) tariffs, typical energy charges in the UK are 6 to 8 c/kWh for the weekday non-peak period, compared to the 'pool price' of around 3 to 4 c/kWh. Other benefits are:

- industrial organisations should be able to get finance more cheaply than a wind energy developer, as the risks are lower;

- there may be fewer problems with planning permission, as the development can be seen by local people as directly benefitting a local employer, rather than a remote faceless wind development company;
- the effect on visual appearance may not be as contentious as on a rural site.

Clearly, wind speeds will not be as high as upland or rural sites, and it is not known if the number of industrial sites with good daily and annual demand profiles in reasonably windy areas adds up to a significant market.

A study to investigate the economics of such arrangements is currently in progress, funded by the UK Department of Trade and Industry. Initial findings are:

- On-site generation under STOD tariffs is more attractive than under Maximum Demand tariffs, as the presence of intermittent generation may not significantly reduce the site maximum demand in any month;
- most industrial customers now purchase their electricity through negotiated contracts, rather than under published tariffs. Although details of contracts are confidential, it appears that the cost of energy under such contracts is of the order of 4.5 c/kWh, so the potential savings are reduced.

It may also be the case that, because the load factor of a customer with on-site intermittent generation will undoubtedly become worse, the fixed elements of contracts with an electricity supply company will become more expensive.

2.3 Green pricing

The aim here is to allow customers to pay more for electricity from non-polluting sources if they wish. In principle, this is currently possible in the UK for customers with a demand over 100 kW (a limit due to be removed altogether in 1998). In practice, it is hard to do because the flow of energy from supplier to customers has to balance over each half-hour: if it doesn't, 'top-up' units have to be purchased or 'spill' units sold. The costs of doing this are high. The situation is worst for highly variable generation sources (such as wind) and customers with poor load factors (such as domestic consumers). Industrial consumers are more attractive, but ecological and moral arguments may carry less weight than with domestic consumers.

The green power market currently becoming established in Sweden is more hopeful because:

- consumer pressures are forcing industries to buy green electricity;
- the sites for wind generation are closer to the load centres than the hydro stations that form a major part of Swedish generation, thus saving losses;
- possibly because of the large hydro component, the energy purchased from non-polluting sources only needs to be balanced with that supplied to consumers over the long term.

This latter point represents a significant economic benefit for green power supply companies.

3 CONCLUSIONS

Wind energy development in the rural and upland areas of Europe has to consider the particular technical issues of connection to weak electricity networks. These issues also apply elsewhere in the world, where very large wind farms with dedicated connections to transmission systems are not possible because of land usage, population density or market structure. The commercial factors for the sale of wind-generated electricity emerging within Europe may also be applicable elsewhere in the world, particularly where electricity markets are being deregulated.

Acknowledgements

Most of the technical issues discussed above were studied in detail in a collaborative project [3], and Garrad Hassan are pleased to acknowledge the contributions made by the collaborators, in particular UMIST (Manchester, UK) and IIT (Madrid, Spain).

References

1. DEFU (Research Association of Danish Electricity Utilities)
DEFU 77.

2. EN 50160
Voltage characteristics of electricity supplied by public distribution systems.

3. Gardner P, Jenkins N, Allan RN, Saad-Saoud Z, Castro F, Roman J, Rodriguez M.
Network connection of large wind turbines
Proc. 17th British Wind Energy Association Conference, July 1995, pp161 - 166
Mechanical Engineering Publications, ISBN 0 85298 961 X.

4. Mirra C (Ed)
Connection of fluctuating loads
Intenational Union for Electroheat, July 1988.

5. Electricity Association
Engineering Recommendation P28
Planning limits for voltage fluctuations caused by industrial, commercial and domestic equipment in the United Kingdom.

6. Vereinigung Deutscher Elektrizitätswerke (VDEW)
Technische Richtlinie
Parallelbetrieb von Eigenerzeugungsanlagen mit dem Mittelspannungsnetz des Elektrizitätsversorgungsunternehmens
1st Edition, 1994. ISBN 3-8022-0408-5

7. Pedersen TK.
Semi-variable speed operation - a compromise?
Proc. 17th British Wind Energy Association Conference, July 1995, pp249 - 260
Mechanical Engineering Publications, ISBN 0 85298 961 X.

8. Craig LM, Jenkins N
Impact of a medium sized wind turbine on a weak rural network
Proc. 17th British Wind Energy Association Conference, July 1995, pp333 - 338
Mechanical Engineering Publications, ISBN 0 85298 961 X.

9. Warren JG, Hannah P, Hoskin RE, Lindley D, Musgrove PJ.
Performance of wind farms in complex terrain
Proc. 17th British Wind Energy Association Conference, July 1995, pp17 - 23
Mechanical Engineering Publications, ISBN 0 85298 961 X.

Utility-Scale Variable-Speed Wind Turbines Using A Doubly-Fed Generator With A Soft-Switching Power Converter

Claus H. Weigand, Dr. Hian K. Lauw, Dallas A. Marckx
Electronic Power Conditioning, Inc.
1895 NW 9th Street, Suite A
Corvallis, OR 97330-2144
USA

1. Introduction

Utility-scale wind turbines operating at variable RPM have been studied for a considerable period of time. Whereas the increase in energy output originally has been considered the principal benefit of variable-speed operation, the ability to tightly control the drive-train torque by electronic means is becoming another very important cost factor, especially for turbine ratings above 500 kilowatts. This cost benefit becomes even more significant as optimum turbine ratings today are approaching (and surpassing) 1 Megawatt. Having identified the benefits for the turbine, the designer is confronted with the task of finding the most cost-effective variable-speed generation system which allows him to make use of the benefits, yet does not introduce well-known electrical problems associated with state-of-the-art variable-speed generator controls, such as drastically reduced generator winding life, excessive harmonics on the utility, and poor utility power factor. This paper will indicate that for high-power (> 500 kW), utility-scale wind turbines a doubly-fed generator system in connection with a soft-switching resonant power converter is the least-cost variable-speed generation system offering all of the desired benefits, yet avoids the introduction of the potential electrical problems stated above.

2. Benefits of State-of-the-Art Variable-Speed Generation Systems

Before the decision is being made to incorporate a variable-speed generation system in a new turbine design or retrofit an existing design, a rigorous cost-benefit analysis is mandatory. The reason for that is that any variable-speed option may add to the capital cost of the generator. The added cost should be outweighed over the lifetime of the turbine by

- additional energy production,
- reduced capital cost of the gearbox due to accurate drive-train torque-control,
- reduced wear and tear on other drive-train components,
- the ability to meet acoustical noise limits without costly blade-designs, and
- financial incentives by the (utility) customer to supply reactive power on demand.

The cost-benefit analysis must also consider the elimination of certain electrical switchgear which fixed-speed turbines require (such as soft-starters and power-factor correction equipment).

The following items must be factored into the calculation of additional energy production:

- Net energy output of the blades due to $C_{P,max}$-operation
- Efficiency of the gearbox (gearbox-efficiencies during variable-speed operation need to be investigated, no data available so far)
- Efficiency of the electrical system (see Figure 3 below)

3. Description of the Doubly-Fed Generation System

The doubly-fed generation system uses a three-phase wound-rotor generator. The rotor windings are connected to a power electronic converter via slip-rings. The stator windings are directly connected to the grid (Figure 1). The instantaneous mechanical RPM is determined by the frequency of the currents which the power electronic converter injects into the rotor windings. The power-factor on the generator stator is determined by the amplitude of the rotor currents. The doubly-fed system is capable of operating at leading and lagging stator power-factor, and is capable of generating power at any RPM. A microprocessor-based digital control system has been developed to give the generator system its desired dynamic behavior, i.e., allow accurate generator torque control, maintain the required utility power-factor, and operate the turbine at $C_{P,max}$. This includes automatic generator synchronization at cut-in, as well as delayed turbine shut-down at cut-out wind-speed in order to avoid "pendeling" of the turbine.

The main difference between the doubly-fed generation system and a standard variable-speed power conditioning system (induction generator with fully rated power conditioner, see Figure 2) is that only a fraction of the total power generated flows from the rotor windings through the power-electronic converter to the utility grid. That means the power-electronic converter has to be rated only a fraction of the total system power, which has very favorable implications on the overall system cost. For the same reason the overall electrical system efficiency is higher compared to the power conditioning approach. It must be kept in mind that a variable-speed generation system with a poor electrical efficiency can almost zero out the additional energy gained from $C_{P,max}$ operation of the turbine.

The doubly-fed generation system must not be confused with a slip-recovery system which also incorporates a wound-rotor generator. The slip-recovery system uses a phase-controlled rectifier on the rotor and inverts the rotor power onto the utility grid. It always draws reactive power from the grid through the stator and can generate power only above synchronous RPM.

4. Power Electronic Converter Considerations

Irrespective of the variable-speed generation system topology under consideration, the power electronic converter used must meet the following electrical requirements:

(1) Capable of 4-quadrant operation (electrical power has to be able to flow from the generator to the grid, and vice versa)
(2) Have high power-conversion efficiency
(3) Fast dynamic response to control inputs in order to allow accurate generator torque control
(4) Must not cause early failure of the generator winding insulation due to the voltage waveforms applied to the generator
(5) Must allow more than 150 ft. of cable between the generator and the converter
(6) Must meet power quality specifications such as IEEE 519, IEC 555 (Europe), or similar on the utility grid side. Individual customer(s) may have more stringent specific requirements
(7) Capable to supply reactive power to the customer (utility) highly desirable. Penalties may apply if utility has to supply reactive power to the turbine.

State-of-the-art power converters, such as bidirectional pulse-width modulated inverters, have been used extensively for variable-speed generator controls. However, hardware filters were required in order to bring them into compliance with requirements (4), (5), and (6), which further increased the cost of the converter.

Bidirectional pulse-width modulated inverters (also known as "hard-switching" converters) are trading off modulation frequency, which directly determines the size and cost of the hardware filters, against power conversion efficiency. In fact, due to the switching losses in the semiconductors, there is an upper modulation frequency limit at which these converters are able to operate.

VARIABLE-SPEED GENERATION SYSTEM TOPOLOGIES

FIGURE 1

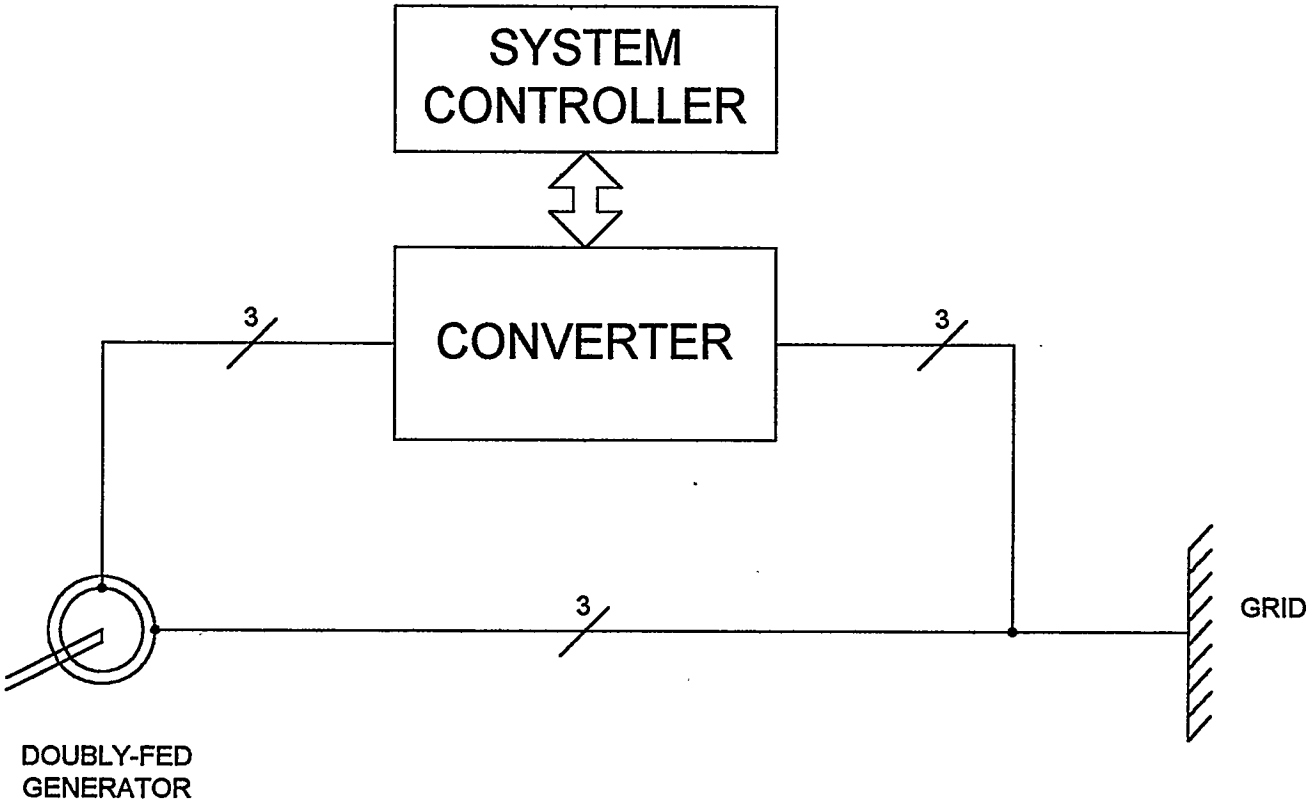

FIGURE 2

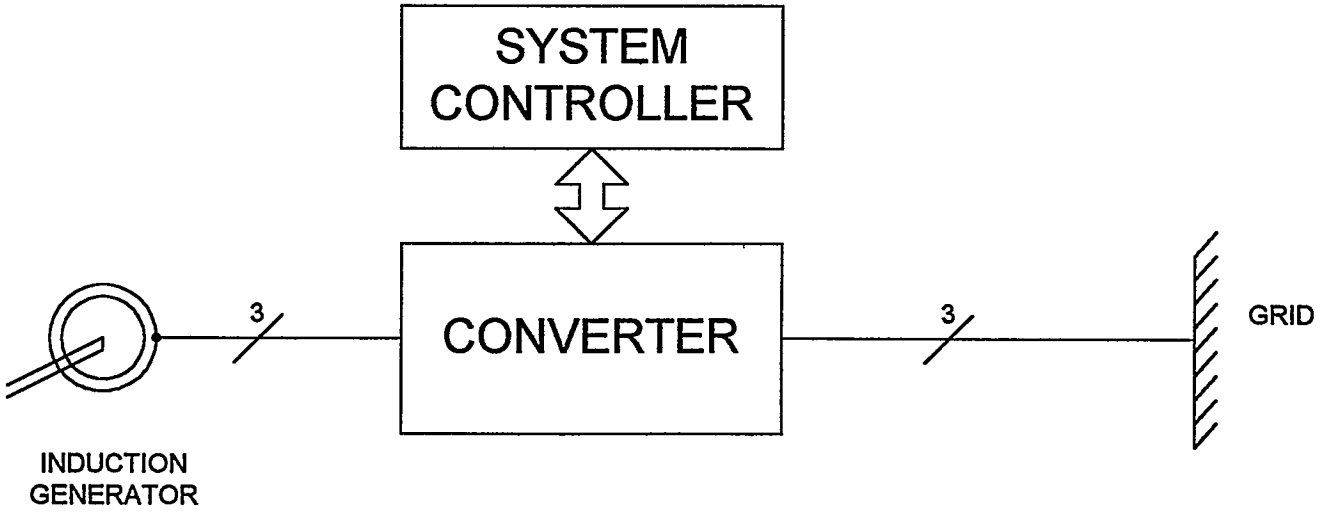

Two different resonant power converter topologies (series and parallel resonant converters) have emerged which allow an increase in modulation frequency of three to ten times compared to the standard pulse-width modulated inverter. High-frequency resonant circuits are being used to accomplish "soft-switching" operation of the semiconductor switches. This enhancement virtually eliminates all semiconductor switching losses, thus allowing operation at much higher modulation frequencies. The size and cost of the utility grid filters are considerably reduced. The electrical waveforms applied to the generator windings are benign and do not cause early winding insulation failure. Cable lengths between the generator and the converter are no longer critical.

Series resonant converters are supplying purely sinusoidal voltages (and, thus, currents) to the generator windings. Parallel resonant converters apply waveforms similar to pulse-width modulated inverters to the generator. However, the voltage rise and fall times are well within acceptable limits for the generator windings not to be prematurely damaged.

Engineering prototypes of high-power series and parallel resonant converters are now in the laboratory and field testing stage at rated power.

5. Variable-Speed Generation System Development Status

Under EPC's NREL contract (Innovative Subsystems), the power-electronic converter (series resonant type) and the variable-speed system controls were designed, assembled, and individually tested in EPC's laboratory. A 375 kW variable-speed wind turbine simulator was used for this purpose.

The microprocessor-based variable-speed generator control system has been tested separately on a 80 kW test turbine during fall and winter of 1995.

A second laboratory test was performed at the test-facility of the manufacturer of a 750 kW generator, in order to determine the overall system efficiency and power quality of this larger installation. Figure 3 shows the efficiency (= electrical output power to utility grid/mechanical shaft power) test results. Mechanical input power settings and RPM settings were taken from a cubic power-RPM characteristic. Output power quality was found to be in compliance with the harmonics limits of the IEEE 519-1992 standard.

FIGURE 3: VSGS ELECTRICAL EFFICIENCY

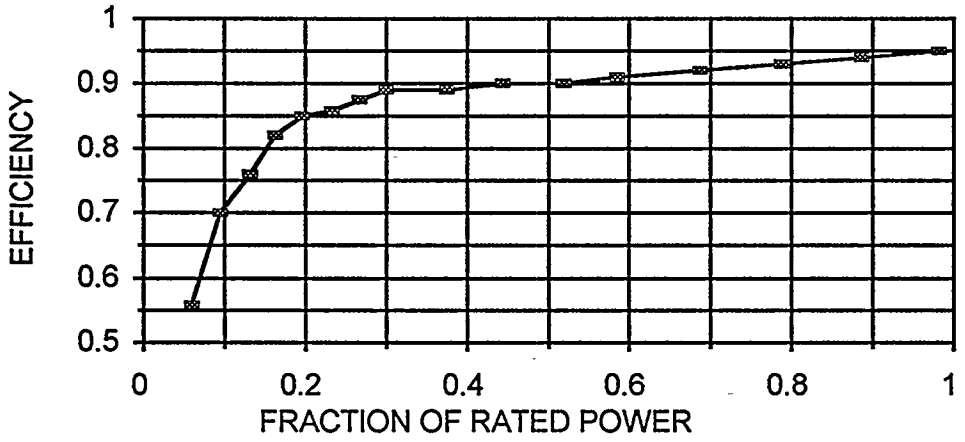

This larger system was installed recently on a prototype turbine in Tehachapi, CA. Even though all test results are preliminary and a substantial amount of testing is yet to be done, the following findings have been made so far:

- The turbine synchronizes reliably, even if started up in very high winds
- 3p output power oscillations which are a given for comparable 3-bladed fixed-speed turbines have been virtually eliminated

6. Variable-Speed Generation System Cost Estimations

The two major components required by any type of variable-speed generation system (doubly-fed or standard power conditioning system) are the generator and a power-electronic converter. Of these two the power-electronic converter cost is anywhere between 200% and 250% of the generator cost on the basis of installed kVA. Therefore, a variable-speed generation system topology requiring a power-electronic converter which is rated at a fraction of the turbine rating has a substantial cost advantage compared to a system requiring a fully rated converter.

Unlike the case for low-power systems (± 100 kilowatts) the doubly-fed generator is not substantially more expensive than a standard induction generator. The reason for this is that at power levels in excess of 500 kilowatts even a standard induction generator is a custom-made generator due to

- the low production volume,
- the specified features required for the wind turbine application (slip-behavior and high efficiency at partial load), and
- the large amount of labor involved in the manufacturing process.

The additional cost for a doubly-fed generator at this power level is in the magnitude of 15 to 20 percent. According to operating experience on existing prototype machines, the presence of brushes in the doubly-fed generator does not create a maintenance issue and, therefore, does not noticeably affect the O&M-cost.

The following is a sample cost calculation comparing a conventional fixed speed system (baseline) with a conventional variable-speed system and a doubly-fed variable-speed system. All cost-figures consider a substantial production-volume (at least 100 units/year).

Component Costs (550 kW sample system)	Topology		
	Fixed-Speed Baseline	Full Power Conversion	Doubly-Fed
Generator Cost	$21,000	$21,000	$24,100
Switchgear/Power Converter Equipment Cost	$7,500	$64,250	$23,000
Total System Cost	$28,500	$85,250	$47,100
Cost Relative to Baseline	1	2.99	1.65

Power Converter Cost Calculation:

- Full Power Conversion: Power Converter Cost = 550 kW * 1.15 * $100/kW + $1000 = $64,250
- Doubly-Fed: Power Converter Cost = 550 kW * 0.4 * $100/kW + $1000 = $23,000

Both variable-speed systems would allow precise torque-control on the drive-train and, therefore, may allow the use of a lower-cost gearbox. In addition, the implementation of a dynamic breaking algorithm may allow the downsizing of the mechanical brake. In that case, the generator controller would increase the generator torque for a brief period of time beyond the blade torque and reduce the RPM to the minimum generator operating RPM. At that point the mechanical brake would take over and bring the turbine to a complete stop. Since the sizing of the brake is related to the energy which it has to dissipate under worst-case conditions, and the brake-energy in turn is related to the square of the RPM, a reduction of RPM by means of the generator from, i.e., maximum to minimum operating RPM may result in a substantial amount of energy which the brake does not need to dissipate.

7. Conclusions

Even though the doubly-fed generator concept is by no means new, in conjunction with the most advanced power-electronic converters it emerges as the least-cost option for utility-scale variable-speed wind turbines at power-levels above 500 kW. The soft-switching resonant power-electronic converters which were briefly introduced are directly hardware-compatible with the generator and the utility-grid, requiring no or only minimal hardware filtering. A microprocessor-based digital system controller performs the overall system management and the high-speed dynamic generator control ensuring smooth generator torque. Therefore, the electrical system satisfies all the requirements imposed on it by a least-cost mechanical turbine design.

References

"Variable-Speed Wind System Design"; Dr. H. K. Lauw, C. H. Weigand, D. A. Marckx, Electronic Power Conditioning, Inc.; final report under contract # DE-AC79-93BP99893, prepared for U.S. Department of Energy, Bonneville Power Administration; October 1993

"Experimental Evaluation of a Variable-Speed, Doubly-Fed Wind-Power Generation System"; C. Brune, R. Spée, A. K. Wallace, Dept. of Electrical and Computer Engineering, Oregon State University; 1993 IEEE Industry Applications Society Annual Meeting

"A High-Efficient Variable Speed Wind-Power Generating System Using Doubly-Excited Brushless Reluctance Machine"; L. Xu, Y. Tang, Ohio State University; Windpower '93 Proceedings

APPLICATION OF BSTRAIN SOFTWARE FOR WIND TURBINE BLADE TESTING

Walter D. Musial
Melissa E. Clark
National Renewable Energy Laboratory
1617 Cole Blvd.
Golden, Colorado 80401

Toby Stensland
3112 South Independence Court
Lakewood, Colorado 80227

Abstract

The National Renewable Energy Laboratory (NREL) currently operates the largest structural testing facility in the United States dedicated to the testing of wind turbine blades. Recently, a completely new data acquisition system was developed to measure blade response and monitor test status. The system is based on a National Instruments (NI) software package, LabVIEW, and NI hardware components. The NREL custom program is called BSTRAIN (**B**lade **S**tructural **T**est **R**eal-time **A**cquisition **I**nterface **N**etwork) [1]. The objectives of the new software were to develop a robust, easy-to-use computer program that could automatically collect data from static and fatigue blade tests without missing any significant events or overloading the computer system with excess data. The program currently accepts inputs from up to 32 channels, but can be expanded to over 1000 channels. In order to reduce the large amount of data collected during long fatigue tests, several options for real-time data processing were developed including peak-valley series collection, peak-valley decimation, block decimation, and the option for continuous data recording of all data. Other features of BSTRAIN include automated blade stiffness checks, remote terminal access to blade test status, and automated VCR control for continuous test recording. Results from the tests conducted with the software have revealed areas for improvement including test accuracy, post-processing analysis, and further data reduction.

Introduction

For more than five years the National Wind Technology Center (NWTC) at NREL has operated a structural test facility for the testing of wind turbine blades. The first test bay was developed in 1990 when demand for blade testing was relatively low. Until then, laboratory testing of wind turbine blades was not commonly practiced in the United States. This was because it was considered adequate for most wind turbine designs to be proven through prototype field testing and trial and error production experience. Also, there were no other incentives, such as design or type certification, to require companies to test their blades. But perhaps the most significant reason was that the facilities required to test blades did not exist in the United States.

Demand for blade testing has risen sharply in recent years. More facilities with larger and more sophisticated capabilities are in demand due to several factors. First, the current generation of blade designers recognize the limitations of their design tools and the difficulty of implementing a design in production. They have a better understanding of the uncertainties associated with predicting extreme stochastic load events. Thus, the recent trend has been toward laboratory verification and component testing to simulate the entire life under accelerated loading. With this trend has come an increase in the number of blades tested.

The recent shift to international markets for wind energy has also added complexity and urgency to the blade testing issue. Turbine manufacturers wishing to export their turbines to various countries abroad are often required to certify their design in accordance with the established national standard for wind turbine certification. Frequently a blade test must satisfy both the designer, who is interested in verification of design criteria, and a particular code or design standard that may not have been part of the original design requirements. Generally, the influence of certification has mandated higher quality standards for testing and has increased the complexity of testing procedures, demanding more quantifiable results.

Finally, the size of wind turbine blades is increasing. During the past ten years the average blade length has more than doubled with corresponding weights increasing exponentially. These larger blades require higher actuator forces and greater displacements which both drive up the cost of the test equipment and increase the time required to perform a test.

Realizing that structural testing of wind turbine blades can be too expensive for most companies to do on-site, NREL has continued to expand its facilities to meet the growing demand. Presently, the NWTC structural testing laboratory includes two blade test labs. A new 34 meter (120 ft) bay with capabilities to test blades up to 30 meters (100 ft) long will soon be available. The NWTC laboratory has performed full scale structural tests on over forty wind turbine blades from six different turbine manufacturers. The testing capabilities include fatigue testing, static testing, and non-destructive evaluation using several techniques.

One component of the recent facility enhancements includes the development of a new data acquisition system. The primary challenge was to develop a system with the capabilities to sample the real-time data continuously and save only necessary data. For static testing this is fairly straightforward since the test is generally conducted over the span of a few hours. A fatigue test, however, can run for several months, and the amount of data passing through the signal conditioning would overload any system if they were all recorded and stored. The BSTRAIN software was developed as a solution to this problem. The software was designed to minimize the amount of data collected without missing any data that could be needed in evaluating the test.

System Architecture

The Blade Structural Testing Real-time Acquisition Interface Network (BSTRAIN) was developed for the NWTC structural testing laboratory. The development approach was to build a fully integrated data acquisition system using the latest hardware and software available. The new system addresses many problems previously limiting the test lab capabilities ranging from missed data to poor user interfaces. The current system specifications are listed in Table 1.

A schematic showing the NREL fatigue test facilities is shown in Figure 1. The facility uses a closed loop servo-hydraulic system to apply fatigue loading to wind turbine blades. Hydraulic actuators load the blade at a point along its span according to an operator defined displacement profile. The displacements are correlated during quasi-static tests to establish equivalent load levels. A typical fatigue test can last up to several months and several million load cycles. The static testing facilities are identical on the data acquisition side, but use an electric crane attached to a whiffle tree to apply distributed static loads across the length of the blade.

TABLE 1 - BSTRAIN SYSTEM SPECIFICATIONS

General Information

Number of Channels	32 (software limited)
Sampling Frequency	Fatigue -120Hz/channel
	Static - 5 Hz/channel

Signal Conditioning

Gain	1 - 500
Bridge Completion	provided in SCXI module
Bridge Excitation	3.3 Volts
SCXI Filtration	10 kHz
Shunt Calibration	Software programmed

A/D Board

Resolution	16 bit
Speed	100 kHz
Input Range	± 5 Volts

Data Storage

Hard Drive	1.2 Gb
Archive	CD ROM read only
	Erasable Optical Disc

Data Storage (cont.)

Data Files	Binary Data - 2 bytes/sample
	ASCII Header

BSTRAIN Software

General Features	Graphical User Interface
	Continuous Test Monitoring
	Real-time Display - Graphical and Numerical
Static Testing	Standard Deviation and Mean
Fatigue Testing	
	Real Time Peak/Valley Processing
	Real Time Decimation
	Remote Test Monitoring via Modem
	Continuous Loop VCR Control
	Automated Stiffness Checking
	Automatic Signal Zeroing
	Test Shut Down Triggers - 3 channels
	Automatic Operator Notification

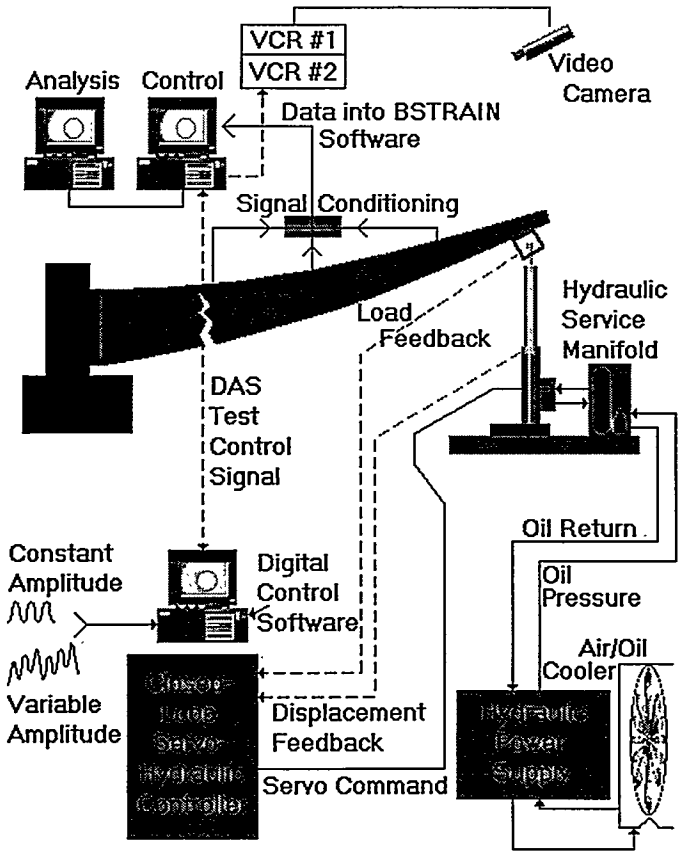

FIGURE I - SCHEMATIC OF NREL FATIGUE TESTING FACILITIES

Each testing laboratory contains a complete system consisting of signal conditioning, a plug-in data acquisition board, and two networked PC's, one for data collection (DAQ) and one for data analysis. The system operates on a NI hardware and software platform. Custom BSTRAIN software, written in LabVIEW, is run on the DAQ computer. Figure 2 shows the generic layout of the Signal Conditioning eXtension for Instrumentation (SCXI) based data acquisition system used. The BSTRAIN software was specifically designed to receive data in real-time during structural testing of wind turbine blades. Because static tests and fatigue tests differ considerably with respect to their duration and thus the quantity of data collected, the BSTRAIN program treats these tests separately.

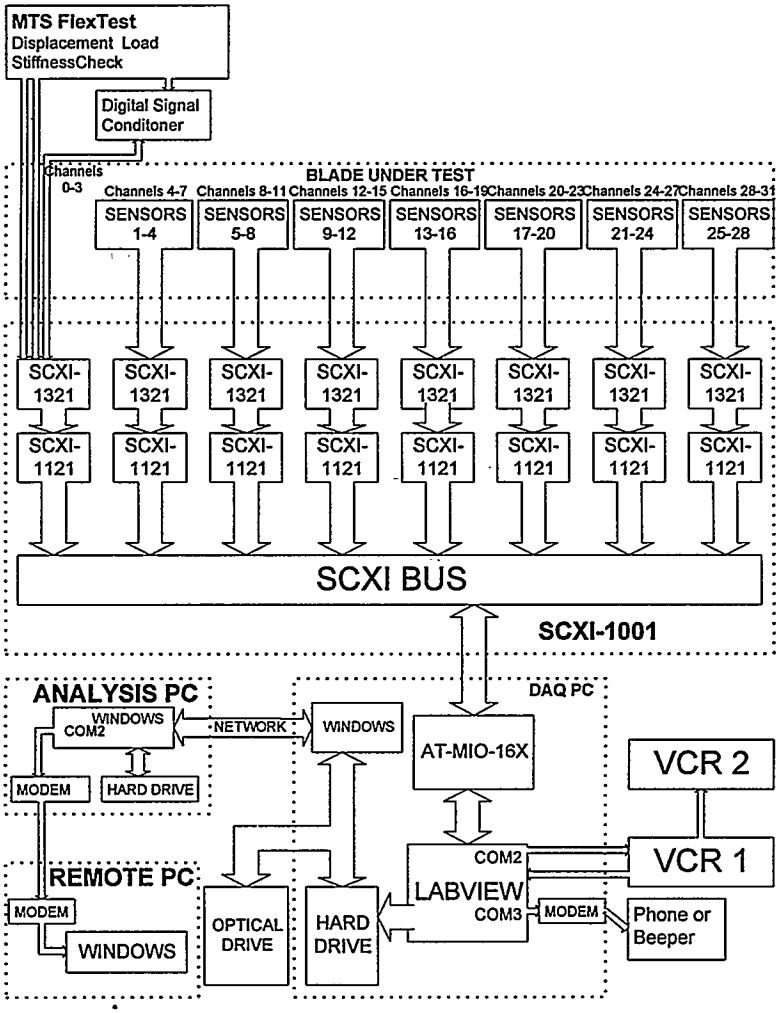

FIGURE 2 - SCHEMATIC OF DATA ACQUISITION SYSTEM

Static Testing

A static blade test usually is conducted to determine the blade's ability to withstand extreme loading. This is done by distributing concentrated point loads along the blade length in a manner which approximates either the blade's design load shape or the blade's design strength distribution. Typically, the loading is increased until a static failure is caused. The results give information on the ultimate strength of the blade, buckling sensitivity, and other likely failure modes. It is extremely important that data is taken continuously without gaps during a static test.

The BSTRAIN static test algorithm collects binary data continuously in real time at a user specified sample rate (typically 2 to 5 Hz) throughout the test. As many as 32 strain gage signals are scaled and shunt calibrated during the initial program set-up. The static load is applied in discrete steps during the test. Displacements are measured and photographs are taken at the plateaus. A time-series file from a typical static blade test is shown in Figure 3. The load measured at the top of a whiffle tree with a three-point distribution is plotted against time for the test duration. The plot shows the increasing blade load steps at regular intervals until failure occurs. Note that the test begins at a non-zero load due to the tare weight resulting from the test fixtures and the weight of the blade itself. The duration of maximum load for this test at the peak load was less than three seconds before failure occurred. It is known that the strength of Douglas Fir, for example, under constant load decreases significantly (8% per decade) with load duration [2]. Therefore, the minimum duration of the target test load should be specified for a static test to avoid ambiguous results.

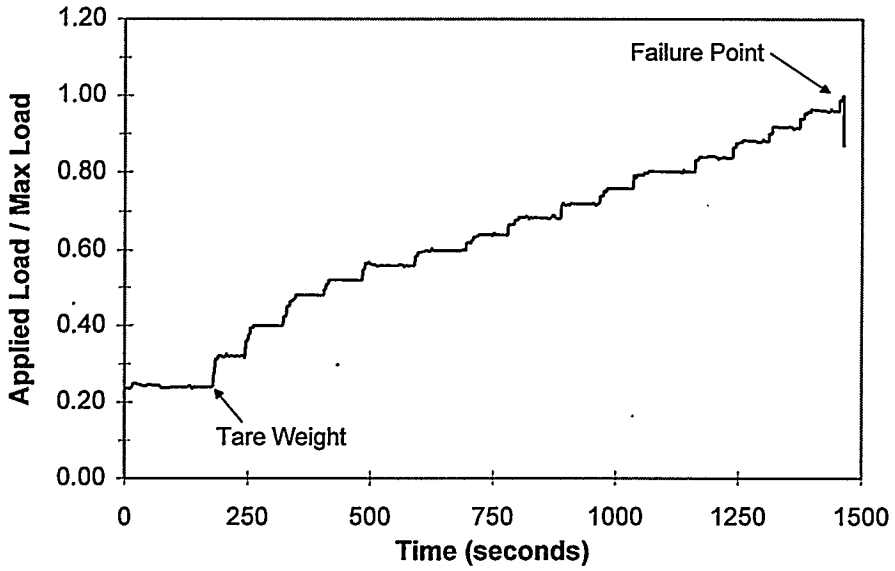

FIGURE 3 - STATIC TEST LOAD TIME HISTORY

In Figure 4, strain measurements are shown on a blade as a function of the normalized applied load during a static blade test. These strains were measured approximately 2.54 cm (1 inch) from the failure location on the compressive side using a rectangular strain gauge rosette for three measurement directions, 0° (longitudinal), 45°, and 90° (transverse). Note that the strain is linear with load at low load levels, but near failure the non-linearity of the strain increases dramatically. The 0° gage shows the greatest non-linearity and some obvious creep behavior at the higher load plateaus.

One useful feature in the BSTRAIN static program is the ability to monitor standard deviations of the measured signals during the test. The program averages each consecutive block of ten samples and computes the mean and standard deviation. Often this additional information provides advanced warning to the test operator of a failure about to occur. For the test data in Figure 4, taken near the static buckle zone, standard deviations increased by more than an order of magnitude in the few minutes before the failure occurred. This gave test operators advanced indication of the failure location, allowing time to make better observations of the final failure.

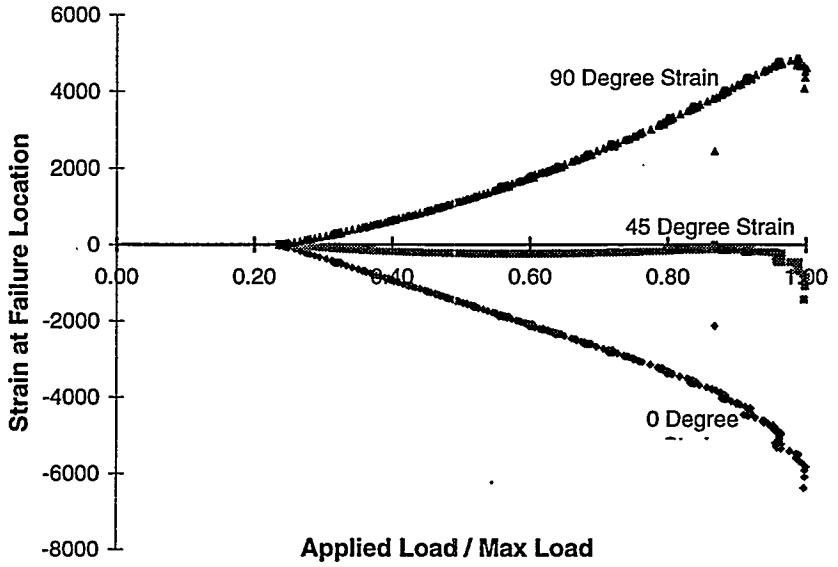

FIGURE 4 - STATIC TEST - STRAIN MEASURED AT FAILURE LOCATION.

Fatigue Testing

A fatigue test is conducted to verify the blade's ability to withstand a spectrum of operating loads that is representative of its design life. Commonly the blade design life is up to thirty years consisting of nearly 10^9 cycles. To achieve a test that is representative, the load is usually amplified to accelerate the test and reduce the number of cycles. Typically this is between 10^6 and 10^7 load cycles. Even with this acceleration, fatigue tests can run for several months. The type of data acquisition program that is required for fatigue tests is therefore quite different than that for static testing.

The primary objective of the fatigue test software was to reduce the amount of data to a reasonable quantity that would not overload the available disk space on a standard PC, but without missing any events that might be important. The minimum requirement was defined as the acquisition of data peaks and valleys for each channel. Although this still results in a large quantity of data, the primary goal was met. Data is stored in 1.4 Mb file sizes in binary format. A FORTRAN conversion routine was written to convert the binary data to ASCII format and download them into an EXCEL spreadsheet.

Normally it is necessary to control the actuator movement and position during a test using displacement rather than load. This is because the actuator force is usually not correlated well with blade strain in the range of frequencies at which blade tests are normally run. As the test frequency approaches the natural frequency of the test specimen, the required load input decreases and the repeatability of load from cycle to cycle is poor [3]. These effects usually make the load signal an unreliable reference for dynamic test control. Therefore, the algorithm is based on the assumption that blade displacement is correlated with blade strains at any cycle frequency. It uses the displacement channel as the master channel to trigger its search for peaks and valleys on the other data channels.

The load, however, is a very important parameter during a fatigue test. Ultimately, the actuator movement is defined by the force applied to the blade under static conditions. To establish the test parameters, displacements are measured statically under the specified test load. The dynamic loading is specified for these statically derived displacement parameters under true load.

The global blade stiffness can be calculated by determining the load required to move the blade a given distance at the load application point under static conditions. As the blade is cycled, this stiffness parameter typically decreases. Rapid drops in stiffness can often be related to a blade failure in progress. Generally, stiffness drops of more than 5% to 10% of the original value will indicate a complete blade failure. Monitoring the blade stiffness is one way to track the health of the test specimen. BSTRAIN has a built in routine for checking the stiffness of a blade during fatigue tests. The operator programs the controller to produce a slow, quasi-static cycle at a prescribed interval during the test. Commonly, this interval is around 1000 cycles. If the slow cycles are applied significantly below the normal cycle frequency, dynamic effects are negligible and an accurate measurement of load versus displacement can be obtained. This is usually 10% of the operating frequency.

The BSTRAIN program computes the stiffness value and writes it to a separate file. During the stiffness check, the MTS program also instructs the actuator to move the blade through its zero strain position. BSTRAIN finds the zero position and corrects all the data channels for any drift that may have occurred. This procedure is illustrated in Figure 5.

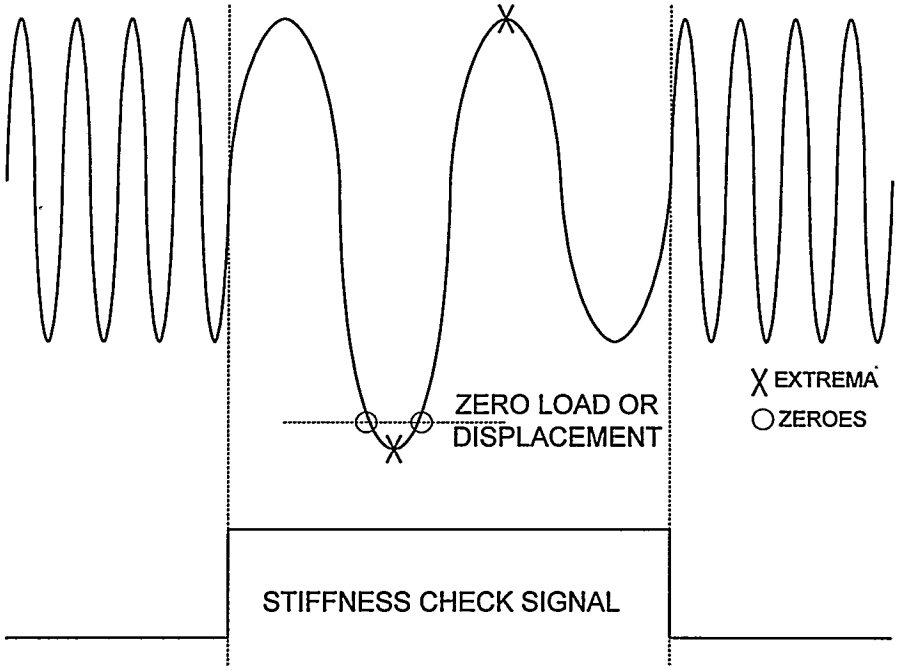

FIGURE 5 - STIFFNESS CHECK AND AUTOZERO

Figure 6 is a plot of the blade stiffness file for an entire blade test. Blade stiffness is normalized about the initial stiffness level. The data illustrate a drop in stiffness of approximately 7% over the test duration. Note that the blade was able to carry the test load for more than 2 million load cycles with a steady but slow decline in stiffness. Near the end of the test, a more overt failure mode caused an accelerated decline in the stiffness which led to the final failure.

One phenomenon noted during the test shown in Figure 6 is the periodic fluctuations that occur approximately every 60,000 cycles. These fluctuations correspond to a diurnal effect caused by thermal effects. Some of this may be due to changes in the blade temperature during ambient day/night cycles, but some is the result of oil temperature changes which affect the LVDT displacement transducer in the actuator. This problem will be thoroughly investigated in the future.

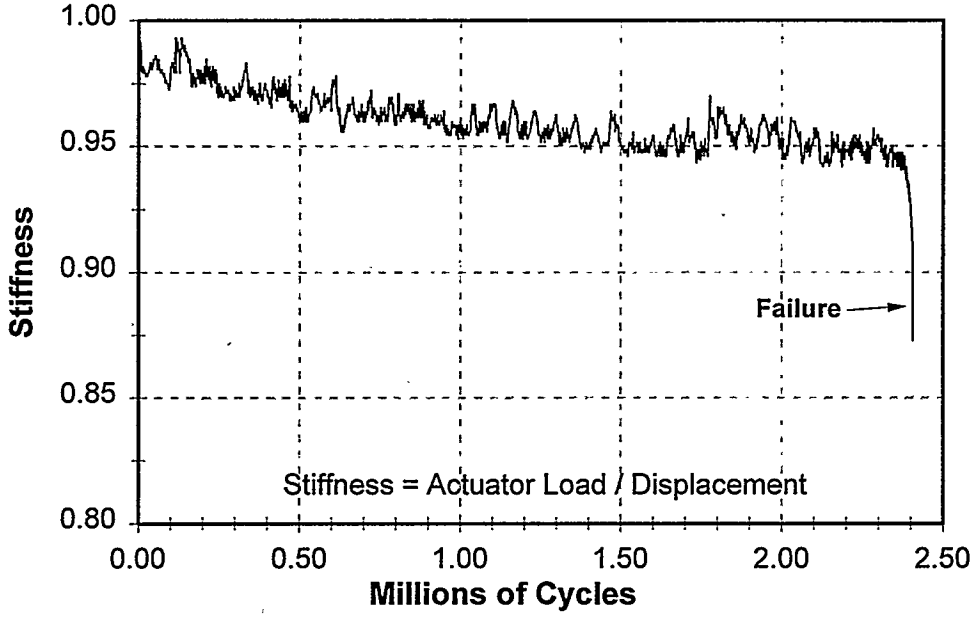

FIGURE 6 - FATIGUE TEST - STIFFNESS TIME HISTORY

Another useful feature allows the operator to print a status file summary printout from the control screen of the BSTRAIN program at any time during the test. This file gives the current values of all the data channels and the current status of the test conditions. This is the fastest way to learn what is happening with a test at any given time. A sample of the status file summary is shown in Figure 7.

BSTRAIN also allows the operator to access the most recent status file of a blade fatigue test from a remote terminal via modem. An additional custom software package called BSTATUS was developed so that the remote user would not need to install LabVIEW in order to retrieve a status file. During a fatigue test, BSTRAIN writes a status file containing the cycle number, stiffness values, peak/valley channel data, VCR status, and other pertinent information about the state of the test. This file is updated approximately every five seconds, depending on the scanning frequency. In addition, the software can be directed to notify a specified person by telephone if the test is shut down for any reason.

For both static and fatigue tests, continuous video recording of the blade test is controlled by BSTRAIN. For fatigue tests, which run even when no one is present to monitor the test (at night, on weekends, etc.), the software controls two looping VCRs so that no event will be missed due to the rewinding or changing of video tapes. When a major event occurs in the test, such as a sudden drop in stiffness, the test will be automatically shutdown and the VCRs stopped so that the event can be viewed at a later time.

Conclusions and Future Work

Full scale blade testing for design verification and to speed certification approvals will likely become a standard part of the design process and a requirement for international marketing. The BSTRAIN program described in this paper uses the latest technology to boost the quality of blade tests conducted at the NWTC.

As more experience is gained with the current software and data system its limitations have become apparent. Efforts to reduce data to a peak-valley series compression were sufficient for managing

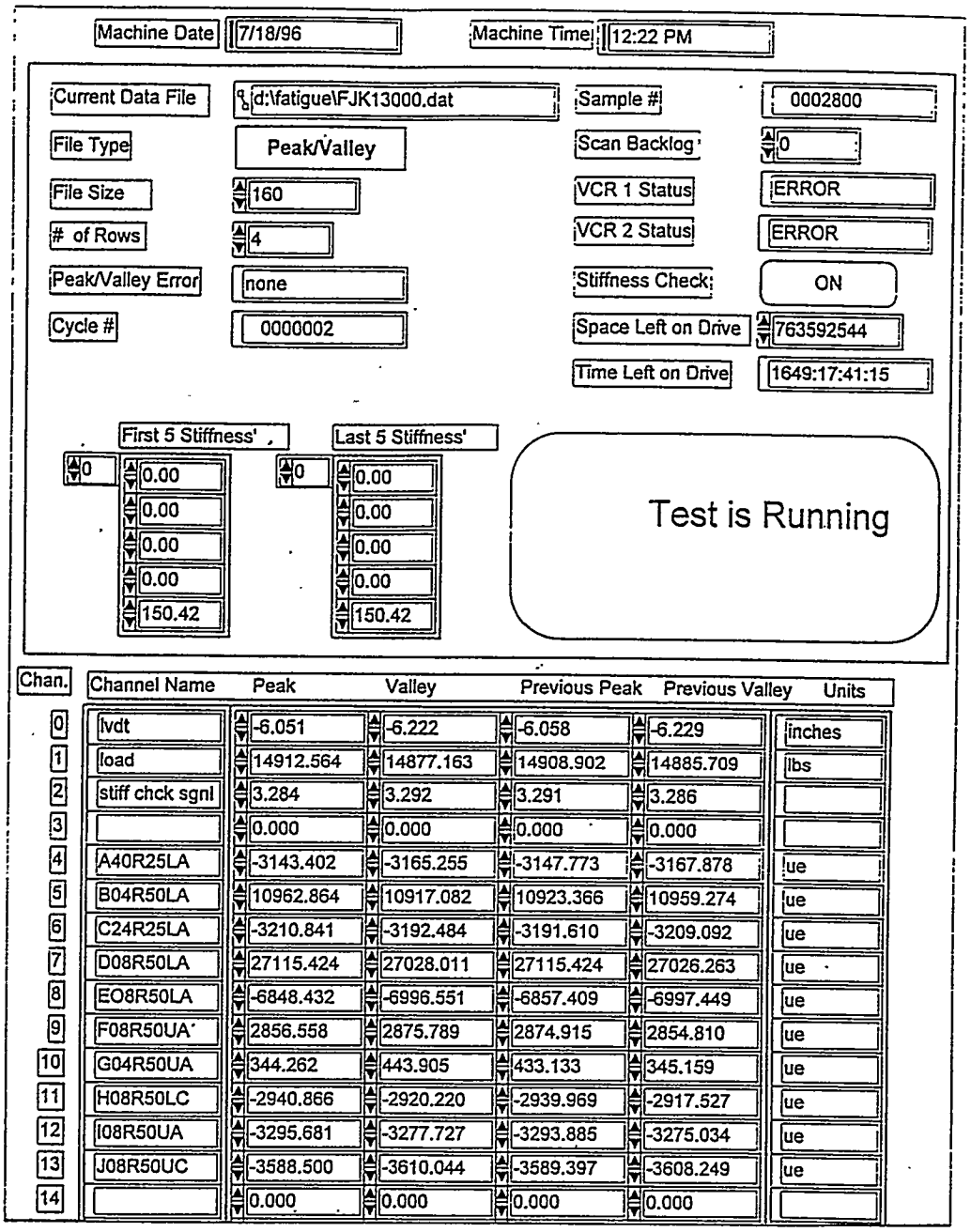

FIGURE 7 - AN EXAMPLE OF A STATUS FILE SUMMARY PRINTOUT

the data stream into a standard PC but the quantity of data is still too cumbersome. Additional data compression routines are still needed to expedite the dissemination of the data to customers and to allow quick trend analyses to be performed. Quick status file summaries are not sufficient.

Future enhancements that are presently being developed for the next version of BSTRAIN include real time rainflow counting and histogram generation for data channels. Histograms will provide a fast and accurate count of the true cycle count at critical channels. The peak/valley and time series data will still be preserved in case sequence effects or discrete events need to be analyzed. Data channels will also be included as part of the stiffness file checks. This will guarantee that a compressed record of the data will be kept throughout the test.

Acknowledgments

The authors would like to thank the many people who made contributions to this work. Jim Johnson, Mike Jenks, Darren DeShay, Zach Hawkins, Jack Allread, Bob Keller, and Bill Gage were all involved in the success of this project and without them the work could not have been completed. Finally, we would like to thank the U.S. Department of Energy for their funding of this project and their continued support of the these activities.

References

1. BSTRAIN Manual - Version 1.6, Unpublished Software Documentation. Available at the National Renewable Energy Laboratory, National Wind Technology Center, 1996.

2. Youngs R.L., and Hilbrand H.C., "Time-Related Flexural Behavior of Small Douglas Fir Beams Under Prolonged Loading," Forest Products Journal, June 1963, Vol. XIII, No. 6, pp. 227-232.

3. Musial W.D., Allread J. " Test Methodology and Control of Full-Scale Fatigue Tests on Wind Turbine Blades" Proceedings of the Twelfth ASME Wind Energy Symposium, January 31 - February 4, 1993, Houston, Texas, SED-Vol. 14, pp. 199-206.

Wind Turbine Performance:
Methods and Criteria for Reliability of Measured Power Curves

Dayton A. Griffin
Advanced Wind Turbines Incorporated
425 Pontius Avenue North, Suite 150
Seattle, Washington 98109

Abstract

In order to evaluate the performance of prototype turbines, and to quantify incremental changes in performance through field testing, Advanced Wind Turbines (AWT) has been developing methods and requirements for power curve measurement. In this paper, field test data is used to illustrate several issues and trends which have resulted from this work. Averaging and binning processes, data hours per wind-speed bin, wind turbulence levels, and anemometry methods are all shown to have significant impacts on the resulting power curves. Criteria are given by which the AWT power curves show a high degree of repeatability, and these criteria are compared and contrasted with current published standards for power curve measurement.

Introduction

The R. Lynette & Associates (RLA) Next Generation Innovative Subsystems (NGIS) program is designed to develop innovative subsystems which can be used to improve the performance and cost effectiveness of the AWT-26 wind turbine and which may be usable on other advanced wind turbine designs. RLA is working cooperatively with the National Renewable Energy Laboratory (NREL) and Advanced Wind Turbines Incorporated (AWT) on the program.

The program included the development and testing of the AWT-27 wind turbine, as well as an investigation into the use of vortex generators for performance augmentation of the AWT-26 turbine (Ref. 1). Both of these projects required measurements of the turbine performance, evaluated in terms of electrical power output versus wind speed (power curve). In addition to the NGIS program, AWT has conducted other performance testing of its prototype turbines in the past year, as indicated in Table 1.

Table 1. Recent Field Tests Conducted by AWT

Model	Designation	Test Objectives	Standards Used
AWT-26	P1	quantify incremental change in performance due to application of vortex generators	AWT, internally developed
AWT-26	P2B/C	measure AWT-26 performance for BPA/CARES Columbia Hills project	ASME (Ref. 2)
AWT-27	P4	quantify variation in performance with changes in blade pitch angle	AWT, internally developed
AWT-27	P4	measure AWT-27 performance for certification of power curve	IEC (Ref. 3)

As part of the performance tests, site calibrations were measured for the P1, P2B/C, and P4 test sites. Additionally, several side-by-side and 'round-robin' tests of NRG Maximum 40 cup-style anemometers were conducted, to evaluate and correct for any systematic bias between the instruments.

Note that Table 1 indicates 'AWT internally developed' as the measurement standards used for the NGIS tests. This is not meant to imply that AWT has adopted a single set of fixed standards for power curve measurement. In an effort to increase the reliability of its performance measurements, AWT engineers have compared historic (AWT) methods for power curve measurement with standards as published by IEC, ASME, and AWEA (Ref. 4). This paper presents field test data to illustrate some of the issues and trends which have resulted from this work. Table 1 should perhaps read 'AWT internally developing,' which is really the topic of this paper.

Test Configuration

Testing of the AWT-27, P4, was conducted at the AWT test site in Tehachapi, CA. The P4 turbine is a downwind, free-yaw machine. The rotor a teetered, two-bladed, fixed-pitch, stall-regulated design, which achieves high efficiency through the use of NREL S815/S809/S810 airfoils. The blades are made of wood-epoxy laminates, reinforced with carbon fiber. It has a diameter of 27.4 m (90 ft) and a nominal speed of 53 rpm. For the test results shown in this paper, the blade pitch was set to 0.0°, where the pitch is measured at the blade tip, and positive pitch angles are towards feather. The rotor is connected directly to the gearbox mainshaft, and the gearbox increases the mainshaft speed to 1800 rpm, driving a three-phase, 60 Hz, 480 volt, induction generator.

The AWT test site is on a ridge at an approximate elevation of 1430 m (4700 ft) near Cameron Peak, and is part of a FloWind wind power plant. In prevailing winds, (300° magnetic) there are no wind turbines upwind of P4. However, because of the proximity of the AWT-26 unit P1, and the FloWind units T340 and T341, valid performance data was limited to azimuths between 272° and 335°.

A meteorological tower (MET) is located 68.6 m (225 ft) from the P4 tower at a bearing of 349° (magnetic), and is instrumented to measure wind speed and direction at P4 hub height. Instruments at the MET tower are connected by cable to the data system at the control house. Ambient temperature and pressure are measured at the control house. Table 2 summarizes the type and locations of the instruments used during the P4 performance test.

Wind speeds were measured using two calibrated anemometers at 42.7 m (140 ft) AGL mounted in a 'rabbit-ear' configuration at the top of the MET tower. This mounting arrangement minimizes flow distortion due to the presence of the MET tower. The lateral separation of the anemometers was 80 cm (31.5 in) to centers, which is five instrument diameters, and is sufficient to minimize flow interference between anemometers for all valid azimuths.

Table 2. P4 Performance Test Instruments

Sensor Type	Make / Model	Location	Calibration / Date
Anemometers:	Maximum 40, Serial #1651	42.7 m, MET Tower	OTECH, 06-21-95
	Maximum 40, Serial #2172	42.7 m, MET Tower	OTECH, 03-30-95
Wind Vane:	NRG 200P	40.2 m, MET Tower	factory standard
Power Transducer:	OSI W-006C	Turbine Switchboard	factory, 08-04-95
Temperature Sensor:	NRG 110S	2.4 m, Control House	factory standard
Pressure Sensor:	NRG BP20	1.5 m, Control House	factory standard

A site calibration was performed to account for any flow variation at the P4 test site (Ref. 5). Simultaneous measurements were made of wind speed and direction at the P4 MET tower, and wind speed at the P4 hub location. Subsequently, the anemometer which was used to measure P4 hub wind speeds was flown side-by-side with the P4 MET anemometer, in the rabbit ear configuration described above. In this side-by-side arrangement, simultaneous measurements of wind speeds were used to identify a consistent bias between the two anemometers. A correction was applied to account for this bias prior to calculating the final correlation between P4 Met and turbine wind speeds. For the valid wind directions, the measured correlation factors ranged from 1.000 to 1.022 (winds from zero to 2.2% higher at the turbine than at the MET).

Data Acquisition and Processing

An NRG 9300 Data Logger was used to record data from the rotor, nacelle, ground control cabinet, and MET tower, with a sampling rate of 1 Hz, and data stored as 1-minute averages. The raw data files were converted into engineering units using the NRG 9300 conversion software. The converted files were then imported into a Quatro Pro spreadsheet, where the power levels were corrected to 1.06 kg/m^3 air density, and plotted in both time-series and scatter-plot formats.

Figure 1 shows an example of time-trace and scatter-plot data from the P4 power curve measurement. The file shown was measured over a 63 hour period, and the time-trace shows that the turbine cycled through four normal low-wind starts and stops. Note that the data shown in Figure 1 was density corrected, but had not yet been sifted for valid directions, or had the wind speeds adjusted per the measured P4 site calibration. Both of these steps were accomplished during the 'method of bins' procedure. Initial data selection was done at this stage. Visual inspection of the plots was combined with information from the test-site logs to select valid data sets with the following criteria:

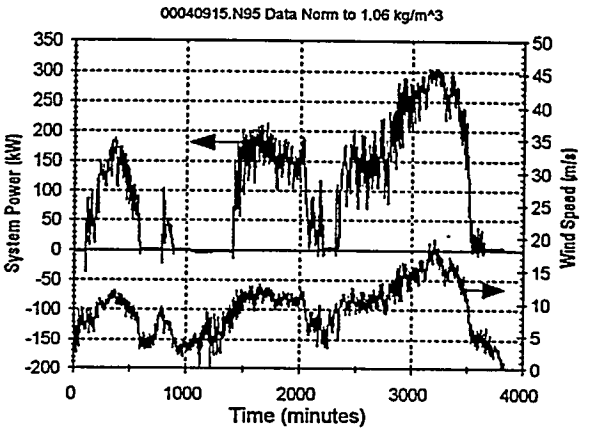

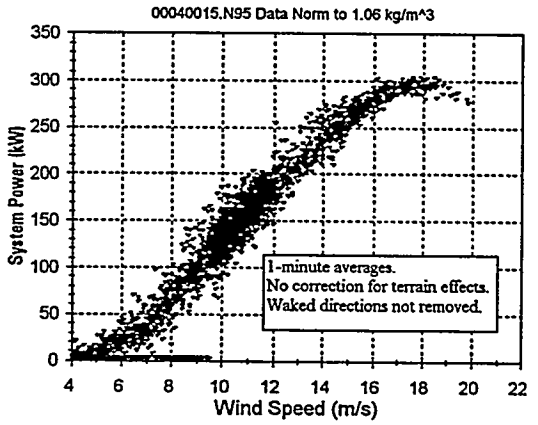

Figure 1. Power Curve Data, P4 Performance Test

1. For a valid test run, the turbine must have been in normal on-line operation for at least 60 minutes.

2. For each test run, end points which were associated with normal start and stop sequences, or turbine fault conditions (e.g. low performance fault due to blade icing) were removed.

3. Data was removed if rain, snow, or blade icing conditions had resulted in excessive scatter of the data, or premature stall of the turbine blades.

Once the valid data sets had been selected, they were grouped into larger sets prior to binning. The binning process was accomplished using a FORTRAN code, which performed the following operations:

1. The average MET wind speeds (the arithmetic mean of the two MET anemometers) were adjusted to calculate turbine wind speeds according to the P4 site calibration.

2. Data points were sorted, according to adjusted wind speeds, into bins 0.9 m/s (2.0 mph) wide, with bin centers at odd mph increments (11, 13, 15,..., 49 mph).

3. For each wind speed bin, averages were calculated for all physical quantities, including air density which was calculated from measured atmospheric pressure and temperature by the Ideal Gas Law.

4. The average air densities calculated in step 3 were used to correct power data to a standard air density of 1.06 kg/m^3.

Note that the average wind speeds which result from this process were not exactly at the original bin centers. To facilitate comparisons between measured power curves, and to allow the combination of multiple data sets, a linear interpolation was applied to calculate the power output at the original bin centers. When multiple data sets were combined, a time-weighted average was used for each wind-speed bin.

Repeatability of Power Curves

The issue of power curve repeatability was first raised in the context of evaluating performance changes during field testing (e.g. AWT-27 at various pitch settings, AWT-26 with and without vortex generators). The test modifications were expected to yield small percentage changes in power production, and this could only be measured if the baseline power curves showed very good repeatability. Two criteria were used to evaluate the repeatability of power curves, the variation of power output at each wind-speed bin, and the percentage variation of annual energy production (AEP) as calculated for various Rayleigh wind-speed distributions (assuming uniform distributions at turbine hub-height and 100% availability).

Figure 2 shows four P4 power curves, each containing from 50 to 80 hours of binned data, with the number of 1-minute averages and power variation per bin given in Table 3. In terms of kilowatts, the variation between the curves is largest where the bins are sparsely populated. However, at the 10.3 m/s bin the most sparse curve contains 96 minutes of data, and the power variation is nearly 11%. At the 12.1 m/s bin, the most sparse bin contains 230 minutes of data, and still the power varies by over 5%.

The power curves of Figure 2 were obviously measured during different wind conditions. Files #8 and #9 were collected during predominantly high winds, and the 1-minute average power output tends to be high in moderate winds. The converse is true of files #4 and #5. These trends have been observed repeatedly for the P4 and P1 (AWT-26) turbines. P1 data which was collected the same days as files #8 and #9 had similarly above-average power levels at moderate wind speeds. The strong correlation of this trend between the P1 and P4 turbines implied a global phenomenon, with wind turbulence identified as the most likely cause. Data from the files of Figure 2 was used to evaluate wind turbulence intensity during the measurement periods. The turbulence intensity was calculated for each 1-minute period as the ratio of the standard deviation to the average wind speed, where the standard

Table 3. P4 Power-Curve Variation by Bin, 50-80 Hour Data Sets

Wind Speed Bin		Number of 1-Minute Averages				Maximum Variation
(m/s)	(mph)	File #4	File #5	File #8	File #9	in Power Output (%)
4.9	11	10	65	0	0	45.8
5.8	13	58	225	0	0	28.0
6.7	15	217	213	0	0	16.5
7.6	17	326	365	15	8	31.1
8.5	19	336	589	53	29	21.6
9.4	21	375	756	86	105	11.8
10.3	23	381	722	96	231	10.9
11.2	25	366	517	148	313	6.9
12.1	27	265	467	230	471	5.3
13.0	29	292	418	387	529	2.3
13.9	31	265	425	586	566	2.9
14.8	33	89	207	690	492	2.7
15.6	35	2	44	559	283	4.5
16.5	37	0	1	473	225	7.7
17.4	39	0	0	278	355	1.0
18.3	41	0	0	195	248	0.5
19.2	43	0	0	75	122	0.0
20.1	45	0	0	7	27	1.0
21.0	47	0	0	0	1	NA

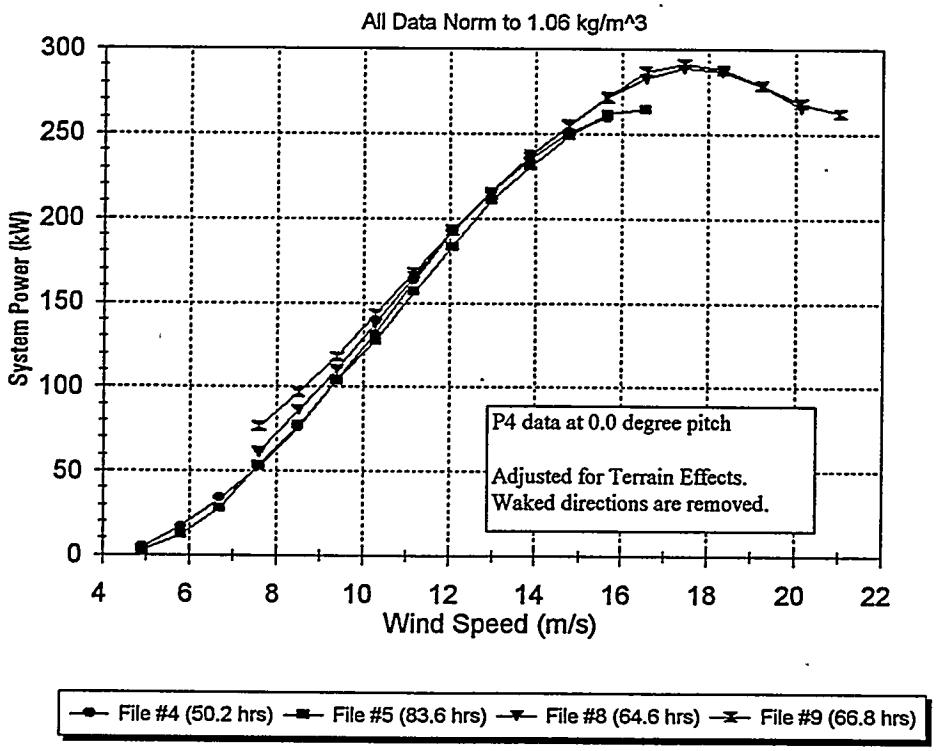

Figure 2. Variation of Measured P4 Power Curves, 50-80 Hour Data Sets

deviations were based on 1-second samples of wind speed. To within the ability of the anemometer cup to respond to turbulent fluctuations, this is a measure of the turbulence intensity in the prevailing wind direction. The results are shown on Figure 3. For the wind speed range between 10 and 14 m/s, the turbulence intensity was 20 to 30% higher for files #8 and #9 (high-wind days) than for files #4 and #5 (low-wind days). This is the same range over which all the file bins had relatively large amounts of data, yet still deviated significantly in terms of power output. While not conclusive, the data of Figure 3 supports the idea that wind turbulence levels were responsible for these variations.

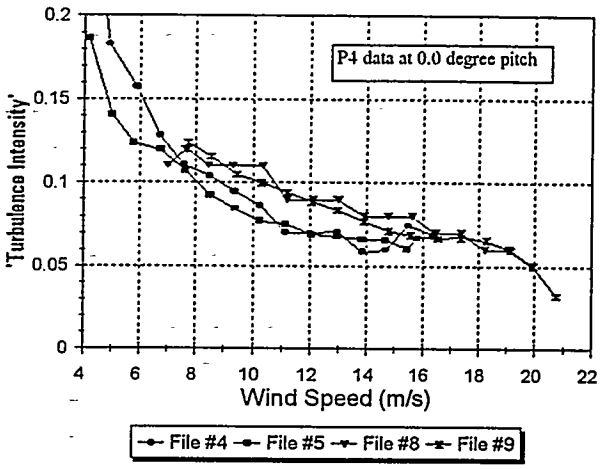

Figure 3. Turbulence Intensity During P4 Power Curve Measurements

Figure 4 shows a larger data set from the same measurement period, where 488 hours of data has been grouped into two files of approximately 250 hours each. The file grouping was done in such a way as to have similar bin distributions of high-wind and low-wind data. The 250-hour curves show excellent repeatability, with power output varying by less than 2.5 kW for all wind speeds between 4.9 and 15.6 m/s. Above 15.6 m/s, the power variations are less than 1.4%, and annual energy production (AEP) for the curves agrees to within 0.4% for Rayleigh wind speed averages between 5.4 and 8.5 m/s. This trend has been observed repeatedly during recent AWT tests, for P4 at both 0.0° and -1.0° pitch settings, for clean-blade P1 performance at two different pitches, and for P1 with vortex generators installed on the rotor (Ref. 1). The power curves showed significant variation for smaller data sets (50 to 100 hours), and a high degree of repeatability for curves containing data on the order of 300 hours.

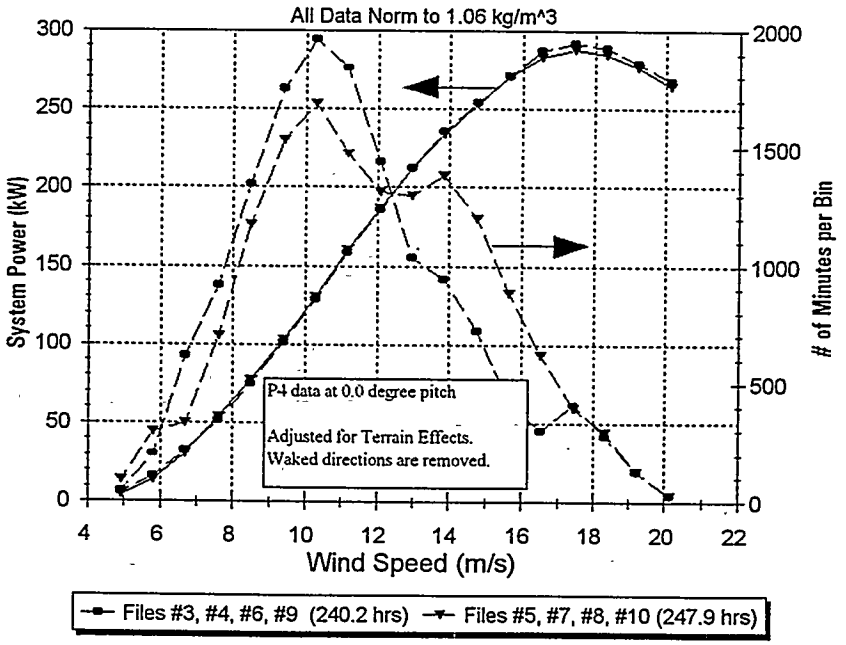

Figure 4. Repeatability of P4 Power Curve, 250 Hour Data Sets

Effect of Averaging Period and Bin Width

The data sets presented above were all based on 1-minute averages and bins widths of 0.9 m/s (2 mph). During two recent tests of AWT turbines, different averaging periods and bin widths were used. One test specified 6-minute averages with 0.9 m/s bins, and the other required 10-minute averages with 0.5 m/s bins. To demonstrate the effect of varying averaging periods and bin widths, the data set shown in Figure 4, has been converted to 10-minute averages, and then binned using bin widths of both 0.9 and 0.45 m/s (2.0 and 1.0 mph). In the comparisons which follow, percent variations in power are all referenced to the original curve which was calculated from 1-minute averages and 0.9 m/s wide bins.

Table 4 summarizes the results, in terms of the number of samples per bin, and the effect on the average power at each bin center. Converting from 1-minute to 10-minute averages greatly reduces the amount of dwell time in both the highest and lowest wind-speed bins. In the middle bins, dwell time is increased, but the impact on power output is very subtle. In the low wind-speed bins the power output is significantly lowered for the 10-minute averages. This is because it rarely blows a steady 5.8 m/s for a 10-minute period at the Tehachapi test site. Therefore, 10-minute averages in the 5.8 m/s bin are likely to contain several 1-minute averages when the turbine is motoring in light winds. The loss of high-wind bins is for a similar reason, the Tehachapi winds rarely blow 20 m/s over a 10-minute average, without having a 1-minute average that exceeds the turbine's cut-out wind speed.

An additional effect is seen in going from 0.9 to 0.45 m/s bin widths. Although the 4.9 m/s bin contained 131 1-minute data points, only two 10-minute averages are retained for the smaller bin width. Similarly, the 20.1 and 19.7 m/s bins only retain one 10-minute average each.

Anemometry Issues

During data analysis, the MET wind speed was calculated as the average of the two anemometers. The major advantage of this procedure is in being able to make periodic comparisons between wind speed measurements of the two instruments, thereby insuring that the anemometers are functioning properly, and are holding their calibrations. Additionally, round-robin tests of Maximum 40 anemometers conducted at the AWT test site have shown small, but consistent bias between instruments, even when calibrated. As there is no way to confirm which of the anemometers is reading closer to the true wind speed, the averaging of two instruments should reduce bias errors.

Figure 5 is from a data record of the present test (from power-curve file #4), and illustrates a benefit of redundant MET anemometers. The figure shows a time-trace of the anemometer signals with a 350 minute duration. For the majority of the file, the two signals agreed almost exactly, but for a 17 minute period the MET 1 signal read unreasonably low. The air temperature was too warm for icing conditions, and no cause was established for the bad signal. The trace shows that the readings returned to normal behavior, and it was observed that the instruments performed well during subsequent data collection periods.

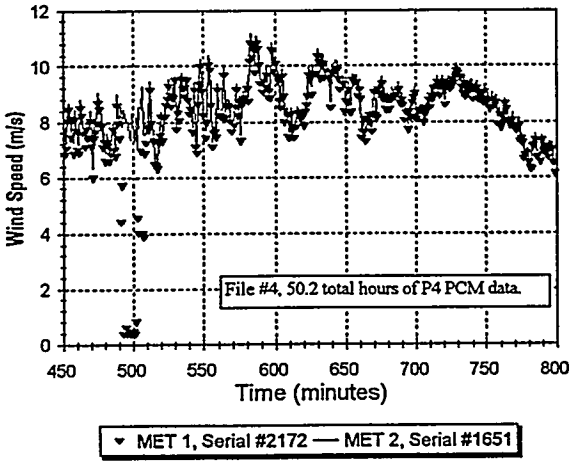

Figure 5. Time-Trace of P4 MET Anemometer Signals

Table 4. Effect of Averaging Periods and Bin Width on P4 Power Curve Data

Wind Speed Bin		Bins 0.9 m/s (1 mph) Wide			Bins 0.45 m/s (2 mph) wide	
(m/s)	(mph)	# of 1-min. averages	# of 10-min. averages	Change in power (%)	# of 10-min. averages	Change in power (%)
4.9	11	131	7	-13.9	2	-3.5
5.4	12				12	
5.8	13	497	39	-6.8	16	-3.3
6.3	14				32	
6.7	15	952	74	-8.4	32	-8.1
7.2	16				58	
7.6	17	1618	167	-2.9	77	-5.1
8.0	18				117	
8.5	19	2521	251	-1.7	123	-2.5
8.9	20				144	
9.4	21	3288	349	-1.0	175	-2.6
9.8	22				192	
10.3	23	3654	393	+1.0	193	+0.7
10.7	24				183	
11.2	25	3321	307	+0.2	154	+0.6
11.6	26				153	
12.1	27	2763	261	0.0	139	-0.6
12.5	28				113	
13.0	29	2339	239	-0.2	108	-0.1
13.4	30				128	
13.9	31	2331	244	0.0	125	+0.3
14.3	32				120	
14.8	33	1926	200	+0.1	104	+0.4
15.2	34				75	
15.6	35	1313	127	+0.2	68	+0.2
16.1	36				47	
16.5	37	927	77	-0.2	36	+0.2
17.0	38				40	
17.4	39	810	100	-0.5	55	-0.5
17.9	40				44	
18.3	41	573	53	-0.8	20	-0.7
18.8	42				21	
19.2	43	259	17	0.0	8	-0.9
19.7	44				1	
20.1	45	57	1		1	+4.2
20.6	46				0	
21.0	47	5	0		0	

By comparing the two anemometer signals in 1-minute averages, this anomaly was easily caught, and the data points removed from the files prior to binning. Note that when the data of Figure 4 was converted to 10-minute averages, the bad signal was significantly masked (as 10-minute averages tended to contain both good and bad 1-minute averages).

Another issue which was raised in the present work was the effect of anemometer calibrations. During side-by-side and round-robin tests of calibrated NRG Maximum 40 anemometers, it was observed that some pairs showed improved long-term agreement with each other when the nominal slope-only conversion factor was applied, rather than the slope-offset conversion that was measured during the instrument calibration.

Table 5 shows the calibration constants for the instruments used in the present work, as measured by OTECH in an atmospheric test (Ref. 6). The slope-offset conversion factors on Table 5 were used for all power-curve data previously shown in this paper.

Table 5. Calibration Constants For P4 MET Anemometers

Anemometer	Calibration Constants
MET 1 Serial # 2172	Slope = 1.654 mph/pulse/sec. Offset = 0.850 mph Slope = 1.689 mph/pulse/sec. Zero Offset
MET 2 Serial #1651	Slope = 1.670 mph/pulse/sec. Offset = 0.945 mph Slope = 1.708 mph/pulse/sec. Zero Offset

For purposes of comparison, the total average P4 power curve of Figure 4 was recalculated using the slope-only calibration constants shown in Table 5. The power curves obtained by this method saw significant improvement at low wind speeds. Relative to the baseline curves, calculations showed AEP increases of 7.1 and 5.3%, respectively, for Rayleigh averages of 6.3 and 7.6 m/s (14 and 17 mph).

Conclusions

AWT Engineers have recently conducted several performance measurements of their prototype AWT-26 and AWT-27 turbines. A specific data set containing 488 hours of binned AWT-27 power-curve data has been used to illustrate some of the issues and trends identified during this work.

Power curves containing 50-100 hours of data have been found to vary significantly, with wind turbulence levels identified as a likely cause. For all performance tests, the AWT prototypes showed improved repeatability with additional data hours. Excellent repeatability has been found for 250-300 hour data sets. Averaging periods and bin widths have been shown to effect the number of data points in the upper and lower wind-speed bins, and can significantly impact the average power at the low-wind bin centers.

As long as they are properly mounted to avoid interference effects, the use of two anemometers should reduce errors due to bias, and provide a method for ensuring that the instruments are functioning properly. Power curve results are shown to be very dependent on the form of conversion constants used, and the accurate calibration of cup-style anemometers for atmospheric testing appears to be an important ongoing concern.

With regard to published standards for power curve measurement, the IEC standards are the most explicitly rigorous, requiring a minimum of 30 minutes of data per wind-speed bin, and a total duration of 180 hours. Data requirements of this level are strongly supported by the present test results. The AWEA standards (10 hours total duration, 10 minutes and less dwell time per bin) are clearly insufficient for reliable power curve measurement. The ASME guidelines allow the test parties to agree on requirements for both dwell time per bin and total data collected, thus allowing the degree of rigor to match the test resources and objectives.

Acknowledgments

The present work was supported by NREL, under Subcontract # ZAA-5-12272-05, monitored by Paul Migliore. The author would like to thank Paul and others at NREL for their support on this project, including many helpful discussions. Robert Poore, Tim McCoy, and Richard Beckett all made significant technical contributions to the present work. Most of all, thanks are due to the AWT test-site engineers and crew, who have conducted these tests year-round in the often extreme Tehachapi environment. This paper is a direct result of their professional and dedicated work.

References

1. Griffin, D.A., *Investigation of Vortex Generators for Augmentation of Wind Turbine Power Performance*, NREL/TP-440-21399, Golden CO: National Renewable Energy Laboratory, publication pending.

2. International Electrotechnical Commission IEC TC88(WG6) 24/1-95, *Wind Turbine Generator Systems Power Performance Measurement Techniques,* 1988.

3. American Society of Mechanical Engineers ASME/ANSI PTC 42-1988, *Wind Turbines Performance Test Codes*, 1988.

4. American Wind Energy Association Standard AWEA 1.1-1988, *Standard Performance Testing of Wind Energy Conversion Systems*, 1988.

5. *AWT-27 Power Curve Design Book*, DB273011, April, 1996

6. Obermeier, J.L., *Calibration Test Results of the Maximum #40 Anemometer*, American Wind Energy Association Proceedings, Minneapolis, MN, May, 1994.

TEST RESULTS OF NREL 10M, SPECIAL-PURPOSE FAMILY OF THIN AIRFOILS

Kenneth L. Starcher
Dr. Vaughn C. Nelson
Jun Wei

Alternative Energy Institute
West Texas A&M University
P.O. Box 248 W.T.
Canyon, Texas 79016

ABSTRACT

Two Carter Wind Systems, 25 kW units were tested at the Alternative Energy Institute to determine performance differences between production blades and rotors with NREL Special Purpose Thin Airfoils. Blade design, mold preparation, blade production, and testing were all conducted by AEI. Design tools were created for computer modeling of the blade. This computer program (ROTOR) for the design and production of modern HAWT rotors is now used by blade manufacturers in the wind turbine industry. The blades had the same twist, taper, and length as production blades. Flap natural frequency was adjusted to be as similar as possible between rotors, as was blade mass, blade center of gravity and rotor moment of inertia. Data collected were; wind speed at hub height, blade root flap & edgewise loads, main shaft torque, azimuth position, teeter angle, yaw angle and electrical power. These data were collected at 128 Hertz for data sets of eight seconds. This data set was then written to hard disk and the cycle repeated resulting in a file containing five and one half minutes of data. A data run consisted of; preflight checkout/warm-up of equipment, preflight calibration/verification of all sensors on both turbines, collection of five files of data (about thirty minutes of data), post flight calibration/verification of sensors. During this high speed data collection period there were a total of twenty-four data runs collected.

Data were collected for wind speeds in the range about 7, 10 and 13 m/s. A data matrix was filled for clean, medium and heavy surface roughness. Baseline power curves, parametric pitch variation runs to establish testing pitch settings, high speed data collection runs with and without applied surface roughness were completed and analyzed. Data were compared using simple arithmetic mean, Fast Fourier Transform (FFT) analysis, rainflow counting algorithms and wavelet analysis. The NREL airfoils showed much less sensitivity to surface roughness. There were minimal root bending load differences. Annual energy production during long term operation is being determined.

INTRODUCTION

A significant effort of the federal wind energy program has been the development of new technology for improved performance of wind turbines [1]. Aerodynamic studies have developed into improved predictions of rotor performance as well as prediction of the operational characteristics of airfoils with computer modeling rather than expensive wind tunnel testing [2,3]. The combination of these two modeling techniques were used to develop new families of wind turbine blades to improve energy output under dirty surface conditions and reduce blade root bending to increase blade life. New blades with the new airfoils were tested at three separate test facilities. The NREL composite test facility used a set of S809 blades, with no twist and no taper. A side-by-side test in California compared a production rotor (Aerostar) to a redesigned rotor using the thin airfoil series [4]. This test did not directly compare identical rotors since the NREL rotor had different twist, taper, length and mass from the production rotor. The third test, was at the AEI Wind Test Center. AEI produced and Composite Engineering fabricated a set of blades that were as much like a production set as possible and operated the pair of rotors under identical conditions and collected high speed strain and meteorological data to determine the load and performance differences at several wind conditions.

DESIGN, FABRICATION, CONSTRUCTION AND TESTING

AEI was involved in the creation and template fabrication of all the rotors for these NREL projects. The S809 (combined experiment) project was designed and built using templates produced from AEI computer programs and cut at the University of Texas, El Paso, Mechanical Engineering Department facilities. The S809 blade was then fabricated at Composite Engineering, Cambridge Mass. They were instrumental in the speedy production of the S809 set of blades. They were also very helpful in monitoring progress of our test blades and supervising the construction stages performed by AEI personnel.

The accuracy from the precise computer calculations was maintained in the production templates through the use of numerical control milling machines. The templates were created in four series. A high density apple plywood was used for the construction templates. An aluminum checking template, slightly oversized female set was produced for each of the four locations of the defining airfoils. A plywood set of female templates were made for checking the finished blade at each

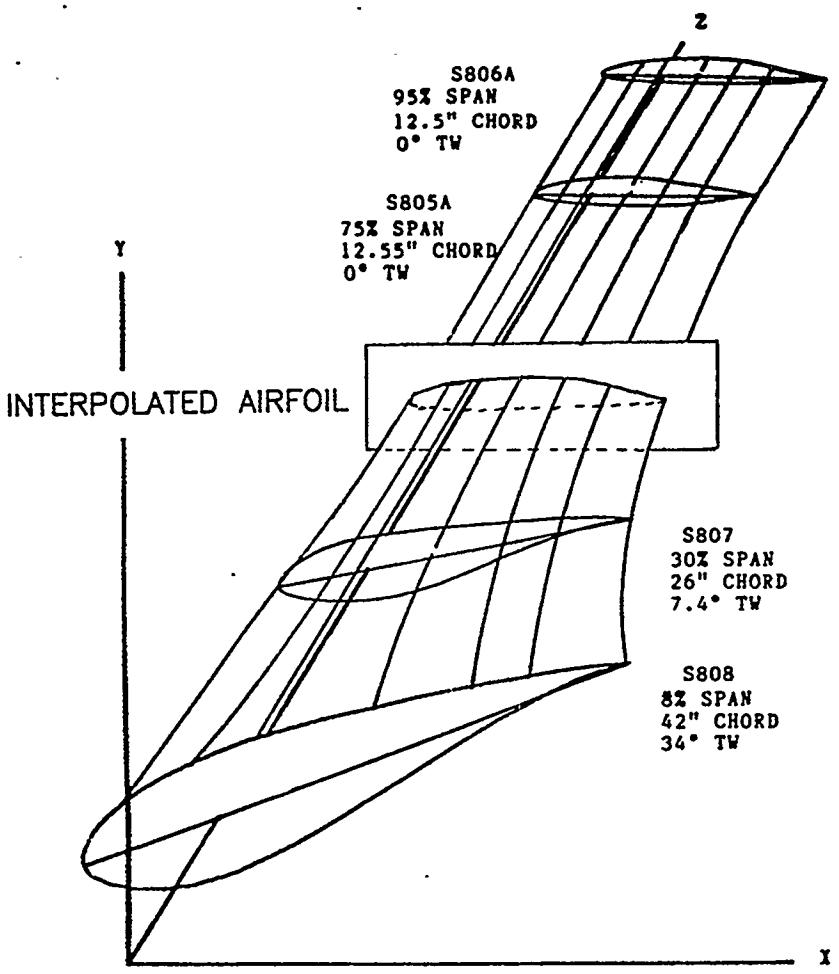

Figure 1. Determination of interpolated airfoils.

station of the outer fifty percent span, as well as selected locations along the inner half of the blade. To aid in mold finishing, a series of male "scraping" templates for verifying the interior surface shape were produced for the outer half of the span. The wood templates had a sighting hole at the 1/4 chord point, used to align each template to the same axis. It also provided an axis for twist alignment. Each scraper template had a one inch offset at the nose and trailing edge that represented the chordline extension past the blade. This was used as a guide on the outer

edges of each mold half to check the mold interior surface for waves or "bumps" that would be hand smoothed out and filled until a uniformly smooth surface was left. The oversized female checking templates were used by NREL personnel during final acceptance tests.

These templates were created using ROTOR, developed at AEI. This software allows designers to specify a given airfoil shape at several spanwise positions and then determines the planform shape at intermediate positions based on the request of the designer. Evenly spaced templates can be created by specifying distance or percent of blade span. The result is a dense set of airfoil coordinates for each of the newly created spanwise coordinates. These virtual templates are then able to be twisted about a axis. This three dimensional surface is then displayed graphically allowing the designer to observe the result for abnormal twisting, waviness or inconsistencies in the blade. Options to the program allow the designer to save the template points in twisted or untwisted form, creation of a template surface offset to allow for a finite blade skin thickness during production, and the use of the quarterchord or any interior point to apply the blade twist about. The computer applies the mathematics technique of the "cubic spline under tension" to determine the surface of the new blade. Then the computer takes a "slice" of the blade at uniform spanwise positions and determines the shape of the airfoil based on the lines striking the plane at that spanwise point (Figure 1). The code, available from AEI, has been used in industry by several designers for visualization of proposed blade designs.

SIMILARITY OF THE BLADES

After the blades were delivered to AEI, they were subjected to measurements to determine any differences between the production rotor and the NREL set. Blade twist and chord distribution were set during production and blade planform matched to within .25 mm (.010"). Mass was added to lower the flap and lead-lag frequencies, tips were repositioned to give the same rotor diameter, then mass was redistributed to obtain similar rotor moment of inertia. In order to establish the power curve to reach peak (25 kW) at the same windspeed and to approximate the same power curve shape, the NREL rotor had to be set at 3.25 degrees while the production blades were set at 0 degrees. This setting was determined to be due to the different zero lift angles of attack of the airfoil series (NACA 230xx and S805A/S806A). Power curves were collected using a central meteorological tower for wind speed input and power transducers for both units. This data was collected at 1 Hz using a Campbell Scientific CR21X, Met-One anemometers, and RIS WV20 Power transducers. Power curves for these settings were essentially the same (Figure 2).

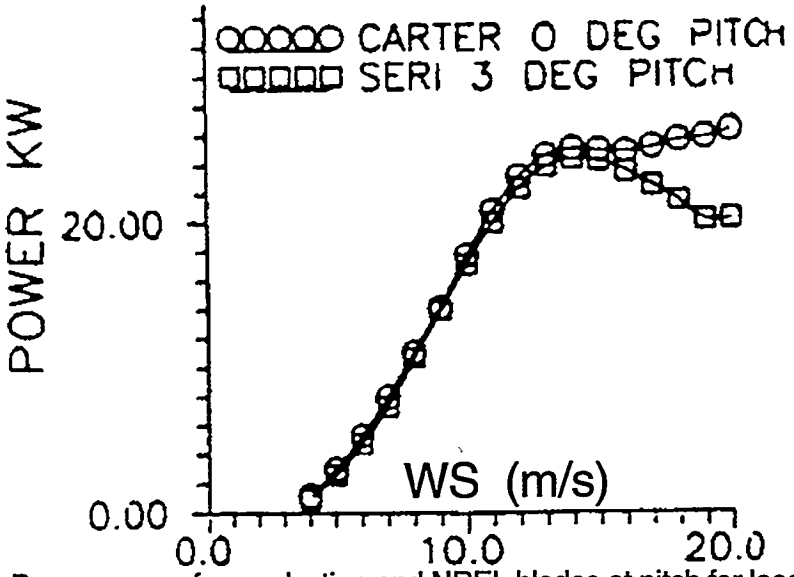

Figure 2. Power curves for production and NREL blades at pitch for loads testing.

HIGH SPEED DATA

The high speed data acquisition system consisted of a 386 DX computer with analog to digital conversion boards. Sensors were purchased or built to measure blade azimuth position, flap strain, lead-lag strain, total main shaft torque, teeter position, yaw direction, wind speed, and wind direction. Sensors were duplicated on both units with common signals coming from the central met tower. Data from individual turbines were transmitted by direct wire runs to the data collection system, using slip rings for rotor based sensors (Figure 3). Data collection consisted of a preflight checkout of all sensors with data collection of verification data and recording of input versus output signals under known loads or deflections. Blades were washed and then the units lifted to run position. Turbines were then allowed to energize and data collection would begin. Typical data sets were combinations of 8 s of continuous data recorded at 128 Hz. Then the data would be recorded to hard disk and an additional 8 s record taken. This continued for 40 sets and then the data file would be closed, a new file opened and the series repeated. A complete run of data would consist of five files of 40 records of 8 s, 1600 s of data taken over 35 minutes of real time. The discrepancy in the real time and the total time recorded is the time needed to transfer data from memory to hard disk, and opening and closing individual data files.

The units were then stopped, lowered and a postflight verification made of sensor drift. Data comparison of the pre and post flights were made to show any change in sensor output with known loads applied. If all data sensors were acceptable then the five files were backed up to floppy diskettes and transferred to our data treatment computer, a 486 DX computer with ASYST software for analysis. Typical treatment of the data consisted of the averaging of the data for each eight second period and then printing these out for binning purposes. The azimuthal average of each eight second period were also created, allowing the signal outputs to be binned by rotor position, creating a composite curve for each sensor, electric power, lead-lag strain, flap strain, shaft torque, teeter angle and yaw position.

MATRIX FOR ANALYSIS

Data were collected for twenty-four runs, then compiled to fill a data analysis matrix. Data were needed at low, medium and high windspeeds for clean, medium and heavy surface roughness conditions. These roughness conditions were simulated with the application of grit in the same manner as in the California NREL side-by-side tests [6]. NREL medium level became our heavy level of surface roughness. Our medium level was determined by operating the production rotor at reduced grit surface densities until rated power output at 10 m/s was reduce 40%, equivalent to power reductions observed during long term field operation of Carter turbines at U.S.D.A. Bushland, Texas [7]. These power reductions were due to bug buildup on leading edges of the rotor during bug hatches. By replicating this level of roughness on both rotors, a comparison to natural conditions could be quickly made without concerns about differences of natural bug distribution between rotors. Sufficient data were collected during the twenty-four runs to fill each cell of the matrix. Data were required in each cell to show conditions where wind speeds were stable (less than 1m/s change centered about the desired speeds), yaw orientations were the same for both turbines, minimal wind shear ($\alpha < .14$), and turbulence intensity values were low. Data were not collected unless the wind direction was within fifteen degrees of perpendicular to the towers' alignment.

DATA ANALYSIS, RESULTS

The primary result from the extensive data analysis is that delivered power of the NREL rotor at 10 m/s was 35% (Power dirty/Power clean) better under heavy surface roughness , 20% at medium roughness (Figures 3,4). This reduced sensitivity to surface roughness could provide a modification of field maintenance schedules, allowing windfarm operators to reduce blade cleaning to a minimum while still maintaining adequate power production.

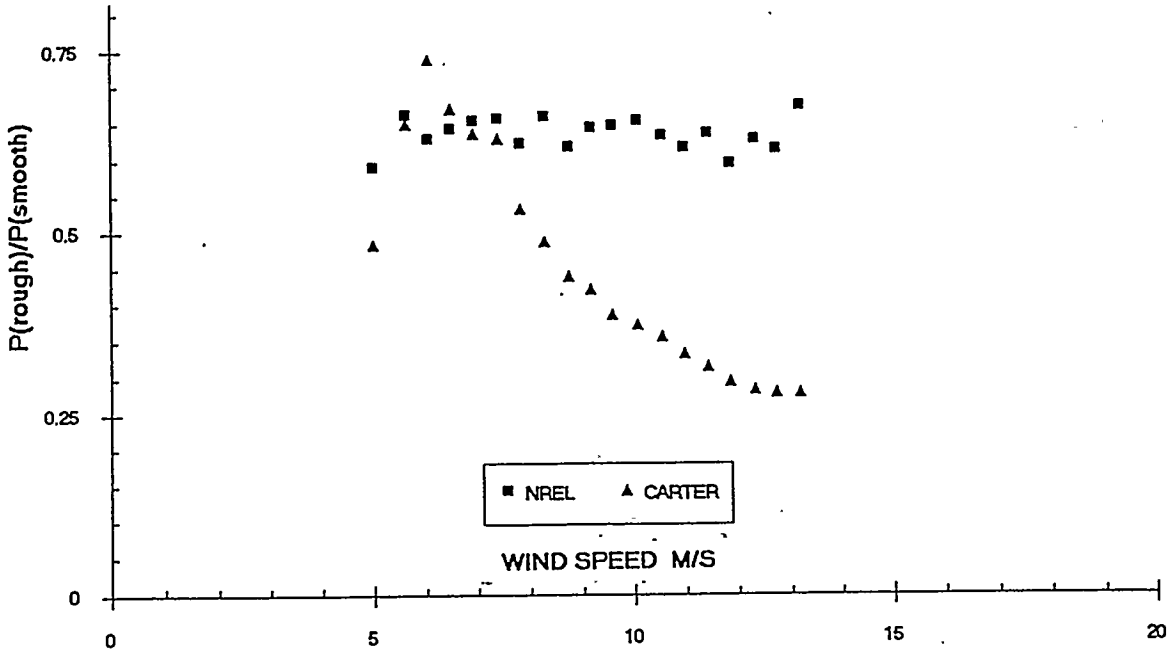

Figure 3. Ratio of power (heavy output/clean output)

As data were found that met the matrix criteria, four second runs of 512 points would be added to a cumulative file for each sensor type (lead-lag, flap, torque, teeter, yaw, power, azimuth position and windspeed) for each unit for the given surface condition. These winnowed files were then treated by ASYST. The results were then formed into composite curves for each data file and then plotted (Figure 4).

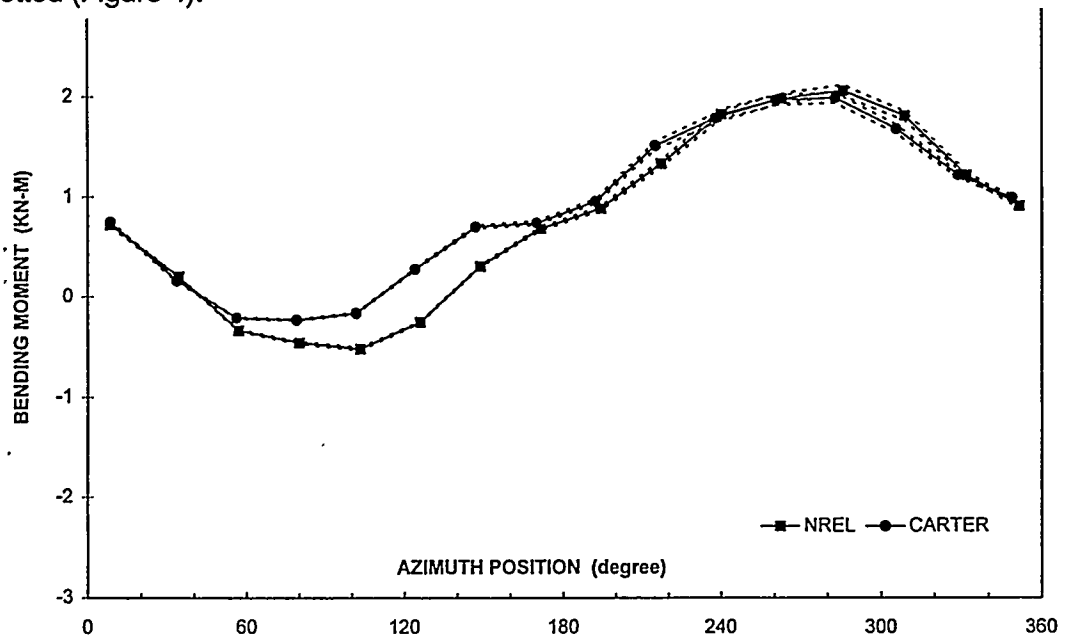

Figure 4. Lead-lag signal composite, both units, 10 m/s, clean blades

Additional analysis of these data, was the application of FFT to these cyclic signals and then taking the composite from the original data, and apply an FFT to these stochastic loads. FFT results show information in the frequency frame that is often unnoticed when examining data in a time or sequential frame. In this instance, the exposure of a noticeable 2P harmonic component in the performance of the Carter blades that has been removed in the NREL rotor (Figure 5).

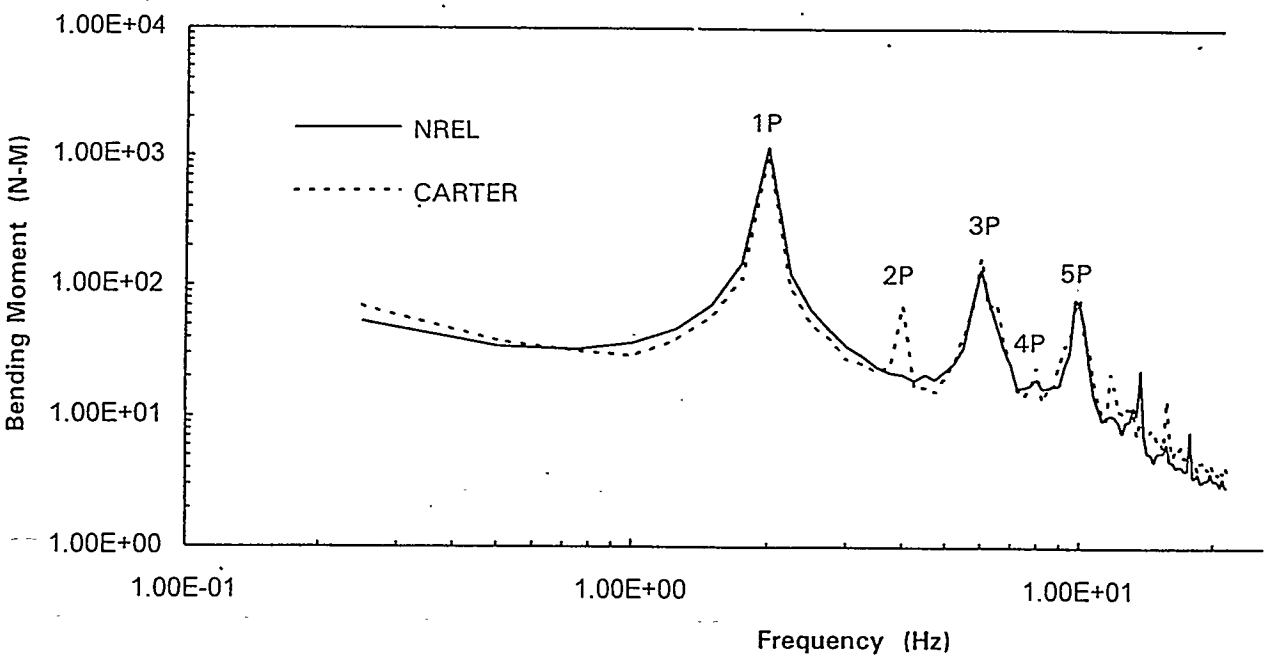

Figure 5. FFT of lead-lag signal, both units, 10 m/s, clean blades.

A third treatment of the data matrix was made using a routine from automotive industry [8] resulting in a matrix of average loads versus load range (peak-to-peak loads) containing the number of cycles counted in each cell. This is displayed three dimensionally on an Excel spreadsheet using bar graphs (Figures 6,7). Comparison of the two turbines for similar conditions then shows definite changes with greater peak-to-peak values in the Carter rotor while the NREL rotor has greater number of cycles at the lower load ranges. This should translate to longer life for the NREL rotor with similar construction and identical hub/spar connection.

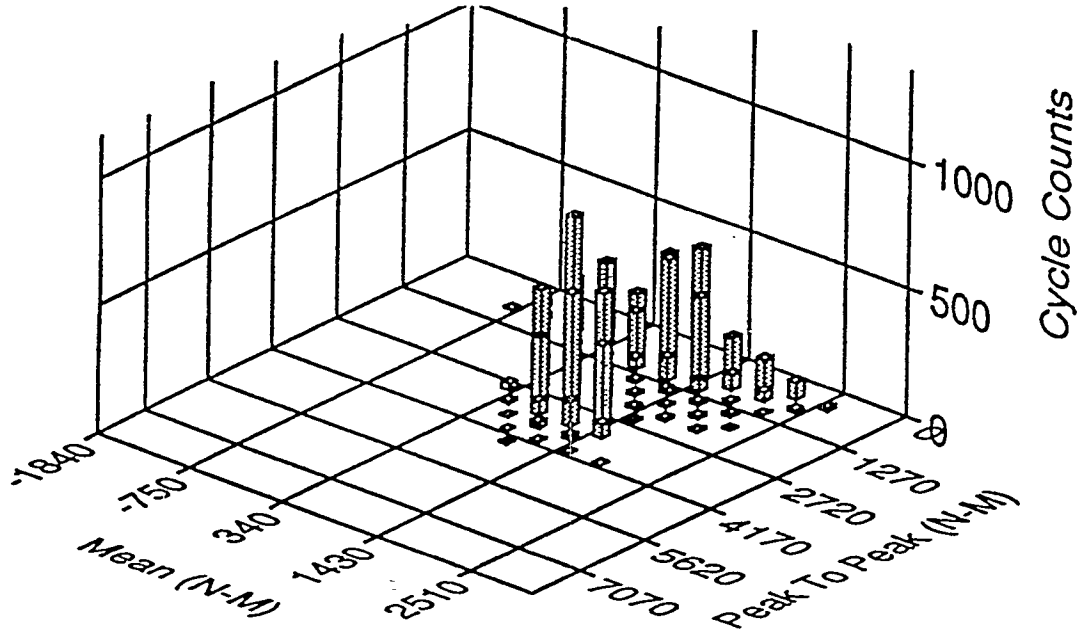

Figure 6. Carter rainflow analysis plot, lead-lag, 10 m/s, clean blades

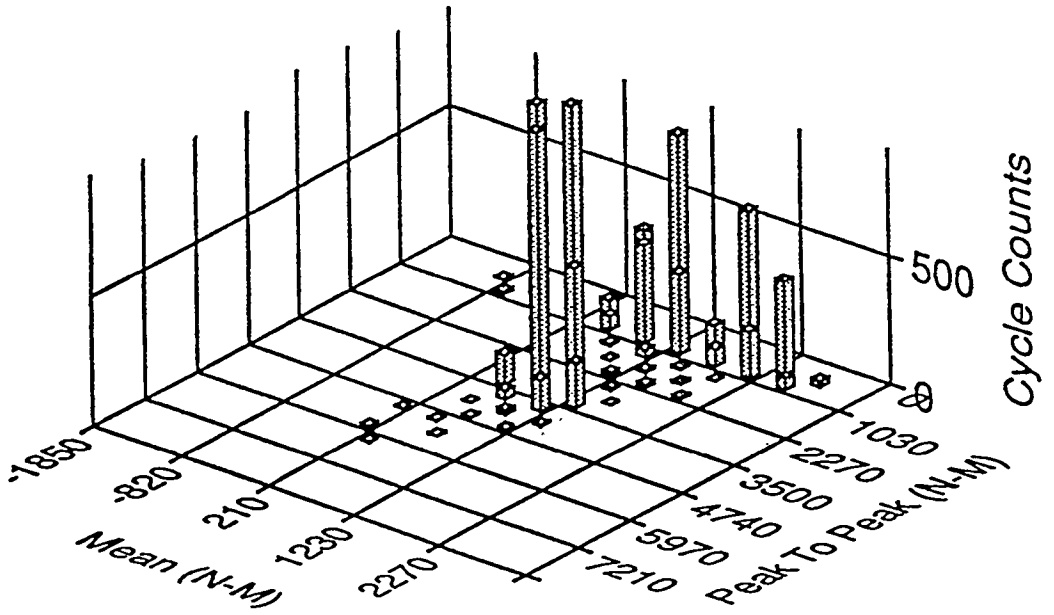

Figure 7. NREL rainflow analysis plot, lead-lag, 10 m/s, clean blades

Wavelet analysis showed differences at high resolution in some of the data for harmonic components of lead-lag and flap bending moments. At some instances, sharp peaks occurred in the data for the NREL blades that were not present in the Carter rotor during the same time period. The wavelet analysis made it possible to analyze both sets of data during specified time frames. The sharp peaks were possibly due to a quicker response to wind speed gusts affecting the NREL blades more than the Carter rotor.

CONCLUSIONS

The airfoil performed well in the field tests and continued long term comparison will be made in the upcoming years. The basic results from the field comparisons were [9];

1) A computer program was developed for blade design that will give a faired blade with distinct airfoil shapes at different span locations.
2) In conjunction with Composite Engineering, a blade tooling/fabrication technique was developed and refined. This allows for the fabrication of blades with very high tolerances without the expense of constructing and master plug.
3) The NREL Special Purpose Thin Airfoil family performs much better than NACA 230XX series airfoils with surface roughness.

This new family of airfoils performs closely to the predictions from computer codes, giving greater confidence of blade designers in these codes. It also means that design work can be performed with computer simulations as long as the exact design is accurately replicated in the final production blade.

REFERENCES

[1] J. Tangler and D. M. Somers, "Advanced Airfoils for HAWTS," American Wind Energy Association, Windpower '85, Proceedings, San Francisco CA. August 27-30, 1985. p.45-51.

[2] Joe McCarty, "PROP 93: Interactive Editor and Graphical Display," Wind Power '93, American Wind Energy Association, San Francisco, CA, July 12-16, 1993, p. 495.

[3] R. Eppler and D. Somers, "A Computer program for the Design and Analysis of Low Speed Airfoils," NASA TM-80210, Hampton, VA: NASA Langley Research Center, 1980.

[4] J. Tangler, B. Smith, D. Jager, T. Olsen, "Atmospheric Performance of the Special-Purpose SERI Thin-Airfoil Family, Final Results," Proceedings of European Wind Energy Conference, Spain, 1990.

[5] B. Andrews and K. VanDoren, "A Method for Geometric Modeling of Wind Turbine Blades," Seventh ASME Wind Energy Symposium, New Orleans, LA, Jan. 10-13, 1988, p. 115.

[6] J. Green, "Artificial Roughness Testing," Interoffice memorandum, National Renewable Energy Laboratory, April 7, 1992.

[7] W. Pinkerton, "Long Term Test: Carter 25," Proceedings, Wind Energy Expo '83 and National Conference, American Wind Energy Association, Oct. 17-19, 1983, San Francisco, CA, p 307.

[8] "Fatigue Design Handbook," 2nd Edition, Society of Automotive Engineers, Inc.

[9] Kenneth L. Starcher, Atmospheric Test of Special-Purpose Thin Airfoil Family, Master Thesis, West Texas A&M University, August, 1995.

ACKNOWLEDGMENTS

This work was done under contract to the Solar Energy Research Institute, currently called National Renewable Energy Laboratory, SERI Agreement # ZK-7-06091-1. The test design engineer, Dr. Forrest Stoddard, was instrumental in the proposal preparation, design of the test plan and initial operation of the test site. Bruce Andrews devoted many hours of labor in the blade construction and parametric pitch operation as well as initial operation of the highspeed data acquisition system. Composite Engineering, Cambridge, Massachusetts, expertise was required to fabricate the blades to tolerance. To all these, our thanks.

Testing of a direct drive Generator for Wind Turbines

Lars M. Søndergaard
The Test Station for Wind Turbines
Department of Meteorology and Wind Energy, AMV-762
Risø National Laboratory, P.O.Box 49, 4000 Roskilde, Denmark
Phone: +45 4677 5040, Fax: +45 4237 2965, E-mail: PFV-LMSQ.RISOE.DK

Abstract

The normal drive train of a wind turbine consists a gearbox and a 4 to 8 poles asynchronous generator. The gearbox is an expensive and unreliable components and this paper deals with testing of a direct drive synchronous generator for a gearless wind turbine. The danish company Belt Electric has constructed and manufactured a 27 kW prototype radial flux PM-generator (DD600). They have used cheap hard ferrite magnets in the rotor of this PM-generator. This generator has been tested at Risø and the test results are investigated and analyzed in this paper. The tests have been done with three different load types (1: resistance; 2: diode rectifier, DC-capacitor, resistance; 3: AC-capacitor, diode rectifier, DC-capacitor, resistance).

1. Technical data for the generator

The main data for the direct drive PM-generator is draw up in table 1.

Table 1. Technical data for the direct drive PM-generator (DD600)

Outside diameter	1200 mm	Bearing lubrication	Grease
Outside length	450 mm	Number of phases	3
Number of pair of poles p	25	Thermal protection system	1 Pt 100 + 3 klixon
Nominal rotation speed n_N	68.0 rpm	Connection	Star
Nominal frequency f_N	28.3 Hz	Cooling	Natural wind
Magnet type	Hard ferrit	Insulation class	F (155 °C)
Weight of electro-magnetic	570	Degree of protection	IP65
Bearing types	Spherical roller	Ambient temperature	-15 °C ... +40 °C

The generator is designed for a 27 kW gearless wind turbine.

2. Measurements

The equipment for testing of the generator are described. The PM-generator is connected mechanical to a asynchronous motor by a gearbox. The asynchronous motor is fed by a three phase frequency inverter and the rotation speed of the PM-generator can be change from zero to 68 rpm. Moreover is the PM-generator electrical connected to a load through a three phase power analyzer (VOLTECH PM3000A). The torque at the generator shaft is measured with a calibrated force transducer (DYNAFOR 2T).

The equipment for testing of the PM-generator is outlined in figure 1.

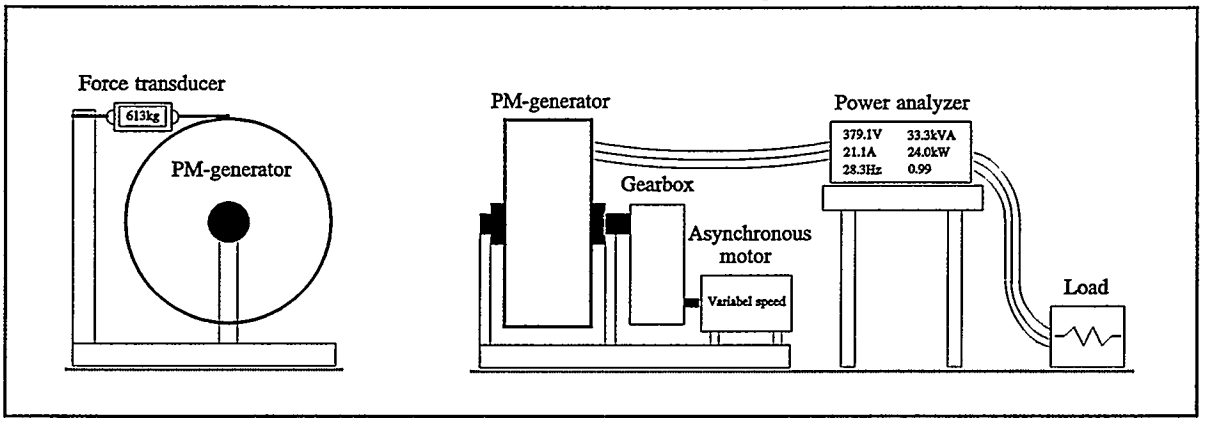

Figure 1. Equipment for testing of the PM-generator

All tests are made at stationary conditions and all the electrical parameters are only valid for a star coupled machine.

2.1. Equivalent diagram for the PM-generator

The equivalent diagram (line to zero) for a star coupled PM-generator is shown in figure 2.

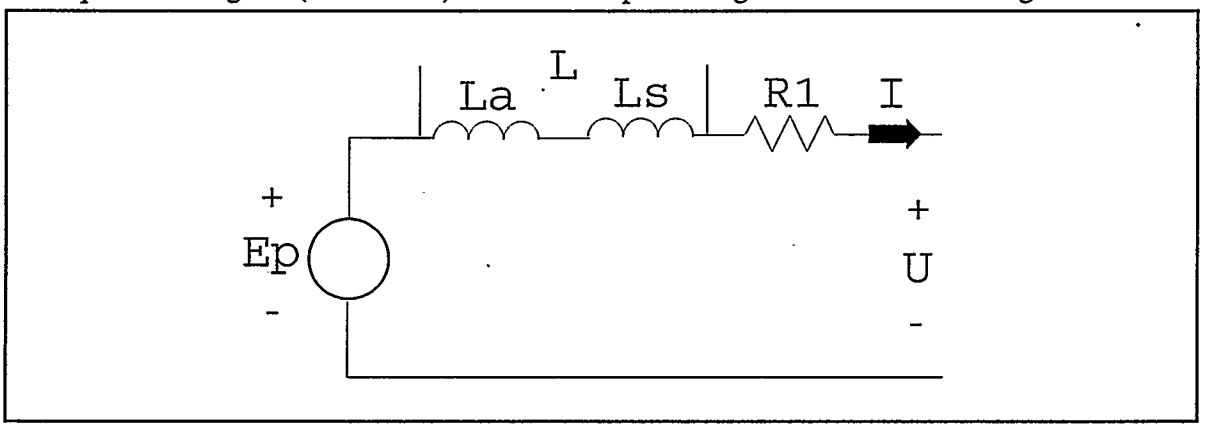

Figure 2. Equivalent diagram (line to zero) for the PM-generator. Resistance R_1=2.23 Ω, Inductance $L=L_a+L_s$=85 mH, E_p = Electromotive force, U = voltage and I = current

2.2. Testing of the generator without an electrical load

It is assumed that the sum of the mechanical loss such as the friction loss and the cooling loss is much smaller than the sum of the copper loss and the iron loss for a direct drive PM-generator.

Therefore at no electrical load is the power given by:

$$P_m = m_d \omega_r = P_e + P_{loss} \approx P_e + P_{cu} + P_{fe} \qquad (1)$$

No load: $P_e = 0 \Rightarrow P_{cu} \approx 0 \Rightarrow P_m \approx P_{fe}$

where: m_d = torque, ω_r = angular velocity, P_e = electrical power, P_m = mechanical power, P_{loss} = loss, P_{cu} = copper loss, P_{fe} = iron loss.

The iron loss and the electromotive force are measured when the load is disconnected from the PM-generator. The measurement results are draw up in table 2.

Table 2. The electromotive force E_p, the mechanical torque m_d and the iron loss P_{fe} as function of the speed n

n [rpm]	E_p [V]	m_d [Nm]	P_{fe} [W]
0.0	0.0	59	0.0
16.9	130.4	96	169
21.8	168.6	96	219
29.0	223.5	96	291
33.8	260.5	96	340
43.3	333.2	96	435
57.2	441.8	102	611
68.4	528.8	102	731

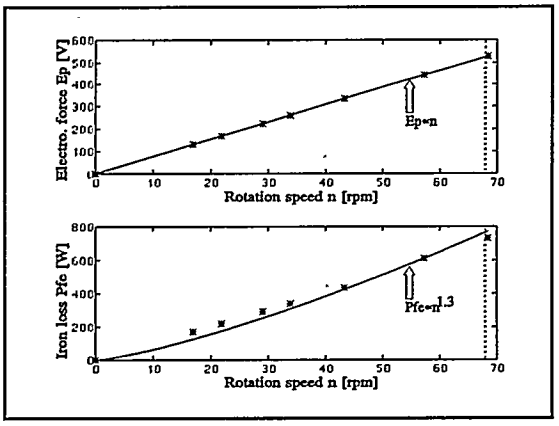

Figure 3. The electromotive force and the iron loss are measured as a function of the speed. (The nominal speed is indicated with a dash line)

The same results are also graphic illustrated in figure 3. Firstly, the electromotive force E_p increase linearly with the speed n. Secondly, the iron loss is less than 800 W which is under 3 % of the nominal power. Finally, the standstill torque is only 59 Nm which is less than 2 % of the nominal torque.

2.3. Testing of the generator with a resistance load

Three 25.6 Ω resistances were connected to the PM-generator in this test. The load diagram is outline in figure 4.

The electrical power and the mechanical power for the PM-generator are measured as function of the rotation speed. It is possible from this measurement to calculated the efficiency of the PM-generator. The results are shown in table 3 and in figure 5.

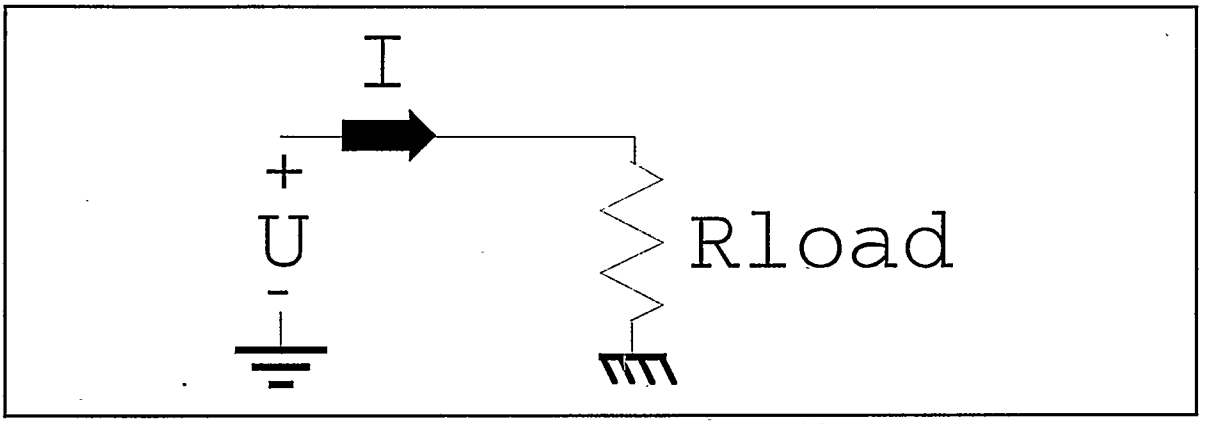

Figure 4. Diagram of the (line to zero) load. The load is a standard resistance (25.6 Ω)

Table 3. Measurement of the mechanical and the electrical power for the PM-generator when the load is a resistance

n [rpm]	U [V]	I [A]	P_e [kW]	P_m [kW]	η [%]
13.1	93.3	3.63	1.01	1.3	80.0
21.6	152.3	5.87	2.68	3.2	84.3
29.2	203.7	7.87	4.81	5.6	85.7
35.4	244.0	9.45	6.92	8.0	86.4
43.0	291.5	11.3	9.90	11.4	86.7
50.2	334.9	13.0	13.1	15.1	87.0
57.3	375.3	14.7	16.5	19.0	87.0
68.6	434.7	17.0	22.2	25.4	87.1

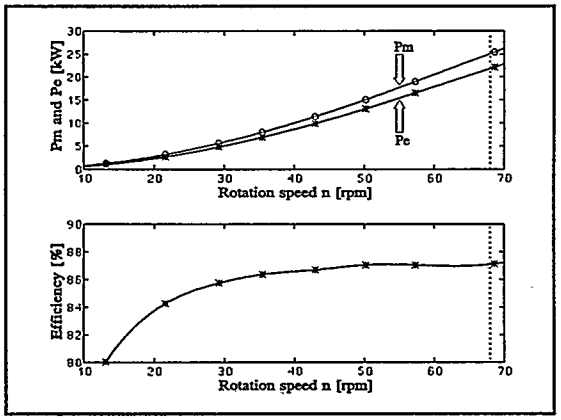

Figure 5. The mechanical power, the electrical power and the efficiency are measured as a function of the speed. (The nominal speed is indicated with a dash line)

The efficiency for the PM-generator is greater than 80 % when the electrical power P_e is higher than 1 kW.

2.4. Testing of the generator connected to a diode rectifier, a DC-capacitor and a resistance

The resistance load is change to a three phase diode rectifier (SKD60/08, 800 V/60 A) connected to a DC-capacitor (367 μF, 900 V) and a resistance (10.5 Ω), see figure 6.

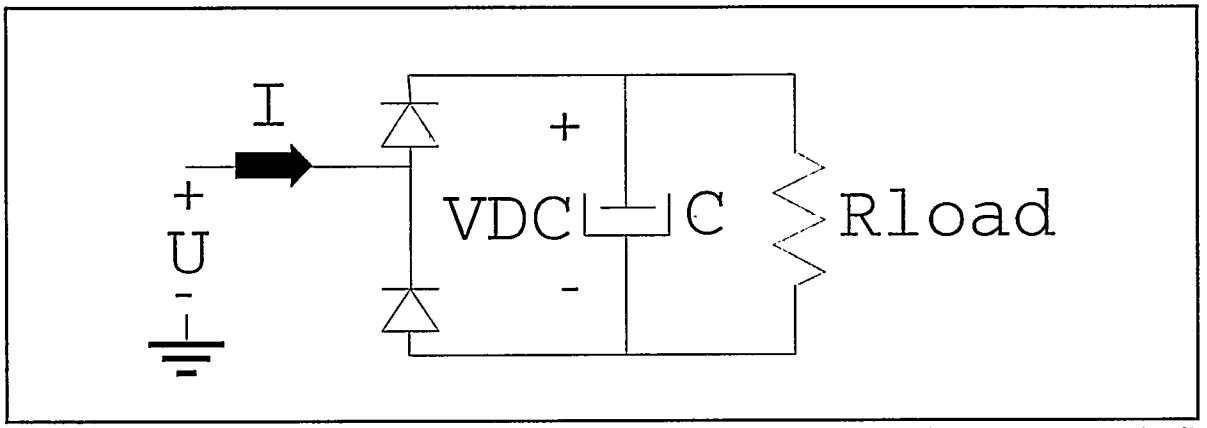

Figure 6. Diagram of the (line to zero) load. The load is a diode rectifier, a DC-capacitor (367 μF) and a resistance (10.5 Ω)

The diode rectifier and the DC-capacitor have to simulated an AC/DC-converter in a normally frequency inverter which will be connected to the PM-generator when it is used in a wind turbine. Table 4 and figure 7 shows the test results.

Table 4. Measurement of the mechanical and the electrical power for the PM-generatoren when the load is a diode rectifier, a DC-capacitor (367 μF) and a resistance (10.5 Ω)

n [rpm]	U [V]	I [A]	P_e [kW]	P_m [kW]	η [%]
14.6	98.9	5.46	1.52	1.9	80.1
22.1	147.1	7.93	3.29	4.0	82.1
36.3	231.9	12.2	7.96	9.6	83.3
43.5	270.6	14.1	10.7	12.8	83.7
50.6	307.2	15.8	13.7	16.3	83.9
57.9	342.4	17.4	16.8	20.0	84.0
67.7	384.4	19.6	21.3	25.4	83.8

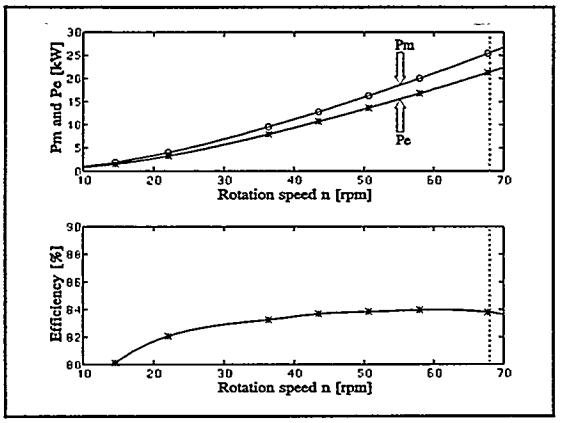

Figure 7. The mechanical power, the electrical power and the efficiency are measured as a function of the speed. (The nominal speed is indicated with a dash line)

The efficiency for the PM-generator at nominal power and speed is reduced 3 % from 87 % to 84 % when the load is change from a resistance to a diode rectifier plus a DC-capacitor and a resistance, see table 3 and table 4.

The efficiency decreased because a diode rectifier together with a DC-capacitor generate harmonics in the phase current which is increasing the copper loss in the stator windings.

3. Optimizing of the AC-capacitor

A three phase AC-capacitor (68 μF) is connected parallel with the load in chapter 2.4 for increasing the DC-link voltage (V_{DC} in figure 6 and figure 8), the nominal electrical power and the efficiency of the PM-generator, see figure 8.

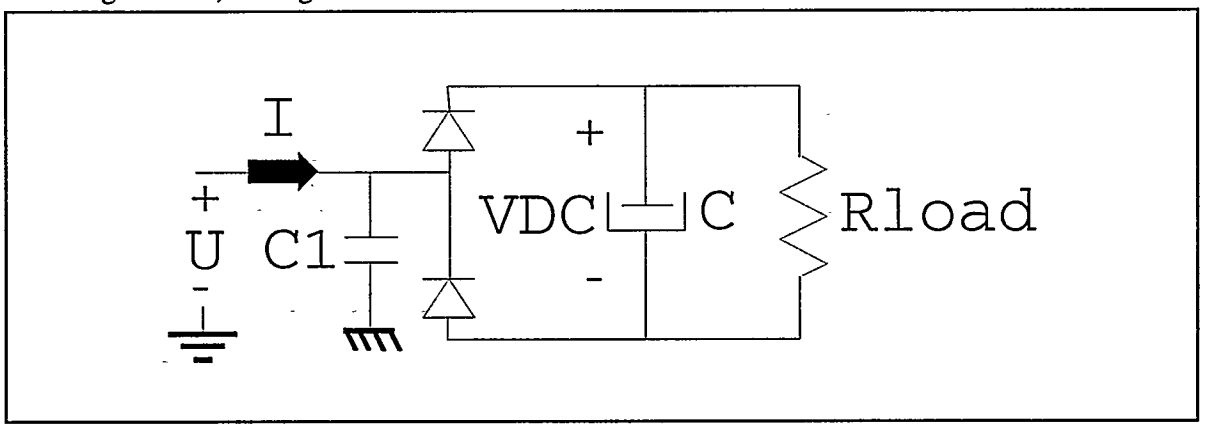

Figure 8. Diagram of the (line to zero) load. A three phase AC-capacitor (68 μF) in parallel with a diode rectifier, a DC-capacitor (367 μF) and a resistance

The test results with and without a three phase AC-capacitor are shown in table 5.

Table 5. Testing of the PM-generator with and without a three phase AC-capacitor (C_1=68 μF) when the electrical power P_e is 20.1 kW. Top: Without C_1, Bottom: With C_1

n [rpm]	U [V]	V_{DC} [V]	I [A]	P_m [kW]	η [%]
63.9	356.8	753	19.9	24.0	83.6
63.9	508.5	1126	15.6	23.1	87.1

The effect of the AC-capacitor is radically because the DC-link voltage V_{DC} increase from 753 V to 1126 V and the efficiency of the PM-generator rise from 83 % to 87 %. A simulation program for optimization of the AC-capacitor is developed. The load resistance in the simulation is choose so the electrical power is proportional with the rotation speed in third because it looks like the power characteristic for a wind turbine. The calculations proved that 68 μF is close to a optimum value for the AC-capacitor, see figure 9.

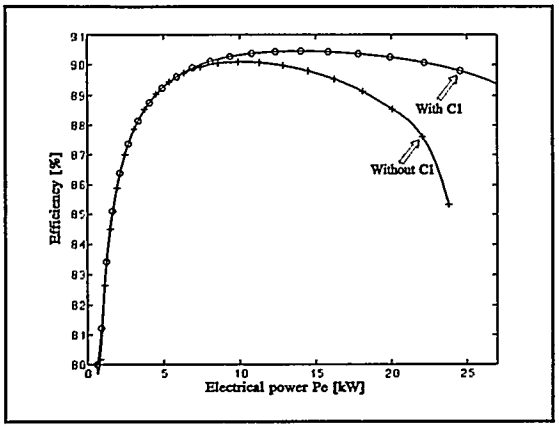

Figure 9. Efficiency for the PM-generator with and without a three phase AC-capacitor (C_1=68 μF) as function of the electrical power

The nominal electrical power and the nominal current at nominal speed can be calculated when a three phase AC-capacitor is connected to the PM-generator.

The calculation is given by:

$$I_N = 21.1A \quad , \quad E_p = 525.5V$$

$$P_{e,N} = 28.0kW \quad , \quad P_{m,N} = 31.6kW \qquad (2)$$

$$\Rightarrow \quad \eta = 88.6\%$$

The rated electrical power for the PM-generator increase more than 19 % from ***23.6 kW*** to ***28.0 kW*** because of the three phase AC-capacitor.

4. Conclusion

The measurements has indicated that this 27 kW prototype PM-generator works properly. The main test results are:

1: The losses at no load are less than 3 % of the nominal electrical power,
2: The torque at standstill is less than 2 % of the nominal torque,
3: The efficiency is greater than 82 % (without AC-capacitor) when the electrical power is over 8 % of the nominal electrical power.
4: The maximal efficiency is better than 90 % when a three phase AC-capacitor is used.

The direct drive PM-generator is suitable for wind turbines because at low load is the efficiency relative high compere to a standard drive train with a gearbox and an asynchronous generator.

Acknowledgments

This paper presents selected results from the project *Testing of a Direct Drive Generator BELT (DD600) for Wind Turbines*. The author acknowledges the financial support to the project from the Danish Ministry of Energy.

References

Søndergaard L., Testing of a Direct Drive Generator BELT DD600 for Wind Turbines, July 1995, Risø-I-908

AIRFOIL AND BLADE OPTIMIZATION FOR A DIRECT-DRIVE, PERMANENT MAGNET WIND GENERATOR

Paolo Dini
Department of Physics and Astronomy, Carleton College, Northfield, MN

Elliott Bayly
World Power Technologies, Inc., Duluth, MN

Abstract

A new blade is designed for a small, variable-speed wind turbine by relying on available theoretical design and analysis methods. The performance predictions are compared to field test measurements and are found to be optimistic. This feedback sheds light on the interpretation of the theoretical results and is used to refine the design method.

Introduction

To meet the needs of the 2.5 billion people without electricity in the world today, it is important to develop an efficient and low-cost wind generator. Because in many parts of the world electrical power is used primarily for lighting, a low-wattage wind turbine is adequate and helps meet the low-cost requirement. This paper is concerned with the optimization of the blade for the Whisper 600 turbine, a 600 Watt, horizontal axis, variable rpm, direct drive, permanent magnet wind turbine with a 2.1 meter diameter rotor. The optimization favors the two-bladed configuration over the three-bladed, again to minimize the cost.

While for this market reduction in size is certainly justifiable from a power demand and economic point of view, it complicates the design process because aerodynamic efficiency deteriorates with a decrease in scale of the rotor and blades. The dynamical scale of a flow is characterized by the Reynolds number, a dimensionless parameter with respect to which the equations of motion of the flow exhibit a convenient similarity. The Reynolds number of a particular blade section, or airfoil, is defined as

$$Re = \frac{cV}{\nu} \tag{1}$$

where c is the chord of the airfoil, V is the velocity relative to the blade at the corresponding radial position, and ν is the kinematic viscosity of the air, or the ratio of the air viscosity μ to its density ρ. Physically, the Reynolds number can be thought of as the ratio of inertial to viscous forces of a flow. As the size of the rotor and blades decreases, the Reynolds number tends to decrease. For the rotor size and rpm characteristic of this 600W turbine, the mean blade Reynolds number varies between Re = 100,000 at cut-in and Re = 500,000 at 25 mph, when the turbine governs out of the wind.

In this regime the drag of the airfoils is susceptible to large increases caused by the so-called laminar separation bubble. As a full discussion of this phenomenon is provided in Ref. 1, it is sufficient here to give a brief description. The creation of lift, and therefore torque for a wind-turbine rotor, depends to a large extent on the pressure recovery afforded by the turbulent boundary layer in the aft-portion of the

blade airfoil. To minimize drag without losing the lift, we want airfoils with as long a laminar region as possible in front and with a short and efficient turbulent pressure recovery in the back. This objective is generally straightforward to achieve at high Reynolds numbers because the boundary layer becomes unstable more easily and, therefore, transition from laminar to turbulent flow occurs over a small portion of the airfoil chord. As the chord Reynolds number decreases, however, the damping effect of viscosity becomes more important relative to the inertial forces of the flow, and the boundary layer becomes more stable. Below Re = 2,000,000, laminar separation usually takes place before the boundary layer has had a chance to transition to turbulence, such that it detaches from the airfoil surface and becomes a free shear layer. Due to its greater instability, the shear layer transitions to turbulence relatively quickly and the flow reattaches through a very dissipative process over a very short distance, forming the laminar separation bubble. As the Reynolds number decreases the bubble becomes progressively longer and thicker until, at Re = 100,000, the drag due to the bubble can be equal to or greater than the drag due to the rest of the airfoil. Because of these facts, below Re = 50,000 it is very difficult to produce lift by means of a stationary wing or blade without making recourse to unsteady vortex shedding–which is what small birds and insects have to do to fly.

A permanent magnet generator charging a battery is essentially freewheeling and presents little load to the rotor up to a cut-in rpm where the rectified output of the generator reaches the battery voltage. The generator input power is then a fairly linear function of rpm up to a point somewhat less than rated power of the wind generator, where the generator goes into current saturation and further increments in rpm result in progressively smaller increases in both input (i.e. absorbed) and output (i.e. produced) generator power. As shown in Fig. 1a, beyond the optimum C_p (15 mph) the rotor rpm increases linearly with wind speed, while the corresponding rotor power increases as the cube of rpm. Thus, matching of generator input power curve and rotor power curve as a function of either wind-speed or rpm is at best a compromise. The resulting behavior of the rotor is well characterized by a tip-speed ratio which is maximum at cut-in, declines to a minimum at a mid-range wind speed, and then climbs again to a maximum permissible in terms of noise and safety, at which point the wind generator must govern out of the wind. In a small wind generator designed for home and farm, reflecting the typical medium to average wind speeds available, the cut-in wind speed is 6-7 mph (2.5-3.5 m/s), the lowest tip-speed ratio of the rotor occurs at 12-16 mph (5.5-7 m/s), and the governing wind speed is 25-30 mph (11-13 m/s). The result is that efficiency of both generator and rotor are highest in the range of moderate wind speeds from 9-20 mph (4-9 m/s), where much of the usable wind energy occurs.

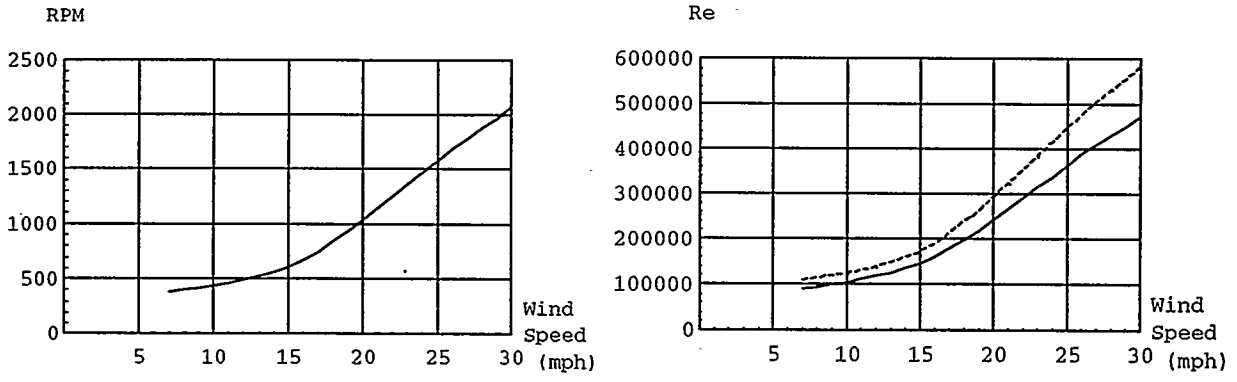

Fig. 1. Typical variation of rpm and of root (solid) and tip (dashed) Reynolds number with wind speed for the Whisper 600 turbine.

Since the airfoil Reynolds number depends on the relative wind, it is affected more by the rpm than by the actual wind speed, causing direct drive turbines to operate most of the time at the low end of the Reynolds number range of their airfoils. Fig. 1b shows the variation in Reynolds number of representative root and tip airfoils for the Whisper 600. Therefore, it becomes especially important for this size turbine to design an airfoil that minimizes the effects of the laminar separation bubbles. A direct consequence of the increase in rpm at the higher wind speeds is that, unlike what happens with constant rpm, stall-regulated rotors, the angle of attack of the relative wind increases between cut-in and approximately 15 mph and then *decreases* beyond 15 mph. Therefore, since the airfoils operate almost entirely within the low-drag laminar "bucket" of the drag polar, a weakly interactive boundary-layer analysis method is sufficient to analyze the airfoils for this type of rotor. The laminar separation bubble model developed in Ref. 1 relies precisely on such a weak interaction analysis method. Another important insight afforded by Fig. 1b is that the Reynolds number does not change significantly between the root and the tip of the blade; rather, the whole blade experiences a significant variation in Reynolds number over its operating envelope. Therefore, it is important to design an airfoil that performs well over the desired Reynolds number range but, unlike what happens for larger, fixed-rpm rotors, it is sufficient to design a single airfoil for the whole blade.

In this paper we discuss the criteria used to determine a "good" low-Reynolds number airfoil for this size turbine, as well as the blade geometry that best matches the airfoil and the overall performance requirements. We then discuss the results of field tests conducted with the optimized geometry and compare them to the performance of a different blade utilizing a Wortmann airfoil.

Design Criteria

The main criterion we used to determine when a rotor design is optimum is the monthly energy production assuming an average wind speed of 9 mph (4 m/s) and a Weibull distribution with a shape factor of 2. The permanent magnet alternator input power curve is given. Other design constraints were required as follows:

a) minimum blade thickness of 12% for strength requirements
b) rotor diameter of 7 ft (2.1 m) for manufacturing purposes
c) cut-in shall be no greater than 7 mph for customer satisfaction
d) maximum L/D (maximum efficiency) should occur at about 15 mph or less to assure good production in low-wind months
e) rpm at governing (25 mph) shall not exceed 1500 rpm for safety and noise concerns
f) starting torque must be sufficient to start turning the rotor and alternator at 7 mph or less, but must be no higher in order not to compromise the holding power of the electrodynamic brake
g) a low-torque, high-rpm design is generally favored to minimize the cost of the generator

Design Methods

The airfoil and blade were both designed using the multi-point inverse design approach originally developed by Eppler and Somers[2] and extended by Selig and Maughmer.[3] Simply put, in this methodology desired performance parameters are specified as input and the geometry that achieves them is returned as the output. It is not quite as clean as that, to be truthful. In both cases the inverse problem is complicated by the fact that no general *direct* solution to the viscous flow equations is known–much less an inverse solution, which is always harder. Nonetheless, the current physical understanding and the available

approximations have been harnessed in remarkably ingenious ways to produce very effective and efficient design methods.

In Eppler's method, characteristics of the inviscid velocity distribution for different operating conditions are prescribed for different segments of the airfoil surface and the airfoil geometry is returned as the solution. Eppler's viscous analysis method then predicts the section characteristics, much as a wind-tunnel test would. Based on the feedback from the viscous analysis, the designer modifies the inviscid characteristics until the desired performance characteristics are achieved. With the Profoil code,[3] Selig extended the inviscid design part by allowing many more parameters to be specified as input, and also allowed some of the boundary-layer properties to be prescribed as well. This is achieved by allowing as many variables to change as there are specified constraints, within the context of a multi-dimensional Newton iteration. In the present design it was especially helpful to be able to fix the desired maximum thickness and moment coefficient at zero lift while iterating on other airfoil characteristics. The blade design program Propid,[4] on the other hand, is based on a direct analysis method as its core, the Prop[5] code. This analysis method utilizes 2-D airfoil data to calculate the induced drag due to the finite length of the blade by means of a blade element method. As the blade geometry is changed, the Prop code calculates the resulting power produced by the rotor in the form of power coefficient as a function of tip-speed ratio. Also Propid uses a multi-dimensional Newton iteration to satisfy as many constraints as are imposed by the designer.

It is clear that, although they are very ingenious and very powerful, these design methods are not independent of the analysis methods or flow models. By making very efficient use of what we do understand about aerodynamics, these programs cut down design time by several orders of magnitude. Yet, without reliable analysis methods (or wind-tunnel tests) to verify the performance, their usefulness is limited. The original Eppler analysis method is an adequate analysis tool for high Reynolds number flows at low angles of attack. As the angle of attack increases, however, the conventional boundary-layer approximations break down and it becomes necessary to utilize viscous/inviscid interaction methods such as those of Refs. 6 and 7. In the present case, the angles of attack are always small over the outer two-thirds of the blade, but the Eppler analysis method breaks down due to the presence of large laminar separation bubbles that form around the mid-chord, since it cannot analyze them. In Ref. 1 the Eppler analysis method is supplemented with a bubble model to take the effects of bubbles into account down to Reynolds numbers of 50,000. This model utilizes the transition prediction method described in Ref. 8. The Bubble code was used both to generate feedback on the performance of candidate airfoils during the airfoil design process as well as to generate the 2-D data used by Propid.

If the Bubble code is to be used as a wind tunnel, to differentiate between good and bad candidate airfoils, then we need to make sure that its predictions are accurate and reliable. In addition to the comparisons presented in Ref. 1, Fig. 2 shows the drag polars of the Clark-Y and S4233 airfoils at Re = 100,000 and 200,000. The agreement between the theoretical predictions and the measurements is very good. It should be noted that, since the Bubble code does not use a global viscous/inviscid iterative method, adjacent angles of attack are entirely independent and the resulting drag polars are not necessarily smooth. This effect is magnified at lower Reynolds numbers by the presence of large bubbles. The Clark-Y does much better than the S4233, but that is mainly due to the different thickness: 11.8% of the Clark-Y vs. 13.7% of the S4233. The actual experimental coordinates were used for the analyses. The somewhat thicker trailing edge of the S4233 causes the formation of very thick bubbles on the lower surface, near the trailing edge. Such bubbles can extend far into the wake and, at Re = 100,000, are mainly responsible for the large "bump" in the drag that can be observed in the middle of what should be the low-drag bucket of the polar. In other words, at these low Reynolds numbers ensuring a very thin and sharp trailing edge is absolutely crucial.

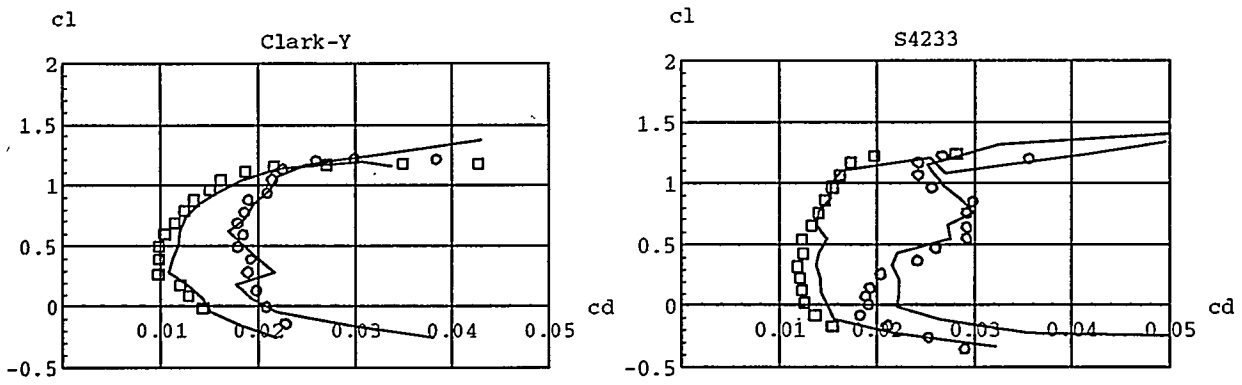

Fig. 2. Comparison of the aerodynamic characteristics of the Clark-Y and the S4233 airfoils predicted by the Bubble code (solid line) with the data of Ref. 9 (symbols) at *Re* = 100,000 (circles) and 200,000 (squares).

Analytical Results

The blade of the Whisper-600 turbine currently utilizes the Wortmann FX 63-137 airfoil. Although the power generated is satisfactory, this is a high-lift airfoil. It was felt that a lower lift airfoil than the FX 63-137 could both improve power output and electrodynamic brake effectiveness of a high speed permanent magnet alternator. It seemed beneficial, therefore, to conduct a careful study of the aerodynamic characteristics necessary to satisfy the desired performance constraints and to design an airfoil and blade taylored to this turbine. Because the angle-of-attack operating envelope of the airfoils for this type of turbine is fairly narrow, we can take advantage of the lower drag produced by a thinner airfoil since its narrower laminar bucket does not harm the performance. A thickness of 12%, as opposed to the 13.7% thick FX 63-137 airfoil, is adequate for structural strength. The design was conducted by generating a candidate airfoil with the Profoil code and producing 2-D drag polars with the Bubble code. Keeping to the specified constraints while optimizing the theoretical performance indices resulted in the PD1204 airfoil. As shown in Fig. 3, this airfoil has a much lower drag than the FX 63-137 at *Re* = 100,000. Its lower lift and lower drag resulted in the prediction by Propid of a significantly higher tip-speed ratio.

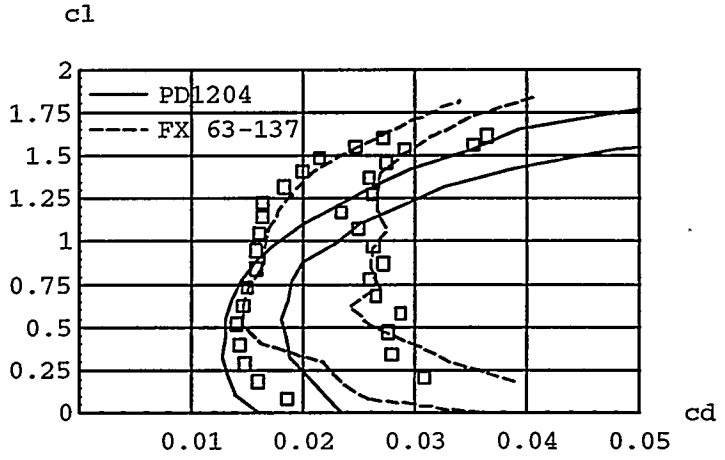

Fig. 3. Comparison of the predicted aerodynamic performance of the PD1204 and the FX 63-137 airfoils. Predicted performance of the FX 63-137 airfoil is also compared to the measurements of Ref. 9.

For a fixed blade geometry, these data were then utilized in the Propid code run in the direct or analysis mode. Because at low Reynolds numbers the drag coefficient changes so drastically with variations in Reynolds number, the operating range was subdivided into twenty-four different Reynolds number intervals corresponding to wind speeds between 7 and 30 mph in 1-mph increments. The variation of Reynolds number with wind speed follows that shown in Fig. 1b. For each Reynolds number, Propid produced a different power coefficient vs. tip-speed ratio curve, as shown in Fig. 4. Once these curves were translated into power vs. rpm curves, Fig. 5, they could be matched to the generator input power curve, thereby obtaining the rotor power curve vs. wind speed. Finally, utilizing the assumed wind regime discussed above and an assumed generator efficiency of 80%, we could estimate the average monthly power output for the airfoil in question. The monthly power output of the rotor utilizing the PD1204 blade was predicted by Propid to be 94 kWh, as opposed to 86 kWh of the FX 63-137 blade.

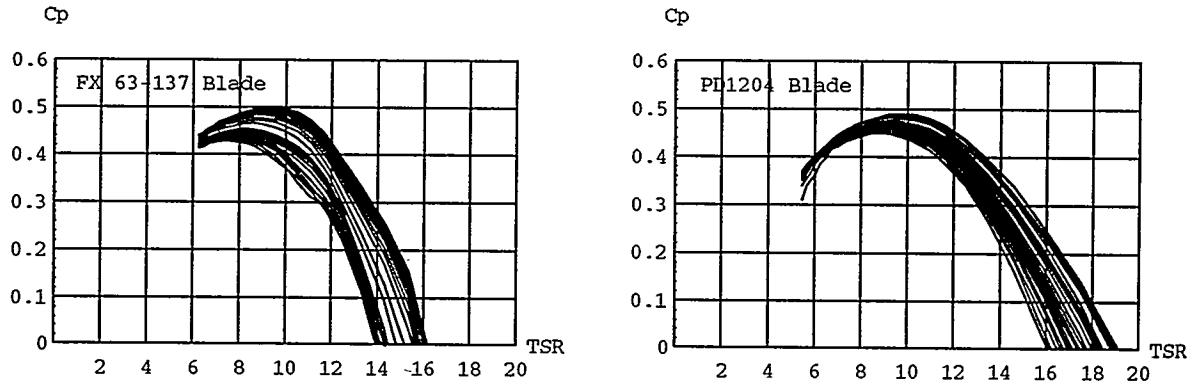

Fig. 4. Power coefficient vs. tip-speed ratio at various Reynolds numbers for the FX 63-137 and the PD1204 rotors.

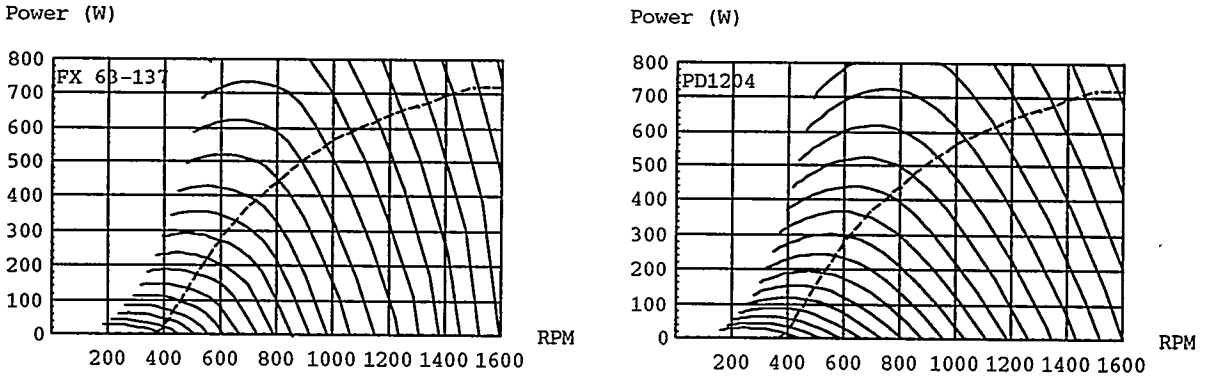

Fig. 5. Power vs. rpm at various wind speeds for the FX 63-137 and the PD1204 rotors. Dashed line is the generator input power curve.

Once the theoretical predictions indicated that the airfoil had been optimized, we could turn to the blade shape. The blade was approximated by 10 elements and Propid was used to optimize the twist and chord of each element. This was done essentially in two steps: the twist was adjusted incrementally for each element, Propid was run in the direct mode, and the average monthly power output was used as a figure of merit. As expected, the resulting twist distribution is such that each blade element is operating near the maximum performance angle of attack (max L/D) most of the time. The chord distribution was then

obtained by utilizing the inverse design capability of Propid, i.e., it was made to depend on a desired distribution of axial induction factor. The axial induction factor is defined as

$$a = \frac{U - V}{U} \tag{2}$$

where U is the wind velocity and V is the velocity at the plane of the rotor, and gives a measure of the blockage that the rotor presents to the oncoming wind. Thus, lowering the axial induction factor causes Propid to generate a blade with a smaller chord. The axial induction factor of each blade element was varied, again using the monthly power output to determine when the optimum value for each element had been reached. The overall limit on how small to make it was set by the maximum allowable rpm of 1500 at 25 mph. As shown in Fig. 6, this process resulted in an almost constant distribution of a at the maximum performance condition of the rotor, while at higher rpms a increases in the outer portion of the rotor. In geometrical terms, this means that the effective solidity of the rotor changes both as a function of radial location along the blade and of rpm.

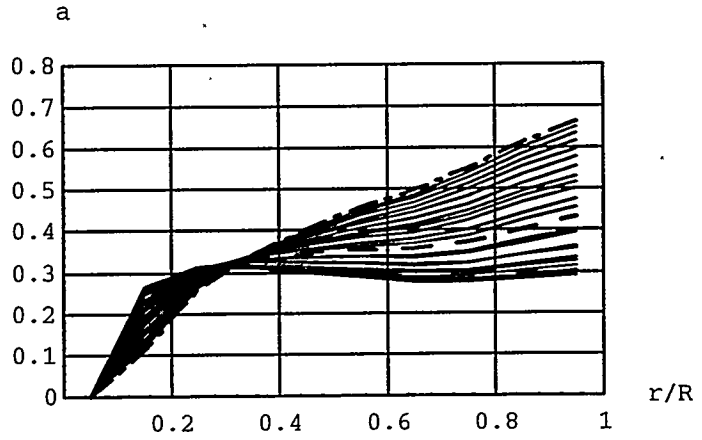

Fig. 6. Distribution of axial induction factor for the PD1204 blade at different rpms between cut-in (dashed) and govern (dot-dashed).

Field Test Results

The possibility to verify the theoretical predictions with field tests has greatly enhanced the effectiveness of this study. As shown in Fig. 7, we did not obtain the expected performance improvement using the PD1204 instead of the FX 63-137 airfoil. The size of the symbols is indicative of the scatter of the test data. Part of the difference we attributed to a very turbulent wind test location that resulted in frequent starting and stopping of the rotor. This favored the heavier FX 63-137 blade with its greater inertia and its greater start-up torque. Another factor we had failed to consider was that the lighter weight of the PD1204 blade caused the Whisper 600 to govern at a slightly lower wind speed than when the same machine was mounted with the FX 63-137 rotor. At the time of publication testing was being moved to the much better wind conditions at the main Wind Power Technologies test site where we intend to defeat the governor (the Whisper 600 survives winds over 40 mph full into the wind) during data gathering. We will run several different sets of the PD1204 blades, both 2- and 3-bladed rotors, to check whether or not shape differences due to manufacturing tolerances are affecting results.

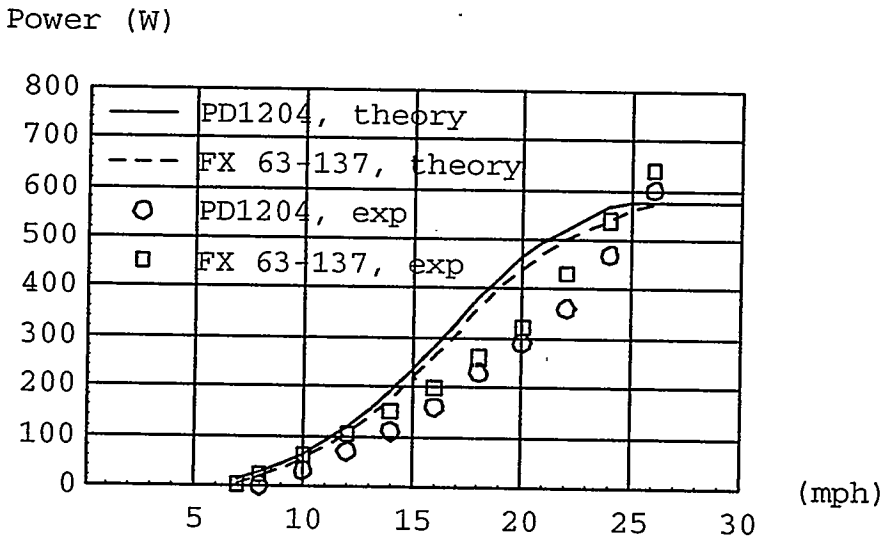

Fig. 7. Comparison of theoretical predictions of power curves with field test data for the PD1204 and the FX 63-137 blades.

These measurements highlighted the weaknesses of the theoretical model. The main weakness appears to be the fact that the Prop code, and therefore Propid also, both assume steady-state conditions; thus, they cannot account for the start-up behavior of the rotor. For this turbine, this means that whenever the wind is at the cut-in speed the program assumes the rotor to be spinning at the cut-in rpm (~370). If the wind is not steady, however, the rotor may spend a significant fraction of the time at a lower rpm. At such a lower rpm, in turn, the relative angle of attack of the flow is much higher than what the 2-D data account for. Thus, some judgement and experience must be used in estimating the necessary start-up torque for the corresponding unsteady and high-lift conditions of the blade. Accordingly, a new airfoil was designed, the PD1271. As shown in Figs. 8-10, this airfoil lies about half-way between the PD1204 and the FX 63-137, yet it still has the low drag of the PD1204. Fig. 9 shows the L/D ratio of the three airfoils discussed, at *Re* = 100,000 and 200,000. Although at the time of this writing no test data were yet available for the performance of the PD1271 blade, the predicted monthly power output of the PD1271 rotor is 93 kWh.

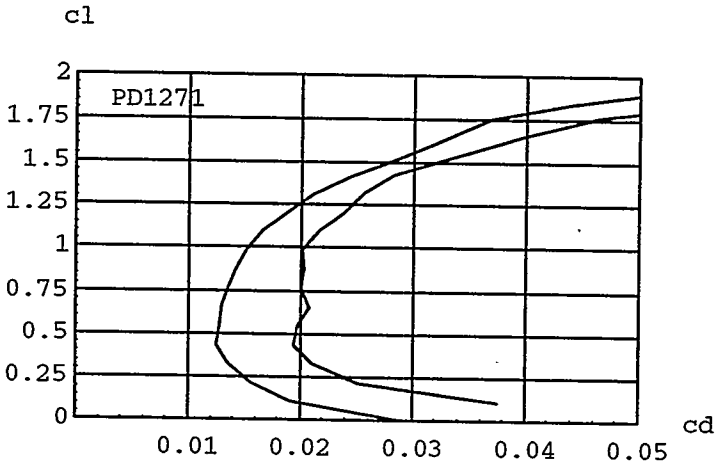

Fig. 8. Aerodynamic characteristics of the PD1271 airfoil at *Re* = 100,000 and 200,000.

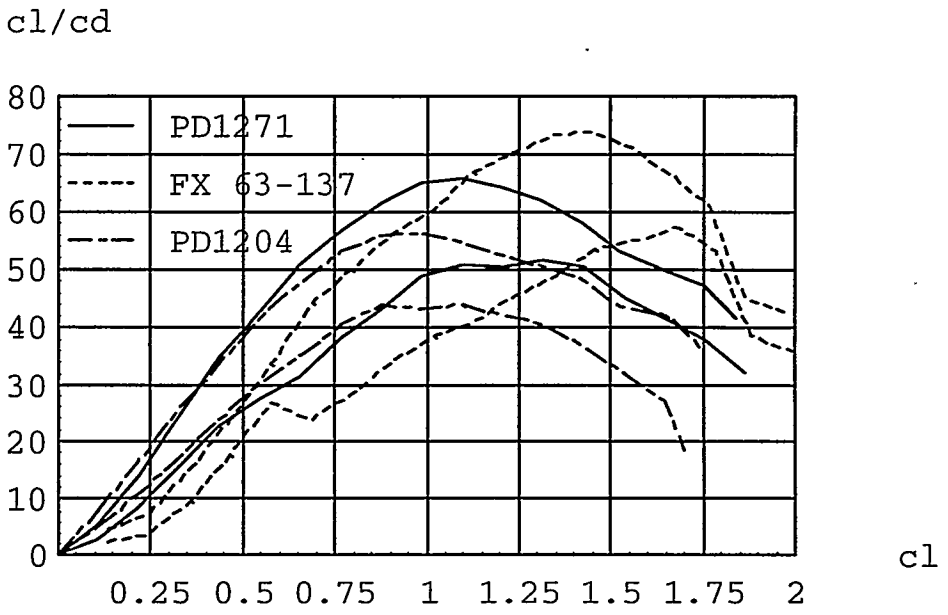

Fig. 9. Comparison of the theoretical lift-drag ratio for the three airfoils discussed, at *Re* = 100,000 and 200,000.

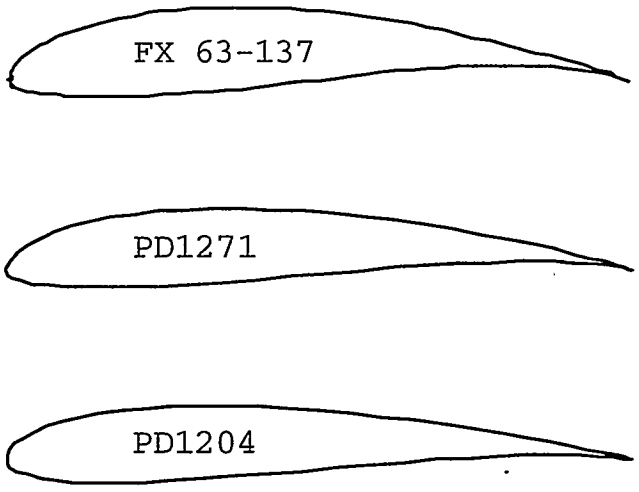

Fig. 10. Comparison of the geometry of the three airfoils discussed.

Conclusion

In this study we have developed a design process for variable rpm, horizontal axis, permanent magnet wind generators. We find that the design of an efficient low-Reynolds number airfoil is crucial for the size turbine examined. Comparison of the theoretical predictions to the measured power generated indicates that the rotor performance prediction model should be improved in its ability to account for start-up and unsteady conditions. This feedback was very valuable in developing a new airfoil and blade, and additional test data for the new blade will be used to refine further the calibration and interpretation of the model. As an interesting general result we found that, because of Reynolds number effects, the Whisper 600 is near the smallest-size turbine possible for achieving a meaningful return on the capital cost in power production.

Acknowledgement

This research was supported by World Power Technologies, Inc.

References

1. Dini, P., and Maughmer, M. D., "Locally Interactive Laminar Separation Bubble Model," *Journal of Aircraft*, Vol. 31, No. 4, July-August 1994, pp.802-810.
2. Eppler, R., and Somers, D. M., "A Computer Program for the Design and Analysis of Low-Speed Airfoils," NASA TM-80210, 1980.
3. Selig, M. S., and Maughmer, M. D., "Generalized Multi-Point Inverse Airfoil Design," *AIAA Journal*, Vol. 30, No. 11, November 1992, pp. 2618-2625.
4. Selig, M. S., and Tangler, J.L., "Development and Application of a Multipoint Inverse Design Method for Horizontal Axis Wind Turbines," *Wind Engineering*, Vol. 19, #2, 1995. pp. 91-105.
5. Tangler, J.L., "Horizontal-Axis Wind Turbine Performance Prediction Code PROPSH," Wind Energy Research Center, Rocky Flats Plant, Golden, CO, 1983.
6. Drela, M., and Giles, M. B., "Viscous-Inviscid Analysis of Transonic and Low-Reynolds Number Airfoils," *AIAA Journal*, Vol. 25, No. 10, October 1987, pp.1347-1355.
7. Dini, P., and Coiro, D., P., "The Prediction of Airfoil Stall," Status Report to the National Renewable Energy Laboratory, September 1995.
8. Dini, P., Selig, M. S., and Maughmer, M. D., "Simplified Linear Stability Transition Prediction Method for Separated Boundary Layers," *AIAA Journal*, Vol. 30, No. 8, August 1992, pp. 1953-1961.
9. Selig, M. S., Donovan, J. F., and Fraser, D. B., *Airfoils at Low Speeds*, Soartech 8, H. A. Stokeley Publisher, 1989.

CUSTOMIZED DSP-BASED VIBRATION MEASUREMENT FOR WIND TURBINES

Niels E. LaWhite
Kenneth E. Cohn,
Second Wind Inc.
366 Summer Street
Somerville, Massachusetts 02144
USA

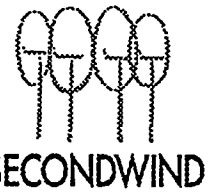

ABSTRACT

As part of its Advanced Distributed Monitoring System (ADMS) project funded by NREL, Second Wind Inc. is developing a new vibration measurement system for use with wind turbines. The system uses low-cost accelerometers originally designed for automobile airbag crash-detection coupled with new software executed on a Digital Signal Processor (DSP) device. The system is envisioned as a means to monitor the mechanical "health" of the wind turbine over its lifetime. In addition the system holds promise as a customized emergency vibration detector.

The two goals are very different and it is expected that different software programs will be executed for each function. While a fast Fourier transform (FFT) signature under given operating conditions can yield much information regarding turbine condition, the sampling period and processing requirements make it inappropriate for emergency condition monitoring.

This paper briefly reviews the development of prototype DSP and accelerometer hardware. More importantly, it reviews our work to design prototype vibration alarm filters. Two-axis accelerometer test data from the experimental FloWind vertical axis wind turbine is analyzed and used as a development guide. Two levels of signal processing are considered. The first uses narrow band pre-processing filters at key fundamental frequencies such as the 1P, 2P and 3P. The total vibration energy in each frequency band is calculated and evaluated as a possible alarm trigger. In the second level of signal processing , the total vibration energy in each frequency band is further decomposed using the two-axis directional information. Directional statistics are calculated to differentiate between linear translations and circular translations. After analyzing the acceleration statistics for normal and unusual operating conditions, the acceleration processing system described could be used in automatic early detection of fault conditions.

BACKGROUND

Second Wind has been supplying computerized windfarm monitoring hardware and software called the Second Wind System since 1985. Collectively, these systems now monitor over 3,000 wind turbines worldwide performing numerous functions.[1] In 1993, with support from the National Renewable Energy Laboratory (NREL), Second Wind began development of a completely redesigned and enhanced wind farm monitoring system which is called the Advanced Distributed Monitoring System (ADMS). The ADMS is comprised of: the on-site Supervisor computer, the off-line Project Analyst software, Communicating Turbine Monitors (CTMs) at wind turbines, meteorological stations, and electrical substations, and the system communications network. The Supervisor communicates with the CTMs in the field and Project Analyst in the office so that managers can respond as quickly and as effectively as possible to operational issues as they arise. In conjunction with the development of the ADMS, Second Wind is designing a vibration monitoring system for installation at each wind turbine at the option of the customer. The DSP and accelerometers are thus the core of an enhanced ADMS capable of providing a wide range of new functions.

A DSP is a specialized type of microprocessor designed to perform digital math at high speed. The type of DSP used in the monitoring system is from the family of low-cost high-production devices that are at the heart of a growing number of consumer products. The DSP used in the ADMS is optimized for integer math and is capable of 10 million integer operations per second.

The accelerometers used are low-cost due to their high volume application in automobile air-bag systems. They incorporate multiple microscopic masses suspended on etched silicon suspension beams. The mass deflection is proportional to acceleration. The multiple masses are electrically connected to form one pole of a capacitor. The second pole is formed by stationary silicon masses each proximate to a deflecting element. Together, the system measures acceleration using a circuit with generates a frequency controlled by the varying capacitance.

ADMS VIBRATION MONITOR OVERVIEW

Figure 1 shows a typical ADMS with an integrated vibration monitor. This configuration is typical of those envisioned for a commercial system but the computer architecture is open. While this case shows the DSP and turbine controller as separate devices, they can be combined. In addition to the DSP, the system uses a low-cost microprocessor which is needed to handle user I/O and to store and transmit data. The first prototype DSP system designed adds a modest amount of I/O sufficient to control a wind turbine. So in the first prototype the controller is the DSP vibration monitor. For this prototype, delivered to FloWind Corporation (FloWind) of San Rafael, California, the controller/DSP also monitors three phases of generator current and voltage. The DSP/controller/vibration monitor also derives power, frequency, phase angle, et. al. and performs all of the typically required utility monitoring/generator control functions. Since the DSP measures generator power with an effective response of about 25 Hertz, it can discern power /torque fluctuations due to torsional vibrations. The concurrent use of the DSP to monitor power/torque in the generator is yet another aspect of the ADMS project. Many of the signal processing concepts introduced here in connection with vibration monitoring will also be used for power/torque monitoring in the completed system.

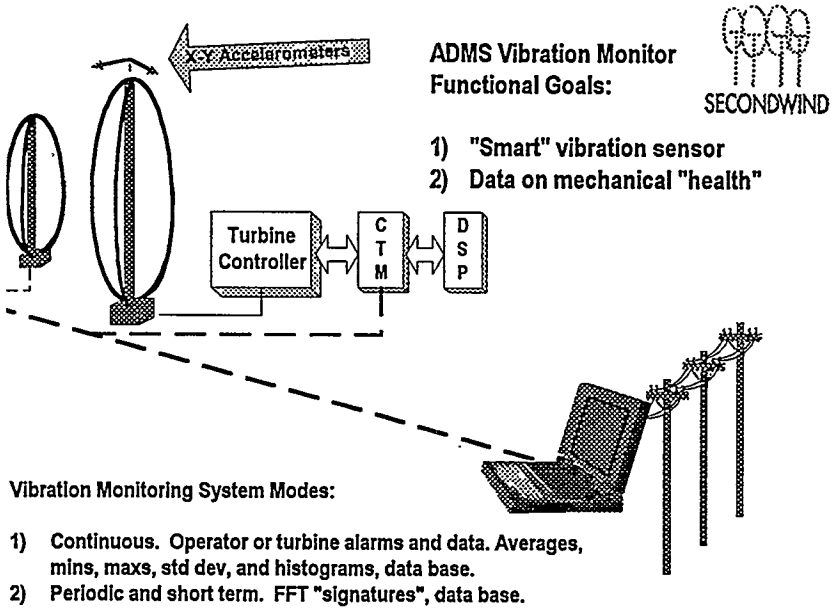

Figure 1. ADMS Vibration Monitor Overview

As shown in Figure 1, the ADMS uses a communications network to link the system nodes to the computer we call the Supervisor. In the completed and fully implemented ADMS, the Supervisor collects data from all of the individual turbines CTMs and DSP nodes throughout the life of the project. Collected data is then always available to the facility operator or owner.

The vibration measurement sensor is a two-axis accelerometer mounted at or near a mainshaft bearing. For the horizontal axis wind turbine (HAWT) case, the sensor would be mounted as close to the rotor as possible. For the vertical axis wind turbine (VAWT) there are two possibilities, corresponding to the upper and lower torque tube/tower bearings. There are advantages to sensing rotor modes at the upper bearing but potential maintenance costs as well. The FloWind field tests of their new Extend-Height-Diameter (EHD) turbine include a sensor of this type at the top bearing. FloWind has shared this test data with Second Wind to help in the development of the ADMS vibration monitor. The analysis of the FloWind EHD test data forms the basis of the results reported here.

For both HAWTs and VAWTs, the active plane of the sensor is the horizontal plane. One axis is aligned with the turbine bedplate for the HAWT case. The second measurement axis is 90 degrees from the first: cross-wind for a properly operating turbine. The two axis device is connected to input channels of the DSP through an Analog to Digital (A/D) conversion stage. The DSP is capable of signal processing tasks such as FFTs, filters, or histograms. However, the DSP serves as a dedicated preprocessor and is not user configurable. At any point in time, the DSP must be operating in one of a small number of pre-defined modes.

There are two functional goals for the system; "smart" vibration sensing and the collection of data on mechanical condition. Collection of data on mechanical condition or "health" can be handled on periodic and short term basis. For this purpose, the vibration monitor will, under control of the central computer Supervisor, load and execute code to perform FFTs or histograms for the relevant signals. This will be stored in the data base for later use. The more challenging goal is to create a "smart" vibration sensor. The primary purpose of the system is to protect the turbine from a potentially catastrophic or otherwise damaging failure. The secondary purpose is to provide maintenance personnel with a new and continuous source of information on the vibration characteristics of their equipment.

The balance of this paper is a description and report on the software which we propose as the core of the DSP-based smart vibration sensor. The basis of this work is a complete software model of the system written on a PC using MatLab. We have implemented a development environment for the DSP for which the MatLab simulation software faithfully produces the same outputs that would have been generated by the DSP board installed in the turbine. The input for the simulation was the data from FloWind's field tests.

MATHEMATICS OVERVIEW OF DIGITAL FILTERS

Figure 2 presents an overview of the mathematics implemented by the DSP system. The X and Y acceleration channels are sampled by the 12-bit A/D converter at 10.5 kHz. The sampling "layer" software applies anti-alias and offset-null filtering. The balance of the software calculates numerous results corresponding to the different functions. These functions are total acceleration intensity (low pass filtered), band pass filtered frequency components, and directional decomposition of filtered frequency components.

The most fundamental functional result is the continuous calculation of total acceleration intensity. Figure 2 shows this value calculated for the range between 0 and 10 Hertz because the FloWind data was taken at

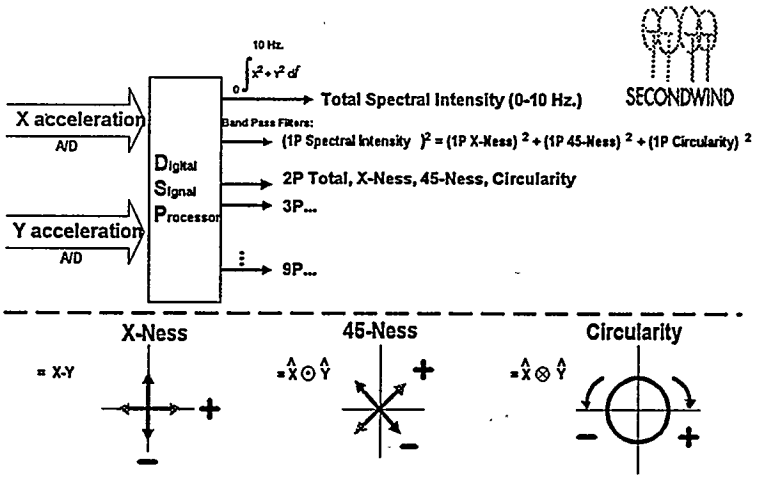

Figure 2. DSP Mathematics Overview

20 Hertz. Since the filtered acceleration measurement response of the actual DSP system will be 25 Hertz, the total spectral intensity calculation will span 0 to 12.5 Hertz. (Note that the selection of accelerometer sensors with good response to 0 Hertz is critical for large slow-moving wind turbines.) The physical interpretation of this signal is a slowly changing value corresponding to the magnitude of the total (two-axis) acceleration vector.

The simulated DSP is also calculating band pass filtered frequency components at a selected set of frequencies. For this work we selected only basic nP turbine operating frequencies. The EHD can operate at two speeds but we selected operating data for one speed only. The rotor speed is approximately 51.8 RPM so the 1P frequency is 0.86 Hertz. As an initial test of these concepts, we selected the 1P, 2P, 3P, 4P, 5P, 6P, and 9P frequencies for this three-blade VAWT. Fifth order Butterworth filters with 0.1 Hz. roll-off were selected after considerable experimentation. The first result calculated is total (two-axis) acceleration intensity for each of the nP frequencies. The physical interpretation of this signal might be the filtered value of the magnitude of the two-axis acceleration vector corresponding to the specific nP frequency

So far the DSP calculations have taken the X and Y directional components and computed total intensities with magnitude only. However, since our goal is to retain the important directional information in the X and Y acceleration signals a means to compute and summarize this was needed. We chose a method used which decomposes the time varying directional information (phasors for X and Y acceleration) into three mutually orthogonal values which uniquely summarize the physical measurements. In the decomposition, each nP total intensity is furthered processed to calculate values which we call "X-Ness", "45-Ness", and "Circularity". X-Ness is the difference between the energy in the X acceleration signal and the energy in the Y acceleration signal, $|X^2| - |Y^2|$. Its physical interpretation is depicted in the lower left section of Figure 2. Positive X-Ness means translation along the X axis, from left to right. Negative X-Ness is vertical translation, up and down in this case. 45-Ness is calculated as the phasor dot product of the X and Y components. Its physical interpretation is depicted in the center section of Figure 2. Positive 45-Ness indicates translation along the diagonal from upper right to lower left. Negative 45-Ness is diagonal translation from upper left to lower right as shown in the figure. Lastly, Circularity is calculated as the magnitude of the cross product of the X and Y phasors. Positive circularity is shown in Figure 2 as circular motion in the clockwise direction and negative as counter-clockwise. As the decomposition is orthogonal, it can be shown mathematically that each total nP intensity squared is the sum of the squares of the three

decomposed signal intensities

RESULTS FROM PROCESSING OF FLOWIND EHD TEST DATA

FloWind supplied data for turbine operation throughout a wide range of wind speeds in blocks of about three minutes for each test file. The sampling and recording rate was 20 Hertz. For each test run, we passed the raw X and Y accelerometer data through our MatLab simulation. The program output the time series values for the filtered data at the eight nP frequencies and also for the total acceleration intensity. Each nP frequency value was also decomposed as described above. The MatLab program also processed the power signal data for which it calculated the same nP band pass filter values. This was done to evaluate the power/torque system discussed above. The results of the DSP simulation are quite interesting. For each filtered time series value, we computed the average over the three minute interval and plotted these results as a function of increasing (average) wind speed.

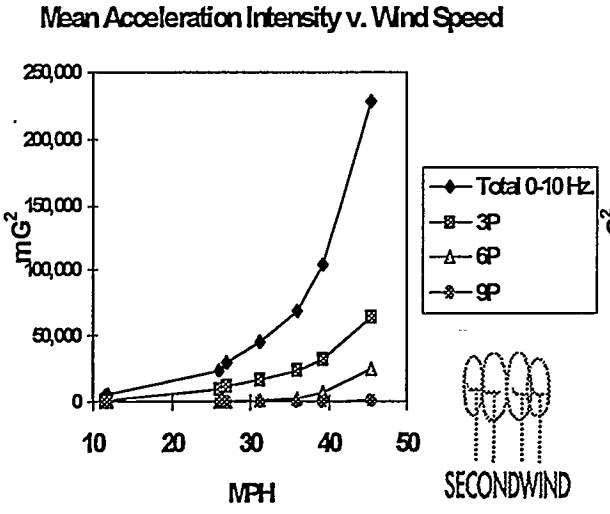

Figure 3. Total, 3P, 6P, and 9P Band Pass Filters

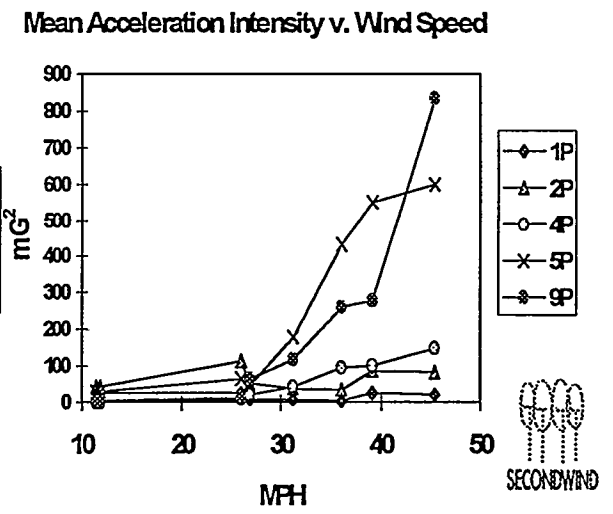

Figure 4. Low Level nP Filter Intensities

Figure 3 plots the total acceleration intensity and the 3P, 6P, and 9P filtered intensities. Since the intensity values range from 220,000 milli-G^2 (units of Gravity^2/1000) to less than 50 depending upon the nP filter frequency, the plots are divided among the higher and lower signal levels. The results show that the total, 3P, and 6P filters have intensities which increase geometrically with wind speed.

Figure 4 plots the same results for the 1P, 2P, 4P, 5P, and again for the 9P on a much finer scale in accordance with their levels. It can be seen that the 9P also increases geometrically but on a much smaller scale. The signal intensity for the 5P filter does not follow the same pattern but does markedly increase. The 1P, 2P, and 4P signal intensities change very little as the wind increases. The lowest level signal is the 1P suggesting a rotor well balanced throughout the range of wind speeds.

Figure 5 plots the results for the averaged decomposed X-Ness for the 3P, 6P and 9P signals. The other signals have very small levels. Both the intensity and sign of the X-Ness characteristics change for this data. The physical interpretation and level of significance of this result is not known.

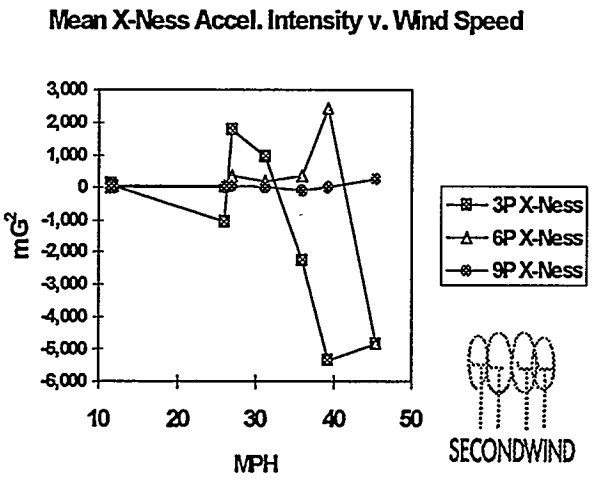

Figure 5. Mean X-Ness Intensities

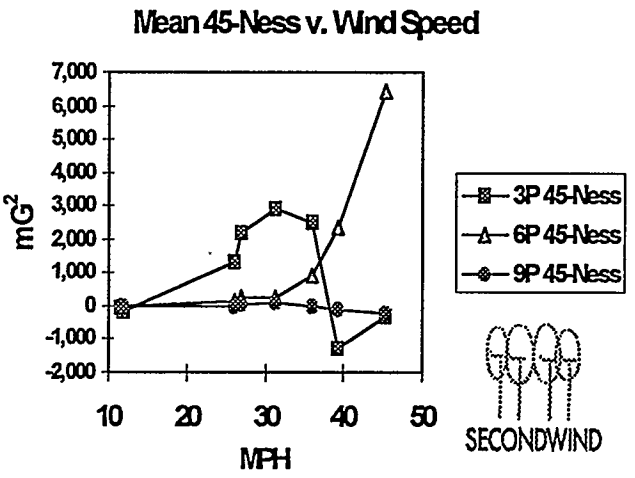

Figure 6. Mean 45-Ness Intensities

As above, Figure 6 plots the 3P, 6P, and 9P results for 45-Ness. As above the other signals have very small levels. Note the 6P signal increases geometrically whereas the 3P signal shows varying behavior. Again, we do not yet know the physical significance of this result.

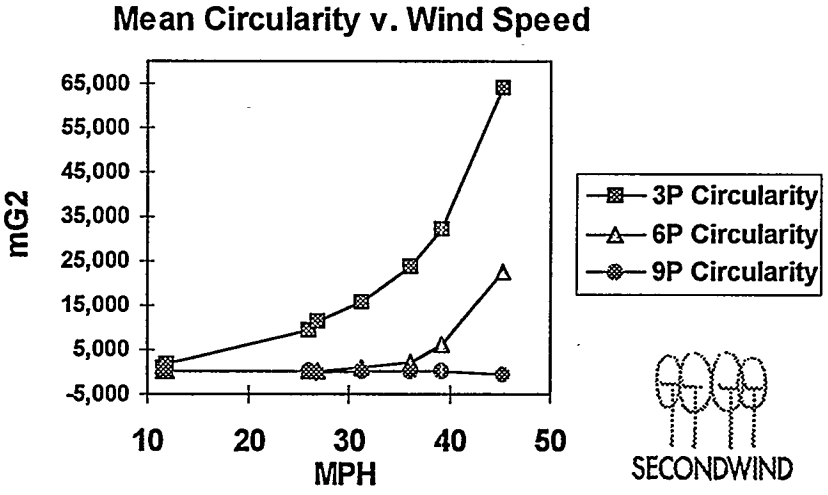

Figure 7. Mean Circularity Intensities

Figure 7 plots the 3P, 6P, and 9P results for Circularity. Note the 3P and 6P signal increases geometrically with the 3P dramatically greater in intensity. So we see that the 3P circularity clearly dominates, a logical result for a three-blade vertical axis machine.

SIGNAL PROCESSING TO DERIVE SIGNATURES

Following traditional concepts in the mechanical engineering literature of vibration monitoring[2], we wrote

a program to generate a polar plot or "Lysajous" signature for the two-axis FloWind data. As input, the program takes the band-pass filtered frequency components; as output, the program creates a simplified average acceleration signature as an X-Y plot for the time interval of one revolution period. Since these plots account for the average activity at only the selected frequencies, the effects of noise and stochastic

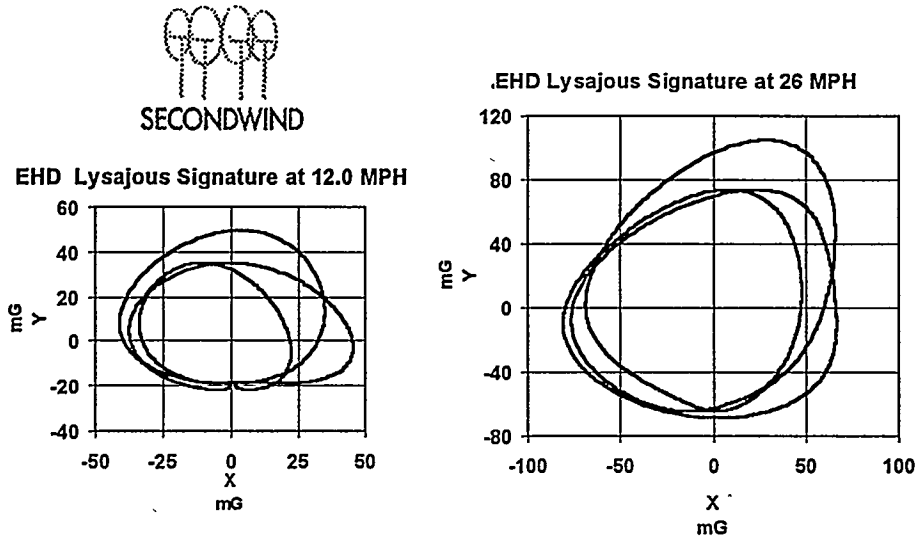

Figure 8. EHD Turbine Signatures for 12 and 26 MPH Winds

events are filtered out. What remains represents the behavior of the system. These plots are a convenient visual representation of system activity, one that can be easily used by the ADMS (windfarm) operator. The results for four wind speed values are presented in Figures 8 and 9. For all cases, including the two for the lower wind speeds (Figure 8), the plots provide visual confirmation that the 3P circularity mode dominates system behavior. This is seen as the three generally circular traces. As the wind speeds increase,

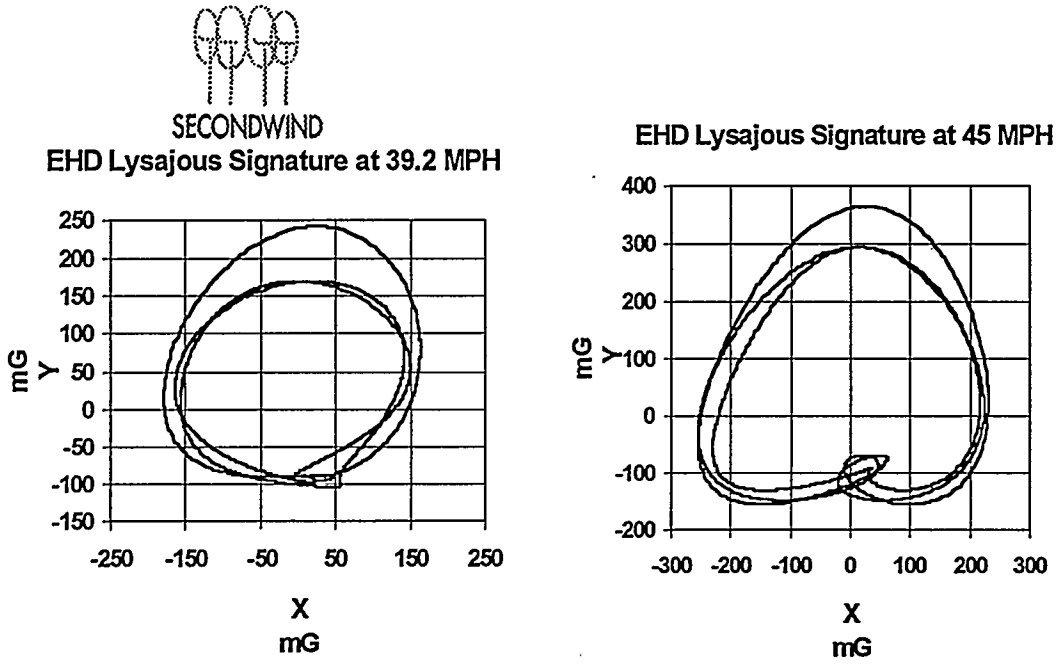

Figure 9. EHD Turbine Signatures for 39 and 45 MPH Winds

the magnitude of the accelerations increase but a 6P circular mode also appears. This is seen as three tiny loops each super-imposed on the 3P main loops. For the 45.6 MPH plot we note that there is a flat spot in the 6P loops. We have been advised that this flat spot may correspond to the system encountering a physical constraint, a limit of travel. This could occur if, for example, the guy wires are too tight.

DISCUSSION

The results suggest that these filtering methods could provide powerful new tools for both emergency vibration detection and mechanical health monitoring. The 1P filter alone could provide the wind turbine designer with a new and effective means to detect rotor imbalance. It also appears that the nP filter (where n is the number of turbine blades) will prove most useful. The additional capability to further decompose filtered accelerations into X-Ness, 45-Ness, and Circularity will provide a new opportunity to define emergency vibration criteria. We envision a table of values of these criteria, resident in the DSP, which represents the combined results of controlled testing and field operation. In essence, the DSP has the capability of storing and comparing the summarized results of field test data to current operational conditions. The filter frequencies could also be specified for tower and blade frequencies. In a fully implemented ADMS vibration monitor, it could be possible to track the magnitude of specific vibration modes of the turbine throughout their lifetime. As the machines encounter particular events or failures, the ADMS operator could catalog their particular signature. Eventually, this capability could lead to the detection of imminent failures.

CONCLUSIONS

The more advanced aspects of the ADMS vibration monitor have been simulated in software and the results are promising. This has been accomplished without the need for field testing which will soon follow at NREL's National Wind Test Center. In addition, prototype DSP hardware has been fabricated and is now in the field controlling a FloWind EHD turbine. The results suggest that this system can provide new and important functions.

FURTHER WORK

With additional field testing experience we hope to learn how to tailor this new system to horizontal axis wind turbines of different designs. We believe that the Lysajous data presentation may be a most effective way to display vibration mode information to the ADMS operator. The data presented here is the first pass and needs refinement. We envision the need to write a software module to support this concept. We need to design and test filters for blades, tower, and turbine system natural frequencies.

ACKNOWLEDGMENTS

We thank NREL for its support and technical guidance, without which this work would not have been possible. Outside NREL, our technical advisors for the mechanical engineering aspects of the ADMS are Craig Hansen of Windward Engineering and Lee Pellum of Kaman Aerospace; we thank them for their help. Thanks go to FloWind Corporation for its cooperation and generous sharing of valuable test data. Finally we thank Brian McNiff of McNiff Light Industries for his observations and interpretation of the Lysajous figure for high winds, and for his affable and inexpensive commentary.

[1] Cohn, K.E., "Insights from Computer-Aided Windfarm Management," *Proceedings of Windpower '87*, American Wind Energy Association (AWEA), Washington DC 1987, pp. 130-136.

[2] Collacott, Ralph A., *Vibration Monitoring and Diagnosis*, published by George Godwin Ltd., London, in USA by Halsted Press division of John Wiley & Sons, 1979.

LABORATORY IMPLEMENTATION OF VARIABLE-SPEED WIND TURBINE GENERATION

D. S. Zinger
Northern Illinois University
DeKalb, IL 60115

A. A. Miller
University of Idaho
Moscow, ID 83843

E. Muljadi C. P. Butterfield M. C. Robinson
National Wind Technology Center
National Renewable Laboratory
1617 Cole Blvd.
Golden, CO 80401

ABSTRACT

To improve the performance of wind turbines, various control schemes such as variable speed operation have been proposed. Testing of these control algorithms on a full scale system is very expensive. To test these systems simulation, we developed programs and small scale laboratory experiments. We used this system to verify a control method that attempts to keep the turbine operating at its peak power coefficient. Both the simulations and the experiments verified the principle of operation of this control scheme.

INTRODUCTION

With the need for reducing the cost of energy generated from wind turbines comes an increased need for improving their efficiency and performance. One method of increasing the performance is to run the turbine at variable speed. Advantages of running an induction machine in this manner include increased compliance to variations in wind, better energy capture, and less aerodynamic noise than systems with pitch control. These advantages come at the price of increased complexity in the system [1].

At the National Renewable Energy Laboratory (NREL),engineers are developing new wind turbine control strategies. Many of these controls are concerned with variable speed generation. In order to advance these control schemes in a cost efficient manner, it is necessary to verify the operation of the control before implementing them in the field. This requires a comprehensive set of simulations and laboratory experiments.

Previous simulations modeled the mechanical system well but basically approached the electrical systems from a steady state point of view. To achieve variable speed, however, the control of the electric machine becomes important, therefore making it necessary to have a dynamic model of the electrical system.

Experimental testing of generators consists of using a dynamometer to turn an electric machine. The dynamometers previously did not have the capability of

simulating the behavior of the wind turbine, making their usefulness in testing variable speed controls schemes very limited

NREL developed computer simulations and a small dynamometer system to simulate the behavior of a wind turbine system. The simulations include the full dynamic behavior of the electric machines, and the dynamometer can be controlled to simulate the characteristics of a wind turbine. The dynamometer system in the Power Electronics Laboratory at the National Wind Technology Center consists of off-the-shelf power converters and a standard motor dynamometer set. The system has been shown to be effective in the preliminary study of variable speed wind turbine power control.

VARIABLE SPEED WIND GENERATION

The power developed through a wind turbine is dependent on the wind speed and a power coefficient (c_p). The power delivered to the motor is given by

$$P_T = 0.5 c_p \rho A V^3 \tag{1}$$

where

ρ is the air density
A is the cross-sectional area of the turbine
V is the wind velocity.

The power coefficient is not a constant and is dependent on the tip-speed ratio (Λ) given by

$$\Lambda = \frac{\omega_T R}{V} \tag{2}$$

where

R is the radius of the turbine.

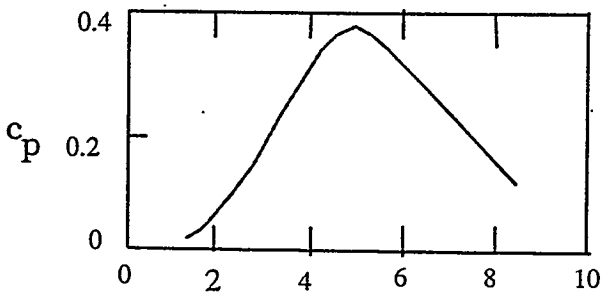

Fig. 1. Power coefficient as a function of tip-speed ratio

A typical relationship between c_p and Λ is complex as seen in Fig. 1. From this relationship there is clearly a value of Λ that will give a maximum c_p and thereby maximize the power for a given wind speed. As Λ is directly related to the turbine speed, there is a turbine speed that corresponds to a maximum power for a given wind velocity. This is illustrated in Fig. 2.

With varying wind speed, it is necessary to vary the turbine speed in order to operate at the maximum value of c_p. To track the maximum c_p power curve shown in Fig. 2, an algorithm was developed that appropriately adjusts the output power of the induction machine using the slip frequency. In an induction machine, slip frequency is the difference between the applied frequency and the mechanical speed of the machine seen by a set of magnetic poles. With an induction machine run at a constant V/Hz, power is related to the slip frequency. The relationship between slip frequency and power is such that a particular frequency could be found that delivers a given power at the desired speed. To implement this control, it is necessary to have the induction machine connected to a variable frequency source.

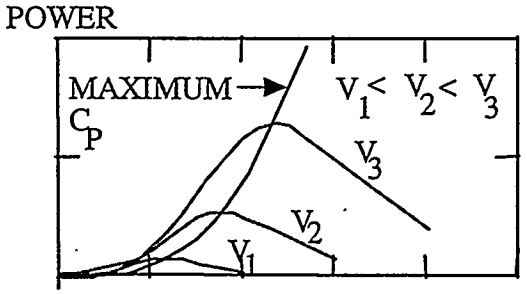

Fig. 2. Typical turbine power relationship for various wind speeds

Although it is generally desirable to have the turbine follow the maximum cp curve, during times of excessive wind gusts it is necessary to limit the speed and power of the turbine. With speed and power limitations, the desired speed power characteristic would appear as shown in Fig. 3. To limit speed, when the maximum speed is reached, the frequency to the induction machine is not allowed to increase. When the maximum power level is reached, the frequency is decreased to move away from the peak power point of the turbine, thereby reducing the overall power generated.

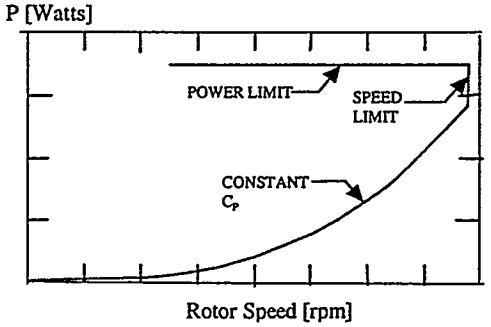

Fig. 3. Desired power speed relationships for induction machine

Development of control systems like the one described is impractical using a full scale system. Therefore it is necessary to use computer programs and small scale systems to develop these control systems. Software simulations and a small scale laboratory

experiment were used at NREL to help verify the behavior of maximum c_p curve control strategy.

SOFTWARE SIMULATION

Computer simulations were first used to determine if the control strategy would perform as desired. The computer program used the Advanced Continuous Simulation Language (ACSL). Although many computer languages could have been used, we chose this language because script can be written similar to other computer programs while containing built-in commands especially useful for control systems.

The computer program uses a dynamic model of the system in the simulation. The induction motor is modeled as a fifth order system with four electrical state variables and one mechanical [2]. The turbine was modeled as a simple system with a large inertia and a torque generated by the appropriate wind speed. The power generated by the turbine was calculated using a third order polynomial representation of the c_p curve. Although relatively simple models were used in this simulation, they proved to be effective for operating conditions modeled in the preliminary studies. The program is also very flexible and the complexity of the system model could easily be increased.

To perform the simulation in ACSL the system is basically described in standard state variable form. In addition, constraint and control equations are used as part of the dynamic model. Once the initial conditions are established, ACSL uses numerical integration techniques to determine the behavior of the system. Although ACSL has various integration techniques, the default forth-order Runge-Kutta was used for these simulations.

POWER ELECTRONICS LABORATORY

To further verify the behavior of a system it is usually desirable to have some experimental verification. In the early stages of system development it is not realistic to use a practical turbine to verify the control operation. Therefore, NREL has developed a small scale laboratory model to test new control algorithms.

The laboratory system consists of power electronics modules that can easily interface with small electric machines. The power electronic modules include a voltage source inverter, a current source inverter, a phase controlled rectifier, and a rectifier bridge. These electronic converters are each capable of handling power of up to 15 kW.

The electric machines in the laboratory are small machines typically rated around 250w. The machines include squirrel cage induction machines, wound rotor induction machines, and dc machines. The machines can all be loaded using a dc machine connected as a dynamometer.

It should be noted that the electronic power converters are rated considerably higher than the electric machines. This allows for easy transfer to the next higher level of testing.

For a typical application the dynamometer is used as a prime mover in place of the wind turbine. When operating in this manner the machine is powered from a phase controlled converter with a current feedback control. By controlling the current on the dc dynamometer, the torque of the dc machine can be directly controlled. Command currents are fed into the control based on its speed of rotation and an externally fed wind speed command. Using this method the speed torque characteristics of the wind turbine can effectively be simulated.

SCALING FACTORS

A problem associated with small scale laboratory implementations is that the system being modeled usually does not scale linearly. Thus it is not possible to have the behavior of the small system match that of the large scale system in all aspects. With proper selection of parameters for the system it is possible demonstrate the principle of operation of a conventional sized system.

As an example in the system described above it is desirable to have the small scale experiment match the c_p characteristic of a larger turbine. For a given turbine the maximum value of c_p would occur at a given value of tip-speed ratio (Λ_{max}). The limits on the small machine are the rated power and speed of the machine. To appropriately compare these values combine (1) and (2) under the conditions the machine operates at c_{pmax} to get

$$P = 0.5\pi\rho c_{p\max}\left(\frac{\omega_t}{\Lambda_{\max}}\right)R^5. \qquad (3)$$

Using a power and speed operating point for the machine, the scaled radius of the turbine can be calculated. With this and the definition of tip-speed ratio (2) the equivalent wind velocity for these operating conditions can be calculated.

EXAMPLE EXPERIMENT

The laboratory facilities were used to examine the variable speed control scheme that follows the maximum c_p power curve. The experiment was set up as shown in Fig. 4. The dc machine and converter were used to simulate the wind turbine. The induction machine and the converter connected to it were used as the power generating device. An input voltage is used to represent a wind speed while the system was controlled with a microcontroller.

The turbine being evaluated has a c_{pmax} of 0.5 at a Λ_{max} of 0.95. For our setup, we desired that the small machine follow the maximum c_p curve to 1300 rpm (23 rpm at the turbine with a gear ratio of 30:1) with a power of 75 w. From this it was determined that the turbine's radius would be about 4 m while the wind velocity for this point would be 2 m/s. In the simulations and experiments, speed was limited to 1300 rpm and power to 130 w. These limits were chosen to keep the machine well within its speed, power ,and current ratings.

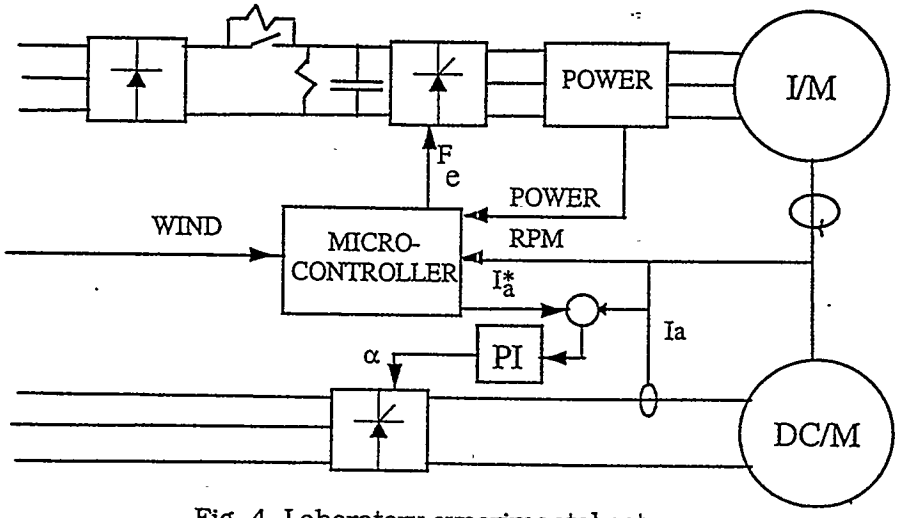

Fig. 4. Laboratory experimental setup

Before running the experiment, we ran computer simulations to test the basic algorithms. In the simulation, wind speed was ramped up to 4 m/s and back down to zero. With this range of wind speeds the system would run beyond the speed and power limits. The results are shown in Fig. 5 in which the power is plotted as a function of speed. In this plot it is seen that the power curve follows nearly the same shape as the ideal power curve shown in Fig. 3. The target power (Ptarget) is the desired power with the machine operating at maximum cp. For this simulation, the power into the generator exactly follows the target power until the speed limit occurs. After the speed limit is reached the speed is maintained at the desired speed of 1300 rpm. In the region where the control is in the power limit, power is seen to fluctuate in a region slightly above the power limitation. Generally this simulation shows that the system behaves as expected.

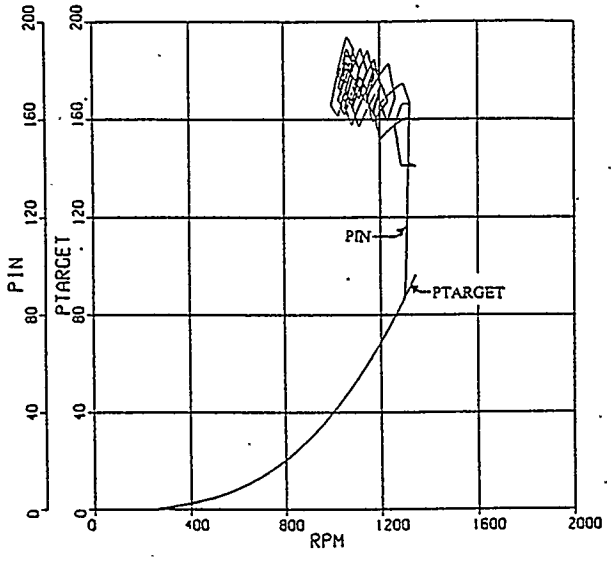

Fig. 5. Comparison of mechanical input power to the generator and targeted power as a function of generator rpm for simulated ramped wind speed

After verifying the basic operation of the algorithm with software, we implemented the hardware. A speed command for the system was input to the microcontroller. From this input the microcontroller determines a current command that creates the desired torque on the dc machine for that wind speed and the present motor speed. The current is regulated using a PI controller external to the microcontroller. In this way the dc machine behaves like the wind turbine.

The microcomputer also controlled the ac generator. The algorithm was the maximum c_p algorithm already described with the desired speed and power limits. To find the proper frequencies for the given speed conditions, a third order polynomial was used. The coefficients of the polynomial were generated in advance based on generator and turbine characteristics. During the experiment the microcontroller calculated the proper frequency using the polynomial and motor speed.

The results of the experiment are plotted in Fig. 6 along with the desired power characteristics. From this data it is seen that the steady state behavior of the system basically follows the desired curve. The power tracks the maximum c_p curve until the speed limit is reached. In the power limit region the power is confined to a value close to the set limit.

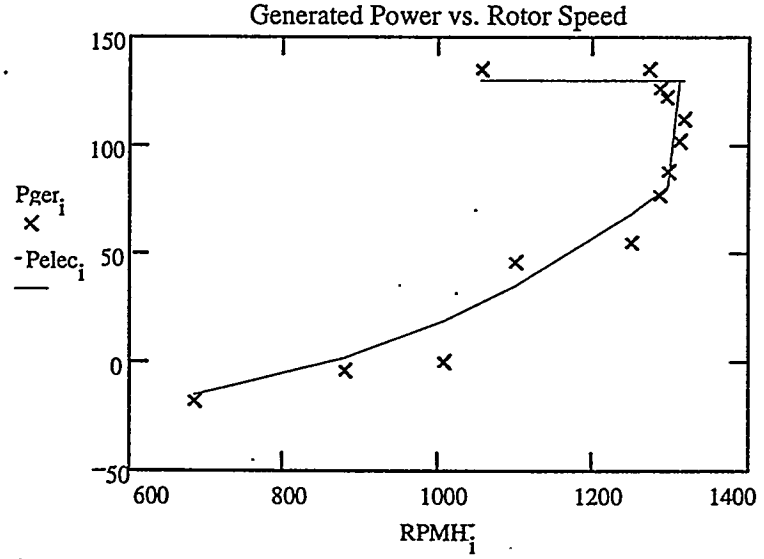

Fig. 6. Experimental steady state power generated (Pgen) compared to desired electrical (Pelect) for a given rotor speed

CONCLUSION

Before implementing new control algorithms for wind turbines it is advantageous to verify the operation of the algorithm in advance using software simulations and small scale laboratory models. We developed simulation software and a small scale laboratory setup for this purpose.

One way of optimizing the power converting capabilities of a wind turbine is to run the turbine at its peak power coefficient. An algorithm was developed for this type of

control using a variable speed wind turbine. The algorithm was simulated and run using the small scale laboratory equipment. Both the computer simulations and the laboratory showed this control algorithm to be viable.

REFERENCES

[1] P. Novak, T. Ekelund, I. Jovik, and B. Schmidtbauer, "Modeling and Control of Variable-Speed Wind-Turbine Drive-System Dynamics," *IEEE Control Systems*, August 1995, pp. 28-38.

[2] P. C. Krause, O. Wasynczuk, and S. D. Sudhoff, *Analysis of Electric Machinery*, New York: IEEE Press, 1995.

VARIANCE ESTIMATES OF WIND PLANT CAPACITY CREDIT

Michael R. Milligan
National Renewable Energy Laboratory
1617 Cole Boulevard
Golden, Colorado 80401
U.S.A.

ABSTRACT

As the utility industry adapts to meet the changing regulatory and business climate, it is becoming increasingly important for utilities to identify and quantify the risks in various aspects of doing business. To reduce the risk of depending too heavily on one specific type of generation or fuel, generation expansion planning techniques are incorporating methods of portfolio diversification theory. Financial option theory is also used to evaluate the relative costs of building now or building later. Applying these theories to utility planning helps utilities assess risks in the emerging competitive environment.

Risk is typically measured as a variance. For example, the risk associated with an investment can be characterized by the rate-of-return variance. Many studies that calculate the capacity credit of a wind plant do not calculate its variance, and therefore ignore risk. A capacity credit that is calculated in this way can be far different than the long-term average value. This problem is compounded by the usual method of calculating capacity credit, which depends very heavily on the level of wind generation during the system peak hours. A small change in wind power during the peak can have a dramatic effect on the capacity credit.

This problem is further compounded by the limited availability of multi-year wind data sets that can be used in utility production cost modeling. For example, a study that uses a single year of data and finds a 30% capacity credit may be based on a wind generation pattern that is not at all typical. Although the preferred approach would be to use many years of wind data to obtain a range of capacity credit estimates, this is not always possible.

This paper describes a technique that can help generation planners evaluate the variance of the capacity credit for wind power plants when there is limited wind data, and also shows some results of these calculations.

INTRODUCTION

One of the most frequently asked questions about wind power plants is whether such a plant has a capacity value, and if so, how much. Unfortunately, the answer to this question is rarely obvious, although it is often framed with the statement that capacity value depends heavily on the wind regime, utility load characteristics, and the utility's existing generation mix. There are also different methods that can be used to calculate capacity credit. Utility capacity expansion models and reliability models differ in their assumptions, algorithms, and their ability to properly account for a resource that is highly variable on both ends of the time scale. Utilities generally use 2 broad types of models: production cost and reliability. Generation expansion models are often built on the framework of production cost and reliability models. In some cases, the same model can be used to produce both reliability and power production cost outputs.

One of the most critical shortcomings of standard techniques used to measure wind plant capacity value is due to the variability of the resource and the lack of adequate wind data. This makes it difficult for the models to adequately measure capacity credit, so that capacity credit results may have little meaning. Because of the temporal interactions between load, wind power, and conventional generating capacity, wind plant capacity credit

measures are often little more than random draws from a probability distribution whose characteristics are largely unknown. To properly account for the exceedingly large number of potential interactions, some form of Monte Carlo simulation appears to be necessary. An excellent discussion of this technique in the context of chronological production cost models can be found in Marnay and Strauss (1990). However, in spite of the falling cost of computing resources, many production cost models have limited, if any, Monte Carlo capability. This paper uses a Monte Carlo technique that is carried out exogenously from the production cost/reliability model, which is then executed for many scenarios. Although this is not as computationally efficient as it would be if the capability were part of the production/reliability model, it can be applied to a wide variety of models that possess the capability of running a large number of scenarios.

It is also possible, if not likely, that long-term measures of capacity credit will differ from short-term measures. The focus of this paper is on long-term measures that would be appropriate for utility planners or investors who are evaluating a potential future wind plant. Short-term capacity credit, although outside the scope of this paper, will be mentioned again briefly below.

The usefulness of the concept of "wind plant capacity credit" has recently been questioned (Utility Wind-Modeling Planning Meeting, 1996). Citing the evolving deregulation of the utility industry, critics have argued that utility planning and capacity expansion will be influenced only by the market, reducing or eliminating the need for traditional capacity analysis. Under this scenario, capacity credit is determined by the pool or independent system operator (ISO) and not by traditional utility analysis. However, the final outcome of the deregulation process is not anything if not unclear. Although a number of states have begun moving toward a competitive market for electric utilities, the incentive to deregulate appears to be somewhat dependent on the price of electricity. States in the northeast and California generally pay the most for electricity, and that is where much of the deregulation effort has progressed significantly. The extent of federal regulatory involvement is also unclear. This could result in a patchwork of competitive and quasi-competitive markets for electricity.

If we assert that competition will indeed be pervasive and consistent, who plans for additional generating capability? It is the investors who are driven by the market. Investment in new generation would be driven by the expected rate of return that can be earned by the productive resource. To evaluate alternative investments, the potential investor must carry out calculations that allow the comparison of returns on these possible investments. This would most certainly include an estimate of the capacity payments that could be earned by a wind (or any other) power plant. If the investor is a generating company, the calculations that are carried out could conceivably be the same as those outlined in this paper.

METHODS USED TO MEASURE CAPACITY CREDIT

The focus of this paper is to examine capacity credit in the context of generation planning or investment. However, it is important to link the concepts of planning capacity credit and operational capacity credit. Planning capacity credit is the value given to a generating plant over a long time horizon, and is typically in the context of utility generation planning. Operational capacity credit is the capacity value that could be specified in a transaction between utilities. Utility A might agree to provide Utility B with 50 MW according to a pre-arranged schedule during a particular day or week. If this capacity can be provided by a wind plant, then the wind plant is said to have an operational capacity credit of 50 MW during the appropriate period. This section provides a short discussion of both types of capacity credit.

The standard techniques that are used to evaluate the reliability of power systems and how these techniques are used to measure planning capacity credit are based on Billinton & Allan (1984). Most methods of assessing the capacity credit of a wind plant are based on a reliability measure called loss of load expectation (LOLE). Most production cost and generation expansion models calculate the LOLE or a related measure, such as loss of load hours or expected unserved energy. Although these measures are not equivalent, they are measures that capture

the possibility that the generating system is not adequate to meet the system load. Of course the goal of the utility is to keep this probability as small as possible, given the trade-off between cost-minimization and reliability. A standard rule-of-thumb is to maintain an expected loss-of-load expectation of 1 day in 10 years.

There are other ways in which a utility can gauge its reliability. Another approach is to maintain a reserve capacity margin that exceeds peak load by a given percentage. Although there is no direct formula for converting between reserve margin and LOLE, higher reserve margins correspond to a lower LOLE and hence a more reliable system.

Using the concepts and techniques from reliability theory (Billinton and Allan, 1984), we want to provide a measure of generating plant capacity credit that can be applied to a wide variety of generators. Although no generator has a perfect reliability index, we can use such a concept as a benchmark to measure real generators. For example, a 500-MW generator that is perfectly reliable has an effective load carrying capability (ELCC) of 500 MW. If we introduce a 500-MW generator with a reliability factor of .85, or equivalently, a forced outage rate of .15, the ELCC of this generator might be 390 MW. In general, the ELCC value cannot be calculated by multiplying the reliability factor by the rated plant output — the ELCC must be calculated by considering hourly loads and hourly generating capabilities. This procedure can be carried out with an appropriate production-cost or reliability model.

To find the ELCC of a new generator, one must evaluate the reliability curve at various load levels prior to adding the new generator to the system. This can be done by running the reliability model, altering the load, and plotting the resulting points in a graph such as that in Figure 1, below. The graph shows the increasing risk of not meeting load, as measured with LOLE, that results from load increases. In the figure, the system load-carrying capability is just under 1,100 MW, assuming a risk level of 1 day in 10 years. The utility that finds itself above its preferred level of risk would add generation to its system. The new generator would shift the reliability curve to the right. This is depicted in Figure 2. The level of load increase that can be sustained at the same reliability level is the distance between the 2 risk curves, evaluated at the preferred risk level. Later discussion in this paper will use this method to determine the ELCC of a wind plant.

The determination of short-term operational capacity credit is a different process. If a wind-plant operator contracts with a utility to provide capacity on a given schedule for a given day, it is in the best interest of the wind-plant operator to possess a consistently accurate forecast of the wind, and hence windpower availability, during the day in question. In the unlikely but optimal case, the wind forecast is known with absolute certainty.

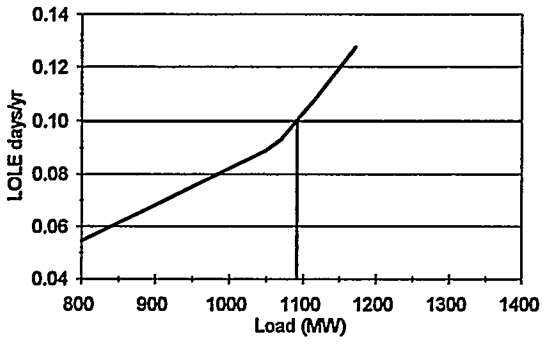

FIGURE 1. RELIABILITY CURVE FOR A FICTITIOUS UTILITY

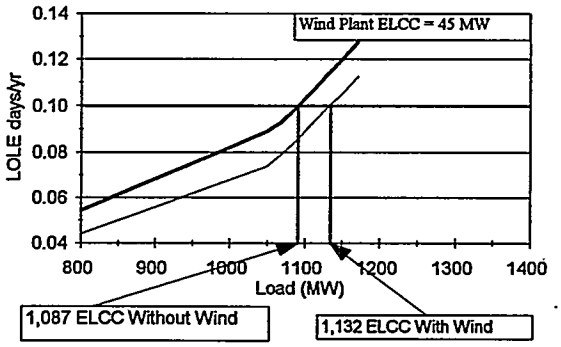

FIGURE 2. RELIABILITY CURVES FOR CALCULATING ELCC OF WIND PLANT

In that case, the wind-plant operator would contract for the full available capacity. In this case, the capacity value of the wind plant is equal to the capacity level that can be sold on a firm basis for the day (or any appropriate time interval) in question. During windy periods of the year, this capacity level is likely to be relatively high, whereas in the calm seasons this capacity level will be lower. The operational capacity credit can therefore vary throughout the year, and can be summarized by a suitable annual average, along with a variance measure. Of course, the forecast will contain an error component. The contract negotiators must quantify the relative risks of aiming too high or too low. A more detailed discussion can be found in Milligan, Miller, and Chapman (1995). However, in the "long run" we would expect that the average of the operational capacity credits would approach the long-term capacity credit, as measured later in this paper.

WIND PLANTS AND RELIABILITY

Adequately representing wind power systems in hourly reliability and production cost modeling can present a challenge, particularly if the model uses the load duration curve (LDC) approach. As computing platforms have become more powerful over the past few years, there has been additional interest in chronological models. However, much of the early work of calculating wind plant capacity credit was done with LDC models. In the LDC framework, loads are grouped into subperiods that consist of some reasonable partitioning of the hours in a week or month. The loads are sorted, and used to calculate a probability density function that is used to find the economic dispatch or reliability values of interest. This process eliminates a significant computational burden, but does so by sacrificing the chronological nature of the load data. Because the correlation between wind power and customer load is important to capture in the modeling, analysts have typically subtracted the hourly available wind power from the load. The result of this set of calculations is the remaining load, which is then met with the usual rules of unit commitment and economic dispatch (although the latter is not typically found in reliability models).

A similar technique for calculating net equivalent load can be used with chronological models. The justification is that a least-cost dispatch strategy will always take an inexpensive variable-cost resource, such as wind, before more expensive options. After wind power is accounted for, the conventional generating resources can be called upon to meet the remaining load. The chronological model overcomes the time-scale limitation of the LDC model. However, treating wind power as a deterministic reduction in load poses the same problem for chronological models as with LDC models.

Capacity credit results depend heavily on what happens during the utility's peak hour or several peak hours. Wind speed varies significantly from year to year and from hour to hour. Capacity credit estimates that are based on a single year of data and modeled without taking this variation into account should be suspect. Some analysts have corrected for this problem (Percival and Harper, 1982), whereas others did not (Bernow, Biewald, Hall, and Singh, 1994). A recent paper by Billinton, Chen, and Ghajar (1996) takes an approach that is similar to this paper. Ignoring this problem can be perilous, and can result in significantly over- or under-estimating capacity credit.

As an example of the wide potential variation in year-to-year wind energy capture, I have done a brief analysis of a 14-year data set from a regional air quality monitoring program (RAMP) site in North Dakota. It is important to note that this site would not be judged as suitable for a wind power plant, because of its low average wind speed and other factors. However, the data series is composed of many years, and until more multi-year data sets are publicly available from potential or actual wind plant sites, it is useful to look at this series.

To illustrate the possible variation in annual energy capture, this 14-year data set was used to calculate annual energy for a fictitious wind plant. The results are presented in Figure 3.

As the figure indicates, there is wide variation in annual energy capture. In 1983, for example, annual energy

produced from this site would be less than 60% of that produced in 1988. This clearly points out the fallacy of using a single year of wind data for meaningful analysis. When several years of data is not available, what then? That question is addressed in the remainder of this paper.

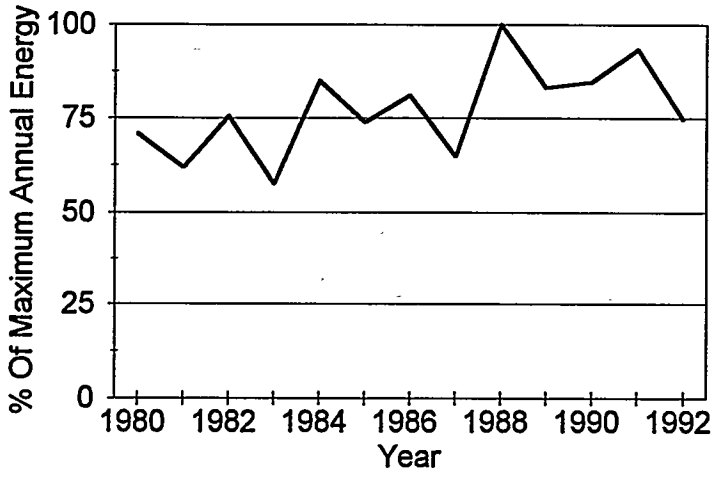

FIGURE 3 - ANNUAL SIMULATED ENERGY PRODUCTION, RAMP DATA SITE

MODELING APPROACH

To provide a plausible analysis of wind plant reliability and ELCC, I apply a Markov (Hillier and Lieberman, 1974) wind-speed simulation tool to a single year of wind data. The wind data is from the U.S. Department of Energy Candidate Wind Site program (Sandusky et. al. 1983). The site chosen for this work is from Romero Overlook, scaled to match the Altamont Pass site. For the utility's peak month, a state transition matrix is calculated. Then multiple realizations of the data are calculated by repeatedly sampling from the state transition matrix. This technique preserves some of the time-scale properties of the wind speed data and also provides an estimate of the variation that could be expected from a wind site. This method suffers from an obvious limitation—only a single year of wind data is used to calculate the state transition matrices. Including additional wind data, if available, would increase the accuracy of these calculations.

This analysis focuses on the month of the utility system peak, although the method could be used on any appropriate time-frame. Some utility control areas, pools, or reliability regions estimate generating plant capability on a monthly basis, so the choice of time-frame is consistent with those approaches. Once the multiple wind speed series have been simulated, I can calculate the hourly wind power output for the month from a hypothetical wind plant from each realization. The hypothetical wind plant is then applied to a reliability model, which is executed for each wind plant realization, and the results are combined. From this process I obtain the ELCC of each wind plant realization, which can then be summarized for further analysis.

The tools used in this study include Wind Power Simulator, described in some earlier work (Milligan & Miller, 1993), and the Elfin production cost model (Elfin is a product of the Environmental Defense Fund). For these cases the economic dispatch logic of Elfin was overridden so that I could focus on installed reliability using all generating resources. Additional software tools were used to simulate the multiple wind speed realizations and summarize the multiple Elfin outputs. The utility data is from an actual utility, modified appropriately for this study. Figure 4 below provides a graphical depiction of the process.

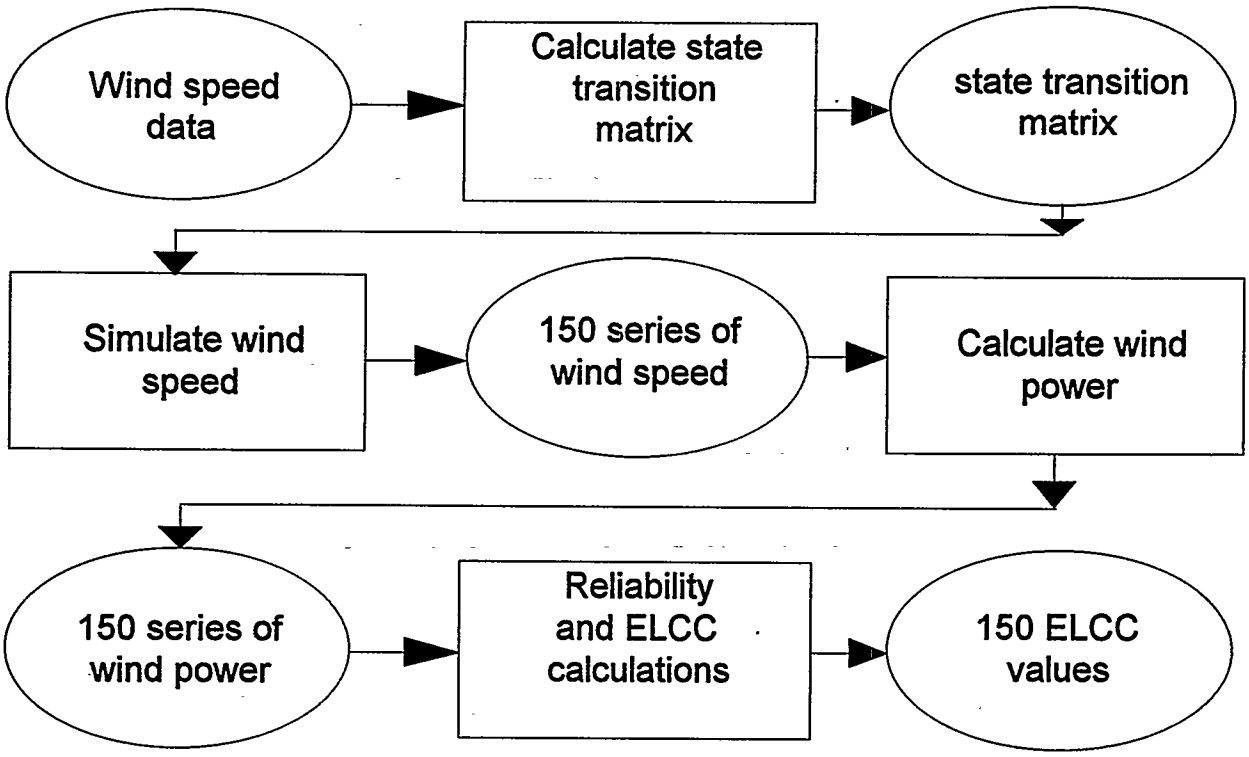

FIGURE 4. FLOWCHART OF THE MODELING PROCESS

Modeling wind power plants in production cost or reliability models requires the modeler to make many decisions about how the plant should be characterized for the model itself. One of the most important decisions is whether the wind plant capacity should be counted as "firm" or "non-firm." A generating unit that is modeled as a non-firm unit can't contribute to the utility's commitment target. By definition, non-firm resources do nothing to improve the reliability calculation, even though they may marginally improve actual reliability. If a unit is treated as non-firm its output is likely to be curtailed on very short notice. Although this situation does not arise often in practice, it implies that another unit must carry spinning reserve to cover the potential outage. Assuming a partially accurate wind forecast, wind plants should not be modeled as non-firm. The purpose of this study is to determine the capacity value and its variation. The designation of a firm vs. a non-firm resource tells the model how a particular resource should be treated for the reliability calculation. For this study, the wind plant was modeled as a firm resource, indicating that its full hourly capacity should be counted in the reliability calculation. Because I calculate a full range of possible outcomes with multiple wind data sets, this procedure allows me to capture such measurements as average capacity on peak or variation of capacity on peak. It also allows me to perform the capacity credit calculation based on the many cases that have been run. For a more detailed discussion of firm and non-firm treatments of wind plants and the relationship to operational capacity credit and wind forecasting, see Milligan, Miller, and Chapman (1995).

RESULTS

The peak-month state transition matrix appears in Figure 5. The three-dimensional graph shows the probability density function for each pair of successive wind velocities. The location of the peaks on the density graph shows a high level of auto-correlation in the wind-speed series.

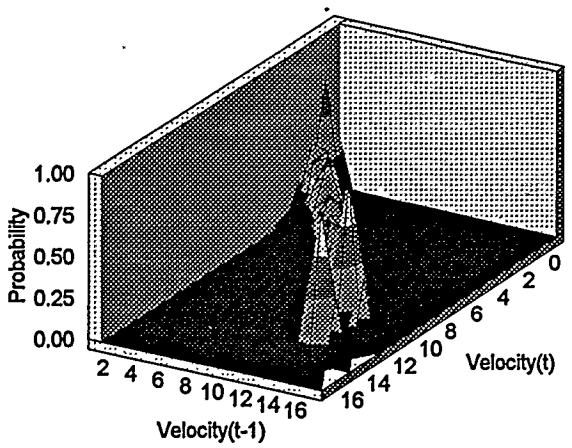

FIGURE 5. PEAK MONTH STATE TRANSITION MATRIX

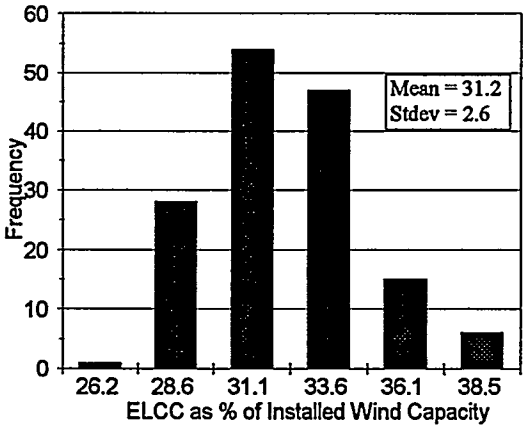

FIGURE 6. CAPACITY CREDIT DISTRIBUTION FOR 150 RUNS

Figure 6 captures the results of the multiple simulations. For each of the 150 runs, ELCC was calculated as a percentage of installed wind plant capacity. The data from these calculations is what the figure summarizes. The intervals were chosen to approximate the standard deviation of the ELCC value. As the figure indicates, most of the ELCC values are within 1 standard deviation of the mean value of 31.2%, with approximately 20 values outside that range. The ELCC values for this wind plant range from a minimum of 25.6% to 37.7%, a difference of 40% of the mean ELCC value.

I have developed reliability curves for several cases. The first case is the mean case, and it shows the simulation case whose ELCC value most closely approximates the mean ELCC value. The second and third cases, respectively, are those whose ELCC values most closely match the mean plus or minus the sample standard deviation. These reliability curves are combined in Figure 7. The distance between these cases at the risk level of 1 day/10 years is the variation in ELCC, which appears in Figure 6.

It is also useful to look at the reliability curves for other extreme cases. Figure 8 shows the average ELCC case along with both the maximum and minimum cases. It should be apparent from this graph that decision-makers

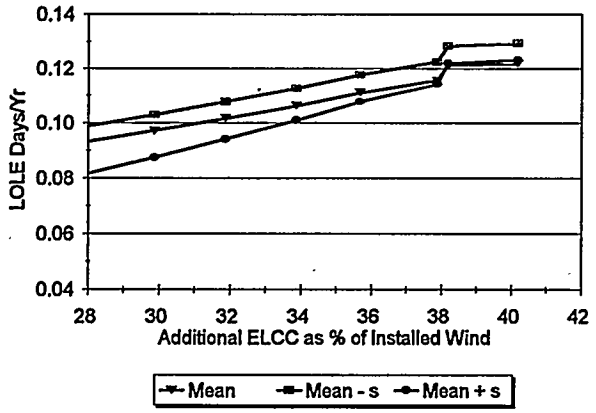

FIGURE 7. RELIABILITY CURVES WITHIN ONE STANDARD DEVIATION OF MEAN

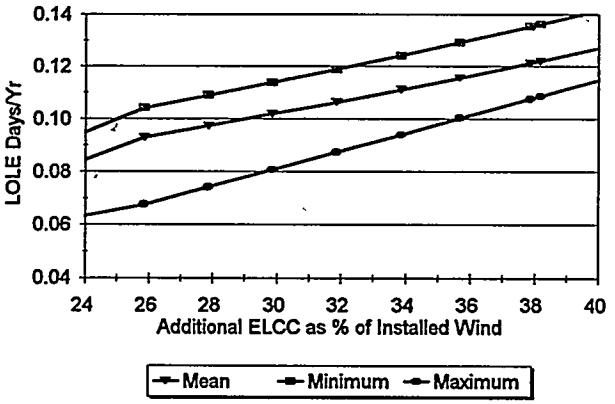

FIGURE 8. RELIABILITY CURVES FOR MEAN, MINIMUM, MAXIMUM ELCC CASES

and analysts should be extremely cautious about representing the capacity value of a wind plant as a single, fixed value.

It is also of interest to examine the convergence of the ELCC calculations as the number of scenarios (or iterations) increases. Adopting a method similar to that used by Billinton, Chen, and Ghajar (1996), I calculate the cumulative average and standard deviation of ELCC for each iteration. The ratio of the standard deviation to the cumulative mean is calculated. This ratio is called the convergence factor, and is graphed in Figure 9.

It is apparent from Figure 9 that a near steady-state value is reached in less than 100 simulations. Although the cost in computer run-time for this number of iterations is somewhat expensive, there is clearly an important benefit derived from running even a smaller number of iterations, as one can obtain a better idea of the possible variation in capacity credit. Figure 10 shows the percentage change in the convergence factor as a function of the number of iterations.

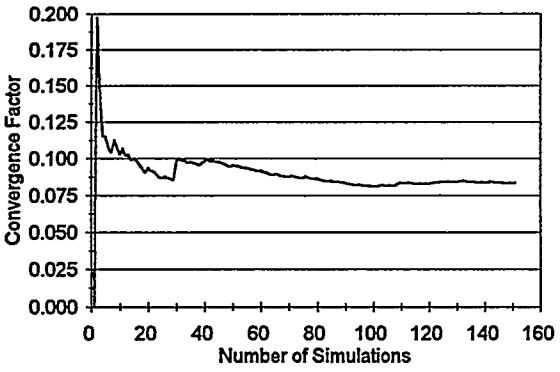

FIGURE 9. CONVERGENCE OF THE SIMULATIONS

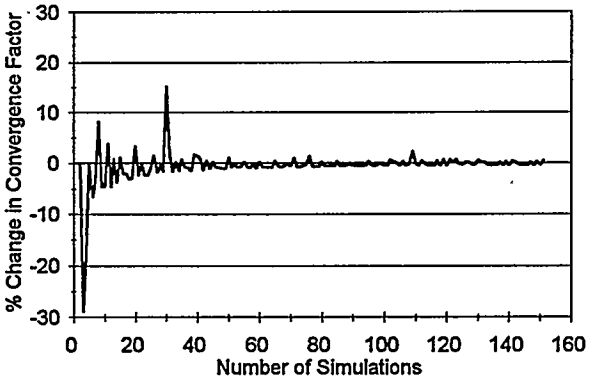

FIGURE 10. PERCENT CHANGE IN CONVERGENCE FACTOR

These results are similar to those in Billinton et al., but these results converge much faster. The Billinton wind-speed model is based on an autoregressive moving average (ARMA) model, described as an ARMA(3,2) process. A simpler form of the ARMA model, the AR(1) model, is a special case of the Markov model. It is possible that the ARMA model more accurately characterizes the time series data, which might explain the large number of iterations required by the ARMA model to converge—about 6,000.

CONCLUSIONS

This paper illustrates a Monte Carlo simulation technique that can be used to estimate the capacity value of a wind plant when there is limited wind data available. It is apparent that a single-year sample of wind data is inadequate to properly evaluate capacity credit unless some form of repeated sampling is used. The Markov wind-speed model used in this paper provides a relatively simple procedure to examine potential variation in capacity credit. The technique can also be applied to any other model output of interest, such as production cost or fuel usage. However, the use of multi-year data sets to calculate the state transition matrix would likely introduce more variation into the capacity credit measure than I have calculated here.

The case study results indicate that wind power plants do indeed have capacity value, and that this value is subject to a reasonably wide variation. Of course the specific results are influenced by the wind regime, utility loads, other conventional generation, and other characteristics of the utility.

REFERENCES

Bernow, S., B. Biewald, J. Hall, D. Singh (1994), "Modelling Renewable Electric Resources: A Case Study of Wind." Tellus No. 91-187. Boston, Massachussetts. Tellus Institute.

Billinton, R. and R. Allan (1984). *Reliability Evaluation of Power Systems*. Plenum Press. New York.

Billinton, R. H. Chen, and R. Ghajar (1996), *A Sequential Simulation Technique for Adequacy Evaluation of Generating Systems Including Wind Energy*. IEEE/PES Winter Meeting, January 21-25, 1996. Baltimore, Maryland.

Hillier, F. and G. Lieberman (1974), *Operations Research*. Holden-Day. San Francisco.

Jarass, L., L. Hoffmann, A. Jarass, G. Obermair (1981), *Wind Energy: An Assessment of the Technical and Economic Potential*. Springer-Verlag. New York.

Marnay, C. and T. Strauss (1990). *Variance Reduction in Monte Carlo Chronological Production-cost Modeling*. California Public Utilities Commission.

Milligan, M. (1996). *Alternative Wind Power Modeling Methods Using Chronological and Load Duration Curve Production Cost Models*. NREL/TP-441-8171. Golden, Colorado. National Renewable Energy Laboratory.

Milligan, M. (1996). "Measuring Wind Plant Capacity Value." *WindStats Newsletter; Vol. 9, No. 1;* Knebel, Denmark. NREL/TP-441-20493. Golden, Colorado. National Renewable Energy Laboratory.

Milligan, M. and J. Klarner (1995). *Wind Data Replacement Algorithms*. Seminar presented at the National Renewable Energy Laboratory, Golden, CO, 19 December.

Milligan, M. and A. Miller (1993). "The Value of Windpower: An Investigation Using a Qualified Production Cost Model." *Windpower '93 Proceedings; July 12-16, 1993;* San Francisco, California. Washington, DC: American Wind Energy Association; pp. 74-81.

Milligan, M., A. Miller, and F. Chapman (1995). "Estimating the Economic Value of Wind Forecasting to Utilities." *Windpower '95 Proceedings; March 27-31, 1995;* Washington, DC. Washington, DC: American Wind Energy Association.

Percival, D., and J. Harper (1981), *Value Analysis of Wind Energy Systems to Electric Utilities*. SERI/TP-732-1064. Golden, Colorado: Solar Energy Research Institute.

Sandusky, W., J. Buck, D. Renne, D. Hadley, O. Abbey, S. Bradymire, J. Gregory (1983), *Candidate Wind Turbine Generator Site Cumulative Meteorological Data Summary and Data for January 1982 Through September 1982*. PNL-4663. Richland, Washington. Pacific Northwest Laboratory.

Utility Wind-Modeling Planning Meeting. (1996). National Renewable Energy Laboratory, Golden, CO, 22-23 February.

A REVIEW OF NOISE DATA COLLECTION AT THE CENTRAL AND SOUTH WEST WIND FARM IN TEXAS

by

Emil Moroz
The University of Texas at El Paso
El Paso, TX 79902

TERMINOLOGY

- A - weighting: Internationally used method to account for a human ear's response to the frequency spectrum, commonly used in environmental noise control.
- Annoyance: Annoyance is the negative subjective reaction to noise on the part of an individual or group.
- Background noise (sometimes referred to as "ambient" noise): Taken to be an important criterion level which indicates the underlying noise level upon which other more intermittent noises are superimposed. To represent the background noise the International Standards Organization, ISO 1996, recommends the use of L_{95} measured with a "fast" meter characteristic while British Standard, BS 4142 recommends "slow" and the use of the L_{90} metric, while ANSI S12.9-1988 refers to the "residual sound" being "approximated by the percentile level exceeded during 90-95 percent of the measurement period." - Following the Riverside County Ordinance, California, we assumed the background noise to be represented by L_{90} measured with a "slow" response (1).
- Broadband: Broadband noise refers to noise with signals spread across a wide range of frequencies.
- Decibel, dB(A): A logarithmic unit of sound, used to account for the large range of response of the human ear, which indicates the ratio of a measured value compared to some reference value. The "A" in brackets indicates that the level, in this case, is measured using A-weighting. Table 1 indicates the subjective effect of changes in noise levels:

TABLE 1. DEALING WITH DECIBELS

CHANGE IN LEVEL, dB	SUBJECTIVE EFFECT
3	Just perceptible
5	Clearly perceptible
10	Twice as loud

- Landowner: The people referred to as the landowners are related to the landowner and act as custodians of the property. For the sake of simplicity and since a member of their family receives compensation for the use of their ridge for the wind farm, they are referred to as the landowners.
- L_{eq}: Indicates an equivalent continuous A-weighted sound level, which has the same acoustic energy for a constant sound level as for a fluctuating level measured over the same time period. (Sometimes written as L_{AeqT}, where the subscripts indicate A-weighting and the period T.)
- L_{90}: A statistical level indicating in this case the sound level exceeded for 90% of the time, expressed in dB(A).

- Masking: If the frequency components of the background noise are sufficiently loud compared to the noise in question, then this particular noise may become difficult to discern. If this were the case then the noise could be referred to as masked.
- Pure Tones: A pure tone is a single frequency signal. Pure tones are unnatural in nature and are considered more annoying than a steady noise of the same intensity.
- Tonal: A signal with a number of distinct pure tones is sometimes referred to as tonal.

INTRODUCTION

Central and South West Incorporated (CSW), a Dallas based utility holding company, has made a serious commitment to identifying the possible contribution that renewables could make to their large service territory. With the support of the Department of Energy (DOE) and the Electrical Power Research Institute (EPRI), CSW has constructed a 6 MW wind farm near Fort Davis, Texas. The wind farm consists of 12 Zond Z-40 500 kW wind turbines, which utilize ailerons for overspeed control and power regulation. Figure 1 is a topographical map showing the ridge line, the location of the wind turbines and the nearest four dwellings.

To support this project CSW sponsored a number of local Universities to provide information and to monitor certain aspects of the project. The University of Texas at El Paso (UTEP) was selected to provide an understanding of noise issues and to investigate methods for transferring the knowledge learnt at Fort Davis to other wind farm sites.

This paper builds on a 1995, AWEA Conference presentation entitled "Demystifying the Wind Turbine Noise Issue" (2.) That paper dealt mostly with theory and summarized findings from an extensive literature review and discussions with experts. The current paper benefits from: over a years worth of data collection; the tribulations of dealing with the first commercial installation of a new wind turbine; and exposure to affected residents. Given the sponsor's requirement to provide information on how to transfer the lessons learnt at Fort Davis to other potential wind farm sites, this paper looks at the features of three different planning criteria and documents comparisons of noise propagation prediction methods with each other and a sample of field data.

WIND TURBINE NOISE IN CONTEXT

Noise, which is commonly defined as unwanted sound, is a serious concern of environmental agencies throughout the world. In the US a high percentage of the population live with noise levels which make the sounds emitted from a wind farm of well-designed wind turbines seem insignificant, see Table 2.

TABLE 2. A COMPARISON OF COMMON NOISE LEVELS
(Adapted from various sources)

Noise Source	Distance from source ft	Distance from source m	Sound Pressure level dB(A)
Threshold of pain			140
Jet engine	200	61	120
Pneumatic drill (Jack hammer)	20	7	95
Inside sports car			80
Vacuum cleaner	10	3	70
Busy General Office			60
Wind in trees (15 mph wind)	40	12	55
Car at 40 mph	100	30	55
Inside an average home			50
Wind farm (3)	1100	350	35-45
Soft whisper	5	2	30
Rural night-time background (3)			20-40
Sound studio / quiet bedroom			20
Threshold of hearing			0

Typically A-weighting is specified in nearly all community noise regulations. However there are exceptions: these alternative weightings attempt to account for the fact that the greatest energy content of a wind turbine's noise spectrum is in the low frequency range. The contributions, to the overall measured noise level, from low frequency noise are drastically reduced in magnitude by the application of the A-weighting scheme. The Riverside County Environmental Health Department, CA, which has many years of experience with large scale wind farm developments is aware of the above and recommends (4) the use of a metric devised by Neil Kelley (5) to assess the potential of complaint from any low frequency components of the noise spectrum. The current work, however, focuses on the more widely used practices and therefore all measurements discussed in this paper are A-weighted.

DATA COLLECTION

To identify the pre-wind farm noise environment a scheme was devised in which background noise data was to be collected at the closest three residences. However, CSW were reluctant to raise the issue of noise early in the project, based on lack of information at the time. Therefore data collection was restricted to areas controlled by the landowner on who's property the wind farm was to be built. These first sets of data revealed that the background noise in this rural, sparsely populated region was exceptionally low and the threshold (30 dB) of the, only available for rent, noise logger was reached. In an attempt to overcome this limitation a survey of other available noise loggers was conducted. This identified the Larson Davis 820 as having the lowest available noise threshold, at a reasonable price. This logger was purchased and integrated into a custom long term noise logging system including: an outdoor pre-amplifier; a Nomad meteorological information logger; solar power supply; and custom built microphone stand and equipment enclosure. The system was placed in the vicinity of the landowner's property and later in a neighbor's front garden in order to record the pre- and post- wind farm noise environment. Figure 2. represents a schematic of this system.

Average noise and meteorological data at the 1.2m above ground level microphone at the property being investigated was synchronized with meteorological equipment set at 10m above the ground and located towards the northernmost end of the ridgeline. Ten minute averaged data was collected and correlation's made between the 10 m height wind speed on the ridge and the noise levels in the valley. The noise logger allowed a number of different descriptors to be collected simultaneously, these being selected so that the final data sets could be compared with various county, state and European regulations. The meteorological logger, located near the microphone, was used to identify any noise data that was corrupted by relatively high local wind speeds blowing over the microphone. The ASTME "Standard Guide for Measurement of Outdoor A-Weighted Sound Levels" (6) advises against noise measurements when the continuous wind speed is greater than 20 km/hr (12 mph.) Overall the noise logging system was reliable and provided good data, although on a few occasions the time synchronization slipped by a number of minutes and some minor damage occurred during a freak 100 mph wind storm.

A COMPARISON BETWEEN DIFFERENT TYPES OF NOISE LIMIT AND FIELD DATA

According to Righter (7) the wind industry, having overcome many technical difficulties, still depends on cultural acceptance of wind farms for it's future. Thus developers have a responsibility to ensure that they site wind farms sympathetically to minimize any potential annoyance. The issue of noise should be addressed early in the planning stages, so as to avoid costly changes after the wind farm is constructed. Thus some sort of planning criteria is required. Since no such criteria or noise regulations exist to limit developments in rural areas near the small town of Fort Davis, TX, it was decide to investigate how the wind farm noise compared with other regulations. A literature survey revealed that there were three distinct types of constraint that could be used to regulate noise producing developments. These are discussed below and comparisons are made with experience gained on the project:

1. Minimum Separation Distance

A minimum separation distance is the simplest form of project regulation. At the start of the project various articles referred to a minimum separation of 350 to 400m as being adequate. However this appears to be a useful guide only on flat terrain such as in Denmark, subsequent discussions with developers in the UK, where wind farms have been situated on hill tops in relatively complex terrain, have revealed the need for minimum separations of at least 800m. Regardless of the actual number chosen, this type of simplistic rule does not account for noise emissions from different types or numbers of machine and is at best a very approximate guide.

2. Absolute Noise Limit

The Absolute Noise Limit is the most commonly found regulation and refers to a specified noise limit that should not be exceeded in a specified time interval. These absolute noise limits for wind farms have been set in a number of different ways. In California absolute limits have been set which cannot be exceeded for any wind speed at the boundary of a proposed wind farm. In Minnesota absolute limits are applied only in the vicinity of a residence, again applicable for all wind speeds. While in Denmark noise from wind turbines is limited to 45 dB(A) in rural areas when measured at a wind speed of 8 m/s measured at a height of 10 m.

Table 3 compares actual measured noise data with a number of different regulations, collected in neighbor, "N's" (see Figure 1,) front garden at the CSW wind farm. The data being compared is the average value of noise described by different descriptors, appropriate to different regulations. It was measured over a three week period, during the local windy season and represents conditions when most of the 12 turbines were

available for operation. In five out of the six cases shown the Fort Davis data is below the required value. Only in Kern County, CA, with the strictest descriptor (i.e. L(8.3) which requires that the specified noise level of 45 dB(A) shall not be exceeded for more than five minutes in any one hour) is a regulation exceeded. In this case by only a small amount.

TABLE 3. AVERAGE NOISE LEVELS AT NEIGHBOR
(All data expressed in dB(A))

Descriptor	Average Noise Level at Ranch	Regulations		
L(eq)	43.8 (whole period) 39.9 (@ 8m/s on 10m mast, 6pm to 7am)	Denmark:	Rural L(eq)	45
L(8)	46.4	Kern County:	L(8.3)	45
L(10) L(50)	46.0 (24 hour 42.5 averaged value)	Minnesota:	Rural: Day 65 Night 55 Rural: Day 60 Night 50	
L(90)	39.7	Riverside County:		45
L_{DN}	51.85	EPA Guidelines		55

3. Relative Noise Limit

The British Noise Working Group (NWG) are about to publish a comprehensive document covering suggested best practice for dealing with wind turbine noise and have recommended relative noise limits as being the most appropriate for complex terrain. A relative noise limit requires that the new noise not exceed a certain margin, typically 5 dB, above background. The NWG final report can be obtained by making a request to the Renewable Energy Enquiries Bureau, ETSU, UK (8).

The following applies the NWG method, as laid out in (9), and reveals how noise limits could be set for residences L and N at Fort Davis. Reference 9 contains detailed guidance and justification for the process. It is beyond the scope of this paper to attempt to repeat the NWG's explanations and therefore the application of a relative noise level is only outlined. Interested readers are referred to the original source for more information. The objective of the relative noise limit is not to totally exclude the new noise but rather to limit it to an acceptable level that will not disturb sleep or stop the resident from enjoying the immediate area around their dwelling. Reference 9 discusses the need for both a daytime and nighttime noise limit, but offers the opportunity to combine these two limits into one should the variation in background noise be small between these two periods. This combined approach has been selected for the following case study.

The first step in determining a relative noise limit is to measure the pre-wind farm noise levels and to relate those levels to the 10 m height wind speed relevant to the wind turbines (mast on the ridge in the CSW case.) Figure 3 is an example of the pre-wind farm background noise, collected at the landowner's ranch and sorted to show the most noise sensitive period of the day, when people might be relaxing or sleeping: the hours from 6 p.m. to 7 am.

Figure 4 compares curve fits of background noise data collected at L with that of N. It can be seen that there are significant differences. Property L, being tucked into a relatively narrow valley is more sheltered from the wind and therefore has a relatively lower rate of change of background noise. Property N is, on the other hand, in a more exposed location and has a steeper rate of change of background noise with wind speed. However because access to N was not obtained during the pre-wind farm measurement phase, their background noise data curve had to be derived from a combination of two nights of recent noise data with the wind farm shut down and from background noise data collected in a similarly exposed location, prior to wind farm construction. Ideally any such assumptions should be avoided and actual pre-wind farm data collected at each affected dwelling (or at a house representative of a group of dwellings.)

It was the very low measured level of background noise, less than 20 dB, that gave most reason for concern during the early stages of this project. Similar low noise levels also occur at British wind farms. However, the NWG argues that protection down to such levels would be very restrictive on development of new wind farms and therefore suggest a range of lower daytime limits, 35-40 dB(A), $L_{A90,T=10\,min}$ (9,) applied up to the point where this lower limit intersects with the line defining the margin above background. In our case 40 dB has been selected as the limiting noise level for the neighbor N's ranch, see Figure 5. A higher minimum limit of 45 dB and a potential to increase the margin above background is suggested by the NWG for properties belonging to people with a financial stake in the development, see Figure 6. This provision for a more lenient noise limit, during low wind speeds, for those with a financial interest appears to be justified by personal impressions of the reaction of the "landowners" who, although not happy, appeared to be more accepting of the project, despite the wind farm being quite audible to them. While the affected neighbor, N, whose noise and visual environment had been changed without their being consulted or their benefiting from some financial gain, was much more negative about the intrusion into their world.

Since the "landowner" requested that the noise logging equipment be removed from their property before the wind farm's teething problems had been resolved no data is available for comparison with the limit in Figure 6. However three weeks of data with all twelve turbines operational was collected for the affected neighbor's dwelling and this is shown in Figure 7. At first glance it looks like the NWG relative noise limit has not been exceeded throughout the whole operating range considered. However it can be observed that the operating wind farm background noise dips below the supposed pre-wind farm background noise line. This suggests that the assumptions about the pre-wind farm noise may have been incorrect or that the data used is only applicable for another season of the year, and that the background noise upon which the limit is to be based should be closer to that of the "landowner." If this were true then the relative noise limits would have to be amended and may therefore be exceeded.

In summary, using a relative level above background is the most comprehensive way of looking at noise of the three approaches discussed and may be the appropriate approach to determine whether a neighbor has a legitimate reason for complaint.

PENALTIES FOR THE CHARACTER OF THE NOISE

It is important to note that both the absolute limits and the relative noise limits need to be adjusted if a noticeable tone exist or should the character of the noise be such as to cause undue disturbance. This type of analysis is normally very complex and can be quite subjective, see (10.) However in order to maintain objectivity and yet to account for these issues, a software program for automatic tonal analysis, recently developed by Renewable Energy Systems (RES) of the UK, was purchased. (For further information contact Rachel Ruffle at RES on Tel # (011 44 1442) 242222.) This program reads recorded noise information, originally collected on a digital audio tape, via a suitable program such as LabView and associated A/D board and allows tonal analysis to be conducted according to a menu of selectable options.

These menus allow selection of different tonal analysis methods based on the Joint Nordic Method. In the case of measurements collected at the neighbor's ranch it was found that no audible tones were reaching their garden.

COMPARISON WITH NOISE PROPAGATION MODELS

To plan a wind farm's layout in order to avoid noise issues, one must have reliable noise propagation models. During this project two techniques were investigated. One involved a relatively complex commercial software package, the Environmental Noise Model (ENM), and the other was a relatively simple IEA recommended hemispherical spreading model. The interested reader is referred to the work of Dr Bass for a more complete discussion, see Reference 11. ENM gives the opportunity to use the ENM algorithm, based on theory, or to purchase other optional algorithms. In our case the empirical CONCAWE algorithm, developed by the Oil Companies International Study Group for the Conservation of Clean Air and Water, was purchased. The ENM software package which is supposed to be able to deal with complex terrain and meteorological effects such as wind speed and direction is distinguished by these features from the IEA model, that only accounts for hemispherical spreading over a flat plane and the attenuation due to atmospheric absorption. Table 4 shows a comparison between the various methods and their relationship to the suggested relative noise limits and to limited field data.

TABLE 4. NOISE PREDICTION COMPARISONS
(Affected Neighbor, N : West Wind , All L(90) dB(A))

Hub Height Wind Speed (m/s)	10m Mast Wind Speed on Ridge (m/s)	CONCAWE algorithm (corrected for background)	ENM algorithm (corrected for background)	IEA equation (corrected for background)	Field Data (12 turbines operating)	Relative Limit as suggested by NWG (9)
4	3.28	35.6	43.9	36.4	33.7	40
8	6.56	40.2	54.2	40.9	38.9	40
12	9.84	48.3	57.8	48.5	41.4	52.3

Reference 11, entitled "Noise Propagation at Wind Farm Sites," found that a number of prediction models, including ENM, CONCAWE and the IEA method, resulted in large errors (up to 15 dB) when compared to a known source being measured in very complex terrain. The results in two out of the three models evaluated, in this study, gave reasonable results. It can be seen that the ENM algorithm over predicts the field data and that the error increases with wind speed, agreeing with Reference 11. Both IEA and CONCAWE follow each other closely, but are slightly conservative in low wind speeds, but over predict by about 7 dB when background noise is added. This, perhaps, being another indication that the estimated background noise being used should be revised. Thus it appears that the relatively simple IEA model can provide a cheap and relatively quick estimate of wind farm noise imission at any designated point. Dr Bass suggests its use for preliminary planning at sites with hard ground and Garrad and Hassan have incorporated such an algorithm into their wind farm optimization software.

CONCLUSIONS

Relative noise limits offer the most comprehensive approach to regulating noise and allow each location to be treated independently.

The IEA hemispherical spreading model appears, from the limited comparisons made, to be a useful planning tool. The CONCAWE algorithm should be used in preference to the ENM algorithm if a complex modeling software is to be used.

Although absolute noise levels of the Fort Davis wind farm are low compared to an urban environment, annoyance has been expressed by a neighbor. Thus it appears that it is not necessarily the absolute noise level but, perhaps, attitude that is governing the response to the project.

Preemptive measures such as sympathetic wind farm layout with respect to noise and early community involvement are necessary steps to ensure cultural acceptance of this clean and sustainable energy source.

ACKNOWLEDGMENTS

This work was sponsored by EPRI, DOE and CSW. The support of all those experts in the field of noise, especially Dr. J Bass(RES, UK)and Mr. W Reddon (Riverside Co. Environmental Health Dept., CA), who took time to share their experiences and give guidance, is much appreciated. I would also like to acknowledge Brian Champion of CSW who helped me obtain the data and oversees the wind farm in Fort Davis.

Any opinions or conclusions expressed in this paper are those of the author and do not necessarily reflect the views of CSW or any of the sponsoring agencies.

REFERENCES

1. Riverside County Ordinance, "Resolution No. 93-378, Amending and Superseding Resolution No. 86-180 Adopting Technical Specifications and Criteria for the Measurement and Projection of Noise from Commercial WECS Projects," Riverside County, CA, 1993.
2. Moroz, E. "Demystifying the Wind Turbine Noise Issue," Proceedings of AWEA Windpower'95 Conference, Washington D.C., 1995.
3. British Government, "PPG22, Planning Policy Guidance Note: Renewable Energy," Department of the Environment, Welsh Office, Feb. 1993.
4. Reddon, W.D. "DRAFT: Noise Elements of the Wind Implementation Monitoring Program, Phase IV," Riverside County Department of Environmental Health, Riverside County, CA, Jan 1996.
5. Kelley, N.D. "A Proposed Metric for Assessing the Potential of Community Annoyance from Wind Turbine Low-Frequency Noise Emissions," SERI/TP-217-3261, Nov. 1987.
6. ASTME "Standard Guide for Measurement of Outdoor A-Weighted Sound Levels," Report ER 1014 - 84.
7. Righter, R. W. "Wind Energy In America,"University of Oklahoma Press, Norman, OK, 1996.
8. Renewable Energy Enquiries Bureau, ETSU, Harwell, Oxfordshire, OX11 0RA,Tel: (011 44 1235) 433601 or 432450.
9. Legerton, M "Preliminary Recommendations of the Noise Working Group," Proceedings of the BWEA Conference, Warwick, UK, 1995.
10. Ruffle, R., Bass, J. and Bullmore, A. "Removing the Subjectivity from Tonal Noise Assessment," Proceedings of the BWEA Conference, Warwick, UK, 1995.
11. Bass, J., "Noise Propagation at Wind Farm Sites," Proceedings of the Institute of Acoustics Vol. 16 Part 1, 1994.

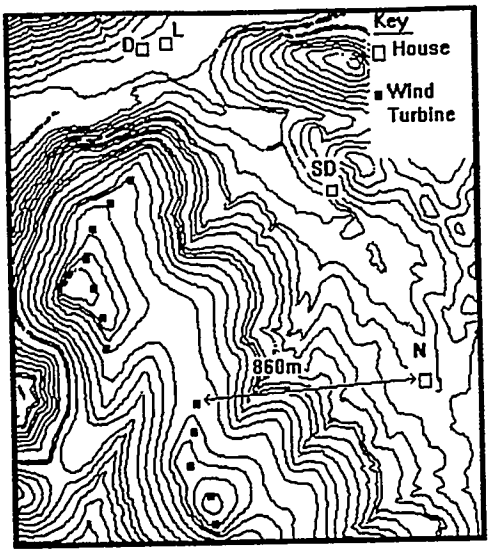

Figure 1. Topographical Map of Wind Farm Site

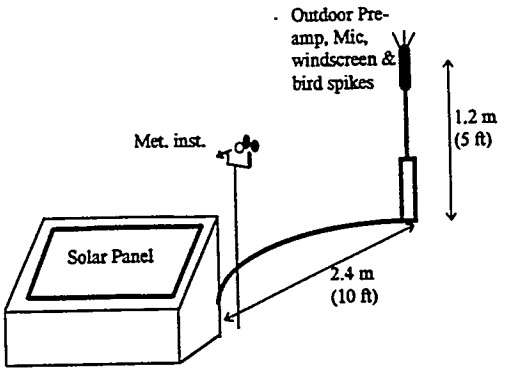

Figure 2. Long Term Noise Logging System

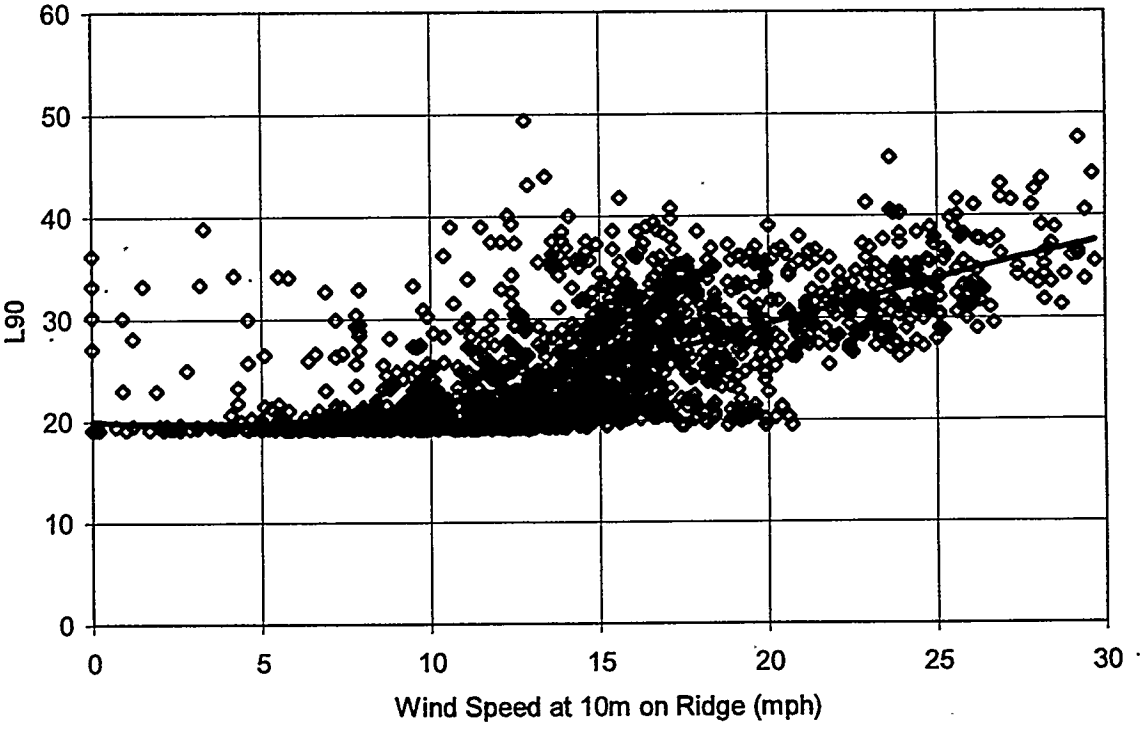

Figure 3. Pre-Wind Farm Background Noise at "L"

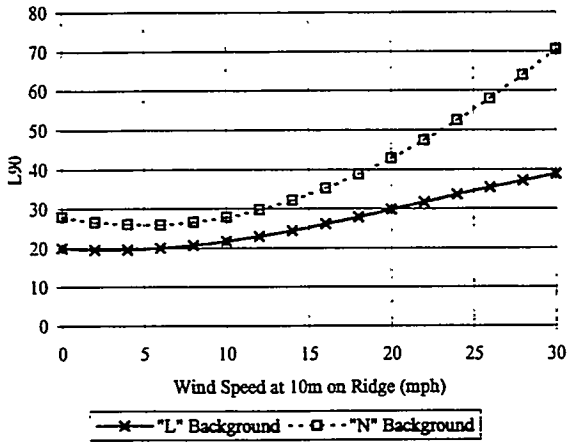

Figure 4. Comparison of Background Noise Levels

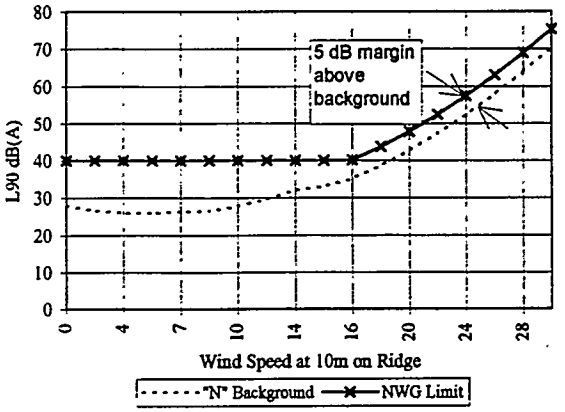

Figure 5. Relative Noise Limit for Affected Neighbor

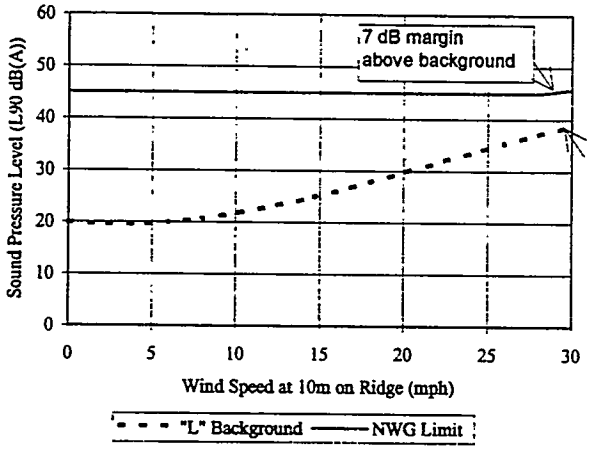

Figure 6. Relative Noise Limit for Financial Involvement

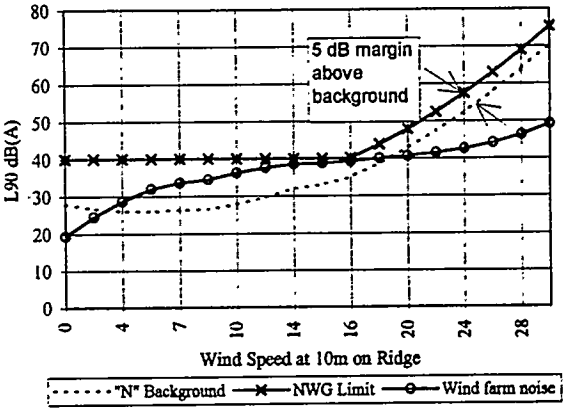

Figure 7. Turbine Noise Superimposed upon Neighbor Scenario

GREEN PRICING: A COLORADO CASE STUDY

Eric Blank, Land and Water Fund of the Rockies
James R. Udall, Community Office for Resource Efficiency

Introduction

As the costs of wind, solar, and geothermal technologies continue to fall, renewable energy is becoming an increasingly economic way for utilities to meet growing electric demands. Renewable resources protect utilities from fuel price escalation and reduce air pollution, acid rain, and climate change. Despite the promise of these technologies, the threat of industry restructuring is discouraging many electric utilities from making new investments in them. As a result, the commercialization of key renewable technologies will be delayed unless new approaches, institutions, and funding mechanisms are developed.

Green pricing offers a new strategy for accelerating the acquisition of renewable resources based on free-market principles, customer choice, and the differentiation of a new product — the clean kilowatt-hour. Numerous surveys have shown that a large majority of utility customers are willing to pay more on their electricity bills to protect the environment. For many, this is the easiest and least-cost way to reduce the environmental impacts associated with their energy use. For example, by paying an additional $6 per month to replace coal with wind power, a typical Colorado household could eliminate annually the need to burn 3,600 pounds of coal, the resulting air pollution, and as much carbon dioxide as is produced by driving 9,000 miles.

At least three utilities have developed "green pricing" programs that attempt to tap into customer desires to purchase cleaner energy. To date, however, these programs have not raised nearly enough funds to make a meaningful difference in commercializing key technologies. Several factors appear to explain this reality. For one, these green pricing programs have focused exclusively on obtaining funding from a relatively small number of residential customers. In addition, the utilities running these programs have not yet developed a "green product" that provides sufficient value to interest business and commercial customers. Finally, utilities have not partnered with community groups capable of conveying the message to a broader audience.

This proposal seeks to remedy these shortcomings by creating a partnership between a local community group, a renewables advocacy group, and several Colorado utilities. The goal of this partnership is to develop a model green pricing program targeted primarily towards larger customers. It is our belief — supported by some initial discussions — that many Colorado businesses including ski areas, municipalities, and high-tech companies would pay somewhat more to purchase clean power. By focusing on larger customers, our analysis shows that utilities could acquire roughly an order of magnitude more renewables compared to existing green pricing programs.

The Rocky Mountain region represents an ideal place to develop and implement such a model. Indeed, the only investor-owned utility currently running a green pricing program is in Colorado. Moreover, the region has a large need for new capacity (due to rapid growth) and attractive renewable opportunities. The two organizations supporting this proposal have extensive working relationships with key utilities, regulators, and customers both within and outside the region. As a result, we are well-positioned to develop a successful model program.

I. Promoting Renewable Resources in an Increasingly Competitive Industry

Renewable resources — solar, wind, and geothermal power — offer attractive economic and environmental opportunities for meeting growing electric demands. Although their initial capital costs are relatively high, these technologies have no fuel expenses and produce little adverse environmental impacts. As a result, renewable resources can help protect utilities from fuel price escalation and environmental risks and should therefore be an important part of utility resource portfolios.

In addition to their long-term fuel diversification and environmental risk minimization benefits, the costs of renewable resources have declined substantially in recent years. For example, the levelized cost of wind power, over 15 cents (¢) per kiloWatt-hour (kWh) a decade ago, has now fallen below 5 cents. The 1992 Energy Policy Act's (EPAct) establishment of a 1.5 ¢/kWh production incentive to encourage new solar, wind, and geothermal development further improves the economics of renewables. Thus, from a resource planning perspective, renewables provide attractive opportunities for utilities and regulators interested in an environmentally and economically sustainable mix of energy alternatives.

The long-term role renewable resources will play in meeting growing electricity demands will likely be determined, in large part, over the next five years in many sections of the country. In the Desert Southwest and Rocky Mountains, for example, projected growth in demand will create an estimated need for 10,000 Megawatts (MW) of new electrical generating capacity by the year 2010 — enough to power ten million new homes at a cost of roughly $10 billion. Renewable resources could cost-effectively capture ten to twenty percent of this need. However, for that goal to be achieved, an extensive infrastructure involving utilities, manufacturers, and customers must be built relatively quickly. There now exists a short, four year window of opportunity within which to begin commercializing key renewable technologies before the EPAct tax incentives expire in 1999.

Despite this opportunity, however, recent changes in the electric power industry are discouraging utilities from acquiring renewable resources. The threat of retail competition — the possibility that existing customers could leave their local utility supplier — has fundamentally changed utility attitudes toward renewable resource acquisition. In the new regulatory environment, utilities have no guarantee of recovering the costs of prudent long-term investments if customers can seek alternative suppliers in the near future. Under these circumstances, utilities are reluctant to invest in projects with high initial costs, however profound the long-term benefits may be. This fear of "stranded assets" threatens to block any new investment in renewable energy.

Because of these financial concerns, utility investments in renewables have been smaller than warranted given their resource planning benefits. To illustrate, a large investor-owned utility in the Rocky Mountain region recently acquired close to 500 MW of new gas-fired capacity and only 10 MW of renewables even though the economics of the two projects were almost comparable. In sum, given the financial constraints under which most utilities operate, key renewable technologies are not likely to be commercialized within the current industry structure without the development of new approaches, institutions, or funding mechanisms.

A. Toward a New Paradigm: Utility-Sponsored Green Pricing Programs and their Problems

Numerous polls and surveys sponsored by utilities and others have shown that the majority of utility customers want to purchase electricity generated by cleaner sources. (Farhar). Moreover, these same studies also show that many of these customers are willing to pay somewhat more for clean, environmentally friendly power.

Given this market data, a number of utilities — including Southern California Edison, Niagara Mohawk, Public Service Company of Colorado, Portland General Electric, and New York State Electric & Gas — have studied a new approach, called "green pricing", for tapping into this customer desire for cleaner power. The premise behind green pricing is that consumers will pay between 5-20% more for cleaner, environmentally friendly power generated by renewable resources.

For many customers, participation in a utility-sponsored green pricing program may be the easiest and least-cost way to reduce the environmental impacts associated with their energy use. For example, by paying an additional $6 per month to replace coal with wind power a typical Colorado household could eliminate annually the need to burn 3,600 pounds of coal, the resulting air pollution, and as much carbon dioxide as is produced by driving 9,000 miles in a 20 mile-per-gallon car. Few pollution prevention measures have an equal cost-benefit ratio.

B. Utility Experience with Green Pricing Programs

Among IOUs, only Public Service Company of Colorado (PSCO) has started a green pricing program, although Niagara Mohawk is on the verge of doing so. PSCO is a 4,000 MW investor- owned utility with $1.2 billion in annual revenues serving over a million customers in Colorado. PSCO's Renewable Energy Alternatives Program (REAP) encourages residential customers to make monthly contributions to a renewable energy fund. After the monies have been collected, a pre- selected group of customers then chooses small renewable energy projects for development. PSCO supplements the REAP program with approximately $1000/KW in avoided cost savings. Although PSCO initially believed that REAP would raise $2 million annually, after its first year of operation the program has raised less than $200,000 — not enough to have much relevance in PSCO's resource planning process. PSCO is currently working with key stakeholders, including the LAW Fund, to improve the program.

Two municipal electric utilities have also started green pricing programs. Sacramento Municipal Utility District's (SMUD) "PV Pioneers Program," begun in 1993, is the oldest and best known. There, 240 utility customers pay an additional $6 per month to host 4 kilowatt, grid-connected PV arrays. In this program, the customer contributions are used to fund PV arrays on the roofs of participants. As a result, participants are truly receiving green power from their own roofs. (Osborn)

Last year 230 residential customers of Traverse City Light and Power, a municipal utility in Michigan, signed up for a green pricing program. In this program, participants pay 1.58 ¢/kWh extra for electricity produced by a 500 kilowatt wind turbine two miles west of town. Since that turbine is just being installed, it may be too early to proclaim the Traverse City experiment a success. To date, though, it seems to be the most cost-effective program of its kind. Unlike the PV panels in Sacramento, whose cost is subsidized by grants and SMUD ratepayers, Traverse City's turbine is being purchased with green pricing funds. (Smiley)

In sum, green pricing does not yet have an extensive track record in this country. The record it does have is mixed. Of the nation's 3,000-some utilities, only three have green pricing programs. Fewer than 2,000 people are participating, and their contributions have bought less than 1.5 Megawatts of renewable generation — not nearly enough to help commercialize these technologies. The concept of green pricing clearly appeals both to utilities and to their consumers, but the idea has had difficulty gaining a toehold.

Several factors appear to explain the problems associated with utility-sponsored green-pricing programs. For one, these green pricing programs have focused exclusively on obtaining funding from a relatively small number of residential customers. In the residential class, the transaction costs of dealing with individual customers is high. As a result, a substantial amount of utility overhead is necessary. Moreover, the overwhelming majority of residential customers remain unaware that a green pricing program even exists. For example, PSCO determined at one point that less than 2% of its residential customers were aware of its REAP program.

In addition, the existing programs have recruited program participants primarily through bill inserts, press releases, and similar outreach. This traditional, if somewhat passive, approach to design and marketing appears to have been partly responsible for the dramatic drop-off between the public's willingness to pay, as determined by market research, and actual participation rates in practice. (Byrnes).

We believe that the electric utility industry has barely begun to harness the potential of green pricing programs. Now that a significant number of market research studies have been completed, and some real world experience gathered, new lines of inquiry suggest themselves. The time is right to refine the model, target larger customers, develop second generation green pricing programs, and implement them on a bigger scale in order to acquire renewable resources in amounts that will help commercialize these key technologies.

II. Developing New Methods To Create, Market, And Sell Clean Kilowatt-Hours.

Research suggests that willingness to participate in green pricing programs correlates with a customer's level of income, education, environmental understanding, and program awareness. (Niagara Mohawk). While the first two factors are relatively fixed, the last two are fluid, and could theoretically be enhanced with creative marketing, advertising, and outreach.

Monopoly service territories and the invisible, fungible nature of electricity itself have limited product differentiation in the utility industry. (Nakarado). But as choice and competition appear on the horizon, and as the price of renewable energy continues to fall, it has become possible to conceive of a fundamentally new utility product — the clean kilowatt-hour — and new institutions to produce, market, and sell it.

Although a number of sophisticated studies have analyzed customer willingness to participate in green pricing programs, little research exists on how best to differentiate and sell clean power as a product in the green marketplace. In other words, there is a lot of market research, but little research on *marketing*. What insights from the marketing of organic cotton clothing, recycled paper, dolphin friendly tuna, and other products are potentially applicable to clean power? The question merits more study.

A 1994 paper contends that consumers do not buy products, they buy product benefits. (Taylor). This insight has important ramifications. Although renewable energy has a quantifiable economic value to a utility, its value to a consumer is an attributed value. That is, the value of clean power is based more on intellectual belief and environmental understanding than on the physical properties of an invisible force. Marketing clean kilowatt-hours as a consumer good, making their purchase chic and fashionable, requires more than snazzy advertising. It will take imagination, consumer education, and community outreach.

To date, it has been assumed that utilities would market clean power. Who else could? But perhaps in the same way that energy services companies are beginning to succeed in helping to market energy efficiency, utility efforts to sell cleaner renewable power could be greatly supplemented by outside entities. Indeed, it is not clear that utilities have the institutional desire, entrepreneurial acumen, and financial incentive to successfully market a new product — particularly one whose appeal subtly undercuts their standard offering. If not, the future of green pricing may be stunted unless a marketing alternative can be devised.

In the view of some, most utilities view green pricing more as public relations gesture than as a business opportunity. (Smiley). This may not change until customer choice (in the form of retail wheeling) is sanctioned by law. From the utility perspective, green pricing renewables is less risky than rate-basing them. But if, from the utility perspective, there is little risk to green pricing, there is also correspondingly little financial reward — and thus little incentive to ensure that such programs succeed.

Even if utilities wanted to sell clean power, they might have difficulty doing so. Many IOUs lack credibility in terms of environmental stewardship. (Niagara Mohawk). And green consumers, the prime audience for clean power, often mistrust utilities the most. This may be why many utilities, such as PSCO, have considered forming "Citizens Advisory Boards" to give green pricing a seal of approval. (Walther; Niagara Mohawk).

From a public policy perspective, clean power and green pricing are valuable tools to accelerate the deployment of renewable energy. To date, their fate has been left largely in the hands of an industry which has little investment in whether such innovative tools succeed or fail. In this situation, it may make sense to explore another assumption: that for green pricing to achieve its full promise, utility efforts to market clean power need to be actively supplemented by a consumer coalition composed of grassroots citizen groups, civic and political leaders, business people, and environmental organizations. Specific questions we will address in Colorado include:

*How can a clean kilowatt-hour best be advertised, positioned, and marketed?

*What lessons have other utilities learned about marketing clean power? What lessons from marketing other green products are applicable to clean power?

*What is the most effective method for recruiting green pricing participants?

*Most green pricing programs have targeted residential customers. Could commercial and industrial customers be recruited as well? How? What are the key factors that would attract such customers?

*How could a grassroots effort to market clean power be financed? Could community organizations partner with utilities to achieve higher participation rates than current green pricing programs project?

*What are the essential elements of a clean power marketing campaign?

*Finally, in what new ways could clean power be marketed? Could, for example, partnerships be formed with local business groups (Chambers of Commerce), professional organizations (Rotary, Lions), national non-profits (the Girl Scouts, Sierra Club, Recreational Equipment, Inc.), or credit card companies (Working Assets) to make buying clean power easier?

III. Overcoming Institutional, Regulatory, and Financial Barriers That Impede Investor-Owned Utilities From Offering Customers An Option To Buy Clean Power.

Although a number of large, investor-owned utilities (IOUs) have investigated green pricing, some efforts have been delayed due to institutional, regulatory, and financial barriers. (Walther). Designing green pricing programs and securing regulatory approval has been time consuming. Niagara Mohawk, for example, has needed three years to study green pricing, do market research, design a program, and gain regulatory approval. This raises a number of questions. How can such barriers be overcome? Can standardized methods be developed to avoid delays and assist utilities in launching green pricing programs?

Other specific questions we will address include:

* What regulatory and economic barriers have delayed the initiation of green pricing programs at other IOUs?

*What contractual arrangements need to be developed if larger customers are going to participate in green pricing programs? Does the future possibility of retail wheeling change the nature of these contracts?

*What contribution arising from a utility's avoided cost savings should be used to supplement funds raised through a green pricing program? Who should decide this question? Regulators? The utility?

*What renewables projects should be selected for funding? Who should decide what projects get selected? Should this question be resolved before utilities approach their customers?

*Once a project is identified for funding, how much money should it get? Again, who decides?

*Who owns any generation purchased as a result of a green pricing program? The utility? An independent power producer? The participating customers?

*Is it possible for utilities to cooperate with other entities in the development of green pricing programs? For example, can a large, investor-owned utility wheel clean power to smaller utilities who are its wholesale customers?

*What renewable resources can be developed with relatively small customer contributions? How is that power wheeled?

*What needs to happen to make a local green pricing program a reality? How much money, at a minimum, is needed to get started?

*If initial efforts are successful, how does one build on them? Is it possible to develop a guide to the practical implementation of green pricing that would help other utilities overcome similar problems?

IV. Devising Strategies For Using Green Pricing To Accelerate The Deployment Of Renewable Energy On A State And Regional Level.

Although green pricing is sometimes viewed as undercutting efforts to deploy renewables through Integrated Resource Planning and other typical utility resource acquisition processes, the two approaches should be complimentary. Moreover, green pricing programs could be combined with other efforts to mobilize support behind renewable resource acquisitions. In our Colorado case study, we intend to address these questions:

*Can the 1999 deadline to qualify for the Energy Policy Act's production tax incentives be paired with green pricing to mobilize state or regional efforts to develop renewable resources?

*What is the exact relationship between utility IRP processes and green pricing programs?

*How can green pricing programs be developed so that they fit into utility IRP processes and make possible an overall coordinated effort to systematically acquire renewables?

*Do green pricing programs influence the outcome of ongoing regulatory proceedings involving utility incentives and cost recovery associated with renewables investments? If so, how?

*Can IRP and other proceedings offer an attractive opportunity for transferring information about green pricing programs among different states?

* Could, for example, a green pricing "citizens challenge," issued by a state's Public Utility Commission, Governor, legislature, utility industry, and/or business community be used to obtain additional funding for renewable resources?

*How might such a challenge work? ("If citizens and businesses commit to buying five Megawatts in the next six months, the utility will fund another five.")

V. A COLORADO CASE STUDY

As we develop a new model for green pricing, we intend to test its key assumptions with a real-world case study in Colorado. To do this, we propose creating a partnership between ourselves and at least two, and perhaps more, Colorado utilities. The Land and Water Fund of the Rockies brings decades of utility and regulatory experience to bear in helping to solve the institutional and other issues that are

likely to arise in developing and implementing a green pricing program through a partnership with electric utilities. In addition, through its ongoing work in utility IRP and other regulatory proceedings, the LAW Fund is well-situated to transfer the lessons learned about green pricing to other utilities and jurisdictions in the region and nationally.

CORE, the second partner in this case study, is a community-based non-profit organization. It can help its local utility market a green pricing program to residential, business, and commercial customers. Indeed, through CORE's work we propose to create a new, consumer-driven green pricing program based on community outreach, grassroots marketing, and an aggressive public education campaign organized by a citizen-based "clean power alliance."

This case study hopes to develop a green pricing program that is substantially different from any utility program that has occurred to date. This pioneering green pricing program will target both residential *and* commercial customers, including ski areas, municipalities, and high-tech companies. Our initial work suggests that these companies are interested in presenting themselves as purchasers of green power. Moreover, this approach should greatly reduce the transaction costs associated with green pricing while raising the dollars collected and the profile of the program.

Once this work is completed, we will produce a draft white paper that describes our conclusions. This paper will then be distributed for peer review. Comments, criticisms, and suggestions will be incorporated in the final report. In this final report we will describe the lessons learned. If our approach is successful, we will try to identify the key reasons for our success. If we are unsuccessful, we will explain how and why we think we failed. We will also incorporate our insights into a practical guide for implementing green pricing.

A. Utilities Involved

Our preliminary work has focused on Holy Cross Electric Association (Holy Cross). In addition, we have also had discussions with Public Service Company of Colorado (PSCO), Holy Cross' primary power provider, and with Aspen Municipal Electric Utility, whose service territory adjoins Holy Cross. All three utilities are currently assessing the green pricing concept.

No final decisions have been reached, but it appears likely that Holy Cross and PSCO will cooperate so that Holy Cross can offer a green rate to its 38,000 customers. In addition, through discussions with the LAW Fund and other key stakeholders, PSCO is exploring ways of improving its green pricing program. Finally, Aspen Municipal has had discussions about green pricing with its wholesale supplier, the Municipal Energy Agency of Nebraska.

Several factors combine to make these Colorado utilities an almost ideal opportunity for creating a new approach for green pricing. Holy Cross Electric Association is a 185 Megawatt, transmission-and-distribution rural electric cooperative serving 38,000 customers in western Colorado. The utility's largest customers are Vail and Aspen ski areas, which purchase about $4 million of the approximately $50 million worth of electricity Holy Cross sells each year. With growth rates averaging 8%, the utility is one of the fastest growing in the country.

Holy Cross buys 10% of its power from the Western Area Power Administration. The remaining 90% is purchased from PSCO under a "requirements" contract. Holy Cross's residential rates are 7 cents/kWh, about average for Colorado. Its avoided costs under its purchased power contract with PSCO are about 4 cents/kWh. Moreover, through PSCO, Holy Cross has access to the output of a Class VII wind site near Arlington, Wyoming which is due to be brought online by 1996.

Although the utility's managers are opposed to funding renewables with monies collected from all customers, they strongly support the principle of customer choice and free market solutions to environmental problems. The area Holy Cross serves is generally affluent and well-educated; Pitkin County ranks in the top ten counties nationwide on household income and average education levels. Based on research that demonstrates a correlation between income, education, and willingness to invest in renewables, such measures bode well for a green pricing program in this area. In addition, Holy Cross provides power to Garfield County which tends to be more representative of the Western U.S. and can thus serve as a model for other utilities.

Under these circumstances, we believe Holy Cross offers an almost ideal opportunity to develop and implement a new approach for green pricing through a partnership with outside entities: the utility wants to experiment with green pricing, but lacks the expertise; it has high avoided costs; it is located near an extremely cost-effective renewable resource; its customers are both educated and environmentally aware, but also, in many instances, representative of the broader regional population; a local community group, CORE, is positioned to partner with the utility; the utility and the community are small enough that a new program can be developed relatively quickly; and, if successful, the results can almost immediately be transferred to PSCO which has over a million customers in Colorado. Moreover, the lessons learned can be transferred throughout the region relatively quickly through the LAW Fund.

B. Lead Organizations

The Land and Water Fund of the Rockies ("LAW Fund") is a non-profit environmental organization that promotes environmentally sound energy policies in a six-state region in the Rocky Mountains and Desert Southwest. Our six states include Arizona, Colorado, Nevada, New Mexico, Utah, and Wyoming. To promote environmental goals, we generally intervene in public utility commission or other administrative proceedings. Our approach has been to work with utilities to make it profitable for them to promote environmentally sound alternatives such as energy efficiency and renewable resources. To be effective in this work, we have pulled together an inter-disciplinary team of lawyers, economists, engineers, and accountants. Moreover, our staff, coming from a wide variety of backgrounds, has extensive experience working with utilities, consulting firms, consumer counsel offices, government, and regulatory agencies.

The LAW Fund has participated in a wide range of utility proceedings in our region involving resource planning, financial incentive, plant siting, and industry restructuring issues. We have also been an active player in a variety of regional processes which include the Federal Energy Regulatory Commission, the Western Area Power Administration, and the Grand Canyon Visibility Transport Commission. All told, over the past four to five years the LAW Fund has been involved in both collaborative and administrative processes that have produced roughly $50 million in annual utility investments in energy efficiency and similar, but smaller, expenditures on solar and wind power. The LAW Fund will deal with all utility and regulatory issues associated with this project proposal.

The Community Office for Resource Efficiency ("CORE") is a 501(c)3 nonprofit organization funded by an unusual coalition of three local governments and three utilities. Those sponsors include Pitkin County, the City of Aspen, Snowmass Village, Holy Cross Electric Association, Aspen Municipal Electric, and Rocky Mountain Natural Gas. CORE's mission is to promote water and energy efficiency in the Roaring Fork Valley.

CORE was established due to the efforts of the Energy 2000 Committee, a grassroots advocacy group interested in resource issues. CORE and the Energy 2000 Committee co-sponsor an annual Energy Town Meeting in Aspen, Colorado; the fourth such meeting in the fall of 1994 attracted 300 participants. The group's work has been recognized in two recent publications: *Renewables Are Ready*, published by the Union of Concerned Scientists and the *Community Energy Workbook: A Guide to Building A Sustainable Economy*, by Alice Hubbard and Clay Fong of Rocky Mountain Institute. CORE and the Energy 2000 Committee would spearhead the grassroots, citizen outreach program to market clean power that is proposed in this study.

Individuals interested in more information on this project may contact Eric Blank at (303) 444-1188 or James Udall at (970) 544-9808.

PLAYING THE ODDS: CLIMATE CHANGE RISKS TRANSFORM UTILITY PLANS

Michael W. Tennis
Union of Concerned Scientists
Two Brattle Square
Cambridge, MA 02238-9105

Electric utilities are in much the same situation today that they were during the late seventies. In the seventies, the environmental science regarding acid rain and smog formation was developing rapidly while environmental policy implementation lagged. Utilities who choose low sulfur coal over high sulfur coal or low-NOx burners over high NOx boilers in the seventies delayed or all together avoided costly retrofits of emission control technologies under the Clean Air Act. In so doing, utility decisionmakers protected their ratepayers and shareholders from foreseeable financial risks and position their companies as good corporate citizens.

Looking back over the first twenty five years of environmental regulation, it is clear that the serious concerns that environmental scientists had about acid rain and smog formation in the 1960's and 1970's made it possible, indeed, likely that some sort of environmental performance regulation would follow. Today, environmental science of climate change is advancing rapidly while climate change policy lags. It is clear that climate change issues pose potentially serious environmental and ultimately financial risks. Given the current and growing scientific consensus on climate change impacts and the continued, unequivocal, support of voter's worldwide for strong environmental protection, it is likely that policy measures controlling greenhouse gas emissions will be enacted within the next five to twenty years.

Should uncertainty about the timing or exact nature of climate change policy be an excuse for inaction? Should a "no regrets" strategy for dealing with issue of climate change impacts really be a combination of "no bucks" and "pass the buck" actions as many contend? Analysis conducted jointly by the Union of Concerned Scientists and World Resource Institute suggests not. Investments now in low carbon emitting energy resources could pay large dividends in a climate change constrained future without raising costs significantly today. The size of those dividends depends on how likely climate change regulations are.

NO REGRETS? PASS THE BUCK?

The Intergovernmental Panel on Climate Change (IPCC) has identified a host of actions that it deems as "no regrets" actions that control emissions of greenhouse gases (GHG). The IPCC has also stated that climate change science supports industrialized nations taking actions over and above these "no regrets" actions. In general, utilities and utility regulators have not integrated systematic procedures for integrating climate change mitigation measures beyond "no regrets" into their plans. For example, in its most recent resource plan covering the period from 1996 to 2010, a large investor-owned utility in the upper midwest, discusses three options for mitigating the risk of future climate change regulations. The first dubbed "no regrets" means that it will pursue only those resources, such as very low-cost demand-side management (DSM), that are cost effective today based on their non-climate benefits. This approach is better described as "no bucks" because the utility has decided, a priori, that no investments over its current low avoided cost should be made now as insurance against climate change regulation risks.

The second approach endorsed by the utility is one where the risk of climate change compliance costs for new power plants is passed contractually to the power plant builders who theoretically will add a risk premium to their bids to account for this potential risk. This approach completely ignores the major contribution that existing fossil-fired plants are making and will continue to make to its carbon emission inventory. For this utility, CO2 emissions from its existing generating inventory account for 88% of the total annual emissions as late as 2010.

A third strategy is one the utility company rejects as not practical due to the uncertainties of the future. Under this approach, it would acquire additional low carbon emission resources like wind power, biomass, or energy efficiency, accepting some costs over and above today's market price for conventional, fossil-fueled power. This cost increase could be thought of as an "insurance premium" against the risks of climate change.

It is troubling that while no stockholder, bank, or board of directors would support a company whose management did not purchase fire insurance, power industry management, stockholders, and boards essentially ignore the risk of climate change. Insurance against climate change problems should be a component of sound utility management as surely as fire insurance is for property management.

The critical question for utility decisionmakers is how to evaluate and justify investments in "climate change insurance".

UTILITY PLANNING - EVALUATING AND JUSTIFYING INVESTMENTS IN "CLIMATE CHANGE INSURANCE"

OVERVIEW

Operating a utility today is more akin to playing the stock market than it is to traditional utility operating principles. Concepts like Portfolio Management, Decision Trees, Options Theory, Risk-adjusted Discount Rates, and Capital Asset Pricing, more familiar to stock brokers and investment councilors, are beginning to be applied to utility planning.

A few utilities, notably, the New England Electric System and Sacramento Municipal Utility District have begun to act aggressively using these new concepts and criteria to position themselves more effectively for an uncertain future. Their recent resource acquisitions have included a variety of thoughtful investments to bring renewable energy resources and advanced DSM into their resource portfolios. The resource plans resulting from these new approaches are not necessarily the "least-cost" based on traditional, deterministic criteria, rather they are robust and stable over a wide range of future conditions protecting shareholders and ratepayers from extremely poor performance under foreseeable conditions and leaving managers with flexibility in responding to unanticipated circumstances. Under this advanced planning paradigm, a "no regrets" approach might very well include investments in above market renewable resources today rather than the "no bucks" approach proposed by other utilities.[1]

[1] Utilities like NEES and SMUD also justify these investments as part of a strategy to commercialize these low-emission, renewable generating technologies so that they are more readily available and cheaper in the future.

UCS/WRI ANALYSIS

As part of a larger WRI project to identify sustainable options for major industries in the U.S.[2], WRI and UCS developed a case study of a midwest, investor-owned utility. The purpose of this case study was to shed light on the dilemma facing the electric industry and policy-makers over whether to take action in the near term to anticipate future carbon constraints. To do this, UCS expanded the utility modeling capability developed for *Powering the Midwest*[3] to cover the years 1995 to 2050 and to include more power resource choices including energy efficiency, wind, and biomass.

To conduct the analysis, two strategies for meeting future electric resource requirements in the face of climate change uncertainty were developed and compared. In each, the mix of resources is chosen to minimize the cost of meeting projected electric demand and generation requirements. Under one strategy, which we designate "wait-and-see" (WAS), the utility does nothing to anticipate the imposition of future carbon restrictions. Rather, it simply waits until the carbon restriction, represented by a carbon tax, is imposed and then alters its investment decisions based on the changed fuel price conditions. This path corresponds closely to the base case resource plans for a number of midwest utilities.

The other strategy, which we designated "act-then-learn" (ATL) explicitly anticipates a possible carbon restriction before one is actually imposed and makes least-cost resource acquisitions based on a postulated carbon tax. To accomplish this, we assumed that a $100/ton of carbon dioxide tax on all fossil fuel used would be phased in between 2010 and 2020.

Since we are uncertain whether or not carbon dioxide emission control policies will be put in place, we assess both strategies with and without the carbon tax actually imposed. In the "wait-and-see" strategy where the utility does not anticipate a carbon tax, the resource acquisition pattern changes abruptly only if the carbon tax is actually implemented. Conversely in the "act-then-learn" strategy where the utility anticipates a carbon tax, resource acquisitions change when the utility determines that carbon tax is not going to be implemented. The costs of the two strategies under two futures, one with a carbon tax and one without, defines their financial performance at the limits of our analysis.

Policy-makers can to begin to assess the different resource acquisition strategies by examining the expected value of a strategy under different futures with different probabilities of occurrence. This type of approach pushes the analysis and discussion of uncertainty to a more useful level providing a quantitative basis for selecting a resource acquisition strategy that may not be "least cost" for a conventional "base case" resource plan.

UCS/WRI RESULTS

Table 1 summarizes the results under the four possible cases in terms of cost and CO2 emissions.

---

[2] Dower, R., Kozloff, K., MacKenzie, J., Ditz, D.; Johnson, N., Faeth, P., A Sustainable Future for the United States, World Resources Institute, Summer 1996.

[3] Brower, M., Tennis, M., Denzler, E., Kaplan, M., Powering the Midwest - Renewable Electricity for the Economy and the Environment, Union of Concerned Scientists, March 1993

TABLE 1, Summary UCS/WRI Climate Change Analysis

Scenario	Tax	Present Value Costs (1995 $ Billions)	Cumulative CO2 Emissions 1995-2050 (million tons)	2050 Emissions (% of 1995 levels)
WAS	NO	19.7	2,215	290%
WAS	YES	30.1	446	10%
ATL	NO	20.9	2,006	169%
ATL	YES	28.6	356	8%

There are three sweeping conclusions evident from this table. First, if current trends remain in effect and carbon dioxide emissions reductions are not pursued, then CO2 emissions from midwest utilities could nearly triple by 2050. Second, our analysis suggests that in the midwest, utilities should have sufficient low-carbon/renewable and energy efficiency resources to dramatically reduce CO2 emissions. Given the conservative technology and fuel price assumptions in our analysis, replacing the majority of the conventional fossil-fueled generating resources with renewable resources could raise the levelized cost of electricity by about 30% - 40%, raising rates by 10% to 20%.[4]

Under the "wait-and-see" case with no carbon tax, the utility's current path, carbon dioxide emissions nearly triple by 2050 over 1995 levels. The generating mix remains dominated by coal-fired generation throughout the period. Gas-fired generation grows in importance early in the study period however increasing natural gas fuel prices ultimately limit the fraction of generation that it provides. Wind energy becomes the second largest generator in our analysis increasing quickly to our predetermined penetration limit of 20% of total generation by 2020 and remaining there through 2050. With no carbon tax, neither higher cost DSM nor biomass capture a significant portion of the resource mix.

Under the "act-then-learn" case with no carbon tax, the resource acquisitions in the years 2000 through 2020 are dominated by wind energy and DSM rather than natural gas as in the WAS no tax future. The generating mix remains dominated by coal-fired generation throughout the period. Wind energy becomes the second largest generator in our analysis increasing quickly to the penetration limit of 20% of total generation by 2020 and remaining there through 2050. Gas-fired generation grows in importance between 2010 and 2020, but again, increasing natural gas fuel prices ultimately limit the fraction of generation that it provides.

When a carbon tax is imposed on the "wait-and-see" strategy, dramatic changes occur between 2010 and 2020. The $100/ton carbon tax makes the operating cost of existing coal-fired generation higher than the cost of installing and operating advanced biomass-fired systems. As a result, biomass quickly dominates generating mix in the post 2020 period. Wind generation and DSM are fully implemented. Natural gas-fired resources are relied upon for only a small fraction of generating requirements by the year 2050.

[4] Energy costs account for between 30% to 50% of retail rates today.

The ATL strategy with a carbon tax is very similar to the WAS strategy by the year 2050. Biomass, wind, and DSM dominate the generating mix with natural gas carrying an even smaller fraction of the load. A carbon tax of $100/ton clearly moves all available low carbon resources high penetration levels.

The UCS/WRI estimates of carbon emissions in the years 2010 and 2050, cumulative emissions 1995 - 2050, and present value costs are shown in Table 1. Under a future with no carbon tax, the WAS strategy results in carbon emissions 290% of 1995 levels. Pursuing an "act-then-learn" strategy when a carbon tax is not implemented slows carbon emissions increases somewhat compared to the "wait-and-see" strategy however total carbon emissions for the midwest utility still rise to 169% of 1995 levels. By 2050, a carbon tax of $100/ton drives carbon emissions well below 1995 levels in both the "wait-and-see" (10.4%) and "act-then-learn" (8.5%) strategies.

Changing investment patterns in response to an actual or anticipated $100/ton carbon tax would raise power costs under the technology and fuel price assumptions that we used in our analysis. The net present value of costs from 2000 to 2050 is calculated to increase by $8.9 billion for the ATL strategy and $10.4 billion for the WAS strategy. The impact of adding zero carbon resources in the early years of the ATL strategy increases its present value by $1.2 billion or 6% over the WAS strategy when no carbon tax is imposed.[5] Our analysis shows that ATL raises annual electricity costs by 1 to 3 mills/kWh in the years prior to the imposition of a carbon tax in exchange for cost reductions of 6 to 8 mills/kWh after a $100/ton carbon tax is imposed.

The benefits of climate change emission reductions are external to a utility's accounting. This means that although society benefits from reduced CO2 emissions, the utility does not see any monetary benefit from its CO2 control efforts. To account for the difference between the utility and societal perspectives, we analyzed the climate change tradeoffs in two different ways. To represent a utility perspective, we valued the CO2 emission reductions at zero and discounted the costs of the plan at a real discount rate of 6.2%/yr. To represent society's perspective, we valued the CO2 emission reductions at $100/ton and discounted the costs at a societal discount rate of 3%/yr. Tables 2 and 3 show the net present value (costs-benefits) of the wait-and-see and act-then-learn strategies under futures with and without a $100/ton carbon tax imposed in 2020. For clarity, these values were referenced to the net present value (NPV) of the WAS no tax scenario cost of $19.7 billion.

TABLE 2, Net Present Value (Costs-Benefits) in 1995 $ billions
Utility Perspective: Benefits = 0; Discount Rate = 6.2% real

SCENARIO	TAX	NO TAX
WAS	10.4	0
ATL	8.9	1.2

If the carbon tax is imposed, the cost increase of the WAS strategy is $10.4 billion while the ATL strategy is only $8.9 billion. If no carbon tax is imposed, the cost of the ATL strategy is 1.2 billion or 6% higher than the WAS no tax case.

[5] The ATL strategy is one where the utility would choose to make some investments in the years prior to resolution of the climate change policy development in return for benefits later.

Figure 1 shows the climate change trade-off from the perspective of the utility company. This figure shows the "expected" value of each strategy as a function of the probability that a $100/ton carbon tax is imposed in the 2020.

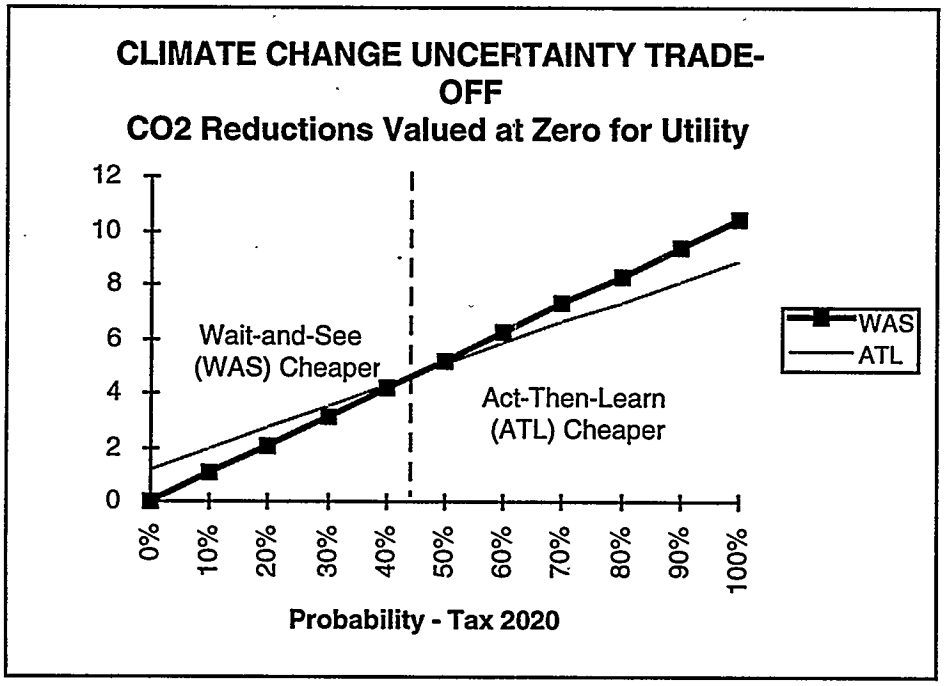

If the probability of this carbon tax is approximately 45% or higher, the ATL strategy will be cheaper than the WAS strategy from utility's perspective. If the probability of the carbon tax is less than 45%, then the WAS strategy is cheaper.

When society's perspective is considered, that is, the savings from reduced carbon emissions are explicitly given a monetary value, the imposition of a carbon tax reduces society's net costs of dealing with climate change. When no tax is imposed we assume that climate change is not an issue and CO2 emissions have no value. When no tax is imposed, the ATL strategy costs society $3.2 billion in net present value terms.[6] If a carbon tax is imposed and emission reductions are valued at $100/ton, the benefits of carbon reductions exceed the costs of adopting low carbon electricity resources by $37.1 billion using the WAS strategy and $47.7 billion using the ATL strategy.

[6] The difference between the $3.2 billion calculated here and the $1.2 billion calculated from the utility's perspective is due to the different discount rates used for the calculations.

TABLE 3, Net Present Value (Costs-Benefits) in 1995 $ billions
Society Perspective: Benefits = $100/ton; Discount Rate = 3% real

SCENARIO	TAX	NO TAX
WAS	-37.1	0
ATL	-47.7	3.2

Figure 2 is the climate change trade-off chart from society's perspective.

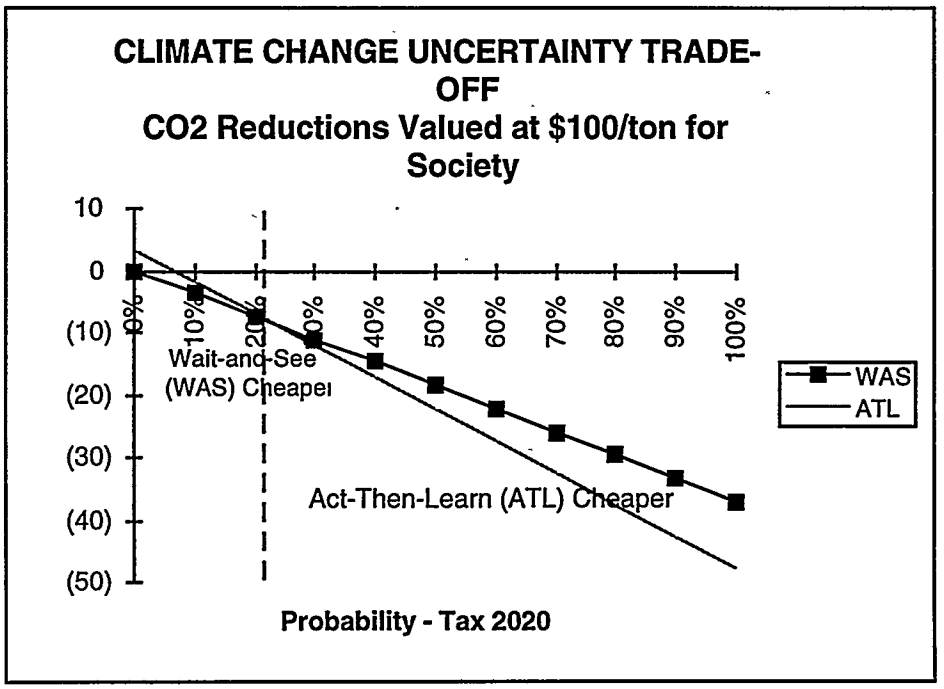

Not surprisingly, when carbon emission reductions are credited with some monetary benefit, the rationale for adopting an act-then-learn strategy to climate change is much more compelling. From society's perspective, we need only assign a probability of 20% or more, roughly 1 chance in 5 or better, that a carbon tax will be imposed and the ACL strategy is preferred over the WAS strategy.

Analyses like these allow policy-makers to begin to assess the robustness and stability of different resource acquisition strategies by examining the expected value of a strategy under different futures with different probabilities of occurrence. They also help illuminate the important differences between the perspective of a utility company and that of society as a whole on an issue like climate change. In the analysis presented here two important policy implications are clear. Explicit consideration of climate change uncertainty can provide an economic justification for investing in low carbon resources at above market costs. In our example, policymakers need only accept the notion that there is a 50/50 or better chance that a carbon tax policy will imposed before an act-then learn strategy is preferred.

The second major implication of this analysis for policymakers is that an analysis of the climate change issue from a utility perspective where carbon emission reductions have no monetary value, consistently understates the societal value of an act-then-learn strategy. In the examples presented here, policymakers taking a societal approach to the issue of dealing with climate change need only assign a 1 in 5 probability or better probability that carbon tax policy will be imposed before an act-then-learn strategy is preferred. From the utility perspective, this probability must be 50/50 before ATL is preferred. It is in society's interest for a utility to "err" on the side of adding more low carbon resources to their resource mix than are justified based on cost and uncertainty analysis from the Company perspective.

RECOMMENDATIONS

Determining the expected value of the resource plan as a function of the probability of a particular uncertain parameter can be very informative and provide a compelling rationale for adopting a resource plan that is something other than strictly least cost under some predetermined base case scenario. Without this type of uncertainty analysis, utilities will always prefer to adopt their least cost, base case resource plan.

The analysis and discussions presented in this paper strongly support several recommendations regarding the utility resource planning.

- Utilities and regulators should develop a consistent and systematic process that can be used to explicitly include consideration of climate change impacts in their resource planning. Uncertainty must be considered explicitly so that this type of analysis can be used to develop an economic rationale for including low carbon resources that may be above market price in utility resource portfolios.

- In the midwest, a policy of planning as *if climate change matters* could open many opportunities for climate friendly resources like wind energy and energy efficiency without exposing consumers to significant near-term costs.

- It is the uncertainty of the future that gives energy efficiency and renewable resource options their extra value. Unless uncertainty is accounted for explicitly in a benefit cost assessment, above-market-cost resources will not survive a benefit cost test.

- The fact that climate-friendly resources are consistently more valuable from society's perspective than from the utility's perspective, suggests that policymakers adopt incentive mechanisms that better align the utility's interests with those of society as a whole. The current production incentive payments and tax credits for renewable energy production are examples of this type of incentive. Energy efficiency and renewable resources would produce additional benefits for society if additional incentives were in place.

INDUSTRY GUIDELINES FOR THE CALIBRATION OF MAXIMUM ANEMOMETERS

Bruce H. Bailey
AWS Scientific, Inc.
3 Washington Square
Albany, NY 12205

INTRODUCTION

The measurement of wind speed is a fundamental step when evaluating the feasibility of wind energy development. Because of the non-linear, cubic relationship between the wind's speed and power content, small speed measurement errors equate to relatively large errors in the estimation of a wind turbine's energy output. Vachon (1985) summarizes the sources of measurement error and their impact on uncertainties in predictions of wind turbine output. It is safe to say that a goal of all wind measurement programs is to ensure that measurement-related uncertainties are limited to levels within a user's tolerance. Ultimately, minimizing measurement uncertainty minimizes the planning, siting, and financing risks of a wind energy project. Since the anemometer is one source of measurement uncertainty, calibration is a way to define and control this uncertainty.

The purpose of this paper is to report on a framework of guidelines for the calibration of the Maximum Type 40 anemometer. This anemometer model is the wind speed sensor of choice in the overwhelming majority of wind resource assessment programs in the U.S. It is generally regarded as being low-cost, low-maintenance, and durable. Despite this sensor's popularity, there is a lack of consensus regarding the appropriate calibration method, or even whether it needs to be calibrated. In fact, in a survey conducted by the author of 17 resource assessment consultants, organizations and sensor vendors, the majority of Maximum anemometers used for wind resource assessment purposes are <u>not</u> calibrated. This situation challenges the wind resource assessment community to define and defend the accuracy of its wind speed data.

These guidelines were established by the Utility Wind Resource Assessment Program (U*WRAP) on behalf of the U.S. Department of Energy and several U.S. utilities (Bailey and McDonald, 1995). The need for these guidelines was prompted by several developments:

- First, is the recent establishment of organized national wind resource assessment programs, such as U*WRAP and the Cooperative Network for Renewable Resource Measurements (CONFRRM). Both programs, which employ this particular anemometer model, have adopted standardized measurement protocols and rigorous quality assurance programs, including anemometer calibration.
- Second, is the growing pressure on the U.S. wind energy industry to conform with international standards for wind energy technology-related certification activities, which include wind speed measurement.
- Third, is a discrepancy between the results of the two most popular calibration techniques practiced by the wind energy industry.

By addressing current concerns over anemometer calibrations, these guidelines aim to minimize avoidable measurement uncertainty and improve the overall quality of wind speed data.

BACKGROUND

The Maximum Type 40 anemometer is a 3-cup design incorporating 51 mm (2.0 in) diameter conical cups which sweep a 190 mm (7.5 in) outer diameter. The cups are made from one piece injection-molded black polycarbonate plastic (Lexan). The beryllium copper shaft is mounted on a modified Teflon, self-lubricating bearing. Rotation of the cups spins a four pole magnet past a stationary coil, producing a sine wave voltage. Each revolution of the cups generates two sine wave cycles at a frequency that is linearly proportional to the wind speed. The voltage output varies in amplitude from 0.5 to 6.0VAC, corresponding to about 0.9 m/s to 45.8 m/s. Other instrument specifications as reported by the manufacturer:

Starting threshold: 0.78 m/s (1.75 mph)
Distance constant: 3.0 m (10 ft)
Operating temperature: -55°C to 60°C (-67°F to 150°F)
Operating humidity range: 0 to 100%

Wind turbine siting guidelines established by the American Wind Energy Association (AWEA) recommend that wind speed measurement systems have an uncertainty no greater than ±3 percent (AWEA Standard 8.2 - 1993). This means that the uncertainties contributed by all of the measurement system components — anemometer, signal wire, data logger, electrical grounding, support structure — should combine to fall within this narrow range. Measurement practices designed to satisfy this recommendation are described in AWEA Standard 8.2 as well as in AWEA Standard 8.1 (1986) — *Standard Procedures for Meteorological Measurements at a Potential Wind Turbine Site* — which is currently undergoing revision.

There are two generally practiced calibration techniques for anemometry: wind tunnel and moving vehicle testing. Both have their advantages and disadvantages. Wind tunnels offer controlled, laminar flow test conditions and, when properly operated, provide accurate and precise test conditions. Standard procedures for wind tunnel testing have been established by the American Society of Testing and Materials (ASTM, 1990). In a round robin comparison of several U.S. wind tunnel facilities, Lockhart (1991) found that carefully calibrated wind tunnels can generate winds at speeds known to a relative accuracy of about one percent. However, laminar flow conditions are not completely representative of the turbulent flow conditions typical of the lower atmosphere. Moving vehicle calibration consists of moving a set of calibrated reference and test anemometers on a vehicle through relatively still air and has been described in several papers (Obermeier 1990, 1994; Obermeier & Blittersdorf, 1996). This procedure, which has demonstrated a high degree of precision, is conducted in the open atmosphere in a manner that has been shown to avoid the influence of the wind flow distortion caused by the vehicle. Neither technique has been shown to be superior.

CALIBRATION HISTORY

The results of wind tunnel and open vehicle calibrations of over 3,000 Maximum anemometers have been documented. Second Wind, Inc., a major supplier of calibrated anemometers, utilizes the Wright Brothers Wind Tunnel at the Massachusetts Institute of Technology (MIT) to perform its calibrations. In a revised version of a paper presented at AWEA's Windpower '94 Conference, the results of over 400 new anemometer calibrations, conducted in 1993 and 1994, were presented (Sass, 1994). Second Wind determined the average relationship between wind speed and anemometer pulses (expressed as pulses per second, or Hz) as follows:

wind speed = 0.77 m/s per Hz + 0.5 m/s
= 1.73 mph per Hz + 1.08 mph

In these tests, the standard deviation of the distribution of slope values was approximately one percent. The difference between the maximum and minimum slope values gave a range of approximately nine percent. The standard error for the offset was approximately 0.08 m/s (0.2 mph).

Since 1987, vehicle test calibrations have been conducted in California by Otech Engineering on behalf of NRG Systems, Inc. (Obermeier, 1990, 1994; Obermeier & Blittersdorf, 1996). Over 2,500 anemometers have been calibrated using a mounting rig attached to a moving vehicle. The mounting rig has evolved in design over the years to locate the test anemometers outside the measurable influence of the vehicle's bow wake. In 1994, the average relationship between wind speed and anemometer output was reported to be:

wind speed = 0.76 m/s per Hz + 0.3 m/s
= 1.70 mph per Hz + 0.7 mph

Since vehicle calibrations began, the standard deviation of the distribution of slope values has decreased from 1.2 percent to 0.6 percent, and the range of slope values from maximum to minimum has decreased from about seven percent to three percent. The standard error for the offset has decreased by a third, from 0.16 to 0.05 m/s (0.36 to 0.12 mph). This favorable trend may be due to refinements in the calibration procedure or to improved quality control practices implemented by NRG Systems in the assembly and pre-shipment inspections of the Maximum anemometer, or both.

Despite the apparently sound experimental techniques demonstrated by both calibration methods, the moving vehicle method produces a consistently lower (approximately 4 percent) anemometer output to wind speed relationship (Obermeier & Blittersdorf, 1996). This finding is based not only on comparisons with the MIT wind tunnel tests, but also on wind tunnel tests from R.M. Young's facility, which were commissioned by Otech Engineering. Transfer constants derived from the two wind tunnels are in fact in close agreement (within 0.5%). To achieve wind tunnel traceability (and traceability to the National Institute of Standards and Testing, formerly the National Bureau of Standards), Otech Engineering includes a wind tunnel-calibrated *propeller* anemometer in all of its vehicle calibrations. Obermeier & Blittersdorf (1996) raise the possibility that use of a propeller anemometer reference, rather than a cup anemometer reference, as the wind tunnels use, may be a source of the observed differences. It is also suggested that even the reference cup anemometers may respond differently in laminar compared to turbulent flow conditions when subjected to the same *average* wind speed.

This disparity in results is a source of concern for wind energy interests because two apparently valid calibration techniques are not in close agreement; their difference exceeds the ±3% AWEA specifications. Over the years, even outside the wind energy community, it has been shown that anemometer calibration in different environments can produce different results. In relatively turbulent, real-world environments, potential sources of error may become significant. These include the anemometer's dynamic response, flow distortion due to terrain and obstruction effects (i.e., non-horizontal flow), and ambient turbulence. Unfortunately, the source(s) of the discrepancy between the wind tunnel and open vehicle tests have not yet been defined. Consequently, wind speed data taken by anemometers calibrated by different techniques may not be directly comparable. A priority of the wind resource assessment community should be to resolve this discrepancy.

THE USE OF NON-CALIBRATED ANEMOMETERS AND DEFAULT VALUES

The previous studies of calibrated anemometers indicate that the variability between sensors has a standard deviation of approximately one percent, or three percent at the 99% confidence level (3 standard

deviations). A user may choose not to calibrate the sensors used within a monitoring program if this range of uncertainty is acceptable. This implies that, when exposed to a true wind speed of, say, 8.0 m/s (17.9 mph), non-calibrated anemometers employing certain default values may indicate speeds of between 7.8 and 8.2 m/s (17.4 and 18.4 mph). (Beware that one percent of anemometers will fall outside this range!) The user should keep in mind when interpreting these results that reported differences among anemometers may not reflect true differences in wind speed. Consequently, wind speed results should be expressed as the reported value and an uncertainty range (i.e., 7.8 m/s ± 0.5 m/s).

When using non-calibrated anemometers, the user has at least three sets of "default" transfer constants to choose from. Two, representing average values from calibration tests, were cited earlier. A third is recommended by NRG Systems in the form of a slope and zero-offset, as follows:

wind speed = 0.76 m/s per Hz
= 1.708 mph per Hz

The zero-offset version is a simplified approximation of the true slope and offset and thus inherently introduces some error. The slope-offset description of the regression line determined by the anemometer calibration is calculated to be the relationship that introduces the least error in the description of the data. Forcing the intercept through zero introduces larger errors.

Table 1 shows how the three sets of transfer constants compare at four different anemometer outputs (pulses per second, or Hz). The table shows that the NRG default always yields the lowest reported wind speeds. Differences between the Second Wind and NRG default values are consistently the largest, with speed ratios ranging from about 8 to 4 percent over the output range of 10 to 25 Hz, respectively. Between Otech and NRG, and between Second Wind and Otech, the differences are approximately 4 to 2 percent over the same output range. An anemometer output of 10 Hz indicates a wind speed at which a wind turbine delivers roughly 30 percent of its power rating. An output of 15 Hz corresponds to approximately 95 percent of a turbine's power rating. Therefore, wind speed errors occurring between the cut-in and rated speeds of wind turbines deserve the most attention. At many sites, more time will be spent nearer the 10 Hz level. In the case of the Second Wind-NRG comparison of default values, the average difference in the turbine cut-in to rated range of wind speeds is on the order of seven percent. If the wind speeds from both default values were used to estimate a wind turbine's energy production, the differences in energy production would be approximately 15 percent. McDonald et. al. (1995) illustrated in greater detail the impact of reported wind speed differences on wind turbine simulations in a comparison of Maximum anemometers using calibrated and default values.

These results illustrate the disconcerting degree to which the same model anemometers can disagree when using different defaults to define the "same" wind. The range of differences can be reduced by half simply by only using non-zero offset default values. However, a more basic problem is the "accepted" practice within the U.S. wind industry of using default values for anemometer transfer constants. Beyond the uncertainty associated with the anemometers themselves, there is an even larger uncertainty with using default values. Given that many measurement programs have utilized only non-calibrated sensors, this suggests that large volumes of wind speed data may have a larger uncertainty than previously thought. If it is assumed that the average difference in indicated wind speed across the relevant range of anemometer outputs using different default values is as high as seven percent, and the range of variability in anemometers is as high as nine percent, combined speed uncertainties larger than 15 percent are very possible.

Table 1 - Comparison of Indicated Wind Speeds For Different Anemometer Outputs
Using Three Different Default Values For Slope and Offset

	Speed Relationship	10 Hz	15 Hz	20 Hz	25 Hz
A. Second Wind	.77 m/s per Hz + 0.5 m/s	8.2 m/s	12.1 m/s	15.9 m/s	19.8 m/s
B. Otech	.76 m/s per Hz + 0.3 m/s	7.9 m/s	11.7 m/s	15.5 m/s	19.3 m/s
C. NRG	.76 m/s per Hz	7.6 m/s	11.4 m/s	15.2 m/s	19.0 m/s
ratio A/C		1.08	1.06	1.05	1.04
ratio B/C		1.04	1.03	1.02	1.02
ratio A/B		1.04	1.03	1.03	1.02

CONCLUSIONS AND RECOMMENDATIONS

The calibration of anemometers is recommended to define and control wind speed measurement uncertainty. Several industry standards related to wind turbine testing require that anemometers be calibrated (AWEA, 1988; Curver and Pedersen, 1989; IEC, 1995). Within the U.S. wind resource assessment community, except for recent organized national monitoring networks, the use of calibrated anemometers is *not* a standard practice. This situation should raise general concern over the quality and comparability of wind speed measurements and their application to wind energy development planning and economics. For an additional minimal cost of approximately $100 for an anemometer to be calibrated, the uncertainty in wind speed measurements can be reduced by about half, and uncertainties in wind turbine energy production estimates can be reduced by a factor of four! This is an exceptional value considering that multi-million dollar wind energy investment decisions may be at stake.

The U.S. wind industry relies primarily on the Maximum Type 40 anemometer for wind speed measurement. It is a simple yet durable instrument that can provide years of reliable service. A comparison of the two most popular anemometer calibration facilities has found that they employ good experimental techniques, but that their average transfer constants disagree consistently by a few percent. A priority of the resource assessment community should be to resolve this disagreement. At this time, neither technique should be considered the "right one". A recommended step toward resolution is a direct comparison of facility outputs using a common calibrated reference anemometer.

In the meantime, sound anemometer calibration practices should be followed using the following guidelines:

1. Use the same form of calibration for anemometers to be used on the same monitoring tower and within the same network of monitoring towers. This will avoid a significant source of uncertainty.

2. When considering a wind tunnel or open-vehicle calibration facility, select one where documented error distributions have been small. Calibration procedures should be NIST traceable.

3. Use measured slope and offset values for the anemometer transfer constants.

4. Calibrate anemometers before and after the measurement program. Experience shows that the Maximum Type 40 sensor retains its calibration with prolonged exposure. However there is no guarantee that environmental factors such as sand or dust will not change the sensor's performance.

5. Reported wind speed data, and other results derived from wind speed data (such as wind turbine output estimates), should be qualified with a total uncertainty estimate that incorporates all known or estimated measurement error sources.

As for non-calibrated anemometers, they have their place in resource assessment as long as the user understands their larger measurement uncertainty. They are more appropriate for general wind prospecting uses where great accuracy is not required. Once the disagreement between calibration techniques is resolved, the industry should adopt one set of default values (with a non-zero offset) for all non-calibrated anemometers.

ACKNOWLEDGMENT

This paper was supported in part by NREL Subcontract No. TAT-5-15283-01 as part of the Utility Wind Resource Assessment Program. The author appreciates the constructive feedback from the following reviewers of this paper: Robert Baker, Impact Weather; Daniel Bernadett, AWS Scientific, Inc.; David Blittersdorf, NRG Systems, Inc.; Ken Cohn, Second Wind Inc.; Tom Gray, American Wind Energy Association; Tom Lockhart, Meteorological Standards Institute; Ed McCarthy, WECTEC; Scott McDonald, AWS Scientific, Inc.; John Obermeier, Otech Engineering; and Marc Schwartz, NREL.

REFERENCES

American Society for Testing and Materials, 1990: **Standard Test Method for Determining the Performance of a Cup Anemometer or Propeller Anemometer**. D5096-90, Philadelphia, PA, 5 pp.

American Wind Energy Association, 1993: **Recommended Practice for the Siting of Wind Energy Conversion Systems**. AWEA Standard 8.2-1993, Washington, DC, 24 pp.

American Wind Energy Association, 1988: **Standard Performance Testing of Wind Energy Conversion Systems**. AWEA Standard 1.1-1988, Washington, DC, 31 pp.

American Wind Energy Association, 1986: **Standard Procedures for Meteorological Measurements at a Potential Wind Turbine Site**. AWEA Standard 8.1-1986, Washington, DC, 18 pp.

Bailey, B.H. and S.L. McDonald, 1995: The Utility Wind Resource Assessment Program. **Proc. Windpower '95 Conference**, American Wind Energy Assoc., Washington, DC, March 27-30, 1995.

Curver, A. and T.F. Pedersen, 1989: **Recommendations for a European Wind Turbine Standard on Performance Determination.** Netherlands Energy Research Foundation, ECN-217, 65 pp.

International Electrotechnical Commission, 1995: **Wind Turbine Generator Systems; Part 12 - Power Performance Measurement Techniques**. Interim standards document prepared by Working Group 6, 39 pp.

Lockhart, T.J., 1991: Relative Accuracy of Wind Tunnel Calibration Speeds. **Proc. Seventh Symposium on Meteorological Observations and Instrumentations. Amer. Meteor. Soc.**, New Orleans, Jan. 14-18, 1991, 73-76.

McDonald, S.L., B.H. Bailey, D.W. Bernadett, M.J. Markus and K.V. Elsholz, 1995: A Field Comparison of Popular Wind Monitoring Systems. **Proc. Windpower '95 Conference**, American Wind Energy Assoc., Washington, DC, March 27-30, 1995.

Obermeier, J. and D. Blittersdorf, 1996: Quality, Precision and Accuracy of the Maximum #40 Anemometer. **Proc. Windpower '96 Conference**, Denver, CO., June 23-27, 1996, American Wind Energy Assoc.

Obermeier, J.L., 1994: Calibration Test Results of the Maximum #40 Anemometer. **Proc. Windpower '94 Conference**, Minneapolis, MN. American Wind Energy Assoc., 747-759.

Obermeier, J.L., 1990: Results of a Moving Vehicle Calibration Test of the Maximum Anemometer. **Proc. Windpower '90 Conference**, Palm Springs, CA. American Wind Energy Assoc., 151-155.

Sass, W.L., 1994: Results of Large Scale Calibration of Maximum Anemometers *(Revised)*. **Proc. Windpower '94 Conference**, Minneapolis, MN. American Wind Energy Assoc., 761-770.

Vachon, W.A., 1985: Critical Issues Involved in Making Proper Wind Measurements for Wind Energy Production Estimates. **Proc. Windpower '85 Conference**, San Francisco, Amer. Wind Energy Assoc., 1-7.

A GIS-ASSISTED APPROACH TO WIDE-AREA WIND RESOURCE ASSESSMENT AND SITE SELECTION FOR THE STATE OF COLORADO

Michael C. Brower
Brower & Company
154 Main Street
Andover, MA 01810

Patrick Hurley
RLA Consulting
18223 102nd Ave., NE, Suite A
Bothell, WA 98011

Rich Simon
Consulting Meteorologist
80 Alta Vista Ave.
Mill Valley, CA 94941

ABSTRACT

This paper describes the methodology and results of a wide-area wind resource assessment and site selection in Colorado. This was the first phase in a three-part assessment and monitoring program conducted for the State of Colorado Office of Energy Conservation and several collaborating utilities. The objective of this phase was to identify up to 20 candidate sites for evaluation and possible long-term monitoring. This was accomplished using a geographic information system (GIS), which takes into account such factors as topography, existing wind resource data, locations of transmission lines, land cover, and land use. The resulting list of sites recommended for evaluation in Phase 2 of the study includes locations throughout Colorado, but most are in the eastern plains. The GIS wind siting model may be modified and updated in the future as additional information becomes available.

BACKGROUND

Geographic information systems are well suited to the large-area screening of prospective sites for wind power development. Wind speeds at the height of a wind turbine depend strongly on terrain elevation, exposure, slope, and orientation to prevailing winds, all factors which can be calculated from a GIS-based digital elevation model (DEM). In addition, with the appropriate data bases, a GIS can account for other factors that affect wind site suitability, such as the distance to nearby transmission lines, proximity to protected areas (such as national parks), and type of vegetation cover. Although nothing can replace on-site investigation, a thorough evaluation of local meteorological

phenomena, and monitoring, a GIS can provide efficient, systematic coverage and screening of potential sites in a large region.

Since the application of GIS to wind resource assessment is relatively new, the methods being employed are in a state of evolution. One of the first efforts in this field was reported in *Powering the Midwest: Renewable Electricity for the Economy and the Environment* (Cambridge, Mass.: Union of Concerned Scientists, 1993). That project surveyed wind resources in a 12-state region from Missouri to Ohio. It took as its starting point the *Wind Energy Resource Atlas of the United States* (Golden, Colo: National Renewable Energy Laboratory, 1987). Two parameters were used to modify the atlas: relative elevation above surrounding terrain (referred to as exposure) and surface roughness (related to vegetation cover). Since most Midwestern states are quite flat, these two parameters were regarded as adequate to identify sites likely to have better-than-average winds.

The large-area analysis of Colorado presented additional challenges requiring substantial modifications to the GIS methods developed for the Midwest. The most significant challenge was to deal with the very complex terrain of the Rocky Mountains. Not only was it necessary to estimate wind speeds within the Rocky Mountain chain, on mountain tops and slopes and in the valleys; it was also important to account for the shadowing effect of the Rocky Mountains on winds in the eastern plains. Since the plains region and the Rocky Mountain region are so different topographically, we developed different approaches to estimating wind resources in these two regions. The approaches were subsequently melded together to form one wind resource map.

In addition, we developed a new approach to ranking and screening candidate wind sites. Rather than basing the screening entirely on the expected cost of energy production (as was done in the UCS Midwest study), we considered non-cost factors which may affect the feasibility of wind power development, such as distance to national parks and forests. After identifying and weighting each of the pertinent factors, we developed a suitability ranking of all prospective wind sites in Colorado. The sites selected for further evaluation in Phase 2 were chosen from areas that ranked relatively high on this suitability scale.

DEVELOPMENT OF THE WIND RESOURCE MAP

See the box at the end for a description of the GIS software and data sources.

Eastern Plains

The starting point for the eastern plains analysis was the *Wind Energy Resource Atlas*. The atlas indicates that Class 3 and 4 (annual average) wind speeds are found on the high plains and uplands of eastern Colorado. The winds in these areas are driven by pressure gradients resulting from seasonal temperature differences across the plains. The predominant wind direction is out of the north and northwest, except in the southeast portion of the state, where it is out of the south. Near the Wyoming border, even higher winds may be found because winds are channeled and accelerated through the Great Divide Basin between Laramie and Lander, Wyoming. In low-lying areas and areas under

the shadow of the Rocky Mountains, however, winds are predicted to be no better than Class 1 or 2.

These estimates are generally confirmed by summary data for individual wind measurement stations. The National Climatic Data Center (NCDC) data indicate that Denver, Colorado Springs, Pueblo, Fort Carson, and Trinidad—all of which are within about 30 kilometers of the Front Range—should be ranked Class 1. On the other hand, Akron, the only NCDC station well to the east of the Front Range, appears to have stronger winds, perhaps Class 3 or 4. (Akron is located on high ground to the south of the South Platte River.) Data collected by the Western Area Power Administration (WAPA) also indicate that Class 3 and 4 winds may be found in favorable locations to the south and east of Sterling, in the central high plains, and on high ground to the northeast of Colorado Springs.

The data and atlas indicate that two factors play a predominant role in determining the wind speed at well-exposed sites: relative elevation and distance from the Front Range. Our analysis made use of this qualitative observation to construct a new wind resource map for the eastern plains by means of linear regression fit to the predicted wind power densities of the wind atlas. The dependent (or y) variables were obtained by taking a random sampling of the wind atlas classes throughout the eastern plains and then converting these classes to a density-corrected mean wind speed.

Regression coefficients were then obtained for three independent (or x) variables sampled at the same points: the distance to the Front Range (defined as where the terrain relief exceeds 1000 meters), the same distance squared, and the upper-air wind speed extrapolated to ground level. Note that if upper air winds at the same elevation were constant across the state, then the last variable would be directly proportional to elevation. The spatial variation of upper air winds introduces an additional independent effect which we believe partially accounts for the spatial variation in wind speeds observed near the ground. The r^2 regression coefficient was 0.50, indicating that the three x variables explain half of the expected variation in wind speeds across the eastern plains.

Mountains

According to the *Wind Energy Resource Atlas*, the very tall peaks and ridges of the Rocky Mountains experience Class 6 and stronger winds. However, the mountains also exert a strong sheltering effect, so that one can expect wind speeds to drop very rapidly off the main peaks. This behavior is confirmed by measurements taken at several sites. Among the NCDC stations, Grand Junction, Eagle, and Alamosa are all at relatively low elevations compared to the surrounding mountains, and all display relatively low wind speeds (Class 1 in the first two cases, Class 2 in the last). In addition, three US Forest Service wind monitoring stations near Berthoud Pass indicate a sharp decline in wind speed just a few hundred meters below mountain peaks. One site, on the 3,800 meter summit of Mines Peak, has an annual average wind speed of at least 10 m/s, whereas the other two sites, which are 200 m and 600 m below the peak, have annual average wind speeds (extrapolated to 40 meters) of 8 m/s and 4.7 m/s, respectively.

It was assumed that the mountain peaks and ridges experience wind speeds that are about as strong, or somewhat stronger, than free-air winds at those elevations. First, the free air wind speeds for the highest elevations in the mountainous areas were calculated by a linear extrapolation of the average annual upper-air wind speeds at the standard 700 mb and 500 mb pressure levels. The resulting mountain-peak wind speeds were then adjusted as follows:

- For mountains along and to the east of the easternmost main ridge line, the speeds were increased by a factor of 10% multiplied by the ratio of the local relief to the maximum relief in the Rocky Mountains (about 2190 m). Thus, for example, at a location where the relief is 1000 meters, wind speeds at the maximum elevation were increased by 4.5% (1000/2190 x 10%). The rationale was to adjust for down-slope acceleration resulting from mountain air flowing into the plains.
- Winds were enhanced by an additional 10% on ridge lines oriented predominantly in a north-south direction and with a typical slope near 30 degrees (regarded as optimal for wind acceleration over ridges). The ridge correction was calculated in a manner similar to that used to develop digital shaded relief maps, by scaling to the cosine of the terrain aspect angle and to the slope.

Once the mountain-peak wind speeds were defined, a quadratic relationship was used to estimate wind speeds off the main peaks and ridges. The quadratic-equation coefficients were defined so that wind speeds would decrease rapidly near the peak and would asymptotically approach a minimum in the valley floors. The minimum wind speeds were estimated by a fit of the wind data at Grand Junction, Eagle, and Alamosa, to the local terrain relief.

This approach did not account for possible drainage flows from high mountain basins into the valleys (except for the easternmost ridges as noted above).

The resulting map predicts much lower wind speeds than does the national wind atlas on certain ridges west of the main line of the Rockies, such as Grand Mesa and Uncompahgre Plateau. This reflects the fact that these ridges are both relatively low (3200 m and 2800 m, respectively) and located near a minimum of the distribution of upper air wind speeds across the state. In addition, neither ridge is oriented perpendicular to the prevailing westerly winds.

Composite Map

The two wind maps were subsequently combined to produce composite map for the entire state. Below a maximum elevation of 2500 m the eastern plains map was used, whereas above a maximum elevation of 3500 m, the mountains map was used. For areas falling in between these two regions, the wind speeds from both maps were combined in a linear interpolation. The result of this process was to increase the wind speed estimates in the Front Range foothills and other intermediate-size ridges and hills (such as Grand Mesa

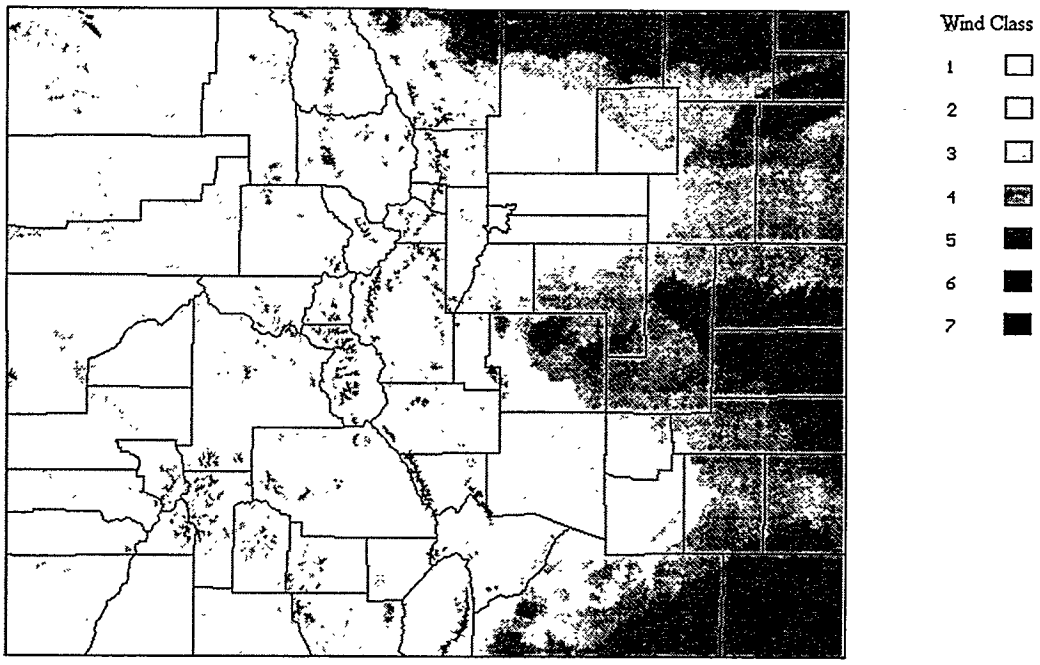

FIGURE 1. COLORADO WIND MAP

and Uncompahgre Plateau) compared to what was obtained using the mountain approach alone.

The final map is shown in Figure 1.

Comparison with Observations

In any computer-assisted assessment of wind resources, it is essential to verify predictions with direct measurement. Unfortunately, few solid data are available for comparison with predicted wind speeds from the map, although this will change once data from 10 recently installed monitoring stations become available. Nevertheless, we have plotted the predicted annual average wind speeds against observed annual average wind speeds for the available sites: 8 NCDC stations listed in Appendix C of the Wind Energy Resource Atlas, 16 WAPA stations, and the three Forest Service stations near Berthoud Pass (Figure 2). All wind speeds assume 40 m tower height.

With some exceptions, the predicted wind speeds match the Berthoud Pass and NCDC data fairly well (the average error is approximately 10 percent). Most of the WAPA points fall well below the line, however, suggesting either that the exposure of these sites is relatively poor, or that the predicted wind speeds in the eastern plains region (where most of the WAPA stations are located) are too high. The latter hypothesis cannot be tested at this stage, but there is evidence of poor exposure at a number of the WAPA sites. The average relative exposure of the sites (defined as the site elevation minus the

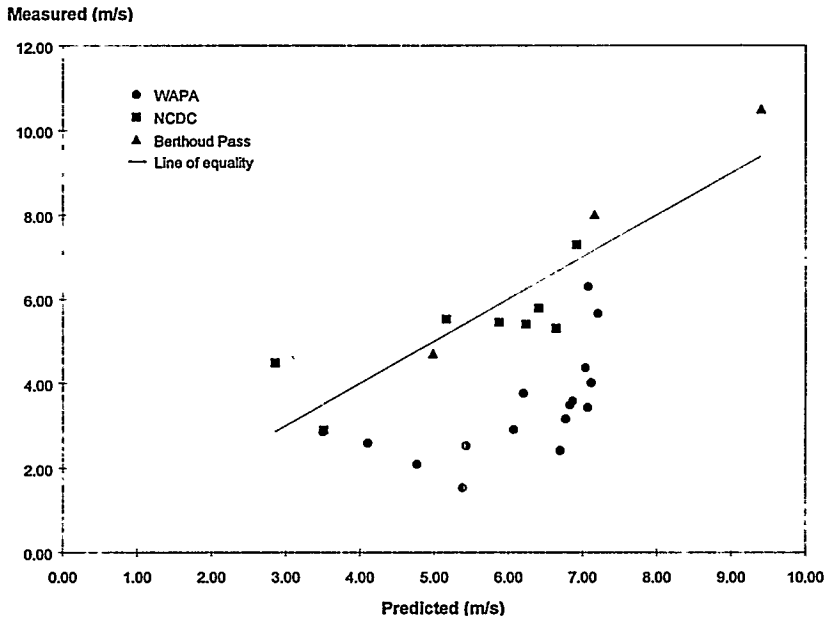

FIGURE 2. PREDICTED AND MEASURED WIND SPEEDS

local minimum elevation divided by the local relief) is 0.6, indicating that most are not located at the highest points in their surroundings. In contrast, the two WAPA stations showing relatively strong wind speeds, Matheson and Phillips, have relative exposures of 0.82 and 1.0, respectively.

DEVELOPMENT OF SUITABILITY MAP

The next task was to develop a ranking of prospective wind sites according to their suitability for wind power development. The method, known as multi-criteria evaluation (MCE), involves several steps.

Identify Significant Factors and Constraints

Constraints are areas excluded from development, whereas factors are variable parameters given a specific weight in the suitability ranking. The following areas were treated as constraints: national parks, forests, wildlife refuges, and military reservations; lakes and other water bodies; cities, towns, and other built-up areas; and areas outside Colorado state boundaries.

The factors weighed in the suitability ranking are shown in Table 1. (The ranges and weights are explained below.) Most—including wind speed, air density, terrain slope, distance to transmission, and land cover—have a direct and obvious bearing on cost of energy. Distances to large or small towns and to protected areas such as national parks are

included because they affect the feasibility of obtaining permits and securing public support for wind projects. The distance to *any* town is intended to account for additional transportation and labor costs for distant projects. The relative exposure is included to help narrow the choice of sites for field assessment.

TABLE 1. FACTORS AFFECTING SUITABILITY RANKING

Parameter	*Range*		*Weight*	
	Worst	*Best*	*Absolute*	*Normalized*
Wind speed (m/s)	6	11	1.59	0.600
Air density	0.75	1.10	0.35	0.132
Terrain slope	55%	0%	0.02	0.007
Cost-distance to transmission	188 km	0 km	0.23	0.087
Distance outside large towns	0	>16 km	0.05	0.019
Distance outside small towns	0	>8 km	0.05	0.019
Distance from any town	212 km	0 km	0.01	0.004
Distance from national park, forest, large lake or stream	0	>8 km	0.05	0.019
Land cover	Forest	Grass/shrub	0.10	0.038
Relative exposure	0.5	1.0	0.20	0.076
Total Weight			2.65	1.000

Create Standardized Suitability Maps for Each Factor

Multi-criteria evaluation involves the linear weighted combination of several maps, each representing a factor scaled to a standard suitability index (such as 1 to 100), with higher numbers referring to more suitable areas. For example, the maximum wind speed predicted in Colorado might be accorded a score of 100, since higher wind speeds are better for wind generation.

The suitability maps in this study were scaled from 0 to 254 (the maximum range for single-byte integers). The ranges spanned by each map, from best to worst, are shown in the second and third columns of Table 1. The distances around large and small towns and protected areas establish buffer zones within which wind development is assumed to become progressively more difficult as one approaches the protected boundary.

Assign Weights to the Suitability Factors

Relative weights were then assigned by estimating the change in cost of energy for a wind power plant over the full range of each factor. For those factors with no clear cost impact—such as distance to ecologically sensitive areas—a subjective weight based on experience with the siting and permitting of wind power plants was chosen. The air density weight is intended to reflect not only the cost impact of air density, which affects energy production, but also the effect of icing at higher elevations on wind turbine performance. (Icing is 10% of the total 35% weight assigned to this factor.) The weights

were subsequently normalized to one. The normalized weights are shown in the last column of Table 1.

Produce the Suitability Map

The final step was to calculate the suitability ranking for each point in Colorado through a weighted combination of the individual suitability maps. The resulting combined map is also on a 0 to 254 scale, where 0 represents the worst and 254 the best for wind power development. Of course, no site received a perfect score, since every location has at least some less-than-ideal characteristic. For example, mountain sites tend to have very strong winds but are usually located relatively far from transmission lines, close to protected parks or forests, and on sloping, forested terrain. Well-exposed locations in the eastern plains tend to have very good access to transmission and few terrain or land cover constraints, but generally experience lower wind speeds than the mountain peaks and ridges. The multi-criteria analysis procedure effectively balances these various factors to come up with an overall suitability ranking for each point on the map.

Figure 3 shows the resulting map. As expected, most of the more promising areas are concentrated in the eastern plains. Many locations in the east central plains appear attractive because their relatively high elevation (situated between the valleys of the South Platte and Arkansas rivers) imply strong winds, and they have good access to transmission and few exclusionary constraints. Similarly attractive areas appear on the south side of the South Platte River near Sterling and Akron, where the land rises up to 300 m or so above the river valley; near the Wyoming border, where relatively high elevations and strong upper air winds create likely Class 4 to 6 conditions; and on some intermediate-size peaks and mesas in the south near the New Mexico and Oklahoma borders.

The great majority of good mountain wind sites are excluded from consideration because they are located within national parks, forests, or wildlife refuges. However, a few promising mountainous areas do appear on the map, most notably the Culebra Mountains (a north-south ridge near the New Mexico border), which received by far the highest suitability ranking in the state (191) despite difficult terrain and relatively poor transmission access. The high ranking is due to the extremely strong annual average wind speeds expected on this mountain ridge—at least 11 m/s—which make this a likely Class 7 wind resource area. In addition, Redcloud Peak and Cannibal Plateau situated in a pocket surrounded by the Rio Grande National Forest; the Waugh Mountain area in Fremont County; and Cold Spring Mountain in the extreme northwest corner of the state appear relatively attractive, although they do not receive as high a suitability score as the Culebra Mountains because of lower predicted wind speeds.

SELECTION OF CANDIDATE SITES

With the suitability map in hand, it was relatively straightforward to select 30 or so sites for further evaluation. The objective was not only to pick areas with a strong suitability rating, but also to choose geographically dispersed sites to ensure adequate coverage of the state. Approximately half of the 39 sites chosen in the preliminary screening were in

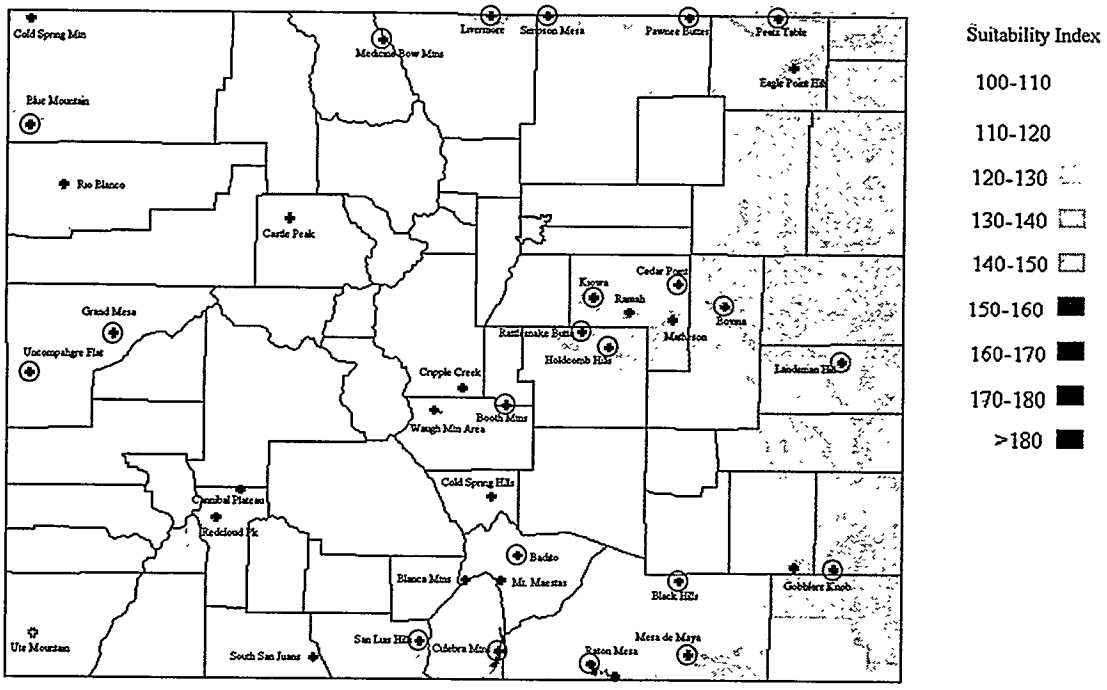

FIGURE 3. COLORADO WIND ENERGY SUITABILITY MAP

the eastern plains; about a third were in the easternmost portion of the Rockies, including the Culebra Mountains and the Waugh Mountain area, and the rest were in the western part of the state. Since the characteristics of federally owned land vary, two sites—Pawnee Buttes and Medicine Bow Mountains—were picked from within nominally protected areas, the Pawnee National Grasslands and the Routt National Forest, respectively. These sites were submitted to utility siting experts to get their reaction. In addition, we selected a limited number of sites from areas of relatively low predicted wind speed because of particular features which we felt could possibly enhance wind speeds there. The sites are: Black Hills (a low hill in southeastern Colorado), Badito (situated in a gap that may channel winds coming down from the San Isabel Mountains), and Grand Mesa (on a bluff just to the northwest of Grand Mesa National Forest).

The candidate sites are depicted as crosses on the map in Figure 3. The sites actually chosen for field assessment are circled. These sites were subsequently visited for further evaluation of land ownership, land use, visibility, access, potential avian conflicts, and permitting issues.

In a subsequent effort sponsored by a consortium of Colorado utilities, monitoring equipment has been installed at ten of the sites identified in this study. None of the mountain sites were instrumented due to difficulties associated with access, permitting, and land use. Consequently, all of the sites fall in the area east of the Front Range.

CONCLUSIONS

This study has demonstrated the utility of computer mapping and analysis tools for wide-area wind resource assessment and site selection in a region of highly complex and variable terrain. About a quarter of the sites deemed promising in the GIS assessment were subsequently selected for monitoring. Data to be obtained from the monitoring stations should be very useful for testing the accuracy of the wind map. The wind resource model has been turned over to the State of Colorado Office of Energy Conservation, where it may be modified as a result of new data.

BOX 1. GIS SOFTWARE AND DATA SOURCES

GIS Software. IDRISI, a PC-based package of programs developed at the Graduate School of Geography at Clark University in Worcester, Massachusetts.

Upper Air Wind Speeds. National Climatic Data Center, *Global Upper Air Climatic Atlas* (CD-ROM). Provides measurements of scalar and vector wind speeds on a 2.5 degree grid at 13 standard atmospheric pressures ranging from 1000 mb to 30 mb over a twelve-year period of record (1980 to 1991).

Digital Elevation Model. US Geological Survey, *Conterminous US AVHRR Companion Disc*, a CD-ROM available from the EROS Data Center in Sioux Falls, South Dakota. Resolution: 1:2,000,000 (1 km grid square). To calculate terrain exposure, elevations were averaged over a 27-kilometer square grid.

Land Cover. US Geological Survey, *Conterminous US Land Cover Characteristics Data Set 1990 Prototype*. The 26 land cover types were grouped into five summary classes: forest, woodlands, mixed woodland/cropland, cropland/grassland, and water.

Administrative Boundaries. Digital line graph (DLG) files from *Conterminous US AVHRR Companion Disc* CD-ROM. The boundaries include state and county borders, national parks and grasslands, national and state forests, national wildlife refuges, and military reservations.

Transmission Lines. AutoCAD file from Rocky Mountain Power Pool (RMPP). Although possibly less accurate than other available maps, it has the advantage of displaying transmission lines down to 69 kilovolts.

Lakes and Rivers. DLG files from the *Conterminous US AVHRR Companion Disc* CD-ROM.

Cities and Towns. Defense Mapping Agency, *Digital Chart of the World*, CD-ROM.

TURBULENCE ASSESSMENT AT POTENTIAL TURBINE SITES

Anders Daniels
Department of Meteorology, University of Hawaii
Honolulu HI 96816
U.S.A.

ABSTRACT

As opposed to a fixed anemometer, the Tala kite is free to move in the air. The motion of the kite is not random, it moves with or against the speed gradient towards the center of passing turbulence events of higher or lower speeds thus allowing the kite to measure event maximum or minimum speed rather than the speed at some unknown distance from the event center like a fixed anemometer. This behavior is confirmed both by a theoretical aerodynamics analysis of the kite motion and by data from a field study where kite and hot film anemometer (HFA) events, defined by the rain flow count method, were compared with flap events on a rotating turbine blade. The HFAs simulated too few events lasting too long while the kites reproduced both the number of events and event periods remarkably close. It is concluded that the kite is the optimal tool for measuring turbulence at potential turbine sites. Kite turbulence can form the bases for economic return estimates and an example is given where less windy sites could be more economical than other more turbulent higher speed sites.

INTRODUCTION

Most meteorological wind energy research has been directed towards estimating long term mean wind speeds to predict potential economic returns of wind turbines and the majority of potential sites have probably been identified and documented. Turbulence at potential sites has, however, received relative little attention and it has simply been assumed that, within economic projections, turbines would handle the turbulence. This has proven incorrect for a number of projects where unexpectedly high turbulence levels have resulted in excessive maintenance, premature failures, and early retirement of turbines. It seems therefore pertinent to now also examine turbulence at potential sites in an attempt to include this factor in economic return calculations to produce a more realistic estimate of the value of a project. This is becoming more important as most low turbulence area with easy access and close power lines have already been exploited. Future sites are likely to be more expensive to develop and may have higher turbulence levels. In

addition, the economic climate for wind energy is now rather severe, at least here in the US, which reinforces the need for more accurate economic projections for potential wind farm projects. But turbine research has progressed significantly; not only are better turbines available, but they may now, at least to some degree, be designed for and tuned to different degrees of turbulence at potential sites. This should allow a turbine to be selected for a site based not only on the mean wind speed but also on the turbulence. This paper presents a method to estimate site turbulence and suggests a procedure to incorporate the results in economic projections.

NATURE OF TURBULENCE

Before proceeding, it is necessary to define turbulence. Turbulence can be viewed as three-dimensional lumps or events with varying amplitudes of faster or slower moving air with a definite spatial and temporal extent. It is important to realize this discrete three-dimensional nature of finite turbulence events as e.g. found by Connell (1988). Assume that an event with a 5 m/s excess speed at its center passes near a stationary anemometer. The anemometer may register the event as having an amplitude of say only 0.5 m/s, corresponding to the speed at the event periphery where the anemometer most likely is measuring. A moving turbine blade, slicing through the event, will, however, not respond to the speed registered by the anemometer, but rather to that at the event center which, in this case, is ten times higher. While it is true that a fixed anemometer will sometimes measure at the event center, it will, in general, severely underestimate the turbulence that a rotating turbine blade experiences. The best method to get a true picture of the structure of turbulence would be to employ a large array of closely spaced anemometers but this is of course totally impractical. There is, however, a instrument that will do the next best thing - the strain gauged meteorological or TALA kite.

THE TALA KITE

The original Tala kite system consists of a 25 by 35 cm sled kite connected via a non-stretching kevlar string to a visually read spring calibrated in wind speed units. The system is light weight, easy to use, and requires no power. A major disadvantage is that an operator is required, which limits its use to short period surveys. Below 5 m/s, the kite will not fly well and may crash, while at winds above 20 m/s, the kite may be lost or damaged. Though mainly used for short-period mean wind speed surveys (Daniels and Schroeder, 1988), the kite has also been used to measure vertical salt profiles (Daniels, 1989) and turbulence. Kite turbulence measurements were made by Baker and Walker (1985) and Hogstrom et al. (1988). These, and other similar studies, all showed that kites register higher turbulence levels than did nearby anemometers

(Hassan et al., 1989). As it is difficult to make precise high-rate visual observations, an automated kite system was developed by the Department of Meteorology at the University of Hawaii under a licensing agreement with TALA. The system measures wind speed by a strain gauge mounted in a gimbals configuration with the angles of both orthogonal planes monitored by potentiometers.

KITE AERODYNAMICS

FWG Associates (Huang et al., 1981) developed the equations of motion for the kite in a coordinate system with one axis along the wind speed relative to the kite, V_a, (the vectorial difference between the kite motion speed and the wind speed relative to the ground, W) and the other, γ', perpendicular (Figure 1).

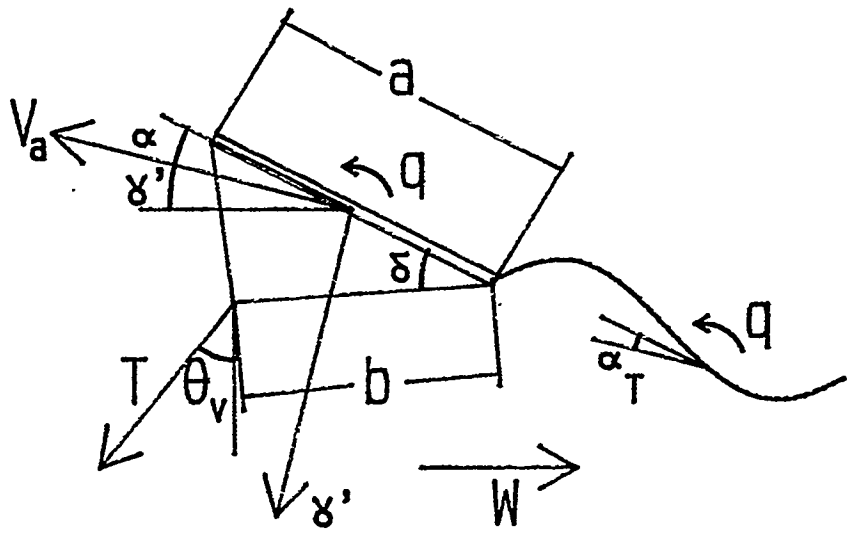

FIGURE 1 COORDINATE SYSTEM FOR THE TALA KITE EQUATIONS OF MOTION

The forces and accelerations along these axes are as follows:

$$m\, dV_a/dt = - D - m\, g \sin\gamma' + T \sin\theta_v \cos\gamma' - T \cos\theta_v \sin\gamma' - m\,(dWx/dt \cos\gamma' - dWz/dt \sin\gamma') - F1 \cos(\theta_T - \gamma') - F2 \sin(\theta_T - \gamma')$$

$$m\, V_a\, d\gamma'/dt = L - m\, g \cos\gamma' - T \sin\theta_v \sin\gamma' - T \cos\theta_v \cos\gamma' + m\,(dWx/dt \sin\gamma' + dWz/dt \cos\gamma') - F1 \sin(\theta_T - \gamma') + F2 \cos(\theta_T - \gamma') \quad (1)$$

where L is the kite lift force, D the drag force, g acceleration of gravity, m the kite mass (the kite weight / g), T the tether force,

θ_v the kite string angle from the vertical, γ' the angle from the horizontal of the V_a axis, dWx/dt and dWz/dt the time change of the wind speed components at the kite, $\theta_T = \alpha_T + \gamma'$, α_T the tail attack angle, and F1 and F2 forces acting on the tail defined as follows:

$$F1 = D_T \cos\alpha_T - L_T \sin\alpha_T + m_T\, g \sin\theta_T + m_T\, lk\, q_T^2$$

$$F2 = D_T \sin\alpha_T + L_T \cos\alpha_T - m_T\, g \cos\theta_T + m_T\, lk\, dq_T/dt \qquad (2)$$

where D_T is the drag force of the tail, L_T the tail lift force, m_T the mass of the tail, lk half the length of the tail, q_T the rotational speed of the tail and dq_T/dt its acceleration.

The rotational accelerations of the tail, q_T, and the kite, q, around their respective centers are

$$dq_T/dt = lk\ (\ -D_T \sin\alpha_T\ - L_T \cos\alpha_T\ + m_T\, g \cos\theta_T\ )\ /I_T \qquad (3)$$

$$\begin{aligned} dq/dt = {} & (\ T \sin\theta_v\ (\ a/2 \sin\theta - b \sin(\theta - \delta)\ ) \\ & - T \cos_v\ (\ b \cos(\theta - \delta) - a/2 \cos\theta\ ) \\ & + F1 \sin(\theta_T - \theta)\ a/2 - F2 \cos(\theta_T - \theta)\ a/2\ )\ /\ I_{yy} \end{aligned} \qquad (4)$$

where I_T is the moment of inertia of the tail around its center, $\theta = \alpha + \gamma'$, a the cord length of the kite, b another side of the kite (Figure 1), δ the angle between the two sides and I_{yy} the moment of inertia of the kite around its center.

The equation for dq/dt describes the rotational acceleration of the kite in the absence of a vertical wind speed gradient. Such a gradient adds the following term to the right side of the equation:

$$VGR = \rho\ CM\ ka\ W\ dW/dz \sin(\gamma' + \alpha)\ /\ 2\ /\ m \qquad (5)$$

where ka is the kite area, W the horizontal wind speed, dW/dz its gradient in the vertical, ρ the air density (the weight / volume divided by g) and CM is the moment coefficient defined as:

$$CM = -\ (\ CL \cos\alpha + CD \sin\alpha\ ) \qquad (6)$$

where CL is the kite lift coefficient and CD the drag coefficient, defined as the ratio between the lift or drag force and the kinetic energy of the wind summed over the kite area.

The V_a and θ' accelerations have components along the string equal to the strain gauge spring constant times the change in tension. Perpendicular components yield kite motions in the horizontal and the vertical. To numerically solve these four equations requires curves for the kite and tail lift and drag coefficients as function of attack angles, α and α_T, as well as curves for the tension, T, the string angle, θ_v , kite attack angle, α and tail attack angle, α_T, all as functions of the wind speed, W. The string tension curve is provided by the Tala company and the kite string angle curve was taken from measurements (Daniels, 1994), Figure 2. Using these two curves and known tail lift and drag curves (determined for a cylindrical wire), the remaining curves can be calculated for equilibrium (Huang el al., 1981), Figures 2 and 3.

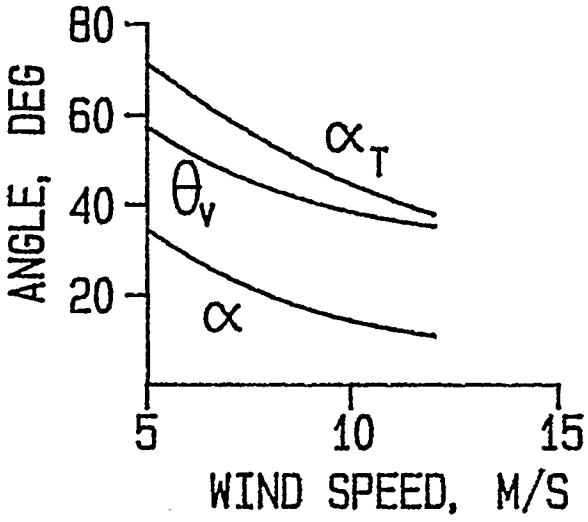

FIGURE 2 KITE STRING ANGLE, θ_v, ATTACK ANGLE, α, AND TAIL ATTACK ANGLE, α_T, VERSUS SPEED

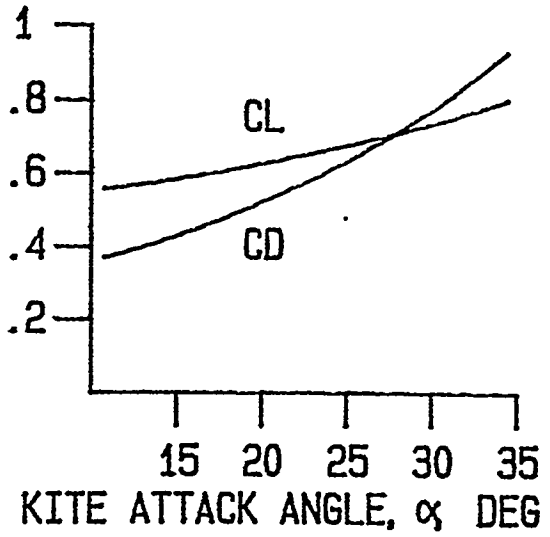

FIGURE 3 KITE LIFT, CL, AND DRAG COEFFICIENT, CD, VERSUS WIND SPEED

Figure 4 shows a numerical simulation of the kite responding to an approaching 3-m diameter elliptical turbulence element. The event amplitude is +/- 3 m/s with the speed excess ratio squared equal to 1 - the square of the distance to the event center divided by the event radius. The mean speed is assumed to be 8 m/s. The kite encounters the event at the upper or lower event boundary. The figure shows the kite travel for a negative event approaching below the kite, NEB, a positive event below, PEB, a negative event above, NEA and a positive event above, PEA.

As can be seen, the kite travels to the center of the event in all four cases and thereby registers the maximum speed of the event. Though the simulations have the kite moving more slowly into events below, measurements do not show an appreciable difference. Speeds calculated from the kite string tensions agree closely with input speeds as was also found by Huang et al. (1981). The simulations

demonstrate that the kite moves into the center of passing turbulence events and thus measures event maximum or minimum speed.

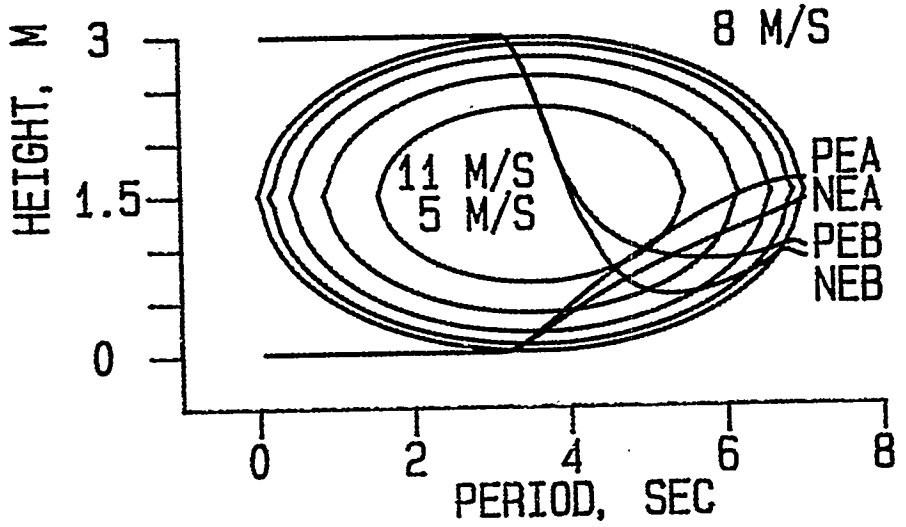

FIGURE 4 NUMERICAL SIMULATIONS OF THE KITE RESPONSE TO A NEGATIVE TURBULENCE EVENT BELOW THE KITE, NEB, A POSITIVE EVENT BELOW, PEB, A NEGATIVE EVENT ABOVE, NEA AND A POSITIVE EVENT ABOVE, PEA. THE WIND SPEED IS 8 M/S AND EVENT CENTER SPEED IS 5 M/S FOR A NEGATIVE EVENT AND 11 M/S FOR A POSITIVE EVENT. 0.5 M/S ISOTACS ARE SHOWN.

FIELD TESTING THE KITE SYSTEM

The kite heads were initially used during turbulence surveys in Hawaii in connection with wind turbine siting surveys (Daniels and Oshiro, 1982). Spectral analyses showed the kite consistently registering many more high frequency gusts than cup anemometers nearby. In connection with acceptance tests of wind turbines in Hawaii in 1987, several Gill UVW anemometers were installed on a tower immediately upwind of a turbine. On eight occasions we flew a strain gauged kite at hub height between the instrumented tower and the turbine. Ten-Hz data from the anemometers were recorded together with turbine blade strain and kite winds (Daniels, 1993). The kite again revealed much more turbulence than the anemometers. Using a measured anemometer speed to blade flap conversion curve, blade flap was simulated by kite and anemometer wind data and compared with measured blade flap based on the rain flow count (RFC) method. The kite simulated many more large amplitude events than the anemometer, much more in line with measured flap.

In 1991 we were given an opportunity to compare the kites to fast responding hot film anemometers (HFA) during a survey at Alsvik on the island of Gotland in the Baltic, where four 170 kW turbines are located (Daniels, 1994). The turbines have a hub height of 30 m, a rotor diameter of 23 m, and a rotational speed of 42 rpm. The fetch

was undisturbed for the prevailing off ocean winds. Ten-Hz data were collected from nine kites flying in an approximately 10 m by 10 m array perpendicular to the wind upwind of a turbine at 20, 30 and 40 m. A nearby tower had HFAs at the same heights. Turbine blade root moments were recorded at 30 Hz together with power produced. During half of fourteen 45-minute runs the kites were in the wake of an upwind turbine which produced interesting wake data (Daniels, 1995). Turbulence events were again identified in wind speed time series using the RFC method. Five-Hz rotational time series were constructed from eight kites (not using the array center kite) and the three HFAs. Corresponding time series were also constructed for blade flap converted to wind speed using a linear flap-turbine power curve and the turbine power-wind speed curve. The number of measured rotational kite, HFA and flap events and event periods are shown in Figures 5 and 6.

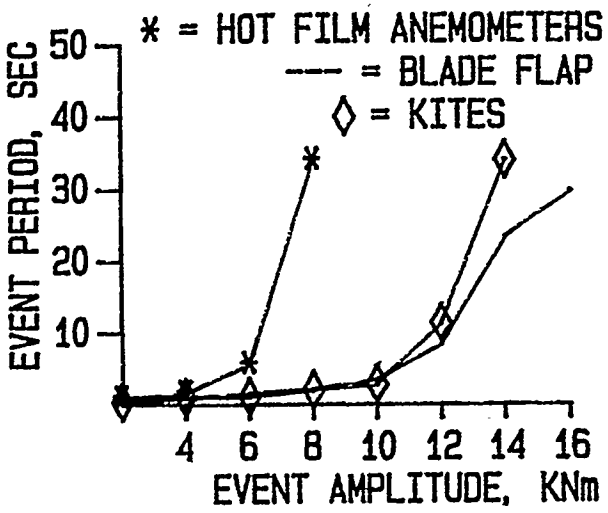

FIGURE 5 MEASURED KITE, HFA AND BLADE FLAP RFC EVENT PERIODS

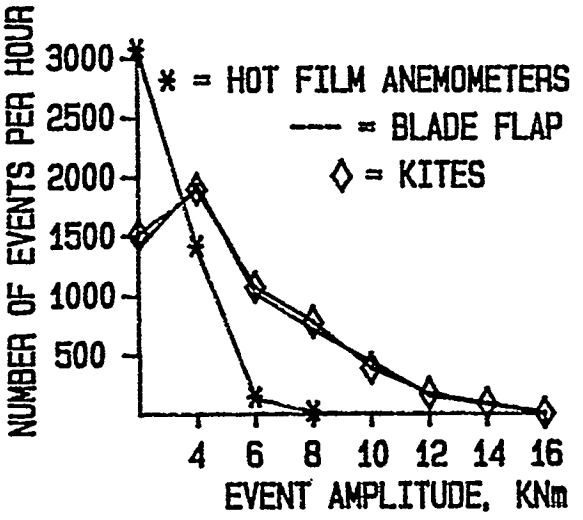

FIGURE 6 MEASURED NUMBER OF KITE, HFA AND BLADE FLAP EVENTS

Compared to measured flap, the rotating HFA severely underestimates the number of blade flap events and have them lasting too long while the number of rotating kite events are remarkably close and their durations almost the same at least up to 8 m/s events. Thus, a comparison with a rotating turbine blade clearly supports the proposition that the kite is the most realistic method to make turbulence estimates for wind energy applications.

INCLUDING TURBULENCE IN ECONOMIC RETURN CALCULATIONS

In 1993 the Department of Meteorology at the University of Uppsala, Sweden, conducted a wind energy survey at a coastal location some 75 miles NW of Gotheborg, Sweden. The site is fairly representative of the northern half of Sweden's North Sea coast with numerous

small islands, a rather narrow beach plane followed by 25 - 50 m high cliffs leading into a flat sparsely vegetated coastal plane with protruding bare hills. Turbine sites were envisioned in three areas: small islands or the beach, the coastal plain immediate behind the cliffs, and the higher plain inland. Each area has its advantages and disadvantages: islands or beach areas are relatively few and often difficult to reach but should have strong and low turbulent winds; coastal plain locations are more plentiful but might have much higher turbulence levels and considerable wind shear; inland protruding hill sites are easy to reach, plentiful and closer to roads and power lines but have probably lower winds. In order to quantify these differences, half-day kite surveys were conducted at eleven sites. Three kites remained at the beach during the survey flying ten meters apart at the same altitude as a nearby tower anemometer. At the other sites, the kites flew roughly above each other at 30, 40 and 50 m. During the 1991 survey we had noticed that the kites registered progressively lower winds speeds compared with tower anemometers as the wind speed dropped below 8 m/s and progressively higher speeds above. This discrepancy was confirmed by the 1994 survey. Kite winds were therefore adjusted using a linear curve moving a 4 m/s kite wind speed to 4.5 m/s and reducing an 11 m/s reading to 10.5 m/s. After this correction, tower and kite speeds agreed fairly well.

The damage by a turbulence event depends on the speed at which it occurs as well as on the amplitude of the event. A IEA expert group, assembled to standardize methods for comparing turbine performance, recommends the use of so called S-N curves for fatigue damage based on the Palmgren-Miner rule which relates the number of stress cycles of a specified amplitude and mean speed to the allowed number of cycles before failure (IEA, 1982). Let the allowed number of cycles with an amplitude, i, at a mean speed, u(i), be N_i. The total fatigue damage, d, is then simply the sum of the damage in each speed class, d_i, from n_i such cycles:

$$d = \Sigma\, d_i(u(i)) = \Sigma\, n_i(u(i)) \,/\, N_i(u(i)) \qquad (8)$$

The value for $N_i(u(i))$ depends both on wind speed and stress amplitude. Parabolic S/N curves are recommended, but no absolute values were given as the curves are blade specific. Measurements indicated that the number of stress cycles are, at least to a first approximation, an inverse linear function of wind speed (Poppen and Dahlberg, 1992) making the fatigue damage linearly proportional to the wind speed i.e., $N_i(u(i))$ can be written as $N_i \,/\, u * u_{ref}$ where u_{ref} is some reference wind speed and N(i) is now independent of wind speed. The allowed number of cycles, N_i, is often assumed inversely proportional to the cycle amplitude to the tenth power. Thus, a relative damage factor, rdf, can be written as

$$rdf = \Sigma\, u(i) \,/\, amp(i)^{10} \qquad (9)$$

where u(i) is the mean speed during the i:th event, amp(i) the amplitude of that event.

Relative damage factors were calculated for the eleven sites based on 10-min period RFC event statistics. Least mean square lines, drawn through about fifteen values for each site, are shown in Figure 7. As can be expected, damage increases with wind speed, but more so for some of the sites. Sites with the largest increase are inland while those with the smallest increase are coastal sites.

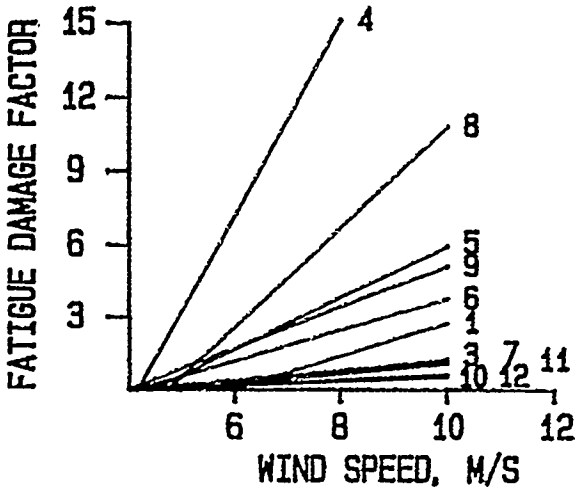

FIGURE 7 FATIGUE DAMAGE FACTORS CALCULATED FOR 11 SITES DURING A WIND SURVEY IN LYSE, SWEDEN, 1994

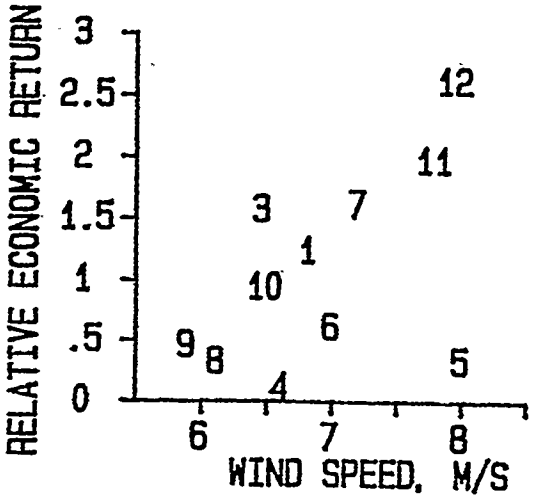

FIGURE 8 RELATIVE ECONOMIC RETURN RATIOS FOR THE 11 SITES DURING THE 1994 LYSE SURVEY

There are, of course, also other factors that fatigue a turbine blade, such as regular start-and-stop cycles (which could be calculated from wind data) and emergency stop damage or damage to the blade while parked which can't be estimate from wind speed measurements alone.

Site wind power was assumed to be proportional to the square of the ratio between site mean speed and tower mean speed during the site run period. Relative economic returns for the sites, proportional to the ratio between site wind power and the average (speed frequency weighted) relative damage fatigue factor, are plotted versus wind speed in Figure 8. As can be seen, sites 11 and 12, which are well exposed coastal cliff sites, are likely the most economical ones. Sites 3 and 7 are the second most economical ones in spite of having lower speed estimates than other sites. This shows that it might not be sufficient to consider only wind speed when estimating the relative return of turbines at different potential locations.

REFERENCES

Baker, R. W. and S. N. Walker, 1985: "Wake velocity deficit measurements at the Goodnoe Hills Mod-2 site", Report BPA 84-15, DOE/BP/29182-15.

Connell, J. R. 1988: "The wind lumps that bump a rotor", Proc. Windpower'88. Am. Wind Energy Assoc., Honolulu, HI, pp 452-461.

Daniels, A. and N. Oshiro, 1982: "Kahuku kite wind survey III: Turbulence analysis", UHMET 82-3, Department of Meteorology, University of Hawaii, Honolulu, HI 96816, USA

Daniels, A. and T. Schroeder, 1988: "Siting large wind turbines in Hawaii", Wind Engineering, 12, 5, 302-310.

Daniels, A., 1989: "Measurements of atmospheric salt concentrations in Hawaii using a Tala kite", Tellus, 41B, 196-206.

Daniels, A., 1993: "Turbulence measurements by anemometers, kites and turbine blade strain", Journal of Solar Energy Engineering, 115, 4, 228-230.

Daniels, A., 1994: "Kite turbulence measurements at Alsvik", Wind Energy Report WE 94:1, Dept. Meteor., Univ. Uppsala, Sweden, 39 p.

Daniels, A., 1995: "Turbine wake measurements using the meteorological kite", Wind Engineering, 19, 5, 1995.

Hassan and partners, 1989: "Characteristics of wind turbine wake turbulence and its implications on wind farm spacing", Report ETSU WN 5096, Energy Technology Support Unit, UK Department of Energy.

Hogstrom, U, D. Asimakopoulos, N. Kambezidis, C.D. Helmis and A. Smedman, 1988: " A field study of the wake behind a 2 MW wind turbine", Atmospheric Environment, 22, 803-820.

Huang, K. H., C. F. Shieh and W. Frost, 1981:" Analysis of a kite anemometer", US DOE Report, DOT/ET/20242-81/2.

IEA, Programme for Research and Development on Wind Energy Conversion Systems, 1982: "Recommended Practices for Wind Turbine Testing and Performance". Expert Group Study. (International Energy Agency, 2 Rue Andre Pascal, F-75775, Paris, Cedex 16, France)

Poppen, M. and J-A Dahlberg, 1992: "Fatigue loads on wind turbine blades in a wind farm", FFA-Vindenergi Report FFA-TN 1992-21, P.O. Box 11021, S-16111, Bromma, Sweden, 31 p.

ACKNOWLEDGEMENTS

I would like to express my sincere gratitude to the Department of Meteorology at the University of Uppsala, Sweden and its chairman, Dr Ulf Hogstrom for financial and moral support during the survey.

SPECTRAL COHERENCE IN WINDTURBINE WAKES

Jørgen Højstrup
Department of Meteorology and Wind Energy
Risø National Laboratory
DK4000 Roskilde, Denmark

INTRODUCTION

Turbulent velocity fluctuations in different positions in space will be correlated to varying degrees, dependent on the orientation of the line connecting the two points relative to the winddirection, and depending on the characteristic scale of the turbulence. This correlation will obviously have some influence on the loads sensed by structures of some spatial extent, subjected to the turbulent wind. Traditionally the spectral coherence of the windspeed fluctuations in the two points has been used as a quantitative measure of the amount of correlation as a function of frequency (or spatial scale). The coherence is an important parameter when translating Eulerian spectra into spectra in a rotating frame of reference as 'seen' by a rotating windturbine blade (Kristensen and Frandsen 1982, Kristensen 1983).

The coherence at frequency f of two timeseries $B_1(t)$ and $B_2(t)$ can be described as the maximum relative amount of variance of signal B_1 at the frequency f that can be retrieved from signal B_2 by a linear filtering process.

Unfortunately in the literature there exists two different definitions on the coherence, the definition employed here will be

$$Coh(f)=\sqrt{\frac{Q(f)^2+Co(f)^2}{S_1(f)S_2(f)}} \qquad (1)$$

where Q(f) is the quadrature spectrum, Co(f) is the cospectrum, and S1(f) and S2(f) are the power spectra. The other definition sometimes used is the square of eq. 1 and is also called the 'squared coherence'.

The behaviour of the coherence is quite well known from many field experiments in equilibrium turbulence, but not much is known about the coherence in the non-equlibrium turbulence that exists in a windturbine wake, where the turbulence statistics can be seriously altered by the local generation of turbulence caused by the strong shear introduced by the extraction of energy from the mean flow (Højstrup et al 1993). In a windfarm where other windturbines will be operating in the wakes of upstream turbines, this phenomenon could be of some significance. Therefore an experiment was set up as part of the measurements in a Danish windfarm to investigate the lateral and vertical coherences of alongwind speed fluctuations.

SITE AND INSTRUMENTATION

The Nørrekær Enge II Windfarm, containing 42 x 300 kW Nordtank turbines, is located in the North Jutland, on the south bank of the Limfjord, about 36 km west of Ålborg and 8 km north east of Løgstør. The terrain is old seabed and extremely flat, about 1 m above sea. The local terrain is however surrounded by small villages and significant terrain, with features up to 40 m in height, immediately to the south of the site. West of the site are farm buildings, rows of trees and the other windfarm : the

Nørrekær Enge I Windfarm, with 36 x 150 kW Nordtank turbines. Immediately north of the site there is water, Limfjord (see fig.1). The power and thrust curves for the windturbines are shown in fig.3.

Mast 1 at A1 is placed on the row of turbines A1 - A7, 55 m south of turbine A1. The Mast 2 at F6 is placed on the line between F6 and E5 (orientation 35.83°), 55 m from F6 and the booms on both masts are perpendicular to the line F6 - E5.

The two meteorological masts are instrumented primarily for measuring profiles of mean speed, turbulence and temperature. For the prevailing south-westerly wind direction, mast1 is an upstream mast, unaffected by wakes from wind turbines. In contrast mast2 is deep in the park and typically experiences wakes from a number of wind turbines. These two different roles are reflected somewhat in the instrumentation of the masts, with significantly more turbulence instrumentation on the wake mast (mast2). The standard instrumentation for each of the two masts are described below.

Mast 1

Cup anemometers (3,10,23,31,44,58m)
Boom arrangements : Pointing 312°.
Wind direction vanes (10,31m)
Temperature difference (23-3m, 58-3m)
Absolute temperature (3m)
Rain

Mast 2

Cup anemometers (3,10,16,23,31,31S,44,44S,58m)
Boom arrangements : pointing 306°
Wind direction vanes (34m)
Sonic anemometers (23,58m)

During some month in 1991-92 the standard instrumentation was supplemented by two cupanemometers mounted on the opposite sides of the m2 (fig.2), such that we could make coherence measurements at 2D downstream of turbine F6, and 7.5D downstream of turbine E5. For reference we also looked at data from the 14.5D wake of turbine D5.

DATA

Data were selected from three cases, signifying different spacings, 2D, 7.5D and 14.5D. For the 7.5D and 14.5D cases undisturbed upstream measurements were also available. Because of the limited amount of data available, it was not possible to get on-axis data for the 2D case. The measurements are 7, 11 and 9° degrees off axis (37°) for the three cases, but we should still be well within the wake, as the wake width of the 2D wake is about 50° (Højstrup et al 1993). The data was further subdivided into windspeed categories, 6-8 m/s, 8-10m/s and 10-13m/s, in the following called '7m/s', '9m/s' and '11.5m/s' cases. The windspeed used for the selection was the windspeed in the wake at hubheight+D/2. A total of 15 2D cases, 12 7.5D cases and 62 14.5D cases were available, where each case was a 30 minute timeseries. The main parameters of all of the categories are shown in table 1.

A linear trend was removed before the FFT-computation was done on the first 1024 seconds of each series. Power spectra and coherences were calculated, band averaged (bandwidth 0.07 decades), upon which the power spectra and coherences in each category were averaged together.

TURBULENCE INTENSITIES

The turbulence intensities for the two heights used here are plotted in fig. 4 together with the corresponding winddirection standard deviations, both as a function of normalized distance to the windturbine. The undisturbed upstream values have been plotted quite arbitrarily at 25D, assuming that at 25D the wake influence will be quite insignificant.

The turbulence in the near-wake case is very large, at hubheight about 25%, at the upper tip position even heigher, about 30%, then decreasing monotonously for increasing spacing towards a value of 11-13%, which is characteristic for undisturbed flow for the type of terrain seen here with expected roughness lengths of a few centimeters. We also note that the relative change in turbulence intensity diminishes with increasing windspeed, as expected, caused by the decrease in thrust coefficient with windspeed, decreasing the wake wind shear for increasing wind speed, i.e. the turbines become more transparent to the wind as the windspeed increases. A similar behaviour can be observed in the standard deviations of winddirection fluctuations also in fig.4.

The main conclusion from these plots is that the turbulence is still somewhat affected, even at 14.5D, although the wake influence here otherwise seems to be minor.

VELOCITY SPECTRA

In figure 5 are plotted the averaged power spectra from both heights and all cases. At hubheight 7m/s we can very clearly observe that the wake turbulence is being input at high frequencies, at scales comparable to the crosswind dimensions of the wake, pushing the dominant scale of turbulence towards much higher frequencies than seen in the free free stream. At the highest level we see a broadening of the wake variance spectra, probably caused by meandering of the wake caused by slow winddirection fluctuations, since we are near the top of the wake, these will cause the wake to be moved in and out of the position, where the cupanemometer is placed. Wake turbulence level decrease with increasing windspeed and increasing distance from the turbine as expected.

We still see some influence even at 14.5D as mentioned above for the turbulence intensities.

LATERAL COHERENCE

The lateral coherences were calculated from band-averaged FFT-values for all runs in each speed and distance category. The coherences were then averaged together in each category. The results are shown in figure 6 together with a simple model for the coherence:

$$coh(f) = \sqrt{\exp\left(-\frac{asf}{U}\right)} \qquad (2)$$

where

f:	frequency [Hz]
s:	Separation [m]
U:	Mean speed [m/s]
a:	$12 + 11(z_2-z_1)/z_{average}$

From fig.6 we can draw som general conclusions:

- The model provides a fair fit to 'no-wake' data (which are 14.5D-data)
- The 7.5D coherences are very similar to the model also
- The near wake 2D data show a coherence dropping off much faster with frequency than the model

VERTICAL COHERENCE

Similarly we can look at the vertical coherences in fig. 7, where we have compared with the model in eq. 2. We note a more rapid decay because of the larger separation, and we also note that

- The model fits all data well except for higher frequencies which was to be expected
- For two lowest speed categories there is some indication of less coherence for the near wake case.

CONCLUSIONS

- The turbulence is somewhat influenced by the wake even at 14.5D, or maybe rather from the aggregated wakes from the many upstream turbines further away.

- Lateral coherence (separation 5m) seems to be unaffected by the wake at 7.5D, but the flow is less coherent in the near wake.

- Vertical coherence (separation 13m) seems to be little influenced by the wake.

It looks as if simple conventional models for the coherence like eq. 2 are adequate descriptions also for wake turbulence except for the near wake situation.

ACKNOWLEDGMENTS

The Nørrekær Enge measurements were supported by the EU-JOULE program, project JOUR-0064 and by the Danish Ministry of Energy (the EFP-program). We also gratefully acknowledge the cooperation of Nordtank.

REFERENCES

Højstrup, J., M.S.Courtney, C.J.Christensen, P.Sanderhoff (1993): Full scale measurements in Wind-turbine arrays. Nørrekær Enge II. CEC/JOULE. Risø-I-684.

Kristensen, L. and S.Frandsen (1982): Model for power spectra measured from the moving frame of reference of the blade of a wind turbine. J.Wind.Eng.Ind.Aerodyn., 10, pp 249-262

Kristensen, L. (1983): Power spectra and cross-spectra as seen from the moving blade of a wind turbine. J.Wind.Eng.Ind.Aerodyn., 12, pp. 245-250.

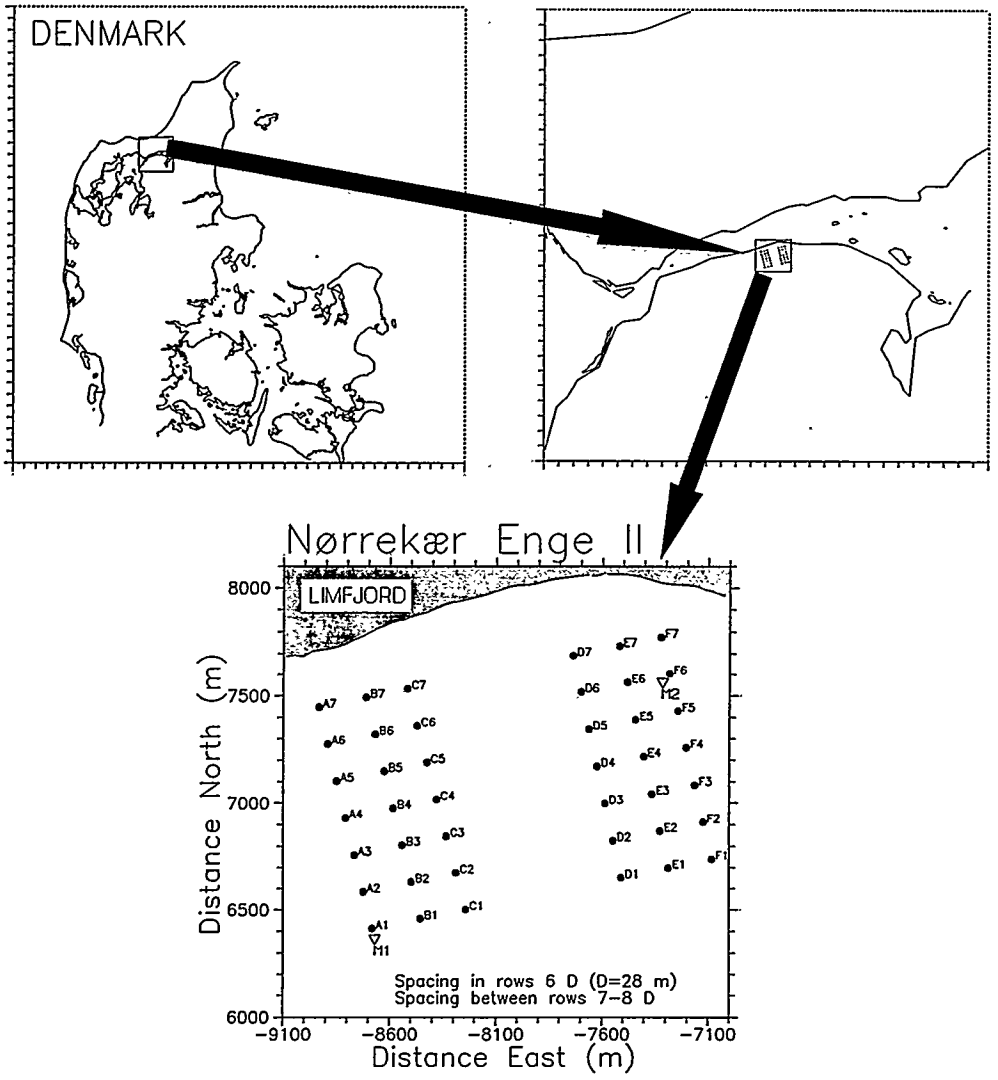

***Figure 1** Zooming site maps. On the last frame (2.1km * 2.1km) the masts are shown as open triangles denoted M1 and M2, and the turbines are shown as black dots.*

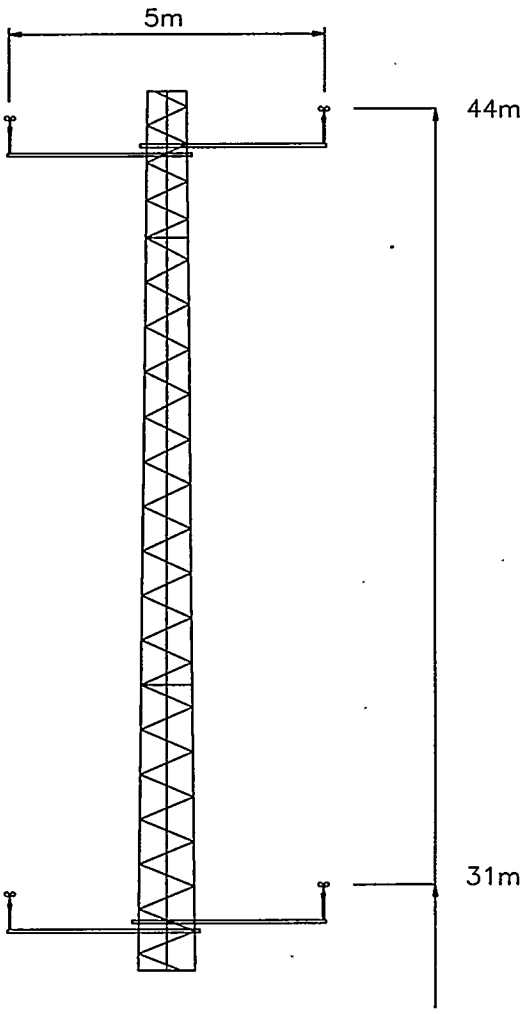

Figure 2 Mast section, showing the double anemomenter positions.

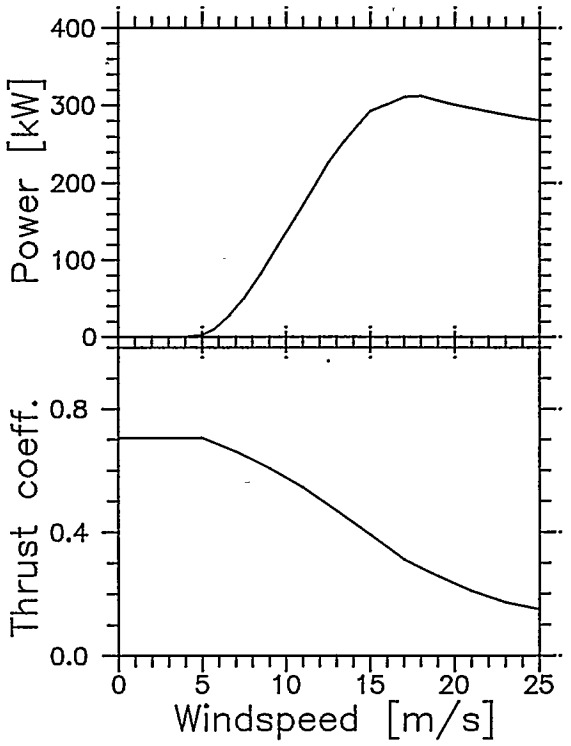

Figure 3 Power curve and thrust coefficient for the Nordtank 300 kW

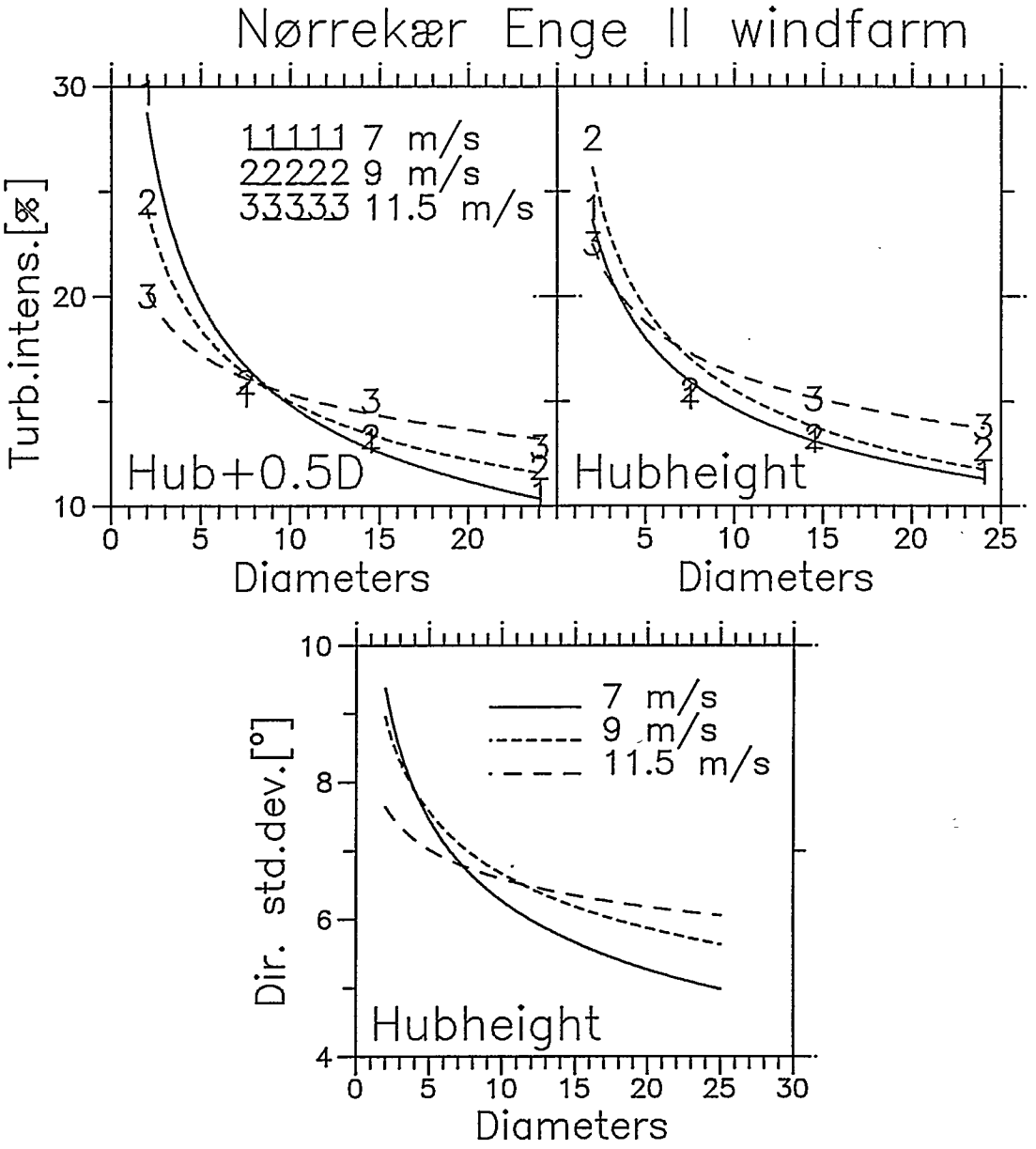

Figure 4 *Top: Turbulence intensities as a function of downstream distance at top of mast (left, hubheight+0.5D) and at hubheight (right). Bottom std. dev. of direction fluctuations.*

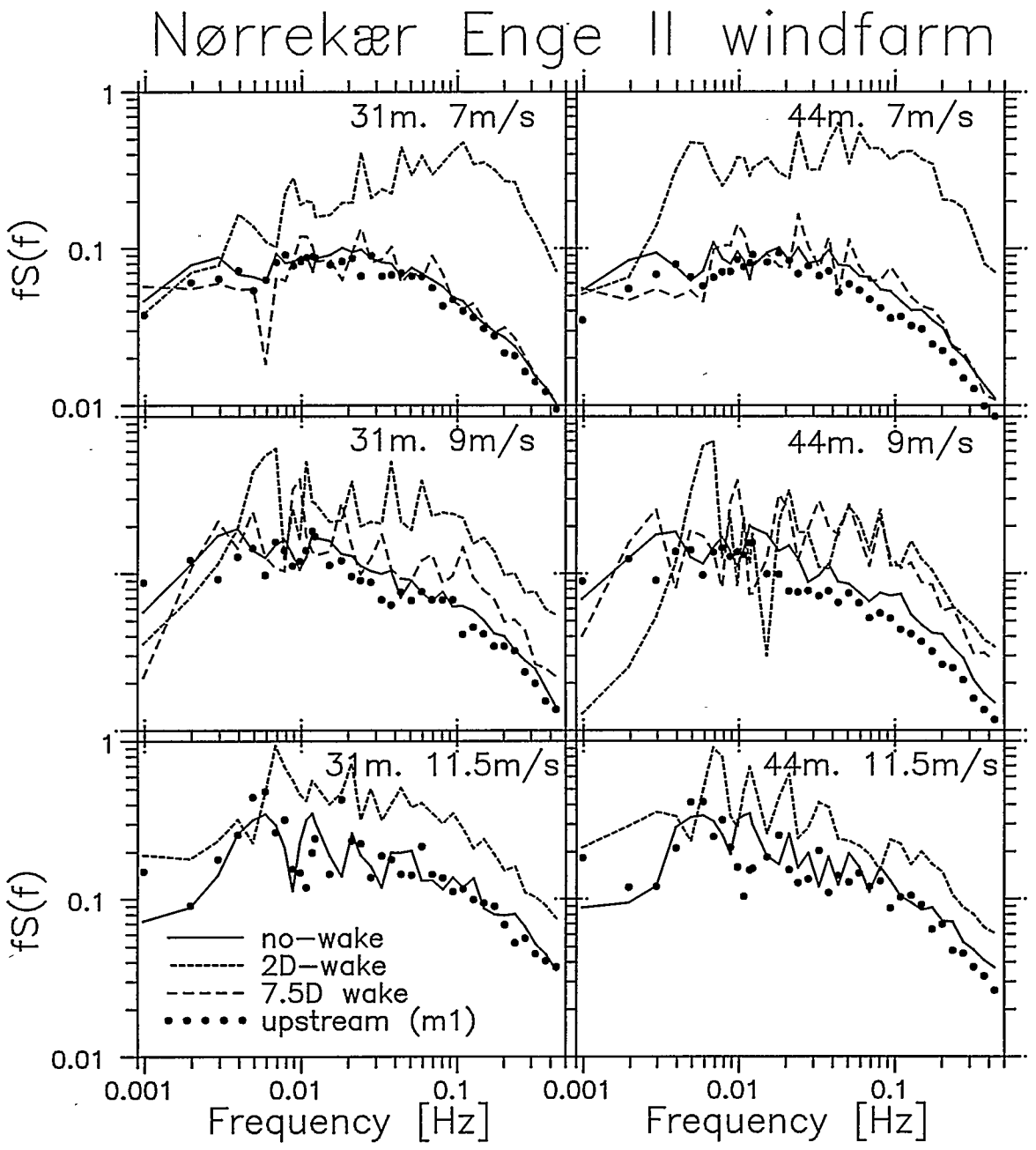

Figure 5 *Velocity spectra at two heights, three speed categories and at wakes at 2D, 7.5D, 14.5D ('no-wake') and undisturbed upstream for reference.*

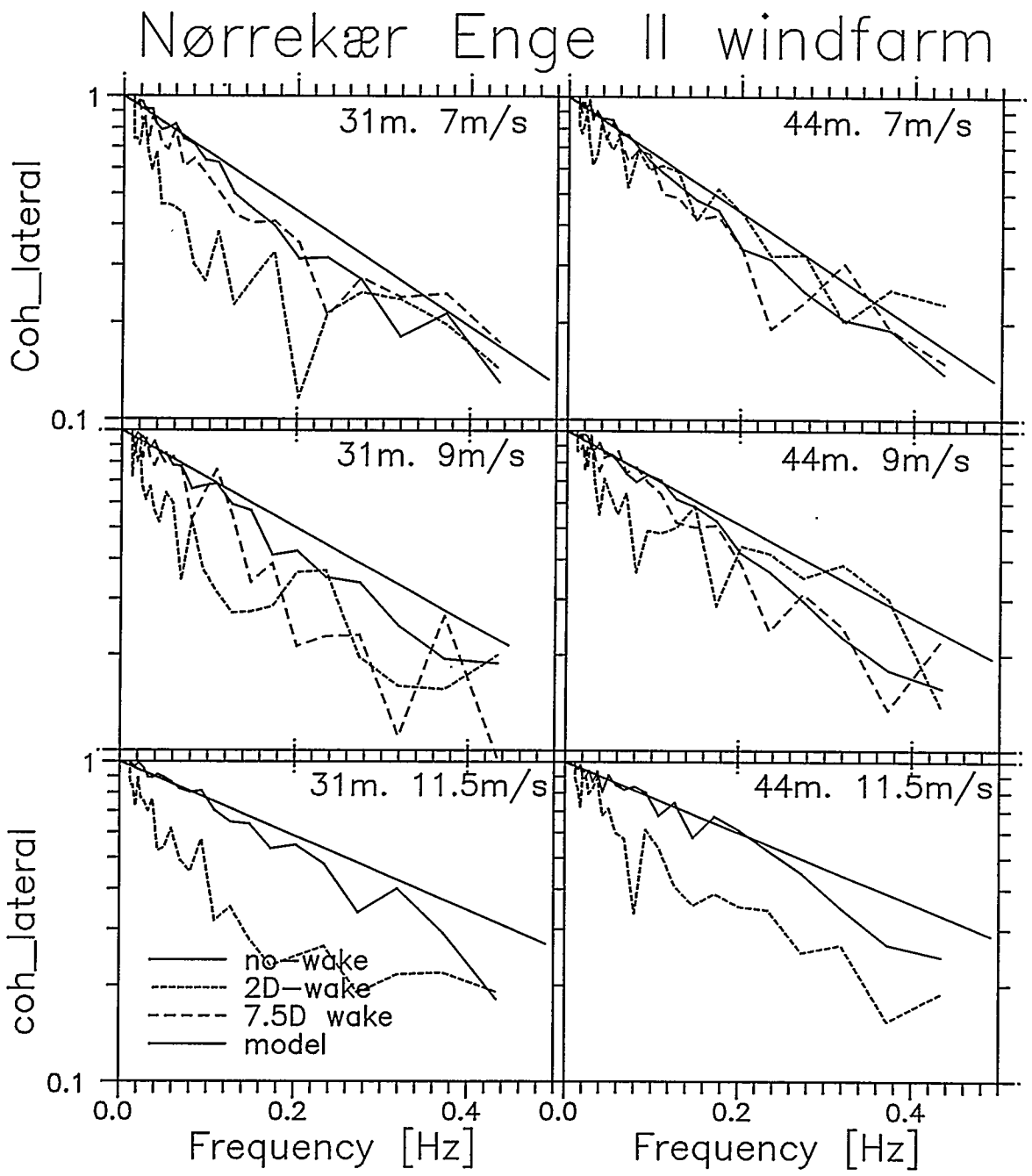

Figure 6 *Lateral coherence at two heights, three speed categories and in 2D, 7.5D, 14.5D wakes. The straight line is a model for the coherence (eq. 2).*

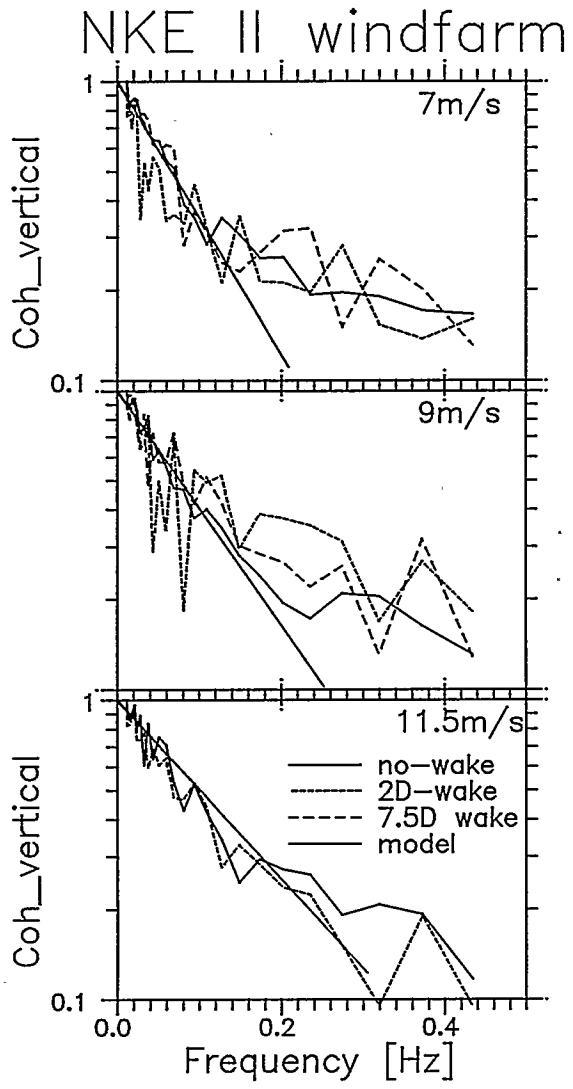

***Figure 7** Vertical coherence for 13m separation, in wakes at 2D, 7.5D and 14.5D distances.*

Number of cases	Wake	INSIDE WINDFARM						UNDISTURBED UPSTREAM				P_{F6}
		M2 U_{44m} [m/s]	M2 σ_{44m} [m/s]	M2 U_{31m} [m/s]	M2 σ_{31m} [m/s]	M2 θ [°]	M2 σ_{θ} [°]	M1 U_{44m} [m/s]	M1 σ_{44m} [m/s]	M1 U_{31m} [m/s]	M1 σ_{31m} [m/s]	[kW]
33	14.5D	7.8	1.02 13%	7.4	0.97 13%	242	5.8	8.4	0.89 11%	7.9	0.92 12%	54
22	14.5D	9.1	1.21 13%	8.8	1.17 15%	241	6.4	9.7	1.14 12%	9.3	1.18 13%	96
7	14.5D	11.9	1.78 15%	11.4	1.72 15%	245	6.5	12.3	1.58 13%	11.7	1.61 14%	195
6	2D	6.3	1.87 30%	6.9	1.67 24%	31	9.8					127
3	2D	8.9	2.18 24%	7.3	2.01 28%	16	9.3					134
6	2D	11.6	2.32 20%	10.3	2.32 23%	18	7.6					232
9	7.5D	7.2	1.10 15%	6.9	1.05 15%	221	6.1	7.9	0.83 11%	7.5	0.82 11%	40
3	7.5D	8.7	1.38 16%	8.4	1.30 15%	221	6.4	9.5	1.20 13%	9.1	1.29 14%	85

Table 1.

Quality, Precision and Accuracy of the Maximum #40 Anemometer

John Obermeier, P.E. and David Blittersdorf
Otech Engineering NRG Systems Inc.
418 Scripps Drive 110 Commerce St.
Davis, CA 95616 Hinesburg, VT 05461

ABSTRACT

This paper synthesizes available calibration data for the Maximum #40 anemometer. Despite its long history in the wind industry, controversy surrounds the choice of transfer function for this anemometer. Many users are unaware that recent changes in default transfer functions in data loggers are producing output wind speed differences as large as 7.6%. Comparison of two calibration methods used for large samples of Maximum #40 anemometers shows a consistent difference of 4.6% in output speeds. This difference is significantly larger than estimated uncertainty levels. Testing, initially performed to investigate related issues, reveals that Gill and Maximum cup anemometers change their calibration transfer functions significantly when calibrated in the open atmosphere compared with calibration in a laminar wind tunnel. This indicates that atmospheric turbulence changes the calibration transfer function of cup anemometers. These results call into question the suitability of standard wind tunnel calibration testing for cup anemometers.

INTRODUCTION

The Maximum #40 three cup anemometer is the defacto standard anemometer for wind energy siting purposes in the United States. Design features that have made it particularly suitable for use in wind energy siting programs include reliable data collection in conditions where many other anemometers fail; low sensor cost where high numbers of sensors are required; consistent performance even after long use; and a linear response in the wind speed range of 4.7 to 27 m/s (10 to 60 mph). The Maximum #40 is a 3-cup design using conical cups, injection-molded as one piece from black polycarbonate plastic (Lexan). These molded parts provide high levels of consistency in the cup shape and dimensions. A beryllium copper shaft rotates between an upper and lower Teflon self-lubricating bearing. This simple, low cost design avoids the maintenance problems associated with ball bearings. Although these bearings have relatively high starting friction, the effect on very low wind speeds (below 4.7 m/s) is of little concern for wind energy applications.

Following are updates to a moving vehicle calibration method, changes in the quality control process of assembling the Maximum #40 and comparisons of wind tunnel calibration data.

MOVING VEHICLE CALIBRATION TEST -- OVERVIEW AND UPDATE

NRG Systems (NRG), an instrument manufacturer, began working with Otech Engineering (Otech), a consulting engineering company, in the late 1980's to develop a method of calibrating cup anemometers that combined low unit cost and high volume. The goal was to improve quality control in the wind measurement process.

The quality control process for wind energy measurement followed distinct stages. Initially, attention was focused on issues related to surviving harsh environmental conditions while still measuring the wind

speed reliably. These conditions included extreme high speed gusts, ice storms and desert sand. Otech evaluated a number of different anemometers and recording systems and found no other anemometer that survived as well as the Maximum #40. With survival issues addressed, attention shifted to questions of comparability -- the need to know how consistently one anemometer reported wind conditions at one site relative to another. Measures of comparability were most often done with side-by-side sensor comparisons in atmospheric test conditions. Finally, the issue of accuracy was addressed -- that is, how the output signals of the Maximum #40 compared with a standard for measuring wind speed. Collaborative work on the moving vehicle test project was done to address both the comparability and the accuracy issues.

Comparing Different Anemometer Transfer Functions

Anemometer transfer functions are normally calculated from a least squares fit of measured calibration data. The least squares calculations can force the intercept to zero, giving a single parameter for each anemometer. Single parameters are convenient for comparing groups of test data as Obermeier [1,2] has done, but the single parameter form always produces higher errors in the estimate of the output wind speed. For this reason, it is advisable to use the two parameter form (slope plus intercept) of the transfer function. This paper uses only the two parameter form of transfer functions. A graphic format comparing the slope with the intercept is used for its visual simplicity, but even this does not convey accurate information about differences in estimates of the wind speed from different transfer functions. Following is the method used for making direct comparisons of transfer functions for wind energy applications.

The comparison method used the wind speed range of interest for wind turbine energy estimates, 4.7 to 27 m/s (10 to 60 mph). A Weibull probability density function is used to provide weighting factors for each wind speed class interval. This density function estimates a typical wind speed frequency distribution for wind turbine sites. In this case, a Weibull shape factor, $k = 2$, is used and a scale factor is selected so that the mean wind speed is 6.7 m/s (15 mph). (This is equivalent to a Rayleigh distribution with a 6.7 m/s (15 mph) mean wind speed). These calculations are performed on a spreadsheet program which also calculates the estimated annual energy production of a generic 500 kW wind turbine. Input parameters include the base transfer function parameters (slope and intercept) and the comparative slope and intercept. The spreadsheet then calculates the average percent difference in estimated wind speed and the overall percent difference in the wind turbine energy. This calculation method is used throughout this paper for direct comparisons of the effect of different anemometer transfer functions on wind speed measurements.

Slope versus Intercept Graph of Calibration Test Data

The moving vehicle test process has been described in previous papers by Obermeier [1, 2]. A summary of test data from three configurations of the moving vehicle method is presented in Figures 1, 2 and 3. The format of these figures uses a direct comparison of the slope value (horizontal axis) with the intercept value (vertical scale). This type of presentation allows an immediate visual grasp of the comparison of large numbers of tests using both parameters. It also presents a visual analogy to a target, in which the concept of precision has to do with the amount of scatter in the data and the concept of accuracy has to do with the relative location of the central value of a set of test data. However, this target analogy is limited because changes in location on the graph are not uniformly consistent in their effect on changes in output wind speeds. Specifically, the distance between data points lying along the upper left to lower right direction have a small effect on output wind speed (low sensitivity). Distance

between data points lying along the lower left to upper right direction are highly sensitive to changes in output wind speeds.

Figure 1 includes data for the period from 14 Mar 1991 to 14 Apr 1994. The test configuration for this period used one 22 cm polystyrene propeller anemometer at the center of the test bar with four Maximum #40 anemometers. The cup anemometer height above the 2.54 cm (1 inch) test bar was 22.2 cm (8.875 inches). This reference propeller anemometer was tested in the National Center for Atmospheric Research (NCAR) wind tunnel in a side by side comparison with the Meteorological Standards Institute (MSI) Round-Robin #1 anemometer (Lockhart [6]).

The Figure 2 data, from 28 Apr 1994 to 11 Nov 1995, used a 17 cm diameter polypropoleyne propeller at the test bar center with four cup anemometers. This propeller was tested in the R.M. Young wind tunnel, making it traceable to the Round-Robin #1 anemometer. This configuration also measured cross flow in a dual 45 degree configuration at the right side (from the driver's view) of the test bar. All cup anemometers were raised up to 29.8 cm (11.75 inches) above the mounting bar. This change in height was in response to Pedersen, et.al. [3] who pointed out the influence of mounting arrangements on the accuracy of cup anemometer measurements. This change placed the cup anemometers at a height more than ten times the width of the mounting bar.

Figure 3 shows a summary of data from 14 Nov 1995 to 02 May 1996. This test configuration was changed to two different reference anemometers, one on each side with the 45 degree cross flow pair in the center. Both reference anemometers use the same black polypropoleyne 17 cm R. M. Young propellers. Both complete anemometer units were tested by the R. M. Young wind tunnel and are directly traceable to the MSI Round-Robin #1 anemometer. The use of two reference anemometers reduces the distance between the tested cup anemometers and the reference anemometers to 35 cm (13.8 inches). Additionally, the reference anemometers are compared with each other on each run. The data analysis software was changed to include the option of reporting the longest possible dwell time per interval, which is normally between 40 and 50 seconds. Printed data reports now include the option of a residual plot and a difference frequency distribution as well as the standard linear regression scatter plot. The software changes also include more filtering of data to remove the non-steady transition times between measured intervals

Results in Figures 1, 2, and 3 are summarized in Table 1. These show that precision of the test data, as indicated by the standard deviation of each parameter (slope and intercept) has improved in each test period. At the same time, the mean value of the slope and intercept have remained essentially constant. In quality control language (Aguayo [4]), this is a test process that is "in control". Changes to the process have steadily reduced the amount of scatter in the final result without shifting outside an acceptable range of uncertainty.

Table 1: Summary of Moving Vehicle Test Results Showing Consistent Reduction in Standard Deviation of Transfer Function Constants

Time Period	Mean Slope m/s /Hz (mph/Hz)	Std.Dev. Slope m/s /Hz (mph/Hz)	Mean Offset m/s (mph)	Std. Dev. Offset m/s (mph)
Mar 91 - Apr 94	0.752 (1.683)	0.0085 (0.019)	0.36 (0.81)	0.098 (0.22)
Apr 94 - Nov 95	0.749 (1.675)	0.0058 (0.013)	0.35 (0.79)	0.094 (0.21)
Nov 95 - May 96	0.747 (1.672)	0.0054 (0.012)	0.39 (0.87)	0.058 (0.13)

QUALITY PROCESS APPLIED TO MANUFACTURING, TESTING AND OPERATION

During the same time that Otech was improving the calibration test process, other changes to the Maximum #40 anemometer were made in the manufacturing, assembly and distribution process by NRG and Maximum, Inc. In 1993, NRG took over the final assembly of the Maximum #40 and implemened a formal quality system (ISO 9001). Product design changes have also been made. Starting in 1996, the anemometer is being marketed exclusively as the NRG #40.

During the calibration test process, Otech observed that many of the extremes in the test data were due to anemometers that had obvious problems. These were easily detected by listening for a noise or feeling unusual friction when spinning the cups. Before 1994, Otech detected such occurrences at a rate of about one per 100 to 200 units. Since 1994, Otech observed no manufacturing or assembly related defects -- clearly a result of the quality process at the assembly level by NRG. Observed improvements in the test results shown in Table 2 are attributed to a combination of improvements in the test method and in the assembly quality control process.

Table 2: Summary of Standard Deviation of Different Calibration Tests of the Maximum #40 Anemometer

Figure No. & Label	Std. Dev. of Slope	Std. Dev. of Intercept
1 Otech 1991 - 1994	0.0085 m/s per Hz (0.019 mph/Hz)	0.098 m/s (0.22 mph)
2 Otech 1994 - 1995	0.0058 m/s per Hz (0.013 mph/Hz)	0.094 m/s (0.21 mph)
3 Otech 1995 - 1996	0.0054 m/s per Hz (0.012 mph/Hz)	0.058 m/s (0.13 mph)
4 Second Wind 1994	0.0089 m/s per Hz (0.020 mph/Hz)	0.085 m/s (0.19 mph)
5 R.M. Young Co 1992 - 1996	0.0058 m/s per Hz (0.013 mph/Hz)	0.089 m/s (0.20 mph)
6 NIST 1988	0.0045 m/s per Hz (0.010 mph/Hz)	0.125 m/s (0.28 mph)

Extending the quality concept to wind energy measurement programs requires that installers be trained in proper handling of the Maximum #40. The bearing spindle can be damaged by rough handling or improper packing during transport to the site. Otech's experience, that simple inspection of the anemometer can be related to measurable differences in calibration, suggests that similar inspections in field operations are worthwhile. NRG advises users to inspect the anemometer by a simple torque test using a one half gram weight, like a paper clip, attached to the outside of the cup. With the anemometer axis in the horizontal position, this weight should easily turn the shaft.

WIND TUNNEL TEST RESULTS FOR THE MAXIMUM #40

Figure 4 is a summary of wind tunnel data from 411 new Maximum #40 anemometers tested by Second Wind in the MIT Wright Brothers wind tunnel. Sass [5] described the test method, which used an R.M.Young Gill 3-Cup anemometer as a secondary reference. This test method differed significantly from standard wind tunnel calibrations because it tested nine cup anemometers at a time. Like the moving vehicle test, it was designed to produce high volume calibration results at low cost.

Figure 5 is a summary of wind tunnel data from 21 different Maximum #40 anemometers tested in the R.M.Young wind tunnel. (Five of the 21 units were "40-H" type anemometers, having the same physical construction with a Hall-effect output signal).

Figure 6 is a summary of wind tunnel data for nine different Maximum #40 anemometers tested in the National Institute for Standards and Technology (NIST) wind tunnel. NIST was formerly known as the National Bureau of Standards (NBS).

All of these calibration tests show a relatively wide range of scatter in the data. Because these tests used different samples of anemometers from different periods of time, it is difficult to draw conclusions from the data. The Second Wind data from 1994 has approximately the same standard deviations as the Otech data for the same time period. Seven of the nine units tested by the NIST wind tunnel appear to have very little scatter, but the remaining two anemometers were far from the central value. The R.M.Young data covered a similarly lengthy span of time but has standard deviations equal to the most recent Otech tests. The data clearly show that the Otech test method has precision levels comprable to the best wind tunnel results.

Test Repeatability

In an effort to quantify the measurement precision, Otech has consistently repeated a test of one Maximum #40 anemometer known as serial number (s/n) 300. This same anemometer was first calibrated in the NIST wind tunnel in 1988. When this repeated test was first done, Otech reported finding one standard deviation in the slope of ± 0.002 m/s/Hz (± 0.004 mph/Hz) and one standard deviation in the intercept of ± 0.045 m/s (± 0.10 mph) based on five sequential repeated tests. This was initially thought to be a measure of the test precision and was interpreted to mean that a statistical statement could be made about typical measurements of slope and offset. Other sequentially repeated tests have produced results similar to the above example.

However, repeated tests selected at random showed no such consistency. As a way of selecting "random" repeated tests, only those tests performed on different days were analyzed. These random test results are summarized in Figure 7. The standard deviation of random tests showed the same trend as the other Otech data, that is, the test standard deviation values reduced over time. But the magnitude of the random repeated standard deviation is about the same as the variation in the sample population. This result makes it difficult to distinguish between test variability and product variability. Anecdotal evidence from wind tunnel operators supports the observation reported here that random repeated tests vary much more than same-day or sequential repeated tests. Unfortunately, no repeatability data from wind tunnels was available.

RELATIVE ACCURACY AND THE MAXIMUM #40 ANEMOMETER

The term "accuracy" is commonly used to indicate how well a measurement "transfers" from an agreed upon standard to other measurement applications. Differences from the agreed standard value are called accuracy errors, or bias. Calibration is the type of measurement process intended to eliminate (or reduce to acceptable levels) bias errors. This use of accuracy is also called absolute accuracy. When measuring an unknown quantity, such as the transfer function for a Maximum #40 anemometer, no one fixed standard value exists, so "relative accuracy" is used to indicate the distribution of measurements about a mean value. Since no fixed standard ("true") value is known, there are differences between measurements rather than errors.

A common reference for many air flow applications is the National Institute for Standards and Technology (NIST) wind tunnel. Consistent measurement of air flow is difficult and wind tunnels do not necessarily always agree with each other. Lockhart [6] suggests that there is no need to certify wind tunnels, but intercomparison tests should be performed to locate a wind tunnel within a sufficiently small error distribution. Such an intercomparison test is being performed for meteorological purposes, and is referred to as the Round-Robin Test. All Otech tests since 1991 have referred to the Round-Robin anemometer by tracing its reference sensors directly to the Round-Robin experiment. It was felt that tracing the reference directly to the Round-Robin anemometer avoided the confusion inherent in using a specific wind tunnel as a standard of reference.

The Accuracy Dilemma for the Maximum #40

A summary of different measurements of the Maximum #40 anemometer transfer function is presented in Figure 8. This graph retains the same scale for slope and intercept used in prior graphs. Most of the values indicated on the graph are the result of calibration tests performed by the indicated agency. Where multiple tests were performed, the indicated point represents the average value of the transfer function slope and intercept for the indicated test population. "Logger default" refers to a pre-programmed transfer function embedded in the firmware of a data recording device. Both NRG Systems and Zond Systems use a slope with zero intercept value in their data loggers. These constants are consistent with historical use of the Maximum #40 dating to the early 1970's. The average value of the Second Wind test results is used by that company as a "logger default" transfer function.

In order to characterize Figure 8 in terms of differences in measured wind speeds, a summary of the same information is listed in Table 3. Speed differences are based on the comparison method described in this paper where the arbitrary reference is the average NIST transfer function. This value was chosen based on its central location among all available data. Table 3 information is listed by decreasing rank order of the wind speed estimate.

Table 3: Rank Order of Relative Difference of Various Estimates of Maximum #40 Transfer Function

Rank Order	Calibration Source	Serial No	Test Date	Slope+Offset (m/s per Hz)	Slope+Offset (mph/Hz)	Wind Speed Difference	Energy Est. Diff.
1	Second Wind (MIT Wind Tunnel)	411 units	1994	0.774+0.48	1.732+1.08	+2.7 %	+5.4 %
2	R.M. Young Company	21 units	1992 - 1994	0.781+0.38	1.747+0.86	+2.2 %	+4.7 %
3	Eindhoven University of Tech.	Max 4		0.768+0.51	1.718+1.12	+2.1 %	+4.2 %
4	National Wind Turbine Center	None	19 Jan 1994	0.766+0.47	1.713+1.04	+1.4 %	+2.7 %
5	Eindhoven University of Tech.	Max 8		0.767+0.40	1.716+0.89	+0.7 %	+1.4 %
6	National Engineering Laboratory	212-104	17 May 1990	0.760+0.45	1.699+1.01	+0.4 %	+0.7 %
7	Royal Dutch Met. Institute	Max 8		0.773+0.30	1.729+0.67	+0.1 %	+0.5 %
8	National Inst. for Standards & Tech.	9 units	10 Aug 1988	0.765+0.37	1.711+0.82	+0.0 %	+0.0
9	National Wind Turbine Center	None	08 Mar 1989	0.750+0.46	1.678+1.02	-0.7 %	-1.6 %
10	Otech Engineering (Avg. since 1991)	2,343 units	1991 - 1996	0.750+0.36	1.678+0.81	-1.9 %	-3.8 %
11	University of Hamburg	OTC-623	05 Apr 1993	0.767+0.18	1.716+0.40	-2.1 %	-3.9 %
12	NRG Systems Inc. (Logger default)		1985 - 1996	0.764+0.00	1.708+0.00	-4.9 %	-9.1 %
13	Zond Systems Inc. (Logger default)		1985 - 1996	0.758+0.00	1.695+0.00	-5.6 %	-10.8 %

A surprising discovery from Table 3 is the range of differences in interpretation of the output data from a Maximum #40 anemometer. Data collected from an NRG data logger and a Second Wind data logger

mounted side by side, with each using their respective default settings, will report a differences in wind speed averaging 7.6% (+2.7% to -4.9%)! If the same data is then used to estimate wind turbine energy production, with all else the same, the turbine estimates will differ more than 16%.

For the most part, data represented in Figure 8 and Table 3 are from different anemometers, so this is not a well controlled comparison. Nonetheless, the Otech and Second Wind data are based on sufficiently large samples so that the difference in the average values indicates a significant difference in opinion of the transfer function. The indicated difference of 4.6% (-1.9% to +2.7%) is wider than the one standard deviation range seen in wind tunnel variation. These differences would produce differences in wind turbine estimates of approximately 9%.

UNDERSTANDING MAXIMUM #40 CALIBRATION DIFFERENCES

To try and understand this difference, a simple experiment was conducted by Otech and NRG. Three instruments, an R.M.Young propeller anemometer, a Gill 3-Cup anemometer and a Maximum 3-cup anemometer were mounted on a crossbar. First, the cross bar was mounted on the Otech calibration vehicle and data were taken on June 5, 1996. The transfer functions developed by independent testing were used to express the anemometer rates of rotation in miles per hour. While all the transfer functions can be traced to NIST, that is not important for this experiment. Relative comparisons are sufficient.

The second part of the experiment used the same anemometer configuration in the 1.5 meter by 2.1 meter (five foot by seven foot) test section of the NIST wind tunnel. NIST provided tunnel wind speed and output data for the three anemometers. The rates of rotation and voltages were converted to speed using the same transfer functions. The preliminary analysis simply compared the speed measured by the cup anemometers to the speed measured by the propeller anemometer, making the propeller the standard of comparison. Any differences would be a result of the type of air flow, particularly the turbulent component. In an absolute sense, the linear regression slopes are a challenge to the transfer functions. Observing any changes in the slopes as a result of the calibration environment is the main goal of the experiment.

Figure 9 is a plot of the speed-range averaged 3-second samples taken by Otech Engineering on June 5, 1996. The speed differences were calculated by subtracting the propeller speed from the Gill 3-cup speed and the Maximum speed based on their respective transfer functions.

Figure 10 is the same plot as Figure 9 based on the readings from the NIST wind tunnel test. NIST data were recorded as 100 samples over 40 second periods. The only difference is that Figures 9 data is from the Otech calibration vehicle and Figure 10 is from the NIST wind tunnel. The difference between the two is largely the difference between turbulent flow and laminar flow.

There is an apparent difference between calibrations using an instrument mount moving through the air and an instrument mount in a wind tunnel. Summaries of comparisons of the indicated speeds are listed in Table 4. In the Otech atmosphere test, the Gill 3-Cup slope differed from the reference propeller by 4.1% and the Maximum s/n 300 slope differed from the propeller slope by 2.8%. In the NIST wind tunnel, the Gill 3-Cup slope differed from the propeller by 0.5% and the Maximum s/n 300 slope differed from the propeller by 4.9%. If these tests are representative, they show that the Gill 3-Cup output increases by 3.6% when going from laminar flow to turbulent flow and the Maximum cup output decreased by 2.1% when going from laminar flow to turbulent flow. When a Maximum anemometer is calibrated in a laminar wind tunnel using a Gill 3-Cup as the standard of comparison, and the same pair

of anemometers is then calibrated in Otech's open atmosphere facility, one should expect to see a 5.7% difference between the two test results. This may account for the difference between transfer function values reported by Otech Engineering and those from Second Wind's wind tunnel where the Gill 3-Cup anemometer was used as a secondary calibration reference.

Table 4: Results of Direct Comparison of Three Instruments In an Otech Open Atmosphere and NIST Wind Tunnel Environment Using the Propeller Anemometer as a Standard of Reference

Test & Cup	Slope	Intercept	Std. Err. Y Est.
NIST Test Gill 3-Cup	0.5 % above Prop.	0.02 m/s (0.05 mph)	0.06 m/s (0.14 mph)
NIST Test Max Cup	4.9 % above Prop.	0.01 m/s (0.03 mph)	0.07 m/s (0.16 mph)
Otech Test Gill 3-Cup	4.1 % above Prop.	-0.03 m/s (-0.07 mph)	0.05 m/s (0.11 mph)
Otech Test Max. Cup	2.8 % above Prop.	0.02 m/s (0.05 mph)	0.07 m/s (0.16 mph)

SUMMARY AND CONCLUSIONS

Otech Engineering started calibration testing of Maximum #40 anemometers in the mid 1980's in response to inconsistencies in calibration reports from different wind tunnels. (Those inconsistencies are now being addressed by the Round Robin Test run by Meteorological Standards Institute). NRG Systems Inc. began working with Otech because of their own interest in quality improvements to the wind measurement process. Despite the consistency of current Otech test results, there is no consensus regarding appropriate transfer function values for the Maximum #40. This controversy has challenged us to continue looking for causes of various discrepancies. What began as a frustration with inconsistent wind tunnels gave us incentive to develop an alternative approach performing calibration tests in the atmosphere. Now differences between our results and wind tunnel data have uncovered fundamental behavior characteristics of cup anemometers that were unknown prior to development of the open atmosphere calibration test method.

Five years of moving vehicle calibration results for the Maximum #40 are summarized and compared. Precision, as measured by standard deviation of the slope and intercept, is shown to be comparable with various wind tunnel results. The summaries show that precision of the overall results has improved over the five year period. It is unclear whether improved precision can be attributed to changes in the test method, or to simultaneous changes in quality improvements in the assembly process. Both test improvements and assembly quality changes are thought to play a role. The moving vehicle test method has produced consistent average estimates of the Maximum #40 transfer function over this period. These are positive steps toward the goal of improving quality in the wind speed measurement process.

A summary of Maximum #40 calibration results from different sources and a survey of default transfer functions embedded in datalogger firmware show a surprisingly wide range of variation. One specific example compares the effect of making wind speed measurements using default values in two commonly available data loggers. Differences in wind speed estimates are 7.6% and associated differences in estimates of wind turbine energy production exceed 16%.

A test comparing behavior of three anemometers in a wind tunnel and open atmosphere environment is described. The test was conducted so that measured differences are due entirely to the test environment rather than other factors. Results show that the tested cup anemometers have different linear transfer

functions in the two environments. The differences are thought to be due to differences between laminar and turbulent air flow. This difference in transfer functions demands that the practice of recommending conventional wind tunnel tests to calibrate cup anemometers be re-evaluated. This difference may account for observed differences between calibrations performed in the atmosphere and those performed in wind tunnels.

ACKNOWLEDGMENTS

The R.M.Young Company and Second Wind Inc. shared test data for this summary. The dedication and assistance of Tom Lockhart of Meteorological Standards Institute is appreciated. Work described here would not have been possible without the support and participation of NRG Systems Inc.

REFERENCES

[1] Obermeier, J.L., "Results of a Moving Vehicle Calibration Test of the Maximum Anemometer", presented at the American Wind Energy Association National Conference "WindPower '90" in Washington D.C. 27 September 1990. Published in AWEA conference proceedings.

[2] Obermeier, J.L., "Calibration Test Results of the Maximum #40 Anemometer", presented at the American Wind Energy Association National Conference "Wind Power 1994" in Minneapolis, MN, May 13, 1994. Published in AWEA conference proceedings.

[3] Pedersen, B.Maribo, Kurt S. Hansen, Stig Oye, Michael Brinch, Ole Fabian, "Some Experimental Investigations of the Influence of the Mounting Arrangements on the Accuracy of Cup-Anemometer Measurements", Technical University of Denmark, Danish Maritime Institute, Tripod Wind Data Aps, Denmark

[4] Aguayo, Rafael, Dr. Deming: The American Who Taught the Japanese About Quality, Simon & Schuster, New York, New York, 1990.

[5] Sass, Walter L., "Results of Large Scale Calibration of Maximum Anemometers", ", presented at the American Wind Energy Association National Conference "Wind Power 1994" in Minneapolis, MN, May 13, 1994. Published in AWEA conference proceedings.

[6] Lockhart, T. J., "Relative Accuracy of Wind Tunnel Calibration Speeds", Procedings of the Seventh Symposium on Meteorological Observations and Instrumentation. Amer. Meteo. Soc., New Orleans, LA. Jan. 14-18, 1991, Pp 73-76

CALIBRATION TEST RESULTS OF GROUPS OF MAXIMUM #40 ANEMOMETERS BY A MOVING VEHICLE METHOD AND THREE WIND TUNNELS

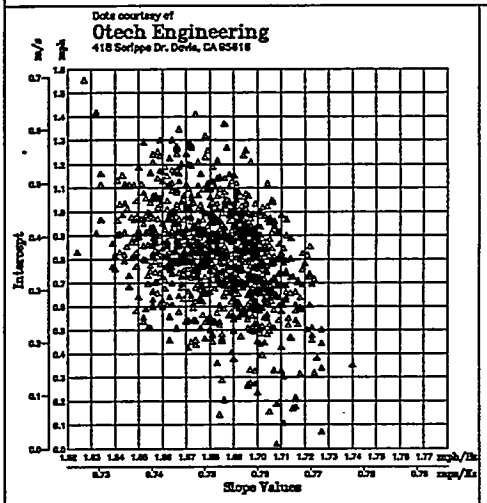

FIGURE 1
OTECH TEST RESULTS
FOR 1991 – 1994

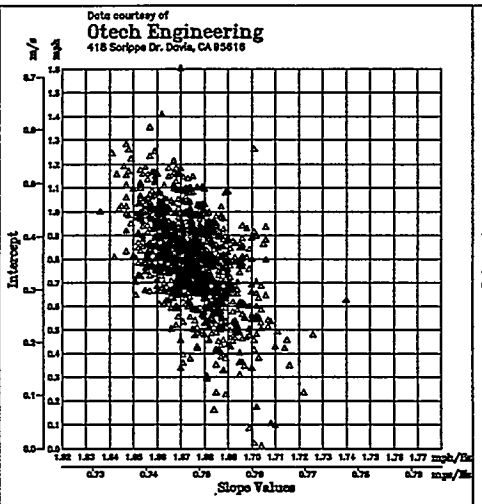

FIGURE 2
OTECH TEST RESULTS
FOR 1994 – 1995

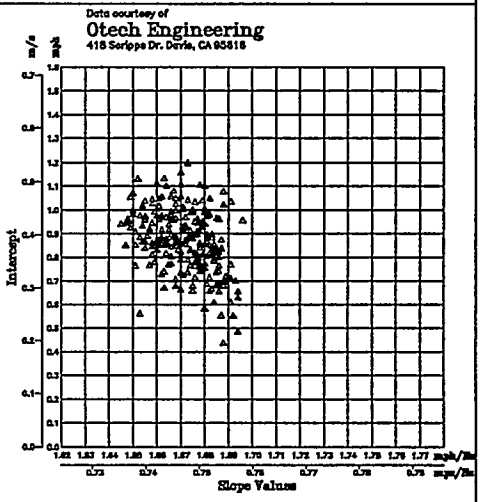

FIGURE 3
OTECH TEST RESULTS
FOR 1995 – 1996

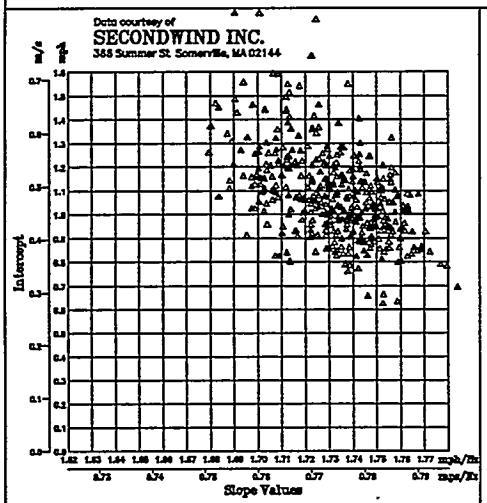

FIGURE 4
SECOND WIND TEST RESULTS
1994 MIT WIND TUNNEL

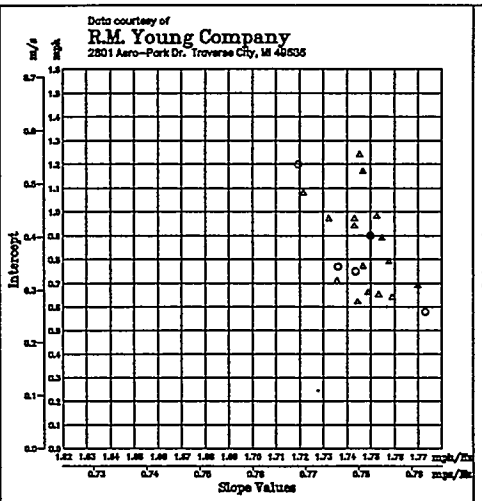

FIGURE 5
R.M. YOUNG TEST RESULTS
1992 – 1996

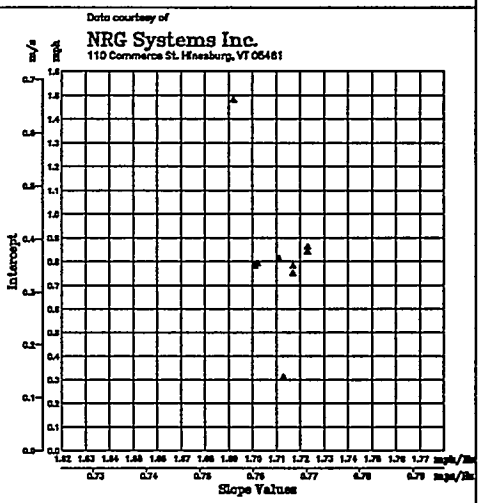

FIGURE 6
NRG TEST RESULTS
NIST WIND TUNNEL 1988

AWEA–1.DW2

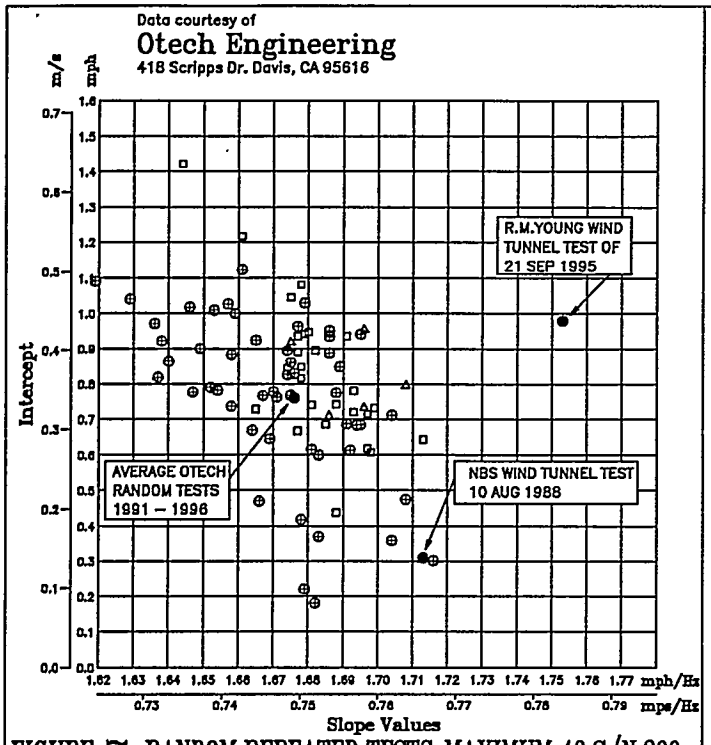

FIGURE 7: RANDOM REPEATED TESTS, MAXIMUM 40 S/N 300

Symbol	Time Period	No. Tests	Slope + Std.	Intercept + Std.
⊕	14 Mar 91 – 14 Apr 94	51	1.671 0.021	0.77 0.22
△	28 Apr 94 – 11 Nov 95	26	1.683 0.014	0.83 0.20
□	14 Nov 95 – 02 May 96	5	1.692 0.011	0.82 0.10
●	COMPARISON OF DIFFERENT TESTS OF S/N 300			

Date : 13 June 1996

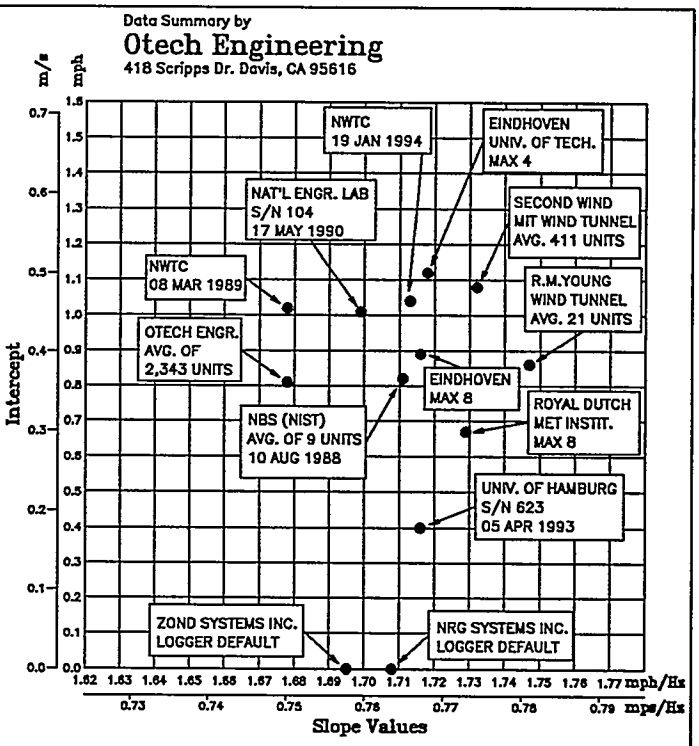

FIGURE 8: VARIATION IN MAXIMUM 40 ANEMOMETER TRANSFER FUNCTION USED IN WIND ENERGY SITING APPLICATIONS

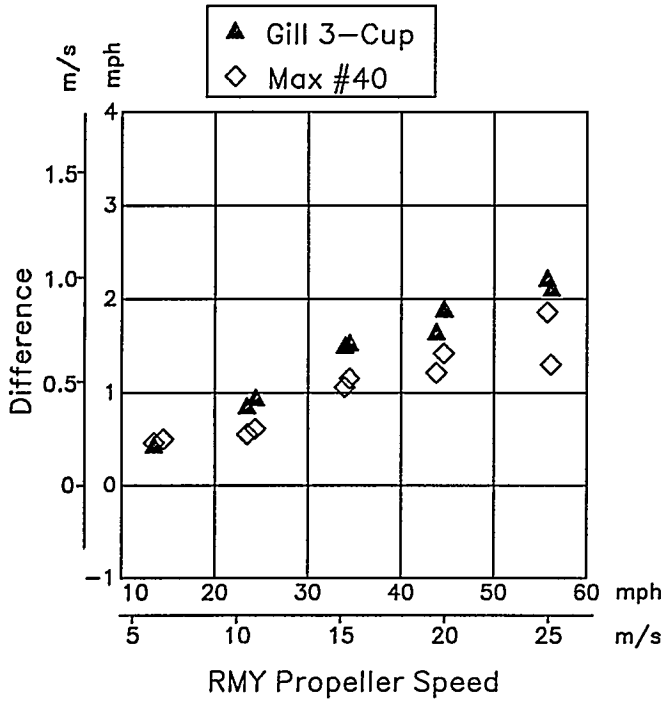

FIGURE 9: OTECH OPEN ATMOSPHERE TEST OF THREE ANEMOMETERS

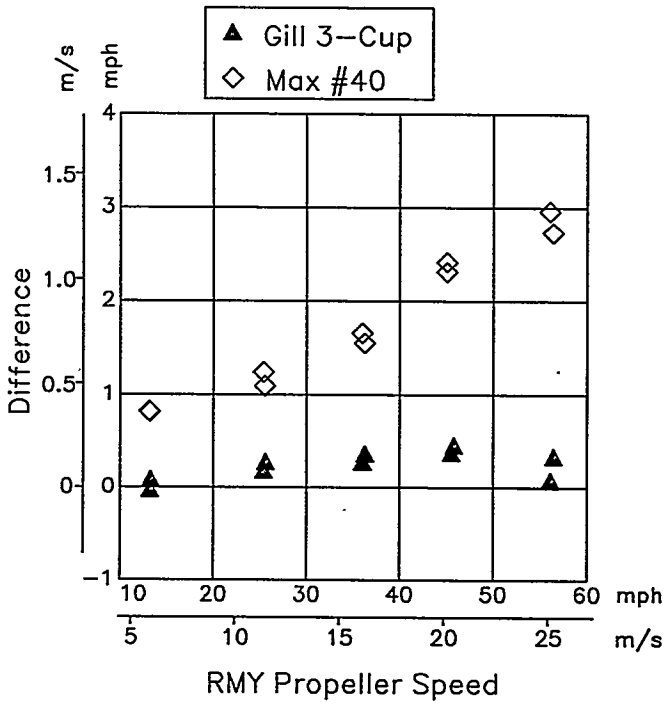

FIGURE 10: NIST WIND TUNNEL TEST OF THREE ANEMOMETERS

AWEA–2.DW2

DATABASE ON WIND CHARACTERISTICS

Jørgen Højstrup
Department of Meteorology and Wind Energy
Risø National Laboratory
DK4000 Roskilde, DENMARK

Kurt S. Hansen
Department of Energy Engineering
Fluid Mechanics Section
Bld. 404, DTU
DK2800 Lyngby, DENMARK

ABSTRACT

Wind data with high temporal resolution exist from a variety of sites, and is in demand by windturbine designers and wind engineers. Unfortunately it has always been a problem to gain access to a suitable amount of this data, because they are available from many different sources in different formats and with very different levels of documentation and quality control. We are now in the process of gaining access to a large amount of this type of data, checking the quality of the data and putting the data at the disposition of the windturbine designer community through easy Internet access. Online search will use summary statistics calculated for each series to help in the selection of data. The selected data can then be downloaded directly to the user.

1. INTRODUCTION

Wind data with high temporal resolution exist from a variety of sites, and is very much in demand by windturbine designers and wind engineers to be used as input for load models. Unfortunately it has always been a problem to gain access to a suitable amount of this data, because they are available from many different sources in different formats and with very different levels of documentation and quality control. It was often in the past discussed how to make it possible to use some of the vast amount of data that we all know exist. Now the technical developments in data storage and data transmission have made it possible to achieve this goal within a reasonable cost.

We are now in the process of gaining access to a large amount of such data, checking the quality of the data and putting the data at the disposition of the windturbine designer community through easy Internet access to a large database. Our aim is to provide online search, using summary statistics calculated for each series to help in the selection of data. The selected data can then be downloaded directly to the user or put on CDROM's and sent by mail in the case of large amounts of data.

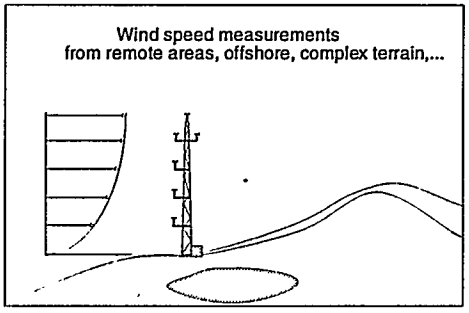

Figure 1 Wind data from many different site types will be included in the database.

2. OBJECTIVES

The objectives of this project are

- to build a database consisting of a large number of timeseries from many different sources. The initial body of data will be composed of data already available, while updating from ongoing and future measurement programs will be carried out on a

regular basis to complement the database.

- to make available tools for efficiently searching through the data, to select the cases needed.

- to set up access to this database through Internet for online search and downloading of selected timeseries for use in the models for the design of windturbines (or other structures or buildings)

3. DATA TO INCLUDE IN THE DATABASE

- Existing timeseries of windspeeds, 10 - 60 minutes lengths, sampling at 1-25 Hz (dependent on instrument time- and spatial resolution), from sites in different terrain types: homogeneous, offshore, coastal, mountainous, in windfarms. Measured at heights of interest for windenergy: 15-100m. Data should include 3-D measurements of the windvector where available.

- 1-10 min. statistics, mean, std.dev., extremes, derived from the timeseries, maybe supplemented with other statistics such as windshear, atmospheric stability and power output of nearby turbines in wake situations. This table also includes information on timeseries availability.
- Accurate site descriptions.
- Climatological descriptions of sites, windspeed distributions, wind roses ....

4. ORGANISATION OF THE DATABASE

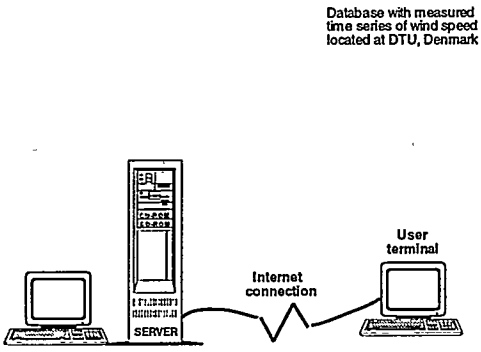

Figure 2

The data will be organized in three databases

#1 Database containing the fast sampled timeseries in a common file format.

#2 Database containing relevant statistics for the timeseries data in '1', that can be used for indexing the timeseries data.

#3 Database containing descriptions of the sites, measurement setup and other relevant information about the data.

All three databases will be located on one or several fileservers accessible through the Internet and part of the databases would be available on CD-ROMs.

5. USE OF DATABASE

The database will be useful as a supporting tool to identify

- rare meteorological events in terms of occurence, durability, extent, strength and shape
- wind shear
- extreme values
- spatial structure of turbulence
- spacing parametres in wind farms
- other meteorological issues

at different site types [homogeneous, offshore, coastal, mountain, windfarm] around Europe.

The intended main users of the databases are:

- Researchers and/or engineers, defining wind turbine loadcases.
- Designers [manufacturers] performing wind turbine load calculation evaluation for remote sitings with extreme wind conditions.
- Research institutions.
- Meteorologists
- Software developers [for load calculations].
- Researchers and/or engineers, defining loadcases for buildings.

The participants in this project represents both researchers, manufacturers and meteorologists.

6. SITES

We are aiming for receiving data from each member country of the EU from two categories

- Typical sites
- High turbulence sites or other 'unusual' sites, which could be sites exhibiting extreme climatic situations, extreme windprofiles or even very low turbulence sites.

7. CATEGORIES OF DATA

From each site data will be requested for a number of different categories, selected on the basis of windspeed, winddirection and other typical features, i.e. wake/nowake, summer/winter etc. Clearly great care must be taken into defining these categories in the initial phases of the project, such that on the one hand we do not get flooded with data, but on the other hand still get a representative coverage of the possible conditions.

A standardized description of each site will also be stored if available. This includes

- WASP type description of surrounding terrain, possibly supplemented by photographs
- Measured mean wind speeds, wind roses and distributions
- References to other available measured meteorological data

A description of the measurement system setup will also be included :

- Site layout, maps with locations of meteorological masts and wind turbines
- Instrument mounting, boom layout and boom direction
- Instrument descriptions, types, locations
- Instrument calibrations, factory or user calibrated.
- System operational reliability, errors ...
- Reference to available publications based on the measurements

8. SCREENING AND INDEXING OF DATA

We will assume that the data we receive from the participants are good data with no errors in them, but since it is well-known that the statistics calculated on the basis of these timeseries can be quite sensitive to errors in the data, like spikes, noise or drop-outs, we will set up automatic data-screening procedures before the data is entered

into the database.

The procedures when receiving data will be

- Conversion to a standard format
- Screening for errors
- Calculations of the statistics for indexing the timeseries, i.e. mean, std.dev., extremes, length scales ....
- Checking of site descriptions
- Statistics table, other info like stability, windshear, power output of a nearby windturbine, atmospheric pressure, temperature, precipitation, geographic location ... are entered into the index table
- Site descriptions are entered into their respective tables
- Timeseries data are stored

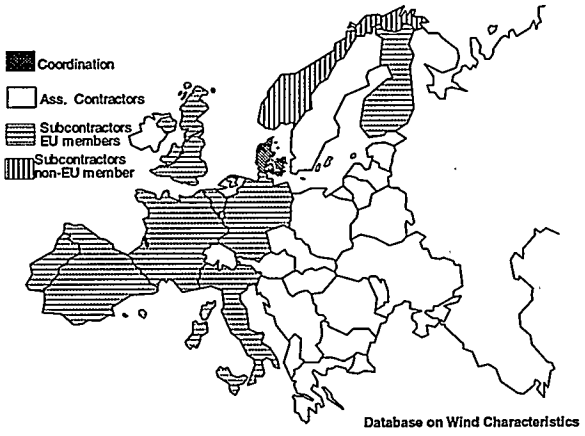

Figure 3 Data is available from nearly all member countries.

9. ACCESS TO DATA

The database will be accessed online by Internet, and the primary access will be through the index database. Using interactive search and selection programs, a list of relevant data can be created.

The user specifies a number of search parameters, i.e.

- Location [World, Europe, USA, ...]
- Site type [homogeneous, offshore, coastal, mountain ...]
- general conditions [normal, instationary, violent events ..]
- specific conditions [windspeed, gust, winddirection, time of year, time of day, temperature, windshear, wake - nowake,.....]
- data types [distributions, averages, timeseries,...]

The utility programs then use the statistics information as index information to search out the cases that are needed, then allowing the user to narrow down the selection/widen the selection depending on the results of the search and finally downloading the selected information to a user specified ftp-site or if large amounts of data are needed, providing the data on some suitable medium for mailing.

Possibilities for plotting of the statistics data will also be available to help the user selecting 'interesting' situations.

After the selection has been finished, the user now has a number of choices

- If the statistics data are sufficient for the present purpose, selected portions of statistics and/or other descriptions are being downloaded to the user's machine.

- The user wants timeseries for his own analysis, and dependent on the amount of data that is needed he can either

    - download the timeseries directly (small amounts of data)
    - request data downloaded to a specified ftp-server, whereupon the data automatically will be downloaded by the server (medium amounts of data)
    - request data sent by mail on some high capacity medium, typically a CD-ROM or the coming high capacity equivalents.

10. SOFTWARE FOR HANDLING OF DATA

The software packages that will be developed/modified consist of

- Graphical user interface for the Internet
- Database software for storage of index data and selection of subsets of data
- Software for retrieval of stored timeseries and automatic downloading of the data or writing to permanent media.
- Software that the user can download to be used for doing simple operations on the data, like transformation to a general format from the (packed) format in which the data will be delivered.
- Programs for simple statistical operations on the data, fourier decomposition, plotting.

11. HARDWARE

The necessary hardware consists of a medium speed workstation with large disk capacity to be used for the development of the system. The final server to be used for interactive access by the end users must be a fast speed workstation with very large harddisk capacity. Both systems also need a suitable selection of large capacity devices for data backup and transfer of data. We estimate a total amount of storage space needed of at least 50 Gbytes.

MORE INFORMATION

Updated information on the database can be found at our WEB-page: **http://www.afm.dtu.dk/wind/database**

ACKNOWLEDGMENTS

This project is being supported by the European Union, DG XII, contract JOR3-CT95-0061.

ORGANIZATION

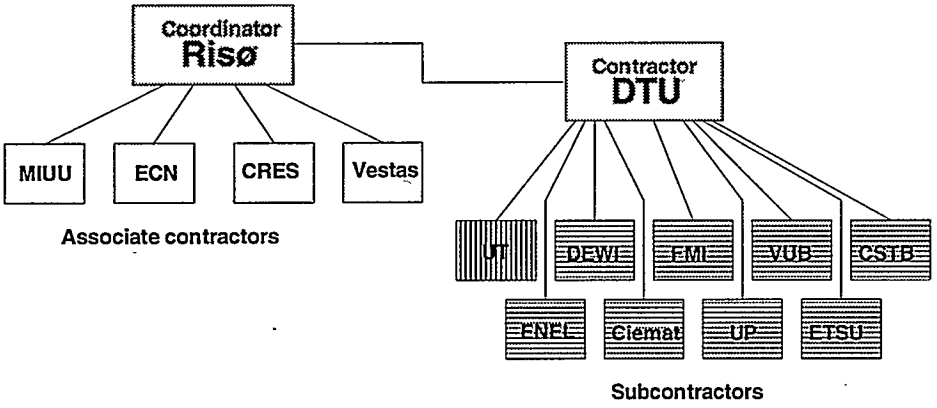

Database on Wind Characteristics

TIME SCHEDULE

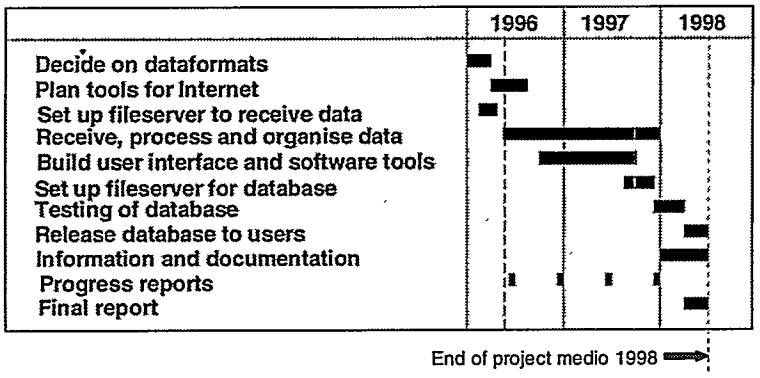

Database on Wind Characteristics

NEBRASKA WIND RESOURCE ASSESSMENT
FIRST YEAR RESULTS

Patrick J. F. Hurley
Rana Vilhauer
RLA Consulting, Inc.
18223 102nd Avenue NE, Suite A
Bothell, Washington 98011 USA

David Stooksbury
High Plains Climate Center
University of Nebraska - Lincoln
Lincoln, Nebraska 68583-0728 USA

ABSTRACT

This paper presents the preliminary results from a wind resource assessment program in Nebraska sponsored by the Nebraska Power Association. During the first year the measured annual wind speed at 40 meters ranged from 6.5 - 7.5 m/s (14.6 - 16.8 mph) at eight stations across the state. The site selection process is discussed as well as an overview of the site characteristics at the monitoring locations. Results from the first year monitoring period including data recovery rate, directionality, average wind speeds, wind shear, and turbulence intensity are presented. Results from the eight sites are qualitatively compared with other midwest and west coast locations.

BACKGROUND

RLA Consulting (RLA) has been retained by the Nebraska Power Association to identify the most promising sites for wind energy development in the state of Nebraska, and to collect high quality wind resource data at the eight most promising locations for which such data are not currently available. Funding for the project is provided by the Nebraska Wind Energy Task Force which consists of representatives of the Nebraska Power Association (an affiliation of the state's public electric utilities), the Nebraska State Energy Office, Nebraska Citizen's Action, the state legislature, and the Union of Concerned Scientists.

The Task Force established sixteen areas of interest based primarily on wind resource predictions, terrain considerations, and transmission access. Within those areas, RLA identified more than 30 promising sites for further investigation and conducted a field survey during which each of the sites were visited and evaluated. The sites were ranked based on their suitability for wind energy development. Finally, eight high-ranking, geographically-diverse locations were selected for monitoring that would compliment any existing wind resource data and characterize the most promising available sites.

Monitoring activities began in April 1995 and are anticipated to continue for approximately four years. RLA contracted with Zond Systems Midwest Regional Office to install and maintain the monitoring stations, and with the University of Nebraska High Plains Climate Center for data collection, quality control, and archiving. RLA manages the monitoring program, performs the data analysis, replaces missing or erroneous values, and reports results to the Task Force. This monitoring program was recently incorporated into the US DOE's Utility Wind Resource Assessment Program (U*WRAP) monitoring network.

MONITORING SITE IDENTIFICATION AND SELECTION

The Task Force established sixteen broad areas of interest based primarily on wind resource predictions, terrain considerations, and transmission access. For their screening, wind resource data were based on the *Wind Energy Resource Atlas of the United States* (PNL, 1991) with terrain considerations accounted for according to the method utilized by the Union of Concerned Scientists in *Powering the Midwest* (UCS, 1994). The area boundaries were established so that all potential sites would fall within roughly 16 kilometers (10 miles) of major transmission lines.

Within those areas, RLA identified more than 30 promising sites for further investigation based on a review of the available wind data, wind resource maps, and topography within each area. RLA conducted a field survey during which each of the identified sites were visited and evaluated. Site characteristics evaluated were grouped in the following general categories:

Wind Resource	local sources of measured data, vegetation and terrain indicators, exposure to prevailing winds, terrain enhancements
Land Availability	extent of available land similar in nature and exposure to the potential monitoring location
Terrain Suitability	suitability of terrain for construction and maintenance activities
Utility Access	proximity, capacity and voltage of nearby transmission lines
Physical Access and Logistical Support	proximity, type, and condition of nearby roads, as well as the proximity, population, and services available in nearby towns and cities
Public and Environmental Sensitivity	habitat or existence of threatened or endangered species, protected areas, scenic areas, or other causes of public concern
Owner Acceptance	disposition of land owners in the vicinity of potential monitoring sites
Communication Access	cellular company and signal strength, or proximity to telephone utility land line and utility company

The potential project sites were first screened based on land availability, proximity to transmission, estimated wind resource, and orientation of local terrain features relative to the prevailing wind direction. The sites were then ranked for consideration according to land owner interest, terrain suitability, environmental and public acceptance issues, and site access. Redundant locations (sites of lesser interest than other locations in their immediate vicinity) were removed from consideration. From the remaining sites, eight were selected with final consideration given to geographical diversity, prior or current wind resource assessment activities, service territories, and proximity to load centers.

The monitoring site locations are regionally distributed throughout Nebraska as follows:

Southwest - Imperial
Panhandle - Kimball, Rushville
North central - Valentine, Springview, Stuart
Eastern - Winnebago, Wahoo

MONITORING EQUIPMENT

Each station was configured to measure the following meteorological parameters at the heights indicated.

Measured Parameter	Height (m)
Wind Speed	10, 25, 40
Wind Direction	25, 40
Air Temperature	10, 40
Solar Radiation	3

The monitoring equipment was supplied by NRG Systems and included a NRG 9300 cellular datalogger, calibrated #40 anemometers, #200 wind vanes, #110S temperature sensors, and a LI-200SA LiCor pyranometer mounted on a 40 meter tower with a 4 foot lightning spike and 8 foot ground rod. A diagram of the basic tower configuration is shown in Figure 1.

Three of the stations (Imperial, Kimball, and Stuart) make use of existing communication towers. These towers have their own grounding and lightning protection system and were each tall enough to allow the installation of an additional anemometer at 50 meters above ground level. Two of the stations (Kimball and Stuart) use NRG 9300 Teleport data loggers to transmit the data over standard telephone lines.

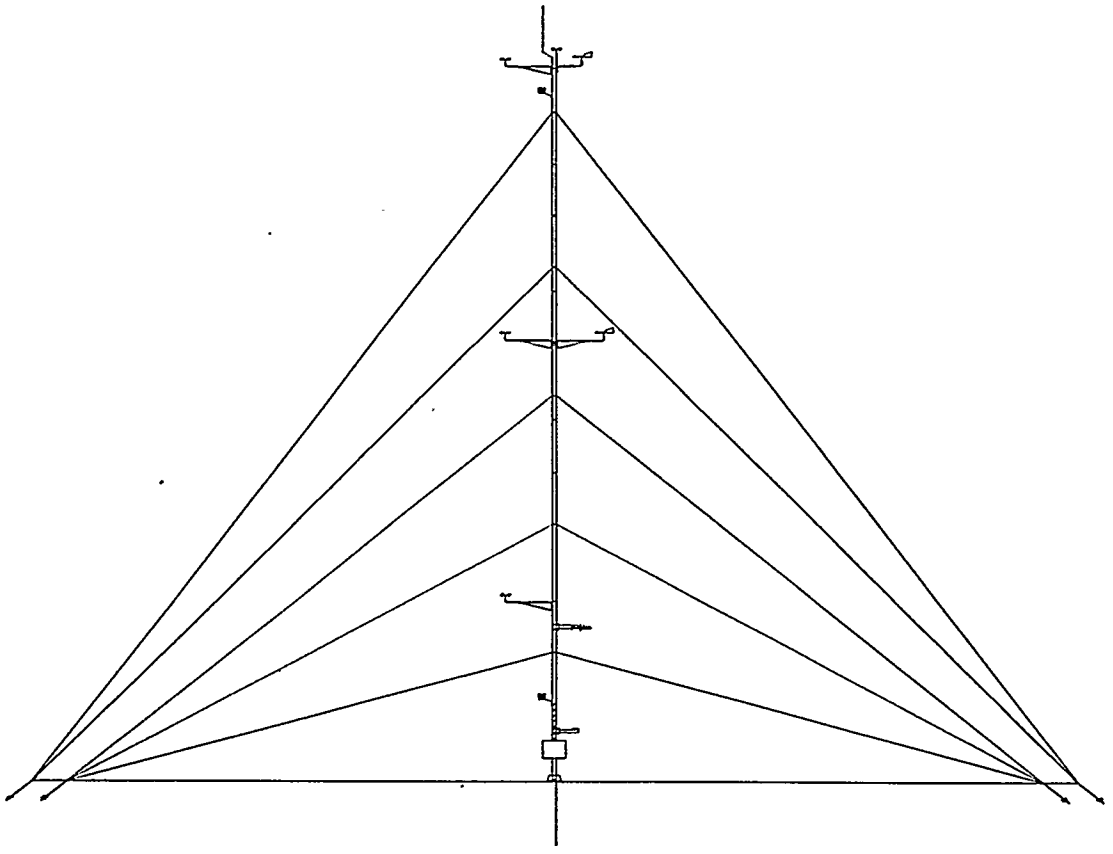

FIGURE 1. MONITORING STATION CONFIGURATION

RESULTS

Data Quality

The quality of data has been reviewed for evidence of any problems due to icing, maintenance, equipment malfunction, lightning, or any other events that may have interrupted data recovery or affected the accuracy of the recorded data. The annual data recovery rate from 40 meter anemometers exceeds 90% at all stations with a system-wide average of 96.9%.

While the average data recovery rate across the monitoring program was high during the first year of operation, all wind speed data noted as missing or erroneous have been replaced. The following methods were used to replace missing data:

- the average of the hour before and hour after (if only a few hours were affected)
- correlation to another sensor at the same monitoring site
- correlation to another nearby wind resource monitoring site
- correlation to nearby meteorological monitoring station
- the measured monthly average wind speed

Erroneous wind direction data values were deleted. No attempt has been made to replace any data values other than wind speed. All of the following results are based on corrected data.

Wind Speed

The annual average wind speed results from all of the monitoring stations are summarized in Table 1. Six of the stations recorded annual average wind speeds of greater than 7 m/s (15.7 mph) at a height of 40 meters above ground level. The average wind power densities at these six sites were higher than 400 W/m^2. The highest average wind speeds were recorded at Valentine (7.5 m/s, 16.8 mph) and Springview (7.5 m/s, 16.7 mph). The lowest values were recorded at Rushville (6.5 m/s, 14.6 mph) and Wahoo (6.6 m/s, 14.8 mph). The terrain and vegetation patterns in the vicinity of the Rushville site are fairly complex and it is possible that there are nearby sites that would exhibit higher average wind speeds. A relatively lower annual average wind speed was anticipated at Wahoo which was chosen primarily because of its proximity to a load center.

TABLE 1. ANNUAL WIND SPEED SUMMARY

	Annual Average Wind Speed in m/s (mph)								Recovery Rate*
	10m		25m		40m		50m		%
Imperial	5.3	(11.8)	6.7	(15.1)	7.2	(16.2)	7.6	(16.9)	99.9%
Rushville	4.5	(10.1)	5.7	(12.7)	6.5	(14.5)			99.1%
Winnebago	5.3	(11.9)	6.3	(14.2)	7.1	(15.9)			98.5%
Wahoo	4.9	(10.9)	5.8	(13.0)	6.6	(14.8)			99.2%
Kimball	4.9	(11.0)	6.2	(13.9)	7.1	(15.9)	7.4	(16.4)	98.8%
Valentine	6.0	(13.4)	6.9	(15.4)	7.5	(16.8)			92.0%
Springview	5.6	(12.5)	6.7	(14.9)	7.5	(16.7)			90.9%
Stuart	5.6	(12.5)	6.5	(14.6)	7.3	(16.4)	7.7	(17.2)	97.1%

* Data recovery based on 40 meter data recovery calculated as: R = (Np - Ne - Nm) / Np x 100%; where R is the data recovery rate, Np the number of possible data values, Ne the number of erroneous data values, and Nm the number of missing data values.

As shown in Figure 2, the seasonal patterns are similar across the State. The winds were the highest during October and February. The winds were the lowest during the summer months and dipped again during November, December, and January. Although the seasonal patterns were similar, the two lowest sites (Rushville and Wahoo) experienced significantly lower dips during the low wind months.

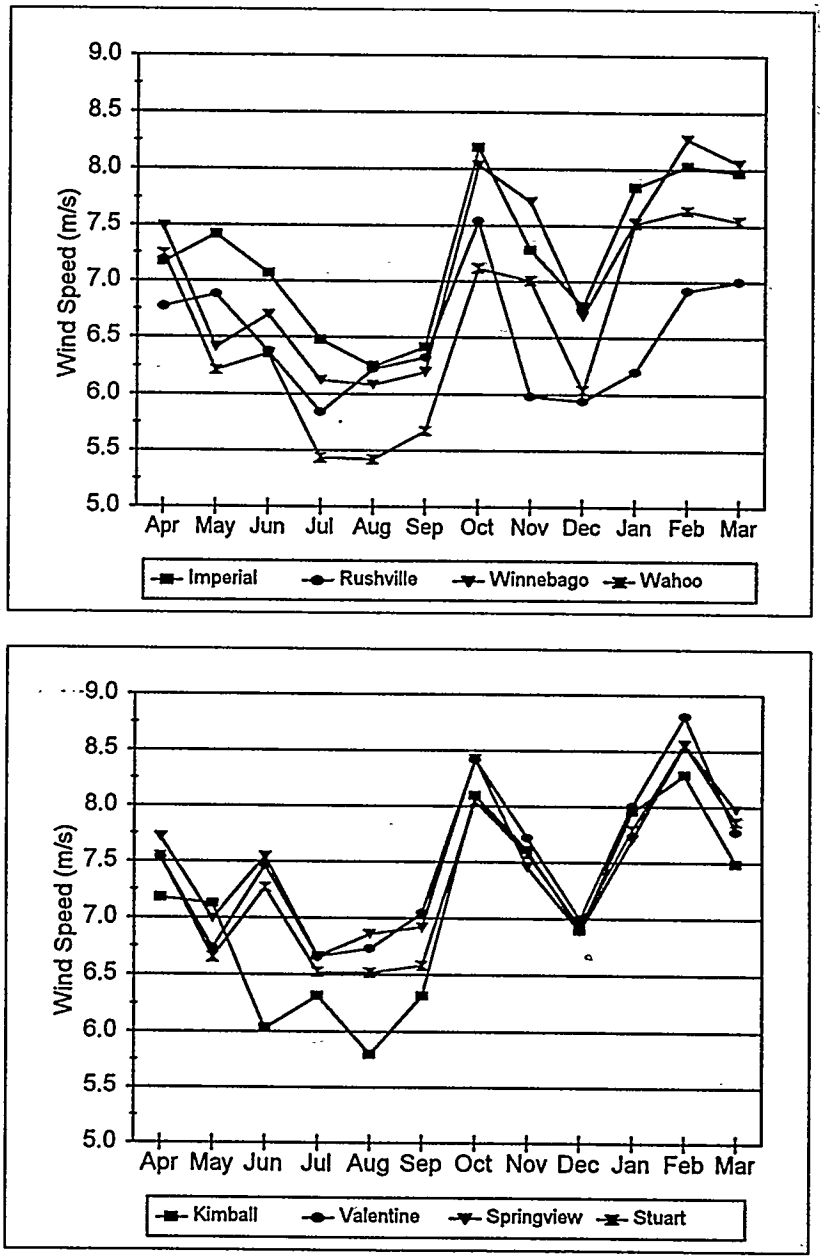

FIGURE 2. MONTHLY WIND SPEED

The North Central sites, Valentine, Springview, and Stuart, all had monthly average wind speeds of greater than 6.5 m/s during the moderate (summer) wind season. These sites have the clearest exposure to the two prevailing wind directions.

The Rushville site compares well with other sites during the summer months when the winds are generally from the south. However, the wind speeds are lower during the winter months when the winds are from the northwest. This difference is likely due to the sites clear exposure to the south and the distribution of forest and more complex terrain to the north.

The annual diurnal patterns are illustrated in Figure 3. As expected, the diurnal pattern is similar between the sites. The most noticeable difference in diurnal patterns is at Imperial and Valentine. The winds at Imperial are the strongest during the late evening to early morning and the strongest winds at Valentine are in the early morning. The other sites tend to have their strongest winds during the early afternoon.

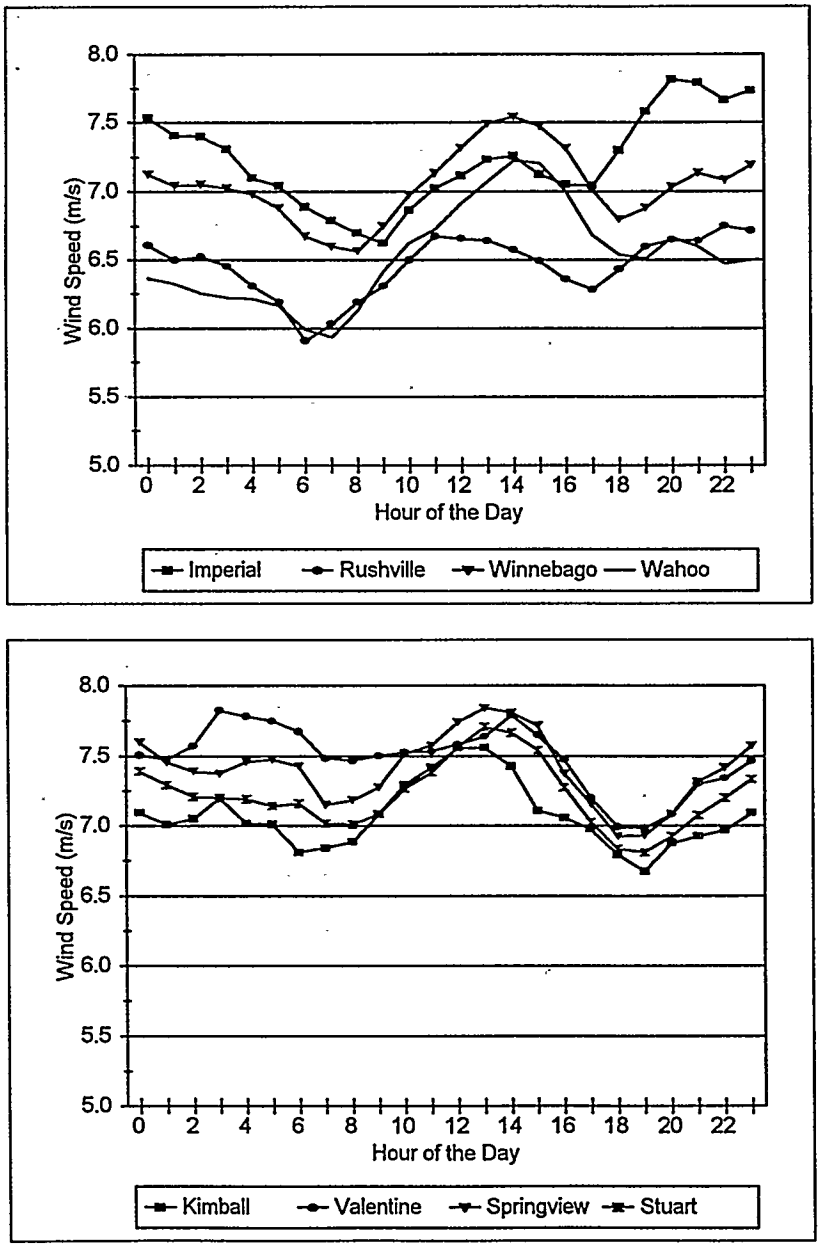

FIGURE 3. DIURNAL WIND SPEED

Wind Direction

Figure 4 provides a summary of the annual wind direction across Nebraska. As seen in the wind rose, the prevailing wind directions are generally from the northwest during the winter and from the south or southeast during the summer. Some variations in the general pattern are observed. The western sites tend to have a NW-SE pattern, while the eastern sites exhibit a stronger southern component to the summer winds.

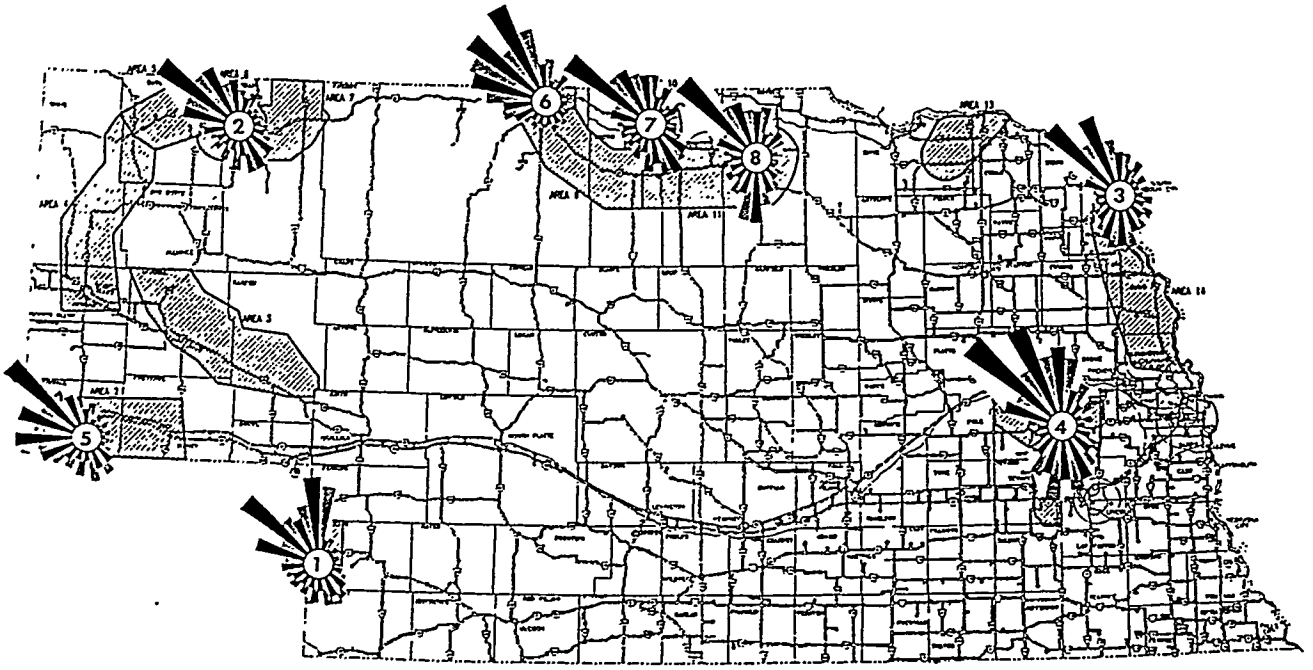

1	Imperial	5	Kimball
2	Rushville	6	Valentine
3	Winnebago	7	Springview
4	Wahoo	8	Stuart

FIGURE 4. WIND DIRECTION PATTERNS THROUGHOUT NEBRASKA

Wind Speed Distribution

The measured wind speed frequency distributions for sites across the state, with average wind speeds ranging from 6.5-7.5 m/s, have weibull-k values from 2.1-2.4. The Springview wind speed frequency distribution is shown in Figure 5 compared to a Rayleigh distribution with the same average wind speed, and a Weibull distribution (k-value of 2.3) with the same average wind speed and average wind power density. The Rayleigh distribution has an average wind power density that is 14% higher than the measured distribution at Springview and is not an appropriate model of the resource.

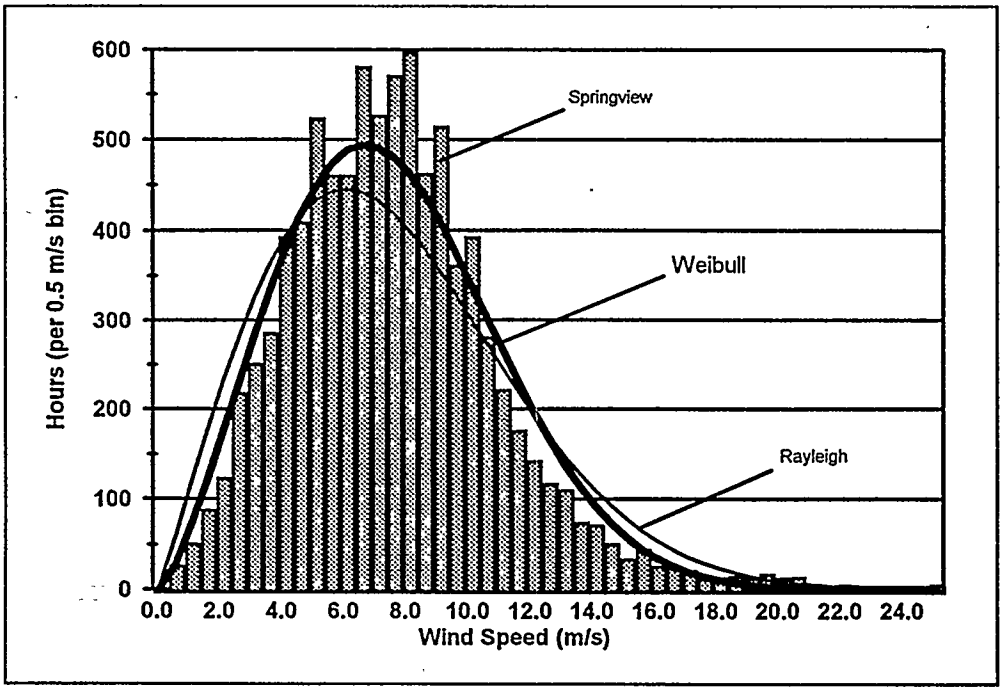

FIGURE 5. FREQUENCY DISTRIBUTIONS

Wind Shear

Average wind shear is calculated based on the power law formulation where the increase in wind speed with height above the ground is assumed to change exponentially with the height above the ground.[1] The theoretically derived value for the shear exponent is 1/7 for a fully developed flow over a smooth surface. At the monitoring sites throughout Nebraska, the wind shear is consistently higher than this theoretical value. Table 2 provides a comparison of the annual average wind shear exponents at the eight monitoring sites. Six of the eight sites had an average wind shear exponent greater than 0.24 when comparing 25m and 40m levels. Where 50m data were measured, the wind shear exponent ranged from 0.16 to 0.21 when comparing 40m and 50m levels. Variations in the wind shear were noted that are assumed to be related to site terrain and surface conditions, wind speed, direction, and seasonal changes.

TABLE 2. WIND SHEAR EXPONENT

	10 - 25 m	25 - 40 m	40 - 50 m
Imperial	0.268	0.155	0.188
Rushville	0.253	0.285	
Winnebago	0.191	0.244	
Wahoo	0.191	0.270	
Kimball	0.253	0.282	0.162
Valentine	0.155	0.180	
Springview	0.187	0.250	
Stuart	0.163	0.248	0.213

[1] For wind speeds (v_1 and v_2) at heights (h_1 and h_2), $v_2/ v_1 = [h_2/h_1]^{\alpha}$, where α is the wind shear exponent.

Turbulence Intensity

Turbulence intensity (TI) calculated as the standard deviation of the wind speed divided by the average wind speed (based on one-second samples over hourly intervals) is a relative indicator of turbulence. Calculated in this manner, TI values of 0.10 or less are relatively low, moderate turbulence is indicated by values of between 0.10 and 0.25, and highly turbulent wind regimes indicated by values greater than 0.25.

The values of TI are similar at stations across the state and generally fall in the low end of the "moderate" range. During the first year of this study, the range of TI from predominant wind directions and at wind speeds of greater than 4 m/s (10 mph) is 0.13 - 0.15. A review of the monthly TI shows that there was no significant seasonal variation.

Summary of Results

The first year data set confirm that Class 3 and 4 wind sites can be found throughout the State of Nebraska. The strongest winds appear to come from the northwest during the winter months, and the diurnal pattern at most of the sites shows a day time peak between 10 am and 4 pm and a night time peak between 10 pm and 6 am. The sites exhibit a relatively high rate of wind shear and low-to-moderate turbulence intensity.

The results presented are for one year only and may not be representative of a typical meteorological year. Analysis of long term data will be conducted later in the program.

OPERATIONAL ISSUES

Installation of data loggers using standard telephone technology proved to be problematic in several of the rural locations due to noise on the phone lines. In addition, the telephone line may be another path open to the influence of lightning induced problems. At least one logger failure was attributed to a surge introduced through the telephone line based on an inspection of the damaged components. Two of the stations were converted from land line to cellular communication.

The system has been subjected to periods of icing and severe thunderstorms. Icing accounts for 1,281 site-hours of missing data, 59% of the total for all causes throughout the system. Lightning accounts for 20% of the total. The remainder of missing data are attributed to equipment malfunction, maintenance, and miscellaneous unexplained causes. In several instances, following thunderstorms passing through the areas, a few loggers have temporarily shut down and rebooted hours or days later. NRG provided retrofit firmware designed to be less susceptible to this type of event.

There has been a persistent problem with the failure of the highest anemometers (40 and 50 meters) that are mounted on booms extending from the towers. Other sensor locations have not experienced the same rate of failure. The failure mode has been identified by NRG as static discharge in the coil windings. The anemometers were installed with movistors across the coil terminals (the movistors were subsequently incorporated into the anemometer design by NRG), two foot lightning spikes and eight foot ground rods. The towers were fitted with longer (four foot) lightning spikes as a trial solution; however, this does not appear to have solved the problem. It has also been suggested that the anodized aluminum sensor booms are contributing to the problem due to their relatively low conductivity. RLA is working with NRG on retrofit solutions to the problem.

Despite the extreme Nebraska weather including severe thunderstorms with lightning and hail, bitter cold winter temperatures, wind driven snow, and tornadoes, high data recovery rates have been attained with six of the eight monitoring stations above 97%. The high data recovery rate can be attributed to the reliability of the equipment, the quality of the installations, and the responsiveness of the entire project team to maintenance events.

OBTAINING THE DATA

Data reports as well as raw and validated data are archived at the High Plains Climate Center and available to the public for a nominal charge. For information regarding the charges and methods of obtaining the data contact the HPCC at (402) 472-6706.

ACKNOWLEDGMENTS

The authors wish to thank the members of the Nebraska Wind Energy Task Force for the opportunity to present the information, Zond Systems Midwest Regional Office for maintenance, and NRG Systems for their after sales support and assistance.

A HIGH SPEED MULTI-TASKING, MULTI-PROCESSOR TELEMETRY SYSTEM

Kung Chris Wu
Mechanical and Industrial Engineering Department
The University of Texas at El Paso
500 W. University Avenue El Paso, TX 79968

1.0 INTRODUCTION

The term "telemetry system" is adopted in this paper as a general term for a data acquisition system with wireless communication capability to collect and transfer data from a site which is not easily accessible. In wind turbine research, a telemetry system is commonly used to collect data about the loads, vibrations, and air pressure of the rotating blades and radio the data to computers on the ground. Conventional telemetry systems utilize a single CPU to perform all functions of the telemetry system in a sequential order. Figure 1 illustrates the flow chart of a typical data collection-radio transmission sequence. The major problems of this "sequential programming" type of system are the limitation on the data acquisition speed and the capability of sampling data continuously for a long period of time. For example, in a typical wind turbine application the telemetry system is required to sample 16 channels of 12-bit or 16-bit data at a speed of 200 Hz per channel, then 51.2 Kbits of data is generated per second (Kbps). If the telemetry system uses a radio-frequency (RF) modem at a rated communication speed of 115.2 Kbps, i.e., a very fast RF modem available in the market for PC computers, then the computer must spend about 0.5 second to transmit the data collected in one second. In practice the data transmission rate between RF modems can be much lower than the rated speed due to the magnetic noise of the generator and interference from other radio equipment operated in the vicinity which uses the same radio frequency. The effective transmission rate has been found to be lower than the rated speed by a factor of 3 in some practical field tests [Wu, et al. 1994]. Furthermore, to ensure data integrity the communication software generally includes handshaking and error checking routines that add computation overhead to slow down the effective transmission rate. Using the sequential programming approach, the data transmission process becomes the bottleneck of the system which limits the maximum data acquisition speed. If a large number of signals must be sampled at a high frequency, say 32 channels of signals at 1 kHz per channel, 512 Kbps of data is generated. A common solution to this problem is to increase the telemetry system's on-board memory to continuously store the sampled data during the test [McCoy 1992; Simms 1992; and Wu, et al. 1994]. After the memory is completely filled, the data collection process is stopped and the sampled data is then transmitted to the remote computer in one batch. This solution has two shortcomings. First, the data collected cannot be monitored in real-time. Second, the duration of the data collected continuously is limited by the amount of on-board memory available.

In addition to sampling data, telemetry systems designed for wind turbine applications must also be physically small and light. Wind turbine rotor blades are generally made of composite materials that are light-weight and flexible. The telemetry system mounted on the rotor must not affect the dynamics of the system. The electric motors driven by the rotor blades produce magnetic noise. Operating the telemetry system in such an environment requires the system to be structurally rigorous to excessive vibration and insensitive to environmental noise.

To address these problems, this paper presents a small size, light-weight, multi-tasking, multi-processor telemetry system capable of collecting 32 channels of differential signals (expandable to 128 channels without a significant increase in cost) at a sampling rate of 6.25 kHz per channel (or 1.56 kHz per channel for 128 channels). This system can be a single-processor system which executes data collection and data transmission in parallel, a multi-tasking system. It can also be a multi-processor system which allows multiple RF modems to transmit data in parallel or execution of data reduction software in real time. The volume of the single-processor system currently implemented measures 16.5 x 18 x 43 cm^3 (see Figure 2) and weighs about 10 kgs (with an AC to DC power transformer for continuous data collection).

2.0 SYSTEM BLOCK DIAGRAM

The computer architecture of a multi-tasking system is designed to achieve high speed data acquisition and RF transmission simultaneously. The block diagram of a two processor system is shown in Figure 3. In this system, Computer-1 is the primary computer which services the data acquisition and transmission tasks. To

avoid the problems associated with the "sequential programming" approach, Computer-1 uses direct memory access (DMA) service routine to execute the data acquisition task in parallel to the data transmission task. DMA is a communication technique to transfer data between peripheral devices and computer memory directly without the control of the CPU. In other words, the DMA controller takes the bus usage privilege from the CPU and transfers data from the peripheral device directly to the memory or vice versa on the system bus. This greatly simplifies the transferring of data at high speed between the peripherals and memories. A typical DMA can transfer data at a speed of 200 to 250 Mhz [Cyber 1993, Wiley 1979] in an 80386sx/25 computer. While the data collection subsystem is sampling data, the CPU is free to transfer data from its memory to the RF modem until one data collection cycle is completed.

For applications requiring on-line processing of the collected data in addition to transmitting data to remote computers, the proposed system uses another DMA service routine to transfer data to other computers directly wired to Computer-1, the Data Acquisition System (DAS). As illustrated in Figure 3, Computer-2 retrieves the collected data from the local memory of Computer-1 through DMA and processes them. The second processor might be equipped with an RF modem which can be used to transfer the processed data to remote computers in parallel to Computer-1.

As shown in Figure 3, Computer-1 has the standard configuration of a DAS computer. It employs a high speed analog to digital converter (ADC) board, HSDAS-16, to accommodate the data acquisition function and a high speed wireless modem, CYLINK128, to transfer the data. An RS-422 interface card is included in Computer-1 to facilitate the RS-422 synchronous communication port required by the CYLINK128 RF modem. Detail of the hardware setup will be discussed in Section 3 of this paper.

2.1 Theory of Operation

After Computer-1 is initialized, the HSDAS-16 board digitizes the analog signals and uses DMA to send the digitized data into a temporary data buffer. When a specified number of data have been sampled, the data collection process stops and an internal DMA complete register is set to one. The CPU will stop its normal operations, transfer the data from the data buffer to the main memory, reset the DMA register, and instruct the HSDAS-16 board to repeat the data collection cycles. While the HSDAS-16 is collecting the next batch of data, the CPU resumes its normal operation which is programmed to transfer the data from its memory to the CYLINK128 RF modem through an RS-422 port. To extend the I/O capacity, a high capacity I/O multiplexer, like the DASMUX 256, can be used to expand the ADC capacity to 256 single-ended or 128 differential inputs. The overall sampling rate of the data acquisition process is controlled by an internal clock on the HSDAS-16 board.

The memory of Computer-1 is configured as a distributed shared memory to support the multi-tasking. The shared memory configuration also permits the local memory of Computer-1 to be accessed by other computers. This feature provides the opportunity of networking a number of computers whose local memories are common to other computers. In other words, the computer architecture supports not only the parallel executions of data collection and transmission, but also supports multi-computer operations. In the two-processor system, the data generated by the ADC board is put into the local memory of Computer-1. Through the multiport shared memory, Computer-2 can access the data and process them in real time. Data transfer among computers are done using the DMA service routines. To transfer data between computers, a 32-bit high speed digital I/O bus is established using the DIO-32F cards (one for each computer).

2.2 Operation Time Allowed for Continuous Data Collection

In summary, the proposed multi-tasking, multi-processor telemetry system provides two major advantages over the conventional systems. First, the multi-tasking arrangement allows continuous data collection and transmission to be executed in parallel with a single CPU. This facilitates the real-time monitoring capacity. If the effective data transmission rate of the RF modem equals or is faster than the data collection rate, the system will run continuously. If the data transmission rate is slower, the total operation time, before the memory overflows, of the system is given by

$$T=M/(D_g-D_t) \qquad (1)$$

where T is the time in minutes

M is the size of the local memory in bytes, D_g is the bytes of data generated per minute,

D_t is the bytes of data transmitted per minute.

Compared to the time allowed by the conventional approach, i.e., fill the whole memory first and transmit

all of the data later,

$$T=M/D_g \quad (2)$$

The proposed system provides significant improvement in the amount of time the data can be collected continuously in addition to the real-time monitoring capability. Second, in the case where the effective data transmission rate of the RF modem is slower than the data collection rate (like in a low cost system), continuous data collection and real-time monitoring can still be realized using the multi-processor feature to multiply the data transmission rate, i.e., multiple RF modems can be used to transfer collected data in parallel.

3.0 DESCRIPTION OF HARDWARE COMPONENTS

The hardware components of the proposed telemetry system can be divided into five sub-systems: the processor boards, the data acquisition sub-system, the RF modem sub-system, the external DMA bus, and the power supply sub-system.

3.1 The Processor Boards

The processor boards selected are an 80486SX/33 single board computer (SBC), referred to as the Processor-1 (or Computer-1 in Figure 3) , and an 80386DX/33 SBC, referred to as the Processor-2 (or Computer-2 in Figure 3), from the Cyber Research Company [Cyber 1994]. The SBCs have several unique characteristics which make them suitable for our system. They have all of the basic functions of the 80x86 desk-top computers, but with only half the size of the standard PC plug-in board. The PC compatibility makes the SBC very easy to program and expand functionally. Each board has an operating system, with 4 Mbyte of RAM memory (expandable to 32 Mbyte on-board), 16 hardware interrupt lines and two DMA controllers on a single board. The single board design allows easy installation and replacement. The industrial-grade SBC can work continuously in a harsh environment at temperatures ranging from 32 to 140 degrees Fahrenheit. The SBC also provides 1.4 Mbyte of flush ROM piggyback disk which can be used as a ROM drive to store the application programs. The ROM disk can sustain much higher vibration than the mechanical disks. This makes it suitable to the telemetry system's high vibration working environment. The SBC uses a single 5 volt power supply which makes it ideal for a telemetry system since the whole system can be powered by a simple rechargeable battery.

There is also a watchdog timer in both the 80486 and the 80386. They can be used to reboot the telemetry system automatically in case of system error. Watchdog is a standard protection and safety method for the industry PC under harsh working environments. It is used to ensure the reliability of the system. The watchdog can reboot the CPU automatically after a system crash due to hardware or software failures.

3.2 The Data Collection Sub-System

The data collection subsystem consists of a high speed ADC board and a multiplexer board. Additional hardware such as programmable active filters and amplifiers can also be included in this system. The HSDAS-16 high speed ADC board from ANALOGIC Company [ANALOGIC 1992] is selected for the data acquisition task. The HSDAS-16 has four independent 16-bit ADC chips on board. Each ADC chip can sample at a maximum rate of 50 kHz. This yields an aggregate sampling rate of 200 kHz for a single input channel. It also features sixteen single-ended or eight differential channels of analog inputs and an internal multiplexer dividing the inputs into groups of four channels. If eight differential channels are sampled together, each ADC must sample two data sequentially during a sampling cycle. This yields a maximum sampling rate of 25 kHz. Table 1 shows the maximum sampling rate provided by the HSDAS-16 board.

TABLE 1. MAXIMUM SAMPLING RATE PROVIDED BY THE HSDAS-16 BOARD

Single channel (single-ended or differential)	200 kHz
2 channels (single-ended or differential)	100 kHz
4 channels (single-ended or differential)	50 kHz
8 channels (single-ended or differential)	25 kHz
16 channels (single-ended)	12.5 kHz

The ranges of the input signals can be programmed independently to be -2.5 to 2.5, -5 to 5, or -10 to 10 volts for each channel. HSDAS-16 has an internal 128-sample First-In-First-Out (FIFO) data buffer. The sampled data can be transferred from the FIFO data buffer to computer memory either through Programmed I/O or through DMA channels. If more than eight differential inputs must be sampled together, additional HSDAS-16's can be used or an external multiplexer like the DASMUX256 (also from ANALOGIC Company) can be used. The DASMUX256 is a programmable 256 single-ended or 128 differential input channel time division multiplex (TDM) multiplexer. When the HSDAS-16 is used with the DASMUX256, it can collect data from up to 128 channels of differential signals at a maximum speed of 1.56 kHz per channel.

3.3 RF Modem Sub-system: Cylink128 Modem and RS 422 Interface

If the data acquisition speed is faster than the speed of the RF modem, the acquired data will eventually overflow the shared memory (as discussed in Section 2). Thus, the speed of the modem dominates the data sampling speed of the telemetry system for a continuous operation. The CYLINK128 from Cylink Corporation can transfer data point-to-point at a distance up to 48 Km using 902 to 928 Mhz frequency range airlinks. It has the remote loop back function and signal quality indicator. It can be designed to function like line modems and can replace wired modems with no effect on the user's application program. When used in synchronous serial communication mode, the CYLINK128 modem provides a communication rate as high as 115.2 Kbps. CYLINK128 uses an EIA-530 synchronous serial communication interface to communicate with computers. Since the EIA-530 interface is not a standard interface provided by 80x86 computers, an RS-422 interface board, which is EIA-530 compatible, was integrated into the telemetry system to accommodate the required interface.

3.4 External DMA Bus: DIO-32F I/O Board

The National Instrument DIO-32F I/O boards are used to finish the data communication function between the processor boards. This board has the following characteristics: (1) high speed parallel data transfer, (2) digital pattern generation, and (3) high speed digital data acquisition [National 1993]. One can access the 32 digital I/O lines of the DIO-32F as four 8-bit ports or two 16-bit ports. This is very suitable to our telemetry system, since the A/D board used in this system has a 16 bit resolution. The high data transferring rate of this board comes from the dual DMA architecture of the DIO-32F board. The data transferring rate of the on-board DMA control circuitry can achieve up to 330,000 32 bit words per second. In buffer mode, its data transferring rate can go even faster: up to 450 Kwords per second. Thus, DIO-32F can outstrip the speed capabilities of most PC's. Here, the data transferring rate has passed the limit of the general PC's DMA data transferring rate which makes the time delay during the data transferring in the DIO-32F negligible.

3.5 Power Supply Sub-system

To make a stand-alone, self-contained telemetry system, a rechargeable battery must be used as the power source. The total power consumption of the main components of the system is estimated to be approximately 5A @5Vdc. The Power-Sonic Company model PS-12280 battery provides 30 AH with a size of 16.5 x 13 x 18 cm^3 and with a weight of 3.7 kgs. Six hours of continuous operation can be realized.

3.6 System Volume Estimate

The physical dimensions of the main components used in the system are listed in Table 2. According to the individual sizes of the components of the system, the volume of the system including battery is estimated to be 25 x 18 x 43 cm^3. The system implemented in this project measures 16.5 x 18 x 43 cm^3 which includes an AC to DC power transformer instead of a battery.

TABLE 2. PHYSICAL DIMENSIONS (IN cm) OF THE COMPONENTS

Board Name	CPCC486-33S	HSDAS-16	DIO-32F	RS422	Cylink 128	Battery
Dimension	10x15	20x30.5	20x30.5	10x15	3x15x35	16.5x13x18

3.7 DC Drift and Electronics Noise Reduction Consideration

The electronics noise, not to be confused with the environmental noise, in the telemetry system can be classified into two types: the white noise and the charge-pump or accumulated noise. The charge-pump noise becomes more serious due to the capacitors and distributed capacitors in the A/D system when used

with the TMD multiplexer. In order to ensure the precision of the A/D result, the following steps can be taken during data acquisition operations: (1) All unused channels must be grounded properly. (2) Apply the optical-electrical isolator to each data acquisition channel. (3) In order to decrease the effect of the accumulated noise, two steps can be taken. First, the DC ground of the telemetry system must be properly grounded to earth. Since the telemetry system is a stand-alone system which might not be connected to earth, an alternative measure can be used to eliminate the accumulated noise. In a pre-programmed time-interval, the HSDAS-16 & DASMUX64 can be programmed in the disconnected mode from the measured signals. A "white" measurement is made. Clearly, the value measured represents the DC drift and the accumulated noise. Three measurements are then taken for each data point. The actual measurement is then calculated by subtracting the "accumulated noise" from the average calculated from (3). Notice that the extra measurement and the arithmetic computation time further reduces the effective sampling rate.

4.0 WORKING WITH OTHER MEASUREMENT SYSTEMS

Another problem that must be considered is the problem of synchronization when different data acquisition systems work together. In general, the absolute synchronization of the different systems using a global signal is not easy to achieve. It is generally done by using a common reference to start the data acquisition simultaneously and check for the synchronization periodically. In this case, we should first build up the handshake between the telemetry system and the ground computer, and the handshake of other measurement systems with the ground computer. A batch of necessary parameters, such as the number of points in one measurement cycle and timer constants, should be sent both to the telemetry system and other measurement systems, followed by a starting signal. This signal starts all the data acquisition systems simultaneously. After a measurement cycle, the two systems have to be re-synchronized.

There are two reasons to cause the time drift during the measurements. One is the starting time drift. The other is the time drift due to the independent timer used in each system. Because the computer on the ground sends the starting signals to the telemetry system and another measurement system sequentially, there can be a four-instruction delay, roughly speaking, in the two way serial starting procedure. Thus, this delay equals 4 x 10 x 0.1 μs, i.e., 4 μs. Here, we assume the instruction length is ten instruction cycles and the clock frequency is 10 Mhz. This delay is negligible compared with the tolerant time drift which is in the magnitude of a millisecond. The number of synchronizations can be decided by the tolerant time skew between the same measurement point of the two systems and the precision of the timer [Ilenkovic 1979]. Clearly, the precision of the timer is decided by the precision of the crystal oscillator and the timer constant, which is decided during the design stage. In general, it can reach 10 nanoseconds. If we require the time drift between the same measurement point of the two systems to be within 1 ms, then the number of synchronizations during a four hour measurement cycle should be:

$$N1=0.001 / 0.00000001 = 100000 \quad (3)$$

$$N=(4 \times 60 \times 60) / (0.001 / 0.00000001)=144 \quad (4)$$

It means that the telemetry system and the other measurement system should be synchronized 144 times, with 100,000 measurement points in each cycle, during a four hour measurement routine in order to ensure the required synchronization degree.

5.0 SYSTEM INTEGRATION AND EXPERIMENTAL RESULTS

The basic configuration of the proposed system has been implemented and tested successfully in the laboratory environment. The implemented system (see Figure 2) is a single-CPU system programmed to collect 16 channels of differential signal at the rate of 1 kHz per channel. The collected data is transferred to a remote computer at a rate 115.2 kHz. The system has not been tested at a wind turbine site so the effective data transmission rate of the RF modem is yet to be determined.

5.1 Shared Memory and Memory Management

In the new telemetry system, data communication and exchange between the data collection and transmission and between processor boards, which are executed in parallel, are facilitated through the use of shared memory. In our distributed shared memory system, the local memory of each processor can only be written by its owner. However, they can be read by any other processors. When multiple processors are used, a First-Come-First-Service load buffer is maintained in each local memory which stores the load

requests from the other processors to ensure the data integrity. For a two processor system, the data integrity is guaranteed, as long as the target processor finishes the load action before it acknowledges the load request from the other processor [Huang 1994]. Load requests and data transfer are accommodated through the DIO-32F I/O external bus.

5.1.1 Realization of Shared Memory and FIFO Policy

In our system, a First-In-First-Out (FIFO) data buffer is set up in the local memory of each processor board. The function of the data buffer is to store the new arriving sample data and a FIFO policy is used to deal with the data overflow. Each element in the data buffer contains two status bits: a dirty bit indicating fresh data is ready to be read and a trash bit indicating the status of the previous data stored in this location. The data stored in the FIFO buffer is the 16-bit data generated by the HSDAS-16 boards. The status bits are implemented using the least two significant bits of the 16-bit data without losing the accuracy of the ADC conversions. Table 3 shows the four possible statuses of the data.

TABLE 3. STATUS BIT PATTERN AND ITS MEANING

Trash Bit	Dirty Bit	Status
0	0	Fresh data ready to be read, previous data is trashed.
0	1	Data has been read, previous data is trashed.
1	0	Fresh data ready to be read, previous data is stored in the hard disk, memory overflow detected.
1	1	Memory overflow detected. Data collection process has been stopped momentarily at this point.

5.1.2 Read-Write Privilege

For a read, the read request is acknowledged by the data owner, and a copy of the data is returned. The dirty bit is then marked to 1. The receiving processor will check the trash bit. If the trash bit is 1, it signals the receiver that previous data at the same memory location was not read by any processor and is not available. Equivalently speaking, the data just received can be invalid data.

For a write, if the data in the target memory location has been read by any other processor, i.e., the dirty bit is 1, the status bit of the data is reset to 00 and the data is written to the memory location. If the dirty is 0, a memory overflow has occurred, and one of the two FIFO policies can be implemented.

(1) Replacement strategy. Once a memory overflow has been detected, the system should make sure that the data will not be lost. If losing data is not permitted, one of the practical methods is to transfer the data which will be replaced to an external storage disk. The trash bit of the new data is set to 1 and written to the memory. (2) Stop sampling data momentarily. This memory overflow routine will stop the data collection process by a fixed amount of time to allow the load process to catch up. All of the new data will be lost during the waiting time.

5.2 The Software

The flow chart of the main program of Computer-1 is depicted in Figure 4. At the beginning of the program, Computer-1 initializes the internal watchdog timer, initializes the data buffer, disables the read requests from Computer-2, initializes the Cylink 128 RF modem, and remains in the idle mode waiting for the data collection parameters to be transmitted from the ground computer. Once the ground computer is initialized, the ADC operation parameters are obtained from the operator, i.e., number of ADC channels and sampling rate. These parameters will be sent to the telemetry system. The telemetry system initializes the ADC subsystem accordingly and puts the system in a wait state until a read request is transmitted to the telemetry system from the ground computer. This start-up procedure is shown as the initialization process in the flow chart.

In the data collection/transmission process, the ADC subsystem is activated to collect a number of data specified in the ADC parameters. The sample data will be stored in a temporary array through the DMA method. Immediately after the ADC subsystem is activated, Computer-1 starts requesting data from the FIFO buffer and checks for the status bits. If valid data is available, it is transferred to the RF modem and the cycle repeats. At the end of each data transfer, Computer-1 checks the DMA status register of the HSDAS-16 board to see if the data collection cycle has been completed. If so, Computer-1 stops the data

transmission process and transfers the data from the temporary array to the data buffer. If multiple processors are used, Computer-1 also pulls the DMA status register of the DIO-32 Card to see if Computer-2 has requested data transfer from Computer-1 (this has not been implemented in the current system). The status bits of the new data will be set according to the FIFO policy discussed earlier. At the end of the service routine, the data collection cycle is reactivated and Computer-1 resumes its data transmission task. Figure 5 shows the flow chart of the DAS/DMA service routine.

Two possibilities can happen in this protocol. One possibility is the data writing speed is lower than the data reading speed, i.e., the data sampling rate is relatively slow compared to the data transmission rate. In this case, all new data will be transferred to the ground computer without overflowing the data buffer. The other possibility is the data writing speed is greater than the data reading speed. The data buffer will overflow in the end. At this time, the processor will give the status bits a pattern of 10 or 11 according to the FIFO policy.

5.3 Experimental Results

The system implemented has been tested in the laboratory for data collection at 1 kHz per channel for 16 channels. A sinusoid signal of 200 Hz is routed to input channels 1, 3, 5, 7, 9, 11, 13, and 15. Another sinusoid signal of 100 Hz is routed to input channels 2, 4, 6, 8, 10, 12, 14, and 16. Figure 6 shows the input signal and the digitized signals at channels 1 and 5. Figure 7 shows the input signal and the digitized signals at channels 2 and 6. The computer has 4 Mbyte of RAM and only 1 Kbyte is used for a data buffer. The system is powered by ac outlet and no data buffer overflow has occurred during a two hour test.

6.0 COST ANALYSIS

Except for the software development cost, the hardware cost for the proposed telemetry system amounts to $13,175 dollars for a 32 differential channel capability. This yields an average of $412 per channel. Cost break down of the hardware components is listed in Table 4.

TABLE 4. COST BREAK DOWN FOR THE TELEMETRY SYSTEM (PRICE QUOTED IN JUNE, 1996)

ITEM	UNIT COST	QUANTITY	TOTAL
CPXJ486-100	$1,245	1	$1,245
CPXB386-40S	745	1	745
HSDAS-16	1,695	1	1,695
SMUX64	920	1	920
DIO32F	595	2	1,190
AirLink 128 Modem	2,995	2	5,990
RS-422 Board	195	2	390
Case, Battery, Misc. Hardware (Hard-disc, keyboards, etc.)			1,000

7.0. SUMMARY AND CONCLUSIONS

The computer architecture of a multi-tasking, multi-processor, high speed telemetry system is discussed in this paper. This new telemetry system provides several advantages over the conventional ones. First, its multi-tasking design allows data acquisition and transmission to be executed in parallel. Thus the sampling rate of the system is significantly improved without an increase of cost. Second, the parallel processing allows the data collection process to be monitored on the remote computer in real time. Third, the amount of time the system can be used to sample data continuously is greatly improved without an increase of cost (see Equation 1). Fourth, the sampling rate is no longer limited by the speed of the RF modem since multiple RF modems can be used in parallel to transmit data in a multi-processor system. Last, it should be pointed out that the computer architecture of the proposed system is an open system. That is, although a two-processor system is used as an example in this paper, additional processors can be incorporated into this system to satisfy the further need of research, i.e., processors to process the data in real-time. A one-processor telemetry system has been implemented. It is capable of collecting 32 channels of differential signals at 1 kHz per channel (at a cost of $412 dollars per channel) and transmit the collected data to a

remote computer via an RF modem continuously. This system uses only 1 Kbyte of data buffer and no data overflow in the data buffer has occurred in a two hour test run in the laboratory.

ACKNOWLEDGMENT

The author wishes to extend his gratitude to the National Renewable Energy Laboratory (NREL) for the financial support of this study under Contract No. XAH-3-13203-02.

REFERENCES

ANALOGIC Corporation, PC-based Data Acquisition System, 1992.

Cyber Research, PC Systems Handbook, 10th edition, 1993.

Cyber Research, Half Size 486SX/33 With Flash/ROM Disk, User Manual, 1994.

Wiley, R., Intel DMA Controller, John Wiley & Sons, 1979.

Huang, K., Advanced Computer Architecture, McGraw-Hill,1994

Ilenkovic, M., Update Synchronization in Multiaccess System, UMI Research Press, 1979.

Lamport, L., "How to Make a Multiprocessor that Correctly Execut Multiprocessor Programs," IEEE Transaction on Computer, Vol. C-28, No.9, September, 1979.

McCoy, T.J., "Development of a High Performance Data Acquisition System," Proceedings of Windpower '92, Seattle, Washington, October, 1992.

National Instrument, AT-DIO-32F User Manual, 1993.

Simms, D.A., and Cousineau, K. L., "An Advanced Data-Acquisition System for Wind Energy Projects," Proceedings of Windpower '92, Seattle, Washington, October, 1992.

Wu, K.C., Swift, A.H., and Depauw, T.C., "Instrumentation and Control of the UTEP Teetered Rotor Test Bed Wind Turbine," SED-Vol. 15, Wind Energy - 1994, ASME, pp. 233-239.

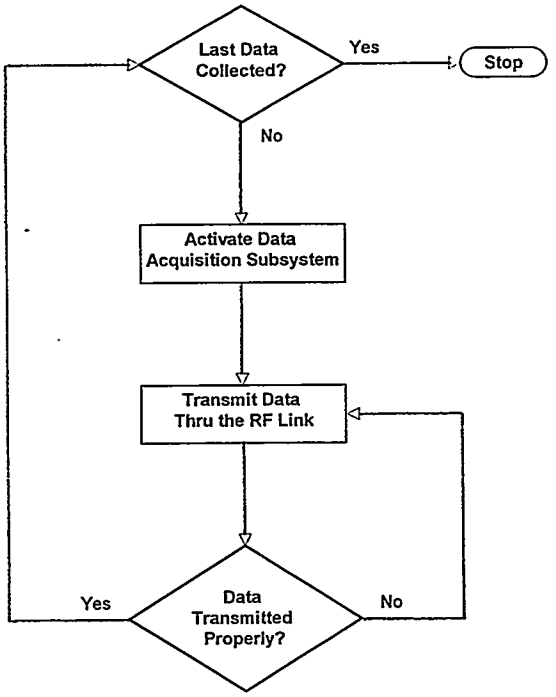

FIGURE 1. FLOW CHART ILLUSTRATING THE SEQUENTIAL PROGRAMMING TECHNIQUE ADOPTED IN THE CONVENTIONAL TELEMETRY SYSTEMS.

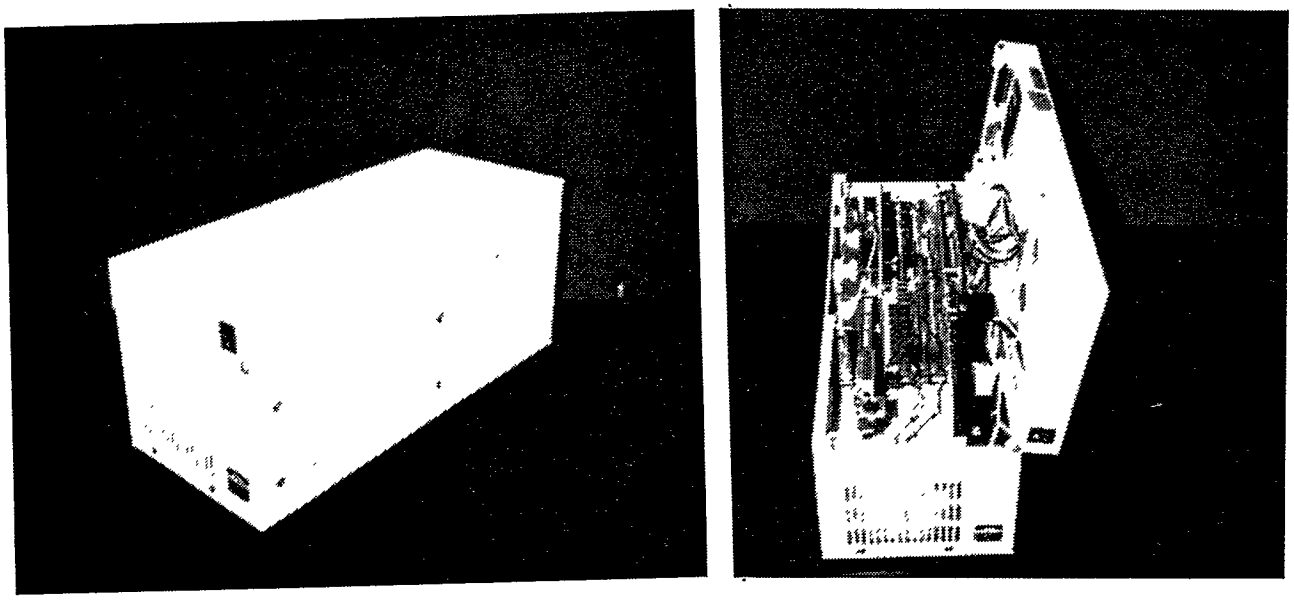

FIGURE 2. COMPUTER-1, THE HIGH SPEED MULTI-TASKING DAS SYSTEM WITH SKYLINK 128 RF MODEM.

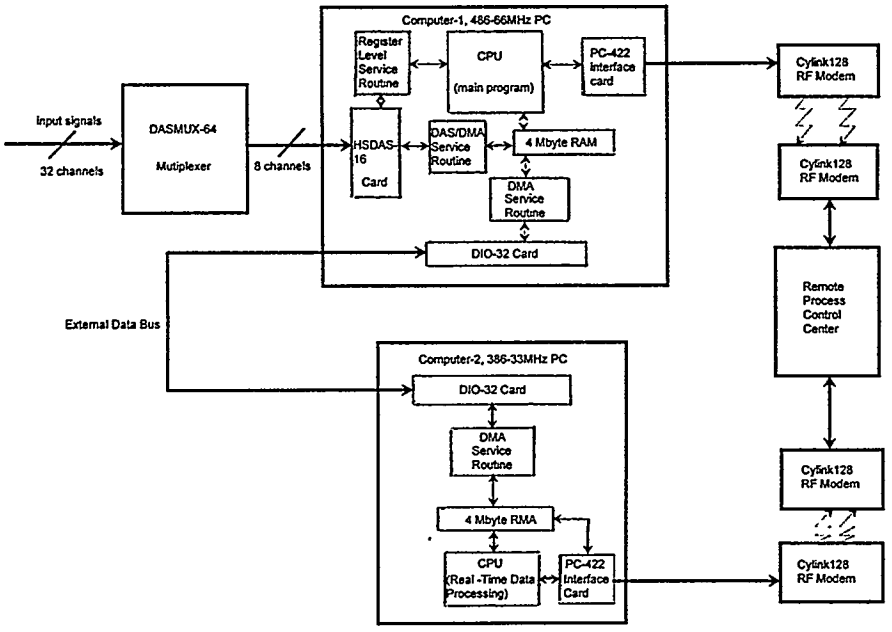

FIGURE 3. BLOCK DIAGRAM OF THE PROPOSED MULTI-PROCESSOR, MULTI-TASKING TELEMETRY SYSTEM.

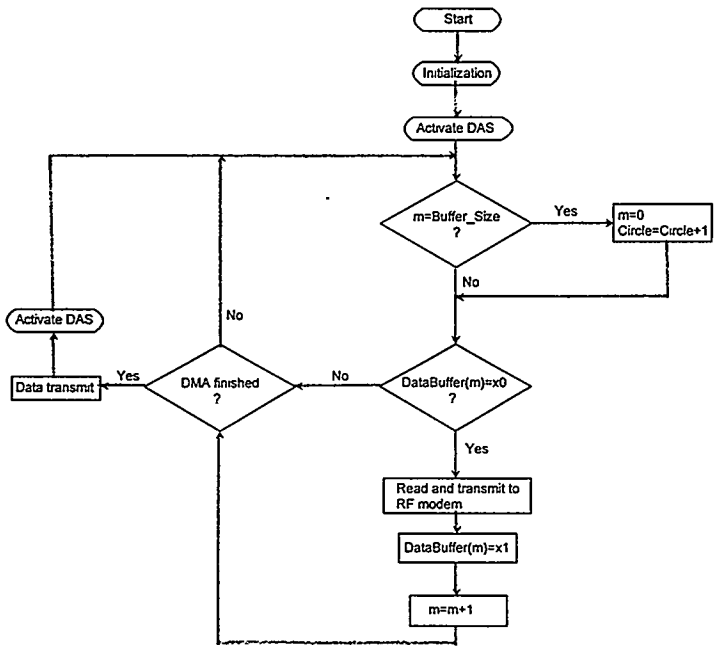

FIGURE 4. FLOW CHART OF THE DATA COLLECTION/TRANSMISSION PROGRAM.

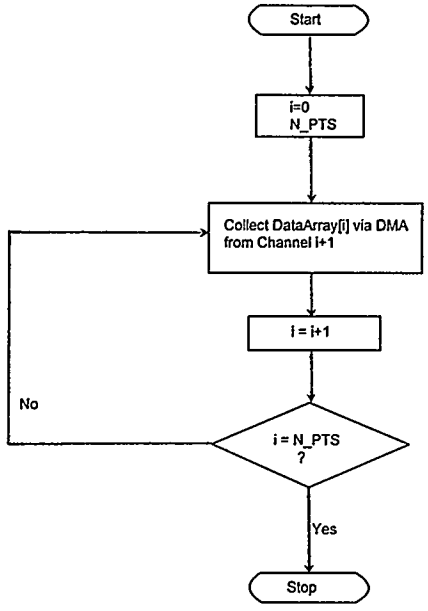

FIGURE 5. FLOW CHART OF THE DAS/DMA ROUTINE.

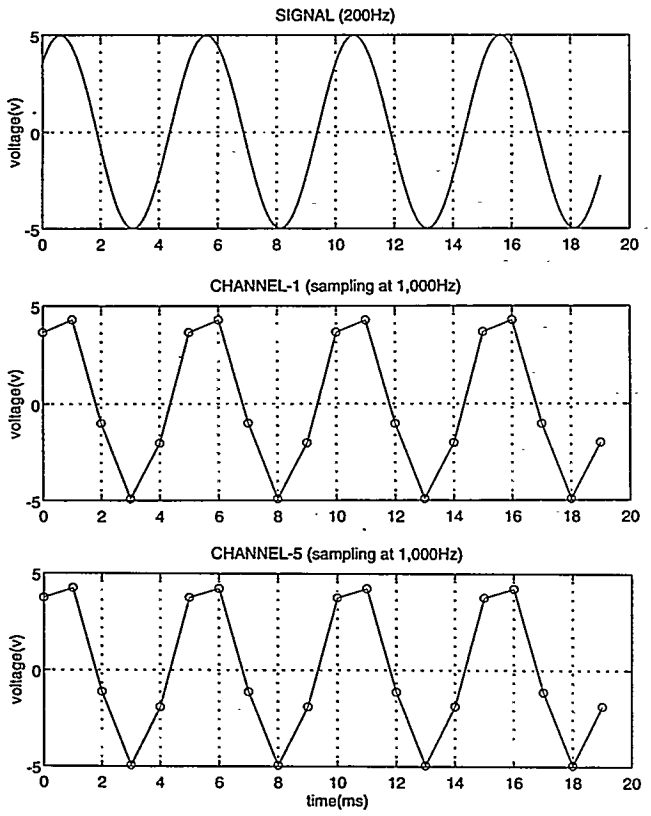

FIGURE 6. LAB TEST RESULTS OF THE TELEMETRY SYSTEM.

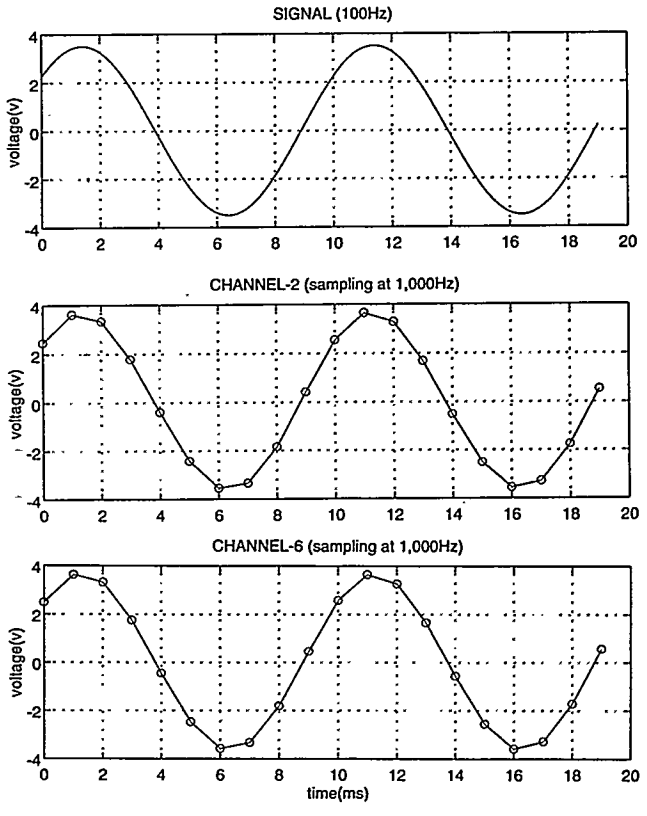

FIGURE 7. LAB TEST RESULTS OF THE TELEMETRY SYSTEM.

WIND SPEED POWER SPECTRUM ANALYSIS FOR BUSHLAND, TEXAS

Eric D. Eggleston, Engineer
USDA-Agricultural Research Service
Conservation and Production Research Laboratory
PO Drawer 10
Bushland, TX 79012

ABSTRACT

Numerous papers and publications on wind turbulence have referenced the wind speed spectrum presented by Isaac Van der Hoven in his article entitled *Power Spectrum of Horizontal Wind Speed Spectrum in the Frequency Range from 0.0007 to 900 Cycles per Hour* (Journal of Meteorology, Vol. 14, 1957, p. 160). Van der Hoven used data measured at different heights between 91 and 125 meters above the ground, and represented the high frequency end of the spectrum with data from the peak hour of hurricane Connie (13 August 1955). These facts suggest we should question the use of his power spectrum in the wind industry. During the USDA - Agricultural Research Service's investigation of wind/diesel system power storage, using the appropriate wind speed power spectrum became a significant issue. We developed a power spectrum from 13 years of hourly average data, 1 year of 5 minute average data, and 2 particularly gusty day's 1 second average data all collected at a height of 10 meters. While the general shape is similar to the Van der Hoven spectrum, few of his peaks were found in the Bushland spectrum. While higher average wind speeds tend to suggest higher amplitudes in the high frequency end of the spectrum, this is not always true. Also, the high frequency end of the spectrum is not accurately described by simple wind statistics such as standard deviation and turbulence intensity.

INTRODUCTION

How big are your wind gusts and how often can you count on one? Looking through the literature, one finds many different papers and books on wind power, wind/diesel storage, or wind turbulence that cite directly, or indirectly, a paper by Isaac Van der Hoven [1]. The Van der Hoven spectrum is reproduced in Figure 1.

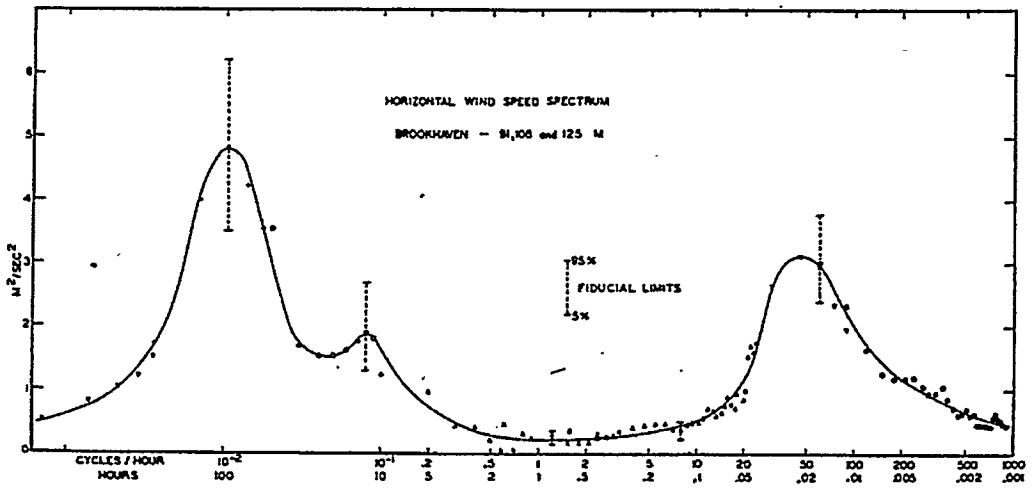

FIG. 1. Horizontal wind-speed spectrum at Brookhaven National Laboratory at about 100-m height. (See table 1 for date and time.)

Van der Hoven's spectrum suggests there is a substantial amount of wind energy that might be captured with storage capacities of about 6 minutes. This size would catch the 1 cycle/minute high frequency peak and it's skirts. The spectral gap suggests that storage capacities from 6 minutes to about 6 hours would not be very effective. Twelve hours to 5 days of storage could be very effective.

TABLE 1. Portions of horizontal wind-speed spectrum of fig. 1.

Height	Date and time	Reading average	Frequency range	No. of lags	Degrees of freedom*
108 m	6/25/55–4/30/56	5-day	0.0007–0.0042 cy/hr	6	19
108 m	8/9/55–2/25/56	1-day	0.0035–0.021 cy/hr	6	65
108 m	8/9/55–9/18/55	5-hr	0.01–0.1 cy/hr	10	38
108 m	0000, 8/20/55–0200, 8/22/55	½-hr	0.1–1.0 cy/hr	10	19
108 m	0000, 8/20/55–0200, 8/22/55	10-min	0.5–3.0 cy/hr	10	58
125 m	0730, 8/13/55–1400, 8/14/55	75-sec	0.8–24 cy/hr	30	96
91 m	0730, 8/13/55–0830, 8/13/55	20-sec	15–90 cy/hr	6	58
91 m	0730, 8/13/55–0830, 8/13/55	2-sec	30–900 cy/hr	30	118

* Number of unrestricted and independent variables entering into statistic. Tukey [8] has shown that spectrum estimates are distributed according to chi square divided by degrees of freedom, degrees of freedom being defined by $[2N - (3/2)m]/m$, where N is total number of observations and m is number of lags.

From the above table you can see that most of the high frequency peak of the Van der Hoven spectrum is backed by one hour of data. Also, measurement heights varied from 91 to 125 meters above the ground at the Brookhaven National Laboratory. In addition, Van der Hoven did not have the benefit of modern computational power in 1956. Still, his paper must have been remarkable at the time.

Van der Hoven recognized limitations of his results in the following two paragraphs quoted from his paper:

> "An anomalous wind situation was purposely chosen to represent the high-frequency end of the spectrum shown in fig. 1. The data were taken during hurricane Connie, with winds averaging 13 m/sec during a 30-hr interval and averaging 20 m/sec during the peak hour (0730 to 0830 EST 13 August 1955) of the hurricane. The effect of the high wind speeds was to increase greatly the

amplitude of the high-frequency end of the spectrum. More normal situations, such as the 14 horizontal wind-speed spectra shown by Van der Hoven and Panofsky [2], seldom show a spectral amplitude above 1.0 m^2/sec^2 and none above 2.0 m^2/sec^2. Fig. 1 shows a peak amplitude of 3.1 m^2/sec^2 in this range.

If fig. 1 can be considered representative, the spectrum of horizontal wind speed seems to have two eddy-energy peaks, one at a period of 4 days and the other at a period of 1 min. with a spectral gap at a period of 1 hr. Very little energy is thought to be present outside the range shown in fig. 1. A measurement of the area under the spectral curve shows 60 per cent of the total variance at frequencies of less than 1 cy/hr, and 40 per cent at frequencies greater than 1 cy/hr. However, the relatively large percentage found at higher frequencies is peculiar to a very windy day."

Its possible that the Van der Hoven spectrum has limited application to the wind power industry. It certainly is not applicable to all wind sites or measurement heights.

ANALYSIS

Because of the implications for wind power storage, I wanted to know the wind speed spectrum for my Bushland, Texas site, 10 meters above the ground. Using GPP (a general purpose postprocessor available from the National Renewable Energy Laboratory) I processed 10 meter height Bushland data: hourly average from 1983 through 1995, five years of 5 minute average data, and five months of 1 Hz average data.

The 1 Hz average data was collected using a Teledyne Geotech anemometer with a distance constant of 1.5 meters and an accuracy of ±1%. Due to the huge size of 1 Hz data, it was collected in files of about 2 days each before reduction. Raw data was converted to two column files: time (hrs) and wind speed (m/s). Then, I imported it to GPP and computed the wind speed average, standard deviation, turbulence intensity (standard deviation/wind speed average), and power spectral density (PSD) for each file. Since the output units of each PSD were $(m^2/sec^2)/(cycle/hr)$, all the spectral estimates were multiplied by their frequency; yielding just m^2/sec^2 for each estimate. Portion of the output frequencies from the high and low end were discarded to eliminate problems of resolution and aliasing.

BUSHLAND RESULTS

Figure 2 shows the Bushland, TX spectrum of wind speed with roughly the same scales as Van der Hoven. It comes from 13 years of hourly average data, one year of 5 minute average data, and one file (about 2 days) of 1 Hz average data all measured in meters per second. In fact, the file chosen to represent the high frequency end of the Bushland spectrum (s10696) had the highest amplitude of any 1 Hz data file yet recorded at Bushland. Data from "average" wind files are much flatter and less interesting.

The large fundamental spike is on a period of once per 24 hours -- the daily spike. It is interesting that the lessor spikes of higher frequencies are harmonics of the daily spike: once per 12 hours, once per 8 hours, once per 6 hours, etc. In all, there are about 7 noticeable harmonics of the daily spike. Its possible the harmonics are artifacts of the daily spike due to data processing with no actual physical meaning. The Bushland spectrum confirms Van der Hoven's spectral gap centered around a period of once per hour. His high frequency peak was found, but

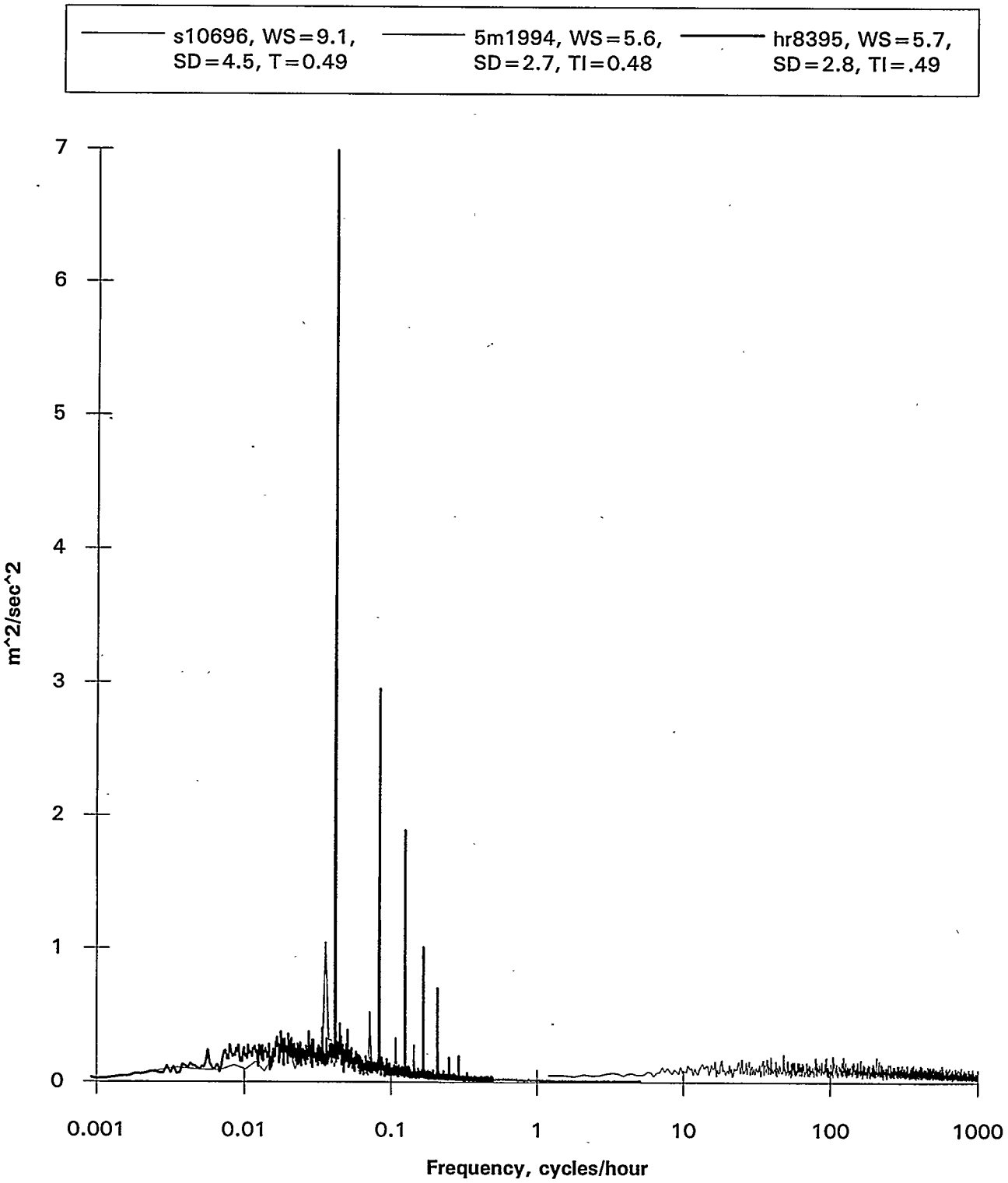

Figure 2: BUSHLAND WIND SPEED SPECTRUM

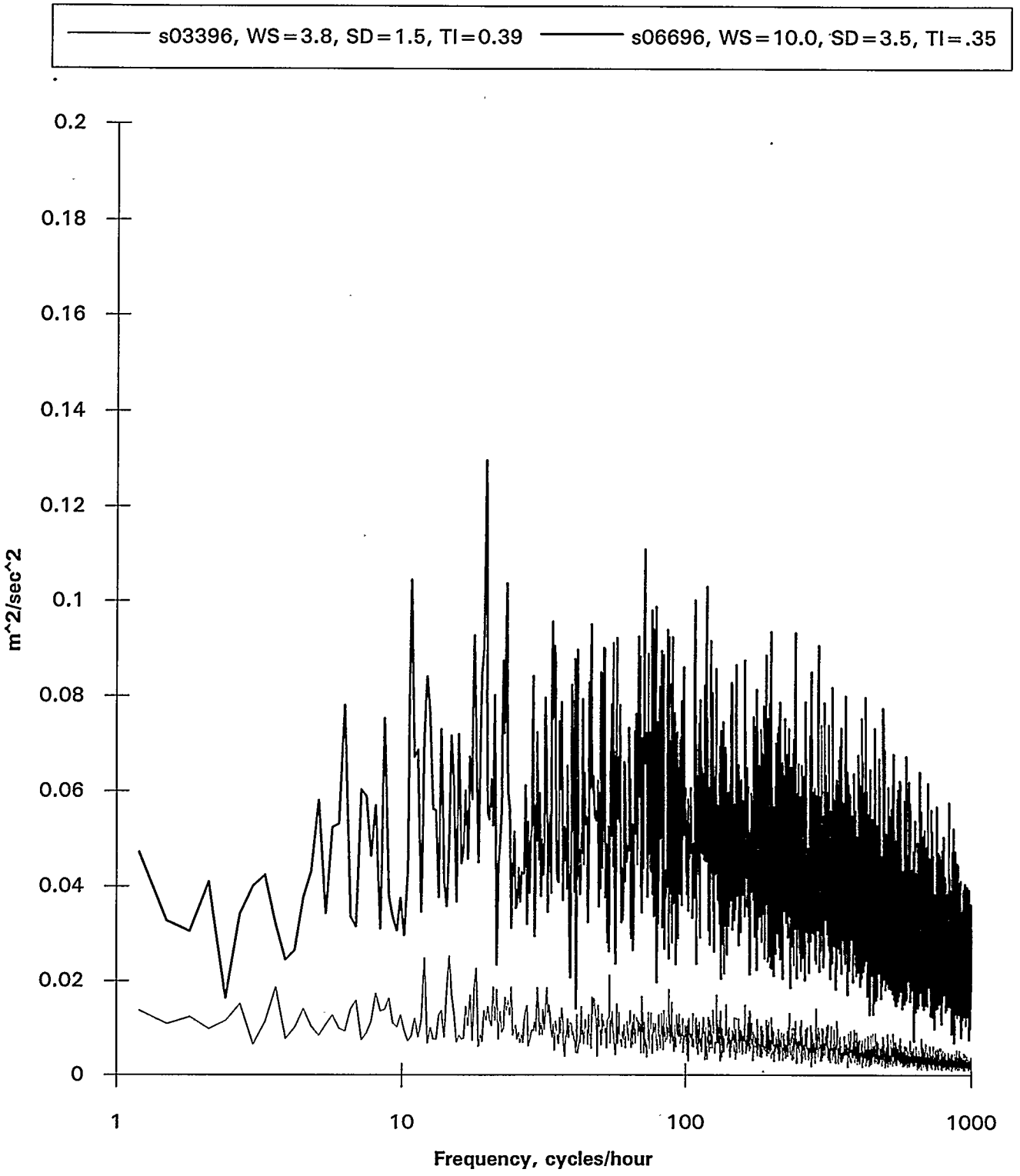

Figure 3: LOW AND HIGH WIND BUSHLAND HIGH FREQUENCY SPECTRUM

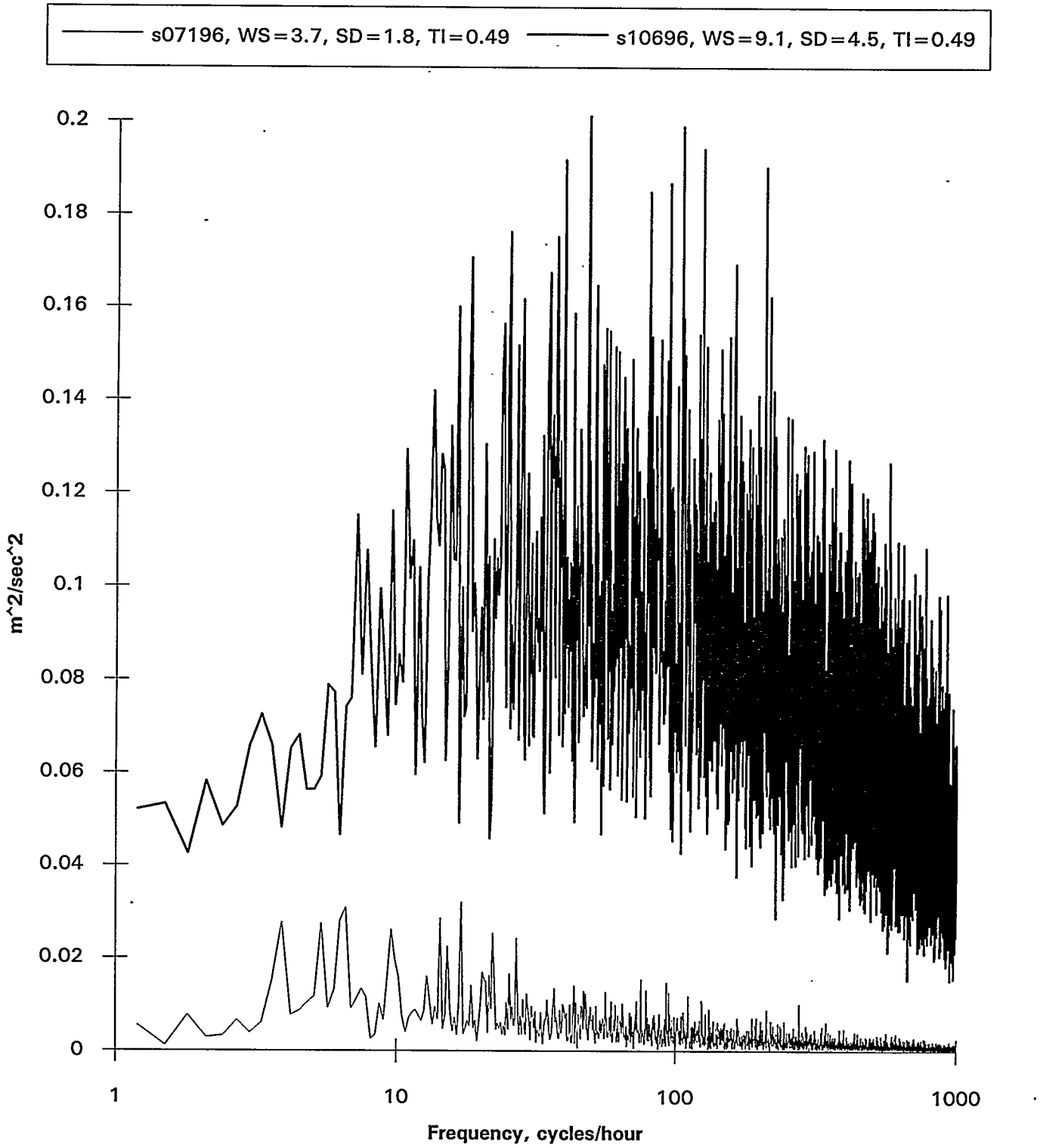

Figure 4: FILES WITH EQUAL TURBULENCE INTENSITY

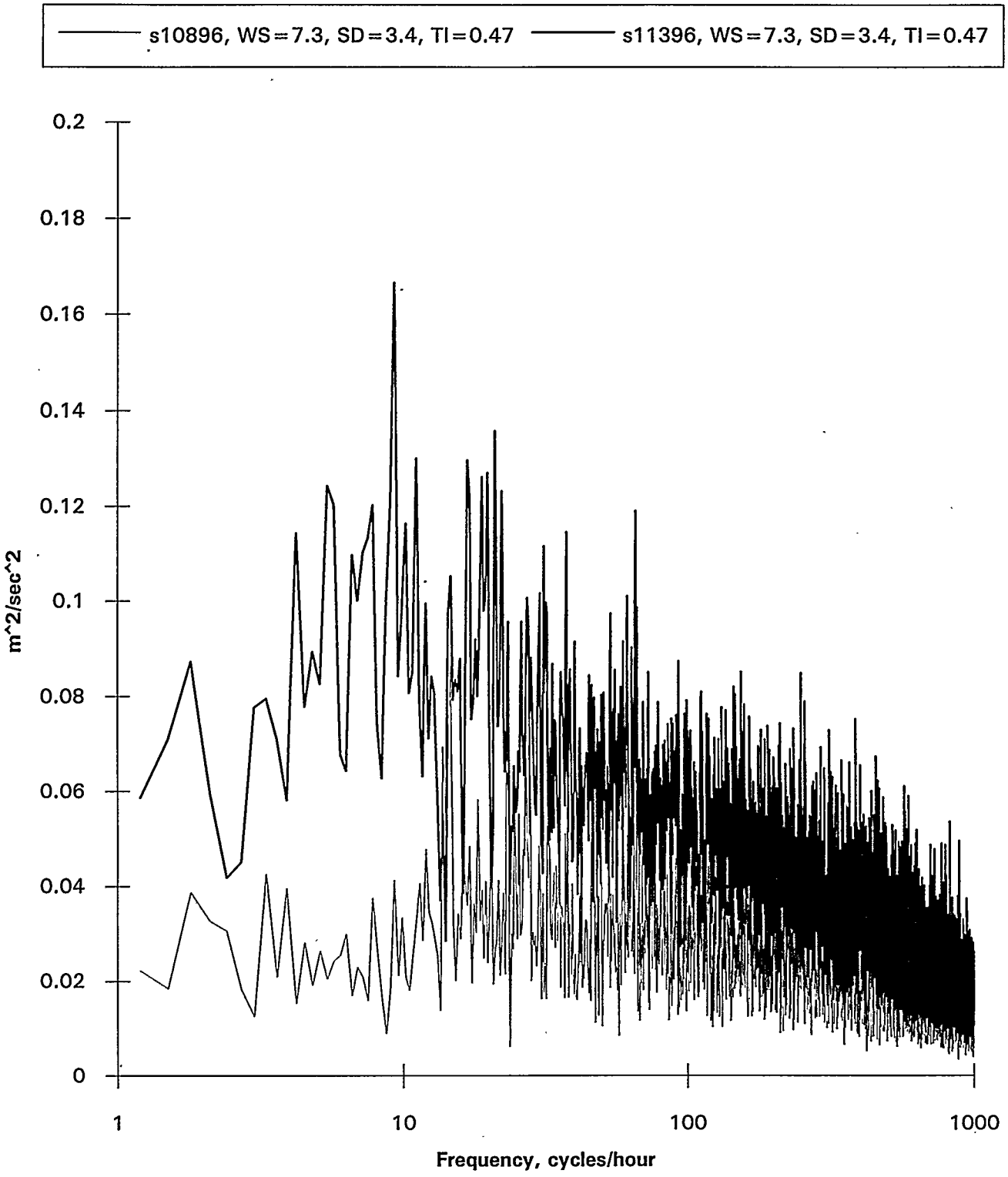

Figure 5: FILES WITH SAME WS, SD, & TI

no where near the amplitude he reported from his site. Van der Hoven's once per four day peak was absent. Yet, there is a very strong daily peak in Bushland wind speeds. The Bushland spectrum suggests that high frequency Bushland gusts do not come in particular frequencies and may not contain large amounts of energy. They are also peculiar to windy days and are largely absent the rest of the time.

All of the power spectral densities were performed by GPP on Bushland data used band smoothing. Van der Hoven used a three point form of band smoothing on his data. GPP uses a six point form of band smoothing. The number of frequencies output can be chosen using this feature of GPP, which proved very convenient in reducing the output from one file from 12.5 megabytes to about 200 kilobytes -- choosing only 6,000 output frequencies. Processing the same data presented in Figure 2, using a cosine "Hamming" window did not change the shape of the spectrum -- just the amplitude of the peaks. The daily peak shot up from about 7 m^2/sec^2 to about 182 m^2/sec^2, and the harmonics were in the same proportion. The high frequency peak also increased to about .5 m^2/sec^2 -- still pretty low when compared to the Van der Hoven spectrum.

Figure 3 shows two 1 Hz files of low and high average wind speeds. The higher wind speed file has much more energy in it's gusts than the low wind speed file. Examination of many high frequency spectra from different files, shows that the amplitude of the high frequency end of the spectrum tends to increase with the wind speed average. Given files with similar average wind speeds, the one with the higher standard deviation tends to have larger amplitude in the high frequency end of the spectrum. While these tendencies are often true, they are not always true.

Figure 4 shows two 1 Hz files with exactly the same turbulence intensity, and one is much higher that the other. Turbulence intensity alone, will not show which file has higher amplitude in the high frequency end of the spectrum. In addition, Figure 5 shows another two 1 Hz files with the exact same wind speed average, standard deviation, and turbulence intensity -- their spectrums are quite different. Both figures suggest that simple wind statistics do not accurately describe the spectrum of wind gusts encountered or the energy they may contain.

CONCLUSION

The Van der Hoven spectrum from 1957 is of little use to the wind turbine industry because it was measured too high above the ground and at different elevations, was of low resolution, and represented the high frequency end of the spectrum with unusually gusty high wind data. It is not applicable to all wind farm sites or height above the ground. The Bushland spectrum confirms some of the shape found by Van der Hoven, but few of his peaks. Bushland shows a very pronounced daily peak in wind speed. While higher average wind speeds tend to suggest higher amplitudes in the high frequency end of the spectrum, the high frequency end of the spectrum is not accurately described by simple wind statistics such as standard deviation and turbulence intensity.

ACKNOWLEDGMENTS

I wish to express my appreciation to the US Department of Energy and the US Department of Agriculture - Agricultural Research Service that fund my research and to Dr. Nolan Clark for choosing me for the job. I wish to thank my colleague, Ron Davis, for providing years of data and helping collect more. Without the assistance of Marshall Buhl of the National Renewable

Energy Laboratory by providing a special version of the GPP program, the large 1 Hz average wind data files would have remained just data -- with no results.

REFERENCES

1. Van der Hoven, I. 1957, *Power Spectrum of Horizontal Wind Speed Spectrum in the Frequency Range from 0.0007 to 900 Cycles per Hour*, Journal of Meteorology, Vol. 14, April, 1957, p. 160).

2. Van der Hoven, I. and Panofsky, H. A., 1954: *Statistical properties of the vertical flux and kinetic energy at 100 m.* [Final report, Contract # AF19(604)-166], University Park, Pennsylvania State University, p. 55.

Update of Wind Resource Assessment Activities at NREL

Dennis L. Elliott and Marc N. Schwartz
National Renewable Energy Laboratory
1617 Cole Boulevard
Golden, Colorado 80401
United States

ABSTRACT

The goal of the wind resource assessment activity at the National Renewable Energy Laboratory (NREL) is to improve the characterization of the wind resource for regions where there are market opportunities for U.S. wind energy technology. A variety of wind resource assessment activities have recently been undertaken at NREL in support of this effort.

The major tasks during the past year include aiding the establishment of new wind measurement programs in the United States, the development of updated comprehensive meteorological and geographical data bases to be used for resource assessments in the United States and abroad, and designing progressive wind resource mapping tools to facilitate products used in support of emerging markets.

BACKGROUND

The wind resource assessment activity has been an integral part of the U.S. Department of Energy (DOE) Wind Energy Program for approximately twenty years. The activity was located at Pacific Northwest Laboratory in Richland, Washington until 1994 when it was transferred to NREL. The activity's location at the National Wind Technology Center promotes direct interactions between the resource assessment staff and personnel involved with wind energy projects such as wind-hybrid system design, wind turbine design, certification and standards, and utility integration.

The wind resource activity is led by key personnel who have extensive experience in wind resource assessment activities over the past 20 years. The staff also has conducted research in other aspects of wind characterization including wake characterization, array losses, turbulence characterization, and wind forecasting. At present, the expertise of the group is primarily in meteorology, wind climatology, computer mapping using Geographic Information System (GIS), software development using FORTRAN and C programming, and management of large data bases. The computer equipment used for wind resource assessment activities include personal computers and advanced UNIX- based operating systems on Sun Workstations.

NREL's wind resource assessment tasks are also ably supported by expert private consultants and subcontractors. Areas of support include wind monitoring station installation and operation, analysis of wind and other meteorological data, wind resource assessment training and presentation, and technical assistance in support of utility/industry requests.

NEW MEASUREMENT PROGRAMS

During the past year, DOE, through NREL, initiated three new cost-shared U.S. wind measurement programs. These programs are the Utility Wind Resource Assessment Program (U*WRAP), the Sustainable Technology Energy Partnerships (STEP), and the Cooperative Networks for Renewable Resource Measurements (CONFRRM). The goal of these programs is to accelerate multi-regional U.S. market penetration of wind systems and to move the United States towards being the world leader in the development and use of advanced wind turbine technology. The programs are designed to form partnerships with diverse types of organizations including state and tribal energy offices, private and public utilities, universities, research institutions, the financial community, and private consultants that wish to help accelerate the commercial development of wind energy.

Most of the previous assessments of wind energy resources in the United States have been accomplished by the use of existing meteorological data from National Weather Service (NWS) stations located at airports. Though the data are useful in characterizing the wind resource over broad areas as illustrated in the *Wind Energy Resource Atlas of the United States* (Elliott et al. 1987), the wind energy community has special measurement needs that the NWS stations were not designed to meet. There have been special programs designed for wind energy resource evaluation in the past such as the DOE Candidate Wind Turbine Site program (Sandusky et al. 1983) but much more of that type of valuable data are needed. These programs are designed to provide long-term data bases that meet the needs of the wind energy community by providing minimum standards for equipment specifications and data quality control. In addition to contributing to wind resource assessment, these data bases will also be useful for wind characterization projects such as climatological adjustment and wind forecasting. A brief description of the three measurement programs and their progress follows.

U*WRAP is a program designed to technically and financially support private and public utilities conducting wind resource assessments. This program will increase the quantity of wind data available to utilities, and enlarge the qualified workforce that can conduct a skilled resource assessment program. The development of U*WRAP has been a collaborative process among several organizations: DOE, the Edison Electric Institute, the Electric Power Research Institute, and the American Public Power Association. U*WRAP is administered by The Utility Wind Interest Group, Incorporated (UWIG). UWIG is a non-profit corporation with a mission to accelerate the appropriate integration of wind power for utility applications through the coordinated efforts and actions of its member utilities in collaboration with wind industry stakeholders. The results from the U*WRAP program will give utilities the means to assess their wind resources and wind electric potential, identify candidate development areas, target the most compatible wind turbine designs, and assess the economics of wind-based generation. Six utilities were chosen in 1995 to participate in U*WRAP with a total of 34 new wind measurement stations to be established in 1995 and 1996. The data collected by the utilities under this program will be proprietary for 5 years after the start of the measurements because the utilities are cost-sharing one-half of the cost of U*WRAP.

STEP seeks to meet the needs of states, industry, and localities in accelerating the commercialization of renewable energy technologies. DOE and NREL work directly with state, territorial, and tribal energy offices to foster research, boost economic development, create jobs, and advance working partnerships between the government and the private sector. One of the areas of interest of the STEP program is wind resource assessment. The STEP program actively supports the establishment of new measurement stations in areas being considered for wind plants and analysis of existing wind data using GIS techniques leading to detailed areal resource characterization. At present, six states are participating in Phase 1 of this program.

CONFRRM is designed to improve the assessment of solar and wind energy resources in the United States. CONFRRM supports the establishment of long-term wind benchmark stations at locations with high wind

energy potential. The benchmark stations are located at sites that are representative of areas where wind technology applications are feasible. There are no restrictions on the type of organizations that are responsible for the operation and maintenance of the benchmark stations. The data collected from the stations will be in the public domain and will be made available through NREL's Renewable Resource Data Center. Twelve wind benchmark stations will be established in 1996.

Figure 1 shows the distribution of the twelve individual states that presently have projects under these three programs. The states are concentrated in the Great Plains and Rocky Mountains, the region with the highest overall wind resource in the United States, but other sections of the country, such as the Northeast and the Great Lakes states, with promising wind resource are also represented. Additional states are likely to be funded in the near future. The three cost-shared programs should significantly increase detailed wind resource assessments and accelerate the commercialization of wind energy in the United States.

NREL also provides technical assistance to wind resource assessment programs run by non-federal agencies such as state and tribal offices and utilities. The assistance, based on past NREL experience, can include reviewing the station siting approach and procedures, offering historical perspectives on wind resource assessment activity in a region, and offering advise on enhancing wind measurement programs.

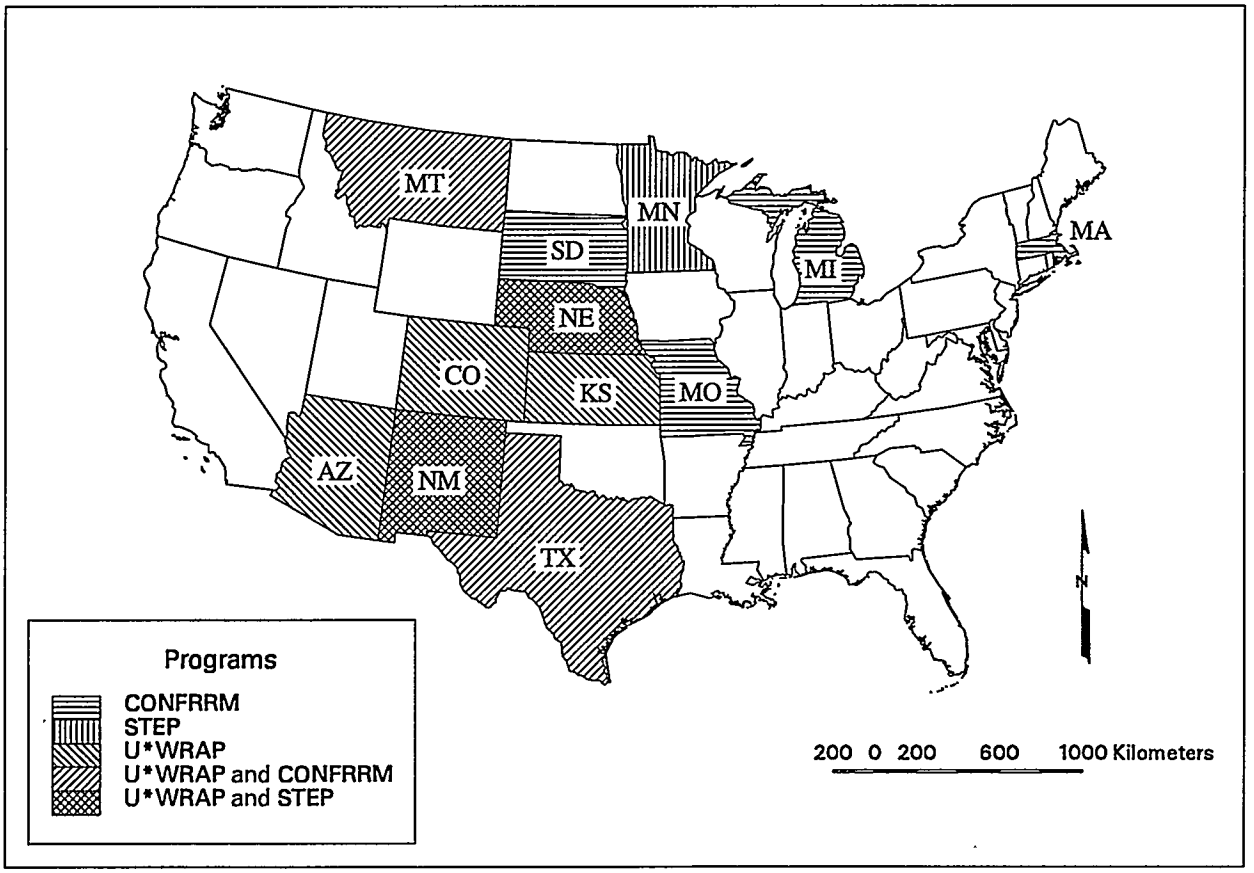

FIGURE 1: MAP OF STATES HAVING PROJECTS UNDER DOE WIND MEASUREMENT PROGRAMS

METEOROLOGICAL and GEOGRAPHICAL DATA BASES

A key component of the wind resource activity at NREL is the development of updated comprehensive global data bases to be used in resource assessments in the United States and abroad. These data bases contain the meteorological and geographical information that are the building blocks for sophisticated wind resource mapping projects.

NREL has data from a variety of meteorological and topographical data sets. These data are necessary both to produce and use the most sophisticated techniques of estimating the wind resource. The principal meteorological data sets at NREL are a global surface Climatic Database, the global upper-air (weather balloon) wind data, and the marine wind data from ship observations. These data sets were used in the Mexico wind resource assessment project (Schwartz and Elliott, 1995). These data are supplemented by surface data from new measurement programs undertaken in areas shown by NREL's original wind maps to have good-to-excellent wind resource. The major type of geographical data used in our assessments are digital elevation data. For U.S. resource assessment activities, NREL has access to the data set produced by the U.S. Geological Survey. For international assessment efforts, the data set used most frequently is the Digital Chart of the World. The elevation data are especially important in the production of advanced wind mapping tools.

NREL has continued to seek and purchase the most useful new types of data sets to supplement and/or supplant existing ones. During the past year, NREL has purchased several data sets that promise to enhance future wind resource assessment work. The most promising of these is a data set of 10-meter ocean winds derived from polar orbiting satellite measurements. The data cover the period from 1987-1994. The ocean wind speeds are derived from the reflectivity of the ocean surface as measured by sensors on the satellite. The satellite ocean wind speed data set's advantage over the historical ship data is the much more even coverage. The historical ship data was concentrated in the primary shipping lanes. Thus, ocean areas outside the shipping lanes frequently had a minimal amount of data, which increased the difficulty of accurately estimating the wind resource at offshore and coastal sites in those regions. NREL is currently comparing satellite ocean wind data to ship data from data-rich regions. Preliminary results show a good match in the wind speed patterns between the ship and satellite data, with the satellite data proving more detailed resolution of these patterns. An example of satellite ocean wind data is shown in Figure 2. Other data sets recently obtained by NREL include global vegetation index data that can eventually be used for delineation of land cover, more detailed elevation data for several areas of the world, and pre-1970 surface observations for locations in the United States and regions abroad. NREL is also currently exploring whether it is possible to obtain gridded average surface temperature data.

The rapidly changing and expanding market opportunities demand that any quality wind resource mapping project be accomplished as quickly as possible. In-depth analyses of the meteorological data, necessary for the production of the wind map, require that raw data from the comprehensive data sets be transformed into a visual form that can be easily examined. Therefore, the development of an efficient method of processing and archiving the extensive data sets is one of the wind resource assessment group's major tasks. Several advanced processing and archiving tools have been developed in the past few months. Software was written to rapidly process twenty-plus years of raw weather balloon upper-air data into summarized graphical and tabular output. The time to process the raw data for a particular upper-air station or group of stations was previously measured in days. Now, data can be processed and usable output can be produced in a matter of minutes. The evolution of a similar type of tool for the global surface data is underway. This is a challenging venture because of the volume of raw data (250 GB) in the global data set and the need to address issues such as the changing locations and identification numbers of many surface stations. The completion of this task in the near future will improve the accessibility of the processed surface data and accelerate the process of producing the wind maps. The work to integrate the newer data sets into the NREL data base is on-going and will continue to be emphasized in the future.

DEVELOPMENT OF WIND MAPPING TOOLS

One of the chief goals of the wind resource group at NREL is to help the U.S. wind energy industry accelerate the deployment of wind energy by producing the most progressive and sophisticated wind maps possible. A necessary component of the production of these maps is the development of progressive wind resource mapping tools.

Advanced analysis techniques using information from the updated NREL data sets are quite important in more accurately assessing the quantity of the wind resource in a particular area (whether it is for utility or rural power applications). A key task is to evolve a conceptual model that explains what causes the wind to blow in a certain region. The scale of the meteorological factors that cause the wind flow can vary from several hundred kilometers (storm-scale) to only a few kilometers when local circulations (eg. sea-land breeze, mountain-valley circulation) predominate. The availability of a variety of meteorological data sources at NREL makes the process of conceptualizing wind patterns in most regions of the world easier. Many regional wind patterns can now quickly undergo three dimensional analysis because of the wide variety of data sources. The diversity of the wind data sources also enables poor quality or suspect data from one data set to be checked and screened against data from other sources. A more rigorous and improved wind resource analysis is now applied as one of the major inputs to the wind resource maps.

The most ambitious plan at NREL for wind resource mapping is to eventually automate the entire wind mapping process. This will be accomplished using a GIS system to create computerized wind maps. The wind resource estimates from advanced analysis techniques will be combined with digital elevation models (DEM) created by GIS software to produce wind maps showing good-to-excellent resource areas as determined by the various algorithms in the software. The computer mapping system developed by NREL uses an analytic approach and is designed to portray the distribution of wind resource over a large area. The computerized mapping technique greatly reduces the effort needed to create a wind map as compared to the old style manual analysis that had characterized wind mapping in the 1980s and early 1990s. This is especially true in areas of complex terrain. Under the old style of manual analysis, the distribution of the wind resource had to be physically drawn in for topographic features such as ridge crests and elevated plateaus. Naturally, this process was time consuming, subjective, and prone to inconsistencies in the analysis. Utilizing computer mapping techniques considerably reduces the time it takes to produce a wind resource map in complex terrain. The analysis of the distribution of the wind resource is also treated consistently throughout the region of interest.

A prototype of NREL's computer generated wind resource maps is presented in Figure 3. Figure 3 is a resource map of Nan'ao Island, a small island a few kilometers off the southeast coast of China. This map was developed as part of a special wind resource assessment project that NREL participated in at the request of the World Bank. This island, for several reasons, proved to be the ideal subject for the first effort at producing computerized wind maps. First, NREL had access to detailed terrain data on the island, which made the production of an accurate DEM quite straightforward. Second, the small size of the island, plus access to sufficient meteorological data from the island and the nearby mainland, enabled the analysis of the wind resource to be integrated with the terrain data in a few steps. NREL has received favorable comments about the realism of the mapped distribution of the wind resource from people familiar with wind energy development on Nan'ao Island.

Another computer wind resource map has been produced for the island of Sumba in southeastern Indonesia. The process of producing a computerized wind resource map of Sumba was more complex than Nan'ao Island. This island is considerably larger with more varied terrain than Nan'ao Island, and there is not as much available wind data in the surrounding region. The time needed to produce the Sumba map was substantially longer than the Nan'ao map because of a more difficult analysis of the wind regime and additional steps in integrating the wind and terrain data in the computer model. The prototype Sumba map can be used to identify

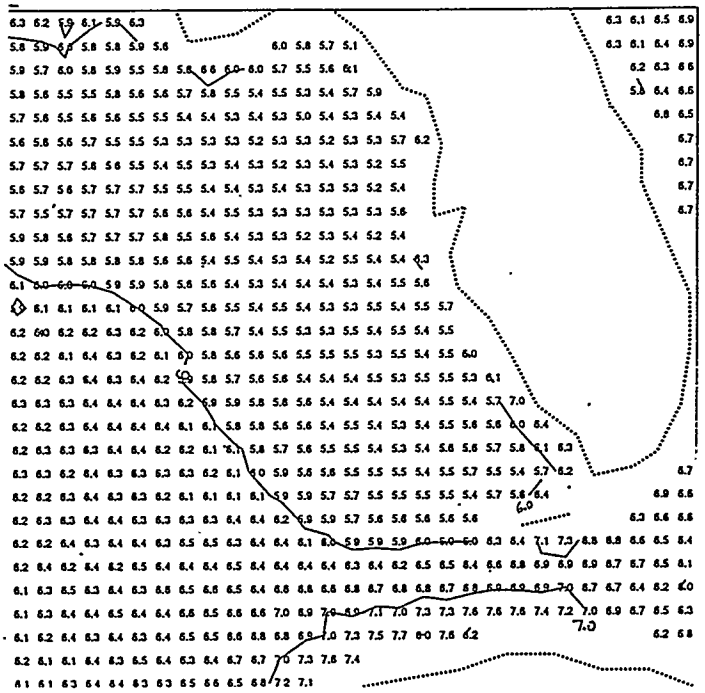

FIGURE 2: 1993 ANNUAL AVERAGE OF SATELLITE DERIVED 10 M WIND SPEEDS (M/S) FOR EASTERN GULF OF MEXICO

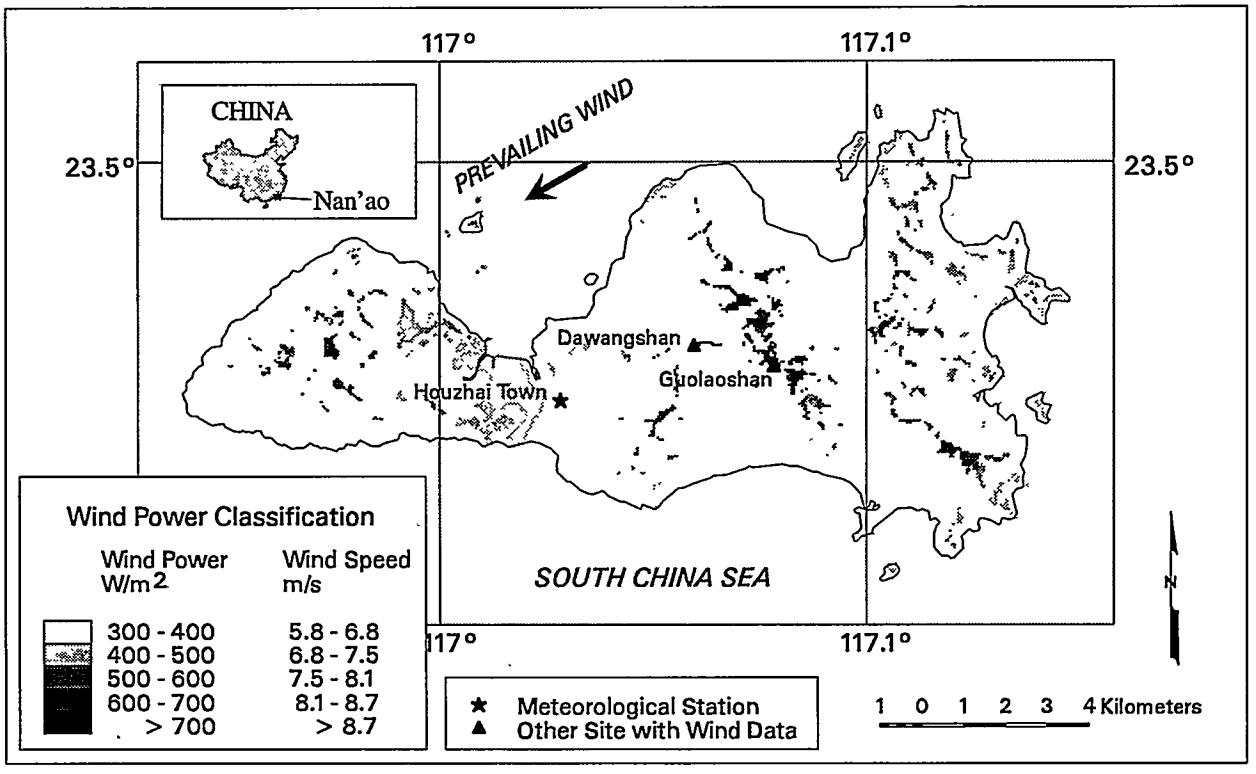

FIGURE 3: COMPUTERIZED WIND RESOURCE MAP OF NAN'AO ISLAND, CHINA

and target sites for wind measurements that ultimately will accelerate wind energy development on that island.

Nan'ao Island and Sumba represent, both from a meteorological and topographic point of view, relatively simple regions to map via computer techniques. Other regions in the United States and abroad present more complex wind flow regimes and topography. Additional routines to account for these complexities will be added to the computer mapping system in the future. Another activity that NREL plans on performing is verification and sensitivity research on the results of the computer mapping. This will enable the mapping system to be modified and result in more accurate wind resource maps. The advanced computerized technique will be applied as part of current or planned wind mapping projects in several areas of the world in support of U.S. wind energy interests. These include specific regions of Mexico, Chile, Argentina, China, and Indonesia.

CONCLUSION

The wind resource assessment group at NREL is involved in a variety of activities designed to accelerate the deployment of wind energy by boosting knowledge of the wind resource. NREL will continue to work with the U.S. industry, and state and other governmental organizations to improve the wind characterization in the United States and develop the comprehensive data bases and advanced wind mapping techniques that will ensure NREL's standing as leader in wind resource assessment.

ACKNOWLEDGMENTS

We would like to thank George Scott and Ray George for their software and data processing development, and Steve Haymes for his work on creating the GIS mapping system. This paper was written at the National Renewable Energy Laboratory in support of the U.S. Department of Energy under contract number DE-AC36-83CH10093.

REFERENCES

Elliott, D.L.; Holladay, C.G.; Barchet, W.R.; Foote H.P.; Sandusky, W.F. (1987). *Wind Energy Resource Atlas of the United States*. DOE/CH 10093-4, Golden, Colorado: Solar Energy Research Institute.

Sandusky, W.F.; Renne, D.S.; Hadley, D.L. (1982). *Candidate Wind Turbine Generator Site Summarized Meteorological Data for the Period December 1976 Through December 1981*. PNL-4407, Richland, Washington: Pacific Northwest Laboratory.

Schwartz, M.N.; Elliott, D.L. (1995). *Mexico Wind Resource Assessment Project*. Prepared for Windpower '95, NREL/TP-441-7809, Golden, Colorado: National Renewable Energy Laboratory.

TRAILING EDGE DEVICES TO IMPROVE PERFORMANCE AND INCREASE LIFETIME OF WIND-ELECTRIC WATER PUMPING SYSTEMS

By Brian D. Vick and R. Nolan Clark
USDA-Agricultural Research Service
Conservation and Production Research Laboratory
P.O. Drawer 10
Bushland, Texas 79012

ABSTRACT

Trailing edge flaps were applied to the blades of a 10 kW wind turbine used for water pumping to try to improve the performance and decrease the structural fatigue on the wind turbine. Most small wind turbines (10 kW and below) use furling (rotor turns out of wind similar to a mechanical windmill) to protect the wind turbine from overspeed during high winds. Some small wind turbines, however, do not furl soon enough to keep the wind turbine from being offline part of the time in moderately high wind speeds (10 - 16 m/s). As a result, the load is disconnected and no water is pumped at moderately high wind speeds. When the turbine is offline, the frequency increases rapidly often causing excessive vibration of the wind turbine and tower components. The furling wind speed could possibly be decreased by increasing the offset between the tower centerline and the rotor centerline, but would be a major and potentially expensive retrofit. Trailing edge flaps (TEF) were used as a quick inexpensive method to try to reduce the furling wind speed and increase the on time by reducing the rotor RPM. One TEF configuration improved the water pumping performance at moderately high wind speeds, but degraded the pumping performance at low wind speeds which resulted in little change in daily water volume. The other TEF configuration differed very little from the no flap configuration. Both TEF configurations however, reduced the rotor RPM in high wind conditions. The TEF, did not reduce the rotor RPM by lowering the furling wind speed as hoped, but apparently did so by increasing the drag which also reduced the volume of water pumped at the lower wind speeds.

INTRODUCTION

A clean water supply continues to be an illusive goal for people and livestock throughout the world. In much of the third world, a grid connected supply of electricity is not available or economically feasible, so stand-alone renewable energy powered water pumping systems are sometimes the only option. Throughout the world many farmers and ranchers are still reliant on mechanical windmills to provide water for their livestock and domestic use. Many of these mechanical windmills are 50 to 60 years old and maintaining this aging equipment is becoming costly. For the above mentioned needs, wind-electric water pumping systems appear to be the best choice for areas with a good wind resource (Clark and Mulh, 1992 and Vick and Clark, 1996).

At the USDA Conservation and Production Research Laboratory, Bushland, Texas, stand-alone wind-electric water pumping systems have been researched and tested since 1988. For the past few years, research and testing has concentrated on improving the overall performance of the wind-electric water pumping system. Ways to improve the controller performance (Vick and Clark, 1995) and selection of the proper pump (Clark and Vick, 1994) were presented in earlier work. Selection of the proper motor for different wind-electric systems was also investigated by Clark and Vick, 1995. In that paper, considerable off time was discovered in moderately high wind speeds (10 - 16 m/s) on the Bergey[1] Excel-PD (10 kW) wind-electric water pumping system.

[1] The mention of trade or manufacture names is made for information only and does not imply an endorsement, recommendation, or exclusion by USDA - Agricultural Research Service.

In contrast, the Bergey 1500 (1.5 kW) is almost always online in the wind speed range of 10 - 16 m/s because it starts furling at a wind speed of 13.5 m/s (unloaded) when it reaches the high frequency cut-off. The Bergey Excel was designed in 1982 before a market for wind turbines for pumping water was realized and therefore was designed with a fairly high furling wind speed of 16 m/s. The Bergey 1500 was designed in 1989 and at that time a market for wind-electric water pumping was seen which resulted in the design of a lower furling windspeed for the Bergey 1500. The furling wind speed on the Bergey 850 (0.85 kW) water pumping system is also around 16 m/s, but using a higher capacitance in parallel with the motor will result in almost 100% availability in the 10 to 16 m/s wind speed range. Increasing the capacitance and other changes in the controller were investigated to improve the performance in the 10 - 16 m/s wind speed range on the Bergey Excel-PD, but no satisfactory solution was found. A modification of the furling mechanism could be made to reduce the furling wind speed, but would potentially be a major, expensive retrofit. Therefore, it was decided to try to lower the furling wind speed with some type of trailing edge device as a quick inexpensive alternative.

THEORY

Figure 1 is a drawing of the Bergey Excel-PD which demonstrates the furling mechanism of the wind turbine. Since the centerline of the rotor is offset from the tower centerline, when the thrust force on the blades gets high enough, the wind turbine will furl (rotor turns out of the wind). The thrust component on the blade can be represented by the following equation:

$$(1) \qquad \text{Thrust} = \text{Lift}\cos\phi + \text{Drag}\sin\phi \text{ (where } \phi = \text{angle of attack} + \text{pitch angle)}$$

As long as the flow is attached (i.e. air flow over the wind turbine blade doesn't separate), the lift force will be much higher than the drag force. Therefore, if the lift force is increased the thrust force will increase and the wind turbine rotor will furl at a lower wind speed. If aft camber is added to an airfoil the lift force will increase as long as the flow stays attached. Aft camber can be added to an existing blade in various ways (trailing edge flap, gurney flap, trailing edge wedge). Based on personal communication with Karl Bergey at Bergey Windpower and a wind tunnel test comparison of trailing edge flaps to gurney flaps (Bloy and Durrant, 1995), trailing edge flaps were selected. The trailing edge flap was limited to the outboard 20% of the blade span since most of the torque in furling comes from this part of the blade.

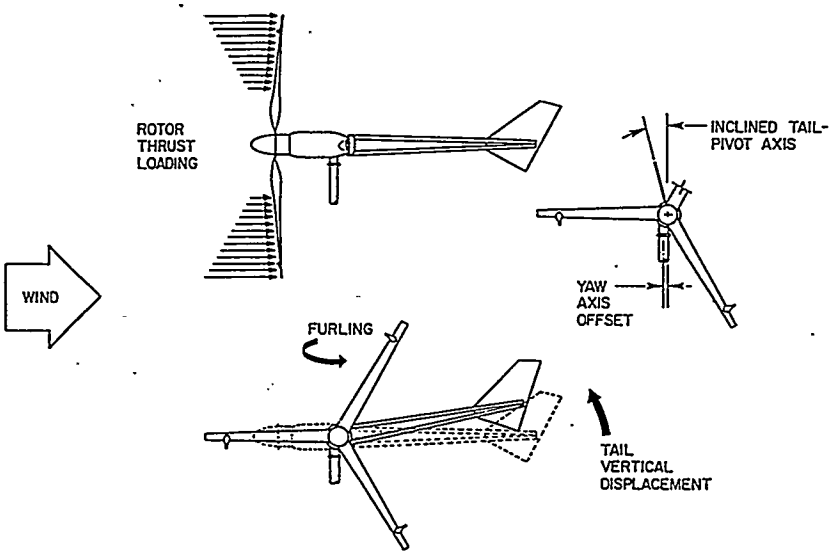

Figure 1. Horizontal furling of Bergey Excel-PD 10 kW wind turbine (Bergey Windpower).

BERGEY EXCEL-PD OPERATION

In order to understand why the high furling wind speed results in reduced daily water volume in the 10 -16 m/s wind speed range on the Bergey Excel-PD, a discussion of the operation of the Bergey Excel-PD is necessary. The Bergey Excel-PD wind turbine has a permanent magnet alternator whose rotor speed varies with the wind speed. The varying rotor speed results in a constant angle of attack of the wind turbine blade which, if the wind turbine is designed correctly, will maximize the lift-to-drag ratio of the blade over a broad wind speed range. The following parameters were kept constant during the testing:

1) 3.8 kW (5 hp) motor
2) 3.8 kW (5 hp) 5 stage pump
3) 35 meter pumping depth
4) 150 μf/phase capacitance
5) Turbine height = 20 meters

The size of the motor recommended by Bergey Windpower for the Bergey Excel-PD is 5.6 kW (7.5 hp). However, as can be seen in Clark and Vick, 1995, the pumping performance is similar for both the 5.6 kW (7.5 hp) and 3.8 kW (5 hp) motors. The Bergey Excel-PD controller during the testing had the following settings:

1) Low frequency cut-in = 40 Hz
2) High frequency cut-out = 85 Hz
3) High frequency cut-in = 85 Hz
4) Low frequency cut-out = 35 Hz
5) High current cut-out = 23 amps
6) Automatic or manual reset after high current cut-out = automatic

When the wind turbine reaches a frequency of 40 Hz, the solenoid relay in the controller closes and the wind turbine electricity is switched to the submersible motor powering the centrifugal pump. The wind turbine will continue to pump water as long as:

1) The frequency doesn't drop below the low frequency cut-out.
2) The frequency doesn't exceed the high frequency cut-out.
3) The high current cut-out is not exceeded for an extended period of time.
4) The wind turbine doesn't lose synchronization with the motor.

The wind turbine will reach 85 Hz when the wind speed is between 13 and 14 m/s. When the high frequency cut-out is exceeded, the solenoid relay will open and the frequency of the unloaded wind turbine will immediately exceed 100 Hz. If the wind speed exceeds 16 m/s, the wind turbine will furl and the frequency will slow to around 60 Hz (high frequency cut-in is 85 Hz so the solenoid relay will close during furling) and the wind turbine and motor will synchronize and begin pumping water again. However, while the wind turbine and motor were synchronized prior to reaching the high frequency cut-out, they don't synchronize when the high frequency cut-in is reached. It is not until the frequency gets down to about 65 Hz (for the Bergey Excel-PD this occurs at a wind speed of about 10 m/s) that the wind turbine will synchronize with the motor and then begin pumping water. Although little water is pumped as the wind turbine rotor slows down from 85 Hz to 65 Hz, the load of the motor spinning does help to slow the wind turbine down to 65 Hz. However, if the winds pick back up again before reaching 65 Hz, the wind turbine will not synchronize with the motor, and when the high frequency cut-out of 85 Hz is again reached, the solenoid relay will open and the unloaded wind turbine will exceed 100 Hz again. If there is no head on the pump and motor, the wind turbine will synchronize with the motor at 85 Hz, so synchronization at high frequencies after the wind turbine goes offline is a function of pumping depth.

TESTING

Testing of the trailing edge flaps was begun on March 13, 1996 at the USDA Conservation and Production Research Laboratory in Bushland. Figure 2 shows a drawing of the trailing edge flap on the Bergey Excel-PD blade. There is no twist in the blade except for the small amount of twist caused by the pitch weight at higher rotor speeds. The three configurations that were tested were:

1) No Flap (Baseline)
2) Trailing Edge Flap #1 (TEF #1 - 8% chord & 45 degree deflection angle)
3) Trailing Edge Flap #2 (TEF #2 - 4% chord & 45 degree deflection angle)

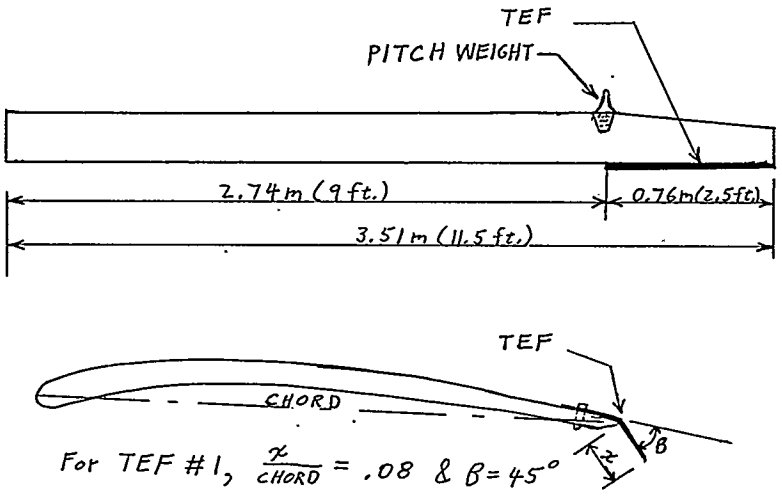

Figure 2. Drawing of Bergey Excel-PD blade showing location of trailing edge flap.

The first trailing edge flap (TEF #1) selected had an 8% chord and a deflection angle of 45 degrees. At the beginning of the test, the trailing edge flaps were fabricated from 1 mm thick aluminum sheet, each weighing 85 grams (3 ounces). The trailing edge flaps were attached to the blade with three screws after drilling holes through the blades. A special double sided tape was also used to help secure the flaps to the blades. The nuts used to attach the screws stuck up 4 mm above the aluminum plate on the upper surface and were 8.7 mm in diameter. The chord of the Bergey Excel-PD blade varies from 15.875 cm (6.25 in.) at the tip to 23.18 cm (9.125 in.) at the pitch weight. Therefore, for an 8% flap chord the chord varied from 1.27 cm (0.5 in.) at the tip to 1.91 cm (0.75 in.) at the pitch weight. The flap did not extend inboard of the pitch weight because of the reduced torque generation of that part of the blade. Because of a bevel on the lower surface which resulted in a sharp trailing edge, the trailing edge flaps were attached to the upper surface. Since the soft aluminum trailing edge flaps tended to fatigue at the screw heads after 10 - 30 days of testing, a stainless steel material was used to make the subsequent flaps, including a remake of the original aluminum configuration. The stainless steel flaps were stiffer and heavier, weighing 227 grams (8 ounces) each. The second TEF configuration (TEF #2) was 4% of the chord and had a deflection angle of 45 degrees. Therefore, for TEF #2 the chord varied from 0.64 cm (0.25 in) at the tip to 0.95 cm (0.375 in) at the pitch weight. TEF #2 was selected when TEF #1 resulted in a significant decrease in flow rate compared to the Baseline for wind speeds below 10 m/s. TEF #2 was also closer to the chord size presented in Bloy and Durrant, 1995. The testing presented in this paper lasted from March until May, but additional configurations are currently being tested.

RESULTS

Figure 3 shows the wind distribution for an entire year (4/01/93-3/31/94) for Bushland, Texas at a 20 meter height. Also shown in Figure 3 is the energy per unit area for Bushland. It is evident from this figure that about 50% of the wind energy in Bushland occurs above a wind speed of 10 m/s, so improvements in this wind speed range would significantly improve the pumping performance provided there is no performance degradation at lower wind speeds. Figure 4 shows the wind distributions that were collected for the three configurations tested. It's important to match wind distributions in the 10 to 16 m/s wind speed range when making pumping performance comparisons otherwise incorrect conclusions can be drawn.

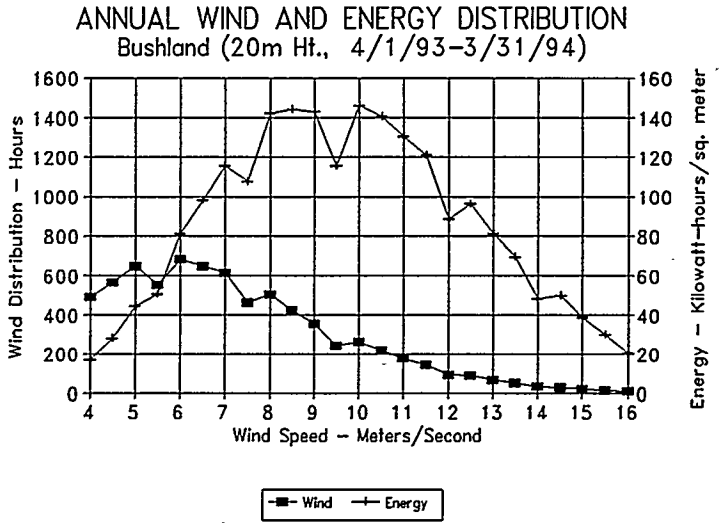

Figure 3. Annual wind and energy distribution for Bushland at a 20 meter height.

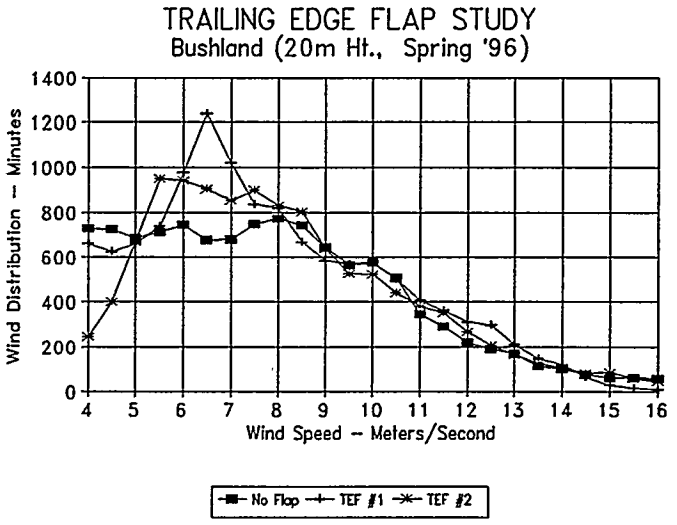

Figure 4. Wind distributions for all three Bergey Excel-PD configurations.

Figure 5 shows the "ON" time (load connected and pumping) for the three configurations. While both TEF #1 and TEF #2 decreased the "ON" time at wind speeds below 6.5 m/s compared to the Baseline, there was an improvement in "ON" time for the wind speed range of 10 - 14 m/s. There also appears to have been a degradation in the "ON" time in the 14 - 16 m/s wind speed range for both TEF #1 and TEF #2 compared to the Baseline. It should be mentioned that the Baseline and TEF configurations would be online 100% of the time for a wind speed range of 7 - 13 m/s if the wind speed never exceeded 13 m/s based on observation of several days of data.

Figure 6 shows the rotor speed for all three configurations as a function of wind speed. There is a noticeable

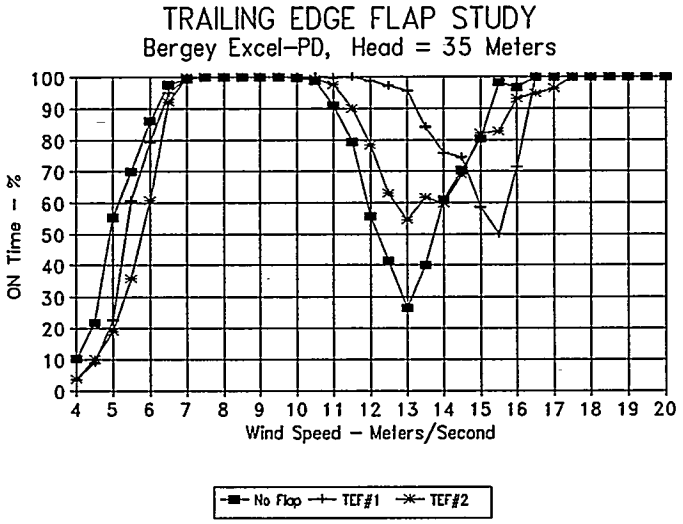

Figure 5. Effect of trailing edge flaps on "ON Time" for Bergey Excel-PD.

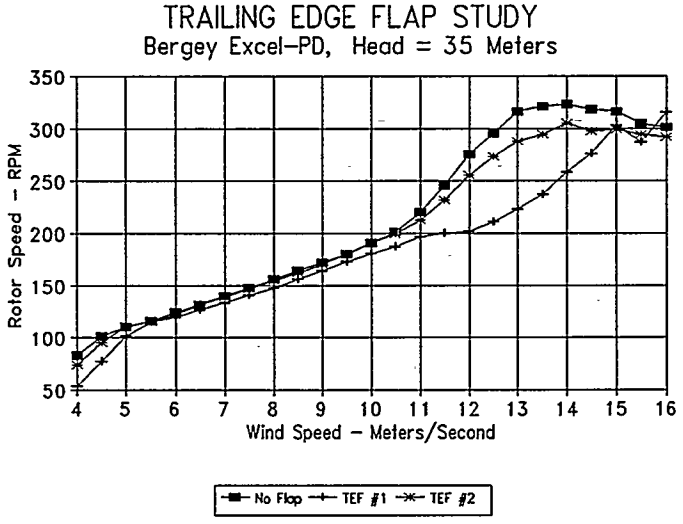

Figure 6. Effect of trailing edge flaps on rotor speed for Bergey Excel-PD.

decrease in rotor speed for TEF #1 compared to the Baseline and TEF #2 in the 11 - 15 m/s wind speed range. This is why the TEF #1 configuration stayed online longer. When the wind turbine goes off line, the rotor RPM immediately increases. TEF #2 shows some decrease in rotor RPM compared to the Baseline above 11 m/s. TEF #1 also has a somewhat lower RPM than the Baseline and TEF #2 in the 6 - 11 m/s wind speed range and probably is a result of the additional drag of TEF #1.

Figure 7 shows the effect of trailing edge flaps on the voltage to frequency ratio. Since the motor and pump are off-the-shelf items, they are designed for 230V and 60 Hz. As long as the voltage/frequency ratio is approximately 230V/60Hz = 3.8, the pumping efficiency will be maximized. The V/F ratio for all three configurations is virtually the same for wind speeds below 10 m/s. At higher wind speeds the trailing edge flap configurations have a different V/F ratio than the Baseline, but the V/F ratio stays around 3.8 for all three configurations.

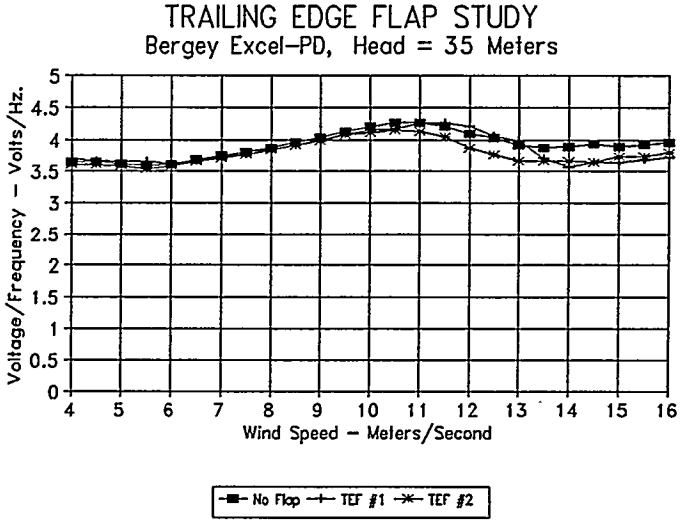

Figure 7. Effect of trailing edge flaps on voltage to frequency ratio.

Figure 8 shows the flow rate and system efficiency of all three configurations. The flow rate of TEF #1 is below that of the Baseline and TEF #2 for wind speeds below 11 m/s. This is probably due to the additional drag caused by TEF #1. For the wind speed range of 11 - 14 m/s, TEF #1 had a much higher flow rate than either the Baseline or TEF #2.

Figure 9 shows the average daily volume of water that would be pumped at Bushland for all three configurations at a 20 meter hub height. The daily water volume was obtained by multiplying the monthly wind distribution (Clark and Vick, 1994) by the flow rate in figure 8 and dividing by the number of days in each month. The Baseline configuration has the highest daily water volume, so the higher flow rate at the higher wind speeds of TEF #1 was cancelled out by the lower flow rate at the lower wind speeds.

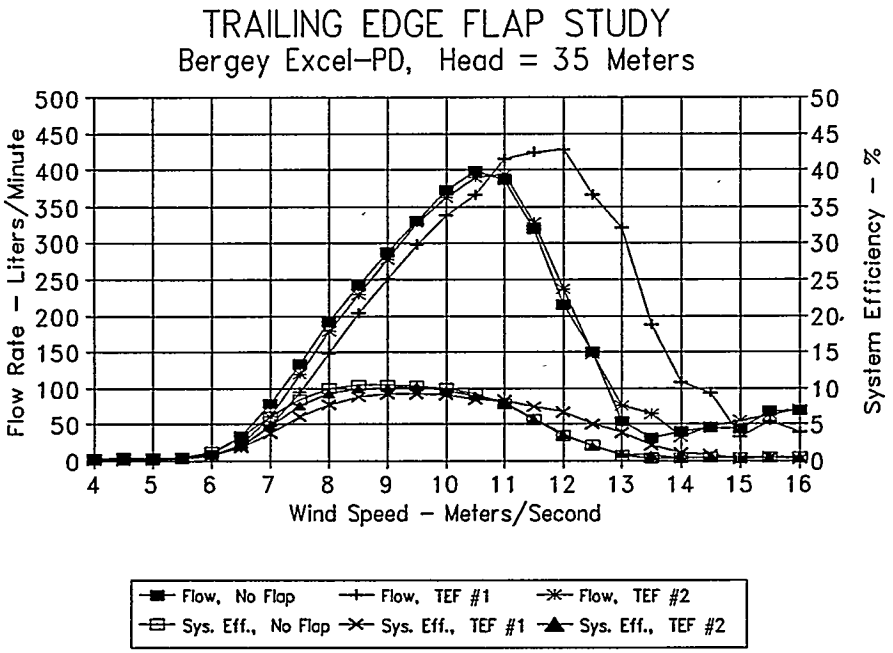

Figure 8. Effect of trailing edge flap on flow rate and system efficiency.

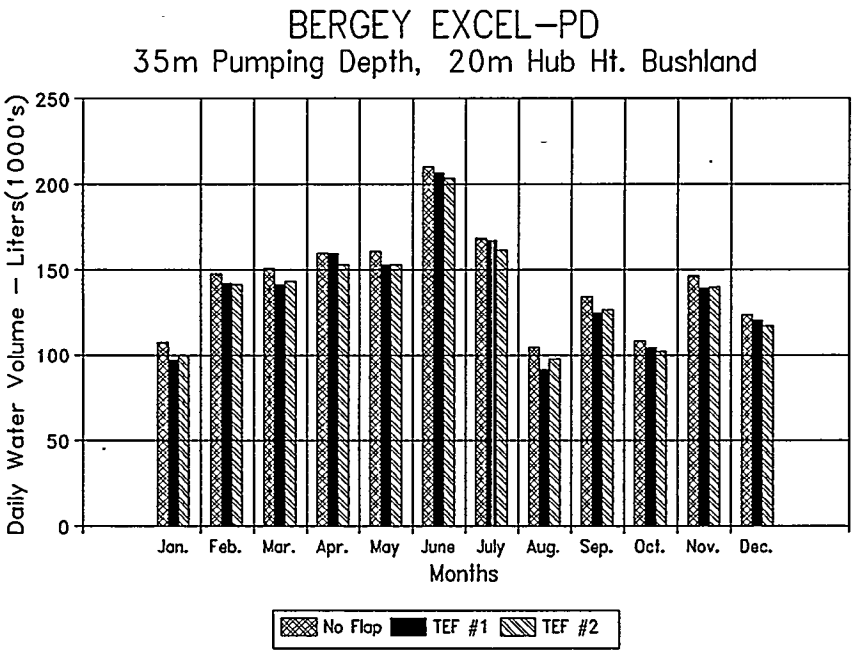

Figure 9. Effect of trailing edge flaps on daily water volume at Bushland for a 20m hub height.

CONCLUSIONS

Trailing edge flaps were shown to improve the flow rate of the Bergey Excel-PD wind turbine at wind speeds above 10 m/s, but they also resulted in a decrease in flow rate at wind speeds below 10 m/s. The trailing edge flaps also reduced the rotor speed at higher wind speeds, noticeably reducing the amount of vibration in the wind turbine, tower, and guy wires. The reason for the reduced vibration with the trailing edge flaps is the wind turbine is running unloaded at higher wind speeds less often. On January 17, 1996 one of the upper guy cables broke on the Bergey Excel-PD when there were wind gusts above 25 m/s, and if not for the quick action by the wind energy group at USDA, there probably would have been a complete failure of the wind turbine and tower. The failure in the big grip guy cable termination appeared to be fatigue related, and the wind turbine running off line in high wind speeds could have contributed to this failure. Another possible contributing factor to the big grip failure is the turbulent site the Bergey Excel-PD is located in at Bushland.

The original intent of the trailing edge flaps was to lower the furling wind speed, so the wind turbine would furl before reaching the high frequency cut-out and the pump would continue to operate. Observations of the operation of the wind turbine in high winds indicate that the trailing edge flaps do not make the wind turbine furl at a lower wind speed but create additional drag which slows the rotor down allowing the turbine to stay on line at higher wind speeds as well as allowing the high frequency cut-in to be reached quicker once the load is disconnected. Why the trailing edge flaps are not making the wind turbine furl sooner is not known. Too thick a boundary layer washing out the effect of the flap due to a lower Reynolds number can't be the reason since the Reynolds number varied between 0.6 and 1.2 million for the flap portion of the blade which was greater than the 0.55 million tested in Bloy and Durrant, 1995. However, flow separation on the blades at the higher wind speeds making the flap ineffective in increasing the thrust vector is a possibility.

We are continuing to test other trailing edge flap configurations to see if an improvement in water flow rate can be made at higher wind speeds without incurring a decrease in flow rate at low wind speeds. Vortex generators may be used to try to reattach the flow if the air flow over the blade is separated. Flow visualization using tufts would help decide whether the use of vortex generators is warranted. Also, Bergey Windpower has developed a new winding for the Excel stator which may also improve the pumping efficiency in the 10-16 m/s wind speed range.

ACKNOWLEDGMENTS

We would like to thank Mike and Karl Bergey, Bergey Windpower for their consultation during this study. We also would like to thank Ron Davis, USDA for fabricating and changing the trailing edge flaps.

REFERENCES

1. Bloy, A. W. and Durrant, M. T., 1995, "Aerodynamic Characteristics of an Aerofoil with Small Trailing Edge Flaps," Wind Engineering Vol. 19 No. 3 1995, pp. 167-172.

2. Clark, R. N. and Mulh, K. E., 1992, "Water Pumping for Livestock," Windpower '92 Proceedings, Seattle, WA., pp. 284-290.

3. Clark, R. N. and Vick, B. D., 1994, "Wind Turbine Centrifugal Water Pump Testing for Watering Livestock," ASAE Paper No. 94-4530, Atlanta, GA.

4. Clark, R.N. and Vick, B. D., 1995, "Determining the Proper Motor Size for Two Wind Turbines Used in Water Pumping," 14th ASME Wind Energy Symposium, Houston, TX., pp. 65-72.

5. Vick, B. D. and Clark, R. N., 1995, "Pump Controller Testing on Wind Turbines Used in Water Pumping" Windpower '95 Proceedings, Washington, D.C., pp. 465-474.

6. Vick, B. D. and Clark, R. N., 1996, "Performance of Wind-Electric and Solar-PV Water Pumping Systems for Watering Livestock," Energy Week '96 Book VIII Conference Papers, Houston, TX., pp. 198-203.

THE MEASURED FIELD PERFORMANCES OF EIGHT DIFFERENT MECHANICAL AND AIR-LIFT WATER-PUMPING WIND-TURBINES

J.A.C. Kentfield
Department of Mechanical Engineering
The University of Calgary
Calgary, Alberta, Canada T2N 1N4

ABSTRACT

Results are presented of the specific performances of eight, different, water-pumping wind-turbines subjected to impartial tests at the Alberta Renewable Energy Test Site (ARETS), Alberta, Canada. The results presented which were derived from the test data, obtained independently of the equipment manufacturers, are expressed per unit of rotor projected area to eliminate the influence of machine size. Hub-height wind speeds and water flow rates for a common lift of 5.5 m (18 ft) constitute the essential test data. A general finding was that, to a first approximation, there were no major differences in specific performance between four units equipped with conventional reciprocating pumps two of which employed reduction gearing and two of which did not. It was found that a unit equipped with a Moyno pump performed well but three air-lift machines had, as was expected, poorer specific performances than the more conventional equipment.

INTRODUCTION

Although small mechanical water-pumping wind-turbines have been available commercially for nearly 150 years it is only in fairly recent years that test stations have been created to perform unbiased performance, endurance, reliability and structural testing on a continuing basis. One of the first of the facilities capable of providing such services is the USDA station at Bushlands, Texas. Another, similar, facility was the Lethbridge Wind Research Test Site at Lethbridge, Alberta, Canada. This site, operated by the Alberta Department of Agriculture, was later developed to carry out test work on solar water-pumpers in addition to wind operated units. Early in 1992 the Lethbridge Wind Research Test Site was moved to a superior, and more suitable, location west of Lethbridge near the town of Pincher Creek, Alberta. The relocated facility was then renamed the Alberta Renewable Energy Test Site (ARETS). The prime task of ARETS remains the performance and reliability evaluation of wind and solar pumpers. The management of ARETS is in the hands of Mr. Rick Atkins of the Alberta Farm Machinery Research Centre, Lethbridge, Alberta, Canada (phone (403) 329-1212, Fax (403) 328-5562) who can provide more information than can be presented here.

During the life of the Lethbridge site, and more recently ARETS, the performance characteristics have been established, sometimes over a time span of more than one year, of a number of wind and solar water-pumping systems. Some of the wind system performance characteristics that were established are reported here in summary form. It has also been possible to verify, experimentally, during the course of the performance test work some performance features expected on the basis of theoretical considerations.

THEORETICALLY BASED CONSIDERATIONS

There are a number of theoretically based considerations that directly or indirectly reflect in the nature of experimentally obtained water-pumping wind-turbine performance characteristics. These relate to the start up of machines equipped with single-cylinder, single acting, lift pumps, the correct matching of the pump with the wind-turbine prime mover, the influence of internal leakage on pump efficiency and the efficiency expectation of air-lift pumping systems.

Counterbalancing Reciprocating Pumps

If no attempt is made to balance a single acting single cylinder lift pump, the type of pump normally used in the majority of simple wind-driven water-pumpers, sufficient torque must be generated by the turbine rotor to raise the pump plunger, or piston, during the pumping stroke. If suitable load balancing of the pump is provided the work input to raise the pump piston will not, of course, be reduced but will, in theory, be distributed over a pump cycle that includes both the up, or pumping, stroke and the subsequent downstroke. This implies that the rotor start-up torque necessary is reduced to half that needed when counter-balancing is not employed. However since rotor torque is, for a prescribed operating condition in this case that at start-up, proportional to the square of the wind speed counterbalancing offers the potential of reducing the cut-in, or start-up, wind speed to $1/\sqrt{2}$, or 71%, of that required when counterbalancing is not used. Ideally the counter balance should balance all the mechanical components of the pump, less buoyancy forces, plus half the pumping load.

Counterbalancing can be applied in several ways. One technique is to employ suitable return springs pushing upwards on the pumping mechanism. Another technique involves the use of a buoyant pump rod and although this can serve to frustrate the downward movement of the pump plunger, a motion for which reliance is normally placed upon gravity. A third technique, preferred by the writer, is to employ a counterbalanced beam in the manner shown in Fig. 1. Two of the water pumpers, one with reduction gearing the other without, the performances of which are reviewed here employ counterbalanced beams to minimize their cut-in wind-speeds without resorting to the use of smaller pumping cylinders.

Undersized Pumping Cylinders

It is tempting, in order to achieve a low cut-in wind speed, to employ an undersized pumping cylinder relative to what might otherwise be termed a pumping cylinder of optimum size. However this practice can be very costly in terms of lost performance potential. This point can be illustrated relatively simply with reference to the performance characteristics of the rotor of a typical water-pumping wind-turbine presented in Fig. 2. It can be seen from Fig. 2 that the torque coefficient, which is defined as the rotor torque divided by the dynamic pressure of the wind and also divided by the product of the rotor projected area and diameter, is reduced by approximately 50% when the rotor tip-speed ratio is unity and the turbine efficiency is at a maximum. Bearing in mind that a typical lift pump represents, for a running turbine, where the rotor acts as a flywheel, an essentially constant torque load and torque is proportional to the square of the wind speed it can be deduced that the peak rotor efficiency occurs at a wind-speed only about $\sqrt{2}$ times that at cut-in.

Thus for a 2 m/s (4.5 mile/h) cut-in wind speed peak rotor efficiency occurs at only 2.83 m/s (≃ 6.3 mile/h). When the torque coefficient has dropped to about 1/16 of the initial value, ie. approximately 0.05, the wind speed is only four times the cut-in value or, say, 8 m/s (≃ 17.9 mile/). It can, therefore, be seen that at this wind speed even a reduction of pump torque to zero will have only a marginal influence on rotor tip speed ratio. Thus it is clear that a reduction of pump size to reduce the cut-in wind-speed is by no means compensated by an automatic increase in rotor speed. Figure 3 illustrates this point which shows experimental results, obtained in 1992 at ARETS, using the same diameter and stroke of pump on a specific water-pumping wind-turbine with pump lifts of 15 m (49 ft) and 30 m (98 ft). It can be seen that the lesser lift does indeed increase the flow rate, but only slightly relative to that with the 30 m (98 ft)[1] lift. The most noticeable increase in flow rate occurs at low wind speeds. The increase in the expected cumulative flow rate, due to reducing the lift by 50%, based on the assumption of a Rayleigh wind-speed distribution and a thirty day month is approximately 43% for a low average monthly wind speed of 3 m/s (6.7 mile/h) and about 12% for an average monthly wind speed of twice that value. It should, in principle be possible to double the flow rate by halving the lift provided the pump-cylinder size is adjusted appropriately.

Influence of Pump Internal Leakage

Internal pump leakage past the valves or the piston of a reciprocating pump serves to decrease the pump volumetric efficiency to zero at sufficiently low pump speeds. Internal leakage is not normally a problem with most reciprocating pumps that employ a soft-seal bucket type plunger and compliant valves. In some cases pump internal leakage was arranged to occur deliberately, by means of a small passage short-circuiting the delivery and suction faces of the pump plunger, to unload the pump in order to assist the machine to start up. This technique was used by the former Dutch group CWD. CWD employed a simple, low cost, light weight, turbine rotor which did not produce a high torque coefficient at start-up conditions. A more sophisticated, and efficient, system employing a floating pump delivery valve was also used by CWD. Descriptions of both the bypass passage and the floating delivery valve has been given by Cleijne et al[2].

Where unwanted internal leakage can prove to be a problem is with Mono, or Moyno, type progressive cavity, rotary, positive displacement pumps. A diagrammatic cross-sectional view of such a pump is presented in Fig. 4. The sinuous rotor not only rotates but also makes an orbital motion. The leakage problem arises because the rotor only makes nominal line contact with the elastomeric stator. Leakage can be minimized by arranging for a heavy, or interference, contact between the rotor and the stator. However this can increase greatly the starting torque required. Hence it is necessary to adjust the rotor-stator interference judiciously to provide a satisfactory compromise between acceptable leakage and minimally excessive starting torque. One of the water-pumping wind-turbines the performance of which is reviewed here employs a rotary progressive cavity pump of the type depicted in Fig. 4.

Efficiency Expectation of Air-Lift Pumps

The important advantages of air-lift pumping systems are the elimination of submerged moving parts requiring periodic maintenance and the ability of such a system to withstand operation, without problems, in a well that has been pumped dry. A shortcoming is the depth of submergence required below the level of the water table, typically equal to about 80% of the pump lift. This, therefore, implies the need for a much deeper well than would be necessary for a conventional lift pump. Another shortcoming is the relatively low efficiency of air-lift pumps.

A portion of the low efficiency is attributable to the operation of an air-lift eduction system itself with the remainder of the irreversibilities occurring in the wind-turbine-driven compressor supplying the air to the eduction system. Stepanoff[3] has shown that losses with the eduction system are such that, as shown in Fig. 5, the peak efficiency with which the compressed air is utilized is typically less than 60% and that a 50% efficiency is all that can be expected over a reasonable operating range. It appears that most of the eduction losses are due to water run-back and subsequent repumping. The compressor isothermal efficiency, even with a well-cooled compressor cannot reasonably be expected to be greater than about 60-70%. Hence the combined efficiency of the compressor and eduction system is not likely to be greater than 30-40% at best. The corresponding efficiency of typical conventional lift pumps, including drive-train losses, is normally in the range 75-85%. Three of the turbines the performance of which is reviewed here incorporate air-lift systems.

TEST CONDITIONS

All the test data reported were obtained, and processed, by test site staff at ARETS or at the earlier, but similar, Lethbridge Wind Research Test Site. Both sites incorporated an array of water-pumping wind-turbine test beds. Suitable tower-mounted anemometers are provided to measure wind speeds corresponding to a range of hub heights. Provision was also made to measure barometric pressure and temperature. Test

data were recorded digitally, including water flow rates, and machine performances were established using bining techniques in accordance with Canadian Standard F417-M91 "Wind Energy Conversion Systems (WECS) Performance".

For all the tests, other than for the results presented in Fig. 3, the pump lifts were 5.5 m (18 ft). Also, because both the Lethbridge and ARETS locations are elevated the ambient pressures for all tests were approximately 90 kPa (13.1 lb_f/in^2 absolute). Since the tests were generally run only between spring and fall, to avoid freeze-up problems, the average ambient temperature applicable to the test data was in the region of 293 K (20°C or 68°F). A more detailed description of the test-site procedures and data processing techniques is available[4].

TEST RESULTS

All the comparative test data presented were obtained from commercially manufactured production units or from commercially manufactured prototype machines. In order to eliminate the direct influence of unit size on the performance data the test data, consisting of water flow rates versus wind speed and monthly, cumulative, flow rates versus monthly average wind speeds, are expressed per unit of rotor projected area. For example water flow rate in litres/(minute, square metre of rotor disc area).

Figure 6 compares the specific performances of two geared, multi-bladed, units namely an Aermotor of 2.44 m (8 ft) rotor diameter with a 6.4 m (21 ft) rotor diameter Wind Baron Softwind machine. The Aeromotor performance was that recorded during the 1992 test season and that of the Softwind was obtained during the 1991 season[5]. The Wind Baron Softwind employed a counter-balanced pump whereas the Aermotor did not. Figure 7 compares the performances of two non-geared units each equipped with a lift pump driven directly from the turbine-rotor shaft. One unit, the Chinook of 7.5 m (24.6 ft) rotor diameter, featured a relatively low solidity multibladed rotor. The design of the Chinook unit was derived from a design by IT (Intermediate Technology) Power in the United Kingdom. The other non-geared unit was a Delta 16 machine manufactured by Dutch Industries of Regina, Saskatchewan, Canada. This unit had a perimeter bladed rotor of 4.815 m (15.8 ft) diameter. A detailed description of this machine is available elsewhere[6]. The Delta 16 employed a balanced-beam pump drive similar to that shown in Fig. 1 whereas the Chinook did not feature a balanced pump. The Chinook performance was established in 1988[7] and that for the Delta 16 during the 1990 test season[8]. It is interesting to note, from a comparison of Fig. 7 with Fig. 6 that in the wind speed range from about 4 m/s to 8 m/s (13 to 26 ft/s) the specific performances, in terms of water flow rate, of the direct drive machines increase much more rapidly than those of the geared units. If the performance comparisons of Fig. 6 and 7 were to be based on rotor blade area instead of rotor disc area it becomes necessary to multiply the ordinates of Fig. 6 and 7 by the inverses of the rotor solidities. For the Aeromotor, Softwind, Chinook and Delta 16 units these values are, approximately, 1.3, 1.3, 1.7 and 2.9 respectively.

Figure 8 presents the performance of a Canadian built Maverick Windmotor turbine equipped with a directly driven progressive cavity, positive displacement pump of the Mono or Moyno type. This turbine is provided with a downwind delta-wing-bladed rotor coupled to the submerged pump by means of a flexible-cable drive shaft. This machine has been described in more detail elsewhere[9]. The specific performance results presented where obtained during the 1992 ARETS test season[1]. Since the pump inertia effects, so important with reciprocating pumps, are absent with the rotary pump furling does not occur until the wind speed reaches 15 m/s (49 ft/s).

The final diagram, Fig. 9, compares the performances of three air-lift systems. One system, the Praire PD8-6, is a true, simple, air lift arrangement with no submerged moving parts. The Bowjon Rancher unit employs

a submerged diaphragm pump and hence is more complicated than the Praire system. The Koenders machine incorporates a special air-operated pumping unit. The exhaust from this unit serves to aerate the pond, or source, from which the water is being pumped. With the Praire and Bowjon machines the pumped water, only, becomes aerated. As can be seen by comparing Fig. 9 with Fig. 6, 7 and 8 the air-operated systems all have inferior specific performances to those employing positive displacement, mechanically driven, pumps. The results presented for the Praire unit were obtained during the 1990 test season[8], those for the Bowjon unit were obtained in the time frame 1985-1987[10] and the Koenders results more recently during the 1994 test season[4].

DISCUSSION

Although not apparent from the performance data presented here the use of a properly counter-balanced reciprocating pump permits very smooth operation of wind-turbines so equipped at wind-speeds only slightly greater than the cut-in value. The importance of correctly matching the pump size to the wind-turbine prime mover is emphasized in Fig. 3. With a pump sized correctly to suit the lift the water flow rate of a prescribed wind water-pumper should be doubled, for a prescribed wind-speed, by halving the lift. Clearly, from Fig. 3, that was not the case when the lift was halved without changing the pump size. It can also be seen, from Fig. 3, that halving the lift had but a very minor influence on the cut-in wind-speed. This was probably due to the use of a counter-balanced pump drive which was not adjusted to suit the reduced lift operating condition. The counter-balance mass should, for the case where the lift was reduced by 50%, have been approximately halved.

The performance differences noted from comparison of the curves of Fig. 7 with those of Fig. 6, namely that the water flow-rate versus wind-speed curves for the non-geared machines of Fig 7 are steeper than those for the geared unit contributing to the corresponding curves of Fig. 6 appears to be an artifact of turbine rotor performance characteristics. Both the high solidity multibladed turbines driving the geared pumps, the performance of which is presented in Fig. 6, have performance characteristics of the kind presented in Fig. 2. However, with regard to Fig. 7, both the relatively low solidity multibladed rotor of the Chinook machine and also the perimeter bladed rotor of the Dutch Delta 16 have torque-coefficient versus tip-speed ratio characteristics that are convex such that the torque-coefficient falls-off from, the cut-in value, with increasing rapidity as the tip-speed ratio increases. Hence for a given multiple of the cut-in wind speed these turbines tend to run faster, and hence deliver more water, than would be the case with essentially linear torque characteristics of the kind depicted in Fig. 2.

The specific performance of the Maverick Windmotor machine equipped with a progressive cavity, positive displacement, rotary, pump is fairly similar to that of the Wind Baron Softwind machine as can be ascertained by comparing Fig. 8 with Fig. 6. This despite a small measure of internal leakage occurring within the rotary pump. A particular advantage attributed to Mono, or Moyno, pumps, in addition to their employment of rotary rather than reciprocating motion, is an ability to accept dirty or gritty water without suffering internal damage such as scouring.

In general terms the performances obtained with various forms of air-lift pumping systems are in agreement with expectations based on theoretical considerations. Another point to note from Fig. 9 is that the best air-lift performance is that of the most simple of the systems studied. It appears that adding a pneumatically operated water pump to an air-lift system does not seem, on the basis of the results presented in Fig. 9, to be a promising concept from the viewpoint of improving system efficiency.

CONCLUSIONS

The following conclusions can be drawn from the work in relation to wind-driven water-pumpers:

(a) Balancing single cylinder lift-type pumps offers the opportunity to lower, by about 30%, the cut-in wind-speed and permit smoother operation in weak winds.

(b) It is very important from the performance viewpoint to match, correctly, a water pump with the wind-turbine prime-mover and to avoid the use of an undersized pump.

(c) Geared and non-geared wind-driven water-pumpers are essentially comparable in performance. The non-geared units have the advantage of eliminating the need for speed-reducing gearing in the pump drive train.

(d) A water-pumping wind-turbine employing a positive displacement, rotary, progressive cavity, pump was shown to be competitive in performance with more traditional concepts employing reciprocating pumps.

(e) In accordance with theoretically based expectations, air-lift systems normally have much poorer performances than direct-drive mechanical systems. However air-lift pumping systems can be implemented without any submerged moving parts. They also permit pumping the well, or sump, dry without sustaining damage and also the installation of the wind-driven compressor remotely from the wellhead.

REFERENCES

1. Anon, Sept. 1993, "Summary Report 703, 1992 Test Season", Alberta Farm Machinery Research Centre, Lethbridge, Alberta, Canada, T1K 1L6.
2. Cleijne, H., Smulders, P., Verheij, F. and Oldenkamp, H., 1986, "Pump Research by CWD: The Influence of Starting Torque of Single Acting Piston Pumps on Water Pumping Windmills", Report R815D, Technical University Eindhoven, The Netherlands, Faculty of Physics, Laboratory of Fluid Dynamics and Heat Transfer, (Note: also presented at the 6th European Wind Energy Conference, Rome).
3. Stepanoff, A.J., 1966, "Pumps and Blowers, Selected Advance Topics", John Wiley and Sons Inc., New York.
4. Atkins, R.P. and Baker, D.R., April 1995, "Alberta Renewable Energy Test Site 1994 Wind System's Test Results", Alberta Farm Machinery Research Centre, Lethbridge, Alberta, Canada, T1K 1L6.
5. Anon, Jan. 1992, "Summary Report 692, 1991 Test Season", Alberta Farm Machinery Research Centre, Lethbridge, Alberta, Canada, T1K 1L6.
6. Kentfield, J.A.C., 1989, "A Prototype Water-Pumping Wind-Turbine Based on a New Design Philosophy", Proceedings, Windpower '89, American Wind Energy Association, pp. 291-297.
7. Atkins, R.P. and Proctor, R.J., Sept. 1993, Consumers Guide to Wind Powered Water Pumping", Development Project DL 0693, Alberta Farm Machinery Research Centre, Lethbridge, Alberta, Canada, T1K 1L6.
8. Anon, June 1992, "Summary Report 683, 1990 Test Season", Alberta Farm Machinery Research Centre, Lethbridge, Alberta, Canada, T1K 1L6.
9. Kentfield, J.A.C., 1992, "A Downwind Application of a Delta-Turbine Rotor to Water Pumping", Proceedings, Wind Energy '92, pp. 209-220, Canadian Wind Energy Association, Calgary, Alberta, Canada, T2L 2K7.
10. Paterson, B.A., Baker, D.R. and Jensen, N.E., 1988, "Lethbridge Wind Research Test Site Evaluation of Wind and Solar Pumping Systems 1985-1987, (Appendix A)", Alberta Farm Machinery Research Centre, Lethbridge, Alberta, Canada, T1K 1L6.

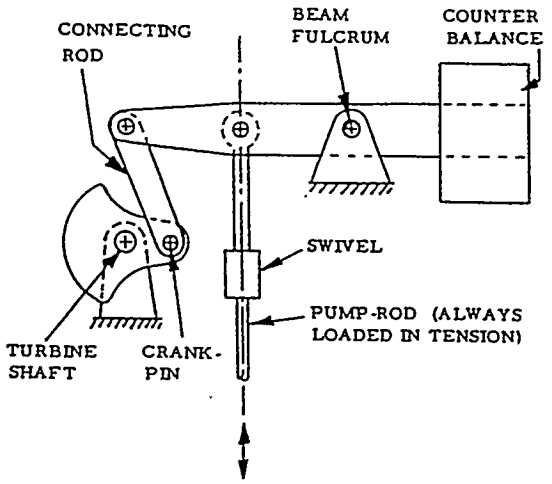

Fig. 1 Pump load-torque balancing beam (diagrammatic).

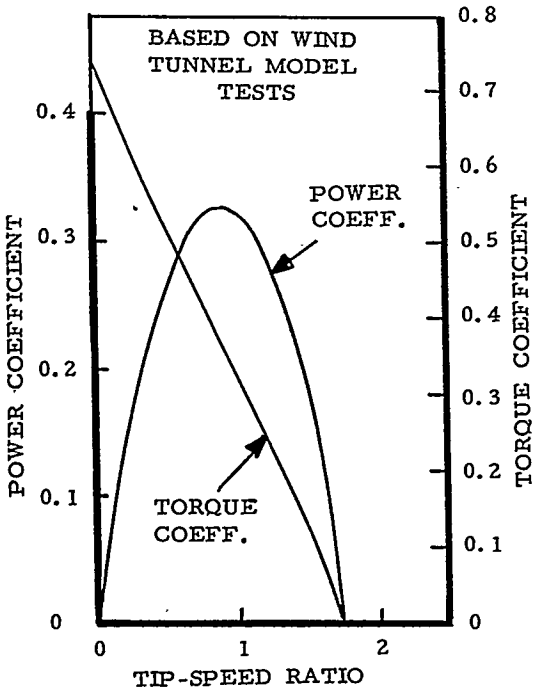

Fig. 2 Performance characteristics of a typical multibladed wind-turbine of the type frequently used in wind water-pumpers.

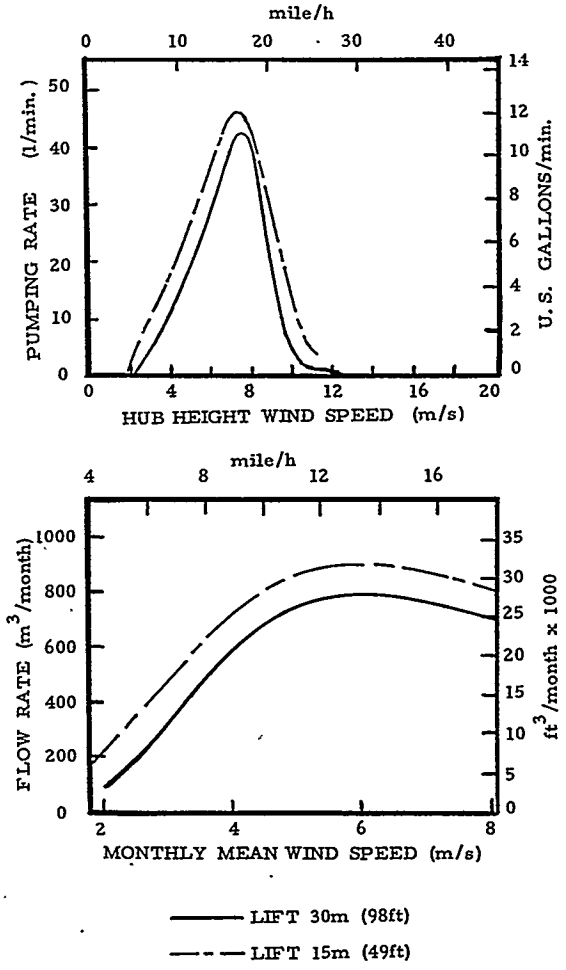

Fig. 3 Field performances of a wind-turbine water-pump combination for two different lifts. The water-pump is of prescribed bore and stroke.

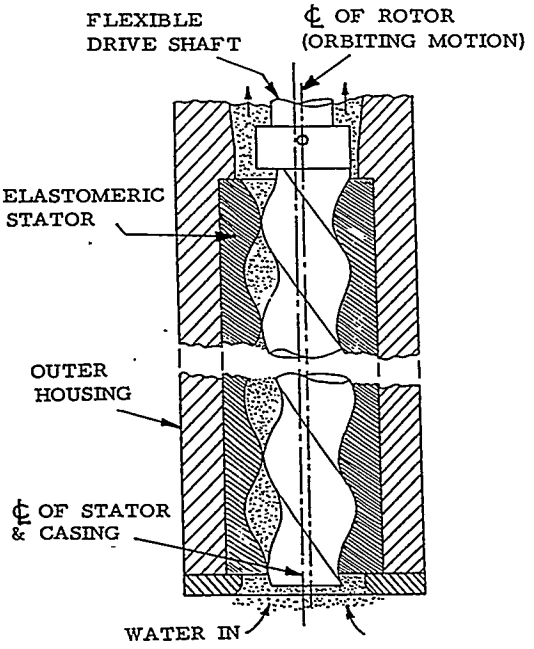

Fig. 4 A rotary, progressive cavity, positive displacement pump of the Mono, or Moyno, type (diagrammatic).

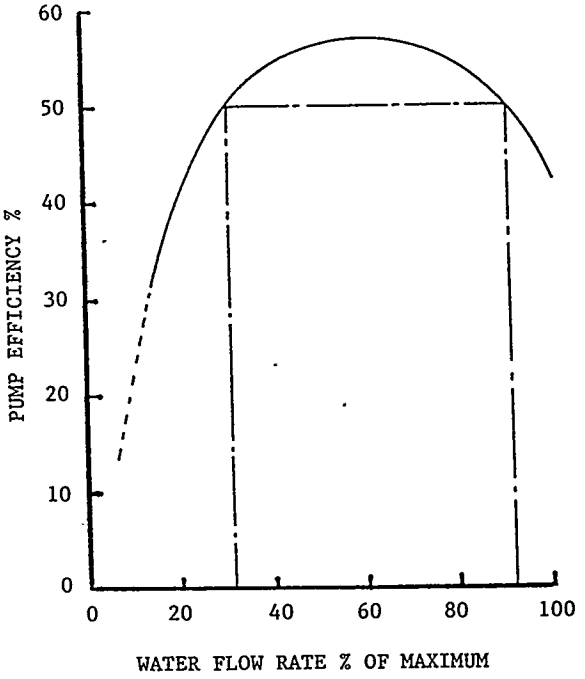

Fig. 5 Performance of a typical air-lift eduction tube type pump (after Stepanoff[3]).

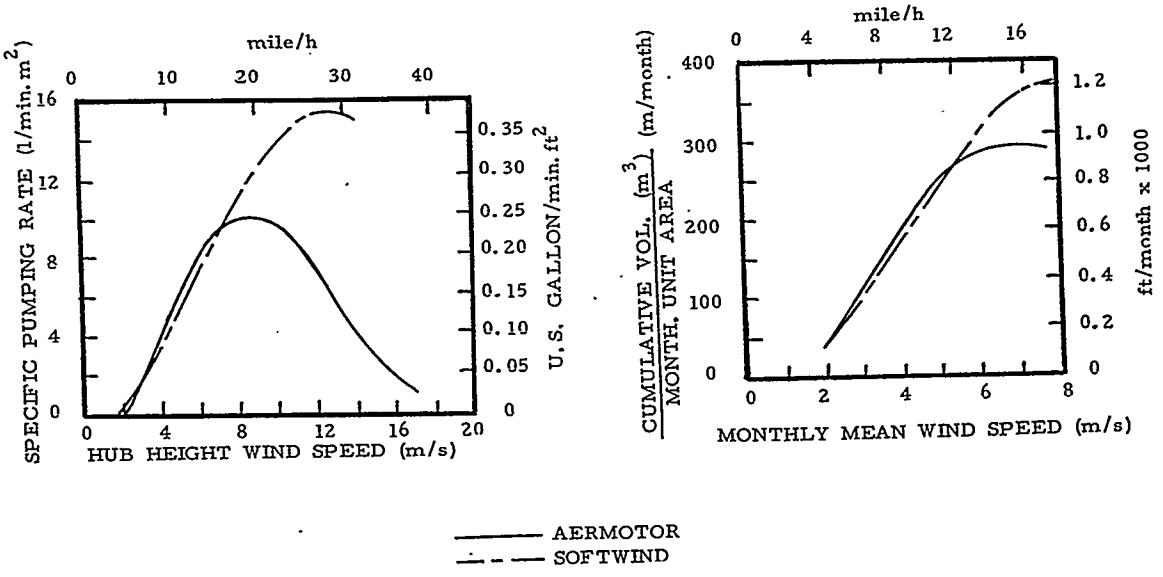

Fig. 6 Field performances of two multibladed wind water-pumpers employing reduction gearing and reciprocating lift pumps: lift 5.5 m (18 ft).

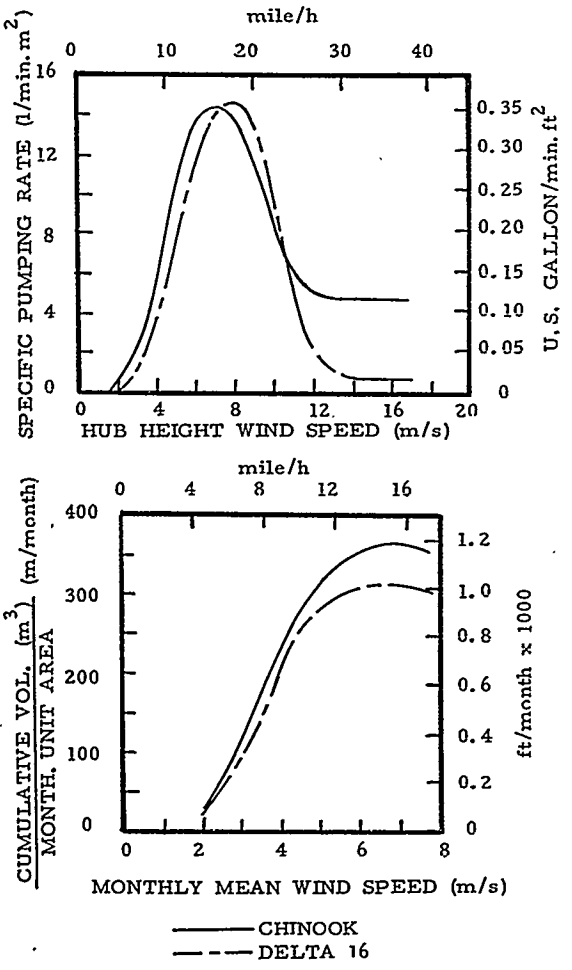

Fig. 7 Field performances of two wind water-pumpers, without reduction gearing, employing reciprocating lift pumps: lift 5.5 m (18 ft).

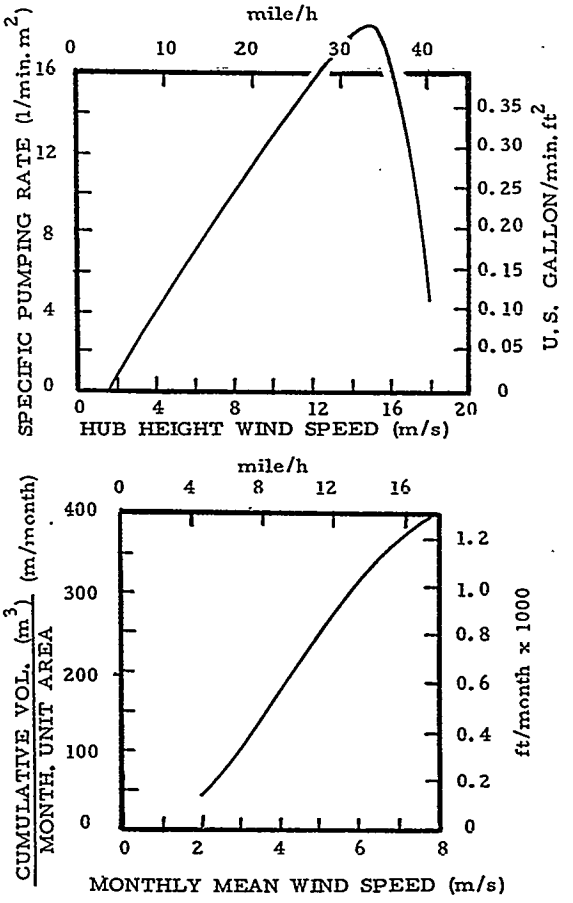

Fig. 8 Field performance of a Maverick Windmotor wind water-pumper employing a rotary, positive displacement, progressive cavity pump: lift 5.5 m (18 ft).

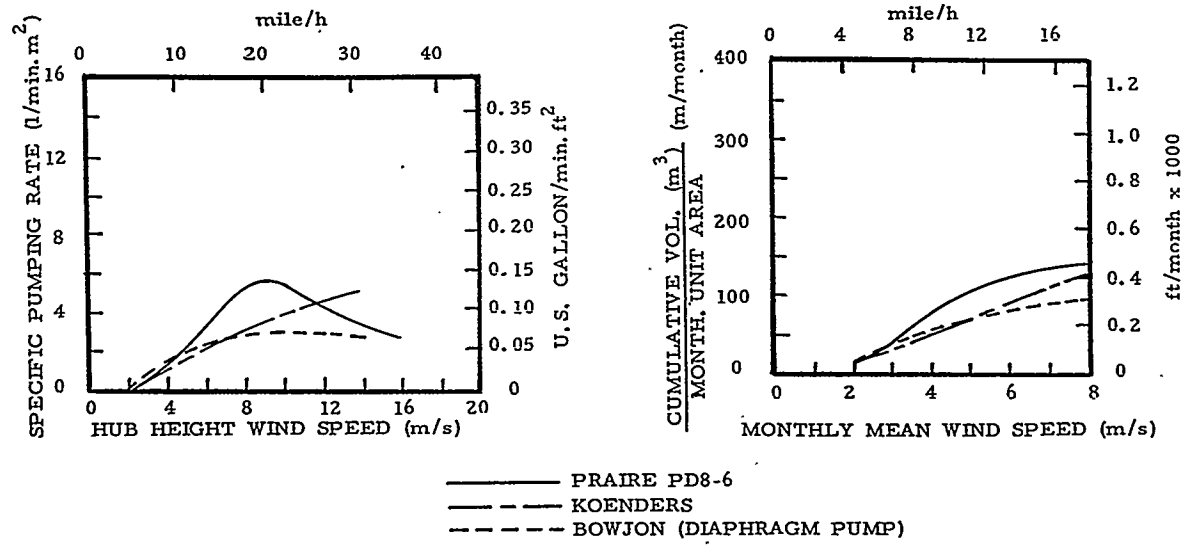

Fig. 9 Field performances of three air-lift type wind water-pumpers: lift 5.5 m (18 ft).

THE UTILIZATION OF EXCESS WIND-ELECTRIC POWER FROM STOCK WATER PUMPING SYSTEMS TO HEAT A SECTOR OF THE STOCK TANK

John E. Nydahl and Bradley O. Carlson
Department of Mechanical Engineering, University of Wyoming
P.O. Box 3295, Laramie, Wyoming 82071

ABSTRACT

On the high plains, a wind-electric stock water pumping system produces a significant amount of excess power over the winter months due to intense winds and the decreased water consumption by cattle. The University of Wyoming is developing a multi-tasking system to utilize this excess energy to resistively heat a small sector of the stock tank at its demonstration/experimental site.

This paper outlines the detailed heat transfer analysis that predicted drinking water temperature and icing conditions. It also outlines the optimization criteria and the power produced by the Bergey 1500 wind electric system. Results show that heating a smaller insulated tank inserted into the larger tank would raise the drinking water temperature by a maximum of 6.7 °C and eliminate icing conditions. The returns associated with the additional cattle weight gain, as a result of the consumption of warmer water, showed that system modification costs would be recovered the first year.

INTRODUCTION

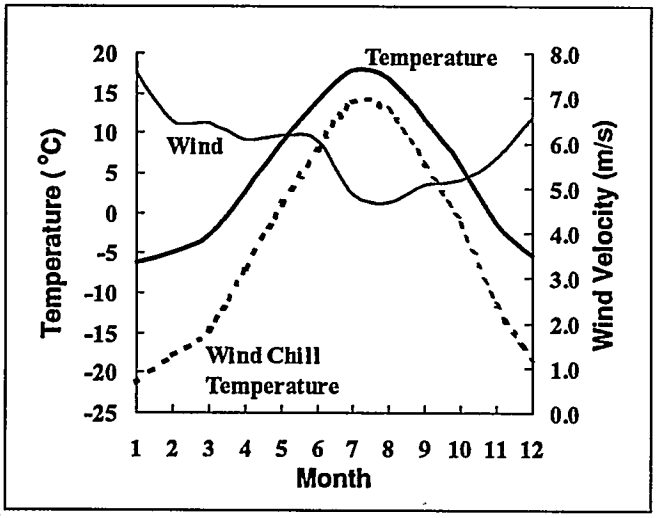

FIGURE 1. LARAMIE, WY MONTHLY MEAN TEMPERATURES AND WIND SPEEDS [MARTNER, 1986]

This paper reports on part of a feasibility study directed toward assisting rural, high-plain cattle ranchers implement cost effective alternative stock watering systems. The acquisition and maintenance of stock water systems represent a significant investment for ranchers and reliable operation in severe freezing and windy conditions is imperative. This relates directly to Wyoming which is one of the coldest and windiest states in the nation as a consequence of its high elevation and interior location. *Figure 1* illustrates this fact by plotting Laramie's mean monthly dry bulb temperature, wind speed and wind chill temperature.

Mechanical windmills are still used extensively to pump many of the approximately 50,000 stock watering wells in Wyoming. This is due, in part, to the high cost to extend power lines (≈$9300/km) and the availability of wind power. For instance, Laramie has an average wind speed of 5.7 m/s which correlates to an estimated annual average wind power of 200 - 250 W/m^2.

The Engineering College of the University of Wyoming has embarked on a program to both demonstrate recent significant technological developments in Wind Electric Pumping Systems (WEPS) [Clark, 1995]

and to investigate possible uses of any excess power to improve their overall performance. These new systems are based on allowing the voltage and frequency of the produced power to vary; therefore, utilizing relatively inexpensive three phase/220 V motors in these systems.

The costs for mechanical and electrical wind pumping systems with the same diameters are approximately the same. For example, the University of Wyoming's test site has a 3 m Aermotor pumping system driving a pump at a 10.7 m depth. The estimated replacement cost of this system is $7830. A Bergey 1500 powers a 40S10-3 Gnundfos submersible pump and motor located at approximately the same depth in this well. The cost of this complete pumping system was approximately $8590. This cost included 210 m of three phase cable between the turbine and the well, as well as the copper grounding wires around the tower and along the three phase line.

The advantages of wind-electric pumping systems have been well documented by Clark and Mulh [1992]. For example, the University of Wyoming's wind generator is located on top of a knoll 210 m from the well. This demonstrates the siting flexibility advantage that wind electric systems have over mechanical systems. Clark's tests also indicate that the Bergey 1500 wind-electric pumping system has an average overall operating efficiency between 9-12% as compared to 6% for the mechanical system which correlates to significantly larger volumes of water being pumped by the wind-electric pumping system. In addition, wind-electric pumping systems have lower maintenance costs and the option to utilize a portable electric generator when the turbine is off line.

Due to the unpredictability of the wind, most stock water tanks are sized to hold a five days supply of water and windmills are sized for the low wind power months during the summer. This implies that a wind-electric pumping system should produce a significant amount of excess electric energy during the windier winter months. *Figure 2* shows some of the possible multi-tasking options that could utilize this excess power and augment the wind-electric pumping system by powering bubblers, resistive heaters or charging batteries. The battery energy could be used to power thermal solar collectors, warning systems, electric fences, etc. Our recent efforts have been directed toward developing resistive and thermal solar stockwater heating systems and this paper presents the results of a feasibility study for resistive heaters.

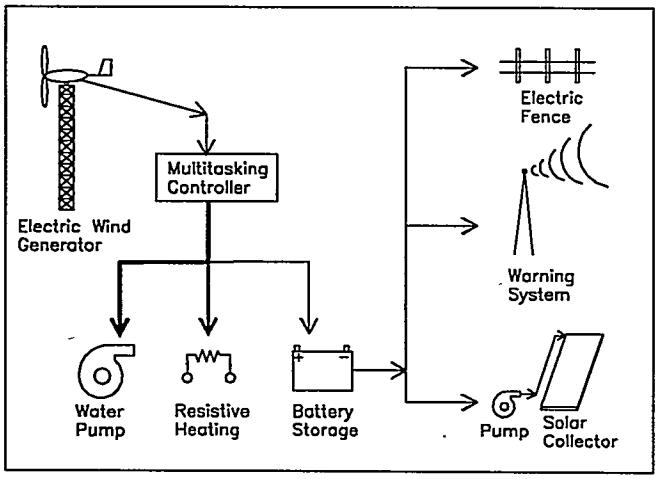

FIGURE 2. MULTITASKING OPTIONS FOR A WEPS

STOCK WATER HEATING

To maintain access to water in this severe winter climate, cattle are typically confined to pastures close to the ranch. Bubblers, gas and electric heaters, solar collectors, the practice of overflowing the stock tank into retaining ponds, and the labor intensive mode of just breaking and removing the ice layer are all utilized. The University of Wyoming, for instance, operates around forty small 500 Watt heated stockwater tanks at its stock farm facility. On occasion, these tanks have frozen even though their exposed water surface area is less than 0.3

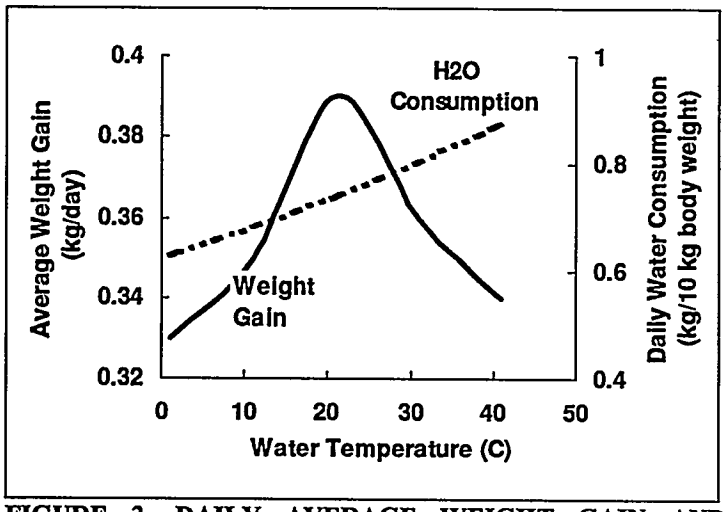

FIGURE 3. DAILY AVERAGE WEIGHT GAIN AND WATER CONSUMPTION OF WEANLING HEIFERS VS. WATER TEMPERATURE [Rice, 1979]

m^2 and their sides are insulated. It should be noted that these small heated tanks have an advertised capacity of 70 head of cattle and cost around $700.

Besides the extremely low *wind chill temperatures* that range cattle must endure, the consumption of cold water during the long *cool season*, that lasts from September through May, exasperates the thermal stress they suffer.

This is reflected in a comprehensive study by Rice [1979] that was carried out at the United States Department of Agriculture, Science and Administration, Central Plains Experimental Range, Nunn, Colorado located just south of Cheyenne, Wyoming. The drinking water temperature was found to have a significant effect on the weight gain and water consumption of weanling Hereford heifers. Although most of the weight gain occurred during the *warm season* of June through August, *Figure 3* implies that the weight gain during the *cool season* can be increased by as much as 15% for range cattle consuming 21°C instead of freezing water. Results of Luken and Hamilton [1962] also indicate that cattle consuming warm water during the cold season can show winter weight gains of the order of 10% whereas cattle drinking unheated water require substantially greater amounts of winter feed just to maintain their weight. Rice's data also showed that the water consumption rate for the "warm season" was at least 50% higher than the average *cool season* water consumption rate.

WIND ENERGY RESISTIVE HEATING SYSTEM

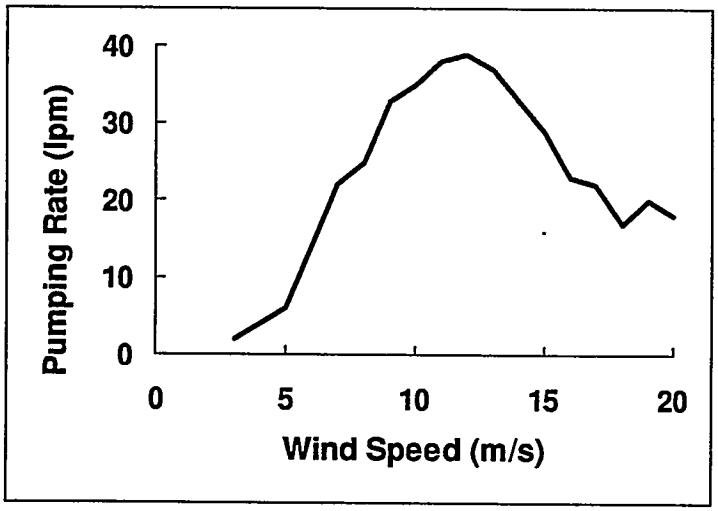

FIGURE 4. BERGEY 1500 PUMPING RATES VS WIND SPEED FOR 17 m PUMPING HEAD [Clark, 1994]

To service a given herd size, the load demands of a wind-electric pumping system which is operated on a year around basis are cyclical depending on the season. The water consumption rate decreases in the winter while there is a significant increase in the wind's magnitude (*Figure 1*). To estimate how much excess energy could be produced at our Laramie site during the winter, the required flow rate was set to a typical value of 5000 l/day. The maximum amount of water that could be pumped each month was then ascertained through the use of the pumping curve presented in *Figure 4*.

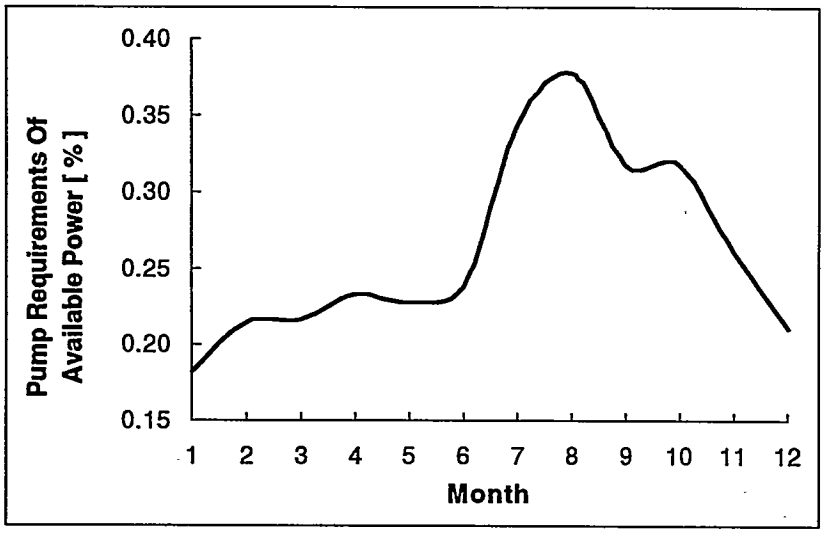

FIGURE 5. FRACTION OF DAILY PUMPING CAPACITY REQUIRED TO PUMP 5000 l/DAY

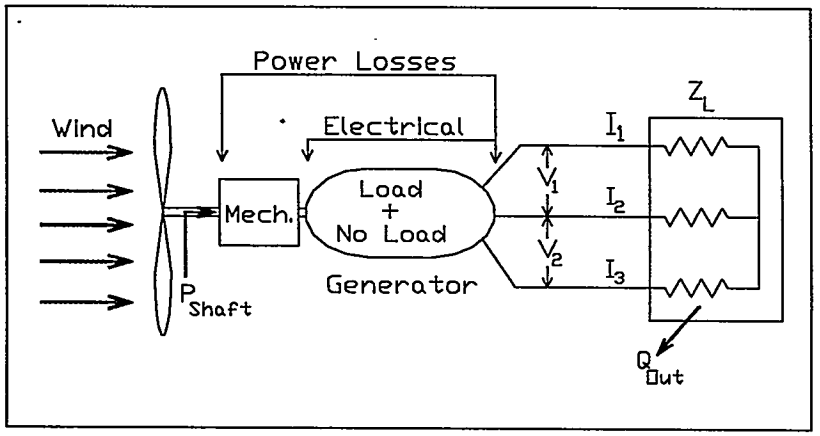

FIGURE 6. SCHEMATIC OF POWER LOSS MODEL AND RESISTIVE LOAD

The pumping curve in *Figure 4* was combined with the Rayleigh wind distribution based upon monthly average wind speeds (*Table 1*), instead of Laramie's annual value [Cliff, 1977], to estimate the average daily pumping capacity for each month. *Figure 5* presents the fraction of the Bergey's monthly pumping capacity that is required to meet a 5000 l/day demand. The hours in each wind velocity bin for pumping were determined by assuming that a uniform fraction of bin hours was removed from every bin above 3 m/s. The remaining hours in each bin were then summed over all bins and used for the resistive heating power.

Figure 6 illustrates the system losses. Dynamometer tests were performed utilizing both resistive and pump loads to ascertain the electrical characteristic of the turbine. Correlations for the no load mechanical, $P_{M,L}$, and electrical, $P_{E,L}$, losses were determined for angular velocities greater than 250 RPM. The turbine's output power P_o for a resistive load is equal to $3*I^2*Z_L$ where I is the phase current and Z_L is the load impedance. The phase current was correlated in terms of RPM, Z_L and the generator's inductance L_s and load resistance R_a. Equating the electrical output plus the loss terms to the aerodynamic power gives the required relationship between wind velocity and output power.

$$\tfrac{1}{2}\rho_{air} A V^3 C_p = 3I^2(Z_L + R_a) + P_{M,L} + P_{E,L} \qquad (1)$$

where ρ_{air} is the air density, A is the rotor's swept area and C_p is the power coefficient of the wind turbine which is a function of the tip speed radio, TSR. The tip speed ratio is the turbine blade tip speed divided by the wind velocity. The manufacturer was unable to supply its own C_p information so Clark's [1994] data were used in this analysis. *Figure 7* indicates that these data showed a maximum C_p near 0.43 at a TSR of 6.4 and this curve is surprisingly similar to data for the world's largest wind turbine, the Mod-5B, which has a 97.5 m rotor diameter [Spera].

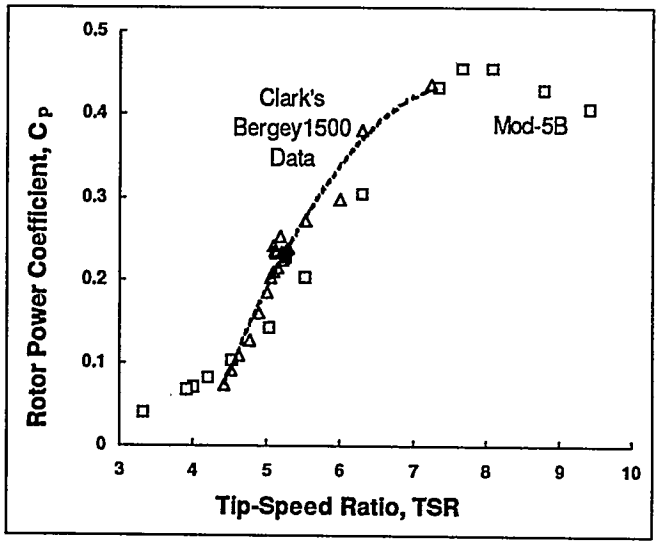

FIGURE 7. TURBINE C_P VS TSR COMPARISON BETWEEN THE ASSUMED BERGEY 1500 AND MOD-5B

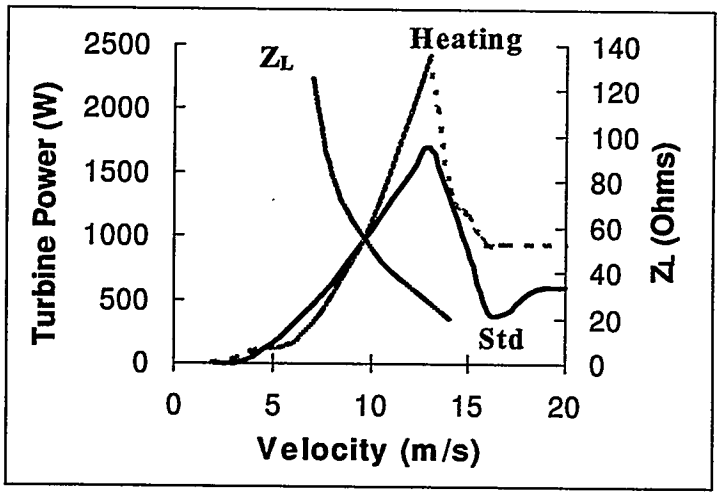

FIGURE 8. ESTIMATED OPTIMUM Z_L AND RESISTIVE & STANDARD POWERS FOR A BERGEY 1500 VS WIND SPEED

The above information permitted the determination of how Z_L and RPM should vary with wind speed to maximize the resistive heating. Maximum constraints for the optimization program were placed at 600 rpm, 6.4 TSR, 7 amps per phase and 250 volts. The results of this calculation are presented in *Figure 8* and indicate the impedance should decrease from 84 to 20 ohms as the velocity increases from 7 to the furling velocity of 13 m/s. The resistive load power increased from 315 to 2425 W over this same interval. As expected, these optimization calculations indicated that the turbine should operate at its maximum C_p at the higher wind velocities. The optimum TSR began dropping for velocities below 6 m/s and the model predicted no power below 4.5 m/s. It was later determined that Clark's C_p data were based on output power rather than aerodynamic power which makes the above calculations overly conservative. These results where retained for velocities from 5 to 13 m/s and Clark's data were utilized with no density correction to estimate powers for velocities below 5 m/s and above the furling velocity.

The heating (excess) power is detailed in *Table 1* and has a maximum available monthly heating power varying from 4.1 to 11.7 kWhr/day with a 7.5 kWhr/day average over the *cool season*. It should be noted that the maximum value is equivalent to a 500 W heater.

HEAT TRANSFER MODEL AND OPTIONS

A hypothetical case was formulated to estimate the costs and the resulting effects that various passive and active options have upon water temperature, weight gain and ice thickness. Rice's weanling Hereford heifer data (*Figure 3*) were used to determine water consumption and weight gain with respect to water temperature. The herd size was assumed to be 175 with an initial September mass of 204 kg/cow. The galvanized tank dimensions were 6.1 m and 0.66 m for the diameter and height, respectively.

A steady state mass and heat transfer analysis was performed on the tank to calculate the equilibrium water temperature and icing condition that the stockwater would obtain when exposed to the mean ambient conditions for each month. The calves' monthly water consumption and mass were also predicted. The analysis was similar to that utilized in DoE's *Energy Smart Pools* software package that estimates the cost-benefits for various pool coverings and thermal solar collector options. The major difference between these two models was that the absorption of solar radiation by the water was handled in a more comprehensive manner. This analysis also modeled the absorption of solar radiation by ice and its effect on the conduction of energy through the ice. *Figure 9* illustrates the various heat and mass transfer components evaluated in this model.

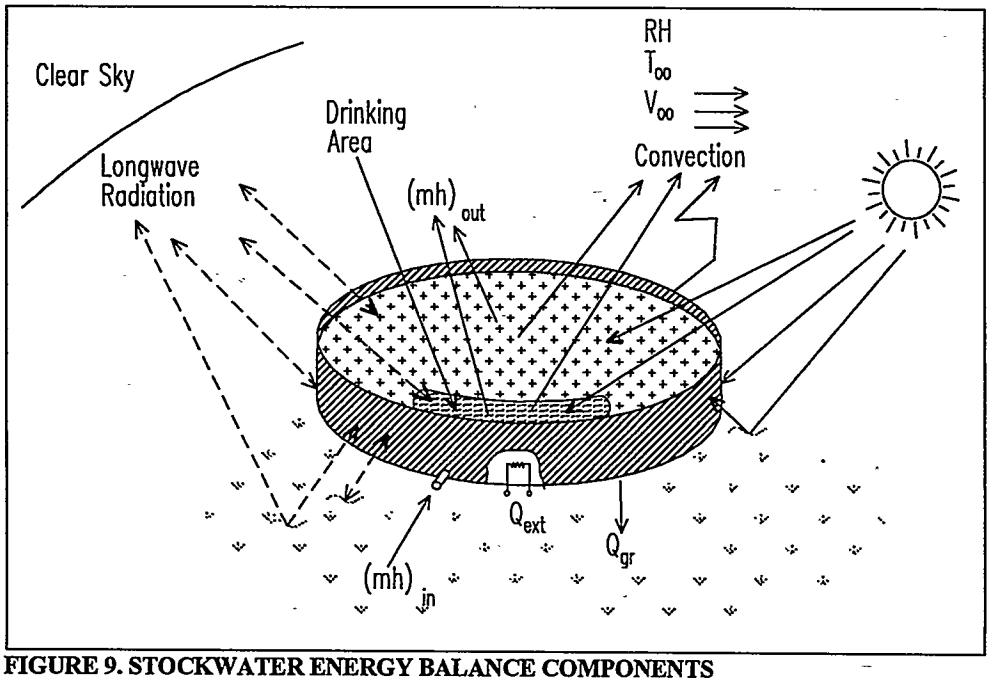

FIGURE 9. STOCKWATER ENERGY BALANCE COMPONENTS

Cheyenne's measured monthly average daily solar horizontal irradiation G_{SH} [Martner, 1986] was used for the horizontal input. The mean solar irradiation to the side of the tank G_{SV} was obtained from ASHRAE's radiation model [ASHRAE HANDBOOK]. The local estimated atmospheric clearness numbers ranged between 0.74 and 0.8 so the calculated daily horizontal irradiation matched the measured values (*Table 1*). A clear sky radiation correlation was used to calculate the sky radiation [Idso and Jackson, 1969]. This somewhat overestimates the longwave losses since skies for the Laramie region are only totally clear around 30% of the time in the winter months.

Three tank configurations were considered with and without heating from the wind electric system.

I. An unmodified tank used as the reference configuration.

II. A tank with a 0.5 m^2 drinking hole and the remaining water surface covered with weathered galvanized metal floated on plywood sheets (*Figure 9*). It was assumed that the floating cover provided no conductive insulation.

III. A smaller insulated tank that could hold a one day supply of water was inserted into the larger tank. The vertical walls of the insert were assumed to be constructed of 5 cm of foam insulation encased in 1.3 cm thick fiber reinforce concrete. Water from the well flows into the insert tank before entering the larger tank. The insert tank has a 0.5 m^2 drinking hole with the remaining water surface being insulated with 5 cm of foam and a galvanized cover. It was assumed that the inserted section would receive the same average G_{SV} as the larger tank. The larger tank's water surface was covered

except for a drinking hole. The cattle were assumed to drink from the warmest tank, and if the larger tank froze its ice temperature was set to the ambient temperature.

If resistive heating was used, the excess electric power indicated in *Figure 8* was assumed to be uniformly supplied to the liquid water. In Case III, all power was added to the insert tank.

RESULTS

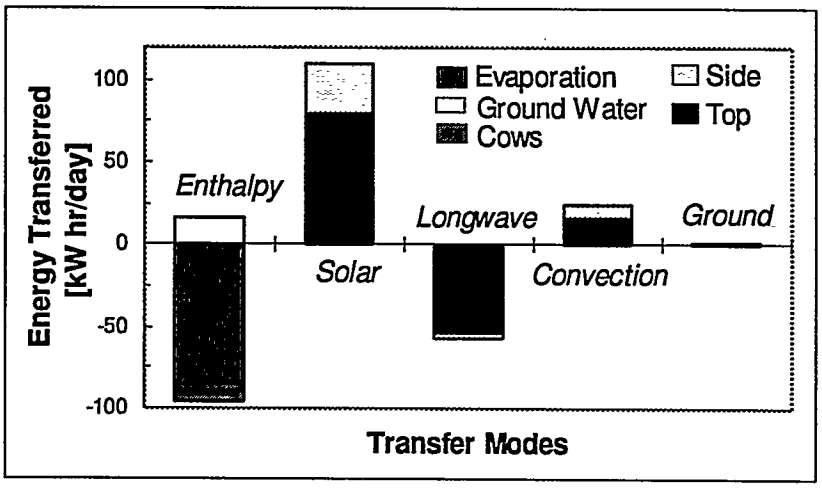

FIGURE 10. OCTOBER ENERGY COMPONENTS FOR THE REFERENCE TANK (CASE I)

Table 1 details the monthly results that were obtained and *Figures 10* and *11* indicate the magnitudes of the various components in the energy balance. As expected, evaporative cooling is very large in October, especially due to Laramie's low humidity that averages around 50%. One should note the long wave losses from the side of the tank are relatively small in comparison to its solar gain whereas the longwave losses for the water surface offset much of its solar gain. This is due to the fact that a weathered galvanized tank is somewhat of a selective surface in that its solar absorptivity and emissivity are 0.80 and 0.28, respectively. This illustrates how the floating galvanized surface mitigates both the evaporative cooling and the longwave losses from the water surface.

Figure 11 indicates the relationship between these energy terms when the tank is frozen and evaporation is no longer a significant component. Note that the long wave losses from the ice (top) are still large.

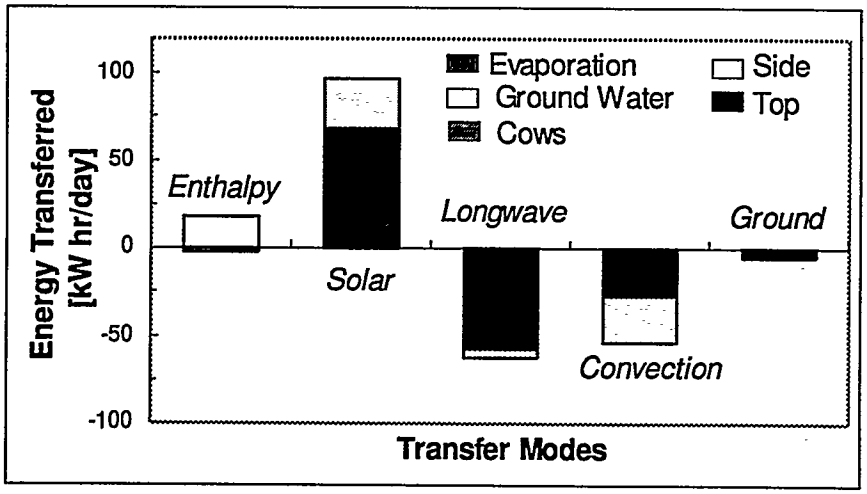

FIGURE 11. FEBRUARY ENERGY COMPONENTS FOR THE REFERENCE TANK (CASE I)

The steady state analysis predicts that the unmodified tank should be completely frozen during the months of December and January (*Table 1*). To estimate how long it takes to obtain an ice layer of thickness H_i, the one-dimensional, transient energy equation, that neglects the internal energy change within the ice itself, was applied to the ice slab. Also assuming a linear ice temperature profile with a constant top surface temperature T_s and a bottom

temperature equal to freezing water T_w resulted in the differential equation

$$\frac{dH_i}{dt} = \frac{k_i(T_w - T_s)}{\rho_i h_{sf} H_i} \quad \text{which implies that } t = \frac{\rho_i h_{sf} H_i^2}{2k_i(T_w - T_s)} \text{ for } H_i(0) = 0. \qquad (2)$$

Here k_i, ρ_i, h_{sf}, and H_i are the thermal conductivity, density, latent heat of fusion, and thickness for ice, respectively. Since the actual ice surface temperature T_s varies from an initial value of T_w to a value greater than the air temperature T_a for large time, a lower bound on time can be calculated by replacing T_s with T_a in the above equation. This implies that it takes approximately 26 days to freeze a 0.3 m thick ice layer for January's mean ambient temperature. However, the time required for the ice depth to reach 1.3 cm is only 1.2 hours. This implies that daily ice removal is require for the drinking hole and that the remaining portion of the tank must be cleared at least once a month during December and January.

CONCLUSIONS

A review of *Table 1* shows that both meaningful increases in weight gain and decreases in ice thickness can be obtained by all the passive measures. This was especially true with the insulated insert case which resulted in a weight gain increase of 3.8% and the elimination of freezing in this tank. Heating the tank had a major effect on equilibrium ice thicknesses and produced some additional weight gain for the galvanized cover case and a notable increase for the insulated insert case. The *cool season* water consumption rate varied from 3640 l/day to 2670 l/day. These rates are well below the 5000 l/day used to calculate the power available for resistive heating. Thus, the total calculated heating energy of 2000 kWhr over the *cool season* (7.5 kWhr/day average) should be a very conservative estimate since higher flow rates and lower C_p

TABLE 1. ENVIRONMENTAL CONDITIONS, RESULTS AND OPERATING CONDITIONS

Model	Month	Sept.	Oct.	Nov.	Dec.	Jan.	Feb.	March	April	May	Weight Gain/cow	% Increase
	Ta (C)	11.8	6.1	-1.3	-5.2	-6.2	-5.0	-2.7	2.8	8.9		
	Wind (m/s)	5.1	5.2	5.7	6.6	7.6	6.5	6.4	6.1	6.2		
	Gsh (kWhr/m^2/day)	5.3	3.9	2.4	2.1	2.3	3.3	4.6	5.7	6.1		
	Gst (kWhr/m^2/day)	3.4	3.0	2.2	2.3	2.3	2.8	3.2	3.2	3.3		
	Excess Power (kWhr/day)	4.1	4.4	6.0	9	11.7	8.7	8.5	7.4	7.8		
1p	Tw (C) or Hi (cm)	9.3	4.2	2	>66 !	>66 !	37	0*	2.6	7.2	89.9	0
2p	Tw (C) or Hi (cm)	17.3	10.6	2.1	58	>66 !	8	3.4	9.2	14.5	92.5	2.9
3p	Tw (C) or Twh (C)	17.2	10.5	4.1	3.4	3.1	3.7	4.2	9.0	14.4	93.3	3.8
1a	Tw (C) or Hi (cm)	9.3	4.2	1.0	43	50	16	0*	2.6	7.2	89.9	0.0
2a	Tw (C) or Hi (cm)	17.5	10.8	2.3	30	0.43	0.2	3.7	9.6	14.9	92.8	3.2
3a	Tw (C) or Twh (C)	17.4	10.7	5.7	5.8	6.1	5.9	6.3	9.3	16.6	94.1	4.7

OPERATING CONDITIONS

	p = Passive	Tw = Water Temp.	Twh = Heated Tank Temp.	! = Tank is Completely Frozen
	a = Active Heating	* = Partial Ice Cover	Hi = Ice Thickness	
1p	Standard tank			
2p	Floating weathered galvanized cover, 0.5 m^2 drinking hole			
3p	Floating weathered galvanized cover, 0.5 m^2 drinking hole, insulated 0.2*Vol. insert			
1a	Standard tank with excess turbine power			
2a	Floating weathered galvanized cover, 0.5 m^2 drinking hole, excess turbine power			
3a	Floating weathered galvanized cover, 0.5 m^2 drinking hole, excess turbine power, insulated 0.2*Vol. insert			

values were used. The maximum possible water temperature increase that 7.5 kWhr/day can produce at the minimum flow rate of 2670 l/day is 2.4 °C, which corresponds to an additional *cool season* weight gain of around 1.94 kg/cow.

TABLE 2. OPTION COST SUMMARY

Option	Cost [$]	Return [$]	Yield [$]	Frozen Months	Ice_{Depth} [cm]	T_{avg} [°C]
Reference Tank (1p)	0	0	0	4	56	2.6
Galvanized Cover (2p)	600	750	150	3	44	6.3
Cover & Insert (3p)	880	980	100	0	0	7.7
Power, Ref. Tank (1a)	90	0	-90	4	36	2.6
Cover & Power (2a)	700	840	140	2	10	6.6
Cover, Insert, Power (3a)	970	1220	250	0	0	9.3

An economic evaluation of the passive and active optional systems was conducted. The average ice thickness and water temperatures along with the option costs, returns and yields are presented in *Table 2*. The cost to implement all options are for material costs only and returns are based strictly on additional weight gain. Weight gain as a function of water temperature was compared to the reference weight with the excess considered to be the benefit of that option. An assumed selling price of 1.65 $/kg was used to determine the return of each option.

The results presented in *Table 2* show that the implementation costs for all options, except adding excess power to an unmodified tank, would be recovered in the first year. The maximum average *cool season* temperature increase of 6.7 °C occurred with the covered tank with an insulated insert and excess power from the wind turbine. This option also increased the weight gain the most as well as eliminated the need for any ice removal.

Additional benefits of these options would be the reduction of labor costs for ice removal, extended grazing days in remote areas and reduced feeding days. These costs can be significant as the minimum cost to feed hay to 175 cows is around $30/day. Therefore, any additional time that an optional system allows a rancher to utilize his remote grasslands will be financially beneficial.

Current controllers for wind-electric pumping systems cost around $1000 and use either voltage or frequency to determine the turbines cut in and out points for a given load. More sophisticated controllers are now starting to be introduced that utilize both voltage and frequency to determine its operation envelopes [Clark and Vick, 1996]. It is expected that the extension of these modern controllers to also handle impedance loads can be done at a minimal additional cost.

ACKNOWLEDGMENTS

We would like to thank Nolan Clark and Brian Vick at the United States Department of Agriculture, Bushland, Texas for their cooperation and input and the DoE/Wyoming Department of Commerce Sustainable/Renewable Energy Demonstration Program for its financial support.

REFERENCES

ASHRAE HANDBOOK, 1985 FUNDAMENTALS SI Edition, American Society of Heating Refrigerating and Air-Conditioning Engineering, Inc.

Clark, R. Nolan and Brian Vick," A smart controller for wind electric water pumping systems," 15th ASME Wind Energy Symp., Houston, TX. 1996. *Proc. Windpower'96*, pp 204 - 208.

Clark, R. Nolan, "Performance of small wind-electric systems for water pumping," *Proc. Windpower'954* AWEA, 1994, pp 627-634.

Clark, R. Nolan and K.E. Mulh, "Water pumping for livestock" *Proc. Windpower'92* AWEA, 1992, pp 284-290.

Cliff, W.C., *The Effect of Generalized Wind Characteristics on Annual Power Estimates from Wind Turbine Generators,* PNL-2436, Richland, Washington:Battelle Pacific Northwest Laboratory, 1977.

Climate of Laramie Wyoming, Climatography of the United States NO. 20., NOAA, Department of Commerce, 1976.

Energy Smart Pools, Assumptions & Calculations, Version 2 for Windows, U.S. Department of Energy, Denver Regional Support Office.

Idso, S.B. and R.D. Jackson, "Thermal Radiation from the Atmosphere," *Journal of Geophysical Research*, Vol. 74, 1969.

Lukens, A.M. and M.E. Hamilton, *Solar Warmed Water for New Mexico Cattle, Bulletin No. 25*, Engineering Experiment Station, New Mexico State University, 1962.

Martner, Brooks E., *Wyoming Climate Atlas*, University of Nebraska Press, 1986.

Rice, I.G., *Optimum Temperature of Drinking Water for Hereford Heifers on Range Land*, Ph.D. Thesis, Colorado State University, 1979.

Spera, David A., Ed., *Wind Turbine Technology, Fundamental Concepts of Wind Turbine Engineering*, ASME Press, 1994.

TRNSYS HYBRID WIND DIESEL PV SIMULATOR

P.J.A. Quinlan
J.W. Mitchell
S.A. Klein
W.A. Beckman
N.J. Blair

Solar Energy Laboratory
University of Wisconsin-Madison
1500 Engineering Drive
Madison, Wisconsin 53706
USA

ABSTRACT

The Solar Energy Laboratory (SEL) has developed a wind diesel PV hybrid systems simulator, UW-HYBRID 1.0, an application of the TRNSYS 14.2 time-series simulation environment. An AC/DC bus links up to five diesels and wind turbine models, along with PV modules, a battery bank, and an AC/DC converter. Multiple units can be selected. PV system simulations include solar angle and peak power tracking options. Weather data are Typical Meteorological Year data, parametrically generated synthesized data, or external data files. PV performance simulations rely on long-standing SEL-developed algorithms. Loads data are read as scalable time series. Diesel simulations include estimated fuel-use and waste heat output, and are dispatched using a least-cost of fuel strategy. Wind system simulations include varying air density, wind shear and wake effects. Time step duration is user-selectable. UW-HYBRID 1.0 runs in Windows®, with TRNSED providing a customizable user interface.

BACKGROUND

TRNSYS (pronounced "transis"), commercially available since 1975, was initially designed to simulate the transient performance of thermal energy systems. Each physical component in a system, such as a pump or solar collector, is represented by a FORTRAN subroutine. The subroutines are then linked into a compiled executable code. An input text file coordinates the linking of the subroutines, and also describes the performance parameters for each subroutine. All TRNSYS users have access to the FORTRAN source code and can create their own subroutines and simulations of physical systems. This has resulted in a diversity of simulations, from solar photovoltaic (PV) pumps and vehicles, to dairy farms, to regional utility dispatching analyses (Cragan, 1995).

In recent years, TRNSYS has become more widely used in building energy analyses (Thornton, 1991), PV systems analyses (Al-Ibrahim, 1996), and utility renewables planning (Trzesnieski, 1996). TRNSYS is also used extensively in Europe, with development and distribution activities in Sweden, France, Germany and Belgium. Two separate front-end applications also now run TRNSYS code under different user-interfaces (SEL, 1996a).

TRNSYS

TRNSYS relies on a modular approach to solve energy system simulations and requires an input file in which the user specifies the components that constitute the system, and the manner in which they are connected. Each of the TRNSYS components has inputs and outputs which represent the weather data, energy flows, and control signals of the physical counterparts. All the subroutines are linked and

then controlled by the main TRNSYS program. The input file sends parameters and initial values to each system component, and describes how the different system components are linked together. For each component, a number of parameters (variables that do not change with time), inputs (variables that change with time and may come from other components) and initial values are entered into the input file.

TRNSYS users are able, through this input file, to completely describe and monitor interactions between system components. The process of system simulation is therefore open to the user and straightforward. Built-in capabilities include plotting routines, output-file data routines, on-screen plotting during processing, and parametric operation.

A user initiates the simulation process by entering an editing environment program called TRNSHELL (pronounced "transhell"). Figure 1 shows an example TRNSHELL screen. This editing environment includes cut/copy/paste and search/replace options; context sensitive help; plotting routines; and houses the various TRNSYS utilities, including video, printing and compiler settings. The user can create a new input file or edit existing input files to define a simulation. The user then runs the simulation by selecting "Calculate" from a pull-down menu. During the simulation creation phase of a project, TRNSHELL is used for debugging, for viewing run-time plots and for viewing post-simulation plots of selected variables. TRNSHELL is also used to create the help files for the simulated devices.

With the specification of input files complete, a user may wish to distribute a simulation to users who may have less expertise in the operation of the simulated system. In this case, a run-time front-end application, TRNSED (pronounced "transed"), can be employed. The expert user can choose which variables are available for editing in the TRNSED input file. Detailed help, unit conversion, and input checking for each item is provided. A screen from a TRNSED user interface is shown in Figure 2. TRNSYS and its component applications run in DOS as well as Windows® 3.1, 95, and NT.

In many instances, a user may wish to explore the sensitivity of system performance on an input variable. If so, the user may post any of the TRNSYS variables displayed in the user-interface to a

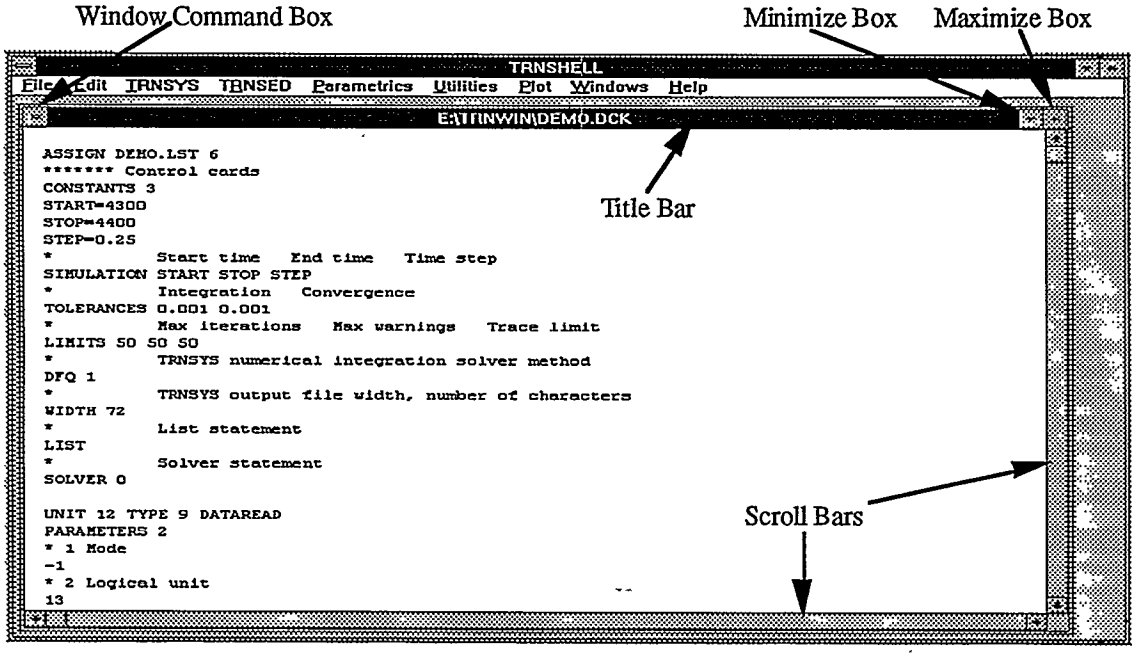

FIGURE 1. EXAMPLE TRNSHELL SCREEN.

Parametric Table. By selecting the number of runs and a range across the runs, the user has the capability to create a "batch" of simulations. This allows the user to set up unattended repeated operation of a complex simulation, or to carry out detailed optimization studies. Plotting and output data capabilities can be applied to the Parametric Table results to allow examination of results across runs.

TRNSYS also allows the display of 10 variable values in a plotting window while a simulation progresses. This window has the ability to pause the TRNSYS simulation while running, change the scale of the plot, hide one or more variables on the plot, and zoom into the display.

TRNSYS COMPONENT LIBRARIES

TRNSYS components are available in two major libraries. The first is provided with the program, and contains the components developed at the Solar Energy Laboratory. This library includes the core components used in most simulations, as well as more complex components developed at SEL. The second source of information is the library of "user-written" components shared with SEL by the user community. This library is maintained on the Internet (SEL 1996b). Existing components from these libraries which are used by UW-Hybrid 1.0 are:

- TMY Data Reader — *Reads in weather data from a "Typical Meteorological Year" file.*
- Text File Reader — *Reads in loads values and other text file data.*
- Hourly Printer — *Sends values of variables to an output file each hour.*
- Solar Radiation Processor — *Determines temperature and incident solar radiation.*
- Photovoltaic Array — *Calculates PV array power each hour.*
- Storage Battery — *Simulates operation of a lead-acid battery.*
- On-Line Plotter — *Shows values on screen during simulation.*
- Quantity Integrator — *Integrates hourly data for monthly results.*
- Histogram — *Creates histograms of selected variables.*

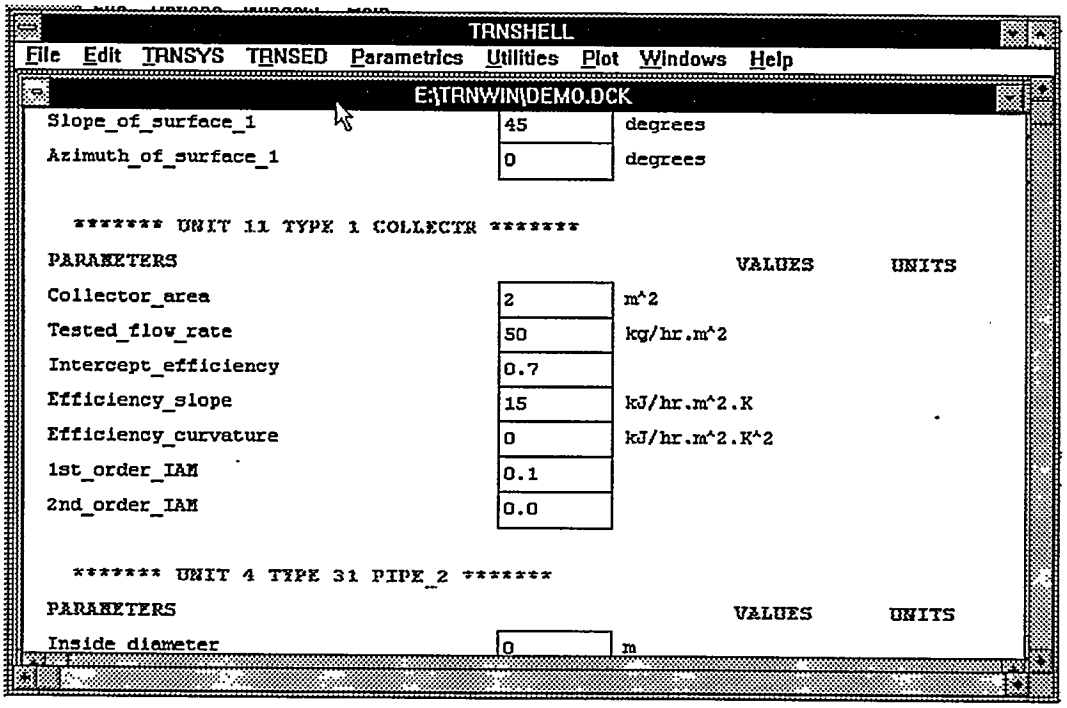

FIGURE 2. EXAMPLE TRNSED USER INTERFACE.

TRNSYS WIND DIESEL HYBRID COMPONENTS

Recently, as additions to the TRNSYS library of components, the authors have created new components for the wind diesel PV hybrid systems simulator. These components are:

- Single Wind Turbine — *Estimates performance of single wind turbine.*
- Wind Turbine Cluster — *Estimates performance of multiple turbines in cluster.*
- Diesel Generator — *Estimates performance of single diesel generator.*
- Diesel Dispatcher — *Selects least-cost combination of diesels to match load.*
- AC/DC Converter — *Determines efficiency of energy AC/DC conversion.*

Each of these components is described further in the paper. In each case, the component was designed in such a way as to simulate the performance of the device in the context of its role as a part of a larger system simulation. For example, the simulation of the wind turbine produced outputs of power output, coefficient of performance, on/off status, etc.

Single Wind Turbine Component

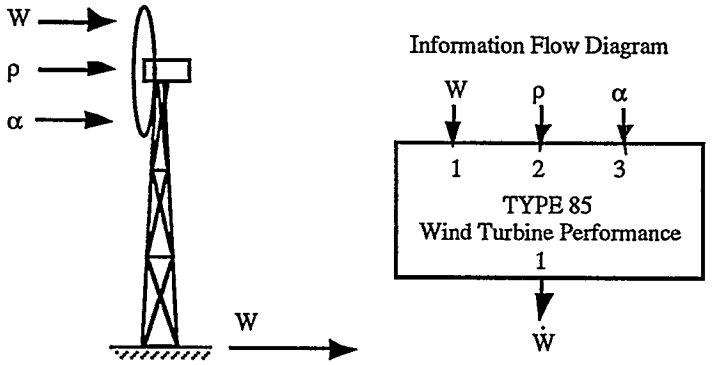

The single wind turbine component simulates the performance of a wind turbine in either of two modes: parametric or empirical. For each timestep, both modes rely on algorithms to determine shear corrections, air density, and resulting air density effect on the power curve. Shear corrections are based on a power-law model, with exponent values derived from a time-series, calculated from available data, or input by the user. Air density is calculated using the ideal gas law and a temperature lapse rate model (White, 1994).

The empirical calculation mode estimates wind turbine performance by linear interpolation of values from a power curve table. Air density corrections for empirical power curves are applied using the AWEA / IEA methodologies (AWEA, 1988) (IEA, 1982).

The parametric performance model creates a wind turbine power curve based on cut-in wind speed, rated wind speed, cut-out wind speed, and rated power output. The parametric model constructs the portion of the power curve between cut-in and rated wind speed based on a quadratic model. (Koeppl, 1982).

Wind Turbine Cluster Component

The TRNSYS wind turbine cluster component is the first implementation of a cluster array loss model in a time series context. The TRNSYS cluster model employs the wake deficit model developed and verified by the U.S. Department of Energy (Veenhuizen, 1988).

Information Flow Diagram

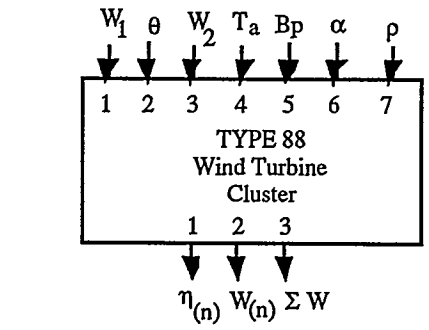

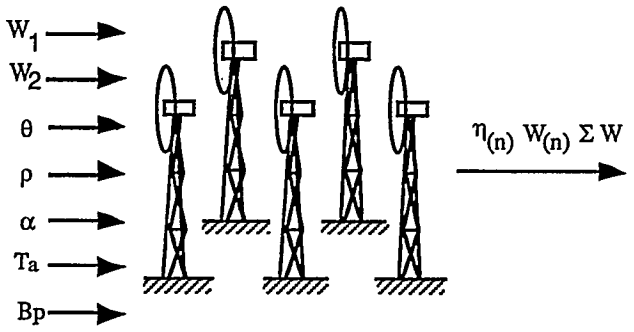

Parameters:

1. Input Units
2. Output Units
3. Wind Data Height*
4. Air Density Mode
5. Air Density**
6. Wind Shear Mode
7. Wind Shear***
8. X coordinate (turbine n)
9. Y coordinate (turbine n)
10. Z Site Elevation (turbine n)
11. Hub Height (turbine n)
12. Power Curve Mode (turbine n)
16. Power Curve File (turbine n)*
17. Rotor Diameter (turbine n)
18. Rotor Center Height (turbine n)

* Optional; only if data height differs from rotor center height.

** If 1, $\rho = \rho(t)$
if 2, $\rho = \rho(Ta, Bp)$
if 3, $\rho = \rho(Ta, Elevation)$
if 4, then user input,
else ρ = STP.

*** If 1, $\alpha = \alpha(t)$
if 2, $\alpha = \alpha(W1,W2)$
if 3, then user input,
else $\alpha = 1/7$.

In order to maintain adequate processing speed, the cluster wake deficits are preprocessed by TRNSYS prior to time-series modeling. At the beginning of the simulation, TRNSYS calculates the power output of each turbine as a function of wind speed and wind direction. During time-series simulation, TRNSYS interpolates the data array.

The cluster model proceeds along the following process to calculate performance:

1. Input turbine x, y, z location and power curve data.
2. For each wind direction, from 0 to 350, in ten degree increments:
   A. Transform coordinates to new a downwind, crosswind system.
   B. For each wind speed, from cut-in to cut-out:
      - Calculate wake deficit per turbine location due to all turbines. (Calculate rotor averaged wind speed at its location in wake.)
      - Apply all deficits to wind speed to obtain a turbine net local wind speed.
      - Calculate power output of the turbine at the net local wind speed.
      - Sum wind turbine power outputs to determine cluster totals at that speed.

The net result is a FORTRAN array dimensioned by wind turbine, wind speed, and wind direction. TRNSYS then interpolates the array per turbine, per timestep.

Diesel Generator Component

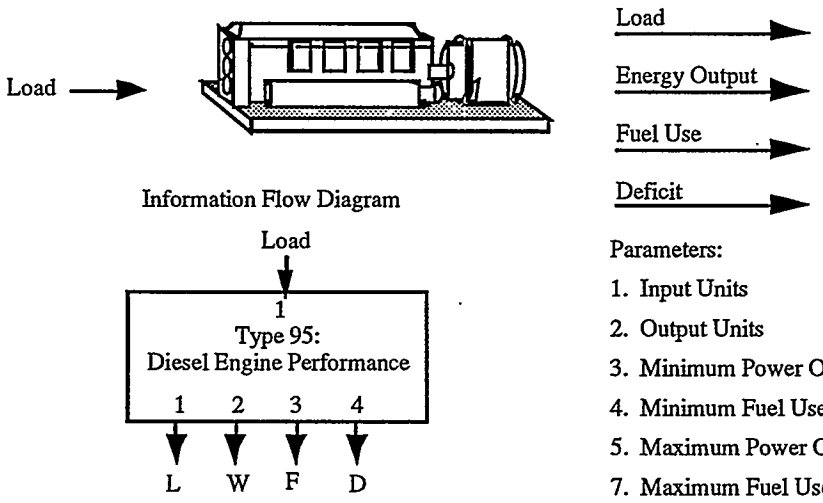

The diesel generator component estimates the amount of fuel, waste heat, and power output of the generator as a function of load. The model is parametric, in that two points on a specific fuel-use line are input to the component. These values are:

- Minimum power output, kW, and specific fuel use at minimum power, kg/kWh
- Maximum power output, kW, and specific fuel use at maximum power, kg/kWh.

Below the minimum power output, all values are set to the minimum. Above maximum power output, all values are at the maximum. In this way, the system simulation results in calculations of levels of dump energy or unmet load, as shown in Figure 3 below.

The TRNSYS diesel component also calculates waste heat produced by the engine generator. This is determined based on the heating value of diesel fuel, rate of fuel use, and net output of the generator. This is valuable information because, in many hybrid power systems, the waste heat is put to use in a cogeneration application.

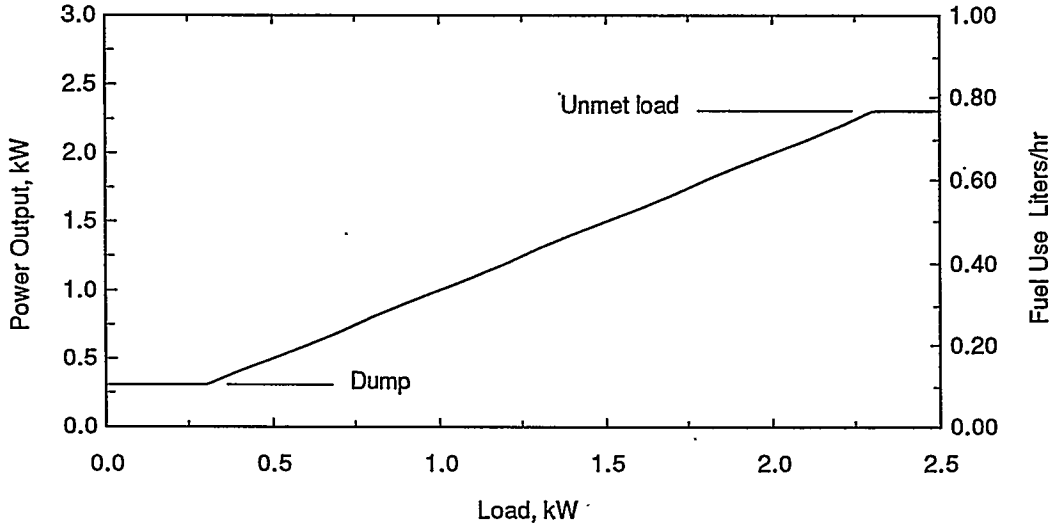

FIGURE 3. EXAMPLE DIESEL OUTPUT AND FUEL USE AS A FUNCTION OF LOAD.

Diesel Dispatcher Component

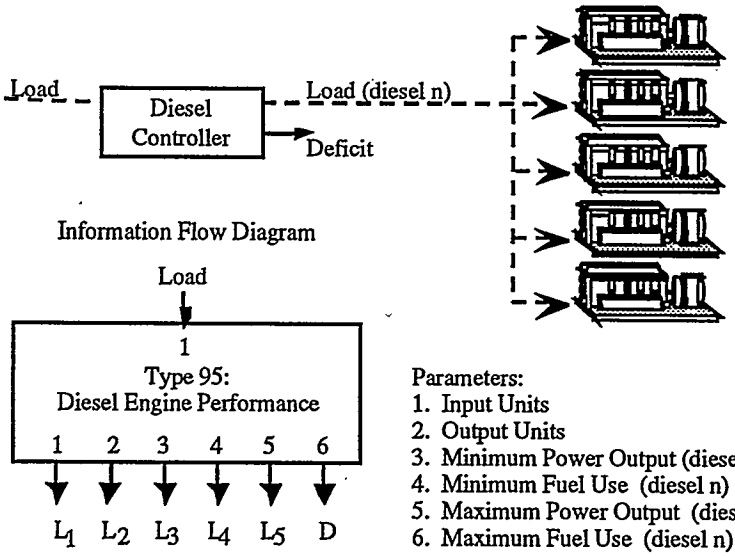

The diesel dispatch component can handle up to five different diesel generators. The strategy employed by the dispatcher, stated simply, is:

Select the least-cost combination of units able to meet demand.

The dispatcher determines least cost based on the specific fuel values given in the file for each diesel it controls. The component programs itself by reading in the performance characteristics data files which describe each engine it controls. In operation, this strategy results in plots such as given in Figure 6 below. Total output in Figure 4 does not equal demand due to accounting for losses.

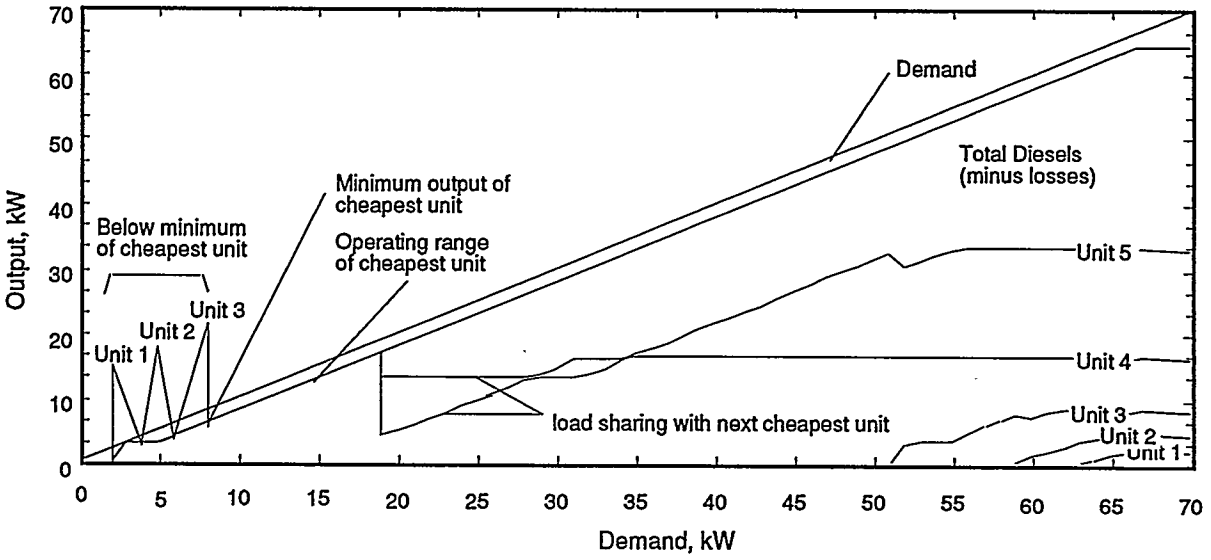

FIGURE 4. EXAMPLE DISPATCH PLOT FOR FIVE DIESEL GENERATORS.

The production envelope of combined diesel operation exhibits the following regions:

Below the minimum rating of the "cheapest diesel." In this region, the component searches through the operating characteristics of each diesel to find the cheapest combination.

Operating range of the cheapest diesel. Cheapest diesel follows the load.

Operating range of the cheapest diesel, minus the minimum output of the "next cheapest diesel". In this region, output of the cheapest diesel is reduced in order to allow for the minimum output of the next cheapest to be included.

Operating range of the next cheapest diesel, plus maximum of cheapest diesel. In this region, the output is simply equal to the cheapest unit plus the load following in the range of the next cheapest unit.

This pattern is repeated for the remaining diesels. Any wind or solar power serves to reduce the apparent load to the diesels. When there is stored power available, the diesels operate whenever the state of charge falls below a user-defined setpoint.

AC/DC Converter Component

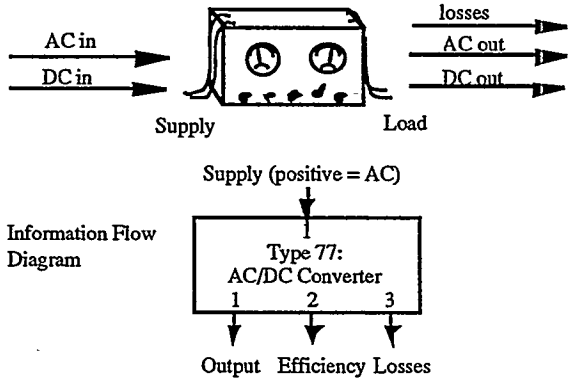

Parameters:
1. Input Units
2. Minimum Inverter Load
3. Efficiency at Inverter Minimum Load
4. Maximum Inverter Efficiency
5. Load at Maximum Inverter Efficiency
6. Rated Inverter Load
7. Efficiency at Rated Inverter Output
8. Minimum Rectifier Load
9. Efficiency at Rectifier Minimum Load
10. Maximum Rectifier Efficiency
11. Load at Maximum Rectifier Efficiency
12. Rated Rectifier Load
13. Efficiency at Rated Rectifier Output

The AC/DC converter creates an efficiency curve based on three points: minimum output, most efficient output, and rated output. An efficiency curve, as shown in Figure 5, is created using a variation of the formulation employed by (Jennings, 1996).

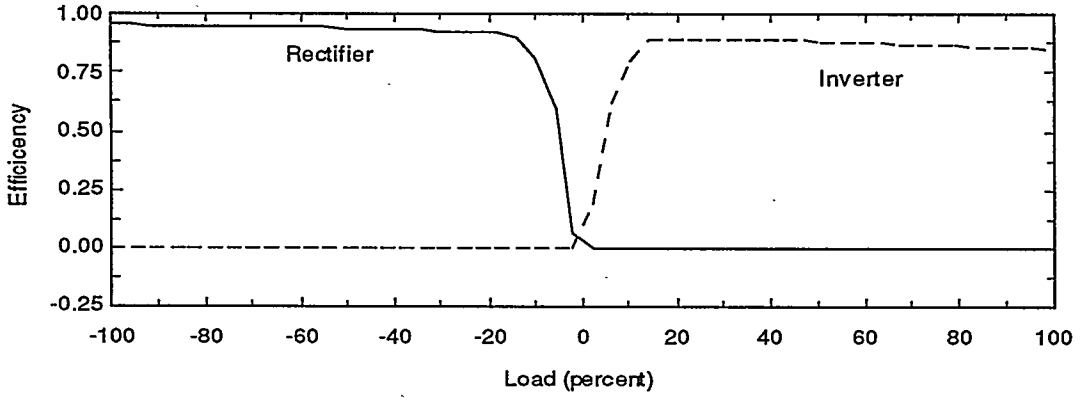

FIGURE 5. TYPICAL AC/DC CONVERTER EFFICIENCY CURVES.

HYBRID SYSTEM SIMULATIONS

In UW-Hybrid, an AC/DC bus links up to five diesels and wind turbine models, along with PV modules, a battery bank, and an AC/DC converter. Multiple units can be selected. PV system simulations include solar angle and peak power tracking options. Weather data are Typical

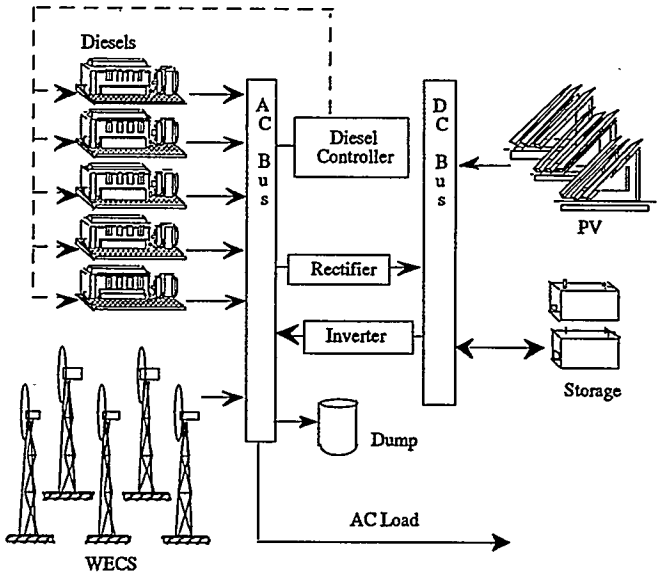

Meteorological Year data, parametrically generated synthesized data, or external data files. PV performance simulations rely on long-standing SEL-developed algorithms. Loads data are read as scalable time series.

Using the standard data readers, radiation processor, integrators and output printers, the TRNSED implementation features: user-selectable weather files and loads files; user-selectable commercial PV modules and number and orientation of modules; user-selectable commercial wind turbines, number, shear, losses, etc., and up to five user-selectable diesel gensets.

Figure 6 shows the output for a simulated week of operation of a Hybrid system in Wisconsin. It can be seen in the figure how wind turbine output reduces the diesel requirement to meet load.

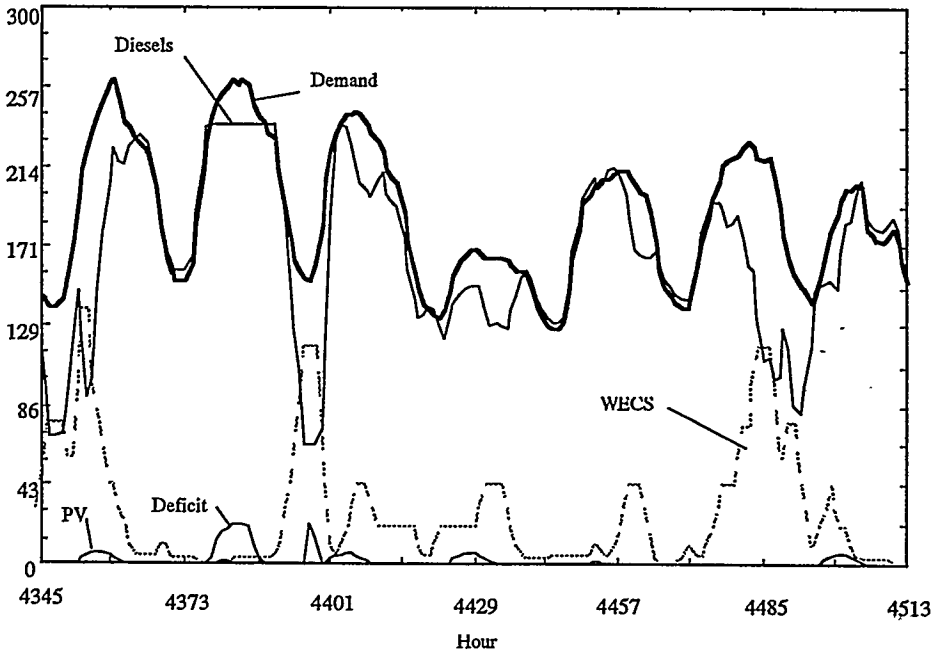

FIGURE 6. SIMULATED WEEK OF OPERATION OF HYBRID SYSTEM IN WISCONSIN.

Performance

A one year simulation of five turbines, five diesels and a bank of PV modules is completed in about three minutes on a 100 MHz Pentium, and seven minutes on a 100 Mhz '486 PC. The software is compiled FORTRAN code, with user-interface elements created in Pascal using Delphi.

FUTURE ACTIVITIES

SEL will continue to improve the wind turbine model and other new components contained in the UW-Hybrid simulation. This will include verification and validation of the components, as well as the overall hybrid system simulation. Other contemplated projects include a utility valuation study similar to (Trzesnieski, 1996) and a simulation of a municipal wind turbine project in Wisconsin.

ACKNOWLEDGMENTS

Work on this project was supported, in part by the Wisconsin Department of Administration: Wisconsin Energy Bureau, and by the University of Wisconsin-Madison. The authors would like to also thank the U.S. Department of Energy for continued support of the TRNSYS program.

REFERENCES

Al-Ibrahim, et al. (1996) "An Investigation of Photovoltaic Powered Pumps in Direct Solar Domestic Hot Water Systems." In *Proceedings, Solar 1996*. Boulder Colorado: American Solar Energy Society. pp. 141-152.

American wind Energy Association. (1988) Standard Performance Testing of Wind Energy Conversion systems. AWEA Standard 1.1 Washington, D.C.: American Wind Energy Association.

Cragan, Keary, E. (1994) "Impact on a Utility of An Ensemble of Solar Domestic Hot Water Systems." MSc. Thesis. Madison, Wisconsin: Solar Energy Laboratory, University of Wisconsin-Madison.

International Energy Agency (1982) *Recommended Practices for Wind Turbine Testing: 1. Power Performance Testing*. Sten Frandsen, et al., editors. Roskilde, Denmark: Risø National Laboratory.

Jennings, S.U., et al. (1996) "RESIM, A Simulation Program for Determining the Viability of Renewable Energy Power Supply Systems." draft document number 96-04-12 1894. Murdoch, Australia: Murdoch University Energy Research Institute.

Koeppl, Gerald W. (1982) *Putnam's Power From the Wind: Second Edition.* New York: Van Nostrand Reinhold Company. pp. 316-317.

Solar Energy Laboratory. (1996a) *TRNSYS 14.2, A Transient System Simulation Program: Featuring IISiBat and PRESIM*. Madison, Wisconsin: Solar Energy Laboratory, University of Wisconsin-Madison.

Solar Energy Laboratory. (1996b) http://www.engr.wisc.edu/centers/sel/sel.html

Thornton, Jeff William. (1991) "Supermarket Refrigeration Systems." MSc. Thesis. Madison, Wisconsin: Solar Energy Laboratory, University of Wisconsin-Madison.

Trzesnieski, Jason, et al. (1996) "Impact of a Solar Domestic Hot Water Demand-Side Management Program on an Electric Utility and its Customers." In *Proceedings, Solar 1996*. Boulder Colorado: American Solar Energy Society. pp. 366-373.

Veenhuizen, Scott D., et al. (1989) "Verification of Numerical Model for Predicting Array Performance in Complex Terrain." In *Proceedings, Wind Power 1988*. Wash.D.C.: American Wind Energy Association. pp. 413-422.

White, Frank. (1994) *Fluid Mechanics: Third Edition.* New York: McGraw Hill, Inc. p. 57.

Hybrid2 - The Hybrid Power System Simulation Model

E.I. Baring-Gould, H.J. Green, V.A.P. van Dijk
National Renewable Energy Laboratory
1617 Cole Boulevard, Golden, CO 80401 USA

J.F. Manwell
Renewable Energy Research Laboratory
Department of Mechanical Engineering
University of Massachusetts
Amherst, MA 01003 USA

ABSTRACT

There is a large-scale need and desire for energy in remote communities, especially in the developing world; however the lack of a user friendly, flexible performance prediction model for hybrid power systems incorporating renewables hindered the analysis of hybrids as options to conventional solutions. A user friendly model was needed with the versatility to simulate the many system locations, widely varying hardware configurations, and differing control options for potential hybrid power systems. To meet these ends, researchers from the National Renewable Energy Laboratory (NREL) and the University of Massachusetts (UMass) developed the Hybrid2 software. This paper provides an overview of the capabilities, features, and functionality of the Hybrid2 code, discusses its validation and future plans. Model availability and technical support provided to Hybrid2 users are also discussed..

INTRODUCTION

With the increasing need for electrical generation in the developing world, the market potential for renewable based hybrid power systems is emerging. In order to address this emerging market, an analysis tool was required by industry, researchers, and development institutions to accurately model the performance and economics of alternative hybrid designs. This analysis tool would require enough versatility to model the many system locations, widely varying hardware configurations, and differing control options for potential hybrid power systems. In response to this need, researchers from the National Renewable Energy Laboratory (NREL) and the University of Massachusetts (UMass) developed the Hybrid2 software. Hybrid2, like its predecessor HYBRID1, is a time-series/probabilistic model that uses time-series resource and load information, combined with statistical analysis, and manufacturers data for hybrid system equipment to accurately predict the performance and cost of hybrid power systems. Hybrid2 is also a user friendly tool that allows for the direct comparison of many different renewable and non-renewable power system designs.

Hybrid2 was designed to study a wide variety of hybrid power systems. The hybrid systems may include three types of electrical loads, multiple wind turbines of different types, photovoltaics, multiple diesel generators, battery storage, and four types of power conversion devices. Systems can be modeled on the AC, DC, or both buses. A variety of different control strategies/options may be implemented which incorporate detailed diesel dispatch as well as interactions between diesel gensets and batteries (Barley, 1995) . An economic analysis tool is also included that calculates the economic worth of the project using many economic and performance parameters. The Hybrid2 code employs a user-friendly Graphical User Interface (GUI) and a glossary of terms commonly associated with hybrid power systems. Hybrid2 is also packaged with a library of equipment to assist the user in designing hybrid power systems. Each piece of equipment is commercially available and uses the manufacturers' specifications. In addition the library includes sample power systems and projects that the user can use as a template. Two levels of output are provided, a summary

and a detailed time step by time step description of power flows. A Graphical Results Interface (GRI) allows for easy and in-depth review of the detailed simulation results.

The validation and verification of the Hybrid2 code is ongoing and very positive. Comparisons have been made among a number of operational hybrid power systems and the Hybrid2 code with validation efforts continuing during the summer of 1996. The Hybrid2 code is also heavily based on its predecessor, HYBRID1, which has been extensively validated (Manwell et al., 1994; Baring-Gould, 1995). The validation of the Hybrid2 code is discussed in greater detail later in this document.

CODE OVERVIEW

Hybrid2 was designed to be a very flexible and easy to use tool to conduct predictions of potential hybrid power system long-term performance and cost. The developers have provided enough structure to allow users with limited knowledge of hybrid systems to evaluate them as one of the electrification solutions while also facilitating detailed analysis for those with more design experience. Hybrid2 is not a complete system design tool, but a middle step to provide a preliminary system performance predictions before the final system design is completed. Hybrid2 is not a dynamic model and will not account for system transients and stability on the order of 30 seconds or less. The Hybrid2 user interface is divided into five modules that comprise a project. The project is a specific power system applied to a particular community or site. The five modules are the community loads, the site/resource information, the proposed power system, an all-diesel power system for comparison and system economics. Each of these modules are discussed below.

Loads Module

Hybrid2 allows for a system to contain loads on both the AC and/or DC buses. The code also provides for the use of three types of loads, primary, deferrable and optional.

The primary load is used to specify the load served on-demand for the community under analysis. The primary load is made up of time series data. An inter-time step variability or standard deviation can also be included which allows for a more accurate prediction of the power systems operation. The primary load must be supported by the power system and any load that is not met is reported. If time series data is not available, Hybrid2 includes a matrix load generator that may be used. This allows the user to specify the average load for each hour of a typical day, generated with a separate worksheet provided with Hybrid2, and a monthly scale factor. The user is still required to specify the variability in the load.

Deferrable and optional loads are two forms of managed loads that can have economic value on small electric grids. Deferrable loads are electrical load that contains a limited amount of storage and thus may be deferred to utilize excess energy. If the deferrable load is not met over a given time period the load is treated as a primary load and must be supplied. Examples of a deferrable loads are an icemaker or water cistern. An optional load represents a useful application for excess electricity that is never served as a primary load, such as space or water heating. If no excess energy is available to meet such a load then it is either unserved or met by other means.

Site/Resource Module

The Site/Resource Module allows the user to merge a combination of resource data and site parameters to include in different projects. There are three types of resource input data that can be used in simulation runs of Hybrid2: wind speed, solar insolation and ambient temperature. Each of these types of resource data take the form of time series averages. The wind resource may also include an inter-time-step standard deviation or variability. Key parameters that affect those resources, such as wind turbulence, and ground reflectivity may also be specified.

Power System Module

The Hybrid2 code is based on a two bus system (AC and DC) but also can model a "coupled diesel" system, in which a diesel is directly connected to a rotary converter. The diverse structure of the model allows for many combinations of wind turbines, photovoltaic arrays, diesel generators, power converters, and battery storage, both in AC, DC, or two-bus systems, as shown in Figure 1. Both buses may be active in a given system with loads and generating sources applied to each bus simultaneously. The power system is defined with components selected from the on-line library. Each type of component is included in a subsystem that is used to define all of the relevant parameters associated with that technology. For example; a specific photovoltaic module from the Hybrid2 library is inserted into the PV subsystem where all the parameters associated with the PV array are defined. This component methodology allows for a wide flexibility in the definition of a power system, as well as giving users the ability to include new components in project analysis.

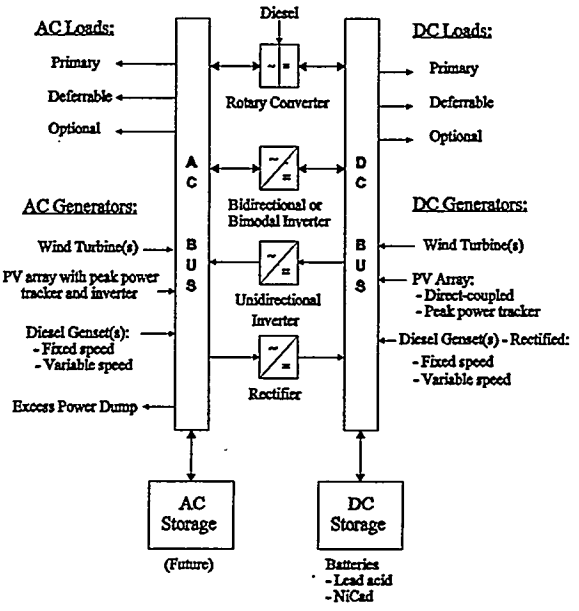

FIGURE 1. CONFIGURATIONS FOR HYBRID2 POWER SYSTEMS

Hybrid2 allows for many different control strategies for systems that contain battery storage and/or diesels. Since the renewable power output and the load are given for a specific simulation, the only true control questions are in the operation of the diesel generator, the battery bank, and any interaction between the two. Hybrid2 allows for more than 180 different dispatch configurations considering questions such as these: How the batteries are used? When does the diesel start? At what power level is it operated when running? When is it shut down (Barley, 1996)? The model also allows the user to specify dispatching specific to each diesel.

Base Case Module

The Hybrid2 code allows for the specification of a base case all-diesel system to use as a comparison to the hybrid system. The base case system is described by one or more diesels, some operation criteria, and a dispatch order. This module is not required to run Hybrid2 simulations.

Economics Module

Hybrid2 includes a detailed economic model that allows the user to determine basic economic figures-of-merit for a particular project. It has been provided to allow for comparisons between differing power system options and to determine approximate system costs. The economics engine uses performance information from a simulation run and economic data supplied by the user to calculate parameters such as payback period, internal rate of return, cash flow, and equipment replacement expenses. The user has wide flexibility in determining the expenses of the project and what detail of inputs to include. Parameters such as grid extension, import tariffs, system administration costs, and taxes can be included in the analysis. Economics simulations can be conducted independently of the simulation engine to make it possible to conduct wide ranging parametric analysis of any economic input without repeating performance simulations.

CODE STRUCTURE

The program is structured in four blocks. The first is the GUI in which the project to be analyzed is specified and created. The second block consists of the simulation engine in which the performance of the system is calculated. The third block is the GRI in which the user can plot and view both the system performance and inter-system component interaction. The user may preform an analysis of the performance output and then modify the original project and conduct additional simulations if required. The final block is the economics module in which an analysis can be conducted varying certain key economic parameters. Both performance and cost simulations can be repeated until an acceptable design is achieved. Hybrid2 is not an optimization software and presently parametric analysis must be conducted manually.

Graphical User Interface

The GUI allows the user to create all aspects of the hybrid system project and start the simulation in a user-friendly windows-based environment. The GUI also performs range checking and a completeness check to insure that each section is complete before the user is allowed to continue. In addition, prior to the execution of the project simulation, Hybrid2 performs a consistency check on the project.

The GUI includes three main features that assist in the creation, use, and storage of projects. First an on-line library includes sample projects, time series data, sample power systems, and manufactures data on system components. The user may use the existing library records, modify library records to update performance information, or enter data for components not presently included in the NREL library. All user records become part of the library and can be used at a later date and in multiple projects. All of the component records that make up the Hybrid2 library are defined by information that is usually provided on a manufacturer's specifications sheets. This library allows users to easily create, combine and, reuse whole modules and individual components. Second, a Glossary is provided to help the user by providing on-line definitions of all of the parameters used in the Hybrid2 code. The glossary also provides, if applicable, an example, default values, recommended ranges and hard limits for all code input. Third, an Import/Export function has been included that not only allows the user to transfer projects and components to other copies of Hybrid2 but also allows for the backup and long term storage of projects that are not currently being analyzed. The GUI is described extensively in Baring-Gould, 1996.

Simulation engine

Hybrid2 uses an energy balance approach within each time step such that the sum of the average outputs of all the energy sources (such as wind, PV, gensets, and storage output) must equal the sum delivered to all the energy sinks (typically loads, storage input, and losses). A probabilistic method is used within each time step to account for the short-term fluctuations in the load and renewable resources (Manwell et al., 1996). These inter-time-step fluctuations, which are input by the user, can have a significant impact on diesel dispatch and subsequently the performance of a system. The spacing between turbines in a multi-turbine system is also considered to account for the power smoothing effect of multiple wind turbine arrays (Beyer et al., 1989). Hybrid2 can use time steps typically between 5 minutes to 2 hours in length. It should be noted that all of the main component algorithms used in Hybrid2 are based on industry accepted research.

Within each time step of a simulation, system performance is calculated by the following steps. The "Net Load" is determined which refers to all of the load(s) on the system less the contribution of the renewable energy sources. When this value is positive, energy must be supplied by the diesel genset(s), battery storage or both. When the net load is negative, there is extra power available which may go to storage, a deferrable or an optional load. The effect of the probabilistic method is that the net load is not a single value during a time step. Rather it is a distribution of values; in Hybrid2 it is assumed that the values are normally distributed. In extreme cases, the net load may be positive for part of the time, but negative for the rest. The most significant aspects of the net load are its mean and its range (maximum and minimum) which will affect

the determination of which diesels are on line, how much power they produce, and how much fuel they use. Next, the energy flow to or from the battery will be calculated and surplus energy will be made available to either deferrable or optional loads. If the power system is incapable of meeting the load during a time step, the unserved load is tabulated and reported. For power systems configured with fewer components or loads than in the discussion above, this process is simplified appropriately. (Manwell et al., 1996)

Graphical Results Interface

The Hybrid2 code includes a GRI that allows the user to view the results of a simulation from within the Hybrid2 code. Hybrid2 creates two levels of output from the simulation engine, a summary output file and a detailed output file. The summary file is a tab-delineated ASCII text file that reports the general results of the simulation. The detailed files report simulation output and power flows for each time step of the simulation run. These detailed files are space delimited and is used by the GRI or can be imported into a spreadsheet for further analysis. The GRI can be used to quickly look at the results a run just completed or previous simulation runs. The GRI can plot multiple time series data or X-Y plots of different parameters. Plots created with the GRI can be copied and pasted into reports or other documents.

The output for the economics package also comes in a summary and detailed form. The summary file provides all of the economic parameters while the detailed output file includes a year by year breakdown of revenues, expenses, and overhaul expense schedules. The summary and detailed files are readable by standard text editors and spreadsheets respectively.

MODEL TESTING

As with any simulation model, Hybrid2 must be tested to ensure that it is accuracy and to build confidence in the use of the model. The model developers are conducting a test program with three main components: verification, validation, and beta-testing. Expected outcomes of Hybrid2 testing are to establish confidence that the model is technically sound, to demonstrate its effectiveness and usefulness, and to clearly identify limitations of which users should be aware.

Verification is the process of confirming that the selected mathematical models have been accurately expressed in the source code. Essentially, this means debugging the code to ensure that the programming has been done correctly. The verification is conducted by designing probable scenarios for which the output can be determined by hand calculations and comparing these results to those of the simulation.

Validation refers to comparisons of simulated performance to measured performance data from operating systems. Validation is useful to demonstrate the degree of correspondence between the model and real power systems and to identify limitations of the model. Four validations planned for Hybrid2 are noted in Table 1 below. Others may be done as data sets become available and resources permit.

Beta-testing is model testing conducted by individuals outside of the development team. In April 1996, a group of about 20 potential Hybrid2 users were trained to use the model and then asked to exercise the model to simulate power systems of interest to them. Feedback on the models useability, effectiveness, and acceptance was received and incorporated into the software. Beta-test results may be qualitative to a great degree, but they are, nevertheless, an important measure of the overall effectiveness of the model.

TABLE 1. PLANNED VALIDATION EXERCISES FOR HYBRID2.

Source of Measured Data	Power System Description	Length of Data Set, Sampling Rate
Frøya Island, Norway	Wind/Diesel/Battery/Dump Load 50-kW nominal	17 days of 10-minute data
Xcalac, Mexico	Wind/PV/Battery 40-kW nominal	84 days of 1-hour data
New World Power Technology Corp. tested at NREL	Wind/Diesel/Battery/Dump Load 50-kW nominal	Testing underway 2/96, 10-minute data
Wind/Diesel System Test Bed University of Massachusetts	5 Different Configurations of Wind/Diesel/Battery 15-kW nominal	12 data sets, each consisting of 2 hours of 2-sec data

Validation of HYBRID1

HYBRID1, the predecessor to the Hybrid2 simulation code, underwent an extensive validation effort before the code release in 1993 (Baring-Gould et. al., 1994 and Baring-Gould, 1995). Since the Hybrid2 model is a direct outgrowth of the HYBRID1 model, it is our view that the rigorous validation efforts undertaken for the earlier version of the code buttress the ongoing validation of Hybrid2. The validation effort consisted of performing a series of tests with the University of Massachusetts Wind/Diesel System Testbed (WDSTB) and them comparing the results to corresponding predications from HYBRID1. Some of these tests will be repeated as part of the validation process using the UMass WDSTB test data.

Verification

The verification process included performing more than 300 different tests using 68 different system configurations isolating certain code algorithms. Verification tests using data taken during the Department of Energy MOD-0A wind/diesel experiments at Block Island, Rhode Island (Jeffries, 1992) were also conducted. The Block Island data was not detailed enough to be used in a validation test, but did allow valuable tests of the wind turbine and diesel algorithms. This verification work gives us confidence that the system algorithms incorporated in Hybrid2 are correctly implemented.

Validation

Two of the four planned validations have been completed by the time of this report: the validations based on the data from Frøya Island, Norway and Xcalac, Mexico. While the report on Xcalac is in draft form, the complete validation of Frøya Island is described in van Dijk and Baring-Gould, 1996. The final two validation efforts will be undertaken during the summer and fall of 1996. Because each validation effort will be different and depends greatly on the quality of the data and the power system configuration, each individual validation will not cover all aspects of the Hybrid2 code. For this reason, four validation tests will be undertaken so that the overlap between the different validation exercises will give confidence that the model has been thoroughly tested. For each validation, two simulations are done for which the input parameters for the components and dispatch strategy are derived from (1) manufacturers' specifications or (2) the measured data. In the first case, the components and dispatch strategy are modelled using their *expected* performance, according to system design. This demonstrates the accuracy that can be expected when modeling potential systems with the Hybrid2 model. In the second case, the input parameters for each component and the dispatch strategy are derived from the measured data, which shows their *realized*

performance and shows the maximum accuracy of the Hybrid2 system performance model. Due to space limitations only the second series of tests will be discussed here.

The Frøya hybrid power system, which is located on the Norwegian island of Frøya about 100 miles north of Bergen, uses a Wincon 55 wind turbine, a 50-kW Cummins diesel and a 20-kWh NiCad battery bank. The system also contains a BBV, 37.5-kW converter and a dump load. The short-term battery storage covers fluctuations in the load and wind energy, thereby preventing rapid on-off cycling of the diesel generator. When the diesel is off and the battery supplies power, the diesel generator acts as a synchronous condenser to provide reactive power. The data set used included primary load, wind speed, the main energy flows and total fuel consumption. A detailed description of the prototype system can be found in Uhlen, 1989.

The 17-day data set was made available by EFI, the Norwegian Electrical Research Institute of Norway. EFI also provided characteristics of the components and the dispatch strategy, obtained from manufacturers' data or from other measurements. The same data set was used earlier to validate the European Wind Diesel Logistic Modelling Package (WDL) (Infield, 1994). This makes it possible to compare the results of the validation for Hybrid2 with the results for these six models.

TABLE 2. COMPARISON OF THE MEASURED AND THE SIMULATED PERFORMANCE OF THE FROYA SYSTEM WITH HYBRID2.

	Measured	Hybrid2
Primary Load (kWh)	8196	8202
Wind Turbine Net Energy (kWh)	4801	4873 (+1)
- Production	4897	4970 (+1)
- Consumption	96	97 (+1)
Diesel Energy Production (kWh)	4944	5045 (+2)
Dump Energy (kWh)	1261	1297 (+3)
Converter Input Energy (kWh)	223	300 (+35)
Converter Output Energy (kWh)	141	151 (+7)
Diesel Run Time (h)	284	282 (-1)
Number of Diesel Starts	29	22 (-24)
Total Fuel Consumption (l)	1812	1909 (+5)

Note: The values between brackets give the percentage with which the simulated value differs from the corresponding measured value.

Tables 2 compares the Hybrid2 summary results with the measured data while Figure 3 shows time series data for diesel operation, a good indicator of how well a hybrid power system is being modeled. Table 3 shows the results compared to validation tests using the same input as was used for the validation of three of the European WDL models (Infield et al., 1993).

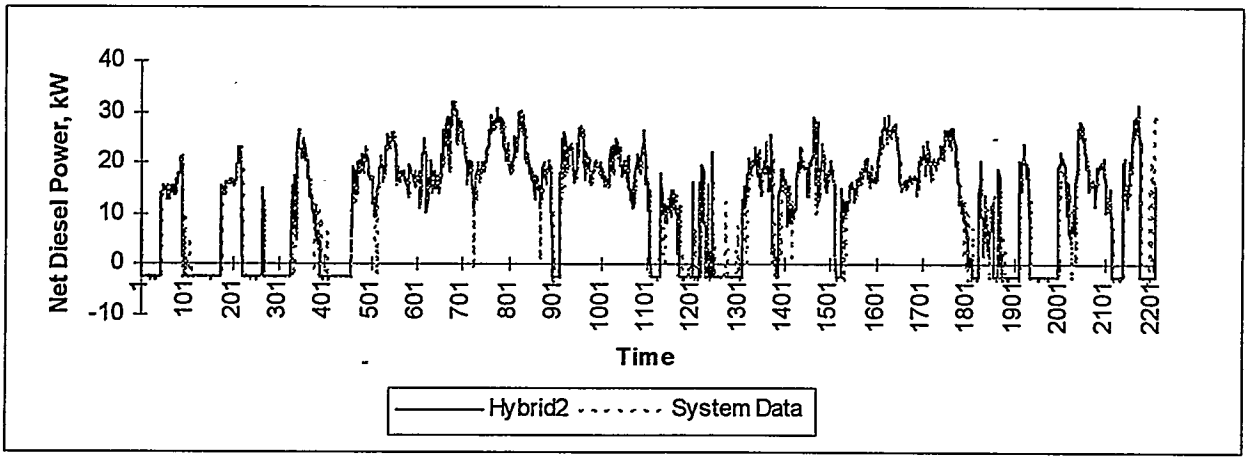

FIGURE 3. TIME SERIES OF FROYA ISLAND DIESEL POWER AND PREDICTION OF HYBRID2.

TABLE 3. HYBRID2 COMPARED TO THE SELECTED EUROPEAN HYBRID SYSTEM MODELS

	Measured Data	Hybrid2	Netherlands SOMES	Denmark WDILOG	Norway VINDEC
Diesel Run Time (h)	284	282(-1)	-	299(+5)	-
Number of Diesel Starts	29	22(-24)	20(-31)	45(+55)	23(-21)
Total Fuel Consumption (l)	1812	1909(+5)	1707(-6)	1919(+6)	1752(-3)

The tables and time series indicate that the model is an excellent predictor of system performance. Further, Hybrid2 compares favorably to the WDL models which are among the best wind-diesel models available.

The specific conclusions of this validation are:

- Hybrid2 can model the performance of a wind turbine to within 1% to 4%. This number will vary depending on the accuracy of the power curve used as the input to the simulation.
- Hybrid2 can model the performance of a diesel genset, either net energy production or fuel consumption, to within 2% to 5%.
- The validation of the battery algorithm in Hybrid2 is inconclusive in this study due to the lack of manufacturer's data for the battery and due to the relatively small (< 2%) contribution the battery subsystem makes to the primary load. It should be noted that even with this lack of knowledge, Hybrid2 predicts the converter power as well as the best European models.
- Hybrid2 does well in modelling the general role of short-term storage and the impact this has on diesel usage. This is evident in the ability of the model to predict the number of diesel starts to an acceptable degree of accuracy, an error of less then one start every two days, as well as the very close approximation of fuel use and diesel operational hours.

Xcalac, Mexico, is a small fishing village on the Yucatan peninsula in southeastern Mexico, about 200 miles south of Cancun, Mexico. The hybrid power system is made up of six Bergey Excel, 10-kW DC wind turbines, a 11.2-kW photovoltaic array of Siemens M75 modules connected in 13 parallel strings, a 125-kW SELMEC diesel generator, and an AES Sinemax 40-kW static inverter. The system also includes a 1738 Ah battery bank made up of 216 GNB Resource Commander 6-75C23 flooded lead acid batteries. The data set that was selected for the validation is comprised of 84 days of data with one day missing. The sensor used to monitor AC power to the loads was not operational during this period. The system is therefore modeled without the diesel and the community load was taken to be the input power to the inverter on the DC bus.

Table 4 shows the comparisons between the Hybrid2 simulation and the actual system performance data. The error in PV array output shows one of the shortcomings of the Hybrid2 code. In an effort to insure that all of the parameters defining each component are easily available, some of the algorithms used to model a component are simple in nature. Because of this, there may be some specific components, like the Siemens M75 PV modules used here, that are not modeled well by Hybrid2. Whether the

TABLE 4. XCALAC MEXICO VALIDATION RESULTS

	Measured	Predicted
DC Primary load (MWh)	23.82	23.82
Unmet load (MWh)	-	2.20
Excess energy (MWh)	-	1.75
Wind turbine output (MWh)	23.30	23.29 (0%)
PV array output (MWh)	3.68	3.01 (-18%)
Net Battery energy (MWh)	3.16	2.97 (-6%)

Note: The values in brackets give the percentage in which the simulated value differs from the measured value. DC Primary load taken from DC power into inverter(code input).

error in the PV performance is due strictly to component mis-modeling, errors in the collection of the resource data or other factors will require further validation exercises and analysis. The code does provide some guidance to the user by pointing out limitations in the model's ability to predict the performance of certain system components.

Clearly, the results of the two simulations discussed here, although indicating areas for improvement and further analysis, demonstrate that the Hybrid2 code does predict the performance of hybrid power systems to a high degree of accuracy. Because Hybrid2 allows so many combinations of system and control structures, it would be virtually impossible to check every possible combination. As Hybrid2 is undergoing its first widespread release, the development team is actively encouraging researchers to report problems and any other comments in regards to the software.

CODE INFORMATION

The code has been made to keep the hardware requirements associated with Hybrid2 as simple as possible. To operate the Hybrid2 code the user is required to have an IBM or compatible 386 PC with a math co-processor. A faster machine will greatly enhance the speed and ease of the code use. The PC must be running under a DOS operating system with Microsoft Windows 3.1 or better, have at least 4 MB of Random Access Memory, 15 MB of free hard disk space, a mouse, a VGA video driver, and a 3.5" disk drive for loading the software. Hybrid2 will function on most laptops and in Microsoft Windows95..

As noted above, NREL would like a more extensive evaluation of Hybrid2. Researchers and users interested in participating in an evaluation should contact the authors at NREL. Evaluation participants must be willing to share modeling experience with NREL and provide feedback on operational problems. The University of Massachusetts is under contract to support the code by offering technical assistance, making code improvements, and providing code updates over the coming year. Participating researchers can obtain the executable code, related manuals and the Frøya Island validation report.

FUTURE PLANS/CONCLUSION

There are plans for the further development of the Hybrid2 code although they are dependent on the future funding of the Hybrid2 program. The first order of business will be to address any bugs uncovered by users. We also plan to improve the code by adding more system consistency checks and including other modules such as micro-hydro power or other types of generators.

The Hybrid2 code provides a very powerful tool that will help those in the hybrid and renewable power industry, funding agencies as well as government agencies assess the potential of incorporating renewable power in their plans for the energy needs of the future.

ACKNOWLEDGEMENTS

The effort reported in this paper has been funded by the U.S. Department of Energy, Wind Energy Program and managed by the National Wind Technology Center at NREL. The authors wish to acknowledge the contributions of a large team who have worked on Hybrid2: Larry Flowers (NREL), Mike Guile (Capital Software), Dennis Barley (Colorado State Univ.), Gannong Deng (UMass), Celso Avelar (UMass), Jon McGowan (UMass), Bill Stein (UMass) and Greg Hayman (UMass).

REFERENCES

Baring-Gould, E.I.. (1996). *Hybrid2; The Hybrid System Simulation Model.* NREL/TP-440-21272, Golden, CO: National Renewable Energy Laboratory.

Baring-Gould, E. I., (1995). "Experimental Validation of the University of Massachusetts Wind/Diesel System Simulator Code, HYBRID1," M.S.M.E. Thesis, Amherst, MA: University of Massachusetts of Amherst, May, 1995.

Baring-Gould, E.I., Manwell, J. F., Jeffries, W. Q., Stein, W. M., (1994). "Experimental Validation of the University of Massachusetts Wind/Diesel System Simulator Code, HYBRID1", Proceedings of the 13th ASME Wind Energy Symposium, New Orleans, LA. January, 1994.

Beyer, H. G., et al. (1989). "Power Fluctuations from Geographically Diverse, Grid Coupled Wind Energy Conversion Systems." European Wind Energy Conference, Glasgow, Scotland: Peter Peregrinus Ltd.

Barley, C. D. (1996). "Modeling and Optimization of Dispatch Strategies for Remote Hybrid Power Systems", Ph.D. Thesis, Fort Collins, CO: Colorado State University; pp. 14-31.

Infield, D., et al. (1994) "Engineering Design Tools for Wind Diesel Systems." Final report on CEC contract JOUR-0078. Report RAL-94-001/007, Didcot: RAL.

Infield, D., et al. (1993) "Engineering Design Tools for Wind Diesel Systems: Presentation and Validation of the Logistic Modeling Package." European Community Wind Energy Conference. Traavemunde: H.S. Stephens & Associates; pp. 316-319.

Jeffries, W.Q., (1992)."A Detailed Investigation of Block Island Wind/Diesel Data" M.S.M.E. Thesis, Amherst, MA: University of Massachusetts of Amherst, May, 1992.

Manwell, J. F., McGowan, J. G., Baring-Gould, E. I., Jeffries, W. Q., Stein, W. M., (1994). "Hybrid Systems Modeling: Development and Validation", Wind Engineering, Vol. 18, No. 5, p. 241, Brentwood, England, Multi-Science Publishing Company, LTD. 1994.

Manwell, J. F., Rogers, A., Hayman, G., Avelar, C.T., McGowan, J.G., (1996). *Theory Manual for Hybrid2 The Hybrid System Simulation Model.* NREL/TP-440-21182, Golden, CO: National Renewable Energy Laboratory.

Uhlen, K., Skarstein, O., Toftevaag, T., Tande, J.O., (1989). "Design and Operation of the Full Scale Norwegian Wind/Diesel Laboratory Model." European Wind Energy Conference, Glasgow, Scotland: Peter Peregrinus Ltd. pp. 209-213.

van Dijk, V., and Baring-Gould, E.I., (1996). *Validation of Hybrid2 with the Frøya Island Data Set.* NREL/TP-441-20976, Golden, CO: National Renewable Energy Laboratory.

Design and Evaluation of Hybrid Wind/PV/Diesel Power Systems for Brazilian Applications

Jon G. McGowan, James F. Manwell, and Celso Ayelar
Renewable Energy Laboratory
Department of Mechanical Engineering
University of Massachusetts
Amherst MA 01002

Cecile Warner
National Renewable Energy Laboratory
1617 Cole Blvd.
Golden CO 80401

ABSTRACT

This paper presents a summary of a study centered on the design and evaluation of hybrid wind/PV/diesel systems for remote locations in Brazil. The objective of this work was to evaluate high reliability hybrid power systems that have been designed for the lowest life cycle costs. The technical and economic analysis of the hybrid wind/PV/diesel systems was carried out using HYBRID2, a computational code developed at the University of Massachusetts in conjunction with the National Renewable Energy Laboratory (NREL). After a summary of a generalized design procedure for such systems based on the use of this code, a systematic parametric evaluation of a representative design case for a village power system in Brazil is presented. As summarized in the paper, the performance and economic effects of key design parameters are illustrated.

INTRODUCTION

The use of hybrid energy systems (wind/PV/diesel/storage) represent an alternative to conventional diesel electrical generating power systems in many developing countries of the world. For such locations, connection to the main electricity grid may be very expensive and not cost effective, thus utilities are using diesel generators to provide electricity. The current diesel systems, generally characterized by high reliability and high fuel costs, have a relatively low conversion efficiency (of a non-renewable resource) and have high maintenance costs. For non grid connected systems, the use of renewable energy in conjunction with a diesel engine can increase the overall efficiency of the system and also allow the optimal use of the diesel engine by applying an optimal control strategy. In order to help make Hybrid Power Systems (HPS) cost effective, engineering tools for the design and techno-economic performance analysis of such systems must be developed. In this light, the University of Massachusetts has been actively involved in the development of modeling and simulation codes for renewable energy based hybrid power systems (McGowan and Manwell, 1995, Manwell and McGowan, 1995). Under NREL support, the result of this work has lead to the development of the HYBRID2 design code (Green and Manwell, 1995). This paper involves the use of this design tool for the design of hybrid power systems for Brazilian applications.

With the largest economy in South America, much interest has been recently generated in Brazil regarding the future growth of electrical energy use. On this subject, much work has been done in the areas of energy conservation (Geller, 1991), or the application of renewable energy technology (Chambouleyron, 1996). For example, as pointed out by the latter author, at the present time, the main customer of PV systems is for communications (TV and radio links). There are numerous isolated communities located in Amazon region of Brazil, many of which do not have any sources of electricity. It can be reasoned that the most cost effective approach to provide the sustainable development needed for these regions is to provide electricity via renewable energy technology. In

spite of high initial costs, hybrid systems can have low maintenance costs an produce relatively little environmental damage.

After the Earth Summit held in Rio de Janerio in 1992, a cooperative agreement was established between the U.S. Department of Energy and Electrobras. Following this, stand-alone PV systems have been installed in about 750 homes and 14 schools in the Brazilian states of Pernambuco and Ceara. Of direct interest, and an example application for this paper, another result of this cooperation is the installation of a hybrid power system supplied by New World Village Power (NWVP) and Bergey Wind Systems in Joanes Village in the Amazon region of Brazil. This hybrid system was evaluated using HYBRID2 with the components and control strategy already established. As summarized in this paper, the objective here was to predict the long term performance of the system.

HYBRID2 CODE DESCRIPTION

HYBRID2 was used as the design tool for the Brazilian rural electrification application summarized in this work. The code is configured such that many different types of hybrid autonomous energy power systems can be modeled including: AC systems with AC or DC load and DC systems with DC or AC load.

HYBRID2 uses a statistical time series approach to obtain a long term performance prediction for the HPS. The code allows the use of two power buses (AC and DC) at the same time. For each time step in the simulation, the net load (Primary Load- Wind Energy - PV Energy) is established on a specific bus. If the net load is positive, then the energy from storage or diesel is calculated based on the average net load, storage availability, and the control strategy. If the net load is negative (excess of energy from wind and PV), the energy is used to charge the battery (if allowed), goes to the other bus, or is used to address different loads (dump, deferrable, or optional). The power fluctuation and short term probability (maximum and average net load) are defined by assuming a normal distribution with the time step. More detail on this code is found in its theory manual (Manwell, et. al., 1996).

SYSTEM DESIGN PROCEDURE

There are many approaches that can be used to carry out a systematic design of an HPS. They include several different sizing methods from handbooks, design charts, or design methods presented by the manufacturers of such systems. In many situations the results of these somewhat oversimplified design techniques are either oversized or undersized systems due to the lack of accuracy in predicting long term performance. It has been found that the most accurate design tools for HPS design involve the use of analytical models that account for loss of load probability or short term probability. At the same time, it is advisable to use practical design information from manufactures who may have years of experience with the installation and performance monitoring of such systems. Thus, with the use of such a powerful design tool as HYBRID2, a simple design using manufacturers recommendations is used as a starting point for the HPS design procedure.

The methodology summarized here is intended to be as general as possible in order to provide a summary of the basic steps involved in the use of the HYBRID2 code. Complete technical details of this code are included in its theory manual (Manwell, et al., 1996). As summarized below and shown schematically in Figure 1, the generic design procedure consists of the following components: 1) Establishment of System Requirements, 2) Collection of Resource Data, 3) Definition of Design Objectives, 4) Initial System Sizing, 5) Parametric Analysis, 6) Economic Analysis, 7) Results Structure, and 8) Decision and Optimum Design. It should also be noted that the design procedure is an interactive process. Therefore, each step can be modified and influenced by other steps.

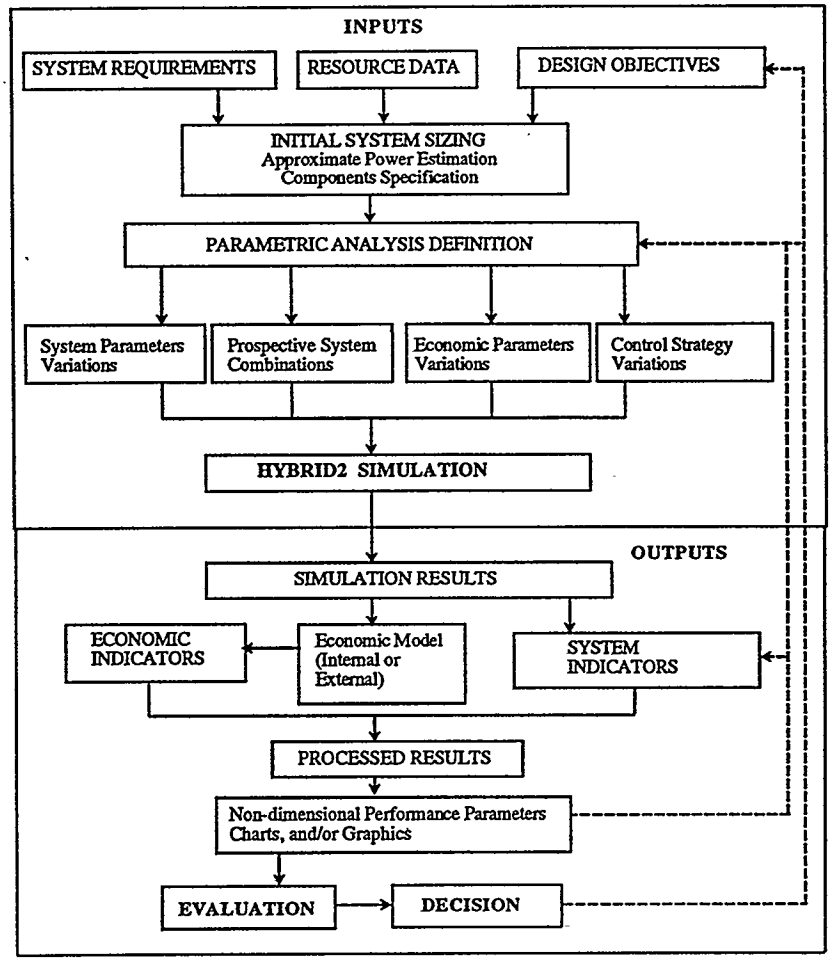

Figure 2 Generic Design Process

1) Establishment of Systems Requirements. As one of the most important steps in the design process, the information provided here will influence many aspects of the system including component size, control strategy, and system autonomy. The following information should be determined in order to characterize the system requirements:
1) Hourly electrical load demand (Fluctuation during the day)
2) Daily electrical load for one year (Seasonal fluctuation)
3) Types of load (Resistive, inductive, or mixed)
4) Type of equipment (AC or DC)
Also, although HYBRID2 is essentially a long term performance model, it is useful to know the transient behavior of the load demand in order to make decisions on the overall structure of the HPS. For example, there are "rules of thumb" on peak load demand that can be applied in the case no high frequency data is available.

2) Collection of Resource Data. In HPS systems design, it is essential to have sufficient information on the wind and solar resource patterns including seasonal trends, daily profiles, and peak values. One of the more difficult and costly tasks is to assemble a complete data set for a whole year (needed for a complete economic analysis). In some cases, however, it is necessary to simulate the period which has resources data available and to make decisions based on that period. In general, the following data should be acquired: 1) Wind speed information, 2) Solar insolation and, 3) Ambient temperature.

3) Design Objectives. The primary objective should be to meet the previously established system requirements, and this can be accomplished in a number of ways. The design objectives should be clearly established because the overall simulation, parametric analysis, and control strategy will be a function of the goals to be achieved with the HPS. In cases where many configurations are to be tested, however, sometimes the goals will be established after simulation and economic analysis. Thus, the objectives are generally defined interactively as the simulation and analysis are performed. In general, the following information should be approximately defined: 1) Renewable power penetration (defined here as the ratio of the energy produced by renewable energy components to the total energy required by the system), 2) Diesel engine penetration, 3) Stand alone or main grid support (utility interface), 4) Existing equipment, 5) System restrictions, 6) Baseline configuration, and 7) Baseline control strategy.

4) Initial System Sizing. In this phase of the design, one should obtain a baseline HPS design using simplified sizing methods. The resulting initial system then serves as a baseline from which a parametric analysis can be performed using the HYBRID2 code. The methodology for establishing an initial design depends on the application of the system, load pattern, and design objectives. A preliminary specification of the candidate components should also be carried out at this point.

5) Parametric Analysis. The parametric or sensitivity analysis can be divided into two subsections: i) Choice of hybrid system combination, and, ii) Investigation of parametric variables for a specific combination. Thus, several configurations can be simulated, each with a different sensitivity analysis. Only one variable is changed at a time to assess the performance effects on the selected system configuration. The level of complexity of this phase of the analysis depends on how much information is available and how important the performance variables are. In general, the parameters can be grouped into the following three categories:
A) System Parameters. These parameters pertain to the energy sources and equipment characteristics. They include, among others: (1) Relative size of renewable components, diesel engine, and batteries, (2) Number of renewable components and diesels, (3) Load scale, (4) Power converter efficiency, (5) Wind turbine height, and (6) Wind speed and solar radiation scale
B) Control Parameters. In many instances the effects of control strategy on the technical and economic performance of an HPS is underestimated. For example, in spite of its high initial cost, a sophisticated control on the diesel may increase the overall reliability of the system, but also can increase the system components' lifetimes. HYBRID2 allows several different combinations on the diesel control operation, with the main control parameters related to the battery and diesel dispatch strategy. The variables include Method of battery use, Boost charge level and interval, Time for diesel operation, Diesel operation methodology and shut down strategy, Battery depth of discharge, and Minimum/maximum battery state of charge.
C) Economic Parameters. Although there is a high degree of uncertainty present in an economic analysis in a developing country, it is important to systematically investigate key economic variables. Examples include fuel cost, renewable components cost, discount rate, inflation rates, replacement costs, components life times, OEM costs, installation and labor costs.

6) Economic Analysis. Although efforts have been made to develop a uniform procedure to evaluate potential investment in renewable energy technology in the public and private sectors, today many different methods exist for the economic analysis of such systems. HYBRID2 contains a variety of internal economic models as well as provision for the use of external models. For this analysis, we used a conventional life cycle analysis external model which yielded the total life cycle cost of the HPS plus a unit energy cost.

7) Results Structure. One must decide on which output should be considered as the relevant parameter to draw a final conclusion on the specified design. The results structure is intimately related with the parametric analysis and the main idea is to determine the effect of one Parametric variable over the Indicators parameter that will define the decision making process. In the process

of developing an "optimum" design for a HPS, new variables can be created and the Indicators become Parametric variables using the simulation results. Although the number of combinations of results is very large, the results (Indicator parameter) structure can be divided into two major groups:
A) Energy Flow and System Performance Indicators. These include: i) Wind, solar, storage, and diesel contributions, ii) Energy into/ out of storage and battery SOC, iii) System autonomy level (unmet load/total load), iv) Diesel operating hours, cycles, and fuel use, and v) Excess energy
B) Economics Performance Indicators. Examples include: i) Capital cost, ii) Total life cycle cost, iii) Levelized cost of energy, and iv) Fuel savings.

The Processed Results (PR) part represents a combination of the Economic and Performance Indicators. That is, the Simulation results can be used as a reference to produce new Parametric variables that provide the necessary data to build Processed results which are the most important source for the Decision making process. Examples could include the following:
A) Renewable Power Penetration (%) vs Time (hour, month, or year)- PR variable: Depth of discharge, Battery size, Minimum diesel power, control strategy, etc.
B) Total Life Cycle Cost ($) vs Renewable Power Penetration (%)- PR variable: Control strategy, Fuel inflation rate, Renewable components cost, etc.

8) Decision and Optimum Design. The final decision on the recommended system configuration depends on the criteria that the designer establishes for the most appropriate system. For example, one criterion could be based on the autonomy of the system with no regards to economics, while another could be based on a simple economic parameter. Obviously, the criteria are related to the overall installation purpose of the HPS, which varies considerably. Also, the most misunderstood and misapplied term in HPS sizing methods using computational tools is optimization. Optimization, in a general sense, requires a more general mathematical formulation- one that could use variational methods to maximize or minimize a specific variable. Thus, it would be necessary to express the indicator variable as a function of system variables (e.g., battery size, renewable source size, control strategy, etc.) in a manner that would incorporate their primary and secondary effects. As it stands, the HPS design presented here using HYBRID2, or any other logistical simulation tool, results in a sensitivity analysis design study of the system. However, it does enable the designer to quantitize the effects of varying basic parameters on system behavior (performance indicators) and system cost (economic indicators). Here, the "optimum" design is one that presents the 'best' indicator values for a specific parametric analysis.

BRAZILIAN HYBRID SYSTEMS DESIGN APPLICATION

1. Village Power System

Recently, NREL and the Brazilian Electrical Research Center (CEPEL) teamed with Brazil's state-owned utilities to install renewable energy systems in areas where the electricity supply is inadequate. One of the applications, to be considered here, was the installation of a hybrid power system to supply electricity to the remote village of Joanes in the Amazon region of Brazil. This AC HPS system is located 17 Km south of a larger town, Salvaterra, on the Island of Marajo, state of Para, Brazil (Lat. 0°50', Long. 48°30').

A) System Requirement and Load Data. As shown in Figure 2, the daily load profile is assumed to remain constant during the simulation period. The daily load from about 700 residential users is 743 kWh.

B)Resources Data. The annual (6 month based) average wind speed at this sits is 6.55 m/s with an average standard deviation of 1.44 m/s, and the average solar insolation is about 4.8 kWh/m^{2}day. The profiles of the daily hourly wind speed for the 6 months of available data are shown in Figure 3. The daily solar radiation profile for each of these 6 months was also obtained.

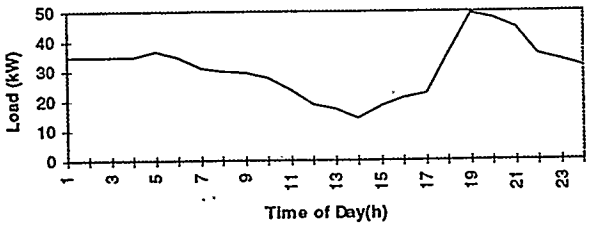

Fig. 2 Daily Load for Joanes Village

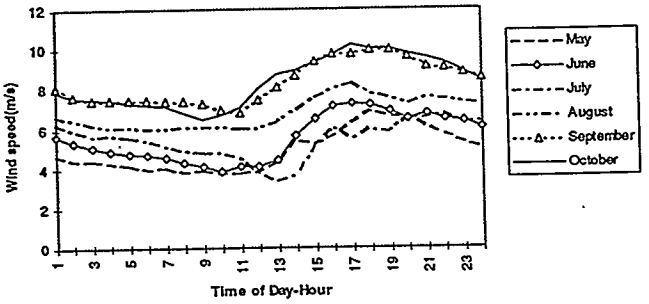

Fig. 3 Hourly Average Wind Speed for Joanes Village

C) Design Objectives. The initial overall design objectives of this HPS included: i) Reduced diesel fuel consumption, ii) Improvement of service quality, iii) Maximum use of renewable power (yearly power penetration ≈ 45%), iv) High reliability, v) Ability to store excess renewable energy for use during peak hours, and vi) A shift in utility peak load demand to off-peak times.

The baseline configuration included: i) 4- 10 kW Bergey wind turbines, ii) 10 kW of Siemens PV modules, iii) NWVP rotary converter (shaft-coupled DC motor and synchronous alternator) and system controller, and iv) Battery storage of 400 kWh. For the baseline control strategy a programmable logic controller (PLC) is used to control the energy flow in the HPS. The main parameters defining the operation of the PLC are: i) Time of day, ii) Utility grid status, iii) Battery state of charge, and iv) Renewable system availability. Three basic operating strategies based on these parameters are: i) Charge Time- The diesel (grid) will charge the battery and meet Joanes load. This is essentially dependent on Time of day, ii) Supply Time- The HPS meets the load. If the load is greater than the HPS plus the battery, the village is connected to the grid and renewable energy is used to decrease the utility load. If battery SOC is less than 50%, the grid will meet the load and renewable energy is used for battery charging, iii) Any Time- Renewable meets the load or charges the battery.

D) Initial System Sizing. For this study, the size and definition of the components were established by the hardware suppliers. A schematic of the Joanes Village HPS is given in Figure 4.

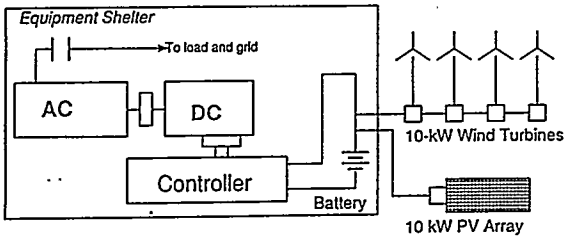

Fig. 4 Schematic of Joanes Village HPS

E) Parametric Analysis Definition. This step is directly related to the Design Objectives for the HPS. A main goal here was to define an appropriate control strategy, using the baseline case as a reference, that minimized fuel consumption. The major parameters that were varied included: i) System Parameter Variation: Storage size, ii) Control Strategy Variation: Battery minimum level, Boost charge, Diesel start strategy, Diesel operation code, Diesel shut down code, and iii) System Combination Variation: PV/Wind/Battery

F) HYBRID2 Simulation. Figure 5 shows the bus scheme configuration used in HYBRID2 for the modeling of the Joanes village hybrid power system. The period of simulation used an artificial year with 166 days (3984 hours) corresponding to 6 months of 'good' data (no missing data). Based on the Parametric Analysis Definition, 20 simulation runs were performed, primarily varying parameters in the baseline control strategy. The approach used to make HYBRID2 reproduce the baseline control strategy included: i) Battery discharge code (1)- all or part of the average load, ii) Battery minimum level (SOC)- 50%, iii) Code for boost charge (2)- forced diesel start, iv) Diesel operating power code (2)- load following with diesel priority, v) Diesel shutdown code (2) - renewables can meet the load, and iv) Forced diesel shutoff period 0,0,18,23.

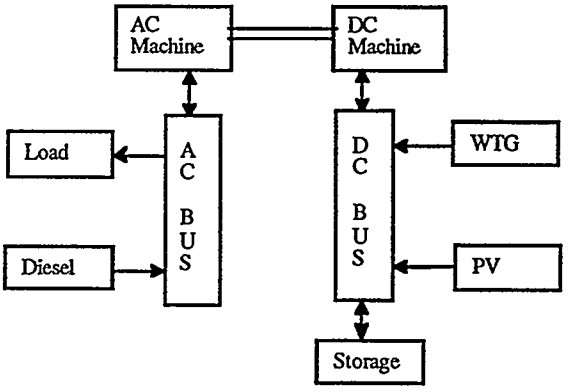

Fig. 5 Bus Scheme of Baseline Configuration for Joanes Village

G) Simulation Results. The long term simulation of the Joanes Village HPS produced analytical results that allowed the time variation of the system performance to be determined. For example, as shown in Figure 6, the energy flows from the diesel and in and out of storage, allows a designer to check the simulation of the desired control scheme (in this case, the baseline control strategy). Similarly, Figure 7 shows a typical result for the battery state of charge as a function of time. In both examples, the supply and charge times can be clearly observed.

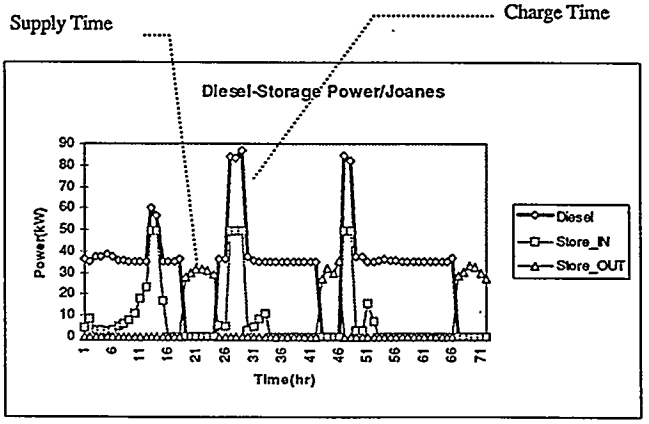

Fig. 6 Diesel and Storage Power Energy Flows

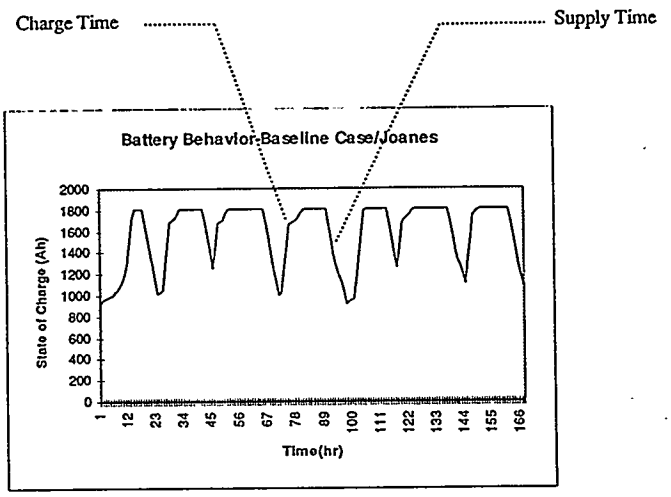

Fig. 7 Battery State of Charge

In addition to these types of results, the main system indicators for this analysis were: i) Fuel consumption, and ii) Diesel on time. The economic model used was an external one based on a conventional life cycle cost analysis with the following major economic indicators: i) Total fuel cost, ii) Total life cycle cost, and iii) Unit energy cost.

H) Processed Results. Based on the results from the simulation runs, a variety of outputs summarizing the performance of the Joanes HPS system can be prepared. For example, Figure 8 gives a summary of the energy production breakdown for the system (201 kWh/day average wind energy and 51 kWh/day average solar energy).

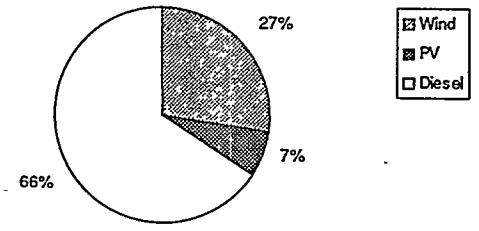

Fig. 8 Energy Production Breakdown

Figure 9 presents the results of a cost sensitivity analysis varying the battery storage size and battery depth of discharge. A major variation is associated with the capital cost for storage size and the replacement cost associated with the depth of discharge (DOD). As shown in this figure, using information for deep cycle batteries (Perez, 1985), increases in the DOD increase cost due to replacement battery cost.

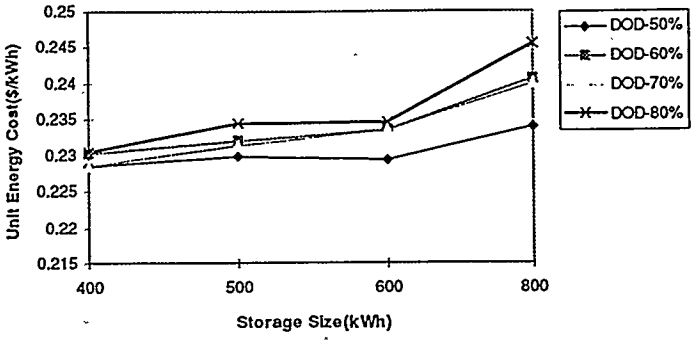

Fig. 9 Cost Sensitivity Analysis Results for Varying Battery Storage Parameters

An example of the processed results for normalized fuel consumption as a function of control strategy variation is shown in Figure 10. For the control strategy variation, 3 basic configurations were simulated using an 800 kWh storage size and a DOD of 80%. Configuration 1 allows the diesel shut down whenever there is energy in storage or coming from renewables. Configuration 2 is the same as 1 without boost charge. Configuration 3 does not have boost charge and does not use forced diesel shut off. The reduced fuel consumption of Configuration 2 should be noted.

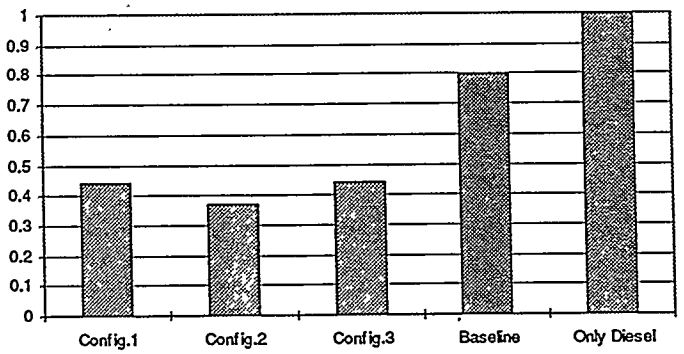

Fig. 10 Normalized Fuel Consumption as a function of Control Strategy

I) Evaluation/ Decision. The techno-economic assessment that has been carried out for the Joanes HPS has yielded valuable information for the establishment of new control strategies and the effects of key parameters on system performance. The importance of determining the first order effects of the parametric variables on the key indicators cannot be understated. It has also been demonstrated that HYBRID2 can accurately model a large variety of control strategies that can be set by the PLC. This analysis focused specifically on the baseline control strategy with the parametric analysis concentrated on battery storage size and DOD. It was found that a higher storage size increases the autonomy of the system, but the penalty is the high replacement cost of the battery. Based on the initial results from this analysis, the following specific recommendations apply to further versions of this HPS system study:

i) Longer term resource data (2 years) should be used.

ii) More detailed information on the installed batteries should be obtained.

iii) The processed results should be established with continuous (instead of stepwise) and non-dimensional technical and economic parameters.
iv) An economic sensitivity analysis should be performed.
v) Field test data should be acquired for system design and code improvement.

SUMMARY/ CONCLUSIONS

This work demonstrates the potential use of powerful simulation tools such as HYBRID2 for assessing different designs of renewable energy based hybrid power systems. The HYBRID2 code provides information of different design scenarios and can be used as a design tool to develop appropriate control schemes. The design methodology summarized here is part of a decision making process that can include many external factors. In general, this can provide the designer with the following analysis tools:
1) An overall technical performance of different system configurations
2) Evaluation of the effects of system parameters on the overall performance of the system
3) A basis to develop an improved control strategy
4) An assessment of the effects of load management
5) An accurate prediction of energy output from the components (Confidence in the prediction of energy output from the renewable components increases with the time run of the simulation)

ACKNOWLEDGMENT

This work was supported by U.S. Department of Energy Subcontracts XL-1-11126 and XAX-6-1573-01 administered by the National Renewable Energy Laboratory (NREL).

REFERENCES

Chambouleyron, I. (1996), "Photovoltaics in the Developing World," Energy, 21, No. 5, pp 385-394.
Geller, H. S. (1991), Efficient Energy Use: A Development Strategy for Brazil, American Council for an Energy-Efficient Economy, Washington, DC.
Green, H. J. and Manwell, J. F. (1995), "HYBRID2- A Versatile Model of the Performance of Hybrid Power Systems," Proc. 1995 AWEA Conference, Washington, D. C.
Manwell, J. F., et al. (1966) "HYBRID2 - A Hybrid System Simulation Model: Theory Summary" UMass/ NREL Report, April.
Manwell. J. F. and McGowan, J. G. (1995), "Wind Diesel System Simulation: A Screening Level Model," Int. J. Solar Energy, 17, pp 223-240.
McGowan, J. G., et al. (1996), "Hybrid Wind/PV/Diesel Power Systems Modeling and South American Applications, " Proc. World Renewable Energy Congress IV, Denver.
McGowan, J. G. and Manwell, J. F. (1995) "Modeling of Wind/Diesel/Hybrid Systems," Energy Environment Monitor, 11, No. 1, pp 47-58.
Perez, R. A. (1985), The Complete Battery Book, TAB books.

ANALYSIS OF VILLAGE HYBRID SYSTEMS IN CHILE

Debra J. Lew
David Corbus
Richard Holz
Lawrence T. Flowers
National Wind Technology Center
National Renewable Energy Laboratory
1617 Cole Blvd.
Golden, CO 80401 USA

J. Andrew McAllister
National Rural Electric Cooperative Association, International
Av. 14 de Septiembre 5080
La Paz, Bolivia

ABSTRACT

Chile recently began a major rural electrification program to electrify those 240,000 families (about half of the rural people) who lack electricity access. In this paper, we discuss a pilot project to electrify three remote villages in Chile's Region IX using wind/genset/battery hybrids. The intent of this project is to demonstrate the reliability and cost-effectiveness of wind/genset/battery hybrids and to encourage replication of these types of systems in Chile's electrification program.

For each village, electricity connections are planned for several residences, and also schools, health posts, community centers, or chapels. Projected average daily loads are small, ranging from 4 to 10 kWh. Using the optimization program HOMER and the simulation program Hybrid2, we evaluated options to maximize technical performance, minimize costs, and gain experience with a variety of systems and components. We find that wind/genset/battery hybrids will be able to provide cost-effective, reliable power for these sites. More importantly, their inherent flexibility allows for variations in load and resource without greatly affecting the cost of energy.

INTRODUCTION

In the summer of 1994, Chile's Comision Nacional de Energia (CNE) met with representatives of the American Wind Energy Association (AWEA), U.S. Department of Energy (DOE), and the National Renewable Energy Laboratory (NREL) and initiated a cooperative program to develop a sustainable approach to applying renewable energy systems to Chile's rural electrification program. As part of this program, a group of pilot projects will be implemented. Region IX (See Figure 1) was selected by CNE for the initial pilot projects, because it is the region with the most unelectrified homes and is central to Regions VII–X, which represent 80% of the unelectrified rural population in Chile. NREL and its regional partner, the National Rural Electric Cooperative Association, have provided technical assistance and training to CNE and the regional utility implementers. DOE and CNE are cost-sharing the pilot installations. The regional private utility Frontel will own, operate, and maintain the systems. NREL will monitor and assess technical performance with site data acquisition systems.

The three sites in Region IX to be electrified are Puaucho, Villa Las Araucarias (VLA), and Isla Nahuel Huapi (INH). Puaucho is a small coastal village with good winds. There is a plan to extend the grid in the next 1 to 2 years, so the system there will be a temporary installation to supply the school and some of the residences until this site can be grid-connected. This system can then be removed and used to electrify another site. INH is an island about 200 m from the mainland in Lago Budi, which is east of Puaucho; because of transportation difficulties, this site needs to be self-sufficient. VLA, the largest of the villages, is located further inland, where the winds are weaker. Because of government resettlement programs, this site is expected to see high growth. Both INH and VLA systems are permanent installations and are expected to last 20 years.

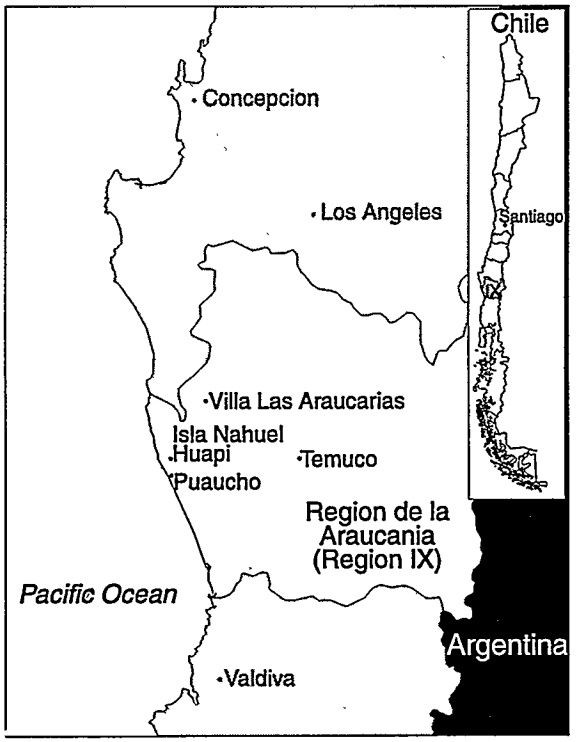

FIGURE 1. REGION IX OF CHILE, SHOWING THE LOCATION OF SITES PUAUCHO, ISLA NAHUEL HUAPI, AND VILLA LAS ARAUCARIAS.

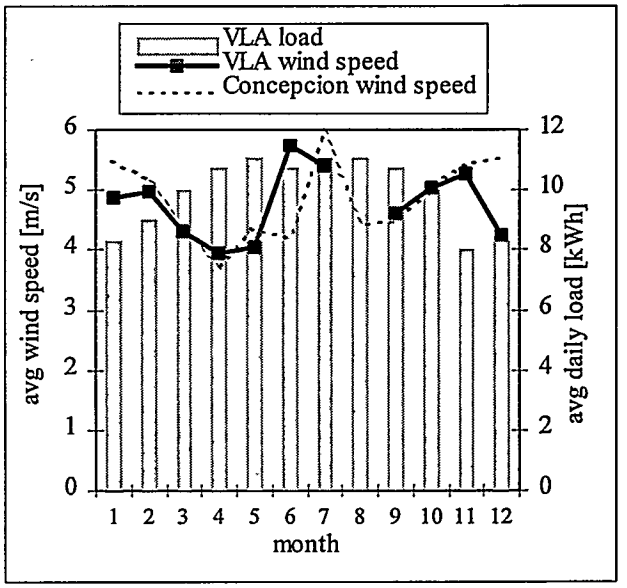

FIGURE 2. MONTHLY AVERAGE WIND SPEEDS (AT 24M HEIGHT) AND DAILY LOADS FOR VILLA LAS ARAUCARIAS, AND CONCEPCION AIRPORT DATA AVERAGED OVER 1977–80.

RESOURCE

As part of this project, anemometers have been installed at four sites in Chile, three of which are in Region IX: Puaucho, Vegas Blancas, and Villa Las Araucarias, and Isla Tac in Region X. The wind resource at Puaucho has been monitored at two heights – 10 m and 24 m – since June 1995. These data, combined with long-term Concepcion airport data, indicate Class 2–3 winds. The Puaucho data set of 7710 hours of wind data was collected from June 1, 1995, to May 21, 1996. Data for the month of August 1995 is missing. This data set is well fit to a Weibull distribution of $v_c = 1.9$ and $k = 6.1$. The average wind speed is 5.3 m/s. Storm-driven winds in the winter months (June–September) result in

high wind speeds with long lulls between storms. The rest of the year is marked by steady, medium winds with the lowest wind speeds in the spring.

Continuous wind data were not available for INH or VLA, so these data sets were derived from the Puaucho data set. Wind speeds at VLA were estimated to be 10% less than that at Puaucho, because VLA is located farther inland. INH is also inland, but on a lake, so wind speeds have been derated by only 5% from Puaucho. Brief periods of simultaneous data taken at both Puaucho and VLA in the fall and in the spring indicate that the VLA wind speeds are 3% and 30%, respectively, less than that at Puaucho. A summary of the data is shown in Table 1.

TABLE 1. WIND RESOURCE ASSESSMENT OF PUAUCHO MONITORED AT 24M HEIGHT FROM JUNE 1, 1995, TO MAY 21, 1996. INH AND VLA DATA ARE ESTIMATED FROM PUAUCHO.

Site	Average Wind Speed [m/s]	Average Wind Power Density [W/m^2]
Puaucho	5.3	190
INH	5.1	165
VLA	4.8	140

Missing data (for example, the entire month of August) were not filled in, so that one year's performance has been extrapolated from a partial year's run. Figure 2 shows the average monthly wind speed for VLA. For the purposes of this graph, monthly averaged wind speeds from 1977–80 from nearby Concepcion airport have been shown.

The solar resource in this area is not good. The daily global horizontal insolation averages 3 kWh/m^2, with highs in the summer of 5.2 and lows in the winter of 1.0 kWh/m^2.

LOAD

A loads analysis was performed for each site and is described in Table 2. Each school, health post and residential connection was evaluated for present energy needs and predicted future needs. The loads represent the greatest uncertainty in the modeling process. It is likely that household consumption will increase after electrification as the villagers acquire appliances and expand lighting usage. In particular, the VLA load is expected to grow quickly, as the population may double in the next few years, due to possible resettlement from the surrounding areas.

TABLE 2. LOAD REQUIREMENTS FOR THE THREE VILLAGES. IN THESE SIMULATIONS, AN ADDITIONAL 5% WAS ADDED TO THE GIVEN ANNUAL LOAD TO ACCOUNT FOR TRANSMISSION LINE LOSSES.

Site	Daily Load [kWh]	Peak Load [kW]	Annual Load [kWh]
Puaucho	4.0	0.7	1470
INH	5.1	0.7	1810
VLA	9.8	1.2	3460

Both VLA and INH are assumed to include continuous-duty refrigerator loads. All loads peak in the evening and have minor peaks in the morning and noontime. Although water pumping would normally operate as a deferrable load, it was included as a primary scheduled load for these simulations. All loads

are based on the use of efficient appliances, such as compact fluorescent light bulbs, which will be purchased by Frontel. Traditional inefficient appliances bought by the users may increase the load estimate by a factor of 2.

TECHNICAL OPTIONS AND DESIGN CONSIDERATIONS

System requirements are for 220 V, 50 Hz delivered power, with a loss of load probability not to exceed 3%. These systems have been designed conservatively for zero loss of load. The basic wind/genset system architecture is shown in Figure 4. A different turbine is used for each site, to gain a variety of operating and maintenance experience in the field. Systems were deliberately oversized to allow for load growth, especially in the case of VLA, where load growth is expected to be most rapid. Local equipment (e.g., towers or gensets) is used wherever possible. The batteries are manufactured in the United States and purchased through a Chilean distributor. The only components that must be purchased from the United States are the turbines and electronics.

TABLE 3. HOMER RESULTS. FIXED CONSTRAINTS ARE SHOWN IN ***BOLDFACE.***

Site	Constraint	COE [$/kWh]	Turbine [kW]	Genset [kW]	Battery [kWh]	Inverter [kW]	Excess Energy [kWh/yr]
Puaucho	none	0.86	0.9	2.3	4.5	0.9	393
	turbine	1.17	**1.5**	0	11.6	1.53	1370
	turbine, genset	1.31	**1.5**	**2.3**	9	1.53	1424
INH	none	0.96	3	0	13.4	3.2	4451
	turbine	0.96	**3**	0	13.4	3.2	4451
	turbine, genset	1.21	**3**	**4**	8	3.2	4562
VLA	none	0.64	3	0	28.8	3.2	2102
	turbine	1.40	**6**	0	28.8	5.6	7516
	turbine, genset	1.52	**6**	**4**	11.7	5.6	7975

Two design tools developed at NREL – HOMER and Hybrid2 – have been used to evaluate the system options. HOMER is an optimization program, which takes load, cost and resource inputs and finds the set of components that minimize the lifecycle cost of energy [Lilienthal *et al.* 1995]. HOMER can constrain part of the system and optimize the remaining parts of the system. These outputs can then be given to Hybrid2, which performs a more detailed simulation of this system with the given load and resource [Green and Manwell 1995].

HOMER was first run with all components completely unconstrained, to find the system that minimized the cost of energy (COE). These results are listed in Table 3.

Turbines

Using the given Puaucho wind data and estimated deratings for INH and VLA, the energy outputs of various turbines (see Table 4) were calculated. For the case of Puaucho, the 850 W turbine output is just enough to cover the load and additional line losses, but the 1.5 kW turbine allows a wider margin of error for load and resource variations. The INH load could also be met by the 1.5 kW turbine, but the 3 kW gives Frontel an opportunity to gain experience with a variety of turbines. This system will have a high-

voltage output with a long wire run to a step-down transformer at the village[1]. The current VLA load is easily met by the 3 kW, but given the strong possibility of load growth, the larger 6 kW is a conservative choice. The VLA system will have a transformer between the turbine and the rectifier[1].

*TABLE 4. ENERGY OUTPUT OF VARIOUS TURBINES AT EACH SITE. THE CHOSEN TURBINE FOR EACH SITE IS GIVEN IN **BOLDFACE**.*

Site	Load + 5% Losses [kWh/yr]	Turbine	Turbine Output [kWh/yr]
Puaucho	1540	850 W	1670
		1.5 kW	**2850**
		3kW	6920
		6 kW	13610
INH	1900	1.5 kW	2290
		3 kW	**5590**
VLA	3630	3kW	4960
		6 kW	**9540**

Gensets

The life of a genset depends on a number of factors including maintenance, run time, and loading. Regular maintenance is assumed. In order to minimize wear and optimize efficiency of the genset, the genset is only started when absolutely necessary to meet the load and charge the batteries; once the genset is on, it is run at full power until the batteries are charged. Finally the total lifetime for these small gensets has been estimated at 3500 hours (about 5 years based on 2 hr/day run times). All of the gensets described for these systems are gasoline-fueled.

Table 3 shows the HOMER results with the turbine choices described above. The choice of turbine especially affects the COE of VLA, where the system is particularly oversized. Detailed Hybrid2 simulations of the winter lulls show that the genset is needed for reliability. The smallest electric start genset manufactured in Chile, a 4 kW unit, is used for INH and VLA. The genset chosen for Puaucho is a 2.3 kW manual-start unit, due to the temporary nature of the system in Puaucho.

Battery sizing and dispatch strategies

For these pilot projects, utility involvement is a major design consideration. Before this project, Frontel's alternatives were a genset-only system or grid-extension. Utilities find hybrid systems potentially attractive for remote areas because of their minimal operations, maintenance, and fuel needs. These requirements are not only problematic for the utility because of the remoteness of the sites but are also costly and involve skilled technicians. In this analysis, solutions have been sought for reduced fuel usage (which is expensive and can involve transportation difficulties, as is the case for INH and Puaucho) and genset starts (which require operator involvement for manual-starting gensets).

The final HOMER run in Table 3, which constrained the turbine and genset selection and evaluated the battery bank sizing, reveals that the necessary storage is quite small. The batteries are U.S.-

[1] The transformer and wire runs are assumed to have losses of 10%.

manufactured deep-cycle batteries, which can be purchased through a local distributor. These batteries have a 2.1 kWh capacity (6V, 350 Ah) and a lifetime throughput of 1225 kWh. However, the bus voltage of the mini-grid is required to be high in order to minimize resistive losses. Bus voltages of 24 V for Puaucho and INH and 48 V for VLA have been chosen. This constrains the number of batteries used.

TABLE 5. HYBRID2 RESULTS OF GENSET OPERATION FOR THE GIVEN TURBINE AND GENSET CAPACITY.

Site	# Batteries	Genset [kWh/yr]	Genset [L/yr]	Genset [h/yr]	Genset [starts/yr]
Puaucho	4	1277	1013	993	108
Puaucho	8	877	541	441	31
Puaucho	12	745	441	344	18
INH	4	701	407	427	82
INH	8	413	191	179	28
INH	12	262	142	145	18
VLA	8	1980	846	754	108
VLA	16	1248	518	452	39
VLA	24	776	356	332	23

In the case of Puaucho, where the load coincides with waking hours, a small manual-start genset is used as a backup. This genset will be run only when the load exceeds the wind power and the batteries are low (30%–35% state of charge), and it will run at full power for about 12 hours until the batteries are fully (95%) charged. Because it will be manually operated, its operating hours will be confined to 8 a.m.–10 p.m. and the system is designed to limit start times. Hybrid2 results with 8 batteries indicate 31 starts per year. Frontel has agreed that about one start or less per week is reasonable, so 8 batteries are used.

For VLA and INH, where there is a constant refrigeration load, an electrical-starting gasoline genset was used. This genset can be run at any time of day or night and the electrical start will minimize interruptions caused by loss of power. This genset will start when the load exceeds the wind power and the batteries drop to a 30% state of charge (SOC), and it will operate at full power until the batteries are charged to 80% SOC. An equalization charge will be performed every 2 to 4 weeks and will charge all batteries to 95% SOC. The fuel consumption for INH drops by about 200 L/yr as the batteries are increased from 4 to 8, but only 50 L/yr as batteries are increased to 12, so 8 batteries were chosen as a reasonable size. For similar reasons, 16 batteries are used for VLA. As the next section will show, the battery bank sizing mostly acts to reduce fuel use and has little effect on the COE.

Inverters

Inverter sizing is tricky using HOMER, because HOMER does not allow for surge capability. Inverters have been sized with a large margin above the current peak demand. INH and VLA both use 3.3 kW sine wave inverters with charging capabilities. Due to the temporary nature of the Puaucho system, the inverter will be a less expensive, modified sine wave inverter/charger with a 2.4 kW continuous rating. It should be noted that although the inversion efficiency of these inverters is quite high, about 85%–90% at full load, the rectification efficiency is much lower, 55%–75%. The basecase system architectures and costs are listed in Table 6.

ECONOMICS

The economics of these hybrid systems have been calculated based on the system configurations described above. These costs include all generation equipment and mini-grid costs. They do not include materials and installation costs for service drops and customer connections. Based on a preliminary study of Puaucho, the costs per residential and school/health post connections are $180 and $420, respectively. Installation costs and all taxes are included (10% shipping charge, 11% import tariff and 18% VAT for imported goods; 18% VAT for domestic goods) in all capital costs.

TABLE 6. SYSTEM CONFIGURATION AND CAPITAL COSTS FOR GENERATION EQUIPMENT.

Site	System Components	Capacity	Installed Cost [$]
PUAUCHO	wind turbine with 24 m tower	1.5 kW	10159
	modified sine wave inverter/charger	2.4 kW	1698
	8 deep cycle batteries and housing	16.8 kWh	2313
	2.3 kW manual-start gas genset	2.3 kW	1770
	Balance of System and Grid costs		3486
	Total Capital Cost of generation		19426
ISLA NAHUEL HUAPI	wind turbine with 24m tower	3 kW	9384
	sine wave inverter/charger	3.3 kW	4416
	8 deep cycle batteries and housing	16.8 kWh	2313
	4 kW electric start gas genset	4 kW	3776
	Balance of System and Grid costs		7891
	Total Capital Cost of generation		27780
VILLA LAS ARAUCARIAS	wind turbine with 24m tower	6 kW	29616
	sine wave inverter/charger	3.3 kW	4416
	16 deep cycle batteries and housing	33.8 kWh	4626
	4 kW electric start gas genset	4 kW	3776
	Balance of System and Grid costs		6931
	Total Capital Cost of generation		49365

Operations and maintenance (O&M) and replacement/overhaul costs were estimated based on limited and varied previous experience and are listed in Table 7. There is a large amount of uncertainty in these values, but as can seen by Figure 5, their contribution to the overall COE of hybrid systems is relatively small.

Figure 5 shows the disaggregated COE for the hybrid systems, assuming an 8.7% constant-dollar discount rate (18.2% current-dollar discount rate and 8.7% inflation rate) and a 20-year system lifetime. The estimated cost of gasoline in these remote regions is $0.56/liter. The hybrid systems are attractive to the utility because utility costs for these hybrids in daily operation (O&M, fuel, replacement, and overhaul costs) are quite low. In comparison, genset-only systems would have much lower capital outlays, but much higher operational costs to the utility. The genset-only systems in Figure 5 and Table 8 are all 2.3 kW gensets, which represent least-cost genset-only systems. The COE of the genset-only system at INH is extremely high because of the continuous load, i.e., refrigerator. This results in long operating hours with a very small load, where generators are most inefficient. It also result in large replacement and overhaul costs. VLA's total fuel and genset overhaul costs are similar, but because the total load served is higher, the COE is lower.

As can be seen from Figure 5, the capital cost of equipment has the greatest effect on the energy generation costs for the hybrid systems. The COE is somewhat dependent on gasoline prices and only slightly dependent upon turbine and genset O&M costs. Table 8 shows that tariffs comprise a significant 25% to 30% of the COE. The mini-grid costs vary from about 5% to 15% of the COE.

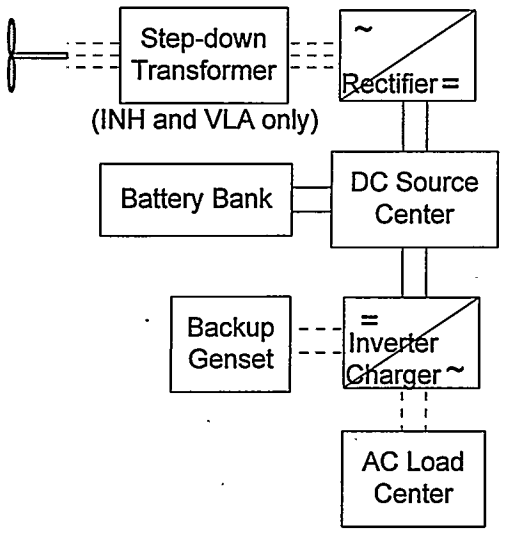

FIGURE 4. SYSTEM DIAGRAM FOR THE WIND/GENSET ARCHITECTURE.

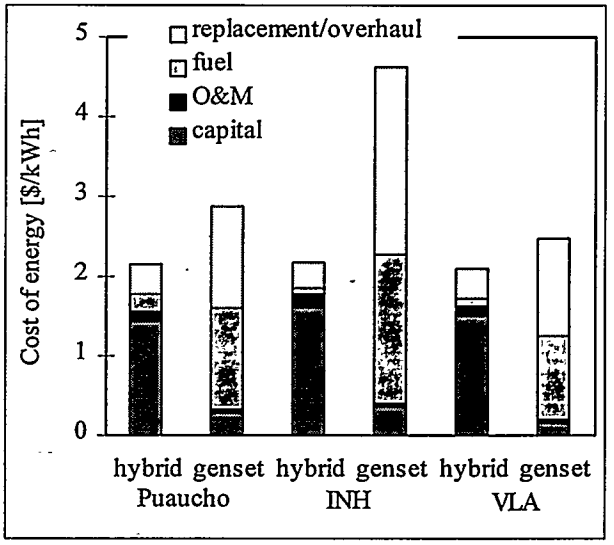

FIGURE 5. COST OF ENERGY FOR THE HYBRID AND GENSET-ONLY SYSTEMS.

TABLE 7. O&M COSTS AND OVERHAUL COSTS USED IN THIS ANALYSIS.

System Component	O&M	Overhaul Cost	Overhaul Period
1.5kW turbine	$0.02/kWh[2]	$1000	10 years
3kW turbine	$0.03/kWh	$1000	10 years
10kW turbine	$0.02/kWh[2]	$2000	10 years
2.3 kW gas genset	$0.05/kWh	$1770	3500 hours
4 kW gas genset	$0.05/kWh	$3776	3500 hours
2.1 kWh batteries	$10/yr	$236	lesser of 1225 kWh throughput or 5 years
2.4 kW inverters/chargers	none	$1588	10 years
3.3 kW inverters/chargers	none	$4129	10 years

Table 8 shows that the given system configurations produce a large amount of excess energy. This can be used for optional loads, such as water-pumping or a battery-charging station, or this can provide for load growth. A battery-charging station is planned for one of the sites. Those villagers who live outside the mini-grid can have their batteries charged with the less expensive, excess electricity from the wind turbine. The economics of this use of excess energy have not yet been determined.

[2] Operations and maintenance costs are assumed to be minimal for these two turbines.

TABLE 8. HYBRID2 RESULTS OF COE AND FUEL CONSUMPTION FOR BASECASE HYBRID AND 2.3 KW GENSET-ONLY SYSTEMS.

Site	Hybrid COE [$/kWh]			Total COE [$/kWh]	Fuel Use [L/yr]		Excess Energy [kWh/yr]
	busbar w/o tax	busbar w/tax	total COE	genset-only	hybrid	genset-only	hybrid
Puaucho	1.62	2.01	2.15	2.88	541	3330	990
INH	1.42	1.93	2.18	4.63	191	6176	3076
VLA	1.56	1.99	2.09	2.48	518	6503	5228

SENSITIVITY ANALYSIS

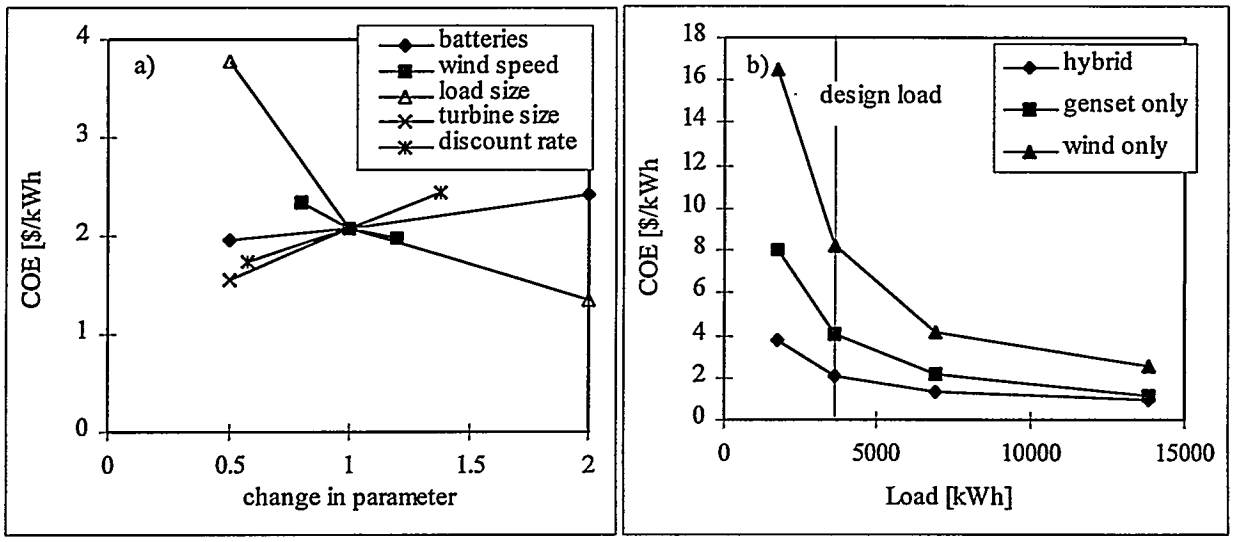

FIGURE 6. SENSITIVITY ANALYSIS OF (A) THE VLA HYBRID SYSTEM AND (B) THE EFFECT OF LOAD SIZE ON THE COE FOR THREE TYPES OF SYSTEMS.

Figure 6a shows the dependence of the COE on variations in storage, annual wind speed, load size, and turbine choice for VLA. Because this particular system has been deliberately oversized, the COE is highly dependent on the sizes of the load and turbine. Doubling the load decreases the COE significantly and halving the load almost doubles the COE. For systems that are sized closer to the load, this effect is less dramatic. A 20–year record of wind data at Concepcion Airport shows a maximum variation in annual wind speed of 20%. A variation of the VLA wind data set by 20% in Figure 6a shows a modest effect on the COE. As the average wind speed increases by 20%, fuel consumption is cut in half, but the COE decreases by about 5%. The same effect occurs with a variation of battery storage. Doubling the number of batteries results in a 15% increase in the COE, because the decreased fuel and genset costs are offset by the increased battery capital and replacement costs. The hybrid system also provides protection from the effects of general inflation and fuel inflation. Inflation is often high and unpredictable in the developing world. Figure 6 shows a modest dependence of the COE on the constant-dollar discount rate, which is a function of inflation.

This illustrates the inherent insensitivity to system uncertainties of wind/genset/battery systems. The COE of a wind-only system would be highly dependent upon storage size and interannual wind variation; these hybrid systems allow for design uncertainty/flexibility, load growth, and lack of long–term resource information.

As an example, Figure 6b compares the effect of load size on the COE for a 4 kW genset-only system, a 24 kW wind/battery system, and the hybrid system. The genset-only and hybrid systems are nearly able to meet the entire load at 14,000 kWh/yr, and for the same COE, but at lower load levels, the hybrid system is more cost-effective. The wind/battery system can only meet 80% of the 14,000 kWh/yr load, and is the most expensive system even at lower loads. This figure clearly shows that for VLA, the hybrid system is best able to cover a wide range of loads for not only the lowest cost, but also for the least variation in cost.

FUTURE PLANS

The pilot projects are intended to demonstrate the reliability of wind–hybrid technology in remote community applications. The process of site identification and evaluation for renewables versus conventional line extension for the replication phase has already begun. Monitoring the performance of these pilots will help identify opportunities for reducing the cost and improving the performance of similar systems in the replication phase. It is expected that as more experience is developed, a lower cost of energy will result through in-country capacity building.

ACKNOWLEDGEMENTS

The authors would like to acknowledge Ramo'n Gala'z Arancibia and Juan Sebastian Barros at CNE; Ramiro U. Pizarro R., Secretariat of Planning and Coordination, Region IX, Chile; and Gustavo Rivero and Rolando Miranda, at SAESA-FRONTEL for their help in all aspects of this project and analysis. We would also like to acknowledge Sergio Castedo and Kevin Rackstraw at AWEA for their work in implementing these projects. Dennis Barley, Michael Bergey, and Peter Lilienthal provided many useful comments.

REFERENCES

Castedo, S., D. Corbus, L. Flowers, R. Holz, D. Lew and A. McAllister. "Wind Hybrid Systems Applications for Rural Electrification: The Case Study of Chile," European Wind Energy Conference, Goteborg, Sweden, May 20-24, 1996.

Green, H.J., J. Manwell. "HYBRID2 – A Versatile Model of the Performance of Hybrid Power Systems," Windpower '95, Washington, DC, March 27-30, 1995.

Lilienthal, P., L. Flowers, and C. Rossman. "HOMER: The Hybrid Optimization Model for Electric Renewables, Windpower '95," Washington, DC, March 27-30, 1995.

Performance Augmentation with Vortex Generators: Design and Testing for Stall-Regulated AWT-26 Turbine

Dayton A. Griffin
Advanced Wind Turbines Incorporated
425 Pontius Avenue North, Suite 150
Seattle, Washington 98109

Abstract

A study investigated the use of vortex generators (VGs) for performance augmentation of the stall-regulated AWT-26 wind turbine. Based on wind-tunnel results and analysis, a VG array was designed for and tested on the AWT-26 prototype, designated P1. Performance and loads data were measured for P1, both with and without VGs installed. The turbine performance with VGs met most of the design requirements; power output was increased at moderate wind speeds with a minimal effect on peak power. However, VG drag penalties caused a loss in power output for low wind speeds, such that performance with VGs resulted in a net decrease in AEP for wind speed sites up to 8.5 m/s.

Introduction

The R. Lynette & Associates (RLA) Next Generation Innovative Subsystems program is designed to develop innovative subsystems which can be used to improve the performance and cost effectiveness of the AWT-26 wind turbine, and which may be usable on other advanced wind turbine designs. RLA is working cooperatively with the National Renewable Energy Laboratory (NREL) and Advanced Wind Turbines Incorporated (AWT) on the program. The program includes a thorough examination of the use of vortex generators to improve the performance of the turbine (Ref. 1). The objectives of the VG project were to:

1. Identify a VG configuration which best augments the performance of AWT turbines, without adversely effecting the turbine dynamics or stall behavior.

2. Gain a greater understanding of the effect of VGs on NREL airfoils, and insight into how VGs may be of use in performance augmentation for a broader class of wind turbines.

An exhaustive literature search was conducted of previously reported work with VGs, and in particular VG applications to wind turbines. Wind tunnel tests were designed to evaluate the effect of VGs on airfoil sections characteristic of the AWT-26 turbine blades. The wind tunnel results, along with insights gained through the literature search, then formed a database from which to design a VG configuration for full-scale testing. The analytic computer code PROPPC (Ref. 2) was used, with wind tunnel data, to conduct performance trade studies for VG sizing and placement, and the effects of various constraints on the design were investigated.

A candidate VG configuration was designed for testing on the AWT-26 prototype, P1. As part of the VG field test, careful measurements were made of the baseline P1 power curve and loads. VG Configuration #1 was then installed on P1, and power curve and loads were again measured. Based on analysis of the performance of the first configuration, it was decided not to test a second VG configuration on P1.

Vortex Generator Aerodynamics

Vortex Generators are typically small wing-like devices which protrude from an aerodynamic surface. The VGs are oriented so they produce longitudinal vortices, which enhance mixing between the free-stream air and the local boundary layer, thinning and energizing the boundary layer so that it can withstand higher adverse pressure gradients prior to flow separation. When used on a airfoil, VGs can delay the onset of stall, increase the maximum lift coefficient (C_{Lmax}), and will result in some drag penalty at low airfoil angles of attack.

VG configurations are of two basic types: co-rotating and counter-rotating arrays. Figure 1 shows airfoils with both array types, with arrows indicating the sense of rotation of the resulting vortices. The co-rotating array produces vortices with the same sense of rotation, while the counter-rotating array produces vortex pairs, with lateral regions of common-flow up and common-flow down. Note that a co-rotating array has a single lateral spacing parameter, d, while the counter-rotating array has two lateral spacing parameters, d ≡ distance between two VGs which form a pair, and D ≡ distance between each pair of VGs. Additional VG parameters are illustrated in Figure 2, where again VGs of the flat-vane type are shown. For this type of VG, a configuration will be completely defined by the parameters shown. Note that all of the spacing parameters may be given in physical dimensions, but will frequently be normalized to another characteristic dimension (e.g. x/c, h/c, d/D).

Wind Turbine Applications

The first reported use of VGs to improve wind turbine performance was in 1983, when counter-rotational VG arrays were installed on the horizontal axis Boeing MOD-2 (Ref. 3). The MOD-2 blade aerodynamics were far from optimal, and so the use of VGs resulted in a large (11%-15%) increase in

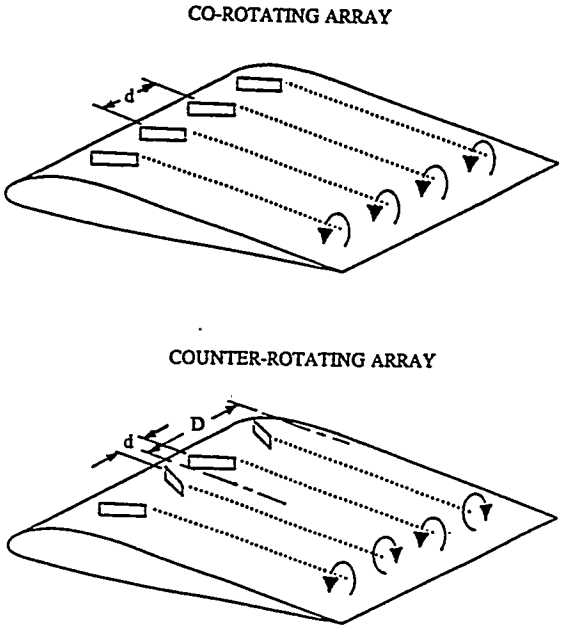

Figure 1. Schematic of Counter- and Co-Rotational VG Arrays

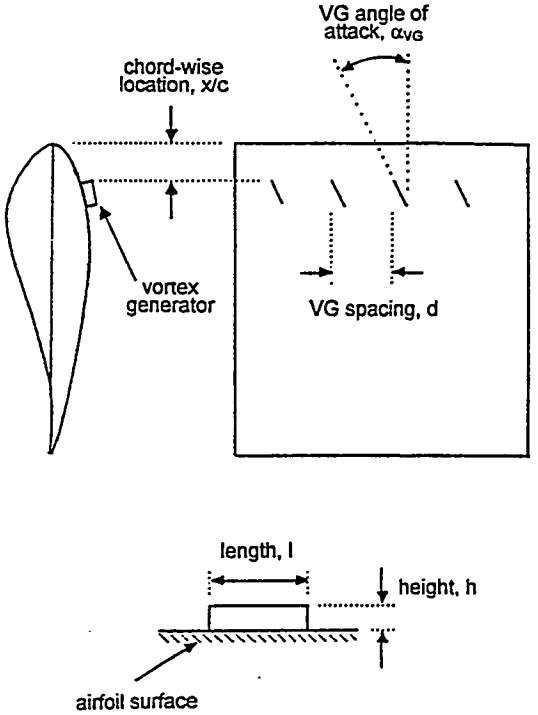

Figure 2. Parameters which Define Vortex-Generator Configurations

AEP for the turbine. Successful VG designs were reported for a Carter Model 25 (Ref. 4) and, and a 50 kW DAF two-bladed Darrieus turbine (Ref. 5), resulting in 20% and 72% increases in peak power output, respectively. Alternately, a very unsuccessful test was reported in 1990, when VGs were applied to several ESI 54 HAWTs (Ref. 6). Although the turbine performance results were initially encouraging, unstable dynamics led to the destruction of one rotor, and a cancellation of the VG test.

The early successes of VG applications to wind turbines had several things in common; the turbines were not stall-regulated, the airfoils of the turbine blades were NACA sections, and the VGs were used to significantly increase the maximum lift coefficient. For the NREL thick-airfoil families designed with low C_{Lmax} for wind turbine applications, and particularly for these airfoils on a stall-regulated rotor, the advantage of using VGs is much less obvious. Use of VGs to delay stall and increase C_{Lmax} seems contrary to both the airfoil and rotor designs.

This study was motivated by the idea that VGs may still be used to improve a stall-regulated turbine using low C_{Lmax} airfoils, although the margin for improvement is admittedly smaller than for early wind turbine applications. The general idea is that with proper sizing and placement, VGs could delay stall and increase lift up to a specified wind speed such that the VGs will become stalled, allowing the turbine to retain its baseline post-stall performance. This is illustrated by Figure 3, which shows an S815 airfoil lift curve, and a possible modification with VGs. Three regions are indicated on the lift curve of Figure 3:

Region A - Here the baseline lift curve is already linear. In this region VGs can not increase lift, and must cause some drag penalty.

Region B - The VGs are delaying stall, causing the lift curve to remain linear to a higher angle of attack, and increasing C_{Lmax}. The VGs will cause a net decrease in drag in this region, as the form drag of the airfoil is decreased.

Region C - Here the airfoil is stalled, with the VGs embedded in the airfoil wake. In this region the VGs should have no effect on either lift or drag of the airfoil.

For VGs to cause a net increase in power production, the lift and drag benefits in region B must outweigh the drag penalty paid in region A. Of additional concern is the increased sharpness of stall between regions B and C. For the case illustrated in Fig. 3, the VGs will be of benefit between 6° and 18° airfoil angles of attack, and the design stall angle is 18°, beyond which the VGs should have no effect. In the present work, the airfoil angle of attack beyond which VGs have no effect is designated the VG stall angle, $\alpha_{VG,stall}$. Note that for a specific turbine blade and pitch setting, the VG stall angle would have a unique corresponding wind speed at each radial blade location.

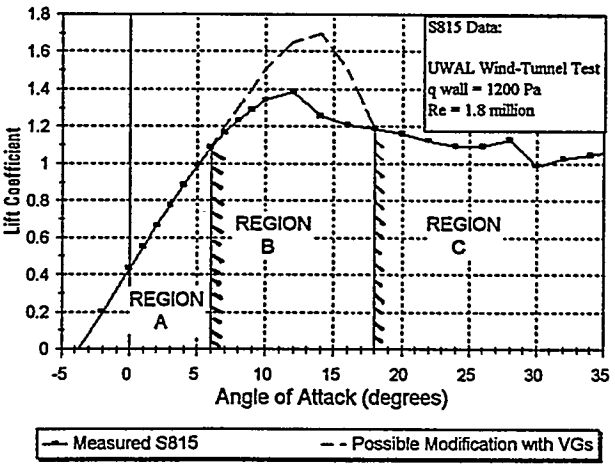

Figure 3. Regions of VG Effect on Airfoil Lift Curve

UWAL Wind Tunnel Experiments

Wind tunnel experiments were designed to provide VG data specific to the NREL airfoil sections which are characteristic of the AWT-26 blade. The experiments were used to quantify the incremental performance improvements and associated drag penalties for airfoils with VG arrays of varying density, height, orientation, and chordwise placement. The wind-tunnel experiments were conducted at the University of Washington Aeronautical Laboratories (UWAL), a subsonic, double-return, closed-circuit tunnel. The UWAL test section is 2.4 m high x 3.6 m wide x 3.0 m long (8 x 12 x 10 ft), vented to the atmosphere. The tunnel can supply dynamic pressures from 47.8-4780 Pa (1-100 psf), and wind-speeds from 8.9-89 m/s (20-200 mph), with approximately zero flow angularity, and 0.72% turbulence intensity.

A modification of the 2.4 x 3.6 m test section for 2-D testing was designed cooperatively by AWT and UWAL. The 2-D insert is formed by 15.2 cm (6 in) thick walls which span from floor to ceiling, extend 0.3 m (1 ft) forward and 0.9 m (3 ft) aft of the 3-D test section, and are mounted with a lateral separation of 1.22 m (4 ft) to centers. Airfoils are mounted between two turntables, which are flush with the 2-D walls, and are in turn supported by the UWAL force balance. The balance struts are embedded in the 2-D walls, and are not impacted by the airflow through the test section.

Three airfoil sections, taken from radial stations along the AWT-26 turbine, were selected for the test. The AWT-2601 was a pure SERI S815 with a thickened trailing edge, and the AWT-2602 and 2603 were hybrids of S815/S809 and S809/S810 airfoils, respectively. The wind-tunnel models of these sections were 61 cm (24 in) long, CNC machined from rolled aluminum plate. The models allowed testing at Reynolds numbers in excess of $Re_c=3x10^6$, equal to or higher than typical for the full-scale turbine.

A rectangular VG planform was selected for testing on the basis of historic effectiveness, simplicity of manufacture, and ease of installation. VG sizing should be such that the desired airfoil performance is achieved, with a minimum of drag penalty. It was expected that heights of 1.0% and 0.5% chord, approximately 6.35 mm (0.25 in) and 3.18 mm (0.125 in), would be of interest.

The standard test run was force measurements, taken at constant dynamic pressure and variable angle of attack. Test runs included 145 unique configurations and conditions, with the matrix constructed from the parameters shown in Table 2. The test was run as a careful sweep through parameter space, with initial results used to identify cases for more detailed study. VG sizing and placement trends were evaluated using co-rotating arrays. Selected counter-rotating configuration were also tested.

Table 2. Wind-Tunnel Test Parameters

Blade Station (Test Model)	35%, 55%, 75% Radius (2601, 2602, 2603)
Array Orientation	Co- Rotating/ Counter-Rotating
VG Height	h = 6.4, 4.8, 3.2 mm
Chord Location	x/c= 0.1, 0.3, 0.4, 0.5, 0.6
Array Density	d/h= 10, 20, 30, 40
Blade Condition	Clean / with LEGR (Ref. 7)
Reynolds #	1.1, 1.8, 2.5, 3.0, 3.4 $x10^6$

Wake-rake measurements were used to measure the profile drag of each airfoil, and to establish a drag tare for skin-friction and interference-drag at the turntables. Having established the tares, all drag measurements were made with the force balance. The UWAL drag measurements showed excellent repeatability, within 1 drag count (0.0001 of a drag coefficient) for repeat runs of the same configuration. Measured lift and drag curves for the clean AWT-2601 were compared with Eppler calculations for the S815 (Ref. 8), and showed very good agreement.

Figure 4 shows that VGs placed at forward chordwise locations on the airfoil gave the greatest increase in C_{Lmax}, and persisted to a higher angle of attack prior to stalling. Forward placed VGs, particularly those at x/c=0.1, also caused a penalty in the linear portion of the lift curve. This was attributed to the VGs triggering early transition, and thus compromising the laminar flow of the airfoils. This trend was observed for all airfoils tested, most noticeably when the VGs were at or forward of x/c=0.3.

The drag caused by the VGs is consistent with the lift curve trends, with the highest drag penalty (about 45 counts) for the furthest forward placement. Note that although the VGs cause a drag penalty at low airfoil angles of attack, they give a drag benefit for airfoil angles greater than 10°, as trailing-edge separation is delayed. Configurations which are most persistent in stall delay will show the largest reductions of form drag, but will also have the largest drag penalties at low angles of attack.

Figure 5 shows that C_{Lmax} is only slightly changed by varying array density, but the effect on the pre-stall lift curve is dramatic. Note also that the angle at which the VGs became stalled appears insensitive to the array density. These density trends were observed throughout the test, for all three airfoils, and all three VG sizes. Another consistent trend was the dependence of drag penalty on VG array density. This is amplified on Figure 6, which shows that a doubling of the array density lead to an approximate doubling of the VG drag penalty.

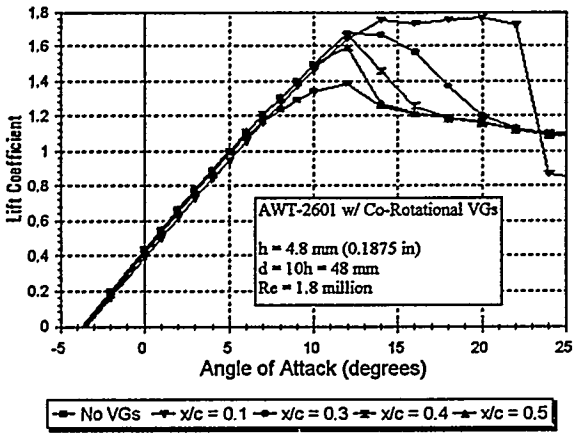

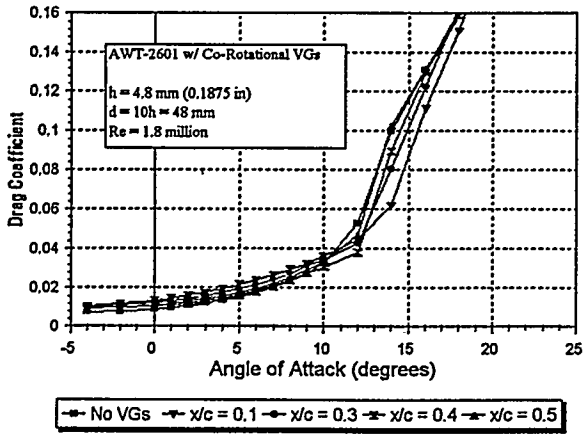

Figure 4. Variation of VG Effectiveness with Chordwise Placement

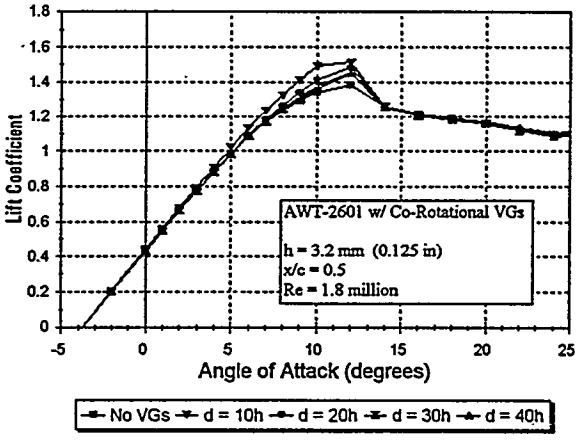

Figure 5. Variation of VG Effectiveness with Array Density

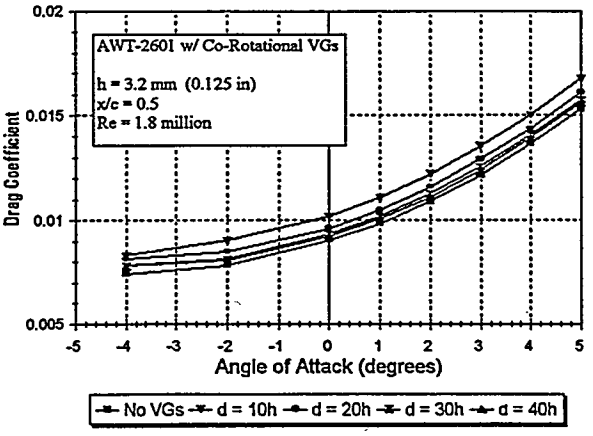

Figure 6. Impact of Array Density on VG Drag Penalty

Design and Analysis

The results of the wind tunnel tests, combined with insights gained through the literature search, were used to design a VG configuration for full-scale testing. Note that this design and analysis has been performed for the AWT-26 rotor, and specific results in terms of VG sizing and placement may not generalize to other rotor designs. However, the design issues, tradeoffs, and methods illustrated in the present work may be applicable to a wider class of wind turbine rotor designs. The goals of this phase of the project were to design a VG configuration which;

1. best augments the performance of the AWT-26 at low-to-moderate wind speeds,
2. does not impact the peak power or peak loads of the turbine,
3. leads to no adverse turbine dynamics.

In predicting performance with VGs, the largest uncertainty was in using measured two-dimensional airfoil data to predict expected three-dimensional blade properties. The UWAL experiments resulted in a database of 2-D ΔC_L and ΔC_D, for a wide range of VG design parameters. Using this database to determine an optimal full-scale design implies knowledge of two things; the 3-D aerodynamic properties of each blade section, and how these properties would be modified by the use of VGs. This distinction is of particular importance to VG design for a stall-regulated wind turbine. Current research shows that the inboard portions of the blade may be seeing significant stall delay, possibly due to centrifugal pumping effects on the boundary layer. If the boundary layer on these blade sections is already modified by 3-D effects, the additional effect of VGs in uncertain. For blade sections experiencing 3-D stall delay, the ΔC_L gained by VGs may be diminished, with similar uncertainties for the 3-D effects on drag and VG stall angle.

PROPPC was used to conduct performance trades, where calculations were performed with a baseline AWT-26 input deck, and with modified decks to simulate possible VG configurations. In modifying the input decks, incremental changes in airfoil properties, ΔC_L and ΔC_D, were applied directly as measured in the UWAL tests. Annual energy production (AEP) calculations were used to evaluate performance gains, for a range of VG heights, chordwise placements, and array densities. In all cases, the performance trades favored a forward chordwise placement of the VGs, the additional drag penalty at low angles of attack being more than offset by the additional persistence of the VGs at moderate to high angles of attack. The calculations showed this trend even when VGs were placed so far forward as to disturb the laminar flow of the airfoil section.

During the PROPPC trades, the only constraint imposed was that the baseline peak rotor power not be exceeded, and the calculations predicted that VGs could result in up to a 4.5% gain in AEP for the AWT-26 rotor. Within this constraint, optimum performance gain was achieved by placing the VGs as far forward on the blade as possible, while still allowing the VGs to stall prior to peak rotor power. If this design could be achieved at each radial blade station, the entire modified portion of the blade would experience a sharp stall at wind speeds between 16.1 and 17.0 m/s (36 and 38 mph). Although in practice 3-D effects may prevent such an abrupt stall of the inboard half of the blade, this is clearly not a desirable design. A safer approach is to design for smooth stall progression along the blade.

PROPPC calculations were used to generate angle of attack versus wind speed tables for each AWT-26 blade radial station. Combining these tables with data for VG stall angles, $\alpha_{VG,stall}$, as a function of chordwise placement and height, a VG array can (in theory) be designed to achieve any specified stall progression. Note that based on the PROPPC performance analysis, designing a VG array for smooth

stall progression will result in less than optimal AEP gains. Based on the analysis described above, the following approach was taken in designing a VG array for full-scale testing:

1. A co-rotational orientation was chosen. The wind tunnel data for counter-rotating VG arrays had an apparent on-design/off-design nature, with some configurations giving superior performance to co-rotating arrays, and some configurations worse. The data for the co-rotating arrays varied more smoothly and predictably with height and spacing, and thus offered increased confidence when interpolating between measured (wind-tunnel) geometries to predict full-scale performance.

2. A full-scale height of 6.35 mm (0.25 in) was selected. For simplicity, reduced cost, and ease of installation, a fixed VG size was desired. Analysis showed a weak performance dependence on VG height, with 6.35 mm scaling close to optimal over the modified portion of the blade.

3. VG angle of attack was nominally chosen as 15°. Wind tunnel data showed no drop-off in VG performance until $\alpha_{VG} < 12.5°$, and an increase in drag penalty for $\alpha_{VG} > 15°$. The easiest method for locating VGs during installation was to use templates with a single preset angle. When applied to the AWT-26 blade, this resulted in all VGs being set near 15°, with the maximum $\alpha_{VG} < 20°$.

4. Lateral spacing was specified as d=15h=9.5 cm (3.75 in). Although the wind-tunnel data and PROPPC calculations indicated that d=10h was superior in performance to d=20h, the d=10h geometry was considered to dense to be practical. The d=15h array was chosen as a compromise, and the performance was calculated by interpolation of wind-tunnel data. A spanwise variation in lateral spacing was considered, but no performance benefit was predicted by the analysis.

5. Lateral extent of the array was limited to 60% radial location. Beyond this radial position, VGs which are placed far enough forward on the blade chord to be effective will delay airfoil stall beyond the desired angle, resulting in increased peak rotor power.

6. Chordwise location of the array was determined to achieve desired stall progression. Wind tunnel data showed that VG effectiveness and persistence are strong functions of chordwise placement. Therefore, even with most parameters specified in steps 1-5 above, the array performance can be strongly influence by this remaining design choice. The present design imposes the constraint that no more than 10% of the blade's radial span become stalled during an incremental increase in wind speed of 0.9 m/s (2 mph). As nearly 60% of the overall blade has been modified, this requires that the VG array become stalled over a minimum of a 5.4 m/s (12 mph) wind-speed range.

The resulting design, VG Configuration #1, is summarized in Table 3. Note that this design is at the boundaries of a constraint. At each radial location the VGs are as far forward as possible without violating the requirement of smooth stall progression. Within this constraint, PROPPC analysis showed that this configuration would be the most effective in terms of performance gains. However, the PROPPC results are dependent on two things: the accuracy of

Table 3. Array Parameters for VG Configuration #1

VG type	Flat-plate vane, with leading-edge radius
VG height	6.35 mm (0.25 in)
VG length	25.4 mm (1.0 in)
VG angle of attack	15° nominal
Lateral spacing	9.52 cm (3.75 in)
Spanwise extent	Blade root to 57.5% radius
Chordwise location	Variable, 10% to 45% chord
Number of VGs	69 per blade (138 total)

the baseline (3-D) input deck, and the assumption that the 2-D ΔC_L and ΔC_D from the wind tunnel test accurately characterize the 3-D performance of VGs on the AWT-26 rotor.

Full-Scale Performance Test

The full-scale VG test was conducted on the AWT-26 wind turbine, P1, located at the AWT test site in Tehachapi, CA. In summary, the P1 turbine is a downwind, free-yaw, fixed-pitch machine which achieves high efficiency through the use of NREL S815/S809/S810 airfoils. The rotor is a teetered, two-bladed, stall-regulated design. The blades are made of wood-epoxy laminates, reinforced with carbon fiber. It has a diameter of 26.2 m (86 ft) and has a nominal speed of 57.1 rpm. For the VG performance test, the blade pitch was set for a peak generator power of approximately 290 kW.

P1 instrumentation for power curve measurement included atmospheric pressure and temperature gages, electrical power measurements, and wind measurements, which were recorded as 1-minute averages using a Power Curve Monitor (PCM). Loads and dynamics data was measured through an Advanced Data Acquisition System (ADAS), and included nacelle accelerations, tower leg loads, and yaw position. A site calibration was used to account for local terrain effects, and measured power was normalized to a reference air density of 1.06 kg/m^3. The selection process eliminated data collected in poor weather (heavy rain, snow), where blade soiling was undesirably high, and when the turbine was off-line for any part of the 1-minute averaging period. Additionally, data was removed for wind directions such that either the P1 turbine or MET tower was waked. Once the valid data sets had been selected, and density corrections applied, the 1-minutes averages were binned by wind speed, with bin centers 0.9 m/s (2 mph) wide. Wind speed, direction, and density-corrected power were then averaged for each bin, resulting in the power curve for the data set. When multiple data sets were combined, a time-weighted average was used for each wind-speed bin.

The VGs were expected to yield small percentage gains in power production, and this could only be measured if the baseline power curve showed very good repeatability. Two criteria were applied to evaluate the repeatability of power curves; the percentage variation of power output at each wind-speed bin, and the percentage variation of AEP as calculated for various Rayleigh wind-speed distributions (assuming uniform distributions at turbine hub height and 100% availability).

The baseline and modified power curves both showed a trend toward improved repeatability with increasing data hours. Figure 7 shows two curves with over 300 hours of binned data per curve. For most bins, the power output of these curves varied by less than 2%, and AEP variation was less than 1% for Rayleigh wind-speed averages above 6.2 m/s (14 mph). With this degree of repeatability, the power curves of Figure 7 were considered to be a high-confidence measure of the baseline P1 performance. The 300-hour curves with VGs showed good repeatability with each other, although not as good as for the baseline P1. For most wind-speed bins the power output varied by less than 3%, and the AEP variation was less than 2% for all Rayleigh wind-speed averages over 6.2 m/s (14 mph).

Figure 8 shows the total average P1 performance, with and without VGs. The curves show a noticeable drop in power output for wind speeds below 11 m/s (25 mph), and an increase in power above this wind speed. The maximum increase in power was just over 4% at 12.8 m/s (29 mph). The increase in peak rotor power was minimal, about 1% at 17.2 m/s (39 mph). From this standpoint, the design goal of increasing power at moderate wind speeds without increasing rotor peak power was met. However, the AEP table on Figure 8 shows that the losses at low wind speeds were not sufficiently offset by performance gains at moderate wind speeds, and the net effect of the VGs was a loss in AEP for annual average wind-speeds up to 8.4 m/s (19 mph).

The slight increase in peak power indicates that the VGs had become largely, but not entirely, stalled at wind speeds above 17 m/s (38 mph). Therefore, the VG array was placed as far forward on the blade as possible, while still retaining the baseline stall behavior. Below 11 m/s, the drag loss in turbine performance was greater than predicted by PROPPC calculations. It appears that the turbine blade did not experience the same amount of lift benefit as measured for the 2-D airfoil sections, yet still saw significant drag penalties. Moving the VGs aft on the blade would decrease the drag penalty, but would also cause the VGs to be less persistent. Therefore, decreasing drag losses by moving the VGs aft would likely compromise some of the performance gains above 11 m/s, with similar logic applicable to either making the VG array less dense, or using smaller VGs. In terms of recovering turbine performance lost to blade soiling, the present design offers little promise, as the most severe soiling occurs on the outboard portions of the AWT-26 blades.

To evaluate the potential for improving on VG Configuration #1, an AEP calculation was performed for the power curve of Figure 8, assuming no drag losses, and retaining all of the benefit above 11 m/s. The results showed performance gains of less than 1.5% for wind-speed averages of 8.4 m/s and below. This confirms that the 3-D effectiveness of the VGs was less than that measured for the 2-D airfoil sections. Based on these results, field testing of a second VG configuration was not deemed worthwhile.

The impact on loads was less conclusive. The available data indicated that the VG array caused an increase in dynamic loads, but the data sets were somewhat limited. Had the performance of the VG design proven more promising, further measurements would have been warranted to better quantify the effects on loads and component fatigue life.

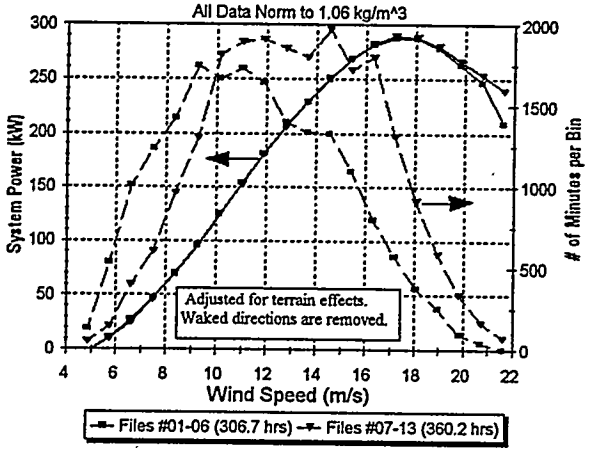

Average Wind Speed (m/s)	Average Wind Speed (mph)	P1 Baseline Files #01-06 AEP (kWh)	P1 Baseline Files #07-13 AEP (kWh)	Variation (%)
5.3	12	235,551	232,291	-1.38
5.7	13	304,826	301,621	-1.05
6.2	14	378,965	375,884	-0.81
6.6	15	456,998	454,144	-0.62
7.1	16	537,169	534,650	-0.47
7.5	17	617,470	615,447	-0.33
7.9	18	696,870	695,574	-0.19
8.4	19	774,291	773,874	-0.05

Figure 7. Repeatability of Baseline P1 Power Curve

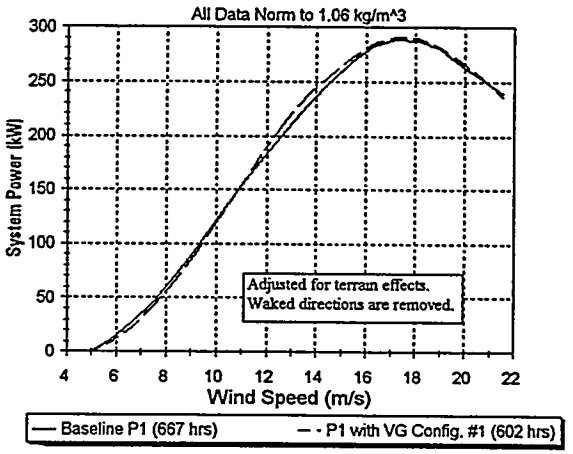

Average Wind Speed (m/s)	Average Wind Speed (mph)	P1 @ 288 kW Baseline AEP (kWh)	P1 with VG Config. #1 AEP (kWh)	Variation (%)
5.3	12	234,829	224,737	-4.30
5.7	13	304,129	294,182	-3.27
6.2	14	378,314	369,090	-2.44
6.6	15	456,466	448,445	-1.76
7.1	16	536,844	530,322	-1.21
7.5	17	617,494	612,641	-0.79
7.9	18	697,459	694,317	-0.45
8.4	19	775,587	774,143	-0.19

Figure 8. Effect of VG Configuration #1 on P1 Performance

Conclusions

While the present work did not lead to improved AEP for the AWT-26 turbine, it does contribute to the understanding of performance augmentation of wind turbines with VGs. Wind tunnel measurements have quantified the (2-D) effect of VGs on NREL S-series airfoils, for a wide range of VG design parameters. The safe design of a VG array for a stall-regulated turbine has been demonstrated, and several issues involving optimal performance with VGs have been identified and addressed.

Acknowledgments

The present work was supported by NREL, under Subcontract # ZAA-5-12272-05, monitored by Paul Migliore. The author would like to thank Paul and others at NREL for their support on this project, including many helpful technical discussions. The large number of configurations tested in the wind tunnel, and the quality of the data, formed a solid foundation for this work. The success of the wind tunnel test was due to the effort of Professors David Russell and Scott Eberhardt, the design assistance of Bob Blair, the machining support of Bill Lowe, and the outstanding work performed by the entire crew of UWAL. Paul Robertson and his engineering staff at Aeronautical Testing Services were invaluable in manufacturing the wind-tunnel models, and providing both materials and advice for the wind-tunnel and field tests. Thanks also to Shawn Lawlor and Richard Beckett, who both contributed much inspiration and insight to this project.

References

1. Griffin, D.A., *Investigation of Vortex Generators for Augmentation of Wind Turbine Power Performance*, NREL/TP-440-21399, Golden CO: National Renewable Energy Laboratory, publication pending.

2. Tangler, J.L., *HAWT Performance Prediction Code for Personal Computers*, Solar Energy Research Institute, January 1987.

3. Sullivan, T.I., *Effect of Vortex Generators on the Power Conversion Performance and Structural Dynamics Loads of the MOD-2 Wind Turbine*, NASA TM, 83680, 1984.

4. Gyatt, G.W., *Development and Testing of Vortex Generators for Small Horizontal Axis Wind Turbines*, AeroVironment Inc., NASA CR-179514, July 1986.

5. Quinlan, P.J., Scheffler, R.L., and Wehrey, M.C., *Performance Test Results of Vortex Generators Attached to a Vertical Axis Wind Turbine*, 7th ASME Wind Energy Symposium, January 1988.

6. Haller, M.E., *Vortex Generator Field Tests on ESI 54 WTGs (modified), an Empirical Approach*, SeaWest Altamont, Inc., July, 1990.

7. Ramsay, R.R., Hoffmann, G.M., and Gregorek, G.M., *Effects of Grit Roughness and Pitch Oscillations on the S815 Airfoil*, Midwest Research Institute Contract Number XF-11009-3, August, 1994.

8. Tangler, J.L., National Renewable Energy Laboratory, Golden CO, personal communications, 1995-1996.

Influence of Pitch, Twist, and Taper on a Blade's Performance Loss Due to Roughness

J. L. Tangler
National Renewable Energy Laboratory
1617 Cole Boulevard
Golden, Colorado 80401-3393

ABSTRACT

The purpose of this study was to determine the influence of blade geometric parameters such as pitch, twist, and taper on a blade's sensitivity to leading edge roughness. The approach began with an evaluation of available test data of performance degradation due to roughness effects for several rotors. In addition to airfoil geometry, this evaluation suggested that a rotor's sensitivity to roughness was also influenced by the blade geometric parameters. Parametric studies were conducted using the PROP computer code with wind-tunnel airfoil characteristics for smooth and rough surface conditions to quantify the performance loss due to roughness for tapered and twisted blades relative to a constant-chord, non-twisted blade at several blade pitch angles. The results indicate that a constant-chord, non-twisted blade pitched toward stall will have the greatest losses due to roughness. The use of twist, taper, and positive blade pitch angles all help reduce the angle-of-attack distribution along the blade for a given wind speed and the associated performance degradation due to roughness.

INTRODUCTION

Unlike aircraft which fly at high altitudes, wind turbines operate within the earth's lower boundary layer (0 to 300 meters) where their blades are exposed to various contaminates. During early spring, insect hatches can severely contaminate an airfoil leading edge. In desert regions, blowing sand also erodes the blade's leading edge. Particulates resulting from the local use of fossil fuels also accumulate on turbine blades. Airfoil roughness adversely affects the energy production of a wind turbine, particularly stall-regulated wind turbines. Performance losses due to leading-edge roughness vary with turbine type. These losses have been found to reduce annual energy production from 5% to 10% for variable-rpm rotors, 5% to 20% for variable pitch rotors, and up to 20% to 30% for stall-regulated rotors (Reference 1).

Rotor performance losses due to roughness were first addressed in the mid 1980's at the Solar Energy Research Institute (SERI), now the National Renewable Energy Laboratory (NREL), through the design of new airfoil families. Environmental roughness effects were simulated with grit (Reference 2 and 3) in the region of the leading edge. Atmospheric tests of stall regulated blades using NREL custom-tailored airfoils demonstrated significant reductions in the energy loss due to roughness (Fig.1). These tests, for both clean and rough surface conditions, also suggested that roughness losses may be related to blade geometric parameters such as pitch, twist, and taper. The first of these tests in 1990 (Reference 2) was a side-by-side comparison between three-bladed, Micon 13/65 wind turbines operating in the San Gorgonio Pass, one with AeroStar 7.4-meter blades and one with NREL/Phoenix 7.9-meter blades. At the same location, a later side-by-side test in 1991 (Reference 4) included a comparison between three-bladed, Micon 108 wind turbines, one with AeroStar 9.1-meter blades and the other with NREL/Phoenix 9.7-meter blades. The measured performance loss due to severe roughness effects versus wind speed is shown in Fig. 2 for the Micon 65 and Micon 108, respectively. A comparison of these tests yields several interesting trends for the roughness losses that appear to be correlated with blade angle of attack.

For the Micon 13/65, the roughness loss at low wind speeds is close to 45% for both rotors and drops off at higher wind speeds to around 25% for the AeroStar 7.4-meter blade and 11% for the 7.9-meter NREL/Phoenix blade. The lower loss for the 7.9-meter blade is attributed to the use of NREL airfoils, more blade twist (20° versus 8.4°), a more favorable 75% radius blade pitch (4.2° toward feather for the 7.9-meter blade versus 0.5° toward feather for the 7.4-meter blade), and possibly thinner airfoils. The annual-energy improvement of the 7.9-meter NREL blade relative to the 7.4-meter AeroStar blade was measured to be 30% as tested on the Micon 65. On a Bonus 65 turbine, tested in Altamont, this relative improvement was dropped to 20%. This difference appears to be due to the higher rpm of the Bonus (54 rpm versus 48 rpm for the Micon) which requires a more negative blade pitch angle to control peak power, which in turn contributes to greater roughness losses.

For the Micon 108, the roughness loss (Fig.2) at low wind speeds is 0% to 15% and continuously increases with wind speed to 28% for the 9.1-meter blade and to 23% for the 9.7-meter blade. This trend is opposite that of the Micon 13/65 test for the following reason. The smaller roughness losses at low wind speeds for the Micon 108 appear to be largely due to it's 45 rpm, single speed, operation. The Micon 65 has two speeds, 30 rpm at low wind speeds and 48 rpm at medium to high wind speeds. Although the low speed enhances energy output, it also results in a higher angle of attack at low wind speeds which increases roughness losses. The greater twist of the 9.7-meter NREL/Phoenix blade relative to the 9.1-meter AeroStar blade (20° versus 16°) results in a roughness loss close to zero at low wind speeds. A minimal roughness sensitivity improvement of 5% is seen for the 9.7-meter NREL/Phoenix blade relative to the 9.1-meter AeroStar blade. This small difference appears to be due to blade pitch and possibly airfoil thickness differences. The 9.1-meter blades were pitched to -1.5° degrees for a 115 kW peak power; whereas, the 9.7-meter blades had to be pitched more toward stall to -1.9° for 115 kW peak power. The following parametric studies will show that negative blade pitch angles toward stall significantly contribute to roughness losses.

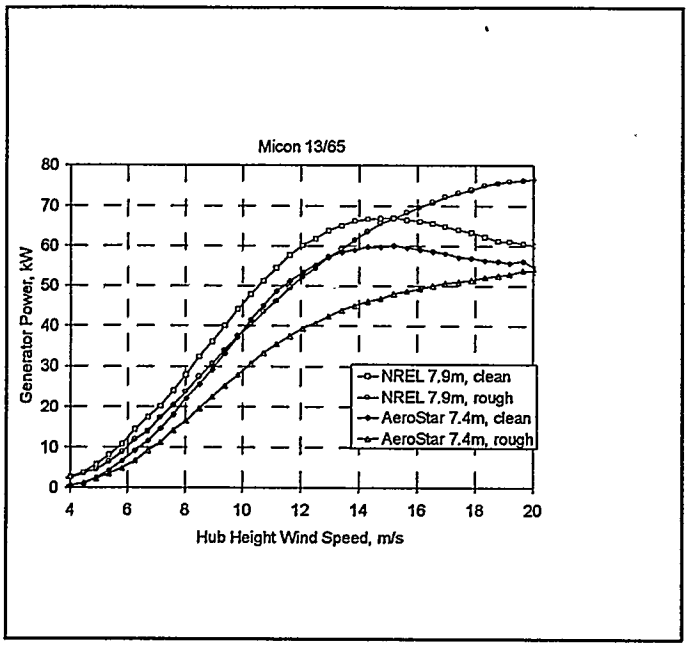

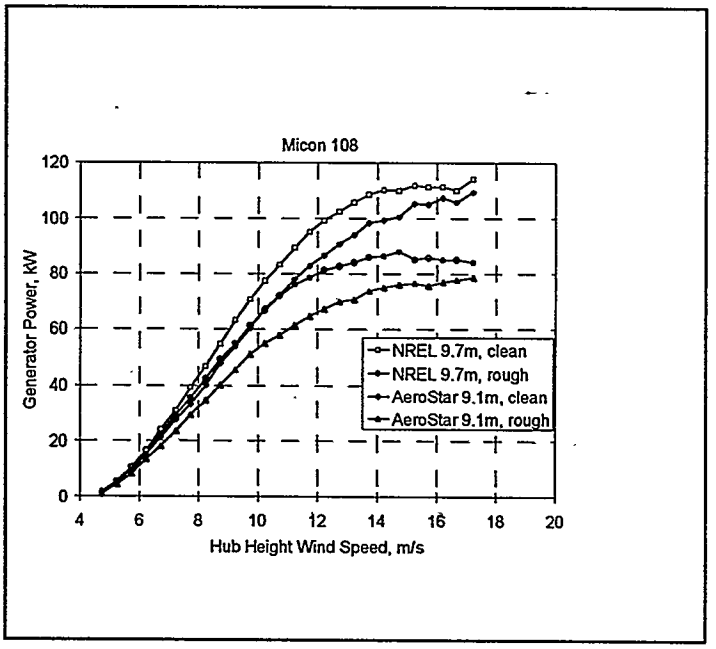

Fig. 1. Micon 13/65 and Micon 108 power curves for clean and rough blades

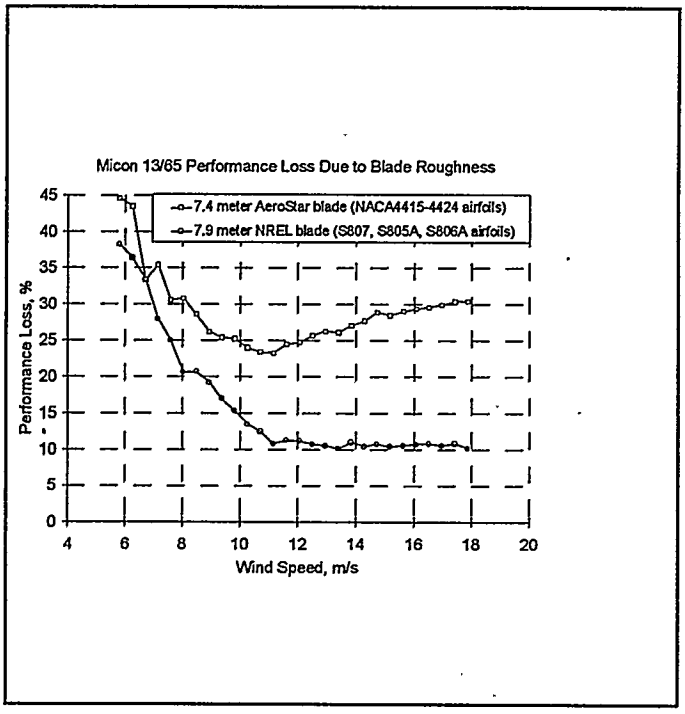

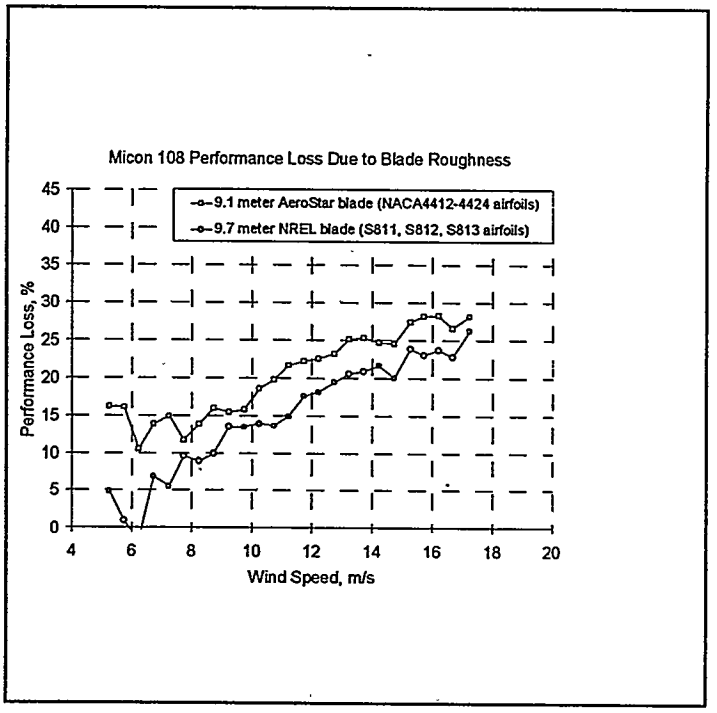

Fig. 2. Micon 13/65 and Micon 108 performance loss due to blade roughness

A third test was conducted by Zond Systems was with a Vestus 65 wind turbine, in which the performance of the NREL/Phoenix 7.9-meter blade was compared to that of the LaCadre 7.9-meter blade (Reference 7). These tests for clean and rough surface conditions yielded performance differences that can be traced to both differences in the airfoils and blade geometric parameters such as pitch and twist.

Recent two-dimensional, wind-tunnel studies (Reference 5 and 6) have also indicated that thicker airfoils may be more sensitive to roughness effects. These studies showed that the decrease in maximum lift coefficient ($c_{l,max}$) from simulated severe roughness was 25% for the S814 (thickness/chord, t/c=0.24), 18% for the S812 (t/c=0.21), and 12% for the S813 (t/c=0.16). These airfoils also have different $c_{l,max}$ that range from 1.4, to 1.2, to 1.1 for the S814, S812, and S813, respectively, which makes it difficult to isolate the effect of airfoil thickness on roughness sensitivity. Further refinements to custom tailored airfoils are planned through a better understanding of the influence of airfoil thickness and $c_{l,max}$ on roughness sensitivity.

Field test data indicate that when new roughness-tolerant airfoils are incorporated into a blade design, geometric blade parameters such as pitch, twist, and taper also affect the blade sensitivity to roughness, particularly for stall-regulated blades. The following section of the paper will explore and quantify how these blade geometric parameters affect roughness-induced performance losses.

ANALYTICAL ANALYSIS

Leading edge roughness degrades airfoil lift characteristics in two ways. The most significant effect is the reduction in the $c_{l,max}$. As the angle of attack increases and the lift coefficient approaches $c_{l,max}$, the adverse pressure gradient on the suction surface of the airfoil becomes more severe and the boundary layer thickens. An airfoil's lift curve slope is also adversely affected by roughness. Roughness increases the thickness of the airfoil's boundary layer on the suction surface more than on the pressure surface. This difference in boundary layer thickness effectively decambers the airfoil, which results in a reduction in the lift curve slope. The decambering effect becomes larger with angle of attack and can be expected to be larger for airfoils having a high $c_{l,max}$. Roughness also leads to greater airfoil drag. These factors are the primary contributors to an airfoil performance loss due to roughness.

The measured performance trends observed for clean and rough blades for the various atmospheric tests were confirmed with the PROP93 blade-element/momentum theory performance prediction code. This was accomplished through parametric studies in which the pitch, twist, and taper were varied for clean and rough airfoil performance characteristics. Airfoil performance characteristics for the LS(1)-0417MOD airfoil, which was used on several first generation machines in the 1980's, were obtained from two-dimensional, wind-tunnel tests conducted in Ohio State's 3' X 5' wind tunnel. These two-dimensional data are shown in Fig. 3a and in Fig. 3b with three-dimensional post stall modifications.

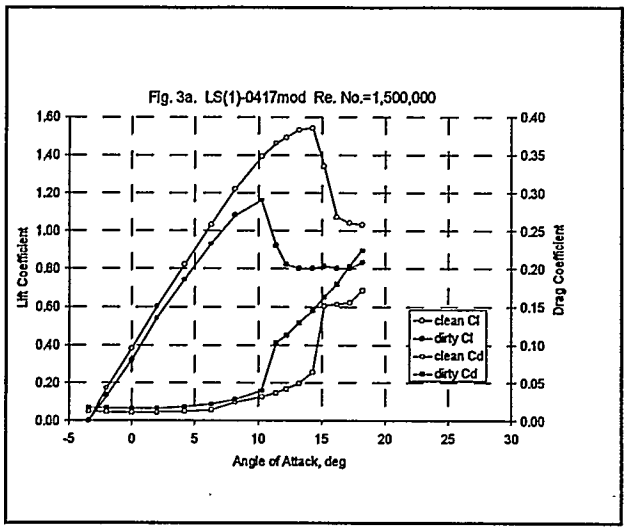

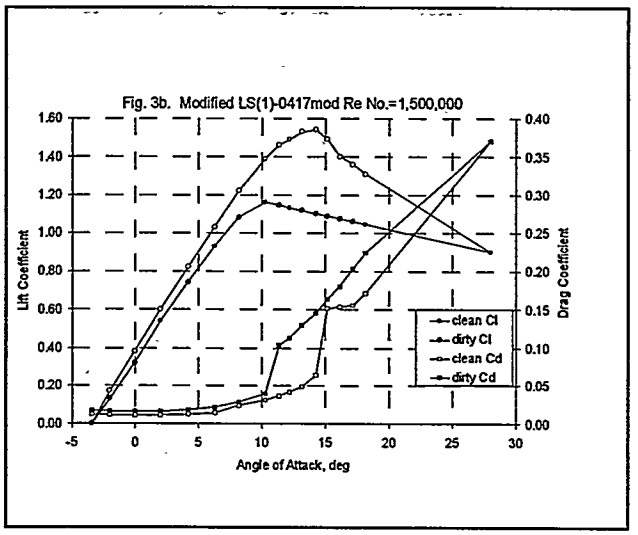

Fig. 3. Clean and rough surface airfoil performance characteristics for the LS(1)-0417MOD

As shown above, the primary effect of roughness is to reduce the $c_{l,max}$, decrease the lift curve slope, and increase the drag. Performance losses derived from the blade geometry parametric studies are intended to reflect these changes in airfoil performance characteristics. The two-dimensional airfoil data of Fig.3a show airfoil stall to occur with a sharp drop in $c_{l,max}$. However, in the three-dimensional atmospheric environment of an operating rotor, stall occurs more gradually. To better approximate the post stall lift coefficient, $c_{l,max}$ is faired into an approximation of flat plate post stall characteristics as shown in Fig 3b. This approximation largely neglects the influence of roughness on the post stall airfoil characteristics. Consequently, these parametric studies are considered qualitatively valid only for low to moderate wind speeds.

To analyze the effect of twist and taper on roughness sensitivity, the following combinations of these parameters, as illustrated in Fig. 4 for a two-bladed rotor, were modeled in PROP93 (Reference 8). The 3-to-1 linearly tapered blade used in the comparison has the same chord at 80% radius as the constant-chord blade. This provides a similar torque-weighted equivalent chord and power curve. The twist distribution is rather generic, with the high twist toward the blade root. The blade pitch angles of -2°, 0°, and +2°, which cover the normal operating range for most rotors at moderate wind speeds, are referenced to the three-quarter radial location. The rotor diameter is 14.8-meters (48-ft.) and the rotor operates at 77 rpm. One airfoil data table was used along the entire blade for lack of airfoil characteristics at Reynolds numbers corresponding to the blade root and tip.

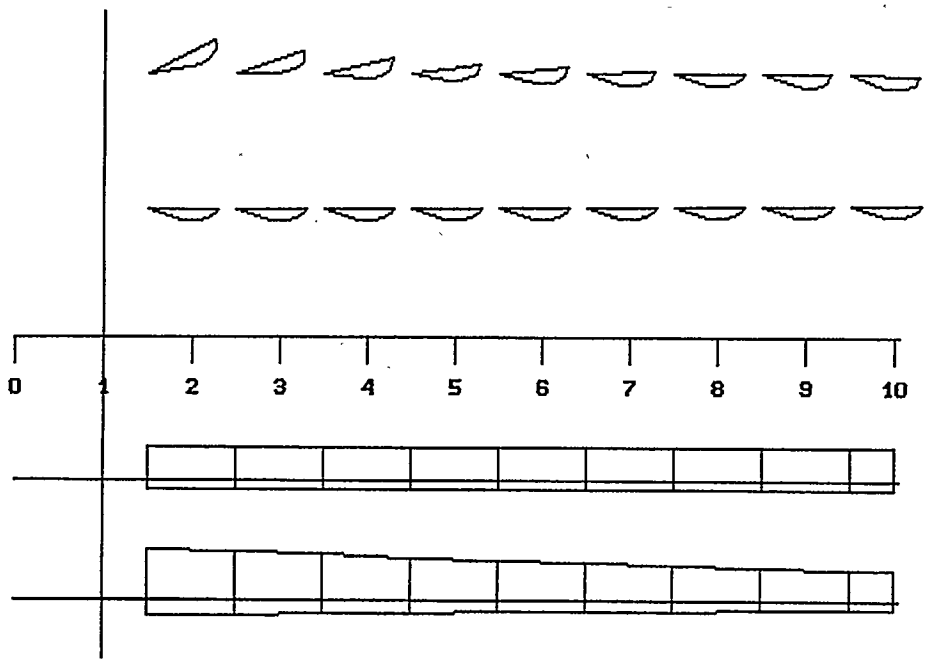

- **constant-chord/zero-twist**
- **constant-chord/twisted**
- **tapered-chord/zero-twist**
- **tapered-chord/twisted**

Fig. 4. Constant chord and tapered chord blade geometries with and without twist

INFLUENCE OF PITCH, TWIST, AND TAPER

To quantify the effect of pitch, twist, and taper, the non-twisted, constant-chord, constant-airfoil, blade was used as a baseline. The gains achieved with favorable pitch, twist, and taper are directly proportional to the reduction in angle of attack over the blade span for a given wind speed. The power loss due to roughness is shown in Fig 5. for blade pitch angles of -2°,0°, and +2°. The general trends show the tapered/twisted blade has the lowest power loss due to roughness effects followed by the twisted, constant chord blade. Taper by itself provides some reduction in power loss due to roughness at low wind speeds. The magnitude of the roughness loss reductions and the wind-speed range over which these improvements occur becomes greater going from a blade pitch of -2° toward +2°, with the exception of taper which appears to be most beneficial at 0°. The general trends shown in this comparison are considered to be valid but the specific differences are likely due to inaccuracies in the numerical calculations in PROP. In addition, differences above 9 m/s will be influenced by the post stall approximation which does not account for roughness effects, particularly at -2° pitch.

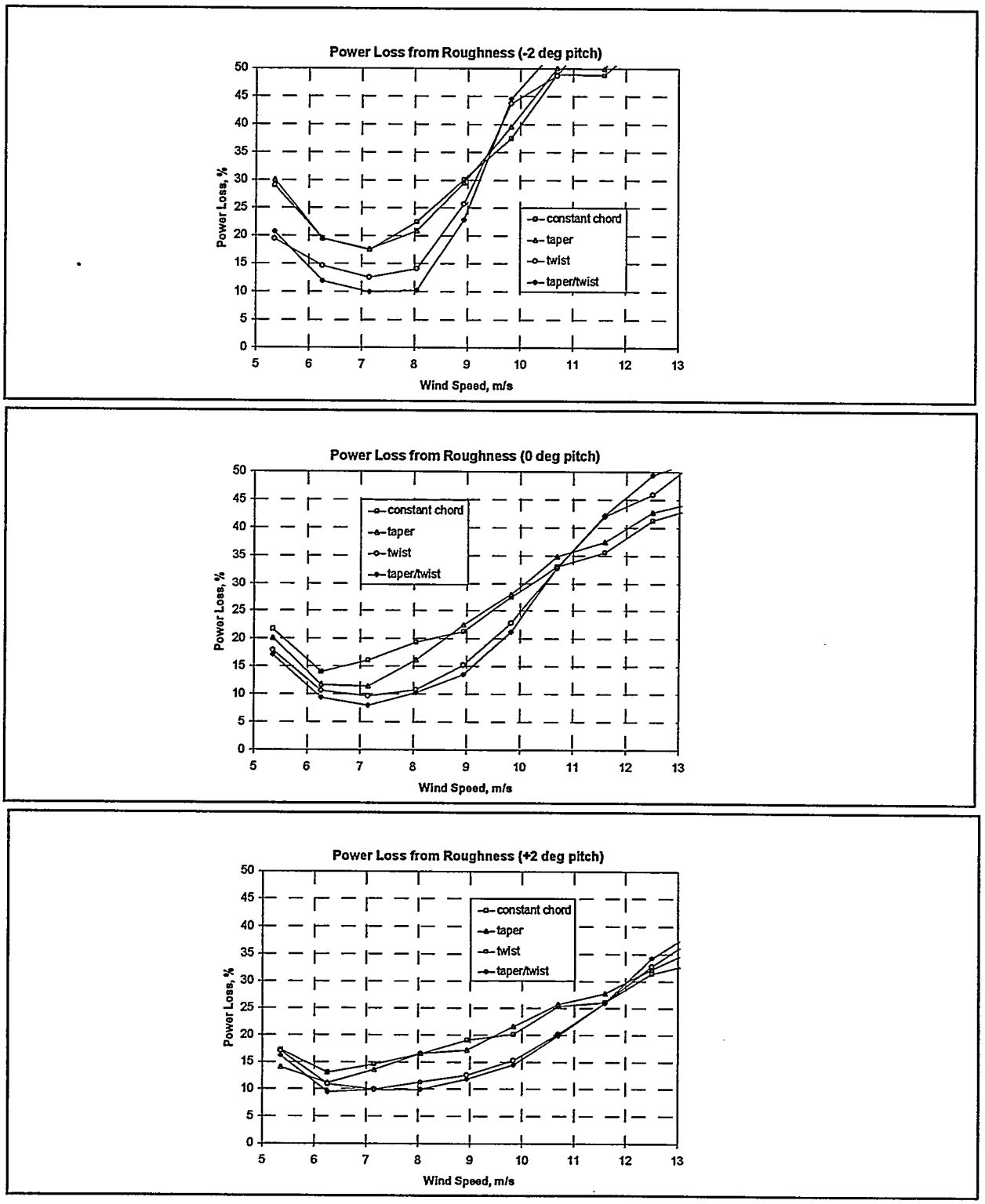

Fig. 5. Power losses from roughness for various blade geometries and pitch angles

These trends have one common characteristic- roughness losses decrease as the angle of attack along the blade decreases for a given wind speed. Blade pitch is the most effective means of decreasing the angle of attack followed by blade twist. The effect of blade taper on angle of attack distribution is less obvious. Relative to an equivalent constant chord blade, taper increases the induced velocity inboard and decreases it outboard. This results in a corresponding angle of attack decrease inboard and an increase outboard. The inboard reduction is beneficial because it delays stall, which begins at the blade root and propagates outboard with wind speed. The greatest improvement is achieved with a favorable combination of twist, pitch, and taper. These trends, which are shown in Fig.6 for pitch angles of -2° and +2°, are most important at wind speeds of greatest energy production. For most wind sites these speeds are close to 9 m/s. Fortunately, tailoring the blade for optimum clean blade performance also leads to minimal sensitivity to roughness effects. As demonstrated in previous studies, additional gains are achieved by using new NREL airfoils designed to be more tolerant to roughness (Ref. 1). Several of these new airfoil families result in a decreasing $c_{l,max}$ from blade root to tip which favorably simulates additional blade twist. This is achieved by using low $c_{l,max}$ tip airfoils such that the zero c_l intersection of the airfoil's lift curve slope moves toward positive angles of attack from blade root to tip.

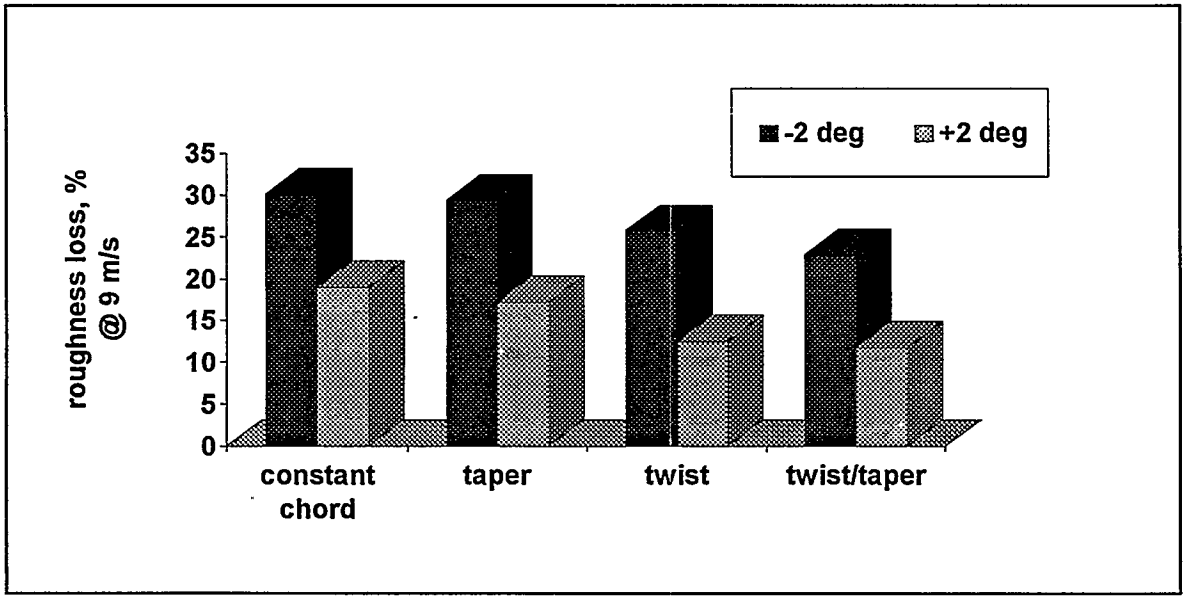

Fig. 6. Influence of blade geometry parameters on roughness loss at a wind speed of 9 m/s

CONCLUSIONS

Blade roughness losses are machine dependent; stall regulated machines are the most sensitive to leading edge roughness. Variable pitch (toward feather), constant rpm machines have less sensitivity to roughness effects but are known to be more susceptible to power spikes. Variable rpm machines are least sensitive to roughness. Due to these differences the guidelines to reduce roughness effects most benefit stall regulated machines.

A blade's sensitivity to roughness, through a loss in $c_{l,max}$, is influenced most strongly by the blade pitch setting and twist and less so by blade taper. A stall regulated rotor stalls from root to tip with increasing wind speed. The stall can be delayed by pitching the blade away from stall and by increasing the blade root twist. However pitching the blade away from stall must also be tempered by the need to control peak power on a stall regulated rotor. Achieving the right balance involves consideration of both the blade geometric parameters and airfoil characteristics along the blade. The latter can best be addressed with new roughness-tolerant airfoils and airfoils having a $c_{l,max}$ distribution along the blade that is compatible with peak power limits and structural requirements.

RESEARCH NEEDS

The influences of airfoil thickness and $c_{l,max}$ are also thought to affect roughness sensitivity. Further exploration of these parameters is needed through two-dimensional, wind-tunnel testing to quantify their effects. These influences need to be understood when selecting current airfoils, and to provide direction for the design of new airfoil families. Wind-tunnel testing for two-dimensional, airfoil performance characteristics and three-dimensional atmospheric testing should include the effects of roughness, particularly when a stall-regulated rotor is concerned.

REFERENCES

1. Tangler, J., and Somers, D., "NREL Airfoil Families for HAWTs," Presented at Windpower '95, Washington D.C., 27-30 March, 1995.

2. Tangler, J., et al., "Atmospheric Performance of the Special-Purpose SERI Thin-Airfoil Family: Final Results," Presented at European Wind Energy Conference, Madrid, Spain, September 1990.

3. Jager, D., "Artificial Roughness Testing," NREL Interoffice Memorandum, 1992

4. Tangler, J., et al. "Atmospheric Performance of the Special-Purpose SERI Thick-Airfoil Family," Windpower '91, Palm Springs, CA., 24-27 September, 1991.

5. Reuss, R., et al., "Effects of Surface Roughness and Vortex Generators on the LS(1)-0417MOD Airfoil," NREL/TP-442-6474, December 1995.

6. Janiszewska., et al., "Effects of Grit Roughness and Pitch Oscillations on the LS(1)-0417MOD Airfoil," NREL/TP-442-7819, January 1996.

7. Mikhail, A. S., "Existing Wind Farm Performance Enhancement and Load Analysis," NREL Subcontract No. AO-2-11101-5, 1993 (available from NREL).

8. McCarty, J., "PROP93 Interactive Performance Prediction Code with Graphics," Alternative Energy Institute, 1993, ($50 to order, phone 806-656-2295)

Design Improvements to the ESI-80 Wind Turbine

T. Rogers, A. Kleeman*, J. Manwell, J. McGowan
Renewable Energy Research Laboratory
Department of Mechanical Engineering
University of Massachusetts
Amherst, MA 01003

ABSTRACT

This paper describes two investigations of related to possible improvements to the University of Massachusetts Renewable Energy Research Laboratory's (RERL) ESI-80 wind turbine. One of them involved modeling the tip flaps during braking. The other was a study of the turbine behavior with various delta-3 angles. These topics are of interest since the UMass turbine is a two-bladed, teetered, free-yaw machine with tip flaps and an adjustable delta-3 angle.

Tip flaps are used for slowing the turbine during shut down and as an emergency system to insure that the rotor does not go into an overspeed condition in the event of failure of other parts of the system. Upon deployment, the tip flaps are exposed to a number of varying forces including aerodynamic, damper, spring, centripetal, and gravitational forces and forces at the hinged connection to the blades. For maximum braking the angle of tip flap deployment needs to be as large as possible with out striking the blades in overspeed conditions and when covered with ice. To investigate tip flap design tradeoffs, the RERL has developed a dynamic model of the tip flaps on the modified ESI-80 turbine. Results include a determination of the effect of the addition of weight to the flap, overspeed conditions, and of changes in damping coefficient.

Teeter motion of a teetered two bladed rotor is a complex process that is governed by aerodynamic and gyroscopic moments acting on the system. Changes in the delta-3 angle can be used to couple pitching and flapping motions, affecting both teeter and yaw behavior. These effects have been investigated using a modified version of YawDyn. The effects of changes in the delta-3 angle on the teeter and yaw behavior of the modified ESI-80 wind turbine were investigated. Results show that increased teeter excursions in steady high winds can be reduced by increasing the delta-3 angle. Increasing the delta-3 angle may also increase yaw motion in low wind speeds. Results suggest that the optimum delta-3 angle for improved performance may be substantially greater than the presently used angle of zero degrees.

INTRODUCTION

The University of Massachusetts' research wind turbine, a modified ESI-80 wind turbine, is a two-bladed, teetered, free-yaw machine with tip flaps and an adjustable delta-3 angle, described in Manwell, et al. (1993) and Baring-Gould, et. al. (1995). The tip flaps are hinged surfaces perpendicular to the end of the blades. Tip flaps are used for slowing the turbine during shut down and as an emergency system to insure that the rotor does not go into an overspeed condition in the event of failure of other parts of the system. Upon deployment, the tip flaps are exposed to a number of varying forces including aerodynamic, damper, spring, centripetal, and gravitational forces and forces at the hinged connection to the blades. For maximum braking the final resting angle of the tip flaps after deployment needs to be as large as possible. Overshoot needs to be minimized to keep the tip flaps from striking the blades in overspeed conditions and when covered with ice. Teeter motion is a complex process governed by aerodynamic and gyroscopic moments.

*Presently at the University of Karlsruhe, Germany

The delta-3 angle in a teetered rotor is the angle between the span of the blades and the normal to the teeter axis. Changes in the delta-3 angle can be used to couple pitching and flapping motions, affecting both teeter and yaw behavior. The dynamics of each of these systems has been investigated, with the goal of improving behavior and reliability of the turbine. Tip flap dynamics were investigated using a model developed for this purpose at the University of Massachusetts. Teeter dynamics and the effects of changing the delta-3 angle have been investigated using a modified version of YawDyn (Hansen, 1994).

TIP FLAPS

The tip flaps on the ESI-80 are hinged surfaces at the end of the blades, held in place by a magnet and hinge pin when not in use. In overspeed conditions or when power to the magnets is interrupted, the tip flaps deploy, rotating about the hinge pin to present a large surface to the prevailing wind to slow the rotor down. The dynamics of the deployment are governed by the acceleration of the flap center of mass, the aerodynamic drag on the tip flap, and the forces from a set of return springs, a damper, and the hinge pin. A schematic of the layout of the tip flap and related equipment showing the forces on the flap is shown in Figure 1. The tip flaps have been used in overspeed conditions and for a while, as a regular part of the braking procedure. After incurring some tip flap damage, when the tip flaps apparently attempted to move more than 90 degrees and struck the blades, attempts were made to determine the cause of the damage. Possible causes are the reduction of clearances between the tip flap and the blades due to ice buildup, changes in the tip flap mass or center of gravity due to ice, faulty design, and overspeed. Previous work, including a study by Lawlor (1992), did not consider all of the aspects of the design that we wanted to study, so a dynamic model was developed to explore the possible causes of the damage. The model can be used to explore the sensitivity of the design to:

- The location of the tip flap center of gravity and center of pressure
- Damper behavior
- Spring force
- Tip flap area
- Air density
- Additional weight on the tip flap due to ice or water in the flap
- Overspeed conditions
- The effect of gravity at different azimuth angles
- Simultaneous braking

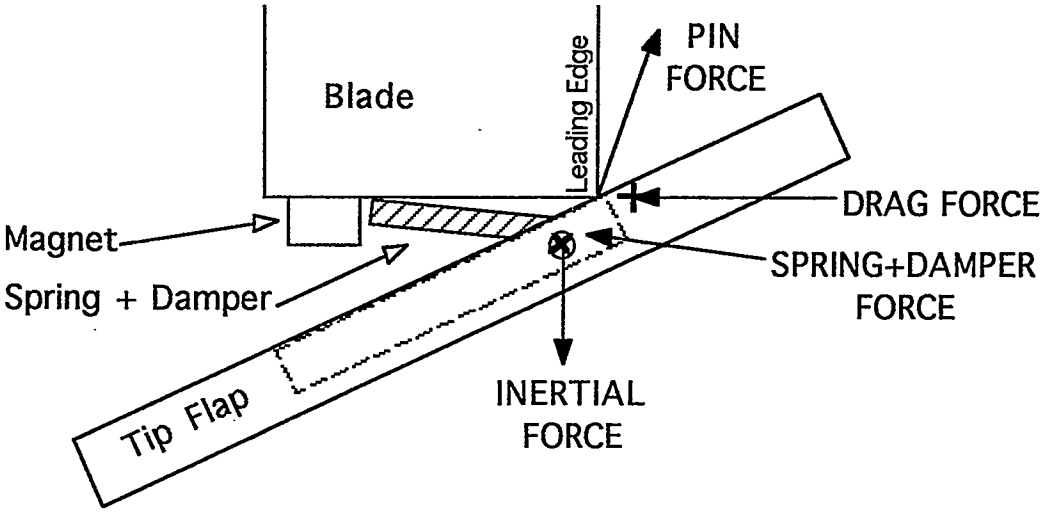

FIGURE 1. TIP FLAP SCHEMATIC INCLUDING FORCES

TIP FLAP COMPUTER MODEL

The tip flap is defined by its mass, inertia about its center of gravity, area, the location of the center of gravity, and the location of the resultant of the aerodynamic forces on the flap (the center of pressure). The distances of the centers of mass and pressure both along the blade and into the blade are separately specified. In the model the center of pressure is assumed to be fixed at one point on the tip flap. Blade behavior is determined by the blade inertia about its center of mass, and its mass and dimensions.

The forces due to the drag on the tip flaps, due to the springs and the dampers, and due to gravity and the wind on the rotor are all calculated at the beginning of each time step. The spring and damper forces are assumed to be collinear. The damper can be modeled as a classic viscous damper or by using a custom-made damper model. The spring is considered to be a massless spring with a fixed spring constant. The tip flap drag force assumes that the flap is a flat plate with an area equal to the flap cross section perpendicular to the motion of the end of the blade. Wind power input is modeled with an aerodynamic moment determined from the Cp-lambda curve for the machine.

Inputs allow for the addition of mass to the present design to change the flap mass, center of mass, and inertia. Additional input parameters include air density, initial rotor position, initial rotor rpm, and a constant braking torque.

GOVERNING DYNAMIC EQUATIONS FOR TIP FLAP

Three different coordinate systems were used in the calculations (see Figure 2). The x3y3 system is an inertial system fixed at the center of the main shaft. Thus, the model does not include any yawing of the machine. The x2y2 system is fixed on the blade with its origin at the center of gravity of the blade. Finally the x1y1 system is fixed on the tip flap with its origin at the center of gravity of the tip flap.

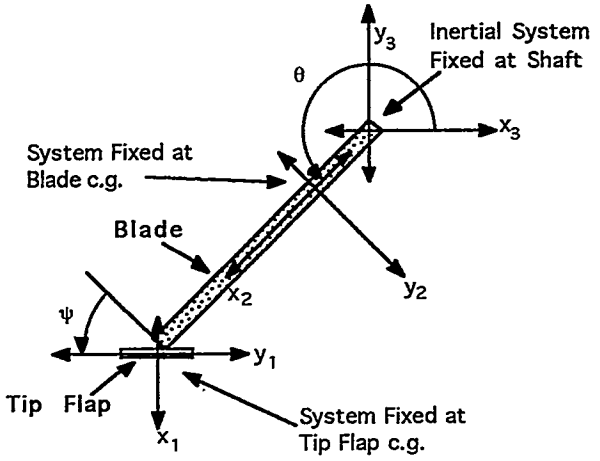

FIGURE 2. DIAGRAM OF COORDINATE SYSTEMS USED IN MODEL.

The governing equations for the flap then, become:

$$\sum \bar{F}_f = m_f\left(s\ddot{\theta}\sin\psi + cgy\left(\ddot{\theta}+\ddot{\psi}\right) - s\dot{\theta}^2\cos\psi - \left(\dot{\theta}+\dot{\psi}\right)^2 cgx\right)\hat{x}_1$$

$$+ m_f\left(s\ddot{\theta}\cos\psi + cgx\left(\ddot{\theta}+\ddot{\psi}\right) - s\dot{\theta}^2\sin\psi - \left(\dot{\theta}+\dot{\psi}\right)^2 cgy\right)\hat{y}_1$$

and $$\sum \bar{M}_f = I_f\left(\ddot{\theta}+\ddot{\psi}\right) .$$

The governing equations for the blade are: $\sum \bar{M}_b = I_b\ddot{\theta}$ and

$$\sum \bar{F}_b = m_b\left(b\ddot{\theta}\sin\psi - b\dot{\theta}^2\cos\psi\right)\hat{x}_1 + m_b\left(b\ddot{\theta}\cos\psi - b\dot{\theta}^2\sin\psi\right)\hat{y}_1 .$$

In these equations θ is the azimuthal position, ψ is the tip flap rotation angle. Mass is designated by m, inertia about each body's center of mass by I, the forces on the centers of gravity by F, and the moments about the centers of gravity by M. Subscripts f and b indicate the tip flap and blade, respectively. The distance of the flap center of gravity from the pin in the x and y directions are designated cgx and cgy. Finally, the blade center of gravity is a distance b from the main shaft and the blade span is s. The forces on the tip flap includes forces from the pin, damper, spring, gravity, and aerodynamic drag. The moments on the flap includes moments from the pin, damper, spring, and aerodynamic drag. The forces on the blade includes forces from the pin, damper, spring, gravity, and the main shaft. The moments on the flap includes moments from the pin, damper, spring, wind, and the main shaft. These equations are solved for the reaction forces at the pin and shaft and the angular accelerations of the rotor and flap.

TIP FLAP RESULTS

Inputs. All of the parameters required for modeling of the tip flap behavior can be accurately determined except for the location of the center of pressure, the magnitude of the aerodynamic drag, and details of the existing damper behavior. In reality, the location of the center of pressure is probably a function of the angle of the flap and the rotor speed, and, thus, is not necessarily fixed in the flap. Similarly the drag may not be a simple function of the flap cross section to the prevailing flow. Dynamic damper behavior over the range of speeds encountered in operation has not been adequately determined. Nevertheless, known operating conditions have been used to determine approximate values for these variables.

Determination of the effective center of pressure. The steady state angle of the tip flap at 60 rpm is known to be about 70 degrees. In the model the steady state angle of the tip flap is a function of the spring force, the tip flap area, the drag coefficient (Cd), center of pressure, and center of mass. The only unknown variables are the center of pressure and the drag coefficient. By assuming a drag coefficient of 2 we can adjust the location of the center of pressure until the model predicts the correct resting angle at a known rpm. Doing this, we can determine an effective location for the center of pressure that applies for the most important conditions - when the tip flap is fully deployed and slowing the turbine down. The value determined from this method is with 0.3 inches of the area centroid of the flap.

Determination of the effective damping coefficient. The model has been used to determine the sensitivity of the tip flap system to changes in a variety of conditions, given that the exact damping is unknown. It is known that the tip flap has at some time hit the blade. A chosen starting point, therefore, assumed that the maximum teeter excursion is 90 degrees at an overspeed condition of

72 rpm. Once the location of the center of pressure is known, the viscous damping coefficient can be adjusted in order to achieve this. The resulting damper coefficient is 35 lb/(in/sec).

Baseline Tip Flap Deployment. To investigate the effects of various tip flap conditions a baseline condition was assumed: that the tip flap just touches the blade at overspeed conditions starting at 72 rpm. The tip flap angle and rotor speed results for the baseline conditions are illustrated in Figures 3 and 4. The wind speed, unless otherwise noted, is assumed to be 17.8 m/s (40 mph). For the baseline conditions the tip flaps take about a quarter of a second to fly out and slowly come in as the rotor speed decreases. The rotor speed does not go much above 72 rpm and decreases in 5 seconds to half of the initial speed. Baseline conditions were varied to determine the effect of different wind speeds, rotor speed, damping coefficients, air temperatures, mass distributions, and gravity on the results.

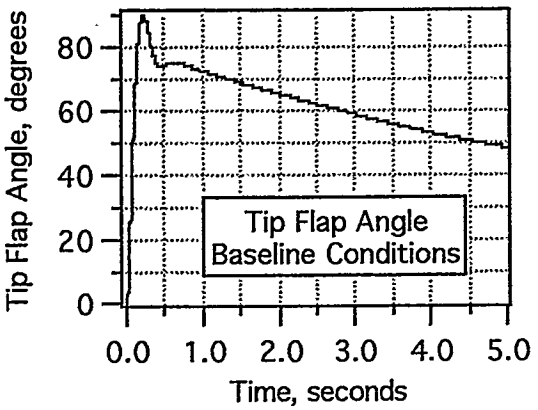

FIGURE 3. BASELINE TIP FLAP ANGLE.

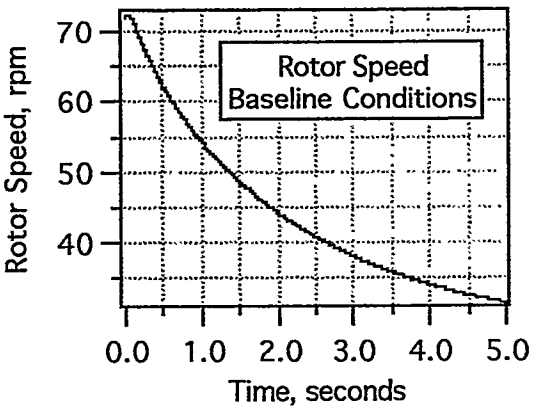

FIGURE 4. BASELINE ROTOR SPEED.

Wind Speed. Increasing wind speed actually decreases the maximum tip flap excursion. The higher wind speed causes the rotor to decelerate more slowly, decreasing the opening moment on the tip flap from the hinge pin. Increasing the wind speed from 9 m/s (20 mph) to 27 m/s (60 mph) decreased the maximum tip flap excursion from 93 degrees to 89 degrees.

Rotor Speed. Overspeed conditions significantly affected the maximum tip flap excursion. The tip flaps of the baseline configuration just touch the blade at 72 rpm. At 60 rpm (operating speed) the tip flaps only reached 79 degrees, while at 84 rpm the tip flaps reached 100 degrees (see Figure 5).

Damping Coefficient. Significant changes in the maximum tip flap excursion also occurred with very small changes in damping coefficient. If the damping coefficient was increased from 6.13 kN/(m/s) (35 lb/(in/sec)) to 8.76 kN/(m/s) (50 lb/(in/sec)), the tip flaps only reached 80 degrees. If damping coefficient was decreased from 6.13 kN/(m/s) (35 lb/(in/sec)) to 3.50kN/(m/s) (20 lb/(in/sec)), the tip flaps reached 112 degrees (see Figure 6).

Air Temperature. All the tests were run assuming a temperature of 0 C (32 F). If a temperature of 38 C (100 F) is assumed, the less dense air affects both the wind moment on the blades and the drag of the tip flaps, with changes in tip flap drag dominating. Increasing the air temperature to 38 C (100 F) resulted in a maximum flap excursion of 96 degrees, six degrees more than the baseline case.

Ice Buildup. Ice buildup can occur in many ways. Ice could coat the flap increasing its weight with little change in the location of the center of mass, ice could coat only one end or the other, adding little weight, but significantly affecting the location of the center of mass, or water could

build up in the damper well and freeze, changing both the mass and the center of mass of the tip flaps. A number of conditions were investigated. An increased weight of two lb. centered at the center of mass decreases the maximum tip flap excursion by 9 degrees to 81 degrees. On the other hand, one pound of ice in the well at 10 inches from the pin (along the $-y_1$ axis of the tip flap) increases the maximum angle to 96 degrees.

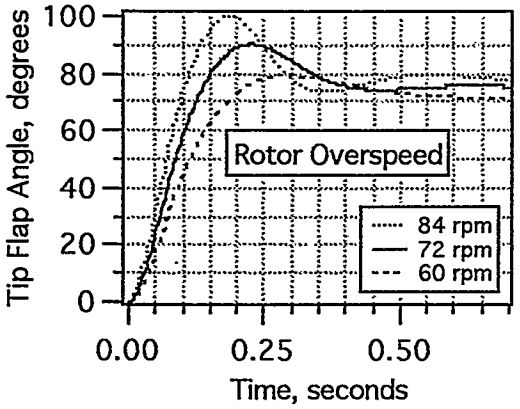

FIGURE 5. TIP FLAP ANGLE. WITH OVERSPEED

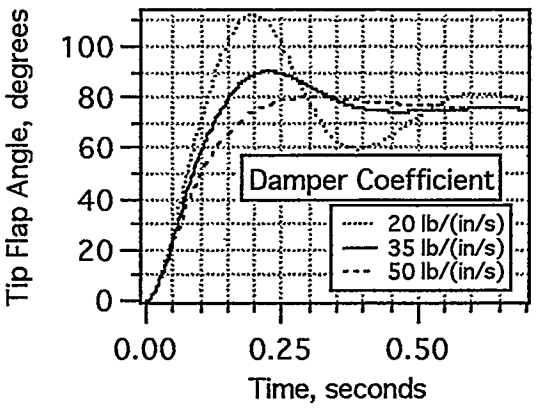

FIGURE 6. TIP FLAP ANGLE . WITH DIFFERENT DAMPING.

Center of Mass. In general tip flap dynamics appear to be very sensitive to the location of the center of mass. The addition of 0.45 kg (1 lb) 0.41 m (16 inches) from the pin along the $+y_1$ axis decreases the maximum excursion to 73 degrees. An additional 0.45 kg (1 lb) at that location decreases the maximum tip flap angle to 47 degrees! The additional weight also significantly reduces the steady state tip flap angle, and thus the rotor braking (see Figures 7 and 8).

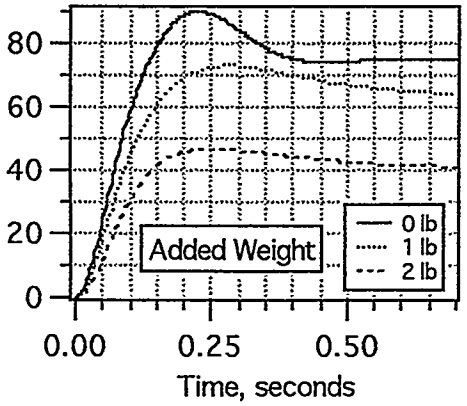

FIGURE 7. TIP FLAP ANGLE. WITH ADDED WEIGHT

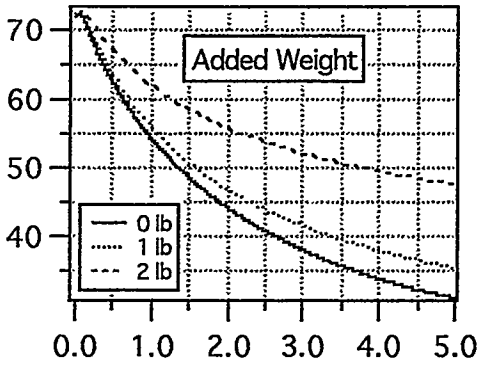

FIGURE 8. ROTOR SPEED . WITH ADDED WEIGHT.

Gravity Effects. Tip flap deployment at different azimuth angles results in different maximum flap excursions due to the different direction of the gravitational force vector with respect to the flap. This effect amounted to less than +/-1.3 degrees from the average excursion of 90 degrees.

DELTA-3 OPTIONS IN TEETERED ROTORS

On two bladed machines, teetered rotors are used to reduce blade and shaft loads due to imbalances in flapwise blade root bending moments. The University of Massachusetts wind turbine on Mt. Tom has a teetered rotor with no constraints on the teetering motion over a range of about +/- 3 degrees. Beyond this point a teeter damper, which includes a spring, constrains the motion. Teeter motion is physically limited at about +/-7 degrees. The delta-3 angle in a teetered rotor is the angle between the span of the blades and the normal to the teeter axis. Changes in the delta-3 angle can be used to couple pitching and flapping motions, affecting both teeter and yaw behavior. The University of Massachusetts wind turbine allows the delta-3 angle to be changed in steps of 18 degrees. Given the consistent wind shear and high wind occurrences at the Mt. Tom site, YawDyn has been used to investigate the tradeoffs in operation with various delta-3 angles.

TEETERED ROTOR ANALYTICAL MODEL

The teeter motion of a teetered two-bladed rotor is a complex process that is governed by aerodynamic and gyroscopic forces and moments acting on the system. Teetered rotors allow for two degrees of freedom: teeter motion and yaw motion. Thus, the dynamics of both teeter and yaw must be included in an analysis of a teetered rotor wind turbine. A modified version of the YawDyn code developed by Hansen (Hansen, 1994) was used in this work. Confidence in the model was generated by previous work at UMass (Bywater and Manwell, 1993), and input data was provided from previous SERI/EPRI experiments with the ESI-80 (Musial, et al., 1985; and Wright and Butterfield, 1992).

Two major modifications were made to the YawDyn code to accommodate the analysis of the effects in non-zero delta-3 angles: The equation for the flap angle, β was modified to become

$$\beta = \beta_0 + \tau \cos \delta_3$$

where β_0 is the coning angle, and τ is the teeter angle. The new angle of attack is

$$\alpha = \Phi - \Theta - \tau \sin \delta_3 \text{ , if } \tau > 0 \quad \text{and} \quad \alpha = \Phi - \Theta + \tau \sin \delta_3 \text{ , if } \tau < 0$$

where Φ is the inflow angle, the angle between the plane of rotation and the inflow angle, and Θ is the pitch angle. The new flapwise moment of inertia was also determined to be

$$I_{b\delta 3} = I_b \cos^2 \delta 3 \ .$$

This correction ignores moments of inertia in other directions and any cross terms.

Steady winds were used for much of the analysis. For a study of teeter behavior with turbulent winds, some runs were made including dynamic stall part and turbulent wind data generated by the SNLWIND code (adjusted for Mt. Tom conditions) developed at NREL (Kelley, 1993).

TEETERED ROTOR RESULTS WITH INCREASED DELTA-3 ANGLES

Before using YawDyn to analyze possible changes in the delta-3 angle, YawDyn was first used to analyze the behavior of the teetered turbine with a delta-3 angle of zero. As expected, the teeter angle increases approximately linearly with increasing wind speed, (3.11) and also increases approximately linearly with increasing wind shear coefficient (3.18). The simulations also showed

that sudden wind direction changes affect the yaw rates and teeter angles much more at high wind speeds. All of these effects have been observed at the Mt. Tom site. A number of aspects of turbine behavior with different delta-3 angles were investigated in the course of this study. The results covered in this paper include changes in turbine response to different wind speeds and sudden wind direction changes, and turbine response to turbulence.

Influence of delta-3 on turbine response to different wind speeds. A set of simulations with a vertical linear wind shear of 0.2 were performed to study the effect of the delta-3 angle on turbine response to different steady wind speeds. Figure 9 shows maximum teeter angles for different wind speeds with three different delta-3 angles, 0, 36, and 54 degrees. The data for delta-3=0 is approximately linearly related to the wind speed above the cut in wind speed of 5.8 m/s (13 mph). Above about 11 m/s (25 mph) increasing delta-3 angles decrease the maximum teeter excursions dramatically. Figure 10 illustrates the effects of delta-3 changes on mean yaw errors for different wind speeds. Below about 11 m/s (25 mph) increasing delta-3 angles increase the mean yaw error dramatically, but over most of the operating range of the turbine the mean yaw error remains about zero for all choices of delta-3 angle.

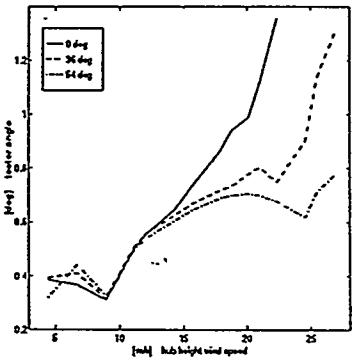

FIGURE 9. MAXIMUM TEETER ANGLE VS. WIND SPEED.

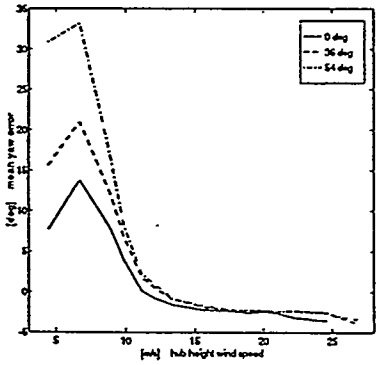

FIGURE 10. MEAN YAW ERROR VS. WIND SPEED.

Influence of delta-3 on tower shadow effects. Winds of 18 m/s (40 mph) with a vertical linear shear of 0.2 were used to study improvements in turbine behavior due to the tower shadow. Figure 11 illustrates the improvement in angle of attack as the blade goes through the tower shadow. The resulting improvement in maximum teeter angle is illustrated in Figure 12.

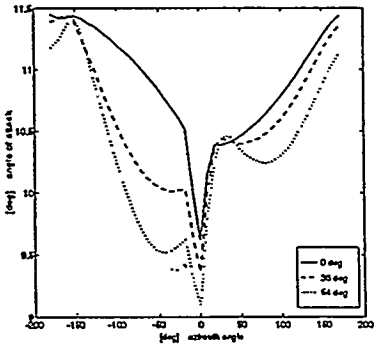

FIGURE 11. ANGLE OF ATTACK VS. AZIMUTH ANGLE.

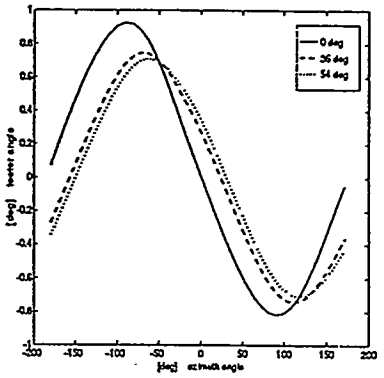

FIGURE 12. TEETER ANGLE VS. AZIMUTH ANGLE.

Influence of delta-3 on initial yaw position response. The sudden imposition of a yaw error significantly different from zero corresponds to turbine behavior with a sudden change in wind

direction. A set of simulations using a constant wind speed of 22.3 m/s (50 mph), a vertical shear coefficient of 0.3 and an initial yaw error of 10 degrees was used to investigate the effect of delta-3 angle on turbine response. In each case the yaw angle asymptotically approaches similar steady state yaw errors (see Figure 13). The negative delta-3 angle results in the smoothest response. The response with other delta-3 angles includes decreasing oscillations for about the first 10 revolutions that are most pronounced with a delta-3 angle of 18 degrees. Yaw response is about the same for delta-3 angles of 0, 36, and 54 degrees. Teeter angles (Figure 14) are also much larger for a delta-3 angle of 18 degrees than for a delta-3 of 0 degrees, but teeter angles are lower with a delta-3 angle of 54 degrees than with a zero delta-3 angle. Thus, delta-3 angles of 0 and 54 degrees give the same yaw response to an initial yaw error, but the larger delta-3 angle results in much lower teeter excursions.

Turbulent wind input response. Turbulent wind data generated by SNLWIND was used to investigate turbine response under conditions similar to those on top of Mt. Tom. The mean wind speed used was 20 m/s (45 mph) with a power law exponent of 0.143 and a surface roughness length of 1.091 m (43 in). In general the teeter angles were slightly higher for higher delta-3 angles (see Figure 15), except during a rapid reversal in yaw rate over a 2 second period, between 30 and 32 seconds in Figure 16. During this sudden change in yaw rate, the teeter angle for delta-3 angles of 36 and 54 degrees remained much lower than with lower delta-3 angles.

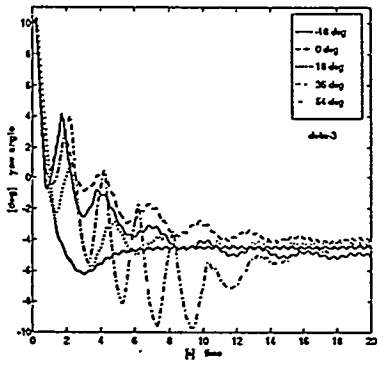

FIGURE 13. YAW TRACKING RESPONSE WITH YAW ERROR OF 10 DEGREES

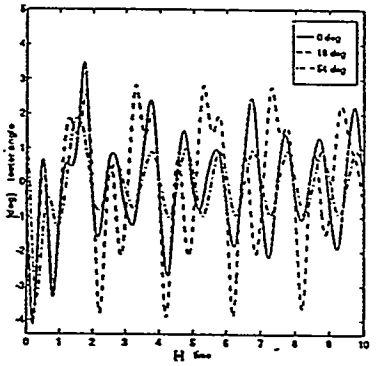

FIGURE 14. TEETER ANGLE WITH YAW ERROR OF 10 DEGREES

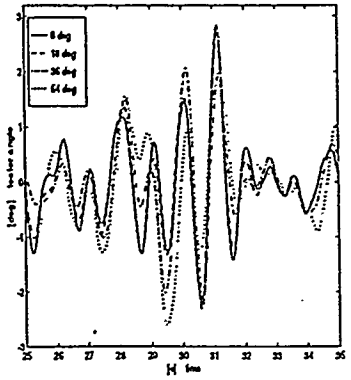

FIGURE 15. TEETER ANGLE WITH TURBULENT WINDS

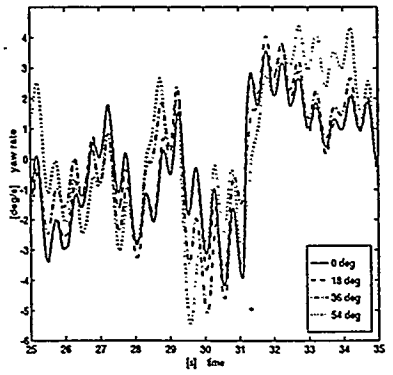

FIGURE 16. YAW RATE WITH TURBULENT WINDS.

CONCLUSIONS

We have found that the tip flap model can effectively simulate tip flap behavior for the parameters of interest, even though more calibration is needed for quantitative predictions. Experience with

water and ice buildup in the well of the tip flaps shows a better flap design is needed. The model has helped to identify design issues to be considered, specifically, overspeed, weight distribution, damping, and the possibility of ice buildup. After measurements of tip flap motion to determine the effective damper coefficient modifications to the tip flaps will be considered.

While the delta-3 results must be considered preliminary, they are encouraging, suggesting that teeter excursions can be decreased under important operating conditions by changing the delta-3 angle. Teeter analysis results confirm that increasing the delta three angle reduces teeter excursions in steady high winds and excursions due to the tower shadow. It is also clear that more analysis is needed, as the large changes in mean yaw error in low winds could be a significant problem. Yaw damping and active yaw control still need to be investigated. We have found that YawDyn can be modified to give plausible results. Upon further investigation, field experiments should be considered.

REFERENCES

Bywaters, G. L. and Manwell, J. F. (1994), "Teeter Dynamics in Complex Terrain," ASME Wind Energy 1994, ASME SED- Vol. 15.

Hansen, A. C. (1994) Users Guide to the Yaw Dynamics Computer Program, Version 9.0, University of Utah Report.

Lawlor, Shawn P., "An Investigation of Tip Brake Performance Characteristics," 11th ASME Wind Energy Symposium, Houston, TX, January, 1992.

I. Baring-Gould, A. F. Ellis, J. F. Manwell, and W. Stein, (1995) "Bringing Wind Power Back East: Redesign, Installation and Initial Operating Results for the ESI-80 in Massachusetts, " Proc 1995 AWEA Annual Conference.

Kelley, N. (1993), "Full Vector (3-D) Inflow Simulation in Natural and Wind Farm Environments using an Expanded Version of the SNLWIND (Veers) Turbulence Code," ASME Wind Energy 1993, ASME SED- Vol. 14.

Manwell, J. F., Stein, W. M., and McNiff, B. P. (1993) "Bringing Wind Power Back East: A New Life for the Original ESI-80 in Massachusetts",Proceedings of the AWEA Annual Conference.

Musial, W. D., et. al. (1985), "ESI-80/EPRI Test Program: Final Report," EPRI Research Project RP1994-14.

Wright, A. D. and Butterfield, C. P. (1992), "The NREL Teetering Hub Rotor Code: Final Results and Conclusions," ASME Wind Energy Synposium, ASME SED- Vol 12.

TEST AND ANALYSIS RESULTS FOR TWO SYNERGY POWER CORP. WIND TURBINES

Dean Davis and Craig Hansen
Windward Engineering, L.C.
Salt Lake City, UT 84117
USA

Introduction:

For the past 18 months Windward Engineering, L.C. has been field testing prototypes and validating computer models of Synergy Power Corporation wind turbines. Synergy Power Corp. designs, manufactures and installs remote area power systems, including small wind turbines they have designed and fabricated. Their headquarters are in Hong Kong, with engineering offices in Kuala Lumpur and Seattle. They have installed over 135 small turbines throughout the world. Recently they have designed and fabricated prototypes of turbines with rotor diameters of 10.3m and 12.8m. The testing and modeling of these turbines is the subject of this paper.

The Synergy wind turbines all utilize passive rotor tilt to limit power output, rotor speed and blade and tower loads in high winds. Figure 1 shows a prototype of the Synergy SL turbine at a test site near Spanish Fork, UT. The distinctive tail boom and tailplane are used to tilt the rotor towards a horizontal plane as wind speed increases above the rated speed. In very high winds the rotor plane becomes horizontal and the power output is nil.

The passive tilt motion of the Synergy turbine cannot be analyzed by most wind turbine dynamics codes. However, the ADAMS code is ideally suited for this analysis. The free-yaw, variable rotor speed, startups, and shutdowns of the Synergy systems are also readily analyzed using ADAMS. Synergy recognized the value of design analysis and contacted Windward Engineering to seek assistance in the design of the larger prototypes. We used the ADAMS code linked with the AeroDyn subroutines developed at the University of Utah to provide the analyses that were needed.

The AeroDyn routines had not been validated for large tilt angles. So this project became a dual effort of 1) validating the code using test data that we obtained from prototypes, and 2) using the code to calculate design loads, optimize the tilt configuration and help interpret test results.

This paper will focus primarily on the ADAMS model predictions. Some of these predictions will be plotted against test data as a validation of the computer modeling. Other predictions which are shown were used for load prediction used in the design. One such example shows blade loading during an IEC Standard gust condition.

Description:

The Synergy SL:
The Synergy SL wind turbine is a 3-bladed, rigid rotor, with a rotor diameter of 12.8 m. It has been designed to operate on a distributed grid system in Class 2 wind regimes and has a rated power of 30 kW. We believe there is a need for turbines in this size range that are designed for lower wind regimes and that can be utilized in more widely dispersed locations. This differs from the focus towards wind farms which has dominated the wind energy industry for several years.

The passive tilt system uses aerodynamic drag on the tailplane to generate a force to overcome the gravity and rotor aerodynamic moments when the wind increases above 10 m/s. At this wind speed or

higher the turbine will begin to tilt. Because of this the power will be limited (or regulated) as the wind continues to increase above 10 m/s.

The rotor uses fixed-pitch, twisted and tapered blades with NREL S806, S807 and S808 airfoils. An induction generator is connected to the grid using an Enerpro auto synchronous controller. The SL system operates at constant rpm (unlike all previous Synergy systems, which use variable-speed alternators). The rotor and tail structure are downwind of, and yaw freely about a guyed pole tower. The tower is hinged at the base and can be raised and lowered for maintenance using a winch and gin pole. Dual, independent disc brakes on the low speed shaft are used to stop the rotor in the event of overspeed and for routine maintenance.

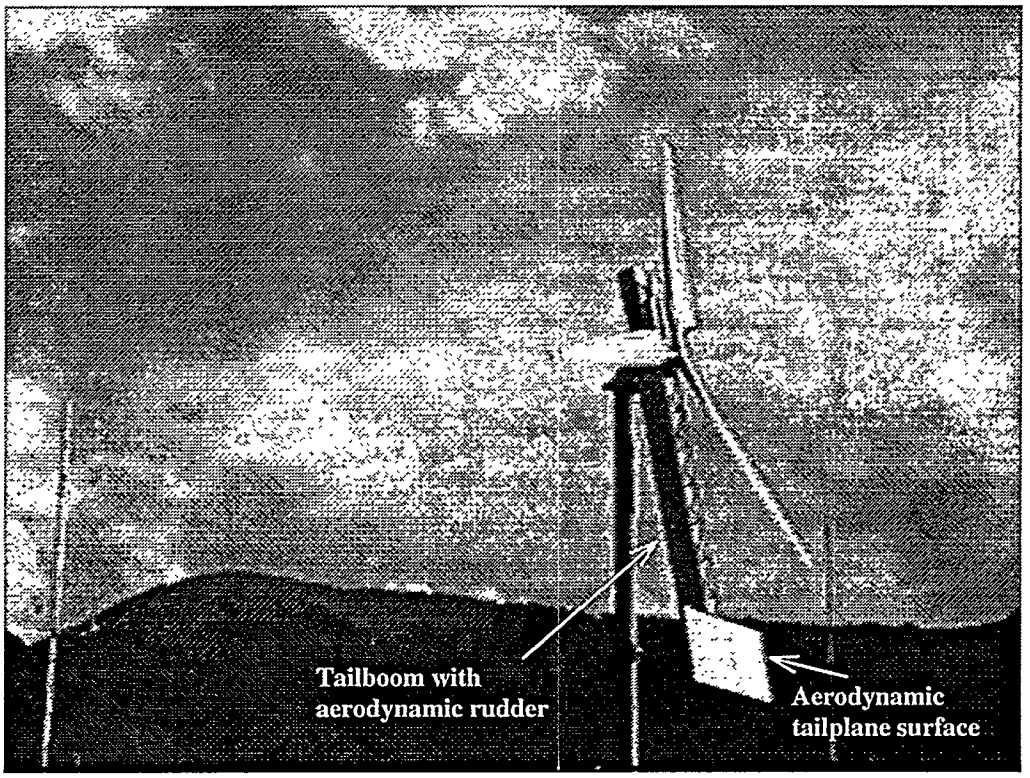

Figure 1. Synergy SL wind turbine operating in moderate winds (10-11 m/s).

The Synergy S-50000:
This earlier prototype turbine was tested for approximately 6 months. It was slightly smaller than the SL, with a rotor diameter of 10.3 m. It used Advanced Aero Technologies blades and a variable speed alternator. The system was tested with a range of constant resistive loads. Results from this turbine are shown to demonstrate that ADAMS can model this variable speed rotor with reasonable accuracy.

The test site:
The test site is located in Spanish Fork, UT on property owned by the City of Spanish Fork. The site is managed by the Utah Municipal Power Agency, which has graciously consented to our use of the site and provided a utility interconnection at no cost. The SL turbine is still under test at the site. The site is located at the mouth of Spanish Fork canyon where canyon (diurnal) winds are a regular occurrence. The winds have proven to be very consistent at the site. A typical wind schedule starts a few hours after sundown. The wind will generally increase during the night and reach a maximum around 15 m/s by

midnight. These winds will continue until dawn when they will start to taper off. Within 4-5 hours after sunrise the winds will die completely and switch up canyon until night fall. The midday winds are typically very light, approximately 0-5 m/s. This makes the site ideal for prototype testing in that it is easy to work on the turbines during the calm of the midday with reasonable assurance of a wide range of wind speeds every night. The only interruption of this routine is caused by passing storms, which can bring strong winds from other directions.

The computer model:
The primary computer modeling was done with the ADAMS / AeroDyn software package. ADAMS allowed us to model the variable rotor speed (as on the S-50000) as well as the tilt degree of freedom. A few modifications were required to the AeroDyn aerodynamics subroutines. These subroutines link to ADAMS and calculate the rotor aerodynamic forces and moments. In short, the subroutines use turbine component velocities and displacements from ADAMS, combine them with wind inputs from data files, and calculate aerodynamic forces. The subroutines include dynamic stall and skewed wake effects that have been shown to be significant to rotor aerodynamics with tilted or yawed flow. While modeling the Synergy wind turbines we needed to add the aerodynamics of the tailboom, tailplane, and tail rudder. These aerodynamic surfaces are primary to the tilt and yaw behavior.

These aerodynamic surfaces were added to ADAMS with the addition of an "SFORCE" user-written subroutine. The subroutine calculates the wind speed and angle of attack of each surface in a similar fashion to that found in the AeroDyn subroutines. With the use of an input file for surface area and airfoil tables, we could calculate a force and apply it internally to the ADAMS model.

All results shown in this report (except the IEC wind modeling) used measured wind data from the test site to drive the dynamic model. The meteorological tower is fitted with the 7 wind sensors listed in Table 1. The Somat data acquisition system limits us to monitoring 5 of the 7 channels at any given time. Channels 1, 2, 3, 4, & 7 were recorded for the results shown herein. For the modeling, the three cup anemometers were used to calculate a mean hub height wind speed. These three anemometers were also used to calculate a vertical shear coefficient. The wind direction was input into the model as a delta angle for the wind and the vertical wind was also used as an input. The limited instrument array provides no information on the horizontal shear across the rotor disc, so we assumed zero horizontal shear in the modeling.

Table 1 Wind measurements for anemometer tower.

Channel	Description	Location
1	top cup anemometer	hub height + R (rotor radius)
2	hub height cup anemometer	hub height
3	bottom cup anemometer	hub height - R
4	wind direction	hub height
5	u prop anemometer	hub height (facing up canyon)
6	v prop anemometer	hub height (facing cross canyon)
7	w prop anemometer	hub height (facing vertical)

The SL wind turbine is instrumented for measurement of the following parameters: true electrical power output, low-speed shaft torque, rotor speed, blade root flap and edgewise bending moments, tilt angle, yaw angle, brake pneumatic pressure, gearbox temperature, tailboom strain, and accelerometers that can be placed in a number of locations. The instruments are connected to a Somat data acquisition system. The NREL GPP software package and a variety of commercial software are used for data analysis.

Results:

Since ADAMS had never been used to model a free-tilt, free-yaw wind turbine we first used test data for validation of the modeling code. This modeling started originally on the Synergy S-20000 system and continued with the S-50000. As might be expected, it was critical that we predict the tilt since an inaccuracy in the tilt prediction results in inaccuracies in power, rpm, flap loads, and yaw. We quickly found that the rotor plays an important role in the tilt behavior. Much like a free-yaw, downwind turbine generates a stabilizing aerodynamic yaw moment, the tilted rotor generates a moment that tends to reduce the tilt angle in most situations. This moment is smaller than the moment generated by the aerodynamic force on the tailplane, but it is not negligible. Of course, the rotor moment depends strongly upon the rotor speed and the wind speed.

As a result the prediction of tilt motion of a variable speed rotor becomes tightly interwoven with the rotor speed. The rotor speed depends upon the tilt angle and vice versa. The single most pressing question at the beginning of the testing was whether the ADAMS/AeroDyn code could accurately predict this dynamic behavior.

The analysis is further complicated by the gyroscopic coupling of the rotor tilt and yaw motions. We were more confident that ADAMS could handle this situation accurately if we could determine the aerodynamic forces on the tail structure.

Figures 2 and 3 show ADAMS predictions against test data for the S-50000. These model predictions used measured wind data as inputs to the model. The test data (both from the turbine and the wind) was collected from the instrumented turbine and anemometer tower at the Spanish Fork test site.

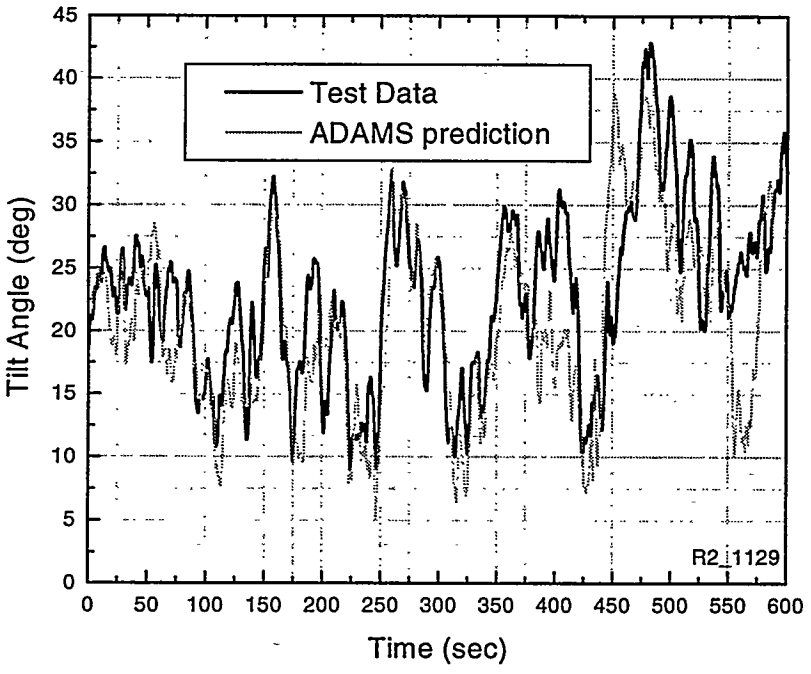

Figure 2. Tilt angle comparison for the S-50000 turbine during a 10 minute test. Tilt angle is zero when the rotor plane is vertical (in the normal run position).

Results such as these gave us confidence that the model could accurately predict the free tilting behavior of the turbine.

As noted before, the interdependence of the tilt, power, and rpm was a difficult (though manageable) aspect of the modeling. The Synergy SL turbine alleviated some of the difficulty in the modeling because it is a grid-connected, constant RPM turbine. With the RPM constant there was one less variable to influence the tilt angle. Below are results from the ADAMS modeling of the Synergy SL turbine.

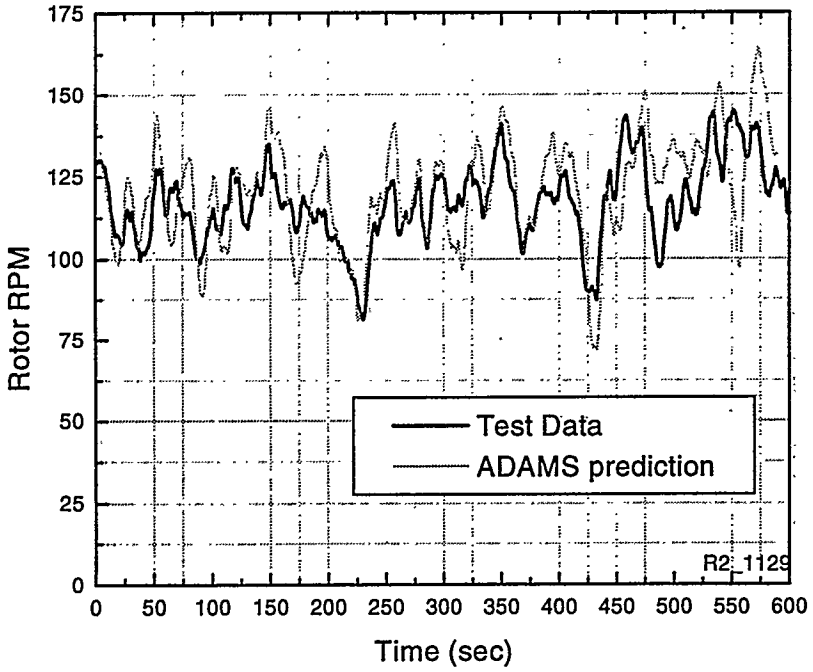

Figure 3. Rotor RPM comparison for the S-50000 turbine.

The ADAMS model was used extensively in the design of the SL turbine. Design loads for the blades, hub, shaft, tower, and yaw column were calculated using the model. It was also used to specify the location of the tilt axis and the size of the tail surfaces to give the desired tilt and yaw behavior. After the first prototype was installed the model was used in further validation studies. This was done to gain additional confidence in the codes before designing the second generation prototypes (20 of which have now been shipped to India for installation).

The first model validations for the SL prototype were of the performance characteristics. Once the performance parameters such as the tilt, and power had been validated, some loads were measured and compared to the ADAMS predictions. Eventually the model was validated enough to be used for load and performance predictions in modeling winds such as turbulence or IEC winds. Plots associated with all of these cases follow.

Figure 4 shows a time-series comparison for power prediction. The plot only shows 200 seconds of the data. More data makes the plot more difficult to decipher. The actual data set was a total of 1000 seconds. Figures 5-7 show the histograms for the entire 1000 second test. Here we can see that the model was quite accurate when compared to the test data.

With good accuracy from the modeling we continued to use the modeling for design refinement and verification. One example was to run IEC wind conditions and model the turbine response as well as loads. We ran 23 IEC Standard 1400-1 wind conditions. Some were in conjunction with a system fault, such as a loss of grid, while others were during normal operation with an extreme gust or other unusual wind condition. Figures 8 and 9 show the turbine response for one of these wind conditions. This case uses the IEC ECD_N wind. This acronym represents a extreme coherent gust with direction change at rated wind speed. The "_N" denotes that the direction change was in the negative direction. This case has the wind direction shift by 160° while a gust increases the wind speed from 10 m/s to 25 m/s. These changes are applied within a 10 second time span.

Figure 8 shows the predicted turbine response to the IEC wind. This plot shows how the rotor power, yaw angle; and tilt respond to the wind. As expected the power increased slightly before the tilt angle could respond. After approximately 8 seconds the tilt and yaw start responding. In 15 seconds the turbine is fully tilted and yawed back downwind while the power has dropped to nearly zero.

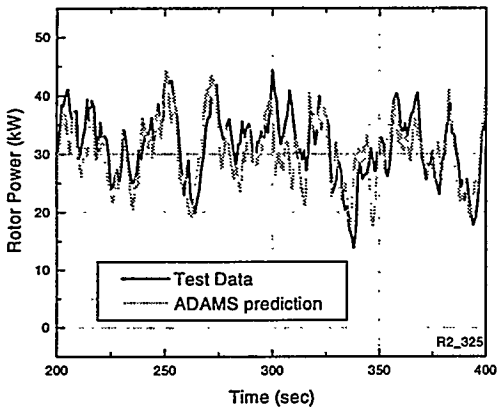

Figure 4 Time series plot of power for the SL turbine.

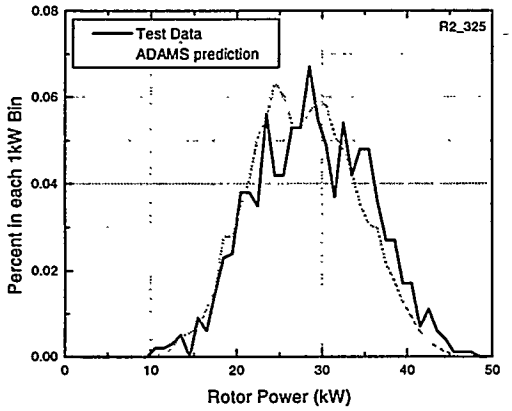

Figure 5 Rotor power histogram for the entire 1000 second test of the SL turbine.

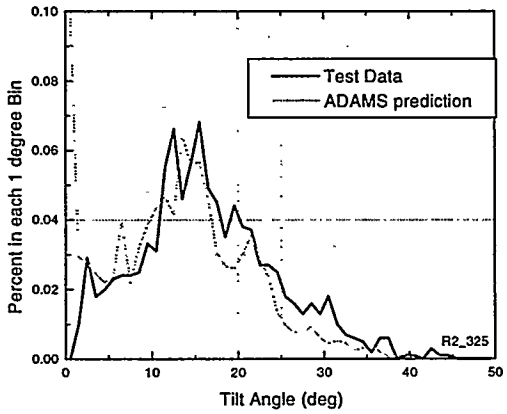

Figure 6 Tilt angle histogram for the entire 1000 second test of the SL turbine.

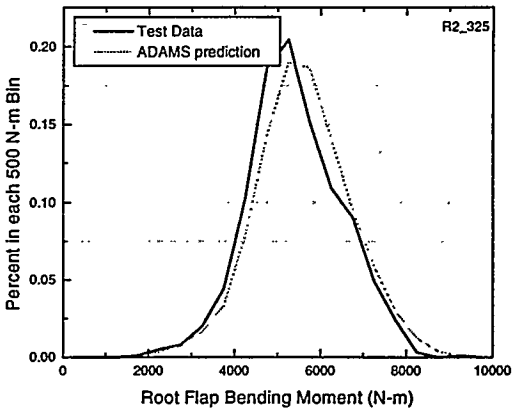

Figure 7 Root Flap Bending Moment histogram for the entire 1000 second test of the SL turbine.

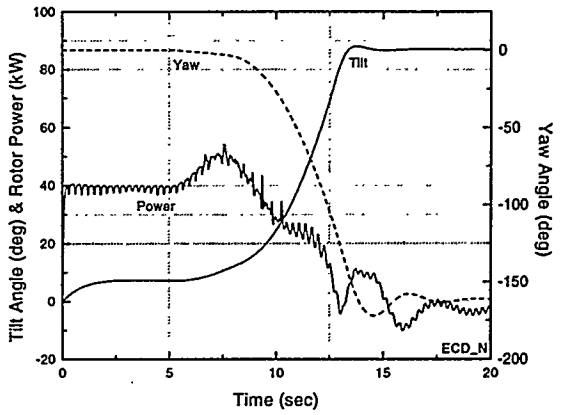

Figure 8 ADAMS prediction of SL turbine response due to IEC wind condition (ECD_N).

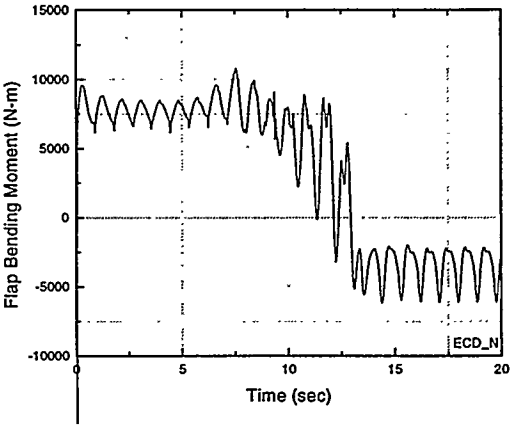

Figure 9 ADAMS prediction of the Synergy SL root flap bending moment during IEC wind condition (ECD_N).

Figure 9 shows how the flap moment responded to this IEC wind condition. For this case the up-tilt significantly reduced the flap moment. The free-tilt/free-yaw configuration prevents very large cyclic flap moments due to gyroscopic effects.

Another use of the model was to determine the effect of air density on the power curve. For a fixed tilt wind turbine the density correction is typically not a difficult calculation. We would expect the power to increase linearly with a change in density up to rated power. With the tilting turbine the correction is not as simple. We did not know how the change in density would influence the tilt behavior and therefore how it would alter the power curve. This correction was necessary since the test site is located at an altitude of 5000 ft and has approximately 15% lower air density than sea level.

To determine the effect of air density on the power curve we ran a very long ADAMS simulation. First an 11 hour data set was used as the baseline. This data set was ideal since it had widely varying winds during the 11 hour period. For the control run we ran ADAMS, using the measured wind and measured air density. Both the test data and this baseline ADAMS run were then binned to obtain a power curve. (see Figure 10). Because the power measurement from the test data was electrical power we needed to assume an efficiency (gearbox and generator losses) for calculating electrical power with the ADAMS data. Figure 10 shows the system power curve for three power train efficiencies which bracket the expected range (over the entire range of output power). These three efficiency curves are shown because we do not know the actual power train efficiency as a function of load. Note also that this is a small sample for an actual power curve measurement (only 11 hours of data) and is only shown to quantify the accuracy which ADAMS was able to predict the measured power output.

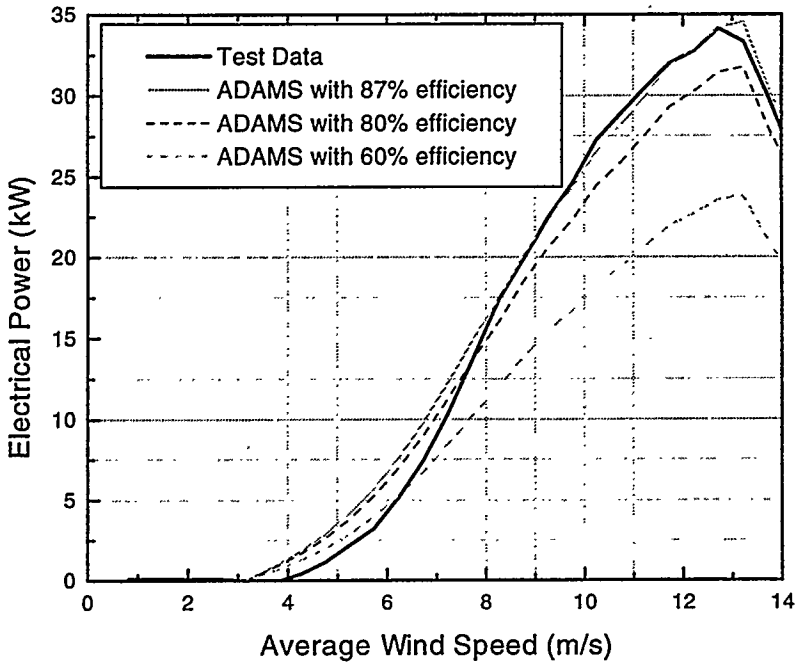

Figure 10 ADAMS power prediction plotted against measured power curve. Three different efficiencies are plotted which bracket the expected range.

After seeing the level of agreement between the model and the data, ADAMS was run again. This time everything was exactly the same except the air density was increased to standard sea level air density. This ADAMS data was then binned and compared with the non-corrected power curve.

This plot (Figure 11) also shows a conventional density correction (with the power ratio equal to the density ratio as if this turbine were not tilting). From Figure 11 we see that the effect of changing air density is less for the tilting turbine than for a conventional turbine. This is primarily because the higher air density generates larger aerodynamic forces on the tilting surfaces such as the tailplane and tailboom. Figure 12 shows that the sea level air density resulted in a higher tilt angle at a given wind speed.

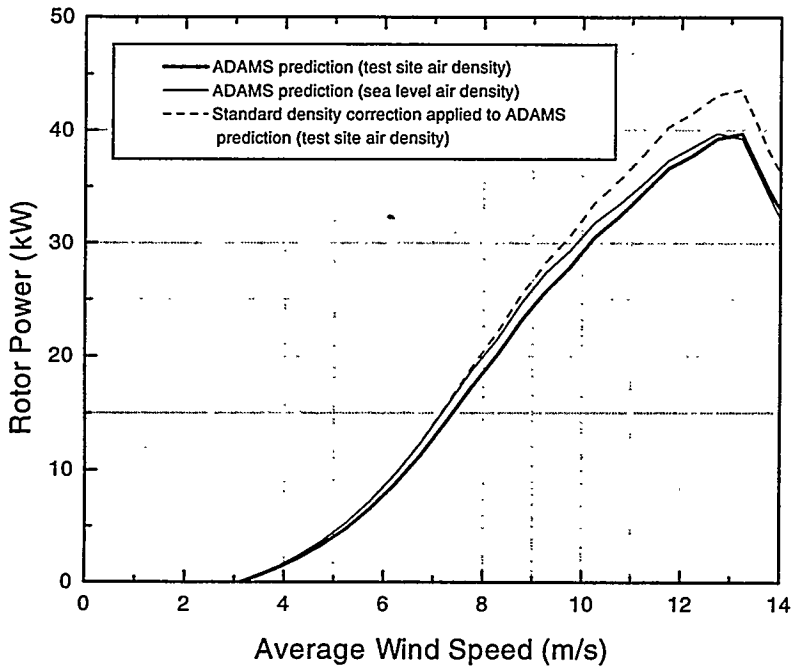

Figure 11 Density correction for power curve. The first (wide solid) line is the power binned from the 11 hour ADAMS prediction (using test data air density). The second (thin solid) line is the binned data for the 11 hour ADAMS prediction using sea level density. The third (dashed) line shows a conventional density correction applied to the first line.

Another design case which we considered was an emergency shutdown (E-stop) while the turbine was tilted. When the rotor is tilted the braking torque has a component in the yaw direction. This yaw moment will yaw the tail upwind unless the rudder produces sufficient drag to keep the tail downwind. Figure 13 shows an E-stop event where the turbine yawed upwind. This figure also shows the ADAMS prediction of this emergency stop.

In this ADAMS run we selected a braking torque time history that produced the correct RPM history. This was necessitated by the difficulty in predicting the dynamics of the brake application. As in the actual turbine, the braking torque produces a yaw moment and a corresponding yaw rate. A gyroscopic moment causes the turbine to tilt. The amount of yaw is dependent upon the braking torque and the opposing force generated from the aerodynamic rudder. Once the tail is pointed upwind the aerodynamic force on the tailplane combines with the gravity moment to start accelerating the tailboom downward. During this particular event the tail eventually hit the down-tilt stop.

We feel these model predictions are quite good considering the complexity of the combined gyroscopic, braking, aerodynamic and gravity moment interactions.

It was shown that the wind during an emergency stop was a key player in the turbine response. This is primarily because the yaw behavior is so strongly dependent on the rudder aerodynamic forces. Using the model we were able to estimate a worst case scenario. This case used a turbulent wind where the wind speed dropped as soon as the turbine started to yaw upwind. Once the turbine was yawed upwind the wind would increase forcing the tail down more rapidly.

Not only was the modeling used to identify a worst case it was also used to determine an effective way to ensure the tilt rate would not become excessive. By making changes in the model (such as larger rudder surfaces) we could easily and quickly determine the benefits of the modification. A combination of a larger tail rudder and some tilt damping was selected. Figure 15 shows test data (for the current turbine configuration with a tilt damper and larger rudder) showing that the turbine now yaws (back) downwind before the tilt nears the down stop.

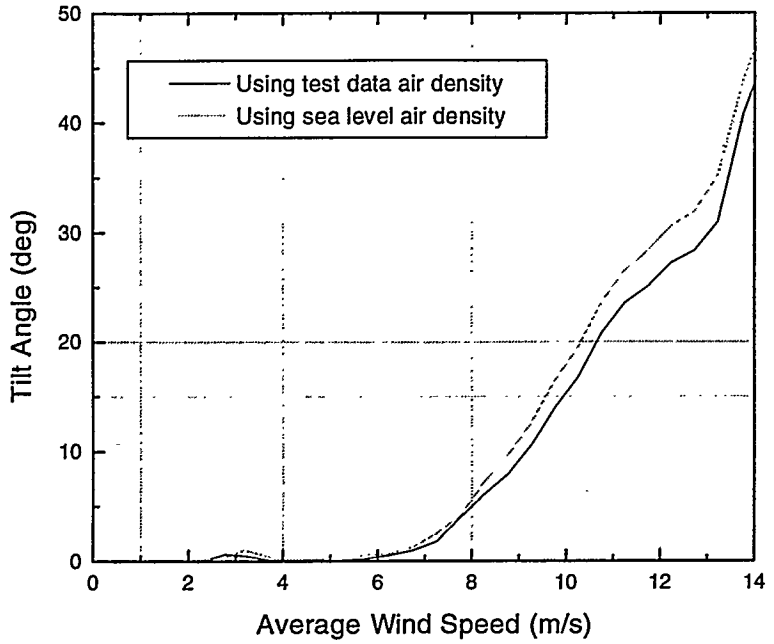

Figure 12 Tilt angle vs. wind speed for two ADAMS simulations. The first run was for the test site air density while the second run was for sea level air density.

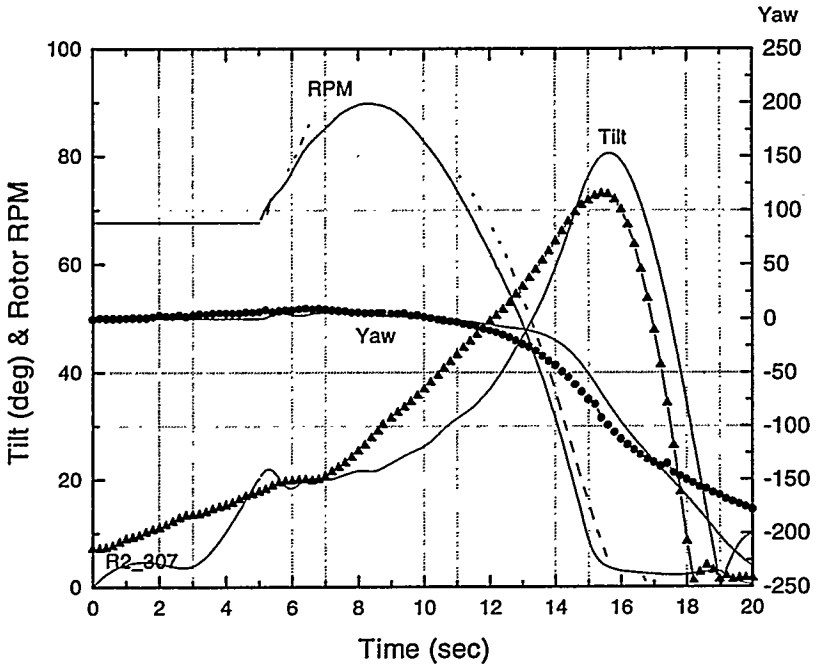

Figure 13 ADAMS model prediction compared to test data during an emergency shutdown. Test data shown with data symbols. ADAMS prediction shown with solid lines.

Conclusion:

The Synergy SL wind turbine is operating successfully at the test site near Spanish Fork, UT. The turbine was designed by Synergy Power Corporation with the assistance of computer modeling by Windward Engineering, L.C.

The ADAMS model has been shown to accurately predict performance characteristics and loads for Synergy Power Corporation free-tilting turbines. These predictions have been validated against test data for two prototype wind turbines. The first (S-50000) is a variable speed rotor while the other (SL) is a constant speed rotor.

Modeling of the S-50000 wind turbine proved to be somewhat more difficult than modeling of the SL turbine. This was primarily because of the variable speed rotor. These predictions showed that the tilt was dependent on the rotor speed and that the rotor speed was dependent on the tilt angle. ADAMS was found to be relatively successful in modeling the free tilt and variable speed rotor.

The modeling has shown that the tilting behavior of the turbine is not only dependent on the aerodynamic surfaces (such as the tailplane) but also on the restoring moment

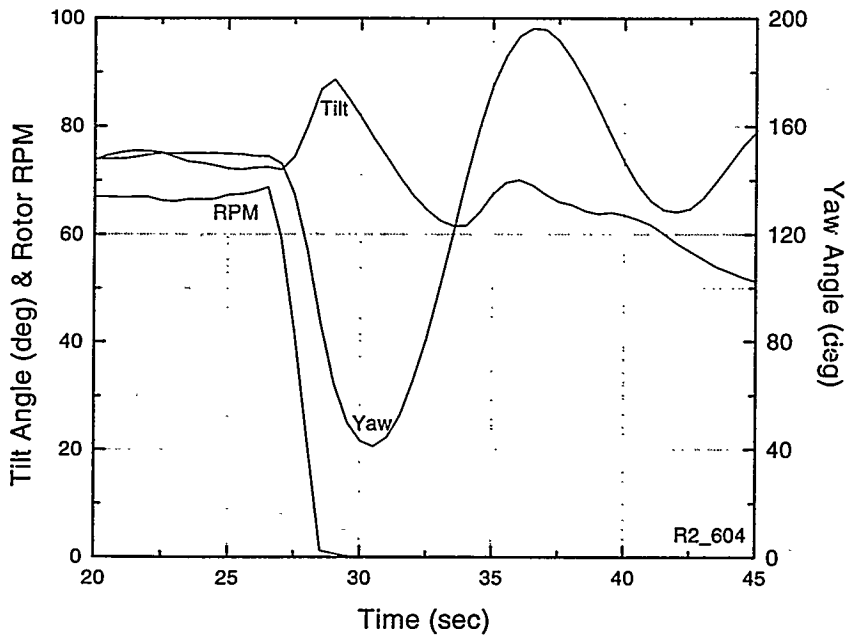

Figure 15 Current turbine configuration reduces the maximum tilt rate during emergency shutdowns.

from the aerodynamics of the rotor. This knowledge, as embodied in the model, has been used to specify the tailplane size and tilt pivot location which will result in the desired power regulation. The successful SL geometry was specified with the use of the computer modeling and avoided the costly trial-and-error solution that would be necessary in the absence of a model.

We have also used the ADAMS model to determine the effect of changes in air density upon the power curve. This calculation, although simple for a conventional turbine, is much more detailed for a free tilting turbine. Long ADAMS simulations have given insight into density correction calculations.

The modeling has also been invaluable for load predictions. Blade fatigue loads were generated using turbulent wind conditions. Maximum blade loads were generated using IEC extreme wind conditions. These loads could not have been accurately estimated without a (free) tilting model.

Finally, the modeling has proven helpful for analysis of a yaw / tilt behavior which arises during some emergency stops. By modeling this event we could choose a simple and economical way to limit tilt rates.

Acknowledgments

We would like to thank Synergy Power Corp. for granting permission to publish this information. We are grateful for their willingness to share this information with the wind energy community. We also would like to thank the Utah Municipal Power Agency and the City of Spanish Fork for the use of their wind energy demonstration site where all of these tests were conducted.

A Graphical Interface Based Model for Wind Turbine Drive Train Dynamics

James F. Manwell, Jon G. McGowan, Utama Abdulwahid, and Anthony Rogers
Renewable Energy Research Laboratory
Department of Mechanical and Industrial Engineering
University of Massachusetts
Amherst MA 01003

Brian McNiff
McNiff Light Industry
Blue Hill ME 04614

ABSTRACT

This paper presents a summary of a wind turbine drive train dynamics code that has been under development at the University of Massachusetts, under National Renewable Energy Laboratory (NREL) support. The code is intended to be used to assist in the proper design and selection of drive train components. This work summarizes the development of the equations of motion for the model, and discusses the method of solution. In addition, a number of comparisons with analytical solutions and experimental field data are given. The summary includes conclusions and suggestions for future work on the model.

INTRODUCTION

Understanding drive train behavior in wind turbine applications is facilitated with the application of dynamic models. Such models may be particularly useful in investigating startup and stopping loads [1, 2], control system development [3-5], and component fatigue. It may also be useful for brake sizing and system configuration selection.

The drive train model discussed in this report is based on an earlier UMass version written in MATLAB [6]. Although able to approximate the behavior of real drive trains in a number of ways, the original model also had a number of limitations. First of all, it required the user to have, and be familiar with MATLAB. Second, it was difficult to add complexity and non-linear effects. The earlier model also did not include any representation of the generator or rotor aerodynamics.

Because of the limitations of the original MATLAB model, and to provide a framework for a model which could be expanded in the future, a completely new model has been written in Visual Basic. The new model contains a differential equation solver which allows it to operate independently of other software packages. In addition, this new model was designed to incorporate the following features: (1) Simple component models, (2) An interactive user interface, (3) An accurate and fast solver routine, and (4) Graphical output.

DESCRIPTION OF ANALYTICAL MODEL/ COMPUTATIONAL CODE

1) Overview

As previously noted, the present code has been developed from an earlier UMass drive train model. Added provisions include modeling of rotor aerodynamics, aerodynamic brakes, a generator, and a user specified control sequence. In its present form, components modeled include the turbine rotor, aerodynamic brakes, shafts, gearbox, couplings, mechanical brake, and an induction generator. A model of 3 springs and dampers and 4 inertias is used with optional braking at any of 4 locations. A control option allows the user to specify the time at which: i) the

generator is connected to the line, ii) the aerodynamic brakes are deployed, iii) the generator is disconnected, and iv) the mechanical brake is applied.

The resulting code, DRVTRNVB, operates in a free standing Visual Basic version working under a PC/ Windows environment. It allows the user to configure and assemble a wide variety of drive train formats to investigate the impact of such choices on system dynamics and loading. Normal operation with a variety of wind flow inputs is available to the operator, as are various types of start-ups and stops. A built in editor allows easy preparation of input files. An efficient solution engine is invoked that offers results in a favorable processing to simulation time with a 486 processor. A unique back end is utilized for processing and graphic output of time series, histograms and rain flow cycle counting of the results. This can be performed without exiting the program.

A control option allows the user to specify the time at which: i) the generator is connected to the line, ii) the aerodynamic brakes are deployed, iii) the generator is disconnected, and iv) the mechanical brake is applied.

The output from the model consists of time series of displacements, velocities, torques, and torsion. A built in graphical option allows the display of X-Y plots, histograms, and cycle counts.

2) Analytical Model

A lumped parameter model is used to define the system. As shown schematically in Figure 1, the drive train is represented by four nodes, connected by three shafts. It is assumed that the nodes correspond to the rotor, the gearbox, the generator and the brake. The brake can be located at any plausible place on the drive train. All mass is concentrated on the nodes and all stiffness and damping coefficients are defined in the connecting shafts. In order to facilitate analysis a geared system is reduced to its single-shaft equivalent on the low speed side.

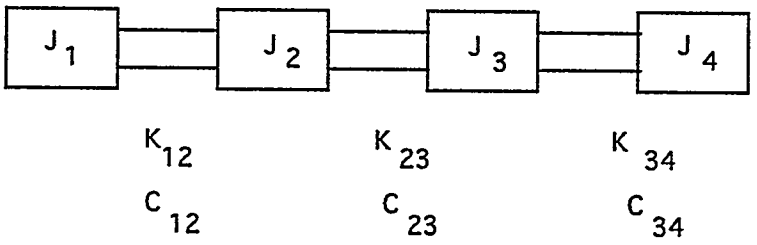

Figure 1 : Sample nodal configuration

The equations of motion were developed for each node based on the sum of all torques (Q):

$$\Sigma Q = J\ \ddot{\theta} \qquad \text{where:}$$

J is mass moment of inertia and $\ddot{\theta}$ is angular acceleration

Using Figure 1, and assuming that the brake is on the far side of the generator, for each node this equation becomes:

1) $Q_{Wind} - Q_{12} = J_{Rotor}\ \ddot{\theta}_1$

2) $Q_{12} - Q_{23} = J_{Gear}\ \ddot{\theta}_2$

3) $Q_{23} - Q_{34} = J_{Generator} \ddot{\theta}_3$

4) $Q_{34} - Q_{Brake} = J_{Brake} \ddot{\theta}_4$

where:
JRotor = Rotor inertia (node 1)
JGear = Gear box inertia (node 2)
JGenerator = Generator inertia (node 3)
JBrake = Brake inertia (node 4)
$Q_{i,j}$ = Torque in shaft connecting nodes i and j

In the above equation it is also assumed that rotor, gearbox, generator, and brake correspond to nodes 1, 2, 3 and 4 respectively, but the actual model allows the relative location of the various components to be varied.

The torque at each node can also be expressed as a function of angular deflections (θ_i) and velocities

5) $Q_{12} = K_{12} (\theta_1 - \theta_2) + C_{12} (\dot{\theta}_1 - \dot{\theta}_2)$

6) $Q_{23} = K_{23} (\theta_2 - \theta_3) + C_{23} (\dot{\theta}_2 - \dot{\theta}_3)$

7) $Q_{34} = K_{34} (\theta_3 - \theta_4) + C_{34} (\dot{\theta}_3 - \dot{\theta}_4)$

It should be noted that the component stiffness (K_{ij}), damping (C_{ij}), and masses (J_i) are located and described in Figure 1. During processing of the inputs, these coefficients are reduced to the low speed shaft (LSS) by the square of the gear ratio.

3) Component Models

A) Rotor. The rotor is characterized by an inertia and a torque due to the wind.
The rotor mass moment of inertia may be known already and input directly or it may be calculated by the program. In the latter case, it is found from the geometry and mass of the blades and hub. The contribution to rotor inertia from the blades is made by assuming a uniform density and using the chord and thickness distribution to determine the radial mass distribution. The parallel axis theorem is used to determine the effect of the location of each segment of the each blade. The total inertia is found by adding the hub inertia to the product of the number of blades and the inertia of each of them. The mass of a blade is required for the program to carry out this calculation.

Rotor torque due to wind, Q_{wind}, is found from wind speed and rotor rpm, in accordance with a power coefficient vs. tip speed ratio curve. The latter is an input to the program, and is used to determine a rotor torque coefficient relation. Mechanical loss, as a function of rotation speed, may be applied to modify the rotor torque.

B) Aerodynamic Brakes. Aerodynamic brakes may be either tip flaps or ailerons. The aerodynamic brakes are characterized by: i) mean radius to the brakes, ii) brake area, iii) number of blades, iv) average drag coefficient, v) maximum deployment angle, and vi) rate of deployment.

The braking torque, Q_{Flap}, is found from:

$$Q_{Flap} = (1/2)\, C_D\, N_B\, A_{Flap}\, \rho\, \Omega^2\, (R_{Flap})^3 \sin(\phi_{Flap})$$

where:

C_D = drag coefficient

N_B = number of blades

A_{Flap} = aerodynamic brake area, m^2

ρ = air density, kg/m^3

Ω = rotor speed, rad/s $(\Omega = \dot{\theta})$

$\phi_{Flap} = \max\{\dot{\phi}_{Flap} * t_D, \phi_{Flap,max}\}$

R_{Flap} = mean distance to a flap, m

with: $\dot{\phi}_{Flap}$ = deployment rate, deg/s

t_D = deployment time, s

$\phi_{Flap,max}$ = maximum deployment angle, deg

When the tip flaps are deployed, their effect is to reduce the torque produced by the rotor. The adjusted (net) rotor torque is then used by the rest of the model, i.e., $Q_{wind} = Q_{wind} - Q_{Flap}$. When ailerons are used, the inputs (i.e. drag coefficient, deployment rate, maximum deployment angle, etc) must be chosen carefully so that their effect is appropriate.

C) Gearbox. The gearbox is modeled as an inertia and a speed up ratio. The gearbox stiffness is one of the primary determinants of the system natural frequency. There is no explicit gearbox model in the program, but its effect on the natural frequency can be included by setting the shaft stiffness according to the following empirically determined equation [7]. Note that this relation is most appropriate for parallel shaft gearboxes.

$$K = 2.26 \times 10^6 * \frac{W}{R}$$

where : W = tooth width, cm

R = bull gear pitch radius, cm

K = stiffness, N m/ rad

D) Generator. The generator is modeled as an induction machine, which is the most common type in grid connected wind turbines. The schematic of the conventional electrical model [8] used is shown in Figure 2.

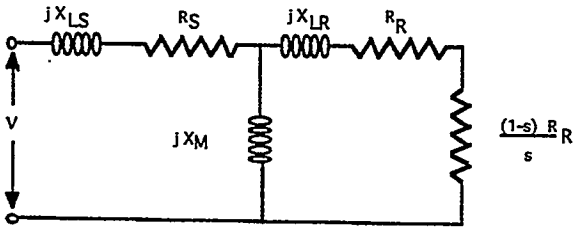

Figure 2 : Induction Generator Equivalent Circuit

where:

V = Terminal voltage, Volt

X_{LS} = Stator leakage inductive reactance, Ohms

R_S = Stator resistance, Ohms

X_{LR} = Rotor leakage inductive reactance, Ohms

R_R = Rotor resistance, Ohms

X_M = Mutual inductance between stator and rotor, Ohms

s = slip = $(n_s - n)/n_s$ with n_s = synchronous speed and n = actual rotational speed

As presently configured, mechanical losses in the generator are not explicitly considered. However, a fixed loss torque may be included in the input, and this may be selected to reflect generator losses. The power converted by the generator at steady state (ignoring losses), P_{in}, is then equal to the power produced by the rotor. A current limiting "soft start" was also included as an option. In electrical terms the converted power is:

$$P_m = I_R^2 R_R \frac{1-s}{s}$$ where the current is found by phasor algebra

Generator torque is given by

$$Q_{Generator} = \frac{P_m}{n_s(1-s)}$$

In general it is difficult to obtain the various constants for an arbitrary generator. Therefore a per unit approach described by Jeffries [9] has been used. This method requires that the user input only the rated generator power, rpm, and voltage. The per unit conversion constant is given by

$$C_{pu} = P_{Rated}/(V_{Rated})^2$$

Per unit leakage reactances, and resistances are used, for both the rotor and the stator (0.08 and 0.01, respectively). The mutual per unit inductance, $x_{m,pu}$, is assumed to be3.0.

The generator inertia may be input directly or it may be calculated based on the generator rotor mass and diameter.

E) Mechanical Brake. The brake is characterized by an inertia, a maximum torque, and an application time. The torque is assumed to increase linearly from zero to full torque during the application time.

$$Q_{brk} = \min(Q_{brk,max} * (\frac{Time_{Current} - Time_{brk}}{Time_{Ramp}}), Q_{brk,max})$$

where,

Q_{brk} = Brake torque, Nm

$Q_{brk,max}$ = Max brake torque, Nm

$Time_{current}$ = Current time, s

$Time_{brk}$ = Time brake started to engage, s

$Time_{ramp}$ = Time required for brake to ramp up to maximum torque, s

F) Shafts and Couplings. By default, the program assumes that each node is connected by a shaft, and that the torsional stiffness of the shaft is found from:

$$k = \frac{JG}{L}$$

where G = modulus of elasticity of the shaft material, N/m^2

L = shaft length, m

J = moment of inertia of shaft, $\pi/(32\ D^4)$, m^{-4} , with D = shaft diameter, m

In reality, other factors may serve to reduce the shaft stiffnesses. These include the gearing in the gearbox and the coupling. The gear box stiffness can be calculated (as described above), or a

shear modulus scaling factor may be used to reduce the stiffness. The damping coefficient value is assigned in the input file. However, based on observations of real data this value changes with direction of rotation. Our contention is that this is due to factors such as gear teeth flexing in the reverse direction and gear lubrication oil damping effect. A reversible damping adjustment factor is introduced to modify the damping coefficient every time the rotation is reversed. This results in the model giving a better fit to real data. These factors need to be investigated further.

G) Control. Four control options are available. The user may specify the time when: i) the generator connects to the line; ii) the aerodynamic brakes are deployed; iii) the generator is disconnected; and/or iv) the mechanical brake is applied.

H) Solution Method. The program employs an adaptive time step Runga Kutta solution technique to step through the drive train operation [10]. Other solution methods are available on an experimental basis in the source code of the program. All inertias, stiffnesses, and damping coefficients are referred to the low speed shaft within the program.

For each node two equations are used, derived for compatibility with the solver. During start up, normal operation and most of braking, all the nodes are allowed to move. This is called the free brake condition. At the end of braking, when the mechanical brake speed is close to zero, the brake is forced to be (and remains) zero. This is called the fixed brake condition.

I) Rainflow counting. A rainflow counting routine [11] was adopted as a predecessor to further work in analyzing fatigue in the drive train. It can be used on any of the recorded data but it is most useful in the analysis of torques.

J) System natural frequencies. Based on the system configuration in the input file, the natural frequencies are calculated using Holzer's method [12]. This calculation is done on the system when it is in the free brake condition and also in the fixed brake condition. Frequencies higher than 30 Hz are excluded.

APPLICATIONS

In this section, two applications of the drive train model are presented that allow a comparison of the results from the analytical model with experimental field data. They include drive train dynamics for an ESI-80 turbine, and a Micon 108 machine.

1) ESI-80

Description

The machine modeled is the ESI-80, a 2-bladed machine rated at 250 kW. It has a planetary gearbox with a 30 to 1 speed up ratio. The original data was taken as part of the ESI-80/EPRI Test Program. The inertias of the turbine components are based on actual weights and estimates from the construction drawings. Shaft stiffnesses are those used by McNiff, Manwell and Xie [6]. Wind speed input was estimated by reference to the mean power before application of the brake. The Cp lambda power curve was based on power curve test data. The timing of the braking sequence was estimated by reference to the test data. Additional data was obtained from the UMass Turbine which is operating at Mt. Tom, Holyoke, Massachusetts.

Input Data

Mass moment of inertias:

Rotor and hub : Calculated by program from blade data (13400 kg m^2)
Gearbox : 169 kg m^2
Generator : Calculated by program from generator mass (250 kg) and diameter (0.21m)

Brake : 1.08 kg m^2

Wind Speed : 10.5 m/s

Component Placing

Node	1	2	3	4
Component	Rotor and Hub	Gearbox	Generator	Brake

Simulation Results

Figure 3 illustrates the rotational speed of the ESI-80 turbine (data from Holyoke, MA) during startup in an approximately 20 mph wind. The brake was released and the turbine was allowed to free wheel up to 150 rpm, at which time the generator was connected to the grid, via the Vectrol soft start. From that point on, it took about 8 seconds to reach operating speed. Figure 4 illustrates a simulated startup of the same turbine, but, the turbine was motored from a stand still. In this case, the entire startup took 16 seconds, but between 150 rpm and operating speed the time was approximately 10 seconds.

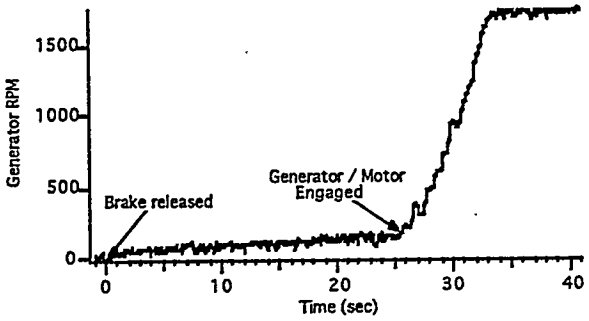

Figure 3 : Field Data (ESI-80)

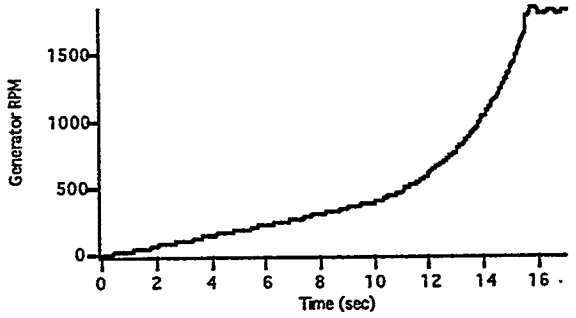

Figure 4 : Simulation (ESI-80)

Figure 5 illustrates the rotational speed of the turbine during a no tip flap braking event (data from Holyoke, MA) in an approximately 10 m/s wind. This stop used only the high speed shaft brake. The peak brake torque was 1.33 kNm (40 kNm when referred to the low speed shaft). The brake ramp time was 3 seconds. The turbine reached a complete stop in approximately 4 seconds. Figure 6 illustrates a simulated braking event, also without use of the flaps. The model also predicted a stopping time of 4 seconds.

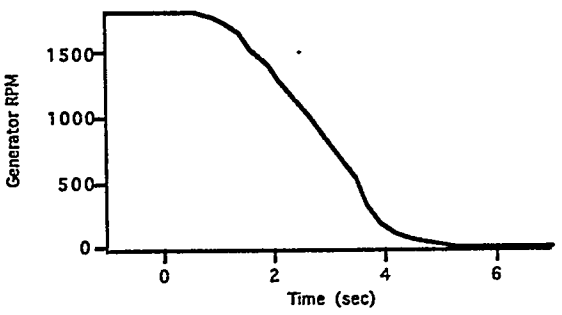

Figure 5 : Field Data (no tip flaps) (ESI-80)

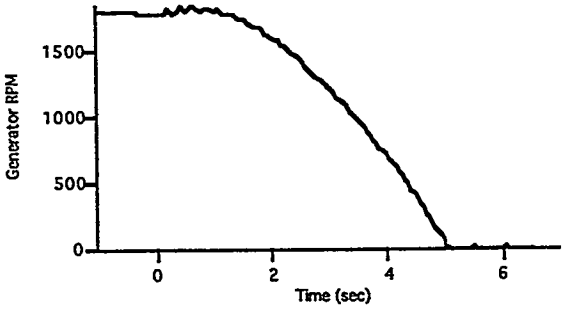

Figure 6 : Simulation (no tip flaps) (ESI-80)

Figure 7 illustrates the low speed shaft torque of the ESI-80 turbine (installed in the Altamont Pass, CA) during a braking event in which tip flaps were used. The sequence of events was: 1) Normal operation, 2) Tip deployment, 3) Release of air from the brake canister to allow the springs to apply the brake, 4) Release of the generator from the grid, 5) Oscillation of torque during brake application, 6) Stopping of the brake, and 7) Oscillation of the rotor against the stopped brake. Features of particular note include: 1) Approximately constant positive torque (with some variation) during normal operation, 2) Sharply dropping, and then negative, torque once the flaps are deployed and the generator acts as a motor, 3) Increasing torque as the generator is released from the grid and deceleration against the increasing torque of the brake begins, 4) Relatively constant torque (with some oscillations) as the brake is fully applied and the rotor continues to decelerate, and 5) Sudden decrease and oscillation of the mean torque about zero once the brake shaft has stopped. The latter oscillation is rapidly damped out.

A simulation of a similar braking event is illustrated in Figure 8. The peak torque was the same as the previous example. The tip flaps were deployed at zero seconds. The brake started to engage at 0.5 seconds and the generator was taken off line at 0.65 seconds. As can be seen, the major events follow a similar pattern, although the details of the real event and the simulated one show some differences. Some of the differences may be attributable to the specific characteristics of the real event as opposed to the simulated one, but others may have to do with limitations inherent in the model in its present form.

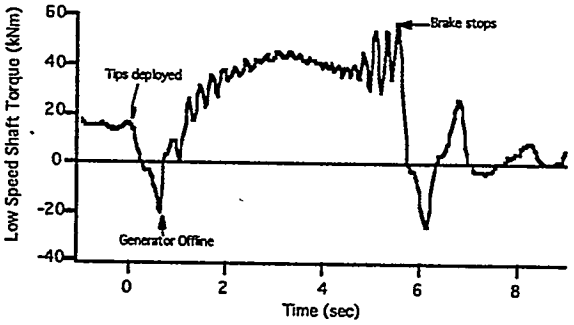

Figure 7 : Field Data (braking) (ESI-80)

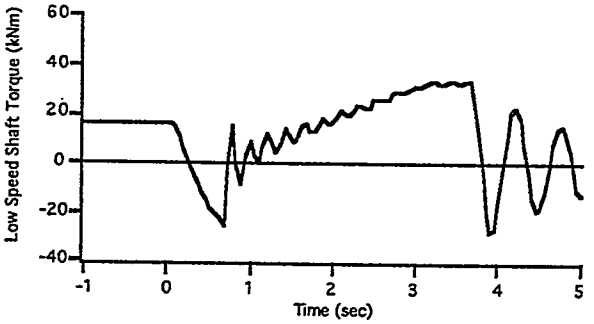

Figure 8 : Simulation (braking) (ESI-80)

2) MICON 108 Turbine

Description

The machine is a three bladed machine rated at 108 kW with a parallel shaft gearbox ratio of 27.7 to 1. The data used is as follows.

Mass moment of inertias:

Rotor and hub : 37500 kg m^2
Gearbox : 1290 kg m^2
Generator : 0.136 kg m^2
Brake : 1.46 kg m^2

Wind Speed : 14 m/s

Brake Strategy

Brake starts to engage : 0 s.
Generator taken off line: 1 s.
Ramp period: 1 s
Maximum brake torque: 40 kNm

Component Placing

Node	1	2	3	4
Component	Rotor and Hub	Gearbox and Brake	Coupling	Generator

Simulation Results

Comparison of real data with the result of a simulation (Figs 9 and 10) shows that the overall characteristics of the results are similar. When the brake is applied and the generator taken off-line the low speed shaft torque is seen to oscillate. As with the ESI-80 data the last set of oscillation prior to the brake stopping is not understood fully and therefore is not modeled. A lower frequency oscillation occurs when the brake is stopped and the dynamic characteristics of the drive train changes. The two oscillation frequencies are very similar between the real data and the simulated run.

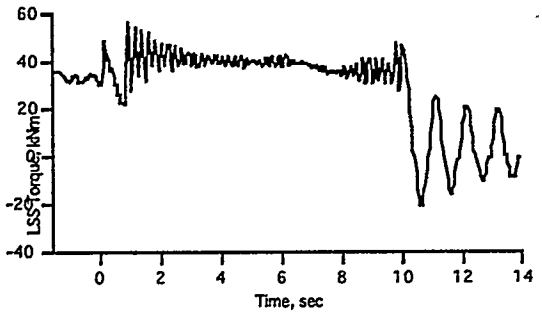

Figure 9 : Field Data (Micon 108)

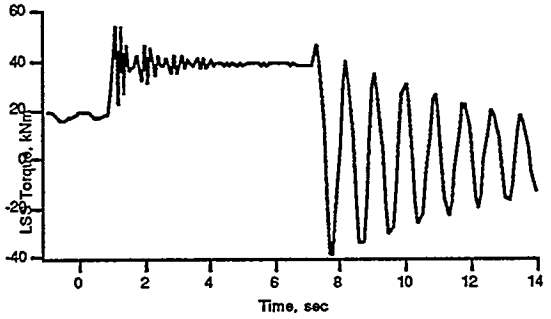

Figure 10 : Simulation (Micon 108)

CONCLUSION AND RECOMMENDATIONS

As seen in the previous examples, the drive train model is able to reproduce a number of significant features of the wind turbine starting and stopping including peak torque and event time. This indicates that the structure of the model is basically sound. The model can not reproduce all the fine structure of the events, however. This suggests that there is still need for creating more detailed component models. This is particularly true in the case of the tip flaps, the gearbox and the controls. As found from field tests, and discussed in Ref. 13, tip flap deployment represents a complex dynamic event, and may include oscillations itself. Gearboxes are complicated structures, and details in their design may significantly affect the natural frequency and damping characteristics of the entire drivetrain. Brake behavior is a function of the details of the actual braking process (such as brake pad performance, pad heating, and its effect on the friction coefficient) and the method of application of the brake (such as via springs or calipers). The generator model is probably adequate for events in the time scales consider so far, but could require elaboration for certain types of transient events. On the other hand, the drive train model in its current form, already requires a significant number of inputs to describe the various components. Many of these inputs are not readily available, and this can be a limitation in carrying out first level simulations. Our experience with the generalized induction generator

model was quite positive, however. This suggests that development of similar generic models for the other components could also be quite useful.

Incorporating more control features into the drive train model would also expand its versatility. In this regard, it should be noted that the core of the drive train model has served as the basis for the development of a "virtual wind turbine" model of the ESI-80. This has been used to facilitate the development and debugging of a new controller for the UMass machine. Future work could result in a generalized virtual wind machine that could be used in conjunction with a variety of turbine controllers.

ACKNOWLEDGEMENT

This work was partially supported at the University of Massachusetts by U.S. Department of Energy Contract No. XL-1-11126-1 administered by the National Renewable Energy Laboratory.

REFERENCES

[1] Clauss, D., and Carne, T., (1981) "Vertical Axis Wind Turbine Drive Train Transient Dynamics", Sandia National Laboratory Report TR--2646 , March.
[2] McNiff, B., Musial, W., and Errichello, R. (1990),"Variations in Gear Fatigue Life for Different Wind Turbine Braking Strategies", Windpower 1990 Proceedings, AWEA.
[3] Novak, P., Jovik, I., and Schmidtbauer, B. (1994), "Modeling and Identification of Drive-System Dynamics in a Variable-Speed Wind Turbine," Proc. Third IEEE Conference on Control Applications, IEEE.
[4] Leithead, W. E., Rogers, M.C., and Agius, P.R.D. (1994), "Dynamic Characteristics of the Drive-Train: Causes and Effects," Proc. 1994 BWEA Conference, BWEA.
[5] Leithead, W. E., and Rogers, M.C. (1995), "Improved Damping by a Simple Modification to the Drive Train," Proc. 1995 BWEA Conference, BWEA.
[6] McNiff, B., Manwell, J.F., Xie, Y. (1994), "Development of a Wind Turbine Drive Train Analysis Code", Windpower '94 Proceedings, AWEA.
[7]. Smith, J. D. (1983), Gears and Their Vibration, Macmillan Press.
[8] Brown, D. and E. P. Hamilton III (1984), Electromechanical Energy Conversion, MacMillan.
[9] Jeffries, William Q. (1994), Analysis and modelling of wind/diesel systems without storage, PhD Thesis (PhD),University of Massachusetts/Amherst.
[10] Sprott, Julien C. (1992), Numerical Recipe Routine and Example in BASIC , Cambridge University Press.
[11] Collins, J.A. (1981), Fracture of Materials in Mechanical Design, Wiley & Sons.
[12] Thomson, William T. (1981), Theory of Vibrations with Applications, 2nd Ed, Prentice Hall.
[13] Rogers, A., et al. (1996), "Design Improvements for the ESI-80 Wind Turbine," Proc. AWEA '96.

MODELING THE EFFECTS OF CONTROL SYSTEMS ON WIND TURBINE FATIGUE LIFE

Kirk G. Pierce
David J. Laino
University of Utah
Department of Mechanical Engineering
Salt Lake City, Utah 84112

ABSTRACT

In this study we look at the effect on fatigue life of two types of control systems. First, we investigate the Micon 65, an upwind, three bladed turbine with a simple yaw control system. Results indicate that increased fatigue damage to the blade root can be attributed to continuous operation at significant yaw error allowed by the control system. Next, we model a two-bladed teetered rotor turbine using three different control systems to adjust flap deflections. The first two limit peak power output, the third limits peak power and cyclic power output over the entire range of operation. Results for simulations conducted both with and without active control are compared to determine how active control affects fatigue life. Improvement in fatigue lifetimes were seen for all control schemes, with increasing fatigue lifetime corresponding to increased flap deflection activity.

INTRODUCTION

Control systems have been incorporated into wind turbine designs throughout history, although the earliest were manual in nature. Aerodynamic brakes, and fantails to point rotors into the wind are the earliest known automatic control systems, utilized as far back as the 16th century (Spera, 1994). Early, modern era wind turbines continued the use of passive controls for yawing and rotor braking. As the size of turbines increased, however, the use of tail vanes and other passive devices became impractical, and the use of active control systems arose. Today, a 100 - 1000 kW wind turbine will often have active pitch control, and in the case of upwind rotors, active yaw control. The future promises to see a further increase in control systems as designs delve into controlling load and power excursions through the use of flaps, tip brakes, and other aerodynamic devices in more complex schemes. Part of the reasoning in choosing this route is in the hope of limiting turbine component fatigue damage. Fatigue failures have plagued modern wind turbines, and can arguably be considered the most formidable obstacle to the next significant reduction in wind turbine operating costs.

At the University of Utah, under funding from the National Renewable Energy Laboratory, the capability to model active control systems has been developed for the YawDyn and ADAMS® dynamic simulation codes (Hansen, 1996). In addition, a fatigue life analysis interface, Dyn2LIFE (Laino and Hansen, 1996) has been developed to assist in producing input for the LIFE2 fatigue life estimation code from YawDyn and ADAMS output. These two capabilities make it possible to analyze the effectiveness of different control systems on the fatigue life of wind turbine components.

In this paper we look into the effects of two control systems on wind turbine component fatigue life. The first is a yaw controller, common in today's upwind machines. The purpose in most cases is strictly to optimize wind energy capture, though it can also be used to regulate power as in the case of the Gamma 60 (Paoli, et. al., 1994). We look at a secondary effect of the yaw controller, how it affects fatigue life of the blades. The second control system analyzed is a flap, or aileron, system used for the control of power output. The industry is showing signs of renewed interest in these aerodynamic control systems that were seen sporadically in the past. We look at how these control systems affect fatigue damage.

FATIGUE LIFE ESTIMATE

LIFE2 was used for estimation of blade root lifetime. LIFE2 is a wind turbine specific fatigue analysis program developed at Sandia National Laboratories (Schluter and Sutherland, 1989). Its capabilities include both stress/strain life, and fatigue crack growth estimation. We use only the former method, which is based on the cumulative damage approach proposed by Miner (1945), now commonly referred to as Miner's rule.

Several inputs are required by LIFE2 to perform a fatigue life estimate: 1) Wind speed distribution; 2) Material fatigue properties; 3) Turbine operational parameters; and 4) Component stress data. For all LIFE2 analyses performed for this report the following *assumptions* regarding these inputs apply:

> Material properties are taken from the Goodman diagram for "GP 0/45" laminates from the FAtigue of Composites for wind Turbines (FACT) database (DeSmet and Bach, 1994).
>
> Stress data is calculated from load data following a procedure similar to that of Sutherland and Kelley (1995). We *assume* the design of the blades calls for the nominal strain to never exceed 0.4%. This strain is *assumed* to occur at twice the sum of the average load measured at 15 m/s (on a ten minute average) hub-height wind speed plus 4 standard deviations. The resulting conversion factor was used in the Dyn2LIFE program to generate rainflow counted stress cycles for LIFE2 from blade flap moment data. A stress concentration factor is later applied to the rainflow counted stress cycles in LIFE2 to achieve lifetimes reasonable for comparison studies.

Other required LIFE2 parameters varied between the different turbines in our study. While our assumptions do not necessarily reflect actual conditions, they are sufficient for comparative purposes.

In the fatigue analyses performed here, ten minute data sets are used to represent each wind speed interval. This is a relatively small amount of data to extrapolate to an entire lifetime of operation, and this must be kept in mind when interpreting the results. The lifetimes reported here are just estimates which may be very sensitive to some parameters. For computer simulations, lifetime estimates can vary by more than 50% just due to changes in the random seed used to generate turbulence. For test data, lifetime differences of a factor of two can be attributed to the more numerous uncontrollable parameters. The results of these comparative studies best serve to show trends in fatigue life sensitivity, while the actual quantitative differences are much harder to judge.

YAW CONTROL

The Micon 65 wind turbine was used for investigation of yaw control. This turbine is an upwind, yaw-driven machine that has been the subject of several previous studies. The data presented here are from performance tests comparing a SERI airfoil- and Aerostar-bladed rotor (Tangler, et. al., 1990). The data used here is from the SERI airfoil bladed turbine unless otherwise noted. In a recent study, Sutherland and Kelley (1995) performed a fatigue analysis of the Micon blade root under different loading spectra. Following their method, we will investigate the affect of yaw error on blade root fatigue life.

The wind speed distribution used for the Micon 65 is based upon the representation given by Sutherland and Kelley (1995) for the San Gorgonio wind park where the test turbine is operated. The turbine is assumed to operate between a cut-in wind speed of 5 m/s and a cut-out of 18 m/s. A stress concentration factor of 3 is applied in the analysis.

The Micon 65 yaw control system adjusts the yaw angle of the machine based on the wind direction measured by a vane atop the nacelle. If the wind direction is measured to be greater than 20 degrees off the rotor axis for 30 *consecutive* seconds, the yaw drive is activated to yaw the machine toward the wind for a specified period of time. A consequence of this simple, "bang-bang" type control system is that the turbine is often oriented at 20 or more degrees of yaw error for extended periods of time. This misorientation not only leads to decreased energy capture, but also significant 1P aerodynamic loading due to the advancing-retreating blade cycle experienced under these conditions. Figure 1 is a plot of blade root flap moment data for the Micon 65 turbine demonstrating predominant 1P (1.25 Hz) cycles. The yaw error over the interval shown ranged from 25 to 65 degrees.

The consequence of this repetitive 1P cycle on blade fatigue loads is evident in the rainflow counted cycles over a 10 minute interval. Figure 2 displays a comparison between 2 ten minute data sets, both with an average hub-height wind speed of approximately 11.5 m/s, one with an average yaw error of only 2.54 degrees, the other 23.9 degrees. The difference is manifested in what Kelley (1994) has termed the low-cycle, high-amplitude (LCHA) range. These large, but relatively rarely occurring loads have been suspected of causing the majority of fatigue damage to composite rotor blades. As can be seen in Figure 2, larger average yaw error yields a greater frequency of LCHA cycles.

Increased LCHA loads due to operation at yaw error was reported by Laino and Kelley (1994) in a study of the Micon 65. Figure 3, adopted from their report, shows how improved agreement to rainflow cycle data was achieved for a model of the Aerostar bladed turbine. Both the overall shape and the cycle counts in the LCHA region agree better with test data when yaw error is accounted for in the model. Conditions over the ten minute data set used for Figure 3 are 15 m/s average wind speed, 21.74 degrees average yaw error.

From the evidence relating yaw error to increased cyclic flap loads, we would expect the fatigue life of a turbine operating extensively at large yaw errors to be lower than if oriented closer to the wind direction. To investigate this hypothesis, we used the LIFE2 program to perform fatigue life estimates for different operating conditions.

Results

Using LIFE2, a lifetime estimate for the Micon 65 blade root was calculated for large and small average

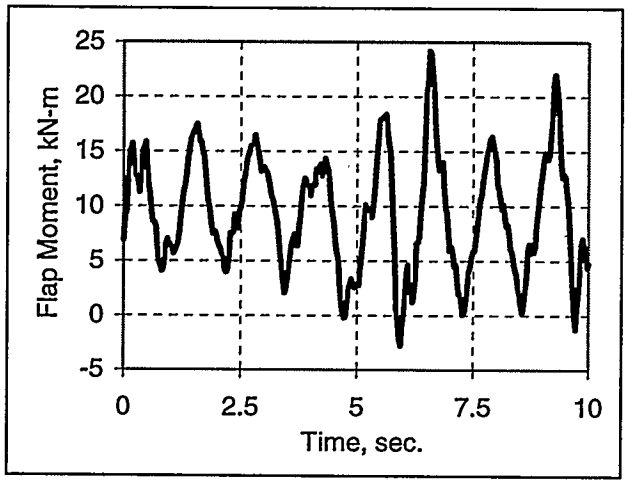

FIGURE 1: MICON 65 BLADE ROOT FLAP MOMENT DATA.

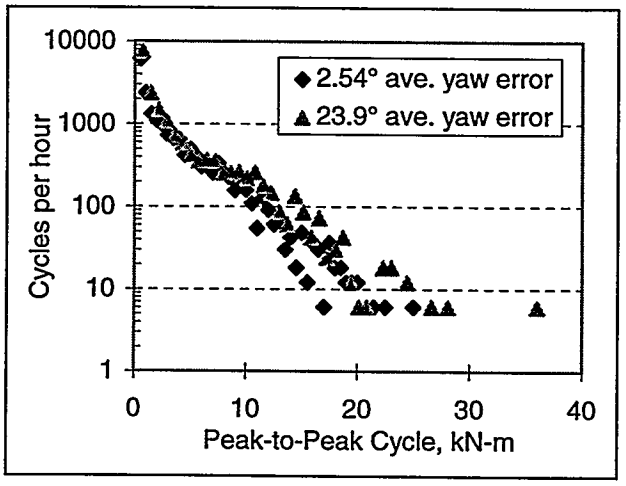

FIGURE 2: MICON 65 RAINFLOW COUNTED FLAP MOMENT CYCLES.

yaw errors. Three data sets are used to represent three wind speed intervals for both calculations. Data sets were chosen based upon similarity in average wind speed and differences in average yaw error. A summary of these statistics and results of the LIFE2 analyses is listed in Table 1.

The results show that operation at smaller yaw error leads to an estimated three-fold increase in fatigue life over operation at larger yaw errors. Notice that 2 of the 3 data sets representing small yaw error operation have yaw errors near 11.5 degrees. We expect that if this yaw error were further reduced, the increase in fatigue life would be even greater. The fact that few data sets exist with truly "small" yaw errors testifies to the yaw controller's inability to keep the turbine aligned with the wind.

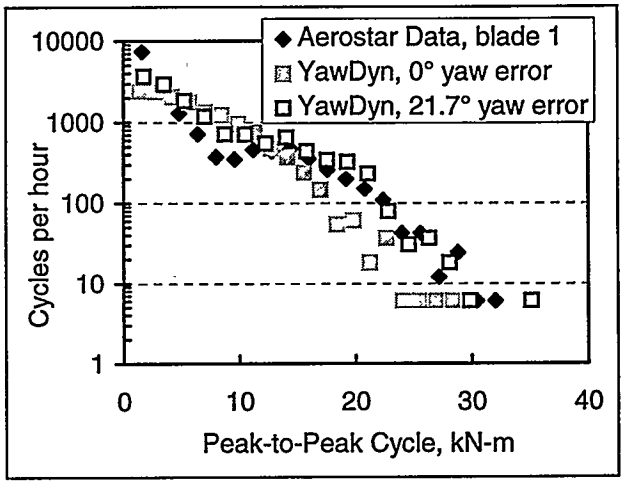

FIGURE 3: RAINFLOW COUNTED FLAP MOMENT CYCLES, FROM LAINO AND KELLEY (1994).

The results shown in this simple study of only six ten minute data sets is far from definitive. The factor of 3 on fatigue life can be attributed to differences in yaw error, but there are also significant differences in mean wind speed, and the turbulence characteristics. To truly reduce these other factors, a larger sample of data would be necessary, but, as mentioned, a large sample of data with limited yaw error does not exist. In the stead of such data, we modeled the behavior of the Micon 65 using YawDyn with simulated turbulence.

YawDyn Analysis

One of the benefits of a computer simulation is the control available over otherwise uncontrollable parameters such as wind. In this study several simulations were run varying only the average yaw error, and thus isolating that parameter. This gives greater confidence that relative differences in the output are indeed due to the yaw error.

For this study 10 minutes of wind was generated using SNLWind-3D (Kelley, 1993) at average wind speeds of 7.6, 11.5, and 14.5 m/s. The results from the YawDyn analyses were then processed in identical fashion to the test data using Dyn2LIFE. The first analysis attempted to reproduce the results of the large yaw error case of Table 1. The result from LIFE2 of only 3.3 years does not compare well with the

TABLE 1 - STATISTICS OF DATA SETS USED FOR YAW ERROR ANALYSIS IN LIFE2 WITH CORRESPONDING RESULTS.

	Wind Speed Interval	Mean Hub-Height Wind Speed m/s	Mean Yaw Error deg.	LIFE2 Estimate yrs.
Large Yaw Error	5 - 9 m/s	7.69	13.84	11
	9 - 13.5 m/s	11.43	23.91	
	13.5 18 m/s	15.09	21.07	
Small Yaw Error	5 - 9 m/s	8.69	11.47	35
	9 - 13.5 m/s	11.50	2.54	
	13.5 18 m/s	14.51	11.86	

result in Table 1, and could probably be improved through more detailed modeling and better matching of turbulence characteristics. For this sensitivity study, however, this result is adequate and will be used to normalize subsequent results.

Table 2 lists the statistics and normalized LIFE2 results for the model in similar fashion to Table 1. In all, four analyses were conducted that clearly show improved fatigue life with decreased average yaw error. While the results show the difference in fatigue life between large and small yaw error is not as great as the factor of 3 determined above, they do agree with the trend of increased yaw error leading to increased fatigue damage.

POWER CONTROL

For investigation of power control using flaps, a two bladed teetering rotor wind turbine model is used. The turbine modeled has a diameter of 26.2 m with a rated power of 275 kW. It is a down wind, stall regulated, passive yaw machine with a hub height of 26 m. Flaps were incorporated on the outer 30% of the span. Flap deflections between 0° and -90° were allowed. The model is implemented in ADAMS coupled with AeroDyn. Three controls systems were implemented to investigate the effect on fatigue lifetime.

The first control scheme is designed to limit maximum power output from the turbine. The controller used for this system is an integrator with additional poles for phase modification at the 2P frequency seen in the output power of the rotor. The -90° phase of a pure integrator amplified the 2P power response of the rotor. An integrator anti-windup was also incorporated into the model to limit control effort when the aileron was at maximum deflection. The desired power for this controller was held constant at 250 kW.

The second controller is designed to reduce the cyclic component of power over the entire range of operation, as well as the maximum output. The integrator described above was used in an IPD configuration with the measured power output fed back with proportional and derivative terms. The power output was estimated from hub height wind speed using a lookup table on a calculated power curve for the rotor. This was then passed through a recursive IIR low pass filter for use as the desired power.

TABLE 2 - STATISTICS OF YAWDYN MODEL DATA SETS USED FOR YAW ERROR ANALYSIS IN LIFE2 WITH CORRESPONDING RESULTS.

	Wind Speed Interval	Mean Hub-Height Wind Speed m/s	Mean Yaw Error deg.	Normalized LIFE2 Estimate
Large Yaw Error	5 - 9 m/s	7.6	13.84	1
	9 - 13.5 m/s	11.5	23.91	
	13.5 18 m/s	14.5	21.07	
Small Yaw Error	5 - 9 m/s	7.6	11.47	1.8
	9 - 13.5 m/s	11.5	2.54	
	13.5 18 m/s	14.5	11.86	
5 degree Yaw Error	5 - 9 m/s	7.6	5	5.7
	9 - 13.5 m/s	11.5	5	
	13.5 18 m/s	14.5	5	
0 degree Yaw Error	5 - 9 m/s	7.6	0	14.6
	9 - 13.5 m/s	11.5	0	
	13.5 18 m/s	14.5	0	

The third control scheme is designed to limit power output from the turbine based on an estimate of the mean power output. In the control systems given above the large 2P cyclic content of the power feeds into the control system. However, it requires considerable control effort to reduce the cyclic component of power, and it may be desirable to limit only the mean power output. For a good estimate of the mean without time delays a digital RLS adaptive filter was used. The RLS filter was implemented in an IIR form, and estimates mean power from hub height wind speed, flap deflection, and the previous estimate of mean power. A section of the mean estimate is shown in Figure 4. The controller used for this system is a proportional plus integral implemented in a digital form with a sampling frequency of 63 Hz. The integral portion of the controller is as given above, transformed to digital form. The desired power for this controller was held constant at 250 kW.

Ten minute simulations were performed at mean wind speeds of 7, 11, 15, and 18 m/s using IEC (International Electrotechnical Commission, 1994) Kaimal turbulence generated from SNLWind-3D. These simulations are used to represent four wind speed intervals in LIFE2. We assumed the turbine operated between wind speeds of 4.5 and 22 m/s at a site with a 7 m/s mean, Rayleigh distributed wind speed. A stress concentration factor of 4 was applied in the fatigue analysis of the blade root.

Results

Using LIFE2 a lifetime estimate was calculated for the blade root for each of the controlled cases and the non-controlled case. Fatigue damage estimates from LIFE2 for each wind speed range are shown in Figure 5. All controllers reduced the fatigue damage, as can be seen in the figure. The expected lifetime for the blade root without control was 26 years. The system for limiting the mean power output produced an expected lifetime of 37 years, reducing damage at the upper wind speeds. The power limiting controller again reduced fatigue damage at primarily the upper wind speeds, producing an expected lifetime of 46 years. The IPD controller reduced damage over the entire range, at the expense of increased flap deflection activity, producing an expected lifetime of 92 years. The IPD controller had the most significant increase in lifetime since it was able to reduce fatigue damage in the 11 m/s range where most of the damage occurred. For design, the increase in lifetime obtained from the different control methods should be weighed against the amount of control effort required. As an indication of control effort for each case, 10 seconds of flap deflection is shown in Figure 6.

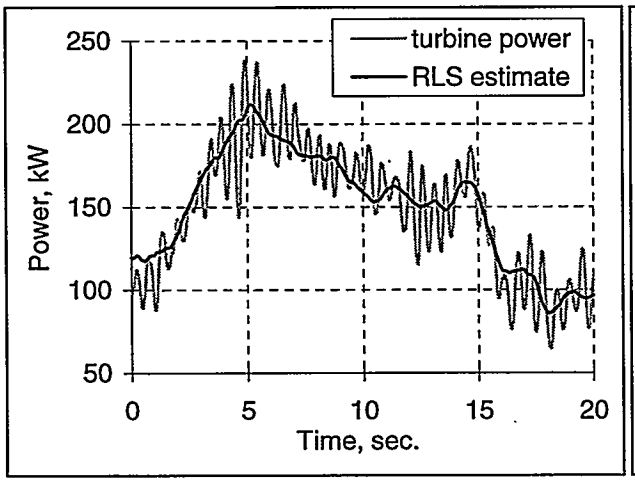

FIGURE 4: RLS ESTIMATE OF MEAN POWER OUTPUT.

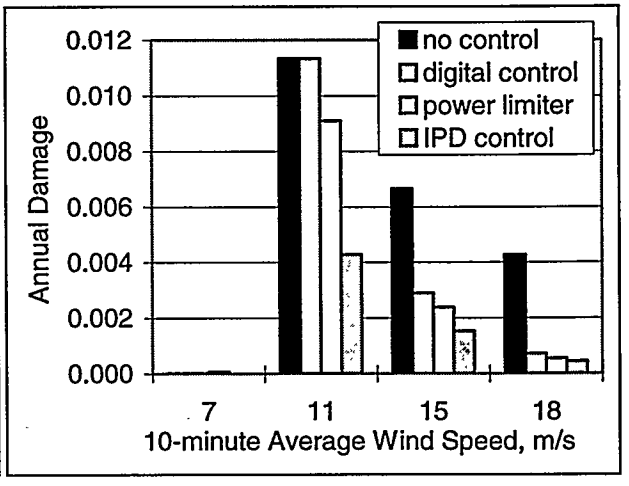

FIGURE 5: FATIGUE DAMAGE FOR EACH WIND SPEED INTERVAL.

Since the same wind was used in all of the cases, the increase in fatigue lifetime obtained from the use of control is considered significant. While the results may change somewhat when using different turbulence the same trends are to be expected. The long runtimes required for the simulations prohibit the use of a large sample of data that would smooth out the variations due to turbulence.

The primary purpose of the flap deflections was to control the power output of the rotor; reduction of blade root fatigue damage was a secondary effect. Further improvements in fatigue life may be achieved by the active control of blade root moments. However, this study illustrates the use of the codes to determine how control choices affect fatigue damage.

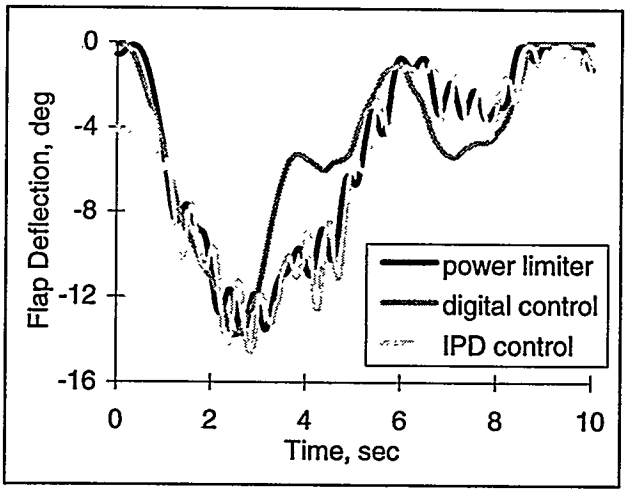

FIGURE 6: FLAP DEFLECTION COMPARISON

CONCLUSIONS

Investigation of the Micon 65 test data suggests the 1P loading due to operation at yaw error is a significant source of fatigue damage to blade roots. Results from the simple analysis performed here imply that even a one half reduction of average yaw - from 20 to 10 degrees - could impact fatigue damage by as much as a factor of 2 to 3. Perhaps a slightly more complex yaw controller - for example, one that responds to the 30-second *average* yaw error rather than 30 consecutive seconds - would reduce the amount of time the turbine spends operating at the 20 degree limit of the yaw controller.

The YawDyn analysis of the Micon 65 served to verify the results of the data analysis regarding the effect of yaw error on fatigue life. If a yaw controller could be made to be "perfect" these results suggest over an order of magnitude improvement in fatigue life of the blade root. This result would need to be weighed against other factors such as the feasibility of such a controller, and the increased number of gyroscopic loads on a rotor undergoing more numerous yaw motions. The study by Laino and Hansen (1996) suggests these gyroscopic loads are a significant source of fatigue damage cycles themselves.

Investigation of flap control of a teetering rotor has shown that choice of control schemes affects the fatigue damage experienced by the blade root. Increased fatigue life may be obtained by the increased use of control, although there is a tradeoff between fatigue reduction and control activity. The control systems modeled here were not specifically designed to reduce blade root fatigue cycles, but were seen to have an effect on the fatigue of the blades nonetheless. The studies performed here illustrate how dynamic simulation and fatigue life estimate codes may be used to determine the way control systems affect fatigue life of wind turbines.

REFERENCES

DeSmet, B.J. and P.W. Bach, 1994, "DATABASE FACT: FAtigue of Composites for wind Turbines," ECN-C--94-045, ECN, Petten, the Netherlands.

Hansen, A.C., 1996, *Users Guide to the Wind Turbine Dynamics Computer Programs YawDyn and AeroDyn for ADAMS®*, Mechanical Engineering Department, University of Utah, Salt Lake City, UT.

International Electrotechnical Commission, 1994, *International Standard: Wind Turbine Generator Systems Part I: Safety Requirements*, IEC 1400-1, First Edition, 1994-12.

Kelley, N.D., 1993, "Full-Vector (3-D) Inflow Simulations in Natural and Wind Farm Environments Using an Expanded Version of the SNLWind (Veers) Turbulence Code," Twelfth ASME Wind Energy Symposium, Houston, TX.

Kelley, N.D., 1994, "The Identification of Inflow Fluid Dynamics Parameters that can be Used to Scale Fatigue Loading Spectra of Wind Turbine Structural Components," *Wind Energy 1994*, Musial, Hock and Berg (eds), SED-Vol. 15, ASME.

Laino, D.J. and A.C. Hansen, 1996, "A Wind Turbine Fatigue Analysis Interface for YawDyn and ADAMS®," *Wind Energy '96*, ASME.

Laino, D.J. and N.D. Kelley, 1994, "YawDyn, Simulated Turbulence, and the Micon 65 Turbine," NREL internal report, Golden CO.

Miner, M.A., 1945, "Cumulative Damage in Fatigue," *Journal of Applied Mechanics*, ASME.

Paoli, P., Botta, G., Falchetta, M. and S. Avolio, 1994, "GAMMA 60 Operational Experiences and Perspectives," *Proceedings of Windpower '94*, AWEA, Washington, DC.

Schluter, L.L., and H.J. Sutherland, 1989, *Reference Manual for the LIFE2 Computer Code*, SAND89-1396, Sandia National Laboratories, Albuquerque, NM.

Spera, D.A. (ed), 1994, *Wind Turbine Technology*, pp. 27 - 29, ASME Press, New York, NY.

Sutherland, H.J. and N.D. Kelley, 1995, "Fatigue Damage Estimate Comparisons For Northern European and U.S. Wind Farm Loading Environments," *Proceedings of Windpower '95*, AWEA, Washington, DC.

Tangler, J., Smith, B., Jager, D. and T. Olsen, 1990, "Atmospheric Performance of the Special Purpose SERI Thin-Airfoil Family: Final Results," SERI/TP-257-3939, Solar Energy Research Institute, Golden, CO.

CONSIDERATIONS FOR AN INTEGRATED WIND TURBINE CONTROLS CAPABILITY AT THE NATIONAL WIND TECHNOLOGY CENTER: AN AILERON CONTROL CASE STUDY FOR POWER REGULATION AND LOAD MITIGATION

Janet G. Stuart, Alan D. Wright, Charles P. Butterfield
National Renewable Energy Laboratory

ABSTRACT

Several structural dynamics codes have been developed at, and under contract to, the National Wind Technology Center (NWTC). These design codes capture knowledge and expertise that has accumulated over the years through federally funded research and wind industry operational experience. The codes can generate vital information required to successfully implement wind turbine active control. However, system information derived from the design codes does not necessarily produce a system description that is consistent with the one assumed by standard control design and analysis tools (e.g., MATLAB® and Matrix-X®). This paper presents a system identification-based method for extracting and utilizing high-fidelity dynamics information, derived from an existing wind turbine structural dynamics code (FAST), for use in active control design. A simple proportional-integral (PI) aileron control case study is then used to successfully demonstrate the method, and to investigate controller performance for gust and turbulence wind input conditions. Aileron control results show success in both power regulation and load mitigation.

INTRODUCTION

Virtually all economic analyses of wind energy point out the make-or-break necessity of the wind industry to reduce its *cost of energy* (COE) in order to compete with other energy options, and to ultimately survive in existing and foreseeable market environments. To make wind energy more cost-competitive, the federal wind program and the wind industry are pursuing critical wind turbine design objectives that enhance fatigue resistance, increase expected lifetimes and decrease costs. One way to achieve these design objectives is to mitigate the damaging loads and responses. Load mitigation can be accomplished through various means, one of which is the use of active control strategies. A few examples of load-mitigating active control strategies are aerodynamic device control, flexible wind turbine dynamics and control, and variable load control using power electronics (variable-speed turbines). These examples demonstrate the wide range of active control options for load mitigation, and imply that the use and selection of a particular active control strategy is highly dependent on wind turbine configuration.

Active control strategies for increasing wind turbine performance (and consequently decreasing the COE) have been proposed, some of which are currently in use. Active control of a dynamic system, however, complicates the system and sometimes destabilizes an otherwise stable, open-loop (i.e. uncontrolled) system. A logical and completely valid question is: why bother implementing active control in the first place? To make a case for continued research in active wind turbine control, one must look at the current performance of existing wind turbines, in terms of cost and design, and offer active control strategies that have a reasonable probability of impacting COE performance to a degree that is worth the effort.

One option for COE reduction is to mitigate the effects of damaging loads, and/or undesirable wind turbine responses, using active control of aerodynamic devices. The resulting control objectives include, but are not limited to, reducing excessive root-flap bending moments and regulating power output to minimize power spikes. It is assumed that minimizing excursions in power consequently reduces the loads caused by power spiking. Therefore, the general motivation for the research presented in this paper is COE reduction via load mitigation through the use of aerodynamic device control strategies.

The development of an integrated controls capability at the NWTC is a potential, long-term research objective currently under evaluation. Toward this end, control system engineers studying the wind turbine problem immediately identify the need for a reasonable dynamic model for use in control design. The body of knowledge existing within the NWTC, in terms of wind turbine structural dynamics design codes, provides valid, detailed dynamics information that can be used for control system dynamic model generation. Correspondingly, these codes must be updated to include control capability for evaluation of control's impact on performance. Therefore, the specific motivation for the research presented in this paper is to demonstrate the use of an existing NWTC structural dynamics design code, namely FAST, together with standard control system design tools, to design a simple aileron controller.

An aileron control case study is used to demonstrate the process of bridging the gap between control system design and analysis software and existing structural dynamics codes, which is the primary objective. In addition, the paper discusses the development of an aileron control strategy for power regulation and load mitigation for a two-bladed, downwind, fixed-speed wind turbine. A FAST model of this turbine is used in conjunction with system identification techniques to characterize aileron power regulation effectiveness for mean wind speeds ranging from 8 to 20 meters/second.

Note that the intention here is *not* to design an "optimal" aileron controller, or even an advanced aileron controller. One can refer to Hinrichsen (1984) and Barton et al. (1979) for PI controllers with additional lead-lag and notch filters for maintaining a constant amount of produced energy and reducing loads, and to Bossanyi (1987, 1989) for an adaptive control scheme that takes into account that the gain from pitch angle to electrical power varies with wind velocity. In this paper, a very simple PI aileron controller is designed to regulate output power. The selected control design objective is to reduce the response time of an aileron-controlled wind turbine when subjected to step changes (i.e. gusts) in wind speed. A single controller design is selected for use over a range of wind speeds and wind input conditions.

DESCRIPTION OF THE FAST CODE AND THE WIND TURBINE EXAMPLE

Code Description. The wind turbine structural dynamics code, FAST (Fatigue, Aerodynamics, Structures, and Turbulence), which was developed at Oregon State University under subcontract to the National Renewable Energy Laboratory (NREL), uses equations of motion based on Kane dynamics (Wilson, 1995). Kane's method is used to set up equations of motion that can be solved by numerical integration. This method greatly simplifies the equations of motion by directly using the generalized coordinates and eliminating the need for separate constraint equations. These equations are easier to solve than those developed using methods of Newton or Lagrange and have fewer terms, thus reducing computation time. For more information on FAST code theory and formulation, see Harman (1995).

Aerodynamic forces are determined using blade element momentum theory. Lift and drag forces on the blades are determined by table look-up of the blade's lift and drag coefficients Cl and Cd. At NREL, there are two versions of FAST in use: a version with the original Oregon State University aerodynamic subroutines and a version with the University of Utah AeroDyn subroutines. The goal was to have the University of Utah develop a stand-alone aerodynamic subroutine package for inclusion into any wind turbine structural dynamics code (Hansen, 1995). This package includes the effects of dynamic stall, dynamic inflow, table look-up of Cl and Cd data, and input of 3-D turbulence (Hansen, 1995). The AeroDyn subroutines have been successfully incorporated into FAST2 and this version was used to generate the results presented in this paper.

In this first-order modeling effort, the effects of the deflected aileron on the blade's overall lift and drag properties, as a function of the degree of aileron deflection, are modeled. Changes in section mass and elastic properties, caused by a shift in the center of gravity of the blade section with the deflected aileron, are not modeled. The objective of this study is to include first order effects only, and then simulate the effects of the ailerons on the overall wind turbine behavior. To simulate this effect, it is necessary to include the modifications of the section lift and drag characteristics into the section airfoil tables at those blade spans employing ailerons. In the airfoil data tables used by the AeroDyn subroutines, multiple columns of Cl and Cd data are inserted corresponding to different discrete aileron angles (or deflections). For any given or prescribed aileron angle, the code interpolates between these columns of Cl and Cd data. These interpolated values of Cl and Cd will then be returned to the main aerodynamics subroutine for calculation of that section's final aerodynamic forces.

To include the PI aileron controller in FAST, one inputs the gains for this control law into the input data-set for the AeroDyn subroutines. The transfer function corresponding to this control law is transformed within this subroutine to a linear differential equation and the states of the controller are integrated along with the rest of the degrees of freedom contained in FAST. In this case, we are regulating power using ailerons, so the input to the aileron control transfer function is the error between the actual power and desired power. The output of the controller (or transfer function) is aileron angle. The calculated aileron angle is then passed to the aerodynamic subroutines, whence the section's lift and drag properties are determined via interpolation as described above.

Turbine Description. A two-bladed, teetering hub, free-yaw, downwind machine was simulated for this study. The 12.1-m (39.7-ft) fixed-pitch blades have a 5.5° pre-twist with a maximum chord of 1.2 m (3.8 ft). They use the NREL thick airfoil family (S809, S810, and S815)[1] designed for 12-m (40-ft) blades. The rotor diameter is 26.2 m (86 ft) with a 7° pre-cone. It sits on top of a free-standing truss tower, with a hub height of 24.4 m (80 ft). The turbine rotates at 57.5 revolutions per minute (RPM) (0.958 Hz) and generates 275 kW of power at rated wind speed (18 m/s, 40 mph). The ailerons are assumed to be attached to the outer 30% of the blade span. Unfortunately, there is no accurate wind tunnel airfoil data for the S810, or any other S8 series airfoil, tested with ailerons. Therefore, airfoil data for other airfoils fitted with ailerons was examined and the general trends of Cl and Cd data for different aileron deflections were followed. The accuracy of the results is obviously affected by this extrapolation. However, it is assumed that the general trends and conclusions that are reached will not be greatly affected by this approximation.

[1] S809, S810, and S815 are trademarks of the National Renewable Energy Laboratory.

OVERVIEW OF AILERON CONTROL STRATEGY AND MODEL REQUIREMENTS

Aileron control is used to regulate power output according to the block diagram shown in Figure 1. The control block, **C**, defines the aileron controller in terms of its transfer function description. The plant model, **P**, characterizes the wind turbine system's output power response to changes in commanded input aileron angle for a given wind speed and corresponding reference power, **Pref.**

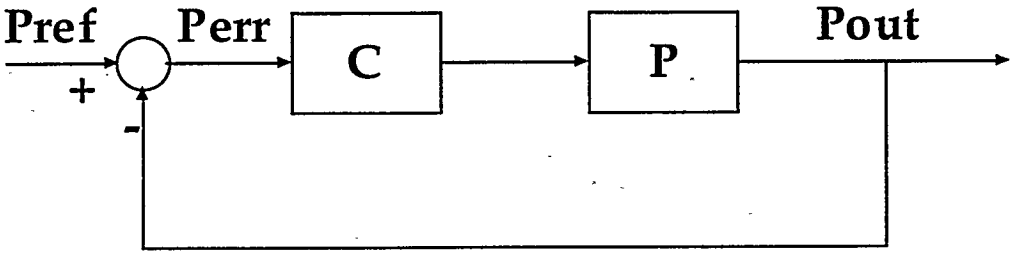

FIGURE 1. AILERON CONTROL BLOCK DIAGRAM FOR POWER REGULATION

The equations describing the conversion of wind energy to electrical energy are non-linear and complex, in that they involve interactions between system elements. Most of the wind turbine active control work, to date, is based on linear control theory. Thus, a linearization about an operating point is required. Operating points, in this case, correspond to various wind speed inputs, and associated turbine power outputs.

Reference power, plant dynamics and possibly controller design, in the case of adaptive control, change as a function of wind speed. Reference power, **Pref**, as a function of wind speed, can be obtained from turbine design specification and/or performance verification. Controller characterization, in **C**, is specified by the control design engineer, and is therefore known. The linearized description of the plant, **P**, as a function of wind speed, however, is more difficult to define. As discussed by Bongers and van Baars (1994), the linear model can be derived in two different ways:

- Given the non-linear model of the wind turbine system, a linearization is performed in one operating condition, resulting in a linear model.
- Using data, measured at a wind turbine, system identification techniques can be applied to obtain a linear description.

For the purposes of integrating active wind turbine control capability into an existing NWTC dynamics code, the system identification option permits the quick generation of a plant model using input and output data generated by the code. Linearization of the code about an operating point is a workable option. However, the magnitude of the work associated with this option, based on the structure of the existing codes and the modifications required to yield the linearization, is significantly greater than the system identification option. (The linearization option is currently being pursued in related research at the NWTC).

The selection of system identification for this problem necessitates the use of modeling tools, in this case, MATLAB® and its system identification toolbox. The theoretical basis for system identification is thoroughly developed by Ljung (1987), and the application of the technique, using the MATLAB® system identification tool box, is also developed by Ljung (1995). MATLAB® control design tools are based on standard definitions, derived from basic principles, and, therefore, require standard inputs. In contrast, wind turbine structural dynamics models have evolved to efficiently handle the complex, non-linear problem, specific to wind turbine dynamics. Extracting the standard inputs required for control system design from the existing codes is greatly simplified by using the system identification capability available in MATLAB® in conjunction with input and output data generated using the FAST code. This method was used to generate linear plant models corresponding to linearizations about four operating points. The operating points selected correspond to wind speeds of 8 m/s, 12 m/s, 16 m/s and 20 m/s.

The plant model description for each operating point was based on input data corresponding to a sine-sweep of aileron input angle, and output data corresponding to the resulting change in power output. The dynamic models produced by system identification analyses of the input-output data were fourth-order for all of the operating points. The plant behavior does indeed vary as a function of wind speed, as seen by the comparison of the open-loop system eigenvalues for the four wind speed cases, shown in Table 1. The open-loop systems are quite stable, as characterized by the eigenvalue with the smallest, negative real value. In the next section, PI control gains are selected to move the negative real values of the closed-loop system further to the left, resulting in a faster system response.

TABLE 1. OPEN-LOOP SYSTEM EIGENVALUE COMPARISON

Wind Speed = 8 m/s		
Eigenvalue	Damping	Freq. (rad/sec)
-4.8894 ± 51.8535i	0.0939	52.0835
-7.4623 ± 18.0724i	0.3817	19.5525
12 m/s		
Eigenvalue	Damping	Freq. (rad/sec)
-4.7123 ± 19.6746i	0.2329	20.2311
-7.0414 ± 60.4978i	0.1156	60.9062
16 m/s		
Eigenvalue	Damping	Freq. (rad/sec)
-5.2675 ± 18.6609i	0.2717	19.3901
-6.9171 ± 61.8496i	0.1111	62.2352
20 m/s		
Eigenvalue	Damping	Freq. (rad/sec)
-1.5580 ± 13.6879i	0.1131	13.7763
-5.1719 ± 54.5658i	0.0944	54.8103

Design. As mentioned previously, this case study focuses on the design of an aileron controller for power regulation. A simple PI controller is designed and the associated gains are selected to meet the control objective of minimizing the aileron-controlled wind turbine's response time when subjected to a step input. The performance of an *initial* aileron controller was the motivation for the design of this simple controller and for the selection of the control objective when simulations of the initial controller showed that it was taking several seconds for the ailerons to respond to gust inputs. The performance of the initial and new controllers are compared in the next section.

Typically, control system performance is characterized by the closed-loop system response to a given input. Impulse and step responses are commonly used to evaluate controller performance. The step input is also a reasonable approximation of a gust input, and was, therefore, selected for the evaluation of PI controller designs. A step/gust wind input profile for use in FAST was created to emulate the standard step input so that MATLAB® and FAST output could be compared. For this FAST input file, a 4 m/s step increase in wind speed occurred over a 0.25 second time period about the mean wind speeds for the four wind input cases.

Controller gains were varied to produce a closed-loop system response that meets the stated objective for the various wind speed operating points. The controller design selected for this case study is specified by the transfer function,

$$\mathbf{C} = \frac{0.1\,s + 10}{s}$$

and the resulting closed-loop systems for the wind speeds of 8, 12, 16, and 20 meters/second are characterized by the eigenvalues shown in Table 2. (Compare with $\mathbf{C} = [0.2s^2+0.5s+2]/[s^2+3s]$ for the *initial* aileron controller). Note that the closed-loop system's stability and response are enhanced through the selection of PI control gains. The smallest negative real values of the closed-loop system (see Table 2.) are further to the left of those for the open-loop system (see Table 1.), resulting in a faster system response.

Simulation. Control design using system identification-based dynamic models was done "off-line" in the MATLAB® environment. The resulting controller design was then put in its transfer function form and integrated into the FAST code as discussed previously. FAST simulations of the controller were used to validate the system identification-based model, and to evaluate performance for the step/gust inputs at the four wind speeds, and for a gust input based on the IEC '88 gust model (IEC, 1994). Simulations of the uncontrolled system's response to these inputs were also conducted for comparison. Simulation output for selected gust input cases are shown in Figures 2, 3, and 4. These figures show power and root flap bending moment as a function of time for controlled and uncontrolled cases. Figure 2 shows power output for both the initial and new aileron controllers for a step/gust input, whereas Figures 3 and 4 show only the new aileron controller's performance when subjected to the IEC '88 gust input. Note that the set-point power for a step gust about a mean wind speed of 8 m/s, as shown in Figure 2, is 58.01 kW for this turbine example. The set-point power for the IEC '88 gust is 241.51 kW, as shown in Figure 3.

Simulations for rough and smooth turbulence inputs, at wind speeds of 14 m/s and 18 m/s, were performed for the controlled and uncontrolled systems. The output for selected turbulence input cases are shown in Figures 5 and 6. Again, these figures show power and root flap bending moment as a function of time for controlled and uncontrolled cases. The simulation results are discussed in greater detail in the next section.

TABLE 2. CLOSED-LOOP SYSTEM EIGENVALUE COMPARISON

Wind Speed = 8 m/s		
Eigenvalue	Damping	Freq. (rad/sec)
-6.3196	1.0000	6.3196
-7.0448 ± 33.5172i	0.2057	34.2495
-7.5454 ± 53.4511i	0.1398	53.9811
12 m/s		
Eigenvalue	Damping	Freq. (rad/sec)
-5.9778 ± 61.0319i	0.0975	61.3240
-6.0129 ± 30.0832i	0.1960	30.6782
-8.4841	1.0000	8.4841
16 m/s		
Eigenvalue	Damping	Freq. (rad/sec)
-5.2644 ± 29.5953i	0.1751	30.0598
-5.9033 ± 62.7378i	0.0937	63.0149
-7.5853	1.0000	7.5853
20 m/s		
Eigenvalue	Damping	Freq. (rad/sec)
-2.0861	1.0000	2.0861
-3.0453 ± 25.1213i	0.1203	25.3052
-4.8039 ± 54.5519i	0.0877	54.7630

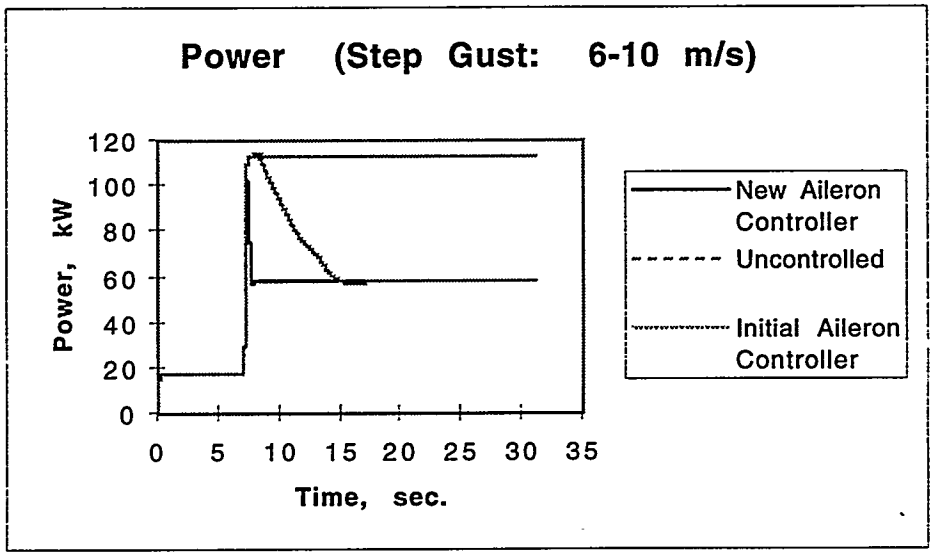

FIGURE 2. SIMULATION OUTPUT FOR STEP INPUT (CONTROLLED AND UNCONTROLLED CASES)

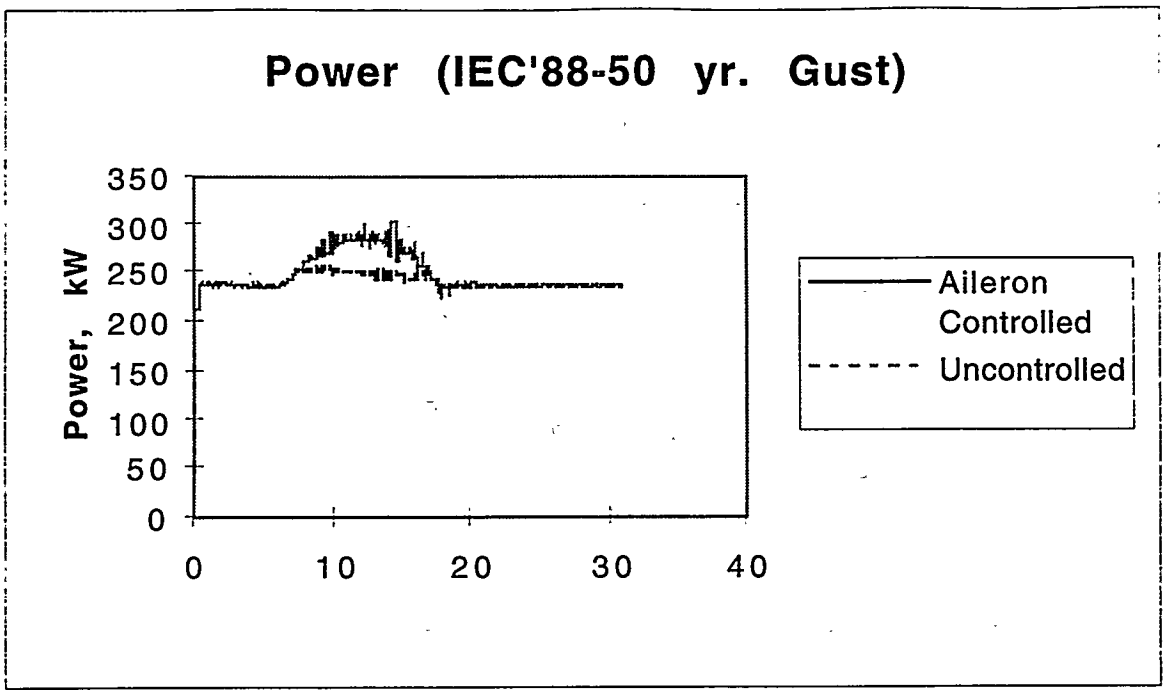

FIGURE 3. SIMULATION OUTPUT FOR IEC '88 GUST INPUT
(CONTROLLED AND UNCONTROLLED CASES)

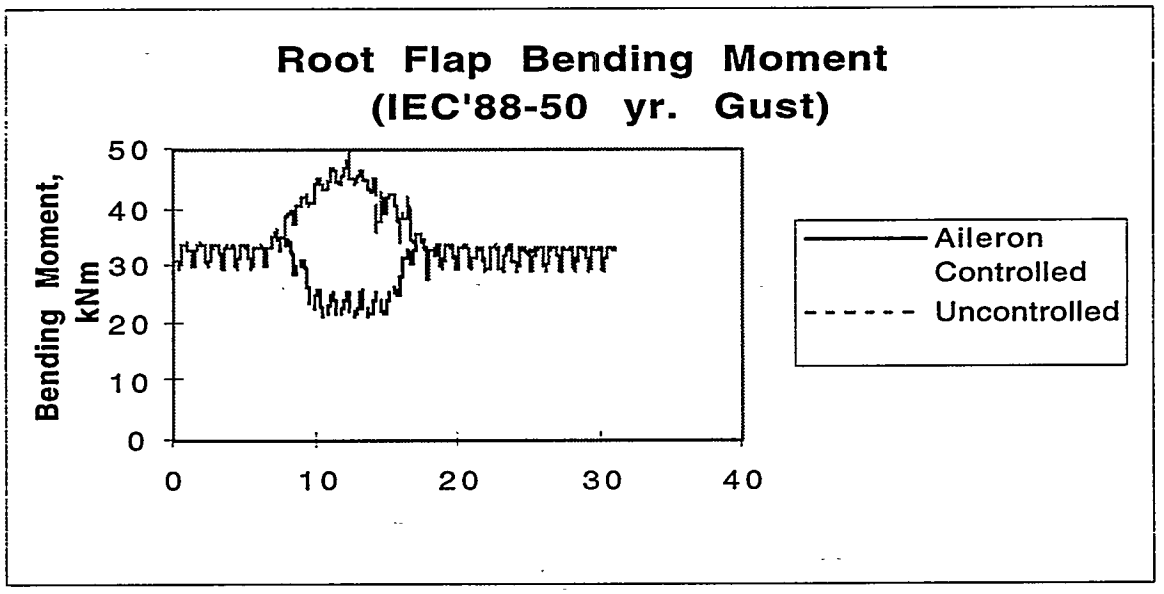

FIGURE 4. SIMULATION OUTPUT FOR IEC '88 GUST INPUT
(CONTROLLED AND UNCONTROLLED CASES)

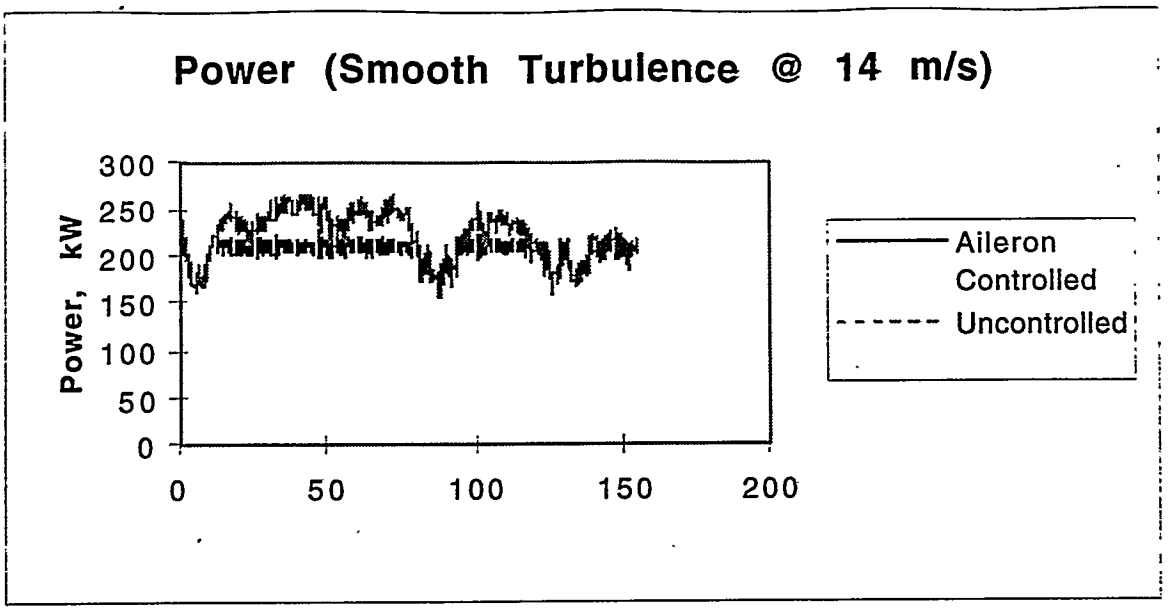

FIGURE 5. SIMULATION OUTPUT FOR TURBULENCE INPUT @ 14 m/s (CONTROLLED AND UNCONTROLLED CASES)

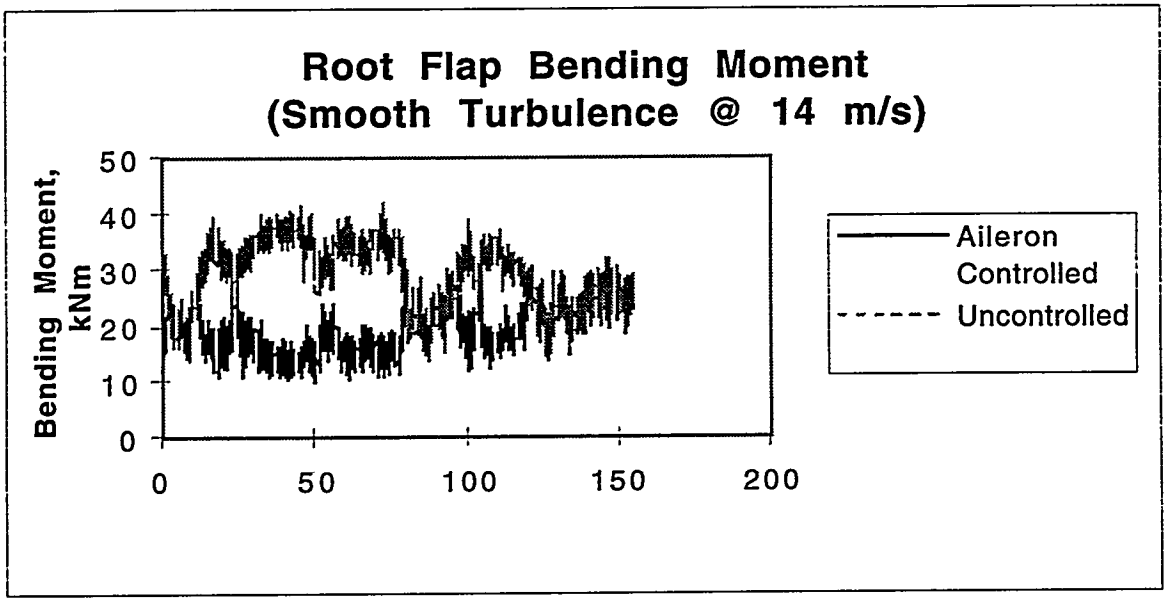

FIGURE 6. SIMULATION OUTPUT FOR SMOOTH TURBULENCE INPUT @ 14 m/s (CONTROLLED AND UNCONTROLLED CASES)

SUMMARY OF SIMULATION RESULTS

A comparison of the performance of the initial and new aileron controllers, as seen in Figure 2., shows that the new controller reduces the response time to a step-gust input by several seconds, thus achieving the selected control objective. This response to the step-gust input validates the aileron controller from a controls perspective. Aileron controller performance, when subjected to the IEC '88 50-year gust, is shown in Figures 3 (power) and 4 (loads).

Power regulation at 250 kW is quite good, especially when compared to the uncontrolled case. The root flap bending moment is also reduced through aileron control. The IEC '88 gust case, therefore, validates the aileron controller from more of a wind industry perspective. The performance of the same aileron controller, when subjected to a smooth turbulence wind input at 14 m/s, is shown in Figures 5 (power) and 6 (loads). Power regulation at the reference power for this wind speed is excellent, and once again, loads are reduced when compared to the uncontrolled case. Note that smooth and rough turbulence at wind speeds of 14 and 18 m/s were also simulated, with similar results, but are not presented here.

CONCLUSIONS AND RECOMMENDATIONS FOR FUTURE RESEARCH

The control objectives for this research were met, namely that the design code, FAST, was successfully used for control system design and analysis using standard control system design tools, and correspondingly, that simple P-I aileron control was successfully implemented in the FAST code. The primary control performance objective was met, i.e. that a new aileron controller was designed to reduce the response time for a step-gust wind input. This simple controller then yielded reasonable performance for a range of wind speeds and input conditions.

The research presented here also served to scope the problems associated with defining a linear system description for use in control system design, and it led to the use of the system identification technique as a viable option worthy of more detailed, future investigation. Background research in aileron control identified the need for the inclusion of actuator dynamics and associated bandwidth limitations in future research. Also, the exciting possibilities of other aerodynamic device control strategies, such as full-span pitch control, both differential and collective, were clearly identified as high-payoff control opportunities. And finally, the utilization of control schemes more sophisticated than PI, and perhaps more appropriate for the challenging wind problem, is another promising control opportunity being evaluated at the NWTC.

REFERENCES

Barton, R.S., Bowler, C.E.J, Piwko, R.J., (1979), Control and Stabilization of the NASA/DOE MOD-1 Two Megawatt Wind Turbine Generator, *Amer. Chemical Society*, pp. 325-330.

Bongers, P.M.M. and van Baars, G. (1994), Control of Wind Turbine Systems to Reduce Vibrations and Fatigue Loading, *Proc. EWEC 94, Vol.1*, 10-14 October. Thessaloniki -Macedonia-Greece,

Bossanyi, E.A. (1987), Adaptive Pitch Control for a 250 kW Wind Turbine, *Proc. 9th British Wind Energy Association*.

Bossanyi, E.A. (1989), Practical Results with Adaptive Control of the MS2 Wind Turbine, *Proc. European Wind Energy Conference,* Glasgow.

Hansen, A. C. (1995), "USER'S GUIDE to the Wind Turbine Dynamics Computer Programs YawDyn and AeroDyn for ADAMS," Program date and version YawDyn 9.3, prepared for the National Renewable Energy Laboratory under Subcontract No. XAF-4-14076-02.

Harman, C. R., Wilson, R. E., Freeman, L. N., and Walker, S. N., (1995), "FAST Advanced Dynamics Code, Two-Bladed Teetered Hub Version 2.1, User's Manual." Draft Report, National Renewable Energy Laboratory, Golden, CO.

Hinrichsen, E.N. (1984), Controls for Variable Pitch Wind Generators, *IEEE Trans. Power Apparatus and Systems*, vol. PAS--103, pp.866-892.

IEC (1994), International Electrotechnical Commission, International Standard, 1400-1, First Edition 1994-12, Wind Turbine Generator Systems, Part 1: Safety Requirements, Modified by 88/7 (Butterfield) 50.

Ljung, L. (1987), *System Identification-Theory for the User*, Prentice Hall, Englewood Cliffs, N.J.

Ljung, L. (1995), *System Identification Toolbox User's Guide - For Use with* MATLAB®, The MathWorks, Inc., Natick, MA.

Wilson, R. E., Freeman, L. N., and Walker, S. N. (1995), "FAST2 Code Validation," presented at the 1995 ASME Wind Energy Symposium, Houston, TX.

ADAMS/WT Advanced Development - Version 1.4 and Beyond

Andrew S. Elliott and Todd R. Depauw
Mechanical Dynamics, Inc.
6530 E. Virginia Street
Mesa, AZ 85215-0736
U.S.A.

ABSTRACT

ADAMS/WT is an wind-turbine-specific shell for the general-purpose mechanical system simulation package ADAMS®. It was developed under the guidance of the National Renewable Energy Laboratory to give engineers and analysts in the wind turbine community access to the analytical power of ADAMS, without having to become expert in its particular technology. The 1.4 version of ADAMS/WT is the most recent upgrade to the package, incorporating the most up-to-date version of the AeroDyn aerodynamic forcing subroutines from the University of Utah. It is also the first version to be made available on the Windows/NT platform. In version 1.4, ADAMS/WT has been significantly improved throughout and runs much faster. Automatic generation of standardized output has been added. The documentation has been extensively augmented with more detailed descriptions, more figures and more examples. ADAMS/WT remains the most powerful analytical tool available for horizontal-axis wind turbine development.

INTRODUCTION

ADAMS/WT (Wind Turbine) is an application-specific version of the well known, general-purpose mechanical system simulation package ADAMS® (Automated Dynamic Analysis of Mechanical Systems). It consists of two main components:

1. a set of ADAMS/View macros and panels which create a customized, highly automated preprocessor for horizontal-axis wind turbine modeling
2. a set of ADAMS/Solver FORTRAN subroutines for computing the highly nonlinear unsteady airloads on the turbine blades.

The package also includes various utility programs used in both pre- and postprocessing, and a complete set of documentation.

USAGE

Over the past five years, ADAMS/WT has been delivered to about 20 sites, including universities, laboratories and commercial wind turbine manufacturers, both in the United States and overseas. Due to the recent elimination of most energy credits for renewable resources, usage in the U.S. is now limited to just a few companies and various laboratories. Usage in Europe, where "carbon taxes" are more common, is fairly widespread.

HISTORY

In early 1991, the Solar Energy Research Institute (SERI) contacted Mechanical Dynamics after seeing an article in Mechanical Engineering magazine about the use of ADAMS for modeling helicopter rotors. A demonstration contract was arranged and in the summer of 1991, Dr. Elliott visited the laboratory in Golden, Colorado. Over the course of two weeks, he constructed an

ADAMS model of the ESI-80 horizontal-axis wind turbine using version 6.0 of ADAMS. This model was validated using existing test data and other, simpler analytical codes.

While SERI was pleased with the results, they believed that turbine modeling in ADAMS was too complicated for the typical wind turbine company to invest in, and would only be useful if access to ADAMS' power could be made easier. They contracted with MDI to create a customized interface to ADAMS which would simplify and automate much of the turbine modeling process. At the same time, they contracted with Dr. Craig Hansen at the University of Utah to create a set of nonlinear aerodynamic forcing routines, called AeroDyn, which could be used with models created by the new ADAMS interface. The combined result of these efforts was ADAMS/WT 1.0, released in the summer of 1993. This version reduced the two-week initial modeling effort to about two days.

Over the next year, the users of WT found various capabilities missing and SERI, now the National Renewable Energy Laboratory (NREL), decided to upgrade the program. NREL believed that although they distributed ADAMS/WT free-of-charge, the base ADAMS program on a workstation was still too expensive for most turbine industry users. Therefore version 1.2 was made compatible with a new version of ADAMS available on the PC. This version was released in the summer of 1994 and was widely distributed. Under WT 1.2, it took about a day to build and run a complete turbine model.

The list of additional capabilities desired for WT continued to grow, along with a call to make it even simpler to use and faster. Version 1.3 was released in July 1995 for ADAMS 8.1. It was the first version to run under Windows-NT. Because of the structural changes to ADAMS between versions 7.x and 8.x, the 1.3 version was not backwardly compatible with the 1.2 code. However, with more and more automation in the View macros, the modeling process was now down to about 2 hours (once the data files were ready).

NREL has continued to support the code. Version 1.4, the current release, was made available in January of 1996. In addition to continued improvements to automation and run times, version 1.4 includes the latest upgrade to the AeroDyn and a greatly enhanced set of documentation including many more examples and details. Currently a turbine model can be built in under 15 minutes, and the amount of real ADAMS expertise required is very minimal.

ADAMS/WT FEATURES

ADAMS/WT consists of a set of macros and panel command files for the ADAMS/View preprocessor and a set of aerodynamics subroutines for ADAMS/Solver analysis engine. The View command files create a complete wind-turbine-specific preprocessor overlay. They are loaded automatically from a single control file called *wt_main.cmd*. The resulting preprocessor contains a variety of new low-level and aggregate elements which greatly simply model development. The aerodynamics subroutines are linked right into the base ADAMS/Solver program to create a special-purpose executable version of the code. This is done using the normal ADAMS commands. Standardized output request creation and plotting are also included.

PREPROCESSOR

When the WT macro and panel files are read into ADAMS/View; the menu structure is enhanced by adding additional elements to some of the standard menus and by adding a complete supplemental hierarchy specifically dedicated to wind turbine modeling. For example, the standard force menus now include a set of special elements, as shown here:

MODEL	CREATE	DIRECT	TAPERED BEAM
PART	MODIFY	BODY	MOTOR-GENERATOR
MARKER	DELETE	ELEMENT_LIKE	SIMPLE AERO FORCE
GEOMETRY	COPY	WT	WIND DUMMY VFORCE
CONSTRAINT	ATTRIBUTES		GUY WIRE
FORCE			
DATA_ELEMENT			
WT			

Selecting "WT" on the main preprocessing menu puts the user into the WT menu structure, but does not remove any of the underlying functionality, power and flexibility of the standard ADAMS/View interface. The main WT menu, which includes options for all the major turbine subsystems, is shown here:

TOWER
NACELLE
POWER TRAIN
ROTOR HUB
ROTOR BLADE
AERODYNAMICS
MAIN MENU
ABOUT WT

Most of these aggregate elements make use of the new low-level elements, as will be shown below.

TURBINE MODELING WITH ADAMS/WT

Instead of going into detail about each of the low-level and aggregate elements in WT, it is more useful to discuss the overall organization of the model and to get a feel for how it goes together. The sections that follow describe some of the basic approaches used in WT, as well as the internal design of the flexible tower and rotor blades, and how the aerodynamics are set up. For more detail on the aggregate entities or the added low-level elements, refer to the ADAMS/WT User's Guide[1]

Basically, a horizontal-axis wind turbine system consists of a tall support tower, a rotating nacelle housing the motor-generator and drive train, some kind of rotor hub and a set of long, thin rotor blades. Optionally, there may be tower guy wires, blade tip brakes, nacelle yawing and pitching mechanisms, etc.

[1] Elliott, A..S., ADAMS/WT User's Guide, Version 1.4, January 1996. Mechanical Dynamics, Inc., Ann Arbor, Michigan.

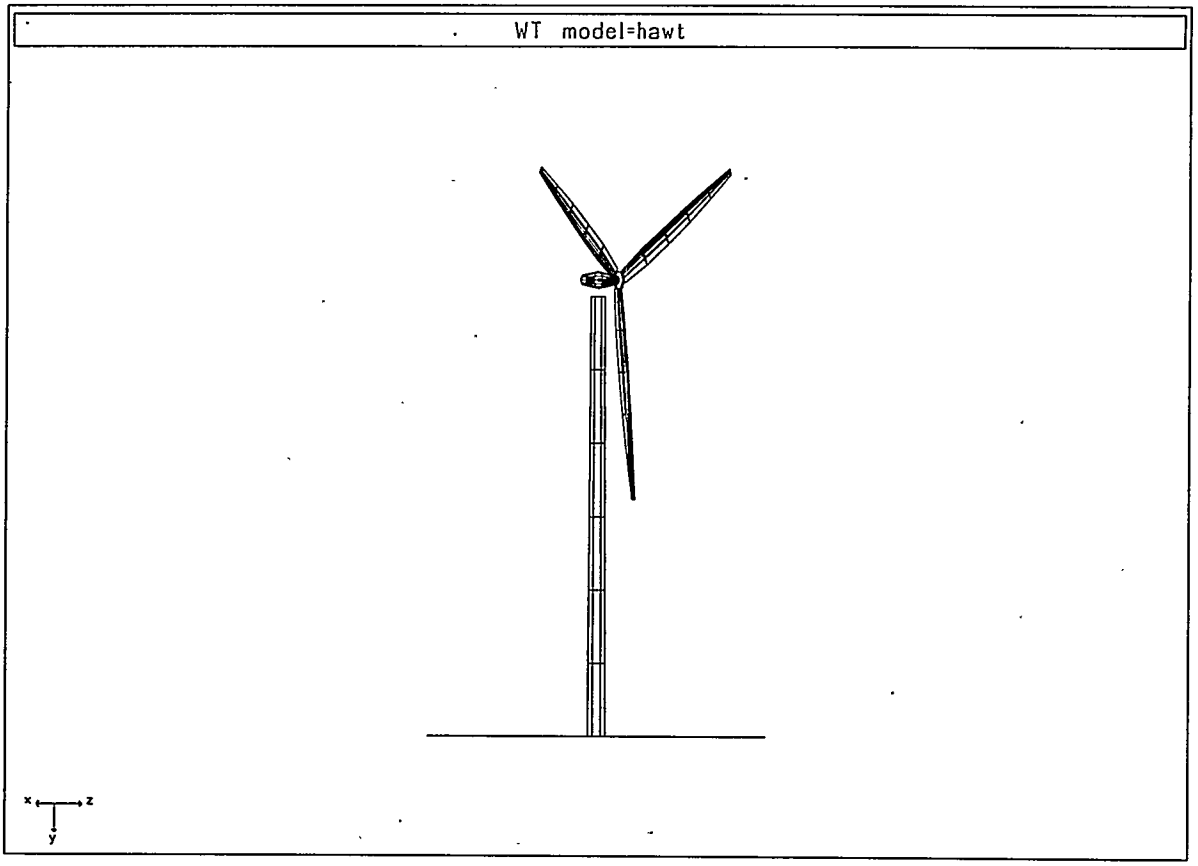

Tower Construction

In ADAMS/WT, the support tower is an aggregate element, modeled as a beam-like structure using the tapered beam and tapered part low-level elements. Details of those elements can be found in WT manual. Like the ADAMS BEAM element, the tower long axis is along the local +x direction of the tower PARTs and FIELDs.

Each pair of parts in the tower is connected by one of the special WT tapered beam FIELD elements, running between the part centers-of gravity. The bottom-most part is connected to ground using a half-length tapered beam element. This is shown in the following figure.

The automation methodology used in ADAMS/WT is based on a standardized naming hierarchy for pieces of the turbine. For example, tower parts are named *twr_sect#*, numbered from the bottom up starting with 1. The special tapered beam FIELD elements are named *twr_tbe#*, again numbered from the bottom up, starting with 0. Each of these is arranged with the J marker for the FIELD on the bottom and the I marker on the top. For example, for *twr_tbe0*, the J marker is *ground.foundation* and the I marker is *twr_sect1.CG*. For *twr_tbe1*, the J marker is *twr_sect1.CG* and the I marker is *twr_sect2.CG*, etc.

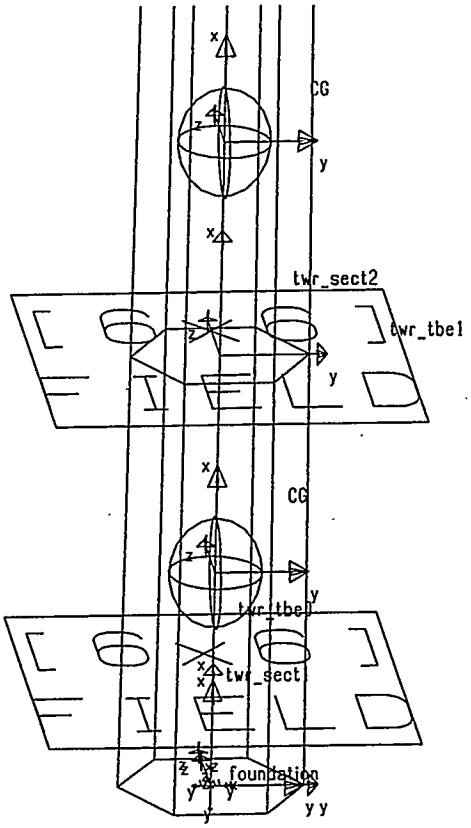

Nacelle and Power Train Construction

The nacelle is treated rather simply in ADAMS/WT. It basically serves as a platform on which to mount the power train and to connect to the tower. It consists of only one part, *nacelle*, which is connected to the tower with a revolute JOINT called *yaw_bearing* and a rotational SPRING-DAMPER called *yaw_damper.* This is shown in the figure below.

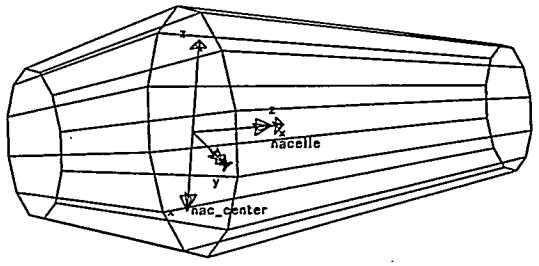

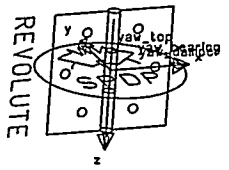

The power train consists of multiple ADAMS entities, including the generator body (a PART), the motor-generator (a rotational SFORCE), high-speed and low-speed shafts (multiple PARTs) and the gearing, if any (a coupler). Depending on the configuration of a particular rotor, some of these components may not be needed in the model.

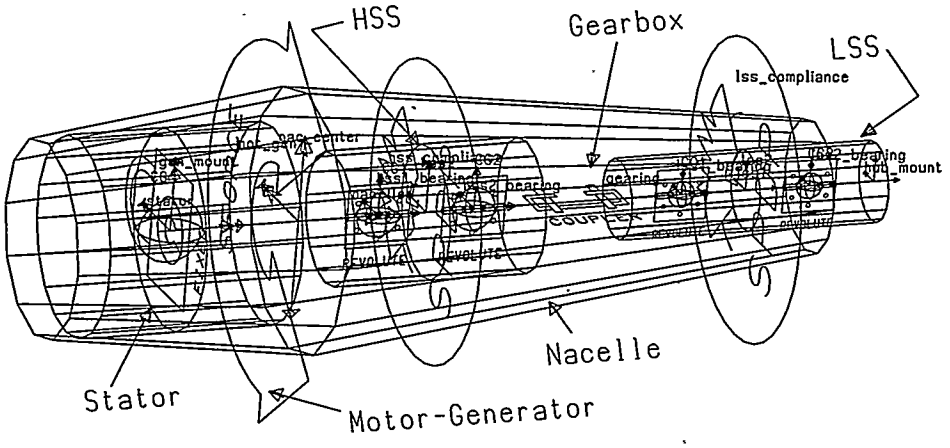

Hub Construction

WT allows for six different hub variations to cover most of the existing and proposed hub designs. You can chose between 2-bladed teetering and 3- or 4-bladed rigid hubs, and can optionally add limited flexibility (at the blade attachment point) to any of the choices.

An example 3-bladed, flexible hub is shown below.

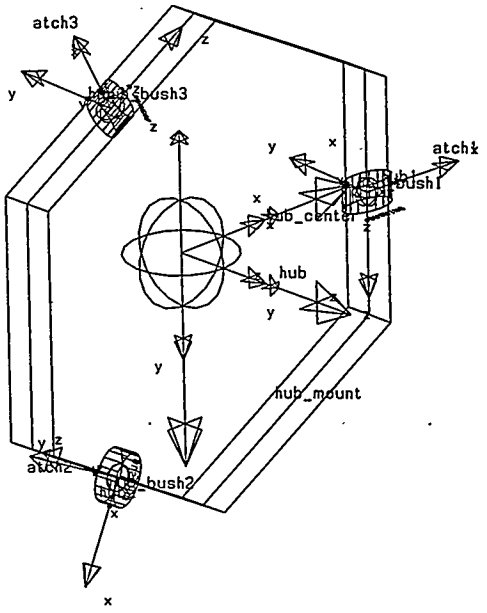

Blade Construction

In WT there are two different types of rotor blades, fully flexible and rigid/hinged. The fully flexible blade is an aggregate element, much like the tower, and is also modeled as a beam-like structure using the tapered beam and tapered part low-level elements. The rigid/hinged blade is a one- or two-part aggregate element with an optional hinge and spring-damper between the parts. This corresponds to the classic rigid flap-only blade that is often used in simpler analytical approximations in other codes.

Regardless of which type of blade is used, the blade's long axis (i.e. radial axis) is along the local x direction of the blade PARTs. The +z direction is toward the leading edge and the +y direction is toward the pressure side (nominally upwind) for a rotor which rotates counterclockwise looking upwind (which is the WT default).

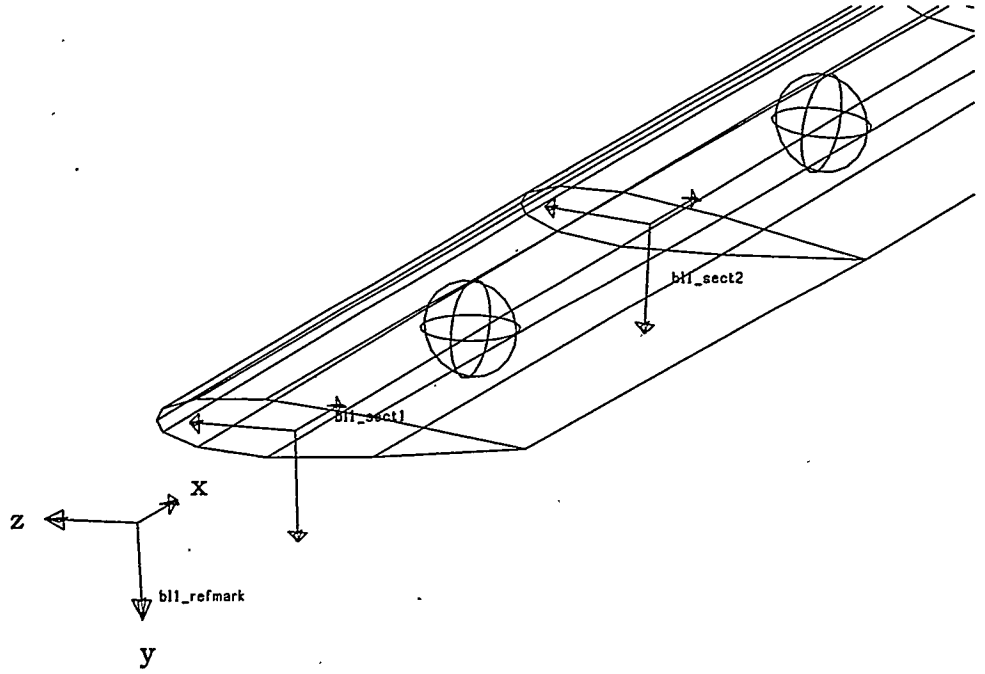

Aerodynamics

Two options are offered for aerodynamics in ADAMS/WT. The first is a very simple, linear, steady aerodynamics algorithm implemented directly as ADAMS functions. The second is the complete 2-D, nonlinear, unsteady aerodynamics from the associated AeroDyn package. Either approach can be automatically added to a blade in WT very simply, basically with one click of the mouse. The automation, however, hides very strict rules for the orientation and placement of the aerodynamic control point markers and the wind definition coordinates.

In version 1.4 of ADAMS/WT, the default rotor configuration is downwind with counter-clockwise rotor rotation looking upwind, i.e. positive about the base frame x-axis..

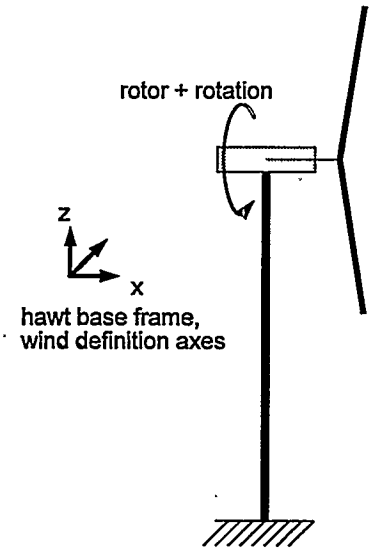

With WT, you have a choice of putting 0, 1 or 2 aerodynamics control points on each blade section. Also, you can define the number of aero markers per section either once for the whole blade or individually on a section-by-section basis. When WT adds aerodynamic control markers to a rotor blade section, it automatically puts them at the Gaussian integration points and orients them correctly, as shown in the two-point blade section here.

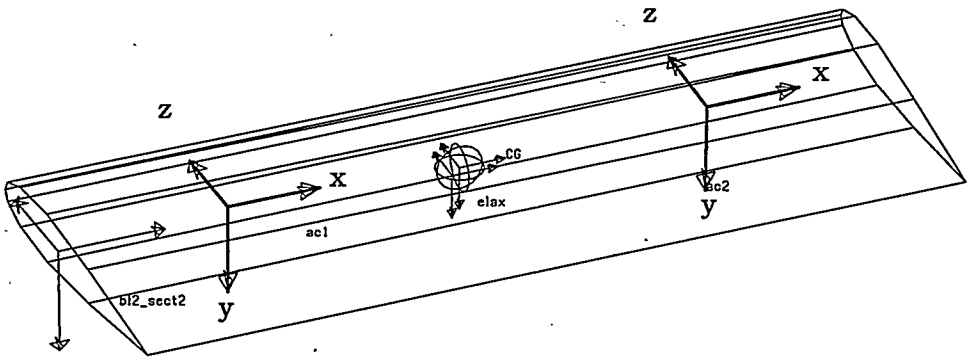

POSTPROCESSING

ADAMS/WT adds a set of pre-defined REQUESTs to the normal ANALYSIS OUTPUT_CONTROL CREATE REQUEST menu. These requests cover all the normally instrumented parts of a wind turbine, and additionally include many things that turbine engineers *wish* they could instrument. In addition, a template plotting command file for View is included to automatically plot and format the results from these requests. This allows easy comparison of run-to-run differences. An example of this automatic plotting is shown here:

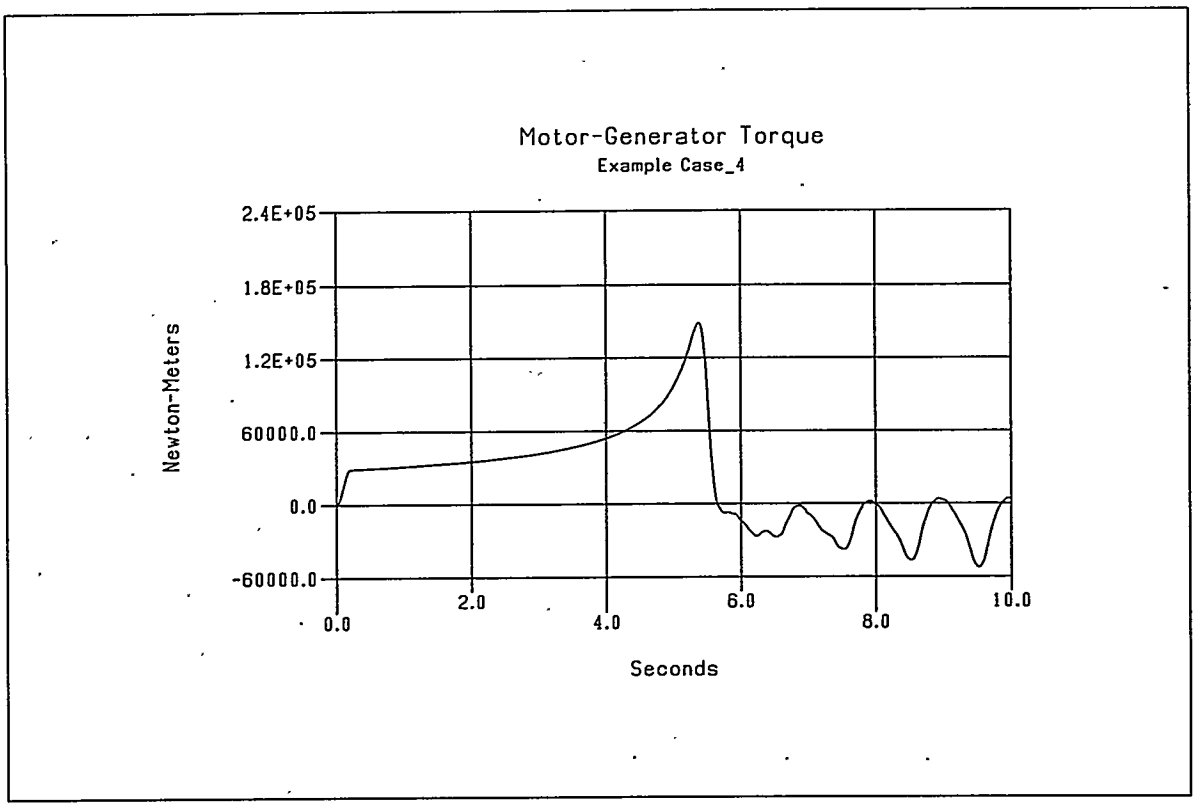

EXAMPLE CASES

As an aid to new users, a series of four example rotors of increasing complexity are included with the ADAMS/WT package and are very completely documented, from staring View and loading WT to what goes into every input field to running the analyses to plotting the results. At each step, screen shots are used to ensure that the user is going the right way. The following cases are included, all using the full, nonlinear AeroDyn aerodynamics:

1. 2-bladed, teetering rotor with rigid blades and rigid drive shaft, but with flexible tower.
2. Same as #1, but with flexible blades and a torsion-only shaft.
3. Same as #2, but with a fully flexible drive train.
4. 3-bladed, rigid hub rotor with flexible blades, shaft and tower.

AVAILABILITY AND SUPPORT OF ADAMS/WT

WT is supplied by MDI completely free-of-charge to interested users, after they have been approved for distribution by the National Renewable Energy Laboratory. To get approval, contact

Mr. Alan D. Wright
National Renewable Energy Laboratory
1617 Cole Boulevard
Golden, CO 80401-3393
Phone: 303/384-6928
e-mail: alan_wright@nrel.gov

ADAMS/WT support is provided by MDI under contract to NREL. For WT-specific problems, contact the author,

Dr. Andrew Elliott
MDI Professional Services
6530 E. Virginia Street
Mesa, AZ 85215-0736
Phone: 602/985-1557
Fax: 602/985-1559
e-mail: aelli@adams.com

FUTURE ENHANCEMENTS

NREL is committed to supporting ADAMS/WT, so that regular enhancements and improvements are being made to the product. In the near future, depending on user requirements, we expect to add the following features to WT:

1. Compatibility with the new 9.0 View interface
2. Different machine configurations
3. Partial DOF lockouts for blades and tower
4. Composite blades
5. Aggregate entity "swapping"
6. Parametric variation capability

BASELOAD, INDUSTRIAL-SCALE WIND POWER: AN ALTERNATIVE TO COAL IN CHINA

Debra J. Lew[1]
Robert H. Williams
Center for Energy and Environmental Studies
Princeton University
Princeton, NJ 08544 USA

Xie Shaoxiong
Zhang Shihui
3, 4/F, South Gate Hua Heng Building,
No. 31 Nanbinhe Road, Guang An Men Wai
Ministry of Electric Power
100053 Beijing, China

ABSTRACT

This report presents a novel strategy for developing wind power on an industrial-scale in China. Oversized wind farms, large-scale electrical storage and long-distance transmission lines are integrated to deliver "baseload wind power" to distant electricity demand centers. The prospective costs for this approach to developing wind power are illustrated by modeling an oversized wind farm at Huitengxile, Inner Mongolia. Although storage adds to the total capital investment, it does not necessarily increase the cost of the delivered electricity. Storage makes it possible to increase the capacity factor of the electric transmission system, so that the unit cost for long-distance transmission is reduced. Moreover, baseload wind power is typically more valuable to the electric utility than intermittent wind power, so that storage can be economically attractive even in instances where the cost per kWh is somewhat higher than without storage.

INTRODUCTION

For the last quarter of a century, China has been operating under a power shortage, which is now estimated to be 20-30 GW. To try to keep up with growing demand, China has been adding capacity since 1980 at an average annual rate of nearly 10%; installed capacity reached 183 GW in 1993. Annual generation increased at an average of 9.4% annually in this period, to 840 TWh in 1993. Three-quarters of the electricity generation is derived from coal. This coal use has resulted in severe local air pollution problems and is contributing significantly to world CO_2 emissions. Chinese CO_2 emissions in 1990 were 680 MtC/year, about 11% of the world total. As China industrializes over in the next thirty years, these emissions are projected to increase to 2400 MtC/year [UNDP/WB, 1994]. By that year, annual world emissions are estimated to range from 6000 to 12,000 MtC/year.

Due to China's air pollution problems, constraints on coal expansion, lack of energy diversity, and climate change concerns, serious consideration should be given to the development of large-scale wind energy in China, as China is richly blessed with wind energy resources. In this report a preliminary assessment is made of the prospective lifecycle costs of wind power in China, with comparisons to the lifecycle costs for coal-based power generation. Particular emphasis is given to a new approach for exploiting good wind resources that are remote from electricity demand centers. Then, the costs for an oversized wind farm/transmission system without storage are examined, followed by an analysis showing how storage can increase the capacity factor of this system and the value of the delivered electricity, at low incremental cost.

[1]Present address: National Wind Technology Center, National Renewable Energy Laboratory, 1617 Cole Blvd. Golden, CO 80401.

a)

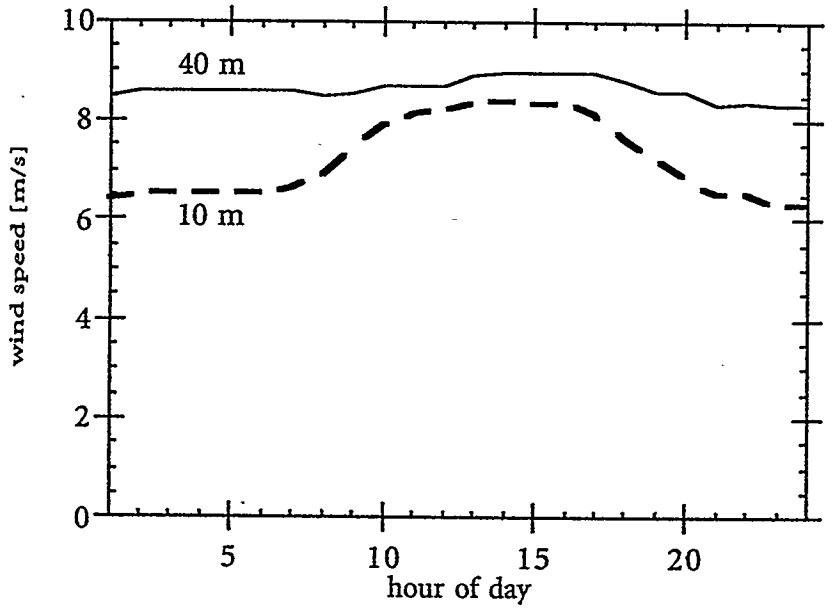

b)

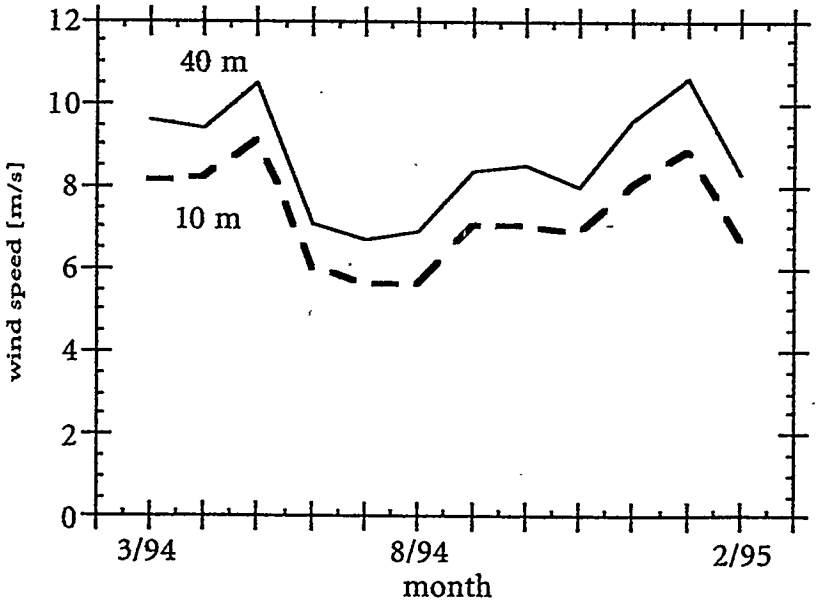

FIGURE 1. (A) DIURNAL AND (B) SEASONAL VARIATIONS IN WIND SPEED AT HUITENGXILE, INNER MONGOLIA FROM MARCH 1994 TO FEBRUARY 1995 [INNER MONGOLIA ELECTRIC POWER PROSPECTING & DESIGN INSTITUTE, 1995].

WIND RESOURCE

The Inner Mongolia Autonomous Region, located in northern China, along the Mongolian border, is home to the largest wind resource in China. The high quality of the wind resource there is evidenced by over 120,000 small scale wind turbines in this region which provide electricity to the rural herdsmen. The winds across these plateaus are generally steady, with little turbulence and few gales. The richest wind area in Inner Mongolia (83,000 km^2 or 0.9% of total land area in all of China) could roughly provide 520 W/m^2 and nearly 7900 usable hours/year at 50 m hub heights. This land area could support nearly a million turbines with more than 500 GW nameplate capacity. Accounting for losses and the intermittency of the resource, the average power produced would be about 200 GW and annual wind electricity production from this region would be nearly 1800 TWh/year.

Huitengxile, located near the region's capital, Hohhot, is one of the best wind sites in Inner Mongolia. The data used in this study and shown in Figure 1 are taken from more than a year of measurements by the Inner Mongolian Electric Power Prospecting and Design Institute [1995]. The measured wind speeds at 10 m and 40 m hub heights have been fit to Weibull distributions with v_c=8.18 m/s, k=2.19 at 10 m and v_c=9.75 m/s, k=2.51 at 40 m. Using the measured wind shear factor of 0.143 and assuming that k=2.51 at a 50 m hub height, a v_c of 10.07 m/s is expected at a 50 m hub height (corresponding to v_{avg}=8.9 m/s and P=584[2] W/m^2). A 600 kW turbine (50m hub height, active pitch controlled, fixed speed) in this wind regime gives a single wind turbine capacity factor of 42%.

EXPLOITING WIND RESOURCES THAT ARE FAR FROM DEMAND CENTERS

Unfortunately, many windy areas, such as those in the Inner Mongolia and Xinjiang Autonomous Regions, are far from most demand centers. For example, Beijing is located about 500 km and Harbin about 1400 km from Huitengxile, Inner Mongolia. For the US, it has been shown that remotely sited wind resources can be exploited so as to provide electricity to distant demand centers that is cost-competitive with electricity from coal, by combining "oversized" wind farms with long distance transmission lines and large-scale electricity storage systems [Cavallo, 1995]. This combination of technologies makes it possible to deliver "baseload wind power" to electricity demand centers.

If the installed turbine capacity of an Inner Mongolian wind farm were set equal to the 1 GW capacity of a transmission line, the number of 600 kW turbines needed would be 1667. For this "normally sized" configuration, assuming 14% array and other losses for the wind farm, the transmission line capacity factor (TLCF) would be the same as for the wind farm, or 36%. Up to 1938 turbines can actually be installed before the peak wind farm output exceeds the transmission line capacity. The output of such a wind farm would appear as in Figure 2a, which shows that the average power output is 42% of the transmission line capacity, i.e., the TLCF can be increased to the capacity factor for a single wind turbine.

The economic analysis for the energy costs is based on assumptions which are detailed in Lew *et al* [1995] and listed in Table 1. Imported turbines are assumed to cost $1000/kW installed. With the large number of turbines required for the wind farm proposed in this report, it is likely that much of the turbines will be manufactured in China. The estimated cost of Chinese-manufactured turbines is based on work by Yang [1995], who analyzed cost reductions in Chinese-manufacture of coal power plant components. A very preliminary assessment of Chinese-manufactured turbines results in a cost of $600/kW installed. The costs for AC transmission lines are cost estimates from China, which are 29% cheaper than US transmission lines; the costs for DC transmission lines are also based on a 29%

[2]The power density for this wind speed is 15% lower than for a wind farm at sea level, due to the low air density of 1.04 kg/m^3 found at the site elevation of 2030 m.

reduction in cost from US DC transmission lines. Since only one CAES plant is required for the proposed system, US CAES costs have been used.

For this wind farm the lifecycle delivered cost of electricity (DCOE) at the end of a 500-km AC transmission line would be 0.180 Yuan/kWh ($0.022/kWh), of which 16% of the cost would be for transmission (see Table 2).

TABLE 1. ASSUMED COSTS FOR THIS MODELING EXERCISE.

Wind Turbine		Transmission Line		CAES	
turbine size [kW] =	600	AC line length	500 km	CAES size[3]	350 MW;h_S=storage hours
50 MW wind farm cost[4][$/kW]		AC capital cost	$130M	porous media	$180 M
domestic =	$600	DC line length	1400 km	salt	$158 M + ($0.4 M) * h_S
imported =	$1000	DC capital cost	$208M	rock	$172 M + ($2.8 M) * h_S
				interest during construction	8.2% * plant cost
owner costs [$/kW]=	5.4% * plant cost			owner costs	2.9% * plant cost
				fuel oil	$3.8/GJ
O&M [$/kWh]=	0.004	O&M	0	fixed O&M	$1.2/kW/yr
				variable O&M	1.5 mills/kWh
Plant car. chg=	0.094	Plant car. chg=	0.094	Plant car. chg=	0.094
OC car. chg=	0.080			OC car. chg=	0.080

If the number of turbines is increased to 4100, the transmission line can be filled more efficiently, as seen in Figure 2b, where the average power output has now been increased to 60% of the line capacity. The lifecycle DCOE for a wind farm of this size is only 16% greater than that for a normally sized wind farm with 1667 turbines and a TLCF of 36%, because much of the additional cost of the turbines is offset by increased power output. There is some spillage of power when the wind farm output exceeds the transmission line capacity. In this case 292 MW, or 33% of the generated wind power is spilled.

Table 2 and Figure 3 show the calculated TLCF and lifecycle DCOE from wind energy by cost component for alternative wind farm sizes. Further increases in number of turbines, however, results in large amounts of spilled power and the resulting increase in the specific cost of delivered electricity from the wind farm (cost/kWh) greatly exceeds the decrease in specific transmission line cost. For 8000 wind turbines in the wind farm, and a TLCF of 68%, the lifecycle DCOE would be 65% higher than for a wind farm with 1667 wind turbines.

[3]Economies of scale apply to CAES capital costs. For example, a 750 MW CAES plant is estimated to cost $275/kW.

[4] For plant sizes other than 50 MW, the costs are assumed to scale with wind farm capacity as $(\text{size}/50\text{MW})^{-0.1}$, based upon work by EPRI [1993].

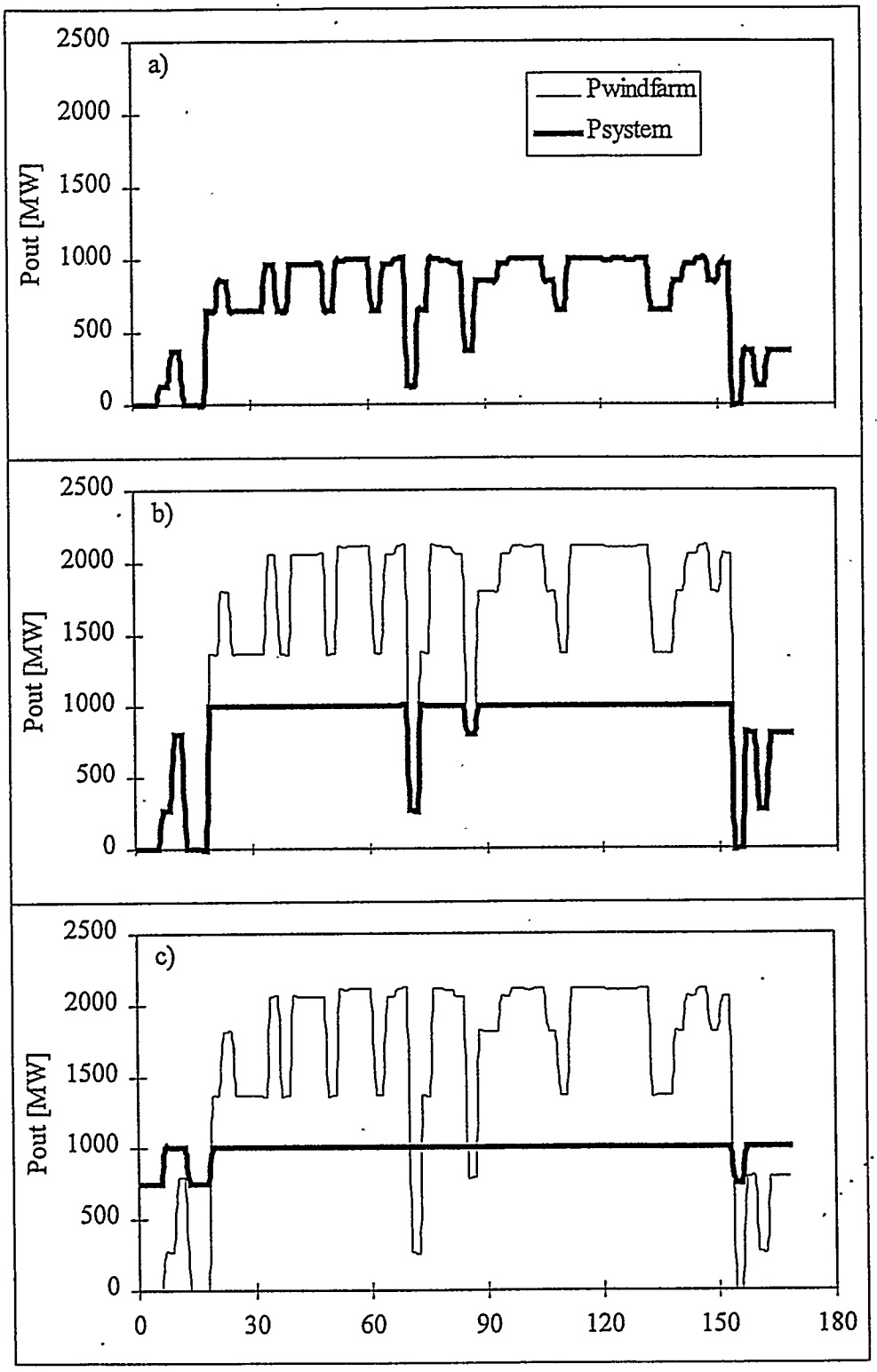

FIGURE 2. SIMULATED HOURLY OUTPUT FOR VARIOUS WIND FARM/STORAGE CONFIGURATIONS CONNECTED TO A 1 GW TRANSMISSION LINE. THE THIN LINE INDICATES THE POWER OUTPUT OF THE WIND TURBINES AND THE THICK LINE REPRESENTS THE DELIVERED POWER OUTPUT OF THE PLANT. A) N=1938 TURBINES, TLCF=42%; B) N=4100, TLCF = 60%; C) N=4100, TLCF = 89%, 750 MW CAES WITH 160 HOURS STORAGE.

TOWARD "BASELOAD" WIND POWER

In order to raise further the capacity factor of the transmission line without incurring large cost increases, the wind farm needs to be combined with a system that provides power when the wind farm output is low. One option is to combine the wind farm with a dispatchable, low capital cost source of electricity generation, such as a natural gas turbine or hydropower plant. Another possibility is some form of energy storage. Storage can utilize the spilled energy and increase the TLCF. For the configuration in Figure 2c, the number of turbines is still 4100, but storage has been added to this system, so that much of the spilled power is recovered by the storage plant to level the transmission line output. In this case, the TLCF reaches 89% and the system effectively produces non-dispatchable baseload power. The TLCF realized with storage is far larger than the value (60%) realizable with the same number of turbines but no storage (shown in Figure 2b). The cost of electricity increases only to the extent that the storage cost is not offset by the cost reductions associated with the increased capacity factor of the transmission line.

There are many kinds of storage, including pumped hydropower, compressed air energy storage (CAES), batteries, superconducting magnetic energy storage, capacitors, flywheels and electrolytic hydrogen. Of these, only pumped hydropower, batteries, and CAES are commercially available. Pumped hydropower is a mature technology that is used worldwide for storage at large scales; in 1990 there were 283 pumped hydro plants with a total capacity of 74 GW. However, the capital costs are high ($1500/kW), and it may not be suitable for many areas due to lack of water. Batteries are commonly used in small-scale applications; however, batteries are costly and have limited lifetimes.

CAES is a commercially ready storage option, based on combustion turbine technology. CAES appears to be well-suited to wind applications in areas where natural gas-based power and hydropower are not readily available as complements to the wind resource. During periods of excess electricity generation, air is compressed and stored in an underground cavern. When wind farm output is low, the compressed air is recovered from storage, heated and expanded through turbines to generate electricity. In the design used in this report, 0.67 kWh of wind farm output plus 4110 kJ (1.14 kWh) of fuel provide 1 kWh of electricity on demand. Distillate oil, syngas, or natural gas can be used as fuel for this system.

An underground airtight space of sufficient volume is needed ~150-1000 meters below the ground for CAES. There are three typical options for this storage volume: solution-mined cavities in bedded or domed salt formations, mined space rock mines, and porous media. The authors have not been able to ascertain whether there are appropriate salt beds in Inner Mongolia, but the Eren basin, a large oil/natural gas basin in central Inner Mongolia, could prove to be a satisfactory porous media site. In addition, there are hard rock formations in these regions.

Several wind/storage configurations were simulated and each simulation was run over one year. Two wind data sets were used. Given the 600kW turbine power curve and the measured wind distribution, the average single turbine capacity factor is calculated to be 42%, so the data sets were scaled to meet this single turbine capacity factor. The initial data set was comprised of randomly generated wind speeds, whose wind speed distribution matched the measured distribution at Huitengxile. Because winds are not random, but are correlated over some time scale, the second data set used three-hourly wind data from the nearby site of Jurh. This was intended to provide the proper seasonal and diurnal variations of the wind resource. Both data sets gave the same results to within a few percent. The sizings for the compressed air energy storage system were arrived at via an hourly analysis of how often the CAES system is used and how much electricity it supplies. The results of the calculations are summarized in Table 2 and Figure 3. It should be noted that by varying the number of turbines and CAES capacity, one can arrive at identical transmission line capacity factors with very different costs. An attempt has been made to arrive at a minimum system cost for each capacity factor.

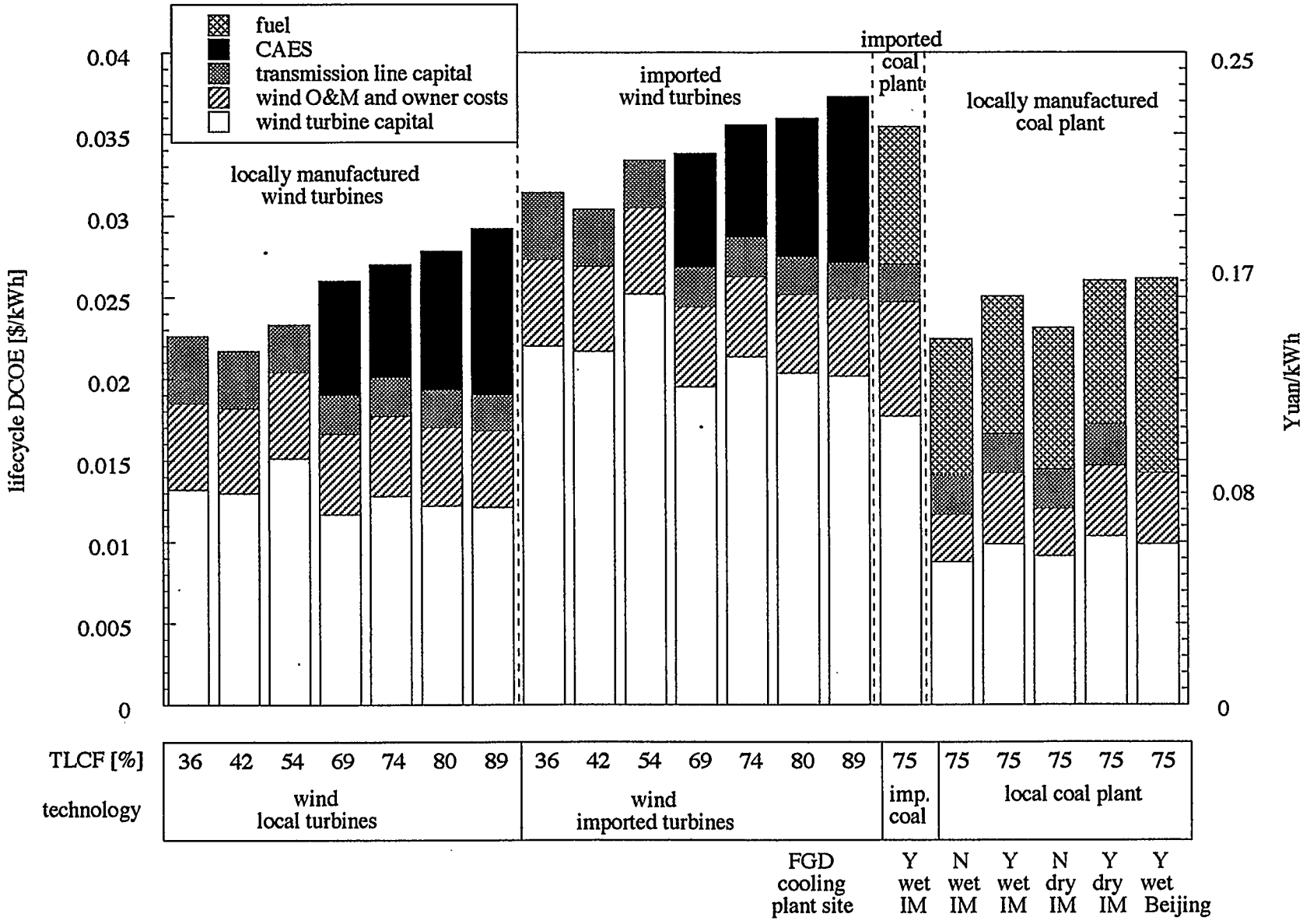

FIGURE 3. COMPARISON OF DCOE FROM HIGH-CAPACITY-FACTOR WIND POWER PLANTS AND COAL POWER PLANTS IN CHINA.

For the situation shown in Figure 2c, where the TLCF is 89% for a wind farm with 4100 turbines, the lifecycle DCOE is 30% higher than for a normally sized wind farm with 1667 turbines (Figure 2a), as shown in Table 2 and Figure 3a. However, the nearly firm electricity provided at high capacity factor with CAES (Figure 2c) is likely to be far more valuable to the electric utility than the highly variable output from a normally sized wind farm (Figure 2a) -- i.e., the utility's "avoided cost" is likely to be much higher.

TABLE 2. SIMULATIONS OF 1 GW WIND/STORAGE SYSTEM FOR VARIOUS WIND FARM SIZES AND CAES CONFIGURATIONS. THE LIFECYCLE DCOE HAS BEEN DISAGGREGATED INTO WIND TURBINE (WT), TRANSMISSION LINE (TL), AND CAES COSTS.

CAES	N	[%] TLCF	[MW] CAES	[hrs] Storg	[%] CAES CF	P_{spill}	Lifecycle DCOE [$/kWh]					
							WT Capital	WT O&M &OC	TL Capital	TL Losses	CAES	Total
no storage	1667	36				0	0.0132	0.0053	0.0039	0.0002		0.0226
	1938	42				0	0.0130	0.0052	0.0033	0.0002		0.0218
	3000	54				115	0.0134	0.0053	0.0030	0.0003		0.0220
	4100	60				292	0.0180	0.0055	0.0024	0.0004		0.0262
	6000	65				649	0.0232	0.0057	0.0022	0.0005		0.0316
	8000	68				1051	0.0287	0.0060	0.0021	0.0006		0.0373
porous media	3000	69	350	160	44	11	0.0117	0.0049	0.0020	0.0004	0.0070	0.0261
	3550	74	350	160	48	87	0.0128	0.0049	0.0019	0.0005	0.0069	0.0270
	3700	80	500	160	45	74	0.0122	0.0048	0.0018	0.0005	0.0085	0.0278
	4100	89	750	160	39	95	0.0121	0.0047	0.0016	0.0006	0.0102	0.0293
salt	3000	67	350	50	38	27	0.0121	0.0049	0.0021	0.0004	0.0066	0.0262
	3500	76	500	50	38	66	0.0123	0.0048	0.0019	0.0005	0.0082	0.0277
	4000	87	750	80	37	88	0.0121	0.0047	0.0016	0.0006	0.0103	0.0293
rock	3000	64	350	25	31	43	0.0126	0.0050	0.0022	0.0004	0.0074	0.0276
	3500	72	500	25	32	88	0.0129	0.0049	0.0019	0.0005	0.0089	0.0291
	3800	79	750	25	28	101	0.0127	0.0048	0.0018	0.0006	0.0106	0.0305
	4000	85	750	50	35	100	0.0123	0.0047	0.0016	0.0007	0.0119	0.0312

OTHER CASES

DC Transmission to Harbin

Since demand centers such as Harbin may be much farther from the wind resource, the feasibility of delivering power over a 1400 km DC transmission line was investigated. The estimated capital cost of a 1400-km HVDC line from the wind site at Huitengxile to the demand center of Harbin would be 60% greater than the cost of the 500-km HVAC line, even taking into account optimistic cost reductions with future Chinese manufacture of the DC technology. However, because the transmission line is a relatively small fraction of the total lifecycle DCOE, the HVDC line would result in only a 3% increase of the lifecycle DCOE to 0.250 Yuan/kWh ($0.030) for the baseload case with a TLCF of 89%.

Geologies for CAES

Due to the large monthly variations, large storage volumes are needed to provide baseload power at the lowest lifecycle DCOE for the Huitengxile site. If suitably sized porous media spaces can be located, this would provide the least expensive option for CAES storage, but salt and rock can also be used. Table 2 shows the cost breakdowns for salt and rock storage for the Huitengxile to Beijing system. For a TLCF of 75%, the lifecycle DCOE with salt is only 2% higher and with rock, 8% higher.

Smaller Systems

A 1 GW wind/storage/transmission system from Huitengxile to Beijing with a TLCF of 75% requires a large capital investment -- about 10.1 billion Yuan ($1.2 billion). This is a large initial cost for a technological system that has yet to be built in an OECD country. Therefore, the feasibility of a smaller wind/storage system, a 200 MW system with 50 MW of CAES capacity, is considered here. Down-sizing the plant to 200 MW affects only the scale economies for the wind farm and the CAES. A 1 GW transmission line already exists between Inner Mongolia and Beijing and is only partially used. Since a new line would not be required, utilization of this existing line is assumed, with 1/5 of the total line capital costs allocated to this wind/storage system. For this 200 MW system, a 50 MW CAES unit is needed for a system with a TLCF of 75%. The wind farm contribution to the lifecycle DCOE increases by 28% and the CAES contribution[5] increases by 20% relative to the lifecycle DCOE for the larger 1 GW Huitengxile/Beijing system. For this system the lifecycle DCOE is estimated to be 0.266 Yuan/kWh ($0.032/kWh) and the total plant cost about 2850 million Yuan ($345 M).

OBSTACLES

What are the major obstacles to building in China industrial-scale wind farms, such as those described in this paper? Surprisingly, perhaps, the construction of large wind farms involving thousands of wind turbines is not a daunting challenge. In fact, more than half of the nearly 8000 turbines in California were installed in three years in the mid-1980s. Construction times for wind farms are nominally one year, but turbines can be erected in far shorter timespans. In 1985, Zond (US) installed 80 MW at four sites in 6 months. Moreover, individual turbines can be operational and generating revenue while the rest of the wind farm is being installed.

Rather the major challenge is to find ways to establish a viable capacity in China for manufacturing high-quality modern wind turbines and related technologies and for managing these technologies at large-scale on electric utility grid systems. Recently, China has sought to develop the needed technological capacity instead via the formation of joint ventures with foreign firms. Industrial consortia organized as joint ventures between foreign vendors and developers and local Chinese companies are promising instruments for accelerating the development of a strong indigenous technological capacity in China for wind power and related technologies such as CAES. China's initial experience with such joint ventures is thus helpful. The key to success with such consortia would appear to be the scale of the activity. Policies that encourage the formation of such consortia for carrying out large wind power projects that involve promising technology transfer arrangements could be very helpful in building the needed indigenous technological capacity.

SUMMARY

This study has provided a preliminary assessment of the prospects for developing remotely located wind resources in China. It showed that if large overbuilt wind farms are combined with compressed air energy storage and long-distance transmission lines, it would be possible to deliver remote wind resources to major demand centers as "baseload" electricity. Moreover, this study has shown that under very reasonable assumptions about the economics of manufacturing modern wind energy equipment in China and about the economies of scale in wind turbine manufacture, large-scale wind energy systems established in remotely located regions of good wind, such as Inner Mongolia, could plausibly provide baseload electricity to demand centers such as Beijing, at delivered lifecycle electricity costs that would be roughly the same as the lifecycle cost of coal-based electricity. This finding, for a region in China in which coal is cheap and plentiful, does not take credit for the reduced greenhouse gas emissions that would result from displacing coal power with wind power.

[5]The Westinghouse costs used in the base case are not appropriate for the smaller 50 MW plant. Costs for this size are based upon the Alabama plant and are estimated to be 4570 Yuan/kW ($550/kW) for the basic above-ground turbomachinery alone [Swensen, 1995]. Based upon this increase, the total CAES capital cost is approximately $1285/kW.

Also, it would be more difficult for wind power to compete with coal if sulfur oxide emissions from coal plants were unconstrained than if they were regulated, as in the West.

ACKNOWLEDGMENTS

The authors are greatly indebted to Al Cavallo for his technical expertise and helpful comments. Fruitful discussions with Gavin Gaul and Paul White were also useful. The authors gratefully acknowledge the W. Alton Jones Foundation, the Rockefeller Foundation and the Merck Fund for their support of this work.

REFERENCES

Cavallo, A.J., *Journal of Solar Energy Engineering*, Vol. 117, p. 137, May, 1995.

EPRI (Electric Power Research Institute), *TAG™ Technical Assessment Guide, Volume 1- Electricity Supply,* Palo Alto, CA, June 1993.

Gaul, Gavin, "Compressed Air Energy Storage Program Status Report," *American Power Conference*, Chicago, IL 13-15 April, 1993.

Inner Mongolia Electric Power Prospecting & Design Institute, *Research Report on Feasibility - First Phase: Engineering Wind Turbine Power Plant*, Hohhot, March, 1995.

Lew, D.J., R.H. Williams, S. Xie, and S. Zhang, "Industrial-Scale Wind Power In China," presented at the Workshop on Wind Power for the China Council for International Cooperation on Environment and Development for the Energy Strategies and Technologies Working Group, Beijing, China, November 1995.

State Statistical Bureau of the People's Republic of China, *China Statistical Yearbook*, Beijing, 1993.

Swensen, Eric, Energy Storage and Power Consultants, personal communication, 1995.

UNDP/WB (United Nations Development Program/World Bank), *China: Issues and Options of Greenhouse Gas Emission Control*, December, 1994.

Yang, Feng, *IGCC and Its Future Market Penetration in China*, Master's Thesis, University of California at Berkeley, May, 1995.

COMPRESSED AIR ENERGY STORAGE SYSTEM RESERVOIR SIZE FOR A WIND ENERGY BASELOAD POWER PLANT

Alfred J. Cavallo, Consultant
289 Western Way
Princeton, NJ

ABSTRACT.

Wind generated electricity can be transformed from an intermittent to a baseload resource using an oversized wind farm in conjunction with a compressed air energy storage (CAES) system. The size of the storage reservoir for the CAES system (solution mined salt cavern or porous media) as a function of the wind speed autocorrelation time (C) has been examined using a Monte Carlo simulation for a wind class 4 (wind power density 450 W m^{-2} at 50 m hub height) wind regime with a Weibull k factor of 2.5. For values of C typically found for winds over the US Great Plains, the storage reservoir must have a 60 to 80 hour capacity. Since underground reservoirs account for only a small fraction of total system cost, this larger storage reservoir has a negligible effect on the cost of energy from the wind energy baseload system.

1. INTRODUCTION

Wind generated electricity currently supplies only a small fraction of total electricity demand even in areas with good wind resources and with public policies that compensate for the failure of the market to recognize the total cost of nuclear and fossil fuel generated electricity [1,2]. At this level of market penetration, utilities can accommodate the intermittent characteristics of wind relatively easily; as still more intermittent generators are added to the system, an increasing amount of effort and capital must be deployed to maintain an acceptable loss of load probability and power quality.

The limitation on the fraction of average demand intermittent wind generators can supply depends on many details of both the wind resource and the utility grid. For example, one such constraint might be the number and type of dispatchable generators or the spinning reserve to which a given utility has access. Another might be the willingness of utility managers to devote an increasing fraction of their time and effort to managing a more difficult system. The load profile of a utility, and the seasonal variation of the wind resource relative to the load profile might be a severe restriction (e.g. a utility with a winter or spring peaking wind resource but a summer peaking load). Finally, transmission lines, which are often difficult and expensive to construct, must be able to supply the demand centers from the remote intermittent generators.

The addition of storage to a wind energy system opens up entirely new possibilities for wind energy utilization [3]. It changes this resource from one that is somewhat awkward and quite eccentric from the point of view of a utility, to one which is entirely familiar and well-behaved. Properly designed, a wind energy system with storage can be used as a baseload or a dispatchable generator, with forced outage rates comparable to those of the best fossil fuel units. In essence, a wind energy system with storage can be engineered so that it is both economical and technically equivalent to an oil, natural gas, coal or nuclear generating station.

For industrial or utility scale systems an ideal candidate for this application is a compressed air energy storage (CAES) system. Several CAES facilities are operational or under construction

around the world [4]. These use compressor and turbomachinery technology which is widely available, reliable and inexpensive; the storage medium - air - is obtainable everywhere at no cost. The underground structures needed for the storage volume such as salt deposits, porous media traps or depleted gas fields, are also widely distributed.

The combination of wind farms with CAES has been modeled using a series of numbers drawn from a Weibull distribution as synthetic wind velocities [5]. This can only be a poor approximation to real wind data since there is a significant correlation between wind velocities several hours apart; that is, the wind velocity at any given time is likely to be similar to that an hour earlier or later in time.

In this paper the impact of the wind speed autocorrelation time on the size of the storage reservoir needed in a wind energy baseload system is examined using a realistic set of synthetic wind speeds.

2. DEFINITION OF THE WIND ENERGY BASELOAD SYSTEM

How a storage system can be coupled most economically to an intermittent wind source can be understood most easily by taking a systems approach to the problem and attempting to minimize the cost of electricity, including the transmission cost, delivered to the consumer. The result of this analysis is an oversized wind farm [3,5], that is a wind farm whose maximum output is much larger than the capacity of the transmission line connecting the wind farm to the demand center; the oversized wind farm is coupled to a CAES system with a charge rate about 1.5 times the discharge rate. At low wind velocities, which occur most frequently, more wind turbines are available to fill the transmission line and thus reduce the per unit cost of transmission. At high wind velocities, power that cannot be transmitted is utilized to compress air which is then stored in an underground reservoir at pressures up to 7.5 MPa (75 atm.); when the output of the wind farm drops below the transmission line capacity, the compressed air is withdrawn from the reservoir, heated and allowed to flow through a turboexpander coupled to an electric generator, adding to the output of the wind plant.

3. WIND TURBINE AND WIND CHARACTERISTICS

The power output of the wind farm is a function of both the wind turbine as well as the wind resource. For this study the wind turbine power output curve is that of the Enercon E-40 [6], a variable speed, variable individual blade pitch, direct drive machine. While this is a more sophisticated and more expensive device than most competitive models, its higher efficiency, due to the variable speed feature, and its lower maintenance costs, due to the absence of the gearbox and the variable speed and pitch, are compelling advantages. Other manufacturers will most likely design and build machines along these lines in the future. Costs are expected to drop as the specialized ring generator is produced in larger volumes.

Wind speed is a stochastic, or random, second-order stationary process, that is, 1) its mean is independent of time, and 2) the correlation between values of the process at different points in time depends only on the time interval (Δt) separating those points. This autocorrelation factor ($A(\Delta t)$) is written as:

$$A(\Delta t) = \exp(-\Delta t / C). \quad (1)$$

Here, C is the autocorrelation coefficient for a given set of wind speeds. Typical values of this parameter for winds over the US Great Plains are between 6 and 10 hours.

In addition, wind speed magnitudes are distributed with a Weibull distribution. The wind speed probability density function is written as:

$$f(v) = \frac{k}{c} \cdot \left(\frac{v}{c}\right)^{k-1} \exp - \left(\frac{v}{c}\right)^{k}, \quad (2)$$

where c is the scale factor and is typically about 1.1 times the average velocity, and k is the shape factor. Values of k are around 2 for winds at 10 m elevation, and between 2.2 and 3.5 for winds at 50 m elevation [3]. For this study a wind power density of 450 W m^{-2} at 50 m elevation with a Weibull k factor of 2.5, both without seasonal variation, is assumed; this describes the wind resource over large areas of the US Great Plains as well as other regions.

To generate wind speed time series with the appropriate characteristics of wind power density, Weibull k factor and autocorrelation time to be used in the simulation, the method outlined in reference 7 was used. Two unit variance Gaussian sequences incorporating the weighting factors that control the correlation in the process are generated using the Gaussian zero mean and unit variance number generator. These two Gaussian time series are combined in an intermediate exponential time series which is one-half the sum of the squares of the Gaussians. The Weibull-distributed wind speeds are then generated using a power law transformation of intermediate time series.

4. SIMULATING A WIND ENERGY BASELOAD SYSTEM WITH STORAGE AND VARIABLE WIND SPEED AUTOCORRELATION TIMES

The system and subsystem parameters, which are representative, not definitive, of the wind energy baseload plant used in this simulation are listed in Table I. Minimum system size is limited by CAES system requirements, such as the costs involved in creating the underground reservoir; CAES systems much below 100 MW are much less economical than larger systems. Different combinations of the number of wind turbines and CAES systems (charge, discharge, and storage volume) can be combined to achieve a given capacity factor; in an actual installation the installed capital cost of the different subsystems and the desired reliability would determine the actual plant configuration.

The wind plant simulation proceeds as follows: for a given wind speed autocorrelation time, 2200 random numbers are generated using the method explained above. The wind power density of the simulated wind data must be within one percent of the 450 W m^{-2} specified for the data to be accepted. This number of data points corresponds to hourly averaged wind data for a three month interval. For each wind speed in the series, the wind turbine output at the given wind speed is determined, then multiplied by the number of wind turbines in the wind farm and the factor (1-L) to account for array and other losses (L). If the wind farm output is greater than the transmission line capacity and the storage reservoir is not full, the excess is (reduced by the factor 0.9 to account for possible mismatches between the compressor capacity and available power) is added to the storage reservoir. When the wind farm output falls below the transmission line capacity and the storage reservoir is not empty, the amount of energy needed or available is multiplied by the energy ratio and withdrawn from the reservoir. Wind plant and CAES system capacity factors, spilled power and fuel consumption of the CAES system are computed for each set of simulated wind data.

TABLE 1 WIND ENERGY BASELOAD PLANT PARAMETERS	
Parameter	Value
Wind Plant Output	200 MW Capacity Factor: 95.4 percent (CAES, Transmission Line Availability 100 percent)
Wind Resource	450 W m^{-2}, Weibull k=2.5, 50 m elevation Wind speed autocorrelation time: 0-20 hours
Wind Turbine	500 kW, 50 m hub height (Enercon E-40 power output curve)
Oversized Wind Farm	1150 wind turbines, 575 MW maximum output Array and Other Losses: 15 percent
Transmission Line	200 MW HVAC Line
CAES System	Charge Rate: 225 MW Discharge Rate: 150 MW Hours of Storage (at Discharge Rate): Variable Energy Input/Energy Output: 0.67 Charging Efficiency: 0.9

Results for the case of C=0 are shown in Figure 1.

This indicates that only three or four hours of storage capacity are required to transform the intermittent wind plant with a capacity factor 61.4 percent without storage to a plant with a capacity factor of over 90 percent, that is a baseload power supply. The storage system functions mostly to cover short term interruptions in output. This is an optimistic and misleading result, since wind velocities are in general not uncorrelated. However, if an area were to have this type of wind over a significant part of the year, such a resource could indeed easily be transformed into something much more manageable, perhaps using above ground storage tanks instead of an underground reservoir.

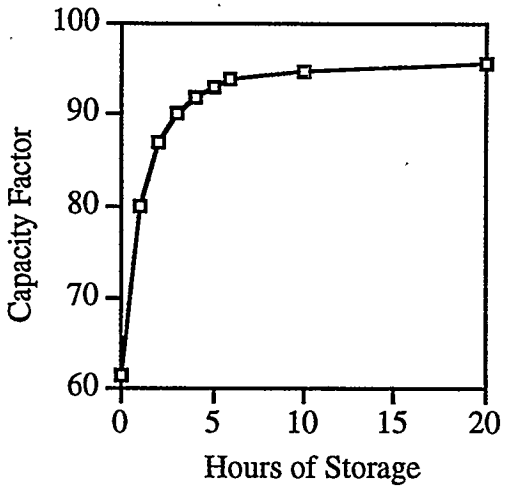

Figure 1. Capacity factor vs Hours of Storage for Uncorrelated Wind (C=0)

For the more realistic example of significant autocorrelation times, the results are quite different (see Figure 2). For the assumed system parameters (TableI I), the plant without storage has a capacity factor of 61.4 percent; for a storage reservoir of 20 hours capacity, the capacity factor decreases from 95.4 percent to about 83 percent as the autocorrelation time increases from C=0

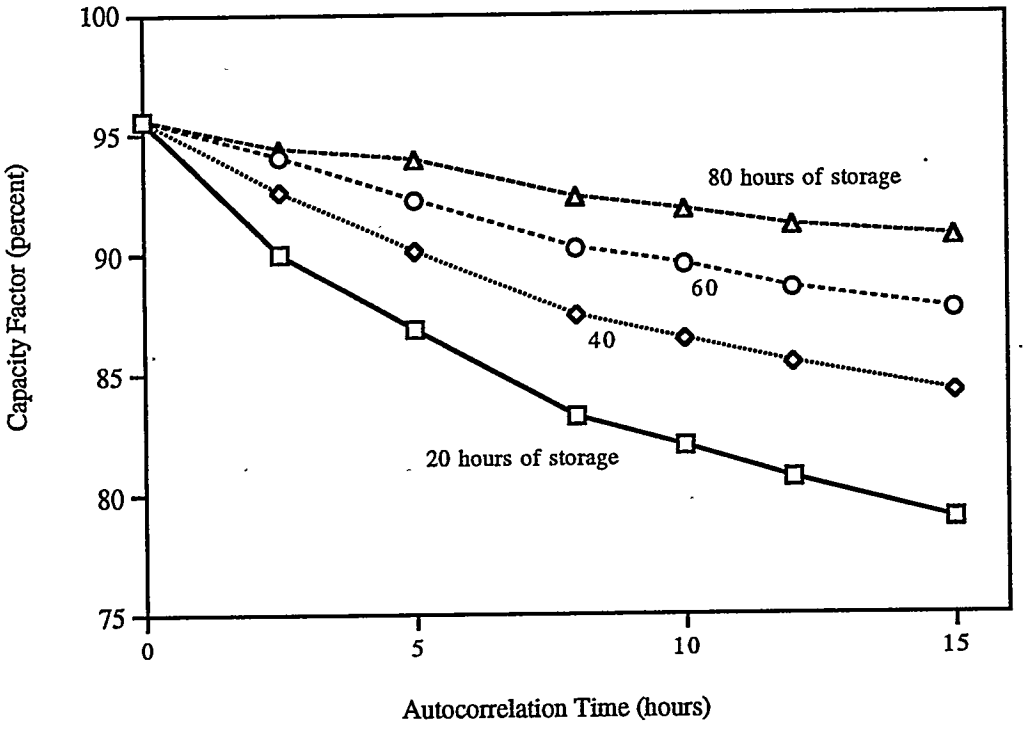

Figure 2. Capacity Factor vs Autocorrelation Time (C) for a wind energy baseload system. The individual curves are for systems with 20, 40, 60 and 80 hours of storage capacity.

to C=10 hours. At least 60 hours of storage is needed if the capacity factor is to remain above 90 percent at an autocorrelation time of 10 hours for the parameters assumed for this wind plant.

5. DISCUSSION AND CONCLUSIONS

The magnitude of the impact of the autocorrelation time on storage system size is surprisingly large and somewhat counter to what might be expected. It might be reasonable to anticipate that a storage system size of about twice the autocorrelation time would be more than sufficient to minimize its effect, but this is not the case at all. It appears that a storage system size of at least five times the autocorrelation time is needed to insure that its impact on system capacity factor is negligible. Thus, even in this simple case in which there is no seasonal variation in the wind resource, a storage reservoir of substantial size is necessary to transform intermittent wind energy to baseload, or constantly available, power.

In a broader sense, these results indicate that unless a storage system has not only a high charge rate but also a large storage capacity, the increase in available energy from the ensemble will be far below what might otherwise be expected. In the example considered here, a system with a 20 hour storage capacity and a wind resource with a ten hour autocorrelation time would only attain 64 percent of its expected increase in capacity factor due to the interaction of the autocorrelated wind with the wind plant-storage system.

Fortunately, the cost of developing large underground storage volumes for CAES systems is not large compared to the cost of the above ground portion of the plant [5], so that there are no real technical or economic obstacles to developing wind energy baseload systems.

ACKNOWLEDGMENT

This work was made possible thanks to a grant from The Energy Foundation. The wind plant simulation was part of the fine work done by Todd Lowpensky of Princeton University as part of his undergraduate independent work.

REFERENCES

[1] H. Hubbard, The Real Cost of Energy, Scientific American, April, (1991) 36.
[2] A. Cavallo, Security of Supply: a Neglected Fossil Fuel Externality, Proceedings, 17th Annual British Wind Energy Association Conference, Warwick, UK (1995) 171.
[3] A. Cavallo, High Capacity Factor Wind Energy Systems, J. Solar Energy Eng., **117**, 137-143, 1995.
[4] R.B.Schainker, B.Mehta and R.Pollak, Overview of CAES Technology, Proceedings of the American Power Conf., Illinois Inst. of Tech, (1993), 992.
[5] A. Cavallo and M. Keck, Cost Effective Seasonal Storage of Wind Energy, Solar Energy Division **16**, Am. Soc. Mech. Eng., New York, NY, (1995) 119.
[6] Enercon, 1993, Dreekamp 5, D-2960, Aurich, Germany.
[7] A.Mcfarlane, P.S.Veers and L.Schluter, Simulating High Frequency Winds for Long Durations, Solar Energy Division **15**, ASME, NY,NY, (1994) 175.

CURRENT AND FUTURE PLANS FOR WIND ENERGY DEVELOPMENT ON SAN CLEMENTE ISLAND, CALIFORNIA

Patrick J. F. Hurley
RLA Consulting, Inc.
18223 102nd Avenue NE, Suite A
Bothell, Washington 98011

S. Brian Cable
Naval Facilities Engineering Service Center
1100 23rd Avenue
Port Hueneme, California 93043-4370

ABSTRACT

The Navy is considering possible ways to maximize the use of wind energy technology for power supply to their auxiliary landing field and other facilities on San Clemente Island. A summary of their past analysis and future considerations is presented. An analysis was performed regarding the technical and economic feasibility of installing and operating a sea-water pumped hydro / wind energy system to provide for all of the island's electric power needs. Follow-on work to the feasibility study include wind resource monitoring as well as procurement and preliminary design activities for a first-phase wind-diesel installation. Future plans include the consideration of alternative siting arrangements and the introduction of on-island fresh water production.

BACKGROUND

San Clemente Island (SCI) is a Navy owned and operated island located 75 miles northwest of San Diego, California. The island supports surface ship and aviation units of the Navy's Pacific Fleet. Federal Executive Order 12902 mandates that Federal agencies implement energy efficiency, water conservation, and renewable energy programs where possible. In response to this order, the Navy has issued a directive to encourage the use of practical and cost effective renewable energy alternatives to current or planned petroleum uses. In response to this directive, the Naval Facilities Engineering Service Center is pursuing options for utilizing wind energy on San Clemente Island.

The Navy has past experience with wind energy on SCI. From July 1983, and sporadically through March 1989, wind speed and direction data were collected from five locations along the island. The locations of these historical wind measurements are shown in Figure 1. In November 1987, a "prototype wind farm" of six 20 kW Jacobs wind turbines were installed, owned, operated and maintained by a third party under lease option arrangements with the Navy. These wind turbines are no longer operated as part of the SCI power system.

In 1995, the Naval Facilities Engineering Service Center completed a concept study for a San Clemente Island Pumped Hydro-Storage / Wind Energy (PHS/WE) System with assistance provided by MCA Engineers, RLA Consulting, Sverdrup Facilities, and TRAK Environmental Group. On the basis of that concept study, a first phase installation of up to 1 MW of wind turbine generation capacity is planned. Future plans include a wind-desalination component, as well as the eventual development of the PHS/WE system.

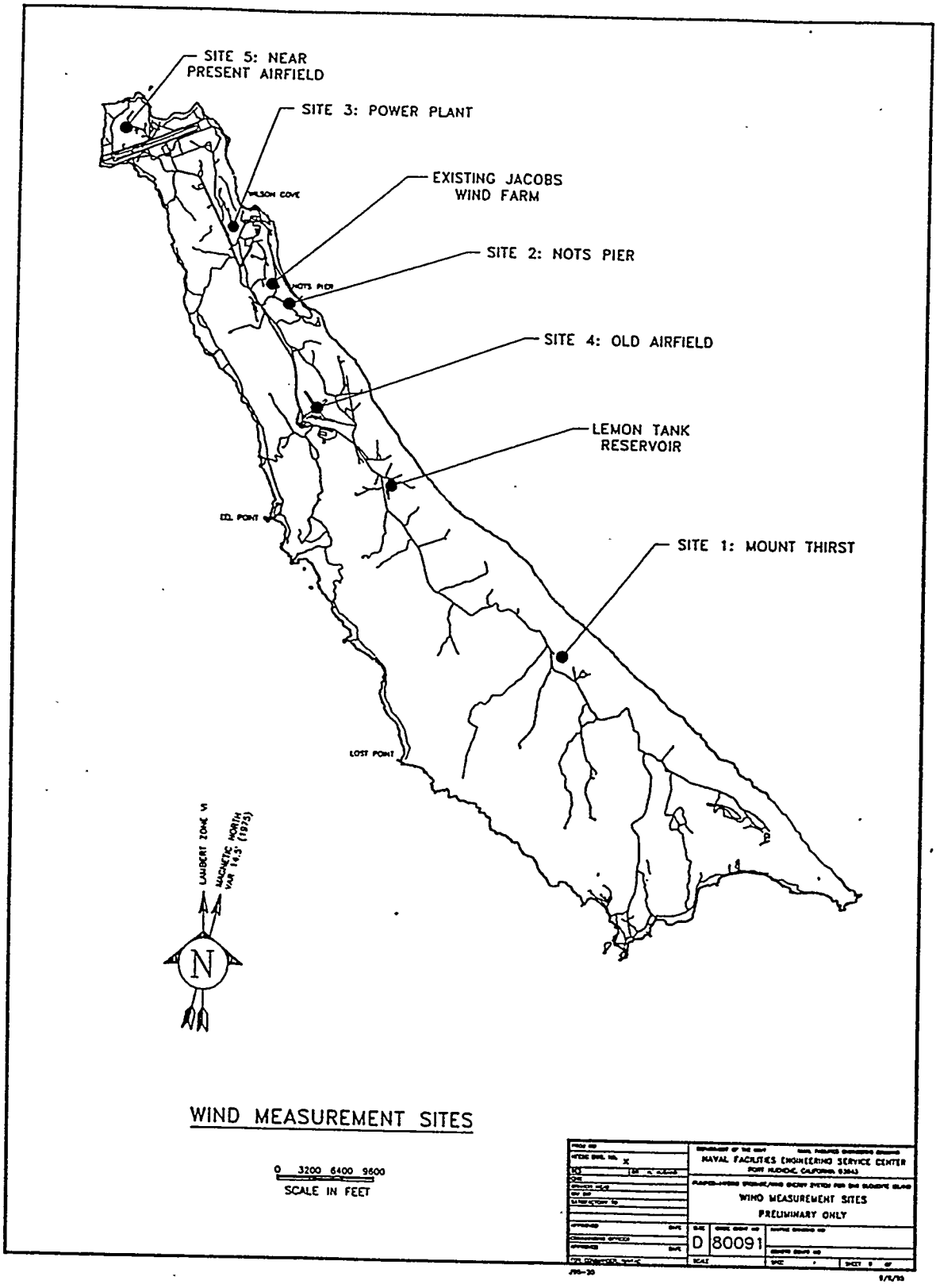

Figure 1. Locations of Past SCI Wind Measurements

SUMMARY OF CONCEPT STUDY

The overall approach used in the concept study was to identify the most appropriate size and configuration of the wind farm, the pumped hydro storage facility, and the power distribution, control, and monitoring subsystems to provide a preliminary design of the most cost-effective system configuration given the operational and physical constraints. The methodology involved the following phases:

1. Assess the island wind resource based on historical data
2. Establish the electrical load requirements based on historical data and projected growth
3. Identify PHS/WE system performance requirements
4. Identify possible sites for wind farm and pumped hydro storage facilities
5. Develop system configurations that meet system requirements
6. Optimize for the most cost effective system configuration based on modeled system performance, and life-cycle costs

Based on a review of the existing wind data, the topography of the island, existing land use patterns, and a rough idea of the wind farm performance requirements, two sites were identified that would suitable and potentially large enough for the PHS/WE wind farm component. Extrapolating data from a monitoring station near to one of the proposed wind farm sites, an estimate of the site wind resource was developed adjusted for long-term representativeness and wind shear. The predicted annual average wind speed at 130 ft above ground level was 5.9 m/s (13.3 mph). Three wind monitoring stations were installed to verify the wind resource at the proposed wind farm locations. Data from these locations are currently being evaluated. An example of the wind speed data collected at one of the new monitoring stations is shown in Figure 2.

Electrical load requirements and system performance requirements were established with the assistance of the Navy personnel from the San Clemente Island utility and Navy Public Works Departments. The maximum allowable utilization of diesel generators was targeted for 400 MWh per year based on current and anticipated emissions requirements and emissions goals.

The NFESC conducted field surveys to assess possible reservoir sites and system configurations. This effort focused on identifying the best configuration based on minimum cost and environmental impact. Alternative options included: (a) converting an existing reservoir into a sea water storage facility, (b) constructing a new sea water reservoir, and (c) constructing a closed loop, two-reservoir system. A utility-scale battery storage system was also considered as an alternative, but was ruled out due to cost and reliability considerations.

The preferred system configuration consisted of a 9 MW wind farm, a 2.4 MW hydroelectric generation and pumping facility, and a new 200 million gallon reservoir excavated and lined with a non-permeable liner and leak detection system. The general arrangement of the preferred PHS/WE system is shown in Figure 3. The energy contribution of various system components according to the performance model is shown in Figure 4.

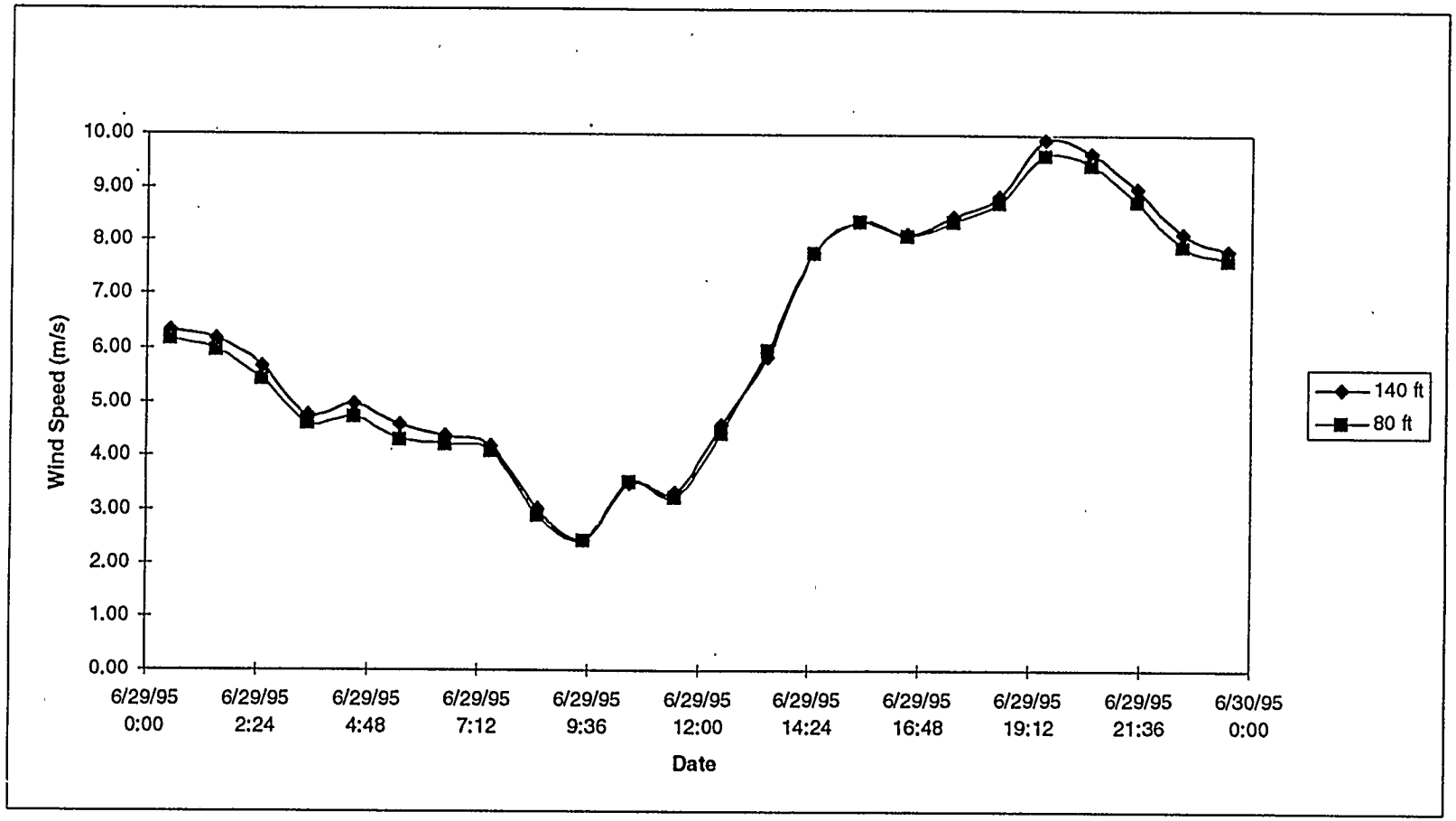

Figure 2. SCI Tower #2 Wind Speed

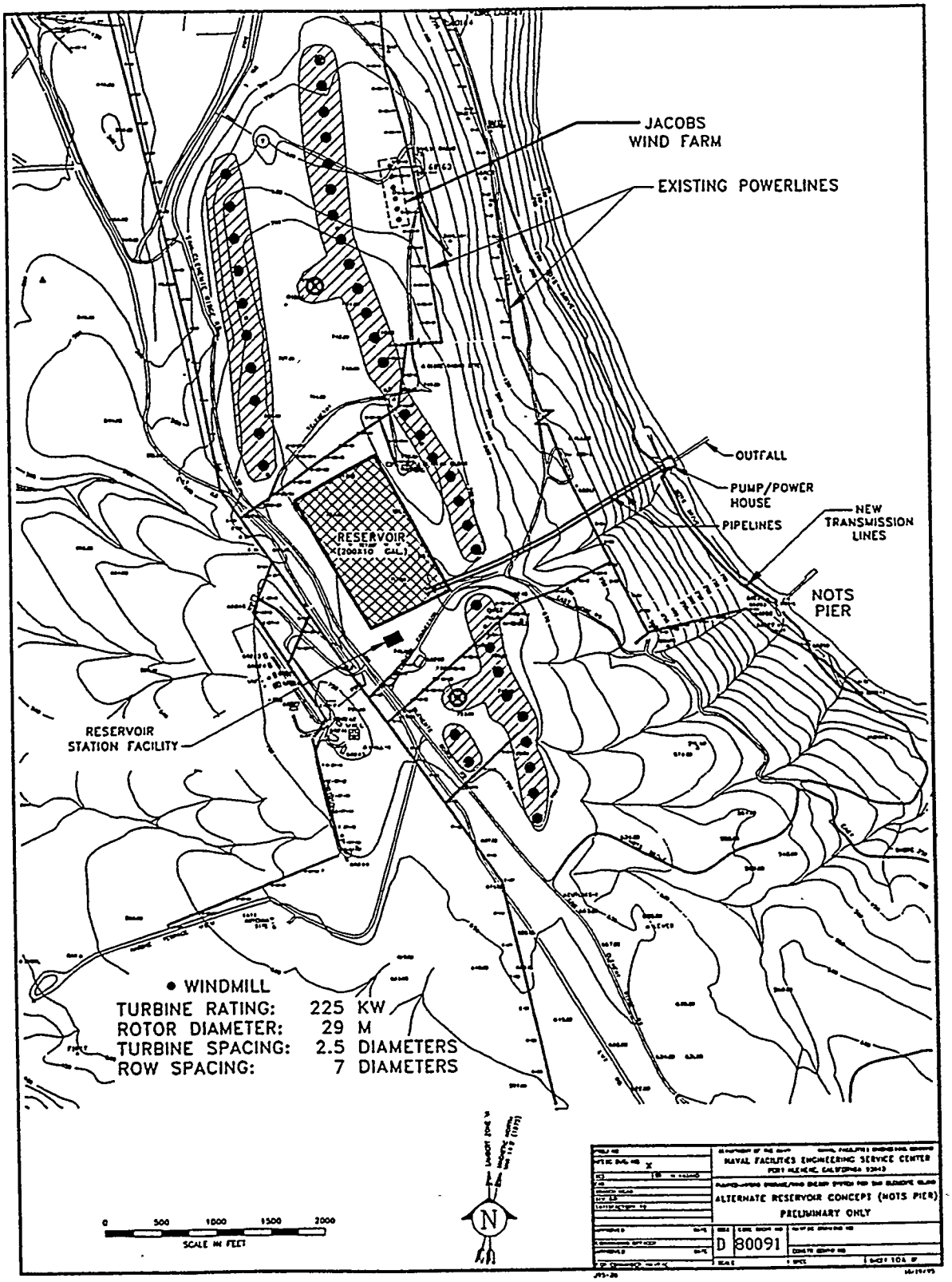

Figure 3. Proposed PHS/WE system

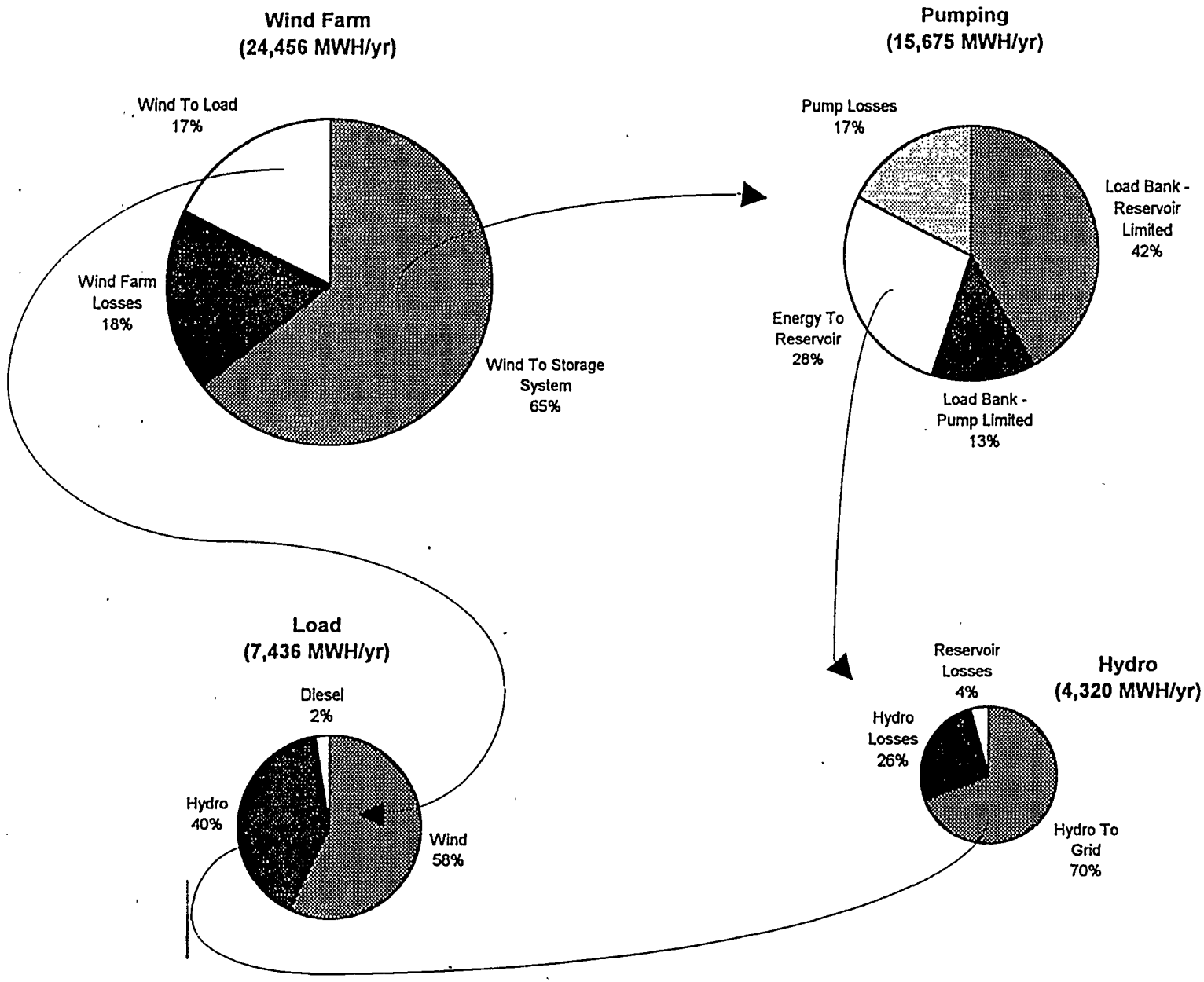

Figure 4. System Energy Balance

The results of the concept study indicate that a PHS/WE system is feasible for San Clemente Island and can meet their energy needs while reducing the Navy's dependence on fossil fuels. The PHS/WE system is based on commercial off-the-shelf technology and would include a 9 MW wind farm, a hydroelectric facility with three 800 kW hydro-turbine generators, and a sea water pumped storage facility. The pumping system would consist of sea water pumps powered from wind generated power in excess of the island electrical loads. The existing SCI diesel electric generators would serve for emergency backup purposes only.

The existing utility system on SCI is powered by a 2.95 MW diesel power plant. Diesel fuel, water, and other goods are barged to the island. The current peak and average electrical loads are 1,200 kW and 850 kW respectively, and the existing power plant produces electric power at $0.39 per kWh.

Benefits of the proposed PHS/WE system include a reduced dependence on fossil fuel, compliance with existing and future Southern California Air Quality Management District emissions requirements, and reduced risk of a hazardous spill during the transportation and handling of diesel fuel.

CURRENT STATUS

- Preliminary design of the PHS/WE System is complete
- Environmental Assessment in progress
- First Phase (up to 1 MW) to be installed in 1997
  - Funding provided through the US Department of Energy's Strategic Environmental Research and Development Program (SERDP)
  - Bidding documents have been released and responses received by several qualified vendors
  - Contract award for First Phase expected in August 1996

FUTURE PLANS

- Proposal submitted to the Navy's Energy Conservation Investment Program for an additional 1 MW Wind / Desalination component
- Funding options being explored by the Navy
- Significant costs savings from Wind / Desalination including delivery of goods:
  - 11 million gallons of water per year at $32.05 per 1,000 gallons
- Alternative to Wind Component
  - 13 ¢ / kWh fuel costs (barging included)
  - $40,529 per year maintenance

ACKNOWLEDGMENTS

In addition to the support of the Ed Cannon, and Ed McKenna from the National Renewable Energy Laboratory, the authors would also like to acknowledge the following concept study contributors: Tom Brule and Zaldy Hidalgo, San Diego Public Works Center; Ken Nicoll, SCI Public Works Department, Bob Miner, NAVFAC Southwest Division; Environmental and Natural Resources, North Island Naval Air Station; MCA Engineers, Sverdrup Facilities, and TRAK Environmental Group.

REFERENCES

Wind Resource Assessment for Naval Auxiliary Landing Field, San Clemente Island, California, TM M-73-86-10, Naval Civil Engineering Laboratory, June 1986

Development of a Prototype Wind Farm at Naval Auxiliary Landing Field, San Clemente Island, California, TM M-74-90-04, Naval Civil Engineering Laboratory, December 1989

Concept Study for a Pumped Hydro Storage/Wind Energy System at San Clemente Island, SSR-2171-E&U, Naval Facilities Engineering Service Center, December 1995.

IMPROVEMENT OF LOW SPEED INDUCTION GENERATOR PERFORMANCES AND REDUCING THE POWER OF EXCITATION AND VOLTAGE CONTROL SYSTEM

N. Budisan
"Politechnica" University of Timisoara, Department of Automation,
Blvd. V. Parvan nr.2, 1900 Timisoara, Romania.
Tel. (011.40.56) 196184 Email: nbudisan@utt.ro

T. Hentea and S. Mahil
Purdue University Calumet, Engineering Department,
Hammond, IN 46323-2094, USA.
Tel. (219) 989-2472. Fax (219) 989-2898.

G. Madescu
Romanian Academy, Timisoara Branch,
Blvd. Mihai Viteazu nr.24, 1900 Timisoara, Romania

Abstract

In this paper we present the results of our investigations concerning the utilization of induction generators at very low speed. It is shown that, by proper design, it is possible to obtain high efficiency and high power factor values. The optimized induction generators require lower reactive power resulting in lower size and price of the excitation control system.

Introduction

In our previous papers [1,2] we presented concepts about equipping autonomous windgenerators and wind, diesel, hydro and mixed systems exclusively with induction generators, emphasizing the advantages in cost, robustness, maintenance and control system simplification. We proposed and studied the following original solutions for induction generator systems: constant capacitance excitation and speed control of the voltage; constant frequency and variable speed; variable frequency, constant speed; constant capacitance excitation and voltage stabilization through load compensators; continuous-variable capacitance excitation; and mixed wind-hydro-thermal motor systems with induction generators only.

The usual trend is to employ low speed generators, as for example, permanent magnet synchronous generators coupled directly to wind turbines. In our opinion, however, induction generators are justifiable even for very low speeds because of their advantages in simplicity, cost, and control opportunity.

The autonomous induction generators, however, have an important reactive power Q relative to machine rated power P_N. For instance [1],

$(Q)_N = 0.6P_N$, at 1 kW, 3000 RPM
$0.46P_N$, at 55 kW, 3000 RPM
$0.96P_N$, at 1 kW, 750 RPM
$0.64P_N$, at 55 kW, 750 RPM
$4.43P_N$, at 1 kW, 250 RPM
$3.71P_N$, at 2.5 kW, 250 RPM

The excitation reactive power of a small power and small speed machine is relatively large. However, these machines are constructed using the existing technologies without considering the possibility of optimization by choosing alternative machine dimensions and technologies.

1. Low speed induction machine design for high efficiency

In view of the above considerations, and because the reactive power is involved in excitation, and additionally it affects the power required and the cost of the voltage control system, it is important to clarify whether it is possible or not to improve the power factor values of low speed induction generators by reducing the excitation reactive power of these machines. This question was addressed for induction machines with large number of poles.

A computer program for optimization of three-phase induction machines was developed by one of the authors, G. Madescu, for ELECTROMOTOR S.A., Timisoara, Romania. The program maximizes the product of efficiency by the power factor ($\eta\cos\phi$) No cost factors were taken into account. The high efficiency of many machines manufactured with specifications determined by this program proves its correctness and utility.

In this paper we present our investigations concerning threephase induction machines with the following rated values and constructive features: power-4 kW, p=12, voltage-380/220 V, winding connection-star, air gap-0.4 mm, D_{1i}= 0,85 D_{1e}, D_{2i}= 0.65 D_{1e}.

For a given external stator diameter D_{1e}, the program finds the optimum values of the following parameters: internal stator diameter, stator/rotor length, slot dimensions, conductor section, etc. The problem is solved for different values of the external diameter D_{1e}. Let denote by λ the ratio between the stator/rotor length L_1 and the pole pitch τ , that is $\lambda = L_1/\tau$. Computations were made for two values of the slots number per pole and phase. The results obtained are plotted in Figure 1 as function of λ. The following notations were adopted: q - number of slots per pole and phase, D_{1e}-external stator diameter, L_1-stator/rotor length, η-efficiency, $\cos\phi$ - power factor, I_N-rated current, I -magnetizing current. x_m-magnetizing reactance, x_{10}-stator dispersion reactance, x_{20}-rotor dispersion reactance, M_K-maximum torque, M_N-rated torque, S-apparent power, Q-reactive power, G_{Cu}-copper weight, G_{Fe}-active iron weight.

From the results given in Fig. 1 the following observations are drawn:

1. For q=2 the external diameter and the length are smaller than in case of q=1 (see Fig.1a,b). Conversely, the parameters η and $\cos\phi$ are greater (see Fig. 1c,d,e);it is, therefore, advantageous to choose values of q equal or greater than 2;

2. Optimum values of the product ($\eta\cos\phi$) are dependent on λ and q (see Fig. 1e); it is preferable to have small values of λ and q > 2. For q=2 high values of the product ($\eta\cos\phi$) can be obtained, namely ($\eta\cos\phi$) > 0.5. In Catalog M11-Siemens-1990 for a motor of 4 kW, 2p=8, the product ($\eta\cos\phi$) = 0.57;

3. The values of the magnetizing current I_μ and of the magnetizing reactance X_m are about equal to those of common machines with 2p=6 and 2p=8 (see Fig. 1f,g);

4. In case of q=2 the dispersion coefficients $X_{1\sigma}/X_m$ and $X_{2\sigma}/X_m$ are acceptable (see Fig. 1h,i) and decrease for small values of λ;

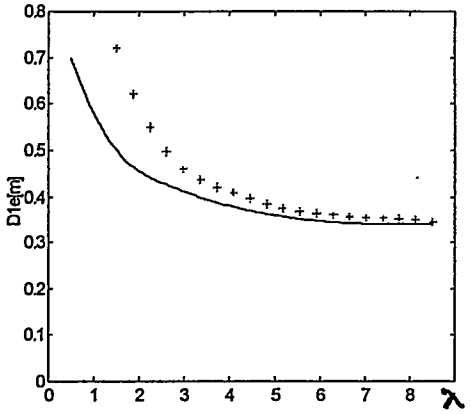

FIG. 1a.EXTERNAL STATOR DIAMETER (q=1 + ; q=2 -)

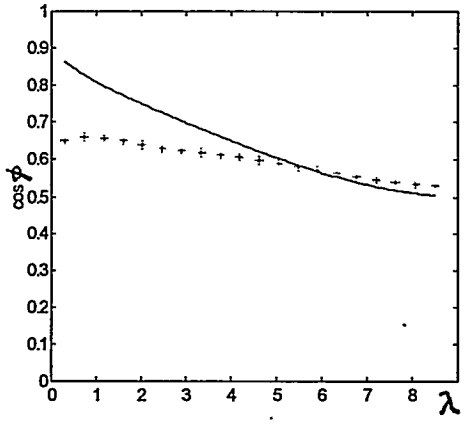

FIG. 1d. POWER FACTOR (q=1 + ; q=2 -)

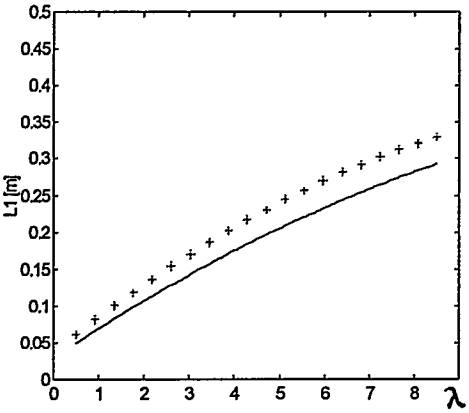

FIG. 1b. STATOR/ROTOR LENGTH (q=1 + ; q=2 -)

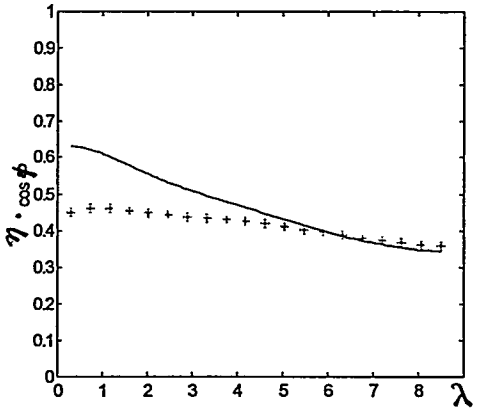

FIG.1e.EFFICIENCYxPWR FACTOR (q=1 + ; q=2 -)

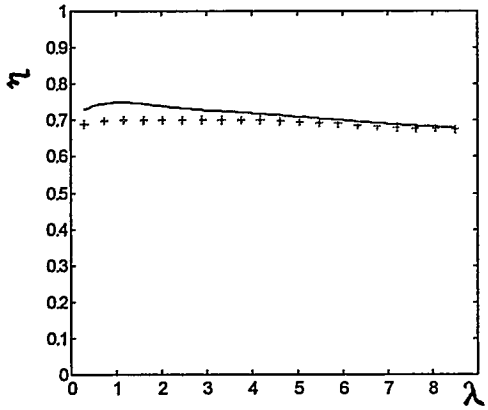

FIG. 1c. POWER EFFICIENCY (q=1 + ; q=2 -)

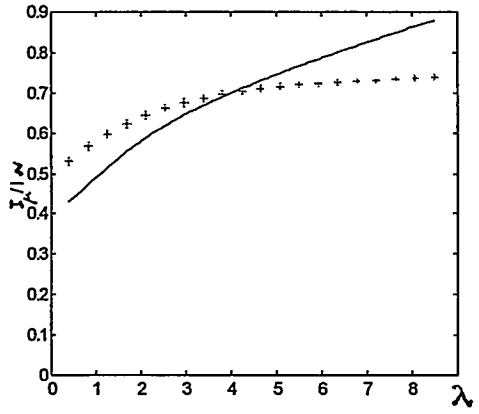

FIG. 1f. MAGNETIZING CURRENT (q=1 + ; q=2 -)

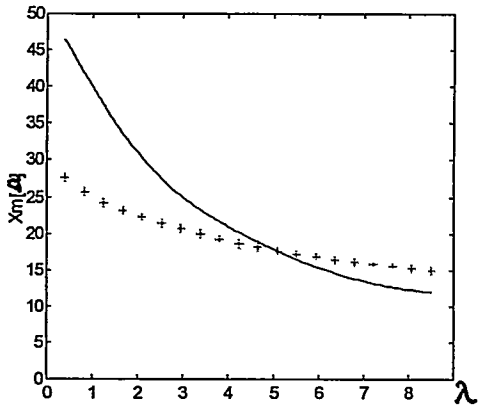

FIG.1g. MAGNETIZING REACTANCE
(q=1 + ; q=2 -)

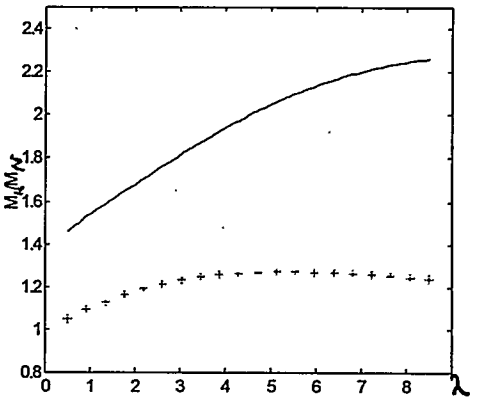

FIG. 1j. TORQUE RATIO
(q=1 + ; q=2 -)

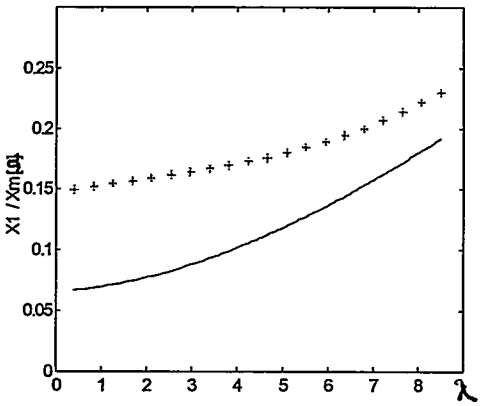

FIG. 1h. STATOR DISPERSION
(q=1 + ; q=2 -)

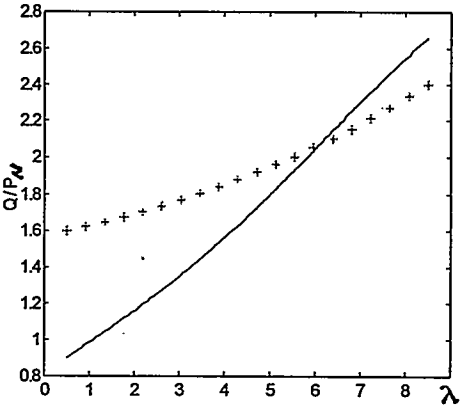

FIG. 1k. REACTIVE POWER
(q=1 + ; q=2 -)

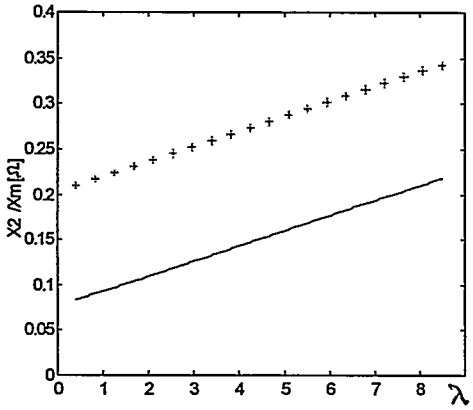

FIG. 1i. ROTOR DISPERSION
(q=1 + ; q=2 -)

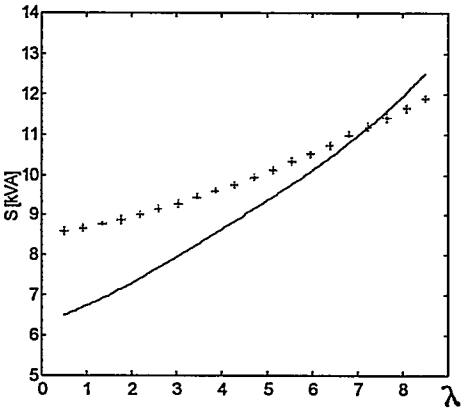

FIG. 1l. APPARENT POWER
(q=1 + ; q=2 -)

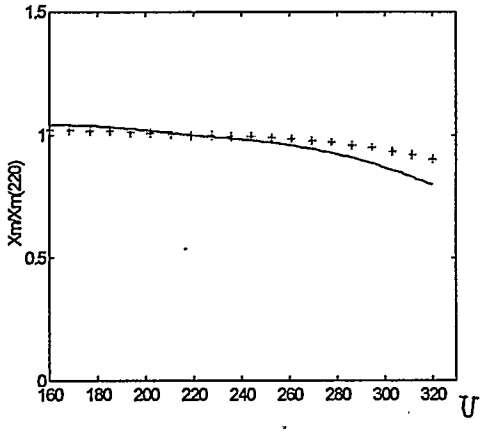

FIG.1m.MAGNETIZING REACTANCE
(q=1 + ; q=2 -)

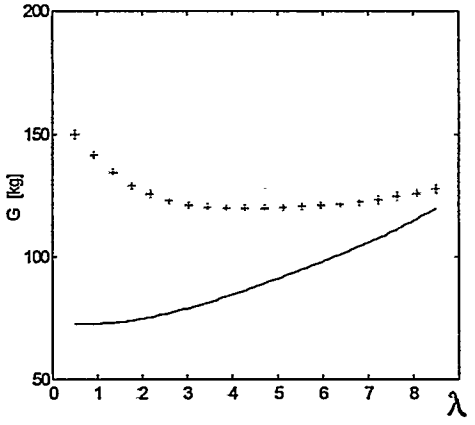

FIG. 1o. IRON WEIGHT
(q=1 + ; q=2 -)

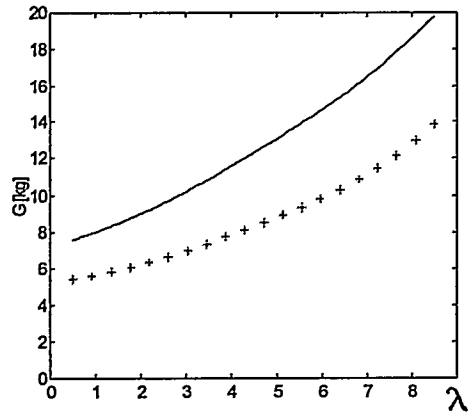

FIG. 1n. COPPER WEIGHT
(q=1 + ; q=2 -)

FIG. 1. OPTIMIZED PARAMETERS AND CHARACTERISTIC VALUES OF SMALL SPEED INDUCTION MACHINES (2p=24, P = 4 KW)

5. In Fig. 1j, it may be seen that the ratio of the maximum torque M_K to the rated torque M_N decreases with λ. Consequently, for an imposed critical torque, the value of λ must not be less than a certain minimum value. Also, in generator regime the critical torque is greater than in motor regime with 40-50% for q=1 and with 70-100% for q=2. Hence, q should be chosen greater than 1.

6. Figures 1k and 1l show the possibility of drastic decreases of the reactive power Q and apparent power S of small speed machines comparatively with those of the existing small speed induction machines; this is, of course, the consequence of higher power factor shown in figure 1d;

7. The Fig. 1n and Fig. 1o show the way of reducing the copper and iron weight by considering small values of λ.

2. Excitation Control System

It is known that the excitation reactive power Q of autonomous induction generators consists of a constant part Q_0 independent of the load, and a varying part ΔQ, which varies with the load. The varying reactive power ΔQ is submitted to the excitation control system and determines the size and cost of that system.

To exemplify, in Figure 2 is given the scheme of our excitation system (Romania Patent NR. 98589, 1987) for autonomous induction generators consisting of a constant capacitance C_0 (battery of capacitors) required at no load and a variable capacitance ΔC required at load. The latter consists of a constant capacitance C and a variable inductance L_{var} magnetic amplifier MA.

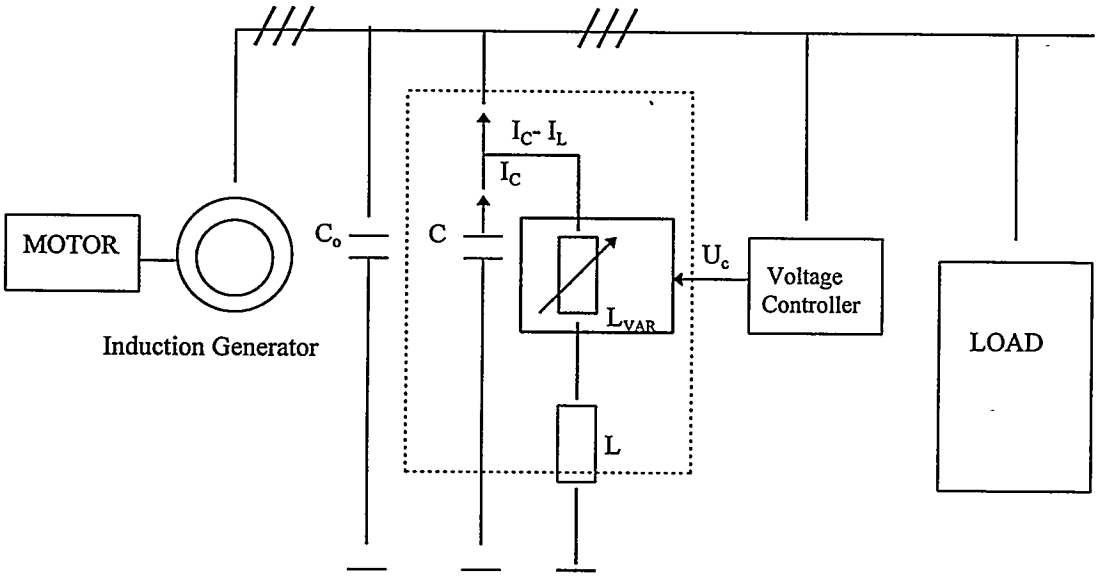

FIG. 2. EXAMPLE OF AUTONOMOUS INDUCTION GENERATOR EXCITATION SYSTEM.

Using an autonomous induction generator equivalent scheme developed by us and presented in [1,2], and proper computer programs, it is possible to determine the working characteristics of the generator for different regimes (n=const, n-controlled, etc.) and different loads, and hence the reactive excitation power and its components Q_0 and ΔQ. For the induction machine of 4 KW, 250 RPM, U=220 V, q=2, λ= 1.5 considered above, at variable power P= (O-4167) W, the following results were obtained:

-at s = 0, P = 0 W Q_0 = 3936 VAR

-at s= -0.035 P = 4167 W Q = 5755 VAR $\cos\phi$ = 0.59

-in the power interval, P, from 0 to 4167 W $\Delta Q = Q - Q_0 = 1819$ VAR, and $\Delta Q / Q_0 = 0.46$, $\Delta Q / P = 0.44$, $Q / P = 1.38$.

The parameters necessary for the excitation system considered in Fig. 2 are: $C_0 = 86.2$ μF, C= 40 μF, L = 254 mH, $I_L = 2.76$ A, $I_{MA} = 2.76$ A.

Conclusions

(1) Adopting proper manufacturing technologies it is possible to obtain high efficiency and high power factor values for small speed induction machines needed for windgenerators. This is equally true for autonomous generators and for generators connected to the grid.

(2) For optimized low speed induction generators the controlled excitation system has, relatively, a small reactive power comparatively to the total reactive excitation power and thus a small size and price.

REFERENCES

1. Budisan, N., S. Stern, and A. Spilca. "Characteristics of the autonomous self-excited generator with voltage stabilization by rotation speed at hydro/wind/diesel plants," Symposium on ***Ecological Small Hydro Power Social and Economic Impact,*** October 5-7, 1993, Timisoara, Romania.

2. Budisan, N., and T. Hentea. "Autonomous hydro, diesel, wind, biogas single or mixed energetical systems with asynchronous generators," ***30th Intersociety Energy Conversion Engineering Conference***, July 31-August 4, 1995, Orlando, Florida, USA.

3. Watson, D.B., and J. Arrillaga. " Controllable d.c. power supply for wind-driven self-excited induction machines," ***Proceedings of the Institution of Electrical Engineers***, vol. 126, no. 12, Dec. 1979.

4. Elattar, M.M.K. "Controllable d.c. power supply from wind driven induction generator," ***Modeling, Simulation, and Control A,*** vol. 26, no. 2, 1990.

INVESTIGATING WIND POWER'S EFFECTIVE CAPACITY: A CASE STUDY IN THE CARIBBEAN ISLAND OF LA MARTINIQUE

Richard Perez, Jean-Michel Germa* and Bruce Bailey
AWS Scientific, Inc.
3 Washington Square
Albany, NY 12205
* La Compagnie du Vent, Paris, France

INTRODUCTION

In this paper, we report on the experimental determination of the effective capacity of wind and photovoltaic (PV) power generation with respect to the utility load requirements of the Island of La Martinique [1]. La Martinique is a French Overseas Department in the Caribbean Sea. The case study spans two years, 1990 and 1991. We consider wind generation at three locations in different wind regimes, and PV generation for fixed and tracking flat plate systems.

The results presented include: (1) An overview of typical solar and wind power output at each considered site, presented in contrast to the Island's electric load requirements; and (2) Effective capacities quantified for each resource as a function of penetration in the utility generation mix.

METHODS

Defining Effective Capacity

The *effective capacity* of a generating resource is its effective contribution to the generating capacity available, utility-system wide or locally, to meet electrical demand. This should not be confused with the commonly used term *capacity factor*, which represents the ratio between the average output of the considered generator and its rated capacity.

Because renewable electrical generation resources such as wind or solar are not dispatchable, they are generally assumed to have no effective capacity, and are considered strictly as energy producers. However, recent studies [2,3,4] have shown that, at least in the case of solar PV production, the effective capacity of the resource may be considerable, because the resource may be highly correlated with peak loads. Effective capacities as high as 80% of rated PV capacity have been observed for several US utilities [3]. In this paper we show that wind power generation may also exhibit sizable effective capacities.

Importance of Effective Capacity

A large portion of the value of a generating resource is a function of its utility-wide and/or localized effective capacity. Indeed, the value of a generating resource to a utility is defined in terms of (1) energy value and (2) capacity value. In addition, when considering distributed generation applications, the resource should also be valued in terms of *transmission and distribution (T&D)*. This value element is largely dependent on the resource's localized effective capacity.

Quantifying Effective Capacity

Several parameters have been introduced to quantify a generator's effective capacity. Here, we use two parameters which offer complementary measures of effective capacity.

The first parameter is the *Effective Load Carrying Capability (ELCC)*. Garver et al. [5] introduced this parameter for non-interconnected utilities. He defined it as the effective increase in the generating capacity available to a utility, due to the added generating resource, at constant loss-of-load capability. A normalized version of this parameter was introduced by the authors [2] -- this assumes a generic loss of load probability that focuses solely on the load-resource relationship. ELCC is reported in terms of percent of installed wind (PV) capacity.

The second parameter is the *Minimum Buffer Energy Storage (MBES)*. This provides a deterministic, worse case measure of the resource's capacity [4]. The MBES is defined as the minimum amount of energy reserve necessary, in addition to the considered resource, to insure an effective capacity of 100% . MBES is reported in system-hours, where "system" represents the wind (PV) installed capacity.

The experimental data necessary to estimate these parameters consist of time-coincident series of power plant output and (utility) load data. A complete year of data is generally preferable, with a data frequency of one hour or less -- in the case of PV, three-hourly data have been shown to offer an acceptable substitute to hourly data if the latter are not available [6].

EXPERIMENTAL DATA

A map of the island is provided in Figure 1. This shows the locations of the considered wind and solar sites. The map includes rainfall isopleths as a qualitative indication of both orography and solar radiation distribution over the island.

PV Production: Hourly PV production for 1990-91 was simulated from global irradiance, temperature and wind speed measured at Le Lamentin (Fig. 1). This site is little affected by orographic clouds that are often found near high elevations. A model (PVFORM 3.0 [7]) was used to simulate PV production from the available input data. The average daily PV output of two-axis tracking and fixed systems is shown in Figure 2.

Wind Production: Hourly wind power production was simulated for a typical variable speed wind turbine, from 3-hourly wind speed measurement at three sites located in different wind regimes: (1) on the upwind shore of the island (La Caravelle) , (2) on a mountain pass (Morne Des Cadets), and (3) off-shore on the downwind side of the island (in the Fort-de-France bay near Le Lamentin measuring station). The off-shore site benefits from orographic enhancement and daily thermal effects. The average daily wind power output profile for each of the wind sites is presented in Figure 3.

Utility Load: Utility load data for 1990 and 1991 were made available to us under the form of printed daily load profile charts. These were digitized into hourly data sets as part of our investigation. The mean and peak daily utility load profiles for 1990 and 1991 are shown in Figure 4.

RESULTS

ELCC Parameter

The effective capacities of the two PV array configurations and of the three wind locations, as quantified by the ELCC parameter, are compared in Figure 5. ELCC is plotted as a function of the resource's penetration on the grid, from 1% to 20% -- note that a 20% penetration for the grid of la Martinique would represent about 25 MW in 1991.

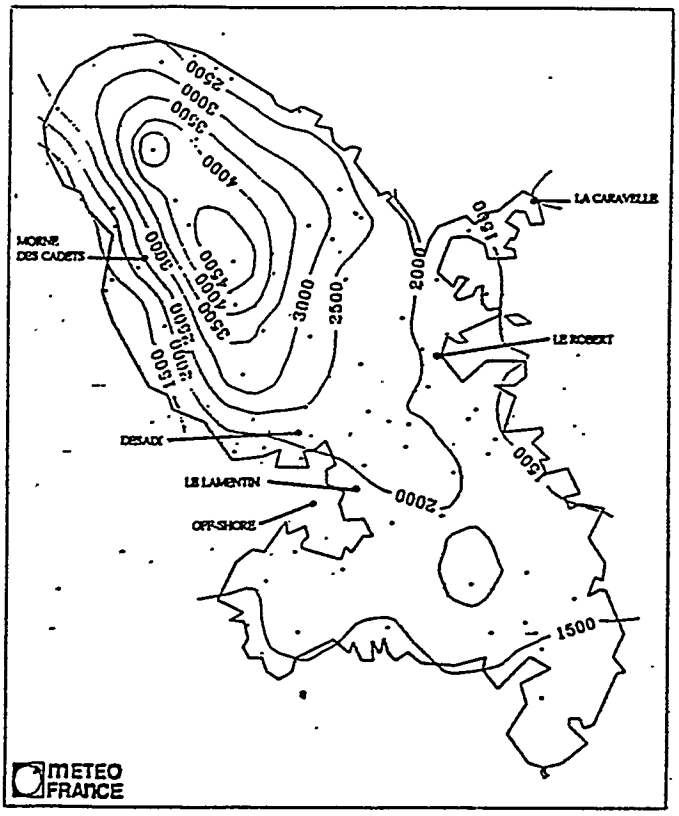

FIGURE 1: ANNUAL RAINFALL IN LA MARTINIQUE

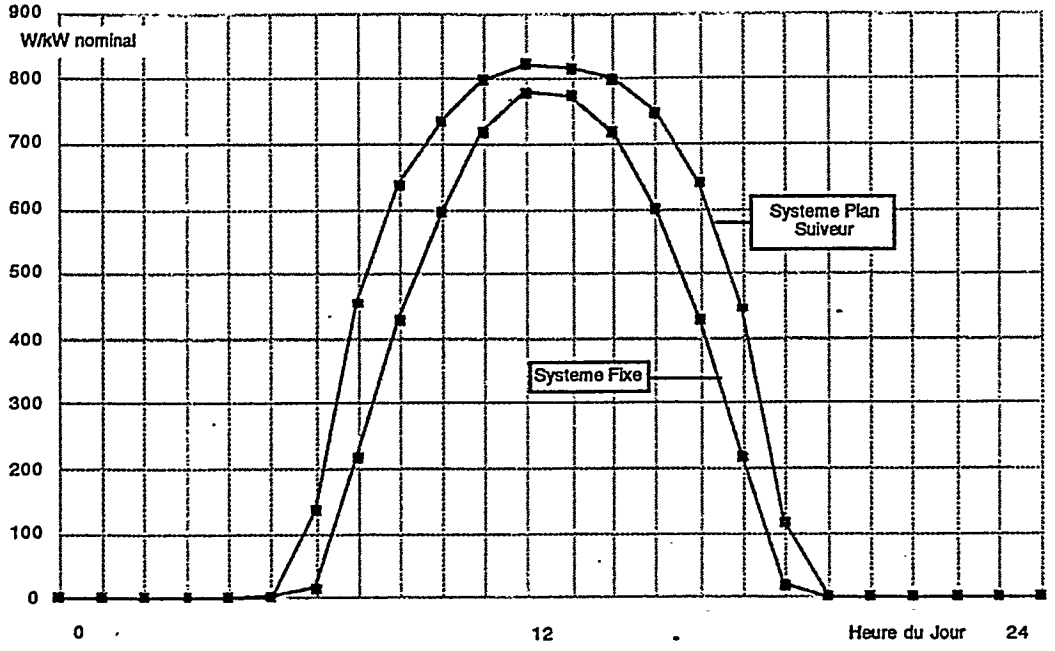

FIGURE 2: AVERAGE DAILY PV OUTPUT IN LA MARTINIQUE FOR FIXED AND TRACKING ARRAYS (1 KW NOMINAL)

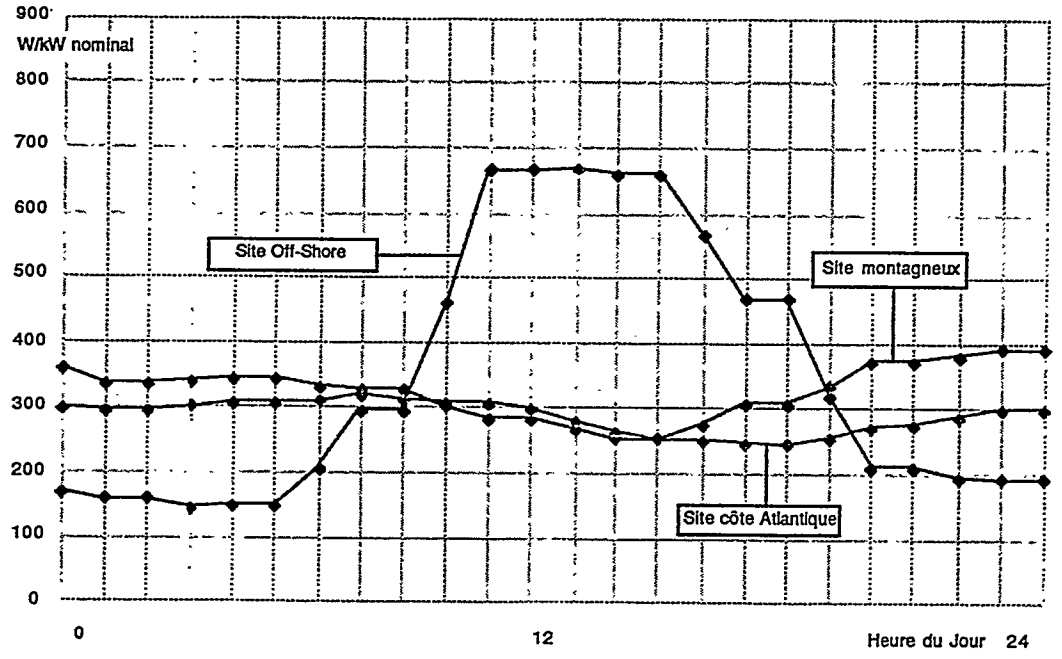

FIGURE 3: AVERAGE DAILY WIND POWER GENERATION AT THREE SELECTED SITES (1 KW NOMINAL)

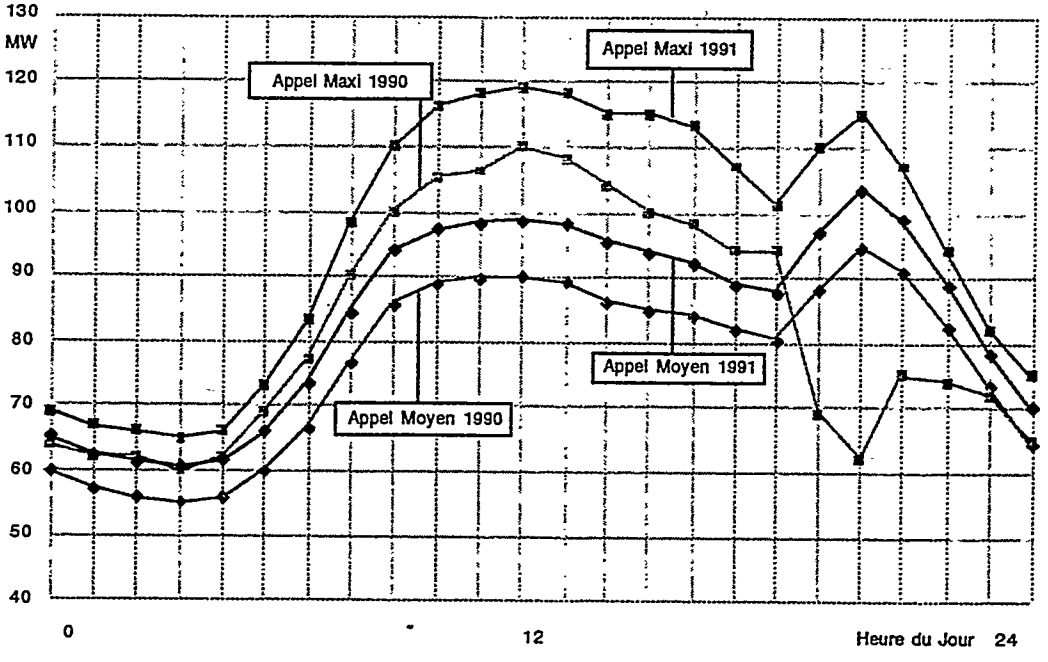

FIGURE 4: AVERAGE AND PEAK DAILY LOAD PROFILES IN LA MARTINIQUE IN 1990 & 1991

With an ELCC approaching 60% at low grid penetration, the effective capacity of PV is found to be substantial for La Martinique.

Wind effective capacities are not quite as high, however, the ELCC of one wind location, which benefits from mid-day thermal enhancement, is considerable and even tends to exceed that of PV as grid penetration increases.

MBES Benchmark

The minimum buffer energy storage necessary to insure 100% ELCC to each considered resource is plotted in Figure 6. Two grid penetration levels are reported, respectively 5% and 15%. The MBES for each resource is compared to the amount of stored energy that would have been necessary to achieve the same 100% ELCC without the help of the wind (PV) resource.

At 5% grid penetration (i.e., installed capacities of the order of 6 MW), only one hour worth of storage (i.e., 6 MWh) would be necessary to insure a 100% capacity credit to the two PV and one of the wind strategies. This is to be compared with almost four hours (24 MWh) worth of energy reserve to meet the same loads without the renewable resources.

Note that the concept of storage is used here as a measure of effective capacity. In practice, one could envision deploying small size storage together with wind/PV, and in cases where storage is already present (e.g., pumped hydro), its load control effectiveness could be greatly enhanced through the deployment of the renewable generation resource.

DISCUSSION

In this paper, we have shown that wind power generation may have a substantial effective capacity. In La Martinique, wind generation has been considered to have serious development opportunity based solely on its energy production value. The added benefit of an effective capacity that may approach 50% should, when properly accounted for, strengthen this opportunity and could make a critical difference between project success and failure.

This case study merits to be extended to other locations, as much remains to be learned about wind's effective capacity. Similar studies should be undertaken for other islanded networks similar to La Martinique -- e.g., other Caribbean islands, international isolated networks, localized loads -- as well as for interconnected US utilities or sub-utilities where localized capacity would constitute a premium.

Results for PV are less surprising today, and given La Martinique's load profile, are found to be fully consistent effective capacities observed for US utilities. Economic implications for the island are also less immediate, because grid-connected PV is not yet near its economic viability threshold -- in part because local electricity retail rates, which are tied to mainland France rates, do not fully reflect local costs. However, with effective capacities approaching 60% -- and 100% with minimized storage systems -- PV could become a very attractive grid support option for the island's grid.

ACKNOWLEDGEMENT

This study was funded by ADEME -- contract No. 1.05.0043/exercice 1991 – Project Officer: Bernard Chabot. Data processing was done by Hand-Made Software, Inc.

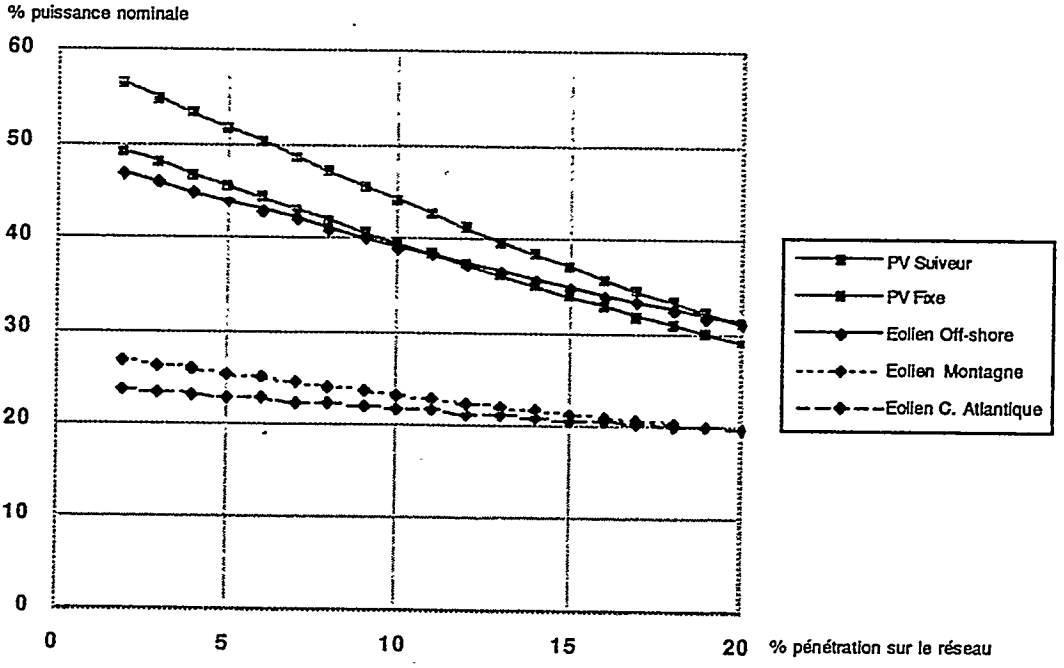

FIGURE 5: ELCC OF PV AND WIND FOR LA MARTINIQUE AS A FUNCTION OF RESOURCE PENETRATION ON THE GRID

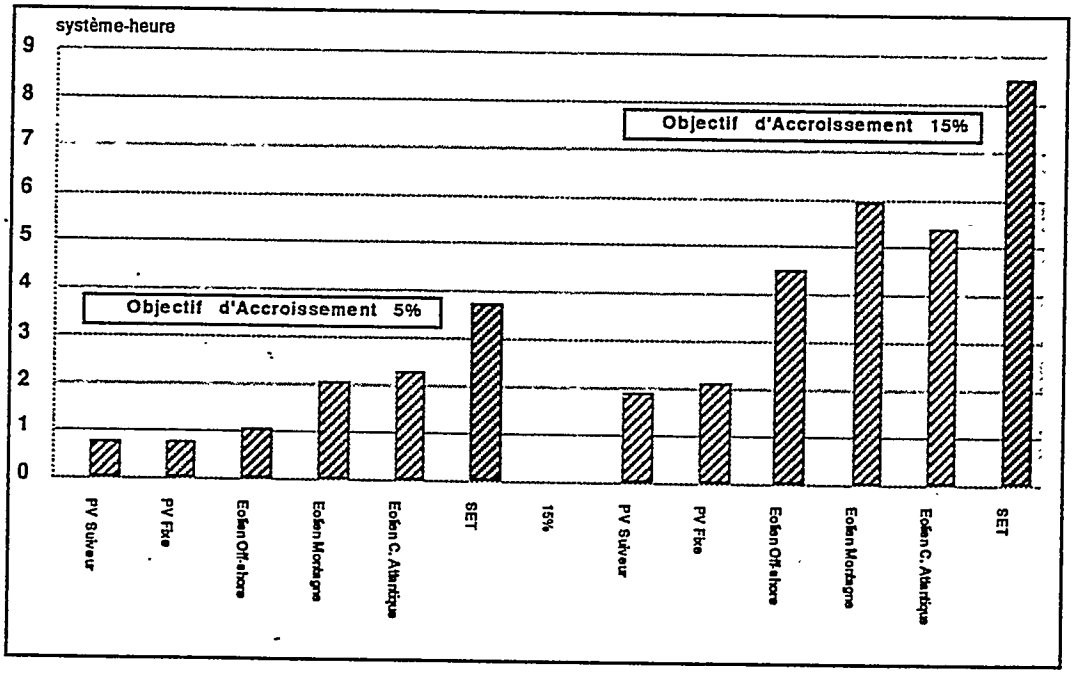

FIGURE 6: MINIMUM BUFFER ENERGY STORAGE FOR TWO GRID PENETRATION LEVELS

REFERENCES

1. Germa J. M. and R. Perez, (1992): Détermination de la Disponibilité Effective de Systèmes Photovoltaïques et Eoliens sur le Réseau Electrique de la Martinique. Report to ADEME (convention No. 1.05.0043 - exercice 1991). ADEME, Sophia-Antipolis, France.

2. Perez, R. Seals and R. Stewart, (1993): Solar Resource -- Utility Load Matching Assessment, Interim Subcontract Report no. NREL/TP-411-6292, NREL, Golden, CO and R. Perez, R. Seals and R. Stewart, (1994): Matching Utility Peak Loads with Photovoltaics, Proc. RENEW-94, (NESEA), Stamford, CT, USA

3. Perez, R., R. Seals and R. Stewart, (1993): Assessing the Load Matching Capability of Photovoltaics for US Utilities Based Upon Satellite-Derived Insolation Data, IEEE Transactions, pp. 1146-1149 (23d. PV Specialists, Louisville, KY).

4. Perez, R. Seals, R. Stewart, (1994): Solar Resource -- Utility Load-Matching Assessment. NREL Report. No. TP-411-6292, 48 pp.

5. Garver, (1966): *Effective Load Carrying Capability of Generating Units*. IEEE Transactions, Power Apparatus and Systems, Vol. Pas-85, no. 8

6. Perez, R. and R. Seals, (1995): Annual Report PV Subcontract Programs -- FY 1994, Solar Resource, Utility Load Matching Program, NREL/TP 410-7995, NREL, Golden, CO.

7. Menicucci and J.P. Fernandez/ User's Manual for PVFORM. *Report # SAND85-0376-UC-276*, 1988, Sandia Natl. Labs, Albuquerque, NM

MARKETING PROSPECT AND ASSESEMENT FOR LOCAL MANUFACTURE OF WIND CONVERTERS IN INDONESIA[1]

Sahat Pakpahan
Head of Applied Technology Division LAPAN[2]
Nenny Sri Utami
Head of Subdirectorate, Development and Utilization of Renewable Energy, DJLPE [3]
Indonesia

ABSTRACT

Wind energy resources in Indonesia provide opportunities to improve the delivery of electricity consumption for small and medium scale applications particularly for rural and remote areas and will be developed as the part of national rural electrification programs. By proper selection of design, this kind of energy source has shown to be a technically proven and affordable means of providing electricity at those areas.

The promotion of WECS technology have been initiated in Indonesia by establishing some pilot projects at selected areas while in comercialization efforts, several private companies are now being involved.

Dissemination of WECS technology should be based on proper selection of WECS types including economic consideration and marketing programs; for obtaning this, manufacturing of some WECS components / parts have been initiated using available materials and components; while other components that's still not producable in Indonesia will be produced by cooperation with industry. In addition, wind resource assesements will be extended sustainably in order to identify more potential areas and locations.

INTRODUCTION

Indonesia, a long archipelago with 13,677 islands (with about 6000 islands are inhabited) and about 73 % of the total population live in estimated 62,000 rural villages with 26 million rural households has various sources of energy but also needs a very large quantity of energy that will be used for fulfill the national energy needs / demands.

This demand will normally increase time by time due to rapid development of industrial and economic sectors, and for achieving this, strongthy efforts in developing other energy resources has been performed including exploiting of renewable energy resources that is

---

[1] Prensented on WINDPOWER 96, DENVER Colorado USA, June, 23-27, 1996

[2] LAPAN - National Institute of Aeronautics and Space

[3] DJLPE - Directorate General of Electricity and Energy Development

particularly aimed at providing electricity for rural and isolated areas and will take contribution to support rural electrifications program. Small scale applications for household lightings, pumpings, ice-making, cold storage, communication systems are potential; but also for larger system with interconnection to existing grids or local generating system such as for pumpings, irrigations, local industries, etc.

Based on the needs for providing energy with these various levels of consumptions, the promotion, marketing and initiation of local manufacture of WECS have been performed and have to be enhanced sustainably; and for obtaining this, measurement activities for identifications of more potential locations should also be extended and improved as one of the main criteria for WECS utilizations.
Promotion of WECS utilizations in Indonesia have to be directed in relation to the site-specificness of areas and locations due to different wind potentials, wind distributions, topographical conditions and applications. In some rural areas, small individual systems for rural electrifications are applicable but other areas need energy with collective use.

For contribution in marketing of WECS products in Indonesia there are now several private companies involved which mainly in the range of small scale WECS up to 10 kW installed capacity; while for procurement and manufacturing, the approach used is to manufacture certain components according to local capabilities, and availability of materials and components.

For demonstrating and evaluating different types of WECS consumers, some pilot projects of the ranges of 50 W to 10 kW installed capacity have been established at several regions in Indonesia; in addition, various utilizations of wind energy converters are also found for various applications.

MARKET APPROACH

Promotion and commercialization of WECS products for actual utilizations, and further dissemination are mainly aimed at providing electricity for some level of consumers particularly in the areas where no electricity available at all, not accessible or will not be accessed by the state electricity grid; or in the areas although there is existing generating sets, but often not in regularly operation due to the lack of fuel, skilled operator and technician for maintenances; other application are for specific users such as communication systems, cold storage etc; while the applications for larger power interconnected to grids are potential for certain areas.

Considering these level of consumers, several approaches have been done and will further be extended, as follows:

a. To evaluate and quantify the role of small up to medium scale wind converters for technical and socio-economic development according to the site conditions and applications.
b. Development of several pilot projects using various types of WECS for various

applications for identifying and approving their performances and reliability.

c. Establishment and development of the necessary technical standards and procedures required for WECS utilizations in Indonesia in order to maximize the utilizations, such as standards for installations, testing and monitoring; standards for wind data measurement and evaluation, general guidance for site selection of WECS installation and selection of WECS products.
d. Technology development for certain components and subsystems (rotor, generator and control) for establishment of prototypes suitable for Indonesian conditions using available local materials and components.
e. To perform the transfer of technology of various aspects of WECS utilizations for gaining capabilities as well as the exchange of informations by maintaning cooperation with various institutions.
f. To gain the cooperation between users, private sector / industry and R & D institutions for commercialization and local manufacture efforts.

For achieving these purposes, some pilot projects have been established using different types of small scale WECS from 50 W - 10 kW installed capacity; while the larger sizes will be developed for centralized system interconnected to existing generating sets or state electricity grid (PLN). Other installations belong to individual or collective consumers for various applications. Such examples of those installations are shown at Fig 1. As well as for public utilizations, some installations are also monitored for their performances and energy production.
Making national standards on wind energy have been initiated since 1989 and there are 6 (six) standards have been published; while in technology development, several prototypes of rotor and control have also been fabricated. For supporting this program, some cooperations have been performed and to be enhanced.

In addition to the marketing efforts, resource assessment is one of the main factor for identifying potential locations according to wind potential and demands, and international cooperations will support for this program. Several institutions that have performed cooperation with this program are DLR Germany, UNIDO (United Nations of Industrial and Development Organization) and WINROCK International. It is expected that with more cooperations and due to the numerous number of remote islands in Indonesia, this target for wind mapping could be accelerated.

MARKET POTENTIAL

a. Consumers with small scale WECS.

Main requirement of energy supply at rural and isolated areas in Indonesia are for household and public lightings, radio and televisions, water pumpings for drinking water, plantation irrigation and rice field irrigation; while at certain areas could be for ice production, medicine storage, aerators for shrimp plantation, remote communication and local home industry. Energy demands for distric areas are different and larger and hence the hybrid with existing generating sets or solar photovoltaic could increase the performances.

Referring to this, potential utilizations of WECS in Indonesia are both for individual or

collective uses, centralized or decentralized, stand-alone or hybrids. The individual system is usually used with one turbine for one to three households using small 50 W - 250 W turbines with 12 Vdc power; and the ranges from 500 W to 1000 W are for collective use by 4-10 households with additional for public facility and electronic equipment such as radio and television.

b. Interconnection system

For larger system with bigger capacity, the WECS system should be interconnected to the exixting state electricity grid (PLN) with the main application for centralized electricity supply, public water pumpings, irrigations, etc. There are some areas in Eastern Indonesia are suitable for these applications where the areas are located high above sea level. Using the tower of minimal 30 m height are also recommanded for producing higher energy. For these applications, the recommended wind converters are of the ranges of 10 kW -100 kW installed capacity and should be managed by professional institution.

c. Communication system

Application of solar photovoltaic for power supply of small communication system have been developed in some areas; and hence the similar system with wind energy could also be applicable particularly for remote communications in the areas where there is no electricity. From technical aspect, a wind turbine used for telecommunication power supply must be mechanically reliable and rugged due to the possibility of extreem weather conditions and notorious turbulent. In addition, they must be designed for higher wind speeds, withstand higher fatigue loading and protected against lightning strikes. The required cut-in wind speed should at least 3.0 m/s and rated at 8.0-12.0 m/s. Since most small turbines have rated power output from 10-12.0 m/s where using AEO (Annual Energy Output) calculation will give the capacity factors from 15-40 %; the turbines will generate power for 50-80 % of the time. Other requirement is that the tower of wind turbine should be from 15-30 m.

d. Decentralized battery charging system

There are many rural areas in Indonesia with undensed population where the distances between two households at one village are relatively far and make distribution lines costly; therefore, the application with decentralized battery charging system are become more economic such as for household lightings, radio and television compared with centralized system.

The battery charging power station which's equipped with battery bank should be located at a strategic side of consumers; therefore the users can bring their own batteries for recharging (each user should have at least two batteries that can be recharged alternatively). Main configuration of power station consists of wind turbine, rectifiers, controller, battery bank and distribution.

e. Autonomous system

In certain areas using small local generator sets for providing electricity, the supply of solar fuel could be difficult as well as maintenance; therefore, to reduce diesel oil consumption in this already existing power generation, the use of wind conversion system to cover the main load and diesel generator as a back up to cover peak loads or during the periods of low wind

speed could increase efficiency. This system is preferably be used for the periods where the load patterns show high peak loads (2 - 10 times higher than average) and only for 1 or 2 hours per day. Diesel generator set requires remote start device which can be activated by the automatic start/stop system under specified conditions. Additional equipment are inverter and small battery bank.

Such potential markets for this application are South Maluku and East Nusa Tenggara where diesel generator sets are used for electric generating system. Combination of existing generating sets with wind turbines are one of the recommended system for optimizing the energy production.

f. Hybrid system

Combination with pv modules equipment with battery bank as storage subsystem become an alternative solution for the areas where both sources of energies are complementary.

g. Wind Electric Pumping Systems.

Main application of wind electric pumping systems in Indonesia are for drinking water, water lifting, plantation and ricefield irrigations, salt water pumping, and aerators. For practical and economic use, the pumping system should not use batteries or inverters but need simple contactors to turn on and of the pump.

There are some installed wind electric pumping system in Indonesia such as Bergey Wind Power at Jepara and Oesao NTT, and there are more applications using mechanical multiblade windmills.

Referring to these markets, potential applications are shown at Fig 2.

LOCAL MANUFACTURE AND APPROACH

The availability of WECS products in market is one of the main factor to support the dissemination of technology applications; therefore, local manufacture with well-planned strategy should be initiated. For achieving this, the following approaches are needed:

a. From technical point of vieuw, implementation with appropriate technology to be one of the main criteria due to the large number of rural and isolated areas in Indonesia with different topographical conditions.
   For this reason, a WECS must be selected according to :
   (i) Simplicity with easiness in installation, operation and maintenance to compensate for the lack of skilled person at locations.
   (ii) Low cost, reliable and long life time.
   (iii) Easy to transport and to handle due to remote areas where the infrastructure could be not supportive.
   (iv) Availability of materials and components for spareparts and further manufacture.

b. From stages of manufacture/production, the most advantage solution could be choiced from the following alternatives :

(i) To manufacture/production of certain components in Indonesia by lisence methode and using available local components for the remain system.
(ii) To produce certain parts of a component or subsystem in Indonesia by lisence and to be completely made in Indonesia; or using available components in markets according to lisence method while the necessary facilities and equipment for production, testing and quality control are required.
(iii) Manufacture of suitable WECS in Indonesia with 100 % components availablility.

c. There must be strong cooperation among related institutions in disseminating the following informations :
(i) Information about potential areas including wind data and useful informations should come from R & D institutions.
(ii) Establishment of the most appropriate types of WECS to be manufactured based on laboratory and field testings and development works, i.e : that will give higher efficiency or energy yields at low wind regimes.
(iii) Market prospects based on actual study and assessment.
(iv) Informations about the capability of local suppliers to provide materials, components, machinaries, equipment for manufacturing, testing equipment, quality control, etc.

These mentioned approaches have been used to evaluate the prospect for local manufacture of WECS in Indonesia and the following results are obtained:
a. Evaluating of some WECS products in market for the most approriate use in Indonesia by field testing and capacity factor calculations.
b. List of available materials and components for manufacturing and testing of WECS as well as equipment and machines.
c. List of local capability for manufacture of components or certain components, construction, installation, testing, operation and maintenance.
d. List of international suppliers of certain WECS components, equipment and machines. including possibility of corporation for design and manufacturing.

Some aspects concerning local capabilities are shown at Fig 3.

RESOURCE ASSESSMENT : IDENTIFICATION OF POTENTIAL AREAS.

Up to 1996, LAPAN has monitored 50 locations and other measurements done by certain organizations. There is at least 10 measurements done by WINROCK INT'L at East Nusa Tenggara (NTT) in the program of WECS promotion and utilization at these areas; and all of these programs will contribute to support wind mapping and WECS utilizations in Indonesia. The BMG (the Agency for Meteorological and Geophysics) are also used as reference data. Several measurements with related data are shown at Fig 4. For the purpose of impoving the measurement system to obtain more reliable informations by including topographical conditions, the measurement technique will be extentded using wind Atlas Programs (WASP).

Identification of potential areas based on these measurement results are based on the minimum average wind speed of 3.0 m/s and show optimum power in the range of 4-12 m/s; and related to actual applications, the energy is calculated for 30 m hub height. Using these conditions the areas are generally classified into 4 (four) classed as follows: Class I (poor) : 0-75 W/m^2; Class

II (Useful) : 75-150 W/m^2; Class III (Good) : 150-250 W/m^2; Class IV (Excellent) : 250-500 W/m^2. Respective areas related to these classifications are shows: at Fig 5 and Fig 6.

DISCUSSIONS AND CONCLUSIONS

a. Potential participation of private sectors to develop market, commercialization and further local manufacture of WECS has good prospects especially for small and later medium scale WECS. Some development on hybrid, interconnection and optimization of rotor to lower cut-in wind speed, hence increasing efficiency should also be performed.
b. There are several thousands of villages located on the coastlines or remote islands need electricity; for which the renewable source of energy are most applicable. For these market, selection of appropriate technology must be done due to the site-specificness of WECS applications which must be acceptable to local people and suit the local basic needs where the technology is developed. In addition, the financing scheme for facilitating the the commercialization process as well as of responsible institutions with skilled personnel should be established. The operational strategy should include cooperation with related organizations, local governments, or selling the electricity to PLN.
c. Research and assessment on renewable energy have been done more extensively with taking consideration on technical, economic and operational aspects; doing these programs, more experiences and capabilities have been gained

ACKNOWLEDGMENTS

I am grateful to LAPAN for the assistance making us to join this WIND POWER 96 and would like to thank AWEA for the invitation. We also thank WINDROCK Int'l for the support in our participation in this workshop.

REFERENCES

1. Sahat Pakpahan and Eko Budi Purwanto; Wind Energy utilizations in Indonesia; presented at Enhancing the Commercialization of Renewable Energy in Indonesia; Jakarta, June 21-23,1995.
2. Nenny Sri Utami; Renewable Energy Development in Indonesia; APRES - The Asia Pacific Renewable Energy Symposium'95; Australia, July, 26 - August, 2,1995.
3. Sahat Pakpahan and Soeripno; Pengembangan dan Pemanfaatan Teknologi Energi Angin Dalam Upaya Meningkatkan Kontribusi Energi Terbarukan untuk Mendukung Program Listrik Pedesaan di Indonesia; National Seminar on Aerospace, Jakarta, Oct-1995.
4. Zuhal (Director General of Electricity and Energy Development, Ministry of Mines and Energy, Indonesia); Dissemination and Implementation on Renewable sources of Energy in Indonesia, presented at Grand Solar Challenge Int Symposium, Tokyo, October, 7, 1995.
5. LAPAN; Wind Data for 10 (ten) locations in Indonesia; LAPAN, 1995.
6. Ariono Abdulkadir and Sahat Pakpahan; Wind turbines Feasibility For Commercial Use in Indonesia; presented at "Asean Experts Group Meeting on NRSE, Jakarta,9-11,1996.
7. Michael L.S Bergey; An overview of Wind Power for Remote Site Telecommunication Facilities; Renewable Energy Power Supplies for Telecommunication Conference, BWEC, London, Sept, 25, 1989.

Figure 1 : WECS INSTALLED

WECS Type / Diameter (m)	Number Installed	1996 Installed
72 W / 0.5	5	10
100 W / 2.0	25	149
250 W / 1.7	5	-
300 W / 2.5	6	146
1000 W / 3.0	24	-
1,3 kW / 5.0	1	-
1500 W / 3.05	3	-
2500 W / 5.0	7	-
3000 W / 5.8	1	-
10 kW / 7.0	4	10
	81	315
	Total	396

Fig. 2 : POTENTIAL MARKET

WECS	Application
1. Small scale from 50 W - 250 W with 12 Vdc power	-Individual application -Household lightings, radio, small TV
2. Small scale from 250 - 1000 W with 12 Vdc power	-Collective use with 3-10 consumers -Radio and TV -Small local industri -Battery charging, etc -Communication system -Medicine storage -Small pumping, etc
3. Small scale from 1000 W - 25000 W with 220 Vac power	-Application forlighting,pumping,compressor, home industry, etc (may need small genset for back-up).
4. Small scale from 2.5 kw - 10 kW with	-Collective use for lightings, pumping, local industri, aerator, etc (need back-up syatem)
5. Interconnecting system	-Centralized system interconnected to grids for lightings, industries, pumping and irrigation.
6. Communication system	-Power supply (12 Vdc or 24 Vdc) of communication system at remote areas.
7. Battery charging power station	-Mainly in isolated areas for small size applications (radio, TV, house lighting).
8. Hybrid System	-Electricity supply

Fig. 3a : MATERIAL AVAILABILITY

No	Component	Material	Availability
1.	Rotor Blades	-Fiberglass	V
		-Galvanized carbon iron	V
		-Stainless steel	V
2.	Generator	-Housing and mounting	-
		-Rotor shaft	-
		-Stator	V
		-Diode block	V
		-Cabling	V
		-Slip ring	V
3.	Orientation/tail unit	-Nylon bearings	V
		-Bearings	V
		-Tail vane and frame material	V
4.	Rotor head	-Turntable	V
		-Supports	V
		-Bearings	V
		-PVC Tube	V
		-Stainless steel	V
5.	Control unit	-Panel	V
		-Indicator (A,V,f)	V
		-Electronic components	V
		-Coil/heater	V
		-Cables, Wires and connectors	V
		-Heat sinks	V
6.	Tower Up to 30 m	-Material for lattice tower and supports	V
		-Material for tubular tower and support	V
		-Material for platform	V
7.	Storage subsystem	-Battery 12 Vdc, 50-200 Ah	V
		-Deep cycle battery, 12 V	V
		-Clamps	V
		-Battery cabless	V
8.	Users	-dc/ac lamps	V
		-dc/ac pumps	V
		-Various cables	V

Fig. 3b : FABRICATION AND CONSTRUCTION

Component	Status
-Rotor blades up to 10 m diameter	V
-Rotor blades greater than 10 m diameter	X
-Rotor head	V
-Tail and orientation	V
-Lattice tower up to 30-40 m	V
-Tubular tower up to 30-40 m	V
-Control unit up to 1000 W	V
-Control unit > 1000 W	X
-Control panel	V
-Battery regulator	V
-Inverter	V
-Foundations	V
-Lifting equipment (cranes, etc)	V

Fig. 4 : LOCATIONS OF MEASURING SYSTEM

No	Location	Windspeed >3.0 m/s	Remarks
1.	Bulak Baru, Jepara, Central Java	V	LAPAN
2.	Nangalabang, Manggarai NTT	V	LAPAN
3.	Bungaiya, Selayar, South Sulawesi	V	LAPAN
4.	Nangalili, Manggarai, NTT	V	LAPAN
5.	T.N. Komodo, Manggarai, NTT	V	LAPAN
6.	Pasir Putih, Manggarai, NTT	V	LAPAN
7.	Doropeti, Dompu, NTB	V	LAPAN
8.	Bajo Pulau, Bima, NTB	V	LAPAN
9.	Sambelia, Lombok Timur, NTB	V	LAPAN
10.	Tembere, Lombok Timur, NTB	V	LAPAN
11.	Maubesi, Kupang ,NTT	V	LAPAN
12.	Langara Laut, Kendari, Sulawesi Tenggara	X	LAPAN
13.	Tinobu, Kendari, Sulawesi Tenggara	X	LAPAN
14.	Paudean, Bitung, Sulawesi Utara	X	LAPAN
15.	Libas, Minahasa, Sulawesi Utara	V	LAPAN
16.	Palakahembi, Sumba Timur, NTT	V	LAPAN
17.	Watumbelar, Sumba Timur, NTT	V	LAPAN
18.	Universitas Pattimura, Ambon, Maluku	X	LAPAN
19.	Namaelo, Maluku Tengah, Maluku	X	LAPAN
20.	Selayar, Lombok Timur NTB	V	LAPAN
21.	Geligede, Lombok Barat,NTB	V	LAPAN
22.	Nangadoro, Dompu, NTB	V	LAPAN
23.	Pai, Bima, NTB	V	LAPAN
24.	Kute, Lombok Tengah, NTB	V	LAPAN
25.	Sajang, Lombok Timur, NTB	V	LAPAN
26.	Sibowuli, Ngada, NTT	V	LAPAN
27.	Ujung, Manggarai, NTT	V	LAPAN
28.	Papagarang, Manggarai, NTT	X	LAPAN
29.	Karimunjawa, Jepara, Jawa Tengah	V	LAPAN
30.	Statiun Inderaja- LAPAN, Pare-pare, Sul-Sel	V	LAPAN
31.	Dongin, Banggai, South East Sulawesi	X	LAPAN
32.	Bulingkobit, Banggai South East Sulawesi	X	LAPAN
33.	Parangtritis, Central Java	V	LAPAN
34.	Baun, Kupang	V	LAPAN
35.	Ternate, Ambon	V	LAPAN
36.	Pamengpeuk, East Java	V	LAPAN
37.	Tomenas, NTT	V	WINROCK
38.	Netpala, NTT	V	WINROCK
39.	Walakiri, NTT	V	WINROCK
40.	Sakteo, NTT	V	WINROCK
41.	Oilbubuk, NTT	V	WINROCK
42.	Hansisi, NTT	V	WINROCK
43.	Leraboleng, Flores, NTT	V	WINROCK
44.	Lemoleba, Flores, NTT	V	WINROCK
45.	Napu, Sumba, NTT	V	WINROCK
46.	Kolak, Rote, NTT	V	WINROCK

Fig. 5 : WIND RESOURCE ASSESSMENT

Class (W/m^2)	Area
I. 0 - 75 (poor)	-
II. 75 - 150 (useful)	Makdule (Rote); Kupang, Nikiriki (TTS); Malerman (Alor), Nangalili (Manggarai), Komodo (East Sumba), Oilnonon (Kupang).
III. 150 - 250 (good)	Baa (Kupang), Batutuah (Kupang), Baun (Kupang), Oemata (Kupang), Soe (Kupang), Amben (East Timor), Kefamenanu (TTU), Alor, Waiwerang (Adonaro), Riung (Flores), Labuhan Bajo (Flores), Lewapako (Sumba), Rinca Beco (East Timor), Madura, East Lombok, East Bali, Buton (South East Sulawesi), South Maluku; North Sulawesi, South Ternate.
IV. 250 - 500 (excellent)	Eakun (Rote), Nembrala (Rote), Kalbano (Kupang), Sakte (Kupang), Baquia (Sawu), Raijua (Sawo), Oihala (Kupang), Kanenger Kapundu (Sumba), Ruteng (Flores), Nila (Flores), Ende (Flores), Jepara (Central Java), Parangtritis (Central Java), Selayar (South Sulawesi), Southern part of south Sulawesi, Bolon (Sawu).

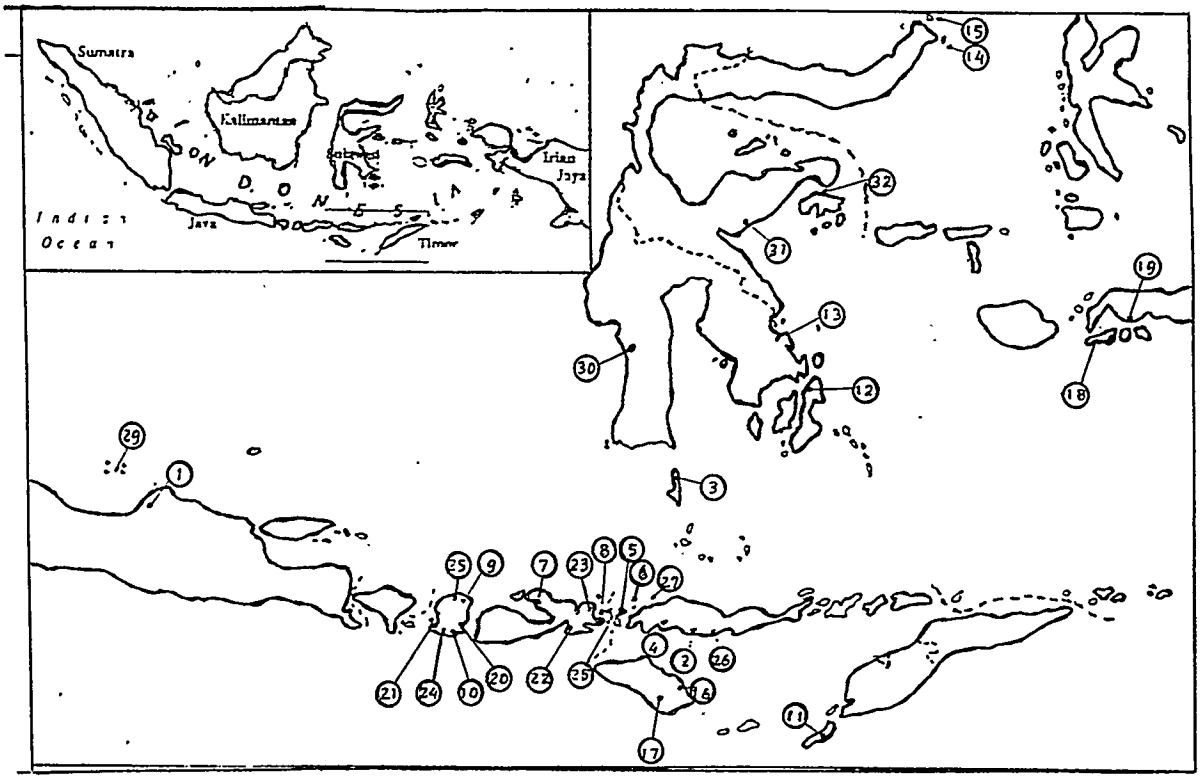
Sumatra
Kalimantan
Sulawesi
Irian Jaya
Java
Timor
Indian Ocean
INDONESIA
1
2
3
4
5
6
7
8
9
10
11
12
13
14
15
16
17
18
19
20
21
22
23
24
25
26
27
29
30
31
32

PRELIMINARY RESULTS OF ARUBA WIND RESOURCE ASSESSMENT

Margo H. Guda
Fundashon Antiyano Pa Energia
P.O.Box 115
Curaçao, Netherlands Antilles

Introduction.

As part of a project to assess the possibilities for wind energy utilitization in the Dutch Antilles islands, windspeed and -direction data were collected in Aruba for two years, from March 1992 to February 1994. Five sites that were estimated to be representative for the islands' wind regimes, were monitored during this period: two sites on the windward coast, one east and one west; two inland sites, again one east and one west, and one site topping the cliffs overlooking the eastern windward coast. Additionally, twenty years' worth of data were analyzed for the reference site at the airport, which is in the middle part of the island, on the leeward coast. Correlation calculations between these data and the data for the project sites were performed, in order to establish a methodology for estimating the long-term behavior of the wind regimes at these sites.

Aruba is a very small island, with the greatest length just about 30 km and the greatest width 8 km, providing a surface area of 193 km^2. Its geographical coordinates are 12°N by 70°W, which situates the island just northeast of the Guajira peninsula in Venezuela, as can be seen in the map shown here.

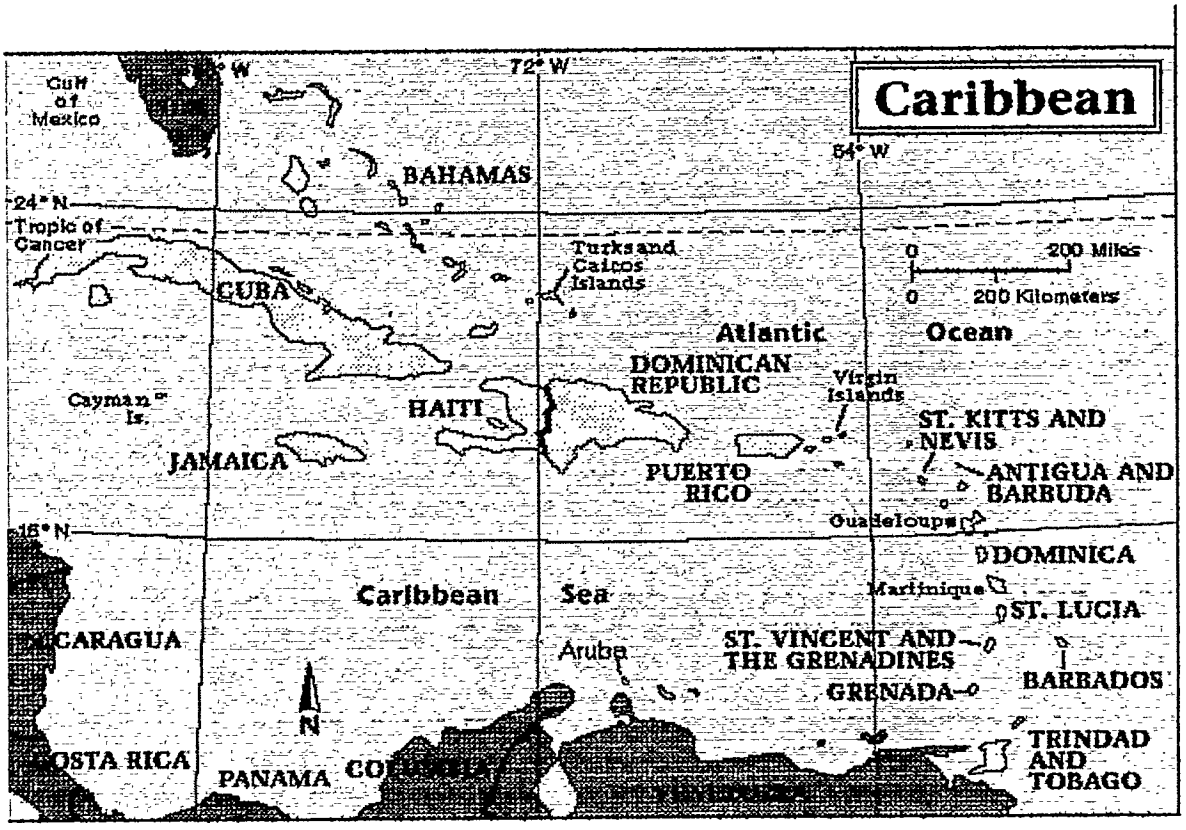

FIGURE 1: ARUBA AND THE CARIBBEAN

Description of measurement sites.

Aruba is dominated by the tradewinds of the Caribbean, which are present year-round, and are usually very strong. Only in October and November does the monthly average windspeed at the reference site not reach 6m/s, and it is usually appreciably higher. The reference site is situated next to the runway of Aruba's Reina Beatrix airport, which is on the southwestern coast of the island. The anemometer is in an exposed spot and faces a kilometers long fetch of flat land with very little vegetation. It is mounted on a meteorological tower at the WMO standard 10 m above ground level. At the project sites, towers of 21 meters height were used, housing two anemometers, one at 10 meters and one at 21 meters above the ground; a windvane was mounted at 10 meters above ground level. The five sites are indicated in the map shown in figure 2.

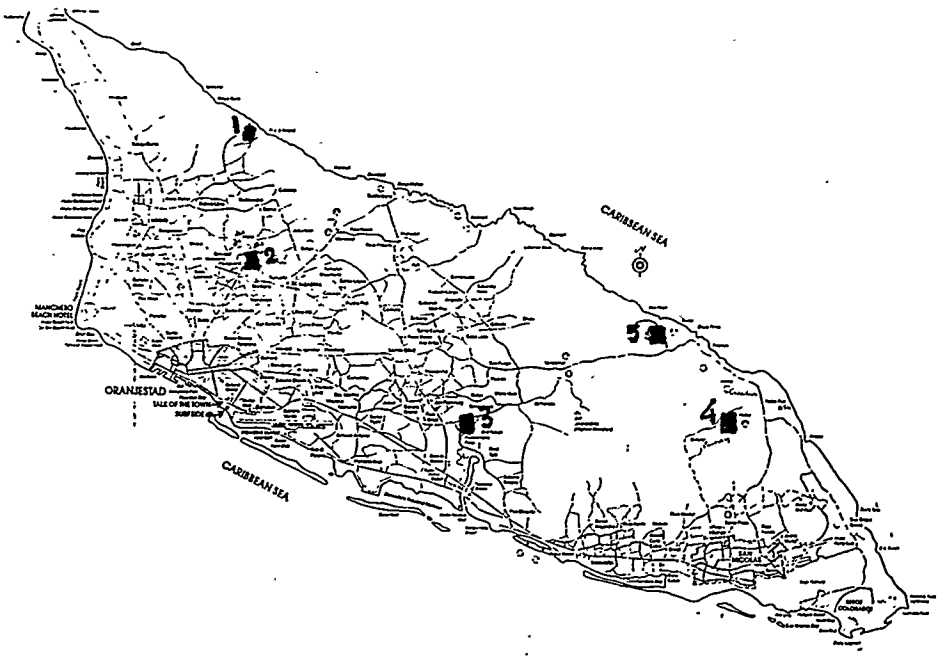

FIGURE 2: MEASUREMENT SITES IN ARUBA

The project sites, numbered 01 through 05, are:
01: Alto Vista, on the northwestern end of the island, about 500 m from the windward coast, in an exposed site close to the ocean. Upwind the land shows low rolling hills with very sparse vegetation, usually not higher than a few centimeters, with isolated thorny shrubs and strongly flagged trees (divi-divi), not higher than 1 meter. Large boulders are strewn about the landscape both upwind and downwind of the tower, as well.
02: Catiri. This was a relatively sheltered inland site in the western part of the island, surrounded by low trees and buildings at a distance of 50 meters or more. The predominant vegetation consists of low trees, not much higher than 3 meters, cactus, and thorny shrubs and desert vegatation to a height of half a meter. Upwind of the site, rolling hills comprise a long overland fetch of complex terrain, made more complicated by isolated large boulders to a distance of 50 meters upwind from the tower, reaching a height of an estimated 4 to 6 meters.
03: Balashi. This was a relatively exposed site near the south coast of the island (the leeward coast). The

land upwind of the tower consists of rolling low hills with the typical vegetation of low thorny trees and cactus, which in the vicinity of the site grew to a height of between 4 and 6 meters. The vegetation is nowhere very dense but rather open and scattered. The area is developed and contains a number of scattered dwellings, usually with large yards surrounding a single-story one-family house. During the measurement period, the area just upwind of the tower (at a distance of 50 meters and more) was being cleared of vegetation by heavy land-moving equipment, although a cactus hedge of maybe 2 meters height surrounding the immediate area around the tower, with a radius of 20 meters, was left standing. Immediately upwind of the tower, vegetation was low, maybe half a meter.
04: Butucu. The tower was situated on the cliffs overlooking the eastern coastal plain, which they overtop at a level of about 30 meters, at a distance of 2 km from the ocean. The tower stood about 600 meters from the edge of the cliff, which runs parallel to the coastline. The land atop the cliff is relatively flat and very sparsely vegetated, with severely flagged very low thorny trees and divi-divi. Trees are no higher than 2 meters generally, and most are even lower. Some of the flagging may be caused by salt spray, which is much in evidence in the area. The ocean is visible from the measurement site, especially from a few meters above ground level.
05: Dos Playa. Half a km from the ocean edge, where the cliffs drop an additional 30 meters to sea level, this site, on the eastern part of the island, was among the most exposed monitored sites. The land rolls very gently and has almost no vegetation ground cover. The winds reach the tower almost straight from the ocean. The land has a very distinctive red color, and some thermal turbulence can be observed by the unaided eye around midday. Isolated large boulders are strewn across the landscape. This site was also very close to the ocean.

The photographs on the next page give an impression of the landscape.

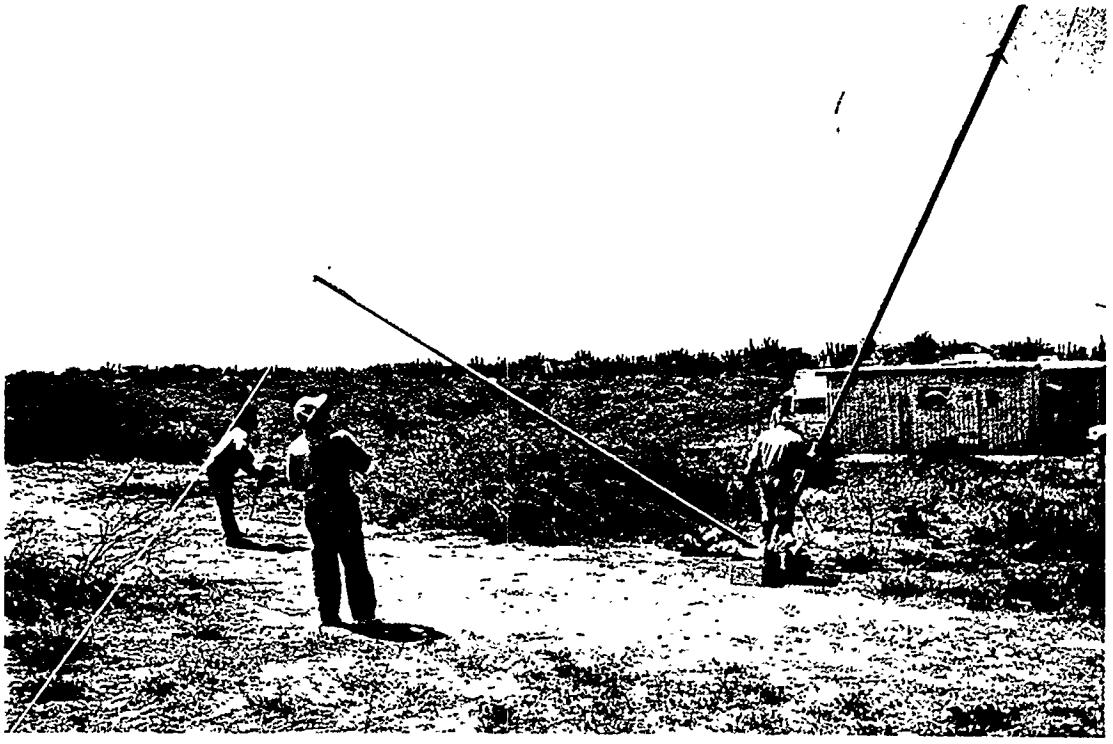

Analysis of long-term wind data for Aruba airport, 1970-1993.

The following are results of the data analysis performed on the windspeed data collected between January 1970 and December 1988 by the Meteorological Service of the Netherlands Antilles and Aruba. The data were collected in the standard way of those days (that is, read off an analog recorder during the last ten minute interval of each hour) and manually entered into spreadsheet files. The data were carefully screened for observer error and data-handling error. The height of the anemometer was 10 meters above the ground.

The following averages were calculated:

- Monthly and annual average diurnal variation and standard deviations;
- Interannual and seasonal variation of hourly averages;
- Distribution and Weibull parameters of windspeeds over aggregate data set.

These data are summarized in the following graphs and tables.

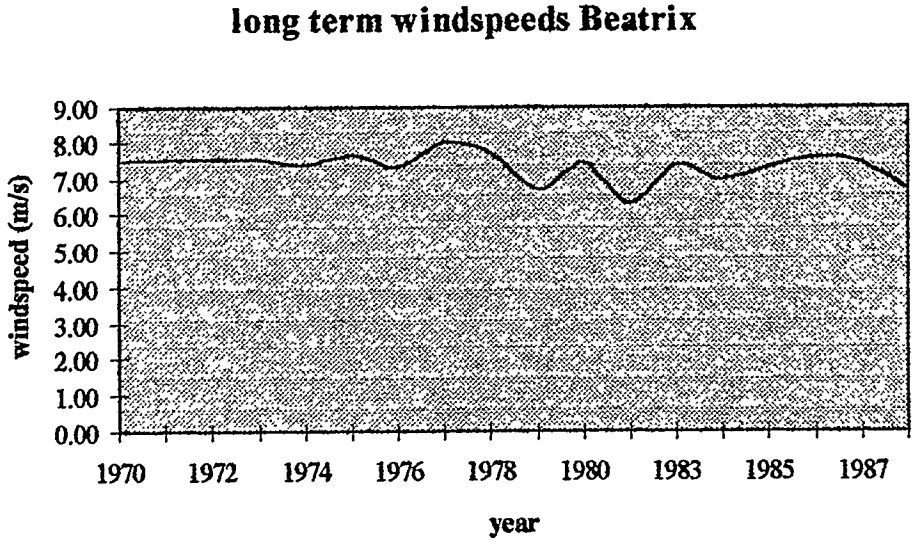

FIGURE 3: LONG TERM ANNUAL AVERAGE WINDSPEEDS

The graph shows the smoothed curve for the long-term annual average windspeed at the airport. The long-term average over the 18 years of data represented here is 7.32 m/s, with a standard deviation of 2.23 m/s. For reference, the data are shown numerically in table 1.

TABLE 1

year	nr of data	annual average	stdev year	avg all data	cum nr of data	log(nr data)	std all data	data recov rate	month	seasonal lt avg
1970	8668	7.46	2.43	7.46	8668	9.07	2.43	0.9895	jan	6.98
1971	8451	7.52	2.18	7.49	17119	9.75	1.55	0.9647	feb	7.63
1972	4987	7.55	2.32	7.50	22106	10.00	2.31	0.5677	mar	7.75
1973	8757	7.52	2.10	7.51	30863	10.34	2.25	0.9997	apr	7.66
1974	8756	7.34	2.02	7.47	39619	10.59	2.21	0.9995	may	7.92
1975	8760	7.67	1.94	7.51	48379	10.79	2.16	1.0000	jun	8.63
1976	8752	7.31	2.39	7.48	57131	10.95	2.20	0.9964	jul	8.39
1977	8760	8.00	1.83	7.55	65891	11.10	2.16	1.0000	aug	7.80
1978	8641	7.72	2.09	7.57	74532	11.22	2.15	0.9864	sep	7.13
1979	8758	6.67	2.39	7.47	83290	11.33	2.20	0.9998	oct	5.95
1980	8777	7.42	2.18	7.47	92067	11.43	2.20	0.9992	nov	5.86
1981	8760	6.30	2.23	7.37	100827	11.52	2.22	1.0000	dec	6.49
1983	8760	7.34	1.92	7.37	109587	11.60	2.20	1.0000		
1984	8751	6.98	2.14	7.34	118338	11.68	2.20	0.9962		
1985	8760	7.31	2.38	7.34	127098	11.75	2.21	1.0000		
1986	8760	7.57	2.16	7.35	135858	11.82	2.21	1.0000		
1987	8736	7.43	2.39	7.36	144594	11.88	2.22	0.9973		
1988	8784	6.71	2.21	7.32	153378	11.94	2.23	1.0000		
avg	**8521**	**7.32**	**2.18**					**0.9720**		

This table also shows that even though data recovery was spotty for some years, still the long-time aggregate average is remarkably stable, although from 1981 the aggregate average seems to be declining. The annual average does show some variation, but the standard deviation of this series is only 0.42 m/s, very small compared with the long term standard deviation of all hourly values. This would suggest a rather constant long-term average windspeed.
Also apparent from this table is the long-term seasonal variation in windspeed. It can clearly be seen from the rightmost two columns of the table that while it is generally windy most of the year, the months June and July stand out. But the windy period can be seen to start in February, on average, and it lasts until September. Still, differences between windy and low-wind months are relatively small. The worst month is November, when the monthly average windspeed is 5.86 m/s. Still, if compared with long-term data for Curaçao, which were collected in roughly the same period, the winds in Aruba would seem to be stronger.[1]

From the same set of data, a long-term frequency distribution of the windspeed at 10 meters above ground level was calculated, and fitted to a Weibull distribution, using simple linear regression of the expression

$$\ln(-\ln(1-F(v))) = k\,(\ln(v)-\ln(c))$$

where F(v) is the cumulative Weibull distribution and c and k are the parameters of the Weibull distribution. The regression calculation was performed using a spreadsheet program. In order to estimate visually how well the actual data fit the fitted curve, both were plotted (see figure 4). Additionally, the two Weibull parameters can be calculated using an experimental approximation for the form parameter, which can then be used to estimate the scale parameter from the expression $\langle v \rangle = c * \mathrm{Gamma}(1+1/k)$. The form parameter k is calculated from $k = a * (\mathrm{sigma}/\langle v \rangle)^{x}$, where sigma is the standard deviation of {v}, and a and x are experimentally fitted constants.

$$a=0.9714,\ x=-1.114.$$[2]

[1]Meteorologische Dienst Nederlandse Antillen: Beknopt overzicht van het klimaat van de Nederlandse Antillen. Curaçao, 1982.

[2]Lysen, personal communication; Margo H. Guda: Curaçao wind resource assessment, 1992.

The calculated and fitted distributions are shown in figure 4.

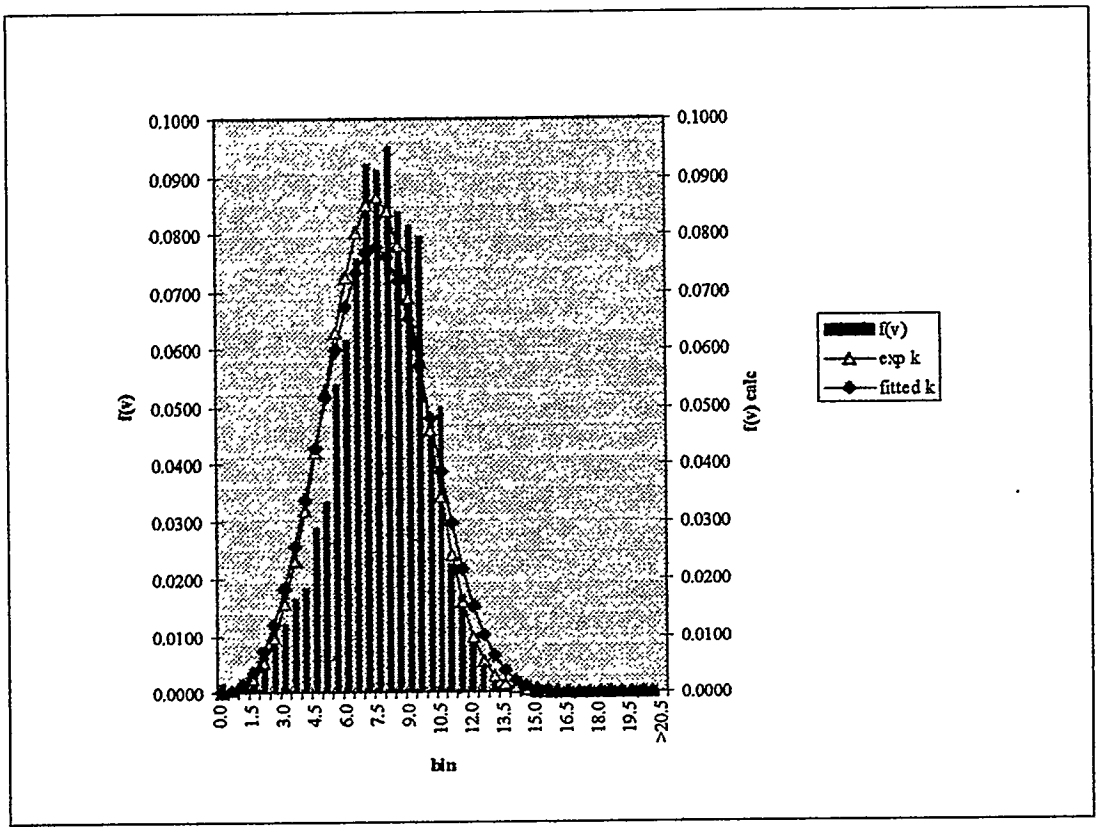

FIGURE 4

From this figure it can be seen that both Weibull fits approximate the actual data remarkably well, although the theoretical curves do not catch the slight right skew in the actual distribution. The curve calculated from the linear regression seems to slightly overestimate the extremes of the curve, while it yields a form parameter slightly smaller than the experimentally found expression. The long-term energy density that can be calculated from these parameters also differs, with the experimental expression for k yielding an annual energy density of 285 W/m^2, while using the parameters found by linear regression gives an energy density of 314 W/m^2.

The results of the curvefit exercise are shown in table 2.

TABLE 2

<v>=	7.32					7.43	from c*gamma(1+1/k)	
sigma=	2.23							
k=	3.66	(calculated with Lysen's approximation)				3.33	from regression	

Five windregimes of Aruba.

Figures 5 to 8, and Table 3 show a summary of the wind regimes measured at the five sites.

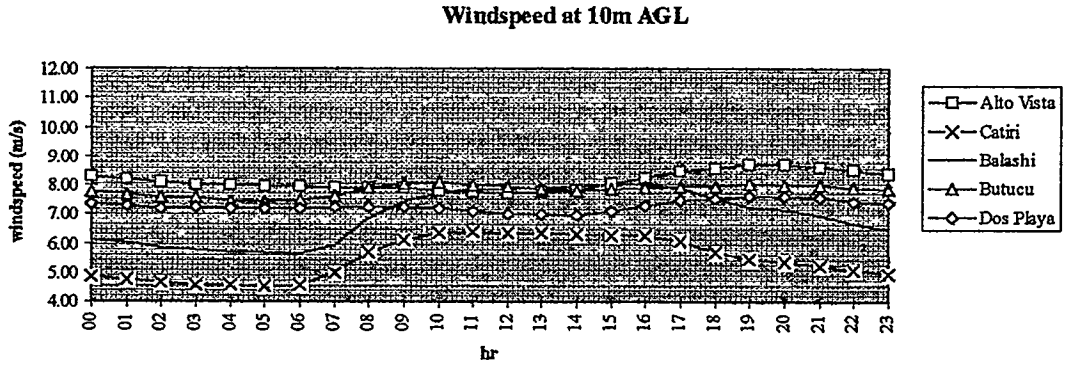

FIGURE 5

Figure 5 gives the windspeed at 10 meters above ground level, and figure 6 shows average windspeeds at 21 meters above the ground. The numerical values are shown in Table 3.

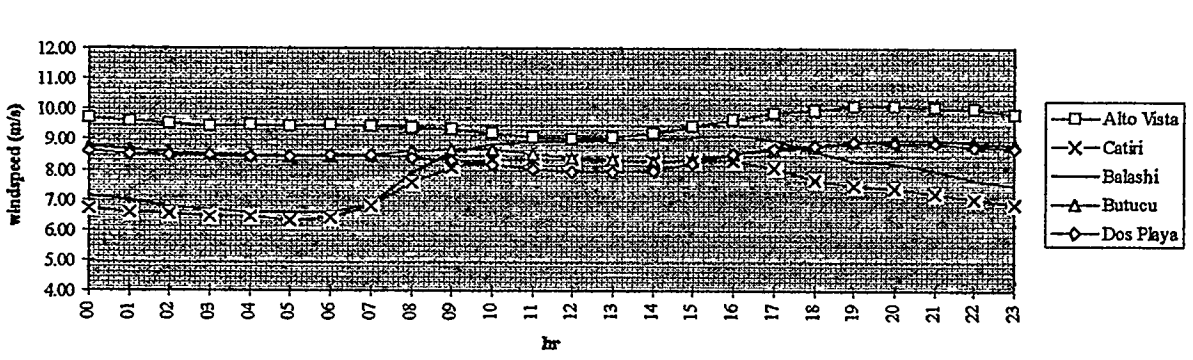

FIGURE 6

Windspeed was measured at two anemometer levels, 10 meters and 21 meters above the ground; winddirection was measured only at 10 meters AGL, to enable comparison with the long-term reference site at the airport, for which data are only available at 10 meters above ground level; turbulence intensity was calculated from logged hourly standard deviations of the windspeed, again at 10 meters AGL.
The five sites were chosen to provide a representative sample of expected windregimes in the small island. Three of the sites - Alto Vista, Butucu, and Dos Playa - are exposed, upwind coastal sites with varying characteristics of overland fetch; one, Catiri, was a relatively sheltered inland site surrounded by low shrubs, trees, and buildings, and one site - Balashi - was situated inland not too far from the downwind coast. The long-term reference site is on the downwind coast on an exposed site along the 2.7 km runway of the airport, which was built in the early 1960s on reclaimed land.
The windregimes at these six studied sites show some variation, although this variation is not as large as that found in Curaçao[1]. As can be seen from Table 3, what varies most are the windspeeds at the two anemometer heights. In this table, the extent of the diurnal variation is expressed as the standard deviation

[1]Margo H. Guda: The Curaçao Wind Resource Assessment Project, March, 1994.

in the set of hourly averages, expressed as a percentage of the overall annual average. At 10 meters, it ranges from a low 2.55% at Butucu, to a high 13.9% at Catiri. At Alto Vista, this diurnal standard deviation is 3.9%. This site, which has a typical coastal windregime, has the highest average windspeeds we have measured. At 10m AGL we found an annual average windspeed of 8.14m/s, which increased to 9.55m/s at 21 meters above the ground, with a diurnal standard deviation of 3.6%. This site, which was the westernmost site, was situated in an exposed area on the windward coast, with an estimated half kilometer of overland fetch. Windspeeds are lowest around midday; after twelve noon they show a marked increase, while they reach their maximum value one to two hours after sunset, around 8PM.

TABLE 3

Windspeed (m/s) at 10m							Windspeed (m/s) at 21m				
Site name		Alto Vista	Catiri	Balashi	Butucu	Dos Playa	Alto Vista	Catiri	Balashi	Butucu	Dos Playa
	hr.										
	00	8.28	4.85	6.14	7.78	7.34	9.70	6.71	7.13	8.76	8.61
	01	8.18	4.77	6.04	7.69	7.28	9.59	6.57	6.96	8.66	8.53
	02	8.11	4.65	5.85	7.58	7.22	9.51	6.51	6.76	8.55	8.46
	03	8.02	4.58	5.77	7.55	7.22	9.43	6.43	6.68	8.53	8.46
	04	8.00	4.56	5.69	7.46	7.21	9.46	6.43	6.60	8.46	8.45
	05	7.95	4.51	5.67	7.45	7.20	9.44	6.32	6.59	8.44	8.43
	06	7.96	4.55	5.66	7.47	7.20	9.45	6.38	6.59	8.45	8.46
	07	7.92	4.99	5.93	7.63	7.24	9.41	6.80	6.86	8.50	8.47
	08	7.93	5.70	6.85	7.89	7.26	9.38	7.58	7.89	8.60	8.40
	09	7.91	6.12	7.45	8.05	7.26	9.33	8.06	8.55	8.66	8.31
	10	7.83	6.35	7.71	8.08	7.19	9.18	8.32	8.83	8.63	8.16
	11	7.75	6.38	7.84	8.01	7.10	9.05	8.35	8.92	8.52	8.02
	12	7.73	6.35	7.86	7.94	7.03	9.01	8.34	8.94	8.40	7.95
	13	7.74	6.35	7.90	7.88	7.00	9.06	8.31	8.96	8.33	7.94
	14	7.83	6.31	7.96	7.81	6.97	9.19	8.29	9.01	8.24	7.96
	15	8.02	6.28	8.00	7.84	7.08	9.42	8.31	9.07	8.33	8.20
	16	8.25	6.25	8.06	7.93	7.31	9.64	8.31	9.14	8.51	8.51
	17	8.45	6.05	7.91	7.94	7.46	9.87	8.08	8.99	8.65	8.69
	18	8.56	5.69	7.52	7.94	7.54	9.98	7.66	8.60	8.76	8.80
	19	8.69	5.46	7.23	8.03	7.63	10.10	7.49	8.30	8.93	8.91
	20	8.72	5.37	7.15	8.02	7.63	10.12	7.37	8.20	8.98	8.90
	21	8.62	5.21	6.94	7.98	7.59	10.04	7.21	7.97	8.95	8.87
	22	8.51	5.07	6.70	7.90	7.45	10.01	7.02	7.68	8.88	8.75
	23	8.40	4.95	6.47	7.85	7.41	9.84	6.86	7.46	8.85	8.70
Annual	Avg	8.14	5.47	6.93	7.82	7.28	9.55	7.41	7.94	8.61	8.46
Annual	StD	1.56	1.29	1.76	1.58	1.56	2.08	1.66	2.00	1.83	1.75
diurnal	StD	3.90%	13.01%	12.90%	2.55%	2.60%	3.59%	10.45%	12.10%	2.42%	3.53%

From the above figures, we can see that the other two exposed sites, Butucu and Dos Playa, on the windward coast show a similar diurnal pattern as that found at Alto Vista; the two inland sites show a very marked diurnal variation, especially Catiri, which was most sheltered. At all sites except Dos Playa, at 21m AGL the diurnal variation decreases as a fraction of the average windspeed.

Wind direction is shown in Figure 7. It also shows little variation; the wind mostly blows from somewhat south of east at all sites. At Alto Vista the average wind direction is 100°. The diurnal standard deviation of the average wind direction for this site is 7.8°. The wind ranges in direction from easterly (88° in the early evening, when speeds are greatest) to south-easterly (110° at midmorning, when speeds are close to their minimum). The winds at the other sites show a similar pattern, although in these sites the diurnal variation (as expressed by the diurnal standard deviation) is even less.

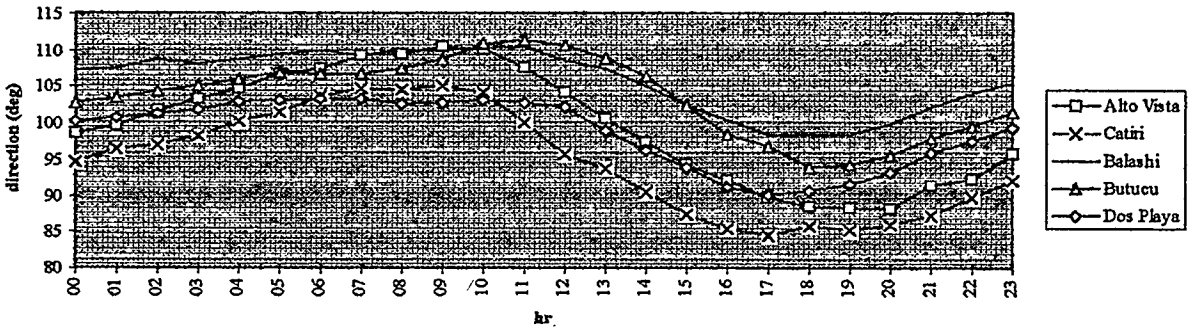

FIGURE 7

Figure 8 shows the turbulence intensity at 10 meters above the ground at the five sites. Turbulence intensity, which is defined as the standard deviation in the hourly average divided by the hourly average windspeed, is a measure for the very short-term variability of the wind, and gives some indication of the forces a windturbine placed at the site will experience. The five sites show considerable variation in turbulence intensity, but at each site, this variable seems remarkably constant. The windward sites generally show the least turbulence intensity, while the more inland sites show larger values. This would seem to indicate two main causes for turbulence in Aruba that contribute equally to the total. Sites with an appreciable overland fetch show considerable thermal turbulence; all sites also show marked mechanical turbulence, due to roughness changes and topographical effects.

One can also see from the graph that at the more exposed sites turbulence intensity shows almost no diurnal variation, echoing the lack of diurnal variation of the windspeed at these sites, while the more sheltered sites turbulence intensity varies markedly during the day. There, turbulence intensity decreases after sunrise, when windspeeds are larger and mechanical turbulence decreases in importance compared to thermal turbulence, while at night, mechanical turbulence dominates.

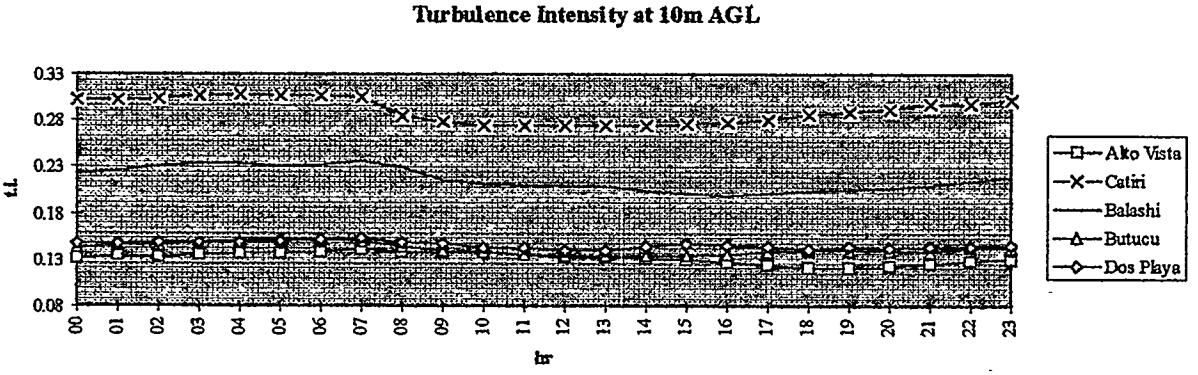

FIGURE 8

SYNCHRONOUS GENERATOR WIND ENERGY CONVERSION CONTROL SYSTEM

Armando L. R. Medeiros - Wind Energy Group/CTG/UFPE
Av. Acad. Hélio Ramos, sn - CDU - CEP. 50740-530 - Recife/PE - Brasil
A. M. N. Lima, C. B. Jacobina, F. J. Simões - DEE/CCT/UFPB
Av. Aprígio Veloso, 882, Bodocongó, CEP. 58109-970 - Campina Grande/PB - Brasil

ABSTRACT
This paper presents the performance evaluation and the design of the control system of a WECS (Wind Energy Conversion System) that employs a synchronous generator based on its digital simulation. The WECS discussed in this paper is connected to the utility grid through two Pulse Width Modulated (PWM) power converters. The structure of the proposed WECS enables us to achieve high performance energy conversion by: i) maximizing the wind energy capture and ii) minimizing the reactive power flowing between the grid and the synchronous generator.

INTRODUCTION

A simplified scheme of the WECS under analysis is shown in Figure 1. This structure has been labeled as VSCF (Variable Speed Constant Frequency) strategy conversion (Smith [1]). The turbine velocity is transmitted to the synchronous generator by a multiplier (M) having a transmission ratio i. The magnetic excitation of the synchronous generator is supplied by a single phase PWM converter (INV3). The two solid state PWM inverters (INV1 and INV2) constitute the link between the utility grid and the synchronous generator. With this arrangement, the power flow between the grid and the WECS may be bi-directional, i. e., the synchronous machine may operate either as a generator or as a motor.

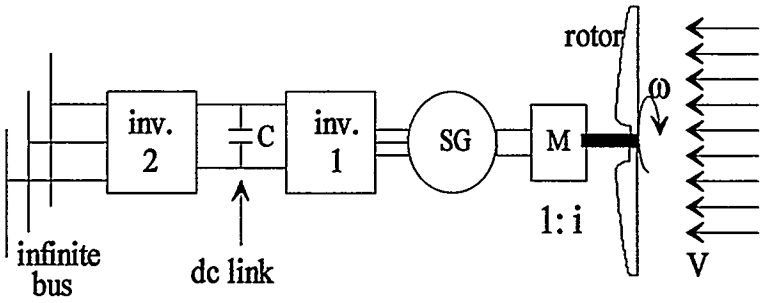

Figure 1 Simplified scheme of the WECS

SYSTEM DESCRIPTION AND MODELING

The amount of electrical power generated by the WECS in steady state, is assumed to follow a cubic profile for $V_{in} \leq V \leq V_r$. For $V_r \leq V \leq V_{out}$, it is assumed $P=P_r$ as depicted in the figure 2.

In the modeling of the WECS one has to take into account two important conditions: i) the start-up condition and ii) the blackout of the utility grid.

Start-up. In the start-up condition the synchronous machine has to run as motor since with low tip speed ratios the aerodynamic torque (Q) does not suffice to accelerate the large inertial load of the turbine. The start-up wind speed V_{st} may be approximated by (Lysen [2]):

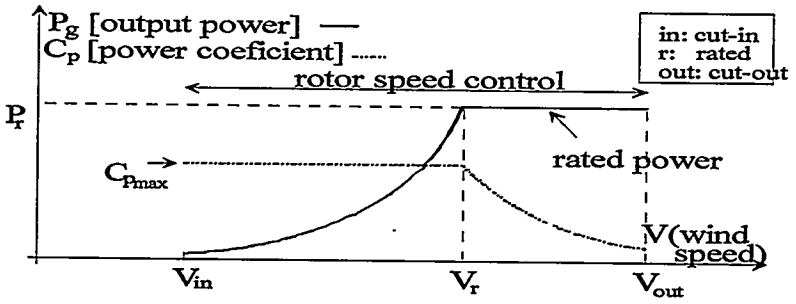

Figure 2 Power output and power coefficient of the WECS.

$$C_{q_{st}} = \frac{1}{2\lambda_d^2} \Rightarrow V_{st} = 2\lambda_d \sqrt{\frac{T_{at}\, i}{\rho A R}} \qquad (1)$$

where Cq_{st} is the starting torque coefficient of the rotor, λ_d is the design tip speed ratio, T_{at} is the friction torque, "i" is transmission ratio, ρ is the air density, "A" is the rotor area and "R" is the rotor radius. Using $V_{in} \cong V_{st}$, in a first approach, the synchronous machine works as a motor since $V \geq V_{in}$ and $\omega \leq \omega_{min}$. The value of ω_{min} depends upon the rotor characteristics. In this simulation it was used the value: $\omega_{min} = 0.5\ V_{in} / \lambda_d R$.

Blackout of the utility grid. On the other hand when a blackout occurs the WECS has to be damped. This is achieved by a dump load that absorbs the generated power. This load is connected as depicted in the figure 3.

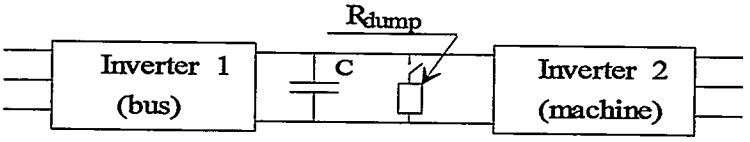

Figure 3 Dump load scheme

Control scheme description. The control strategy of the WECS is implemented on the Control Unit as indicated in the figure 4.

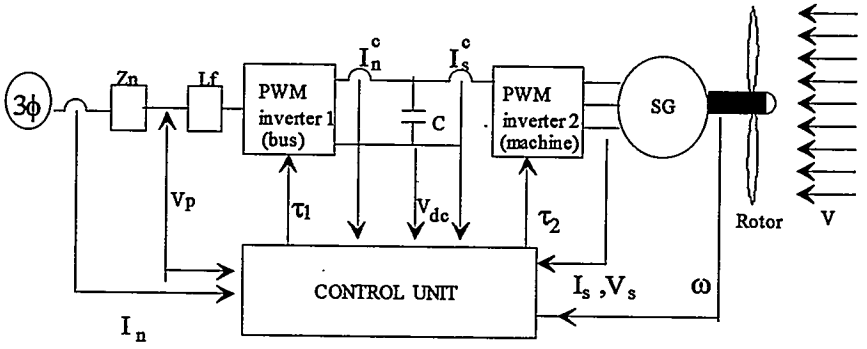

Figure 4 Control scheme of the system

The global control scheme consists of a cascade of six proportional and integral (PI) controllers as shown in the figure 5. The stator current control loop of the synchronous machine takes two of these PI controllers. Their main tasks are assure the electromagnetic torque reference given by the PI controller of

the speed control of the turbine. The synchronous machine control strategy follows the standard indirect field oriented control approach which does not require rotor flux estimation. The grid input current control loop takes also two PI controllers to assure unit power factor. The DC link voltage loop takes also one PI controller.

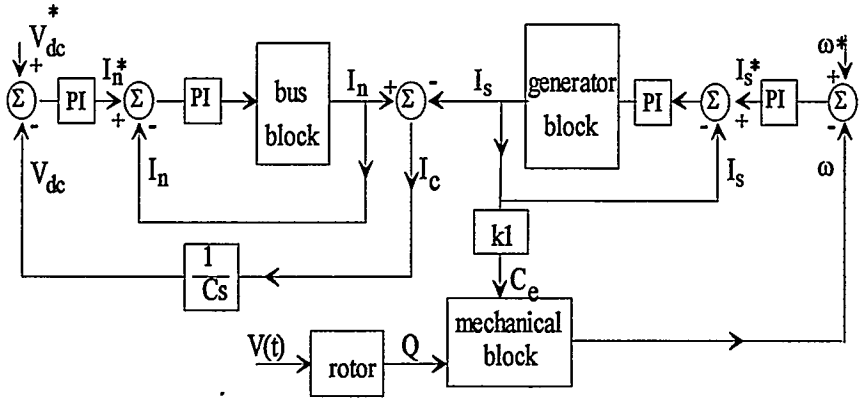

Figure 5 Scheme of the PI controller frame

Optimal rotor speed reference. The control system design of the WECS aims to maximize the wind energy capture by adjusting the turbine shaft speed to keep constant the tip speed ratio at the point where the value of the power coefficient is maximum ($Cp=Cp_{max}$). As shown in the figure 6, the speed control signal is derived from the wind velocity signal that is obtained by a specific sensor. The turbine speed control loop is restricted to operate within the range of the cut-in and cut-out velocities. The constant speed ratio operation is achieved only for $V_{in} < V < V_{out}$.

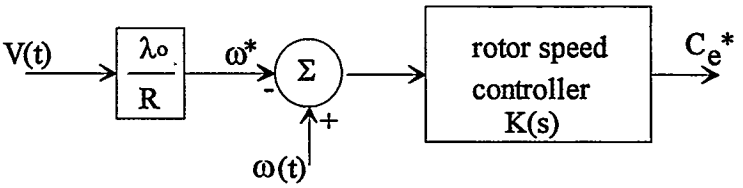

Figure 6 Rotor speed control diagram

PWM voltage Source Inverter. The scheme depicted in the figure 7 was used in the voltage space vector control since it presents the advantage of controlling the power factor. From the point of view of the PWM strategy, each inverter leg can be represented as in the figure 8.

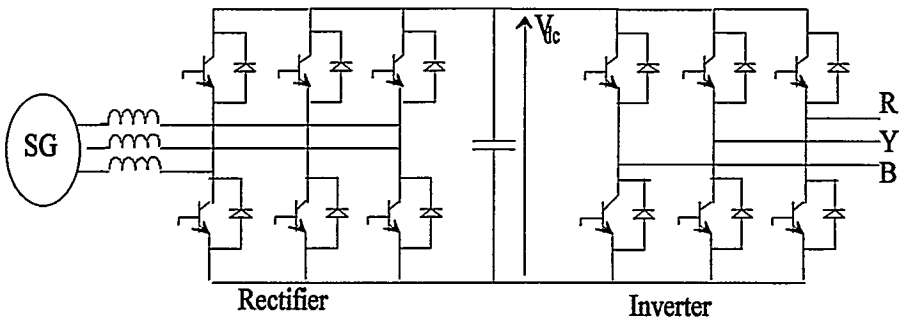

Figure 7 Voltage Source Inverter

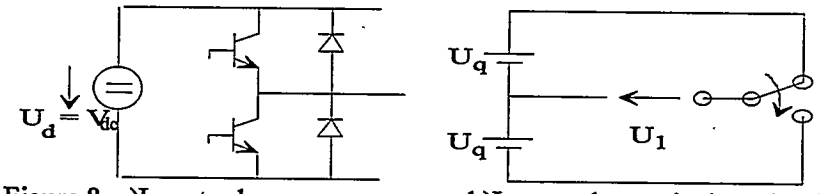

Figure 8 a)Inverter leg b)Inverter leg equivalent circuit

Space vector modulation. The three machine voltages are represented by a voltage space vector U. There are eight states (or switching configurations) available for this vector according to eight switching positions of the inverter which are depicted in figure 9 (Broeck [3]).

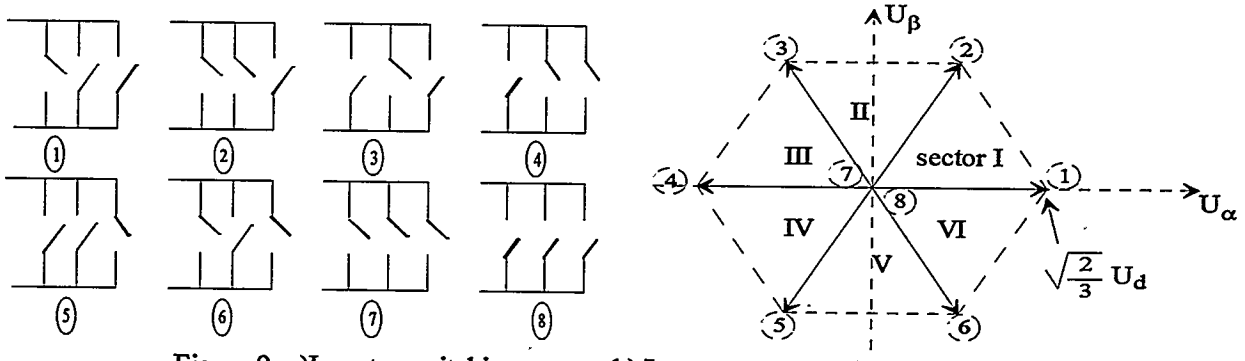

Figure 9 a)Inverter switching states; b) Inverter output voltage space vectors

To obtain minimum switching frequency of each inverter leg it is necessary to arrange the switching sequence in such a way that the transition from one state to another is performed by switching only one inverter leg. If, for example, the reference vector sits in sector I, the switching sequence has to be ...812721812721....and ...72383272383... for the sector II. The switching time for each adjacent space vector is obtained as depicted in the figure 10 for the sector I.

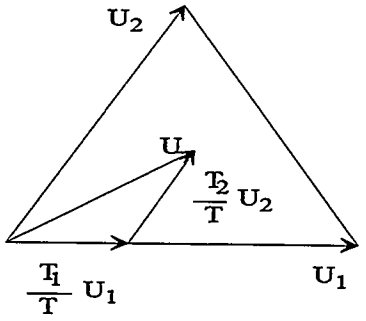

Figure 10 Determination of the switching times

The resultant vector from the application of U_1, U_2 and U_7 for the times T_1, T_2 and T_0 must be equivalent to the application of U for all the time T. The vector equation (2) shows this equivalence [3]:

$$\vec{U}_1 T_1 + \vec{U}_2 T_2 + \vec{U}_7 T_0 = T\vec{U} \qquad (2)$$
$$T_1 + T_2 + T_0 = T \quad \textit{and} \quad U_7 = U_8 = 0$$

Model of the synchronous machine (SM). The dynamic model of the synchronous machine is given by the following equations.

$$v_s^g = R_s\, i_s^g + \frac{d\phi_s^g}{dt} - j\,\omega_g\,\phi_s^g \tag{3}$$

$$v_r^g = R_r\, i_{rq} + \frac{d\phi_r^g}{dt} + j(\omega_g - \omega_m)\,\phi_r^g \tag{4}$$

$$\phi_s^g = l_s\, i_s^g + l_{sr}\, i_r^g \tag{5}$$

$$\phi_r^g = l_s\, i_r^g + l_{sr}\, i_s^g \tag{6}$$

$$C_e = K\, i_s^g\, (\phi_r^g)^* \tag{7}$$

The typical assumptions used when developing this model are borrowed from Chatelain [4]. The g superscript indicates an arbitrary choice for the reference frame. $v_s{}^g$, $i_s{}^g$ e $\phi_s{}^g$ are the stator voltage, the stator current and the stator flux vectors, respectively (the vector definitions are valid for the rotor by changing the s subscript by r). ω_m and ω_g are the synchronous machine speed and the speed of the dq axis, respectively. C_e is the electromagnetic torque. l_s, l_r and l_m are the self and mutual machine inductances. r_S and r_r are the ohmic resistances of the windings. K is a constant that depends on the machine parameters. Using the field reference frame, i. e., aligning the d axis with the rotor flux, $\omega_g = \omega_b$, as shown in the figure 11, the rotor flux components are given by:

$$\phi_{rd}^b = \phi_r \quad e \quad \phi_{rq}^b = 0$$

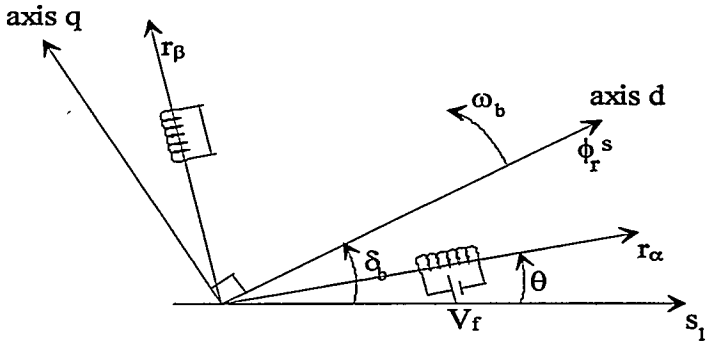

Figure 11 Voltage vector reference frame

So the equation (4) can be rewritten as:

$$v_{rd}^b = \frac{R_r}{l_r}\phi_r - \frac{R_r\, l_m}{l_r} i_{sd}^b + \frac{d\phi_r}{dt} = V_f \cos(\delta_b - \theta) \tag{4a}$$

$$v_{rq}^b = (\omega_b - \omega_m)\phi_r - \frac{R_r}{l_r} l_m\, i_{sq}^b = -V_f \sin(\delta_b - \theta) \tag{4b}$$

For maximum power factor: $i_{sd}^b = 0 \qquad \Rightarrow C_e = K\, \phi_r\, i_{sq}$ (8)

For steady state conditions, the (reference) excitation voltage amplitude V_f^* and the (reference) position of the field axis δ_b^* are given by Medeiros [5]:

$$V_f^* = \frac{\phi_r^*}{T_r}\sqrt{1+a^2} \tag{9}$$

$$\delta_b^* = arctga + \theta \tag{10}$$

$$a = \frac{l_m}{\phi_r^*}\, i_{sq}^{b*} \tag{11}$$

$$\theta = \theta_o + \int_0^t \omega_m\, dt \tag{12}$$

Indirect oriented field control. In the Indirect oriented field control strategy, which basic scheme is depicted in the figure 12, the electromagnetic torque reference C_e^* depends on I_{sq}^*, given by (8). In this case, the rotor flux reference is supposed to be constant. Since $I_{sd}^*=0$, the current components, in the stator reference frame, depends on the position of the field vector δ_b^* given by (10). All strategy details are depicted in the figure 12. The $\exp(j\delta_b^*)$ block represents the coordinate transform from the field reference to the stator reference. The PWM+VSI block controls the stator currents. On the other hand, the excitation is provided by a one leg inverter.

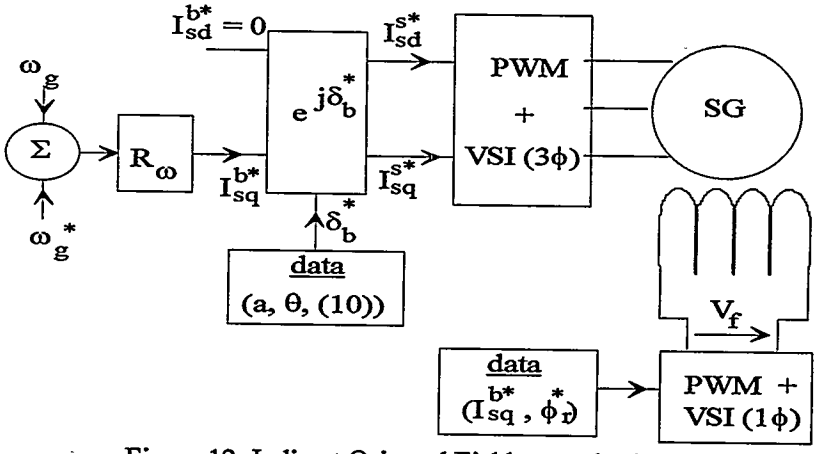

Figure 12 Indirect Oriented Field control scheme

DESIGN OF THE PI CONTROLLERS

Stator current controller. The stator current controllers are designed in according to the dominant pole cancellation technique with placement of complex poles with optimal damping (Buhler [6]). The stator current closed-loop is depicted in the figure 13.

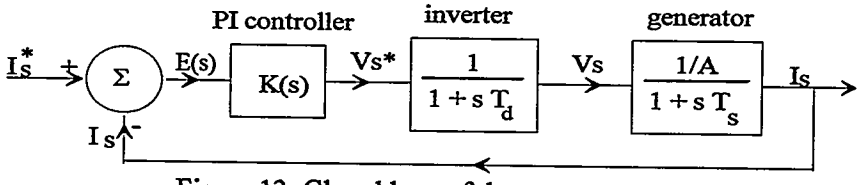

Figure 13 Closed loop of the stator currents

From the figure 13, the open-loop transfer function of the stator current $G_{oi}(s)$ is given by [5]:

$$G_{oi}(s) = \frac{I_s}{E(s)} = \frac{1 + sT_i}{sT_i} \frac{1}{1+sT_d} \frac{1/A}{1+sT_s}$$

$$T_s = \frac{A}{B} = \frac{A}{\sigma l_s} = \frac{r_s + r_r l_m^2 / l_r^2}{(1 - l_m^2/l_s l_r) l_s}$$

where T_d, the inverter time constant, is equal to the half period of one inverter load cycle, i. e., $T_d = T_e/2$. The result after cancellation of the dominant pole at $-1/T_s$ is:

$$G_{oi}(s) = \frac{1/AT_i}{s(1+sT_d)}$$

A simple rule to obtain complex poles with optimal damping or to obtain real poles with the same magnitude, for the closed-loop, it is necessary to follow the rule [6]:

$$T_i = \frac{4T_d}{A} \quad \text{or} \quad T_i = \frac{2T_d}{A} \tag{13}$$

respectively. For discrete control purposes, it is necessary to obtain the equivalent discrete PI controller gains related to a sampling period T_{ei}. Thus, the gains are given by the relations [6]:

$$K_i = \frac{T_{ei}}{T_i} \qquad K_p = \frac{(T_s - T_{ei}/2)}{T_i} \tag{14}$$

Bus current controllers. In the figure 14, L_n and R_n are the inductance and the ohmic resistance related to the local transmission line (Kohlmeier et al [7]). L_f is the filter inductance. The power factor control is carried out in the line side.

The closed-loop diagram of the line (grid) currents is similar to the figure 13. This control loop aims at aligning the line current vector to the voltage V_p. So, in steady state, the phase shift ϕ tends towards zero and the power factor tends towards -1 or +1 depending on the machine is operating as a generator or as a motor respectively.

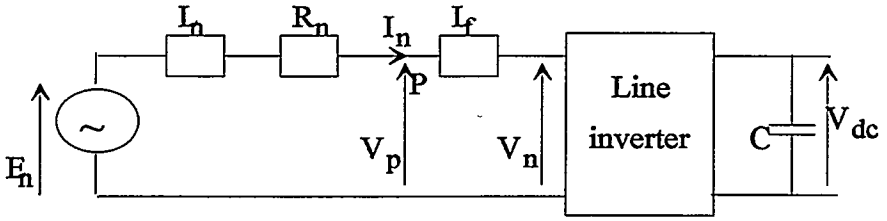

Figure 14 Grid (line) side diagram

The design of the controller gains and the computation of its discrete values follow the same procedure employed in the stator current controller section.

Angular velocity controller. It was assumed a simplified mechanical model with two mass moments of inertia to represent the mechanical behavior of the system. The multiplier inertia is included in J_2 as show in the figure 15.

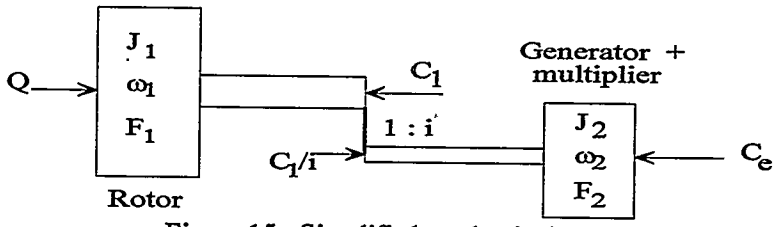

Figure 15 Simplified mechanical model

Although the system is of third degree, it can be approximated by one of order one. Marechal [8] shows that in general this kind of system have a low frequency vibrating mode related to the dominant pole and others two frequency vibrating modes of high frequency, so, the rotor speed controller design can be based on the equation:

$$\frac{d\omega_1}{dt} = \frac{(-Q + i\,C_e - F\,\omega_1)}{J} \qquad F = F_1 + iF_2 \quad and \quad J = J_1 + i^2 J_2$$

In cascade with the rotor speed closed-loop control, the stator current closed-loop control can be represented by a first order transfer function with a small time constant T_p ($=T_{ei}$) and an unit gain so resulting in a scheme similar to the figure 13 where the time constant T_s is replaced by $T_m = J/F$. The gains of the rotor speed controller were calculated based on placement of real poles of same magnitude. Their values for a sampling period T_{ew} are equal to:

$$K_i = \frac{T_{ew}}{T_i} \qquad K_p = \frac{(T_m - T_{ew}/2)}{T_i} \qquad T_i = 4\,T_p / F$$

Dc link voltage controller. The voltage stability in the dc link is very important to the line current control as the amplitude I_n^*, showed in the figure 16, is the output of the dc voltage controller. Fast fluctuations in I_n^* may result in a poor power factor.

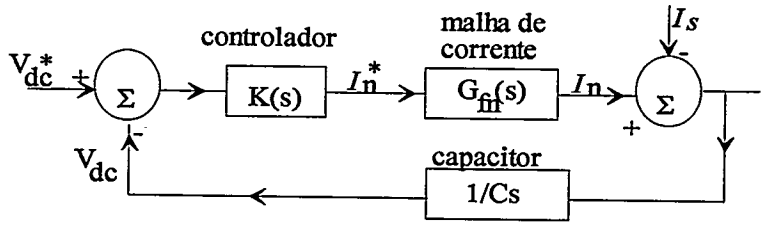

Figure 16 Closed loop of the dc link voltage

On the other hand, as the J_1 (rotor) is much greater then the J_2 (generator) the mechanical dynamics of the systems is very slow independently if the electromagnetic torque can vary fast or not. This can result on easy saturation in the stator current controllers. It may be avoided by limiting the output of the rotor speed controller.

RESULTS

It was chosen three variables to analyze the simulation results of the system. They are : a)rotor power coefficient, b)rotor speed and c)electrical power factor. The input signal of the wind speed was simulated as depicted in the figure 17. The simulation was carried out digital computer with a time increment of 1 μs.

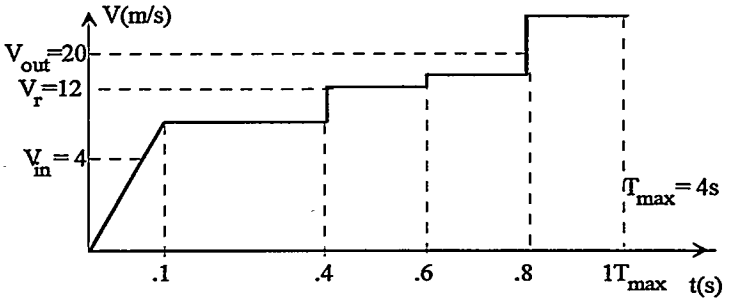

Figure 17 Wind velocity input signal

Power coefficient of the rotor. In the figure 18a, the value of C_p is multiplied by the factor 100% /Cp_{max}. For $V_{in} < V < V_r$ the C_p value tends to 100%, i. e., it tends to Cp_{max}. It can be seen small fluctuations in Cp due to the wind speed transients. In the interval $V_r < V < V_{out}$ the wind power capture is reduced in order to keep constant the output power. So, the maximization on the energy capture from the wind was achieved satisfactorily.

Rotor speed. The rotor speed results show a good first degree behavior with an error lesser than 1% when the system reached the steady state. This signal converges to the steady state reference without overshoot. In part, this is caused by the limit in the signal output of the controllers. In this case, the output of the integral part of the rotor speed controller was strongly limited. The results are shown in the figure 18b.

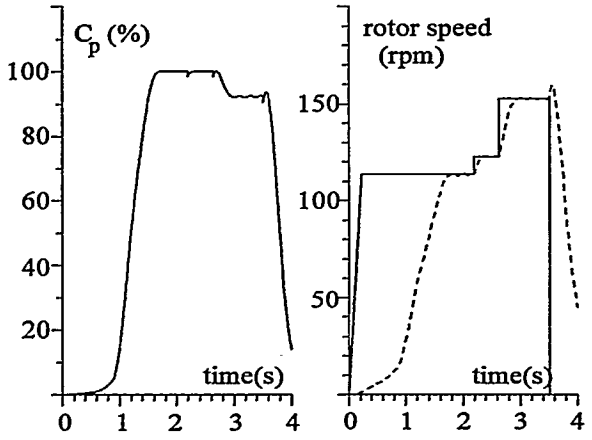

Figure 18 a)Power coefficient b)Rotor speed

Power factor. The power factor measured in the point P of the figure 14 assumes values between -1 and +1 as depicted in the figure 19b. For t ≅ 1s the signal fluctuates with great frequency because the value of the reference of the electromagnetic torque is reduced. Before this moment, the machine is operating as a motor and after that it starts to work as a generator so this is the moment of transition. The final value of the power factor is ≅ -1 after reached the steady state.

Rotor flux. The rotor flux that is controlled by feed forward strategy presents fluctuations when the wind speed varies and during the machine start-up as shown in the figure 19 a.

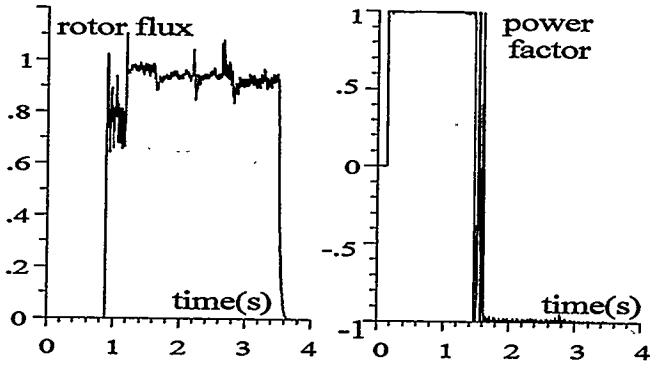

Figure 19 a)Rotor flux b)Electrical power factor

WECS SIMULATION DATA

Generator: r_s=0.5 Ω; r_r=1.5 Ω; l_s=l_r=0.022 H; l_m=0.021 H; p=2; T_s=1.05 ms; T_r=14.67 ms
Rotor: R=9 m; λ_d=8.5; Cp_{max}=0.44; P_r=118 kW; V_r=12 m/s; V_{in}=4 m/s; V_{out}=20 m/s
Dc link: C=5000 μF **Converters:** switching frequency=10 kHz → T_e=0.1 ms
Local grid: R_n=0,4 Ω; L_n=0,01 H; T_n=25 ms; **Sampling period:** T_{ei}=T_{en}=T_{evdc}=1 ms; T_{ew}=10 ms;

REFERENCES

[1] SMITH, G.A. (1989) - Wind Engineering, vol 13, no 2, pp. 88-98.

[2] LYSEN, E. (1984)- "Introduction to Wind Energy". Technical University of Eindhoven, Netherlands.

[3] BROECK, H. W.; SKUDELNY, H. C.; STANKE, G. V. (1988). IEEE Trans. on Industry Applications, Vol. 24, No 1, Jan./Feb., 142-150.

[4] CHATELAIN, J. (1983) - "Machines Eléctriques", Tome I, Dunod & Presses Polytechniques Normandes.

[5] MEDEIROS, A.L.R. - "Dynamic Analysis of a Synchronous Generator Wind Energy Conversion System for performance optimization". Internal research report, UFPB, Campina Grande/PB, Brazil.

[6] BUHLER, H. (1983) - "Réglages Echantilonées". Vol. 1 et 2. Presses Polytechniques Romandes - Ecole Polytechnique Fédérale de Lausane.

[7] KOHLMEIER, H.; NIEMEYER, O; SCHRODER, D. F. (1987) - . IEEE Trans. on Industry Applications, Vol. IA-23, No 6, Nov./Dec., 1001-1009.

[8] MARECHAL, L. (1987) - "Commande Optimale d' un Aerogenerateur a Vitesse Variable". Thése de Doutorat, Université Paul Sabatier de Toulouse,

TESTING OF A 50-kW WIND-DIESEL HYBRID SYSTEM AT THE NATIONAL WIND TECHNOLOGY CENTER

David A. Corbus
Jim Green, April Allderdice, Karen Rand & Jerry Bianchi
National Renewable Energy Laboratory
1617 Cole Blvd.
Golden, CO 80401-3393
United States of America

Ed Linton
New World Village Power
One North Wind Road
PO BOX 999
Waitsfield, VT 05673
United States of America

INTRODUCTION

In remote off-grid villages and communities, a reliable power source is important in improving the local quality of life. Villages often use a diesel generator for their power, but fuel can be expensive and maintenance burdensome. Including a wind turbine in a diesel system can reduce fuel consumption and lower maintenance, thereby reducing energy costs. However, integrating the various components of a wind-diesel system, including the wind turbine, power conversion system, and battery storage (if applicable), is a challenging task.

To further the development of commercial hybrid power systems, the National Renewable Energy Laboratory (NREL), in collaboration with the New World Village Power Corporation (NWVP), tested a NWVP 50-kW wind-diesel hybrid system connected to a 15/50 Atlantic Orient Corporation (AOC) wind turbine. Testing was conducted from October 1995 through March 1996 at the National Wind Technology Center (NWTC). A main objective of the testing was to better understand the application of wind turbines to weak grids typical of small villages. Performance results contained in this paper include component characterization, such as power conversion losses for the rotary converter system and battery round trip efficiencies. In addition, system operation over the test period is discussed with special attention given to dynamic issues. Finally, future plans for continued testing and research are discussed.

System Description

The hybrid power system includes a synchronous generator that provides 3-phase power to the load. This is coupled to a DC machine on one side and through a clutch to a diesel engine on the other side. AC current is converted to DC current when the DC machine runs as a generator, thereby allowing the batteries to be charged. When the clutch is disengaged on the diesel, the batteries may power the DC machine and the DC machine can supply torque to the AC generator. Frequency on the system may be controlled either by the diesel governor (diesel on) or the DC machine and programmable logic controller (PLC) (diesel off). An AOC 15/50 wind turbine is connected in parallel to the load to reduce diesel fuel consumption, with excess wind power charging the batteries or being dissipated by a resistive dump load. Table 1 lists the major components of the system [New World Village Power, 1994], and Figure 1 shows a system schematic with the location of the sensors used in the data acquisition system.

TABLE 1. System Components

Rotary Converter		Diesel Engine
AC Synchronous Machine	**DC Machine**	**Northern Lights Lugger**
480 V, 3 phase, 60 Hz 50 kWe and 62 KVA continuous 75 kWe peak (30 sec)	240 V armature (300 V generating) rated for 309 A @ 200 V 150 V field, 3 A nominal, 6 A maximum 55 kW, 4 Pole Shunt Wound 1800 RPM	75 Hp, 1800 RPM 4 cylinder, turbocharged Radiator cooled
Dump Load	**Controller**	**Battery Bank**
480 V, 3 phase 75 kW continuous Resistive Load Bank	Omron PLC Controller TCP Jr. Local Operator Interface New World Village Power Remote Operator Interface	C&D HD700, valve-regulated, absorbent glass mat, lead-calcium batteries 114 cells, 700 AHr (nominal 5 Hr rating to 1.88 V per cell)

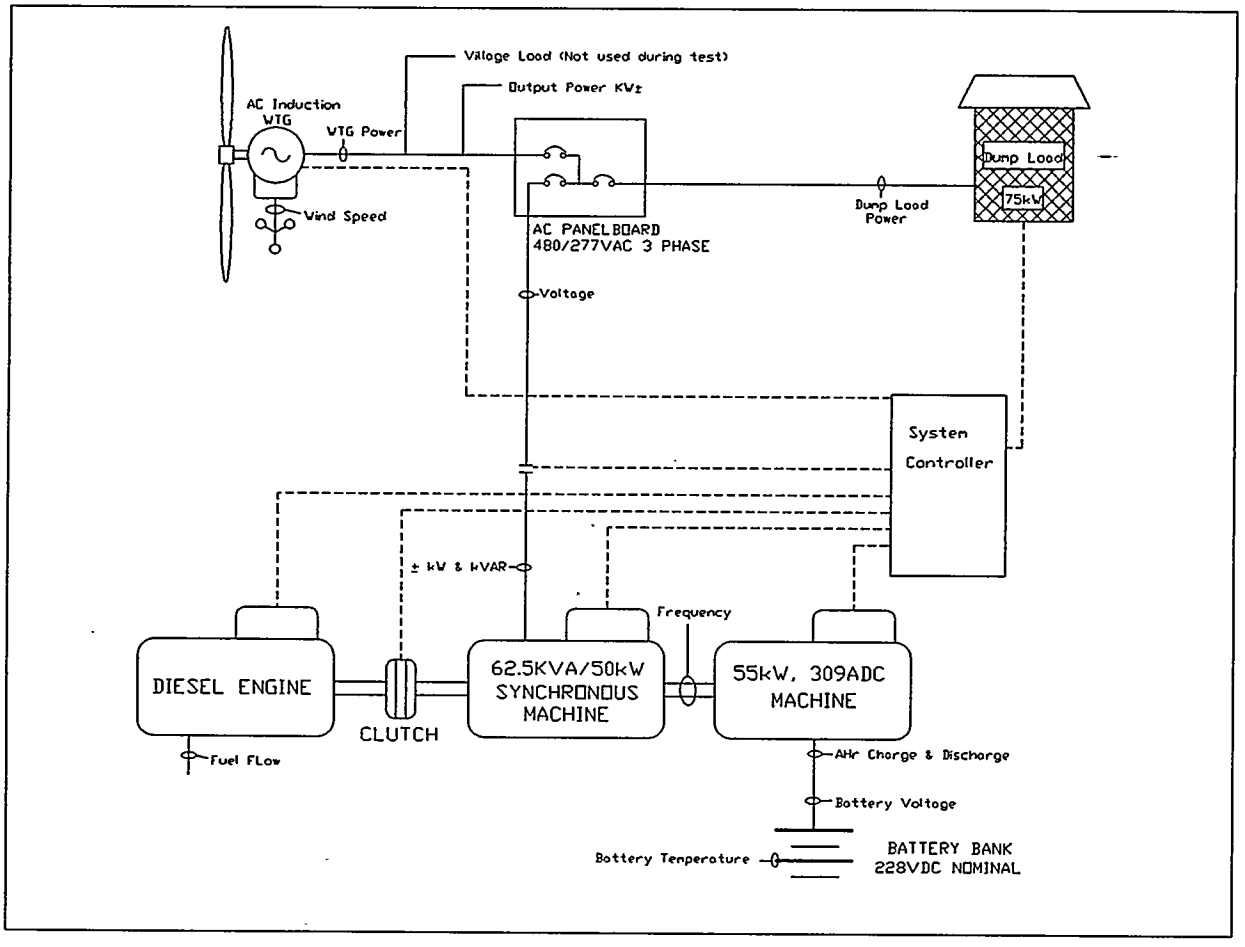

FIGURE 1. System Schematic

COMPONENT CHARACTERIZATION TESTS

The initial hybrid system testing focused on component characterization. We calculated component efficiencies of the rotary converter and battery bank for different operating states, and we measured wind turbine power output. Evaluation of fuel efficiency (i.e., liters/kWh) is pending until installation of a fuel flow meter.

AOC 15/50 wind turbine. The AOC 15/50 is a downwind, stall regulated, 15 meter rotor-diameter turbine that is rated at 50 kW for a 11 meter/sec wind speed. Maximum continuous power output from the turbine, based on the published power curve, is 65 kW [Atlantic Orient Corporation, 1994]. Test data for the 15/50 turbine connected to the utility grid showed maximum peak power of 83 kW for a two-second average wind speed, as shown in Figure 2. Figure 2 also shows minimum power reaching -25 kW. (Because of the air density variation due to the altitude at the NWTC, the average power data shown in Figure 2 differ from the published power curve.)

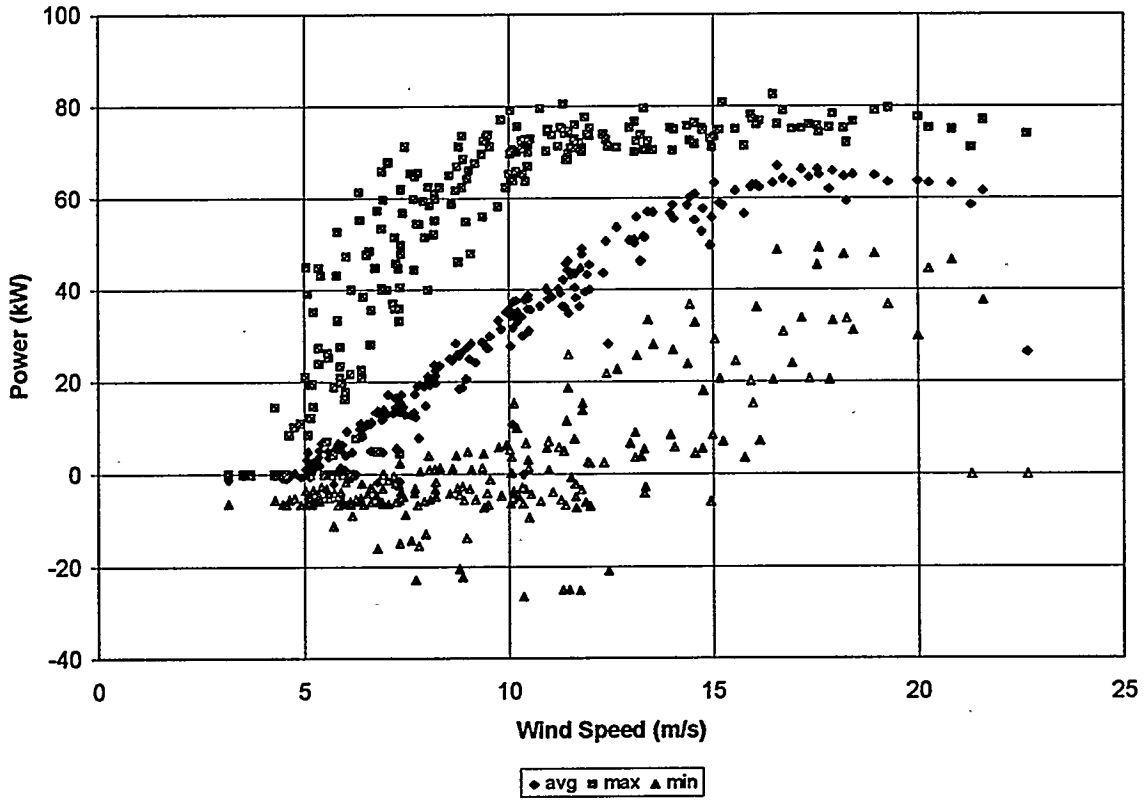

FIGURE 2. AOC Power Output (2 sec. avg.)

Rotary converter efficiency. To evaluate the rotary converter efficiency, we measured power input to and from the AC synchronous generator, power to and from the battery bank, battery bank voltage, and diesel run time (see Figure 1 for sensor locations). The system dump load was used as a power sink for power

out of the AC synchronous generator. Data was taken every tenth of a second and recorded as ten-minute averages.

For energy flowing from the battery bank to the AC bus, a data set of 104 time steps with zero diesel and zero wind turbine run time was used. The graph of power out of the AC machine versus power from the batteries is shown in Figure 3. The performance of the rotary converter was found to obey the relationship:

$$y = 1.135x + 2.98 .$$

For energy flowing from the AC bus to the battery bank, a concatenated data set of 360 time steps with the wind turbine as the source of power was used (i.e., zero diesel run time and zero battery discharge). The graph of power to the battery bank versus power into the AC machine is shown in Figure 4. The performance of the rotary converter was found to be:

$$y = 1.135x + 2.85 .$$

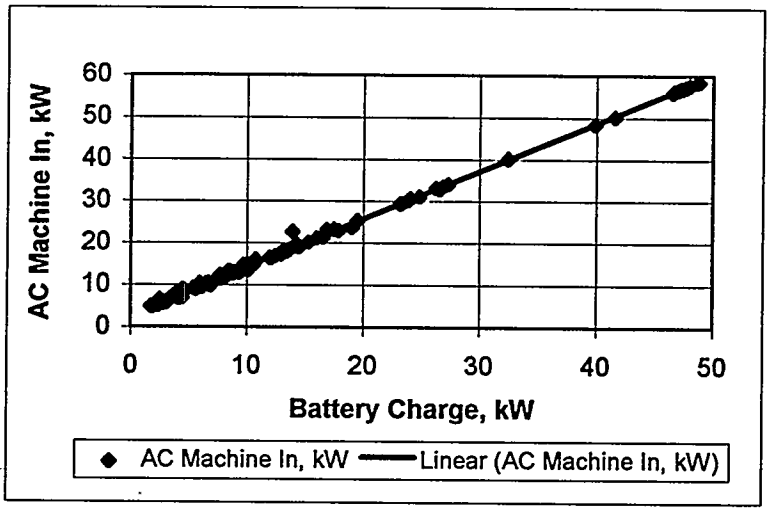

FIGURE 3. Converter Performance AC to DC

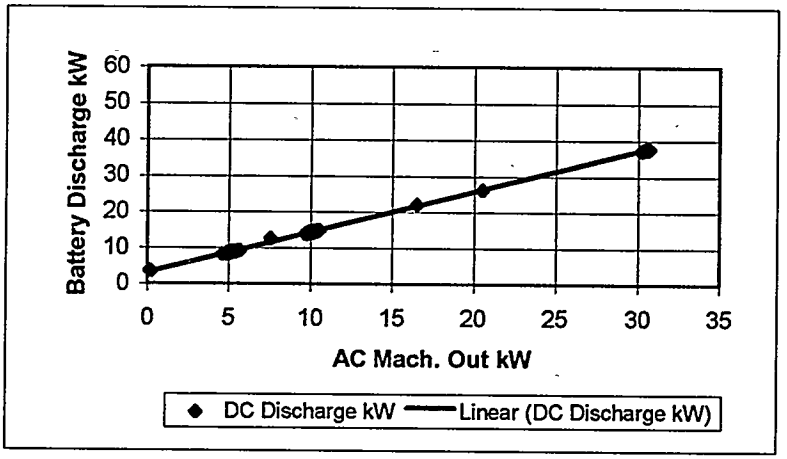

FIGURE 4. Converter Performance DC to AC

In these equations, y is the power input to the rotary converter in kW and x is the power output from the rotary converter in kW. The y-intercept (2.85 and 2.98 kW) represents the fixed losses for the system, or the standing losses, and are constant because the rotary converter operates at a fixed speed. (These losses are slightly different depending on the direction of power flow, i.e., DC-AC or AC-DC, because of the difference in conversion efficiency of the AC and DC machines.) Electrical losses scale with the amount of power through the rotary converter and may be calculated from the slope of the curve in Figures 3 and 4; they are about equal. A graph of overall rotary converter efficiency as a function of power is given in Figure 5.

Battery charging efficiency. The hybrid system uses valve regulated lead acid (VRLA) batteries. The battery efficiency depends on temperature, depth of discharge, length of tapering charge, rate of charge and discharge, age and condition of batteries. We characterized batteries for the actual operating conditions of the system, and this included analysis of the battery efficiency under both a constant load and a preprogrammed diurnal "village" load.

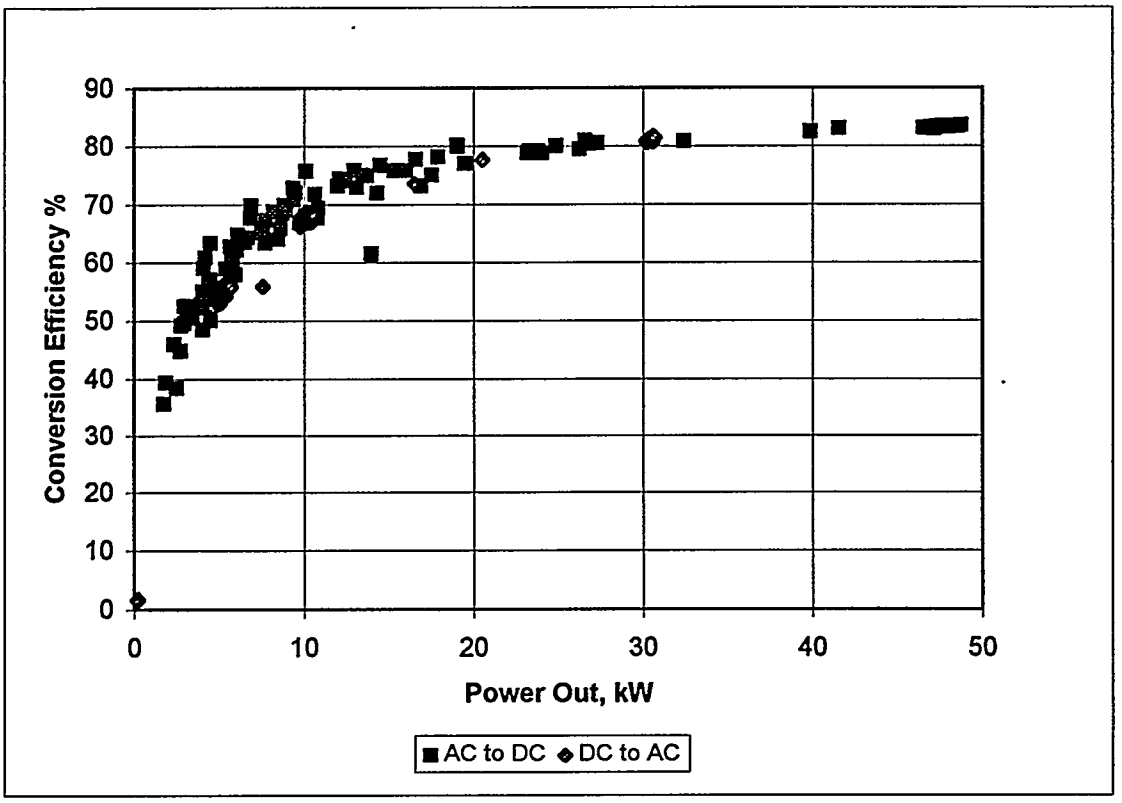

FIGURE 5. Rotary Converter Efficiency

To characterize the battery efficiency for a constant load, the battery bank was charged by the diesel generator at a constant current and then discharged for a constant load for four battery charge/discharge cycles. The batteries performed at a 90% watt-hour efficiency. The temperature of the battery bank measured between 25° and 35° C. When compensated for high temperature, the watt-hour battery efficiency was about 80%, which is within the expected 65%-80% range for VRLA batteries [Berndt, 1993]. A graph of battery voltage, current, and temperature during this test is shown in Figure 6.

Battery performance was also characterized for a simulated village load profile, without using the wind turbine. The batteries performed at an 88% watt-hour efficiency. The temperature of the battery bank measured between 30° and 40° C. When compensated for high temperature, the battery efficiency is also about 80%. A graph of battery voltage, current, and temperature during this test is shown in Figure 7. In both cases, the transducers monitored only the battery bank, so rotary converter losses are not included in these efficiencies.

Overall rotary converter/battery system efficiency. For energy from the wind turbine and passing through the battery bank before meeting a village diurnal load, the system has a round-trip overall efficiency of 62% at full load: 83 * .90 * .83 = .62 (i.e., 83% conversion efficiency one way and battery efficiency of 90%).

EXTENDED OPERATION OF SYSTEM

System Tests. We conducted system testing from December 1995 through March 1996. Because of competing uses for the turbine and dynamic issues associated with operation of the system, testing of the system was intermittent. The majority of the testing was conducted using a typical village load profile that

Battery Round Trip Efficiency over 4 cycles
Load = 20kW

kWh in	kWh out	Net Loss	Efficiency
404.71	365.48	39.23	0.90

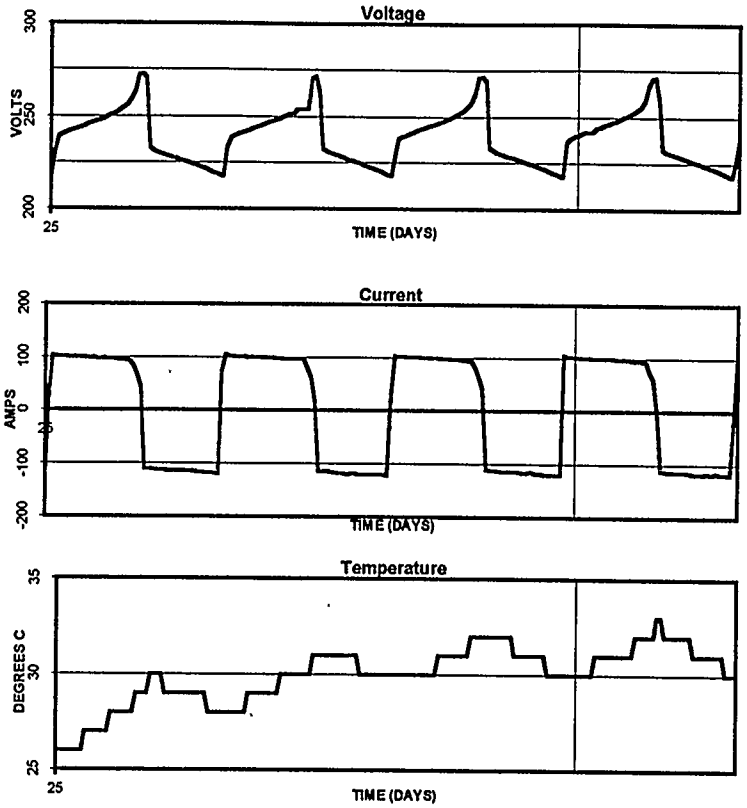

FIGURE 6. Constant Load Condition

Battery Round Trip Efficiency over 5 cycles
Village Diurnal Load

kWh in	kWh out	Net Loss	Efficiency
636.71	559.69	77.01	0.88

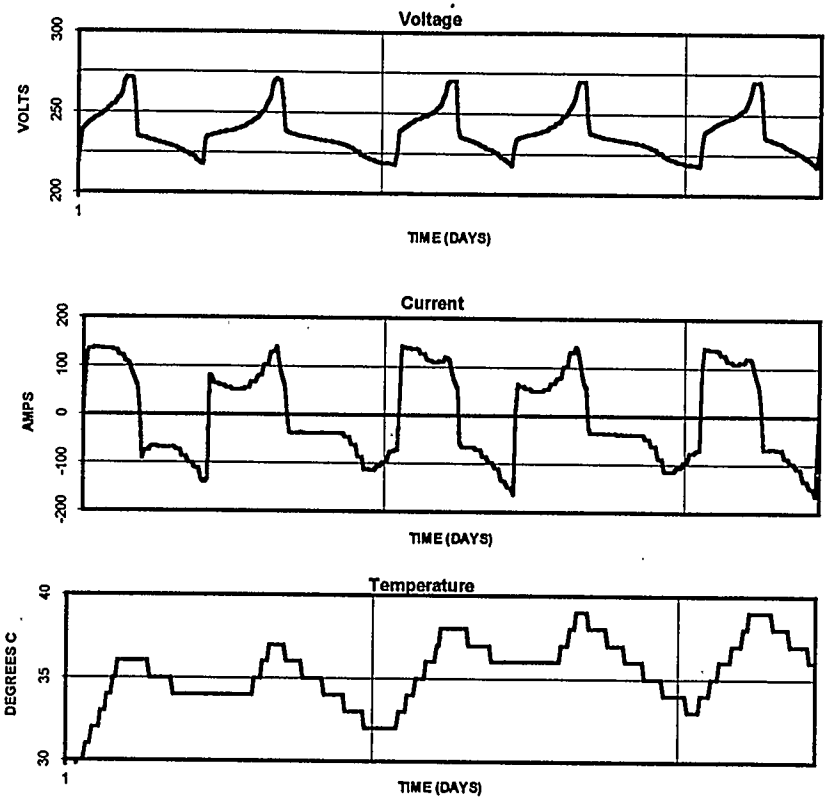

FIGURE 7. Diurnal Load Condition

is shown in Figure 8. The resistive dump load was used to simulate the village load for system testing. Although the dump load comprises resistive elements, the power factor on the system was usually low because of harmonic distortion created by the silicon controlled rectifier (SCR) switches in the phase-controlled dump load controller.

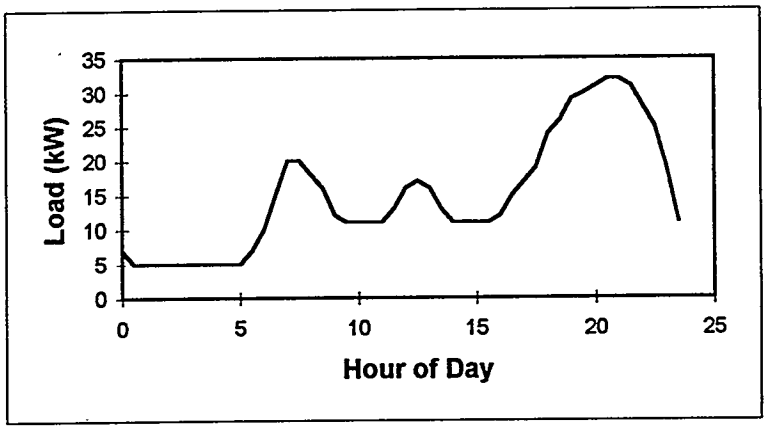

FIGURE 8. Diurnal Load Profile

The data acquisition system recorded operating parameters in ten-minute averages. Based on the ten-minute averages, weekly summaries for the system were produced that show on-line time, diesel run time, total wind turbine energy, total load, dumped energy, diesel starts, and battery cycles. In addition, operating parameters such as wind power, load setting, dumped power, and battery state-of-charge were plotted. An example on one of these plots is shown for 7 days in Figure 9. Note the dumped power is high when the batteries are fully charged and the wind speed is high, and that the system is off when the load power is zero.

Rotary converter. In March 1996, large vibrations were noticed on the AC synchronous generator, so the system was shut down and disassembled. Inspection showed severe wear on the spline connection from the AC generator shaft to the diesel clutch. The AC generator was converted from a single bearing to a double bearing system to reduce transverse loads on the clutch-to-spline connection. The system was up and running again in June, but operating data and analysis results for this paper are included only through March.

Batteries. One of the problems encountered with operation of the batteries was temperature control. Temperature control of VRLA batteries is important, because if cells are allowed to operate at too high a temperature, their lifetime may be shortened as a result of loss of electrolyte. VRLA batteries are "maintenance free," hence their electrolyte cannot be replaced. Although the exact correlation between cell lifetime and operating temperature is poorly understood, it is always prudent to operate batteries near their rated temperature of 25° C.

One of the advantages of VRLA batteries is that they can be stacked on top of one another, thereby reducing the space required to house them. However, the stacked battery cells are harder to keep cool; hence, we will install an air conditioner to keep batteries cool during testing when ambient temperatures are high.

An alternative to VRLA batteries is flooded lead-acid batteries. For systems of this type, especially those installed in warm climates, we recommend that flooded lead-acid cells be considered because of their tolerance of higher temperatures and their reduced costs. Disadvantages of flooded lead-acid batteries are their larger space requirements and need for maintenance. The degree of maintenance (e.g., watering of batteries) varies for different types of flooded lead-acid batteries.

Dynamic issues. Three dynamic issues arose during system testing: negative power from the wind turbine, larger-than-anticipated power transients from the wind turbine, and high battery voltage excursions. The

first two issues are primarily a result of integrating the AOC 15/50 turbine with the NWVP system, while the last issue is more closely related to system control of the rotary converter system.

The first dynamic issue, negative power from the wind turbine, occurred during extremely turbulent, high wind conditions. As shown in Figure 2, power output from the AOC 15/50 wind turbine is negative at times. In fact, negative power excursions as low as -70 kW were observed on the system in very high turbulent wind conditions. (During this testing we did not identify the cause of these extreme excursions; however, we will investigate this in subsequent testing). During the negative power surges, the rotary converter system supplies power to the turbine to motor it, but in many cases the current was over the DC machine rating, so the PLC would shut down the DC part of the system. (During a DC fault, the diesel generator takes over control of the system so that the load continues to be met, which is an important feature of the hybrid system.)

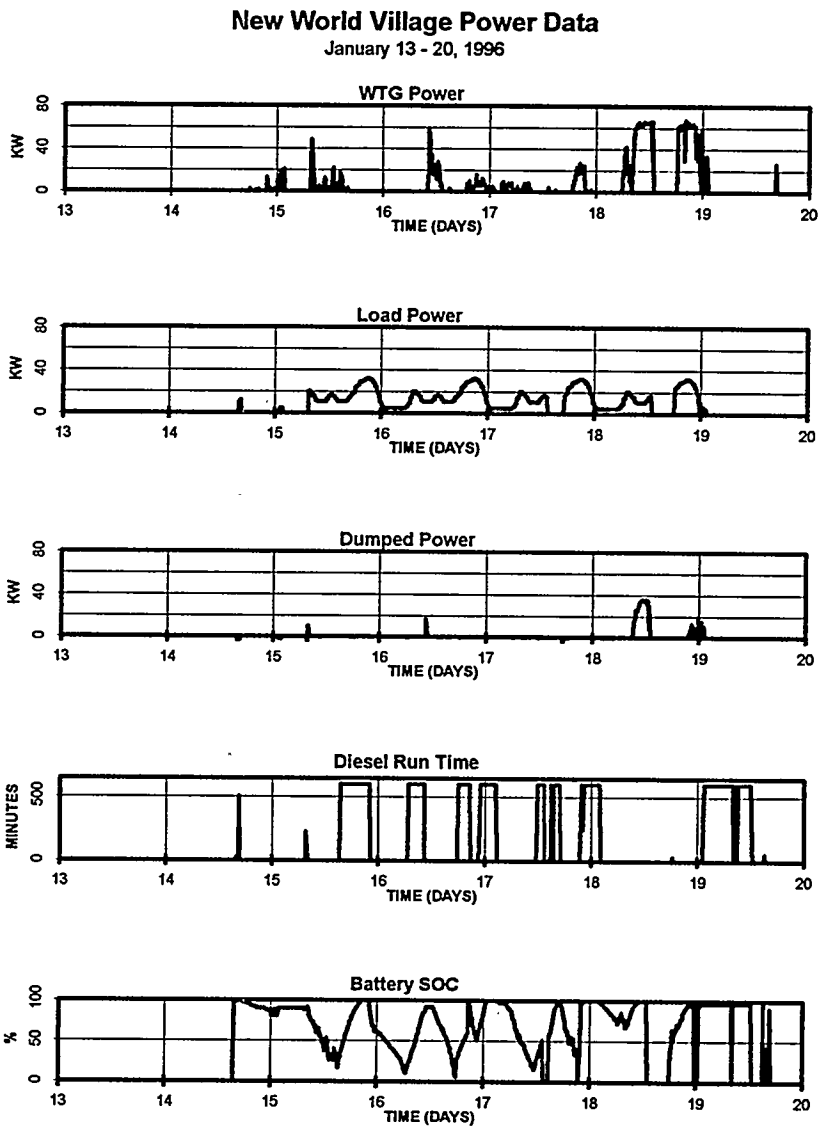

FIGURE 9. NWVP Weekly Summary

We changed the PLC to disconnect the turbine whenever the power went below -10 kW. Although this resulted in significant turbine downtime during periods when the turbulent conditions existed, these *conditions were infrequent*, so overall turbine downtime was not excessive. (Because the testing was intermittent, total downtime from this condition at this site is hard to estimate, but might be on the order of 10 days during the peak four months of wind.)

There are two approaches to mitigate this problem. A high speed tachometer could be added to the turbine to detect transient underspeeding of the turbine and shut it down during negative power events before the hybrid system grid tried to motor the turbine. (The existing turbine tachometer does not have enough resolution to detect very short-term changes in turbine speed and hence could not be used.) The approach would result in a situation similar to the existing solution of cutting the wind turbine out at -10 kW; both could put excessive wear on the turbine breaking system. The second approach is to install an

asynchronous controller on the turbine so that it could go below synchronous speed momentarily and have the power regulated on the grid. These two approaches will be considered in follow up testing.

The second dynamic issue, higher-than-anticipated power output from the wind turbine, was a problem for system testing because the existing 75 kW of dump load capacity could not absorb the peak 83 kW of power from the turbine during extremely high winds. As a result, the turbine would overspeed and shut itself down, although the hybrid power system would continue to operate. The turbine would go into a normal 7-minute cool down before restarting itself and reconnecting to the system. This condition would not be a problem for actual installations in most villages, because a village would have a continuous base load of about 10 kW. However, the higher-than-anticipated turbine output did require the addition of extra test load capacity to the dump load. For village systems, we recommend sizing the dump load for the maximum short-term turbine power output minus the minimum expected base load.

High battery voltage was the third dynamic issue we identified. When the wind turbine is charging the batteries, current is supplied to the batteries until a high voltage set point on the batteries is reached, then the current is supplied to the dump load. However, power spikes from the turbine resulted in transient high battery voltage excursions because the PLC was not able to shift power from the batteries to the dump load fast enough. Although changes to the dump load controller gain were made, further changes are required to mitigate this problem. This could include changing the size of the dump load increments or implementing PID dump load control.

System Startup. In the beginning of the testing the hybrid system grid could not handle a "hard start," (i.e., the hybrid system could not motor the turbine up to synchronous speed), because the in-rush currents to the turbine were too high for the hybrid system grid. Hence, the PLC was changed to allow the turbine to coast up to synchronous speed before connecting to the hybrid system grid.

Dump load. Harmonic noise (20%-25% total harmonic distortion) was created by the phase controlled dump load, and this set off a voltage alarm on the turbine and caused other problems. For future systems, changing to a binary step, zero crossing solid-state-relay dump load should eliminate this problem.

General maintenance. Routine diesel maintenance was required for the system (e.g., changing oil and oil filters). In addition, water was frozen in the breather for the system which resulted in a broken seal on the turbo that had to be replaced. Aside from the major generator retrofit to the double bearing system, equipment maintenance on the NWVP system was low.

FUTURE WORK

We plan to make additional changes to the PLC software to mitigate the high battery voltage events, and to further test the system response to step changes in load, loss of load, and power quality for various events, such as severe phase imbalance and induction motor starts. Short-term power quality measurements will also be performed to help further understand dynamic issues, and we will record fuel flow measurements and estimate fuel efficiency (i.e., liters/kWh) for the system. Finally, the negative power from the AOC 15/50 will be investigated to determine why it is happening and under what type of conditions, and various approaches will be implemented to mitigate the effect that negative power has on the hybrid system grid.

CONCLUSIONS

Testing of the system has demonstrated the challenges of integrating specific wind turbine characteristics into a small, weak grid (i.e., a grid typical of a small village), as is demonstrated by the NWVP 50-kW

system. In our testing, we had to make changes to the NWVP system's controller so that the hybrid system could handle the AOC 15/50's negative power events and so that high battery voltage events caused by transient peak power from the turbine could be minimized. For hybrid systems of this type, a good PLC code is required for system control, and changes to this software will be needed depending on the specific turbine connected to the system.

REFERENCES

New World Village Power. 1994. "Renewable Energy Modules for Village Electrification." Waitsfield, Vermont: The New World Power Corporation.

Atlantic Orient Wind Systems. 1994. "Producing Tomorrow's' Wind Turbines Today. " Waitsfield, Vermont: Atlantic Orient Wind Systems Inc.

Berndt, D. 1993. *Maintenance-Free Batteries*. Somerset, England: John Wiley and Sons.

Wind Farm Production Cost : Optimum Turbine Size and Farm Capacity in the Actual Market

A-R. LAALI*, A. LOUCHE, J-L. MEYER*, C. BELLOT***

*Electricité de France (EDF)
R&D Division - Machines Department
6 Quai Watier 78401 Chatou - France

**Espace de Recherche
et d'ApplicationS en Maîtrise de l'Energie (ERASME)
Route des Sanguinaires F-20000 Ajaccio- France

ABSTRACT : Several studies are undertaken in R&D Division of EDF in collaboration with ERASME association in order to have a good knowledge of the wind energy production costs. These studies are performed in the framework of a wind energy monitoring project and concern the influence of a few parameters like wind farm capacity, turbine size and wind speed on production costs, through an analysis of the actual market trend. Some 50 manufacturers and 140 different kind of wind turbines are considered for this study.

The minimum production cost is situated at 800/900 kW wind turbine rated power. This point will probably move to more important powers in the future. This study is valid only for average conditions and some special parameters like particular climate conditions or lack of infrastructure for a special site the could modify the results shown on the curves.

The variety of wind turbines (rated power as a function of rotor diameter, height and specific rated power) in the actual market is analysed. A brief analysis of the market trend is also performed.

1 - BACKGROUND

The French Ministry of Industry, EDF and ADEME (Energy and Environment Agency) are collaborating to prepare a few call for tenders in order to develop 250-500 MW of wind power over the next ten years in France. EDF is also involved in another important project in Morocco (Tetouan) to develop a 50 MW wind farm to be commissioned in the early 1997.

Several studies are undertaken in R&D Division of EDF in collaboration with ERASME (Research and Application of Rational use of Energy) association in order to have a good knowledge of the wind energy production costs. These studies are performed in the framework of a wind energy monitoring project.

2 - INTRODUCTION

A large number of parameters are involved in the assessment of the production costs of a wind turbines such as performance, operating costs, interest rates, capital depreciation periods, fiscal rules etc. These parameters are different from one country to another and from one company to another and are changing rapidly. The price policy of the manufacturers depends also on different parameters varying from case to case.

Sometimes the utilities need to know the production costs in advance and it is necessary to assess the costs with some average parameters. These costs couldn't be considered as absolute values but are very important to decision makers. In this paper we have tried to derive the market tendencies and to study more specially the influence of different variables.

Some 50 manufacturers and 140 different kinds of wind turbines are considered for this study. The new types of the MW class turbines are also taken into account.

3 - VARIETY OF WIND TURBINES

3.1 - VARIETY OF HEIGHTS & ROTOR DIAMETERS

The wind turbine variety is shown in figures 1 & 2. For the same rated power, different rotor diameters and different heights are proposed due to the wind conditions.

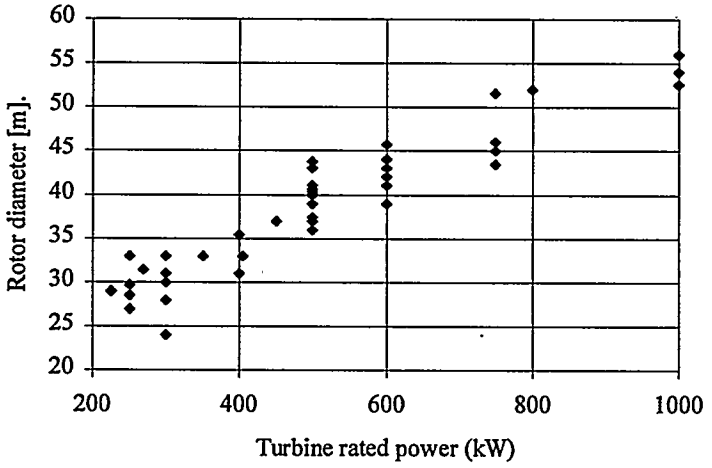

Figure 1 - Rotor diameter as a function of turbine rated power

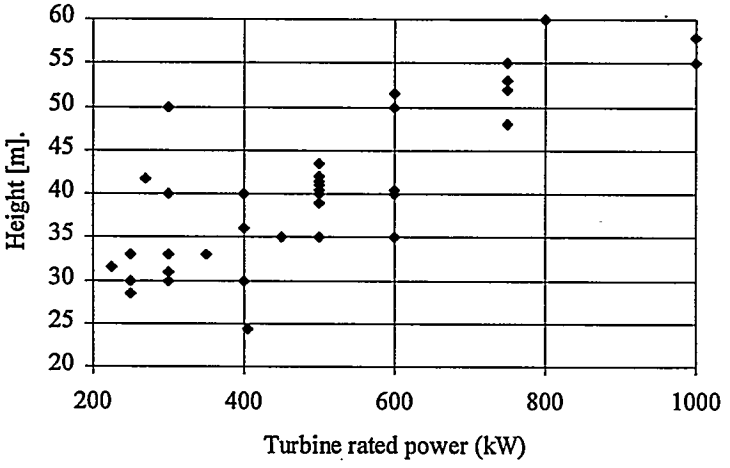

Figure 2 - Height as a function of turbine rated power

3.2 - VARIETY OF SPECIFIC RATED POWER

The variation of Specific Rated Power (W/m^2) for different wind turbines is shown in figure 3. This variety could be considered as rational because there is an optimal SRP, different for each wind potential and due to the choice of optimal economic production or maximum energy production.

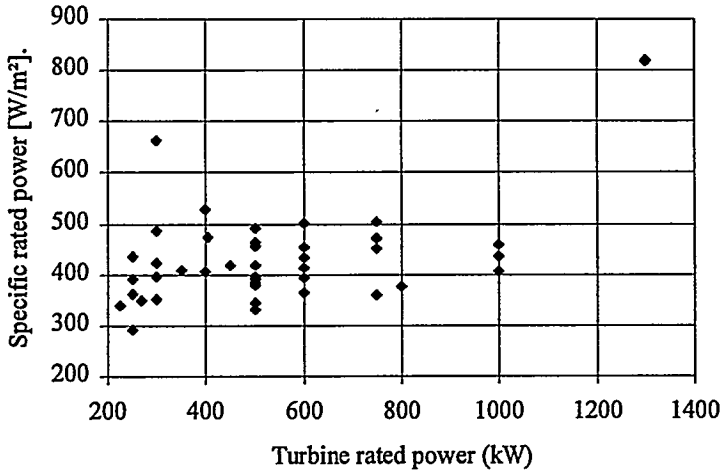

Figure 3 - Specific rated power as a function of turbine rated power

4 - PRODUCTION COSTS ASSESSMENT

The estimated production costs is based on the following assumptions :

Project life time	: 15 years
Capital recovery factor	: 8%
Capacity factor	: 0.30
Equity funding	: 40%
Interest rate	: 10%
Inflation rate	: 3.5%

The calculations are performed with the Weibull wind distribution (shape parameter k = 2). The wind turbine prices are obtained from [1&2]. According to some European experiences and the price trend for 1996, these official catalogue prices are reduced by 20%. The costs of grid connection, project management, civil engineering, erection, land, transport and miscellaneous costs are obtained by studying some European projects.

An example of different investment costs break down is provided in figure 4. The wind turbine represents roughly ¾ of the investment costs of a wind farm. The second important expenditure is the grid connection which varies from case to case. The rate of 10% in the figure gives an idea of these costs. The civil engineering costs are also very variable and the rate of 6% considers that there is no special truck roads to be constructed.

The off-shore installations are not considered in this study. Recent experiences have demonstrated that the costs related to these type of wind farms are 30 to 40% more (for shallow water wind farms).

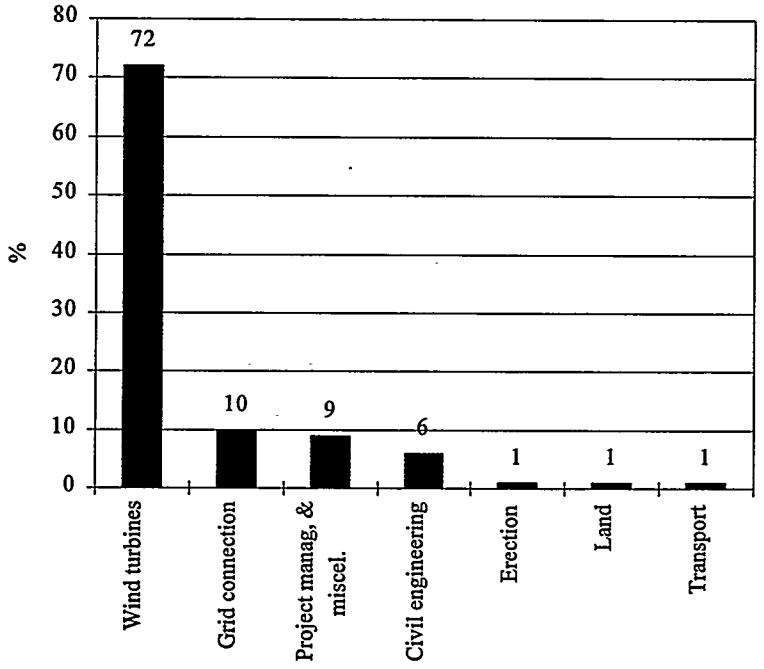

Figure 4 - Wind farm investment costs break down

5 - INFLUENCE OF DIFFERENT PARAMETERS ON PRODUCTION COSTS

Some 50 manufacturers and 140 different kind of wind turbines are considered for this study. The outcomes of this study are presented in figures 5 & 6 (the exchange rate considered in this study : US$ = 5.10 FF).

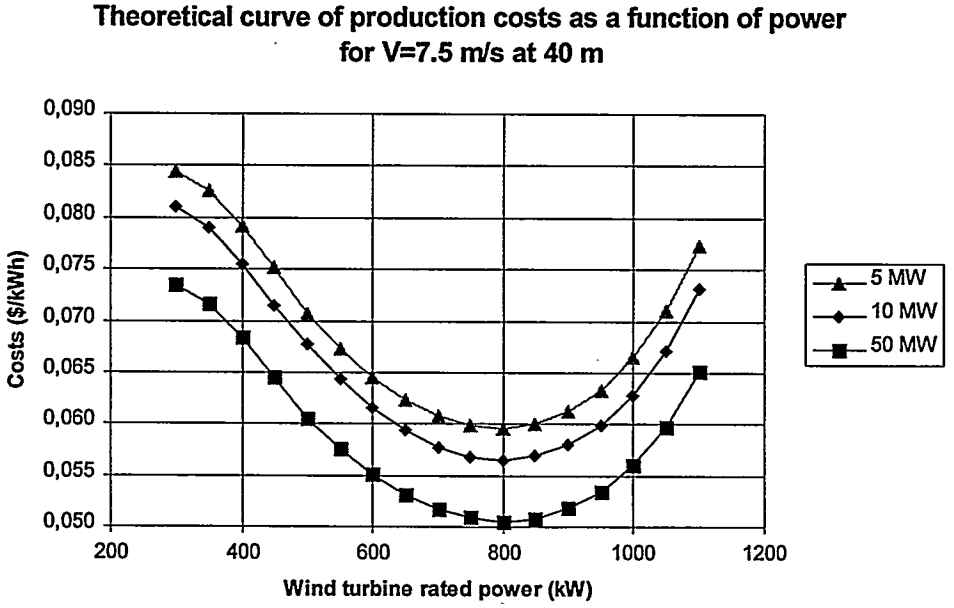

Figure 5 - Production costs as a function of turbine rated power for different farm capacity

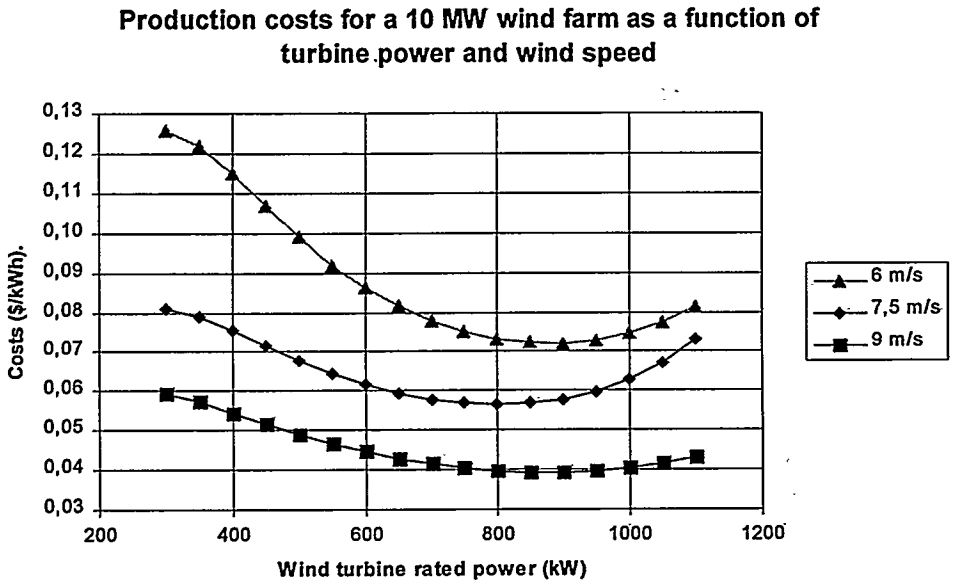

Figure 6 - Production costs as a function of turbine rated power for different mean velocities (Weibull coeff. k=2)

As illustrated in figure 5, by increasing the farm capacity from 5 to 50 MW the production cost will decrease by 20%. The minimum production costs, as could be seen from the curves is situated at 800/900 kW. This point will probably move to more important powers in the future. At 7.5 m/s wind mean velocity, using 800 kW machines instead of 400 kW turbines will generate a drop of 33% on production cost (figure 6). These curves are valid only for average conditions and some special parameters like particular climate conditions or lack of the road infrastructure for a special site could modify the results shown on the curves.

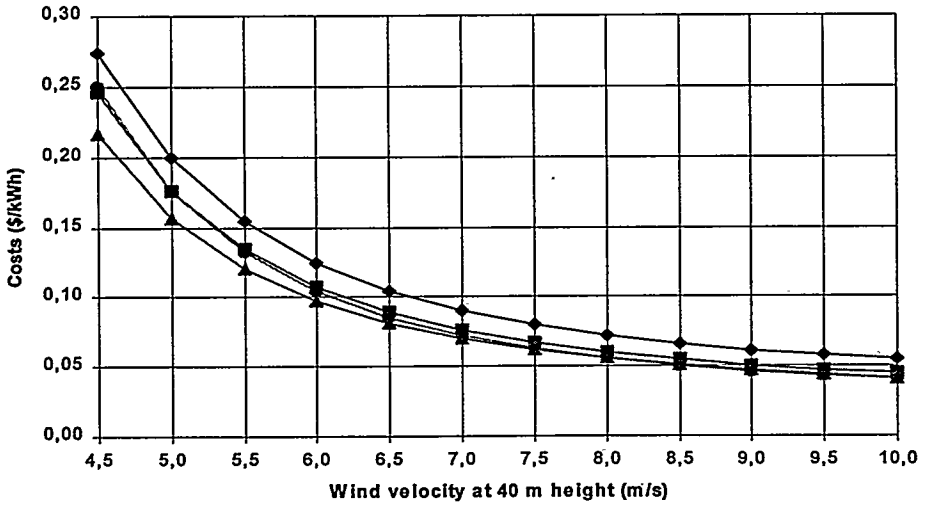

Figure 7 - Production costs of a 10 MW farm as a function of mean velocity (Weibull coeff. k=2) for 4 different wind turbines

The influence of wind velocity on production cost is shown in figure 7 for 4 different wind turbines. It could be seen that the production cost difference for these wind turbines is roughly divided by 2 at high wind speeds.

6 - CONCLUSIONS AND MARKET TREND

In this paper we have tried to shed more light to the problem of costs assessment of a wind farm project and to evaluate the influence of different parameters. The wind turbine market is changing rapidly and the costs presented in this paper are based on some average values of the prices, published in 1994 and 95. Nevertheless we have tried to study more specially the influence of different parameters.

The operation time of the MW class turbines and large industrial applications of these turbines are still not enough and the prediction for best size/production costs for the near future suffers from lack of feedback experience of these turbines over a sufficiently long periods. The turbine cost increases as a function of d^3 (d : rotor diameter) and the power increases as a function of d^2. This law ('square cubic' law) shows that there is an optimum economic size for the wind turbines and we will somehow achieve it in a near future.

But the overall costs for all kind of wind turbines are decreasing continuously. Many experts [5,7] estimate that the costs of wind energy will drop by 20/30% over the next 10 years and the same rate of costs decreasing will be ongoing up to 2010.

REFERENCES

[1] H Gluck
Wind turbine Market 1995 - WINKRA-RECOM, Hannover

[2] European Wind Turbine Catalogue (91-94)
A Thermie programme action (N° WE 15) - European Commission (DG XVII)

[3] A Bossanyi, AG Strowbridge
Operation and Maintenance costs for UK Wind farms -
ETSU Report W/32/00207/REP, 1994

[4] JK Vesterdal
Experience with wind farms in Denmark
EWEA Special Topic Conference '92, sept 1992

[5] DJ Milborrow
Wind farm economics
Proc. Inst. Mech. Eng. Vol 209, 1995

[6] MJ Steadman
Site development costs for wind farm sites
ETSU Report WN 5092, Feb. 1992

[7] Commission of the European Communities,
DG XVII. The European Renewable Energy Study, 1994

WINDPOWER '96 Awards

Utility Award
Central and South West Services, Inc.

Technical Award
Dr. Amir Mikhail
Zond Corporation

Federal Award
Darrell Dodge
National Wind Technology Center

Windsmith Award
Ed Duggan
FloWind Corporation

Academic Award
Dr. John F. Mandell
Montana State University

Wind Industry Person of the Year
Nancy Rader

Lifetime Acheivement Award
Senator Mark Hatfield